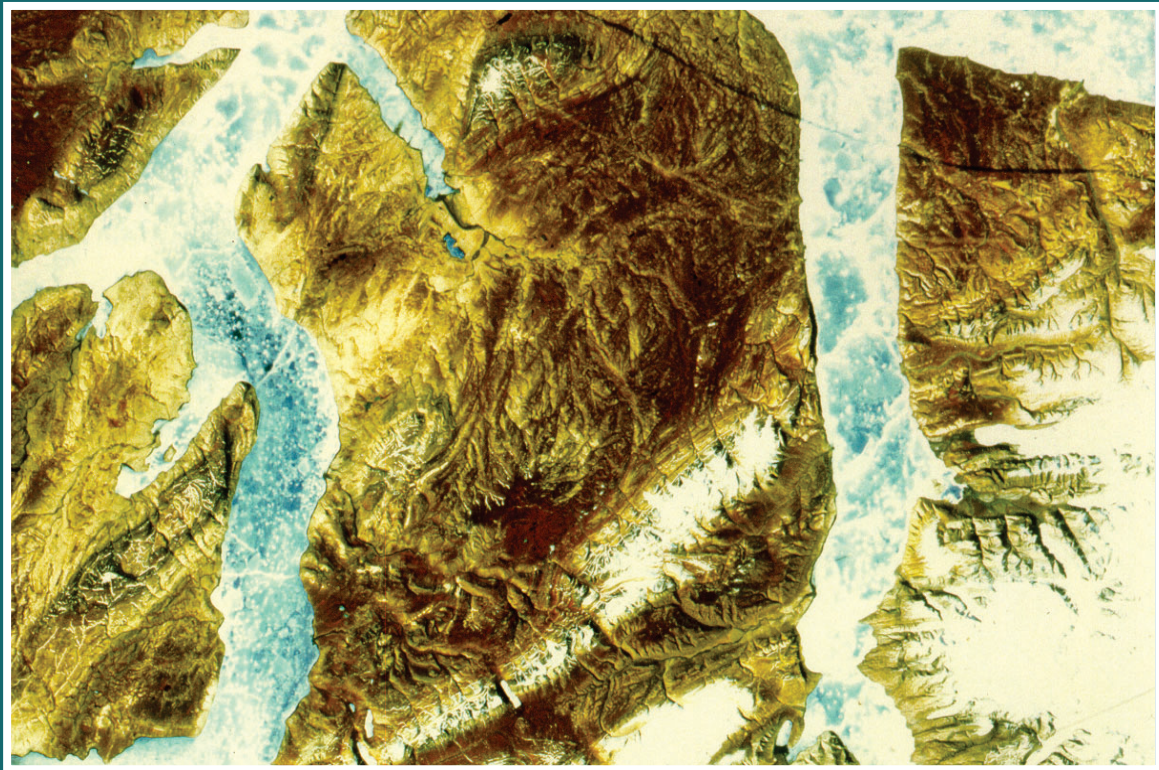




GEOLOGICAL SURVEY OF CANADA
BULLETIN 529

ENVIRONMENTAL RESPONSE TO CLIMATE CHANGE IN THE CANADIAN HIGH ARCTIC

Edited by
M. Garneau and B.T. Alt



2000



Natural Resources
Canada

Ressources naturelles
Canada

Canada

GEOLOGICAL SURVEY OF CANADA
BULLETIN 529

**ENVIRONMENTAL RESPONSE TO CLIMATE
CHANGE IN THE CANADIAN HIGH ARCTIC**

Edited by
M. Garneau and B.T. Alt

2000

©Her Majesty the Queen in Right of Canada, 2000

Catalogue No. M42-529E
ISBN 0-660-18336-6

Available in Canada from
Geological Survey of Canada offices:

601 Booth Street
Ottawa, Ontario K1A 0E8

3303-33rd Street N.W.
Calgary, Alberta T2L 2A7

101-605 Robson Street
Vancouver, B.C. V6B 5J3

A deposit copy of this publication is also available for reference
in selected public libraries across Canada

Price subject to change without notice

Cover illustration

Satellite photograph of Fosheim Peninsula and surrounding area
(Landsat II bands are 4, 5, 7).

Editors' addresses

Michelle Garneau
INRS-Eau, 2800 rue Einstein
C.P. 7500
Sainte-Foy, Quebec
G1V 4C7

Bea Alt
Balanced Environments Associates
5034 Leitrim Road
Carlsbad Springs, Ontario
K0A 1K0

Original manuscript submitted: 1997-12
Final version approved for publication: 2000-02

CONTENTS

Foreword/Avant-propos D.A. St-Onge	vi
Summary/Sommaire	viii
Introduction M. Garneau, B.T. Alt, and S.A. Edlund	1

CURRENT CLIMATE AND MODERN CONDITIONS

MODERN CLIMATE

Overview of the modern arctic climate B.T. Alt and B. Maxwell	17
Automatic weather station results from Fosheim Peninsula, Ellesmere Island, Nunavut B.T. Alt, C.L. Labine, D.E. Atkinson, A.N. Headley, and P.M. Wolfe	37
Modelling July mean temperatures on Fosheim Peninsula, Ellesmere Island, Nunavut D.E. Atkinson	99

MODERN FLORA AND FAUNA

Overview of vegetation zonation in the Arctic S.A. Edlund and M. Garneau	113
Vegetation patterns on Fosheim Peninsula, Ellesmere Island, Nunavut S.A. Edlund, B.T. Alt, and M. Garneau	129
The insects, mites, and spiders of Hot Weather Creek, Ellesmere Island, Nunavut F. Brodo	145

QUATERNARY GEOLOGY OF FOSHEIM PENINSULA

Quaternary geology and glacial history of Fosheim Peninsula, Ellesmere Island, Nunavut T. Bell and D.A. Hodgson	175
Preliminary results on the Quaternary sedimentary environment and benthos of part of Cañon Fiord, Fosheim Peninsula, Ellesmere Island, Nunavut R. Gilbert and A.E. Aitken	197

Distribution and characterization of ground ice on Fosheim Peninsula, Ellesmere Island, Nunavut	
W.H. Pollard	207

***ENVIRONMENTAL CHANGES ON NORTHERN
ELLESMERE ISLAND***

LAKE RECORDS AND CLIMATE CHANGE

Physical, chemical, and biological characteristics of lakes from the Slidre River basin on Fosheim Peninsula, Ellesmere Island, Nunavut	
P.B. Hamilton, K. Gajewski, R. McNeely, and D.R.S. Lean	235

A 6500-year diatom record from southwestern Fosheim Peninsula, Ellesmere Island, Nunavut	
A.P. Wolfe	249

Summary of paleolimnological investigations of High Arctic ponds at Cape Herschel, east-central Ellesmere Island, Nunavut	
M.S.V. Douglas, J.P. Smol, and W. Blake, Jr.	257

Present and past environments inferred from Agassiz Ice Cap ice-core records	
J.C. Bourgeois, R.M. Koerner, B.T. Alt, and D.A. Fisher	271

Peat accumulation and climatic change in the High Arctic	
M. Garneau	283

Late Tertiary plant and arthropod fossils from the high-terrace sediments on Fosheim Peninsula, Ellesmere Island, Nunavut	
J.V. Matthews, Jr. and J.G. Fyles	295

Preliminary results of archeological research on Fosheim Peninsula and in adjacent areas of western Ellesmere and eastern Axel Heiberg islands, Nunavut	
P.D. Sutherland	319

***PERMAFROST DYNAMICS ON
FOSHEIM PENINSULA***

Ground-ice aggradation on Fosheim Peninsula, Ellesmere Island, Nunavut	
W.H. Pollard	325

Thaw-slump-derived thermokarst near Hot Weather Creek, Ellesmere Island, Nunavut	
S.D. Robinson	335

***HYDROLOGICAL SYSTEM ON
FOSHEIM PENINSULA***

Hydrological environment of the Hot Weather Creek basin,
Ellesmere Island, Nunavut
K.L. Young and M-k. Woo 347

Glacier hydrology in the Sawtooth Range, Fosheim Peninsula,
Ellesmere Island, Nunavut
P.M. Wolfe 375

Summary of results and recommendations
B.T. Alt and M. Garneau 391

FOREWORD

Archeology and anthropology teach us that as far back as we can venture to speculate, humans have attempted to predict the future, either to improve their chances of survival or to better their lot. Priests, philosophers, prophets, shamans, charlatans, and other inspired or educated individuals have consulted the stars, the entrails of birds, the wind, and other phenomena; they have used meditation, drugs, trances, or other means 'to reach a higher plane of consciousness' that would allow a glimpse of the future. This is not and should not be surprising given the extraordinary importance of planting crops at the most propitious time of the year or of predicting when and where the caribou herds will move from their summer calving grounds to their winter range.

In the Arctic, being able to predict the weather was crucial to survival 'on the perimeter of the habitable world'. In his 1996 book *Ancient People of the Arctic*, Dr. Robert McGhee argues that the Paleo-Eskimo people that we know as the Dorset developed their remarkable civilisation as a result of a dramatic cooling that began about 2000 BC. This well documented climatic event forced the Dorset people to change from hunting musk-oxen with bows and arrows to harvesting sea mammals with harpoons at the ice-flow edge. McGhee further argues that a warming trend 1000 years ago was largely responsible for the demise of the Dorset culture because it allowed the migration to Arctic Canada of a new civilisation, the Thule, who, because of their superior technology, could occupy the best hunting regions and thus accelerate the demise of the Dorset.

This remarkable example is only one of many where intimate links between a civilisation and climate can be shown convincingly. In a conceptual way, our current preoccupation with 'global change' is certainly not new to the human psyche. It is merely based on different concepts and technology. However, we would be fools indeed if we were to ignore the lessons of the past.

The Global Change Observatory on Hot Weather Creek, Fosheim Peninsula, Ellesmere Island, was established by the Geological Survey of Canada in 1989 to try to understand one small part of the climate change puzzle: by studying the past and attempting to understand the present, could we make reasonable and sound predictions for the future? The present volume includes contributions by numerous scientists, some with decades of Arctic experience, and brings together the results of work in numerous disciplines all linked by the common preoccupation of better understanding the natural environment of a part of the Canadian Arctic. The volume editors, Dr. Michelle Garneau and Bea Alt, deserve our congratulations and gratitude for this compendium of knowledge that will make it possible to better predict the impact of man-induced global changes in the climate of planet Earth.

Denis A. St-Onge
Science Advisor to the Polar Continental Shelf Project

AVANT-PROPOS

L'archéologie et l'anthropologie nous enseignent qu'aussi loin que nous pouvons regarder dans le passé, les êtres humains ont tenté de prévoir l'avenir pour améliorer leurs chances de survie ou leur sort. Les prêtres, les philosophes, les prophètes, les chamans, les charlatans ainsi que d'autres personnages inspirés ou éduqués ont consulté les étoiles, les entrailles des oiseaux, le vent et d'autres phénomènes; ils ont utilisé la méditation, les drogues, les transes ou d'autres moyens pour «atteindre le niveau de conscience supérieur» qui permet d'entrevoir l'avenir. Ceci n'est pas surprenant, et ne devrait pas nous surprendre non plus, étant donné la très grande importance du choix du moment le plus propice de l'année pour les semailles ou encore de la prévision de la date et du lieu de la migration des troupeaux de caribou de leurs aires estivales de mise bas vers leurs habitats d'hiver.

Dans l'Arctique, pouvoir prévoir le temps qu'il fera était essentiel pour la survie dans cet habitat «à la limite du monde habitable». Dans son livre «Ancient People of the Arctic», publié en 1996, M. Robert McGhee présente l'hypothèse voulant que les anciens Inuits, peuple que nous connaissons sous le nom de Dorset, ont développé leur remarquable civilisation à la suite d'un refroidissement dramatique du climat qui s'est amorcé il y a environ 4000 ans. Ce phénomène climatique bien documenté a forcé le peuple de Dorset à changer leur mode d'existence, fondé sur la chasse à l'arc des boeuf musqués, vers une subsistance basée sur la chasse au harpon des mammifères marins à la bordure de la glace de mer. McGhee soutient en outre qu'un réchauffement du climat amorcé il y a environ 1000 ans a été en grande partie responsable du déclin de la

culture Dorset parce qu'il a permis à une nouvelle civilisation, celle de Thulé, de migrer vers l'Arctique canadien. La technologie supérieure de la civilisation de Thulé lui a permis de s'accaparer les meilleurs terrains de chasse et a ainsi accéléré le déclin de la culture Dorset.

Cet exemple remarquable n'est qu'un des nombreux cas où on peut démontrer clairement des liens très étroits entre une civilisation et le climat. Du point de vue conceptuel, notre préoccupation actuelle concernant le «changement climatique» n'est certainement pas un fait nouveau pour l'âme humaine. Elle est seulement basée sur des concepts différents et sur la technologie. Cependant, nous manquerions certainement de sagesse si nous ignorions les leçons que peut nous offrir le passé.

L'observatoire du changement climatique du ruisseau Hot Weather sur la péninsule Fosheim de l'île d'Ellesmere a été établi par la Commission géologique du Canada en 1989 afin d'essayer de comprendre une petite partie du casse-tête que représente le changement climatique : En étudiant le passé et en essayant de comprendre le présent peut-on tenter des prévisions raisonnables et fondées pour l'avenir? Le présent ouvrage comprend des contributions par plusieurs scientifiques, dont certains ont des dizaines d'années d'expérience dans l'Arctique, et il rassemble les résultats des travaux dans de nombreuses disciplines toutes reliées par une préoccupation commune qui est de mieux comprendre l'environnement naturel d'une partie de l'Arctique canadien. Les rédactrices, Michelle Garneau et Bea Alt, méritent nos félicitations et notre gratitude pour ce recueil de connaissances qui rendra possible de meilleures prévisions de l'impact du changement climatique induit par l'action de l'homme sur le climat de la Terre.

Denis A. St-Onge
Conseiller scientifique pour l'Étude du plateau continental polaire

SUMMARY

The interdisciplinary environmental research undertaken by the High Arctic Integrated Research and Monitored Area of the Geological Survey of Canada on Fosheim Peninsula, Ellesmere Island, had two major thrusts: a cryosphere-atmosphere (snow and ice) program that studied past and present atmospheric changes at high latitudes and monitored transport and deposition of pollutants and aerosols, and a geosphere-biosphere (terrestrial) program focused mainly on highly sensitive terrain in the thermally enhanced interior of Fosheim Peninsula. This bulletin comprises 20 papers that present the results of the terrestrial component of this research, exploring the wide range of environmental processes, and one review paper covering the cryospheric component. An attempt is made to provide a spatial and temporal synthesis of the interpretation.

An overview of High Arctic climate, climate change, and climate modelling results provides a background for examining the unique climate of the Eureka intermontane, regional-scale, warm anomaly. The broad, interior lowland (about 1000 km²) of Fosheim Peninsula, represented by the Hot Weather Creek automatic weather station (autostation), experiences further summer heating due to its continental nature. Six years (1989-1994) of daily and monthly autostation data are examined. Mean July temperatures in the interior were 2°C warmer in cold, wet summers and 4.5°C warmer in warm, dry summers than at Eureka. These differences are particularly significant in evaluating past and future environmental change.

A model developed within a geographic information system platform to estimate mean July surface air temperature on a regional scale is discussed. The model quantifying the effect of proximity to the coast and elevation was applied to Fosheim Peninsula. Temperature data from a selection of Polar Continental Shelf Project field stations are used for comparison with the model results.

During quality control and documentation of the autostation data from Hot Weather Creek (and the Sawtooth Range stations) and the supporting metadata, careful attention was given to developing standards for the archiving and release of this type of nonstandard field-station data.

Bioclimatic zones, based on common growth forms of woody plants on mesic soils, are presented as background for the discussions of regional and local vegetation conditions on Fosheim Peninsula. The dense and diverse tundra and sedge-meadow vegetation is characterized by 145 plant species in the Hot Weather Creek area alone and, although it is atypical of its geographic location, it is not atypical of its thermal regime. However, the high percentage cover of vascular plant species cannot be accounted for easily by the meagre

SOMMAIRE

Le projet de recherche environnemental interdisciplinaire qui a été entrepris au Site de recherche et de surveillance intégrées de l'extrême Arctique de la Commission géologique du Canada sur la péninsule Fosheim, dans l'île d'Ellesmere, comprend deux volets principaux: un programme axé sur la cryosphère et l'atmosphère (la neige et la glace) pour l'étude des changements atmosphériques actuels et passés aux latitudes élevées ainsi que pour la surveillance du transport et du dépôt des polluants et des aérosols, et un programme axé sur la géosphère et la biosphère (terrestre) surtout mené dans les terrains fortement sensibles et en voie de réchauffement de l'intérieur de la péninsule Fosheim. Ce bulletin comprend 20 articles présentant les résultats du volet terrestre du projet de recherche et explorant la vaste gamme des processus environnementaux ainsi qu'un article de synthèse couvrant le volet sur la cryosphère. On tente de fournir une synthèse spatiale et temporelle de l'interprétation.

Une vue d'ensemble du climat, du changement climatique et des résultats de la modélisation du climat de l'extrême Arctique fournit l'information de base nécessaire pour l'examen du climat exceptionnel de l'anomalie régionale de réchauffement climatique du bassin intermontagneux d'Eureka. Les vastes basses terres intérieures de la péninsule Fosheim (environ 1 000 km²), que représente la station météorologique automatisée du ruisseau Hot Weather, subissent un réchauffement estival plus intense en raison de leur caractère continental. On examine les données journalières et mensuelles recueillies à la station météorologique automatisée sur une période de six ans (de 1989 à 1994). En comparaison avec celles d'Eureka, les températures moyennes du mois de juillet dans les basses terres intérieures ont été plus élevées de 2 °C lors des étés froids et humides et de 4,5 °C lors des étés chauds et secs. Ces différences sont très significatives pour l'évaluation des changements environnementaux passés et futurs.

On examine un modèle qui a été mis au point à l'aide d'un système d'information géographique pour estimer, à l'échelle régionale, la température moyenne de l'air en surface pendant le mois de juillet. Le modèle, qui quantifie l'effet de la proximité à la côte ainsi que de l'altitude, a été appliqué à la péninsule Fosheim. On utilise les données sur la température issues d'une sélection de stations de terrain de l'Étude du plateau continental polaire à des fins de comparaison avec les résultats du modèle.

À l'étape du contrôle de la qualité et de la documentation des données de la station météorologique automatisée du ruisseau Hot Weather (ainsi que des stations de la chaîne Sawtooth) et des métadonnées les soutenant, on a apporté un soin particulier à l'élaboration de normes pour l'archivage et la diffusion de ce type de données de stations de terrain non standard.

Des zones bioclimatiques, basées sur les formes de végétation ligneuses répandues sur les sols mésiques, sont présentées comme information de base pour la discussion des conditions locales et régionales de végétation de la péninsule Fosheim. La végétation de toundra et de cariçaie est dense et variée (dans la seule région du ruisseau Hot Weather elle comprend 145 espèces végétales) et, quoi qu'elle soit atypique pour l'emplacement géographique, elle n'est pas atypique pour le régime de température. Toutefois, le pourcentage élevé de couverture par des plantes vasculaires ne peut pas facilement être expliqué par les faibles précipitations estivales

summer precipitation reported (<70 mm annually at Eureka). Precipitation and ground-ice melt provide two distinct moisture sources. The precipitation-controlled mechanism operates in years with near-normal temperatures and the ground-ice-controlled regime prevails in warmer years. Relationships between vegetation and hydrological, geomorphic, and eolian processes are investigated.

The insect fauna at Hot Weather Creek is also richer than might be expected at this latitude. At least 226 taxa were recognized. The arthropod diversity is close to the ground, in the vegetation, on or in the soils, or in the very shallow to deeper, fresh-water bodies in the region. The dominant order is Diptera, with the family Chironomidae being the most abundant. Several species that might prove useful for monitoring climate change are identified.

The Quaternary geology and glacial history of Fosheim Peninsula are presented. The reconstruction of the last glaciation shows limited ice buildup attributed to the hyperaridity of the region at the time. The Holocene marine limit reached a maximum elevation of approximately 150 m a.s.l. along northern Eureka Sound and Greely Fiord and fell to the southwest to 139–142 m a.s.l. near the Sawtooth Range. The problems of the magnitude and pattern of Holocene emergence and the pattern and timing of deglaciation are discussed.

Acoustic profiling of the inner 40 km of Cañon Fiord revealed two acoustic facies. The lower facies represents deposition near or beneath glaciers that formerly extended down the fiord and may represent the late Pleistocene ice limit. Overlying these sediments are acoustically transparent to layered sediments up to 50 m thick that are glaciomarine deposits resulting from suspension settling of fine-grained sediments and from gravity flows (probably turbidity currents). Cluster analysis based on mollusc species defines three assemblages. In shallow-water (5–40 m), deltaic environments, a diverse *Astarte* spp. assemblage inhabits substrates of mud, sand, and gravel. Muddy substrates at depths of 10 to 20 m are inhabited by a low-diversity *Portlandia arctica* assemblage. In deep water (40–80 m), a low-diversity *Astarte crenata* assemblage inhabits sandy mud substrates.

The extensive occurrence of ground ice in the Eureka Sound lowlands of western Fosheim Peninsula is described. Of particular importance are the widespread distribution and the thickness of ice-rich sediments and massive ice. In marine sediments, massive ice occurs in two distinct stratigraphic positions, as either shallow bodies of pure ice interbedded with layers of icy sediment, or as deep, thick layers of horizontally layered, clear to white ice. Ground-ice aggradation and degradation contribute to the unique nature and evolution of periglacial ecosystems on Fosheim Peninsula.

observées (<70 mm par an à Eureka). Les précipitations et la fonte de la glace de sol fournissent deux sources d'humidité. Le régime d'humidité contrôlé par les précipitations entre en jeu lors des années aux températures près des normales alors que le régime caractérisé par la fonte de la glace de sol domine lors des années plus chaudes. On examine les relations entre la végétation et les processus hydrologiques, géomorphologiques et éoliens.

La faune d'insectes du ruisseau Hot Weather est également plus riche que celle normalement présente sous ces latitudes. On a y reconnu non moins de 226 taxons. La diversité des arthropodes se manifeste près du sol, soit dans la végétation, sur ou dans les sols ou encore dans les étendues d'eau douce (très peu profondes ou plus profondes) de la région. L'ordre dominant est celui des Diptères, la famille des Chironomidae étant la plus abondante. Plusieurs espèces qui pourraient servir d'indicateurs pour la surveillance du changement climatique sont identifiées.

On présente la géologie du Quaternaire et l'histoire glaciaire de la péninsule Fosheim. La reconstitution de la dernière glaciation montre qu'à cette époque, il y a eu une accumulation limitée de glace dans la région en raison de l'extrême aridité qui y régnait. La limite marine de l'Holocène a atteint une altitude maximale d'environ 150 m ASL le long de la partie nord du détroit d'Eureka et du fjord Greely et une altitude de 139 à 142 m ASL près de la chaîne Sawtooth. On discute de la problématique de la magnitude et de la distribution de l'émergence à l'Holocène ainsi que de la distribution et de la chronologie de la déglaciation.

Des profils acoustiques effectués dans les 40 km intérieurs du fjord Cañon ont révélé deux faciès acoustiques. Le faciès inférieur représente un dépôt près ou sous les glaciers qui s'étendaient autrefois le long du fjord et pourrait représenter la limite glaciaire du Pléistocène supérieur. Ces sédiments sont recouverts par des sédiments acoustiquement transparents ou stratifiés, qui ont jusqu'à 50 m d'épaisseur et qui représentent des dépôts glaciomarins formés par le dépôt de sédiments fins en suspension et par des coulées de masse (probablement des courants de turbidité). Des analyses typologiques des espèces de mollusques définissent trois assemblages. En eau peu profonde (de 5 à 40 m), dans un environnement deltaïque, on retrouve un assemblage varié d'*Astarte* sp. qui colonise les substrats boueux, sablonneux et graveleux. Un assemblage peu diversifié de *Portlandia arctica* habite les substrats boueux de 10 à 20 m de profondeur. En eau profonde (de 40 à 80 m), un assemblage peu diversifié d'*Astarte crenata* habite les substrats de boue sablonneuse.

On décrit la présence généralisée de glace de sol dans les basses terres de la partie ouest de la péninsule Fosheim le long du détroit d'Eureka. La présence généralisée et l'épaisseur des sédiments riches en glace et de la glace massive sont des points particulièrement importants. Dans les sédiments marins, la glace massive se rencontre en deux positions stratigraphiques distinctes, soit à faible profondeur, sous la forme de masses de glace pure interstratifiées avec des couches de sédiments riches en glace ou encore à plus grande profondeur, sous la forme d'épaisses couches horizontales de glace claire ou blanchâtre. L'accroissement et la dégradation de la glace de sol contribuent à la nature unique et à l'évolution particulière des écosystèmes périglaciaires de la péninsule Fosheim.

The chemical composition, nutrients, and diatom diversity of lakes and ponds in the largest watershed, the Slidre River basin, on Fosheim Peninsula were examined. Results show significant changes in lake pH, sodium, calcium and magnesium content, dissolved inorganic carbon, organic content of sediments, and benthic diatom community structure along an elevational transect of lakes through the basin. Water solutes vary from dilute calcium-bicarbonate-dominated headwater lakes to sodium-chloride-dominated lakes at the estuarine mouth. Calcium, sodium, and sulphate levels provide an assessment of the type of surficial materials in the basin and prove to be a useful proxy in defining marine limits in the region.

Information on a new diatom stratigraphy from a small, upland lake on southwestern Fosheim Peninsula contributes to the growing body of paleoecological studies in the area and to defining how High Arctic ecosystems respond to Holocene climate variability. The results of diatom analysis on a sediment core cover approximately 6500 years of continuous deposition. Diatom floras were consistently dominated by *Fragilaria* species. The diatom stratigraphy reveals significant differences between the two warm paleoclimatic periods encompassed by the record, i.e. the relatively wet, early to middle Holocene and the arid twentieth century.

A considerable amount of research on the neolimnology and paleoecology of ponds in the Cape Herschel area has been carried out since 1983. The moderate relief (up to 285 m a.s.l.) and varying exposure of 36 sites result in pronounced, interpond differences in microclimate, as well as variations in water chemistry, vegetation, and drainage characteristics. Marked differences in species composition are evident among the ponds that exhibit degrees of microhabitat specificity. Other biological indicators, such as chrysophytes and invertebrates, are also studied.

Paleolimnological data indicate that diatom assemblages have been relatively stable over the last few millennia, but then experienced unparalleled changes, likely beginning in the nineteenth century. The environmental factors causing these assemblage shifts are related to recent climate warming.

Glaciological investigations that have been underway on Agassiz Ice Cap since 1974 are reviewed. Six surface-to-bedrock ice cores provide long records of past environmental changes. Several shorter cores have been extracted near the deep ice cores and the areas around the sites have been extensively monitored. Melt concentrations and $d^{18}O$ records indicate that summer temperatures were $2^{\circ}C$ to $2.5^{\circ}C$ warmer during the Holocene than now. Since approximately 8000 BP, a gradual cooling has occurred in summer with a minimum about 100 to 200 years ago. Chemistry records reveal an increase in the concentration of contaminants in snow since the middle of the twentieth century,

On a examiné la composition chimique, les substances nutritives et la diversité des diatomées dans les lacs et les étangs du plus grand bassin-versant de la péninsule Fosheim, le bassin de la rivière Slidre. Les résultats montrent des changements importants du pH, des concentrations de sodium, de calcium et de magnésium, de la quantité de carbone inorganique dissous, du contenu organique des sédiments et de la structure de la communauté de diatomées benthiques des lacs le long d'un transect ascendant dans le bassin-versant. Les solutés dans l'eau varient : en amont, les eaux des lacs présentent des solutions diluées de bicarbonate de calcium et près de l'embouchure de l'estuaire, les eaux des lacs sont dominées par des solutions de chlorure de sodium. Les concentrations de calcium, de sodium et de sulfates fournissent une idée des types de matériaux de surface présents dans le bassin et constituent des indicateurs indirects utiles pour définir les limites marines dans la région.

On a tiré des informations sur une nouvelle stratigraphie des diatomées d'un petit lac en altitude au sud-ouest de la péninsule Fosheim, qui s'ajoutent à la masse croissante d'études paléocologiques dans la région et aident à définir la réponse des écosystèmes de l'extrême Arctique à la variabilité climatique pendant l'Holocène. Les résultats de l'analyse des diatomées dans une carotte de sédiments couvrent environ 6 500 ans de dépôt ininterrompu. Les flores de diatomées montrent une dominance constante des espèces de *Fragilaria*. La stratigraphie des diatomées révèle des différences importantes entre les deux périodes de réchauffement paléoclimatiques qu'elle couvre, c'est-à-dire la période humide de l'Holocène inférieur à moyen et la période aride du vingtième siècle.

Depuis 1983, on a effectué de nombreuses recherches sur la néolimnologie et la paléocologie des étangs de la région du cap Herschel. Le relief modéré (jusqu'à 285 m ASL) ainsi que l'exposition variée en 36 sites engendre d'importantes différences microclimatiques d'un étang à un autre ainsi que des variations dans la chimie de l'eau, dans la végétation et dans les caractéristiques du drainage. Il y a des différences marquées dans la composition des espèces dans les étangs qui révèlent divers degrés de spécificité des micro-habitats. On a également étudié d'autres indicateurs biologiques tels que les chrysophytes et les invertébrés.

Les données paléolimnologiques montrent que les assemblages de diatomées ont été relativement stables lors des quelques derniers millénaires mais qu'ils ont ensuite subi de grandes transformations, probablement à partir du dix-neuvième siècle. Les facteurs environnementaux qui ont causé ces variations dans les assemblages sont reliés au réchauffement climatique récent.

On passe en revue les études glaciologiques qui sont en cours sur la calotte glaciaire Agassiz depuis 1974. Six carottes de glace, de la surface jusqu'au substratum rocheux, nous fournissent de longs registres des changements environnementaux passés. Des carottes plus courtes ont été prélevées près des carottes de glace profondes et les régions voisines des sites ont fait l'objet d'une surveillance intense. Les concentrations de fusion et les observations de $d^{18}O$ indiquent que les températures estivales lors de l'Holocène dépassaient les températures contemporaines de 2 à $2,5^{\circ}C$. Un refroidissement graduel des températures estivales a commencé vers 8 000 BP, et un minimum a été atteint il y a environ 100 à 200 ans. Les données chimiques indiquent qu'il y a une augmentation de la concentration des contaminants dans la neige depuis le milieu

which is associated with a marked increase in SO₂ emissions in Europe. Long-range transport of tree and herbaceous pollen is also evident from pollen analyses of the snow layers of the Agassiz Ice Cap. The pollen assemblages show seasonal and annual variations that are compared with meteorological records obtained from automatic weather stations.

Peat has accumulated during the Holocene under the influence of many factors, all of which may vary with climate. In the Hot Weather Creek area, the onset of peat accumulation followed postglacial marine emergence at about 7500 BP. To determine whether peat accumulation has been greater in the past than it is today, 48 peat deposits (modern and fossil) from the present-day surface to the underlying mineral surface were sampled. Results of macrofossil, stratigraphic, and radiocarbon analyses demonstrate that the rate of peat growth varied considerably through the Holocene, although large accumulations of bryophytes formed during the middle Holocene in areas where little peat is accumulating today. For this reason, it is important to consider a combination of allogenic and autogenic factors to understand the presence and persistence of these organic deposits under High Arctic latitudes.

Macroremains of bryophytes, vascular plants, and arthropods have been found at a number of sites in the so-called 'high-terrace sediments' on Fosheim Peninsula. Fossils from these sites not only help to bracket the age of the sediments, but also provide information on late Tertiary environments of the region. The climate was significantly warmer than at present and at times the region was occupied by open forests. The open forests of Fosheim Peninsula, even those forming the treeline, were more diverse than modern taiga, which presently has its northern limit thousands of kilometres farther south.

An archeological survey carried out on Fosheim Peninsula and in the surrounding areas during the summer of 1992 located 237 archeological sites; test excavations were made at six sites. Prehistoric occupation of the region apparently occurred primarily during two periods: approximately 2500 to 1000 BC (4000–3000 BP) and AD 700 to 1700 (1300–300 BP). During both periods, cultural adaptations seem to have been based largely on hunting of land mammals, but there is evidence of increased hunting of sea mammals during the latter period when sea ice was more open. The recovery of paleobiological material from archeological sites in the region indicates the presence in the area of species currently limited to more southern ranges.

On the basis of information obtained from the seven ice-rich areas in the Eureka Sound lowlands, a simple model is proposed for the widespread occurrence of ground ice in western Fosheim Peninsula. Stratigraphic, petrographic, and hydrochemical data suggest that the

du vingtième siècle, qui est associée à une importante augmentation des émissions de SO₂ en Europe. Un transport du pollen des arbres et des plantes herbacées sur de grandes distances est également évident d'après les analyses des couches de neige de la calotte glaciaire Agassiz. Les assemblages de pollen montrent des variations annuelles et saisonnières qui sont comparées avec les observations météorologiques enregistrées aux stations météorologiques automatisées.

La tourbe s'est accumulée pendant l'Holocène et cette accumulation dépend de plusieurs facteurs qui peuvent tous varier avec le climat. Dans la région du ruisseau Hot Weather, l'accumulation de tourbe a commencé après l'émergence marine postglaciaire, vers environ 9 500 BP. Afin de déterminer si les taux passés d'accumulation de tourbe étaient plus élevés que le taux contemporain, on a échantillonné 48 dépôts de tourbe (contemporains et fossiles) depuis la surface actuelle jusqu'à la surface minérale sous-jacente. Les résultats des analyses de la stratigraphie, des macrofossiles et au radiocarbone indiquent que le taux d'accumulation de la tourbe a varié de façon importante pendant l'Holocène, bien que de grandes accumulations de bryophytes se soient formées pendant l'Holocène moyen dans des régions où il y a peu d'accumulation contemporaine de tourbe. Pour cette raison, il est important de tenir compte d'une combinaison de facteurs allogéniques et autogéniques si on veut comprendre pourquoi ces dépôts organiques sont présents et persistants aux latitudes de l'extrême Arctique.

On a trouvé des macrorestes de bryophytes, de plantes vasculaires et d'arthropodes en un certain nombre d'endroits dans les sédiments dits «de la haute terrasse» de la péninsule Fosheim. Les fossiles de ces sites facilitent non seulement une datation plus précise des sédiments mais fournissent également de l'information sur les environnements du Tertiaire tardif dans la région. À cette époque, le climat était beaucoup plus chaud que le climat contemporain et pendant certaines époques la région était recouverte de forêts clairsemées. À la différence de la taïga moderne, dont la limite actuelle se situe à des milliers de kilomètres au sud, les forêts clairsemées de la péninsule Fosheim, même celles qui formaient la limite de croissance des arbres, étaient plus diversifiées.

Un levé archéologique effectué sur la péninsule Fosheim et aux environs lors de l'été 1992 a permis de localiser 237 sites archéologiques; on a effectué des excavations d'essai en six emplacements. Pendant la préhistoire, la région a vraisemblablement été habitée surtout pendant deux périodes : soit de 2 500 à 1 000 ans av. J.-C. (de 4 000 à 3 000 BP) et de 700 à 1 700 ans apr. J.-C. (de 1 300 à 300 BP). Durant ces deux périodes, les adaptations culturelles semblent avoir été surtout basées sur la chasse aux mammifères terrestres, mais il y a des signes que la chasse aux mammifères marins a augmenté pendant la période plus récente alors qu'il y avait plus d'ouvertures dans la couverture de glace marine. Les matériaux paléobotaniques récupérés aux sites archéologiques de la région indiquent la présence d'espèces qui sont actuellement limitées à des répartitions plus méridionales.

En se basant sur l'information recueillie dans les sept régions riches en glace des basses terres longeant le détroit d'Eureka, on propose un modèle simple pour expliquer la présence généralisée de glace de sol dans la partie ouest de la péninsule Fosheim. Les données stratigraphiques, pétrographiques et hydrochimiques

ice is probably the result of rapid permafrost aggradation into recently emergent, marine sediments. The widespread occurrence of stabilized, retrogressive thaw slumps suggests that ground ice was even more common in the past. These data form the basis of a genetic model of ground-ice formation that is compatible with the limited glaciation ('Little Ice') hypothesis suggested for this part of the High Arctic during the late Quaternary and is closely linked to the sea-level history of the region.

Early Holocene marine sediments near Hot Weather Creek contain laterally extensive, massive bodies of ice up to at least 17 m thick. Thermokarst degradation of these ice bodies, mainly in the form of polycyclic, retrogressive thaw slumps, has already affected 12 per cent of the 80 km² study area. Morphological changes and headwall retreat were monitored at nine thaw slumps. A strong correlation between headwall retreat and thawing degree days was found at slumps set in terrain sloping at over 10°. Correlations were weaker at slumps set in flatter terrain (<5°) and poor at thaw slumps with major headwall morphology changes during the thaw season. Maximum retreat at high- and low-angle slumps is predicted to increase to about 18 and 12 m/a respectively under a 4°C summer-warming scenario.

Results from three years of intensive field study in Hot Weather Creek basin demonstrate the large spatial and temporal variability of the basin's hydrological variables. Snowfall and rainfall vary considerably from year to year and their spatial distribution is uneven, being strongly affected by the local topography. Using the small subbasin of Heather Creek, the feasibility of upscaling point values to drainage-basin level by weighting the hydrological quantities for various facets of the terrain is demonstrated. Three field seasons with different hydrological characteristics provide temporal analogues to create scenarios of hydrological responses to climate change. Summer flow tends to be much curtailed under a warmer climate as elevated evaporation rates further reduce the amount of water available to streamflow.

Accumulation on Quviagivaa (4.7 km²) and Nirukittuq (0.4 km²) glaciers in the Sawtooth Range is predominantly in the form of wind-blown snow and is controlled primarily by topography. Superimposed ice formation is a vital factor in the survival of Quviagivaa Glacier. Melt depends on altitude and albedo. A multiple regression of air temperature, wind speed, incoming shortwave radiation, and net radiation hours from the glacier meteorological station produced the best estimates of daily runoff. Precipitation had the most dramatic effect on runoff and measurements on the glacier suggest that precipitation values at the Eureka autostation greatly underestimate the rainfall in the Sawtooth Range.

suggèrent que la glace de sol résulte probablement de l'aggradation rapide du pergélisol dans les sédiments marins nouvellement émergés. La présence généralisée de glissements régressifs dûs au dégel, maintenant stabilisés, porte à croire que la glace de sol était encore plus abondante dans le passé. Ces données forment la base pour un modèle génétique sur la formation de glace de sol qui est compatible avec l'hypothèse que la glaciation a été restreinte dans cette région de l'extrême Arctique pendant le Quaternaire supérieur et qui est rattaché de près à l'historique du niveau de la mer dans cette région.

Les sédiments marins de l'Holocène inférieur de la région du ruisseau Hot Weather renferment des masses de glace de grande étendue horizontale qui ont jusqu'à au moins 17 m d'épaisseur. La dégradation thermokarstique de ces masses de glace a déjà touché 12 p. 100 des 80 km² de la région à l'étude. On a surveillé les changements de morphologie et la retraite du front d'affaissement à neuf glissements dûs au dégel. On a trouvé une forte corrélation entre la retraite du front d'affaissement et le nombre de degrés-jours de fonte aux glissements situés dans un terrain ayant une pente supérieure à 10°. La corrélation était plus faible dans les terrains à pente moindre (<5°) et elle était très faible pour les glissements dûs au dégel présentant de grands changements morphologiques au front d'affaissement durant la saison de dégel. Dans un scénario de réchauffement estival de 4 °C, on prévoit que la vitesse de retraite maximale du front d'affaissement augmentera jusqu'à environ 18 m/a pour les glissements en terrain à forte pente et jusqu'à 12 m/a pour les glissements en terrain moins incliné.

Les résultats de trois années d'études intensives sur le terrain dans le bassin du ruisseau Hot Weather démontrent la grande variabilité spatiale et temporelle des variables hydrologiques du bassin. Les précipitations de neige et de pluie varient considérablement d'année en année et leur répartition spatiale est inégale, car elle est fortement influencée par la topographie locale. En utilisant le petit sous-bassin du ruisseau Heather, on démontre la faisabilité de l'extrapolation des valeurs ponctuelles jusqu'à l'échelle du bassin-versant en pondérant les quantités hydrologiques selon les diverses facettes du terrain. Des observations sur le terrain pendant trois saisons présentant des caractéristiques hydrologiques différentes fournissent des analogies temporelles pour la création de scénarios de réponse hydrologique au changement climatique. L'écoulement estival tend à diminuer considérablement pendant les périodes au climat plus doux alors que des taux d'évaporation élevés réduisent encore d'avantage la quantité d'eau disponible pour le ruissellement.

L'accumulation sur les glaciers Quviagivaa (4,7 km²) et Nirukittuq (0,4 km²) de la chaîne Sawtooth se fait surtout sous la forme de neige transportée par les vents et est principalement contrôlée par la topographie. La formation de glace superposée est un facteur essentiel pour la survie du glacier Quviagivaa. La fonte dépend de l'altitude et de l'albédo. Une régression multiple avec les valeurs de la température de l'air, de la vitesse du vent, du rayonnement incident de courte longueur d'ondes et du nombre d'heures de rayonnement net tel que mesuré à la station météorologique du glacier a fourni les meilleures estimations du ruissellement quotidien. Ce sont les précipitations qui ont l'effet le plus saisissant sur le ruissellement et des mesures effectuées sur le glacier font penser que les valeurs de précipitation mesurées à la station météorologique automatisée d'Eureka sous-estiment grandement les précipitations sous forme de pluie sur la chaîne Sawtooth.

The objectives of the project at the High Arctic Integrated Research and Monitoring Area were to assess the probable geological consequences of environmental changes, to identify where the geological impact of environmental changes is likely to be most severe, and to place general circulation model scenarios of global warming and anticipated process responses within the context of Holocene climatic and environmental changes. Impact analyses based on general circulation model scenarios are invaluable for understanding how climate interacts with other aspects of the environment. In this bulletin, modern climate, vegetation, and faunal (insects) data have been integrated with results from the Canadian general circulation model to predict consequences for ground ice. Hydrological sensitivity demonstrated changes in either direction and identified critical parameters. Research also integrated paleo-environmental information from a variety of sources including lacustrine, marine, and glacial sources, peat cores, and archeological sites. Although records of environmental changes extending to the Late Tertiary are of interest, research emphasis was placed on the Holocene with particular focus on the last centuries.

Les objectifs du projet en cours au Site de recherche et de surveillance intégrées de l'extrême Arctique étaient d'évaluer les conséquences géologiques probables de changements environnementaux, d'identifier des endroits où l'impact géologique des changements environnementaux sera le plus sévère, et de placer les scénarios de réchauffement climatique des modèles de circulation générale et les réponses anticipées des processus dans le contexte des changements climatiques et environnementaux de l'Holocène. Les analyses d'impact basées sur les scénarios dans les modèles de la circulation générale sont irremplaçables pour comprendre les interactions entre le climat et divers aspects de l'environnement. Dans ce bulletin, les données contemporaines sur le climat, la végétation et la faune (insectes) ont été intégrées aux résultats du modèle canadien de circulation générale afin de prévoir les conséquences pour la glace de sol. La sensibilité hydrologique a montré des variations dans les deux directions et a permis d'identifier des paramètres critiques. Les recherches ont également intégré de l'information paléoenvironnementale tirée de toute une gamme de sources comme les lacs, le milieu marin, les glaces, les carottes de tourbe et les sites archéologiques. Bien que les données sur les changements environnementaux allant jusqu'au Tertiaire tardif soient intéressantes, la recherche a surtout porté sur l'Holocène et spécifiquement sur les derniers siècles.



Frontispiece. Trimetrogon photo of the Fosheim Peninsula interior from the west. Note the relative uniformity of terrain between Black Top Ridge (foreground) and Sawtooth Range. Some locations are noted.
NAPL T490R-6

Introduction

M. Garneau¹, B.T. Alt², and S.A Edlund³

Garneau, M., Alt., B.T., and Edlund, S.A., 2000: Introduction; in Environmental Response to Climate Change in the Canadian High Arctic, (ed.) M. Garneau and B.T. Alt; Geological Survey of Canada, Bulletin 529, p. 1–15.

The Geological Survey of Canada's High Arctic Global Change Observatory was established on Fosheim Peninsula to support interdisciplinary studies related to environmental change. The primary objective on west-central and north-central Ellesmere Island was to determine relationships between geomorphic processes and climate to help predict the potential geological impact of global change. Establishing detailed paleoclimatic records for the region was an essential component of these climate-change studies. Paleocological studies (lake and sea records, ice cores, peat cores, and archeological records) along with other methods have been used to outline short-, middle-, or long-term climate variability. From the outset, the project has involved participants from government, universities, and industry.

HISTORY OF EXPLORATION IN THE STUDY AREA

North-central Ellesmere Island

Due to their proximity to Greenland and to northern Baffin Bay (and its open water area 'North Water'), the eastern coasts were the first parts of north-central Ellesmere Island to be explored not only by Europeans, but perhaps also by the Norse. Paleo-Eskimo people, who occupied the area at least 4000 years ago, and the more recent Neo-Eskimo people, who are the direct ancestors of the Inuit, both spread into the area from the west (McGhee, 1978).

In 1616, Baffin became the first European to sight Ellesmere Island; he also named Smith Sound (Fig. 1). His detailed mapping of the bay that now bears his name was not credited until its confirmation in 1818 by John Ross (who entered the area searching for the lost Franklin Expedition). From the farthest point north he reached off the Carey Islands, John Ross named the capes in the far distance at the entrance

to Smith Sound after his ships *Isabella* and *Alexander* (Fig. 1). Inglefield, while on a private expedition in search of Franklin in 1852, reached Cape Herschel and gave Ellesmere Island its name. His surgeon-naturalist, Peter Sutherland, made notes on and sketches of the geology of the coast. Meteorological journals are included in the appendices to Inglefield's narrative (Inglefield, 1853). Many of the features of the east coast of north-central Ellesmere Island were named in 1853 and 1854 by members of the Kane expedition. On the basis of observations of open water in Smith Sound (North Water) and Kennedy Channel made during this expedition, it was thought that the polar sea was open.

While searching for a route to the North Pole, Hayes (1860–1861), Hall (1871–1873), and Nares (1875–1876) charted the remainder of the northeast coast of Ellesmere Island, including Archer Fiord.

In 1881, as part of the First International Polar Year, Greely was left to build a wintering station at Fort Conger and to keep regular meteorological and magnetic records and begin the overland exploration of Ellesmere Island. This included the first crossing of Ellesmere Island from Archer Fiord to Greely Fiord by Lockwood who named the ice cap south of his route 'The Chinese Wall'. Greely later renamed it 'Mer De Glace Agassiz' after Agassiz, the renowned Swiss-American naturalist. It is now often known as the 'Agassiz Ice Cap'.

The mysteries of the complex Bache Peninsula area were solved in the fall of 1898 during two separate expeditions lead by Peary and Sverdrup respectively, who both spent the winter in the area. In 1904, a Canadian expedition under the command of Low of the Geological Survey of Canada landed on Cape Sabine and Cape Herschel and took possession of Ellesmere Island for Canada. A new era of exploration began on north-central Ellesmere Island. Royal Canadian Mounted Police posts were operated on Bache Peninsula from 1926 to 1933 and later at Alexandra Fiord.

¹ INRS-Eau, 2800, rue Einstein, C.P. 7500, Sainte-Foy, Quebec G1V 4C7

² Balanced Environments Associates, 5034 Leitrim Road, Carlsbad Springs, Ontario K0A 1K0

³ Terrain Sciences Division, Geological Survey of Canada, 601 Booth Street, Ottawa, Ontario K1A 0E7

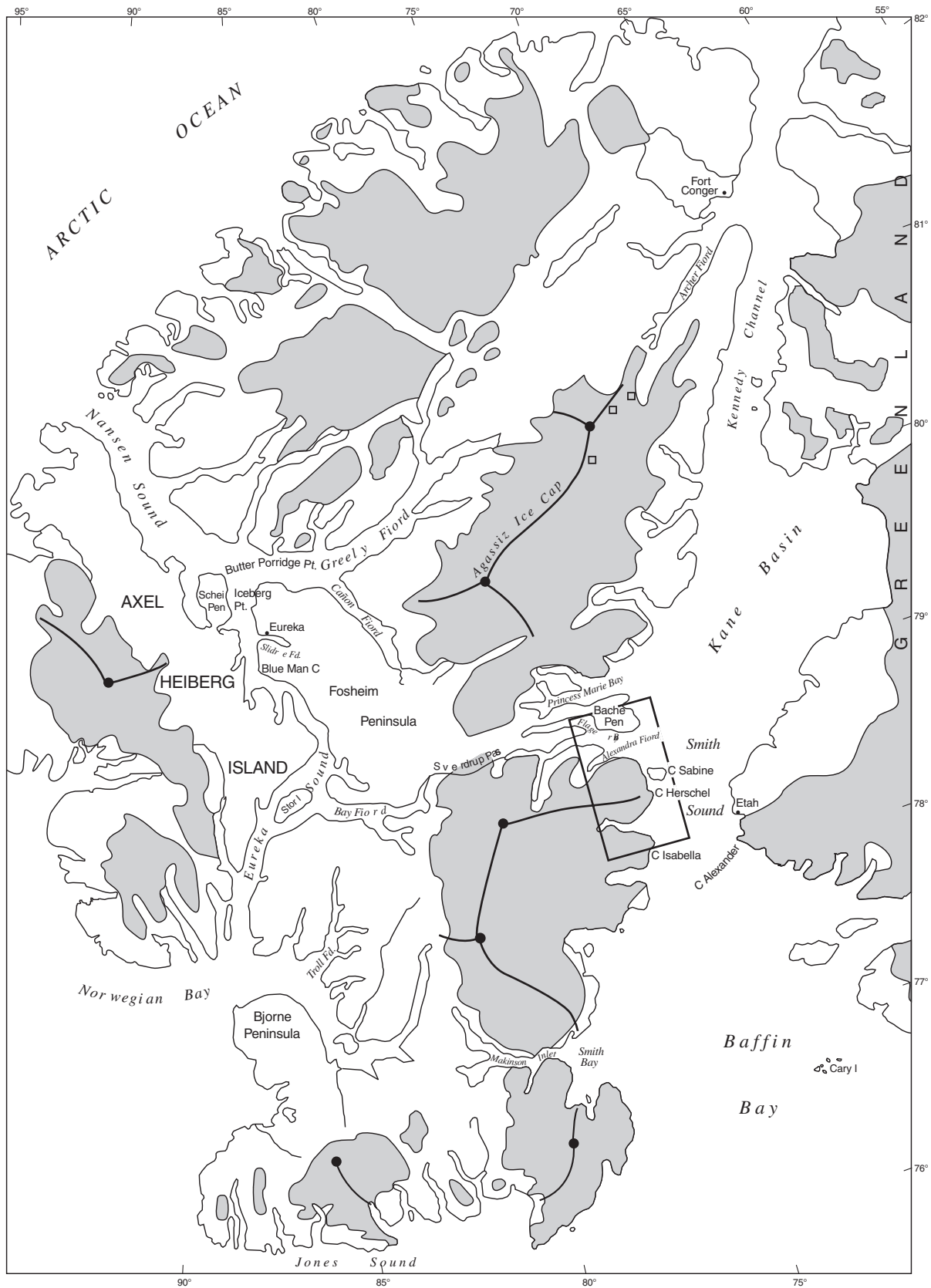


Figure 1. Map of north-central Ellesmere Island showing place names given by early explorers in the Cape Herschel and Agassiz Ice Cap area and Fosheim Peninsula. Solid lines represent Koerner's traverses on Agassiz Ice Cap; dots show the sites of 12 m cores on the traverse; squares indicate the sites of the Agassiz automatic weather station. The square outline shows the general location of the Cape Herschel study area.

Fosheim Peninsula

On April 29, 1899, Sverdrup and Bay reached the head of Bay Fiord, travelling west from Flagler Fiord by way of what is now called ‘Sverdrup Pass’ (Fig. 2). From there, they were

the first to view the mountains of the island they named ‘Axel Heiberg’. Three months later, Peary, having climbed the glacier at the head of Princess Marie Bay, glimpsed Cañon Fiord and Axel Heiberg Island. However, his heart was set on the

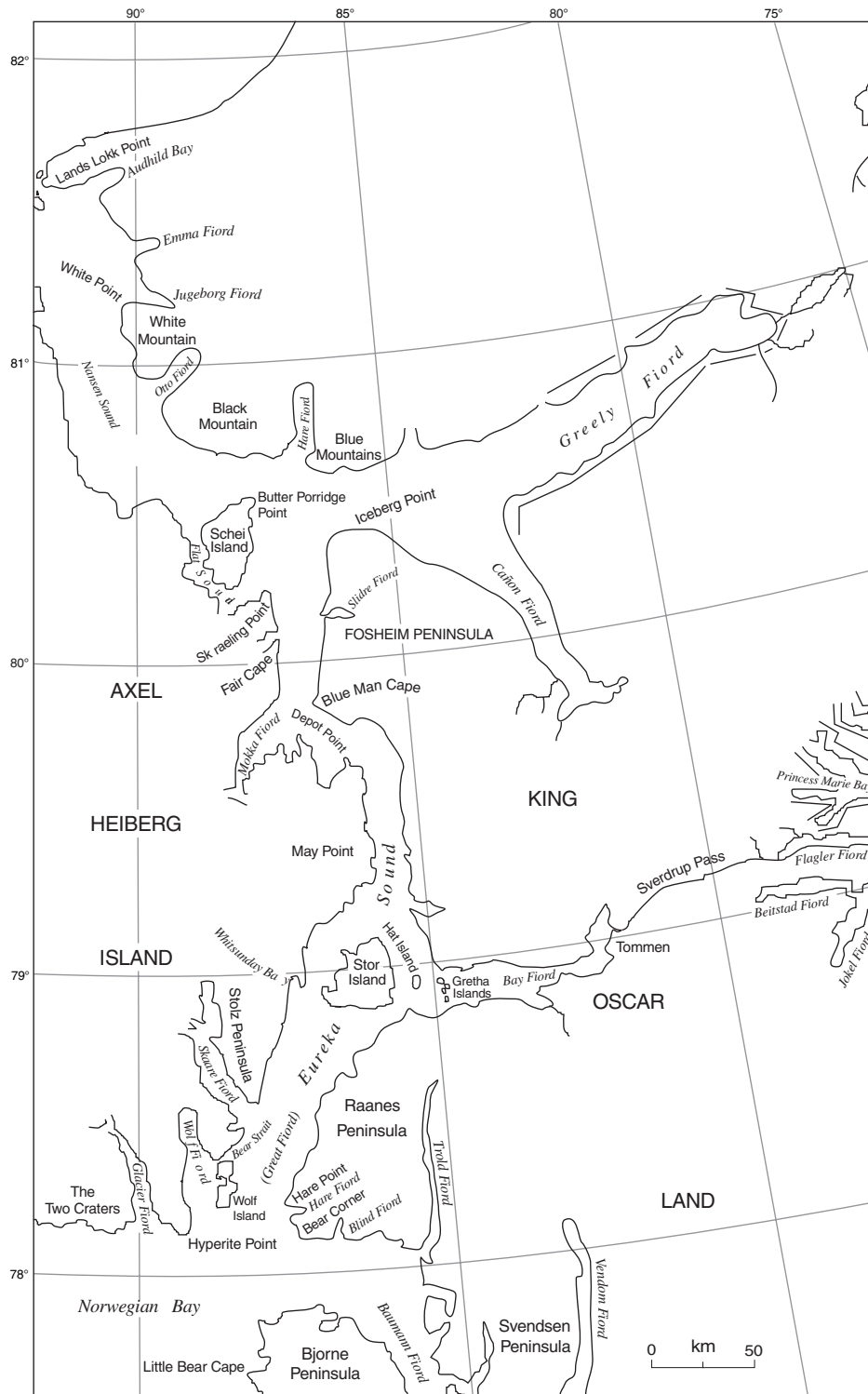


Figure 2. Map prepared by Isachsen, Sverdrup’s cartographer, for the original edition of *New Land* as reproduced in Fairley (1959) showing discoveries in the Eureka Sound area. Coastlines charted by earlier expeditions are indicated by a thinner line along the coastline.

North Pole and it was Sverdrup's party of scientists who "contributed more than any one expedition to the map of Ellesmere Island...." (Dunbar and Greenway, 1956, p. 296). Sverdrup gave up his northern Greenland objective and took his ship, the *Fram*, into western Jones Sound. Extensive exploration was carried out over the next two years. In 1900, Isachsen reached as far north as Stor Island, but mistook it for the head of what he called 'Great Fiord'. The following spring, Sverdrup, along with Fosheim, Schei, and Raanes, made an arduous trip overland from the head of Troll Fiord and west to the mouth of Bay Fiord (Fairley, 1959, Fig. 2, p. 153), rounded the point, "And what did we see? A beautiful large sound extending northward as far as the eye could reach!" (Fairley, 1959, p. 190). "Fosheim was again ready with a name. It had probably been simmering for some time and he came out with it pat, before anybody else had time to make a suggestion. He called it Heureka Sund (Eureka Sound), and this is the name it has kept." (Fairley, 1959, p. 191)

After celebrating the discovery, the party turned north up Eureka Sound. Fosheim and Raanes parted from Sverdrup at Blue Man Cape and travelled north along the east side of Eureka Sound.

They ran across the entrance of a 'smallish fiord running inward in an easterly direction, with lowlands in the background,...which was later called Slidrefiord...' (Sverdrup, 1904, p. 274) and rounded Iceberg point on May 6. Following along the west side of Canyon Fiord, they attempted to cut westward up Wolf Valley near its head directly into Eureka Sound. In this purpose, they were defeated by deep snow and the tortuous course along the narrow valley.

— Taylor, 1955, p. 95

Sverdrup, travelling north in Eureka Sound with Schei, recorded this first description of Fosheim Peninsula as seen from Smorgrautberget (Butter Porridge Point) on 12 May 1901.

Due east of us, on the other side of the sound, stretched extensive lowlands. Where the land ended and the sea began we could not decide, but at any rate we saw enough to tell that a largish fiord cut far into the land south-east of the cape which Fosheim, as we learned later, named Isfeldodden (Iceberg Point).

— Fairley, 1957, p. 197

Sverdrup's expedition and most early expeditions were interdisciplinary. According to Taylor (1957),

Sverdrup's hurriedly written narrative is well done. It is not only full of exciting adventure, but contains many interesting observations respecting archaeology, geology, geomorphology, ice conditions, and sledging techniques. Sverdrup's ability to find food for his dogs and men by hunting allowed him to extend his journeys hundreds of miles beyond what he might otherwise have been able to accomplish. He was part of the beginning of the Stefansson technique of Polar travel.

In a footnote, Taylor points out that Sverdrup (1904) presents "important scientific appendices by Schei (geology), Bay (zoology), and Simmons (botany and meteorology)." He goes on to list the publications coming out of the expedition, which "...include an extremely comprehensive series of 30

reports by Norsk Videnskaps-Akademi (1907-19)" and a long list of additional scientific reports (Taylor, 1957, p. 98). The great value of Schei's collections and observations is frequently acknowledged in the modern literature. (e.g. Taylor, 1957; Blackadar, 1963; Christie and Dawes, 1991).

In 1914, MacMillan passed Fosheim Peninsula on his way to look for the phantom Croker Land northwest of Axel Heiberg Island. Ekblaw, geologist and botanist to the expedition, made a round trip in 1915 from Etah on western Greenland, west via Sverdrup Pass, around Fosheim Peninsula, and returning east by way of Greely Fiord and Lake Hazen. "Ekblaw's account (MacMillan, 1918a, p. 33-70) contains some excellent passages describing the country through which he passed" (Taylor, 1957). MacMillan returned to Etah in 1925, this time with two aircraft and Byrd who, as pilot, was getting his first Arctic experience. Two flights were made across Ellesmere Island.

A number of Royal Canadian Mounted Police patrols, such as that of Amstead in 1929 around Axel Heiberg Island, passed Fosheim Peninsula, but little scientific work was done during these patrols because of the amazing speed at which they travelled. The Danish Thule and Ellesmere Island expedition also skirted Fosheim Peninsula in the spring of 1940. Vibe collected specimens for zoological, botanical, and geological museums in Copenhagen.

The use of aircraft changed the nature of arctic exploration in the post-World-War II period. On Fosheim Peninsula, this was particularly evident in the establishment of a permanent weather station on the north coast of Slidre Fiord by airlift from Thule Greenland (April, 1947). Eureka (Fig. 3), named after Sverdrup's and Fosheim's joyous discovery, was the first of six joint weather stations operated by Canada and the United States. It served as a base for subsequent scientific exploration of the area. The early investigations were restricted to coastal areas around Eureka (Bruggermann and Calder, 1953).

Aerial photography provided the first information from the interior of Fosheim Peninsula, which until then had only been skirted by exploration parties. Dunbar and Greenway (1956) describe the topography of Fosheim Peninsula and illustrate their descriptions with trimetragon photographs taken by the Royal Canadian Air Force in the spring of 1950 (see Fig. 4).

Air support was a major feature of Geological Survey of Canada's Operation Franklin headed by Fortier in 1955 and described by R.L. Christie as "a combined geological and aerial geophysical reconnaissance" (Christie and Dawes, 1991). The first ground observations from the interior of Fosheim Peninsula were made by McMillan (1963) who, accompanied by Marsden and Sims of the Geographical Branch, spent five days in the area on the north side of the Slidre River. His study area extended up the Slidre River 1.6 km past the junction with its tributary, which he called 'Hot Weather Creek' (Fig. 5). Along Hot Weather Creek, he discovered 'fossil forests' with stumps preserved in growth position (Christie and McMillan, 1991). He also reported on the physical features and stratigraphy of the study area. In

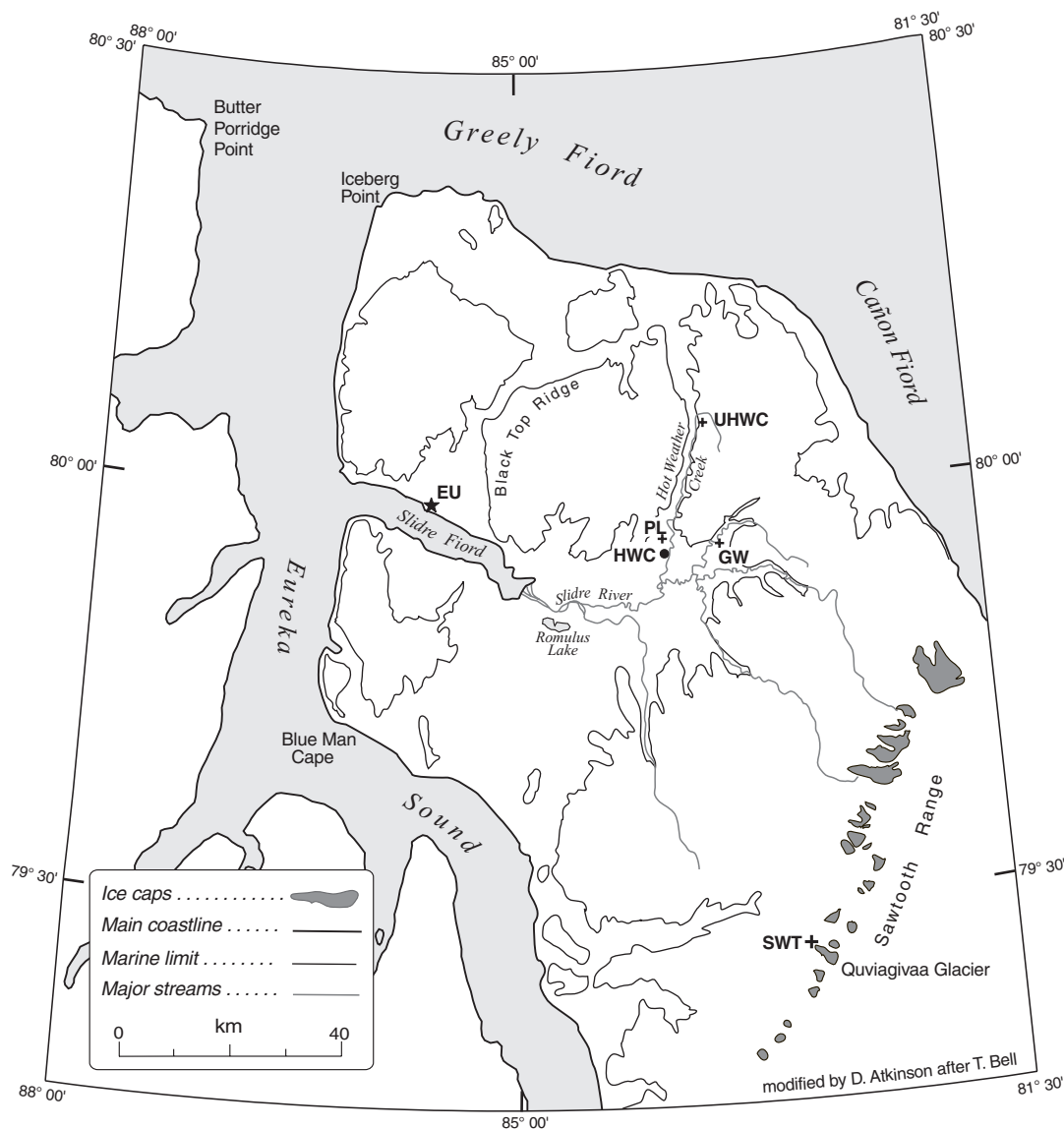


Figure 3. Fosheim Peninsula showing Eureka weather station (EU), Hot Weather Creek (HWC), Upper Hot Weather Creek (UHWC), Picnic lake (PL), and Gemini site (GW).

1961–1962, Operation Eureka, headed by R. Thorsteinsson, resulted in further geological mapping of the area (Thorsteinsson and Tozer, 1970).

In 1972, in response to a proposal to run a pipeline from the newly discovered Romulus well across the Fosheim Peninsula and the ice caps to Makinson Inlet on southeastern Ellesmere Island, Hodgson (1973) began an investigation of the surficial materials concentrated along the proposed route. More extensive mapping was undertaken in 1973 (Hodgson, 1974) and in 1974, Edlund (Edlund and Hodgson, 1975) added a vegetation component to the surficial geology, geomorphology, and terrain disturbance results, all of which are available as a series of preliminary maps (Hodgson and Edlund, 1977). These remain the basic detailed map reference for the area. Bell (1992, 1996) began work in the area in the late 1980s and he and other students have added details to the

original mapping. A continuing effort has been made to unravel the geological and geomorphological mysteries of the area (Hodgson, 1985; Fyles, 1989; Bell, 1992, 1996).

Agassiz Ice Cap

The first scientific investigations (and first crossing) of Agassiz Ice Cap involved four traverses made over snow by a field party of four, headed by Koerner in the spring of 1974 (Fig. 1). Investigations included radioechosounding and mass-balance and oxygen-isotope measurements on transects from sea level to between 1600 and 1800 m a.s.l. (Paterson, 1974; Koerner 1977, 1979). On the basis of the results, a suitable site for ice-core drilling was chosen and, in 1977, the first ice core was drilled at 1670 m a.s.l. near the top of the north-eastern part of Agassiz Ice Cap.



Figure 4. Trimetragon photograph(s) of the interior of Fosheim Peninsula from the west. Note the relative uniformity of the terrain between Black Top Ridge and the Sawtooth Range. Some locations are noted. NAPL T490R-8

THE HIGH ARCTIC GLOBAL CHANGE OBSERVATORY

In 1988, Edlund returned to Fosheim Peninsula and established an interdisciplinary Geological Survey of Canada camp at Hot Weather Creek (aptly named) to study the interaction of vegetation, soil hydrology, and other geomorphological processes in the surprisingly favourable climatic conditions that apparently existed in the interior of Fosheim Peninsula.

Ice-core drilling and surface-snow studies continued on Agassiz Ice Cap and, by 1988, had become an international interdisciplinary program headed by scientists from the Glaciology Section of the Terrain Sciences Division, Geological Survey of Canada.

Automatic weather stations were established in both areas in the spring of 1988. These were co-operative ventures with the Arctic Section of the Atmospheric Environment Service at Hot Weather Creek (Fig. 6) and with Campbell Scientific Canada Corporation on Agassiz Ice Cap (Fig. 1). The location of the Hot Weather Creek automatic weather station was chosen to represent the regional climate of the broad, interior lowland of Fosheim Peninsula. This lowland is shown in Figures 4 and 7. The main Agassiz station was established at the 1977 borehole site. Other stations were established at the 1984 borehole site and at the equilibrium line and in the accumulation zone of an outlet glacier that drains to the northeast (Fig. 1).

Participants in the two multidisciplinary programs, as well as other researchers involved in the area, recognized the need for integrated research and scientific co-operation to address the challenges presented by the unique, north-central Ellesmere region and to evaluate its response to past environmental change, present variability and future potential. Thus, in 1989, the Geological Survey of Canada's High Arctic Global Change Observatory was established. The program had two major components, a terrestrial one and a snow and ice one.

The terrestrial (geosphere/biosphere) component focused on the highly sensitive terrain of Fosheim Peninsula, where the response of landscape to modern climate change was monitored and paleoenvironmental reconstructions were done on the basis of sedimentary and archeological records.

The snow and ice (cryosphere/atmosphere) component studied past and present atmospheric changes at high latitudes using deep ice cores from High Arctic ice caps; it also monitored transport and deposition of pollutants and aerosols in recent snow samples from the surface of the Arctic Ocean and High Arctic ice caps.

Both components were interdisciplinary, international, and multi-agency programs. The breadth of subjects covered is reflected in the bibliography presented in Appendix A and in the different contributions in this bulletin.

PHYSIOGRAPHY

The study areas/sites discussed in this bulletin are mapped on Figures 1, 3, and 5 and, where appropriate, are shown on Figures 4 and 7. Specific aspects of the topography are discussed in the various contributions, but the maps and photographs show that the interior of Fosheim Peninsula is a low, rolling upland (Fig. 4, 7) flanked by the Black Top Ridge to the east and the Sawtooth Range to the southeast.

Fosheim Peninsula has ten distinct hydrometric basins. Lakes, ponds, and wetlands are limited, with lotic systems dominating the freshwater resources. Surface-water retention time for lotic systems is short, with fresh water draining quickly to the fiord especially during snow melt. Conversely, lentic systems are typically basin entrapments with long retention times.

The Sawtooth Range is home to over 35 separate ice fields, valley glaciers, and cirque glaciers, which range in size from less than 0.5 km² to 20 km² and cover approximately 75 km². An 8.7 km², glacierized catchment in the central Sawtooth Range (lat. 79°33.98'N, long. 83°20.48'W) (Fig. 3) was selected for study.

The Agassiz Ice Cap covers approximately 16 000 km² in the central part of Ellesmere Island between latitude 79°45' and 81°N. It is drained by glaciers that penetrate the surrounding mountains; the larger glaciers reach sea level. The series of boreholes was drilled in the northern part of the ice cap, at latitude 80°40'N, longitude 73°30'W. The first core (A77), drilled in 1977 to a depth of 338 m, was taken at an elevation of 1670 m about 1 km downslope from a local ice divide (Fig. 1).

Cape Herschel (lat. 78°37'N, long. 74°42'W), on the east-central coast of Ellesmere Island (Fig. 1), is a rugged peninsula of moderate relief, approximately 2 km wide by 5 km long, with the high point at 285 m a.s.l. It is characterized by a large number of ponds. Cape Herschel lies close to the northern limit of the North Water polynya.

RESEARCH CHALLENGES

The challenges presented to the integrated program were broad; those addressed in this bulletin include a synthesis of the temporal variations seen in the various types of paleoclimatic records and an attempt to define integrated environmental variations over a range of space scales.

One of the most important objectives of the present volume has been to bring together results of multidisciplinary research and evaluate data sets from the area. In some cases, such as macrofossil records, these data represent the accumulated efforts of many years of field activities that have been brought together in this volume. In other cases, such as climate and insect records, the data were collected specifically for the project and are presented here for future use and analysis. In all cases, the aim is to build a reliable database that will be accessible to future interdisciplinary studies in the High Arctic area.

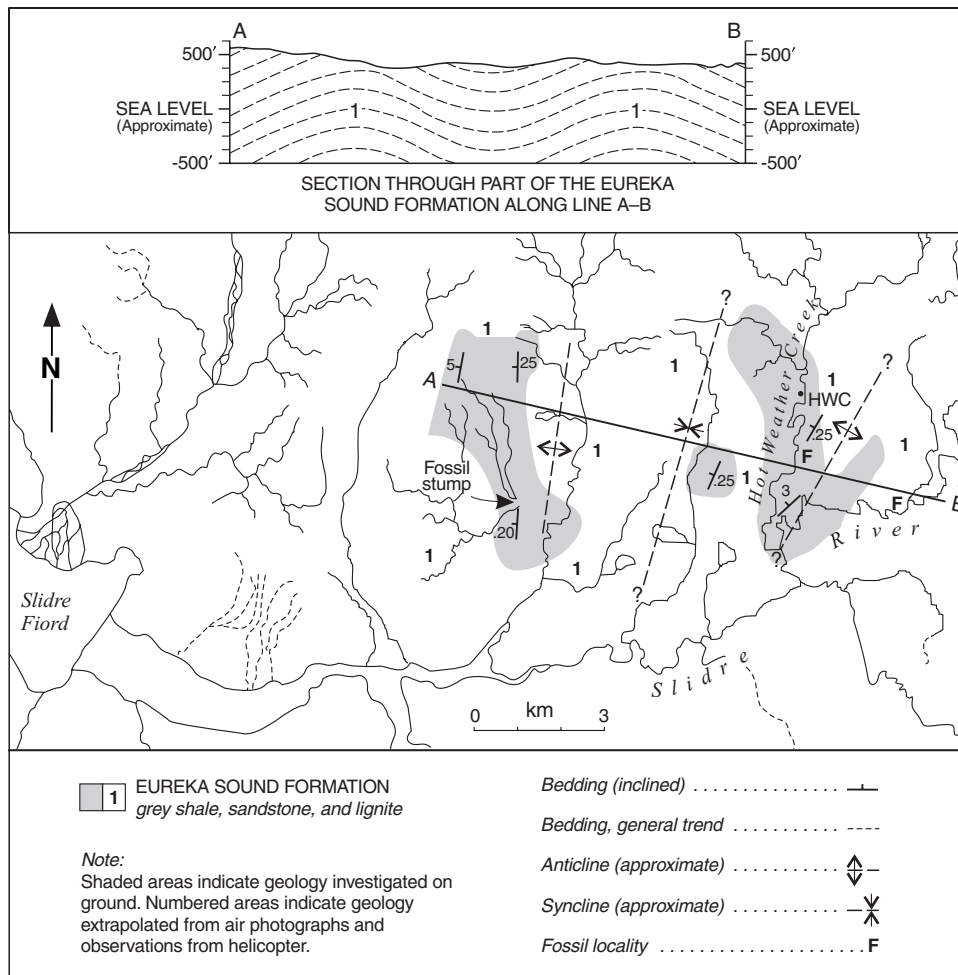


Figure 5. Map with the first reference to Hot Weather Creek and the Hot Weather Creek fossil forest (modified from McMillan, 1963). The location of the current Hot Weather Creek camp has been added.

Figure 6.

Map of study sites near the Hot Weather Creek base camp. AWS = automatic weather station

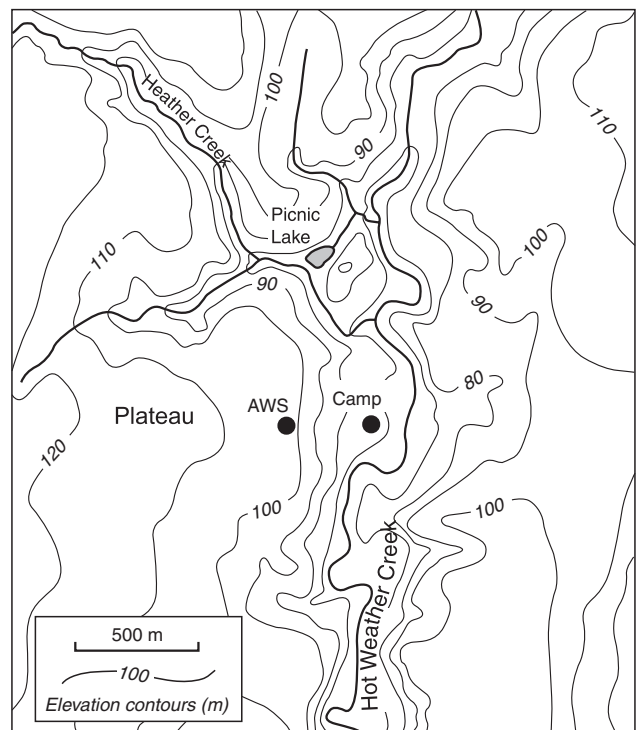




Figure 7. Satellite photograph of Fosheim Peninsula and surrounding area (Landsat II bands are 4, 5, 7).

Specific questions that required the integration of several disciplines include the mechanisms responsible for maintaining the dense and diverse vegetation observed over much of the Fosheim interior in spite of its high latitude and low measured precipitation; the lack of evidence, over most of the peninsula, of ice cover during the most recent glacial advance; the magnitude and pattern of marine emergence, the extent of massive ice, and the most useful proxy and instrumental indicators of climate change.

The final challenge is to assess the impact of change in any given aspect of the environment on the other components of the system, the most obvious being the effect of modelled predictions of climate warming due to increased greenhouse-gas concentrations in the atmosphere. Other types of natural and anthropogenic changes within the atmosphere-geosphere-biosphere are also important. This bulletin considers questions such as the impact of global change on the hydrology of a small basin, the effect of climate warming on vegetation, insect fauna, ground ice, and landscape features, and the increase and source of atmospheric pollutants.

REFERENCES

- Bell, T.**
1992: Glacial and sea level history of western Fosheim Peninsula, Ellesmere Island, Arctic Canada; Ph.D. thesis, University of Alberta, Edmonton, Alberta, 172 p.
1996: The last glaciation and sea level history of Fosheim Peninsula, Ellesmere Island, Canadian High Arctic; Canadian Journal of Earth Sciences, v. 33, p. 1075–1086.
- Blackadar, R.G.**
1963: History; in *Geology of the North-Central Part of the Arctic Archipelago, Northwest Territories (Operation Franklin)*, (ed.) Y.O. Fortier, R.G. Blackadar, B.F. Glenister, H.R. Greiner, D.J. McLaren, N.J. McMillan, A.W. Norris, E.F. Roots, J.G. Souther, R. Thorsteinsson, and E.T. Tozer; Geological Survey of Canada, Paper 48-23, p. 257–264.
- Bruggemann, P.F. and Calder, J.A.**
1953: Botanical investigations in northeast Ellesmere Island, Northwest Territories; *The Canadian Field-Naturalist*, v. 67, no. 4, p. 157–174.
- Christie, R.L. and Dawes, P.R.**
1991: Geographic and geological exploration; in Chapter 2 of *Geology of the Inuitian Orogen and Arctic Platform of Canada and Greenland*, (ed.) H.P. Trettin; Geological Survey of Canada, *Geology of Canada*, no. 3, p. 5–25 (also *Geological Society of America, The Geology of North America*, v. E, p.5–25).
- Christie, R.L. and McMillan, N.J.**
1991: Introduction; in *Tertiary Fossil Forests of the Geodetic Hills, Axel Heiberg Island, Arctic Archipelago*, (ed.) R.L. Christie and N.J. McMillan; Geological Survey of Canada, Bulletin 403, p. xiii–xvi.
- Dunbar, M. and Greenaway, K.R.**
1956: *Arctic Canada from the air*; Queen's Printer, Ottawa, 541 p.
- Edlund, S.A. and Hodgson, D.A.**
1975: Surficial geology, geomorphology, and terrain disturbance, Central Ellesmere Island, District of Franklin; Geological Survey of Canada, Paper 75-01A, p. 411.
- Fairley, T.C.**
1959: *Sverdrup's Arctic Adventures*; Longmans, London, England, 305 p.
- Fyles, J.G.**
1989: High terrace sediments, probably of Neogene age, west-central Ellesmere Island, Northwest Territories; in *Current Research, Part D*; Geological Survey of Canada, Paper 89-1D, p. 101–104.
- Hodgson, D.A.**
1973a: Surficial geology and geomorphology of central Ellesmere Island; Geological Survey of Canada, Paper 73-1A, p. 203.
- Hodgson, D.A. (cont.)**
1973b: Terrain performance, central Ellesmere Island, District of Franklin; Geological Survey of Canada, Paper 73-1A, p. 185.
1974: Surficial geology, geomorphology and terrain disturbance, central Ellesmere Island, District of Franklin; in *Report of Activities, Part A*; Geological Survey of Canada, Paper 74-1A, p. 247–248.
1985: The last glaciation of west-central Ellesmere island, Arctic Archipelago, Canada; Canadian Journal of Earth Sciences, v. 22, no. 3, p. 347–368.
- Hodgson, D.A. and Edlund, S.A.**
1978: Biophysical regions, western Fosheim Peninsula and eastern Axel Heiberg island; Geological Survey of Canada, Open File 501, scale 1:250 000.
- Inglefield, E.A.**
1853: *A Summer Search for Sir John Franklin: with a Peep into the Polar Basin*; T. Harrison, London, England, 232 p.
- Koerner, R.M.**
1977: Ice thickness measurements and their implications with respect to past and present ice volumes in the Canadian high Arctic ice caps; Canadian Journal of Earth Sciences, v. 14, no. 12, p. 2697–2705.
1979: Accumulation, ablation, and oxygen isotope variations on Queen Elizabeth Islands ice caps, Canada; *Journal of Glaciology*, v. 22, no. 86, p. 25–41.
- MacMillan, D.B.**
1918: *Four Years in the White North*; Harper, New York, 426 p.
- McGhee, R.**
1978: *Canadian Arctic Prehistory*; Van Nostrand Reinhold, Toronto, Ontario, 128 p.
- McMillan, N.J.**
1963: Slide River; in *Geology of the North-Central Part of the Arctic Archipelago, Northwest Territories (Operation Franklin)*, (ed.) Y.O. Fortier, R.G. Blackadar, B.F. Glenister, H.R. Greiner, D.J. McLaren, N.J. McMillan, A.W. Norris, E.F. Roots, J.G. Souther, R. Thorsteinsson, and E.T. Tozer; Geological Survey of Canada, Paper 48-23, p. 400–407.
- Paterson, W.S.B. and Koerner, R.M.**
1974: Radio echo sounding on four ice caps in Arctic Canada; *Arctic*, v. 27, no. 3, p. 225–233.
- Sverdrup, O.N.**
1904: *New Land : Four Years in the Arctic Regions*; Longmans, London, England, 496 p.
- Taylor, A.**
1955: *Geographical discovery and exploration in the Queen Elizabeth Islands*; Geographical Branch, Department of Mines and Technical Surveys, Canada, Memoir 3, 172 p.
- Thorsteinsson, R. and Tozer, E.T.**
1991: *Geology, Slide Fiord, District of Franklin*; Geological Survey of Canada, Map 1298A, scale: 1:50 000.

APPENDIX A

Bibliography of High Arctic observatory activities

J.A. Fergusson, S.A. Edlund, B.T. Alt, and M. Garneau

- Alt, B.T.**
1987: Arctic climates; in *Encyclopedia of Climatology*, (ed.) J.E. Oliver and R.W. Fairbridge, New York, p. 82–91.
- Alt, B.T. and Bourgeois, J.C.**
1995: Establishing the chronology of snow and pollen deposition events on Agassiz Ice Cap (Ellesmere Island, Northwest Territories) from autostation records; in *Current Research 1995-B*; Geological Survey of Canada, p. 71–79.
- Alt, B.T. and Maxwell, B.**
1990: The Queen Elizabeth Islands: a case study for arctic climate data availability and regional climate analysis; in *Canada's Missing Dimension — Science and History in the Canadian Arctic Islands, Volume I*, (ed.) C.R. Harington, Canadian Museum of Nature, Ottawa, Ontario, p. 294–326.
- Alt, B.T., Fisher, D.A., and Koerner, R.M.**
1992: Climatic conditions for the period surrounding the Tambora Signal in ice cores from the Canadian high Arctic islands; in *The Year Without a Summer? World Climate in 1816*, (ed.) C.R. Harington, Canadian Museum of Nature, p. 309–330.
- Alt, B.T., Kuchin, V.A., and Maxwell, J.B.**
1993: Investigations into the applicability of the AARI positive anomaly position classification catalogue to mass balance and climate change studies in the Queen Elizabeth Islands; Canadian Climate Centre Report no. 93-5, Atmospheric Environment Service, Downsview, Ontario, 25 p.
- Alt, B.T., Labine, C.L., Headley, A., Koerner, R.M., and Edlund, S.A.**
1992: High Arctic IRMA (Integrated Research and Monitoring Area) automatic weather station field data 1990–91, parts 1 and 2; Geological Survey of Canada, Open File 2562, 101 p.

- Alt, B.T., Labine, C.L., Headley, A., Koerner, R.M., and Edlund, S.A.** (cont.)
 1992: High Arctic IRMA (Integrated Research and Monitoring Area) automatic weather station field data 1990–91, Part 3; Geological Survey of Canada, Open File 2562, 173 p.
- Aitken, A.E. and Gilbert, R.**
 1996: Marine mollusca from Expedition Fiord, western Axel Heiberg Island, Northwest Territories, Canada; *Arctic*, v. 48, p. 29–43.
- Atkinson, D.E.**
 1994: Aspects of local- and regional-scale climatologies in the Canadian Arctic Islands: coastal effect at AES Eureka; Program with Abstracts, 28th Canadian Meteorological and Oceanographic Society (CMOS) Conference, Ottawa, Ontario, May 1994, p. 143.
- Barrie, L.A., Fisher, D., and Koerner, R.M.**
 1985: Twentieth century trends in Arctic air pollution revealed by conductivity and acidity observations in snow and ice in the Canadian high Arctic; *Atmospheric Environment Service*, v. 19, p. 2055–2063.
- Barry, p. and Pollard, W.H.**
 1992: Ground-probing radar investigation of ground ice on the Fosheim Peninsula, Ellesmere Island, N.W.T.; *The Musk-Ox*, v. 39, p. 59–67.
- Bell, T.**
 1992: Glacial and sea-level history of western Fosheim Peninsula, Ellesmere Island, Arctic Canada; Ph.D. thesis, University of Alberta, Edmonton, Alberta, 172 p.
 1992: Pre-last glaciation of west-central Ellesmere Island, Canadian High Arctic; *in* Proceedings, 22nd Arctic Workshop, Institute of Arctic and Alpine Research, Boulder, Colorado, p. 22–23.
 1996: The last glaciation and sea-level history of Fosheim Peninsula, Ellesmere Island, Canadian High Arctic; *Canadian Journal of Earth Sciences*, v. 33, no. 6, p. 1075–1086.
- Bell, T. and England, J.**
 1993: Extensive glaciations of Ellesmere Island: tentative age estimates based on amino acid ratios and paleoenvironmental implications; 23rd Arctic Workshop, Byrd Polar Research Center Miscellaneous Report 28, The Ohio State University, Columbus, Ohio, p. 90–92.
- Blake, W., Jr.**
 1977: Glacial sculpture along the east-central coast of Ellesmere Island, Arctic Archipelago; *in* Report of Activities, Part C; Geological Survey of Canada, Paper 77-1C, p. 107–117.
 1978: Coring of Holocene pond sediments at Cape Herschel, Ellesmere Island, Arctic Archipelago; *in* Current Research, Part C; Geological Survey of Canada, Paper 78-1C, p. 119–122.
 1981: Lake sediment coring along Smith Sound, Ellesmere Island and Greenland; *in* Current Research, Part A; Geological Survey of Canada, Paper 81-1A, p. 191–200.
 1981: Neoglacial fluctuations of glaciers, southeastern Ellesmere Island, Canadian Arctic Archipelago; *Geografiska Annaler*, v. 63A, p. 201–218.
 1982: Coring of frozen pond sediments, east-central Ellesmere Island; a progress report; *in* Current Research, Part C; Geological Survey of Canada, Paper 82-1C, p. 104–110.
 1987: Lake sediments and glacial history in the High Arctic; evidence from east-central Ellesmere Island, Arctic Canada, and from Inglefield Land, Greenland; *Polar Research*, v. 5, no. 3, p. 341–343.
 1989: Application of ¹⁴C AMS dating to the chronology of Holocene glacier fluctuations in the High Arctic, with special reference to Leffert Glacier, Ellesmere Island, Canada; *Radiocarbon*, v. 31, p. 570–578.
 1992: Shell-bearing till along Smith Sound, Ellesmere Island, Greenland: age and significance; *in* Quaternary Stratigraphy, Glacial Morphology, and Environmental Change, (ed.) A.-M. Robertsson, B. Ringberg, U. Miller, and L. Brunnberg; *Sveriges Geologiska Undersökning, Ser. Ca. 81*, p. 51–58 (Festschrift for Professor Jan Lundqvist).
 1992: Holocene emergence at Cape Herschel, east-central Ellesmere Island, Arctic Canada: implications for ice sheet configuration; *Canadian Journal of Earth Sciences*, v. 29, p. 1958–1980.
 1993: Holocene emergence along the Ellesmere Island coasts of northernmost Baffin Bay; *Norsk Geologisk Tidsskrift*, v. 73, p. 147–160.
- Blake, W., Jr., Boucherle, M.M., Fredskild, B., Janssens, J.A., and Smol, J.P.**
 1992: The geomorphological setting, glacial history and Holocene development of ‘Kap Inglefield Sø’, Inglefield Land, North-West Greenland; *Meddelelser om Grønland, Geoscience, Nr. 27*, 42 p.
- Bourgeois, J.C.**
 1986: A pollen record from the Agassiz Ice Cap, northern Ellesmere Island, Canada; *BOREAS*, v. 15, p. 345–354.
 1990: Seasonal and annual variation of pollen content in the snow of a Canadian high Arctic ice cap; *BOREAS*, v. 19, p. 313–322.
- Bourgeois, J.C., Koerner, R.M., and Alt, B.T.**
 1985: Airborne pollen: a unique air mass tracer, its influx to the Canadian High Arctic; *Annals of Glaciology*, v. 7, p. 109–116.
- Brassard, G.R. and Blake, W., Jr.**
 1978: An extensive subfossil deposit of the arctic moss *Aplodon wormskioldii*; *Canadian Journal of Botany*, v. 56, p. 1852–1859.
- Brodo, F.**
 1990: Crane flies (Diptera: Tipulidae) of the arctic islands; *in* Canada’s Missing Dimension — Science and History in the Canadian Arctic Islands, Volume II, (ed.) C.R. Harington; *Canadian Museum of Nature, Ottawa, Ontario*, p. 471–474.
- Brown, K.M., Douglas, M.S.V., and Smol, J.P.**
 1994: Siliceous microfossils in a Holocene High Arctic peat deposit (Nordvestø, Northwest Greenland); *Canadian Journal of Botany*, v. 72, p. 208–216.
- Burn, C.R. and Lewkowicz, A.G.**
 1990: Canadian landforms examples — 17: retrogressive thaw slumps; *Canadian Geographer*, v. 34, no. 3, p. 273–276.
- Doubleday, N.C., Douglas, M.S.V., and Smol, J.P.**
 1995: Paleoenvironmental studies of black carbonaceous particles in the High Arctic: a case study from northern Ellesmere Island; *The Science of the Total Environment*, v. 160/161, p. 661–668.
- Douglas, M.S.V.**
 1989: Taxonomic and ecological characterization of freshwater diatoms from the sediments of 36 High Arctic ponds (Cape Herschel, Ellesmere Island, N.W.T., Canada); M.Sc. thesis, Queen’s University, Kingston, Ontario, 173 p.
 1993: Diatom ecology and paleolimnology of High Arctic Ponds; Ph.D. thesis, Queen’s University, Kingston, Ontario, 161 p.
- Douglas, M.S.V. and Smol, J.P.**
 1987: Siliceous protozoan plates in lake sediments; *Hydrobiologia*, v. 154, p. 13–23.
 1993: Freshwater diatoms from high arctic ponds (Cape Herschel, Ellesmere Island, N.W.T.); *Nova Hedwigia*, v. 57, p. 511–552.
 1994: Limnology of high arctic ponds (Cape Herschel, Ellesmere Island, N.W.T.); *Archiv für Hydrobiologie*, v. 131, p. 401–434.
 1995: Periphytic diatom assemblages from high arctic ponds; *Journal of Phycology*, v. 31, p. 60–69.
 1995: Paleolimnological significance of chrysophyte cysts in arctic environments; *Journal of Paleolimnology*, v. 13, p. 79–83.
- Douglas, M.S.V., Smol, J.P., and Blake, W., Jr.**
 1994: Marked post-18th century environmental change in high arctic ecosystems; *Science*, v. 266, p. 416–419.
- Duchesneau, M.**
 1992: La calotte de glace Agassiz : profil physico-chimique et échanges neige-atmosphère; *The Musk-Ox*, v. 39, p. 86–92.
- Duff, K.E. and Smol, J.P.**
 1988: Chrysophycean statospores from the postglacial sediments of a High Arctic lake; *Canadian Journal of Botany*, v. 66, p. 1117–1128.
- Duff, K.E., Douglas, M.S.V., and Smol, J.P.**
 1992: Chrysophyte cysts in High Arctic ponds; *Nordic Journal of Botany*, v. 12, p. 471–499.
- Duff, K.E., Zeeb, B.A., and Smol, J.P.**
 1995: Atlas of Chrysophycean Cysts; Kluwer Academic Publishers, Dordrecht, 189 p.
- Edlund, S.A.**
 1989: Vegetation indicates potentially unstable Arctic terrain; *GEOS*, v. 18, p. 9–13.
 1989: Vegetation patterns assist in identifying potentially thaw-sensitive terrain on central Ellesmere Island, Arctic Canada; Proceedings, 40th Arctic Science Conference, Fairbanks, Alaska, September 14–16, 1989, 24 p. (abstract).
 1989: The coincidence of regional vegetation distribution patterns and summer temperatures in Arctic Canada; Proceedings, 40th Arctic Science Conference, Fairbanks, Alaska, September 14–16, 1989, 53 p. (poster abstract).
 1990: Woody plants as bioclimatic indicators in Arctic Canada; Proceedings, Symposium: Climate of Northern Latitudes: Past, Present and Future; University of Tromsø, Tromsø, Norway, April 2–4, 1990 (abstract).

- Edlund, S.A.** (cont.)
 1990: Bioclimatic zones in the Canadian Arctic Archipelago; *in* Canada's Missing Dimension — Science and History in the Canadian Arctic Islands, Volume I, (ed.) C.R. Harington; Canadian Museum of Nature, Ottawa, Ontario, p. 421–441.
- Edlund, S.A., Alt, B.T., and Young, K.L.**
 1989: Interaction of climate, vegetation, and soil hydrology at Hot Weather Creek, Fosheim Peninsula, Ellesmere Island, Northwest Territories; *in* Current Research, Part D; Geological Survey of Canada, Paper 89-1D, p. 125–133.
 1989: Vegetation, hydrology and climate at Hot Weather Creek, Ellesmere Island, Northwest Territories; Program, Annual Meeting of the Canadian Committee on Climate Fluctuations and Man, Ottawa, Ontario, January 25–27, 1989, Canadian Committee on Climate Fluctuations and Man Newsletter, v. 5, p. 65 (abstract).
 1989: Vegetation indicates potentially unstable Arctic terrain; GEOS, v. 18, no. 3, p. 9–13.
- Edlund, S.A., Woo, M-k., and Young, K.L.**
 1990: Climate, hydrology, and vegetation patterns at Hot Weather Creek, Ellesmere Island, Arctic Canada; Nordic Hydrology, v. 21, p. 273–286.
- Edlund, S.A., Young, K.L., and Woo, M-k.**
 1990: Aspects of vegetation and soil hydrology of Hot Weather Creek, Ellesmere Island, Arctic Canada; Proceedings, Eighth International Northern Regions Basin Symposium and Workshop, Abisko, Sweden (abstract).
- Egginton, P.A. and Hodgson, D.A.**
 1990: Preliminary assessment of selected drainage basins in western Fosheim Peninsula, Ellesmere Island, as sites for global change studies; *in* Current Research, Part D; Geological Survey of Canada, Paper 90-1D, p. 71–77.
- Fisher, D.A.**
 1987: Enhanced flow of Wisconsin ice related to solid conductivity through strain history and recrystallization; *in* The Physical Basis of Ice Sheet Modelling (Proceedings of the Vancouver Symposium, August 1987), International Association of Hydrological Sciences, publication no. 170, p. 45–51.
- Fisher, D.A. and Koerner, R.M.**
 1986: On the special rheological properties of ancient microparticle-laden northern hemisphere ice as derived from bore-hole and core measurements; Journal of Glaciology, v. 32, p. 501–510.
 1987: The effects of wind on $\delta^{18}\text{O}$ and accumulation give an inferred record of seasonal δ amplitude from the Agassiz Ice Cap, Ellesmere Island, Canada; Bern Symposium on Ice Core Analysis, March/April 1987; Annals of Glaciology, v. 10, p. 34–37.
 1994: Signal and noise in four ice-core records from the Agassiz Ice Cap, Ellesmere Island, Canada: details of the last millennium for stable isotopes, melt and solid conductivity; The Holocene, v. 4, p. 113–120.
- Fisher, D.A., Koerner, R.M., Paterson, W.S.B., Dansgaard, W., Gundestrup, N., and Reeh, N.**
 1983: Effect of wind scouring on climatic records from ice-core oxygen-isotope profiles; Nature, v. 301, p. 205–209.
- Fisher, D.A., Koerner, R.M., and Reeh, N.**
 1995: Holocene climatic records from Agassiz Ice Cap, Ellesmere Island, N.W.T., Canada; The Holocene, v. 5, p. 19–24.
- Fyles, J.G.**
 1989: High terrace sediments of Neogene age, west central Ellesmere Island, Northwest Territories; *in* Current Research, Part D; Geological Survey of Canada, Paper 89-1D, p. 101–104.
- Fyles, J.G., McNeil, D.H., Matthews, J.V., Jr., Barendregt, R.W., Marincovich, L., Jr., Brouwers, E., Bednarski, J., Brigham-Grette, J., Oviden, L.E., Miller, K.G., Baker, J., and Irving, E.**
 1998: Geology of Hvitland beds (late Pliocene), White Point Lowland, Ellesmere Island, Northwest Territories; Geological Survey of Canada, Bulletin 512, 35 p.
- Gajewski, K., Garneau, M., and Bourgeois, J.C.**
 1995: Paleoenvironments of the Canadian high Arctic derived from pollen and plant macrofossils: problems and potentials; Quaternary Science Reviews, v. 14, p. 609–629.
 1995: Postglacial vegetation history of the Canadian High Arctic; conference presented at the 28th Annual Meeting, American Association of Stratigraphic Palynologists, Ottawa; Program with Abstracts, p. A-7.
 1995: Interpretations of High Arctic pollen diagrams; poster presented at the 28th Annual Meeting, American Association of Stratigraphic Palynologists, Ottawa, Ontario; Program with Abstracts, p. A-7.
- Garneau, M.**
 1991: Rapport sur les analyses macrofossiles préliminaires d'une séquence de tourbe de la péninsule de Fosheim, île d'Ellesmere, district de Franklin, Territoires du Nord-Ouest; internal report, Terrain Sciences Division, Geological Survey of Canada, 40 p.
 1992: Analyses macrofossiles d'un dépôt de tourbe dans la région de Hot Weather Creek, péninsule de Fosheim, île d'Ellesmere, Territoires du Nord-Ouest. Géographie physique et Quaternaire, vol. 46, n° 3, p. 285–294.
 1992: Analyses macrofossiles d'une séquence de tourbe holocène dans la région de Hot Weather Creek, péninsule de Fosheim, île d'Ellesmere, Territoires du Nord-Ouest; Programme et résumés, VII^e Congrès de l'Association québécoise pour l'étude du Quaternaire, Rouyn-Noranda, Québec, p. 37 (affiche).
 1993: Analysis of peat deposits in Northeastern Arctic; *in* Proxy Climate data and models of the six thousand years before present time interval: The Canadian perspective, (ed.) A.M. Telko; Incidental Report Series no. IR93-3, Canadian Global Change Program, Royal Society of Canada, p. 12.
 1995: Collection de référence de graines et autres macrofossiles végétaux de taxons provenant de l'Arctique canadien/Reference collection of seeds and other botanical macrofossils from Arctic Canada; Geological Survey of Canada, Open File 3049, 18 p.
- Gemmell, A.M.D., Sharp, M.J., and Sugden, D.E.**
 1986: Debris from the basal ice of the Agassiz Ice Cap, Ellesmere Island, Arctic Canada; Earth Surface Processes and Landforms, v. 11, p. 123–130.
- Gilbert, R., Aitken, A.E., and Lemmen, D.S.**
 1993: The glacial marine sedimentary environment of Expedition Fiord, Canadian High Arctic; Marine Geology, v. 110, p. 257–273.
- Glenn, M.S. and Woo, M-k.**
 1994: Hydrology a High Arctic wetland; M.Sc. thesis, McMaster University, Hamilton, Ontario, 97 p.
 1997: Spring and summer hydrology of a valley-bottom wetland, Ellesmere Island, Northwest Territories, Canada; Wetlands, v. 17, p. 321–329.
- Goto-Azuma, K., Koerner, R.M., Nakawo, M., and Kudo, A.**
 1997: Snow chemistry on the Agassiz Ice Cap, Ellesmere Island, Northwest Territories, Canada; Journal of Glaciology, v. 43, p. 199–206.
- Gregor, D.J., Dominik, J., Vernet, J.-P.**
 1996: Recent trends of selected chlorohydrocarbons in the Agassiz Ice Cap, Ellesmere Island, Canada; *in* Proceedings of the 8th International Conference of the Comité Arctique International on Global Significance of the Transport and Accumulation of Polychlorinated Hydrocarbons in the Arctic, Oslo, Norway, (ed.) R.G. Shearer and A. Bartonova.
- Gregor, D.J., Peters, A.J., Teixeira, C., Jones, N., and Spencer, C.**
 1995: The historical residue trend of PCBs in the Agassiz Ice Cap, Ellesmere Island, Canada; The Science of the Total Environment, v. 160/161, p. 117–126.
- Hamilton, P.B. and Edlund, S.A.**
 1994: Occurrence of *Prasiola fluviatilis* (Chlorophyta) on Ellesmere Island in the Canadian Arctic; Journal of Phycology, v. 30, p. 217–221.
- Hamilton, P.B., Douglas, M.S.V., Fritz, S.C., Pienitz, R., Smol, J.P., and Wolfe, A.P.**
 1994: A compiled freshwater diatom taxa list for the Arctic and Subarctic regions of North America; *in* Proceedings of the Fourth Arctic-Antarctic Diatom Symposium (workshop), Canadian Museum of Nature, Ottawa, Ontario, Canada, September 18–21, 1993, (ed.) P.B. Hamilton; Canadian Technical Report of Fisheries and Aquatic Sciences, v. 1957, p. 57–63.
 1994: A compiled freshwater diatom taxa list for the arctic and subarctic regions of North America; *in* Proceedings of the fourth Arctic-Antarctic Diatom Symposium, Canadian Museum of Nature, Ottawa, Ontario, Canada, September 18–21, 1993, (ed.) P.B. Hamilton; Canadian Technical Report of Fisheries and Aquatic Sciences, v. 1957, p. 85–102.
- Hamilton, P.B., Lean, D.R.S., and Poulin, M.**
 1994: The physicochemical characteristics of lakes and ponds from the northern regions of Ellesmere Island; *in* Proceedings of the Fourth Arctic-Antarctic Diatom Symposium (workshop), Canadian Museum of Nature, Ottawa, Ontario, Canada, September 18–21, 1993, (ed.) P.B. Hamilton; Canadian Technical Report, of Fisheries and Aquatic Sciences, v. 1957, p. 57–63.

- Hamilton, P.B., McNeely, R., and Poulin, M.**
1996: The morphology and distribution of *Neidium distincte-punctatum* Hustedt and its systematic position within the genus; *Diatom Research*, v. 11, p. 59–71.
- Hamilton, P.B., Poulin, P.B., Prévost, C., Angell, M., and Edlund, S.A.**
1994: *Americanarum Diatomarum Exsiccata Fascicle II (CANA)*, voucher slides from 34 lakes, ponds and streams from Ellesmere Island, Canadian high Arctic, North America; *Diatom Research*, v. 9, p. 303–327.
- Handfield, M.**
1992: Seasonal fluctuation patterns of microflora on the Agassiz Ice Cap, Ellesmere Island, Canadian Arctic; *The Musk-Ox*, v. 39, p. 119–123.
- Harry, D.G., French, H.M., and Pollard, W.H.**
1988: Massive ground ice and ice-cored terrain near Sabine Point, Yukon Coastal Plain; *Canadian Journal of Earth Sciences*, v. 25, p. 1846–1856.
- Headley, A.**
1990: A comparison of wind speeds recorded simultaneously at three metres and ten metres above ground; Canadian Climate Centre, Atmospheric Environment Service, Report no. 90-1, 36 p.
- Heron, R. and Woo, M-k.**
1978: Snowmelt computation for a high Arctic site; *Proceedings of the 35th Eastern Snow Conference*, Hanover, New Hampshire, p. 162–172.
- Hodgson, D.A.**
1985: The last glaciation of west-central Ellesmere Island, Arctic Archipelago, Canada; *Canadian Journal of Earth Sciences*, v. 22, no. 3, p. 347–368.
- Hodgson, D.A. and Edlund, S.A.**
1978: Surficial materials and biophysical regions, eastern Queen Elizabeth Islands: part II; Geological Survey of Canada, Open File 501, scale 1:250 000.
- Hodgson, D.A., St-Onge, D.A., and Edlund, S.A.**
1991: Surficial materials of Hot Weather Creek basin, Ellesmere Island, Northwest Territories; *in Current Research, Part E; Geological Survey of Canada, Paper 91-1E*, p. 157–163.
- Howard, S.M.**
1989: The postglacial history and present-day diatom assemblages of Proteus Lake, Pim Island, Canadian High Arctic; B.Sc. thesis, Queen's University, Kingston, Ontario, 42 p.
- Kane, D.L., Hinzman, L.D., Woo, M-k., and Everett, K.R.**
1992: Arctic hydrology and climate change; *in Arctic Ecosystems in a Changing Climate — an Ecophysiological Perspective*, (ed.) F.S. Chapin III, R.L. Jefferies, J.F. Reynolds, G.R. Shaver, J. Svoboda, and E. Chu; Academic Press, Toronto, Ontario, p. 35–57.
- Koerner, R.M.**
1979: Accumulation, ablation, and oxygen isotope variations on the Queen Elizabeth Islands ice caps, Canada; *Journal of Glaciology*, v. 22, p. 25–41.
1989: Queen Elizabeth Islands glaciers; *in Chapter 6 of Quaternary Geology of Canada and Greenland*, (ed.) R.J. Fulton; Geological Survey of Canada, *Geology of Canada*, no. 1, p. 464–473 (*also Geological Society of America, The Geology of North America*, v. K-1, p. 464–473).
1989: Ice core evidence for extensive melting of the Greenland Ice Sheet in the last interglacial; *Science*, v. 244, p. 964–968.
1990: Arctic ice cores: putting present climate into perspective; *in Canada's Missing Dimension — Science and History in the Canadian Arctic Islands*, Volume I, (ed.) C.R. Harington; Canadian Museum of Nature, Ottawa, Ontario, p. 265–272.
1994: Past and present contaminants in the Russian and Canadian High Arctic; synopsis of research conducted under the 1993–1994 Northern Contaminants Program, Department of Indian Affairs and Northern Development, Environmental Studies Series, p. 62–79.
- Koerner, R.M. and Fisher, D.A.**
1982: Acid snow in the Canadian high Arctic; *Nature*, v. 295, p. 137–140.
1990: A record of Holocene summer climate from a Canadian high-Arctic ice core; *Nature*, v. 343, no. 6259, p. 630–631.
1990: Climatic warming, glaciers and sea level; *Annals of Glaciology*, v. 14, 345 p.
1995: The Greenland Ice Sheet record: insensitive to Holocene climatic change?; *in Proceedings, Wadati Conference on Global Change and Polar Climate*, Japan, 1995, p. 74–78.
- Koerner, R.M. and Lundgaard, L.**
1995: Glaciers and global warming; *Géographie physique et Quaternaire*, v. 49, p. 429–434.
- Koerner, R.M., Alt, B.T., Bourgeois, J.C., and Fisher, D.A.**
1991: Canadian ice caps as sources of paleoenvironmental data: advantages and disadvantages; *in Proceedings, Conference on The Role of Polar Regions in Global Change*, Alaska, June 1990, p. 576–581.
- Koerner, R.M., Bourgeois, J.C., and Fisher, D.A.**
1988: Pollen analysis and discussion of time-scales in Canadian ice cores; *Annals of Glaciology*, v. 10, p. 85–91.
- Koerner, R.M., Dubey, R., and Parnandi, M.**
1989: Scientists monitor climate and pollution from ice caps and glaciers; *GEOS*, v. 18, no. 3, p. 33–38.
- Koerner, R.M., Fisher, D.A., and Goto-Azuma, K.**
1999: A 100 year record of ion chemistry from Agassiz Ice Cap, Northern Ellesmere Island, N.W.T., Canada; *Atmosphere Environment*, v. 33, p. 347–357.
- Koerner, R.M., Fisher, D.A., and Parnandi, M.**
1981: Bore-hole video and photographic cameras; *Annals of Glaciology*, v. 2, p. 34–38.
- Koerner, R.M., Fisher, D.A., and Paterson, W.S.B.**
1987: Wisconsinan and pre-Wisconsinan ice thicknesses on Ellesmere Island, Canada: inferences from ice cores; *Canadian Journal of Earth Sciences*, v. 24, p. 296–301.
- Labine, C.L.**
1990: Arctic meteorology and climatology, present state and future direction; *in Canada's Missing Dimension — Science and History in the Canadian Arctic Islands*, Volume I, (ed.) C.R. Harington; Canadian Museum of Nature, Ottawa, Ontario, p. 337–349.
1994: Meteorology and climatology of the Alexandra Fiord Lowland; *in Ecology of a Polar Oasis: Alexandra Fiord, Ellesmere Island, Canada*, (ed.) J. Svoboda and B. Freedman; Captus University Publications, Toronto, Ontario, p. 23–29.
- Labine, C.L., Alt, B.A., Atkinson, D., Headley, A., Koerner, R.M., Edlund, S.A., and Waszkiewicz, M.**
1993: High Arctic IRMA automatic weather station field data 1991–1992. Part 1: Documentation, Part 2: Plots; Geological Survey of Canada, Open File 2898, 52 p.
- Lemmen, D.S., Aitken, A.E., and Gilbert, R.**
1994: Early Holocene deglaciation of Expedition and Strand fiords, Canadian High Arctic; *Canadian Journal of Earth Sciences*, v. 31, p. 943–958.
- Lewkowicz, A.G.**
1990: Morphology, frequency and magnitude of active-layer detachment slides, Fosheim Peninsula, Ellesmere Island, N.W.T.; *in Permafrost Canada: Proceedings of the Fifth Canadian Permafrost Conference*, Quebec City, June 1990; Laval University, Quebec, Centre d'études nordiques, Collection Nordicana, p. 111–118.
1990: Active-layer detachments, Fosheim Peninsula, Ellesmere Island; Annual Meeting of the Canadian Association of Geographers, University of Alberta, Edmonton, Alberta, June 1990, Program with Abstracts, p. 143.
1990: Climatic change and permafrost slope processes; Annual Meeting of the Canadian Association of Geographers, University of Alberta, Edmonton, Alberta, June 1990, Program with Abstracts, p. 143.
1992: Slope hummocks on Fosheim Peninsula, Ellesmere Island; *in Current Research, Part B; Geological Survey of Canada, Paper 92-1B*, p. 97–102.
1992: A solifluctuation meter for permafrost sites; *Permafrost and Periglacial Processes*, v. 3, p. 11–18.
1992: Factors influencing the distribution and initiation of active-layer detachment slides on Ellesmere Island, Arctic Canada; *in Periglacial Geomorphology*, (ed.) J.C. Dixon and A.D. Abrahams; John Wiley and Sons Ltd., Chichester, England, p. 223–250.
1994: Ice wedge rejuvenation, Fosheim Peninsula, Ellesmere Island; *Permafrost and Periglacial Processes*, v. 5, p. 251–268.
- Lewkowicz, A. G. and Duguay, C. R.**
1999: Detection of permafrost features using SPOT panchromatic imagery, Fosheim Peninsula, Ellesmere Island, N.W.T.; *Canadian Journal of Remote Sensing*, v. 25, no. 1, p. 34–44.
- Lewkowicz, A.G. and Wolfe, P.M.**
1994: Sediment transport in Hot Weather Creek, Ellesmere Island, Canada, 1990–1991; *Arctic and Alpine Research*, v. 26, p. 213–226.

Lichti-Federovich, S.

1985: Diatom dispersal phenomena diatoms in rime frost samples from Cape Herschel, Ellesmere Island, N.W.T.; *in* Current Research, Part B; Geological Survey of Canada, Paper 85-1B, p. 391–399.

1986: Diatom dispersal phenomena: diatoms in precipitation samples from Cape Herschel, east-central Ellesmere Island, N.W.T. — a quantitative assessment; *in* Current Research, Part B; Geological Survey of Canada, Paper 86-1B, p. 263–269.

Luckman, B.H., Edlund, S.A., and Harry, D.G.

1988: Active-layer detachments during late summer, 1988, Fosheim Peninsula, Ellesmere Island; CAGONT '88 Permafrost Abstracts; Program and Abstracts; Annual Meeting of the Canadian Association of Geographers Ontario Division, 13 p.

Luckman, B.H., Harry, D.G., Edlund, S.A., and Alt, B.

1989: Global change, ground ice and geomorphic processes: some observations from the Fosheim Peninsula, Ellesmere Island, N.W.T., Canada; Abstracts, 18th Annual Arctic Workshop, April 13–15, 1989, Global environmental change and the Arctic, Lethbridge, Alberta.

Matthews, J.V., Jr.

1990: New data on Pliocene floras/faunas from the Canadian Arctic and Greenland; *in* Pliocene Climates: Scenario for Global Warming, v. 90-64, (ed.) L.B. Gosnell and R.Z. Poore; United States Geological Survey, Open File 29-33.

Matthews, J.V., Jr. and Ovenden, L.E.

1990: Late Tertiary plant macrofossils from localities in arctic/subarctic North America (Alaska, Yukon and Northwest Territories): a review of the data; *Arctic*, v. 43, no. 4, p. 364–392.

McJannet, C.L., Argus, G.W., Edlund, S.A., and Cayouette, J.

1993: Rare vascular plants in the Canadian Arctic; *Canadian Museum of Nature Syllogeus*, no. 72, 79 p.

McNeely, R. and Gummer, W.D.

1984: A reconnaissance survey of the environmental chemistry in east-central Ellesmere Island, N.W.T.; *Arctic*, v. 37, p. 210–223.

Nogrady, T. and Smol, J.P.

1989: Rotifers from five High Arctic ponds (Cape Herschel, Ellesmere Island, N.W.T.); *Hydrobiologia*, v. 173, p. 231–242.

Nriagu, J.O., Lawson, G.S., and Gregor, D.J.

1994: Cadmium concentrations in recent snow and firn layers in the Canadian Arctic; *Bulletin of Environmental Contamination and Toxicology*, v. 52, p. 756–759.

Ovenden, L.

1993: Late Tertiary mosses of Ellesmere Island; *Review of Palaeobotany and Palynology*, v. 79, p. 121–131.

Parsons, D.

1985: Patterns of growth and relative abundance of cladocerans in two high arctic ponds; B.Sc. Honours thesis, Queen's University, Kingston, Ontario, 50 p.

Peters, A.J., Gregor, D.J., Teixeira, C.F., Jones, N.P., and Spencer, C.

1995: The recent depositional trend of polycyclic aromatic hydrocarbons and elemental carbon to the Agassiz Ice Cap, Ellesmere Island, Canada; *The Science of the Total Environment*, v. 160/161, p. 167–179.

Peters, B. and Headley, A.

1992: A comparison of winds at Hot Weather Creek and Eureka, N.W.T.; Canadian Climate Centre, Atmospheric Environment Service, Report no. 92-2, 22 p.

Pollard, W.H.

1990: The nature and origin of ground ice in the Herschel Island area, Yukon Territory, *in* Permafrost Canada; Proceedings of the Fifth Canadian Permafrost Conference, Quebec City, June 1990; Laval University, Quebec, Centre d'études nordiques, Collection Nordicana, p. 23–30.

1991: Observations on massive ground ice on Fosheim Peninsula, Ellesmere Island, Northwest Territories; *in* Current Research, Part E; Geological Survey of Canada, Paper 91-1E, p. 223–231.

Pollard, W.H. and Dallimore, S.R.

1988: Petrographic characteristics of massive ground ice, Yukon Coastal Plain, Canada; *in* Permafrost, Fifth International Conference Proceedings, v. I; Tapir Publishers, Trondheim, Norway, p. 224–229.

Pollard, W.H. and French, H.M.

1980: A first approximation of the volume of ground ice, Richard Island, Pleistocene Mackenzie Delta, N.W.T.; *Canadian Geotechnical Journal*, v. 17, p. 509–516.

Prest, V.K.

1952: Notes on the geology of parts of Ellesmere and Devon islands, Northwest Territories; Geological Survey of Canada, Paper 52-32, 15 p.

Robinson, S.D.

1993: Geophysical and geomorphological investigations of massive ground ice, Fosheim Peninsula, Ellesmere Island, Northwest Territories; M.Sc. thesis, Queen's University, Kingston, Ontario, 171 p.

1993: Massive ground ice in the vicinity of Hot Weather Creek, Fosheim Peninsula, Ellesmere Island, N.W.T., Canada; 23rd Annual Arctic Workshop Program and Abstracts; Byrd Polar Research Centre, Miscellaneous Series Publication no. 322, The Ohio State University, Columbus, Ohio, 102 p.

1994: Geophysical studies of massive ground ice, Fosheim Peninsula, Ellesmere Island, N.W.T.; *in* Current Research 1994-B; Geological Survey of Canada, p. 11–18.

Smol, J.P.

1983: Paleophycology of a high arctic lake near Cape Herschel, Ellesmere Island; *Canadian Journal of Botany*, v. 61, p. 2195–2204.

1988: Paleoclimate proxy data from freshwater Arctic diatoms; *Verhandlungen Internat. Verein. Limnologie*, v. 23, p. 837–844.

Sutherland, P.D.

1989: An inventory and assessment of the prehistoric archaeological resources of Ellesmere Island National Park Reserve; Canadian Parks Service, Microfiche Report Series 431, 388 p.

1996: Continuity and change in the Paleo-Eskimo prehistory of northern Ellesmere Island; *in* The Paleo-Eskimo Cultures of Greenland, New Perspectives in Greenland Archaeology, (ed.) Bjarne Grønnow and John Pind; Danish Polar centre, Copenhagen, Denmark, p. 271–294.

Taylor, A.E.

1991: Holocene paleoenvironmental reconstruction from deep ground temperatures: a comparison with paleoclimate derived from the $\delta^{18}\text{O}$ record in an ice core from the Agassiz Ice Cap, Canadian Arctic Archipelago; *Journal of Glaciology*, v. 37, p. 209–219.

Waddington, E.D., Magnusson, M. M., Fisher, D.A., and Koerner, R.M.

1994: Microclimate at Agassiz Ice Cap, Ellesmere Island, and its implications for ice core studies; *EOS*, v. 69, no. 44, p. 1211.

Wilkinson, A.N., Zeeb, B.A., Smol, J.P., and Douglas, M.S.V.

1997: Chrystophyte stomatocyst assemblages associated with periphytic habitats from High Arctic pond environments; *Nordic Journal of Botany*, v. 17, p. 95–112.

Wolfe, P.M.

1992: Suspended sediment and solute transport in Hot Weather Creek, Fosheim Peninsula, Ellesmere Island, Northwest Territories, 1990–1991; B.Sc. Honours thesis, University of Toronto, Toronto, Ontario, 144 p.

1994: Hydrometeorological investigations on a small valley glacier in the Sawtooth Range, Ellesmere Island, Northwest Territories; M.Sc. thesis; Wilfrid Laurier University, Waterloo, Ontario, 205 p.

Wolfe, P.M. and M.C. English

1995: Hydrometeorological relationships in a glacierized catchment in the Canadian high Arctic; *Hydrological Processes*, v. 4, p. 911–921.

1995: Mass balance of a small valley glacier in the Canadian high Arctic, Ellesmere Island, Northwest Territories; *Zeitschrift Fur Gletscherkunde Und Glazialgeologie*, Band 31 (1995), S. 93–103.

Woo, M-k. and Marsh, P.

1978: Analysis of error in the determination of snow storage for small High Arctic basins; *Journal of Applied Meteorology*, v. 17, p. 1537–1541.

Woo, M-k. and McCann, S.B.

1994: Climatic variability, climate change, runoff, and suspended sediment regimes in Northern Canada; *Physical Geography*, v. 15, p. 201–226.

Woo, M-k. and Young, K.L.

1997: Hydrology of a small drainage basin with polar oasis environment, Fosheim Peninsula, Ellesmere Island, Canada; *Permafrost and Periglacial Processes*, v. 8, no. 3, p. 257–278.

Woo, M-k., Edlund, S.A., and Young, K.L.

1991: Occurrence of early snow-free zones on Fosheim Peninsula, Ellesmere Island, Northwest Territories; *in* Current Research, Part B; Geological Survey of Canada, Paper 91-1B, p. 9–14.

Woo, M-k., Heron, R., Marsh, P., and Steer, P.

1980: Comparison of weather station snowfall with winter snow accumulation in High Arctic basins; *Atmosphere-Ocean*, v. 21, p. 321–325.

Woo, M-k., Marsh, P., and Steer, P.

1983: Basin water balance in a continuous permafrost environment; Proceedings, Fourth International Conference on Permafrost, National Academy Press, Washington, D.C., p. 1407–1411.

Woo, M-k., Rowsell, R.D., and Edlund, S.A.

1992: Effects of manipulation of climate factors on arctic snowmelt; Proceedings of the 9th International Northern Research Basins Symposium/Workshop, Canada, National Hydrology Research Institute Symposium no. 10, p. 627–641.

Woo, M-k., Rouse, W.R., Lewkowicz, A.G., and Young, K.L.

1992: Adaptation to permafrost in the Canadian North: present and future; Canadian Climate Centre, Atmospheric Environment Service, Report no. 92-3, 61 p.

Woo, M-k., Walker, A., Yang, D., and Goodison, B.

1995: Pixel-scale ground snow survey for passive microwave study of the arctic snow cover; Proceedings, 52nd Eastern Snow Conference, Toronto, Ontario, p. 51–57.

Woo, M-k., Young, K.L., and Edlund, S.A.

1990: 1989 observations of soil, vegetation, and microclimate, and effects on slope hydrology, Hot Weather Creek basin, Ellesmere Island, Northwest Territories; *in* Current Research, Part D; Geological Survey of Canada, Paper 90-1D, p. 85–93.

Young, K.L.

1995: Slope hydroclimatology and hydrologic responses to global change in a small High Arctic basin; Ph.D. thesis, McMaster University, Hamilton, Ontario, 167 p.

Young, K.L. and Woo, M-k.

1997: Modelling net radiation in an arctic environment using summer field camp data; International Journal of Climatology, v. 17, p. 1–19.

Young, K.L., Woo, M-k., and Edlund, S.A.

1997: Influence of local topography, soil and vegetation on microclimate and hydrology at a High Arctic site, Ellesmere Island, Canada; Arctic and Alpine Research, v. 29, no. 3, p. 270–284.

Zheng, J.

1995: Electrical conductivity measurements on ice cores from the Canadian Arctic: an analysis of signal variation within and between ice cores; M.Sc. thesis, Ottawa-Carleton Geoscience Centre and University of Ottawa, 99 p.

Overview of the modern arctic climate

B.T. Alt¹ and B. Maxwell²

Alt, B.T. and Maxwell, B., 2000: Overview of the modern arctic climate; in Environmental Response to Climate Change in the Canadian High Arctic, (ed.) M. Garneau and B.T. Alt; Geological Survey of Canada, Bulletin 529, p. 17–36.

Abstract: Fosheim Peninsula is the largest interior lowland of the protected, anomalously warm, dry, Eureka Sound intermontane area, which lies in the circumpolar-vortex-dominated Canadian High Arctic. The climate of this latter region is characterized by high, longitudinal temperature variations, strong, persistent temperature inversions, and widely differing precipitation totals.

Climate and related trends for 1961 to 1990 were used to delineate climate change regions around the circumarctic area and to examine their response to recent global climate conditions. General circulation model results for doubled CO₂ scenarios show least agreement in this geographical area, with only a transient model with a coupled ocean circulation model reflecting the current observed trends.

Because of the anomalous conditions of the Eureka Sound area within the eastern Canadian High Arctic and similarly of the latter region within the circumpolar Arctic, close monitoring and interdisciplinary research are warranted to understand the climate processes involved.

Résumé : La péninsule Fosheim représente la plus grande superficie de basses terres intérieures de la région intermontagneuse protégée et anormalement chaude du détroit d'Eureka, étendue qui est située dans une partie unique de l'extrême Arctique canadien oriental dominé par le vortex circumpolaire. Le climat de la région est caractérisé par de fortes variations de températures suivant la longitude, par des inversions de température intenses et persistantes ainsi que par des accumulations totales de précipitations très variées.

On a utilisé les tendances climatiques et de la période de 1961 à 1990 pour délimiter des régions de changement climatique avoisinant la région circumpolaire et pour examiner leur réponse aux récents changements climatiques mondiaux. Les modèles de circulation générale pour les scénarios de doublement de la concentration du CO₂ concordent le moins bien pour cette région géographique où seul un modèle transitoire couplé à un modèle de la circulation océanique reflète les tendances contemporaines observées.

En raison des conditions anormales de la région du détroit d'Eureka par rapport au reste de l'extrême Arctique canadien oriental et de la similitude de cette région avec l'Arctique circumpolaire, il est nécessaire d'y faire une surveillance intense et de la recherche interdisciplinaire afin de comprendre les processus climatiques aux échelles variées qui sont en cause.

¹ Balanced Environments Associates, 5034 Leintrim Road, Carlsbad Springs, Ontario K0A 1K0

² 103 Langley Avenue, Toronto, Ontario M4K 1B4

INTRODUCTION

It is intrinsic to interdisciplinary investigations of environmental and paleoenvironmental change to understand the present climate. Transfer functions cannot be built without a solid, modern database and fundamental knowledge of the complex interactions of climate and the geosphere-biosphere. Climatic evidence from terrestrial sources and ice cores cannot be compared or mapped without an accurate spatial representation of the present climate with which modern environmental conditions can be compared.

The purpose of this overview is to provide the circumpolar climate background for the interdisciplinary studies in the present volume, to show the relationship between the Fosheim Peninsula (Fig. 1) and circumpolar climate patterns, and to introduce the topics of recent trends and the results of the general circulation model (GCM) doubled CO₂ scenario. It is an attempt to gather together figures and references and make them available for future studies.

CIRCUMPOLAR CLIMATE PATTERNS

The High Arctic is characterized by continuous darkness during several winter months and continuous daylight in the summer, although these extremes are tempered in several ways. Complete darkness does not settle in until at least one month after the sun sets completely in the autumn, creating prolonged arctic twilight. Even during the polar night, moonlight reflected from snow and ice surfaces noticeably lightens the darkness. The moonlight is sometimes strong enough to show up on autostation insolation records (*see below*). In summer, because the days are so long, the total input of solar energy is approximately the same as at lower latitudes. Due to the higher reflectivity of arctic surfaces and the lower sun angle, a smaller percentage of the available energy actually remains to heat the Earth's surface. The arctic atmosphere also loses large amounts of heat to space mainly from the level of the inversion (*see below*) and, in particular, from the tops of clouds and moist layers. Warm advection (warm-air streams) accompanying travelling cyclones makes up for more than half this deficit.

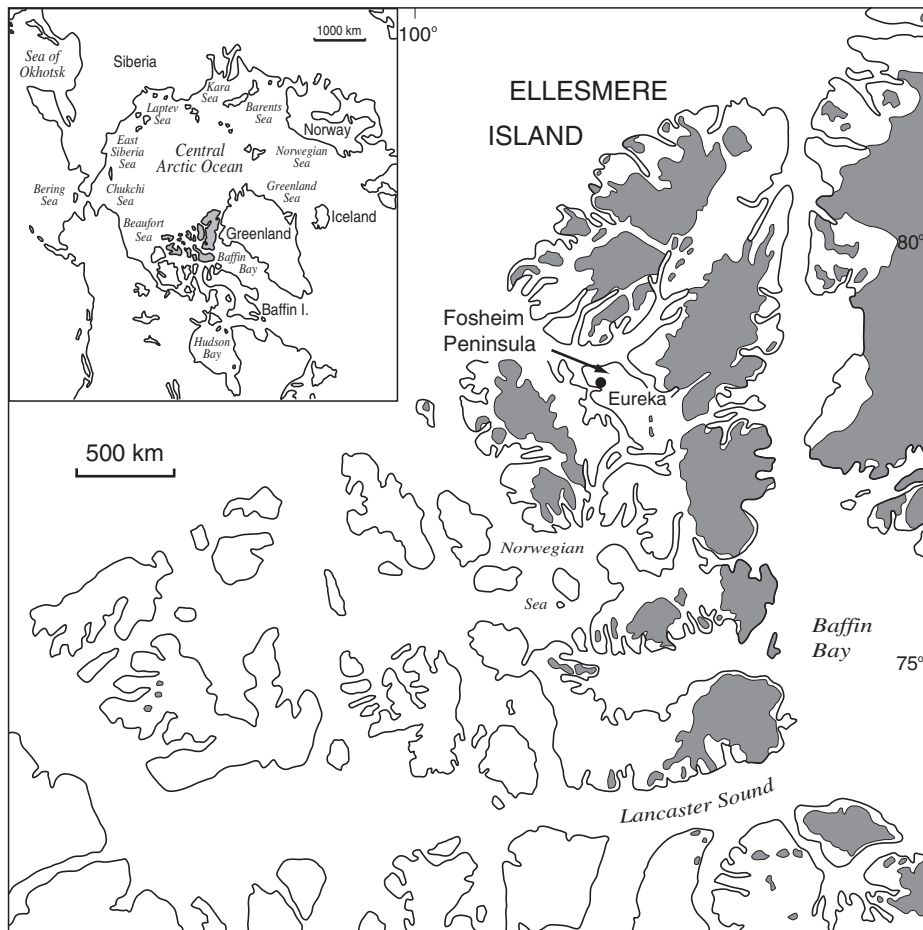


Figure 1. The Queen Elizabeth Islands, showing Fosheim Peninsula. Dark shaded areas are glacier ice. Inset map shows the circumpolar region.

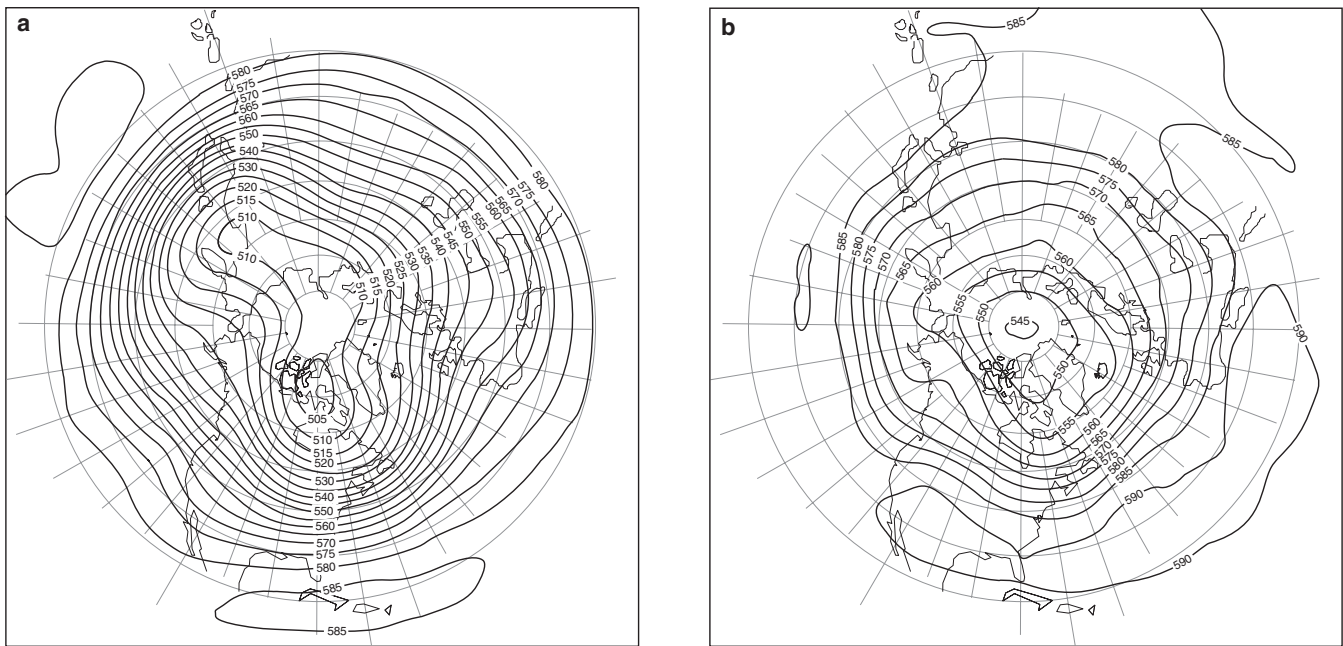


Figure 2. Circumpolar, 50 kPa, mean height pattern for **a)** January and **b)** July, based on the 1949 to 1978 period. Heights, given in decameters (dm) and contoured at 5 dm intervals, represent the elevation above the Earth's surface at which pressure is 50 kPa (modified from Harley, 1980).

Unequal solar heating of the globe, combined with the Earth's rotation, drives general atmospheric circulation, which in turn directs large-scale storm movements. Regional circulation patterns are altered by mountain ranges and by differential solar heating from season to season over different surfaces such as forest, tundra, snow, ice, and water.

In the Arctic, atmospheric circulation is dominated by a deep, cold, low-pressure area known as the 'circumpolar vortex', which extends through the middle and upper troposphere and lower stratosphere (Maxwell, 1992). This feature is illustrated in Figures 2 and 3, which show the mean patterns at the 50 kPa (about 5000 m a.s.l.) and 100 kPa (near surface) levels in the atmosphere. On the 50 kPa maps, the vortex appears as a pronounced area of low heights extending over the North Pole with three distinct troughs, particularly in winter. The two most intense of these are situated over eastern Canada and the Sea of Okhotsk, with the third, somewhat less pronounced, lying over the northwestern portion of Siberia. The two strong troughs are reflected in the surface patterns in the Icelandic and Aleutian lows respectively.

It must be kept in mind that not until 1952 was it possible to address the enigma of High Arctic atmospheric circulation. In the late 1960s, the arctic weather forecaster was still working with one fiftieth of the information available at middle latitudes. Serreze (1995) provides a review of early circulation studies and discusses the reasons and direction for renewed interest in this topic. He has examined cyclone statistics for six regions using output from an automated cyclone detection tracking algorithm.

Quantification of High Arctic temperature-normals patterns (and thus trends in these patterns) is still uncertain in some key areas. Only after 1980 was it possible to obtain 'climate normals' for the Canadian sector of the High Arctic and normals are still not available for the Arctic Ocean as discussed by Kahl et al. (1993b). Surface air temperature patterns for the circumpolar region (Fig. 4) reveal marked differences with latitude in all seasons of the year. For example, at latitude 70°N, the mean January temperature varies from nearly freezing over the Norwegian Sea to as low as -42°C over Greenland and northern Siberia. In summer, the range is somewhat smaller, but still appreciable — from as high as +12°C over northern Norway to -12°C over central Greenland. These variations are a function of the major climate controls, including atmospheric circulation, solar radiation input, physical geography, and the nature of the underlying surfaces (*see* Maxwell, 1980, 1982, 1997, and Alt, 1987 for further discussion).

Temperature inversions (temperature increase with height) are an important feature of the High Arctic temperature regime (Maxwell, 1982). Bradley et al. (1992) examined the annual cycle of surface-based inversions at nine coastal stations in the North American Arctic. They found that inversions in the winter months were most frequently the result of strongly negative net radiation at the surface. In summer, inversions were produced mainly by near-surface cooling of warm air masses. Their results showed the following:

Inversion frequency is at a maximum in winter (generally over 70 per cent of days), when inversions range from about 400 to 850 m in thickness. Inversion thickness and strength (temperature change across the

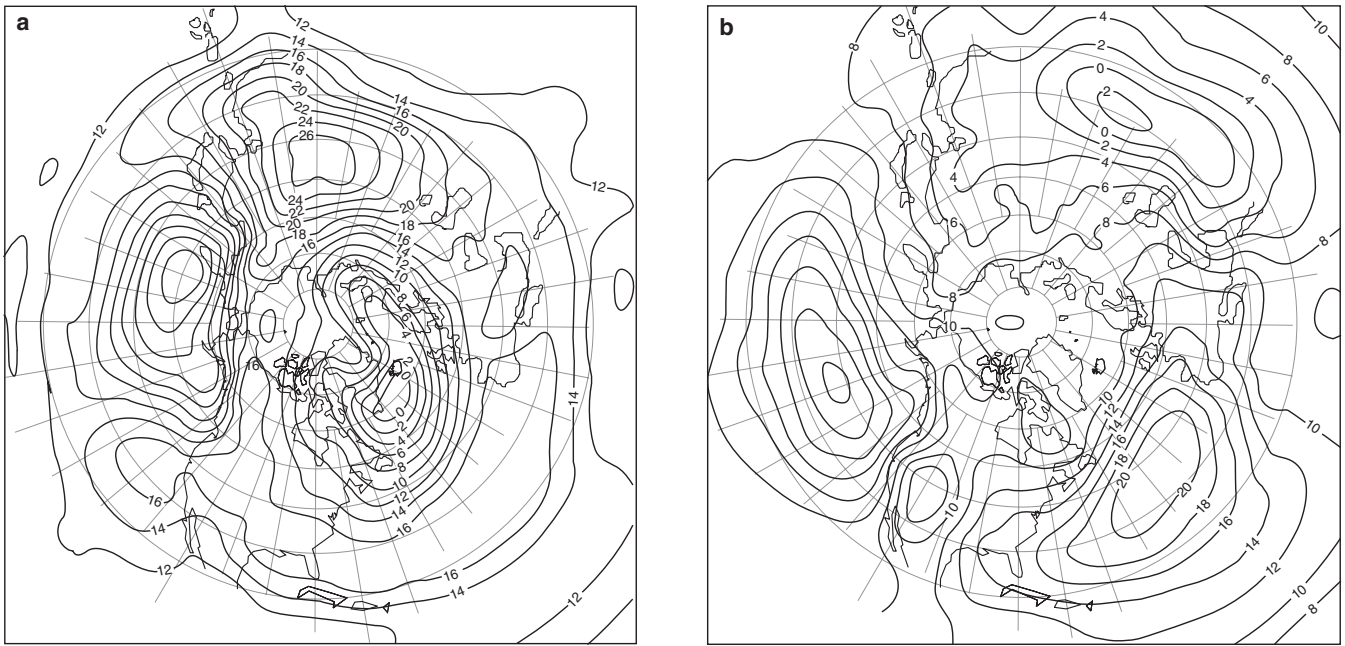


Figure 3. Circumpolar, 100 kPa, mean height pattern for **a)** January and **b)** July, based on the 1949 to 1978 period. Heights, given in decameters (dm) and contoured at 2 dm intervals, represent the elevation above the Earth's surface at which pressure is 100 kPa. The 100 kPa pattern is very much indicative of the mean sea-level pressure pattern (modified from Harley, 1980).

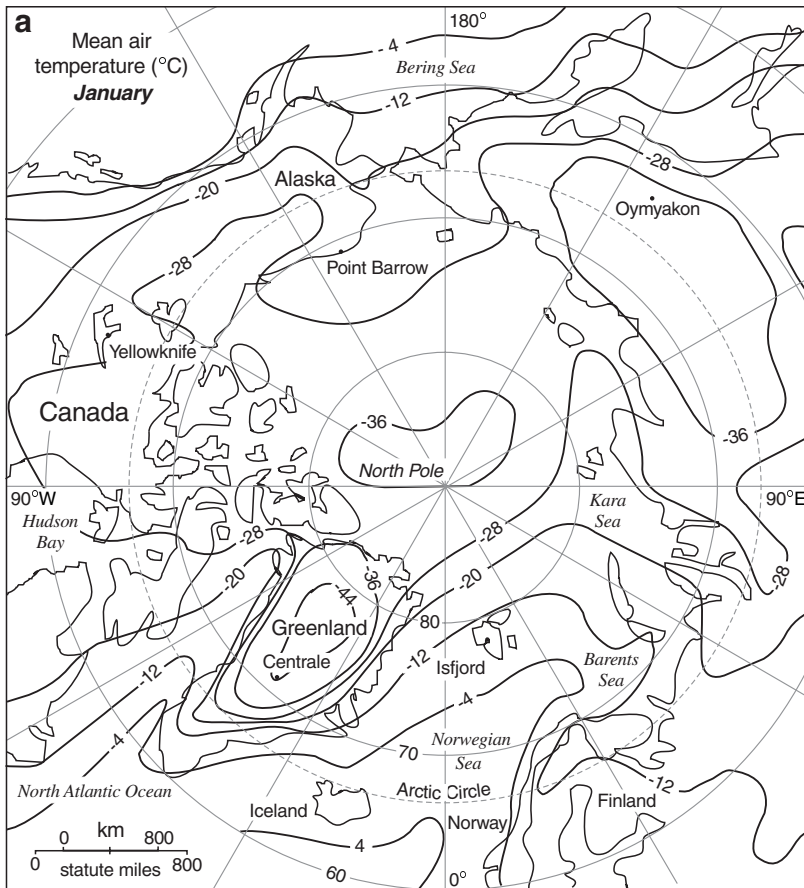


Figure 4. Surface temperature patterns for the circum-arctic region for **a)** January and **b)** July (modified from Central Intelligence Agency, 1978).

inversion) are strongly related to surface temperature. Inversions may involve temperature changes of over 30°C in under 1 km, with gradients of over 6°C/100 m during periods of extreme warm air aloft. Midwinter inversions commonly persist for two to four days, but may remain undisturbed for several weeks, affecting lower tropospheric chemistry.

They further point out that this decoupling of the surface from conditions in the lower troposphere has important implications for energy exchange across the boundary layer and for dispersal of both local air pollutants and long-distance 'arctic haze'.

Precipitation patterns for the circumpolar region suffer from problems associated with measurement techniques. Because of the effects of wind and evaporation, the actual precipitation may be double or more the amount recorded in standard precipitation gauges (Maxwell, 1980, 1982; Woo et al., 1983; Goodison and Louie, 1986). Recently, the World Meteorological Organization completed the 'solid precipitation measurement intercomparison' (Goodison et al., 1994) and Metcalfe et al. (1994) have reported on a corrected precipitation archive for the Northwest Territories. In an attempt to overcome the measurement problems, Serreze et al. (1995b) derived precipitation fields from aerological data. Circumpolar snow-cover patterns are being monitored via

National Oceanic and Atmospheric Association (NOAA) snow-cover charts (Robinson and Dewey, 1990; Robinson et al., 1993, 1995).

As with temperature, the arctic precipitation pattern has a marked regional character. In Canada, for example, over much of the exposed eastern coasts of eastern arctic islands such as Baffin and Devon, total annual precipitation exceeds 300 mm; at comparable latitudes to the west over Victoria and Prince of Wales islands, measured totals are only half that amount or less.

Recently, considerable attention has been focused on circumpolar sea-ice patterns because of the importance of sea-ice concentrations in climate change and general circulation model studies. Barry et al. (1993) and Maxwell (1997) provide reviews of recent results. The annual cycle of sea-ice cover (minimum in September and double the areal extent in March) and regional variability of ice conditions are "controlled by complex interplays between in situ thermodynamic growth and decay and by ice transport, driven in turn by both atmospheric and ocean forcings" (Barry et al., 1993, p. 398). Circumpolar patterns (e.g. Bradley et al., 1993, Fig. 2) are thus a combination of temperature (Fig. 4) and circulation (Fig. 3) patterns. Recently available satellite data combined with field data and drifting-buoy data have enabled progress to be made in the study of these complex interactions.

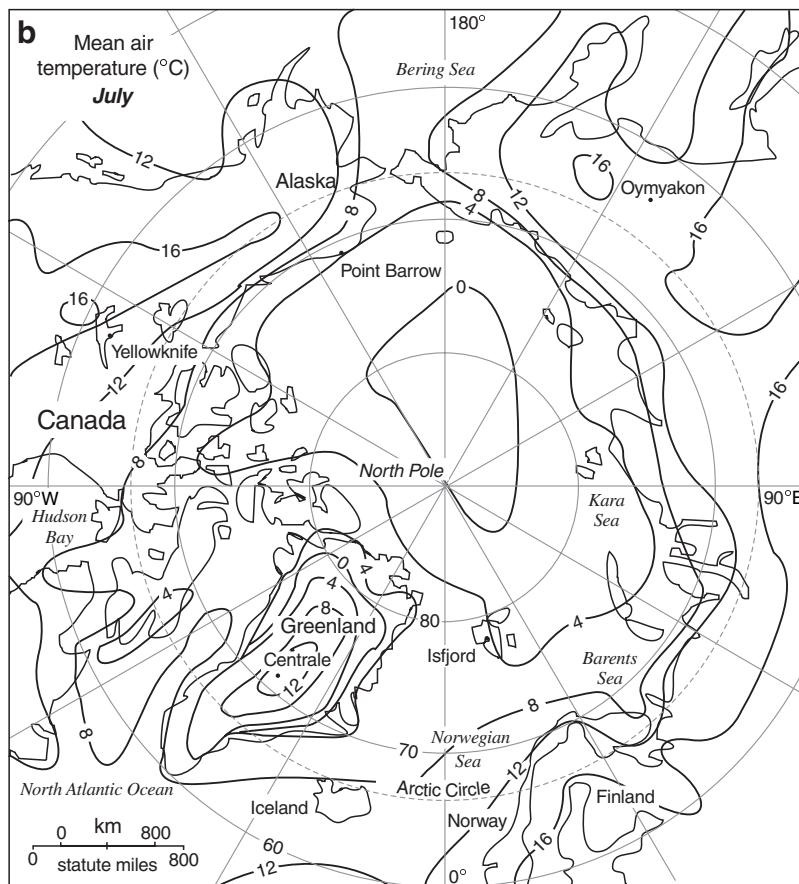


Figure 4. (cont.)

CIRCUMPOLAR CLIMATE CHANGE REGIONS

On the basis of the best-fit linear trends of Chapman and Walsh (1993), Maxwell (1997) identified 11 geographical areas for the Arctic north of latitude 60°N within which temperature trends from 1961 to 1990 have been similar (Fig. 5). To these have been added the western and central Arctic Ocean areas discussed by Kahl et al. (1993a).

Table 1 summarizes the temperature trends on a circumpolar basis with the eleven areas grouped into five major regions and also shows trends observed in other climatic and related elements including precipitation, snow cover, sea ice, and atmospheric circulation (Maxwell, 1997). These trends are generally consistent with each other; for example, in northwestern Canada and Alaska, the increased temperatures and precipitation are both to be expected with the strengthening of the Aleutian low and the resulting increased southerly to southwesterly flow of air over the area. With spring being the season of greatest warming, the trends to decreased spring snow-cover extent and earlier dates of snow-cover disappearance are also to be expected. Conversely, in the eastern Canadian Arctic and Greenland, strengthening of the Icelandic low to the southeast has resulted in increased northerly to northwesterly flow over the area. This is reflected in generally lower temperatures and a trend to increased sea-ice extent. Precipitation, although somewhat increased, is substantially less so than in northwestern Canada and Alaska or the Yamal area of Russia — the two areas of greatest warming in the Arctic.

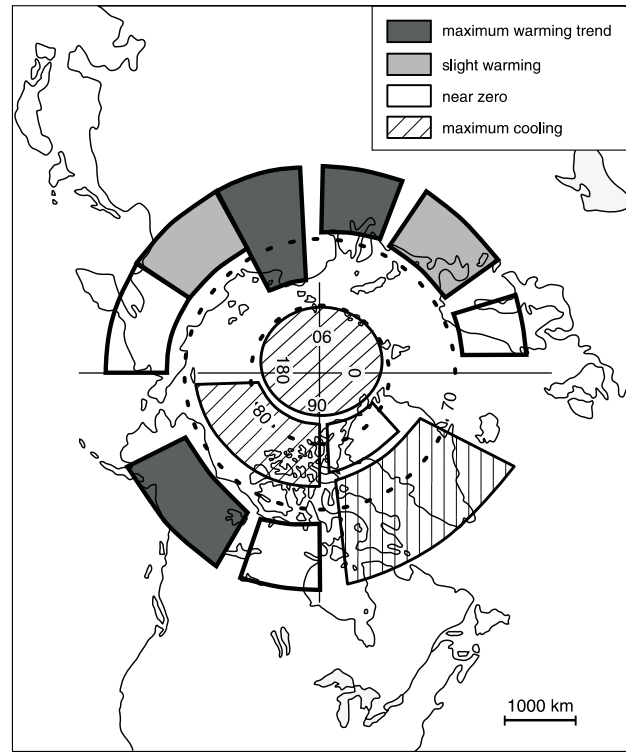


Figure 5. Trend regions: geographical areas for the Arctic north of latitude 60°N within which the temperature trends during the 1961 to 1990 period have been similar (Maxwell, 1997). Data for western and central Arctic Ocean areas from Kahl (1993a).

Table 1. Climate and related element trends by region

	Northwest Canada and Alaska	Eastern Canadian Arctic and Greenland	Scandinavia	North-central Russia (Yamal)	Extreme northeast Russia	Arctic Ocean
Surface temperature						
- annual	increase	decrease	no trend	increase	no trend	decrease
- January	increase	decrease	no trend	increase	decrease	decrease*
- July	increase	no trend	increase	increase	increase	no trend*
Precipitation						
- annual	increase	increase	increase	increase	no trend	
- July	increase	decrease	decrease	increase	increase	
Snow cover extent	North America as a whole		Eurasia as a whole			
- fall	no trend		decrease			
- winter	no trend		decrease			
- spring	decrease		decrease			
Date of disappearance of snow cover	earlier	no trend	no trend			
Sea ice						
- extent	decrease	increase		decrease	decrease	no trend
- thickness						decrease
Atmospheric circulation	Strengthening of the Icelandic and Aleutian lows					
* Trend information from Kahl et al. (1993a). Note: Bold entries indicate statistically significant results.						

Maxwell (1997) further calculated the surface air temperature trends for five areas (condensed from the eleven areas in Figure 5) for June and July and gives time series for each region. Once again, the eastern Canadian Arctic and southern Greenland show little or no change from 1961 to 1990. Briffa and Jones (1993) also produced regional temperature series

for selected areas. Their Greenland (GNLD) and Iceland (ICE) areas show slight cooling trends since 1940, particularly in summer.

Comparisons of the annual and July precipitation anomalies and trends for the five regions (Maxwell, 1997) show that the eastern Canadian Arctic experiences a negative anomaly (difference from long-term means) in July, but has a positive anomaly over the year. Both however, are less than 1 per cent a decade. Considering the large uncertainties in the precipitation record, these results are not at all compelling.

The geographical zones used in the Arctic and Antarctic Research Institute classification of positive pressure anomaly location are shown in Figure 6. They are based on the most frequent locations of ridges and anticyclones and, thus, their dimensions are characteristic of the long-wave pressure patterns (Rossby waves). A strong similarity between the trend areas in Figure 5 and the positive pressure anomaly zones in Figure 6 points to the link between temperature trends and atmospheric circulation. In fact, zones A6 and A7 are dominated by a trough and ridge respectively in all seasons and at all levels from surface to 50 kPa (Fig. 2 and 3). These areas also show the greatest degree of cooling and warming respectively.

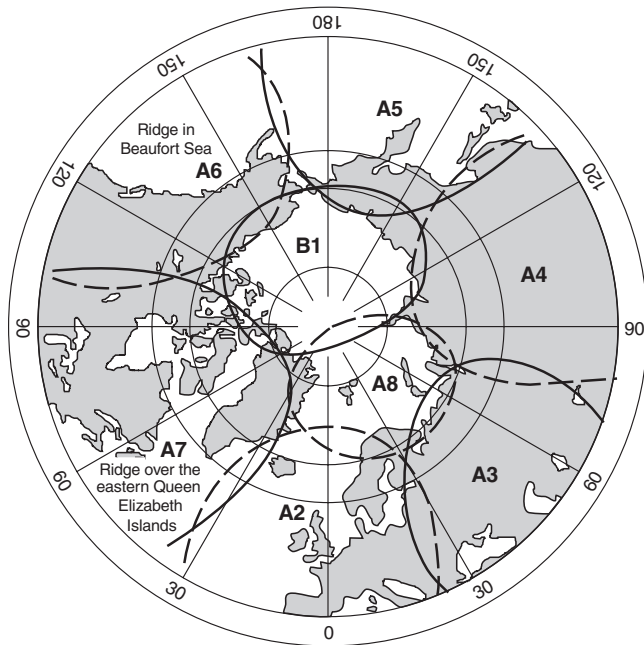


Figure 6. Geographical zones used in the classification of positive pressure anomaly locations (from Alt et al., 1993). These zones are based on the most frequent locations of ridges and anticyclones. Their dimensions are characteristic of the long-wave (Rossby) patterns.

CANADIAN ARCTIC CLIMATE REGIONS: EASTERN HIGH ARCTIC

Figure 7 shows the Canadian climate regions and the distribution of the 131 stations having temperature data in the Historical Canadian Climate Database. The database was constructed from the National Climate Data Archive of the Atmospheric Environment Service, using climate stations that were selected on the basis of spatial distribution, length of record, data continuity, homogeneity assessments, and

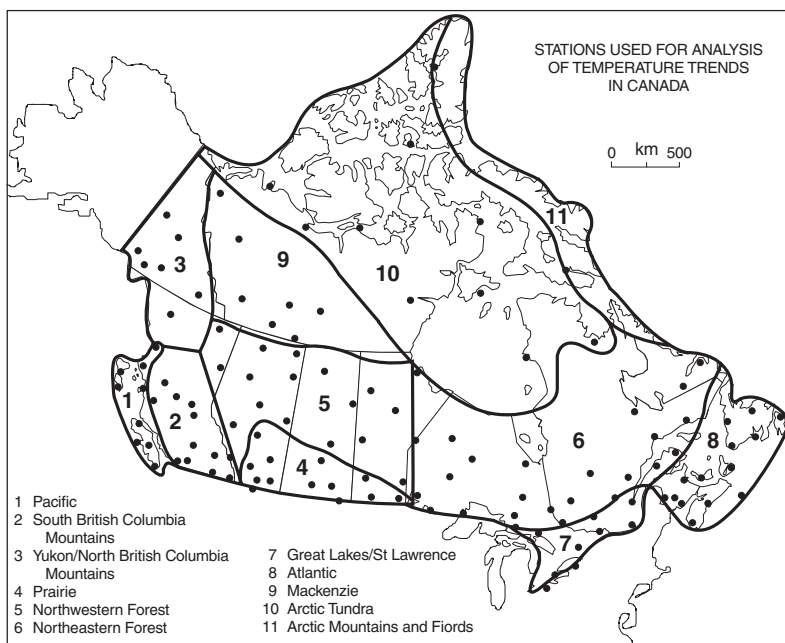


Figure 7.

Canadian climate regions and the distribution of stations with temperature data in Environment Canada's Historical Canadian Climate Database.

other factors. It was assembled to provide climate researchers access to an initial, but expanding, data set that has been rigorously quality controlled, assessed for homogeneity (Gullett et al., 1991), and adjusted, where necessary, to ensure regional representativeness. The data adjustments that were carried out had the effect of filtering out some of the 'local' noise, thereby making the data suitable for use in regional-scale analyses. Departures of annual and seasonal values from the 1951 to 1980 normal were calculated for each location in all climate regions and then averaged, to create regional series of departures from normal. Currently, the data are useful for large, regional- and national-scale analyses over seasonal and annual periods (Skinner and Gullett, 1993).

Figure 8 shows the time series of annual daily mean temperature departures from the 1951 to 1980 average for the four northern Canadian climate regions. These are accompanied by ten-year, running-average filters (ten years being the normal minimum filter period needed to filter out short-term variations) to denote trends. For this analysis, the Mackenzie climate region has been extended beyond the southern boundaries identified in Figure 7 to include the entire river basin, which now includes a large portion of the western half of the Northwestern Forest climate region.

The two western regions, Yukon–North British Columbia and Mackenzie River basin, have longer records than the two eastern regions, Arctic Tundra and Arctic Mountains and Fiords, because of the history of settlement in each of these areas. The two western regions reflect the national pattern of warming into the 1940s, followed by cooling into the 1970s and a resumption of warming through the 1980s. The two eastern regions show similar cooling into the 1970s, but no warming after that. In fact, the Arctic Tundra region has experienced near normal temperatures since that time, whereas the Arctic Mountains and Fiords region has continued to cool.

Figure 9 shows seasonal time series of daily mean temperature departures for the Arctic Mountains and Fiords climate region (represented by only two stations). Time series for this region are shorter, beginning in 1946. In winter, there was a warming trend into the early 1960s followed by a cooling trend until the present. In spring, there has been a cooling trend for the entire period of record. A slight warming trend occurred in the 1980s during the summer. There was no apparent trend during the autumn.

The time series of temperature and precipitation for the High Arctic permanent weather station at Eureka on the Fosheim Peninsula (latitude 80°N, longitude 85°W, Fig. 1) were compared to Arctic and Antarctic Research Institute positive pressure anomaly frequencies (Alt et al., 1993). The

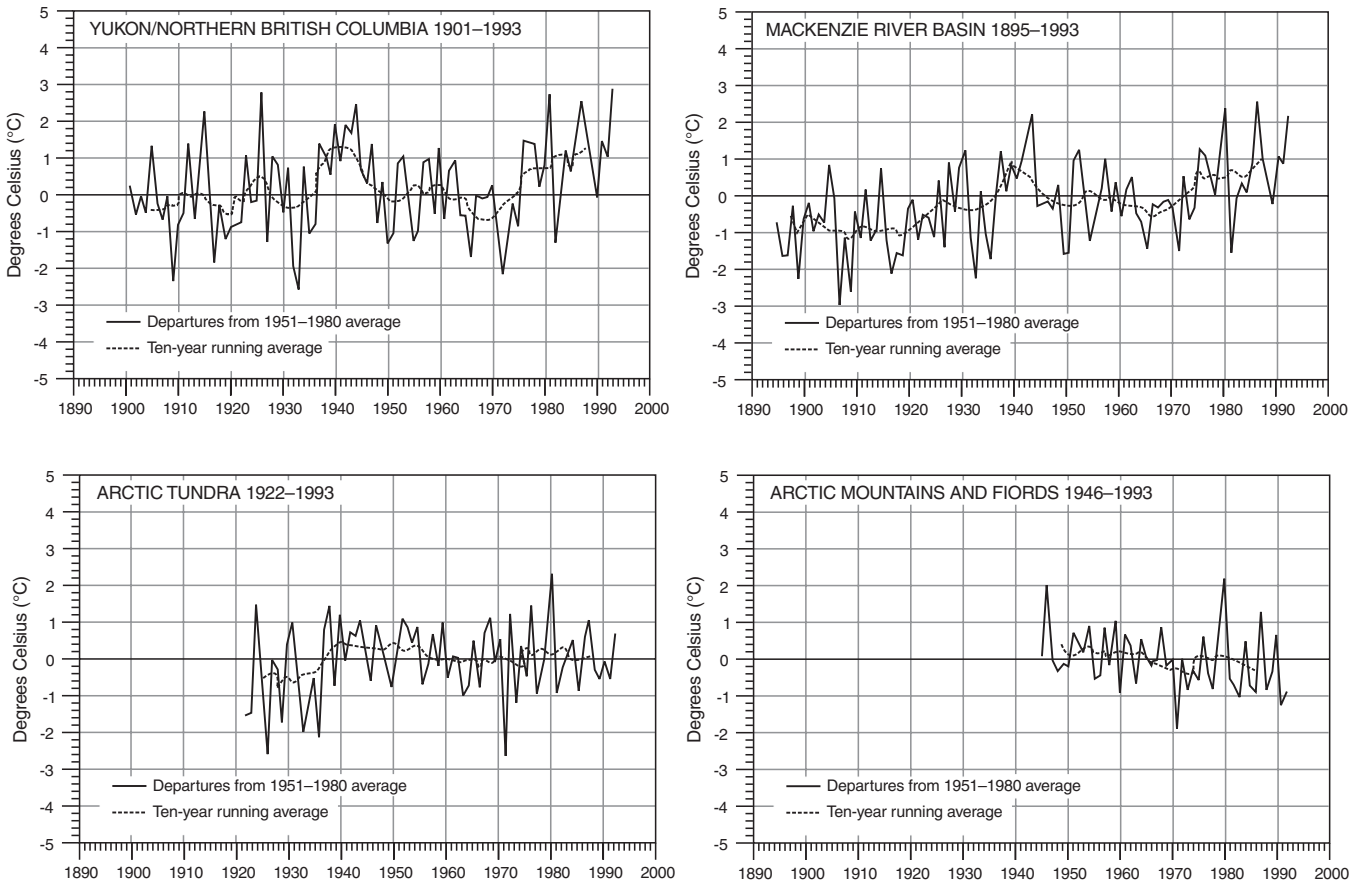


Figure 8. Annual mean temperatures for the four northern Canadian climate regions (data source: Historical Canadian Climate Database, Environment Canada).

five-year running means of summer temperature deviations from the 30-year normals closely resemble the frequencies in Arctic and Antarctic Research Institute geographical zone A7 (Fig. 10). A very warm period occurs in the late 1950s and early 1960s and a cold period, in the 1970s.

There is reasonable agreement between the one-year Eureka winter temperatures (Fig. 11) and positive anomalies in geographical zone B1. Synoptically speaking, this indicates a weakening or displacement of the circumpolar vortex from the central polar region. The lack of positive anomalies in zone A6 (Beaufort Sea) and the presence of anomalies in zone A7 (Baffin Bay) that accompany the peaks in the curve for zone B1 suggest that the vortex slipped southwest to sit over the Mackenzie–Alaska region, pumping warm air and moisture-bearing lows into the islands from the southwest (Alt et al., 1993).

Both summer and winter precipitation at Eureka show some similarity to the plot for zone A6, suggesting that a strong ridge in the Alaska sector would result in flow from the central polar region over the Queen Elizabeth Islands and may be indicative of the positioning of a strong circumpolar vortex over the northern Queen Elizabeth Islands. A study of the daily archive and of the circumpolar vortex archive (Dmitriev et al., 1989) is necessary for detailed analysis of precipitation events.

Further evidence of the uniqueness of the eastern High Arctic

Bradley et al. (1993) examined winter inversion data for the period 1966–1990 and found that a systematic reduction in midwinter, surface-based inversion depths has occurred during that period for North American stations (Fig. 12). Although Eureka does show some reduction in inversion depth, there is no corresponding increase in surface temperature (Fig. 12). The examination of some Russian data suggested that this pattern of decreasing inversion thickness may extend to longitude 104°E (Cape Chelyuskin). These results are generally in agreement with those of Kahl et al. (1993b), who found a warming trend in the 85 to 70 kPa layer (about 1500–3000 m a.s.l.) of the troposphere for the same geographical area of the Arctic. On the other hand, a cooling trend was recorded for that layer over northwestern Russia, Scandinavia, and Greenland.

In their study of atmospheric water vapour at latitude 70°N, Serreze et al. (1995a) found that integrated vapour transport exhibits marked, longitudinal variation. Maximum poleward transport occurred in Baffin Bay (and the Norwegian Sea), but the Canadian Arctic Archipelago was the only sector where mean integrated transport was found to be towards the equator (Fig. 13).

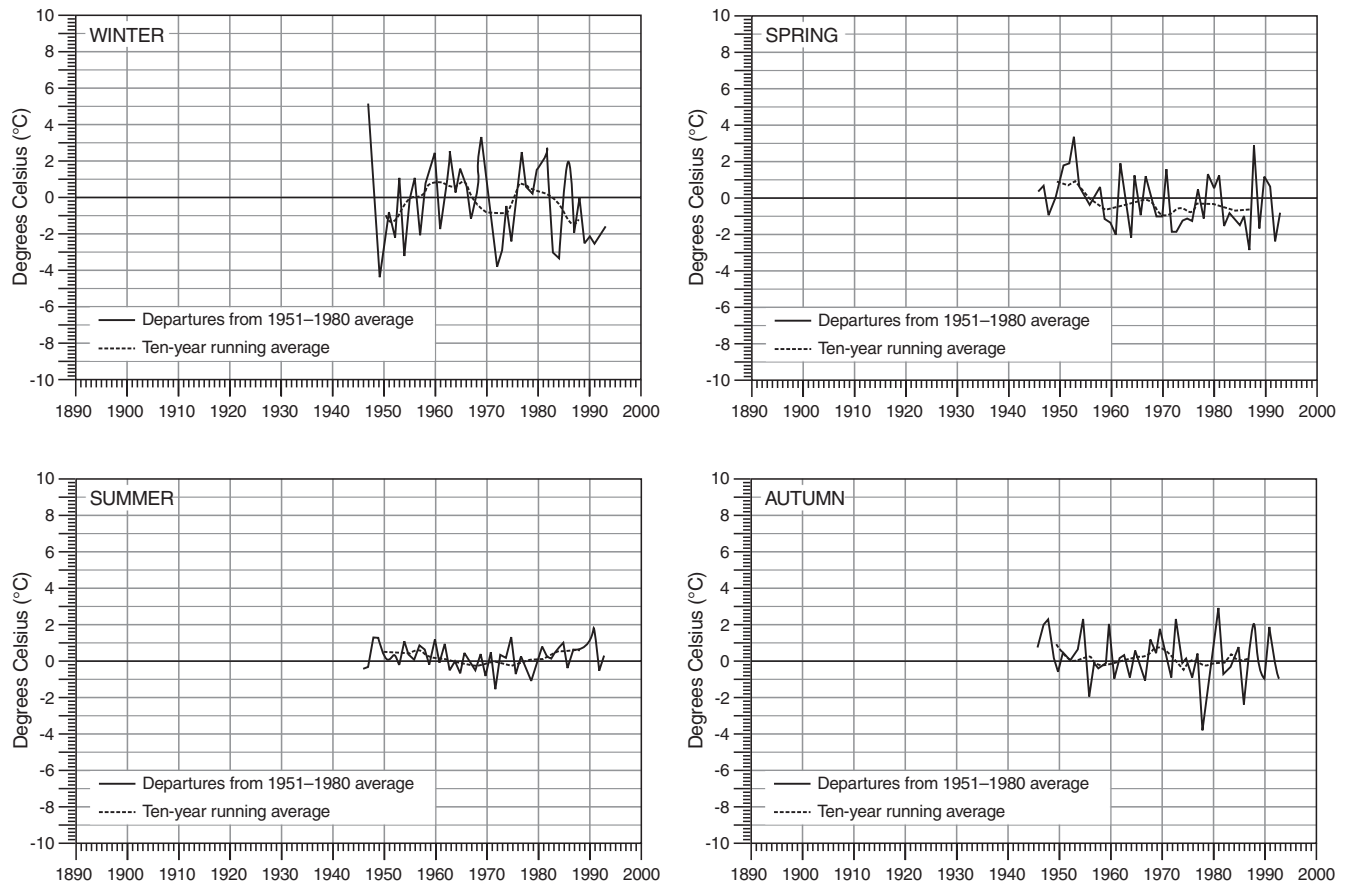


Figure 9. Seasonal mean temperatures for the Arctic Mountains and Fiords climate region, 1946 to 1993 (data source: Historical Canadian Climate Database, Environment Canada).

Maxwell (1997) compares trends for the five circumpolar trend regions (Fig. 5) with general circulation model climate patterns under a scenario of doubling of the atmospheric concentration of carbon dioxide. Two GCM results were considered, the Canadian Climate Centre high-resolution model for a doubled CO₂ equilibrium experiment (Boer et al., 1992) and the National Center for Atmospheric Research community climate model coupled to an ocean general circulation model with CO₂ increasing linearly by 1 per cent a year (Washington and Meehl, 1989). The model results are summarized in Tables 2 and 3 for both winter (December–February) and summer (June–August). Only temperature information was readily available for the summer from the National Center for Atmospheric Research model.

A comparison of these two tables shows general agreement between the model results. The most apparent differences are found in the eastern Canadian Arctic and southern Greenland region where, in winter, the Canadian Climate

Centre model suggests an increase in temperature, a decrease in sea-ice extent, and a decrease in sea-level pressure whereas the National Center for Atmospheric Research model shows results that are opposite for all three elements. The same contrast in temperature trends is also evident in summer.

In comparing the model results with the currently observed trends in the Arctic, those regions where the models are in agreement show current trends that are for the most part consistent with the direction of changes that might be expected under an enhanced greenhouse-gas effect. This shows up for all climate and related elements considered here. In the eastern Canadian Arctic and southern Greenland region where the model results differ, currently observed trends tend to agree with the direction of changes suggested by the National Center for Atmospheric Research model. The fact that the National Center for Atmospheric Research model results presented here are from a transient run (CO₂ changes gradually) and that the model involves a coupled oceanic

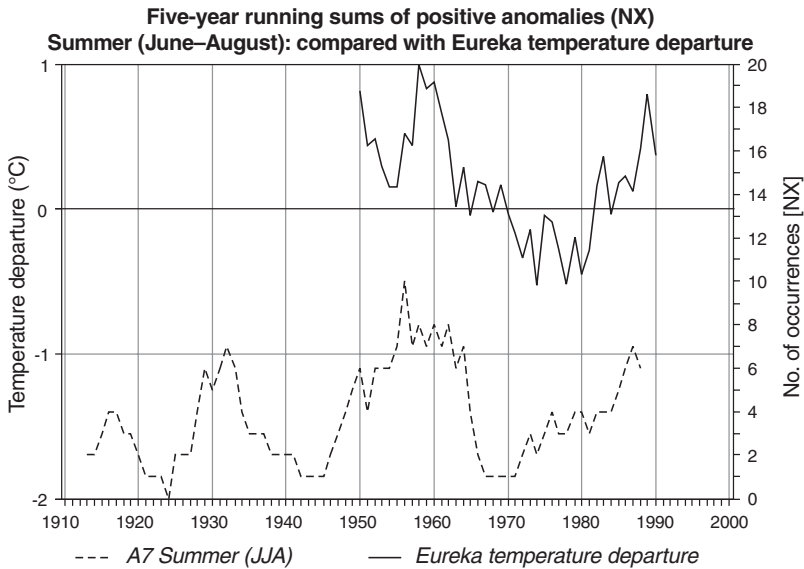
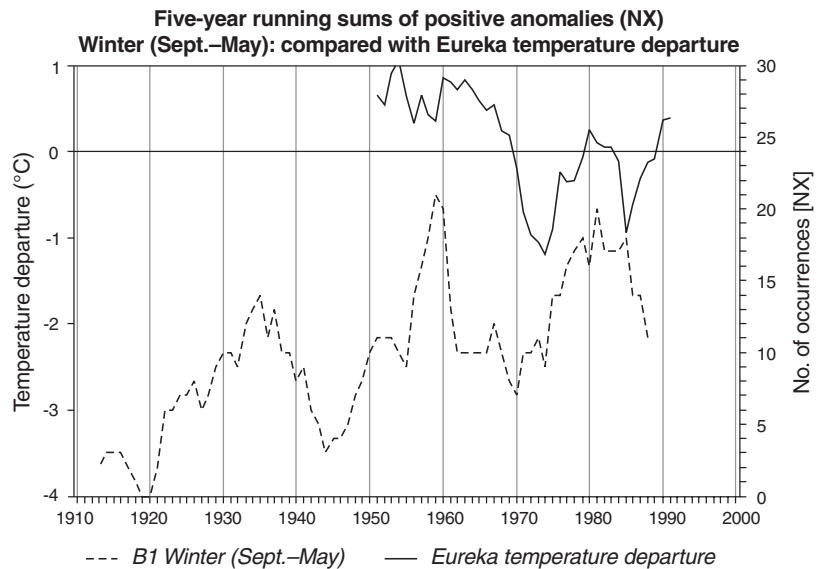


Figure 10.

Frequency of anomalies in zone A7 (positive pressure anomaly in the eastern North American zone) compared with five-year running sums of summer temperature deviation (from 30-year normals) at Eureka.

Figure 11.

Frequency of five-year winter anomalies in zone B1 (positive pressure anomaly in the central Arctic Ocean) compared with Eureka winter temperature deviations.



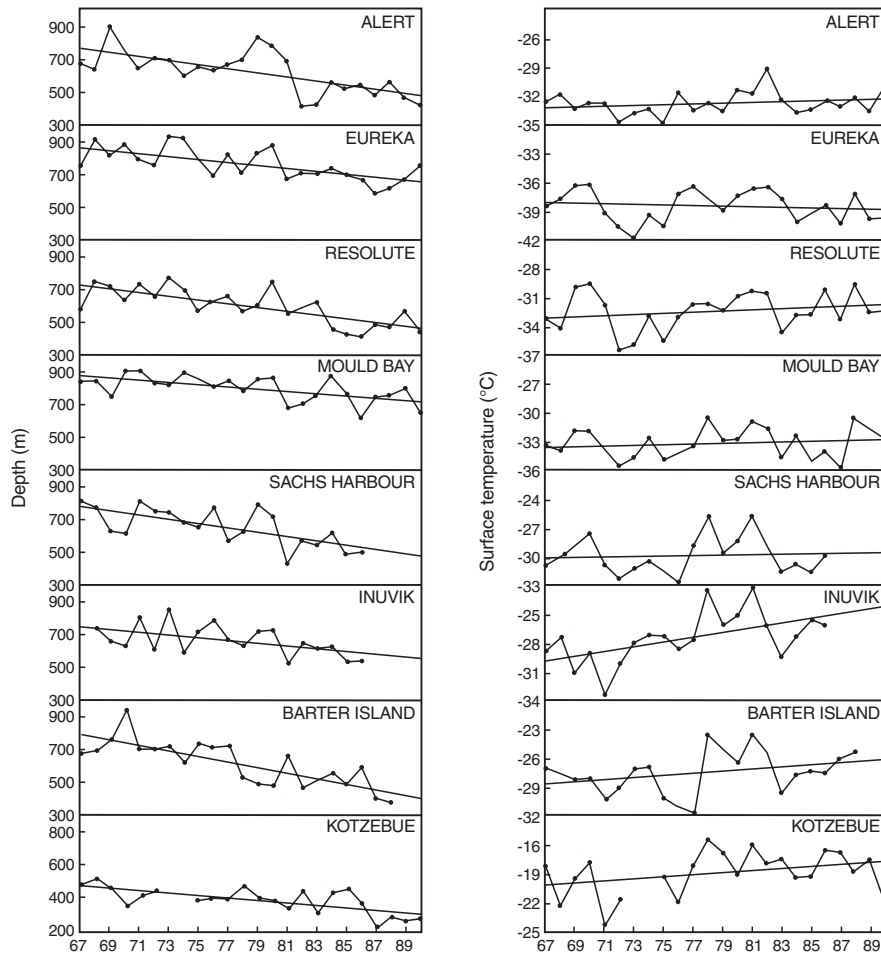


Figure 12. Mean December to March, surface-based inversion depths and mean surface temperatures at the time of each sounding (12:00 h UCT) for the stations indicated. Year given is for each January (i.e. 1953 is December 1952 to March 1953) (from Bradley et al., 1993).

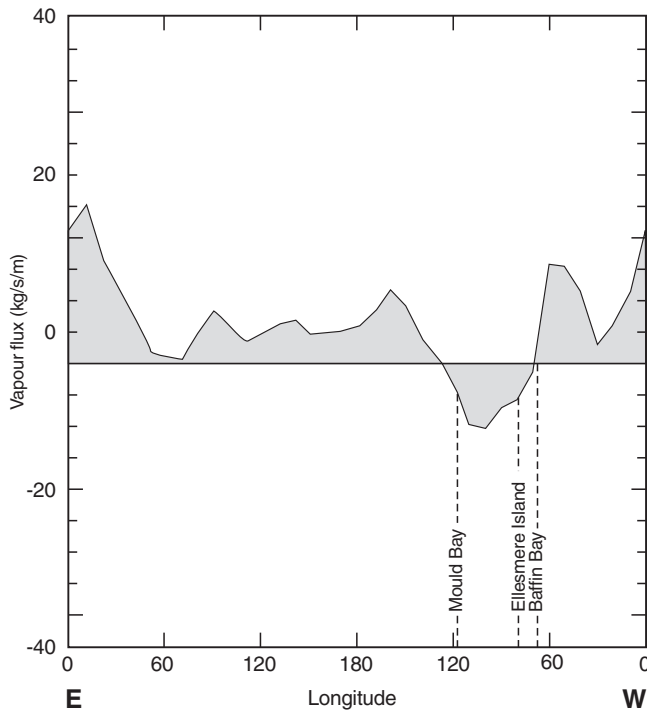


Figure 13. Mean, vertically integrated, meridional vapour flux (kg/m/s) at latitude 70°N at every 10° of longitude (poleward values positive) (modified from Serreze et al., 1995a).

circulation component may suggest that its outputs will be closer to future reality, although the model has other deficiencies (Washington and Meehl, 1989). This suggests that trends for the eastern Canadian Arctic and southern Greenland region may well be a sign of things to come in that region. At the very least, close attention to ongoing conditions in the region is warranted.

***The Queen Elizabeth Islands:
Eureka Sound intermontane region***

The Eureka (Sound) intermontane region (Fig. 14), bounded on all sides by mountain barriers, is a regional-scale feature approximately 400 km long and 120 km wide. It is similar in size to the Columbia Basin in the northwestern United States or the Nechako Plateau between the Coastal Range and the Rockies in British Columbia; it was identified on the basis of

Table 2. General circulation model results for doubled CO₂ scenario (compared with single CO₂ for various arctic regions in winter (CCC = Canadian Climate Centre; NCAR = National Center for Atmospheric Research)

	Northwest Canada and Alaska	Eastern Canadian Arctic and southern Greenland	Scandinavia	North- central Russia (Yamal)	Extreme northeast Russia	Arctic Ocean
Temperature -CCC -NCAR	increase increase	increase decrease	increase decrease	increase no change	increase increase	increase decrease
Precipitation -CCC -NCAR	increase	increase	increase	increase	increase	increase
Snow cover -CCC -NCAR	North America as a whole decrease		Eurasia as a whole decrease			
Sea ice -CCC -NCAR	decrease decrease	decrease increase		decrease no change	decrease decrease	decrease no change
Sea-level pressure -CCC -NCAR	decrease decrease	decrease increase	decrease decrease	decrease decrease	decrease decrease	decrease decrease

Table 3. General circulation model results for doubled CO₂ scenario (compared with single CO₂ for various arctic regions in summer (CCC = Canadian Climate Centre; NCAR = National Center for Atmospheric Research)

	Northwest Canada and Alaska	Eastern Canadian Arctic and southern Greenland	Scandinavia	North- central Russia (Yamal)	Extreme northeast Russia	Arctic Ocean
Temperature - CCC - NCAR	increase increase	increase decrease	increase increase	increase increase	increase decrease	no change no change
Precipitation - CCC - NCAR	increase	no change	increase	increase	increase	no change
Sea ice - CCC - NCAR	decrease	decrease		decrease	decrease	decrease
Sea-level pressure - CCC - NCAR	decrease	no change	decrease	decrease	decrease	increase

regional studies of the congruence of climate and vegetation in the Queen Elizabeth Islands by Edlund and Alt (1989) and Alt and Maxwell (1990), who discuss previous studies in the region and the history of data availability to the end of the 1980s. Summer, defined as the melt or thaw season and represented by June and July monthly mean analysis, was the focus

of these studies. Correction factors were applied to short-term records through comparison with the appropriate, permanent station record to produce values comparable to normals for 1951 to 1980. As seen in Figure 14, despite the addition of field stations, the interior of the Queen Elizabeth Islands is still virtually unrepresented and even in the Eureka Sound

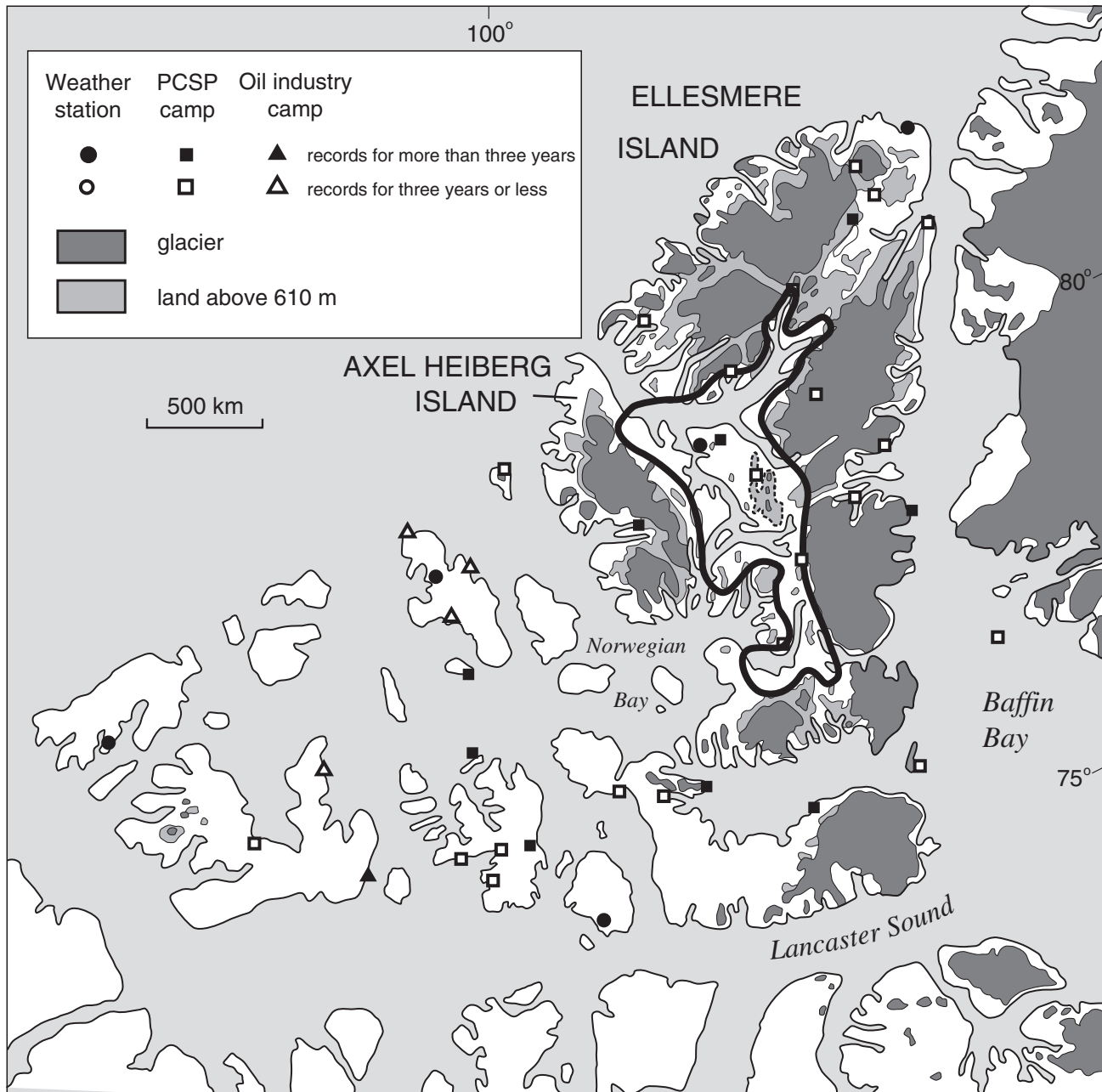


Figure 14. The Eureka Sound intermontane area (heavy outline). The area outlined with a dotted line in the centre encloses the glacierized mountain ranges of eastern Fosheim Peninsula, including the Sawtooth Range. This is not strictly speaking an intermontane area. The Sverdrup Lowlands comprise the low-lying parts of the central and western Queen Elizabeth Islands. Shown are permanent weather stations of the Atmospheric Environment Service, short-duration stations supported by the Polar Continental Shelf Project (PCSP), and oil industry camps. See Edlund and Alt (1989) for station names and references. Light shaded areas are above 610 m a.s.l.

intermontane area, most of the stations are on fiords or lakes. The contours have been drawn through sea-level coastal-station values. For any contour, a range of values exists. For instance, in summer, the lowest values would be found over the ice-bound channels and the highest, at sheltered, interior sites. Inland contours have been drawn only where they represent regional-scale features (i.e. 100 km or more). Contours have not been drawn in mountainous areas (over 600 m, light shading) or over ice caps (shaded). In drawing details of contours, consideration was given to common sea-ice patterns and boundaries. Reference should be made to Maxwell (1980, 1982) for a traditional analysis of these parameters.

Radiation data are still insufficient to produce normal maps at a regional level in the Queen Elizabeth Islands. More solar radiation reaches the top of the atmosphere at latitude 80°N from May to July than at any lower latitude. The amount of solar radiation reaching the ground is largely dependent on cloudiness. The reflective property (albedo) of the surface determines how much global radiation is actually absorbed by the ground. Measurements of surface albedo (Alt and Maxwell, 1990) are available for Resolute and several expedition sites (Holmgren, 1971; Dahlgren, 1974; Alt, 1975; Müller et al., 1976; Courtin and Labine, 1977; Ohmura, 1981; Wolfe, 1994; Young et al., 1995). Although it is not yet possible to draw regional-scale albedo maps, the following generalizations can be made.

Snow remains on the ground throughout June in the central and western Queen Elizabeth Islands and at high elevations in the mountains of Ellesmere and Axel Heiberg islands. Thus, these regions have a high albedo. At Expedition Fiord and in other interior valleys of western Axel Heiberg Island, snow disappears by mid-June (Ohmura, 1981). Snow disappears even earlier in the Eureka Sound intermontane area.

Thus, the low albedos in June increase the total energy absorbed in the interior area, whereas high albedos reduce the absorption of available energy over sea ice and in snow-covered areas in the northwestern part of the islands.

By July, most of the land in the Queen Elizabeth Islands is free of snow. Albedo differences between the Eureka Sound intermontane area and the Sverdrup Lowlands are less pronounced; however, differences in surficial materials, vegetation cover, and moisture content of the ground still result in increased absorption in the intermontane region and reduced absorption in exposed lowlands.

In both June and July, therefore, the gradient of solar radiation absorbed at the ground is not latitudinal. Rather, the highest values are in the interior of Ellesmere and Axel Heiberg islands and the lowest values, west of Isachsen and Mould Bay over the pack ice of the central Arctic Ocean.

The regional distribution of cloudiness in June and July (Fig. 15) is a result of the complex interaction of atmospheric circulation, topography and surface conditions. Overwhelming evidence shows that the Queen Elizabeth Islands (with the possible exception of the east coast of Ellesmere and Devon islands) are dominated at all levels by air moving into the islands from the Arctic Ocean. Previous studies (Alt, 1987; Edlund and Alt, 1989; Alt and Maxwell, 1990) are supported by Serreze et al. (1995a) who demonstrated that the frequency of poleward geostrophic wind events greater than 5 m/s over the entire Queen Elizabeth Islands is less than 1 per cent. It should be stressed that this flow into the Queen Elizabeth Islands from the Arctic Ocean is not associated with tracking cyclones, but rather is a result of the northwesterly flow (Fig. 2, 3) occurring between the Western Canadian

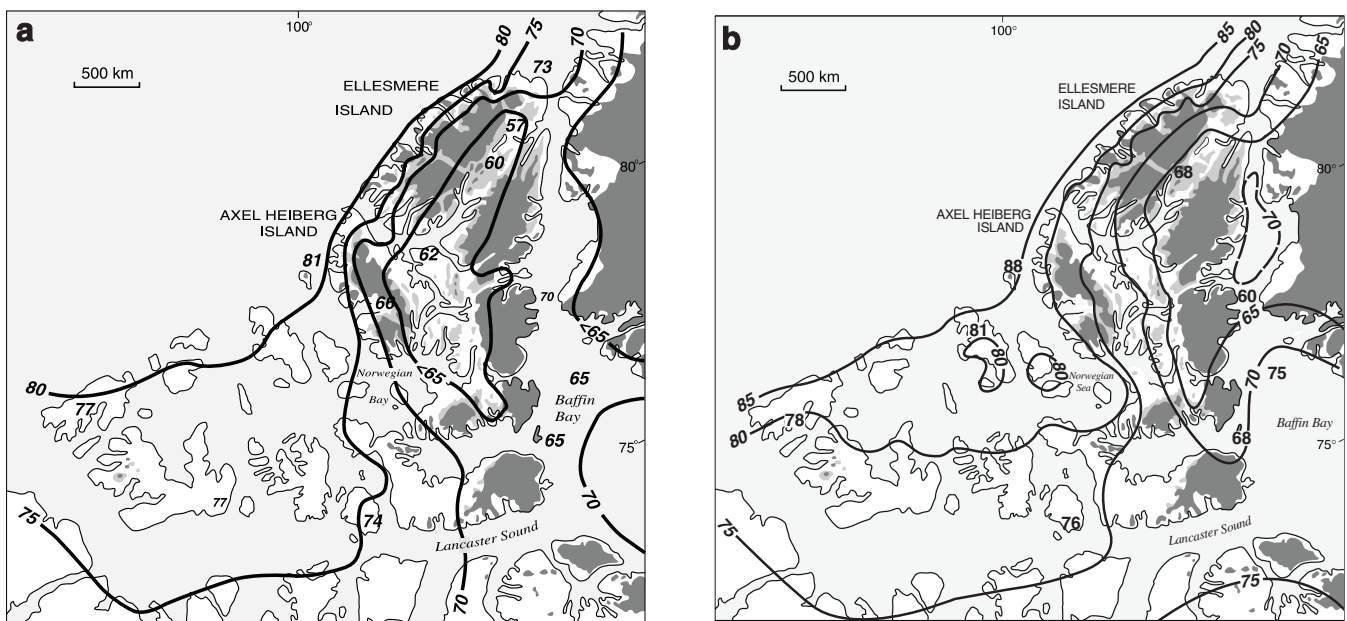


Figure 15. Mean cloud cover (%) for **a)** June and **b)** July, based on the period 1959 to 1979. Where applicable, field-station data were used (corrected as discussed in text).

(Alaska-Mackenzie) Ridge and the Eastern Canadian (Baffin Bay) Trough (Bryson and Hare, 1974; Maxwell, 1980, 1982; Alt, 1987).

In summer, the season considered here, the central Arctic Ocean is the coldest region of the northern hemisphere with a mean July temperature ranging from -1 to 2.5°C . The surface of the moving polar pack ice is extensively puddled and this moisture source maintains a nearly continuous, low-lying layer of stratus and stratocumulus cloud. In the northeastern Queen Elizabeth Islands, the mountains of northern Axel Heiberg and northern Ellesmere islands lie athwart the mean circulation, forming a barrier similar to (although not as extensive nor as high as) the Cordillera in western North America (Bryson and Hare, 1974). The cold, moist Arctic air mass ('continental Arctic' or 'cA' air mass) is either deflected or forced aloft by the mountains. In the former case, the Arctic Ocean stratus and stratocumulus do not reach the sheltered, interior region. In the latter case, the orographically lifted air cools and precipitates much of its moisture; then it descends the lee slope of the mountains with warming due to adiabatic compression and with decreasing relative humidity. It arrives in the Eureka Sound intermontane area (Fig. 14) with dry, mild characteristics, in contrast to the moistness and coldness of the Arctic Ocean (continental Arctic) air masses. A similar process of adiabatic warming due to subsidence affects air entering the region at atmospheric levels above the central mass of the mountains.

These warming processes are observed whenever the prevailing atmospheric flow is forced to cross mountain ranges (Flohn, 1969). On a regional scale, this results in a belt of precipitation on the windward slope, whereas the leeward side of the mountains is characterized by dry conditions. At a local scale, intense and in places isolated occurrences of warm, dry winds in the lee of topographic barriers have been observed. These occurrences are often associated with specific synoptic conditions. In the Alps, these winds have been known for centuries as 'foehn'. Similar in effect, but differing somewhat in extent and synoptic properties, are the 'chinook' (east of the Rocky Mountains), the 'zonda' (in the Argentine Andes), and the dry winds in the eastern lowlands of southern New Zealand. The extent, frequency, and synoptic nature of such conditions in the Eureka intermontane region have yet to be studied, but are doubtless a feature of the area.

It should be stressed that the Eureka intermontane area is sheltered from the low cloud associated with prevailing, low-level, northwesterly atmospheric flow. The mountains do not completely prevent intrusion of a deep, cold-cored low into northern Ellesmere Island. Similarly, the low-level cloud associated with the semipermanent Baffin Bay low will not encroach on the intermontane area, but a deep, cold-cored low moving over northern Ellesmere Island from the cold waters of Baffin Bay will bring middle cloud and possibly low-level moisture to the Eureka intermontane region. Tracking cyclonic systems moving around the upper-level vortex can cross the mountains at upper levels or enter the intermontane area from the southwest up Eureka Sound. These often possess well developed, warm sectors and extensive cloud and precipitation.

The distribution of lower troposphere temperature is shown by the 90 kPa temperatures for July (Fig. 16). Topography was not taken into account when drawing the contours, which were spaced and shaped solely as demanded by the values of the five data points. The intrusion of cold Arctic Ocean (continental Arctic) air over the Sverdrup Lowlands and the sheltering effect of the mountain barriers in the east form an S-shaped pattern similar to the cloud patterns (Fig. 15a, b). This general S-shaped pattern is thus a macro- or synoptic-scale phenomenon; it reaches at least 1000 m into the atmosphere and reflects the impact of regional topography on the lower troposphere.

July temperatures (Fig. 17a) at latitude 80°N over the Sverdrup Lowlands are 4°C colder than similar coastal station in the Eureka Sound intermontane area; in June (Fig. 17b), the 0°C isotherm separates the two areas. A relatively steep temperature gradient exists over northern Ellesmere and Axel Heiberg islands; it broadens in the Sverdrup Lowlands as the cold Arctic Ocean (continental Arctic) air masses there are gradually modified as they travel over the heated land of low-lying islands.

The plots of regional, coastal temperatures (Fig. 17) show that in the intermontane area, coastal temperatures in July exceed 5°C . These are the highest coastal temperatures recorded around the latitude 80°N belt. The distinctive S-shaped pattern is evident in both June and July.

The details of the temperature patterns will undoubtedly change with the addition of new stations and more comprehensive techniques for using field-station data; however, this will not alter the S-shaped pattern or general features of the present synoptic-scale climate configuration. Strong interannual variations do occur, though, and the pattern may be amplified or reversed seasonally and may alter with long-term climate change.

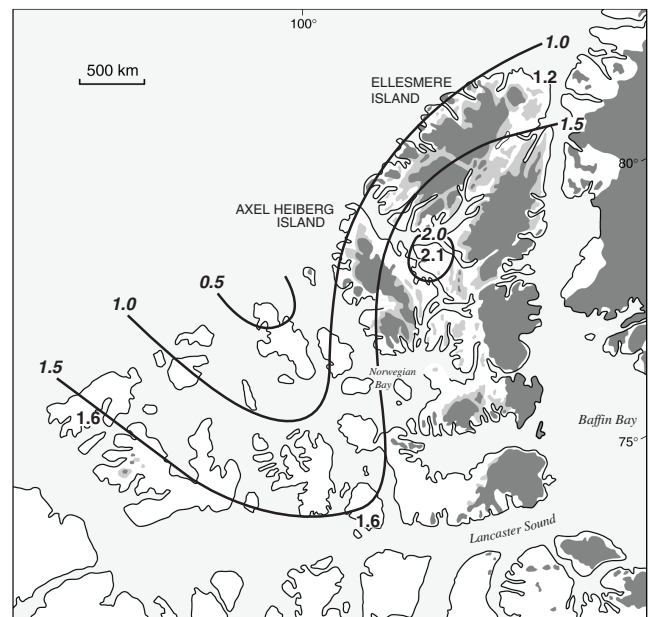


Figure 16. Mean July temperature at 90 kPa (about 1000 m) for 1951 to 1980.

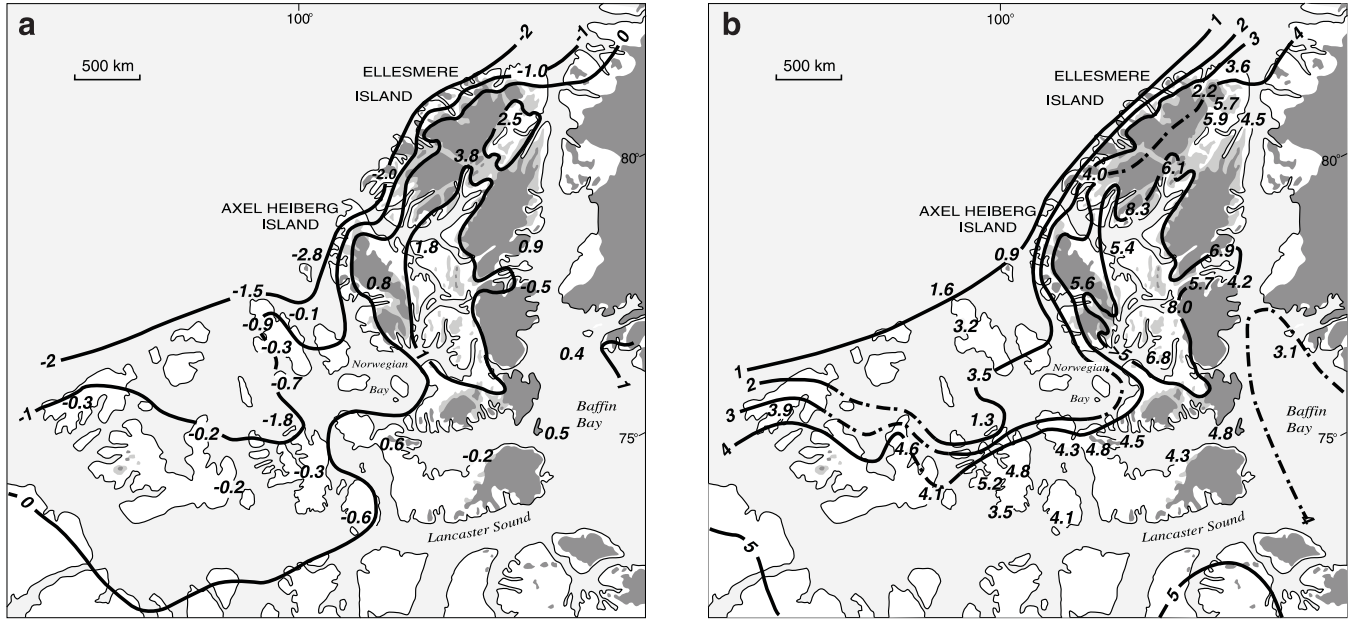


Figure 17. Mean monthly summer temperature (°C) over the Queen Elizabeth Islands for **a)** June and **b)** July. Permanent weather stations and nonstandard weather data were used. Correction factors, developed through comparison with the appropriate permanent weather station records, were applied to the short-term record to produce values for the 1951 to 1980 normal period.

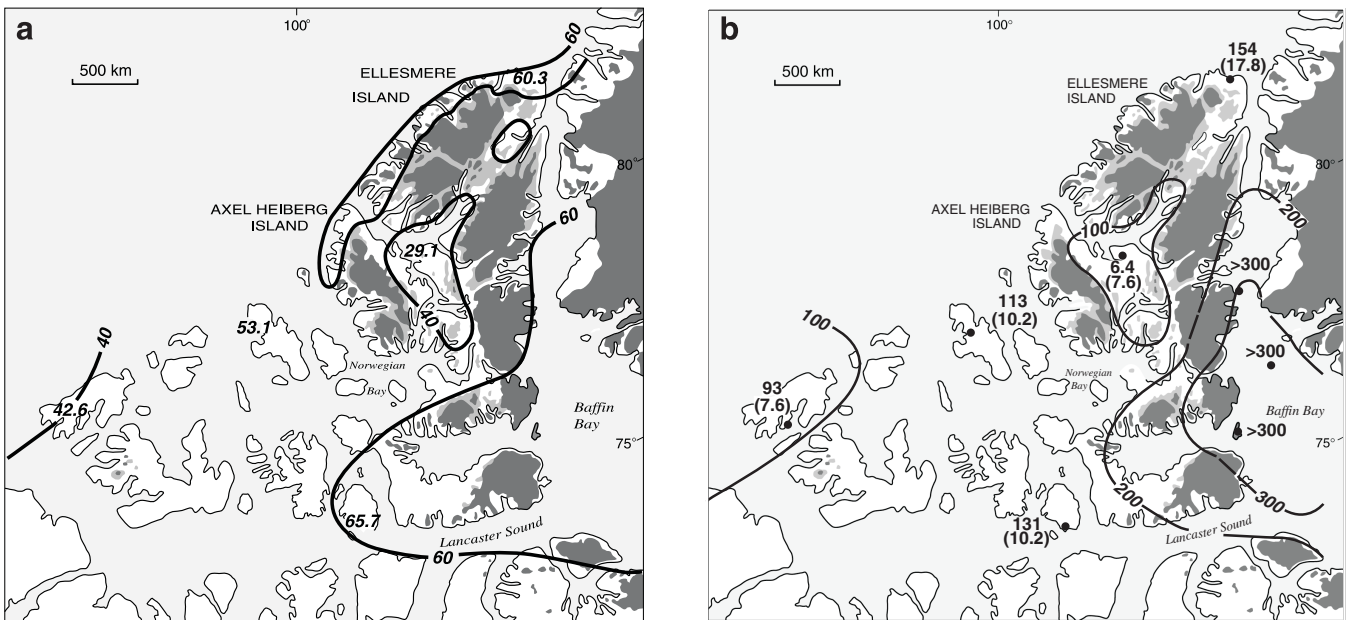


Figure 18. a) Mean total summer (June, July, and August) precipitation in millimetres (mm) for the Queen Elizabeth Islands; **b)** mean total annual precipitation (mm) and snow depth at the end of January in centimetres (in parentheses).

Winter snow accumulation values from the permanent weather stations are underestimated by 40 to 400 per cent (Koerner, 1979; Maxwell, 1980; Woo et al., 1983). Mean total annual precipitation, mean total summer precipitation, and mean snow depth on 31 January have been plotted (Fig. 18a, b). Areas over 600 m a.s.l. (shown in Fig. 14) or covered by ice caps were ignored, to be consistent with the regional (near sea level) temperature analysis.

Total values for summer (Fig. 18a) and annual (Fig. 18b) precipitation and winter snow depth (Fig. 18b) all show similar distributions. The highest precipitation occurs in the area under the direct influence of the North Water Baffin Bay

cyclone. A secondary maximum is found windward of the mountain barriers on Ellesmere and Axel Heiberg islands. Precipitation minima occur in the Eureka Sound intermontane region due to the precipitation-shadow effect and in the far western islands due to the proximity of the persistent surface anticyclone.

Snow accumulation measurements made by oversnow traverses in the spring of 1974 (Koerner, 1979) for the 1973–1974 accumulation season and for the 1962–1974 period (Fig. 19, 20) show a definite precipitation shadow facing the intermontane region.

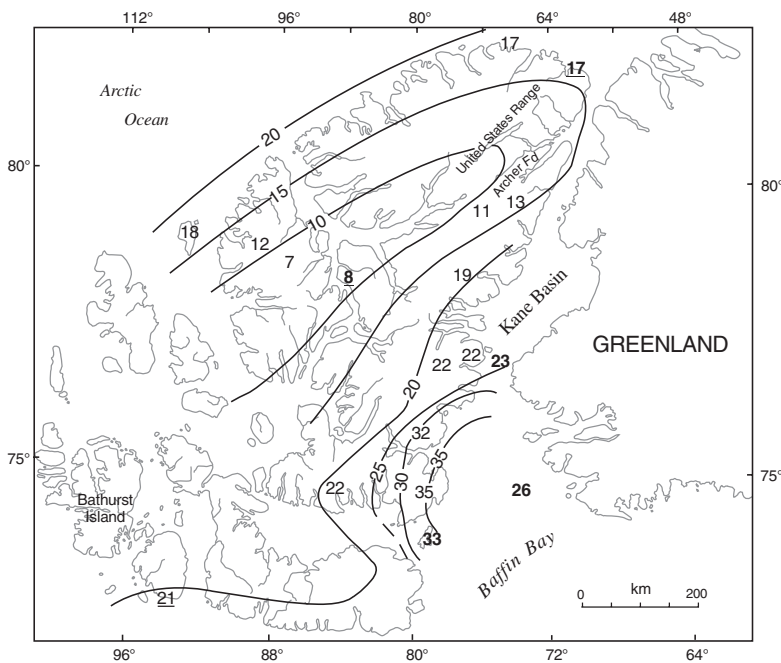


Figure 20.

Snow accumulation ($\text{g}/\text{cm}^2/\text{a}$) for the period August 1962 to August 1973 in the eastern Queen Elizabeth Islands, as calculated from measurements made down to the 1962 summer melt layer in April and May 1974. Bold-faced values are from Hattersley-Smith and Searson (1973) and bold-faced, underlined values are from Müller et al. (1977). The isohyets on Greenland are from Mock (1967); the broken lines are interpolations. (From Koerner, 1979).

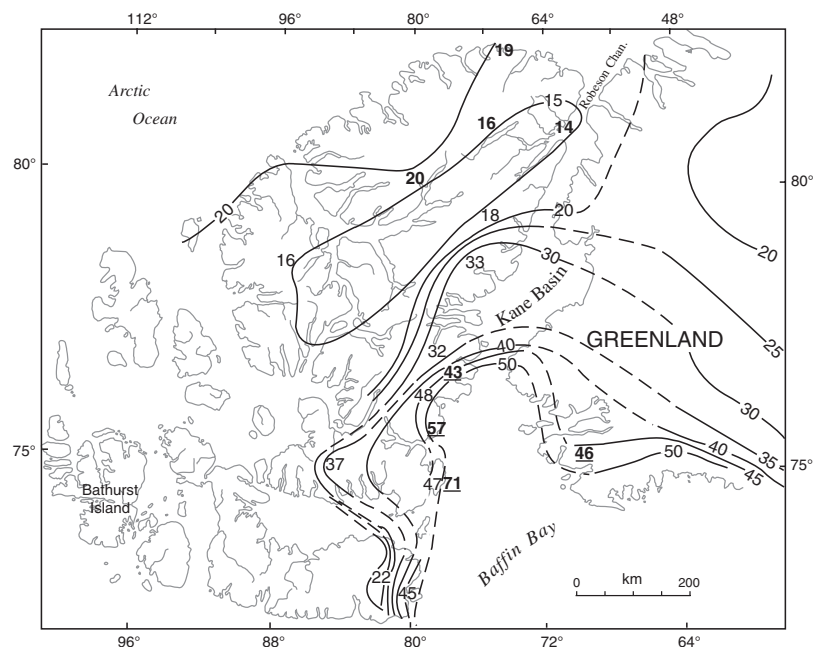


Figure 19.

Snow accumulation ($\text{g}/\text{cm}^2/\text{a}$) for the period August 1973 to June 1974, as calculated from snow-surface measurements in April and May 1974. Underlined, bold-faced values are from the permanent weather stations; bold-faced values are from F. Müller (pers. comm., 1977). (From Koerner, 1979).

Thus, precipitation amounts do not produce the S-shaped pattern seen in the temperature analyses. This indicates that at a regional scale, precipitation amounts are controlled by a different mechanism. Previous studies have also suggested that the major control on precipitation is the frequency and intensity of cyclonic activity and that the interaction of topography and mean atmospheric flow is secondary (Müller et al., 1976; Maxwell, 1980; Bradley and Eischeid, 1985). Considerably more study of the synoptic situations responsible for extreme and significant precipitation events is still necessary, not only to determine the regional patterns and their effects, but also to establish source regions for the moisture, pollen, and aerosols that constitute the precipitation.

Eureka Sound intermontane region: Fosheim Peninsula

Fosheim Peninsula is the largest interior lowland area in the Eureka Sound intermontane region. It is surrounded on three sides by ice-choked fiords. In the southeast, the Sawtooth Range and several parallel ranges separated by narrow, lowland areas merge into the higher mountains of eastern Ellesmere Island. The interior of the Fosheim lowland covers a much larger area than the thermal oases studied by Labine (1994) and others. Thus, it affords an opportunity to study the regional, interior lowland climate of the anomalously warm Eureka Sound intermontane region. Initial results from field studies in the Fosheim Peninsula interior (Edlund et al., 1989) suggested inland July mean temperatures from 2 to 5°C warmer than the coastal means used in the climate and climate change evaluations discussed previously. In addition, these initial studies showed that the coastal-inland difference was considerably greater in the warm summer of 1988 than in the cold, wet summer of 1989.

CONCLUSIONS AND RECOMMENDATIONS

Due to their very nature, trend discussions must be updated annually. It is obvious, however, that for the eastern Canadian Arctic, a comprehensive study is needed to investigate the reasons and mechanisms for its anomalous behaviour in trend analysis and currently available general circulation model results. The regional differences between the western Canadian Arctic and eastern Canadian Arctic are particularly important in light of Mackenzie Basin studies such as the Mackenzie Basin Impact Study and the Global Energy and Water Cycle Experiment. Variations between the Queen Elizabeth Islands, Baffin Island, and Greenland and the relationship between the Eureka Sound intermontane and Sverdrup Basin areas must also be addressed in studies of modern, past, and future environmental relationships.

Alt and Maxwell (1990) have discussed the importance, in interdisciplinary studies, of comparing all processes at similar temporal and spatial scales. The key to successful interdisciplinary studies related to climate change is constant awareness and attention to the appropriateness of the comparisons being made. Young and Woo (2000) point out that in evaluating the impact of global change, much more realistic

results will come from first aggregating meteorological, hydrological, and botanical information defined at a small scale and then moving upward from that point. They and others advocate the point-slope-basin-region approach. The modern climate patterns and trends examined in this arctic overview are, of necessity, based on site data. They are only as representative as the data used to construct them and are presented here to show the relationship of the Fosheim study area to circumpolar conditions.

At a global scale, the Arctic is expected by all general circulation models to experience the greatest warming due to greenhouse gases. At a regional scale, the eastern Canadian Arctic is not exhibiting such a trend, either in the instrumental records or in the transient general circulation model scenarios. At a mesoscale, the Fosheim Peninsula, the area of focus for this bulletin, lies at the centre of the anomalously warm Eureka Sound intermontane region. An understanding of the climate of this broad, inland area would help to characterize the regional interior climate of this anomalously warm, High Arctic region. To this lowland interior climate profile, it would then be necessary to add coastal, elevation, and extreme sheltering influences. Combined with land and sea-ice distribution, these results would allow evaluations of regional averages for use in general circulation model validation, trend studies, and paleoclimatic reconstructions.

REFERENCES

- Alt, B.T.**
1975: The Energy Balance Climate of Meighen Ice Cap, N.W.T., v. 2; Polar Continental Shelf Project, Department of Energy, Mines, and Resources, Ottawa, 101 p.
1987: Developing synoptic analogs for extreme mass balance conditions on Queen Elizabeth Island ice caps; *Journal of Climate and Applied Meteorology*, v. 26, no. 12, p. 1605–1623.
- Alt, B.T. and Maxwell, B.**
1990: The Queen Elizabeth Islands: a case study for arctic climate data availability and regional climate analysis; *in Canada's Missing Dimension – Science and History in the Canadian Arctic Islands*. Volume 1, (ed.) C.R. Harington; Canadian Museum of Nature, Ottawa, Ontario, p. 294–326.
- Alt, B.T., Kuchin, V.A., and Maxwell, B.**
1993: Investigations into the applicability of the AARI positive anomaly position classification catalogue to mass balance and climate change studies in the Queen Elizabeth Islands; Canadian Climate Centre Report no. 93-5, Atmospheric Environment Service, Downsview, Ontario, 25 p.
- Barry, R.G., Serreze, M.C., Maslanik, J.A., and Preller, R.H.**
1993: The Arctic sea ice-climate system: observations and modeling; *Reviews of Geophysics*, v. 31, no. 4, p. 397.
- Boer, G.J., McFarlane, N.A., and Lazare, M.**
1992: Greenhouse gas-induced climate change simulated with the CCC second-generation general circulation model; *Journal of Climate*, v. 5, p. 1045–1077.
- Bradley, R.S. and Eischeid, J.K.**
1985: Aspects of the precipitation climatology of the Canadian High Arctic; *in Glacial, Geologic and Glacio-climatic Studies in the Canadian High Arctic*, (ed.) R.S. Bradley; University of Massachusetts, Amherst, Massachusetts, Contribution no. 49, p. 250–271.
- Bradley, R.S., Keimig, F.T., and Diaz, H.F.**
1992: Climatology of surface-based inversions in the North American Arctic; *Journal of Geophysical Research*, v. 97, no. D14, p. 15699–15712.
1993: Recent changes in the North American Arctic boundary layer in winter; *J. Geophys. Res.* 98, no. D5, p. 8851–8858.

- Briffa, K.R. and Jones, P.D.**
1993: Global surface air temperature variations during the twentieth century: Part 2 implications for large-scale high frequency paleoclimatic studies; *The Holocene*, v. 3 no. 1, p. 77–88
- Bryson, R.A. and F.K. Hare**
1974: *Climates of North America*; World Survey of Climatology, v. 11; Elsevier, Amsterdam, 420 p.
- Central Intelligence Agency**
1978: *Polar Regions Atlas*; United States Government Printing Office, Washington, DC, report GC78-10040.
- Chapman, W.L. and Walsh, J.E.**
1993: Recent variations of sea ice and air temperature in high latitudes; *Bulletin of the American Meteorological Society*, v. 74, p. 33–47.
- Courtin, G.M. and Labine, C.**
1977: Microclimatological studies on Truelove Lowland; *in* Truelove Lowland, Devon Island, Canada: A High Arctic Ecosystem, (ed.) L.C. Bliss; University of Alberta Press, Edmonton, p. 73–106.
- Dahlgren, L.**
1974: Solar radiation climate near sea level in the Canadian Arctic Archipelago. Arctic Institute of North America Devon Island Expedition 1961-62; *Meteorologiska Institutionen Uppsala Universitetet Meddelser* no. 121, p. 1–119.
- Dmitriev, A.A., Sel'tser, P.A., Kondratyuk, S.I., and Kuchin, V.A.**
1989: Makromasshtabnye Atmosfernye Protesessy i Srednesrochnye Prognozy Pogody v Arktike (Macroscale Atmospheric Processes and Medium-Range Weather Forecasting in the Arctic); State Commission of the USSR on Hydrometeorology, Arctic and Antarctic Scientific Research Institute, Leningrad, 197 p.
- Edlund, S.A. and Alt, B.T.**
1989: Regional congruence of vegetation and summer climate patterns in the Queen Elizabeth Islands, Northwest Territories, Canada; *Arctic*, v. 42, no. 1, p. 3–23.
- Edlund, S.A., Alt, B.T., and Young, K.**
1989: Vegetation, hydrology and climate at Hot Weather Creek, Ellesmere Island, Northwest Territories; Canadian Committee Climatic Fluctuations and Man Annual Meeting, Canadian Committee Climatic Fluctuations and Man Newsletter no. 5, p. 65 (abstract).
- Flohn, H.**
1969: General climatology, 2; *World Survey of Climatology*. Volume 2; Elsevier, Amsterdam, 270 p.
- Goodison, B.E. and Louie, P.Y.T.**
1986: Canadian methods for precipitation measurement and correction; *Proceedings of the International Workshop on Correction of Precipitation Measurement*, Zurich, Switzerland, 1–3 April 1985, p. 141–145.
- Goodison, B.E., Elomaa, E., Golubev, V., Gunther, T., and Sevruck, B.**
1994: The WMO Solid Precipitation Measurement Intercomparison: Preliminary Results; World meteorological organization Technical Conference on Instruments and Methods of Observation (TECO-94), Geneva, Switzerland, 28 February–2 March 1994, p. 15–19.
- Gullett, D.W., Vincent, L., and Malone, L.H.**
1991: Homogeneity Testing of Monthly Temperature Series. Application of Multiple-Phase Regression Models with Mathematical Change-points; Canadian Climate Centre Report no. 91-10; Atmospheric Environment Service, Downsview, Ontario, 47 p.
- Harley, W.S.**
1980: Northern Hemisphere monthly mean 50-kPa and 100-kPa height charts; Report CLI 1-80; Atmospheric Environment Service, Downsview, Ontario, 30 p.
- Hattersley-Smith, G. and Searson, H.**
1973: Reconnaissance of a small ice cap near St. Patrick Bay, Robeson Channel, northern Ellesmere Island, Canada; *Journal of Glaciology*, v. 12, no. 66, p. 417–421.
- Holmgren, B.**
1971: Climate and energy exchange on a subpolar ice cap in summer; Part F, On the energy exchange of the snow surface at Ice Cap Station. Arctic Institute of North America Devon Island Expedition 1961–63; *Meteorologiska Institutionen, Uppsala*, 53 p.
- Kahl, J.D., Charlevoix, D.J., Zaitseva, N.A., Schnell, R.C., and Serreze, M.C.**
1993a: Absence of evidence for greenhouse warming over the Arctic Ocean in the past 40 years; *Nature*, v. 361, p. 335–337.
- Kahl, J.D., Serreze, M.C., Stone, R.S., Shiotani, S., Kisley, M., and Schnell R.C.**
1993b: Tropospheric temperature trends in the Arctic: 1958-1986; *Journal of Geophysical Research*, v. 98, no. D7, p. 12825–12838.
- Koerner, R.**
1979: Accumulation ablation and oxygen isotope variations on the Queen Elizabeth Islands ice caps, Canada; *Journal of Glaciology*, v. 22, no. 86, p. 25–41.
- Labine, C.L.**
1994: Meteorology and climatology of the Alexandra Fiord Lowland; *in* Ecology of a Polar Oasis, Alexandra Fiord, Ellesmere Island, Canada, (ed.) J. Svoboda and B. Freedman; Captus University Publications, Toronto, p. 23–40
- Maxwell, B.**
1980: The Climate of the Canadian Arctic Islands and Adjacent Waters. Volume 1; Atmospheric Environment Service, Environment Canada; *Climatological Studies* no. 30, 531 p.
- 1982: The Climate of the Canadian Arctic Islands and Adjacent Waters. Volume 2; Atmospheric Environment Service, Environment Canada; *Climatological Studies* no. 30, 589 p.
- 1992: Arctic climate: potential for change under global warming; *in* Arctic Ecosystems in a Changing Climate: an Ecophysiological Perspective, (ed.) F.S. Chapin III, R.L. Jefferies, J.F. Reynolds, G.R. Shaver, and J. Svoboda; Academic Press, San Diego, p. 11–34.
- 1997: Recent climate patterns in the Arctic; *in* Global Change and Arctic Terrestrial Ecosystems, (ed.) W.C. Oechel, T. Callaghan, T. Gilmanov, J.I. Holten, B. Maxwell, U. Molau, and B. Sveinbjornsson; Springer-Verlag, New York, p. 21–46.
- Metcalfe, J.R., Ishida, S., and Goodison, B.E.**
1994: A corrected precipitation archive for the Northwest Territories; *in* Mackenzie Basin Impact Study (MBIS) Interim Report #2, (ed.) S.J. Cohen; *Proceedings of the Sixth Biennial Atmospheric Environment Service/Department of Indians Affairs and Northern Development Meeting on Northern Climate and Mid Study Workshop of the Mackenzie Basin Impact Study*, p. 110–117.
- Mock, S.J.**
1967: Calculated patterns of accumulation on the Greenland ice sheet; *Journal of Glaciology*, v. 6, no. 48, p. 795–803.
- Müller, F., Blatter, H., Braithwaite, R., Ito, H., Kappenberger, G., Ohmura, A., Schroff, K., and Zust, A.**
1976: Report on North Water project activities, 1 October 1974 to 30 September 1975; Progress Report; McGill University and Swiss Federal Institute of Technology, 149 p.
- Müller F., Stauffer, B., and Schriber, G.**
1977: Isotope measurements and firm stratigraphy on ice caps surrounding the North Water polynya; Symposium, Isotopes et impuretés dans les neiges et glaces; Actes du colloque de Grenoble, août/septembre 1975; International Association of Hydrological Science-Association Internationale des Sciences Hydrologiques publication no. 118, p. 188–196.
- Ohmura, A.**
1981: Climate and energy balance on arctic tundra: Axel Heiberg Island, Canadian Arctic Archipelago, spring and summer 1969, 1970 and 1972; *Eidgenussische Technische Hochschule, Zurich, Zurich Geographische Schriften* 3, p. 1–448.
- Robinson, D.A. and Dewey, K.F.**
1990: Recent secular variations in the extent of Northern Hemisphere snow cover; *Geophysical Research Letters*, v. 17, p. 1557–1560.
- Robinson, D.A., Dewey, K.F., and Heim, R.R., Jr.**
1993: Global snow cover monitoring: an update; *Bulletin of the American Meteorological Society*, v. 74, p. 1689–1696.
- Robinson, D.A., Frei, A., and Serreze M.C.**
1995: Recent variations and regional relationships in Northern Hemisphere snow cover; *Annals of Glaciology*, v. 21, p. 71–76.
- Serreze, M.C.**
1995: Climatological aspects of cyclone development and decay in the Arctic; *Atmosphere-Ocean*, v. 33, no. 1, p. 1–23.
- Serreze, M.C., Barry, R.G., and Walsh, J.E.**
1995a: Atmospheric water vapor characteristics at 70° N.; *Journal of Climate*, v. 8, no. 4, p. 719–731.
- Serreze, M.C., Rehder, M.C., Barry, R.G., Walsh, J.E., and Robinson, D.A.**
1995b: Variations in aerologically derived Arctic precipitation and snowfall; *in* Proceedings, International Symposium on the Role of the Cryosphere in Global Change, Columbus, Ohio, August 7–12, 1994, (ed.) D.A. Rothrock, p. 77–82.
- Skinner, W.R. and Gullett, D.W.**
1993: Trends of daily maximum and minimum temperature in Canada during the past century; *Climatological Bulletin*, v. 27, no. 2, p. 63–77.

Washington, W.M. and Meehl, G.A.

1989: Climate sensitivity due to increased CO₂: experiments with a coupled atmosphere and ocean general circulation model; *Climate Dynamics*, v. 4, p. 1–38.

Wolfe, P.M.

1994: Hydrometeorological investigations on a small valley glacier in the Sawtooth Range, Ellesmere Island, Northwest Territories; Master's thesis, Wilfrid Laurier University, Waterloo, Ontario, 205 p.

Woo, M-k., Heron, R., Marsh, P., and Steer, P.

1983: Comparisons of weather station snowfall with winter snow accumulation in High Arctic basins; *Atmosphere-Ocean* 21, no. 3, p. 312–325.

Young, K.L. and Woo, M-k.

2000: Hydrological environment of the Hot Weather Creek basin, Ellesmere Island, Nunavut; *in* Environmental Response to Climate Change in the Canadian High Arctic, (ed.) M. Garneau and B.T. Alt; Geological Survey of Canada, Bulletin 529.

Young, K.L., Woo, M-k., and Edlund, S.A.

1997: Influence of local topography, soil and vegetation on microclimate and hydrology at a High Arctic site, Ellesmere Island, Canada; *Arctic and Alpine Research*, v. 29, no. 3, p. 270–284.

Automatic weather station results from Fosheim Peninsula, Ellesmere Island, Nunavut

B.T. Alt¹, C.L. Labine², D.E. Atkinson³, A.N. Headley⁴, and P.M. Wolfe⁵

Alt, B.T., Labine, C.L., Atkinson, D.E., Headley, A.N., and Wolfe, P.M., 2000: Automatic weather station results from Fosheim Peninsula, Ellesmere Island, Nunavut; in Environmental Response to Climate Change in the Canadian High Arctic, (ed.) M. Garneau and B.T. Alt; Geological Survey of Canada, Bulletin 529, p. 37–97.

Abstract: Meteorological data collected over six years (June 1988–March 1994) at the Hot Weather Creek automatic weather station on Fosheim Peninsula are presented. Preliminary results are discussed. Metadata and a list of data and value-added data are also provided. Conditions at this inland site and at three stations in the Sawtooth Range are compared with those at the permanent weather station at Eureka, on the coast of Slidre Fiord.

July mean monthly temperatures average 3°C warmer in the interior than on the coast. These differences depend on climatic and synoptic conditions and are particularly significant in evaluating past and future environmental change. Mean monthly winter temperatures are between 1.5°C and 3.8°C colder in the interior than on the coast. The 1988–1994 Hot Weather Creek autostation records offer the opportunity for promising future environmental-change studies based on the integration of synoptic climate analysis and environmental process results.

Résumé : On présente les données météorologiques qui ont été recueillies sur six ans (de juin 1988 à mars 1994) à la station météorologique automatisée du ruisseau Hot Weather sur la péninsule Fosheim. On discute les résultats préliminaires et on inclut les métadonnées ainsi qu'une liste des fichiers de données et de données à valeur ajoutée. On compare les conditions météorologiques de ce site et de trois stations situées dans la chaîne Sawtooth avec celles de la station météorologique permanente d'Eureka, sur la côte du fjord Slidre.

Les températures mensuelles moyennes pour le mois de juillet sont en moyenne plus élevées de 3 °C à l'intérieur des terres que sur la côte. Ces différences de température dépendent des conditions climatiques et synoptiques et sont particulièrement significatives pour l'évaluation des changements environnementaux passés et à venir. En hiver, les températures mensuelles moyennes sont de 1,5 °C à 3,8 °C plus froides à l'intérieur des terres que sur la côte. Les observations météorologiques recueillies de 1988 à 1994 à la station automatisée du ruisseau Hot Weather nous offrent la possibilité de futures études prometteuses des changements environnementaux basées sur l'intégration de résultats d'analyses synoptiques du climat et de processus environnementaux.

¹ Balanced Environments Associates, 5034 Leitrim Road, Carlsbad Springs, Ontario K0A 1K0

² Campbells Scientific Canada Corp., 149 Street, Edmonton, Alberta T5M 1W7

³ University of Ottawa, Department of Geography, Ottawa, Ontario K1N 6N5

⁴ Canadian Climate Centre, Atmospheric Environment Service, 4905 Dufferin Road, Downsview, Ontario M3B 5T4

⁵ Deceased

INTRODUCTION

In this report, preliminary results from the six-year record at the Hot Weather Creek automatic weather station (autostation) are presented to demonstrate the types of data available and the progress made to date in analyzing these data. Recommendations are made for specific future analyses that would complement the national and international paleoenvironmental work currently underway in the Arctic. Most importantly, this report and Alt et al. (2000) will make these data available to the research community. (The data and metadata used to prepare this bulletin are found in Alt et al. (2000).)

As a result of co-operation between the Geological Survey of Canada and the Atmospheric Environment Service, it was possible to maintain an autostation operation that met Atmospheric Environment Service standards to the extent that this was practical for such a remote region (*see* Alt et al., 1992). Untended, year-round autostations represent an important new method of data collection in the High Arctic. They do, however, face a unique set of problems.

Autostation records are being generated at a rapid rate, providing much valuable data and easing the gaps in spatial data. These data are generated with relative ease, once the initial station has been installed (or serviced). There is a real danger that data will accumulate faster than quality control can be performed and the data documented and prepared for release to the public.

This study, along with Alt et al. (2000), introduces the first quality-controlled, well documented, autostation records from the High Arctic. It represents an important contribution to the scientific community that is now coming to depend on such devices and will become increasingly dependent on them as communication links become less expensive and more reliable. An ongoing effort will be needed by industry and researchers to improve autostation sensors, storage systems, and power sources and to standardize quality control and analysis techniques.

Climate plays a role in a large number of the geological and biological processes discussed in this bulletin. In some cases, such as vegetation and other biological investigations, there is a need for processed, analyzed, climate data with which to compare results spatially and temporally. The analyses presented in this paper will address some of these requirements, but additional studies are needed. In other cases, such as hydrological and mass-movement studies, autostation data have already been incorporated into work presented elsewhere. In all cases, the results should be related to the overall climate picture (once both have been completed) if regional and temporal variability are to be placed in context.

In the following pages, the Hot Weather Creek autostation data will be compared with data from the Atmospheric Environment Service manned weather station at Eureka and, for the summer of 1993, with field data from three stations in the Sawtooth Range that were maintained as part of the glacier

hydrology program discussed in Wolfe (2000). One of the main problems faced by researchers undertaking studies that require their field data be related to standard Atmospheric Environment Service station data is the very long lag time involved in obtaining the Atmospheric Environment Service climate data. The delay is due to the quality control and data archiving needed to maintain a climate database that meets World Meteorological Organization standards. These delays are responsible for the missing Eureka data in the figures presented below.

Other sources of meteorological data such as those discussed by Edlund et al. (1990), Lewkowicz (1990), Alt et al. (1992), Edlund and Woo (1992), Atkinson (1994, 2000), and Young and Woo (2000), including the Agassiz Ice Cap station and the Polar Continental Shelf Project network, have not been included because of time constraints. Obviously, analyses incorporating these data should be undertaken as soon as possible.

Detailed station descriptions and maps emphasizing meteorologically significant features of the surroundings are presented for the stations discussed. The Hot Weather Creek autostation location was chosen specifically to represent the climate of the broad extent of the Fosheim Peninsula interior lowland. Conditions at the Eureka manned surface and upper-air station are representative of coastal conditions within the Eureka intermontane region. The Sawtooth Range stations were established for glacier hydrology studies and represent various aspects of the mountain climate.

HOT WEATHER CREEK AUTOMATIC WEATHER STATION

Regional setting and representativeness

The Hot Weather Creek field camp is located on Fosheim Peninsula, 30 km east of the permanent weather station at Eureka (Fig. 1). The automatic weather station (lat. 79°57'54"N, long. 84°26'33"W, 105 m a.s.l.) is situated on the interfluvium about 20 m from the western edge of the narrow strike valley cut by the small, ephemeral, north-south-oriented Hot Weather Creek (Fig. 2). East of the autostation site, the valley slopes downward over an old slump and several terraces to the creek bed 30 m below. The area within a 20 to 25 km radius of the site is characterized by gently rolling terrain dissected by numerous creeks. The elevation of this lowland is about 100 m and valleys are typically 30 m deep except to the northwest, where a series of ridges rise to more than 150 m. The site was chosen to represent this roughly 1000 km² inland lowland area and contrasts with the coastal-fiord location of the Eureka station. Some minor, local effects due to the site's proximity to the edge of the creek valley and the definite north-south orientation of the valley could alter the wind regime. The cross-section in Figure 3 illustrates the greatest differences in relief in the area. Beyond the 20 km radius (about 1000 km²), mountain barriers about 1000 m high fill the central part of the northwest and south

quadrants and all the southeast quadrant. In the remaining quadrants, the terrain slopes downward to ice-filled fiords (Alt and Maxwell, 2000, Fig. 1) beyond which, at a distance of 60 to 80 km, mountain ranges dominate the terrain.

To the east, beyond the creek valley, the 100 m a.s.l. lowland continues as gently rolling terrain cut by the Slide River and a number of creeks that extends to the foothills of the Sawtooth Range, 25 km to the east and southeast. The Sawtooth Range runs northeast-southwest and rises to 1200 m, 35 km southeast of the site. To the northeast, the terrain rises gently and then falls to Cañon Fiord, 20 km

northeast of the site. Beyond, Agassiz Ice Cap is visible on clear days. North of the site, the rolling terrain rises gently for 20 km to the head of Hot Weather Creek at an elevation of 140 m, then falls off for another 20 km to ice-filled Greely Fiord.

About 5 km northwest of the site, the terrain rises to 200 m at the top of a corrugation in the rolling terrain. These roughly 100 m high undulations extend 20 km to the base of Black Top Ridge (about 770 m), which runs north, filling the northwest quadrant of the horizon. Slide Fiord cuts 25 km eastward into Fosheim Peninsula, reaching to within 15 km of the

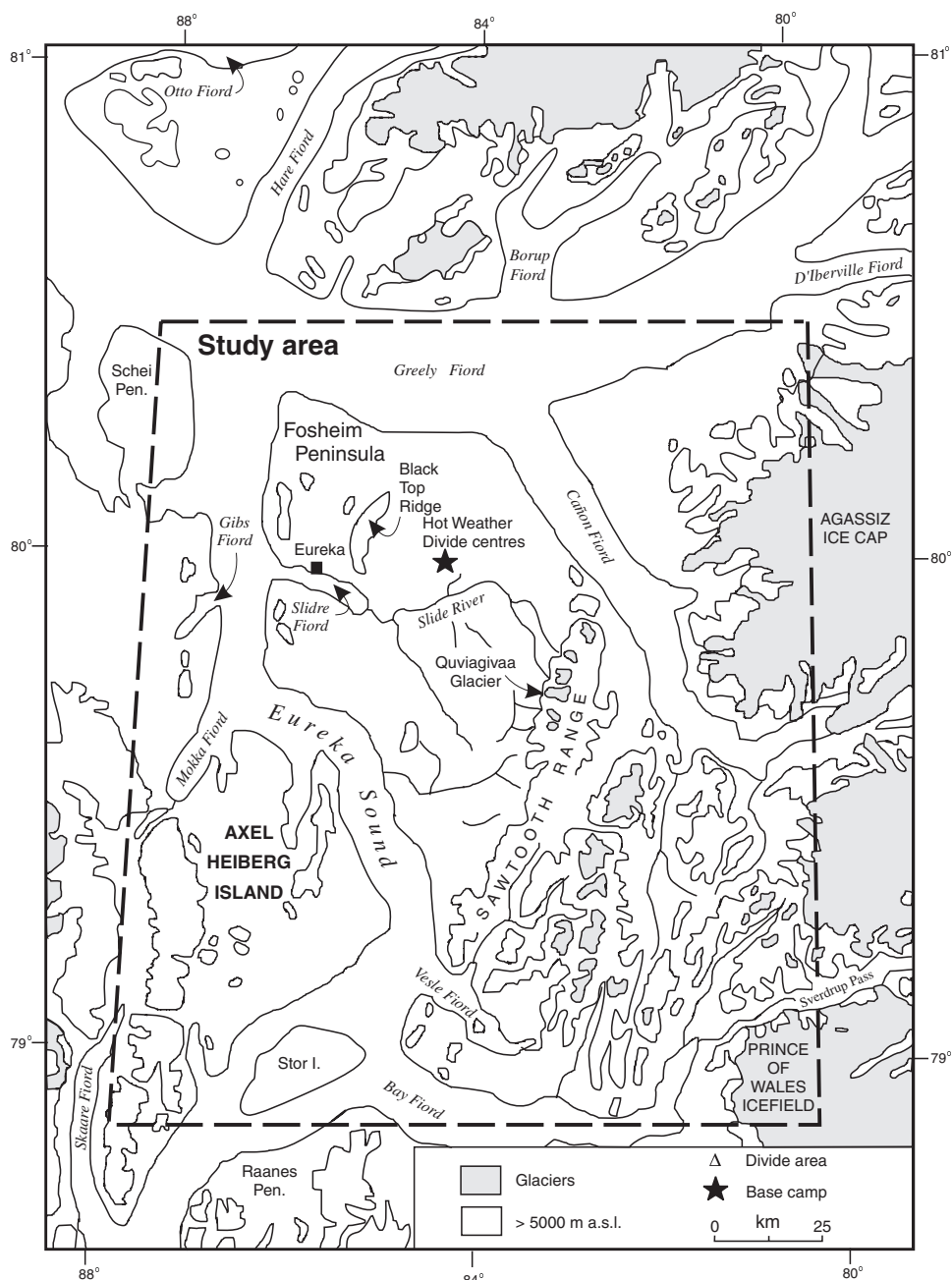


Figure 1. Fosheim Peninsula location map showing Eureka and the Hot Weather Creek and Sawtooth Range study areas.

site south of Black Top Ridge. Eureka, the permanent Atmospheric Environment Service weather station, lies 30 km due west of the site on Slidre Fiord (west of Black Top Ridge).

Less than 5 km south of the site, Hot Weather Creek joins the Slidre River, which drains west into Slidre Fiord. The rolling terrain extends southwestward to Eureka Fiord; 30 km to the south, an unnamed mountain rises to 700 m. To the southeast, the terrain rises to over 300 m some 20 km from the site.

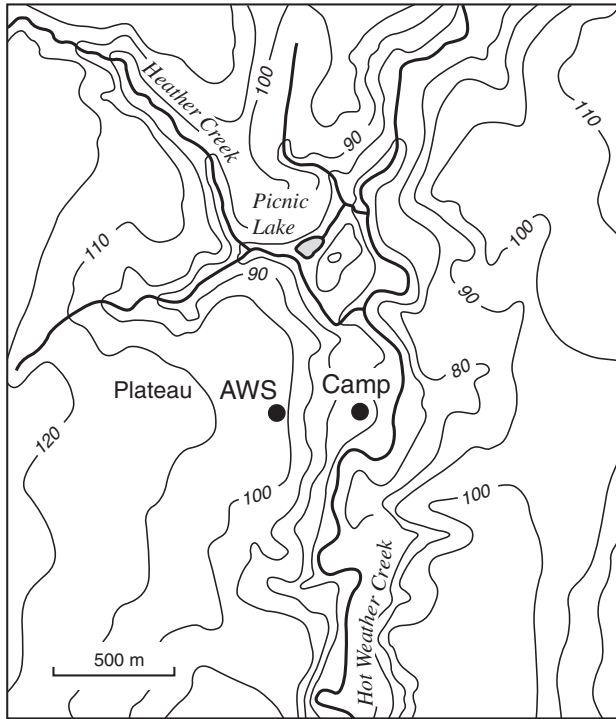


Figure 2. Hot Weather Creek base camp area. AWS = automatic weather station

General site and instrument information

The instrument site was chosen to be representative of vegetation and surface conditions in the broad area of gently rolling terrain (100 m a.s.l.) and not of the valleys or the ridge tops. This terrain is covered by earth hummocks 10 to 100 cm in diameter and by large networks of high-centre, frost-fissure polygons 20 to 30 m in diameter. *Salix-Dryas* hummocky tundra is the most common plant community found on almost all moderately drained, neutral to moderately alkaline soils of the silty lowlands.

The automatic weather station is located near the centre of a large polygon that is covered by typical *Salix-Dryas* broken tundra vegetation.

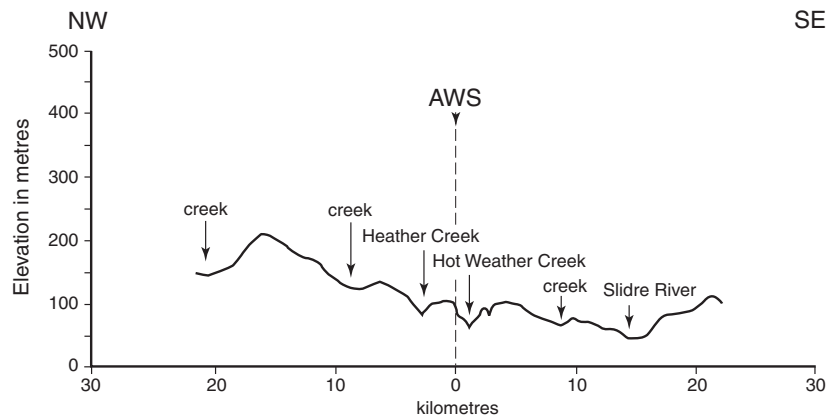
The instruments were originally installed in June 1988 and maintained by the Arctic Adaptation Division of the Atmospheric Environment Service, with field support provided by the Terrain Sciences Division of the Geological Survey of Canada until the summer of 1994. Subsequently, the data were dumped by university personnel when they passed through the area.

The instrumentation and sampling rates do not meet those set out in version 2 of the autostation guidelines (Atmospheric Environment Service, 1992) because of power and storage limitations. The autostation must therefore still be considered a field-camp autostation. It was carefully maintained and serviced every spring from 1988 to 1994; any sensors that had been damaged or had malfunctioned during the winter were replaced. In addition, each season, the wind speed and direction sensors and the pyranometer(s) were replaced so that the sensors could be calibrated annually.

Details of the sensor types and the condition of the overall station and sensors at the time of servicing are provided in Appendix A for each year of the record. The Hot Weather Creek autostation record for June 1988 to March 1994 forms the basis for the discussions in this report.

Figure 3.

Cross-section through the Hot Weather Creek automatic weather station (AWS) site.



EUREKA METEOROLOGICAL STATION

The following description of the Atmospheric Environment Service's Eureka meteorological station (lat. 80°00'N, long. 85°56'W, 10 m a.s.l.; Fig. 4) appeared in the first compilations of data from the High Arctic weather stations, then called 'Joint Arctic Weather Stations' (Department of Transport, 1961; Maxwell, 1980). The early instrument data and general site conditions from this same reference are included in Appendix A along with details of instruments used during the years of the present study (Atmospheric Environment Service, 1991). Maxwell (1982, Appendix 4) includes a discussion of wind instrumentation and a standardized site description in his extensive climatological study of the Canadian Arctic islands and adjacent waters.

The Eureka weather station, the first of the weather stations jointly operated by Canada and the United States in the Queen Elizabeth Islands, was established on Fosheim Peninsula, western Ellesmere Island, on April 8, 1947. It is situated on the north shore of Slide Fiord, about 6 miles [9.6 km] from its mouth [Fig. 4a]. This fiord, one of the numerous deep indentations on the western Ellesmere coast, runs east-southeastward from Eureka Sound and is about 17 miles long and 2.5 [miles] wide.

The site was selected by representatives of the Canadian and United States weather services who made the initial landing on Easter Sunday, April 7, 1947, and reconnoitred the area on foot. The airlift commenced the following day and by nightfall the first building had been erected by the five-man station team working in temperatures of -40°F. Radio communications were established with Thule that evening. Aircraft and air crews were provided by the U.S. Army Air Force.

The terrain near the station consists of rolling hills, less than 800 feet high, but rises abruptly to 2800 feet at Blacktop [sic] Ridge 7 miles to the northeast (Fig. 4a). Twenty miles to the east on a north to south line lies the Sawtooth Range with peaks rising to 6000 feet. To the south of the fiord the land is rolling, with hills rising to 2000 feet near the entrance from Eureka Sound.

The station proper is located on the beach and an adjacent gravel terrace some fifteen feet higher. The exposure for taking meteorological observations is excellent [Fig. 4b].

As the site is surrounded by a large land area except for the comparatively narrow channels of the Eureka and Nansen sounds and the fiords opening into them, the climate is more continental in character with greater extremes of temperature than at the other Joint Arctic Weather Stations. The mountains of Axel Heiberg and of Ellesmere afford some protection to this part of the island so that fog is less frequent, cloudiness is less persistent and precipitation less than at more exposed locations. Although the station is partly sheltered by neighbouring hills, high winds do occur, mainly from a southeasterly or a westerly direction.

The weather programme [sic] consists of three-hourly surface weather observations, two upper-air rawinsonde and two pibal upper wind observations per day. The U.S. Weather Bureau supplies the instruments and balloons for the upper air program and standard Weather Bureau procedures are followed in making these observations. Surface weather observations are taken with Canadian instruments and Canadian procedures are followed.

The Canadian Government is now solely responsible for the station. Eureka is currently the site of a state-of-the-art ozone-monitoring facility and is being considered as a possible site in the Ecological Monitoring and Assessment Network. A number of other scientific programs are operated out of the station. The observing program during the six years

(1988–1993) involved hourly surface observations (except for two missed nighttime hours) and twice-daily upper-air soundings.

DESCRIPTIONS OF STATIONS IN THE SAWTOOTH RANGE STUDY AREA

The regional setting of the Sawtooth Range study area is described in Wolfe (2000). The meteorological data from the glacier, valley, and camp stations are included in Appendix B and are treated in a number of papers by Wolfe (*see* Appendix A in Garneau et al., 2000)

Quviagivaa Glacier meteorological station

The glacier station was located at a middle elevation (875 m a.s.l.) in the centre of the Quviagivaa Glacier (Wolfe, 2000, Fig. 1, 2, 3). The meteorological instruments were placed at 0.5 m (rather than the standard 2 m) as the purpose of the observations was to relate air temperature to melt at the surface of the glacier. The sensors were connected to a Campbell Scientific CR21X datalogger and hourly values of air temperature, wind speed and direction, incoming shortwave radiation, and net radiation were recorded. The sensor model and height are listed in Wolfe (2000, Table 2). Average daily values of these data for the period 30 May 1993 to 10 August 1993 are given in Appendix B and in Alt et al. (2000).

Albedo measurements were made at each ablation station (Wolfe, 2000, Fig. 1) every other day using a portable solarimeter mounted on a 75 cm long wooden rod, from which voltage was read using a multimeter. The solarimeter was held level, approximately 60 cm from the user and 150 cm off the ground, pointing towards the sun so as to avoid the shadow of the user. Measurements were always taken in the late morning, between 09:00 h and 12:00 h to avoid possible 'cosine errors' caused by low sun elevations (Dirnhiem and Eaton, 1975). Surface lowering was measured at the ablation stations throughout the summer as described in Wolfe (2000) and the winter snowcover on Quviagivaa Glacier for the 1992–1993 season was measured on 9 and 11 June 1993 (Wolfe, 2000).

Precipitation was measured using Atmospheric Environment Service standard rain gauges at four sites within the Quviagivaa basin: the camp meteorological station (550 m, *see* below), the glacier terminus (590 m), the glacier meteorological station (875 m), and a ridge top between Quviagivaa and Nirukittuq glaciers (1000 m).

Valley meteorological station

The site is situated at approximately 230 m a.s.l. on a plateau slightly inclined towards the west. Approximately 1 km to the west is the deeply dissected river valley of an unnamed river that flows southwestward into Eureka Sound and whose headwaters are in the central southern Sawtooth Range (including the Quviagivaa Glacier catchment). Quviagivaa Creek flows in a narrow valley 0.5 km south of the meteorological station

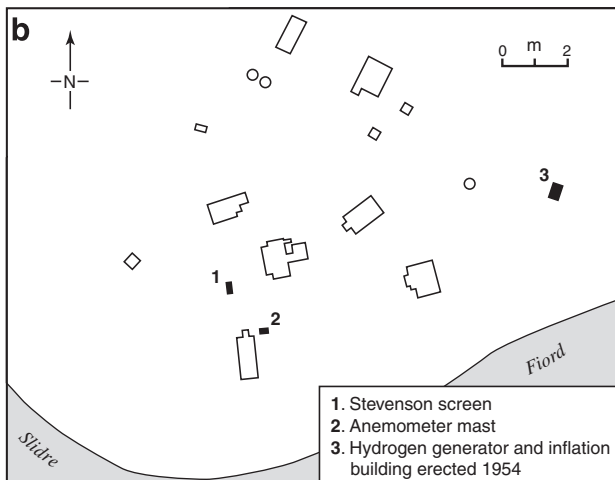
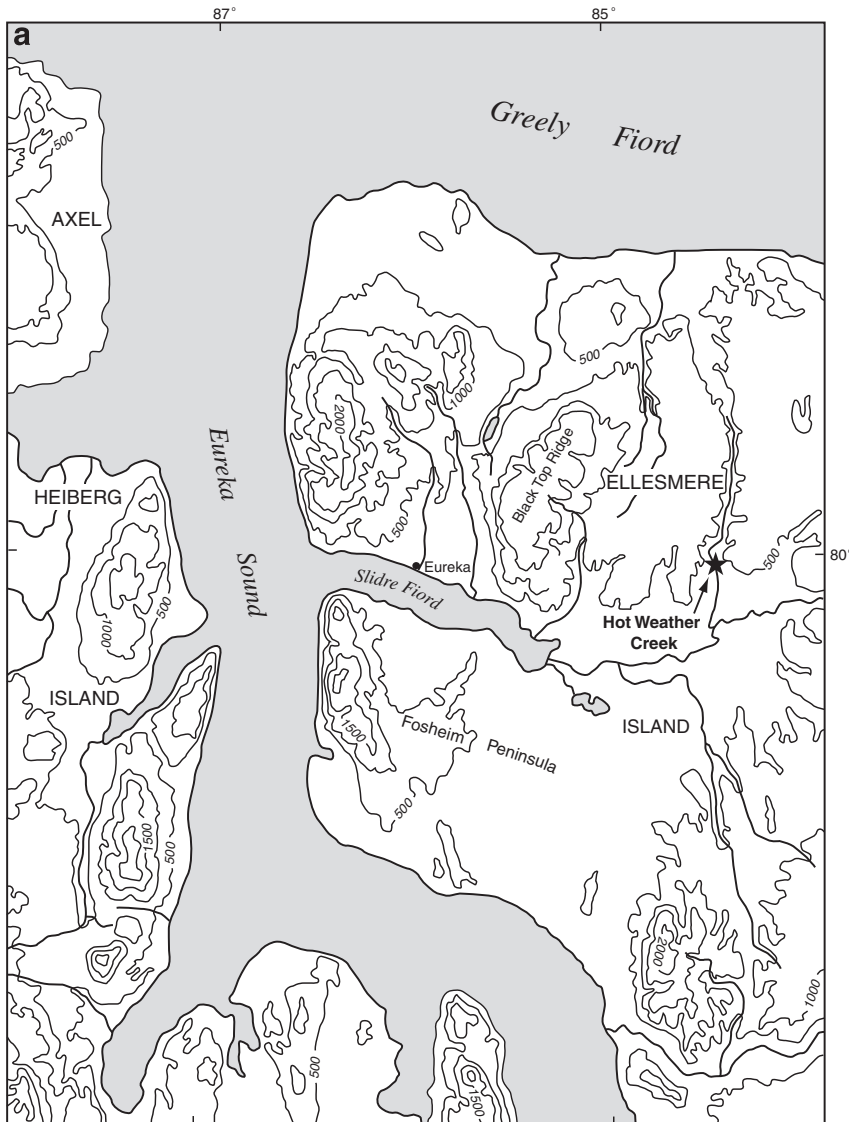


Figure 4.
a) Topography in the vicinity of the Atmospheric Environment Service Eureka permanent weather station. b) Site plan of the Eureka station.

before joining the unnamed river. Another tributary of the aforementioned river occupies a deep, narrow valley 0.5 km to the north. The station should be representative of the mid-level plateaus that stretch from the southwest to the northeast just west of the Sawtooth Range. The sensors and their deployment are shown in Table 1 (Appendix B) and average daily values of the data are given in Table 4 (Appendix B) and in Alt et al. (2000).

Camp meteorological station

The site is located on a small plateau at approximately 550 m a.s.l. A gentle slope rises east-southeastward 1 km to the terminus of Quviagivaa Glacier. To the west-northwest, the elevation gradually drops across a series of valleys and ridges that run parallel to the Sawtooth Range. To the north, the

slope gradually increases for 1 km, then descends into a shallow river valley. The mountains of the northern half of the Sawtooth Range are 5 km to the north and northeast. To the southwest, the sloping terrain resembles the camp meteorological station site and is dissected every kilometre or so by deep stream channels flowing from the mountain peaks and the glaciers of the Sawtooth Range.

Air temperature, wind speed, and wind direction were measured at 2 m using a Davis Instruments Digitar. Maximum and minimum temperatures and wind speeds were recorded every twelve hours. Observations of air temperature, wind speed and direction, cloud height, cloud cover, and cloud type were made daily at 07:00 h and 19:00 h CDT (06:00 h and 18:00 h CST or 12:00 h and 00:00 h UCT) (*see* Table 5 in Appendix B).

Table 1a. Mean monthly values for selected parameters, Hot Weather Creek automatic weather station. Additional parameters are given in the value-added data files in Alt et al. (2000).

YEAR	MONTH	Tmax ¹	Tmin ²	Tmean24 ³	Tmeanxn ⁴	KD ⁵	RH ⁶	SN GD ⁷
1988	7	14.7	8.8	12.2	11.8	23.4	55.5	
1988	8							
1988	9							
1988	10	-11.9	-20.2	-15.7	-16.1	0.4	82.5	102
1988	11	-30.0	-36.8	-33.5	-33.4	0.0	71.2	82
1988	12	-33.1	-41.0	-37.1	-37.1	0.0	68.0	
1989	1	-42.3	-47.4	-45.1	-44.9	0.0	61.0	
1989	2	-34.1	-42.1	-38.5	-38.1	0.0	66.5	99
1989	3	-34.4	-43.5	-39.4	-38.9	0.3	65.4	165
1989	4	-17.7	-30.5	-24.1	-24.1	6.4	73.8	
1989	5	-7.2	-15.9	-11.7	-11.6	21.4	73.9	
1989	6							
1989	7	8.7	4.4	6.6	6.5	15.7	81.3	
1989	8	7.0	2.9	5.0	5.0	9.5	87.4	
1989	9	-4.7	-10.8	-7.4	-7.7	3.9	89.2	119
1989	10	-20.4	-28.8	-24.7	-24.6	0.3	80.5	86
1989	11	-29.5	-37.5	-33.9	-33.5	0.0	72.2	176
1989	12	-34.9	-41.2	-38.1	-38.0	0.0	68.4	180
1990	1	-37.8	-43.6	-40.9	-40.7	0.0	66.3	
1990	2	-39.3	-45.1	-42.4	-42.2	0.0	64.8	144
1990	3	-32.3	-41.1	-36.4	-36.7	3.7	69.3	110
1990	4	-18.4	-28.9	-23.0	-23.6	12.8	76.0	210
1990	5	-2.8	-8.9	-5.4	-5.9	22.5	82.2	90
1990	6							
1990	7	10.8	5.6	8.3	8.2	16.8	64.9	
1990	8	9.2	2.7	6.2	6.0	11.8	72.9	
1990	9	-2.4	-9.4	-5.6	-5.9	3.9	88.0	29
1990	10	-21.7	-29.6	-25.6	-25.7	0.3	79.7	
1990	11	-33.3	-40.0	-36.8	-36.7	0.0	70.1	
1990	12	-34.4	-41.4	-37.9	-37.9	0.0	66.8	
1991	1	-39.4	-45.3	-42.5	-42.3	0.0	64.3	
1991	2	-36.5	-44.2	-40.5	-40.3	0.0	65.3	
1991	3	-29.4	-38.8	-34.6	-34.1	3.8	69.7	18
1991	4	-18.7	-32.8	-26.1	-25.8	13.8	72.1	53
1991	5	-2.1	-11.0	-6.5	-6.6	22.6	79.0	
1991	6	8.2	3.4	5.7	5.8	17.3	76.7	
1991	7	12.7	7.5	10.0	10.1	19.6	65.3	
1991	8	6.7	2.1	4.4	4.4	9.0	84.5	162

METHODS

Data processing and quality control are discussed in detail in Labine et al. (1994, p. 3–6 and Appendix 3). The data documentation files (metadata), quality-controlled data files, and value-added data files are listed in Appendix A for each logger year and the data provided in Alt et al. (2000). In addition to site description and instrumentation information, the metadata include annual files of logger programming, output arrays, SPLIT data-extraction software parameter files, final file formats, and notes on missing data and quality control. The quality-controlled data include separate files for hourly sampled values and daily mean and extreme data generated by the logger for each calendar year within each logger year. The value-added data include daily means and extremes calculated from hourly records, monthly means and extremes based on the hourly, daily, and calculated daily files (where applicable), and a composite record of selected parameters for the whole period (June 1988 to June 1994).

In the following discussion, the seasons are defined as follows:

- melt season (thaw season): the period for which daily temperatures are above freezing, plotted from mid-May to mid-September
- summer and winter: refers roughly to the periods of sunlight and darkness (this is not conventional, but, as will be shown, it is convenient for the presentation of data)
- JJA or summer: as defined for general circulation models and other global change studies (DJF or winter; MAM or spring; and SON or autumn).

The autostation data are identified as HWC or HWC(AWS). The camp data are identified as HWC(CMP). Data from the Eureka weather station are identified as EU or EU(AES). When referring to parameters, the first letter(s) indicate(s) the element and the next, the type of record. For example, ‘Tsamp’ indicates the sampled temperature value, ‘Tmeanxn’, the mean temperature calculated from maximum and minimum temperature, and ‘Tmean24’, the mean temperature obtained by averaging 24 hourly values.

Table 1b.

YEAR	MONTH	Tmax ¹	Tmin ²	Tmean24 ³	Tmeanxn ⁴	KD ⁵	RH ⁶	SN GD ⁷
1991	9	-3.3	-10.4	-6.5	-6.9	4.5	94.9	276
1991	10	-17.2	-25.6	-21.1	-21.4	0.4	84.7	240
1991	11	-25.0	-33.3	-29.2	-29.2	0.0	75.2	240
1991	12	-34.3	-42.2	-38.5	-38.2	0.0	68.6	272
1992	1	-39.8	-45.8	-42.9	-42.8	0.0	65.2	295
1992	2	-37.6	-43.9	-41.0	-40.7	0.0	66.4	361
1992	3	-33.6	-41.4	-37.7	-37.5	0.6	68.7	405
1992	4	-18.3	-34.7	-26.7	-26.5	9.8	75.2	427
1992	5	-7.2	-18.7	-12.9	-12.9	22.3	79.8	271
1992	6	4.9	0.8	2.7	2.7	21.4	76.6	
1992	7	10.2	5.3	7.8	7.7	17.6	72.6	
1992	8	5.4	0.3	2.9	2.8	10.0	86.5	
1992	9	-3.7	-10.3	-6.8	-7.0	3.7	91.0	35
1992	10	-16.5	-25.3	-20.4	-20.9	0.3	82.7	20
1992	11	-29.8	-37.9	-34.1	-33.8	0.0	71.4	25
1992	12	-30.0	-38.5	-34.3	-34.3	0.0	70.8	37
1993	1	-34.7	-42.2	-38.4	-38.4	0.0	67.0	67
1993	2	-32.3	-41.1	-37.0	-36.7	0.1	66.2	25
1993	3	-34.7	-42.3	-38.3	-38.5	3.2	65.7	68
1993	4	-18.5	-30.6	-25.0	-24.6	15.6	71.9	96
1993	5	-3.9	-13.0	-8.5	-8.5	24.7	79.5	
1993	6	8.8	4.3	6.7	6.6	23.0	62.7	
1993	7	14.2	8.8	11.7	11.5	20.3	64.6	
1993	8	6.4	0.6	3.9	3.5	10.3	78.6	
1993	9	-4.9	-12.3	-8.1	-8.6	5.1	89.7	53
1993	10	-15.4	-22.9	-18.8	-19.1	0.5	84.2	37
1993	11	-32.3	-39.4	-35.9	-35.8	0.0	69.2	13
1993	12	-33.7	-40.3	-37.2	-37.0	0.0	68.0	25
1994	1	-29.5	-38.3	-34.1	-33.9	0.0	65.1	16
1994	2	-34.9	-42.0	-38.9	-38.4	0.1	64.3	68
1994	3	-34.9	-43.8	-39.0	-39.4	3.4	63.8	93
1994	4	-20.3	-33.3	-26.7	-26.8	13.7	70.5	146
1994	5	-2.0	-10.7	-6.5	-6.3	22.2	79.1	95

¹Tmax = maximum temperature
²Tmin = minimum temperature
³Tmean24 = mean temperature obtained by averaging 24 hourly values
⁴Tmeanxn = mean temperature calculated from maximum and minimum temperatures
⁵KD = incoming solar radiation
⁶RH = relative humidity
⁷SN GD = snow on the ground

Table 2. a) Mean monthly values for selected parameters, Eureka meteorological station. Additional parameters are given in the value-added data files in Alt et al. (2000).

YEAR	MONTH	Tmax ¹	Tmin ²	Tmeanxn ³	Rain	Snow	Precipitation	SN GD ⁴	KD ⁵
1988	4	-17.5	-25.4	-21.5	0.0	7.7	4.8	13.8	8.4
1988	5	-4.1	-9.9	-7.0	0.0	0.5	0.5	6.4	24.2
1988	6	4.3	-0.2	2.1	3.8	1.8	5.6	0.1	25.3
1988	7	10.6	3.8	7.3	0.2	0.0	0.2	0.0	28.1
1988	8	6.2	1.4	3.8	0.6	6.2	6.6	0.5	14.1
1988	9	-3.6	-8.9	-6.3	0.0	10.0	9.0	1.5	4.0
1988	10	-12.1	-18.9	-15.5	0.0	17.9	13.7	2.2	0.4
1988	11	-29.0	-35.3	-32.2	0.0	7.7	6.9	4.2	0.0
1988	12	-30.6	-38.0	-34.4	0.0	3.5	3.5	9.7	0.0
1989	1	-39.9	-45.1	-42.5	0.0	3.7	3.7	11.6	0.0
1989	2	-32.3	-40.8	-36.6	0.0	14.6	14.6	16.7	0.1
1989	3	-34.8	-42.3	-38.6	0.0	3.6	3.6	20.8	3.4
1989	4	-22.3	-30.1	-26.2	0.0	3.2	3.2	20.2	13.6
1989	5	-10.5	-16.5	-13.5	0.0	2.1	2.1	17.6	29.5
1989	6	4.2	0.1	2.2	6.0	7.2	12.9	0.3	25.1
1989	7	6.6	1.6	4.1	36.0	5.1	40.5	0.0	19.9
1989	8	5.1	1.2	3.2	16.9	1.1	17.7	0.0	11.0
1989	9	-5.4	-10.6	-8.0	0.1	14.7	11.2	2.2	4.5
1989	10	-19.9	-27.6	-23.8	0.0	13.6	9.8	10.8	0.4
1989	11	-27.1	-36.1	-31.6	0.0	20.6	14.2	12.5	0.0
1989	12	-32.7	-40.3	-36.5	0.0	3.5	3.2	20.2	0.0
1990	1	-36.1	-43.1	-39.6	0.0	3.8	2.9	18.7	0.0
1990	2	-37.3	-44.3	-40.8	0.0	3.4	2.8	16.9	0.1
1990	3	-31.3	-39.4	-35.4	0.0	3.6	3.4	14.5	2.4
1990	4	-19.7	-28.3	-24.0	0.0	22.8	19.2	20.0	11.1
1990	5	-4.0	-10.4	-7.2	0.0	5.5	4.7	23.0	22.8
1990	6	15.7	-5.7	4.5		3.2	2.4	0.0	28.2
1990	7	8.6	2.4	5.5	8.3	0.1	8.4	0.0	18.5
1990	8	6.7	1.2	4.0	1.5	6.4	6.9	0.1	11.6
1990	9	-3.3	-8.3	-5.8	0.0	6.4	6.4	1.5	3.9
1990	10	-20.4	-27.1	-23.8	0.0	10.9	10.7	5.8	0.5
1990	11	-31.9	-37.9	-34.9	0.0	3.7	3.7	9.1	0.0
1990	12	-31.6	-38.9	-35.3	0.0	3.2	2.9	7.5	0.0
1991	1	-37.0	-43.1	-40.1	0.0	2.8	2.8	5.3	0.0
1991	2	-34.2	-42.2	-38.3	0.0	3.3	3.3	6.2	0.0
1991	3	-31.2	-37.5	-34.3	0.0	2.2	2.2	7.7	2.3
1991	4	-21.7	-29.6	-25.7	0.0	2.8	2.4	12.6	11.8

All times are given in Central Standard Time (CST), which has been taken as the standard local time for all High Arctic autostations (*see* Alt et al., 1992). The Eureka observations, which were taken in Eastern Standard Time, have been adjusted to CST.

MONTHLY MEANS

Monthly mean values (particularly air temperature) are used extensively in validating and presenting general circulation models, in calculating paleoenvironmental transfer functions, and in relating climate and climate change to geophysical and biological variations and distribution. For this reason, the conditions at the Hot Weather Creek autostation, representing the Fosheim Peninsula interior lowland, and at the Eureka station, representing coastal conditions within the Eureka intermontane region, will first be discussed on the basis of monthly mean values (Tables 1, 2). It must be remembered, however, that an understanding of the trends and variability in monthly mean values is only possible after detailed

analysis of the hourly and daily values from which these are derived. These hourly and daily values must, in turn, be examined in the context of the circulation or synoptic weather conditions from which they are produced before the mechanisms controlling climate change can be understood.

Only after the data have been through the initial quality-control process and subsequently plotted and analyzed in comparison with other stations and parameters to discover inconsistencies can mean monthly values be calculated and released with confidence. Thus, the monthly means should be the final product of a complete analysis of the hourly, daily, and calculated daily data. It is, therefore, possible that further analysis of the data will result in minor amendments to mean values. If more than five days are missing or if three consecutive days are missing, the monthly means have been discarded, following the 'three five'-rule (Atmospheric Environment Service, 1994). The missing observations in the Hot Weather Creek autostation record are listed as part of the Hot Weather Creek camp [HWC(CMP)] documentation in Appendix A. The gaps in the June records are due to station servicing and instrumentation replacement. In the case of

Table 2b.

YEAR	MONTH	Tmax ¹	Tmin ²	Tmeanxn ³	Rain	Snow	Precipitation	SN GD ⁴	KD ⁵
1991	5	-4.5	-10.5	-7.5	0.0	0.9	0.9	10.6	23.0
1991	6	5.2	1.0	3.1	9.4	7.5	16.5	0.0	19.5
1991	7	16.1	0.1	6.3		0.2	12.4	0.0	20.1
1991	8	5.0	1.1	3.1	21.2	5.8	26.9	0.1	9.0
1991	9	-3.4	-7.8	-5.6	0.0	14.3	13.3	2.0	3.8
1991	10	-16.4	-23.5	-20.0	0.0	9.3	9.3	8.5	0.5
1991	11	-23.3	-30.7	-27.0	0.0	6.8	6.8	14.0	0.0
1991	12	-31.9	-39.1	-35.5	0.0	4.5	4.5	16.2	0.0
1991	1	-37.3	-43.9	-40.6	0.0	3.8	3.8	17.8	
1992	2	-34.3	-42.0	-38.2	0.0	4.7	3.0	18.0	
1992	3	-34.0	-40.4	-37.2	0.0	4.5	4.5	19.4	
1992	4	-26.9	-34.9	-30.9	0.0	1.1	1.1	19.8	
1992	5	-11.5	-17.5	-14.5	0.0	3.3	3.3	15.5	
1992	6	2.9	-1.7	0.6	0.1	5.1	5.1	2.6	
1992	7	8.0	2.2	5.2	18.7	5.5	23.9	0.0	
1992	8	3.4	-0.6	1.4	10.1	7.1	17.0	0.0	
1992	9	-4.7	-9.5	-7.1	0.1	5.4	5.5	0.4	
1992	10	-16.5	-24.1	-20.3	0.0	3.2	3.2	2.7	
1992	11	-28.2	-34.5	-31.4	0.0	5.3	5.3	7.3	
1992	12	-29.8	-36.8	-33.3	0.0	4.2	4.2	8.1	
1993	1	-32.9	-39.5	-36.3	0.0	5.0	5.0	11.9	
1993	2	-29.9	-38.4	-34.2	0.0	1.9	1.9	14.0	
1993	3	-33.0	-40.1	-36.6	0.0	4.7	4.7	14.9	
1993	4	-20.4	-28.8	-24.7	0.0	2.0	2.0	15.8	
1993	5	-8.1	-14.4	-11.3	0.0	6.9	7.1	16.8	
1993	6	6.2	0.1	3.2	10.1	0.1	10.2	2.5	
1993 ⁶	7	16.7	1.5	7.3		0.0	10.5	0.0	
1993 ⁶	8	7.4	-3.0	2.2		7.2	10.7	0.0	
1993	9	-4.4	-9.9	-7.2	0.0	8.8	6.3		

¹Tmax = maximum temperature
²Tmin = minimum temperature
³Tmeanxn = mean temperature calculated from maximum and minimum temperatures
⁴SN GD= snow on the ground
⁵KD = incoming solar radiation
⁶from Wolfe (1994) extracted from station records at Eureka, not available from Atmospheric Environment Service (1994)

August and September 1988, the logger overwrote previously collected data because of insufficient storage space. The large gaps in the wind and radiation records are due to environmental conditions such as riming, icing, and solidifying of the lubricant caused by very cold temperatures during the dark season. During the early years, the snow-depth record was particularly power-dependent and spurious readings often occurred during snow storms or blowing snow.

As would be expected, the continental nature of the Hot Weather Creek site produces higher summer and lower winter monthly mean temperatures than at Eureka (Fig. 5a). As soon as incoming solar radiation becomes negligible (Fig. 5b), usually in October, the difference between the two sites (Fig. 5c) becomes negative. This difference varies somewhat more in summer than in winter. The maximum difference in summer monthly means (4.5°C) occurred in July 1988 and the minimum July difference (2.4°C), in July 1989. It should be noted that the mean July temperature of 5.8°C at Eureka quoted by Edlund et al. (1990), as compared to the value of 4.2°C (Atmospheric Environment Service, 1992), was calculated from data copied by hand from the Eureka operational weather sheets on the way out of the field in

August 1989. The additional discrepancy between the July 1989 mean temperature of 4.1°C (Table 2) obtained from the Atmospheric Environment Service data archived after the initial quality control and the Atmospheric Environment Service (1994) value of 4.2°C used in Table 3 emphasizes the problems associated with the use of data that have not been released officially, a common practice because of time constraints placed on the scientific research community.

Thirty-year normals of mean monthly total incoming solar radiation from Eureka (Fig. 6a) show the expected June maximum. Of the years for which data are available (Fig. 6b), departures from normal were highest in 1988. It should be noted that the Atmospheric Environment Service (1994) monthly CD-ROM data summaries only contain values to 1991, which shows some of the problems inherent in making climatic comparisons between field-station data and Atmospheric Environment Service quality-assured station data. The negative insolation differences between Hot Weather Creek and Eureka, with Eureka receiving more incoming solar radiation than Hot Weather Creek, for 1988 and 1989 are surprising in light of the measured temperature

Table 3. Hot Weather Creek July monthly mean temperatures calculated using a linear correlation of the six seasons of July means from the Eureka and Hot Weather Creek weather stations.

YEAR	EUREKA	HOT WEATHER CREEK	HOT WEATHER CREEK	HOT WEATHER CREEK	calculatedHWC-observedEU
	Tmeanxn ¹	Calculated Tmeanxn	Observed Tmeanxn	Calculated-Observed	Difference
1947	5.60	8.66			3.06
1948	6.20	9.72			3.52
1949	5.90	9.19			3.29
1950	6.10	9.55			3.45
1951	5.70	8.84			3.14
1952	6.70	10.61			3.91
1953	4.10	6.01			1.91
1954	5.70	8.84			3.14
1955	3.80	5.48			1.68
1956	5.50	8.49			2.99
1957	6.70	10.61			3.91
1958	5.80	9.02			3.22
1959	6.20	9.72			3.52
1960	6.60	10.43			3.83
1961	4.50	6.72			2.22
1962	7.50	12.02			4.52
1963	5.80	9.02			3.22
1964	3.60	5.13			1.53
1965	4.20	6.19			1.99
1966	5.10	7.78			2.68
1967	4.50	6.72			2.22
1968	6.30	9.90			3.60
1969	4.60	6.90			2.30
1970	5.30	8.13			2.83
1971	7.00	11.14			4.14
1972	4.60	6.90			2.30
1973	4.50	6.72			2.22
1974	4.90	7.43			2.53
1975	4.90	7.43			2.53
1976	5.10	7.78			2.68
1977	6.70	10.61			3.91
1978	6.80	10.78			3.98
1979	5.20	7.96			2.76
1980	5.50	8.49			2.99
1981	5.90	9.19			3.29
1982	5.10	7.78			2.68
1983	5.80	9.02			3.22
1984	5.40	8.31			2.91
1985	6.60	10.43			3.83
1986	4.30	6.37			2.07
1987	6.00	9.37			3.37
1988	7.20	11.49	11.80	-0.31	4.29
1989	4.20	6.19	6.50	-0.31	1.99
1990	5.60	8.66	8.20	0.46	3.06
1991	6.30	9.90	10.10	-0.20	3.60
1992	5.16	7.89	7.70	0.19	2.73
1993	7.30	11.67	11.50	0.17	4.37
mean all	5.58	8.62			3.04
mean	5.42	8.35			2.93
1960–1990					
mean	5.96	9.30	9.30	0.00	3.34
1988–1993					
mean	6.22	9.75			3.54
1958–1962					
mean	6.03	9.43			3.40
1947–1951					

¹Tmeanxn = mean temperature calculated from maximum and minimum temperatures

solarimeter by the wind instrument was first noted by M-k. Woo (pers. comm., 1989). The method used to correct this problem in the early data and the instrumental solution implemented in spring 1992 are discussed in Appendix A. The corrections to the data may have been underestimated, particularly for the predominantly cloudy summer of 1989. Further investigations of the radiation measurements are needed, including detailed comparisons with the results of Young and Woo (1995) and other short-term radiation measurements in the area. Problems with High Arctic radiation measurements are well documented (Holmgren, 1971; Dahlgren, 1974; Courtin and Labine, 1977; Maxwell, 1980; Ohmura, 1981; McKay and Morris, 1985; Alt and Maxwell, 1990).

The diurnal temperature range (Fig. 7a) for Hot Weather Creek shows a distinct peak each April with a secondary maximum in October in some years. These maxima coincide with the periods of transition between 24-hour darkness and 24-hour daylight. Diurnal-range values are lower at Eureka than at Hot Weather Creek and the spring and autumn maxima are less extreme at the coastal station (Fig. 7b). There is considerably more year-to-year variation in the extreme maximum than in the extreme minimum temperatures.

The effect on winter ground temperatures (Fig. 8a) of snow depth (Fig. 8b) is well illustrated by the warm winter means in 1991–1992, which coincide with the highest recorded winter snow cover at Hot Weather Creek. On the other hand, winter snow cover at Eureka for that year was

Figure 5.

a) Hot Weather Creek mean air temperature T_{meanxn} (mean temperature calculated from maximum and minimum temperatures) except for 1988–1989 logger year when T_{mean24} (mean temperature obtained by averaging 24 hourly values) is used (heavy line and asterisk for July 1988) and Eureka mean air temperature T_{meanxn} (fine line); b) Hot Weather Creek monthly mean incoming solar radiation (heavy line and horizontal line for July 1988) and reflected solar radiation (fine line); c) Hot Weather Creek-Eureka temperature difference (bars) and missing months (small vertical lines near x-axis). KD = incoming solar radiation

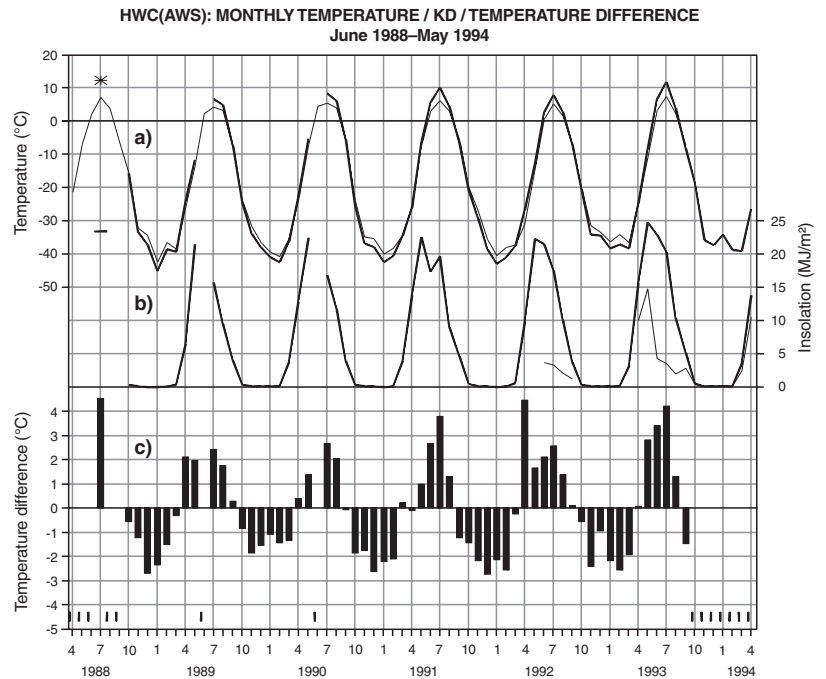
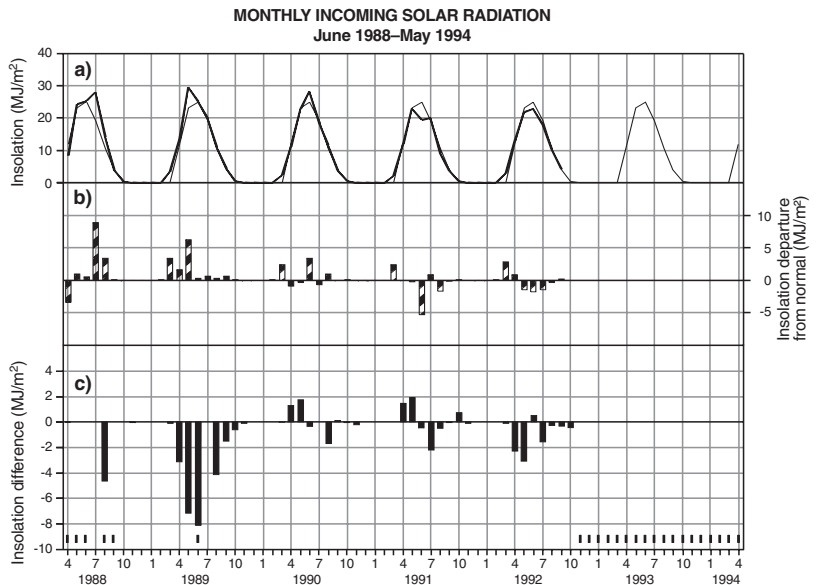


Figure 6.

Monthly means of daily total incoming solar radiation (insolation): a) monthly means (heavy line) and 30-year normal (fine line); b) departure from normal (striped bars); c) Hot Weather Creek-Eureka difference in incoming solar radiation (solid bars).



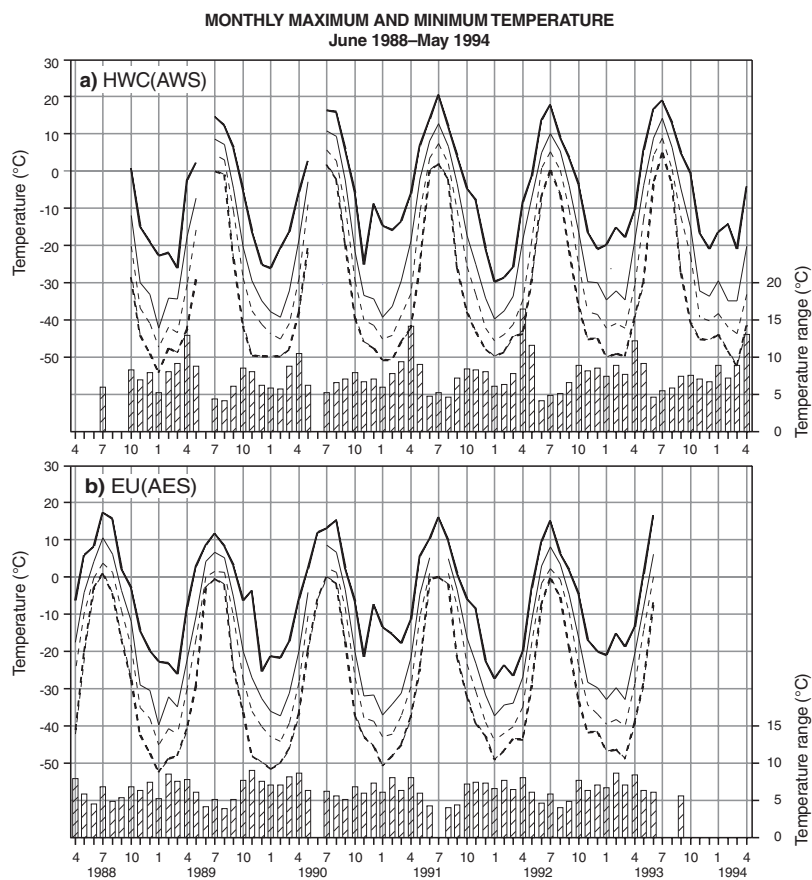
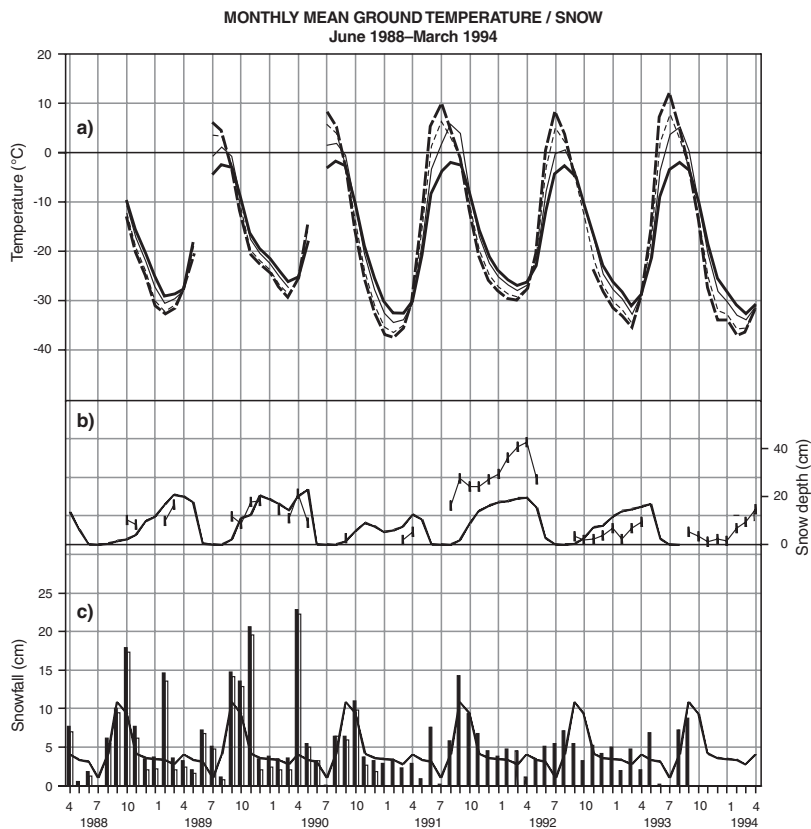


Figure 7.

Monthly extreme maximum temperature (heavy solid line), mean maximum temperature (fine solid line), mean minimum temperature (fine dashed line), and extreme minimum temperature (heavy dashed line) for **a)** the Hot Weather Creek automatic weather station [HWC(AWS)] and **b)** the Eureka permanent weather station [EU(AES)].

Figure 8.

a) Hot Weather Creek monthly mean temperatures in the ground at 0.1 m (heavy dashed line), 0.2 m (fine dashed line), 0.5 m (fine solid line), and 1.0 m (heavy solid line); **b)** snow depth at the end of the month at Hot Weather Creek (vertical lines) and Eureka (solid line); and **c)** snowfall at Eureka calculated from the addition of daily snowfall values using 0.3 mm for trace (solid bars) and from Atmospheric Environment Service (1994) data where a trace is added as 0.0 mm (empty bars) with 30-year normals shown as a solid line.



similar to that of other years in the record. Although there is some concern for the accuracy of the Hot Weather Creek snow-depth data (*see* below), it should be noted that such large intersite variations showed that constructing ground-temperature records for interior sites from Eureka snow depths (as in ground-ice models) would produce erroneous results. The timing of the winter snow accumulation is also critical to ground-ice studies.

The Eureka total monthly precipitation is given in Table 2. Monthly rain, snow, and precipitation totals are often represented as a percentage of normal for modelling studies (Young and Woo, 2000). In the plots, the actual values are shown with the normal curve superimposed (Fig. 8, 9a, b) in order to allow comparison with the snow-depth record from Hot Weather Creek and to illustrate the effect of frequent trace values on the totals. The result of assigning a 0.03 mm value to trace records (Goodison, 1981) rather than ignoring their contribution is shown in the calculated Eureka monthly snowfall (Fig. 8c) and total precipitation records (Fig. 9a) for Eureka. The contribution of trace values is greatest in mid-winter when snowfall is low because of low temperatures. This and other problems of obtaining accurate precipitation values in the High Arctic have been treated at length in the literature (Koerner, 1979; Goodison, 1981; Woo et al., 1983; Metcalf et al., 1994) and still require further field studies and instrumentation development. The summer of 1989 stands out in the total precipitation and rainfall records (Fig. 9) as a very wet summer. Significant amounts of snow were recorded at Eureka in the summers of 1989 and 1992.

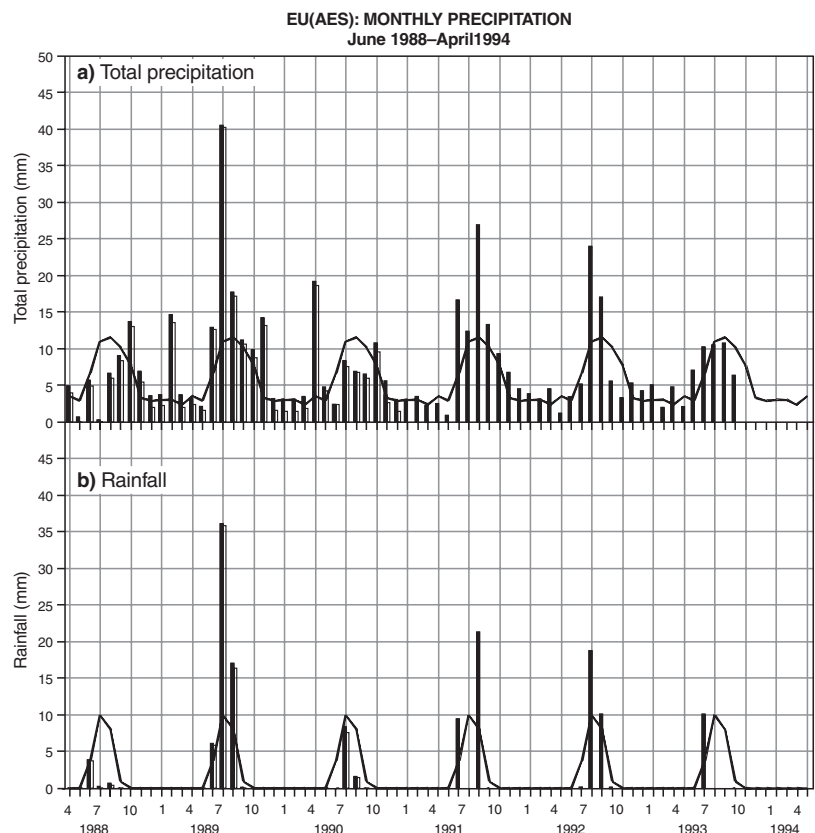
Detailed summer rainfall records for the summers of 1989–1992 taken at Hot Weather Creek by Young are discussed in connection with the hydrological regime (Young et al., 1995; Young and Woo, 2000). The records from the tipping-bucket rain gauge installed in 1992 are not discussed here as they are part of the hydrology program.

Monthly values for wind speed and direction are not included in this report as they require further processing (Atkinson, 2000). The limited Eureka record (Fig. 10) shows strong seasonal variation in wind speed and direction. Headley (1990) studied the effect of placing the wind-recording instruments at 3 m above the ground (Hot Weather Creek autostation), as opposed to the standard 10 m, by comparing simultaneous records from both heights at the Hot Weather Creek site during the summer of 1989. The results of the study showed that, with some noted exceptions, it would be possible to adjust the wind speeds recorded at 3 m to provide an estimate of the wind at 10 m using a mean variation of wind speed with height based on a simplified form of Hellman’s formula.

A detailed comparison of the Hot Weather Creek 3 m wind data for September 1988–June 1991 with the standard record from Eureka was undertaken (Peters and Headley, 1992) as part of the remote field autostation data assessment program initiated by the Atmospheric Environment Service’s Canadian Climate Centre, Arctic Division. The results from this study are illustrated by the wind roses for the complete study period and for the summer (Fig. 11a, b, c). On the basis of their statistical analyses, Peters and Headley (1992)

Figure 9.

Eureka **a)** total monthly precipitation and **b)** total monthly rainfall, calculated from daily values using 0.3 mm for trace (solid bar) and from Atmospheric Environment Service (1994) data (empty bar) with 30-year normals shown as a solid line.



concluded that the Eureka wind data are not representative of the wind field at Hot Weather Creek and that the Hot Weather Creek data are likely to be more representative of the wind field over most of the interior of Fosheim Peninsula.

A detailed knowledge of the wind regime is a critical aspect of synoptic paleoclimate studies (Alt, 1975, 1985). The Eureka wind roses for September 1988–June 1991 (Fig. 11a, b, c) are similar to the normal plots (Fig. 12) given in Maxwell (1980). On the basis of these preliminary results, the total and summer wind roses for Eureka show northwest- and southeast-sector dominance whereas those for Hot Weather Creek show north-sector and southwest- to south-sector dominance. Young et al. (1995, Fig. 10) show a

definite southwest-sector dominance with a secondary peak in the northeast for the summer of 1989. As shown by Alt (1975), it is possible to characterize the synoptic climate of an area and its interaction with other processes by using dominant-wind-direction sectors. This would be an advantageous approach in the present case where the atmospheric flow is being deflected or modified by different physiographic features at the two stations. The sector approach incorporates the topographical differences by dealing with as few as four broad wind sectors, each of which represents conditions at the individual stations in response to overall atmospheric flow. For instance, the total wind roses for Hot Weather Creek and Eureka suggest that winds from the west through northwest

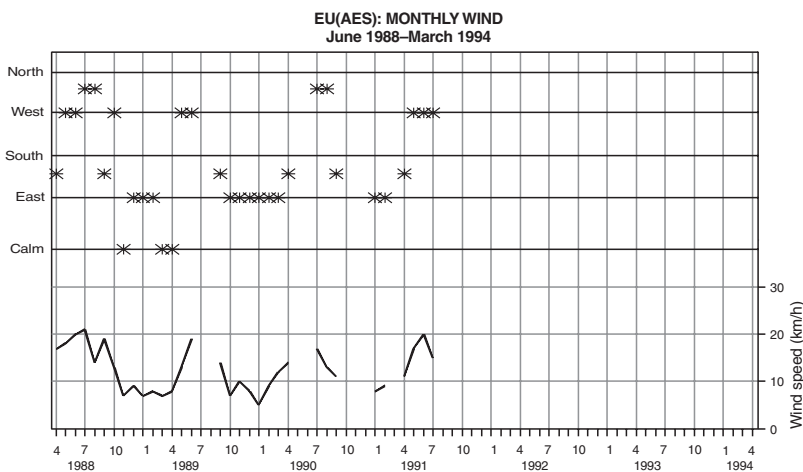


Figure 10.

Eureka monthly prevailing wind direction (eight points) (asterisks) and monthly mean wind speed (solid line).

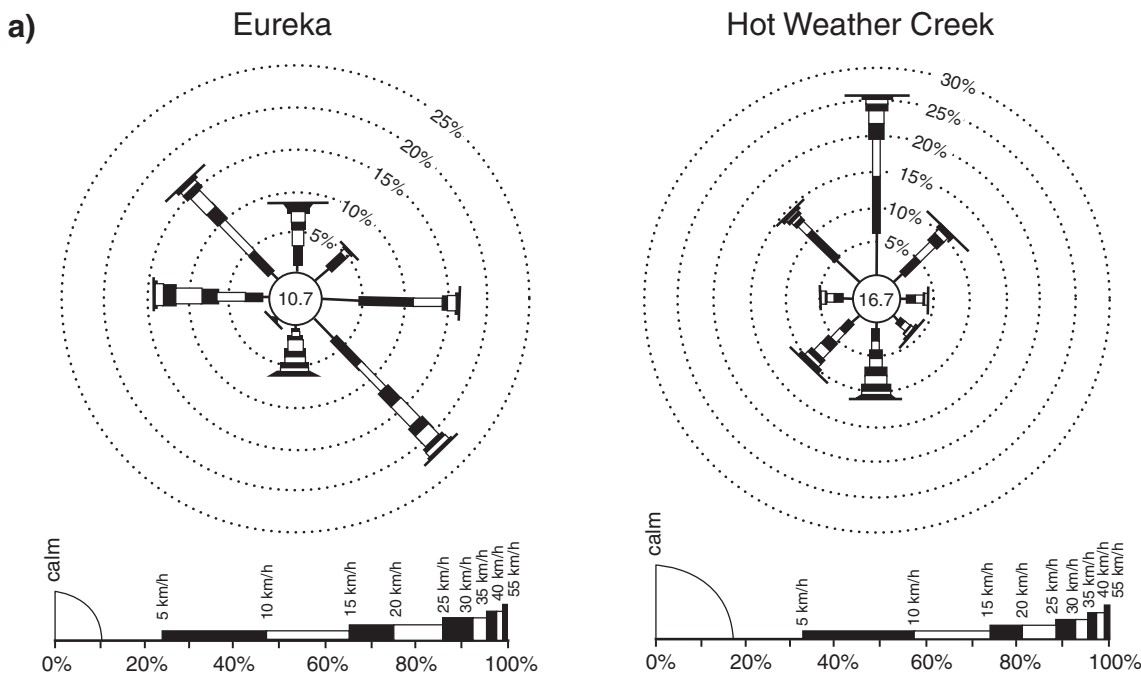


Figure 11. a) Wind roses for Eureka and Hot Weather Creek for September 1988 to June 1991 (after Peters and Headley, 1992). Wind roses for b) Eureka and c) Hot Weather Creek for December–February, March–May, June–August, and September–November for the same years as in a) (after Peters and Headly, 1992).

sector at Eureka are related to winds from the northwest through northeast sector at Hot Weather Creek. The dominant-wind sectors will vary with season.

A detailed study, beginning with the hourly wind record, is needed in order to define the relevant sectors. The preliminary synoptic study outlined in the section 'Discussion, recommendations, and conclusions' would include this type of analysis for July 1988.

TIME SERIES OF DAILY MEANS

The following figures are based on the value-added data in the combined file of selected parameters (Alt et al., 2000). Note that daily values are not available for the logger year 1989–1990. For that year, mean and extreme values were calculated from the 24 hourly values. The maximum and minimum values are therefore not extreme maxima and minima

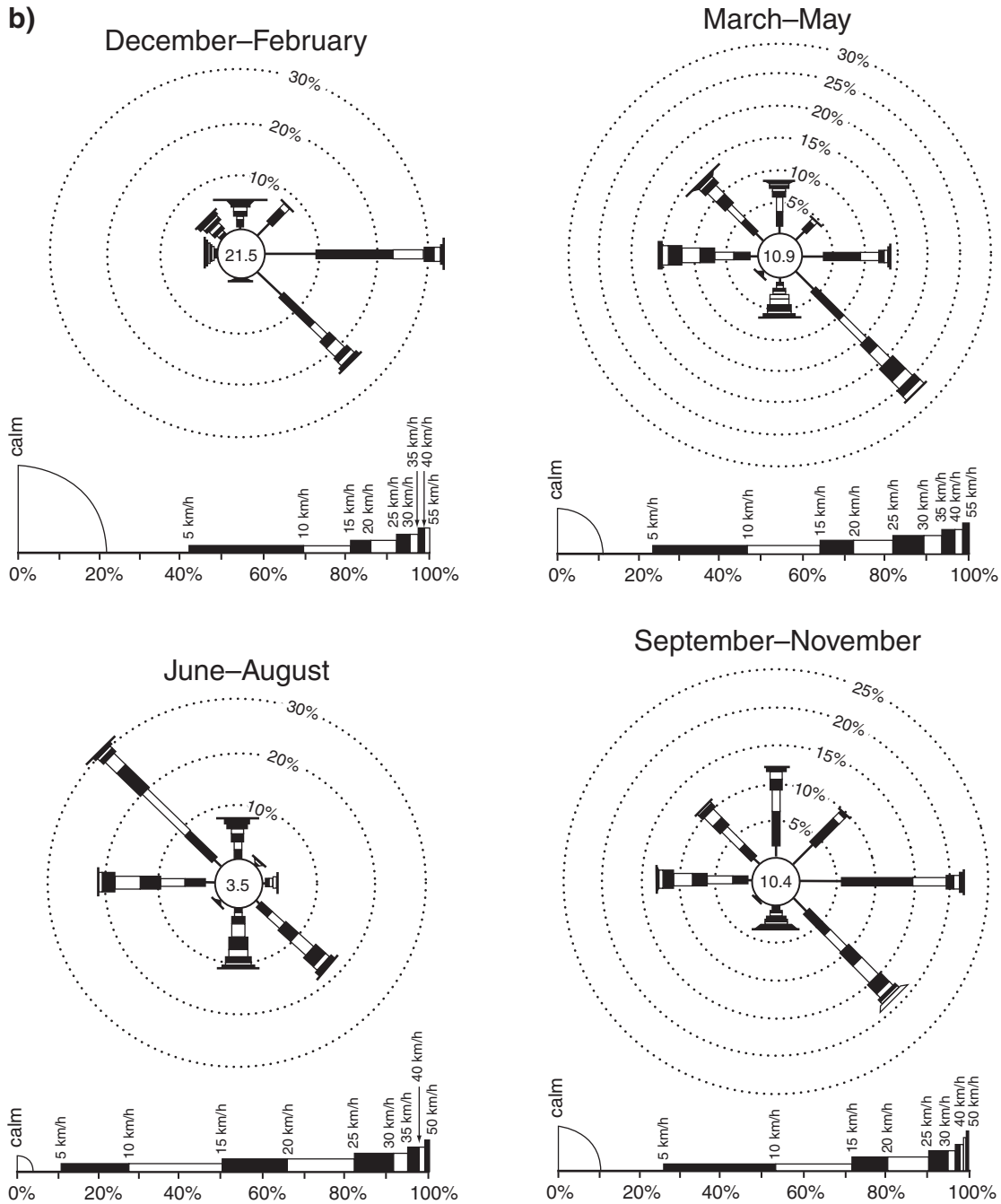


Figure 11b

for the day, but rather the highest and lowest sampled hourly value. The result is lower values of diurnal range for this period than were actually experienced at the station.

The shapes of the daily mean temperature time series for Hot Weather Creek and Eureka are similar, but not identical (Fig. 13a, b). Daily means as high as 18°C are seen in the Hot Weather Creek record, with a significant portion of the mid-summer mean-temperature record above 10°C (except in 1989). Daily means at Eureka barely reach 10°C, even in the warmest summers. Cumulative positive-degree-day plots

magnify the summer differences between Hot Weather Creek and Eureka as first noted by Edlund et al. (1989). Summer conditions are discussed further in the next section.

The most striking features of the Hot Weather Creek and Eureka daily temperature records (Fig. 13a, b) are the rapid rise from and descent into winter and the large, brief intrusions of warm air that occur during the winter. These intrusions are further illustrated (Fig. 14a, b) by the Eureka departures from 30-year smoothed normals (only 1951–1980 normals were available, but the difference from 1961–1990 normals is unimportant at this scale). Summer departures

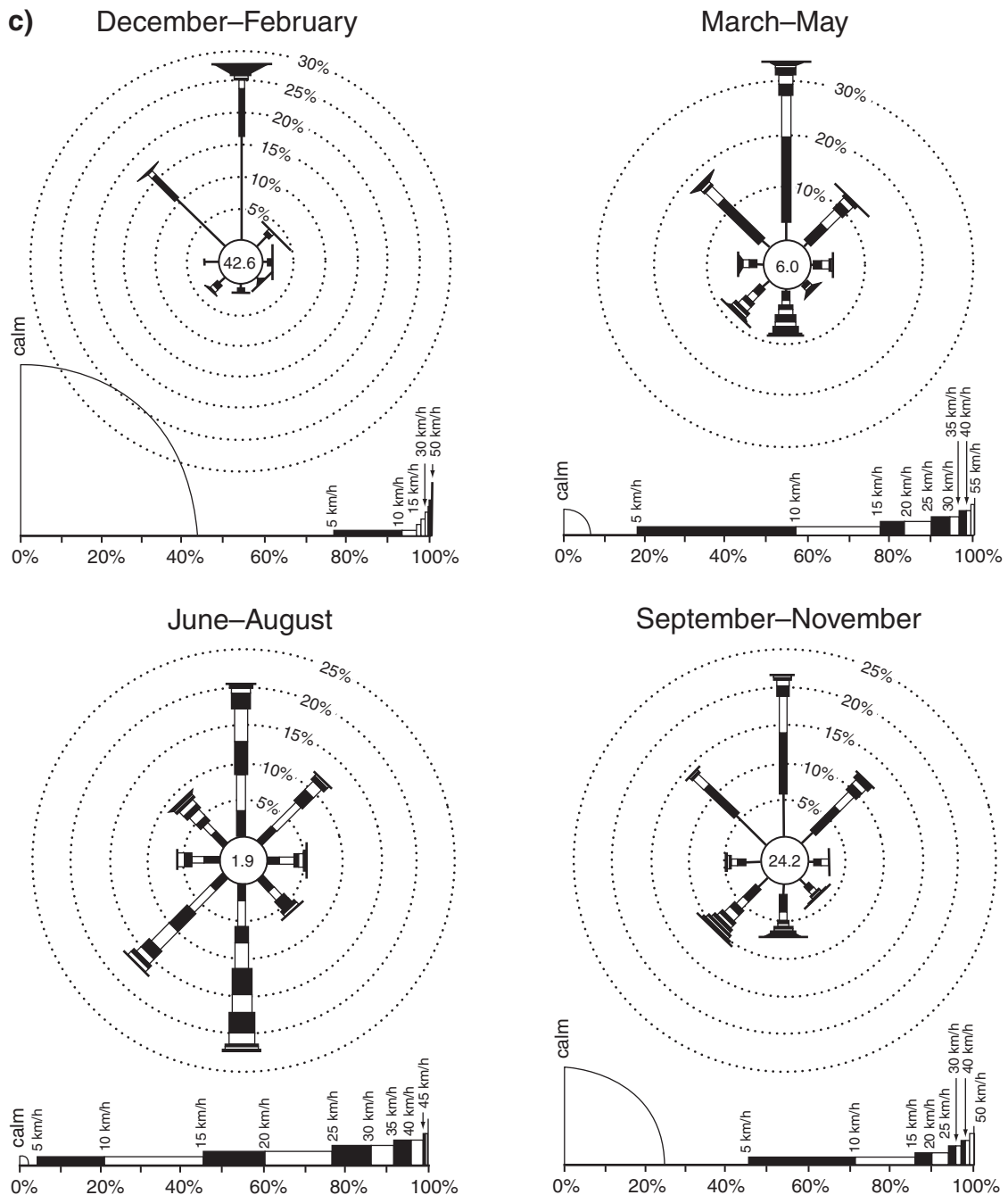


Figure 11c

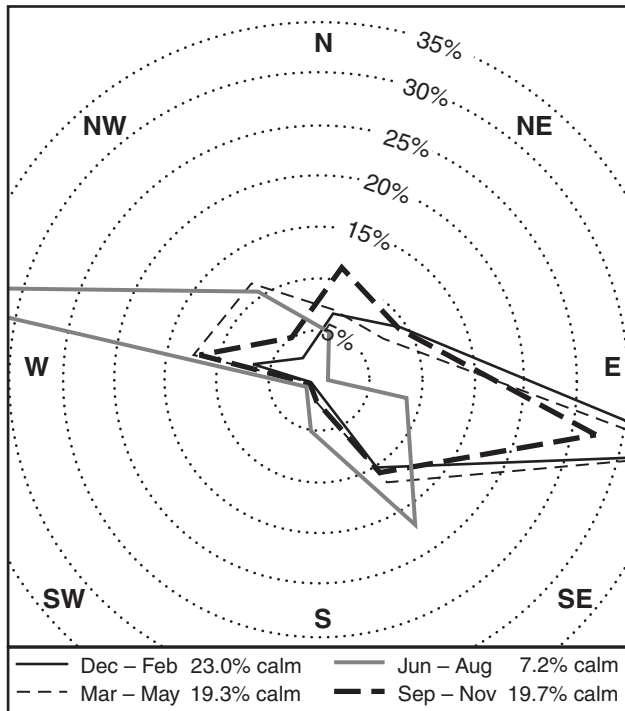


Figure 12. Wind rose for Eureka for June–August 1953–1972 (heavy line) (after Maxwell, 1980).

from normal are not only considerably smaller than winter departures, but they tend to be predominantly in one direction. With the possible exception of winter 1991–1992, winter departures alternate rapidly above and below normal. Winter 1990–1991 shows the strongest winter variability and should be analyzed in detail, which is beyond the scope of this paper.

The daily radiation record for Eureka was not available at the time of writing, but a comparison of the Eureka temperature departures (Fig. 14b) and the Hot Weather Creek radiation record (Fig. 14c) shows that the period of highest variability corresponds to the dark season. This is also the period of maximum surface-based inversions, as noted by Maxwell (1982) and Bradley et al. (1992, 1993). A breakdown of the surface temperature inversion is indicated by these warm screen-level temperatures. Maxwell (1982) states that this breakdown can result from high wind speeds or from cloud cover based at the height of the inversion maximum. Both these conditions would accompany the passage of a storm and might also indicate a change in the dominant air mass.

Plots of the maximum and minimum daily air temperatures for each logger year (Fig. 15) show the reason for the April maximum in monthly diurnal temperature range values (Fig. 7b). During the period when the sun is strong only at midday (i.e. April and October), nighttime temperature

Figure 13.

Mean daily air temperature (fine line) and cumulative melting degree days (heavy line, dashed when estimated) for a) the Hot Weather Creek automatic weather station [HWC (AWS)] and b) the Eureka permanent weather station [EU(AES)] ('m' indicates missing data)

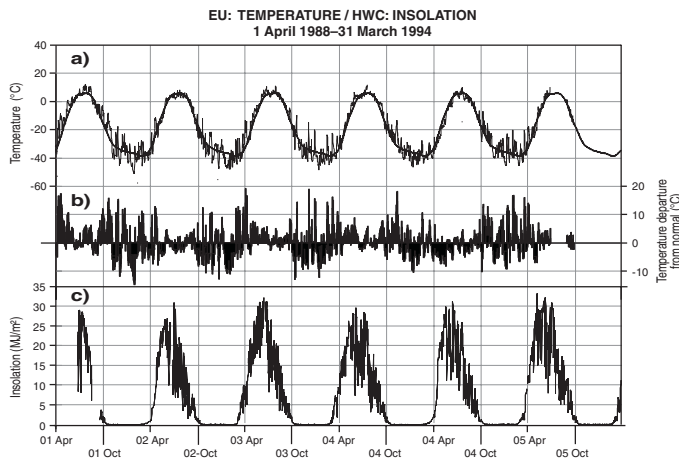
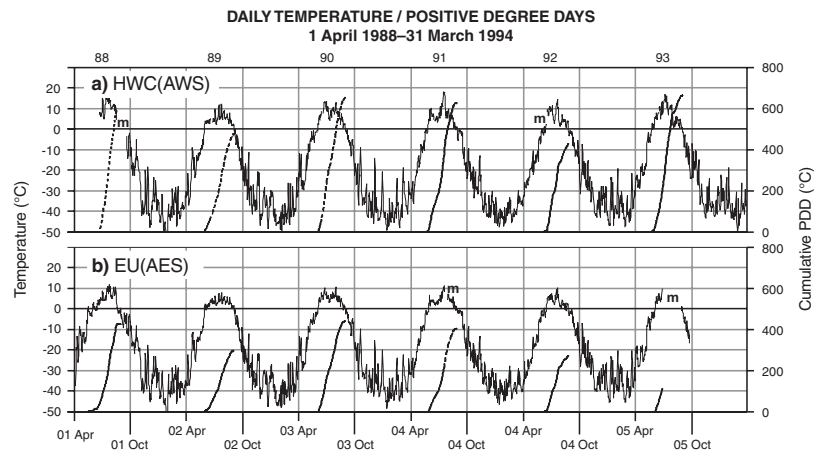


Figure 14.

Mean daily a) Eureka (EU) air temperature (fine line) and normal air temperature (heavy line); b) Eureka departure from normal of air temperature (solid bars); and c) Hot Weather Creek (HWC) incoming solar radiation (insolation).

HWC(AWS): DAILY MAXIMUM AND MINIMUM TEMPERATURES

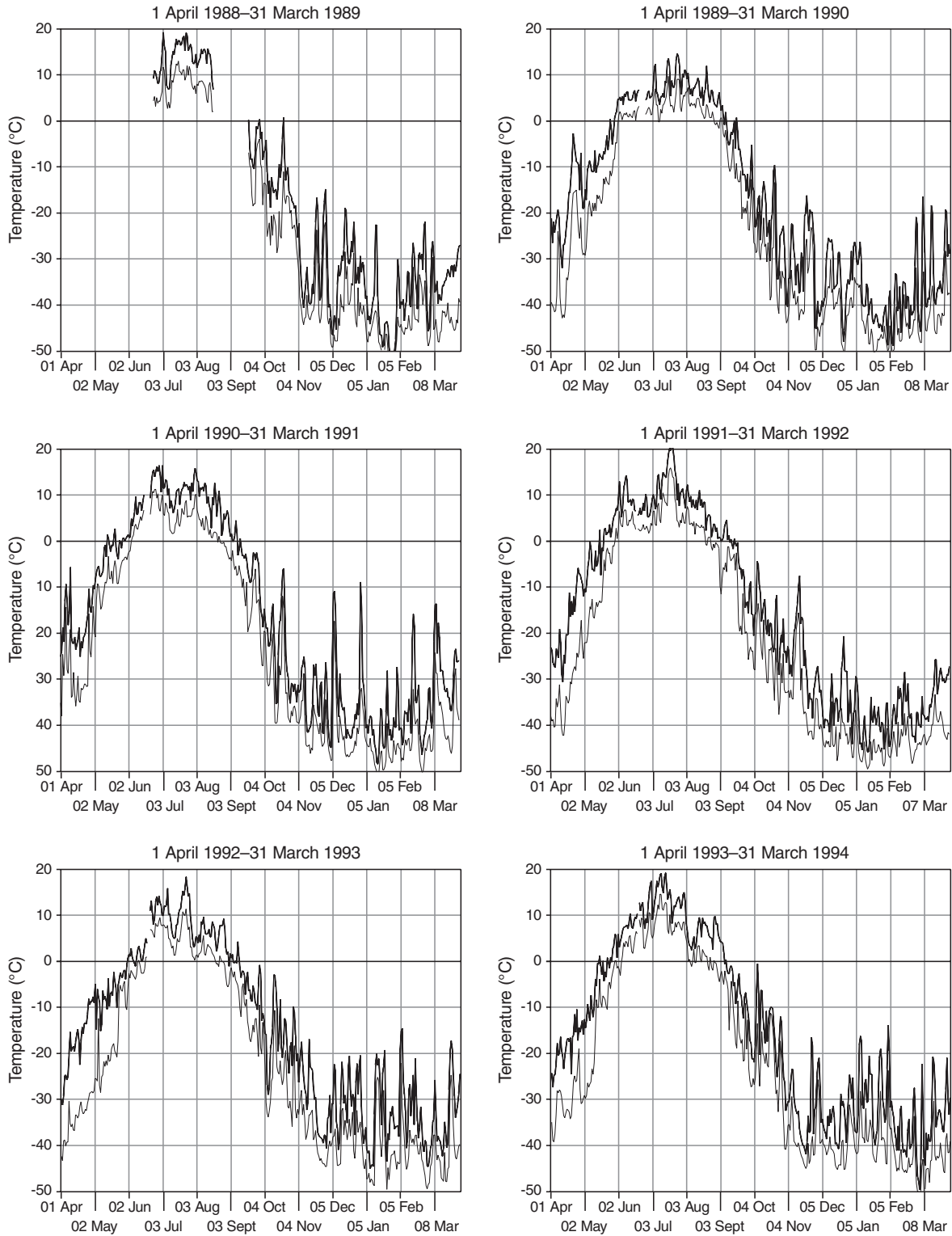


Figure 15. Daily maximum (heavy line) and minimum (fine line) temperatures for years of record at the Hot Weather Creek automatic weather station [HWC(AWS)].

Figure 16.

Daily dark season **a)** maximum, mean, and minimum air temperature and **b)** wind direction and speed at the Hot Weather Creek automatic weather station [HWC(AWS)].

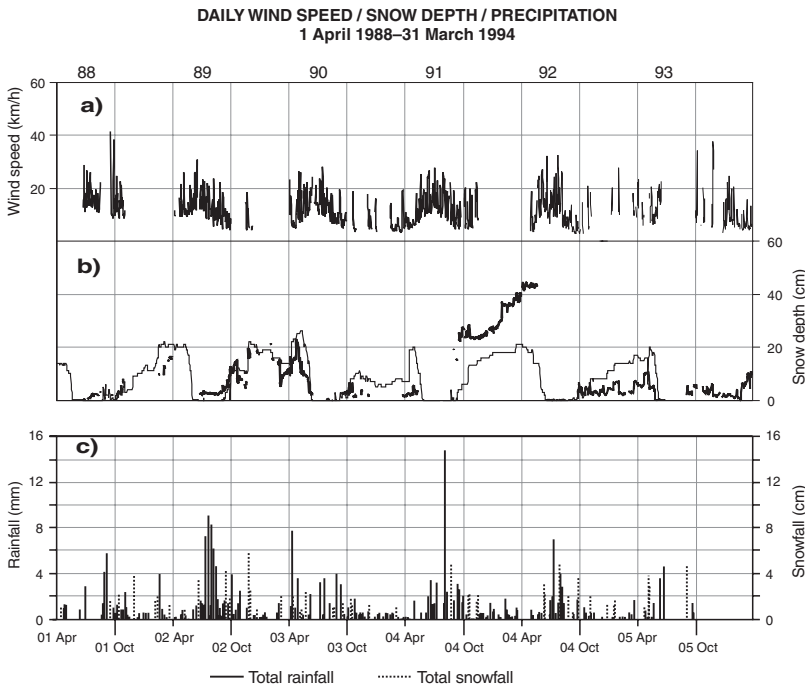
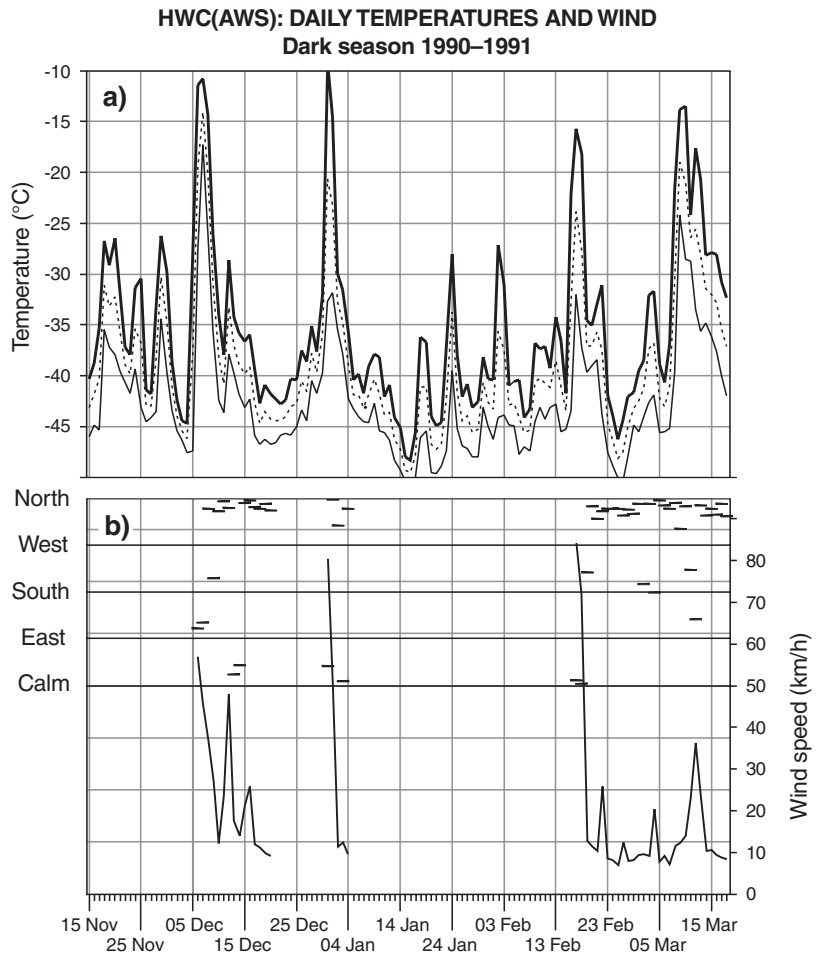


Figure 17.

Daily **a)** Hot Weather Creek mean wind speed, **b)** Hot Weather Creek snow depth (heavy line) and Eureka snow on ground (fine line), and **c)** Eureka rainfall (solid lines) and snowfall (dotted lines).

minima remain low due to long-wave (terrestrial) radiative losses. Brief cloudy sky conditions accompanying storm conditions either prevent these radiative losses, which raises the minimum temperature, as in May 1992, or suppress maximum temperatures by decreasing radiative input or by advection of cold air, as in April 1990. The duration, shape, and intensity of each summer-season temperature regime can also be seen in these plots and are discussed below.

The winter of 1990–1991 stands out again (Fig. 15), with maximum temperatures reaching -10°C several times and temperature fluctuations of as much as 30°C within a few days (*see* Fig. 16). The winter of 1991–1992, on the other hand, was relatively cold from late November until the return of the sun in March. The contrasting ground temperature and snow-cover conditions for these two winters were noted above (Fig. 8).

The winter mean daily wind-speed record (Fig. 17a) has large gaps. Wind data were removed from the record if there was any question as to their validity (*see* Appendix A). The reasons for these instrumental problems are not yet clear (*see* Peters and Headley, 1992, p. 5–6), but what is clear is that at times the anemometer was restarted and thus at least some of the major storm events were recorded. In fact, the dark-season plot for 1990–1991 (Fig. 16) shows that the anemometer restarted at the height of the major temperature peaks and registered maximum winds of 60 to 80 km/h during these periods of high temperatures. A comparison of wind and snow-depth records (Fig. 17a, b) shows that these peak winds can also correspond to abrupt increases (or decreases) in snow depth, suggesting snowfall, drifting, or compaction, and possibly melt.

The winter of 1990–1991 stands out in the Hot Weather Creek wind record (Fig. 17a) and the Eureka ‘snow-on-the-ground’ and snowfall record (Fig. 17b, c), with high wind speeds and low snow cover. The eolian deposition that occurred during this particular winter is discussed in Edlund and Woo (1992):

Significant eolian deposition occurred during winter 1990–91 on western Fosheim Peninsula. Snow-cored barchan dunes coated with sand and gravel developed on the sea ice of Slidre Fiord adjacent to an air strip. Dust was distributed throughout snow layers at many sites and thick blankets of silty clay draped some slopes near [the] Hot Weather Creek base camp. Low regional winter snowfall and the redistribution of snow by strong winds created substantial bare areas which became sources for such deposition. An experiment confirmed that snowmelt could be accelerated by a week by manual dusting of a snow surface. This suggests that dust layers help create the observed zones of early melt. After snowmelt, eolian activity impacts on vegetation by delaying stabilization, by smothering vegetation, or by causing a shift in species dominance.

The importance of such events for the interpretation of marine- and lake-sediment history is also noted.

The ramifications of these periods of high winds, high temperatures, and the breakdown of the surface temperature inversion for the atmospheric transport and deposition of aerosols, contaminants, dust, and pollen in winter snow layers on ice caps (where they become part of the ice-core

record) and on the tundra (where they subsequently melt and are deposited in terrestrial paleoenvironmental records) cannot be ignored. Nor can the question of how these conditions would change with increasing concentrations of greenhouse gases or particulate pollution or from natural global change due to forcing functions, such as solar constant changes or natural changes in the atmospheric transmission coefficient.

These preliminary results show that a detailed synoptic climate study of the contrasting winters of 1990–1991 and 1991–1992 should be undertaken. It should include an evaluation of the frequency of occurrence of such events in the Eureka record and an attempt to identify such seasons in the ice-core and snow-pit records from Agassiz Ice Cap (*see* Bourgeois et al., 2000). The upper-air characteristics of the two contrasting winters should also be investigated along with the Agassiz Ice Cap autostation records.

The most striking feature of the daily snow-depth records (Fig. 17b) is the rapid drop in depth due to spring melt. There is a considerable difference in the pattern of snow-cover buildup among the six years. Buildup is gradual in 1988–1989 and 1992–1993 and reaches maximum winter levels by mid-October in 1989–1990 and 1991–1992. In 1990–1991, however, the snow accumulation is interrupted in midwinter (with the consequences for ground temperature discussed above). The decrease in depth could be a result of drifting or compaction caused by the frequent high winds and temperature peaks that occurred during that winter. It is not until April that normal winter snow depths are reached at Eureka, although the partial Hot Weather Creek record suggests that snow depth on the interior plateau remained low all winter. The Hot Weather Creek snow-depth-sounder record shows many of the same features as the Eureka ruler-measured snow-on-the-ground record, but depths are lower at Hot Weather Creek than at Eureka in some years and higher in others. The contrast between the winters of 1991–1992 and 1992–1993 raises the question of instrumental or programming error at Hot Weather Creek. The snow-depth sensor was upgraded in spring 1992 from the CSMALL to the UDG01. In addition, when the station was serviced in June 1992, it was noted (A. Headley, unpub. rept., 1992) that

...the station had tilted due to settling of the north and southeast legs of the tripod. This settling likely occurred during the spring thaw of this year. The tilt was about 5° from normal to the east-northeast. At the time of arrival at the site, it was still very wet and soft around the station, making it necessary to delay levelling until the ground had dried.

In 1991–1992, as shown above, the warm ground temperatures were consistent with a deep snow cover at Hot Weather Creek, suggesting that the snow-depth record is real. The Eureka daily snowfall records (Fig. 17c) show frequent snowfall events during the autumn of 1991. These could have produced more snow on the ground at Hot Weather Creek than at Eureka because of local drifting or regional snow-distribution characteristics. The very rapid drop in snow depth seen in the partial Hot Weather Creek spring record could be the result of the early warmth of the 1992 season. In 1992–1993, on the other hand, the new sensor gave a

full winter record, but shows almost no increase in snow depth over the winter, although there is a small peak in spring. The 1993–1994 record is similar. These possible discrepancies need more study.

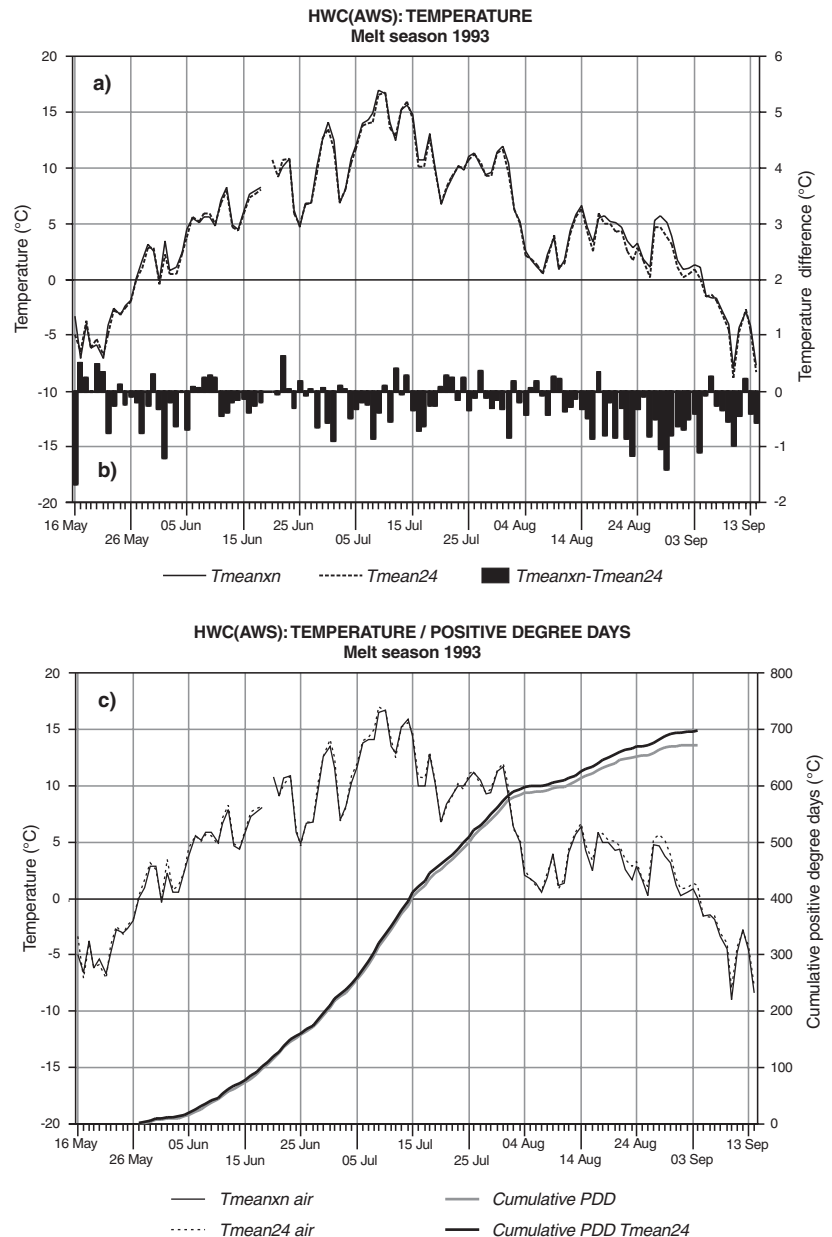
A detailed study, including an examination of the original data file, is necessary. Woo’s snow-course data (Woo et al., 1991) and Young’s results (Young, 1995) must also be incorporated. A comparison of the Hot Weather Creek results with those from the Agassiz Ice Cap autostations would also be useful. Snowfall values should be calculated from the snow-depth data for Hot Weather creek and compared to the Eureka snowfall record (Fig. 8c). These calculations are not straightforward because they must account for drifting and consolidation of the snowpack (see Alt and Bourgeois (1995) and Pomeroy et al. (1997)). The role of sublimation from the spring snowpack during blowing-snow events, as studied by Pomeroy et al. (1997) should also be examined. Strong spring

wind events, such as those seen in May 1992 that were accompanied by strong warming, would provide an opportunity to study these and other factors capable of creating regional-scale snow-distribution differences. Finally, these results should be combined with synoptic weather investigations to determine possible synoptic-scale reasons for the recorded differences. For Hot Weather Creek, once again, a comparative study of the winters of 1990–1991, 1991–1992, and possibly 1992–1993 should be undertaken.

The uncertainties in the snow-depth record illustrate the problems that can be encountered in data from untended, non-standard autostations. They stress the advisability of undertaking a preliminary analysis of all the data, even after it has undergone quality control, before it is released to the public. These questionable snow-depth data have been included in data files in Alt et al. (2000) to allow other researchers to study the apparent inconsistencies.

Figure 18.

a) Hot Weather Creek automatic weather station [HWC(AWS)] 1993 melt season mean daily temperature calculated by standard method T_{meanxn} ($[maximum+minimum] \div 2$) and as an average of 24 hourly values (T_{mean24}); b) difference between these mean values ($T_{meanxn}-T_{mean24}$); and c) daily and cumulative positive degree days calculated from these mean values.



The snow-depth instruments are continuously being improved and provide a new type of precipitation data that may help solve some of the problems associated with measuring precipitation in the Arctic. Interpretation of these records will require considerable caution, experience, and crosschecking.

SUMMER CONDITIONS AND TOTAL POSITIVE DEGREE DAYS

The duration, intensity, and shape of the melt (thaw) season for each year can be seen from plots of maximum and minimum temperatures for each logger year (Fig. 15). Temperatures at Hot Weather Creek did not drop below freezing in July in any of the six years. Minimum temperatures tend to be more conservative than maximum temperatures. Seasonal temperature maxima can occur at any time from late June to early August and approached 20°C in 1988, 1991, and 1993. Several years show two distinct warm periods. A detailed discussion of individual summers and of the interaction of temperature with other available autostation parameters is, unfortunately, beyond the scope of this report, but an outline of the basic analyses still to be completed is provided in the conclusions. In the following pages, the methods of calculating positive degree days and the duration of the melt (thaw) season is discussed and seasonal values are presented. This will allow an evaluation of the position of the six-year Hot Weather Creek record in relation to the long-term record. The melt seasons of 1989 and 1993 (1988) are used to illustrate daily temperature and positive degree-day conditions.

Arnold (1964) first noted the effect, on calculations of positive (melting) degree days, of the method by which mean daily temperatures are calculated. The standard method is to average the maximum and minimum temperature. Arnold proposed that daily means derived from the average of hourly observations (equivalent to 24 hourly sampled values from autostations) gave a more representative mean daily temperature. Both methods were used to calculate mean daily temperatures from Hot Weather Creek autostation data (Fig. 18a, 19a). These data are included in the value-added data files (Alt et al., 2000) and monthly means are given in Table 1. (Similar calculation could not be made for Eureka as two of the hourly observations were missed every night.) The differences between these two calculation methods (Fig. 18b, 19b) can be as high as 2–3°C, but are most frequently in the 0.5–1°C range. They tend to be large and variable in spring and large and negative (i.e. $T_{\text{mean}24}$ is greater than $T_{\text{mean}xn}$) in years when temperature is above normal (e.g. Fig. 18a) and smaller and positive in summers with below-normal temperatures (e.g. Fig. 19a). The highest negative values seem to occur when the diurnal temperature range is greatest (cf. Fig. 19b, e). Thus, it must be cautioned that, in addition to all the possible instrumental and observer errors inherent in measuring temperature, there is also the question of which method of calculating the mean temperatures best represents conditions at a station.

Total positive degree days have been calculated using both types of mean daily temperature (Table 4 and e.g. Fig. 18c). This produces differences of from -4 to +25°C in the seasonal total positive degree days, which is less than 5 per cent of seasonal totals (Table 4). However, the fact that the difference increases in seasons with above-normal temperatures such as 1988 and 1993 is important in climate-change evaluations (Fig. 20).

It was seen above that the difference in July mean temperature between Hot Weather Creek and Eureka during warm summers is almost double that of cold summers (Fig. 20). A comparison of the July mean temperatures and total seasonal positive degree days for the six summers of the Hot Weather Creek autostation record (Fig. 21a and Table 4) is hampered by missing data in the critical 1988 and 1993 seasons (1993 because of the unavailability of Eureka daily temperatures and 1988 because melt began at Hot Weather Creek before the station was established). The total positive degree days from the Hot Weather Creek camp station [HWC(CMP)] have been used to estimate the 1988 value. This is a rough estimate as even the camp station record does not include the very first days of above-freezing temperature. This is partly balanced by the fact that temperatures at the camp are somewhat higher than the autostation site (*see also* Fig. 22). The problem of missing data can be solved once a detailed analysis of the daily and hourly data is complete. These analyses would result in the development of methods to fill in the data gaps. The inefficiency of trying to use monthly mean data before the detailed analyses are complete is once again obvious. The results for positive degree days (PDD) at Hot Weather Creek, when complete, should be compared with those from studies of the biosphere, geosphere, hydrosphere, and cryosphere (i.e. *see* Edlund and Garneau, 2000; Lewkowitz, 2000; Young and Woo, 2000; Robinson, 2000; Wolfe, 2000).

An examination of the duration of the melt season for the warm seasons (Fig. 21b) is hampered by the missing 1988 and 1993 data. For seasons with near-normal and below-normal temperatures, the duration of the melt season is not significantly longer at Hot Weather Creek than at Eureka (Fig. 21b and Table 4). There is some indication that the difference in the duration of the melt season at the coast and in the interior is not as large, even in warm years, as is the difference in the intensity of the positive-degree-day season. This is important in climate-change studies as some environmental factors are more sensitive to melt-season duration and others relate better to intensity. The use of the main melt-season values (*see* Table 4) in Figure 21b results in the low value for 1988 at Eureka. This emphasizes the need for examining the methods used to determine the duration of the melt season in High Arctic regions.

The mean temperatures for July 1993 (Fig. 21a) from the Hot Weather Creek and Sawtooth Range inland stations decrease with elevation; this decrease is not linear because of other geographical influences such as the presence of glaciers. It is interesting to note that the coastal effect at Eureka is

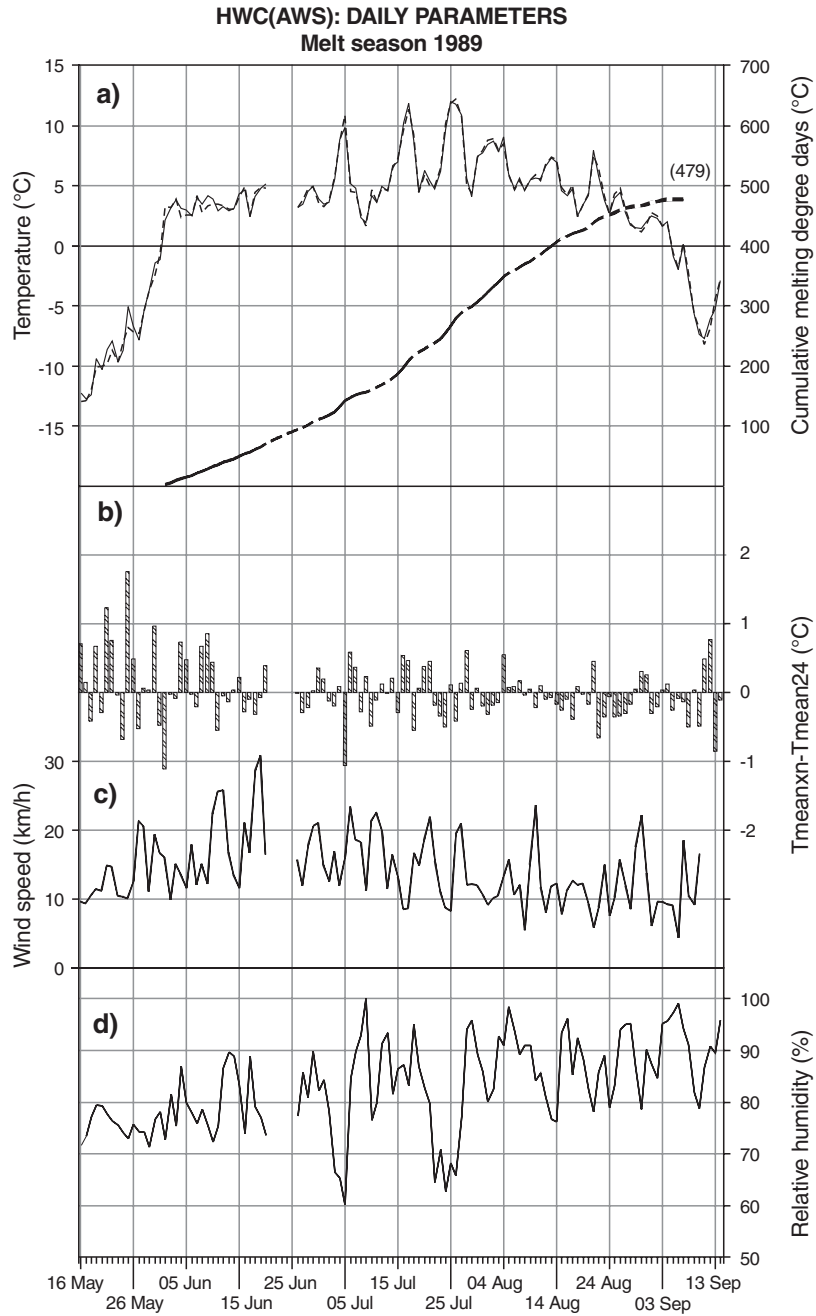


Figure 19. Hot Weather Creek automatic weather station [HWC(AWS)] 1989 daily **a)** T_{meanxn} (solid line) and T_{mean24} (dashed line) and cumulative melting degree days of T_{meanxn} (heavy solid line) and of T_{mean24} (heavy dashed line); **b)** difference in means calculated from the average of maximum and minimum temperatures (T_{meanxn}) and from 24 hourly sampled values (T_{mean24}); **c)** wind speed, scalar means of 24 two-minute scalar mean values; **d)** mean relative humidity; **e)** maximum temperature (heavy solid line), minimum temperature (fine solid line), and temperature range (bars); **f)** total incoming solar radiation; **g)** snow depth.

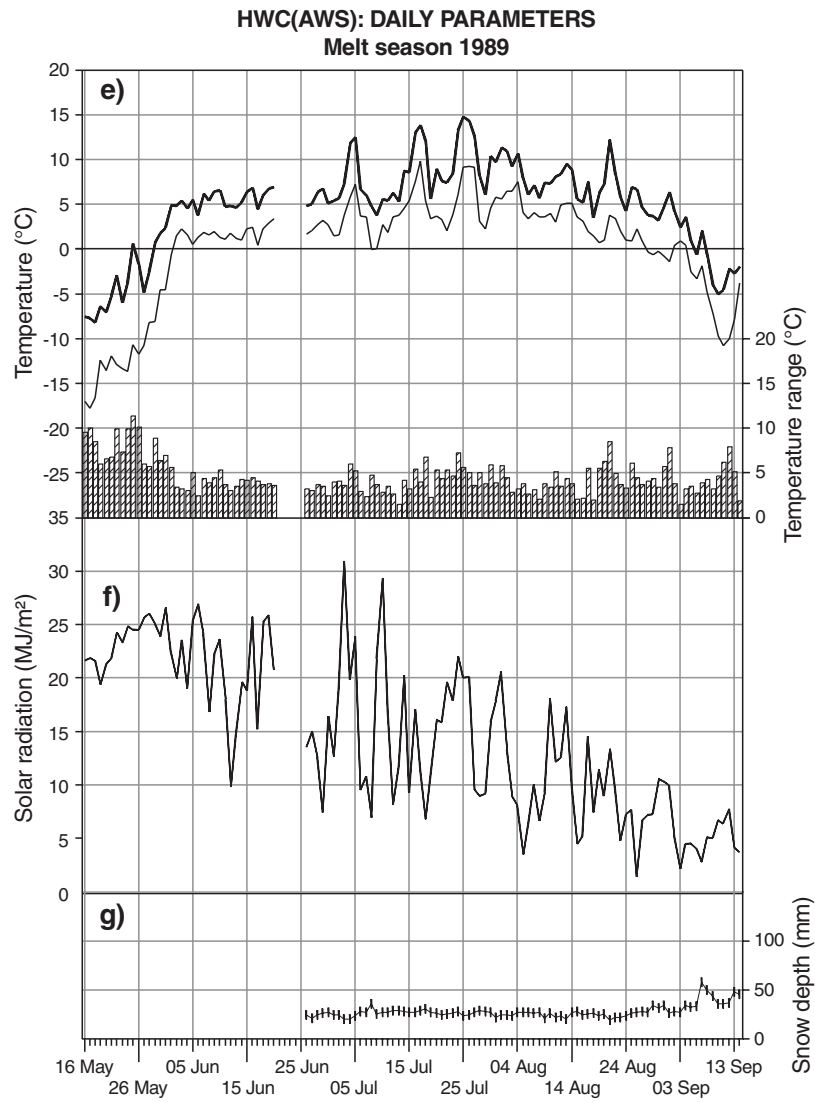


Figure 19e,f,g

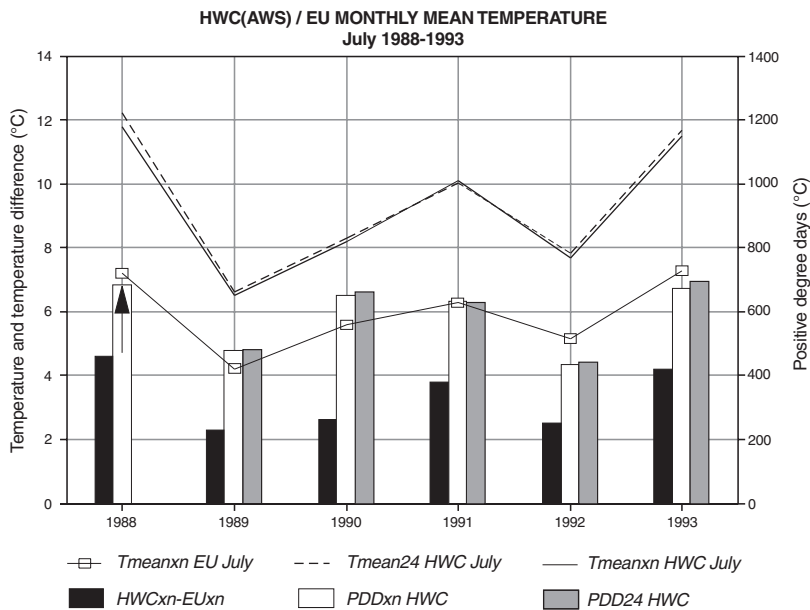


Figure 20.

Comparison between Hot Weather Creek (HWC) and Eureka (EU) July daily mean temperatures (T_{meanxn} and T_{mean24}) and total seasonal positive degree days.

roughly equivalent to an elevation difference of 600 m. The shape of the daily mean temperature curve at the Sawtooth Range camp station is similar to that for the Hot Weather Creek autostation (Fig. 23a), being well above the Eureka daily temperature during periods of above-normal temperatures and falling below Eureka temperatures when temperatures are below normal. Wolfe (1994) calculated daily air-temperature lapse rates between the valley and the glacier meteorological stations for use in estimating ablation. These ranged from 0.0034°C/m to 0.0132°C/m. Variations in the

station-to-station differences for the inland stations are evident from Figure 23b. Temperatures at the valley station approach those at Hot Weather Creek during the peak periods whereas conditions at the Sawtooth Range camp station, nearer the glacier, remain significantly colder. Considerable further study is needed of screen-level air-temperature lapse rates and their relationship to upper-air free-atmosphere soundings from Eureka. These results, in turn, should be related to weather and atmospheric circulation conditions.

Figure 21.

a) Hot Weather Creek (HWC) and Eureka (EU) July mean temperature (T_{meanxn}) and total seasonal positive degree days (PDD) and differences in these parameters between the two stations. July mean temperatures for 1993 at the Sawtooth Range valley [SWT(VLY)], camp [(SWT(CMP))], and glacier [SWT(QC)] stations and the Hot Weather Creek autostation [HWC(AES)] and camp station [HWC(CMP)] and the respective elevations of these stations are provided at the far right of the figure. **b)** Duration of the main melt season and total seasonal positive degree days at Hot Weather Creek and Eureka and differences in these parameters between the two stations.

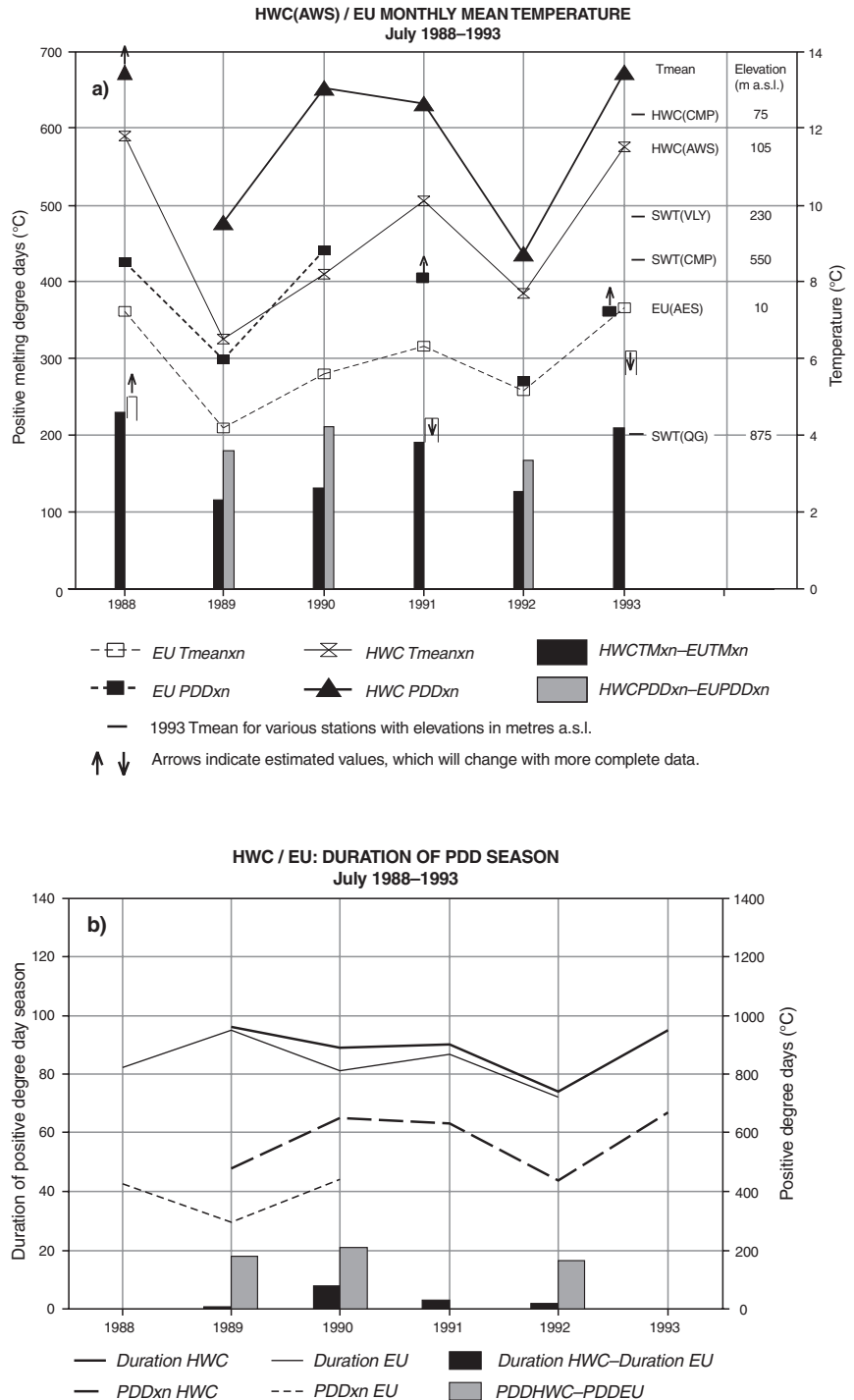


Table 4. For the Hot Weather Creek and Eureka weather stations, total positive degree days (PDD) calculated using Tmeanxn (PDDxn) and Tmean24 (PDD24), duration of the main melt season from the first to the last prolonged period of above-freezing temperatures, and duration of the total melt season from the first to the last period of above-freezing daily mean temperature.

A) Hot Weather Creek [HWC(AWS)]							
Year	PDD PDDxn [PDD24] (°C)	Beginning		End		Duration	
		first (dd/mm) (JD ¹)	main (dd/mm) (JD)	main (dd/mm) (JD)	last (dd/mm) (JD)	main (days)	total (days)
1988	(593)+ ([608])+	()	()	()	()	()	()
1989	477 [479]	01/06 153	01/06 153	04/09 248	07/09 251	96	99
1990	652 [663]	05/06 157	05/06 157	01/09 245	01/09 245	89	89
1991	631 [627]	25/05 145	28/05 148	25/08 237	31/08 243	90	99
1992	437 [441]	10/06 162	16/06 168	28/08 241	28/08 241	74	80
1993	672 [697]	27/05 147	01/06 153	04/09 248	04/09 248	95	101
B) Eureka [EU(AES)]							
1988	426	17/05 138	01/06 153	21/08 234	31/08 244	82	108
1989	298	01/06 152	01/06 152	04/09 247	04/09 247	95	95
1990	441	06/06 157	06/06 157	25/08 237	01/09 244	81	88
1991	(404)	31/05 151	31/05 151	25/08 237	30/08 243	87	93
1992	271	11/06 163	19/06 171	28/08 241	28/08 241	72	78
1993	(361)+	07/06 158	07/06 158	()	()	()	()
Normal 1960-1990	349						

¹ JD = Julian day
² (incomplete) melt underway when record begins and not complete by end (estimated PDDxn is 681+ using the Hot Weather Creek camp [HWC(CMP)] record, which is also incomplete, but longer than the Hot Weather Creek autostation [HWC(AWS)] record.
³ missing days in June were estimated (<6 days)
⁴ (incomplete) 10 days missing in July were not estimated
⁵ estimated from Wolfe (1994), missing final melt period in August (see Fig. 14).

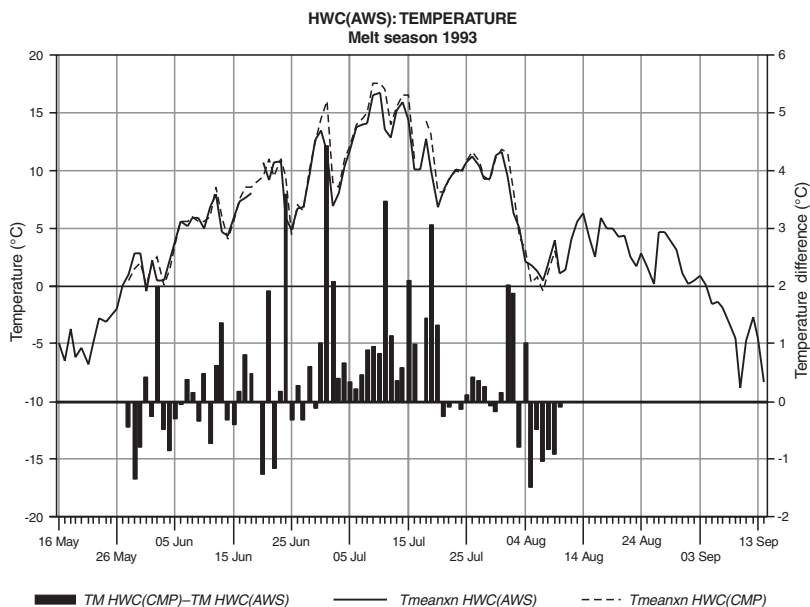


Figure 22.
 Comparison of Hot Weather Creek auto-station [HWC(AWS)] and camp station [HWC(CMP)] mean daily temperatures for the 1993 melt season.

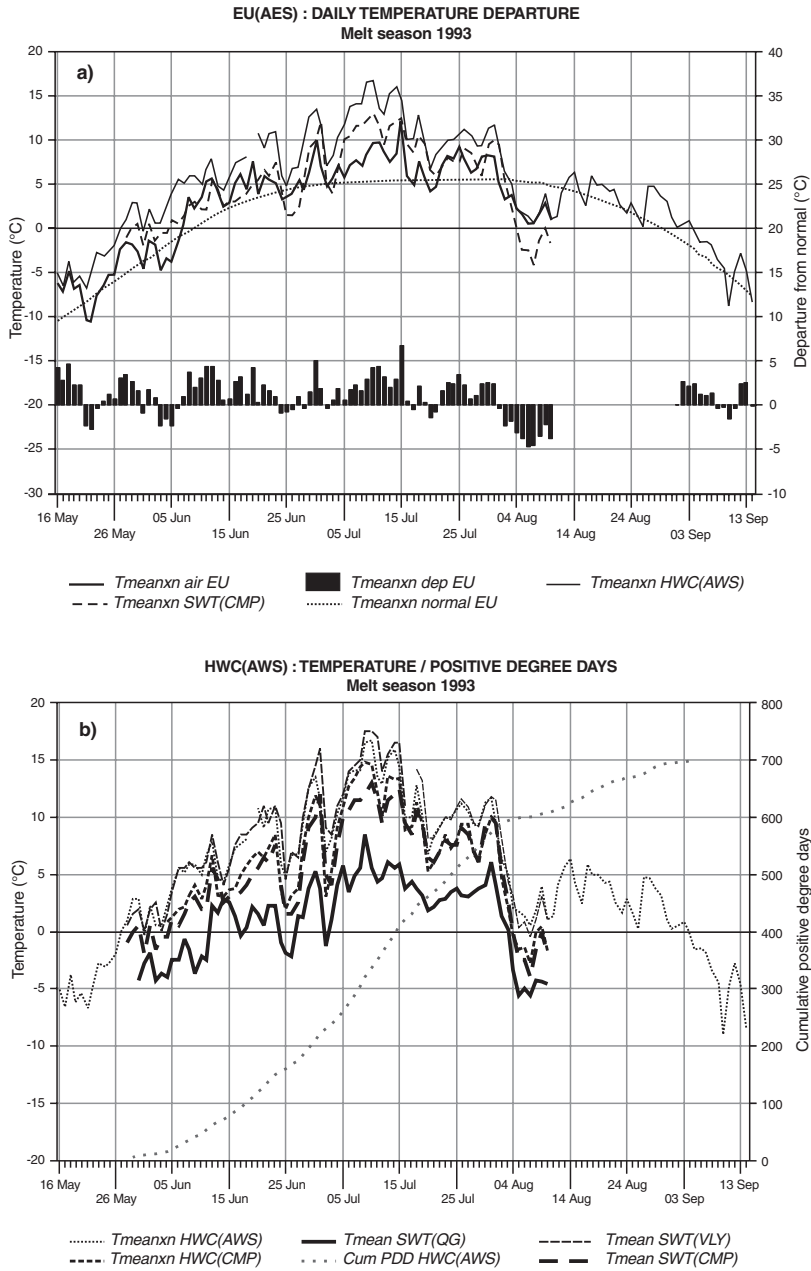


Figure 23. a) Mean daily temperatures for the Hot Weather Creek autostation [HWC(AWS)], Sawtooth Range camp station [SWT(CMP)], and Eureka station [EU(AES)], and 30-year (1958–1980) smoothed daily normal temperature and departure from 30-year normal for the Eureka station. **b)** Mean daily temperatures (tmeanxn) at the Hot Weather Creek autostation and camp station [HWC(CMP)] and the Sawtooth Range valley [SWT(VLY)], camp [SWT(CMP)], and glacier [SWT(QC)] stations, and Hot Weather Creek autostation cumulative positive degree days (PDD) for the 1993 melt season.

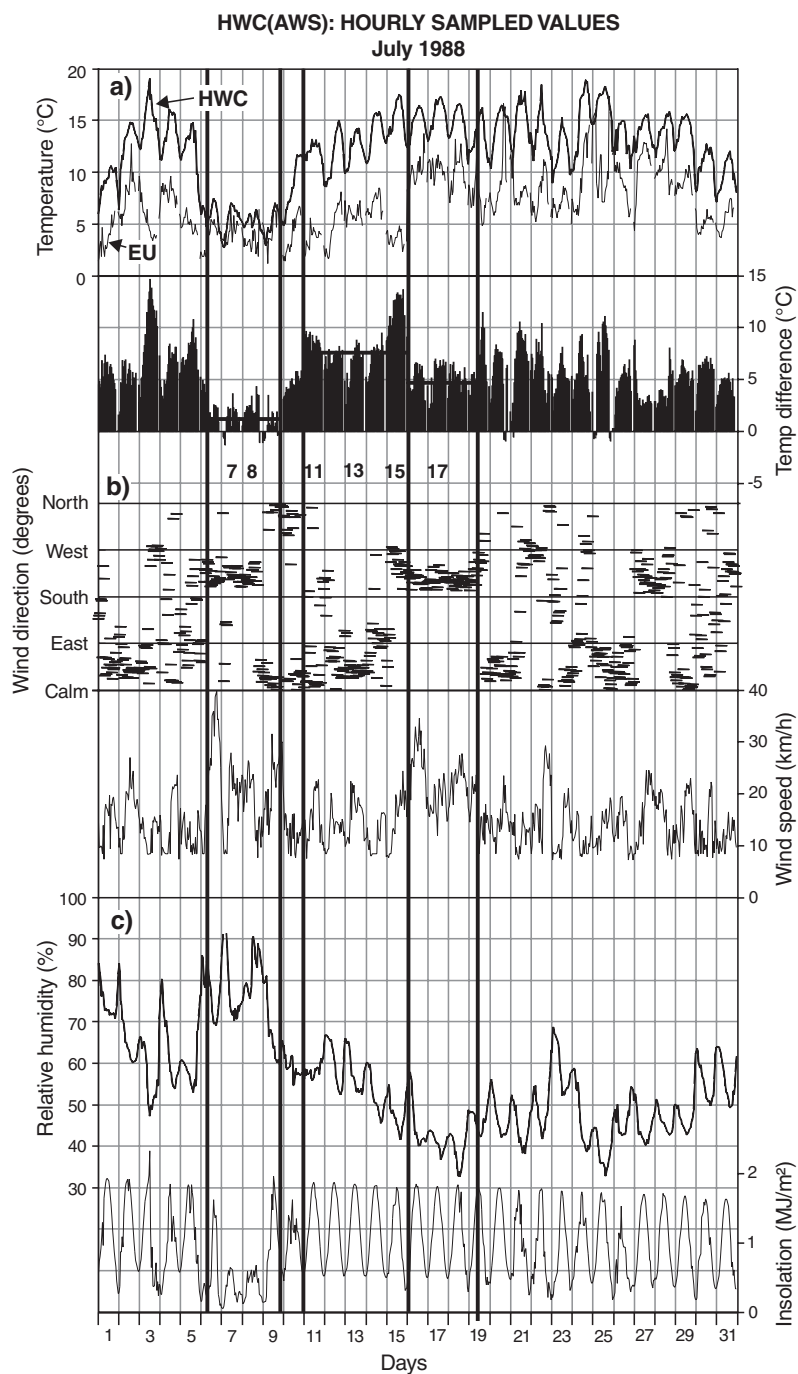


Figure 24. July 1988 Hot Weather Creek autostation hourly sampled values of: **a)** Hot Weather Creek (HWC) air temperature (heavy line), Eureka (EU) air temperature (fine line), and air temperature difference between the two stations with days within the three distinct periods indicated along the horizontal axis; **b)** wind direction, two-minute vector means (horizontal lines), and wind speed, two-minute scalar means (solid line); **c)** relative humidity (heavy line) and incoming solar radiation (fine line). The vertical lines delineate the three periods discussed in the text (July 6–9, 11–15, and 16–18).

Figure 25.

A comparison of Hot Weather Creek (HWC) mean July temperature (T_{meanxn}) and the mean July temperature ($T_{mean calc}$) calculated from Eureka (EU) values using the simple linear regression equation given in the text and by simply adding 3.34°C to the Eureka values. Also shown is the difference between the two stations and the difference between the observed and calculated Hot Weather Creek July temperatures.

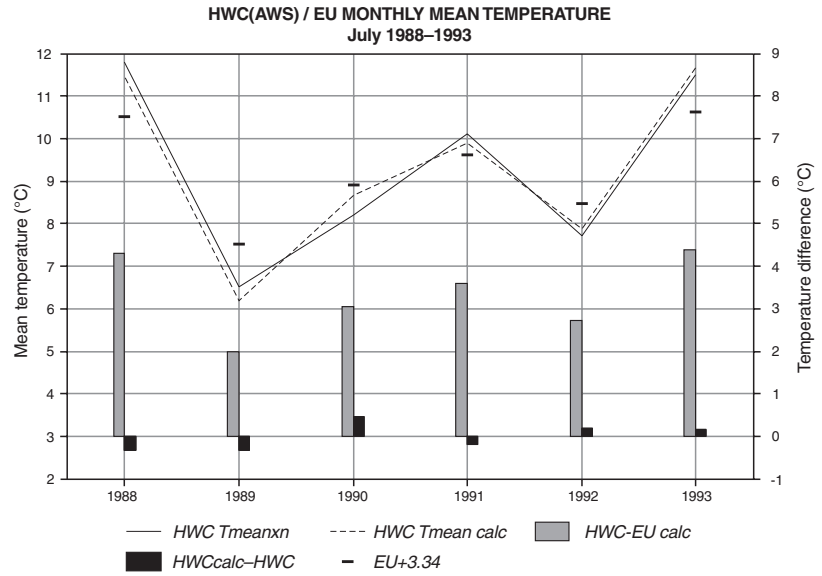
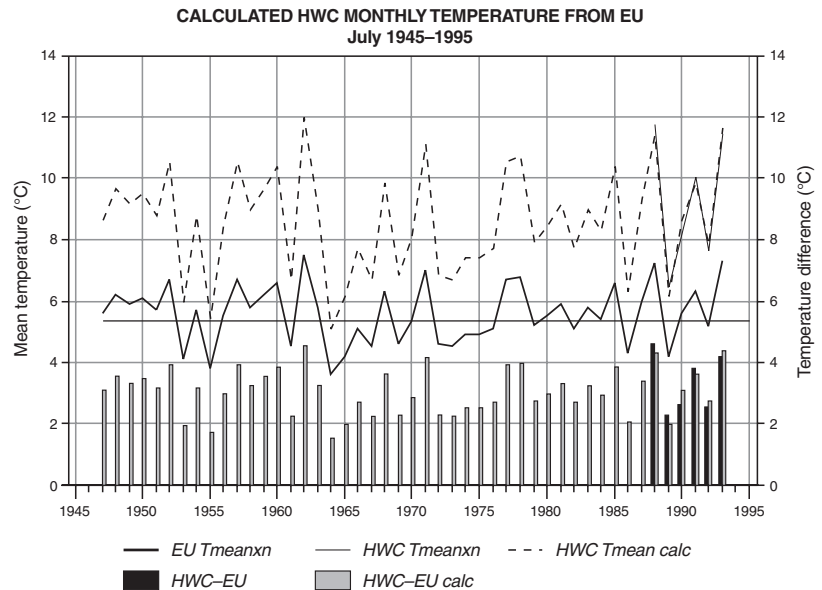


Figure 26.

Mean July temperature for Eureka (EU) and for Hot Weather Creek (HWC) observed and calculated (calc), as well as the difference between the Eureka and the two Hot Weather Creek values for 1948 to 1995.



Edlund et al. (1989, 1990) first documented the environmental extremes experienced during the 1988 and 1989 summer field seasons. In 1988, these included active-layer detachment slides, headwall retreat, streamflow regeneration, artesian-flow features and surface wetting, and second and in some cases third plant flowerings. To this can be added from the Agassiz Ice Cap seasonal pollen studies (Bourgeois, 1990; Alt and Bourgeois, 1995) an extreme maximum in regional pollen influx, and from Canadian arctic island mass-balance studies (Koerner and Lundgaard, 1995), the second most negative combined Devon Ice Cap-Meighen Ice Cap mass-balance conditions in the 30-year record. By contrast, in 1989, many species did not produce seed and there was no stream recharge, moisture being provided as a result of above-normal precipitation and low evaporation. Regional pollen influx was almost nonexistent and mass-balance

conditions were positive. Plots of hourly values from July 1988 (Fig. 24) illustrate the type of meteorological information available for studies of individual seasons. Three periods are delineated in this hourly record. Each shows a distinct relationship between temperature at Hot Weather Creek and Eureka, accompanied by distinct cloud, humidity, and wind conditions.

Detailed synoptic climate analyses of these three periods from summer 1988 and similarly distinct periods from other years in the six-year Hot Weather Creek record are necessary to link environmental events with weather conditions. A proposal for such a study is presented below. For this report, however, it should be noted that the hourly difference between Hot Weather Creek and Eureka varies from almost 0°C to a maximum of 15°C .

SIX YEARS OF HOT WEATHER CREEK AUTOSTATION RECORDS AND LONG-TERM VARIATIONS

In Alt and Maxwell (2000), the application of a preliminary method of extending the available short-term records to 30-year normals allowed the analysis of the June and July regional patterns. In order to examine the relationship between the six-year Hot Weather Creek autostation record and these regional patterns and climate change on various time scales, some attempt must be made to extend the autostation record to cover the 30-year normal period. As a first approximation, a simple linear regression between the six years of Eureka and Hot Weather Creek July mean temperatures produced the following equation:

$$\text{Hot Weather Creek Tmean calc.} = 1.23034 + (1.76675 * \text{Eureka Tmeanxn})$$

The R^2 value for this relationship is 0.89. This is a great improvement over simply applying a mean correction (3.3°C) to the Eureka record as seen in Figure 25. This equation has been used to extend the Hot Weather Creek record to the 45-year Eureka record and allow calculation of an estimated 30-year normal mean July temperature for the Hot Weather Creek autostation (Fig. 26 and Table 3).

A Hot Weather Creek July normal of 8.3°C is consistent with normals from the two interior sites shown for the Eureka intermontane area on the regional-pattern map in Alt and Maxwell (2000, Fig. 17b). It is significant to note that these values are equivalent to July normals at latitude 20°N to the south on the North American and Siberian mainland coasts (Alt and Maxwell, 2000, Fig. 4b).

The six years of the Hot Weather Creek autostation record are a full 1°C warmer than the 1960–1990 normal period (Table 3). However, if the whole period of the Eureka record is examined (Fig. 26), there is no discernable warming trend. Similarly, the Eureka June–August mean temperatures and total positive degree days (Fig. 27) show no trend over the 40-year record. In fact, the estimated mean July temperature for the first six years of the Hot Weather Creek autostation record is 9.30°C , whereas that for the 1958–1962 period is 9.75°C (Table 3). Five-year running means of Eureka June–August and July mean temperature and of calculated Hot Weather Creek July temperature (Fig. 28) all show conditions above the long-term average for the most recent decade; however, the strong warm period of the late 1950s to early 1960s precludes any long-term trend. A comparison of the five-year running sums of Eureka summer-temperature deviations and atmospheric conditions for the 1910–1990 period (Alt and Maxwell, 2000, Fig. 10) suggests that summer temperatures in the early 1930s were similar to those of the six-year record from Hot Weather Creek.

The six-year record from Hot Weather Creek includes the second (1988) and third (1993) warmest Julys in the Eureka record, making it a good record with which to study the effect on the environment of anomalously warm conditions. Fortunately, the record also includes the second coldest July (1989) and the third lowest positive-degree-day summer (1992) and

therefore provides the opportunity to study the effects of below-normal temperatures. Thus, a balanced picture of the range of possibilities for future and past climate change could be obtained from a detailed analysis of the summers in the Hot Weather Creek record.

Similar evaluations need to be performed on other seasons of the year and other parameters. Once the daily and hourly analysis is complete, it should be possible to fill in the missing June days so that a summer (June–August) estimate can be made. It must be stressed that although the estimated Hot Weather Creek autostation 30-year normal July mean given in Table 3 is a great improvement over using Eureka temperatures to relate to a paleosite in the interior Fosheim Peninsula lowland, these means are still not suitable for the creation of meaningful paleoenvironmental transfer functions for several reasons: they represent only part of the thaw season; they do not address the duration or nature (i.e. continuous or interrupted) of the thaw season; they are based only on a six-year record, which is not representative of even the past half century; they are site-specific and thus do not reflect the microclimate of individual sites (*see* Young et al. (1995) and Young and Woo (2000)).

DISCUSSION, RECOMMENDATIONS, AND CONCLUSIONS

It is essential to the study of the complex interaction of the atmosphere, geosphere, and biosphere to have a multiyear record of all the parameters involved. In the case of the meteorological records, the following observations can be made.

A 40-year record is now available from the Eureka meteorological station and includes upper-air soundings. This provides a sufficiently long record for the development of traditional paleoenvironmental transfer functions. However, it has been shown that the Eureka data are not representative of conditions in the Fosheim Peninsula lowland, which covers the largest portion of the peninsula, in contrast to the very narrow coastal belt represented by Eureka. Nor are the differences between Hot Weather Creek and Eureka constant from year to year. In fact, indications are that they are increased by some types of climate change and decreased by others. This is a particularly important consideration for the construction of paleoenvironmental transfer functions because it is from the interior of the Fosheim Peninsula that the terrestrial paleoenvironmental records are obtained.

Two additional studies are needed to complete this very preliminary analysis of the available autostation data. The first should concentrate on the melt season during which the land is free of snow, a thaw zone propagates into the ground (active layer), exposed ground ice melts, and vegetation produces pollen: the time when the tundra awakens. Once again the data used would be from the Hot Weather Creek autostation and the Eureka weather station. The Hot Weather Creek camp records would be added to these and the Sawtooth Range data added to the 1993 record. The emphasis would be on presenting the data for future use and analysis in a format similar to Figure 19. The Hot Weather Creek

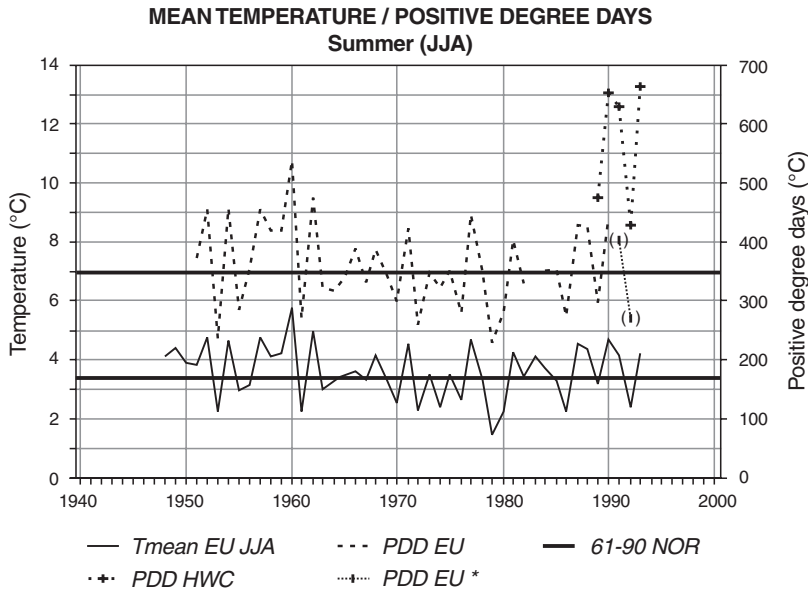


Figure 27.

A comparison of Eureka (EU) June–August mean temperature and Eureka and Hot Weather Creek (HWC) positive-degree-day (PDD) values. The solid lines are the 1961–1990 normal (NOR) values. The 1988 PDD value for Hot Weather Creek is estimated from an incomplete record. The Eureka 1991 and 1993 PDD records are also underestimated because of missing data from these summers.

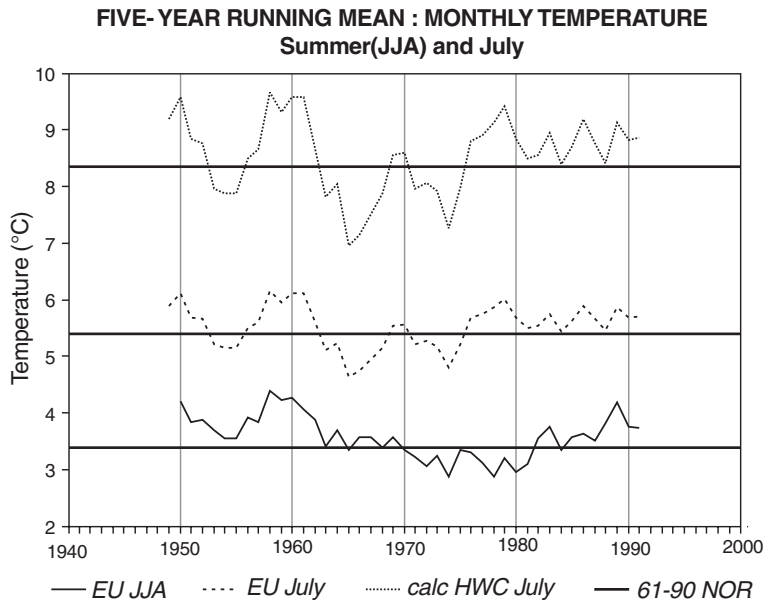


Figure 28.

Five-year running means of temperature for June–August and July at Eureka (EU) and for July at Hot Weather Creek (HWC). The solid lines are 1961–1990 normal (NOR) values.

autostation record is not yet sufficiently long to produce climatic means or to recognize real ‘trends’ in the data. An examination of the range of individual years available in the six-year record (Fig. 19) would, however, point out problems in the data, relationships between stations and parameters, and some interesting possibilities for future study. To understand the mechanisms or processes by which the atmosphere interacts with the hydrosphere, cryosphere, geosphere, and biosphere, particularly in times of rapid change on either a global or seasonal scale, it is necessary to study the system in as wide a range of conditions as possible. Young and Woo (2000) recognized this when they chose to discuss the slope hydrology and spatial energy-balance distribution of two

distinctly different years, the cold, wet year of 1989 and the warm, dry season of 1990. As was seen above, the six summers of the present record, although not representative of the mean conditions over the past half century, do contain individual seasons similar to the extremes within the long-term record. Thus, valuable information would be obtained from a study of the thermal, wind, precipitation, and ground temperature regimes of these six summers.

The second study would examine the magnitude of the differences between Hot Weather Creek and Eureka on an hourly basis (Fig. 24) and the synoptic or atmospheric-circulation reasons for the observed variations in these differences. Synoptic climate studies provide a means

of linking mesoscale climate (*see* Alt and Maxwell, 1990, Table 2) on a spatial and temporal level to global atmospheric circulation (Alt, 1975). This is an essential step in the study of the complex interaction of the atmosphere with the geosphere-biosphere and in understanding regional variability and the extent to which it influences and is influenced by global environmental change. On a spatial level, the hourly data from the Hot Weather Creek autostation would represent the mesoscale climatic conditions of the Fosheim Peninsula lowland. This would be contrasted with the coastal climate of Slidre Fiord as represented by the hourly meteorological data from Eureka. The climate difference between these two areas is not constant as is seen in the daily, monthly, and hourly parameter plots presented above. On a temporal level, the seasons of 1988 and 1989 provide contrasting climatic extremes. Edlund et al. (1990) and Woo et al. (1990) first documented the ramifications of these climatic extremes for the geosphere and biosphere of the Fosheim Peninsula lowland, as discussed above. Indications are that the summers of 1992 and 1993 will also provide interesting contrasts. The preliminary synoptic study would thus begin with a detailed study of 1988 (and 1989) synoptic summer weather conditions and how they influence the differences between Hot Weather Creek and Eureka. These would then be related to global atmospheric conditions.

The initial analyses have also suggested a number of important additional studies using the Hot Weather Creek autostation data, which should be undertaken in support of paleoenvironmental, ground-ice, and other interdisciplinary studies. A comparative synoptic climate study of the winters of 1990–1991, 1991–1992, and 1992–1993 would support studies of modern and past pollen and contaminant transport as well as provide important input into hydrological studies and geological studies of eolian deposition and ground ice. Similarly, a detailed synoptic analysis of May 1992 would allow an evaluation of the role played by extreme events in ice-core and terrestrial records. In support of the development of the Canadian general circulation model's ground surface parametrization model CLASS (Verseghy et al., 1993), a detailed regional albedo study should be undertaken. These studies are in addition to the obvious needs that include the completion of the two studies outlined above, an analysis of the Hot Weather Creek camp station record and of other data-logger and weather records for the Fosheim area, and a study of upper-air data from Eureka and data from the Agassiz Ice Cap. The fact that Eureka is being considered as an Ecological Monitoring and Assessment Network site is encouraging and may provide the mechanism for some of the analyses still to be performed on meteorological data from the area.

The very limited analyses of the monthly means generated by the Hot Weather Creek autostation data and a first look at the daily mean record have shown what valuable information is available in these records. Some of the limitations of the data set have been identified. The quality-controlled data set has been made available in Alt et al. (2000). Additional value-added data have been included. The importance of quality control and careful analysis has been demonstrated and a standard set for processing data from future nonstandard field

autostations. It is hoped that this contribution will provide the rationale for continued support of studies currently underway or in preparation and the impetus to initiate the exciting additional studies suggested by these very preliminary analyses.

ACKNOWLEDGMENTS

First, we would like to thank Dr. Sylvia Edlund who had the vision to pick up the challenge presented as a result of the initiation of a Global Change program by the Terrain Sciences Division of the Geological Survey of Canada. She established, on Fosheim Peninsula, a truly integrated, multi-disciplinary research and monitoring program. To this program she gave one hundred per cent effort at all times. Each of the authors benefited from the financial, moral, and field support she provided. Barrie Maxwell of the former Arctic Section of the Canadian Climate Centre (Atmospheric Environment Service) initiated the establishment of the automatic weather station at Hot Weather Creek and provided his wise council and practical support during all phases of the work. Many people contributed to the autostation field program over the years; the contributions of Dr. M-k. Woo, Dr. A.G. Lewkowicz, and Dr. K.L. Young are particularly appreciated. The contributions of three Terrain Sciences Division subdivision chiefs, Dr. Bernard Pelletier, Dr. Roger McNeely, and Paul Egginton, are gratefully acknowledged. The Polar Continental Shelf Project provided incomparable logistics throughout the program. The value of their support goes far beyond the dollar value of the flying hours. Finally, we are indebted to Michelle Garneau, who took on the daunting task of co-editor of this bulletin and at all times strived to maintain the spirit of the original vision.

REFERENCES

- Alt, B.T.**
 1975: The energy balance climate of Meighen Ice Cap, N.W.T.; Polar Continental Shelf Project, Energy, Mines and Resources Canada, v. 1, 67 p.
 1985: 1550–1620: A period of summer accumulation in the Queen Elizabeth Islands; *in* Climate Change in Canada 5, (ed.) C.R. Harington; National Museum of Natural Sciences, Syllogeus, no. 55, p. 461–480.
- Alt, B.T. and Bourgeois, J.C.**
 1995: Establishing the chronology of snow and pollen deposition events on Agassiz Ice Cap (Ellesmere Island, Northwest Territories) from autostation records; *in* Current Research, 1995-B; Geological Survey of Canada, p. 71–79.
- Alt, B.T. and Maxwell, B.**
 1990: The Queen Elizabeth Islands: A case study for Arctic climate data availability and regional climate analysis; *in* Canada's Missing Dimension Science and History in the Canadian Arctic Islands, Volume 1, (ed.) C.R. Harington; p. 294–326.
 2000: Overview of the modern Arctic Climate; *in* Environmental Response to Climate Change in the Canadian High Arctic, (ed.) M. Garneau and B.T. Alt; Geological Survey of Canada, Bulletin 529.
- Alt, B.T., Labine, C.L., Desrochers, D.T., Young, K.L., and Garneau, M.**
 2000: Climate and ground thermal data, 1988–1994: Hot Weather Creek, Fosheim Peninsula, Nunavut; Geological Survey of Canada, Open File D3783.

- Alt, B.T., Labine, C.L., Headley, A., Koerner, R.M., and Edlund, S.A.**
1992: High Arctic IRMA (Integrated Research and Monitoring Area) automatic weather station field data 1990-91 Part 3; Geological Survey of Canada, Open File 2562.
- Arnold, K.C. and MacKay, D.K.**
1964: Different methods of calculating mean daily temperatures, their effects on degree-day totals in the high Arctic and their significance to glaciology; *Geographical Bulletin*, no. 21; Geographical Branch, Department of Mines and Technical Surveys, p. 123-129.
- Atkinson, D.E.**
1994: Aspects of local- and regional-scale climatology in the Canadian Arctic Islands: coastal effect at AES Eureka; *in* Program and Abstracts, 28th Canadian Meteorological and Oceanographic Society (CMOS) Congress, Ottawa, Ontario, May 30-June 3, 1994, p.143.
2000: Modelling July mean temperatures on Fosheim Peninsula, Ellesmere Island, Nunavut; *in* Environmental Response to Climate Change in the Canadian High Arctic, (ed.) M. Garneau and B.T. Alt; Geological Survey of Canada, Bulletin 529.
- Atmospheric Environment Service**
1991: Observation Site Data: Eureka; Atmospheric Environment Services, Downsview, Ontario, 4 p.
1992: AES Guidelines for co-operative climatic autostations Version 2.0; Canadian Climate Centre, Atmospheric Environment Service, Environment Canada, Guide 91-1, 84 p.
1994: Canadian monthly climate data and 1961-1990 normals. User manual for the CD-ROM data access software V3.0E; Environment Canada, 14 p.
- Bourgeois, J.C.**
1990: Seasonal and annual variation of pollen content in the snow of a Canadian high Arctic ice cap; *BOREAS*, v. 19, p. 313-322.
- Bourgeois, J.C., Koerner, R.M., Fisher, D.A., and Alt, B.T.**
2000: Present and past environments inferred from Agassiz Ice Cap ice core records; *in* Environmental Response to Climate Change in the Canadian High Arctic, (ed.) M. Garneau and B.T. Alt; Geological Survey of Canada, Bulletin 529.
- Bradley, R.S., Keimig, F.T., and Diaz, H.F.**
1992: Climatology of surface-based inversions in the North American Arctic; *Journal of Geophysical Research*, v. 97(D14), p. 15 699-15 712.
1993: Recent changes in the North American Arctic boundary layer in winter; *Journal of Geophysical Research*, v. 98(D5), p. 8851-8858.
- Courtin, G.M. and Labine, C.L.**
1977: Microclimatological studies on Truelove Lowland; *in* Truelove Lowland, Devon Island, Canada: A High Arctic Ecosystem, (ed.) L.C. Bliss; University of Alberta Press, Edmonton, p. 73-106.
- Dahlgren, L.**
1974: Solar radiation climate near sea level in the Canadian Arctic Archipelago. Arctic Institute of North America, Devon Island Expedition 1961-62; Meteorologiska Institutionen Uppsala Universitetet Meddeleleser, no. 121, p. 1-119.
- Department of Transport**
1961: Climatological Summary, Eureka, N.W.T., Canada: June 1947 to December 1953; Meteorological Branch, Department of Transport, Toronto, Ontario.
- Dirmhirm, I. and Eaton, F.D.**
1975: Some characteristics of the albedo of snow; *Journal of Applied Meteorology*, v. 14, p. 375-379.
- Edlund, S.A. and Garneau, M.**
2000: Overview of vegetation zonation in the Arctic; *in* Environmental Response to Climate Change in the Canadian High Arctic, (ed.) M. Garneau and B.T. Alt; Geological Survey of Canada, Bulletin 529.
- Edlund, S.A. and Woo, M-k.**
1992: Eolian deposition on western Fosheim Peninsula, Ellesmere Island, Northwest Territories during the winter of 1990-91; *in* Current Research, Part B; Geological Survey of Canada, Paper 92-1B, p. 91-96.
- Edlund, S.A., Alt, B.T., and Young, K.L.**
1989: Interaction of climate, vegetation, and soil hydrology at Hot Weather Creek, Fosheim Peninsula, Ellesmere Island, Northwest Territories; *in* Current Research, Part D; Geological Survey of Canada, Paper 89-1D, p. 125-133.
- Edlund, S.A., Woo, M-k., and Young, K.L.**
1990: Climate, hydrology and vegetation patterns Hot Weather Creek, Ellesmere Island, Arctic Canada; *Nordic Hydrology*, v. 21, p.273-286.
- Garneau, M., Alt, B.T., and Edlund, S.A.**
2000: Introduction; *in* Environmental Response to Climate Change in the Canadian High Arctic, (ed.) M. Garneau and B.T. Alt; Geological Survey of Canada, Bulletin 529.
- Goodison, B.E.**
1981: Compatibility of Canadian snowfall and snow cover data; *Water Resources Research*, v. 17, no. 4, p. 893-900.
- Headley, A.**
1990: A comparison of wind speeds recorded simultaneously at three metres and ten metres above ground; Canadian Climate Centre, Atmospheric Environment Service, Report no. 90-1, 36 p.
- Holmgren, B.**
1971: Climate and energy exchange on a subpolar ice cap in summer, Part F: On the energy exchange of the snow surface at Ice Cap Station; Arctic Institute of North America, Devon Island Expedition 1961-1963, Meteorologiska Institutionen, Uppsala, Sweden, 53 p.
- Koerner, R.M.**
1979: Accumulation, ablation, and oxygen isotope variations on the Queen Elizabeth Islands ice caps, Canada; *Journal of Glaciology*, v. 22, no. 86, p. 25-41.
- Koerner, R.M. and Lundgaard, L.**
1995: Glaciers and global warming; *Géographie physique et Quaternaire*, v. 49, no. 3, p. 429-434.
- Labine, C.L., Alt, B.A., Atkinson, D., Headley, A., Koerner, R.M., Edlund, S.A., and Waszkiewicz, M.**
1994: High Arctic IRMA automatic weather station field data 1991-1992. Part 1: Documentation, Part 2: Plots; Geological Survey of Canada, Open File Report 2898.
- Lewkowicz, A.G.**
1990: Morphology, frequency and magnitude of active-layer detachment slides, Fosheim Peninsula, Ellesmere Island, N.W.T.; Permafrost-Canada: Proceedings of the Fifth Canadian Permafrost Conference, Quebec City, June 1990, Université Laval, Quebec, p. 111-118.
- Maxwell, J.B.**
1980: The climate of the Canadian Arctic Islands and adjacent waters. Volume 1; Atmospheric Environment Service, Climatological Studies no. 30, 532 p.
1982: The climate of the Canadian Arctic Islands and adjacent waters. Volume 2; Atmospheric Environment Service, Climatological Studies no. 30, 589 p.
- McKay, D.C. and Morris, R.J.**
1985: Solar radiation data analyses for Canada 1967-1976; Volume 6: The Yukon and Northwest Territories, Canadian Climate Program.
- Metcalf, J.R., Ishida, S., and Goodison, B.E.**
1994: A corrected precipitation archive for the Northwest Territories; *in* Mackenzie Basin Impact Study; Interim Report No 2, p. 110-117.
- Ohmura, A.**
1981: Climate and energy balance on arctic tundra: Axel Heiberg Island, Canadian Arctic Archipelago, spring and summer 1969, 1970 and 1972; *Eidgenussische Technische Hochschule, Zurich, Zurich Geographische Schriften*, v. 3, 448 p.
- Peters, B. and Headley, A.**
1992: A comparison of winds at Hot Weather Creek and Eureka, N.W.T.; Canadian Climate Centre, Atmospheric Environment Service, Report No. 92-2, 22 p.
- Pollard, W.H.**
2000: Distribution and characterization of ground ice on Fosheim Peninsula, Ellesmere Island, Nunavut; *in* Environmental Response to Climate Change in the Canadian High Arctic, (ed.) M. Garneau and B.T. Alt; Geological Survey of Canada, Bulletin 529.
- Pomeroy, J.W., Marsh, P., and Gray, D.M.**
1997: Application of a distributed blowing snow model to the Arctic; *Hydrological Processes*, v. 1, no. 11, p. 1451-1464.
- Robinson, S.D.**
2000: Thaw-slump-derived thermokarst near Hot Weather Creek, Ellesmere Island, Nunavut; *in* Environmental Response to Climate Change in the Canadian High Arctic, (ed.) M. Garneau and B.T. Alt; Geological Survey of Canada, Bulletin 529.

Verseghy, D.L., McFarlane, N.A., and Lazare, M.

- 1993: CLASS - a Canadian land surface scheme for GCMs, II. Vegetation model and coupled runs; *International Journal of Climatology*, v. 13, p. 347–370.

Wolfe, P.M.

- 1994: Hydrometeorological investigations on a small valley glacier in the Sawtooth Range, Ellesmere Island, Northwest Territories; Master's thesis, Wilfrid Laurier University, Waterloo, Ontario, 205 p.
- 2000: Glacier hydrology in the Sawtooth Range, Ellesmere Island, Nunavut; *in* Environmental Response to Climate Change in the Canadian High Arctic, (ed.) M. Garneau and B.T. Alt; Geological Survey of Canada, Bulletin 529.

Woo, M.-k., Edlund, S.A., and Young, K.L.

- 1991: Occurrence of early snow-free zones on Fosheim Peninsula, Ellesmere Island, Northwest Territories; *in* Current Research, Part B; Geological Survey of Canada, Paper 91-1B, p. 9–14.

Woo, M.-k., Heron, R., Marsh, P., and Steer, P.

- 1983: Comparison of weather station snowfall with winter snow accumulation in high arctic basins; *Atmosphere-Ocean*, v. 21 no. 3, p. 312–325.

Woo, M.-K., Young, K.L., and Edlund, S.A.

- 1990: 1989 observations of soil, vegetation, and microclimate, and effects on slope hydrology, Hot Weather Creek basin, Ellesmere Island, Northwest Territories; *in* Current Research, Part D; Geological Survey of Canada, Paper 90-1D, p. 85–93.

Young, K.L.

- 1995: Slope hydroclimatology and hydrologic responses to global change in a small High Arctic basin; Ph.D. thesis, McMaster University, Hamilton, Ontario, 167 p.

Young, K.L. and Woo, M.-k.

- 1995: Simple approaches to modelling solar radiation in the Arctic; *Solar Energy*, v. 54, p. 33–40.
- 2000: Hydrological environment of the Hot Weather Creek basin, Ellesmere Island, Nunavut; *in* Environmental Response to Climate Change in the Canadian High Arctic, (ed.) M. Garneau and B.T. Alt; Geological Survey of Canada, Bulletin 529.

Young, K.L., Woo, M.-k., and Edlund, S.A.

- 1997: Influence of local topography, soils and vegetation on microclimate and hydrology at a High Arctic site, Ellesmere Island; *Arctic and Alpine Research*, v. 29, no. 3, p. 270–284.

APPENDIX A

Hot Weather Creek automatic weather station quality control and documentation and Eureka instrumentation documentation

C.L. Labine¹, B.T. Alt², and A.N. Headley³

PART 1: HOT WEATHER CREEK AUTOMATIC WEATHER STATION QUALITY CONTROL AND DOCUMENTATION

Introduction

This appendix contains a hard copy of the metadata that supports the Hot Weather Creek data set. This documentation is also included in Alt et al. (2000). The data and metadata (documentation) file-naming procedures and brief descriptions of the various file types are presented in the following.

File organization and description

There are two basic types of file, data files and metadata (documentation) files.

All file names consist of a three-letter station identifier (e.g. HWC), followed by a numeric code of two or four digits (e.g. 88 or 8889) designating the period covered by the data or metadata. The two-digit code represents data from a calendar year (or part of a calendar year) whereas the four-digit code represents data collected between station servicing and thus from two consecutive partial calendar years. Since the annual site visit usually occurs in mid-season, typically June, the files cover the period from the summer of the first season to the summer of the next (termed 'logger year'). For simplicity, all examples of file-name nomenclature and file description will use 88, the 1988 portion of the 1988–1989 logger year, or 8889, the 1988–1989 logger-year data period. The other time periods are 8990 (1989–1990), 9091 (1990–1991), 9192 (1991–1992), 9293 (1992–1993), and 9394 (1993–1994). Value-added files for the whole period of data collection are designated by the type of data (e.g. COMP for a composite file of selected daily values or MEAN for a composite file of selected monthly mean data). The file extension is used to indicate the type of data file (e.g. .WQ1 for spreadsheet files or .PRN for comma-delimited files) or the type of information in the metadata (e.g. .SFT for data element lists or .DQC for quality control information files).

Data files

e.g. xHWC88xx.WQ1
 xHWC88xx.PRN
 HWCCOMP.WQ1
 HWCMEAN.WQ1

xHWC88xx.WQ1

The spreadsheet data files (file extension .WQ1) have been divided into hourly, daily, and calculated-daily data files. All data files released with this bulletin start with the letter R, which stands for 'revised' and indicates that the data have undergone quality control. All data files are for a portion of a single calendar year. Thus, the hourly files for the 1988–1989 season are RHWC88HB.WQ1 and RHWC89HA.WQ1. The 88HB indicates that this is the hourly (H) data and represents the later part of the year (B) as opposed to the 89HA, which represents hourly data from the beginning of the year to the time of the annual site visit. Similarly, the daily files are RHWC88DB.WQ1 and RHWC89DA.WQ1 and the calculated daily files are RHWC88CB.WQ1 and RHWC89CB.WQ1.

¹ Campbell Scientific Canada Corporation, 11564 - 149 Street, Edmonton, Alberta T5M 1W7

² Balanced Environments Associates, 5034 Leitrim Road, Carlsbad Springs, Ontario K0A 1K0

³ Canadian Climate Centre, Atmospheric Environment Service, 4905 Dufferin Road, Downsview, Ontario M3B 5T4

HWC88xx.PRN

The comma-delimited files .PRN have the same names as the spreadsheet files, but a different extension. Missing or bad data are indicated by -9999.

HWCCOMP.WQ1

This is a combined file of selected elements from the daily and calculated files (including some additional calculated fields such as melting degree days) for the years June 1988–May 1994. Note: the maximum and minimum temperatures for the logger year 1989–1990 are the maximum and minimum of the sampled hourly values, rather than the extreme maximum and minimum (the mean of these, Tmeanxn, is also affected).

HWCMEAN.WQ1

This file contains the monthly means of selected parameters calculated from the daily and hourly files. As in HWCCOMP.WQ1, maximum and minimum temperatures for logger year 1989–1990 are not extreme values. The three-five rule has been used to deal with missing data (*see* HWC.CMB).

File description files

e.g. HWC.STN
 HWC.NST
 HWC8889.LST
 HWC8889.SFT
 HWC8889.DQC
 HWC88.CMB

HWC.STN

This is a station description file that includes topographic information and station representativeness evaluation.

HWC.NST

This includes sensor and other instrumentation information for the years of record, including sensor calibration results and condition of sensors after the wintering-over period.

HWC8889.LST

This is a list of the main data files (both .WQ1 and .PRN) with their start and end times and dates for a particular logger year.

HWC8889.SFT

This is a data-element list for .WQ1 and .PRN files, including units and in some cases sensor type for each logger year.

HWC8889.DQC

This file lists the data quality-control problems that have been discovered for a specific logger year and warns the user of the data gaps that exist for the various measured parameters.

HWC.CMB

This file lists the formats of the HWCCOMP.WQ1 and HWCMEAN.WQ1 files and gives information on calculated parameters and the treatment of missing data.

Sensor description and conditions (HWC.NST)

Sensor	Description
Radiation	Eppley pyranometer for incoming shortwave radiation, uses a thermopile sensing element. The sensor is calibrated and replaced every year.
Temperature	Campbell Scientific Canada Corp. (CSCC) thermistor (207C) for air temperature housed in a small Gill self-ventilating radiation shield. CSCC thermistors (107B) are also used to measure near-surface and ground temperatures.
Relative humidity	Phys-Chem polysulphanated styrene chip that is part of the air (207C) temperature and humidity probe.
Wind speed	Met-One 013A heavy duty three-cup anemometer
Wind direction	Met-One 023A heavy duty wind vane.
Snow depth	Ultrasonic distance sensor, the CSMAL01 (CSCC)

In June 1992, the following changes were made to the sensor configuration.

The main anemometer Met-One wind speed and direction sensors were replaced with an R.M. Young wind monitor (RMY), which measures both wind speed and direction (DIR). The 023A Met-One wind-direction (Met-One) sensor was removed and the Met-One 013A wind-speed sensor was moved to the west side of the station at a height of 3 m.

The snow-depth sensor was changed from a CSMAL01 sensor to a UDG01 sensor. Both sensors use the same type of ultrasonic device. The UDG01 performs the temperature correction using the station's temperature sensor whereas the CSMAL01 had an internal, but poorly shielded, temperature sensor.

An Eppley pyranometer was added to measure reflected shortwave radiation.

A standard Atmospheric Environment Services tipping-bucket rain gauge was added.

Hot Weather Creek 1988–1989**List of data files (HWC8889.LST)**

NAME	STARTS	ENDS
RHWC88HB.WQ1 (.PRN)	17:00, Julian day (JD) 175 (June 23), 1988	06:00, JD 1 (January 1), 1989 (24:00, JD 366 [December 31], 1988) local time
RHWC89HA.WQ1 (.PRN)	07:00, JD 1 (January 1), 1989	21:00, JD 172 (June 21), 1989
RHWC88DB.WQ1 (.PRN)	JD 177 (June 25), 1988	JD 1 (January 1), 1989 (JD 366 [December 31], 1988) local time
RHWC89DA.WQ1 (.PRN)	JD 2 (January 2), 1989	JD 172 (June 21), 1989
RHWC88CB.WQ1 (.PRN)	JD 177 (June 25), 1988	JD 1 (January 1), 1989 (JD 366 [December 31], 1988) local time
RHWC89CA.WQ1 (.PRN)	JD 2 (January 2), 1989	JD 172 (June 21), 1989

Spreadsheet data-element description (HWC8889.SFT) (numbers in parentheses indicate order of element in .PRN files)

Hourly data

A (1)	YEAR
B (2)	JULIAN DAY
C (3)	TIME (HHMM, UTC)
D (4)	AIR TEMPERATURE, °C, HOURLY SAMPLE
E (5)	AIR RELATIVE HUMIDITY, %, HOURLY SAMPLE

F (6)	TWO-MINUTE MEAN WIND SPEED, MET-ONE, km/h
G (7)	TWO-MINUTE WIND DIRECTION VECTOR, RMY DIR, MET-ONE SPEED
H (8)	SAMPLE, SURFACE VEGETATION TEMPERATURE, °C
I (9)	SAMPLE, 10 cm SOIL TEMPERATURE, °C
J (10)	SAMPLE, 20 cm SOIL TEMPERATURE, °C
K (11)	SAMPLE, 50 cm SOIL TEMPERATURE, °C
L (12)	SAMPLE, 100 cm SOIL TEMPERATURE, °C
M (13)	TOTAL INCOMING SHORTWAVE RADIATION, MJ/m ²

Daily data

A (1)	YEAR
B (2)	MONTH
C (3)	DAY
D (4)	JULIAN DAY (one day ahead of date)
E (5)	TIME (HHMM, 06:00 UTC)
F (6)	MAXIMUM AIR TEMPERATURE, °C
G (7)	TIME OF MAXIMUM AIR TEMPERATURE
H (8)	MINIMUM AIR TEMPERATURE, °C
I (9)	TIME OF MINIMUM AIR TEMPERATURE
J (10)	MAXIMUM WIND SPEED, km/h
K (11)	TIME OF MAXIMUM WIND SPEED
L (12)	DIRECTION OF MAXIMUM WIND SPEED
M (13)	TOTAL INCOMING SHORTWAVE RADIATION
N (14)	SNOW DEPTH, mm
O (15)	BATTERY VOLTAGE

Calculated daily

A (1)	YEAR
B (2)	MONTH
C (3)	DAY
D (4)	JULIAN DAY (one day ahead of date)
E (5)	TIME (HHMM, 06:00 UTC)
F (6)	AVERAGE AIR TEMPERATURE, °C
G (7)	AVERAGE AIR RELATIVE HUMIDITY, %
H (8)	AVERAGE WIND SPEED, km/h
I (9)	MAXIMUM SURFACE VEGETATION TEMPERATURE, °C
J (10)	MAXIMUM 10 cm TEMPERATURE, °C
K (11)	MAXIMUM 20 cm TEMPERATURE, °C
L (12)	MAXIMUM 50 cm TEMPERATURE, °C
M (13)	MAXIMUM 100 cm TEMPERATURE, °C
N (14)	AVERAGE SURFACE VEGETATION TEMPERATURE, °C
O (15)	AVERAGE 10 cm TEMPERATURE, °C
P (16)	AVERAGE 20 cm TEMPERATURE, °C
Q (17)	AVERAGE 50 cm TEMPERATURE, °C
R (18)	AVERAGE 100 cm TEMPERATURE, °C
S (19)	MINIMUM SURFACE VEGETATION TEMPERATURE, °C
T (20)	MINIMUM 10 cm TEMPERATURE, °C
U (21)	MINIMUM 20 cm TEMPERATURE, °C
V (22)	MINIMUM 50 cm TEMPERATURE, °C
W (23)	MINIMUM 100 cm TEMPERATURE, °C

Notes on quality control of data (HWC8889.DQC)

In the HWC8889.DAT file, a large data gap exists from 07:00 on Julian day (JD) 232 to 13:00 on JD 262. All data parameters are missing for that period and only the time elements have been kept.

Wind speed and direction

Data have been eliminated for those periods when the sensors are covered with ice or frost and yield no data, i.e. from 21:00 JD 304 to 07:00 JD 113.

NAME	STARTS	ENDS
RHWC89HB.WQ1 (.PRN)	07:00, JD 177 (June 26), 1989	06:00, JD 1 (Jan. 1), 1990 (24:00, JD 365 [December 31], 1989) local time
RHWC90HA.WQ1 (.PRN)	07:00, JD 1 (January 1), 1990	06:00, JD 168 (June 17), 1990
RHWC89DB.WQ1 (.PRN)	JD 178 (June 27), 1989	JD 1 (January 1), 1990 (JD 365 [December 31], 1989) local time
RHWC90DA.WQ1 (.PRN)	JD 2 (January 2), 1990	JD 168 (June 17), 1990
RHWC89CB.WQ1 (.PRN)	JD 178 (June 27), 1988	JD 1 (January 1), 1990 (JD 365 [December 31], 1989) local time
RHWC90CA.WQ1 (.PRN)	JD 2 (January 2), 1990	JD 168 (June 17), 1990

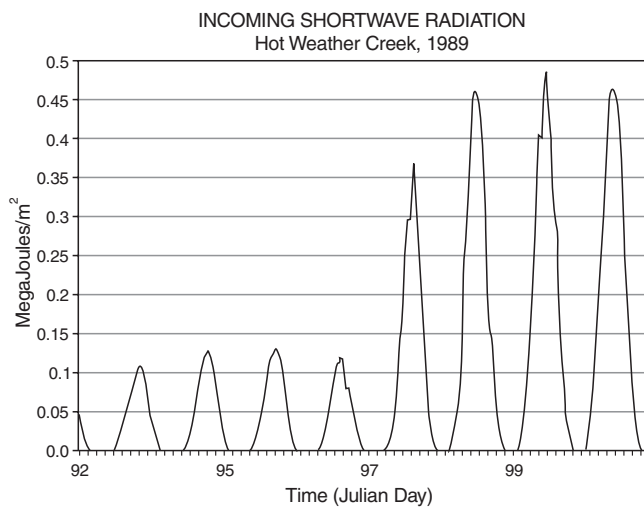


Figure A1. Radiation data showing the effect of snow and/or frost covering the sensor.

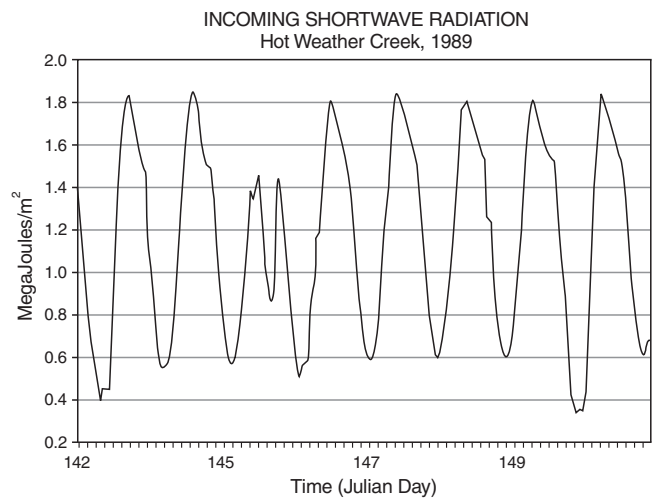


Figure A3. Radiation data, corrected.

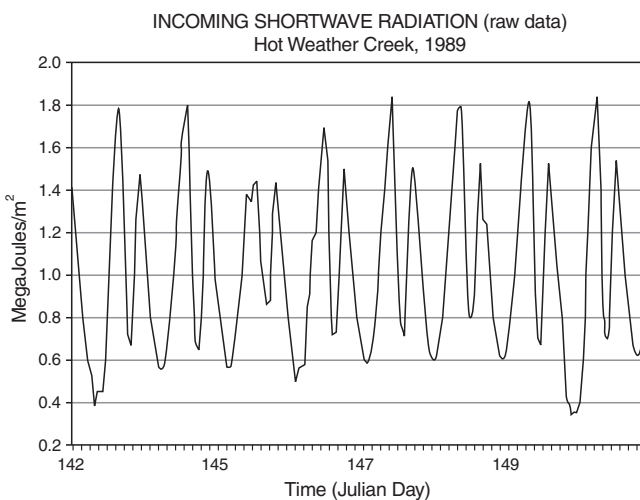


Figure A2. Radiation data, uncorrected.

Snow depth

Throughout the entire period, there are many instances of 0 readings, which means that the snow-depth sensor could not make a reasonable reading. All the 0 readings have been removed and some of the obvious out-of-range noise was also eliminated.

Radiation

The radiation record for the first days of measurement after the return of the sun indicates that the sensor was probably covered in snow up to Julian day 98 (April 8). Figure A1 shows the transition to a cleared sensor, but also shows that for the first several days following sensor clearing, the sensor was not shaded. The shading near the sensor, probably due to the anemometer, is clearly seen in Figure A2. The same data are plotted and

shown in Figure A3, but are corrected to eliminate the shading for clear days only. The data have been corrected for clear days by eliminating the shaded portion of the recorded data and extrapolating the line from the start to the end of the shaded portion of the record. If there was any question that there might be some cloud cover and therefore that the day was not perfectly clear, then the radiation data were left in their original state. The radiation data can best be corrected using a modelling technique as found in Young et al. (1995).

Hot Weather Creek 1989–1990

List of data files (HWC8990.LST)

Spreadsheet data-element description (HWC8990.SFT) (numbers in parentheses indicate order of element in .PRN files)

Hourly data

A (1)	YEAR
B (2)	JULIAN DAY
C (3)	TIME (HHMM, UTC)
D (4)	AIR TEMPERATURE, °C, HOURLY SAMPLE
E (5)	AIR RELATIVE HUMIDITY, %, HOURLY SAMPLE
F (6)	TWO-MINUTE MEAN WIND SPEED, MET-ONE, km/h
G (7)	TWO-MINUTE WIND DIRECTION VECTOR, RMY DIR, MET-ONE SPEED
H (8)	SAMPLE, SURFACE VEGETATION TEMPERATURE, °C
I (9)	SAMPLE, 10 cm SOIL TEMPERATURE, °C
J (10)	SAMPLE, 20 cm SOIL TEMPERATURE, °C
K (11)	SAMPLE, 50 cm SOIL TEMPERATURE, °C
L (12)	SAMPLE, 100 cm SOIL TEMPERATURE, °C
M (13)	TOTAL INCOMING SHORTWAVE RADIATION, MJ/m ²

Daily data

A (1)	YEAR
B (2)	MONTH
C (3)	DAY
D (4)	JULIAN DAY (one day ahead of date)
E (5)	TIME (HHMM, 06:00 UTC)
F (6)	EMPTY
G (7)	EMPTY
H (8)	EMPTY
I (9)	EMPTY
J (10)	EMPTY
K (11)	EMPTY
L (12)	EMPTY
M (13)	TOTAL INCOMING SHORTWAVE RADIATION
N (14)	SNOW DEPTH, mm
O (15)	BATTERY VOLTAGE

Calculated daily

A (1)	YEAR
B (2)	MONTH
C (3)	DAY
D (4)	JULIAN DAY (one day ahead of date)
E (5)	TIME (HHMM, 06:00 UTC)
F (6)	AVERAGE AIR TEMPERATURE, °C
G (7)	AVERAGE AIR R.H., %
H (8)	AVERAGE WIND SPEED, km/h
I (9)	MAXIMUM SURFACE VEGETATION TEMPERATURE, °C
J (10)	MAXIMUM 10 cm TEMPERATURE, °C
K (11)	MAXIMUM 20 cm TEMPERATURE, °C
L (12)	MAXIMUM 50 cm TEMPERATURE, °C
M (13)	MAXIMUM 100 cm TEMPERATURE, °C
N (14)	AVERAGE SURFACE VEGETATION TEMPERATURE, °C
O (15)	AVERAGE 10 cm TEMPERATURE, °C
P (16)	AVERAGE 20 cm TEMPERATURE, °C
Q (17)	AVERAGE 50 cm TEMPERATURE, °C
R (18)	AVERAGE 100 cm TEMPERATURE, °C
S (19)	MINIMUM SURFACE VEGETATION TEMPERATURE, °C
T (20)	MINIMUM 10 cm TEMPERATURE, °C
U (21)	MINIMUM 20 cm TEMPERATURE, °C
V (22)	MINIMUM 50 cm TEMPERATURE, °C
W (23)	MINIMUM 100 cm TEMPERATURE, °C
X (24)	MAXIMUM AIR TEMPERATURE, °C
Y (25)	MINIMUM AIR TEMPERATURE, °C
Z (26)	MAXIMUM WIND SPEED, km/h

Notes on quality control of data (HWC8990.DQC)

The following data elements have data that have been removed from the cleaned spreadsheet data files.

Wind speed and direction

Because of icing of the anemometer, the following data periods contain no data in the spreadsheet data files:

From 05:00, JD 254, to 20:00, JD 257
 07:00, JD 266, to 22:00, JD 266
 10:00, JD 267, to 17:00, JD 268
 14:00, JD 271, to 21:00, JD 273
 00:00, JD 275, to 01:00, JD 1
 07:00, JD 1, to 23:00, JD 95.

Snow depth

The snow-depth sensor baseline was set at 25.4 mm. This value was subtracted from the data in order to obtain corrected snow-depth information. The following time periods have no data because of erroneous data when a measurement was taken during a snowfall event or during periods of blowing snow: Julian day 312 to 319, 323, 327 to 329, 338 to 356, 361, and 363, 1989, Julian day 1 to 35, 39, 40, 45 to 59, 63, 75 and 134, 1990.

Hot Weather Creek, 1990–1991**List of data files (HWC9091.LST)**

FILE	STARTS	ENDS
RHWC90HB.WQ1 (.PRN)	13:00, JD 234 (August 22), 1990	06:00, JD 1 (January 1), 1991 (24:00, JD 365 [December 31], 1990)
RHWC91HA.WQ1 (.PRN)	07:00, JD 1 (January 1), 1991	11:00, JD 235 (August 23), 1991
RHWC90DB.WQ1 (.PRN)	JD 235 (August 23), 1990	JD 1 (January 1), 1991 (JD 365 [December 31], 1990)
RHWC91DA.WQ1 (.PRN)	JD 2 (January 2), 1991	JD 235 (August 23), 1991
RHWC90CB.WQ1 (.PRN)	JD 236 (August 24), 1990	JD 1 (January 1), 1991 (JD 365 [December 31], 1990)
RHWC91CA.WQ1 (.PRN)	JD 2 (January 2), 1991	JD 235 (August 23), 1991

Spreadsheet data-element description (HWC9091.SFT) (numbers in parentheses indicate order of element in .PRN files)

Hourly data

A (1)	YEAR
B (2)	JULIAN DAY
C (3)	TIME (HHMM, UTC)
D (4)	AIR TEMPERATURE, °C, HOURLY SAMPLE
E (5)	AIR RELATIVE HUMIDITY, %, HOURLY SAMPLE
F (6)	TWO-MINUTE MEAN WIND SPEED, MET-ONE, km/h
G (7)	TWO-MINUTE WIND DIRECTION VECTOR, RMY DIR, MET-ONE SPEED
H (8)	SAMPLE, SURFACE VEGETATION TEMPERATURE, °C
I (9)	SAMPLE, 10 cm SOIL TEMPERATURE, °C
J (10)	SAMPLE, 20 cm SOIL TEMPERATURE, °C
K (11)	SAMPLE, 50 cm SOIL TEMPERATURE, °C
L (12)	SAMPLE, 100 cm SOIL TEMPERATURE, °C
M (13)	TOTAL INCOMING SHORTWAVE RADIATION, MJ/m ²

Daily data

A (1)	YEAR
B (2)	MONTH
C (3)	DAY
D (4)	JULIAN DAY (one day ahead of date)
E (5)	TIME (HHMM, 06:00 UTC)
F (6)	MAXIMUM AIR TEMPERATURE, °C
G (7)	TIME OF MAXIMUM AIR TEMPERATURE
H (8)	MINIMUM AIR TEMPERATURE, °C
I (9)	TIME OF MINIMUM AIR TEMPERATURE
J (10)	MAXIMUM WIND SPEED, km/h
K (11)	TIME OF MAXIMUM WIND SPEED
L (12)	DIRECTION OF MAXIMUM WIND SPEED
M (13)	TOTAL INCOMING SHORTWAVE RADIATION
N (14)	SNOW DEPTH, mm
O (15)	BATTERY VOLTAGE

Calculated daily

A (1)	YEAR
B (2)	MONTH
C (3)	DAY
D (4)	JULIAN DAY (one day ahead of date)
E (5)	TIME (HHMM, 06:00 UTC)
F (6)	AVERAGE AIR TEMPERATURE, °C
G (7)	AVERAGE AIR RELATIVE HUMIDITY %
H (8)	AVERAGE WIND SPEED, km/h
I (9)	MAXIMUM SURFACE VEGETATION TEMPERATURE, °C
J (10)	MAXIMUM 10 cm TEMPERATURE, °C
K (11)	MAXIMUM 20 cm TEMPERATURE, °C
L (12)	MAXIMUM 50 cm TEMPERATURE, °C
M (13)	MAXIMUM 100 cm TEMPERATURE, °C
N (14)	AVERAGE SURFACE VEGETATION TEMPERATURE, °C
O (15)	AVERAGE 10 cm TEMPERATURE, °C
P (16)	AVERAGE 20 cm TEMPERATURE, °C
Q (17)	AVERAGE 50 cm TEMPERATURE, °C
R (18)	AVERAGE 100 cm TEMPERATURE, °C
S (19)	MINIMUM SURFACE VEGETATION TEMPERATURE, °C
T (20)	MINIMUM 10 cm TEMPERATURE, °C
U (21)	MINIMUM 20 cm TEMPERATURE, °C
V (22)	MINIMUM 50 cm TEMPERATURE, °C
W (23)	MINIMUM 100 cm TEMPERATURE, °C

Notes on quality control of data (HWC9091.DQC)

The Hot Weather Creek data for this 1990 to 1991 period contain periods of bad data associated with the anemometer and wind vane, the ultrasonic snow-depth sensor, and the radiometer.

Wind speed and direction

The main problem with the wind data occurs when the anemometer set becomes inoperative due to icing. For those periods, the wind-speed and wind-direction data were removed. These data gaps are:

16:00, 276 (October 3) to 16:00, 294 (October 21), 1990
 00:00, 306 (November 2) to 01:00, 341 (December 7), 1990
 13:00, 356 (December 22) to 10:00, 365 (December 31), 1990
 22:00, 6 (January 6) to 14:00, 43 (February 12), 1991

The wind data for the period 50 (February 19) to 86 (March 27) 1991 have been kept, but should be treated with caution since there is a higher frequency of calm winds and wind speeds are generally lower for that period.

Snow depth

The ultrasonic snow-depth sensor will give erroneous readings when taking measurements during periods of snowfall or blowing snow. As a result, all questionable data were removed. These gaps appear throughout the period from August 1990 to March 1991 and again briefly from May to August 1991. The baseline is 150 mm. This offset was probably introduced in June during the annual site visit. Confirmation of the offset will be done during the 1992 site visit.

Radiation

The pyranometer was briefly shaded for part of the day from March 24 to May 30, 1991. The data for clear days have been corrected; the data for cloudy days were not affected because of the diffuse light.

Temperature

All the temperature data have passed the initial quality control with one obvious exception. On July 22 (JD 203), 1991, the 50 cm soil temperature jumped from 2.2°C at 17:00 to 5.6°C at 18:00.

Hot Weather Creek, 1991–1992**List of data files (HWC9192.LST)**

FILE NAME	STARTS	ENDS
RHWC91HB.WQ1 (.PRN)	12:00, JD 235 (August 23), 1991	06:00, JD 1 (January 1), 1992 (24:00, JD 365 [December 31], 1991) local time
RHWC92HA.WQ1 (.PRN)	07:00, JD 1 (January 1), 1992	1700, JD 171 (June 19), 1992
RHWC91DB.WQ1 (.PRN)	JD 236 (August 24), 1991	JD 1 (January 1), 1992 (JD 365 [December 31], 1991) local time
RHWC92DA.WQ1 (.PRN)	JD 2 (January 2), 1992	JD 171 (June 19), 1992
RHWC91CB.WQ1 (.PRN)	JD 237 (August 25), 1991	JD 1 (January 1), 1992 (JD 365 [December 31], 1991) local time
RHWC92CA.WQ1 (.PRN)	JD 2 (January 2), 1992	JD 171 (June 19), 1992

Spreadsheet data-element description (HWC9192.SFT) (numbers in parentheses indicate order of element in .PRN file)

Hourly data

A (1)	YEAR
B (2)	JULIAN DAY
C (3)	TIME (HHMM, UTC)
D (4)	AIR TEMPERATURE, °C, HOURLY SAMPLE
E (5)	AIR RELATIVE HUMIDITY, %, HOURLY SAMPLE
F (6)	TWO-MINUTE MEAN WIND SPEED, MET-ONE, km/h
G (7)	TWO-MINUTE WIND DIRECTION VECTOR, RMY DIR, MET-ONE SPEED
H (8)	SAMPLE, SURFACE VEGETATION TEMPERATURE, °C
I (9)	SAMPLE, 10 cm SOIL TEMPERATURE, °C
J (10)	SAMPLE, 20 cm SOIL TEMPERATURE, °C
K (11)	SAMPLE, 50 cm SOIL TEMPERATURE, °C
L (12)	SAMPLE, 100 cm SOIL TEMPERATURE, °C
M (13)	TOTAL INCOMING SHORTWAVE RADIATION, MJ/m ²

Daily data

A (1)	YEAR
B (2)	MONTH
C (3)	DAY
D (4)	JULIAN DAY (one day ahead of date)
E (5)	TIME (HHMM, 06:00 UTC)
F (6)	MAXIMUM AIR TEMPERATURE, °C
G (7)	TIME OF MAXIMUM AIR TEMPERATURE
H (8)	MINIMUM AIR TEMPERATURE, °C
I (9)	TIME OF MINIMUM AIR TEMPERATURE
J (10)	MAXIMUM WIND SPEED, km/h
K (11)	TIME OF MAXIMUM WIND SPEED
L (12)	DIRECTION OF MAXIMUM WIND SPEED
M (13)	TOTAL INCOMING SHORTWAVE RADIATION
N (14)	SNOW DEPTH, mm
O (15)	BATTERY VOLTAGE

Calculated daily

A (1)	YEAR
B (2)	MONTH
C (3)	DAY

- D (4) JULIAN DAY (one day ahead of date)
- E (5) TIME (HHMM, 06:00 UTC)
- F (6) AVERAGE AIR TEMPERATURE, °C
- G (7) AVERAGE AIR RELATIVE HUMIDITY %
- H (8) AVERAGE WIND SPEED, km/h
- I (9) MAXIMUM SURFACE VEGETATION TEMPERATURE, °C
- J (10) MAXIMUM 10 cm TEMPERATURE, °C
- K (11) MAXIMUM 20 cm TEMPERATURE, °C
- L (12) MAXIMUM 50 cm TEMPERATURE, °C
- M (13) MAXIMUM 100 cm TEMPERATURE, °C
- N (14) AVERAGE SURFACE VEGETATION TEMPERATURE, °C
- O (15) AVERAGE 10 cm TEMPERATURE, °C
- P (16) AVERAGE 20 cm TEMPERATURE, °C
- Q (17) AVERAGE 50 cm TEMPERATURE, °C
- R (18) AVERAGE 100 cm TEMPERATURE, °C
- S (19) MINIMUM SURFACE VEGETATION TEMPERATURE, °C
- T (20) MINIMUM 10 cm TEMPERATURE, °C
- U (21) MINIMUM 20 cm TEMPERATURE, °C
- V (22) MINIMUM 50 cm TEMPERATURE, °C
- W (23) MINIMUM 100 cm TEMPERATURE, °C

Notes on quality control of data (HWC9192.DQC)

Wind speed and direction

Because of icing of the sensors and invalid data, the following time periods contain no wind data:

- 11:00, JD 271, 1991, to 12:00, JD 280, 1991
- 16:00, JD 288, 1991, to 22:00, JD 290, 1991
- 05:00, JD 310, 1991, to 17:00, JD 315, 1991
- 22:00, JD 326, 1991, to 06:00, JD 1, 1992
- 07:00, JD 1, 1992, to 23:00, JD 124, 1992

Soil temperature at 50 cm depth

The 50 cm soil-temperature data show a strong temperature drop from 10:00 to 11:00 on Julian day 270. The data have been left as is.

Snow depth

The snow-depth data have been eliminated throughout the period because of bad readings when the measurements were taken during periods of snowfall or blowing snow.

Hot Weather Creek, 1992–1993

List of data files (HWC9293.LST)

FILE	STARTS	ENDS
RHWC92HB.WQ1	07:00, JD 173 (June 21), 1992	06:00, JD 1 (January 1), 1993 (24:00, JD 366 [December 31] 1992) local time
RHWC93HA.WQ1	07:00, JD 1 (January 1), 1993	14:00, JD 170 (June 19), 1993
RHWC92DB.WQ1	JD 173 (June 21), 1992	JD 1 (January 1), 1992 (JD 366 [December 31], 1992) local time
RHWC93DA.WQ1	JD 2 (January 2), 1993	JD 170 (June 19), 1993
RHWC92CB.WQ1	JD 174 (June 22), 1992	JD 1 (January 1), 1993 (JD 366 [December 31], 1992) local time
RHWC93CA.WQ1	JD 2 (January 2), 1993	JD 170 (June 19), 1993

Spreadsheet data-element description (HWC9293.SFT) (numbers in parentheses indicate order of element in .PRN files)

Hourly data

A (1)	YEAR
B (2)	JULIAN DAY
C (3)	TIME (HHMM, UTC)
D (4)	AIR TEMPERATURE, °C, HOURLY SAMPLE
E (5)	AIR RELATIVE HUMIDITY, %, HOURLY SAMPLE
F (6)	TWO-MINUTE MEAN WIND SPEED, MET-ONE, km/h
G (7)	TWO-MINUTE WIND DIRECTION VECTOR, RMY DIR, MET-ONE SPEED
H (8)	SAMPLE, SURFACE VEGETATION TEMPERATURE, °C
I (9)	SAMPLE, 10 cm SOIL TEMPERATURE, °C
J (10)	SAMPLE, 20 cm SOIL TEMPERATURE, °C
K (11)	SAMPLE, 50 cm SOIL TEMPERATURE, °C
L (12)	SAMPLE, 100 cm SOIL TEMPERATURE, °C
M (13)	TOTAL INCOMING SHORTWAVE RADIATION, MJ/m ²
N (14)	TWO-MINUTE WIND VECTOR SPEED, MET-ONE, km/h
O (15)	TWO-MINUTE MEAN WIND SPEED, RMY, km/h
P (16)	TWO-MINUTE WIND VECTOR SPEED, RMY, km/h
Q (17)	TWO-MINUTE WIND VECTOR DIRECTION, RMY, DEGREES
R (18)	TWO-MINUTE DIRECTION STANDARD DEVIATION, RMY
S (19)	TOTAL REFLECTED SHORTWAVE RADIATION, MJ/m ²
T (20)	SAMPLE, SNOW DEPTH, mm
U (21)	TOTAL HOURLY RAINFALL, mm

Daily data

A (1)	YEAR
B (2)	MONTH
C (3)	DAY
D (4)	JULIAN DAY (one day ahead of date)
E (5)	TIME (HHMM, 06:00 UTC)
F (6)	MAXIMUM AIR TEMPERATURE, °C
G (7)	TIME OF MAXIMUM AIR TEMPERATURE
H (8)	MINIMUM AIR TEMPERATURE, °C
I (9)	TIME OF MINIMUM AIR TEMPERATURE
J (10)	MAXIMUM WIND SPEED, km/h
K (11)	TIME OF MAXIMUM WIND SPEED
L (12)	DIRECTION OF MAXIMUM WIND SPEED
M (13)	TOTAL INCOMING SHORTWAVE RADIATION
N (14)	SNOW DEPTH, mm
O (15)	BATTERY VOLTAGE
P (16)	TOTAL REFLECTED SHORTWAVE RADIATION

Calculated daily

A (1)	YEAR
B (2)	MONTH
C (3)	DAY
D (4)	JULIAN DAY (one day ahead of date)
E (5)	TIME (HHMM, 06:00 UTC)
F (6)	AVERAGE AIR TEMPERATURE, °C
G (7)	AVERAGE AIR R.H., %
H (8)	AVERAGE WIND SPEED, km/h
I (9)	MAXIMUM SURFACE VEGETATION TEMPERATURE, °C
J (10)	MAXIMUM 10 cm TEMPERATURE, °C
K (11)	MAXIMUM 20 cm TEMPERATURE, °C
L (12)	MAXIMUM 50 cm TEMPERATURE, °C

- M (13) MAXIMUM 100 cm TEMPERATURE, °C
- N (14) AVERAGE SURFACE VEGETATION TEMPERATURE, °C
- O (15) AVERAGE 10 cm TEMPERATURE, °C
- P (16) AVERAGE 20 cm TEMPERATURE, °C
- Q (17) AVERAGE 50 cm TEMPERATURE, °C
- R (18) AVERAGE 100 cm TEMPERATURE, °C
- S (19) MINIMUM SURFACE VEGETATION TEMPERATURE, °C
- T (20) MINIMUM 10 cm TEMPERATURE, °C
- U (21) MINIMUM 20 cm TEMPERATURE, °C
- V (22) MINIMUM 50 cm TEMPERATURE, °C
- W (23) MINIMUM 100 cm TEMPERATURE, °C
- X (24) EMPTY
- Y (25) EMPTY
- Z (26) EMPTY
- AA (27) TOTAL PRECIPITATION, mm

Notes on quality control of data (HWC9293.DQC)

Wind speed and direction

Wind data were removed for the following periods when the sensors were frozen by icing:

- For 1992: 07:00, JD 271, to 06:00, JD 272
- 16:00, JD 275, to 10:00, JD 277
- 14:00, JD 278, to 22:00, JD 278
- 23:00, JD 280, to 18:00, JD 286
- 10:00, JD 290, to 08:00, JD 292
- 06:00, JD 293, to 12:00, JD 304
- 03:00, JD 307, to 00:00, JD 308
- 18:00, JD 309, to 19:00, JD 312
- 17:00, JD 315, to 06:00, JD 1

- For 1993: 07:00, JD 2, to 07:00, JD 13
- 04:00, JD 17, to 02:00, JD 20
- 11:00, JD 25, to 23:00, JD 28
- 04:00, JD 30, to 17:00, JD 67
- 15:00, JD 68, to 20:00, JD 80
- 12:00, JD 86, to 15:00, JD 90
- 11:00, JD 93, to 03:00, JD 95
- 10:00, JD 101, to 05:00, JD 109
- 18:00, JD 114, to 06:00, JD 115
- 11:00, JD 118, to 00:00, JD 131
- 13:00, JD 134, to 12:00, JD 135

Snow depth

Throughout the period of measurement, data gaps exist because of bad measurements taken during periods of snowfall or blowing snow. An offset of 31.5 mm was applied to the snow-depth data because of an incorrect offset established when the sensor was installed.

Hot Weather Creek, 1993–1994**List of data files (HWC9394.LST)**

FILE	STARTS	ENDS
RHWC93HB.WQ1 (.PRN)	17:00, JD 171 (June 20), 1993	06:00, JD 1 (January 1), 1994 (24:00, JD 365 [December 31], 1993) local time
RHWC94HA.WQ1 (.PRN)	07:00, JD 1 (January 1), 1994	20:00, JD 169 (June 18), 1994
RHWC93DB.WQ1 (.PRN)	JD 172 (June 21), 1993	JD 1 (January 1), 1994 (JD 365 [December 31], 1993) local time
RHWC94DA.WQ1 (.PRN)	JD 2 (January 2), 1994	JD 169 (June 18), 1994
RHWC93CB.WQ1 (.PRN)	JD 173 (June 22), 1993	JD 1 (January 1), 1993 (JD 365 [December 31], 1993) local time
RHWC94CA.WQ1 (.PRN)	JD 2 (January 2), 1994	JD 169 (June 18), 1994

Spreadsheet data-element description (HWC9394.SFT) (numbers in parentheses indicate order of element in .PRN files)

Hourly data

A (1)	YEAR
B (2)	JULIAN DAY
C (3)	TIME (HHMM, UTC)
D (4)	AIR TEMPERATURE, °C, HOURLY SAMPLE
E (5)	AIR RELATIVE HUMIDITY, %, HOURLY SAMPLE
F (6)	TWO-MINUTE MEAN WIND SPEED, MET-ONE, km/h
G (7)	TWO-MINUTE WIND DIRECTION VECTOR, RMY DIR, MET-ONE SPEED
H (8)	SAMPLE, SURFACE VEGETATION TEMPERATURE, °C
I (9)	SAMPLE, 10 cm SOIL TEMPERATURE, °C
J (10)	SAMPLE, 20 cm SOIL TEMPERATURE, °C
K (11)	SAMPLE, 50 cm SOIL TEMPERATURE, °C
L (12)	SAMPLE, 100 cm SOIL TEMPERATURE, °C
M (13)	TOTAL INCOMING SHORTWAVE RADIATION, MJ/m ²
N (14)	TWO-MINUTE WIND VECTOR SPEED, MET-ONE, km/h
O (15)	TWO-MINUTE MEAN WIND SPEED, RMY, km/h
P (16)	TWO-MINUTE WIND VECTOR SPEED, RMY, km/h
Q (17)	TWO-MINUTE WIND VECTOR DIRECTION, RMY, DEGREES
R (18)	TWO-MINUTE DIRECTION STANDARD DEVIATION, RMY
S (19)	TOTAL REFLECTED SHORTWAVE RADIATION, MJ/m ²
T (20)	SAMPLE, SNOW DEPTH, mm
U (21)	TOTAL HOURLY RAINFALL, mm

Daily data

A (1)	YEAR
B (2)	MONTH
C (3)	DAY
D (4)	JULIAN DAY (one day ahead of date)
E (5)	TIME (HHMM, 06:00 UTC)
F (6)	MAXIMUM AIR TEMPERATURE, °C
G (7)	TIME OF MAXIMUM AIR TEMP.
H (8)	MINIMUM AIR TEMPERATURE, °C
I (9)	TIME OF MINIMUM AIR TEMPERATURE
J (10)	MAXIMUM WIND SPEED, km/h
K (11)	TIME OF MAX. WIND SPEED
L (12)	DIRECTION OF MAXIMUM WIND SPEED
M (13)	TOTAL INCOMING SHORTWAVE RADIATION

N (14) SNOW DEPTH, mm
 O (15) BATTERY VOLTAGE
 P (16) TOTAL REFLECTED SHORTWAVE RADIATION

MONTH	MISSING DAYS (JD)	MONTHLY MEANS
June 1988	up to JD 126 (June 24)	eliminate
August 1988	from 07:00 JD 232 (August 19) to end	eliminate
September 1988	from beginning to JD 262 (September 18)	eliminate
May 1989	one hour of data	ok
June 1989	from 21:00 JD 171 (June 20) to 06:00 JD 175 (June 25) and JD 176 unreliable	eliminate
June 1990	from 06:00 JD 168 (June 17) to 15:00 JD 173 (June 22)	eliminate
February 1991	one hour	ok
June 1991	from 17:00 JD 170 (June 19) to 18:00 JD 171 (June 20)	ok
June 1992	from 17:00 JD 171 (June 19) to 07:00 JD 173 (June 21)	ok
June 1993	from 14:00 JD 170 (June 19) to 17:00 JD 171 (June 20)	ok
June 1994	up to JD 169 (June 18)	eliminate

Calculated daily

A (1) YEAR
 B (2) MONTH
 C (3) DAY
 D (4) JULIAN DAY (one day ahead of date)
 E (5) TIME (HHMM, 06:00 UTC)
 F (6) AVERAGE AIR TEMPERATURE, °C
 G (7) AVERAGE AIR R.H., %
 H (8) AVERAGE WIND SPEED, km/h
 I (9) MAXIMUM SURF/VEG TEMPERATURE, °C
 J (10) MAXIMUM 10 cm TEMPERATURE, °C
 K (11) MAXIMUM 20 cm TEMPERATURE, °C
 L (12) MAXIMUM 50 cm TEMPERATURE, °C
 M (13) MAXIMUM 100 cm TEMPERATURE, °C
 N (14) AVERAGE SURFACE VEGETATION TEMPERATURE, °C
 O (15) AVERAGE 10 cm TEMPERATURE, °C
 P (16) AVERAGE 20 cm TEMPERATURE, °C
 Q (17) AVERAGE 50 cm TEMPERATURE, °C
 R (18) AVERAGE 100 cm TEMPERATURE, °C
 S (19) MINIMUM SURFACE VEGETATION TEMPERATURE, °C
 T (20) MINIMUM 10 cm TEMPERATURE, °C
 U (21) MINIMUM 20 cm TEMPERATURE, °C
 V (22) MINIMUM 50 cm TEMPERATURE, °C
 W (23) MINIMUM 100 cm TEMPERATURE, °C
 X (24) EMPTY
 Y (25) EMPTY
 Z (26) EMPTY
 AA (27) TOTAL PRECIPITATION, mm

Notes on quality control of data (HWC9394.DQC)*Wind speed and direction*

Wind data were removed for the following periods when the sensors were frozen by icing:

For 1993, both anemometers: 11:00, JD 262, to 17:00, JD 265
 10:00, JD 274, to 15:00, JD 278
 07:00, JD 284, to 18:00, JD 294
 21:00, JD 295, to 06:00, JD 300
 22:00, JD 304, to 11:00, JD 306
 12:00, JD 307, to 20:00, JD 328
 07:00, JD 336, to 06:00, JD 364

For 1994, RMY anemometer: 07:00, JD 36, to 06:00, JD 75
 For 1994, Met-One anemometer: 07:00, JD 36, to 16:00, JD 42
 07:00, JD 54, to 06:00, JD 57
 For 1994, both anemometers: 12:00, JD 131, to 12:00, JD 132

Snow depth

Throughout the period of measurement, data gaps exist because of bad measurements taken during periods of snowfall or blowing snow. A correction factor of 31.5 mm was applied to the snow-depth data because of an incorrect offset established when the sensor was installed.

Value added data: combined files of selected data (HWC.CMB) from Hot Weather Creek, 1988–1994**List of missing days in data files (usually at time of station servicing)**

Spreadsheet data-element description (numbers in parentheses indicate order of element in .PRN file)

HWCCOMP.WQ1

A (1) YEAR
 B (2) MONTH
 C (3) DAY (CST)
 D (4) JULIAN DAY (UCT)
 E (5) TIME
 F (6) MAXIMUM AIR TEMPERATURE, °C
 G (7) MINIMUM AIR TEMPERATURE, °C
 H (8) TOTAL INCOMING SHORTWAVE RADIATION, MJ/m²
 I (9) SNOW DEPTH, mm
 J (10) MEAN OF 24 ONE-HOURLY AIR TEMPERATURES, °C
 K (11) RELATIVE HUMIDITY, %
 L (12) AVERAGE WIND SPEED, km/h
 M (13) TOTAL OUTGOING SHORT WAVE RADIATION
 N (14) SURFACE ALBEDO, %
 O (15) MEAN OF MAXIMUM AND MINIMUM AIR TEMPERATURE, °C
 P (16) MELTING DEGREE DAYS FROM T_{mean24} ONE-HOURLY, °C
 Q (17) MELTING DEGREE DAYS FROM T_{mean} MAXIMUM AND MINIMUM TEMPERATURES, °C

Notes

The data begin on 24 June 1988 and end 17 June 1994

The maximum and minimum temperatures for the logger year 1989–1990 are not extreme two-minute values, but rather have been calculated from the 24 one-hourly observations. Thus, the diurnal range is damped. The mean air temperature for this year is also calculated from these damped maximum and minimum temperatures.

HWCMEAN.WQI

A (1)	YEAR
B (2)	MONTH
C (3)	MAXIMUM AIR TEMPERATURE, °C
D (4)	MINIMUM AIR TEMPERATURE, °C
E (5)	MEAN OF 24 ONE-HOURLY AIR TEMPERATURES, °C
F (6)	TOTAL DAILY SHORT WAVE RADIATION, MJ/m ²
G (7)	MEAN RELATIVE HUMIDITY, %
H (8)	MEAN 10 cm GROUND TEMPERATURE, °C
I (9)	MEAN 20 cm GROUND TEMPERATURE, °C
J (10)	MEAN 50 cm GROUND TEMPERATURE, °C
K (11)	MEAN 100 cm GROUND TEMPERATURE, °C
L (12)	SNOW-ON-GROUND AT END OF MONTH, mm
M (13)	TOTAL DAILY OUTGOING SHORTWAVE RADIATION, MJ/m ²
N (14)	MEAN SURFACE ALBEDO, %
O (15)	MEAN OF MAXIMUM AND MINIMUM AIR TEMPERATURE, °C
P (16)	MELTING DEGREE DAYS FROM 24 ONE-HOURLY, °C
Q (17)	MELTING DEGREE DAYS FROM MAXIMUM AND MINIMUM TEMPERATURES, °C

Notes

See above for note on maximum and minimum temperatures in the 1989–1990 logger year.

Snow-on-ground at end of month was extracted from the daily data to match data recorded at Eureka.

PART 2: EUREKA INSTRUMENTATION AND DOCUMENTATION

Surface and upper-air instruments (Department of Transport, 1961)

Barometer

An MSC Kew-Patterson barometer, serial number 85-43, has been used since the station was established. It is installed at an elevation of 2.4 m, on an inside wall, facing north. For each observation, a station pressure card is used, incorporating a reduction to mean sea level as well as corrections for temperature of the barometer, index error, and gravity.

A Friez barograph has been in operation since the station was established, providing a continuous record of pressure variations. It is time-marked and checked against the reading of the mercury barometer every six hours.

Thermometers

Because of breakage and the development of defects during use, a considerable number of thermometers have been used since the station was first established. Thermometers used were MSC ordinary thermometers, mercury-filled, and wet- and dry-bulb thermometers, MSC mercury-filled maximum thermometers, and MSC alcohol minimum thermometers. All were calibrated at the laboratories of the Meteorological Branch of Canada and appropriate correction cards were issued. These were used at the station to obtain a corrected temperature reading from each thermometer for every weather observation taken.

Hygrothermograph

A United States Weather Bureau hygrothermograph has been used to obtain a temperature-humidity record. Unfortunately, difficulties encountered with blowing snow clogging the instrument and clock stoppages in the continuously cold weather in winter have resulted in an intermittent record. The thermograph was never used to measure current temperatures and the hair hygrometer was never used to measure humidity. Both instruments served merely as a check on values of temperature and humidity obtained from the dry- and wet-bulb thermometers.

Stevenson screen

A Stevenson screen with exterior dimensions 61.12 cm by 45.72 cm by 68.27 cm high has been used to house all thermometers and the hygrothermograph. The screen is a double-louvred box painted white, with its base 1.05 m above the ground. Drifting and blowing snow does not normally accumulate around the screen.

Wind equipment

The wind equipment is the standard MSC type 45 equipment consisting of an anemovane, combining a rotating-cup anemometer and a wind vane, a recording anemograph, and a flashing-light wind indicator. The anemovane is mounted on a 7.5 m mast.

Theodolite

A David White type ML 47 theodolite has been used since the station was established. It is mounted in a pibal shelter. An aluminium pibal dome was installed on the shelter in August 1953.

Precipitation-measuring equipment

An 20.32 cm, nonrecording rain gauge is used for measuring the amount of liquid precipitation. Snowfall measurements are made with a 30.48 cm ruler. Precipitation measurements are carried out every six hours.

Upper-air equipment

Eureka has been a full rawinsonde station from the outset. An SCR 658 radio theodolite is housed in an insulated, fabric-covered dome. There is a double installation of Leeds and Northrup Type G Speedomax recorders. In 1955, the installation was improved by the provision of a plastic rawin dome and supporting building, which together will accommodate both the SCR 658 and the recorders at one location.

Current surface instrumentation

The following comments on the instrumentation are recorded in the current site description (Atmospheric Environment Service, 1991):

The instruments are well exposed, some on a flat gravel plain, others on a slight rise to the northeast, in order to take advantage of higher elevation. Airflow from all directions is unobstructed and there should be no vehicle traffic in the vicinity.

Surface observations are performed hourly with the exception of 04:00 and 05:00 UTC. During the operational hours, specials are also performed when significant changes in weather conditions occur. Synoptic observations are performed at six-hour intervals and upper-air observations, at 00:00 and 12:00 UTC.

Table 1 (Atmospheric Environment Service, 1991) gives details of the instrumentation.

Table 1. Instrument and equipment systems

Equipment class	Type or model	Remarks or special notes
1) PRESSURE		
Mercury barometer Altimeter setting indicator Barograph	NCC Kollsman standard	serial number d-496, altimeter thermometer QC77-0043 no edge lighting midscale: 1000 mb
2) CLOUD and VISIBILITY		
Ceiling balloon system Ceiling projector	3° helium 116 vAC	standard cabinete baseline: 305 m
3) TEMPERATURE		
Maximum thermometer Minimum thermometer Thermometer Stevenson screen Remote temperature indicator Psychrometer Dewcel probe Dry thermister	synoptic synoptic ordinary columnar digital RTI plug-in motor AES AES standard	with correction cards with correction cards with correction cards
4) PRECIPITATION		
Ordinary rain gauge Nipher snow gauge Snow rulers Ice accretion indicator	type B surface type IV	rim height: 40 cm; spare graduate on site rim height: 175 cm; aluminium shield mounted on alidade
5) WIND		
Direction detector Speed dectector Display unit Remote processor Wind tower	78D 78D 78D 78D tilting	cupwheel height 10 m cupwheel height: 10 m

REFERENCES

Alt, B.T., Labine, C.L., Desrochers, D.T., Young, K.L., and Garneau, M.

2000: Climate and ground thermal data, 1988–1994: Hot Weather Creek area, Fosheim Peninsula, Nunavut; Geological Survey of Canada, Open File D3783.

Atmospheric Environment Service

1991: Observation Site Data: Eureka; Atmospheric Environment Services, Downsview, Ontario, 4 p.

Department of Transport

1961: Climatological Summary, Eureka, N.W.T., Canada: June 1947 to December 1953; Meteorological Branch, Department of Transport, Toronto, Ontario.

Young, K.L., Woo, M-k., and Edlund, S.A.

1997: Influence of local topography, soils, and vegetation on microclimate and hydrology at a High Arctic site, Ellesmere Island, Canada; Arctic and Alpine Research, v. 29, no. 3, p. 270–284.

APPENDIX B

Sawtooth Range meteorological data

P.M. Wolfe

Table B1. Instrumentation of the valley meteorological station.

Measurement	Instrument and model	Instrument height
Air temperature	Campbell Scientific Inc. 107 temperature probe	2.0 m
Wind speed and direction	R.H. Young wind monitor	0.5 m
Incoming shortwave radiation	Li-Cor LI 200SZ pyranometer	1.8 m
Soil temperature	Campbell Scientific Inc. 107 temperature probe	-0.05 m, -0.1 m, -0.15 m, -0.2 m

Table B2. Average daily meteorological data from the glacier meteorological station, Quviagivaa Glacier, 875 m a.s.l., 1993.

Date	Air temperature (°C)	MDD ¹ (°C)	K down ² (W/m ²)	KDD ³ (W/m ²)	Net Rad. (W/m ²)	NRD ⁴ (W/m ²)	Wind speed ⁵ (m/s)	Wind direction ⁷	Glacier albedo ⁸
30 May	3.5	1	316	7579	-18.2	212			
31 May	-4.2	3	326	7820	-10.7	293			
1 June	-2.5	15	340	8163	-17.7	304			
2 June	-5.3	0	305	7320	-33.8	98			
3 June	5.4	0	349	8368	-37.4	100	2.1	NE-E	
4 June	4.3	5	340	8158	-24.8	226	0.9	NE-E	
5 June	-3.2	6	350	8396	-23.4	256	1	E-SE	
6 June	2.2	5	305	7311	-5.4	306	0.8	E-SE	
7 June	1	7	192	4605	-0.3	124	0.4	NE-E	
8 June	-0.7	11	275	6599	-4.6	189	1.2	NE-E	
9 June	-2.5	3	346	8299	-21.2	289	2.7	NE-E	
10 June	2.6	0	228	5460	-19.1	59	5.4	NE-E	
11 June	-2.1	0	317	7596	-20.9	127	5.7	NE-E	
12 June	1.7	44	299	7185	-9.7	208	2.9	NE-E	
13 June	0.9	22	162	3898	-1.8	103	2.2	NE-E	
14 June	0.2	14	244	5860	6.4	384	1.6	NE-E	0.68
15 June	1	36	239	5743	8.2	298	0.8	NE-E	
16 June	0.2	11	5887	245	5.8	325	1.2	NE-E	
17 June	0.4	5	253	6070	12.1	395	3.4	NE-E	
18 June	0	12	297	7134	-2.7	279	3.3	E-SE	0.67
19 June	1.8	52	343	8221	-3.4	491	1.7	NE-E	
20 June	1.8	47	215	5171	7.6	410	1.2	E-SE	0.61
21 June	0.4	11	235	5639	12	464	3.6	NE-E	
22 June	2.1	54	276	6635	6.6	417	1.1	NE-E	0.61
23 June	2.1	51	243	5822	17.2	570	2.9	NE-E	
24 June	0.6	1	199	4768	5.6	136	2.2	E-SE	0.69
25 June	2.1	0	268	6423	-25.4	27	1.4	SE-S	
26 June	-1.5	0	178	4261	2.3	124	1.3	SE-S	0.73
27 June	0.4	24	143	3432	1.2	97	0.8	SE-S	
28 June	2.1	58	178	4277	11	403	0.6	E-SE	0.61
29 June	4.1	100	311	7467	13.8	732	0.8	E-SE	
30 June	5.1	123	241	5777	29.8	844	1.4	W-NW	0.44
1 July	3.8	92	168	4042	71	1704	1.2	E-SE	
2 July	-1	0	172	4125	56.7	1360	1.1	W-NW	
3 July	0.9	27	166	3973	48.9	1174	1.1	W-NW	
4 July	3.8	90	284	6806	52.7	1379	0.8	E-SE	0.5
5 July	4.9	117	305	7313	17	604	0.8	E-SE	
6 July	3.4	82	199	4771	38.9	1022	1.2	E-SE	0.48
7 July	4.9	119	264	6347	27	811	1.4	E-SE	
8 July	5.8	138	272	6520	41.4	1137	1.7	NE-E	0.41
9 July	7.9	190	301	7233	51.9	1347	1.5	E-SE	
10 July	6.6	158	308	7399	90.6	2277	2.4	E-SE	0.42
11 July	4.2	100	147	3537	50.5	1400	3.1	E-SE	

Table B2. (cont.)

Date	Air temperature (°C)	MDD ¹ (°C)	K down ² (W/m ²)	KDD ³ (W/m ²)	Net Rad. (W/m ²)	NRD ⁴ (W/m ²)	Wind speed ⁵ (m/s)	Wind direction ⁷	Glacier albedo ⁸
12 July	4	97	155	3718	73.4	1762	1.7	E-SE	0.39
13 July	5.3	127	263	6322	84.6	2138	2.1	NE-E	
14 July	5	121	233	5585	76.9	1936	1.3	E-SE	0.38
15 July	6.3	152	265	6362	73.3	1787	1.7	W-NW	
16 July	2.9	69	130	3112	72.4	1743	0.8	E-SE	0.47
17 July	4.1	99	257	6162	82.6	2006	2.5	W-NW	
18 July	3.4	81	147	3537	68.8	1696	1.2	E-SE	
19 July	3.3	80	118	2842	79.1	1898	1.9	SW-W	0.38
20 July	1.9	46	51	1215	52.5	1260	1	SW-W	
21 July	1.7	41	70	1683	63	1511	0.6	E-SE	
22 July	2.5	59	104	2486	60.8	1464	0.7	E-SE	
23 July	3.2	77	125	3001	75.6	1813	0.8	E-SE	
24 July	2.8	66	122	2932	55.9	1347	0.6	SE-S	0.37
25 July	2.6	63	152	3653	67.7	1690	0.6	NE-E	
26 July	2.6	62	124	2970	69.9	1677	0.8	E-SE	0.4
27 July	2.2	52	91	2179	52.4	1258	0.8	E-SE	
28 July	2.9	70	122	2920	61	1464	0.4	NE-E	0.39
29 July	2.7	65	158	3795	54.4	1378	0.7	NE-E	
30 July	4.3	103	203	4862	74.4	1897	1.1	E-SE	0.41
31 July	6	143	173	4155	73.5	1811	1.5	SE-S	
1 August	3.9	93	149	3573	81.7	2049	0.8	E-SE	0.31
2 August	1.3	32	58	1395	44.1	1059	0.3	NE-E	
3 August	0.1	2	72	1739	20.2	486	0.7	SE-S	0.57
4 August	-2.8	0	84	2027	4.2	104	1.7	SW-W	
5 August	-5.5	0	134	3220	-2.3	38	1.1	SE-S	
6 August	-4.9	0	119	2851	-6.2	5	3.3	E-SE	
7 August	-5.9	0	149	3567	4.9	226	1.7	S-SW	
8 August	-4.5	0	129	3096	-8.7	1	3.6	E-SE	
9 August	-4.3	0	115	2749	-5.9	2	5.2	N-NE	
10 August	-4.6	0	124	2987	-5.8	0	2.3	SW-W	

Notes:

Air temperature, net radiation, and wind speed are average values, taken from hourly measurements.

¹MDD is 'melting degree days', the sum of all positive hourly temperatures.

²K down is incoming shortwave radiation.

³KDD is 'K down days', the sum of all hourly incoming shortwave radiation values.

⁴NRD is 'net radiation days', the sum of all positive hourly net radiation values.

⁵Wind speed is an average value from hourly values.

⁷Wind direction is the predominant wind direction for the day.

⁸Glacier albedo is the average albedo using measurements from 6–12 ablation stations.

Italicized values are estimated due to missing data.

Table B3. Glacier meteorological station wind direction frequency by sector, 1993.

Date	Down-glacier winds				Up-glacier winds				% windy
	N-NE	NE-E	E-SE	SE-S	S-SW	SW-W	W-NW	NW-N	
3 June	0%	46%	38%	14%	1%	1%	0%	0%	100.0 0%
4 June	2%	36%	36%	5%	11%	7%	2%	0%	99.99%
5 June	3%	31%	33%	29%	4%	1%	0%	0%	99.99%
6 June	1%	11%	48%	8%	4%	17%	10%	1%	99.98%
7 June	11%	24%	12%	11%	13%	20%	8%	1%	99.99%
8 June	11%	59%	21%	5%	1%	1%	1%	1%	99.98%
9 June	4%	77%	18%	0%	0%	0%	0%	0%	100.00%
10 June	2%	74%	23%	0%	0%	0%	0%	0%	100.00%
11 June	6%	90%	4%	0%	0%	0%	0%	0%	100.00%
12 June	8%	68%	10%	3%	1%	1%	7%	3%	100.00%
13 June	11%	73%	7%	0%	8%	1%	0%	1%	99.85%
14 June	5%	38%	17%	5%	3%	11%	18%	4%	100.35%
15 June	5%	31%	11%	5%	6%	28%	13%	1%	99.99%
16 June	3%	63%	21%	7%	2%	3%	0%	1%	99.87%
17 June	9%	58%	22%	7%	3%	1%	0%	0%	99.99%
18 June	1%	17%	67%	15%	0%	0%	0%	0%	99.98%
19 June	19%	35%	19%	4%	3%	4%	11%	6%	99.86%
20 June	4%	24%	34%	22%	10%	5%	0%	1%	99.99%
21 June	1%	49%	43%	7%	1%	0%	0%	0%	99.98%
22 June	5%	48%	37%	6%	1%	1%	1%	1%	99.72%
23 June	4%	68%	24%	3%	0%	0%	0%	1%	100.13%
24 June	1%	22%	37%	28%	11%	1%	0%	0%	99.98%
25 June	1%	2%	14%	56%	22%	4%	0%	0%	99.97%
26 June	0%	0%	20%	58%	13%	7%	0%	0%	100.00%
27 June	4%	4%	26%	28%	22%	12%	3%	1%	99.98%
28 June	8%	23%	50%	10%	4%	2%	2%	1%	99.85%
29 June	2%	19%	43%	5%	7%	18%	5%	1%	100.00%
30 June	2%	21%	19%	5%	5%	7%	38%	3%	99.98%
1 July	1%	19%	55%	3%	6%	9%	7%	0%	99.98%
2 July	2%	5%	2%	1%	4%	37%	47%	2%	99.99%
3 July	0%	24%	16%	4%	11%	17%	27%	0%	99.99%
4 July	7%	18%	34%	13%	1%	2%	16%	9%	99.85%
5 July	10%	20%	41%	11%	4%	6%	5%	4%	99.97%
6 July	0%	11%	68%	20%	0%	0%	0%	0%	99.99%
7 July	2%	26%	59%	14%	0%	0%	0%	0%	99.99%
8 July	2%	76%	22%	0%	0%	0%	0%	0%	100.00%
9 July	6%	43%	50%	1%	0%	1%	0%	0%	99.98%
10 July	7%	32%	60%	1%	0%	0%	0%	0%	100.01%
11 July	0%	4%	90%	5%	0%	0%	0%	0%	100.00%
12 July	4%	44%	46%	4%	1%	0%	0%	1%	99.98%
13 July	2%	70%	26%	0%	1%	1%	0%	0%	100.00%
14 July	2%	32%	37%	1%	0%	1%	23%	4%	100.00%
15 July	2%	12%	5%	2%	3%	18%	52%	6%	99.98%
16 July	2%	42%	47%	4%	2%	1%	2%	1%	100.00%
17 July	0%	85%	15%	0%	0%	0%	0%	0%	100.00%
18 July	1%	32%	35%	2%	8%	18%	2%	1%	100.00%
19 July	5%	16%	4%	1%	7%	65%	1%	1%	99.98%
20 July	1%	14%	24%	0%	3%	47%	10%	0%	100.00%
21 July	3%	29%	58%	2%	0%	4%	2%	1%	99.99%
22 July	9%	26%	40%	15%	3%	2%	1%	3%	99.98%
23 July	4%	9%	26%	21%	11%	22%	5%	3%	99.98%
24 July	5%	11%	18%	29%	12%	10%	11%	4%	100.00%
25 July	11%	42%	27%	12%	4%	2%	1%	1%	99.84%
26 July	4%	26%	57%	8%	1%	1%	2%	2%	99.74%
27 July	1%	39%	54%	2%	1%	1%	3%	0%	99.85%
28 July	10%	32%	25%	11%	4%	6%	8%	3%	99.71%
29 July	4%	50%	35%	3%	2%	2%	2%	1%	99.86%
30 July	3%	23%	43%	25%	4%	1%	1%	0%	99.98%
31 July	3%	5%	20%	36%	26%	7%	3%	1%	99.85%
1 August	6%	29%	37%	13%	5%	8%	1%	1%	99.98%
2 August	9%	42%	16%	4%	3%	9%	11%	6%	99.99%
3 August	2%	5%	25%	32%	14%	11%	9%	2%	100.01%
4 August	0%	0%	0%	1%	6%	53%	38%	1%	100.00%
5 August	1%	11%	22%	27%	15%	16%	8%	0%	100.00%
6 August	0%	22%	41%	10%	11%	16%	0%	0%	99.98%
7 August	1%	0%	6%	22%	40%	28%	2%	0%	99.98%
8 August	0%	8%	49%	41%	1%	0%	0%	0%	100.00%
9 August	1%	76%	23%	0%	0%	0%	0%	0%	100.00%
10 August	0%	5%	13%	6%	31%	44%	1%	0%	100.00%
Average	3.80%	32.27%	30.77%	10.92%	5.86%	8.93%	6.11%	1.29%	99.97%

Table B4. Average daily meteorological data from the Valley meteorological station, 230 m a.s.l., 1993

Date	Air temperature (°C)	MDD ¹ (°C)	K down ² (W/m ²)	KDD ³ (W/m ²)	Wind speed (m/s)	Wind direction ⁴
4 June	0.8	25	307	7377	0.8	S-SW
5 June	1.2	35	329	7900	1.1	SW-W
6 June	2	48	320	7681	1.1	SW-W
7 June	2.1	50	141	3395	1.9	N-NE
8 June	3.1	74	235	5637	4.3	N-NE
9 June	4	96	329	7905	3.3	N-NE
10 June	2.8	66	144	3448	5.2	NE-N
11 June	4	95	334	8015	8.3	NE-N
12 June	6.6	158	279	6685	4.3	NE-N
13 June	3.1	75	148	3547	2.6	N-NE
14 June	3	73	237	5698	3.1	N-NE
15 June	3.6	87	254	6103	4.3	N-NE
16 June	3.7	88	149	3577	0.8	S-SW
17 June	5	120	221	5293	3.6	NE-N
18 June	5.7	136	281	6749	4.2	SE-S
19 June	6.5	157	331	7946	4.3	NE-N
20 June	7	167	267	6407	3.1	N-NE
21 June	6.5	155	212	5085	2.7	SE-S
22 June	7.3	175	271	6514	1.2	NE-E
23 June	8.4	202	264	6346	3.7	NE-E
24 June	3.6	86	123	2959	3.3	S-SW
25 June	2	49	202	4848	6.1	S-SW
26 June	3.1	75	174	4178	3	S-SW
27 June	3.7	88	140	3363	0.7	W-NW
28 June	7.2	172	196	4694	1	N-NE
29 June	9.9	238	304	7286	1.3	W-NW
30 June	11.9	287	250	5991	1.1	N-NE
1 July	11	265	165	3958	1.6	NW-N
2 July	3	73	184	4424	1.8	NW-N
3 July	5.2	126	155	3712	2.3	N-NE
4 July	9.1	218	267	6401	4.2	N-NE
5 July	10.9	262	310	7445	2.6	N-NE
6 July	12.7	306	334	8010	1.5	W-NW
7 July	13.4	322	272	6539	1.3	W-NW
8 July	14.4	345	293	7038	2	E-SE
9 July	14.8	356	314	7530	2.4	NE-E
10 July	14.6	350	316	7576	3.1	NE-E
11 July	12.1	291	170	4073	2.9	SE-S
12 July	10.1	243	176	4233	1.5	W-NW
13 July	13.6	327	278	6671	2.5	N-NE
14 July	13.3	319	282	6757	1.6	W-NW
15 July	13.4	322	270	6468	4.2	NW-N
16 July	8.9	214	159	3810	1.7	W-NW
17 July	9.2	221	242	5807	2.5	N-NE
18 July	11.3	272	195	4689	1.4	W-NW
19 July	9.3	224	158	3783	1.6	SW-S
20 July	5.3	126	49	1175	0.6	NW-N
21 July	6.1	146	100	2407	0.3	NW-N
22 July	7	168	97	2325	0.6	NW-N
23 July	8.4	202	136	3263	3.8	W-NW
24 July	7.2	172	177	4254	1.7	W-NW
25 July	8	192	201	4813	0.4	NW-N
26 July	9.4	226	148	3555	0.8	E-SE
27 July	9.3	223	111	2670	0.4	E-SE
28 July	6.6	158	162	3883	0.4	NW-N
29 July	6.3	150	174	4168	0.2	NW-N
30 July	8.6	207	217	5197	0.3	NW-N
31 July	9.9	238	177	4246	4	W-NW
1 August	9.6	231	105	2520	2	W-NW
2 August	4.7	113	66	1585	0.2	NW-N
3 August	2	48	69	1647	0.8	NW-N
4 August	-0.4	8	44	1064	1.2	NE-E
5 August	-1.6	0	90	2165	4.3	W-NW
6 August	-1.4	0	97	2338	6.4	W-NW
7 August	-2.7	0	151	3612	10.5	W-NW
8 August	0	19	90	2157	6.6	SW-S
9 August	0.4	13	106	2539	5.8	SE-S
10 August	-1.7	0	91	2181	5.7	W-NW

Notes:
 Air temperature, K down, and wind speed are average values from hourly measurements.
¹MDD is melting degree days, the sum of all hourly temperatures above 0°C.
²K down is incoming shortwave radiation.
³KDD is K down days, the sum of all hourly incoming shortwave radiation values.
⁴Wind direction is the predominant wind direction for the day.

Table B5. Sawtooth Glacier base camp twice-daily meteorological data, May 26 to August 11, 1993.

Date	Time	Sky conditions	Visibility Obs. to Temp. Wind Clouds				Max. (°C)	Min. (°C)	Precipitation (mm)	Remarks
			Visibility	Temp	Wind	Clouds				
May 26	1900	E20OVC	15	-3	0	ST10			T snow	FOG most of day
May 27	700	E30OVC	10 S--	-3	0	ST10			0.5 cm S	
	1900	E30BKN	15	-2	1710	ST8				
May 28	700	E40SCT200OVC	15	-3	0	ST2CS8	0	-4		
	1900	E200-SCT250SCT	15	-2	0	CS2CI1	2	-3		
May 29	700	E200BKN	15	-1	0	CS6	2	-3		
	1900	CLR	15	1	0		3	-1		
May 30	700	E150BKN	15	-1	0	AS7	0	-2		
	1900	E30SCT150SCT	15	-1	3302	SC2AS1	3	-2		ST around mtns during day
May 31	700	CLR	15	-4	0		0	-5		
	1900	E100SCT250BKN	15	-1	0	AS4CI3	1	-5		
June 1	700	E150SCT200SCT	15	-1	0	AS1CI1	1	-3		
	1900	E100SCT200SCT	15	1	2402	AS1CI1	4	-1		
June 2	700	E20OVC	10 S	-4	2707	ST10	2	-4 T		S--drg nite w/cold front pass
	1900	E150SCT	15	-2	0	AS1	-1	-5		
June 3	700	E200SCT	15	-3	1204	CI3	-1	-4		
	1900	E40SCT	15	0	0	SC1	3	-4		
June 4	700	E100SCT	15	-1	0	AS1	1	-3		
	1900	E40SCT200SCT	15	1	1801	SC1CI1	2	-2		
June 5	700	E200SCT	15	1	0	CI1	2	-2		
	1900	E100SCT200SCT	15	2	0	AC3CI1	4	-1		
June 6	700	CLR	15	2	0		3	-2		
	1900	E70BKN	15	2	0	AS7	3	0		
June 7	700	E60OVC	15	1	0	ST10	3	0		
	1900	E60BKN	15	1	3003	SC9	3	0		
June 8	700	E50BKN60BKN	15	2	904	ST5SC3	3	0		
	1900	E60BKN	15	3	3206	SC6	5	2		
June 9	700	CLR	15	3	0		4	1		
	1900	E50SCT	15	4	406	SC2	5	2		
June 10	700	E50BKN100OVC	15	3	714	ST8AS2	4	0		
	1900	E30SCT50BKN	15	1	912	SF3ST5	3	0	0.5 cm S	winds all day gusting 30 kts
June 11	700	E35SCT200SCT	15	1	717	ST1CI1	2	-1		
	1900	E40SCT100BKN	15	5	712	ST1AS4	5	1		
June 12	700	E40SCT100BKN	15	4	709	ST4AS3	5	3		
	1900	E50SCT200BKN	15	6	3208	SC4CI1	8	3		
June 13	700	E35OVC	15	3	2502	ST10	7	2 T		v light rain
	1900	E30BKN	15	4	0	ST9	5	2	2	
June 14	700	E25SCT60BKN	10 S	2	2904	ST2ST7	4	1		
	1900	E30BKN200BKN	15	3	3208	ST5CI2	3	1 T		light snow for 3 hr in aft.
June 15	700	E100SCT200OVC	15	2	3004	AS3CS7	4	0		
	1900	E50BKN100BKN200OVC	15	4	3001	ST6AS3CS1	6	1		
June 16	700	E30SCT100BKN	15	2	0	ST4AS5	4	1 T		light snow this morning
	1900	E40BKN80BKN	15	4	2203	ST5AS4	5	2 T		
June 17	700	E50SCT100SCT200BKN	15	3	811	ST1AS3CS2	5	2		
	1900	E80SCT100BKN	15	5	907	AS2AC3	5	2		
June 18	700	E50SCT100BKN200BKN	15	3	1614	ST3AS2CS2	6	2		
	1900	E50SCT	15	5	1205	SC2	6	3		
June 19	700	CLR	15	4	203		6	2		
	1900	E100SCT200SCT	15	7	3007	AS1CI1	8	3		
June 20	700	E100SCT200BKN	15	5	1003	AS3CS5	7	2		
	1900	E45BKN200BKN	15	9	1803	SC6CI1	9	4		
June 21	700	E45SCT100SCT200BKN	15	4	1202	SC2AC2CI2	9	4		
	1900	E45SCT100BKN	15	4	1013	SC4AC3	7	4		
June 22	700	E45SCT200BKN	15	4	403	SC3CI3	5	3		
	1900	E60SCT180BKN200BKN	15	8	505	SC3CS5CI1	9	3		
June 23	700	E180SCT200BKN	15	6	0	CS3CI2	9	6		
	1900	E45SCT100BKN200BKN	15	7	508	SC2AC5CI1	9	6		
June 24	700	E30OVC	5 FOG	3	703	FOG10	7	3	1.4	
	1900	E30BKN100BKN	10 S	2	1503	ST7AS2	5	1 T		intermittent snow all day
June 25	700	E30BKN100OVC	15	1	1804	ST7AS3	2	0 T		wind gusting 29 kts drg night
	1900	E30BKN100BKN	15	1	1809	SC6AC2	3	0 T		light snow showers in morning
June 26	700	E35SCT50BKN	15	1	2203	ST3ST6	2	0		
	1900	E50SCT100OVC	15	2	1110	ST4AC6	3	1 T		light snow in morning
June 27	700	E35SCT40OVC	15	2	1606	SF1ST9	3	1		
	1900	E30BKN40BKN80OVC	15	4	0	ST5SC3AS2	4	1	0.4	sun dim vis
June 28	700	E40SCT80BKN	15	5	3203	ST3AC5	5	3		
	1900	E80BKN100BKN	15	6	2202	AS5AC4	9	4		

Table B5. (cont.)

Date	Time	Sky conditions	Visibility Obs. to Temp. Wind Clouds				Max. (°C)	Min. (°C)	Precipitation (mm)	Remarks
			Visibility	Temp	Wind	Clouds				
June 29	700	E50SCT	15	6	904	SC2	8	6		
	1900	CLR	15	10	2305		12	6		
June 30	700	E80BKN	15	8	902	AS9	11	7		
	1900	E50SCT100SCT200BKN	15	13	3208	SC1AC3CI3	13	8		
July 1	700	E100OVC	15	10	0	AS10	14	10		
	1900	E80BKN100BKN	15	12	3010	AS5AC4	13	10		
July 2	700	E30BKN	15	0	0	ST9	11	-1	2	
	1900	E35BKN	15	3	3403	ST9	3	0	cold front passage; cling to W	
July 3	700	E20OVC	5	FOG	2	2706	FOG10	3	1	
	1900	E35BKN200BKN	15	6	605	ST6CI2	7	2		
July 4	700	E50BKN100BKN	15	6	606	SC6AC3	7	5		
	1900	E200SCT	15	9	3212	CS1	10	6		
July 5	700	E100SCT	15	8	2703	AS1	10	7		
	1900	CLR	15	11	3007		13	8		
July 6	700	E200SCT	15	10	2203	CI1	12	8		
	1900	E80BKN	15	10	1405	AC7	13	9		
July 7	700	E80SCT100SCT	15	11	903	AS1AC1	13	9		
	1900	E80SCT	15	13	708	AC2	14	10		
July 8	700	E80SCT	15	12	903	AC1	13	9		
	1900	E80BKN200BKN	15	13	607	AC5CI1	14	10		
July 9	700	CLR	15	12	703		13	9		
	1900	CLR	15	14	1006		15	12		
July 10	700	CLR	15	12	1006		15	11		
	1900	E200SCT	15	13	807	CI2	15	12		
July 11	700	E100SCT180BKN200BKN	15	10	708	AS3CC2CI2	14	9		
	1900	E80BKN100OVC	15	10	505	AS6AC4	12	9		
July 12	700	E80BKN100OVC	15	8	0	AS7AC3	10	7		
	1900	E50SCT100BKN200BKN	15	12	0	SC3AS3CI1	12	7	0.3	
July 13	700	E200SCT250BKN	15	11	707	CC1CI5	12	8		
	1900	E50SCT200BKN	15	14	2507	SC4CI1	15	10		
July 14	700	E200SCT	15	10	0	CI1	14	9		
	1900	E50BKN200BKN	15	14	3005	SC6CI1	15	10		
July 15	700	E200SCT	15	12	3006	CI4	15	10		
	1900	E100SCT200SCT250BKN	15	11	2608	AC1CC4CI4	14	11		
July 16	700	E100SCT200SCT250BKN	15	10	0	AS3CC1CI1	12	7		
	1900	E30SCT50OVC	15	7	0	SF2ST8	11	7	v light rain at present	
July 17	700	Indef. Obs.	0.125	FOG	6	0	FOG10	7	4	2.3
	1900	E50SCT	15	11	907	SC2	13	6		
July 18	700	E100BKN	15	9	0	AC7	12	9		
	1900	E50SCT60BKN200BKN	15	11	2407	SF1CU6CI2	12	9	0.8	
July 19	700	E50BKN100BKN	15	9	2505	SC6AS3	12	7	0.9	
	1900	E40SCT60OVC	15	8	2004	SF4ST6	10	8T		
July 20	700	Indef. Obs.	0.125	FOG	5	2402	FOG10	8	5	4.7
	1900	Indef. Obs.	0.125	FOG	5	2802	FOG10	6	5	6
July 21	700	Indef. Obs.	0.125	FOG	5	0	FOG10	5	5	2.4
	1900	Indef. Obs.	0.125	FOG	6	2303	FOG10	7	5	8.2
July 22	700	Indef. Obs.	0.125	FOG	4	2403	FOG10	6	4	2.4
	1900	E40BKN100BKN	15	8	1807	ST5AC4	10	4	1.9	
July 23	700	E40BKN100OVC	15	7	1610	ST8AS2	9	7		
	1900	E50BKN100BKN	15	7	1906	ST6AC3	9	7		
July 24	700	E30SCT50OVC	15	5	0	ST3ST7	8	5		
	1900	E50SCT200BKN	15	8	2005	SC4CS4	10	5		
July 25	700	E100SCT200SCT	15	7	0	AS1CI1	8	6		
	1900	E50BKN	15	8	2202	SC8	9	6		
July 26	700	E50OVC	15	7	0	SC10	10	7		
	1900	E40SCT50BKN100BKN	15	9	1404	ST4SC3AS2	11	7	0.1	
July 27	700	E40SCT50OVC	15	7	802	ST2ST8	9	7	1.5	
	1900	E40SCT50OVC	15	8	2502	ST7SC3	10	7		
July 28	700	E50SCT100SCT200BKN	15	7	0	SCAS1CI 1	9	6		
	1900	E30SCT50BKN100-OVN	15	6	2204	ST1ST6A C3	9	5		

Table B5. (cont.)

Date	Time	Sky conditions	Visibility Obs. to Temp. Wind Clouds				Max. (°C)	Min. (°C)	Precipitation (mm)	Remarks
			Visibility	(°C)						
July 29	700	E60BKN100BKN	15	4	0	ST7AS1	6	3		
	1900	E80SCT100BKN200-OVC	15	8	0	AS2AS6CS2	9	3		
July 30	700	E100SCT200-OVC	15	10	0	AS2CS8	11	7	8.6	
	1900	E150SCT200BKN250BKN	15	9	2502	AC2CS4CC2	12	7		
July 31	700	E150SCT	15	9	1903	AS4	11	7		
	1900	E150SCT180BKN200BKN	15	11	1804	AS2CC3CS3	13	9		winds gusting 20 kts drg aft
August 1	700	E40SCT50BKN200BKN	15	8	1610	ST2SC6CS1	11	8		winds gusting 20 kts drg night
	1900	E50BKN80BKN200BKN	15	8	0	SC5AC3CI1	11	8		
August 2	700	E30OVC	15	5	1802	ST10	8	5 T		v light rain at present
	1900	E28OVC	15	3	1802	ST10	5	3		
August 3	700	E25SCT50OVC	15	1	0	ST4ST6	3	1	0.7	
	1900	E30BKN50OVC	15	3	2204	ST6ST4	4	1		
August 4	700	Indef. Obs.	1FOG +S	0	2205	FOG10	3	0	0.9	v light snow at present
	1900	Indef. Obs.	2S	-3	2502	ST10	0	-3	3.8	snow drg day, S on ground
August 5	700	Indef. Obs.	0.25S	-4	2208	FOG10	-3	-4T		snow was likely > trace
	1900	E25BKN	10 S-	-2	1810	SC9	-1	-4 T		S- drg day, vis 2 miles to N
August 6	700	Part.Obs.E20OVC	0.5 S+BS	-2	1216	SNOW10	-1	-3T		wind 27 kts drg nite, >T snow
	1900	Part.Obs.E20OVC	1S+BS	-3	1710	SNOW10	-1	-4T		light-mod S all day, >T snow
August 7	700	E35BKN	15	-4	1808	ST6	-3	-5T		winds gusting 19 kts drg night
	1900	Part.Obs.E30OVC	2S+BS	-3	1813	SNOW10	-3	-5 T		light snow in afternoon, >T
August 8	700	Part.Obs.E30OVC	5S+BS	-3	1223	SNOW10	-3	-4T		wind gusting 27 kts presently
	1900	E30BKN80BKN180OVC	10BS	1	1220	ST5AS3CI2	1	-3T		wind gusting 32 kts drg aft
August 9	700	Indef. Obs.	0.125S +BS	-2	1020	SNOW10	2	-2 T		wind gusting 30 kts drg nite
	1900	E35SCT50OVC	15	0	612	ST2ST8	1	-2T		wind gusting 36 kts drg day
August 10	700	Indef. Obs.	1S	-2	1802	SNOW10	0	-2		five cm of snow, no drifting
	1900	E40SCT50BKN80OVC	10BS	-4	1615	ST2ST6AS2	-1	5cmS -4T		improved vis to S
August 11	700	E40SCT50OVC	5S	-3	1611	ST2ST8	-3	-4T		sun dim vis, > T snow

Notes:
 Visibility is in miles.
 Restrictions to visibility are: S = snow, S- = light snow, S-- = very light snow, BS = blowing snow, FOG = fog
 Wind is in knots and is in the format: direction, speed
 Precipitation is in millimetres except where indicated

Modelling July mean temperatures on Fosheim Peninsula, Ellesmere Island, Nunavut

D.E. Atkinson¹

Atkinson, D.E., 2000: Modelling July mean temperatures on Fosheim Peninsula, Ellesmere Island, Nunavut; in Environmental Response to Climate Change in the Canadian High Arctic, (ed.) M. Garneau and B.T. Alt; Geological Survey of Canada, Bulletin 529, p. 99–111.

Abstract: Results are presented from a limited test of a model that predicts July mean surface-air temperatures at high spatial resolution using upper-air data from Atmospheric Environment Service stations and a digital representation of topography. Data from the Polar Continental Shelf Project database of nonstandard climate observations were used to assess the accuracy of model predictions. A brief assessment of Polar Continental Shelf Project temperature data was also performed.

The model was tested on Fosheim Peninsula, Ellesmere Island. Results generally agreed with the observational record for most locations except the heads of sheltered fiords, complex terrain, or areas far from the Eureka automatic weather station. Model limitations were reviewed.

The assessment of Polar Continental Shelf Project data revealed the existence of a summertime ‘coastal effect’ with temperatures cooler at coastal locations than at inland sites. It also revealed a general coherence amongst Polar Continental Shelf Project stations and Eureka in the low-frequency components of the temperature trends.

Résumé : Cette étude présente les résultats d’essais restreints d’un modèle qui calcule, avec une grande résolution spatiale, les températures mensuelles moyennes de l’air en surface pour le mois de juillet en utilisant les données de la haute atmosphère provenant des stations du Service de l’environnement atmosphérique combinées avec une représentation numérique de la topographie. On a utilisé des données provenant de la base de données d’observations climatiques non normalisées de l’Étude du plateau continental polaire pour évaluer l’exactitude des prévisions du modèle. On a également effectué une évaluation sommaire des données sur la température de l’Étude du plateau continental polaire.

On a fait l’essai du modèle pour la péninsule Fosheim, île d’Ellesmere. Les résultats du modèle concordent généralement avec les valeurs observées pour la plupart des sites sauf aux extrémités amont des fjords abrités, dans les terrains complexes ou dans les régions éloignées de la station météorologique automatisée à Eureka. On a examiné les limites du modèle.

L’évaluation des données de l’Étude du plateau continental polaire a révélé l’existence d’un «effet côtier» estival caractérisé par des températures plus basses près des côtes qu’aux sites à l’intérieur des terres. Elle a également révélé une cohérence généralisée entre les stations de l’Études du plateau continental polaire et Eureka pour les composantes à basse fréquence des tendances des températures.

¹ University of Ottawa, Department of Geography, 165 Waller St., Ottawa, Ontario K1N 6N5

INTRODUCTION

In the Canadian Arctic, we are faced with the problem of trying to describe climate adequately from relatively short series of observations at too few stations.

— Jacobs, 1990

The screen-level...temperature measurements that are commonly available are our best estimates of the very low-level, free-air temperature. Even so, they may not be representative of areas only hundreds of metres away.

— Maxwell, 1980

Differences between climate records from Eureka and from the other Fosheim locations raise concern regarding the representativeness of climatic records from coastal stations. The scarcity of long records in the Arctic necessitates heavy reliance upon the few coastal weather stations for baseline temporal data against which future climatic changes will be gauged. Results from this investigation demonstrate that point data cannot represent the entire surrounding landscape. Thus much caution must be exercised when extrapolating the coastal station data to a region.

— Woo et al., 1991

A concern raised consistently in results from interdisciplinary studies in the Arctic is the accuracy of climate depiction. At issue are the plots of climate parameters interpolated from data gathered at Atmospheric Environment Service weather stations. Specifically, three problems arise in the context of the High Arctic. First, all Atmospheric Environment Service stations are located on the coast. The localized modification of climate parameters, especially temperature, resulting from proximity to a coastal zone is well known. Contour plots of temperature surfaces using data obtained from coastal stations introduce a systematic bias towards depicting a coastal regime. Second, there are very few stations; those that exist are separated by large distances. Interpolative accuracy decreases with distance from the original data points, thus the greater the distance from a point observation, the less accurate an estimate is likely to be. Third, parts of the High Arctic are topographically complex. Zones within the larger region can be dominated by local factors, such as elevation or proximity to ice fields, that are not represented in a synoptic-scale depiction that is based on data from coastal zones.

In lieu of a station density that is great enough to calculate spatially detailed interpolated surfaces, the option of deriving surfaces of climate elements using physical principles might yield more accurate results. Such a methodology would possess two main components: a model that parametrizes processes affecting climate at the mesoscale and that accounts for systematic bias (e.g. a prevalent coastal signal) in the permanent station record, and some means of independently verifying the model, either a set of observations from various times, or satellite data, or a combination of both. The model would predict values for climate elements at every point in a regular grid over the area of interest.

A model to estimate screen-height temperature has been developed and initial results have been evaluated. The data used for verification are drawn from nonstandard data sets, chiefly the Polar Continental Shelf Project data set of weather observations.

EXISTING METHODS FOR THE SPATIAL REPRESENTATION OF ARCTIC CLIMATE

Contour maps of climate variables can be drawn subjectively or objectively (i.e. using a computer). A variation of the objective approach is to use satellite imagery. The strengths and weaknesses of various approaches are discussed below.

Subjective methods

Subjective methods have been applied to incorporate the effects of elevation, distance from the coast, and nearness to sea ice or open water on point-source data. A primary example in the High Arctic is found in what must be the main reference source for climate in the Canadian Arctic: Maxwell's two volumes entitled *The Climate of the Canadian Arctic Islands and Adjacent Waters* (Maxwell, 1980, 1982), which include a map showing the distribution of July normal temperatures for the period 1941–1970. All existing permanent stations, except for Dewar Lakes on central Baffin Island, are located on the coast. Maxwell's map is based on data from these stations; however, it is supplemented by his own knowledge of the climatic characteristics of the region. He was able to fill subjectively the gaps created by stations whose records show a coastal bias.

In other studies, Jacobs (1990) uses potential temperature to show the elevation effect he knows to be present in climate data gathered on Baffin Island. Alt and Maxwell (1990) apply their experience in a depiction of regional-scale coastal climate patterns. Edlund (Edlund, 1987; Edlund and Alt, 1989), Jacobs and Grondin (1988), and Jacobs (1990) have suggested incorporating vegetation distribution patterns in subjective contouring of climate parameters to increase the areal detail of the depiction and to overcome coastal bias.

Parks Canada (1994) presents a detailed temperature plot for the vicinity of Tanquary Fiord and Lake Hazen on northern Ellesmere Island (Fig. 1). All temperature records available for the area were incorporated. Most stations used to prepare this map, with the exception of Tanquary Fiord and Lake Hazen, were not coincident in time and their records were integrated subjectively.

The temperature map in Figure 1 represents the level of regional detail in a climate analysis that is needed for the rest of the Queen Elizabeth Islands. A weakness with the Parks Canada (1994) analysis, as with the normals plots in Maxwell (1980), is that effects due to coastal proximity and high ground have been estimated qualitatively.

The strength of subjective methods is the opportunity to incorporate all available data and the experience of the analyst, an important consideration in data-sparse areas. Weaknesses are the lack of objectivity (quantification) and the work required to apply corrections to data to compensate for locational biases.

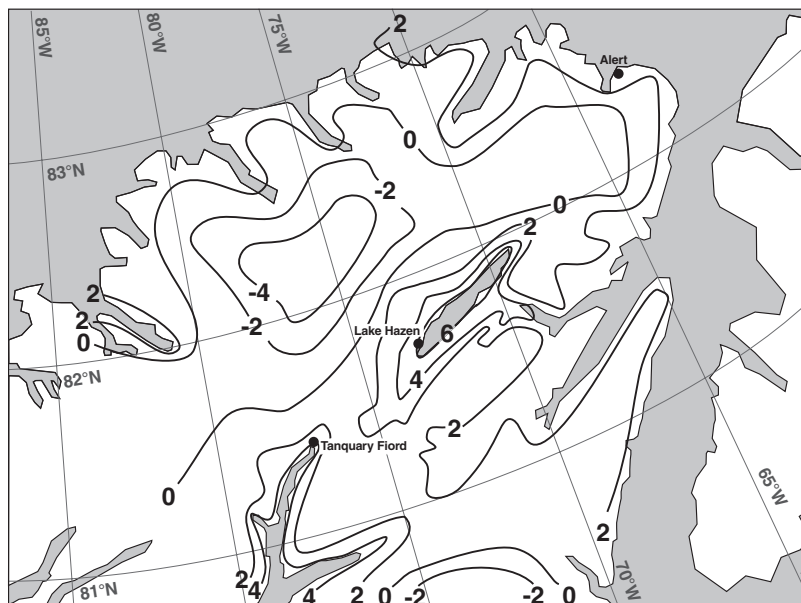


Figure 1.

July mean temperatures for northern Ellesmere Island (after Parks Canada, 1994). Isotherms are in degrees Celsius.

Objective methods

Mapping software performs objective analyses of point data by using computer or mathematical algorithms to interpolate between data points and generate contour lines. Jacobs (1990) uses an automated procedure to integrate data from automatic weather stations (autostations) into objective temperature maps for southern Baffin Island. By producing maps both with and without the autostation data, he evaluated the existing maps of temperature normals and could verify the assumptions Maxwell used to create them. For example, autostation data indicate that the interior of southern Baffin Island can be up to 5°C warmer than what is suggested by interpolating from coastal stations alone. A map of potential temperatures (temperatures from elevated sites standardized to sea level using a predefined rate of temperature change with elevation) did indicate the existence of topographic influence.

Remote sensing

An important technique for gathering spatial climate information, and one that has been suggested as a means of automating the preparation of maps of climate parameters, is satellite remote sensing. However, visible and infrared remote-sensing techniques suffer greatly in the Arctic due to the frequent cloud cover, meaning that any satellite record would possess both temporal and spatial gaps. Radar, which can penetrate cloud cover, cannot provide climatic information. Although techniques and coverage improve, there will still remain a need for ground-truth information to verify and calibrate the remotely gathered data. Even if remote-sensing techniques were able to operate independently of ground-truth support, existing archives of surface-based observations that predate effective remote-sensing coverage still need to be incorporated into arctic climate analyses. As well, surface-based analyses that have been performed since the advent of satellite remote sensing need to be integrated

with remotely sensed data to maintain continuity of record. Thermal infrared imagery, such as that which may be obtained from the National Oceanic and Atmospheric Administration (NOAA), advanced very high resolution radiometer sensor, can play a useful role in verifying the results of a surface-temperature model. Thermal imagery, however, is also adversely affected by cloud cover and, thus, periods of satellite data availability would be limited.

A GIS MODEL TO ESTIMATE SURFACE AIR TEMPERATURE

Introduction

A model was developed to provide spatially detailed estimates of surface air temperature across Fosheim Peninsula that is fully contained within geographic information system (GIS) software. With such a tool, the strengths of objective and subjective methodologies can be combined, in that the prevalent influences the researcher knows about can be modelled and quantified and then applied in an objective and repeatable manner. In a GIS, the region of interest is represented by a grid, with each cell ('pixel' in GIS terminology) having one value for the parameter under consideration. Initial values are assigned to pixels using existing data. The range and magnitude of each influencing factor, such as proximity to the coast to icefields, are resolved on a separate grid. All grids are then overlain, necessary interactions are performed, and the pixel takes the resultant value (Bonham-Carter, 1994).

The Fosheim Peninsula was selected as the site of this study because of ongoing research in the region. Several research projects have had camps in the area, some for several consecutive field seasons. A time-series comparison of twice-daily temperature data from the Atmospheric Environment Service's Eureka station and various Polar Continental Shelf Project stations shows that Polar Continental Shelf Project

data and Atmospheric Environment Service station data are coherent even though the sites are several hundred kilometres apart.

Model development

Screen-height air temperature was selected for modelling. A geographic model was developed to estimate July temperature on the basis of Atmospheric Environment Service data and the influence of two large-scale geographic parameters, topography and distance from the coast.

Model operation centres on two components. First, broad temperature trends are estimated across the region using data from Atmospheric Environment Service stations (Eureka in this case). This step is justified because there exists a certain regional coherency in temperature time-series trends as a result of synoptic climate patterns, so that one station can be used to depict the gross features of another station located at some distant point (Walsh, 1984). The work of Jacobs (1990), in which he presents a model to predict temperature for a given station using data from neighbouring stations, demonstrates the phenomenon of regional coherency in temperature patterns. Second, the preliminary temperature estimates are then improved by overlaying quantified representations of smaller scale influences, such as coastal effect, ice-field

proximity, or altitude. Amplitude differences in the time series that occur between individual stations are a result of such localized influences.

For simplicity, it was decided to limit the modelled influences on temperature to altitude and distance from the coast. Temperature change with altitude is modelled by applying the temperature curve generated by mean rawinsonde ascents (Fig. 2a, b, c). This instrument, carried aloft by balloons, records temperature, wind speed, and wind direction at various elevations during its ascent and is the only indicator of environmental lapse rate available for this region. The use of the dry adiabatic lapse rate — 10°C decrease per 1000 m — was rejected given the potential variability in actual lapse rates (Maxwell, 1982; Bradley et al., 1992; Kahl et al., 1992). The coastal effect is modelled as a logarithmic decay with distance from the coastline; the magnitude is estimated from the rawinsonde temperature curve (Fig. 2c).

The main data inputs consist of rawinsonde ascent data from the closest Atmospheric Environment Service upper-air station, a digital terrain model (Fig. 3), and a vector plot of the coastline.

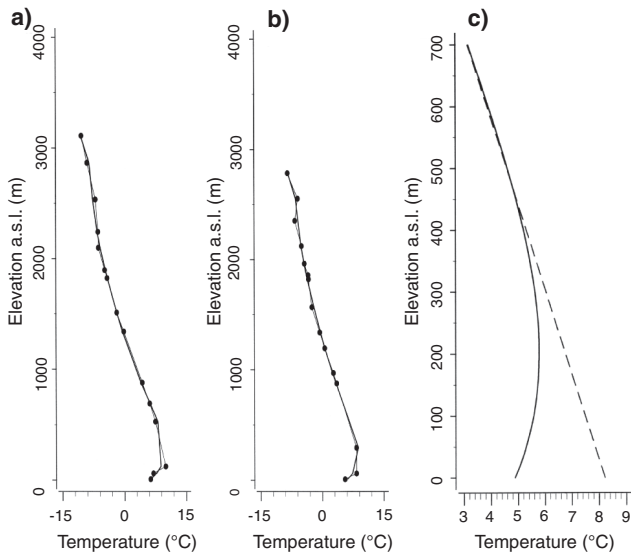


Figure 2. Examples of upper-air temperature profiles derived from individual rawinsonde ascents at AES Eureka. **a)** July 2, 1987, 00:00 h UCT; **b)** July 23, 1987, 12:00 h UCT. The thin line with black dots represents original data points; the thicker line is the polynomial fit. **c)** Mean rawinsonde ascent profiles for July generated by averaging all polynomial estimates for each ascent in the month of July for a given year. The coastal effect is estimated by taking the difference between the surface temperature (solid line) and the hypothetical extrapolation of the straight portion of the curve (dashed line) to the surface.

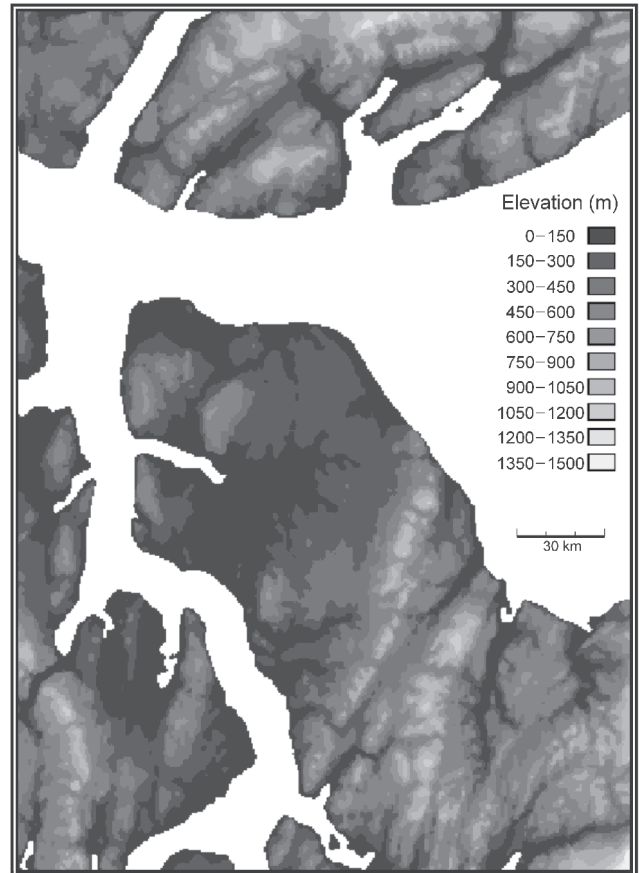


Figure 3. Digital terrain model of Fosheim Peninsula, Ellesmere Island.

Rawinsonde ascent

A polynomial curve was fitted to the temperature data from each rawinsonde ascent (two a day). The form of the equation was as follows:

$$T_z = \beta_0 + \beta_1 z + \beta_2 z^2 + \beta_3 z^3 + \beta_4 z^4 + \beta_5 z^5 + \beta_6 z^6,$$

where T_z is the predicted temperature for a given altitude, z . A sixth-degree polynomial was selected to closely map the form of the original data curve within the range of the original data and not for purposes of extrapolation or physical explanation. A high-order polynomial assured adequate representation of the main features of the temperature-profile curve.

Two example temperature profiles are plotted along with their fitted line in Figures 2a and b. A mean July value for each coefficient β_0 to β_6 was obtained to generate an equation describing the mean profile of temperature variation with altitude (Fig. 2c). The coefficients β_0 to β_6 for the fitted lines in Figures 2a, b, and c are presented in Table 1.

The mean ascent curve described by the equation possessed a surface inversion. It was reasoned that the inversion is caused by coastal effect on the basis of the following. First, although a surface inversion is a prevalent feature of the arctic winter climate, it is present less often in the summer. Radiative heating of the surface produces a positive net energy balance that results in a constant decrease in temperature with altitude unless some other factor, such as proximity to a large body of water, introduces a modifying influence on the temperature near the surface. Second, data taken from a station 30 km inland have shown that, on a clear day when radiative heating does not differ substantially between the sites, the inland site can be as much as 10°C warmer than the coastal site. The only major difference between the two sites is proximity to the coast.

Given that the cause of the inversion may be ascribed to coastal effect, it follows that if this equation were used to predict temperature over the entire region, predictions for lower elevations would be underestimated. To eliminate the coastal effect present in the mean ascent profile, a correction factor was generated by adding the difference between the mean curve and the extrapolated straight line on Figure 2c. This was done at all elevations where there was a difference and the result (Fig. 4) was stored to be added later to the base temperature model.

Table 1. Beta coefficients for the curves presented in figures 5a, b, and c.

	2a	2b	2c
β_0	9.97	6.84	5.75
β_1	3.50E-04	0.01	0.02
β_2	-6.10E-06	-3.10E-05	-4.70E-05
β_3	4.14E-09	2.10E-08	4.24E-08
β_4	-1.90E-12	-7.50E-12	-1.90E-11
β_5	4.93E-16	1.42E-15	4.36E-15
β_6	-5.60E-20	-1.20E-19	-3.90E-19

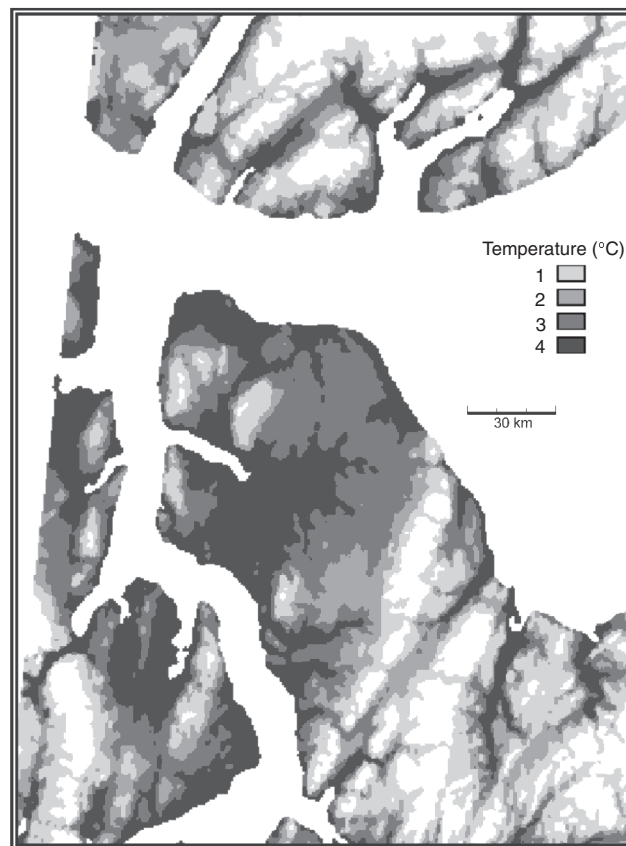


Figure 4. Coastal effect correction factor.

Digital terrain model

Temperature estimates for all elevations were interpolated from the equation. There is an elevation value (z) for each pixel in the digital terrain model. When the values are substituted into the equation, an estimate T_z is generated, transforming the attribute value of each pixel from an elevation value to a surface temperature value. In this manner, the equation is applied to the entire land surface represented by the digital terrain model, creating the base temperature model (Fig. 5).

Vector plot

The magnitude of coastal effect was taken as the difference between the observed surface temperature and an estimation of what the surface temperature would be in the absence of coastal effect. This estimate was based on an extrapolation to the surface of the straight portion of the mean temperature profile curve (Fig. 2c). A straight line relationship describes a typical temperature with altitude profile for a site with a positive net radiation balance at the surface, i.e. with no inversion. Linear distances from the coast were obtained using the vector plot of the coastline (Fig. 6). A series of bands, delineated by exponentially increasing distance from the coast, was established using the data plotted on Figure 6. A linear magnitude decay was applied to the distance bands, falling to zero at

6 km inland (Fig. 7). The 6 km distance was an arbitrary selection. The direction of decay was simplified to be always normal to the coastline. Thus, a temperature value, representing a progressive reduction in the magnitude of coastal effect with distance from the coast, was assigned to each band.

The three resulting maps, base temperature, low-elevation correction factor and coastal effect, were combined to generate the final output (Fig. 8). This mesoscale model is thus based only on topography and distance from the coast. Polar Continental Shelf Project data will be used to verify predictions made by the model.

Model output and considerations

Model output consists of one estimate of the mean July surface-air temperature for each pixel in the original digital terrain model for the selected year. July was selected because it is the month commonly used for climatological study, because it is representative of the arctic summer (i.e. largely free of snow patches or extensive areas of wet ground), and because of the availability of Polar Continental Shelf Project data for model verification. Given that Atmospheric Environment Service temperature and upper-air data records extend over a period long enough to generate true climatic normals

(i.e. a continuous 30-year record), it follows that detailed regional normals could be generated from the geographic model.

The model output for 1980 was contrasted with the available observational record. Many observations agreed to within $\pm 1^\circ\text{C}$ with the model estimates. Stations that did not agree with the model output were located at the heads of sheltered fiords, where a uniformly applied coastal effect might not apply; in complex terrain, such as a narrow valley bordered by ice fields; or far (>200 km) from Eureka, in which case the assumption of regional coherence is weaker than for closer stations.

A number of problems may exist with the assumptions used so far, such as

- the free-air temperature is not necessarily a good estimator of the surface air temperature at the same elevation (Maxwell, 1982);
- the assumption that the surface inversion observed at the Atmospheric Environment Service station is caused by coastal effect has not been validated; and
- the rate and form (e.g. logarithmic, linear) of coastal effect decay for the archipelago is unknown.

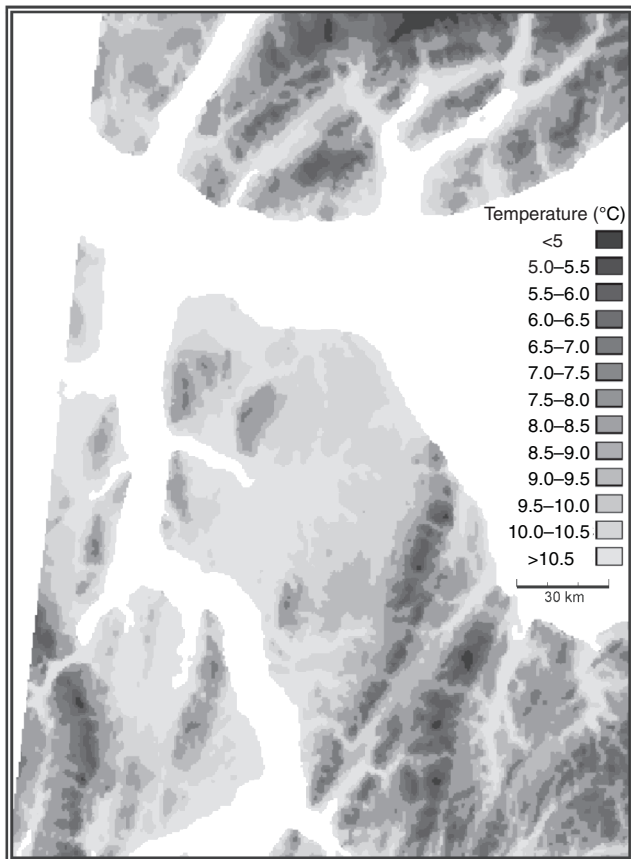


Figure 5. Base model result, after correction for the over-application of coastal effect.

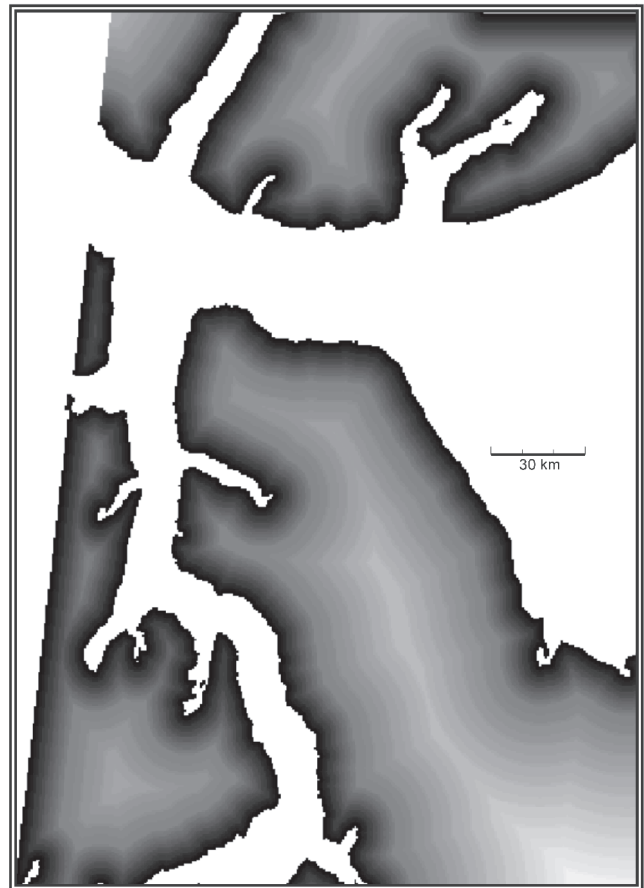


Figure 6. Representation of continuous linear distances from the coast.

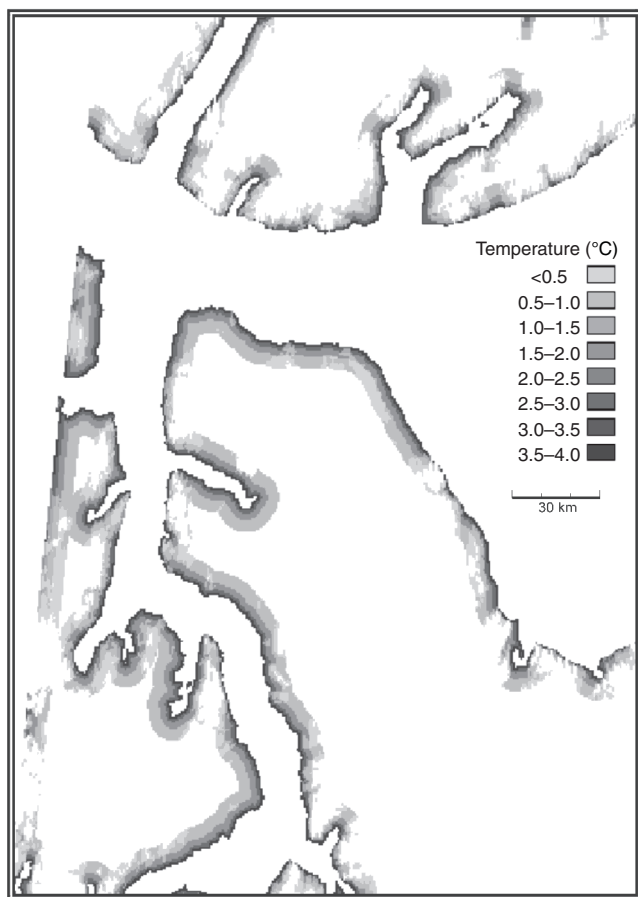


Figure 7. Coastal effect modifier.

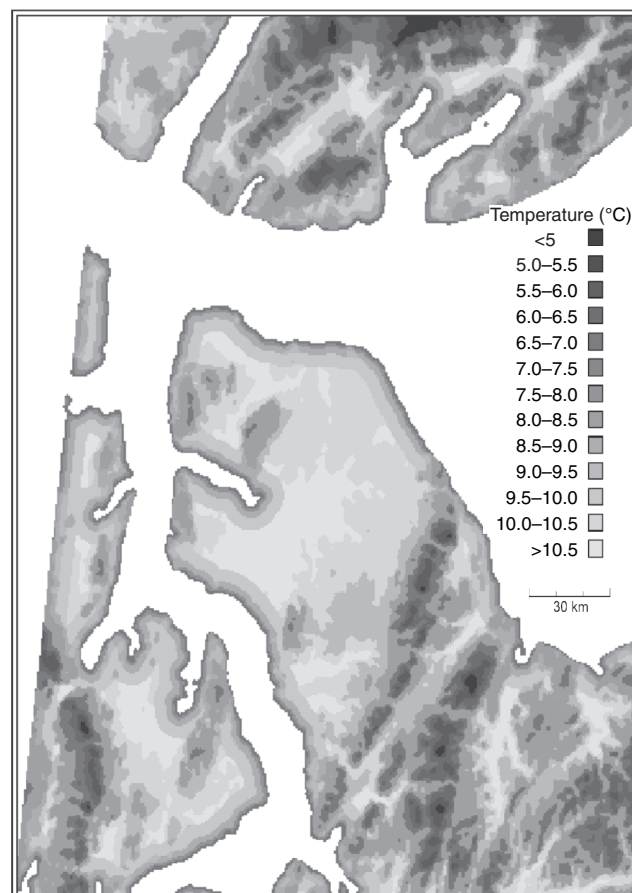


Figure 8. Final model result: mean July air temperatures for 1980.

These assumptions can be tested in part using the Polar Continental Shelf Project data archive.

Various directions are yet to be explored, including the following:

- the use of near-surface (e.g. at the 95 kPa level) winds to refine coastal effect and turbulent mixing considerations;
- the use of upper-level winds and station pressure to apply a synoptic classification (e.g. cloudy, clear);
- further examination of the coastal environment, for example, ice-covered ocean–snow-covered land, ice-free ocean–snow-covered land, ice-covered ocean–snow-free land;
- local effects (glaciers and ice fields, ocean condition, local ground conditions);
- insolation, especially in highlands.

AVAILABILITY OF DATA ON FOSHEIM PENINSULA

Fosseim Peninsula has been the site of numerous studies with the result that many sets of transient climate data exist for the peninsula. When combined with the record from the permanent weather station at Eureka, data are adequate both to drive and verify a geographic model.

Available climate data from the Eureka station include temperature, wind speed, cloud cover, precipitation, and radiation data that have been recorded hourly and summarized in daily and monthly formats. Most elements are available back to 1948. The Eureka station also gathers upper-air wind data twice daily (at 00:00 h and 12:00 h Universal Co-ordinated Time, an international standard). These data, and similar data from Atmospheric Environment Service stations throughout the Arctic, are best summarized in tabular and map form in Maxwell (1980, 1982).

Six years of summer data, 1988 through 1993, are available from a camp at Hot Weather Creek, in the centre of the peninsula (Fig. 9). Data from this site have been generated

Figure 9.

Site map showing the locations of Polar Continental Shelf Project (PCSP) camps. The sites mentioned in this report and some sites with long records are named.



from two sources, an almost continuous record from an automatic weather station operated by the Atmospheric Environment Service and summer data from a campsite about 200 m from the autostation. The autostation records temperature, winds, and radiation hourly, whereas observations on current, maximum, and minimum temperature, winds, weather, and cloud cover were made twice daily at the camp, at 07:00 h and 19:00 h Eastern Standard Time, corresponding to 12:00 h and 00:00 h Universal Co-ordinated Time. The autostation data from Hot Weather Creek have been through a quality control process as discussed in Alt et al. (1992) and Labine et al. (1994). Aspects of the validity of the autostation wind data have been analyzed by Headley (1990) and Peters and Headley (1992) and other climatic elements, by Alt et al. (2000).

Data from the automatic weather station and the camp have been incorporated into various studies undertaken in the area, for example Edlund et al. (1989), Woo et al. (1990), and Alt and Maxwell (2000).

The camp data from Hot Weather Creek are part of a large set of nonstandard data gathered in the spring and summer by researchers at camps operated through the Polar Continental Shelf Project, an organization within the federal Department of Natural Resources that provides logistical support to arctic research. Figure 9 shows some camp locations during the 20 years the Polar Continental Shelf Project weather observation program was in operation; camps with the longest records are labelled. The Polar Continental Shelf Project data are termed 'nonstandard' because they have been gathered by personnel untrained in gathering meteorological data and have not been subjected to the same quality control as the Atmospheric Environment Service data. Also, they are much more temporally and spatially discontinuous than the Atmospheric Environment Service data, since station locations and lengths of observation periods have varied considerably over the years. The camp at Hot Weather Creek has one of the better Polar Continental Shelf Project observation records. In general, these data represent a very useful supplement to the existing

Atmospheric Environment Service climatological data because they are often from sites away from the influence of coastal zones.

Throughout the Queen Elizabeth Islands, the total number of Polar Continental Shelf Project stations has varied from year to year. Twenty to forty stations were in operation in most years, although in some years there were as many as eighty. Nine stations were in operation in 1989 and fifteen in 1993, the lowest years in the record. Thus, the total number of stations per year, their locations, the numbers of observations, and the continuity of site occupancy have varied considerably (Table 2).

Polar Continental Shelf Project data from single stations have been used often to support projects of limited spatial scale, especially botanical studies of the thermal oases found at several locations in the High Arctic (see Courtin and Labine, 1979; Edlund and Alt, 1989; Labine, 1994). The Polar Continental Shelf Project data were also used to produce the Atmospheric Environment Service marine climatological atlases (e.g. Agnew et al., 1987). Alt and Maxwell (1990) have made the most extensive use of the data so far, creating maps that incorporated Polar Continental Shelf Project data to indicate the complexity of regional temperature patterns in the Queen Elizabeth Islands. Young et al. (1995) prepared a detailed radiation model that uses cloud observations from Polar Continental Shelf Project camps. Polar Continental Shelf Project data have also been the subject of several government reports that analyzed various aspects of the program, including the instruments used, the data-gathering process, and archiving of the retrieved data (Alt and Inkster, 1987).

Other sources of arctic climate data exist in addition to Atmospheric Environment Service weather stations, automatic weather stations, and Polar Continental Shelf Project camps. Individual researchers have often gathered more detailed and more frequent observations for their own purposes. These data sets have become more common as the

Table 2. Availability of Polar Continental Shelf Project data for the Queen Elizabeth Islands.

YEAR	Total no. of stations	Total no. of observations	No. of stations >1 week	% stations >1 week	No. stations >1 month	% stations >1 month	Total % weeks + % months
1972	6	3362	3	50.0	3	50.0	100.0
1973	17	3067	5	29.0	7	41.2	65.0
1974	37	5242	4	11.0	20	54.0	65.0
1975	38	5095	12	32.0	21	55.0	87.0
1976	56	3656	23	41.0	21	38.0	79.0
1977	62	3432	26	42.0	21	34.0	76.0
1978	56	3643	22	39.0	22	39.0	79.0
1979	64	3423	30	47.0	21	33.0	80.0
1980	72	3838	28	39.0	27	38.0	76.0
1981	59	3127	21	36.0	22	37.0	73.0
1982	82	2907	34	41.0	14	17.0	59.0
1983	58	3085	26	45.0	17	29.0	74.0
1984	51	1598	21	41.2	8	15.7	56.9
1985	58	1596	22	37.9	10	17.2	55.1
1986	24	942	13	54.2	7	29.2	83.4
1987	20	1294	15	75.0	4	20.0	95
1988	27	1619	12	44.4	12	44.4	88.8
1989	9	479	5	55.6	3	33.3	88.9
1990	47	2448	23	48.9	14	29.8	78.7
1991	24	2075	10	41.7	13	54.2	95.9
1992	26	1662	11	42.3	11	42.3	84.6
1993	15	954	9	60.0	5	33.3	93.3
TOTAL	908	58544	470		304		
MEAN	41	2661	17	43	14	36	79

OVERALL (statistics include all years)
Mean number of observations per station: 65
Percentage of stations with duration of 1 month or more: 36%
Percentage of stations with duration over 1 week and under 1 month: 43%
Percentage of stations with duration under 1 week: 21%
Total percentage of stations with duration over 1 week: 79%
'stations >1 week' indicates stations with at least one continuous week, but less than one month, of observations (14).
'stations >1 month' indicates stations with at least one continuous month of observations (56).

availability of computer-based data-gathering and storage systems has increased. Examples include data sets from upper Hot Weather Creek (Woo et al., 1990; Young et al., 1997), from the east-central part of the peninsula (the Gemini site), and from the southern part of the peninsula in and near the Sawtooth Range (Wolfe, 1994; Wolfe and English, 1995).

INITIAL ANALYSIS OF NONSTANDARD RECORDS

Temperature records from several Polar Continental Shelf Project camps in and around Fosheim Peninsula were compared with the temperature record from the Eureka station. Results are presented in Figures 10 to 17. The plotted data consist of twice-daily observations (recorded at 12:00 h and 00:00 h UCT). The observation times correspond to 07:00 h and 19:00 h locally, thus minimizing problems associated with midday heating and direct radiation of the low-angle, midnight sun into the thermometer screen when it is opened to take a reading.

Several Polar Continental Shelf Project temperature time series were correlated with data from the Eureka station. Support for the following two assumptions used in the model was sought: the extent to which the trend of the data series at any one site is repeated at other sites, i.e. the extent to which the trend at one site can be representative of a larger region, and the magnitude of inland heating-coastal-effect cooling. Magnitudes of mean differences and confidence intervals are given in Table 3.

Figures 10 and 11 compare the temperature record from the Eureka station with that from the Polar Continental Shelf Project Hot Weather Creek station for July and August 1988 and the summer of 1992. Hot Weather Creek is on a low, inland plateau approximately 30 km east of Eureka. Figure 10 shows the comparison for an relatively warm year (1988) and Figure 11, for a relatively cool year (1992). The plots show that both stations exhibit very similar trends, with Hot Weather Creek being continuously warmer during the summer, defined as the period after snowmelt, than Eureka. Before the snow melts, the temperature at Hot Weather Creek does not vary significantly from that at Eureka. The difference between the coast and the interior is not consistent, but is more pronounced during the warmer year and during warm

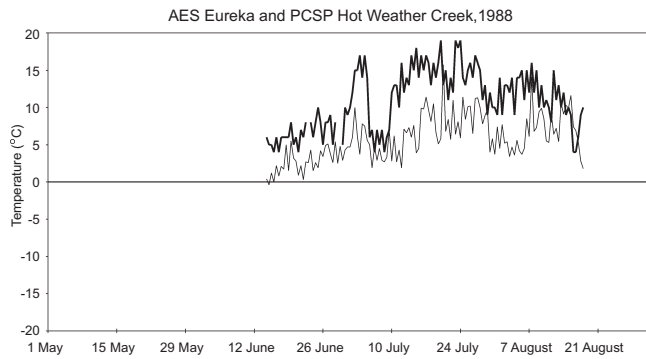


Figure 10. Comparison of temperatures from AES Eureka (light line) and PCSP Hot Weather Creek (dark line), July and August 1988.

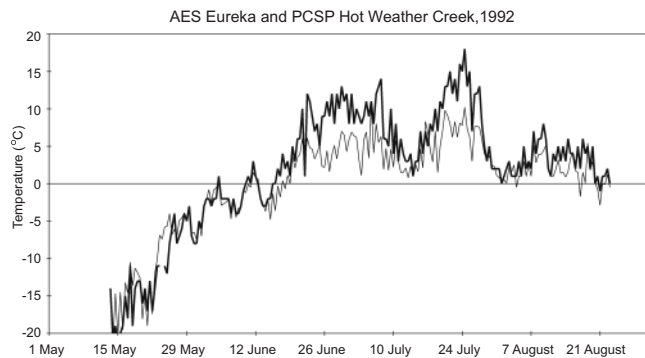


Figure 11. Comparison of temperatures from AES Eureka (light line) and PCSP Hot Weather Creek (dark line), summer 1992.

periods of the warmer year. The difference in temperature between the two stations is attributed to a coastal effect acting to keep temperatures at Eureka low. The effect is not manifested until after snowmelt, when the radiation excess is available to heat the ground rather than being used to melt snow.

Figure 12 compares the temperature record from the Eureka station with that from the Polar Continental Shelf Project station at Expedition Fiord, approximately 150 km west of Eureka, for the summer of 1977. Figure 13 compares the temperature record from the Polar Continental Shelf Project station at Tanquary Fiord, approximately 320 km northeast, with that from the Eureka station for the summer of 1975. Both Polar Continental Shelf Project stations are relatively sheltered, being situated at the heads of long fiords. The difference in temperature between Expedition Fiord and Eureka is slight and less significant than that at most other stations.

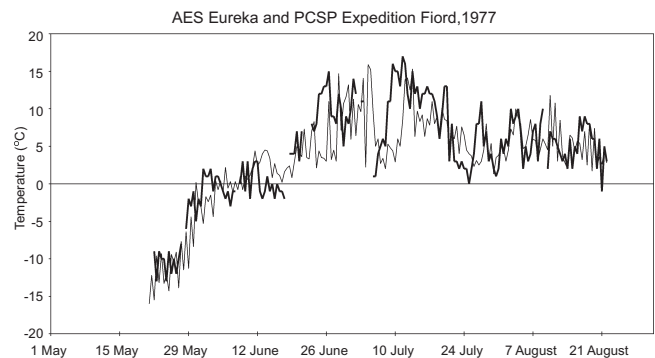


Figure 12. Comparison of temperatures from AES Eureka (light line) and PCSP Expedition Fiord (dark line), summer 1977.

Table 3. Comparison of temperature means between AES Eureka and various PCSP stations for twice-daily observations.

PCSP Station	Year	Temperature difference (°C)	Level of confidence	Distance from the coast (km)	Sheltered fiord ?	Figure
Hot Weather Creek	1988	+5.2	0.99	30	n/a	13
Hot Weather Creek	1992	+1.8	0.99	30	n/a	14
Expedition Fiord	1977	+0.9	0.95	2	Yes*	15
Tanquary Fiord	1975	+4.8	0.99	1	Yes	16
Eastwind Lake	1977	+1.8	0.99	15	n/a	17
Mokka Fiord	1975	+3.1	0.99	1	Yes	18
Mokka Fiord	1977	+3.7	0.99	1	Yes	19
Greely Fiord	1974	-0.8	0.70	<1	No	20

Notes: Comparisons are between PCSP stations and AES Eureka.

Positive values indicate that the PCSP station was warmer.

* Expedition Fiord is on the west side of Axel Heiberg Island. Although the station is situated at the head of a long fiord, it is not as sheltered from the prevailing northwesterly flow as is the AES Eureka area.

This is most likely due to the fact that, despite its sheltered location at the head of a long fiord, the station at Expedition Fiord is on the west side of Axel Heiberg Island, a region that is more exposed to weather and low cloud cover from the Arctic Ocean than Eureka and Tanquary Fiord.

Figure 14 compares data from the Eureka station and from the Polar Continental Shelf Project station at Eastwind Lake, an inland site about 11 km north of Eureka. The temperature at Eastwind Lake is similar to that at Hot Weather Creek and tends to be warmer than at Eureka.

Figures 15 and 16 compare data from the Eureka station and from the Polar Continental Shelf Project's shorter period station at Mokka Fiord, for 1975 and 1977, respectively. Mokka Fiord is approximately 50 km southwest of Eureka and about 1 km inland in the middle of a low plain. Both years show consistent temperature differences between the two stations. This could be an indication of the extent to which coastal influence is effective, i.e. it only affects stations less than 1 km from the coast, although some other local modifier could also be at work. For example, the prevailing wind may have been towards the ocean during the two periods of observation.

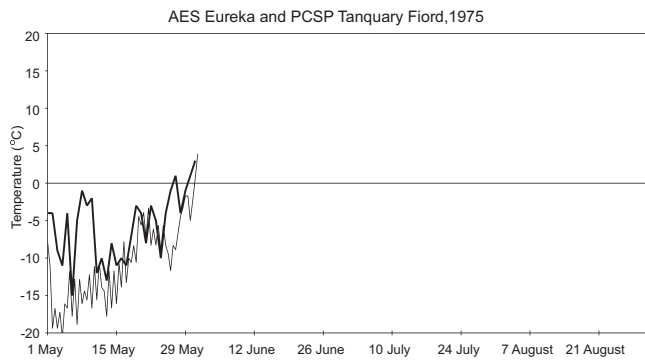


Figure 13. Comparison of temperatures from AES Eureka (light line) and PCSP Tanquary Fiord (dark line), summer 1975.

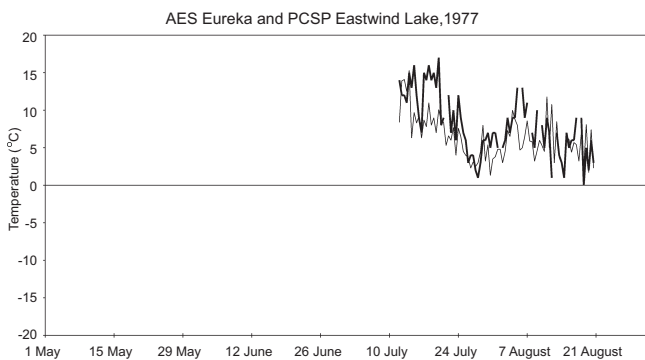


Figure 14. Comparison of temperatures from AES Eureka (light line) and PCSP Eastwind Lake (dark line), summer 1977.

Figure 17 compares data from the Eureka station and from the Polar Continental Shelf Project station at Greely Fiord, approximately 200 km northeast of Eureka, for May and June 1974. Greely Fiord is in an exposed location on the coast and

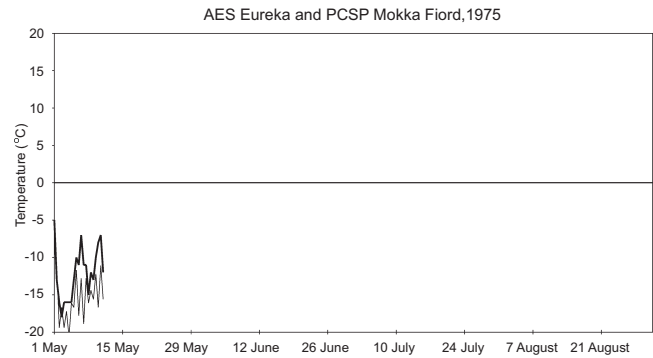


Figure 15. Comparison of temperatures from AES Eureka (light line) and PCSP Mokka Fiord (dark line), summer 1975.

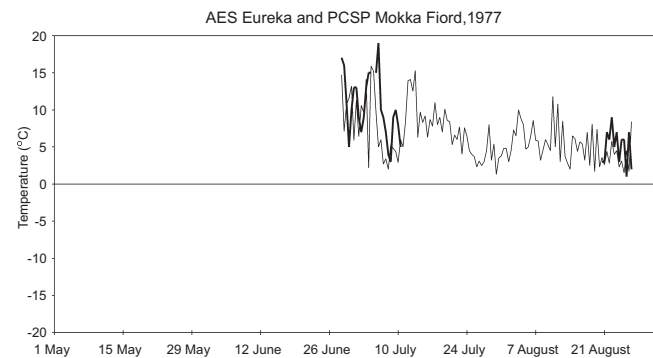


Figure 16. Comparison of temperatures from AES Eureka (light line) and PCSP Mokka Fiord (dark line), summer 1977.

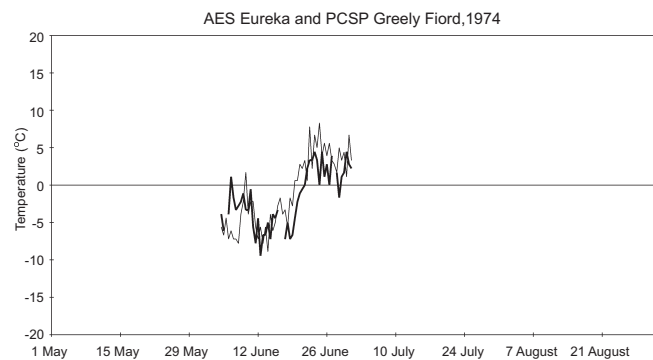


Figure 17. Comparison of temperatures from AES Eureka (light line) and PCSP Greely (dark line), summer 1974.

its temperature record is marginally cooler than at Eureka, although the level of significance is poor (no greater than 70%).

An important point to note is that, in all cases presented, the comparisons show strong coherence, despite differences in relative magnitude.

Overall, the figures show that temperatures are warmer at inland sites than at coastal sites, an observation repeated for various years at various sites. Similarly, the plots comparing data from coastal and near-coastal stations with data from the Eureka station show that proximity to the coast does keep temperatures lower, although a coastal location can be influenced by the length and width of the fiord, for stations located in a fiord, and by position within the archipelago. This series of plots shows that the well documented 'coastal effect' is at work at the Eureka station, a factor that must be considered when applying data from this site to other regions (Jackson, 1959).

The general coherence of the data series, even over large distances, supports the model methodology of using Atmospheric Environment Service stations to provide information on trends and general magnitude and parametrization of local effects to enhance detail. The inclusion of coastal effect in the model is also warranted; however, more work is needed to account for local modifications.

CONCLUSIONS

This model will increase significantly the detail of monthly surface air temperature maps at the mesoscale. It allows the topographic complexity of the archipelago to be fully considered more objectively and in more detail than did previous mapping efforts. In addition, it is applicable in any data-sparse area with a few permanent stations. The use of a geographic information system (GIS) permits incorporation of short-term climatic data to refine model accuracy through either the validation of output or the delineation of the magnitude and extent of local influences that the model is reproducing. A framework for the utilization of transient data will be of use in many regions for which such data records exist and in which there are a few permanent stations. The output of this model can also provide material for studies in other disciplines that require long- or short-term temperature means of high spatial resolution.

For the Canadian Arctic, the inclusion of short-term climatic data into the very sparse permanent record represents an important contribution to understanding the climate. A limited examination of Polar Continental Shelf Project data reveals mesoscale coherence and a strong reflection of local influences, both of which make the data set valuable.

REFERENCES

- Agnew, T., Spicer, L., and Maxwell, B.**
1987: Marine Climatological Atlas — Canadian Beaufort Sea; Atmospheric Environment Service, Canadian Climate Centre, Report no. 87-14, Downsview, Ontario, 196 p.
- Alt, B.T. and Inkster, B.**
1987: Networking, Arctic weather style; GEOS, v. 16, no. 3, p. 6–10.
- Alt, B.T. and Maxwell, J.B.**
1990: The Queen Elizabeth Islands: A case study for arctic climate data availability and regional climate analysis; *in* Canada's Missing Dimension — Science and History in the Canadian Arctic Islands, (ed.) C.R. Harrington; Canadian Museum of Nature, Ottawa, Ontario, p. 294–326.
- 2000: Overview of the modern arctic climate; *in* Environmental Response to Climate Change in the Canadian High Arctic, (ed.) M. Garneau and B.T. Alt; Geological Survey of Canada, Bulletin 529.
- Alt, B.T., Labine, C.L., Atkinson, D.E., Headley, A.N., and Wolfe, P.M.**
2000: Automatic weather station results from Fosheim Peninsula, Ellesmere Island, Nunavut; *in* Environmental Response to Climate Change in the Canadian High Arctic, (ed.) M. Garneau and B.T. Alt; Geological Survey of Canada, Bulletin 529.
- Alt, B. T., Labine, C.L., Headley, A., Koerner, R.M., and Edlund, S.A.**
1992: High Arctic IRMA [Integrated Research and Monitoring Area] Automatic Weather Station Field Data 1990–91; Geological Survey of Canada, Open File 2562, 274 p.
- Bonham-Carter, G.F.**
1994: Geographic Information Systems for Geoscientists: Modelling with GIS; Pergamon Press, New York, 398 p.
- Bradley, R.S., Keimig, F.T., and Diaz, H.F.**
1992: Climatology of surface-based inversions in the North American Arctic; *Journal of Geophysical Research*, v. 97, no. D14, p. 15 699–15 712.
- Courtin, G.M. and Labine, C.L.**
1979: Microclimate studies on Truelove Lowland; *in* Truelove Lowland, Devon Island, Canada: A High Arctic Ecosystem, (ed.) L.C. Bliss; University of Alberta Press, Edmonton, Alberta, p. 73–104.
- Edlund, S.A.**
1987: Plants: living weather stations; GEOS, v. 16, no. 2, p. 9–14.
- Edlund, S.A. and Alt, B.T.**
1989: Regional congruence of vegetation and summer climate patterns in the Queen Elizabeth Islands, Northwest Territories, Canada; *Arctic*, v. 42, no. 1, p. 3–23.
- Edlund, S.A., Alt, B.T., and Young, K.L.**
1989: Interaction of climate, vegetation, and soil hydrology at Hot Weather Creek, Fosheim Peninsula, Northwest Territories; *in* Current Research, Part D; Geological Survey of Canada, Paper 89-1D, p. 125–133.
- Headley, A.**
1990: A comparison of wind speeds recorded simultaneously at three metres and ten metres above the ground; Atmospheric Environment Service, Canadian Climate Centre, Report no. 90-1, 36 p.
- Jackson, C.I.**
1959: Coastal and inland weather contrasts in the Canadian Arctic; *Journal of Geophysical Research*, v. 64, no. 10, p. 1451–1455.
- Jacobs, J.D.**
1990: Integration of automated station data into objective mapping of temperatures for an arctic region; *Climatological Bulletin*, v. 24, no. 2, p. 84–96.
- Jacobs, J.D. and Grondin, L.D.**
1988: The influence of an arctic large-lakes system on mesoclimate in south-central Baffin Island, N.W.T., Canada; *Arctic and Alpine Research*, v. 20, no. 2, p. 212–219.
- Kahl, J.D., Serreze, M.C., and Schnell, R.C.**
1992: Tropospheric low-level temperature inversions in the Canadian Arctic; *Atmosphere-Ocean*, v. 30, no. 4, p. 511–529.
- Labine, C.L.**
1994: Meteorology and climatology of the Alexandra Fiord lowland; *in* Ecology of a Polar Oasis: Alexandra Fiord, Ellesmere Island, Canada, (ed.) J. Svoboda and B. Freedman; Captus University Publications, Toronto, Ontario, 268 p.

Labine, C.L., Alt, B.T., Atkinson, D., Headley, A., Koerner, R.M., Edlund, S.A., and Waszkiewicz, M.

1994: High Arctic IRMA automatic weather station field data 1991–92: part 1, documentation, part 2, plots; Geological Survey of Canada, Open File 2898, 190 p.

Maxwell, B.

1980: The climate of the Canadian Arctic Islands and adjacent waters, v. I.; Climatological Studies no. 30; Atmospheric Environment Service, Environment Canada, Downsview, Ontario, 532 p.

1982: The climate of the Canadian Arctic Islands and adjacent waters, v. II.; Climatological Studies no. 30; Atmospheric Environment Service, Environment Canada, Downsview, Ontario, 589 p.

Parks Canada

1994: Ellesmere Island National Park Reserve Resource Analysis and Description: Chapter 5 – Climate; Canadian Heritage, Parks Canada, Ottawa, Ontario, 78 p.

Peters, B. and Headley, A.

1992: A comparison of winds at Hot Weather Creek and Eureka, N.W.T.; Canadian Climate Centre, Atmospheric Environment Service, Report no. 92-2, 22 p.

Walsh, J.E.

1984: Forecasts of monthly 700 mb height: verification and specification experiments; *Monthly Weather Review*, v. 112, no. 11, p. 2135–2147.

Wolfe, P.M.

1994: Hydrometeorological investigations on a small valley glacier in the Sawtooth Range, Ellesmere Island, Northwest Territories; M.Sc. thesis, Wilfred Laurier University, Waterloo, Ontario, 205 p.

Wolfe, P.M. and English, M.C.

1995: Hydrometeorological relationships in a glacierized catchment in the Canadian High Arctic; *Hydrological Processes*, v. 9, p. 911–921.

Woo, M-k., Edlund, S.A., and Young, K.L.

1991: Occurrence of early snow-free zones on Fosheim Peninsula, Ellesmere Island, Northwest Territories; *in* Current Research, Part B; Geological Survey of Canada, Paper 91-1B, p. 9–14.

Woo, M-k., Young, K.L., and Edlund, S.A.

1990: 1989 observations of soil, vegetation, and microclimate, and effects on slope hydrology, Hot Weather Creek basin, Ellesmere Island, Northwest Territories; *in* Current Research, Part D; Geological Survey of Canada, Paper 90-1D, p. 85–93.

Young, K.L., Woo, M-k., and Edlund, S.A.

1997: Influence of local topography, soil and vegetation on microclimate and hydrology at a High Arctic site; *Arctic and Alpine Research*, v. 29, no. 3, p. 270–284.

Young, K.L., Woo, M-k., and Munro, D.S.

1995: Simple approaches to modelling solar radiation in the Arctic; *Solar Energy*, v. 54, p. 33–40.

Overview of vegetation zonation in the Arctic

S.A. Edlund¹ and M. Garneau²

Edlund, S.A. and Garneau, M., 2000: Overview of vegetation zonation in the Arctic; in Environmental Response to Climate Change in the Canadian High Arctic, (ed.) M. Garneau and B.T. Alt; Geological Survey of Canada, Bulletin 529, p. 113–127.

Abstract: Woody plants can be used as bioclimatic indicators in the Arctic. Northern Canada is divided into seven bioclimatic zones whose limits coincide remarkably well with mean July isotherms. Two zones encompass the transition from treed terrain to tundra. The Northern Boreal Forest coincides with the southernmost extent of the arctic biome. Its biogeographic limit corresponds to the mean position of the arctic front in summer and to the 13°C mean July isotherm. In the Forest-Tundra Transition zone, mean July temperatures fall below 13°C and continuous forest is absent. The other five zones are zones of the ‘true’ or treeless Arctic and are characterized by plant habitat and number of vascular plant species.

Résumé : On peut utiliser les plantes ligneuses comme indicateurs bioclimatiques dans l’Arctique. Le Nord du Canada est subdivisé en sept zones bioclimatiques dont les limites correspondent remarquablement bien avec les isothermes moyens pour le mois de juillet. Deux zones couvrent la transition du terrain forestier à la toundra. La taïga coïncide avec l’étendue la plus méridionale du biome de l’Arctique. Sa limite biogéographique correspond à la position estivale moyenne du front Arctique et à l’isotherme moyen de 13 °C pour le mois de juillet. Dans la zone de transition forêt-toundra, les températures moyennes du mois de juillet tombent sous le seuil de 13 °C et il n’y a pas de forêt continue. Les cinq autres zones sont les «véritables» zones arctiques (sans arbres) et elles sont caractérisées par l’environnement biophysique des végétaux et notamment par un certain nombre d’espèces de plantes vasculaires.

¹ Terrain Sciences Division, Geological Survey of Canada, 601 Booth Street, Ottawa, Ontario K1A 0E8

² INRS-Eau, 2800, rue Einstein, C.P. 7500, Sainte-Foy, Québec G1V 4C7

INTRODUCTION

Vegetation in the Arctic is far from homogeneous. Diversity and plant-community composition vary with summer warmth, soil type, and moisture availability (Bliss and Matveyeva, 1992). Vascular-plant species in the Canadian Arctic reach their maximum diversity (350 species) in the warmest regions close to the treeline and their minimum diversity (fewer than 35 species) in the coldest regions (Young, 1971; Rannie, 1985; Edlund, 1986a; Edlund and Alt, 1989).

Summer warmth has the greatest influence on vegetation diversity. This control is best expressed as summations of total warmth such as melting degree-days or growing degree-days. Such data, however, are generally available only for the sparse network of northern weather stations (Edlund and Alt, 1989; Alt and Maxwell, 2000). The most readily available and widespread measure of summer warmth is the mean temperature for July, the warmest month (Fig. 1).

In the Canadian Arctic, mean July isotherms grade northward from about 10°C near the treeline to 1°C along the northwestern rim of the Queen Elizabeth Islands. This decline is not a simple, linear, latitudinal progression, but rather a complex pattern reflecting the interaction between incoming solar radiation, characteristics of the dominant air mass, topography, and the amount of open water surrounding the islands during the summer (Edlund 1983a, 1986a; Edlund and Alt, 1989). Climate affects the diversity, density, productivity, and growth forms of vascular plants on any given type

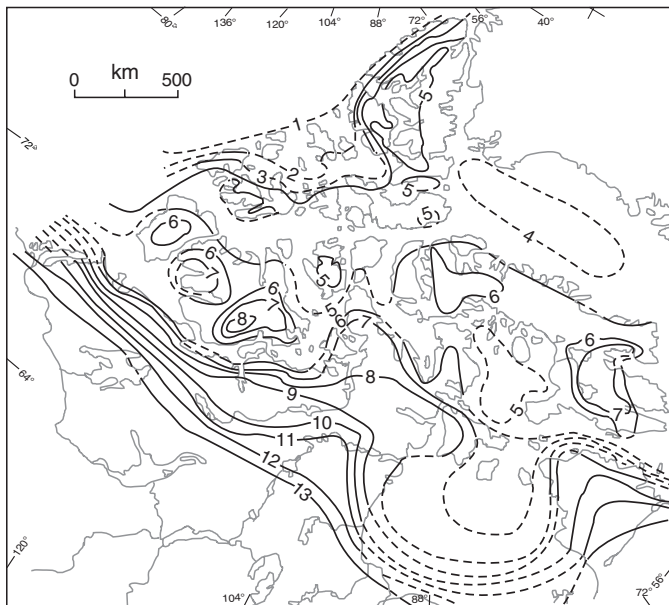


Figure 1. Mean July temperatures in northern Canada, derived from northern weather stations (Atmospheric Environment Service, 1982), community records, and selected, nonstandard weather data collected by the Polar Continental Shelf Project (after Edlund, 1986a).

of substrate by controlling temperature, length of thaw season, variations in precipitation, and intensity and duration of cloud cover.

Many plant species and associations have preferences for, or intolerances to, chemical, textural, and moisture variations in soils (Elevebakk, 1982). Some species prefer weakly to moderately alkaline soils, whereas others do not tolerate such conditions. Similarly, some species have specific moisture requirements. For example, aquatic sedges require poorly drained to saturated soil throughout most of the growing season. Other species cannot tolerate such an abundance of moisture. Therefore, within a given area, each type of parent material supports a suite of plant communities, each favouring a particular moisture regime. In the Arctic, where soils in summer are still underlain by permafrost and differences of a few centimetres in elevation make a great difference in the moisture availability, a mosaic of plant assemblages is characteristic (Polunin, 1960; Bliss, 1975, 1990).

Several broad biogeographic subdivisions of the North American arctic ecosystem have been proposed. Polunin (1951, 1960) and Energy, Mines, and Resources Canada (1973) divided the Arctic into three regions, Low, Mid, and High Arctic, primarily on the basis of the abundance of continuous ground cover and species diversity.

Young (1971) proposed a circumpolar, floristic classification based on species diversity. He created four zones north of the treeline that reflect the progressive impoverishment of vegetation towards the pole. He suggested that the primary ecological factor involved is the available summer warmth. Beschel (1969) numerically showed similar floristic trends on an island-wide scale.

Bliss (1977) divides the Canadian Arctic into two major regions on the basis of density and continuity of vegetation cover and implied soil-moisture characteristics. The Low Arctic encompasses the continental region north of the treeline and the southeastern corner of Baffin Island. The High Arctic includes all islands of the Canadian Arctic Archipelago, as well as Boothia and Melville peninsulas and Wager Plateau in northern Keewatin. Bliss further subdivided the High Arctic into the following three types (Babb and Bliss, 1974): polar desert, polar semidesert, and a complex including polar desert, polar semidesert, and sedge meadows. All three High Arctic zones occur throughout the Arctic Archipelago, although the complex is more prevalent in the more southerly sector of the islands. These subdivisions are compared with the Russian classification system in a recent review (Bliss and Matveyeva, 1992). The arctic vegetation zones of Alexandrova (1971, 1988) are based on floristic composition and plant forms and show a vegetation response to a strong, northward temperature gradient. The Eurasian classification scheme, as illustrated in Bliss and Matveyeva (1992), has four zones north of the Forest-Tundra Transition zone.

Detailed regional maps of plant associations for some areas of Arctic Canada (Edlund 1980, 1982a, b, c, 1983b, c, d, 1987b) revealed several broad vegetation patterns that could not be explained satisfactorily using previously proposed subdivisions. Comparisons with climate patterns, particularly

summer-temperature patterns, revealed great similarities between major vegetation changes and the degree of severity of the summer climate (Edlund, 1983a, 1986a). Because the terms 'Low Arctic', 'Mid Arctic', and 'High Arctic' have been applied to different areas by different authors (Edlund, 1986), they are not used in this paper although in a few regions, some zonal boundaries match. The zones used are named after the dominant vascular-plant growth form on mesic terrain. The nomenclature for vascular plants follows that of Porsild and Cody (1980).

BIOCLIMATIC ZONES IN ARCTIC CANADA

Although coniferous trees (spruce and larch) are absent in the Arctic, woody plants are the major components of most communities on all but the wettest or driest terrain. The mere presence of woody plants as well as changes in diversity and growth forms of woody plants have proven to be useful bioclimatic markers. Thus, major bioclimatic zones have been delineated on the basis of these characteristics of woody species. Great changes in diversity and density of herbaceous (nonwoody) species also occur throughout these zones and help to define them further.

Seven major bioclimatic zones have been recognized (Fig. 2), two of which encompass the transition from treed terrain to tundra. The other five are zones of the 'true' or treeless Arctic and are characterized by plant habitat and number of vascular-plant species and the roughly coincident mean July isotherms. These zones should not be interpreted directly as physically significant temperatures, but rather as relative indicators of regional warmth.

Regional diversity within the seven bioclimatic zones was calculated by overlaying the Canada-wide zones on individual species' range maps (Porsild, 1964; Porsild and Cody, 1980). Recent range extensions are also included. The total flora of a zone was compiled irrespective of the chemistry or drainage characteristics of the soils. As Young (1971) and Rannie (1985) found, the diversity of vascular plants decreases dramatically through the zones with decreasing summer temperatures (Fig. 3). Perennial, herbaceous species make up the largest number of taxa in all zones (Appendix A). Annuals are rare in the Arctic whereas biennials are few and generally restricted to the warmest zones.

The seven major bioclimatic zones represent major shifts in vegetation patterns with increasingly severe summers. Although the zones were named to reflect changes in the growth forms and significance of woody species on mesic terrain, they also represent changes in the density and diversity of herbaceous species in wetlands (Table 1).

Northern Boreal Forest zone

The northern limit of the boreal forest, which coincides with the southernmost extent of the arctic biome, is one of the best known phytogeographic and bioclimatic boundaries. It coincides roughly with the mean position of the Arctic front in summer (Bryson, 1966) and with the 13°C mean July isotherm

(Hare, 1970). Compared with other northern zones, diversity is greatest within the Northern Boreal Forest zone: over 500 vascular-plant species occur near the northern limit of the boreal forest, including over 100 woody species and many temperate genera such as cherry (*Prunus*), currant (*Ribes*), mountain ash (*Sorbus*), dogwood (*Cornus*), silverberry (*Elaeagnus*), blueberry and bilberry (*Vaccinium*), and willow (*Salix*). The erect, single-trunked tree is the dominant vascular-plant growth form in this zone.

Near the northern forest limit, this continuous coniferous forest, which is confined to the northern mainland of Canada, is dominated by spruce (*Picea*). Other conifers such as larch (*Larix*), fir (*Abies*), and pine (*Pinus*) are also present (Rowe, 1972; Ritchie, 1984; Richard, 1987). Tall, deciduous shrubs and small specimens of birch (*Betula*), alder (*Alnus*), aspen (*Populus*), and willow (*Salix*) are also found in this zone (Gill, 1973; Gilbert and Payette, 1982; Ritchie, 1984), often as successional species in opening or disturbed terrain such as river margins. Common juniper (*Juniperus communis*), a coniferous shrub, also occurs in this zone.

Wetlands, dominated by sedges, contain over 170 wetland (growing in poorly drained soils), emergent (growing with lower stems partly submerged), and aquatic (vegetative growth totally submerged) species. A number of woody species and herbs are present on mounds of peat, which afford slightly better drained conditions.

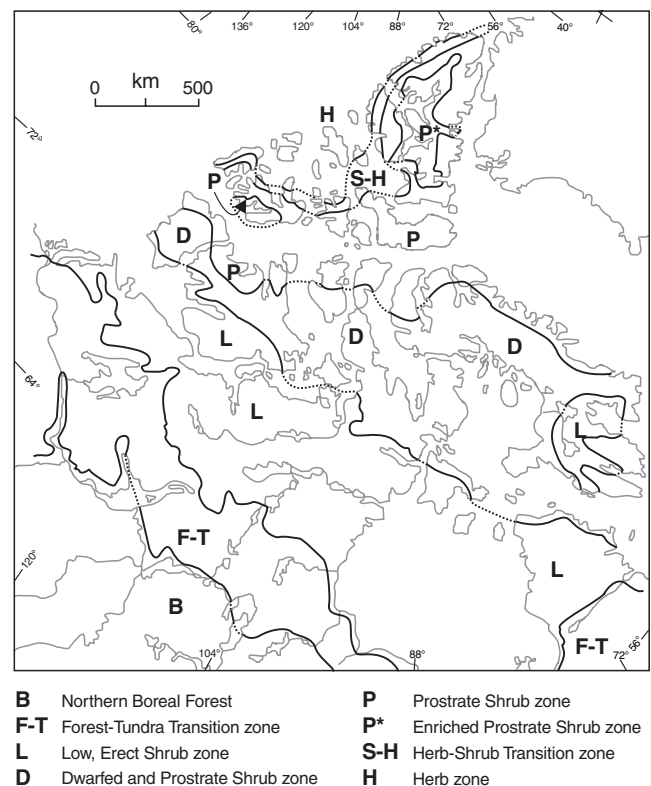


Figure 2. Bioclimatic zones in northern Canada (after Edlund, 1990).

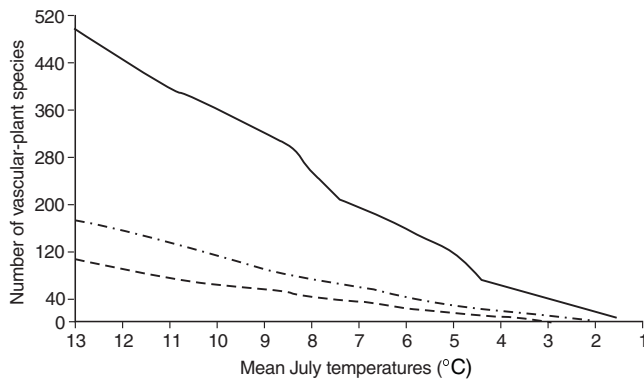


Figure 3. Diversity of vascular plants in the bioclimatic zones. Key: solid line = total number of vascular plant species; dashes and dots = number of wetland aquatic and emergent species; dashed line = number of woody species (after Edlund, 1990).

Forest-Tundra Transition zone

The continuous forest is absent where mean July temperatures fall below 13°C. The tree growth form persists, however, and woody plants continue to dominate all but the wettest terrain. Between the 13°C and 12°C isotherms, trees commonly occur in an open formation; between the 12°C and 10°C isotherm, trees are generally restricted to favourable locations such as sunny slopes and sheltered, well watered valley bottoms. Low, erect shrubs, 25–100 cm high, occur in many parts of this zone in both clumps and dense thickets on moderately to imperfectly drained substrates, although lichens are the common ground cover in some areas of the Canadian Shield. Prostrate (low and sprawling) shrubs are more common on thin, well drained soils and in more exposed sites. Multibranched, small-tree-sized deciduous shrubs such as *Salix* and *Alnus* are found on floodplains and disturbed terrain. Over 400 species of vascular plants, including at least 75 woody species, are found in this zone.

Wetlands contain about 130 wetland, aquatic, and emergent species (still rich by northern standards), as well as a variety of sedges, shrubs, and herbs. Sedges remain the dominant vascular plants.

The treeline, the northern limit of the coniferous-tree growth form and of the Forest-Tundra Transition zone, is found on the continental mainland, but not on any of the Arctic Islands, although it is close to the northern continental margin near the head of Horton and Coppermine rivers and the Mackenzie Delta. It coincides roughly with the 10°C mean July isotherm (Nordenskjöld and Mecking, 1928; Hare, 1970). Many more temperate woody species including small, deciduous trees such as poplar (*Populus*), birch (*Betula*), *Alnus*, a few *Salix* species, and serviceberry (*Amelanchier*), and shrubs such as northern rose (*Rosa acicularis*), shrubby cinque (*Potentilla fruticosa*), bog laurel (*Kalmia polifolia*), sweet gale (*Myrica gale*), spirea (*Spiraea beauverdiana*), soapberry (*Sherpherdia canadensis*), twin flower (*Linnaea*

Table 1. Arctic bioclimatic zones, corresponding mean July isotherms, and vascular plant diversity (modified from Edlund, 1990 and Edlund and Alt, 1989).

Vegetation zone	Mean July isotherm (°C)	Vascular-plant diversity	Woody species	Wetland species
Northern Boreal Forest zone	>13°C	≥500	100	>170
Forest-Tundra Transition zone	10–13°C	>400	75	≥130
Low, Erect Shrub zone	7–10°C	300	50	75
Dwarfed and Prostrate Shrub zone	5–7°C	150–200	17	35
Prostrate Shrub zone	4–6°C	50–150	12	24
Herb-Shrub Transition zone	3–4°C	35–75	2	11
Herb zone	1–3°C	<35	none	none

borealis), common Labrador tea (*Ledum groenlandicum*), cranberry (*Oxycoccus microcarpus*), and common bearberry (*Arctostaphylos uva-ursi*) are also present.

Low, Erect Shrub zone

This treeless region of the Arctic is found immediately north of the treeline in the following areas: the northernmost mainland, southern Banks, Victoria, and Baffin islands, and the islands in Hudson and James bays. Mean July temperatures within this region range from 10°C to 7°C. Over 300 species of vascular plants occur in this zone, over 50 of which are woody. This is the arctic zone with the greatest density and diversity of vascular plants.

Conifers are generally absent except near the treeline, where the low shrub *Juniperus communis* and *Picea*, which occur locally in a severely dwarfed, or 'krummholz' growth form, are found. Woody plants, particularly low, erect shrubs (25 cm to 1 m or more high) such as dwarf birch (*Betula glandulosa*) and *Salix*, as well as ericaceous species such as arctic white heather (*Cassiope tetragona*) and northern Labrador tea (*Ledum decumbens*), are dominant. In the warmest sectors, the low, shrub-thicket canopy (0.5–1.0 m high) can be nearly continuous on sheltered, well watered slopes. In the cooler sectors (at the northern end of the zone), dense, low-shrub thickets (25–50 cm high) are restricted to more sheltered locations such as hollows and protected valleys. Exposed terrain and thin soils are dominated by prostrate shrubs such as arctic avens (*Dryas integrifolia*) and arctic willow (*Salix arctica*), or low, ericaceous species.

Tree-sized (2–7 m high) felt-leaf willows (*Salix alaxensis*) and Betulaceae (birch and alder) are found locally, generally on floodplains near the edges of deep channels and in sheltered locations (Maycock and Matthews, 1966; Edlund and Egginton, 1984). Away from stream margins, the same felt-leaf willow species commonly adopts the more usual low, erect growth form.

Wetlands contain 75 wetland, aquatic, and emergent species. Sedges still dominate and low, erect shrubs and a variety of herbs often occur on slightly better drained terrain within the wetlands. A thick, mossy, peat-forming mat is commonly associated with wetlands. The most continuous coverage of tussock-cotton-grass tundra (mainly *Eriophorum vaginatum*), primarily found on extensive, fine-grained sediments of coastal lowlands, is also found in this zone.

The Low, Erect Shrub zone marks the northern limit of many common arctic shrub species such as dwarf birches (*Betula glandulosa* and *B. nana*), green alder (*Alnus crispa*), andromeda (*Andromeda polifolia*), alpine azalea (*Loiseleuria procumbens*), mountain heather (*Phyllodoce coerulea*), and cloudberry (*Rubus chamaemorus*).

Dwarfed and Prostrate Shrub zone

In regions with mean July temperatures between 7°C and 5°C, the low, erect, shrub growth form is absent, although species capable of erect growth, such as *Salix alaxensis*, *Salix lanata* var. *richardonii*, and *S. niphoclada*, still occur, but rarely form canopy. Their growth form is stunted (less than 25 cm high). These dwarfed species, generally restricted to sheltered, well watered sites, are only a small part of the plant communities.

Mesic soils in the zone are usually dominated by genetically dwarfed shrubs. One such species is the prostrate arctic willow (*Salix arctica*) that has branches sprawling along the ground and that can reach a lateral extent of 1 m or more. Another common species is the matted shrub *Dryas integrifolia*, which is abundant on neutral to moderately alkaline soils. These two species are also present in more southerly areas, but are restricted to thinner soils and more exposed terrain. The Dwarfed and Prostrate Shrub zone contains 150 to 200 species of vascular plants, including 17 woody species.

Wetland communities, dominated by sedges, contain 35 wetland, aquatic, and emergent species. Both dwarfed and prostrate shrub species are present on slightly better drained hummocks. *Eriophorum* tussock-tundra may also occur, although its coverage is not as dense or as extensive as it is in the Low, Erect Shrub zone.

The Dwarfed and Prostrate Shrub zone occurs extensively in the southern third of Arctic Islands, on the mainland on Boothia and Melville peninsulas, and on a strip along the northern coast of Ungava Peninsula. Its northern limit is south of Parry Channel. It generally marks the northern extent of shrub species capable of erect growth, including northern Labrador tea (*Ledum decumbens*), Lapland rosebay (*Rhododendron lapponicum*), several *Salix* species, a number of naturally prostrate, ericaceous species, and *Empetrum nigrum*.

Prostrate Shrub zone

In regions where mean July temperatures range between 6°C and 4°C, plant assemblages are generally similar to those in the Dwarfed and Prostrate Shrub zone, but shrubs capable of erect growth are absent. The woody species *Salix arctica* and *Dryas integrifolia* still dominate on mesic terrain. On the

whole, the flora of this zone is less diverse than in the Dwarfed and Prostrate Shrub zone. Most obviously absent are Leguminosae (particularly *Oxytropis* and *Astragalus*), arctic fireweed (*Epilobium latifolium*), and many Compositae — particularly those with erect flowering stems such as *Senecio congestus*, *Petasites frigidus*, and *Arnica alpina*, as well as the more compact *Antennaria compacta*, *Chrysanthemum integrifolium*, *Crepis nana*, and *Erigeron* spp. *Cassiope tetragona*, the hardiest heath species, is restricted to neutral or acid soils in the warmer sectors with mean July temperatures of at least 5°C. Less obvious are decreases in the number of grass and sedge species. The zone supports 50 to 150 species of vascular plants, including 12 woody species.

Wetlands are still dominated by sedges, although their diversity is reduced to three common species, *Carex aquatilis* var. *stans*, *Eriophorum triste*, and *E. scheuchzeri*. *Eriophorum* tussock-tundra does not occur in this zone, although the species itself may occur locally. Only 24 wetland, aquatic, and emergent species are found in this zone. Grasses, particularly *Dupontia fisheri* and *Alopecurus alpinus*, are common associates in these wetlands and may become dominant locally, particularly on bare mineral soils.

Floral assemblages are exceptionally rich in two widely separated areas within this zone, western Melville Island and west-central Ellesmere Island (Edlund, 1986b). These enriched zones resemble the Dwarfed and Prostrate Shrub zone, except for the absence of species capable of erect shrub growth (e.g. *Salix alaxensis*, *S. lanata*, and *S. niphoclada*). Mesic floras of western Melville Island locally include *Oxytropis* sp., *Astragalus* sp., and a variety of more southerly Compositae as well as *Epilobium latifolium*. These species may, however, have greatly stunted flowering stalks (Edlund 1986b, 1987b).

The enriched zone of west-central Ellesmere Island is similarly enhanced (Bruggemann and Calder, 1953; Brassard and Beschel, 1968; Soper and Powell, 1983; Bridgland and Gillett, 1984). No Leguminosae are present, but six species of shrubs (*Salix herbacea*, *S. polaris*, *S. reticulata*, *Rhododendron lapponicum*, *Vaccinium uliginosum*, and *Empetrum nigrum*) are found at a few sites (Porsild, 1964; Porsild and Cody, 1980). This enriched zone is not only sheltered from the direct effect of air masses originating over the polar pack ice by substantial mountain and plateau barriers, but it also experiences minimum cloud cover and low relative humidity associated with broad subsidence in the lee of the mountains (Alt and Maxwell, 1990). The land is generally free of snow by early to middle June. Temperatures in June are well above freezing. Mean July temperatures of over 8°C are common (Alt et al., 2000). The melt season may be as long as 12 weeks, while the snow-free period is at least 10 to 11 weeks.

These disjunct, enriched zones (Fig. 2) correspond roughly to anomalously warm areas (Fig. 1) in which temperature ranges overlap with those of the Dwarfed and Prostrate Shrub zone, with mean July temperatures of at least 5°C. They may represent outliers of the warmer Dwarfed and Prostrate Shrub zone, since most other associated species thrive

there. Low, erect shrub species may not have been dispersed into these areas because of the distances involved (Edlund and Alt, 1989).

These enriched areas also show enhanced growth and diversity of wetland, aquatic, and emergent species. More southerly species such as *Carex membranacea*, *Hippuris vulgaris*, and *Ranunculus gmelinii* occur in both areas, whereas *Arctophila fulva* and *Caltha palustris* occur only in southwestern Melville Island.

The Prostrate Shrub zone extends from south of Parry Channel well into the Queen Elizabeth Islands. It is found near sea level in the southern island as well as on the northern coast of Devon Island and some of the larger, central islands, generally in the lee of sizable land masses. Snow generally disappears by mid-June and perennial snow beds are present, but not abundant. The melt season is at least ten weeks long and, as the snow tends to disappear rapidly, the snow-free period lasts over nine weeks. The 4°C mean July isotherm coincides roughly with the northern limit of woody plant dominance and with the northern limit of sedge dominance in wetlands.

Herb-Shrub Transition zone

Woody plants are present, but no longer dominant, in regions with mean July temperatures below 4°C. They are replaced by herbs, generally those that were most common in plant communities in the Prostrate Shrub zone to the south. This transition zone, bracketed by the 4°C and 3°C mean July isotherms, contains between 35 and 75 species of vascular plants, including only two species of woody plants. *Salix arctica* and *Dryas integrifolia* are generally restricted to sunny, sheltered locations. *Salix arctica* commonly has an extremely compact growth form instead of its usual sprawling, branched form.

A major change in plant-species composition also occurs in wetlands. Only 11 wetland, aquatic, and emergent species are found. Although present, sedges are no longer dominant. Vascular wetland plants are restricted primarily to grasses, such as *Alopecurus alpinus* and *Dupontia fisheri*. Only a few emergent species such as *Pleuropogon sabinei* and *Ranunculus hyperboreus* survive.

This zone is found primarily in the north-central and northern Queen Elizabeth Islands. It is common near sea level on the leeward sides of the islands, at intermediate elevations in the southern uplands, and at elevations ranging upward of 800 m on the leeward side of the mountains in the northeast. The 3°C mean July isotherm coincides roughly with both the northern limit of the zone and the northern limit of the presence of woody plants. It also marks the northern limit of sedges.

In this zone, the melt season varies from eight to ten weeks and the snow-free period lasts generally only seven to nine weeks. Near sea level, the zone apparently coincides with areas where sea ice in interisland channels breaks up in mid-summer, leaving extensive areas of open water adjacent to the islands.

Herb zone

Vascular-plant assemblages are sparsest, least diverse, and entirely herbaceous in regions where mean July isotherms fall below 3°C. The Herb zone is found in the northwestern and north-central Queen Elizabeth Islands and extends to their northern margins (Edlund, 1980, 1983a). Woody plants, sedges, members of the Compositae, and aquatic and emergent species do not occur in this zone. Fewer than 35 species of vascular and herbaceous plants are found. There are no true wetland species; four vascular species grow on saturated soils, but are also found in somewhat drier habitats. Snow cover persists into early July. Small, perennial snow beds are common on leeward slopes and in ravines. Freeze-up begins as early as mid-August.

Vegetation-free zone

Some sectors characterized by the lack of both vascular plants and cryptogamic vegetation are found on the highlands and plateaus of Melville Island (Edlund, 1985) and Bathurst Island (Edlund, 1982c). Although not yet aerially mapped, the Vegetation-free zone probably also occurs on some ice-free summits of Axel Heiberg and Ellesmere islands (Beschel, 1970), as well as in a narrow band along the coast of the Queen Elizabeth Islands adjacent to the polar pack ice. These sectors are the latest to thaw in the spring, the first to freeze up in late summer, and correspond roughly to equilibrium-line calculations for glaciation levels or freezing levels (Bradley, 1975; Bradley and Eischeid, 1985). Summer temperatures are so low (mean July temperatures near 0°C) that lee-slope snowbanks commonly persist throughout the summer.

Oases

The concept of polar oases surrounded by polar deserts (Bliss, 1977; Svoboda and Freedman, 1981; Henry et al., 1986; Freedman et al., 1994) has been used to characterize "small and discrete oasis of relatively high biological productivity, within the context of the more typically barren polar desert climatic regime" (Labine, 1994). These locally fertile areas can be the result of thermal and/or moisture enhancement (Edlund and Alt, 1989; Labine, 1994). To date, oases have been the most intensively studied areas (Bliss, 1977; Bergeron and Svoboda, 1989; Levesque and Svoboda, 1992; Muc et al., 1994; Nams and Freedman, 1994; Svoboda and Freedman, 1994; Levesque et al., 1997) in the High Arctic. They usually represent the best plant productivity under relatively good conditions for these High Arctic environments. They may be of great local or seasonal importance to fauna. However, oases cannot be taken as representative of the region, for most of them cover a total area of less than 5 km²; they represent a micro- or mesoscale feature rather than a regional one. Regional bioclimatic studies, such as the present climate zonation, provide a background with which oases or locally enriched areas can be compared.

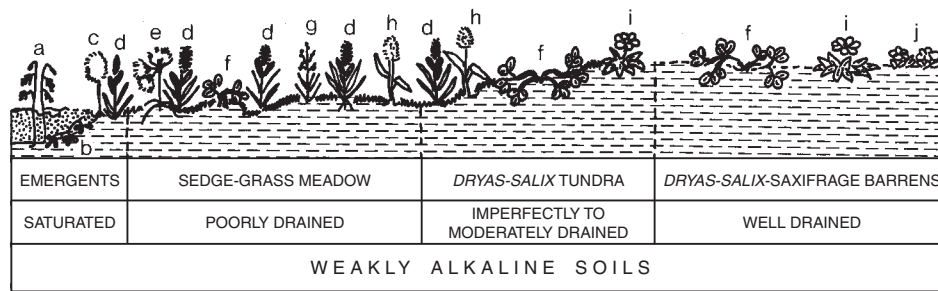


Figure 4. Catena showing the suites of plant communities on weakly alkaline surficial materials for each broad type of moisture regime in an area that supports prostrate shrub communities on moderately to well drained soils and sedge meadows on poorly drained soils. Typical species include the following: a. *Pleuropogon sabiniei*; b. *Ranunculus hyperboreus*; c. *Eriophorum scheuchzeri*; d. *Carex aquatilis* var. *stans*; e. *Eriophorum triste*; f. *Salix arctica*; g. *Arctagrostis latifolia*; h. *Alopecurus alpinus*; i. *Dryas integrifolia*; j. *Saxifraga oppositifolia* (after Edlund and Alt, 1989).

DISCUSSION

The zones outlined above are the end product of extensive island-by-island survey work undertaken over a 20-year period by Dr. Sylvia Edlund as part of the mapping activities of the Geological Survey of Canada in the Canadian Arctic Islands. This work was consolidated in a comparative study of regional vegetation zones and regional climate conditions (Edlund and Alt, 1989). It should also be noted that the definitions of both vegetation and climate patterns were developed independently and combined only after the similarities in the two were noticed. The congruence is most evident when comparing the characteristic S-shaped patterns of vegetation limits (Edlund and Alt, 1989, Fig. 6) with mean July temperatures (Edlund and Alt, 1989, Fig. 11b). It is important to remember that both these patterns were derived on a regional scale and do not take into account the effects of elevation, local topography, and mesoscale climate. The regional vegetation patterns reflect the best possible vegetation that can be expected if materials are capable of supporting plant growth and if adequate moisture is available. The temperature patterns reflect the air-mass temperature as deduced from screen-level temperatures at coastal stations. The following additional aspects of previous research are relevant to the present volume.

Controls of vegetation patterns within regional bioclimatic zones

The regional nature of this bioclimatic zonation system must be stressed. It is not in any way a contradiction of the fact that the arctic vegetation is a mosaic based on local conditions (Bliss, 1977; Bliss and Svoboda, 1984). Edlund (1986a) has pointed out that climate is not the only control upon vegetation in the Arctic. The flora of the Arctic, once thought to be analogous to a pioneer succession stage with a strong random component (Britton, 1958), is a series of regularly repeating plant communities controlled by climate and edaphic factors. The physical and chemical properties of arctic soils influence both vascular-plant species and plant-community distribu-

tions in the Queen Elizabeth Islands (Thorsteinsson, 1958; Tozer and Thorsteinsson, 1964; Edlund, 1980, 1986b, 1989). Some materials are inimical to plant life, as discussed in detail by Edlund (Edlund and Alt, 1989). In soils with chemical properties within the range of tolerance of arctic vascular plants, the degree of alkalinity or acidity greatly influences the distribution of vascular species and communities. This is illustrated in Figure 4 by a catena showing the suites of plant communities on weakly alkaline surficial materials for each broad type of moisture regime in an area that supports prostrate-shrub communities on moderately to well drained soils.

Moisture availability varies with topographic position and proximity to a moisture source (Edlund and Alt, 1989). Results from Hot Weather Creek slope studies (Woo et al., 1990; Young et al., 1997) illustrate this. Even in regions with less than 40 mm of measured, annual precipitation, extensive wetlands can develop in lowlands and downslope from permanent snowbeds. Slight changes in moisture regimes result in changes in plant assemblages. For each type of material, a suite of plant communities reflects changes in local soil moisture availability. Figure 5 illustrates the variation in vegetation within each bioclimatic zone using a catena of species for weakly acidic and weakly alkaline materials over a range of moisture conditions.

Bioclimatic indicators

Bioclimatic indicators are necessary for paleoenvironmental reconstruction. Tree growth form is the best known bioclimatic indicator and the one that is used the farthest north, the northern boreal forest and treeline being traditionally linked to the 10°C and 13°C isotherms respectively. Edlund (1986a) introduced the use of vascular-plant species as bioclimatic indicators for treeless, arctic regions.

Woody plants are among the most useful bioclimatic indicators throughout the Arctic, even though the tree growth form is absent. The presence of coniferous krummholz is an indicator of climatic conditions similar to those found near the coniferous treeline (associated with the 10°C mean July

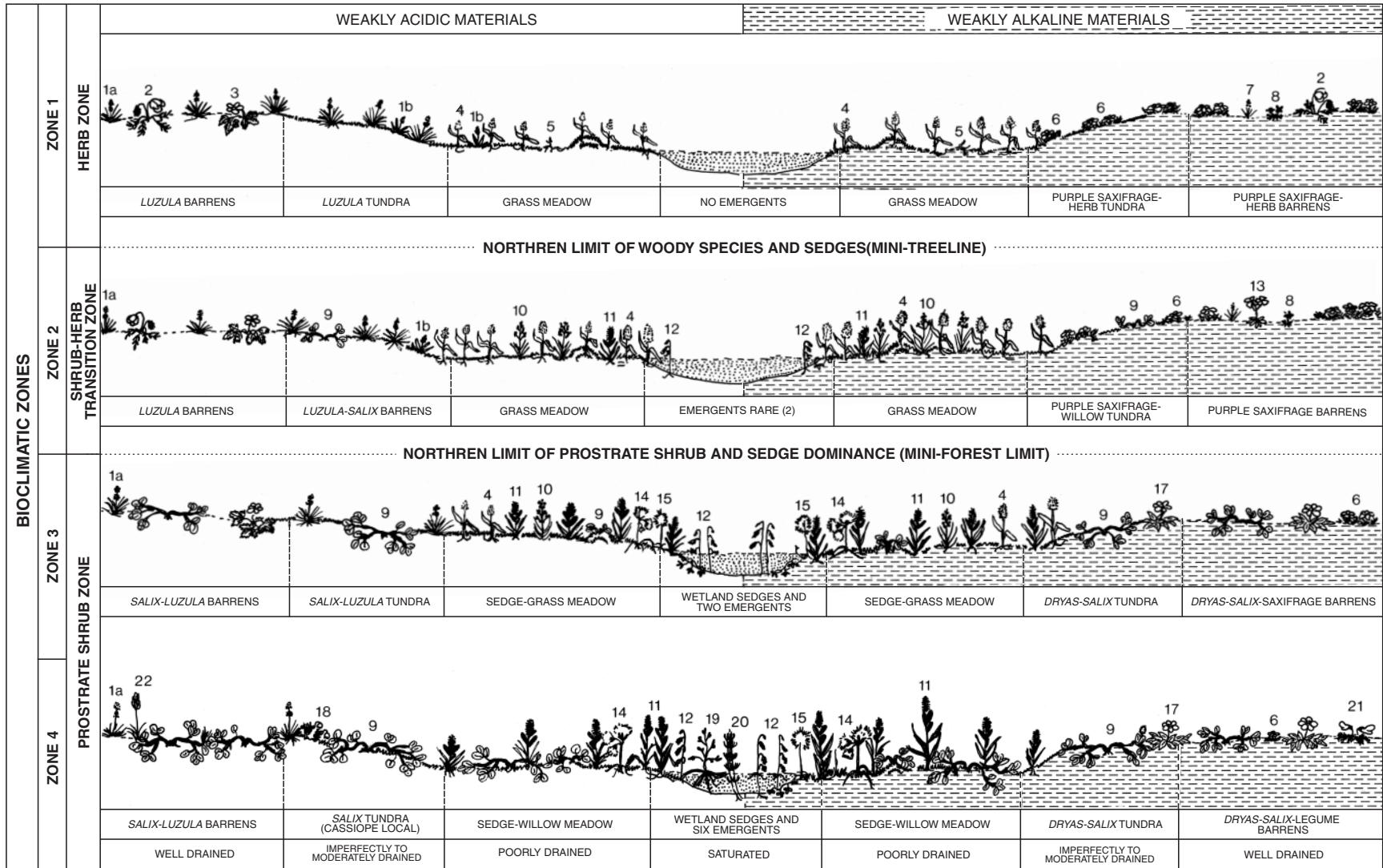


Figure 5. Catena for each vegetation zone. Species illustrated include the following: 1a. *Luzula confusa*; 1b. *Luzula nivalis*; 2. *Papaver radicatum*; 3. *Potentilla hyparctica*; 4. *Alopecurus alpinus*; 5. *Phippsia algida*; 6. *Saxifraga oppositifolia*; 7. *Poa abbreviata*; 8. *Draba* sp.; 9. *Salix arctica*; 10. *Dupontia fisheri*; 11. *Carex aquatilis* var. *stans*; 12. *Pleuropogon sabinei*; 13. *Parrya arctica*; 14. *Eriophorum triste*; 15. *Eriophorum scheuchzeri*; 16. *Ranunculus hyperboreus*; 17. *Dryas integrifolia*; 18. *Cassiope tetragona*; 19. *Arctophila fulva*; 20. *Hippuris vulgaris* (after Edlund and Alt, 1989).

isotherm). The small-tree growth form of several deciduous shrubs, such as *Betula*, *Alnus*, and *Salix*, also indicates that treeline climate conditions occur at least locally.

Where tree growth forms are absent, treeline climate conditions may be indicated by the presence of several, more temperate, woody species such as *Juniperus communis*, *Amelanchier alnifolia*, *Spiraea beauverdiana*, *Myrica gale*, *Ribes* spp., *Ledum groenlandicum*, *Rosa acicularis*, *Rubus strigosus*, *Potentilla fruticosa*, *Linnaea borealis*, and shrubby *Salix* species (Edlund, 1990, Table 1).

Farther north, in the arctic islands, the presence of shrubs with low, erect growth forms (e.g. *Salix alaxensis*, *S. glauca*, *S. lanata*, *S. niphoclada*, *Ledum decumbens*, *Betula glandulosa*, and a variety of ericaceous species; Edlund, 1990, Table 1) indicates a climate comparable to that of the warmest sector of the Arctic — the denser and higher the thickets, the warmer the summer climate.

The pattern of increasing restriction of low, erect, thicket growth to sheltered, well watered places with decreasing temperatures (from 10°C to 7°C) is similar to the pattern displayed by trees in the Forest-Tundra Transition zone. The northern limit of low, erect shrubs corresponds roughly to the 7°C mean July isotherm and is the southern Arctic equivalent of the northern forest limit.

The climatic dwarfing of willows, the deciduous equivalent of coniferous krummholz, is an indicator of regional mean July temperatures ranging from 7°C to 5°C where snow depth is not a factor. The northern limit of species capable of erect shrub growth corresponds roughly to the 5°C mean July isotherm and is the southern Arctic equivalent of the treeline (shrubline or mini-tree line).

Prostrate shrubs thrive from the northern limit of the coniferous forest. They are important, often dominant, species throughout most of the Canadian Arctic Archipelago. In regions with mean July temperatures above 5°C, the branches of *Salix arctica* may spread out to 1 m or more. The diameter of clumps of *Salix arctica* decreases dramatically as mean July temperatures fall below 5°C. Prostrate and matted shrubs lose their dominance when regional mean July temperatures drop below 4°C. The northern limit of woody plant dominance (the northern Arctic equivalent of the northern forest limit) corresponds roughly to the 4°C mean July isotherm. Prostrate and matted shrubs persist locally into regions cooler than 4°C, but their growth forms are extremely compact, which may reflect age and slow growth rather than just the inability to grow larger (E. Levesque, pers. comm., 1992). Clumps of *Salix arctica* may be no more than 10 cm in diameter. The northern limit of woody plants corresponds roughly to the 3°C mean July isotherm, which can be considered the northern Arctic equivalent of the treeline.

Wetlands, too, have several obvious bioclimatic indicators. A high diversity of wetland, aquatic, and emergent species suggests conditions similar to those occurring in the warmest zones of the Arctic. The presence of extensive *Eriophorum* tussock-tundra suggests mean July temperatures of at least 5°C. The presence of low, erect shrubs in the tussock-tundra would indicate mean July temperatures of at least 7°C. The dominance of sedge species in wetlands indicates mean July temperatures of at least 4°C, whereas the mere presence of sedges indicates mean July temperatures of at least 3°C.

CONCLUSIONS

Northern Canada has been divided into seven bioclimatic zones on the basis of the growth form of the dominant vascular plant species. Five of these zones cover the true Arctic. These regional vegetation patterns can be linked roughly to mean July isotherms, as in the northern boreal forest and treeline. Many vascular-plant species show promise as bioclimatic indicators that can assist in extrapolating modern, summer-climate data to treeless regions where there are no climate records and where most vascular-plant species are at or near their physiological limits of tolerance, as is seen in the decrease in the number of taxa in various zones, in the distribution of individual species, in the changes in growth type, and in the dominance of certain growth forms and species.

Regional zonation and the definition of zonal boundaries such as the limit of woody species or the limit of woody species dominance, which can in turn be related to climate parameters, are important indicators for studies of paleoenvironmental and future environmental change. They also provide a definition of regional, potential vegetation to which intensive vegetation mapping of limited areas can be related. This will make it possible to link micro- and mesoscale processes and monitoring studies to global-scale variations, both modelled and monitored.

ACKNOWLEDGMENTS

The logistical support provided by the Polar Continental Shelf Project during the field seasons of 1973–1987 made the vegetation mapping possible. The comments and references provided by Dr. Esther Levesque (Université du Québec à Trois-Rivières) are gratefully acknowledged.

REFERENCES

- Alexandrova, V.D.**
1970: The vegetation of the tundra zones in the U.S.S.R. and data about its productivity; *in* Productivity and Conservation in Northern Circumpolar Lands, (ed.) W.A. Fuller and P.G. Kevan; International Union for the Conservation of Nature, Morges Switzerland, New Series, v. 16, p. 93–114.
1988: Vegetation of the Soviet Polar Deserts; Cambridge University Press, Cambridge, 228 p.
- Alt, B.T. and Maxwell, J.B.**
1990: The Queen Elizabeth Islands: a case study for arctic climate data availability and regional climate analysis; *in* Symposium on the Canadian Arctic Islands, Canada's missing dimension, (ed.) C.R. Harington; Special Publication, National Museum of Natural Sciences, v. I, p. 295–326.
2000: Overview of the modern arctic climate; *in* Environmental Response to Climate Change in the Canadian High Arctic, (ed.) M. Garneau and B.T. Alt; Geological Survey of Canada, Bulletin 529.
- Atmospheric Environment Service**
1982: Canadian climate normals 1951–1980: temperature and precipitation — the North — Y.T. and N.W.T.; Environment Canada, Downsview, Ontario, 55 p.
- Babb, T.A. and Bliss, L.C.**
1974: Susceptibility to environmental impact in the Queen Elizabeth Islands; *Arctic*, v. 27, no. 3, p. 234–236.
- Bergeron, J.-F. and Svoboda, J.**
1989: Plant communities of Sverdrup Pass, Ellesmere Island, NWT; *The Musk-Ox*, v. 37, p. 76–85.
- Beschel, R.E.**
1969: Floristicheskie Sootnosheniya na ostrovakh Nearktiki (Floristic relations of the Nearctic Island); *Botanicheski Zhurnal*, v. 54, no. 6, p. 228–269.
1970: The diversity of tundra vegetation; *in* Proceedings, Conference on Productivity and Conservation in Northern Circumpolar Lands, Edmonton, Alberta, (ed.) W.A. Fuller and P.J. Kevan; International Union for Conservation of Nature, New Series v. 16, p. 85–92.
- Bliss, L.C.**
1975: Tundra grasslands, herblands, and shrublands and the role of herbivores; *Geoscience and Man*, v. 10, p. 51–79.
1990: High Arctic ecosystems: how they develop and are maintained; *in* Canada's Missing Dimension: Science and History in the Canadian Arctic Islands, Volume 1, (ed.) C.R. Harington; Canadian Museum of Nature, Ottawa, Ontario, p. 350–384.
- Bliss, L.C. (ed.)**
1977: Truelove Lowland Devon Island Canada: a High Arctic ecosystem; University of Alberta Press, Edmonton, Alberta, 714 p.
- Bliss, L.C. and Matveyeva, N.V.**
1992: Circumpolar arctic vegetation; *in* Arctic Ecosystems in a Changing Climate: an Ecophysical Perspective, (ed.) F.S. Chaplin III, R.L. Jefferies, J.F. Reynolds, G.R.S. Shaver, J. Svoboda, and E.W. Chu; Academic Press Inc., San Diego, California, p. 59–89.
- Bliss, L.C. and J. Svoboda**
1984: Plant communities and plant production in the western Queen Elizabeth Islands; *Holarctic Ecology*, v. 7, p. 325–344.
- Bradley, R.S.**
1975: Equilibrium line altitudes, mass balance and July freezing level heights in the Canadian High Arctic; *Journal of Glaciology*, v. 14, p. 267–274.
- Bradley, R.S. and Eischeid, J.K.**
1985: Aspects of the precipitation climatology of the Canadian High Arctic; *in* Glacial, Geologic and Glacio-climatic Studies in the Canadian High Arctic, (ed.) R.S. Bradley; University of Massachusetts, Amherst, Massachusetts, Contribution no. 49, p. 250–271.
- Brassard, G.R. and Beschel, R.E.**
1968: The vascular flora of Tanquary Fiord, northern Ellesmere Island, N.W.T.; *The Canadian Field-Naturalist*, v. 82, no. 2, p. 103–113.
- Bridgland, J. and Gillett, J.M.**
1984: Vascular plants of the Hayes Sound region, Ellesmere Island, Northwest Territories; *The Canadian Field-Naturalist*, v. 97, p. 279–292.
- Britton, M.E.**
1958: Vegetation of the Arctic tundra; *in* Arctic Biology, (ed.) H. Hansen; Annual Biological Colloquium, Oregon State University Press, Corvallis, p. 26–61.
- Bruggemann, P.F. and Calder, J.A.**
1953: Botanical investigations in northeast Ellesmere Island, Northwest Territories; *The Canadian Field-Naturalist*, v. 67, no. 4, p. 157–174.
- Bryson, R.A.**
1966: Air masses, streamlines, and the boreal forest; *Geographical Bulletin*, v. 8, no. 3, p. 228–269.
- Edlund, S.A.**
1980: Vegetation of Lougheed Island, District of Franklin; Geological Survey of Canada, Paper 80-1A, p. 329–333.
1982a: Plant communities on the surficial materials of north-central Keewatin; Geological Survey of Canada, Paper 82-33, p. 1–20.
1982b: Vegetation of Cornwallis, Little Cornwallis, and associated islands, District of Franklin; Geological Survey of Canada, Open File 857, scale 1:250 000.
1982c: Vegetation of Melville Island, District of Franklin: eastern Melville Island and Dundas Peninsula; Geological Survey of Canada, Open File 853, scale 1:250 000.
1983a: Bioclimatic zonation in a High Arctic region: central Queen Elizabeth Island; Geological Survey of Canada, Paper 83-1A, p. 381–390.
1983b: Reconnaissance vegetation studies on western Victoria Island, Canadian Arctic Archipelago; Geological Survey of Canada, Paper 83-1B, p. 75–81.
1983c: Vegetation of the Bathurst Island area, Northwest Territories; Geological Survey of Canada, Open File map 888, scale 1:250 000.
1983d: Vegetation of north-central Queen Elizabeth Islands, Northwest Territories; Geological Survey of Canada, Open File 887, scale 1:250 000.
1985: Lichen-free zones as neoglacial indicators on western Melville Island, District of Franklin, N.W.T.; *in* Current Research, Part A; Geological Survey of Canada, Paper 85-1A, p. 709–712.
1986a: Modern arctic vegetation distribution and its congruence with summer climate patterns; *in* Proceedings of Atmospheric Environment Service Workshop: Impact of Climate Change on the Canadian Arctic, (ed.) H.M. French; Atmospheric Environment Service, Downsview, Ontario, p. 84–99.
1986b: Vegetation-geology-climate relationships of western Melville Island, District of Franklin; Geological Survey of Canada, Paper 86-1A, p. 719–726.
1987a: Plants: living weather stations; *Geos*, v. 16, no. 2, p. 9–13.
1987b: Vegetation of Melville Island, District of Franklin, Northwest Territories: western Melville Island; Geological Survey of Canada, Open File 1509, scale 1:250 000.
1990: Bioclimatic zones in the Canadian Arctic Archipelago; *in* Canada's Missing Dimension. Science and History in the Canadian Arctic Islands. Volume I, (ed.) C.R. Harington; Canadian Museum of Nature, p. 421–441.
1991: Climate change and its effects on Canadian arctic plant communities; *in* Arctic Environment: Past, Present and Future, (ed.) M-k. Woo and D.J. Gregor; Proceedings of a symposium held at McMaster University, November 14–15, p. 121–138.
1994: The distribution of plant communities on Melville Island, Arctic Canada; *in* The Geology of Melville Island, Arctic Canada, (ed.) R.L. Christie and N.J. McMillan; Geological Survey of Canada, Bulletin 450, p. 247–255.
- Edlund, S.A. and Alt, B.T.**
1989: Regional congruence of vegetation and summer climate patterns in the Queen Elizabeth Islands, Northwest Territories, Canada; *Arctic*, v. 42, no. 1, p. 3–23.
- Edlund, S.A. and Egginton, P.A.**
1984: Morphology and description of an outlier population of tree-sized willows on western Victoria Island, District of Franklin; Geological Survey of Canada, Paper 84-1A, p. 279–285.
- Elevebakk, A.**
1982: Geological preferences among Svalbard plants; *Inter-Nord*, v. 16, p. 11–31.

Energy, Mines, and Resources Canada

1973: Vegetation regions; *in* National Atlas of Canada; Queen's Printer, Ottawa, p. 45–46.

Freedman, B., Svoboda, J., and Henry, G.H.R.

1994: Alexandra Fiord — an ecological oasis in the polar desert; *in* Ecology of a Polar Oasis: Alexandra Fiord, Ellesmere Island, Canada, (ed.) J. Svoboda and B. Freedman; Captus University Publications, Toronto, Ontario, p. 1–9.

Gilbert, H. and Payette, S.

1982: Écologie des populations d'aulne vert (*Alnus crispa* (Ait.) Pursh) à la limite des forêts, Québec nordique; *Géographie physique et Quaternaire*, vol. 36, n^{os} 1-2, p. 109–124.

Gill, D.

1973: Ecological modifications caused by removal of tree and shrub canopies in the Mackenzie Delta; *Arctic*, v. 26, no. 2, p. 95–111.

Hare, F.K.

1970: The tundra climate; *Transactions of the Royal Society of Canada*, 4th Series, v. 8, p. 393–399.

Henry, G., Freedman, B., and Svoboda, J.

1986: Survey of vegetated areas and muskox populations in east-central Ellesmere Island; *Arctic*, v. 39, n. 1, p. 78–81.

King, R.L.

1981: Das Sommerklima von N-Ellesmere Island, N.W.T. Kanada — Eine Beurteilung von Stationswerten unter besonderer Berücksichtigung des Sommers 1978; *Heidelberger Geographische Arbeiten*, Heft 69, p. 77–107.

Labine, C.L.

1994: Meteorology and climatology of the Alexandra Fiord Lowland; *in* Ecology of a Polar Oasis: Alexandra Fiord, Ellesmere Island, Canada, (ed.) J. Svoboda and B. Freedman; Captus University Publications, Toronto, Ontario, p. 23–39.

Levesque, E. and Svoboda, J.

1992: Growth of Arctic Poppy in contrasting habitats of a polar oasis and a polar desert; *The Musk-Ox*, v. 39, p. 148–156.

Levesque, E., Henry, G.H.R., and Svoboda, J.

1997: Phenological and growth responses of *Papaver radicum* along altitudinal gradients in the Canadian High Arctic; *Global Change Biology*, no. 3 (Suppl. 1), p. 125–145.

Maycock, P.F. and Matthews, B.

1966: An arctic forest in the tundra of northern Ungava, Quebec; *Arctic*, v. 19, no. 2, p. 114–144.

Muc, M., Freedman, B., and Svoboda, J.

1994: Vascular plant communities of a polar oasis at Alexandra Fiord, Ellesmere Island; *in* Ecology of a Polar Oasis: Alexandra Fiord, Ellesmere Island, Canada, (ed.) J. Svoboda and B. Freedman; Captus University Publications, Toronto, Ontario, p. 53–63.

Nams, M.L.N. and Freedman, B.

1994: Ecology of heath communities dominated by *Cassiope tetragona*; *in* Ecology of a Polar Oasis: Alexandra Fiord, Ellesmere Island, Canada, (ed.) J. Svoboda and B. Freedman; Captus University Publications, Toronto, Ontario, p. 75–84.

Nordenskjöld, O. and Mecking, L.

1928: The geography of the polar regions; *American Geographical Society*, Special Publication no. 8, p. 1–359.

Polunin, N.

1951: The real Arctic: suggestions for its delimitation, subdivision, and characterization; *Journal of Ecology*, v. 39, p. 308–315.

Polunin, N. (cont.)

1960: Introduction to Plant Geography and Some Related Sciences; McGraw-Hill, New York, 640 p.

Porsild, A.E.

1964: Illustrated flora of the Canadian Arctic Archipelago; *National Museums of Canada, Bulletin* 146, p. 1–218.

Porsild, A.E. and Cody, W.J.

1980: Vascular plants of the continental Northwest Territories; *National Museums of Canada, Ottawa, Ontario*, 667 p.

Rannie, W.F.

1985: Summer air temperature and number of vascular species in Arctic Canada; *Arctic*, v. 2, no. 39, p. 133–137.

Richard, P.J.H.

1987: Le couvert végétal au Québec–Labrador et son histoire post-glaciaire. Notes et documents; *Département de géographie, Université de Montréal*, n^o 87-101, p. 1–59.

Ritchie, J.C.

1984: Past and Present Vegetation on the Far Northwest of Canada; *University of Toronto Press, Toronto, Ontario*, 251 p.

Rowe, J.S.

1972: Forest regions of Canada; *Canadian Forestry Service, Publication* 1300, p. 1–72.

Soper, J.H. and Powell, J.M.

1983: Botanical studies in the Lake Hazen region, northern Ellesmere Island, Northwest Territories, Canada; *National Museums of Canada, Publications in Natural Sciences* no. 5, p. 1–67.

Svoboda, J. and Freedman, B. (ed.)

1981: Ecology of a High Arctic Lowland Oasis, Alexandra Fiord (78°53'N; 75°55'W), Ellesmere Island, N.W.T., Canada; *Progress Report of Alexandra Fiord Lowland Ecosystem Study; University of Toronto and Dalhousie University, Toronto and Halifax*, 245 p.

1994: Ecology of a Polar Oasis: Alexandra Fiord, Ellesmere Island, Canada; *Captus University Publications, Toronto, Ontario*, 267 p.

Thorsteinnsson, R.

1958: Cornwallis and Little Cornwallis Island, district of Franklin, Northwest Territories; *Geological Survey of Canada, Memoir* 294, 134 p.

Tozer, E.T. and Thorsteinnsson, R.

1964: Western Queen Elizabeth Islands, Arctic Archipelago; *Geological Survey of Canada, Memoir* 332, 242 p.

Vowinckel, E. and Orvig, S.

1970: The climate of the north polar basin, Chapter 3; *in* *World Survey of Climatology*, v. 14, (ed.) S. Orvig; Elsevier, Amsterdam, p. 129–252.

Woo, M.-k., Young, K.L., and Edlund, S.A.

1990: 1989 observations of soil, vegetation and microclimate, and effects on slope hydrology, Hot Weather Creek basin, Ellesmere Island, Northwest Territories; *in* *Current Research, Part D; Geological Survey of Canada, Paper* 90-1D, p. 85–93.

Young, S.B.

1971: The vascular flora of St. Lawrence Island, with special reference to floristic zonation in the arctic regions; *Contributions from the Gray Herbarium*, no. 201, Harvard University, Cambridge, Massachusetts, p. 11–115.

Young, K.L., Woo, M.-k., and Edlund, S.A.

1997: Influence of local topography, soil and vegetation on microclimate and hydrology at a High Arctic site, Ellesmere Island, Canada; *Arctic and Alpine Research*, v. 29, no. 3, p. 270–284.

APPENDIX A

CHECKLIST OF VASCULAR PLANTS ON FOSHEIM PENINSULA,
ELLESMERE ISLAND, NUNAVUT (Porsild and Cody, 1979, and Scoggan, 1979)

S.A. Edlund

EQUISETACEAE

Equisetum arvense L.
Equisetum variegatum Schleich

HORSETAIL FAMILY

common horsetail
variegated horsetail

POLYPODIACEAE

Cystopteris fragilis (L.) Bernh.

FERN FAMILY

fragile fern

GRAMINEAE

Alopecurus alpinus J.E. Smith
Arctagrostis latifolia (R.Br.) Griseb.
Calamagrostis purpurascens R.Br.
Colpodium vahlianum (Leibm.) Nevski
Deschampsia brevifolia R. Br.
Dupontia fisheri R.Br. ssp. *fisheri*
Dupontia fisheri R.Br. ssp. *psilosantha* (Rupr.) Hulten
Agropyron violaceum (Hornem.) Lange
Festuca baffinensis Polunin ssp. *violaceum*
Festuca brachyphylla Schultes
Festuca rubra L.
Hierochloa alpina (Sw.) R.&S.
Hierochloa pauciflora R.Br.
Phippsia algida (Sol.) R.Br.
Pleuropogon sabiniei R.Br.
Poa abbreviata R.Br.
Poa alpigena (Fr.) Lindm. var. *alpigena*
Poa alpigena (Fr.) Lindm. var. *colpodea*
Poa arctica R.Br. ssp. *arctica*
Poa arctica R.Br. ssp. *caespitans*
Poa glauca M. Vahl.
Poa hartzii Gand.
Puccinellia angustata (R.Br.) Rand & Redf.
Puccinellia arctica (Hook.) Fern. & Weath.
Puccinellia bruggemannii Th.Sor.
Puccinellia langeana (Berl.) Th. Sor.
Puccinellia phyrgranodes (Trin.) Scribn. & Merr.
Puccinellia poaceae Th. Sor.
Puccinellia vaginata (Lge.) Fern. & Weath.
Trisetum spicatum (L.) Richt.

GRASS FAMILY

alpine foxtail
polar grass
purple reedgrass
Vahl's alkali-grass
tufted hairgrass
Fisher's dupontia
Fisher's dupontia
violet wheatgrass
Baffin fescue
short-leaved fescue
alpine fescue
alpine holy grass
few flowered holy grass
snowgrass
Sabine's semaphore grass
low spear grass
alpine meadow grass
alpine meadow grass
arctic blue grass
arctic blue grass
glaucous spear grass
Hartz's spear grass
tall Arctic Alkali-grass
arctic alkali-grass
Bruggemann's alkali-grass
reddish alkali-grass
creeping alkali-grass
poa-flowered alkali-grass
sheathed alkali-grass
narrow false oat

CYPERACEAE

Carex amblyorhyncha Krecz.
Carex aquatilis Wahlenb. var. *stans* (Drej.) Boott
Carex atrofusca Schk.
Carex capillaris L.
Carex glacialis Mack.
Carex maritima Gunn.
Carex membranacea Hook.
Carex misandra R.Br.
Carex nardina Fr.
Carex rupestris All.
Carex scirpoidea Michx.
Carex saxatilis L.

SEDGE FAMILY

blunt-nosed sedge
water sedge
dark brown sedge
hair sedge
glacier sedge
seaside sedge
fragile sedge
short-leaved sedge
nard sedge
rock sedge
scirpus sedge
rocky ground sedge

<i>Carex ursina</i> Dew.	bear sedge
<i>Eriophorum scheuchzeri</i> Hoppe	arctic cotton grass
<i>Eriophorum triste</i> (Th. Fr.) Hadac & Love (= <i>E. angustifolium</i> spp. <i>triste</i> (Fries) Hult.)	tall cotton grass
<i>Kobresia myosuroides</i> (Vill.) Fiori & Paol.	Bellard's kobresia
<i>Kobresia simpliciuscula</i> (Wahlenb.) Mack	arctic kobresia
JUNCACEAE	RUSH FAMILY
<i>Juncus albescens</i> (Lange) Fern.	whitish rush
<i>Juncus arcticus</i> Willd.	arctic rush
<i>Juncus biglumis</i> L.	two-flowered rush
<i>Juncus castaneus</i> Smith	chestnut rush
<i>Luzula confusa</i> Lindebe	northern wood-rush
<i>Luzula nivalis</i> (Laest.) Beurl. (= <i>L. arctica</i> Blytt)	snow wood-rush
SALICACEAE	WILLOW FAMILY
<i>Salix arctica</i> Pall.	arctic willow
POLYGONACEAE	SORREL FAMILY
<i>Oxyria digyna</i> (L.) Hill	mountain sorrel
<i>Polygonum viviparum</i> L.	alpine bistort
CARYOPHYLLACEAE	PINK FAMILY
<i>Cerastium alpinum</i> L. s. lat.	alpine chickweed
<i>Cerastium arcticum</i> Lge.	arctic chickweed
<i>Cerastium beringianum</i> Cham. & Schlecht	beringian chickweed
<i>Cerastium regelii</i> Ostf. ssp. <i>caespitans</i>	tufted polar chickweed
<i>Cerastium regelii</i> Ostf. ssp. <i>regalii</i>	polar chickweed
<i>Melandrium affine</i> J. Vahl (= <i>Lynchnis brachycalyx</i> Raup)	arctic bladder campion
<i>Melandrium apetalum</i> (L.) Fenzl ssp. <i>Arcticum</i> (Fr.) Hult (= <i>Lynchnis attenuata</i> Farr)	nodding bladder campion
<i>Melandrium triflorum</i> (R.Br.) J. Vahl. (= <i>Lynchnis triflora</i> R.Br.)	three-flowered bladder campion
<i>Minuartia rossii</i> (R.Br.) House	Ross's sandwort
<i>Minuartia rubella</i> (Wahlenb.) Hiern.	reddish sandwort
<i>Sagina intermedia</i> Fenzl	snowy pearlwort
<i>Silene acaulis</i> L.	moss campion
<i>Stellaria ciliatocephala</i> Trautv. (= <i>Stellaria edwardsii</i> R.Br.)	long-stalked stitchwort
<i>Stellaria crassipes</i> Hult.	long-stalked stitchwort
<i>Stellaria laeta</i> Richards	long-stalked stitchwort
<i>Stellaria humifusa</i> Rottb.	seaside stitchwort
<i>Stellaria longipes</i> Goldie s.str.	long-stalked stitchwort
<i>Stellaria monantha</i> Hult.	long-stalked stitchwort
PAPAVERACEAE	POPPY FAMILY
<i>Papaver cornwallisensis</i> A. Love	Cornwallis poppy
<i>Papaver lapponicum</i> (Tolm.) Nordh. Ssp. <i>occidentale</i> (Lundstr.) Knaben	arctic poppy
RANUNCULACEAE	BUTTERCUP FAMILY
<i>Ranunculus aquatilis</i> L. var. <i>eradicatus</i> Laest.	white water crowfoot
<i>Ranunculus hyperboreus</i> Rottb.	arctic buttercup
<i>Ranunculus nivalis</i> L.	snow buttercup
<i>Ranunculus pedatifidus</i> Sm. var. <i>leiocarpus</i> (Trautv.) Fern. (= <i>R. affinis</i> R.Br.)	birdfoot buttercup
<i>Ranunculus sabinei</i> R.Br.	Sabine's suttercup
<i>Ranunculus sulphureus</i> Sol.	sulphur buttercup
CRUCIFERAE	MUSTARD FAMILY
<i>Braya humilis</i> (C.A. Mey.) Robins. s.l.	northern rock cress

<i>Braya purpurascens</i> (R. Br.) Bunge	purplish braya
<i>Braya thorild-wulfii</i> Ostenf.	Wulff's braya
<i>Cardamine bellidifolia</i> L.	alpine cress
<i>Cardamine pratensis</i> L. var. <i>angustifolia</i> Hook.	meadow bitter cress
<i>Cochlearia officinalis</i> L. ssp. <i>groenlandica</i> (L.) Porsild	common scurvy grass
<i>Draba alpina</i> L.	alpine whitlow grass
<i>Draba cinerea</i> Adams	ashy whitlow grass
<i>Draba corymbosa</i> Holm. R.Br. (= <i>D. bellii</i> Holm)	oblong-fruited whitlow grass
<i>Draba fladnizensis</i> Wulfen	white arctic whitlow grass
<i>Draba groenlandica</i> El. Ekm	Greenland whitlow grass
<i>Draba lactea</i> Adams	ahite arctic whitlow grass
<i>Draba oblongata</i> R.Br.	oblong-fruited whitlow grass
<i>Draba subcapitata</i> Simm.	tiny whitlow grass
<i>Erysimum pallasii</i> (Pursh) Fern.	Pallas' wallflower
<i>Eutrema edwardsii</i> R. Br.	Edward's eutrema
<i>Lesquerella arctica</i> (Wormskj) S. Wats.	arctic bladderpod
SAXIFRAGACEAE	SAXIFRAGE FAIMLY
<i>Saxifraga ceaspitosa</i> L.	tufted alpine saxifrage
<i>Saxifraga cernua</i> L.	nodding saxifrage
<i>Saxifraga flagellaris</i> Willd. ssp.	spider saxifrage
<i>Saxifraga foliolosa</i> R. Br.	foliolose saxifrage
<i>Saxifraga hieracifolia</i> Waldst. & Kit.	large snow saxifrage
<i>Saxifraga hirculus</i> L. var. <i>propinqua</i> (R. Br.) Simm.	yellow marsh saxifrage
<i>Saxifraga nivalis</i> L.	alpine saxifrage
<i>Saxifraga oppositifolia</i> L.	purple saxifrage
<i>Saxifraga rivularis</i> L. s.lat.	brook sSaxifrage
<i>Saxifraga tenuis</i> (Wahlend.) H.Sm.	tiny saxifrage
<i>Saxifraga tricuspidata</i> Rottb.	prickly saxifrage
ROSACEAE	ROSE FAMILY
<i>Dryas intergrifolia</i> M. Vahl. var. <i>canescens</i> Simm.	wooly arctic avens
<i>Dryas integrifolia</i> M. Vahl. s. str.	arctic avens
<i>Geum rossii</i> (R.Br.) Ser.	alpine avens
<i>Potentilla hyparctica</i> Malte	arctic cinquefoil
<i>Potentilla nivea</i> L. ssp. <i>hookeriana</i> (Lehm.) Hiit.	snow cinquefoil
<i>Potentilla pulchella</i> R.Br.	bright cinquefoil
<i>Potentilla rubricaulis</i> Lehm.	red-stemmed cinquefoil
<i>Potentilla vahliana</i> Lehm.	one-flowered cinquefoil
ONAGRACEAE	EVENING PRIMROSE FAMILY
<i>Epilobium latifolium</i> L.	arctic fireweed
<i>Epilobium arcticum</i> Samuelss.	dahurian willow-herb
HALORAGACEAE	MARE'S TAIL FAMILY
<i>Hippuris vulgaris</i> L.	common mare's tail
PYROLACEAE	WINTERGREEN FAMILY
<i>Pyrola grandiflora</i> Radius	large-flowered wintergreen
ERICACEAE	HEATH FAMILY
<i>Cassiope tetragona</i> (L.) D. Don	arctic white heather
<i>Vaccinium uliginosum</i> L.	arctic blueberry
PRIMULACEAE	PRIMROSE FAMILY
<i>Androsace septentrionalis</i> L.	pygmy flower
PLUMBAGINACEAE	LEADWORT FAMILY
<i>Armeria maritima</i> (Mill.) Wild. Ssp.	
<i>labradorica</i> (Wallr.) Hult.	sea pinks

SCROPHULARIACEAE

Pedicularis arctica R.Br. (= *P. Langsdorffii*
ssp. *arctica* (R. Br.) Polunin
Pedicularis capitata Adams
Pedicularis lanata Cham. & Schlecht.
Pedicularis hirsuta L.
Pedicularis sudetica Willd.

CAMPANULACEAE

Campanula uniflora L.

COMPOSITAE

Antennaria ekmaniana Porsild
Arnica alpina (L.) Olin ssp. *angustifolia* (J.Vahl) Maguire
Chrysanthemum integrifolium Richards.
Erigeron compositus Pursh
Erigeron eriocephalus J. Vahl
Taraxacum ceratophorum (Ledeb.) DC
Taraxacum hyparcticum Dahlst.
Taraxacum lacerum Greene
Taraxacum phymatocarpum J. Vahl.
Taraxacum pumilum Dahlst.

FIGWORT FAMILY

arctic lousewort
capitate lousewort
wooly lousewort
hairy lousewort
sudetan lousewort

BLUEBELL FAMILY

arctic or alpine bluebell

DAISY FAMILY

labrador cat paws
alpine arnica
entire-leafed chrysanthemum
cut-leafed fleabane
dwarf fleabane
arctic horned dandelion
arctic dandelion
lacerate dandelion
warty-fruited dandelion
dwarf arctic dandelion

REFERENCES

Porsild, A.E. and Cody, W.J.

1979: Vascular plants of continental Northwest Territories; National Museum of Natural Sciences, Ottawa, Ontario, 667 p.

Scoggan, H.J.

1979: The flora of Canada. Volumes I, II, III, and IV; National Museum of Natural Sciences, Ottawa, Ontario, 1711 p.

Vegetation patterns on Fosheim Peninsula, Ellesmere Island, Nunavut

S.A. Edlund¹, B.T. Alt², and M. Garneau³

Edlund, S.A., Alt, B.T., and Garneau, M., 2000: Vegetation patterns on Fosheim Peninsula, Ellesmere Island, Nunavut; in Environmental Response to Climate Change in the Canadian High Arctic, (ed.) M. Garneau and B.T. Alt; Geological Survey of Canada, Bulletin 529, p. 129–143.

Abstract: On Fosheim Peninsula, dense and diverse tundra and sedge-meadow vegetation is characterized by 145 vascular-plant species in the Hot Weather Creek area alone, in part because of higher than expected summer temperatures. Plant growth is not limited by low polar desert precipitation. Soil moisture comes from atmospheric precipitation (in cold, wet years) and melting of massive ground ice (in warmer years). The activation of the latter regime enables the lush vegetation of Fosheim Peninsula to exist within a region where sparse, polar-desert vegetation would have been expected.

Preliminary phenological results show that very warm summers can produce second and third waves of flowering from the same plant and below-normal summer temperatures limit pollen and seed production. Anomalous wetlands may serve as indicators of local massive ice. The effects of eolian activity and early snow-free areas are examined. The local spatial variability of vegetation, soil, microclimate, and hydrological and geomorphical processes illustrates the complex linkages and feedbacks among environmental variables.

Résumé : Sur la péninsule Fosheim, la végétation de toundra et de cariçaie est dense et diversifiée et est caractérisée par la présence de 145 espèces de plantes vasculaires dans la seule région du ruisseau Hot Weather. Cette situation est attribuable en partie aux températures estivales qui sont plus élevées que ce à quoi on s'attendrait. Les faibles précipitations du désert polaire ne limitent pas la croissance des plantes. L'humidité du sol provient des précipitations atmosphériques (années froides et humides) et l'eau de fonte issue de la glace de sol massive (années plus chaudes). C'est l'activation de cette deuxième source d'humidité qui permet le développement de la végétation fournie de la péninsule Fosheim dans une région où l'on ne devrait trouver qu'une végétation éparse de désert polaire.

Les résultats phénologiques préliminaires montrent que, lors des étés les plus chauds, une plante donnée peut avoir une deuxième et même une troisième floraison alors que pendant les étés de chaleur sous la normale, la production de pollen et de graines est limitée. Les terres humides anormales peuvent indiquer la présence de glace massive locale. On a examiné les effets de l'activité éolienne et des zones de libération précoce du couvert de neige. La variabilité spatiale locale de la végétation, du sol, du microclimat et des processus hydrologiques et géomorphologiques illustre les liens complexes et les rétroactions entre les variables environnementales.

¹ Geological Survey of Canada, Terrain Sciences Division, 601 Booth Street, Ottawa, Ontario K1A 0E8

² Balanced Environments Associates, 5034 Leitrim Road, Carlsbad Springs, Ontario, K0A 1K0

³ INRS-Eau, 2800, rue Einstein, C.P. 7500, Sainte-Foy, Québec G1V 4C7

INTRODUCTION

The Queen Elizabeth Islands of Arctic Canada generally fit the climatological (Bovis and Barry, 1974) and botanical definitions (Bliss, 1977; Alexandrova, 1980; Bliss et al., 1984; Bliss and Matveyeva, 1992) of a polar desert or semidesert. Within this polar desert, local areas of relatively lush vegetation have been identified and studied in detail (Bliss, 1977; Bergeron and Svoboda, 1989; Levesque and Svoboda, 1992; Muc et al., 1994; Nams and Freedman, 1994; Svoboda and Freedman, 1994; Levesque and Svoboda, 1995; Levesque et al., in press). In his mosaic classification scheme, Bliss (1977, 1990) has also identified areas of polar semidesert and areas that he defines as a complex of sedge meadows and polar semidesert within the Queen Elizabeth Islands (Fig. 1). Edlund (Edlund and Alt, 1989; Edlund, 1990; Edlund and Garneau, 2000) developed a regional vegetation scheme for the Queen Elizabeth Islands based on the growth form of the dominant vascular-plant species (Fig. 2). These zones are summaries of patterns seen on 1:250 000 scale vegetation maps (Edlund, 1982a, b, 1983c, d, 1987b). Each of these classifications systems has recognized that within the High Arctic there are botanically rich areas that are not typical for

the latitude at which they are found. This study examines one such area with emphasis on understanding regional-scale biosphere-geosphere interactions.

Fosheim Peninsula on west-central Ellesmere Island has a more dense and diverse tundra and sedge-meadow vegetation than would be predicted for latitude 80°N from the bioclimatic law (Hopkins, 1920); its vegetation is characterized by 145 vascular-plant species in the Hot Weather Creek area alone (*see Appendix A in Edlund and Garneau, 2000*). This contrasts with the vegetation growing in similar surficial materials in the western and central Queen Elizabeth Islands where generally there are less than 35 vascular-plant species. On the basis of Edlund's regional vegetation zonation (Edlund, 1986; Edlund and Alt, 1989; Edlund, 1990; Edlund and Garneau, 2000), the Fosheim Peninsula falls within the Enriched Prostrate Shrub zone (Fig. 2). This vegetation zone, based on dominant vascular-plant species, covers most of the Eureka intermontane region identified in regional climate studies of the Queen Elizabeth Islands (Edlund and Alt, 1989; Alt and Maxwell, 1990, 2000). The mountains of northern Ellesmere and Axel Heiberg islands surrounding the intermontane area create a regional-scale warm anomaly approximately 400 km long and 120 km wide (Alt and Maxwell, 1990, 2000).

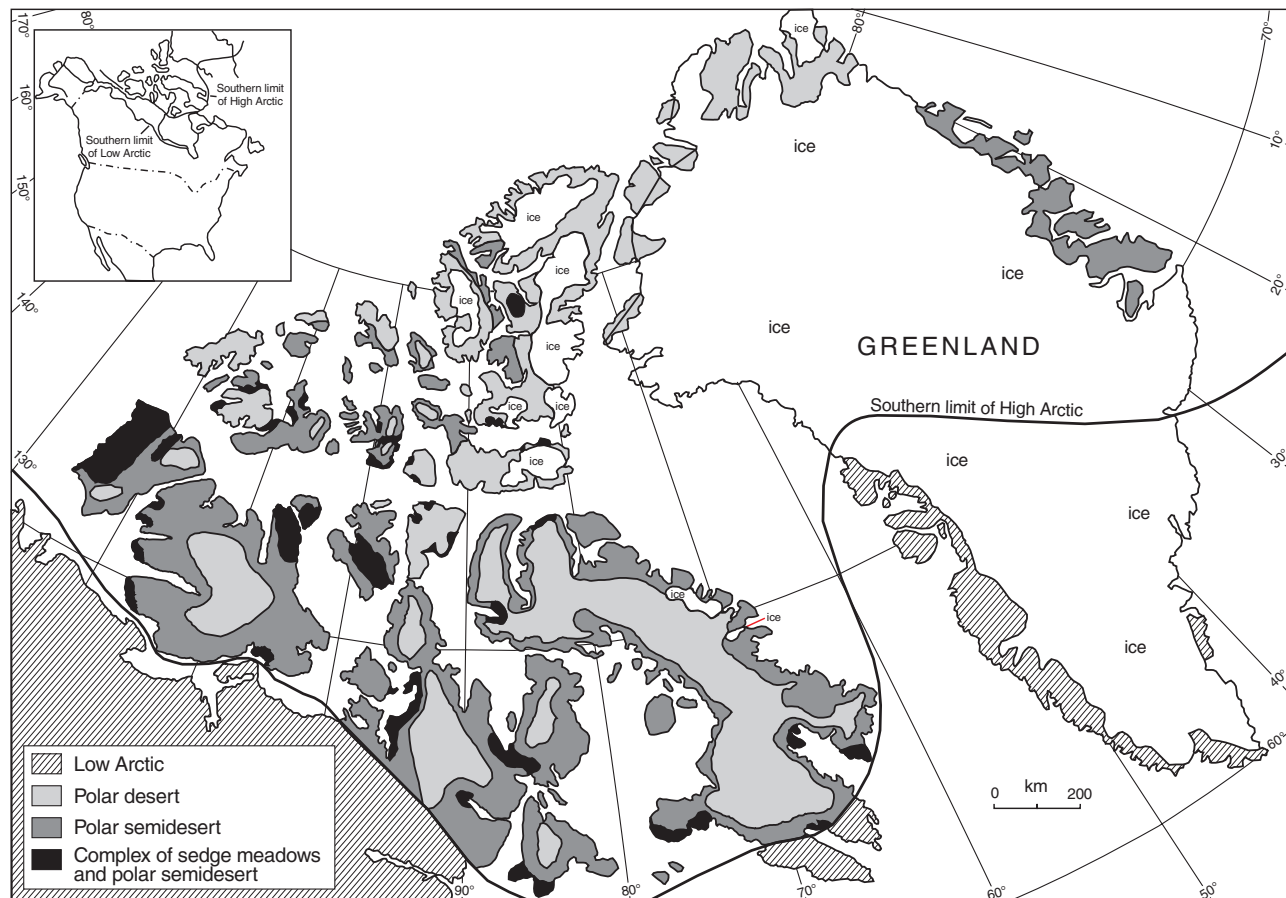


Figure 1. Botanical division of polar desert, polar semidesert, and complex (of sedge meadows and polar semidesert) in arctic North America and Greenland (after Bliss, 1977).

The Hot Weather Creek site (Fig. 3) was selected as the focal point of the High Arctic Global Change Observatory (Garneau et al., 2000) because of its central location on the peninsula, away from large water bodies and mountain ranges, with vegetation density and diversity representative of the best of the region. Detailed plant-community distribution and plant phenology studies were undertaken during the field seasons of 1988–1993. The program afforded the opportunity to study the response of vegetation to climatic, hydrological, and geophysical changes on a regional scale, to assess

the effect on vegetation of the broad-scale thermal enhancement experienced by the sheltered interior of the Eureka intermontane area, and to investigate the use of vegetation patterns to map the regional extent of the warm temperature anomaly.

The Fosheim Peninsula vegetation studies were an integral part of the concurrent investigations of fauna, climate, hydrology, geomorphology, and climate change. Observations of hydrological, geomorphological, and eolian processes, made

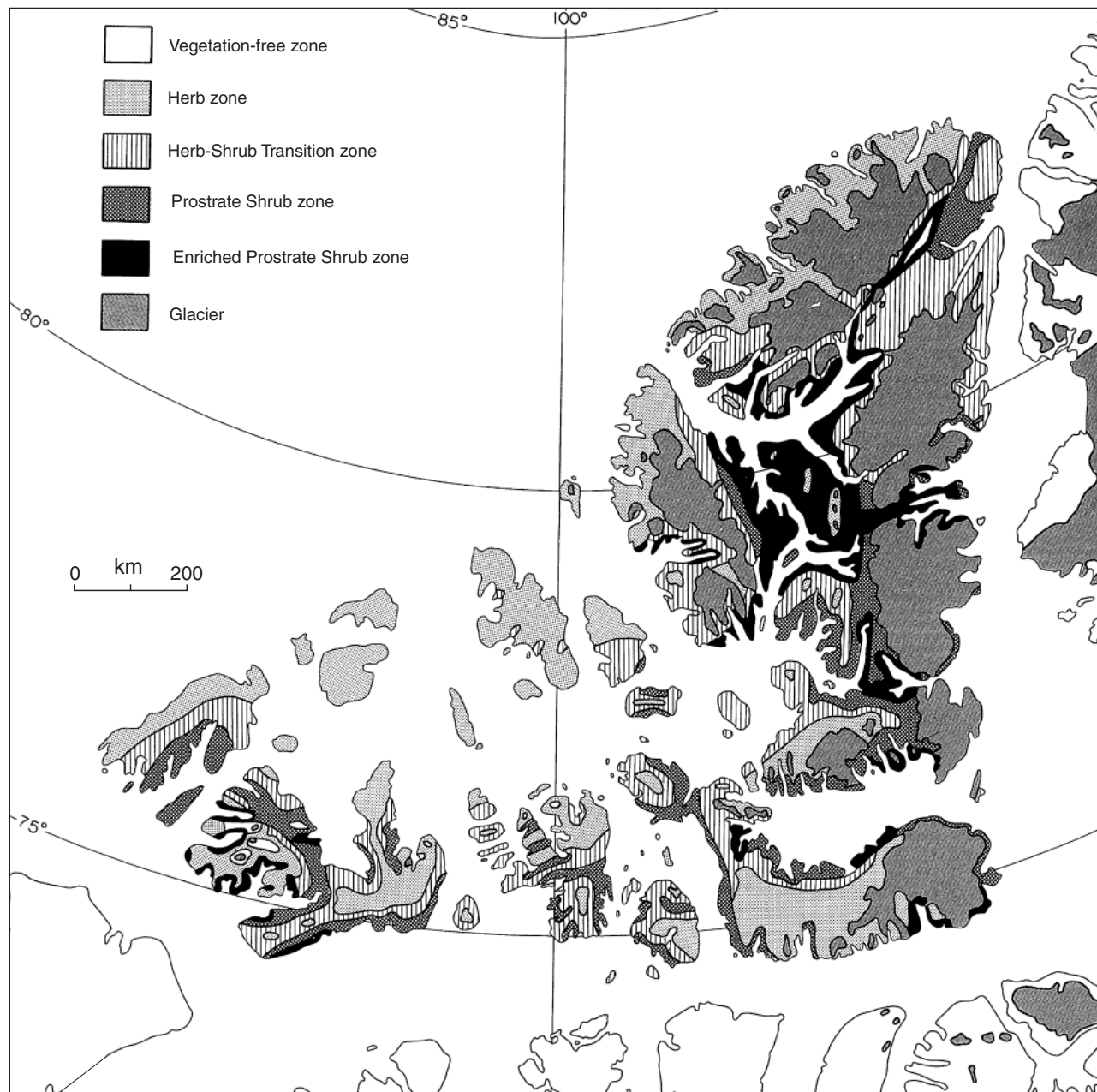


Figure 2. Vegetation zones of the Queen Elizabeth Islands (after Edlund and Alt, 1989) based on the growth forms of the dominant vascular-plant species as described in Edlund and Garneau (2000). The zones are summaries of patterns seen on 1:250 000 scale vegetation maps (Edlund, 1982a, b, 1983c, d, 1987b).

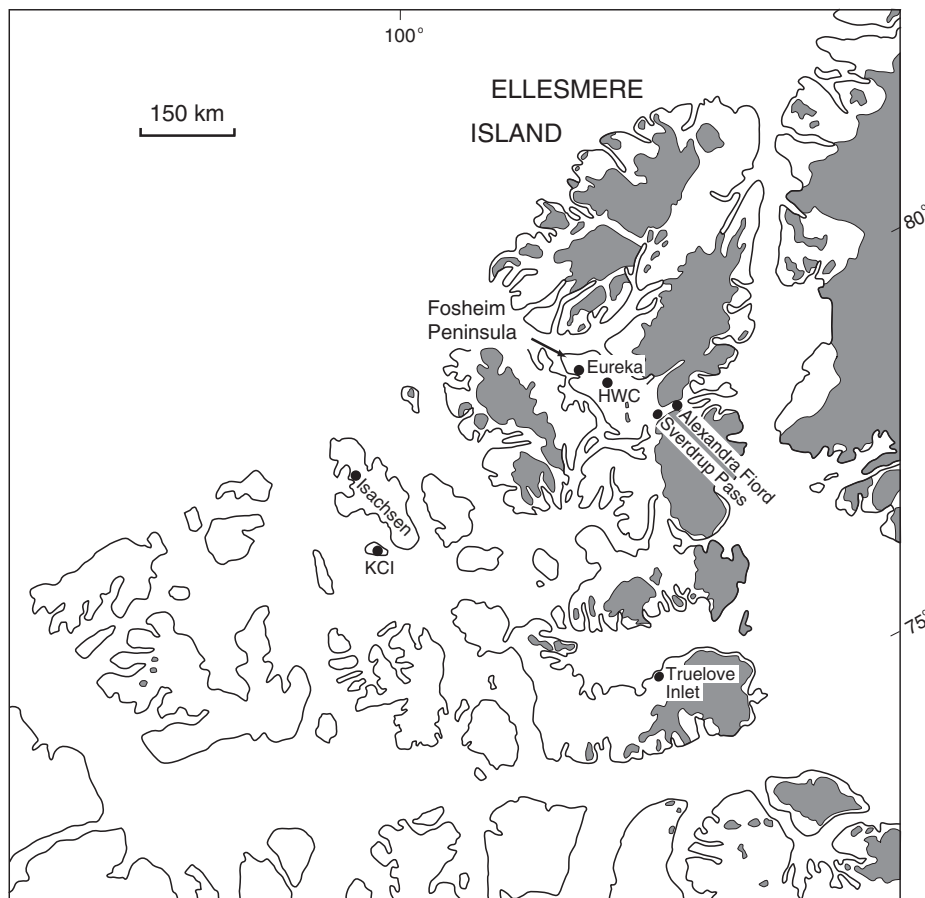


Figure 3. Hot Weather Creek (HWC) site and other sites in the Queen Elizabeth Islands. KCI = King Christian Island

during the initial years of the study, provided insight into the interactions between these processes and vegetation. A few of these early results related to vegetation patterns are also reviewed in this paper.

CLIMATE

An automatic weather station, situated to represent the climate of the broad area of gently rolling terrain (100 m a.s.l.) near the Hot Weather Creek station, has provided six years of records. The preliminary climate analysis (Alt et al., 2000) shows that summer is considerably warmer in the Fosheim Peninsula lowland interior than at Eureka, the long-term coastal weather station, and that the difference between the interior and the coast is considerably enhanced during warm, dry summers. Mean July temperatures at the Hot Weather Creek automatic weather station (autostation) site are also considerably higher than those recorded at polar oasis locations on Ellesmere and Devon islands (Table 1). The lack of concurrent study years at the field stations precludes detailed comparisons, but indications are that even at Sverdrup Pass, located well inland from the coast (Fig. 3), July is 2°C cooler

than at the Hot Weather Creek autostation site. Temperatures at Sverdrup Pass (approximately 300 m a.s.l.) are similar to those at the valley and camp stations in the Sawtooth Range (Fig. 3). Conditions at Alexandra Fiord and Truelove Inlet (Fig. 3) are still very coastal compared with the Hot Weather Creek station, although summer conditions are favourable compared with stations in the west and west-central Queen Elizabeth Islands (referred to by Beschel as a 'barren wedge' [Beschel, 1969; Edlund, 1986] and represented by true polar-desert stations such as Isachsen). Detailed quantitative comparisons are beyond the scope of this study, but there is no question that summers in the Fosheim Peninsula interior lowland are longer (80–100 days) and warmer than those of even the most favourable polar oasis sites. The summer temperatures at the Hot Weather Creek autostation site are, in fact, equivalent to those in the Keewatin on the continent and warmer than at coastal stations in the southern arctic islands such as Cambridge Bay. They fall well within the Low Arctic limits given by Bliss and Matveyeva (1992).

The first two seasons of the program (1988 and 1989) had contrasting climatic regimes (Table 2): hot and dry in 1988 and cold and wet in 1989 (Alt et al., 2000). In 1988, the mean July temperature (11.8°C) at the Hot Weather Creek

autostation site was higher than that (10°C) associated with the mean position of the treeline. In 1989, on the other hand, summer precipitation was more than double the 30-year normal at Eureka. These summers are examined in some detail in the following.

METHODS

Four slopes of different orientation (north, east, south, and west) and a plateau site were chosen for detailed vegetation studies (Edlund et al., 1989, 1990). Other interdisciplinary investigations on these slopes included thaw depth, soil moisture and properties, groundwater level, precipitation, and measured components of the surface energy balance (Woo et al. 1990; Young 1995; Young et al., 1997; Young and Woo, 2000). Details of the methods of measurement and results from these studies can be found in the papers cited.

Percentage vegetation cover was measured in 1988 at the plateau site using line-transect and quadrat methods (Wein and Rencz, 1976). In 1989, per cent cover was measured

along a number of 60 m transects at each site. The transects were parallel to the slope on the oriented sites, but were placed randomly at the nearly level plateau site. Three replicates of entire transects were performed at each site, involving 1 m² quadrat inventories at 5 m intervals along the transects. The study also included a complete survey of the diversity of vascular plants at all sites and vegetation phenology was monitored throughout the summers. Additional inventories in other parts of the basin and adjacent areas of Fosheim Peninsula and Axel Heiberg Island (Edlund et al., 1989; Woo et al., 1990) were made during the study period. All nomenclature for vascular plants follows Porsild and Cody (1980).

Methods used in the snow surveys are described in Woo et al. (1990, 1991), Edlund and Woo (1992), and Young and Woo (2000). Snowmelt experiments and measurements of eolian deposits are discussed in Edlund and Woo (1992). Details of vegetation, meteorological, and snow-ablation measurements at the base site, the upper Hot Weather Creek site, and Eureka as well as evaluation of snow-free patches from satellite images are given in Woo et al. (1991).

Table 1. July 30-year normal, 1993 and 1988 (warm years), and 1989 (cold year) monthly mean temperature, and thawing degree days (PDD) for stations on Fosheim Peninsula and at other sites in the Queen Elizabeth Islands (see Figures 3 and 4 for locations) as well as mainland Low Arctic sites for comparison. KCI = King Christian Island; SWT(CMP) = Sawtooth Range base camp; SWT(VLY) = Sawtooth Range valley station; SWT(QG) = Sawtooth Range glacier station; HWC(CMP) = Hot Weather Creek camp; AGA(A77) = Agassiz Ice Cap 1977 borehole site

JULY Station	Elevation m a.s.l.	Mean temperature		PDD		Mean temperature	
		30 year	1993	30 year	1993	1988	1989
Eureka ¹	10	5.4	7.3	349	361+	7.2	4.2
Hot Weather Creek ¹	105	8.4	11.5		672	11.8	6.5
Sverdrup Pass ²	~300	5.7	(9.6)		462		(5.2)
Alexandra Fiord ³	~20	4.2	*88(6.7)			6.7	
Truelove Inlet ⁴	~40	4.3					
Bathurst Island ⁴	3	4.8					
KCI ⁴	~10	3.5					
SWT(CMP) ¹	550		9.2				
SWT(VLY) ¹	230		9.8				
SWT(QG) ¹	875		3.9				
HWC(CMP) ¹	75		12.4			12.7	6.3
AGA(A77) ⁵	1670		*88(.5)		*88(47)	0.5	-3.5
Mould Bay ⁴	15	3.9					
Resolute Bay ⁴	64	4.1					
Isachsen ⁴	25	3.2					
Alert ⁴	63	3.6					
Cambridge Bay ⁶	23	7.9					
Lady Franklin ⁶	15	6.9					
Shepherds Bay ⁶	51	7.5					
Spence Bay ⁶	13	7.4					
Port Radium ⁶	–	12.4					

*1988 or 1982 value (both warm July months, similar to 1993)
 () estimated values
¹after Alt et. al. (2000)
²after Levesque et al. (in press)
³after Labine (1994)
⁴after Edlund and Alt (1989)
⁵after Bourgeois et al. (2000)
⁶after Edlund et al. (1989)

Table 2. July 30-year normal monthly mean temperatures and thawing degree days (PDD) for individual years in the period of record at Hot Weather Creek. KCI = King Christian Island; SWT(CMP) = Sawtooth Range base camp; SWT(QG) = Sawtooth Range glacier station; SWT(VLY) = Sawtooth Range valley station; HWC(CMP) = Hot Weather Creek camp; AGA(A77) = Agassiz Ice Cap 1977 borehole site

JULY Station	Mean temperature (°C)					
	1988	1989	1990	1991	1992	1993
Eureka ¹	7.2	4.2	5.6	6.3	5.2	7.3
Hot Weather Creek ¹	11.8	6.5	8.2	10.1	7.7	11.5
Sverdrup Pass ²		(5.2)	(6.4)	(7.5)	(6.0)	(9.6)
Alexandra Fiord ³	6.7					
SWT(CMP) ¹						9.2
SWT(VLY) ¹						9.8
SWT(QG) ¹						3.9
HWC(CMP) ¹	12.7	6.3	8.6	10.3	8.2	12.4
AGA(A77) ⁵	0.5	-3.5	-4.5	-3.8	-4.9	
JULY Station	Thawing degree days (PDD °C)					
	1988	1989	1990	1991	1992	1993
Eureka ¹	426	298	441	(404)	271	361+
Hot Weather Creek ¹	593+	477	652	631	437	672
Sverdrup Pass ²		322	476	419	298	462
AGA(A77) ⁵	47	12	16	3	2	
() estimated values			⁴ after Edlund and Alt (1989)			
¹ after Alt et. al. (2000)			⁵ after Bourgeois et al. (2000)			
² after Levesque et al. (in press)			⁶ after Edlund et al. (1989)			
³ after Labine (1994)						

Methodologies, archiving procedures, and results from the plateau automatic weather station are given in Alt et al. (2000). General site location, physiography, and other relevant geographical information are covered in the above references and in Garneau (2000).

VEGETATION PATTERNS

The relative uniformity of the weakly alkaline, silty soils in the Hot Weather Creek area has produced rather homogenous shrub- and sedge-dominated tundra communities. Woody plants dominate the moderately to well drained terrain below 300–500 m a.s.l. on Fosheim Peninsula; *Salix arctica* and *Dryas integrifolia* are the most common species (Fig. 2). *Salix* is ubiquitous on all types of substrates, whereas *Dryas* is most abundant on sandy and gravelly terrain. *Salix arctica* dominates most slopes, generally rooting in shallow troughs, in major cracks between hummocks, and in shallow depressions. *Dryas integrifolia*, the most common associate, occurs on more exposed microhabitats and is more abundant on sandier soils. In some places, *Cassiope tetragona*, *Vaccinium uliginosum*, and the rare *Pyrola graniflora* are found on sheltered, lower slopes.

On low-centred polygons, vegetation is characterized mainly by *Alopecurus alpinus*, *Poa alpigena*, *Salix arctica*, and *Stellaria longipes*. The edges of these polygons are domi-

nated by *Dryas integrifolia* and *Salix arctica* accompanied by *Kobresia myosuroides*, *Polygonum viviparum*, *Stellaria longipes*, *Pedicularis arctica*, and *P. capitata* (Garneau, 1992).

Sparse-grass-dominated, salt-tolerant, herbaceous communities occur on dry, silty knolls and slopes where the surface has salt accumulations. These communities consist of species of *Puccinellia*, such as *P. angustate*, *P. langeana*, and *P. poacea*, several species of *Poa*, including *P. hartzii* and *P. glauca*, plus *Agropyron violaceum*, *Melandrium affine*, *Potentilla nivea*, and *P. pulchella*.

Wetlands are common around lakes and ponds at the heads of creeks. Localized wetlands occur in poorly drained troughs and junctions of troughs, with dense sedge-meadow vegetation and thick bryophytic mats as ground cover dominated by *Drepanocladus* spp., *Calliergon* spp., *Scorpidium scorpioides*, and *Bryum* sp. Forty-eight species of vascular plants are found in wetlands, often dominated by *Carex aquatilis* var. *stans* and/or *Eriophorum scheuchzeri*. In places, these are accompanied by a variety of *Carex* species not normally found at this latitude and by other rare herbaceous species such as *Carex saxatilis*, *C. amblyorhyncha*, *C. capillaris*, *Hierochloa pauciflora*, *Cardamine pratense*, *Saxifraga hieracifolia*, *Cerastium regelii*, and *Epilobium arcticum*. Many perennial ponds and shallow lakes have aquatic and emergent species such as *Hippuris vulgaris*, *Ronunculus aquatilis*, and *Pleuropogon sabinei*, which root in the muddy bottoms.

The floors of some deep, flat-bottomed, narrow valleys, often with limited catchments, support a rich wetland vegetation. There are no channels, but only a series of moss dykes that form terraces. In the spring, their frozen or shallowly thawed ground can be covered by standing water or by overland flow. Active-layer depth is no greater than about 0.3 m because of the insulating properties of bryophytic mats that remain saturated through the summer.

Small patches of wetland communities are found at some slope breaks and on raised berms, well above the summer level of the modern creeks. The presence of these shallow-rooting species indicates that ample moisture is available at or near the surface during most of the growing season.

The experimental sites

The irregular upland surfaces are occupied by high-centre polygons, the middle of which is covered by hummocks 0.1 to 0.3 m high (Edlund et al., 1990). The amount and duration of soil moisture supply during the melt period are the prime controls of the distribution of plant communities (Young et al., 1997). Vegetation on moderately to well drained soils on the slope study plots includes 28 vascular-plant species (Table 3). (Although small wetlands exist nearby, no wetland communities were found at the instrumental sites and wetland species are not included in the site inventories.) Twelve additional species occur on the plateau and on similar slopes in the immediate vicinity, but are often associated with specialized habitats such as enriched sites around animal burrows. The north-facing slope site has the greatest diversity of species (18) because it includes parts of a *Cassiope*-dominated heath community at the foot of the slope and a disturbed zone on the uppermost part of the slope. Vascular plants generally cover over 50 per cent of the slopes, but at each site, percentage cover decreases from bottom to top, corresponding to a decrease in soil moisture (Young et al., 1997).

Phenology

Meteorological results from the automatic weather station near the plateau site are discussed by Alt et al. (2000) and have been related to vegetation and other studies on the slopes by Young et al. (1997) and Young and Woo (2000). Summer warmth parameters are summarized in Tables 1 and 2 and in Alt et al. (2000, Table 2 and Fig. 18a). Total thawing (positive) degree days for the Hot Weather Creek sites are higher than those at all the Sverdrup Pass polar oasis sites reported by Levesque et al. (in press) mainly because of the higher altitude at Sverdrup Pass, but also because of the relative size of the areas. In warm years, positive degree days at the Hot Weather Creek autostation are close to 700°C. In 1989, the coldest season of the period of record (and one of the coldest seasons in the 40-year Eureka record [see Alt et al., 2000, Fig. 23]), they were still considerably higher (477°C) than the 30-year normals (349°C) at Eureka, which is the warmest permanent weather station in the High Arctic. The length of the thaw season at the Hot Weather Creek station ranged from 80 to over 100 days during the study period, beginning in late May in three of the six years studied. By mid-June,

above-freezing mean daily temperatures were recorded, even during the coldest season. Thus, the area takes full advantage of the very high incoming solar radiation available at these latitudes during June. Mean daily temperatures do not fall below 0°C until late August or early September, although below-freezing minimum temperatures have been recorded at screen level in August. Standardization and evaluation of the methods used to calculate the length of thaw season are needed before detailed comparisons can be made with other stations; however, initial results suggest that the length of the melt season at the Hot Weather Creek autostation site and at Sverdrup Pass are similar. Thus, the higher positive degree-day values (thawing degree days) at the Hot Weather Creek autostation are a result of intensity rather than duration of melt season.

The length of the thaw season provides ample time for most vascular plants to break dormancy, flower, and set and disperse seed. In 1988, an unusually warm summer in the Hot Weather Creek area (Edlund et al., 1989; Alt et al., 2000, Fig. 18a, 23), most plants broke dormancy in early to middle June and most had completed their life cycles by early August, starting to senesce even though temperatures were still mild and without any freezing-temperature shock. Several species, including *Braya purpurescens*, *Lesquerella arctica*, and *Dryas integrifolia*, had second and third waves of flowering from the same plant.

Some plants showed the effects of the drought that occurred in early July 1988. The drought was sufficiently severe to delay seed development in cotton-grass (*Eriophorum scheuchzeri*) around some shallow plateau ponds for at least ten days, as compared to development of the same species around nearby lakes where moisture was available throughout the summer. The sudden availability of abundant water after mid-July (see following section) was sufficient to permit *Eriophorum* to produce seed, although one to two weeks later than in communities around the lakes.

In the cool, wet summer of 1989 (Alt et al., 2000), many species did not break dormancy until early July and many early flowering species such as *Dryas* and *Saxifraga oppositifolia* flowered sporadically, in low numbers, throughout July and August. Few mature seed heads were produced on *Dryas* by the end of August. Several species of *Carex* and *Eriophorum* did not produce seed, nor did many grasses and herbs. This may be attributed to below-normal minimum temperatures during most of July.

The results of phenological studies are preliminary. Efforts should be made to analyze the results from subsequent seasons and to complete the necessary field observations to link these with climate records.

OTHER AREAS OF FOSHEIM PENINSULA AND ADJACENT AXEL HEIBERG ISLAND

Below 240–300 m a.s.l., the vascular-plant diversity and plant-community structures in other parts of Fosheim Peninsula are similar to those at Hot Weather Creek. This is particularly so in regions underlain by the Eureka Sound Group,

although plant diversity decreased above elevations of about 180 m. Large areas of southern and southwestern Fosheim Peninsula are more sparsely vegetated, with the typical prostrate-shrub communities dominated by *Dryas* and *Salix*. Where water is abundant, both density and diversity of wetland vegetation are comparable to those in the Hot Weather Creek area.

Few acidic soils (pH under 6.8) occur in the area. Where they are present, *Salix* is the dominant vascular plant, with *Cassiope tetragona* present in abundance. *Cassiope* also occurs locally on weakly alkaline deposits, particularly at the bottom of steep slopes. Above 300 m elevation in the mountainous region between Sawtooth Range and Agassiz and Prince of Wales ice caps, as well as in other east-central ice caps, woody species diminish in abundance. Individual woody plants are smaller and more compact, with branches sprawling for no more than 30 cm. Many individual *Salix* plants failed to flower even in the warm summer of 1988 and showed no signs of flowering in the previous year. Growth was limited to the production of leaves and an extension of

branches by a few millimetres. A few individual plants with catkins were found in early August, but seeds were not mature at that time. At these higher elevations, herbaceous species such as *Luzula confusa* and *Potentilla hyparctica* are abundant on more acidic soils and saxifrages such as *Saxifraga oppositifolia* and *S. caespitosa* dominate the alkaline soils. Several species that are rare at lower elevations, are common to abundant at these high elevations on both weakly acidic and moderately alkaline soils. These include *Saxifraga nivalis*, *S. foliolosa*, *S. flagellaris*, *S. tenuis*, *S. rivularis*, *Cardamine bellidifolia*, and *Phippsia algida*. *Papaver radicum* is also common on all but the wettest soils. In some areas, only a few herbaceous species such as *Papaver radicum*, *Phippsia algida*, and *Saxifraga caespitosa* occur (cover less than 1 per cent). These changes with elevation are reminiscent of the latitudinal changes on the western and central Queen Elizabeth Islands. Communities on the highlands of Fosheim Peninsula are similar, although often denser, than those at sea level on northern Melville Island, the Ringnes islands, and southern Lougheed Island (Edlund, 1980, 1983a, b, c, 1986; Edlund and Alt, 1989).

Table 3. Per cent cover of vascular plants at each study site.

Species	Plateau	North	East	South	West
		Slope			
<i>Alopecurus alpinus</i>	+	-	+	+	+
<i>Armeria maritima</i>	-	+	-	-	-
<i>Braya purpurescens</i>	+	+	+	+	+
<i>Braya thorild-wulfii</i>	+	-	-	+	-
<i>Carex misandra</i>	-	+	-	-	-
<i>Carex rupestris</i>	-	+	-	+	-
<i>Cassiope tetragona</i>	-	35(b)	-	-	-
<i>Cerastium alpinum</i>	+	-	+	+	-
<i>Draba alpina</i>	+	-	-	-	-
<i>Draba cinerea</i>	+	-	-	+	+
<i>Draba corymbosa</i>	+	-	-	-	-
<i>Dryas integrifolia</i>	5 to 15	5 to 15	5 to 10	+ to 5	+ to 5
<i>Kobresia myosuroides</i>	-	+	-	-	-
<i>Lesquerella arctica</i>	-	+	-	+	+
<i>Oxyria digyna</i>	+	+	+	+	+
<i>Papaver radicum</i>	+	+ to 1	+ to 1	+ to 1	+
<i>Pedicularis arctica</i>	+	+ to 1	+	+	+
<i>Pedicularis capitata</i>	-	+	-	-	-
<i>Pedicularis hirsuta</i>	-	-	+	+	-
<i>Pedicularis lanata</i>	+	+	-	-	-
<i>Polygonum viviparum</i>	-	+	+	+	-
<i>Potentilla nivea</i>	+	-	-	-	-
<i>Potentilla rubricaulis</i>	+	-	-	-	-
<i>Puccinellia vaginata</i>	+	-	-	+	-
<i>Salix arctica</i>	25 to 50	10 to 20	40 to 55	30 to 50	15 to 30
<i>Saxifraga oppositifolia</i>	1	1 to 5	1	1	1
<i>Taraxacum hyparcticum</i>	-	+	-	-	+
<i>Vaccinium uliginosum</i>	-	+	-	-	-
Bare ground	35 to 60	25 to 85	35 to 55	45 to 60	65 to 85
Total vascular-species diversity	17	18	12	16	11

* to the nearest 5%; ranges from top to bottom of slope
 + indicates present in the area, but in amounts less than 1% cover
 - indicates not present
 (b) indicates species found only at bottom of slope

HYDROLOGICAL AND GEOMORPHICAL PROCESSES (1988)

The extremely warm, dry summer of 1988 (Alt et al., 2000) saw mean July temperatures (11.8°C) at Hot Weather Creek higher than normal July temperatures south of the mainland treeline (Table 1). Geomorphological and hydrological processes observed during the 1988 field season and their botanical implications provide both a possible scenario for the effect of climate warming and a key to understanding present vegetation density and patterns.

Hydrological processes

Hot Weather Creek exhibits the arctic nival streamflow regime described by Church (1974) with snowmelt being the major source of runoff (Woo and Young, 1997). By 5 to 14 July, flow in Hot Weather Creek and its tributaries had ceased. Small, isolated pools remained in the stream beds, but by 20 July some had disappeared. During the latter part of the summer, flow returned to many tributaries. This renewed flow generally consisted of clear water, which, in the absence of significant precipitation inputs, was assumed to come from melting ground ice. On 29 July, flow began again in the southernmost major tributary of Hot Weather Creek and pools in Hot Weather Creek began to expand. In the first and second weeks of August, all other major tributaries also began flowing into Hot Weather Creek, with the most northerly ones connecting the latest.

After snowmelt, numerous small ponds also appeared at the junctions of frost-fissure troughs on the broad interfluvies. One such pond (Edlund et al., 1989, Fig. 6), instrumented with thermistors, initially had a maximum water depth of 10–20 cm. By the end of the first week of July, many of the ponds had dried, although in some places the water table was at a depth of 10 to 15 cm. By the end of the first week in August, the monitored pond and many other ephemeral ponds contained water again, reaching a depth of 9 cm by 18 August.

Most of the ground surface dried quickly in June, although silty soil contained moisture at 15–20 cm throughout most of late June and to mid-July (Edlund, 1994). By 18 July, damp spots began to appear randomly on silty slopes and on the plain surfaces and they slowly increased in size throughout the rest of the summer. On some dry terraces, some damp areas coalesced into patterns that outlined ice wedges with minimal surface expression, but, in most cases, the damp patterns seemed random. Similar damp spots on silty soils were seen in other parts of Fosheim Peninsula and eastern Axel Heiberg Island during helicopter reconnaissance studies after the end of July.

After 23 July 1988, several local areas were observed where water flowed intermittently to the surface as if under pressure. Such areas were generally on silty materials at or near the crest of hills. Silty water flowed through small (1–3 mm diameter) holes or cracks in the surface. In some places, the flow left concentric rings of wet silt no more than

1 m in diameter and in other areas downslope, flow resulted in tongues of fresh silt up to 2–3 m long and 50 cm to more than 100 cm wide.

Depth of the active layer

Few active-layer depth measurements were made in 1988, but the automatic weather station (on the plateau) showed that at 0.5 m in the ground, temperatures were above freezing after 20 July. Linear extrapolations of temperature between the 0.5 and 1.0 m thermistors suggest that the maximum thaw would have reached 0.75 m. Other active-layer depth measurements were made at the headwall of a retreating, north-facing, ground-ice slump. On 9 July, it was 0.52 m deep, approximately the same as the experimental north slope in 1989. However, the prolonged and intense warmth of 1988 caused further deepening of the active layer to 0.8 m on 28 July and to a maximum of 0.84 m in mid-August (Edlund et al., 1990).

Active-layer detachment slides

The extremely dry, warm summer of 1988 (Alt et al., 2000) triggered many active-layer detachment slides along the slopes of Hot Weather Creek during the third week of July and throughout the first two weeks of August (Edlund et al., 1989). Similar events occurred simultaneously in other places on Fosheim Peninsula and on the adjacent Axel Heiberg Island. The failure planes corresponded with the base of the active layer (0.5 to 0.75 m depth), sometimes revealing massive ground ice. Immediately after such slides, water commonly pooled behind the slumped material. In some instances, water was so abundant that it breached the dam to maintain an ephemeral stream for several days.

Ground-ice slumps

Three large, actively eroding, ground-ice slumps, with headwalls two to five times greater than the thickness of the active layer, were located close to camp and scars of a few inactive ones were found in the watershed of Hot Weather Creek and at numerous places on Fosheim Peninsula. Massive ice was found in the headwalls at the active sites. Two slumps, monitored in 1988 (Edlund et al., 1989), showed progressive retreat of up to 1 m/week through 21 July and noticeable subsurface water seeping along the base of the active layer by 4 August. Subsequent studies were undertaken by Robinson (2000).

Implications

Unusual distribution patterns of small wetlands suggest that, rather than being a phenomenon of unusually warm summers, mid- to late-summer subsurface ground-ice melt may occur with sufficient regularity to support water-requiring plant communities. However, the randomly distributed damp spots found on silty surfaces and water ejection features cannot be linked to any vegetation patterns. Their occurrence suggests that ground-ice thaw in 1988 was much greater than usual.

Ground-ice studies undertaken by Pollard (2000a, b) and Robinson (2000) show the thick, massive ground ice to be extensive within the study area. The magnitude of the contribution made by ground-ice melt to the total summer soil-moisture budget at these sites has not been evaluated. Information regarding the movement of subsurface water in this region is also needed. The upwelling of silty water on hill crests, the sporadic appearance of damp spots, and the mid- to late-summer replenishment of water to small wetlands suggest that piping and subsurface percolation are important means of water movement in this region. The hydrological implications of piping and its significance with respect to arctic hydrology and geomorphology have yet to be examined in the High Arctic and might be particularly important on Fosheim Peninsula.

The surface vegetation provides useful clues to the distribution of subsurface water flow. The conventional wisdom would have plant distribution reflecting soil moisture from precipitation and spring runoff. Our data suggest that mid- to late-summer moisture availability from melting ground ice is also a significant factor in determining patterns of plant communities.

Catastrophic events such as high numbers of detachment slides and activation of ground-ice slumps were restricted, almost without exception, to the vegetation zone dominated by the floristically richest woody plant and sedge communities. Such communities are also coincident with areas of warmest temperature as determined by initial mesoclimate studies. The widespread presence of small wetlands on interfluvies may serve as the only surface manifestation of massive amounts of subsurface ground ice. Their presence may provide another tool by which such thaw-sensitive terrain can be detected.

The long-term effects of prolonged periods of summer warmth of the magnitude experienced in July and August 1988 (Alt and Maxwell, 2000; Alt et al., 2000) are not as easily predicted. Slope instability would continue until a new equilibrium was reached. This could radically change the appearance of the landscape, from both a geomorphological and a biological point of view, and would provide abundant fresh habitats for colonizing plant species. Continued studies of the botanical and geomorphological responses to events of the summer of 1988 should help provide insight into the possible immediate effects of global warming on landscape evolution in this part of the Arctic. These should be related to the results of geomorphological, hydrological, and glaciological studies from 1988 and other warm years in the period of record. A multidisciplinary approach is needed to decipher the complexity of process interaction in this region.

SNOW-COVER DISTRIBUTION AND VEGETATION

In the spring of 1990, the effects of early, snow-free zones on the soil hydrology, microclimate, and vegetation patterns were investigated (Woo et al., 1991). Certain areas on

Fosheim Peninsula became free of snow at an early date. National Oceanic and Atmospheric Association (NOAA) satellite imagery from 17 May 1990 shows dark patches that delineate snow-free areas. This was confirmed by ground observations during snow surveys undertaken on the same day. The base-camp site and Hot Weather Creek autostation site were located in the early snow-free zone, whereas the other two sites studied, Eureka and the upper Hot Weather Creek site (Fig. 4), were still covered by snow at this time.

The largest snow-free zone on 17 May was in the centre of the lowlands on Fosheim Peninsula. This area has a dissected, rolling topography. Other smaller, snow-free zones are associated with steep-sided slopes such as the west slope of Black Top Ridge, 5 km east of Eureka, and another steep scarp facing Eureka Sound, 15 km west of Eureka. The lower slopes and bottoms of steep-walled valleys between the mountain ranges of eastern Fosheim Peninsula also have similar early snow-free areas. Such early snow-free areas developed in 1988 and 1990 in similar locations.

The development of the largest snow-free zone on central Fosheim Peninsula cannot be fully explained at this time. Preliminary observations at the Hot Weather Creek base camp suggest that thinner snow cover, higher air temperatures, and lower albedo may contribute to earlier snowmelt and ground exposure. Wind and sublimation of the dust-covered snow may also play an important part. Young and Woo (2000) discuss experiments undertaken to investigate the effect of dust on snowmelt.

The spatial differences in the microclimate and the snowmelt regime at the three sites were not large enough to modify the floral diversity or dominants within the plant communities. Variability on a local scale among the slopes at each site overwhelms the regional differences so that the effects of early snow-free areas were not apparent from the vegetation surveys undertaken at the three study sites (Eureka, Hot Weather Creek, and upper Hot Weather Creek). This is in contrast to studies such as those of Kudo (1991) who studied the effects of snow-free periods on the phenology of alpine plants. Several theories can be advanced to explain this result. One suggestion is that the temperature is still so low at this time that the advantage of a few more snow-free days is limited (E. Levesque, pers. comm., 1996). Another suggestion is that the growing season is generally (in most years) adequate to support the existing vegetation and thus the added days do not make any difference.

The patterns, instead, testify to the strong control that summer soil moisture and depth and local persistence of snow cover have over vegetation. Heath communities roughly correspond to areas where snow drifts persist several days to weeks after snow has generally disappeared from the area. They also have ample summer groundwater. The saline-tolerant herbaceous community reflects soils that probably never become saturated and that undergo prolonged summer drought. Such soils do not have runoff or rainfall in sufficient amounts to dissolve and remove the salts accumulated at the surface. This suggests that these upper slopes have only a thin snow cover in winter. Woody-plant-dominated

communities reflect conditions where snow cover is continuous during winter and where some soil moisture is present throughout the thaw period.

EOLIAN DEPOSITION AND VEGETATION

Eolian deposition on west-central Fosheim Peninsula commonly occurs as dustings of fine-grained sediments interspersed through the snow, or locally as blankets of silt and

clay. This is not unexpected, since the dominant surficial materials are fine-grained marine deposits and sediments from the generally poorly consolidated Eureka Sound Formation (Thorsteinsson, 1971a, b; Hodgson et al., 1991).

In the winter of 1990–1991, significant eolian deposition occurred on western Fosheim Peninsula. Investigations (Edlund and Woo, 1992) showed that snow-cored barchan dunes coated with sand and gravel developed on the sea ice of Slidre Fiord adjacent to an airstrip. Elsewhere, near lower Hot Weather Creek and south of Slidre Fiord, the regional pattern



Figure 4. Vegetation distribution on Fosheim Peninsula. W = shrub (*Salix* and *Dryas*) tundra (per cent cover > 25%); S = wet sedge meadows; H = herb-dominated tundra; B = barrens (shrubs and sedges rare to absent). Glaciers are shown with a stippled pattern. Climate study sites: UHWC = upper Hot Weather Creek; SWT = Sawtooth Range stations

of snow containing significant dust corresponds to the zone of early spring melt in 1990 and 1991. The extensive, snow-free, poorly vegetated sand and silt in the lower Slidre River floodplain are most likely the source of dust east of Romulus Lake.

The absence of structure within the localized thick eolian deposits at Hot Weather Creek suggests that they were probably deposited during a single strong wind event when there was a period of significant southerly gusts, as well as northerly winds such as occurred on 15–20 February 1991 (Alt et al., 2000). The source of the silty clay is most likely the knoll of marine sediments upslope (Edlund and Woo, 1992).

Evidence of deflation and deposition at this site has been noted each year since 1988. Until winter 1990–1991, however, thin deposition occurred only on poorly vegetated upper slopes near the crest and not on the nearly continuously vegetated lower slopes. This suggests that stronger winds occurred at this site in winter 1990–1991, which moved the sediment downslope beyond the usual zone of accumulation. The sharp trimline on these deposits at the valley bottom suggests that the deposits accumulated on the winter snow cover and were subsequently removed by snowmelt runoff.

Accumulations of leaf litter within snow drifts in some valleys in the area suggest that snow removal was not confined to upper slopes and knolls, but that snow was removed from nearby well vegetated slopes and plateaus. The terrain adjacent to the valleys has extensive *Dryas-Salix* hummocky tundra vegetation. Such communities ordinarily retain a protective snow cover throughout winter, but if exposed in winter, they would readily provide the litter found in the drifts.

Repeated eolian erosion, even on a local scale, retards the development of mature, woody-plant-dominated communities so common on Fosheim Peninsula (Edlund et al., 1989). Upper slopes and crests, which are the source area for eolian sediments, are characteristically found in an early stage of succession, dominated by grasses and herbs (Edlund and Woo, 1992).

If eolian deposition is light and infrequent, most mature plant communities would probably survive with little alteration except for lichens or mosses at the ground surface. Thick sedimentation, however, kills most if not all plants and moderate sedimentation favours some species over others. *Salix arctica*, which can produce substantial increments of branch growth each year, is able to survive major episodes of deposition by growing up through the deposits, whereas *Dryas integrifolia*, the most common plant where hummocks are present, is not.

The extent of terrain vegetated by nearly continuous *Dryas-Salix* tundra communities indicates that the exceptional accumulations of eolian deposits are rare and localized events. Should future climate changes accelerate winter eolian erosion and deposition, either by reducing winter precipitation or increasing wind intensity, there may be an expansion of wind-scoured terrain and early melt zones and an increase in eolian deposition on snow, leading to accretion on slopes. This could result in an expansion of successional

communities, a loss of *Dryas*- and heath-dominated communities, and an alteration of species composition within communities.

DISCUSSION

Mean summer temperatures in the Hot Weather Creek area are in the range expected at Low Arctic locations; in the summer of 1988, July temperatures as warm as those in the Forest-Tundra Transition zone were recorded. The Hot Weather Creek autostation site is at least 2°C warmer in July than Sverdrup Pass, an extensively studied ‘polar oasis’ in central Ellesmere Island.

The diversity of vegetation on Fosheim Peninsula, although atypical of the geographical location, is not atypical for this enhanced thermal regime (Edlund, 1988). However, the high vascular-plant cover cannot easily be accounted for by the meagre summer precipitation reported by the weather stations. One reason is that precipitation is probably inaccurately measured (Koerner, 1979; Woo et al., 1983). Even if precipitation were doubled, the amount still puts the region within the polar-desert climate category. Vegetation, however, is definitely not characteristic of a polar-desert precipitation regime.

Topographic disposition may enhance water supply on a local scale and overcome precipitation shortages. The presence of well developed wetlands in the bottomland and at the break of slope indicates that plentiful moisture is available in all years. However, the presence of wetland vegetation in trough ponds that dried up in early July 1988 suggests that an alternate source of moisture is needed to explain the maintenance of the well established vegetation.

Hydrological and geomorphological observations made during the warm, dry summer of 1988 showed an abundance of subsurface moisture from mid-July to mid-August. The evidence pointing to melting ground ice as the source of this moisture include slumping exposing massive ground ice on many headwalls, damp spots delimiting the ice wedges found abundantly in the troughs of polygons that crisscross the area, soil cores revealing lenses of ice at the base of the active layer after mid-July, and clear water reappearing in dried-up creeks and ponds in mid-July suggesting a subterranean origin. These observations are supported by the results of Robinson (2000) who found bodies of massive ice up to at least 17 m thick in the sediments near Hot Weather Creek.

In 1989, on the other hand, precipitation was frequent and cool, cloudy weather limited surface evaporation (Alt et al., 2000). At the Hot Weather Creek plateau site, 115 mm of precipitation were recorded between 1 June and 22 August. Adequate moisture was available to maintain vegetation and no signs of drought were observed. Seed and pollen production was low due to below-normal temperatures. Active-layer depth at the plateau site was only 0.46 m (Woo et al., 1990).

Soil moisture in the region has two distinct sources: precipitation from weather systems and meltwater from massive ground ice (Edlund et al., 1990). The precipitation-controlled mechanism operates in cold, wet years and the ground-ice-controlled regime prevails in warmer years. The activation of the latter regime enables the lush vegetation of Fosheim Peninsula to exist within a region defined by Bliss (Bliss et al., 1984) as 'polar desert'. The availability of two possible sources of moisture, from above and below the ground surface, offers a fail-safe moisture supply for the vegetation. This enables a relatively dense tundra and wet-meadow vegetation to grow in areas where sparse, polar-desert and barrens vegetation would have been expected.

Preliminary phenological results suggest that very warm summers can produce second and third waves of flowering from the same plant, which would be expected to dramatically increase the 'regional pollen' (Bourgeois et al., 2000) available for transport to the nearby Agassiz Ice Cap. Below-normal summer temperatures on the other hand limit not only pollen, but also seed production. In warm summers, many vascular plants complete their life cycles and start into dormancy while air temperatures are still warm and no climatic cue such as snowfall or freezing temperatures has occurred.

Patterns of plant communities can be used to map the extent of anomalously warm conditions. The local spatial variability of vegetation, soil, microclimate, and hydrological and geomorphological processes illustrates the complex linkages and feedbacks among environmental variables. Eolian activity affects vegetation by delaying stabilization, smothering vegetation, or causing a shift in species dominance. It may help create zones of early snowmelt. Intersite variability precludes the use of floral diversity as indicators of early snow-free zones; however, anomalous wetlands may serve as indicators of local massive-ice bodies, which may aid in the detection of thaw-sensitive areas that would be subject to thermokarst degradation under conditions of climate warming (Robinson, 2000).

Preliminary results of the vegetation component of interdisciplinary investigations undertaken within the Geological Survey of Canada High Arctic Global Change Observatory confirm that vegetation responds to, and thus provides a valuable indicator of, climatological, hydrological, and geomorphological processes at temporal and spatial scales vital to studies of environmental change.

ACKNOWLEDGMENTS

We wish to acknowledge the invaluable logistical support of the Polar Continental Shelf Project. The field assistance of Christine Roncato Spencer (1988) and Sharon Reedyk (1989) as well as that in subsequent years of Paul Wolfe, Kelly Thomsen, and others is gratefully acknowledged. The extensive review and useful suggestions of Dr. Ester Levesque of Erindale College are particularly appreciated.

REFERENCES

- Alexandrova, V.D.**
1980: The Arctic and Antarctic: their division into geobotanical areas (translated from Russian by D. Löve); Cambridge University Press, London, 247 p.
- Alt, B.T. and Maxwell, J.B.**
1990: The Queen Elizabeth Islands: a case study for arctic climate data availability and regional climate analysis; *in* Symposium on the Canadian Arctic Islands, Canada's Missing Dimension: Science and History in the Canadian Arctic Islands, Volume I, (ed.) C.R. Harington; Canadian Museum of Nature, Special Publication, p. 295–326.
2000: Overview of the modern arctic climate; *in* Environmental Response to Climate Change in the Canadian High Arctic, (ed.) M. Garneau and B.T. Alt; Geological Survey of Canada, Bulletin 529.
- Alt, B.T., Labine, C.L., Atkinson, D.E., Headley, A.N., and Wolfe, P.M.**
2000: Automatic weather station results from Fosheim Peninsula, Ellesmere Island, Nunavut; *in* Environmental Response to Climate Change in the Canadian High Arctic, (ed.) M. Garneau and B.T. Alt; Geological Survey of Canada, Bulletin 529.
- Bergeron, J.-F. and Svoboda, J.**
1989: Plant communities of Sverdrup Pass, Ellesmere Island, N.W.T.; The Musk-Ox, v. 37, p. 76–85.
- Beschel, R.E.**
1969: Floristicheskie Sootnosheniya na ostrovakh Neoarctiki (Floristic relations of the Nearctic Island); *Botanicheski Zhurnal*, v. 54, no. 6, p. 228–269.
- Bliss, L.C. (ed.)**
1977: Truelove Lowland, Devon Island, Canada: a High Arctic Ecosystem; University of Alberta Press, Edmonton, Alberta, 714 p.
- Bliss, L.C.**
1990: High Arctic ecosystems: how they develop and are maintained; *in* Canada's Missing Dimension: Science and History in the Canadian Arctic Islands, Volume I, (ed.) C.R. Harington; Canadian Museum of Nature, Special Publication, p. 350–384.
- Bliss, L.C. and Matveyeva, N.V.**
1992: Circumpolar arctic vegetation; *in* Arctic Ecosystems in a Changing Climate: an Ecophysical Perspective, (ed.) F.S. Chaplin III, R.L. Jefferies, J.F. Reynolds, G.R.S. Shaver, J. Svoboda, and E.W. Chu; Academic Press Inc., San Diego, California, p. 59–89.
- Bliss, L.C., Svoboda, J., and Bliss, D.I.**
1984: Polar deserts, their plant cover and plant production in the Canadian High Arctic; *Holarctic Ecology*, v. 7, p. 305–324.
- Bourgeois, J.C., Koerner, R.M., Fisher, D.A., and Alt, B.T.**
2000: Past and present environments inferred from Agassiz Ice Cap ice-core records; *in* Environmental Response to Climate Change in the Canadian High Arctic, (ed.) M. Garneau and B.T. Alt; Geological Survey of Canada, Bulletin 529.
- Bovis, M.J. and R.G. Barry**
1974: A climatological analysis of northern polar desert areas; *in* Polar Deserts and Modern Man, (ed.) T.L. Smiley and J.H. Zumberge; The University of Arizona Press, Tucson, Arizona, p. 23–31.
- Church, M.**
1974: Hydrology and permafrost with reference to northern North America; Proceedings, Workshop Seminar on Permafrost Hydrology; Canadian National Committee, International Hydrological Decade, Ottawa, Ontario, p. 7–20.
- Edlund, S.A.**
1980: Vegetation of Lougheed Island, District of Franklin; Geological Survey of Canada, Paper 80-1A, p. 329–333.
1982a: Vegetation of Cornwallis, Little Cornwallis and associated islands, District of Franklin; Geological Survey of Canada, Open File Map 857, scale 1:250 000.
1982b: Vegetation of Melville Island, District of Franklin: eastern Melville Island and Dundas Peninsula; Geological Survey of Canada, Open File Map 852, scale 1:250 000
1983a: Bioclimatic zonation in a High Arctic region: central Queen Elizabeth Islands; Geological Survey of Canada, Paper 83-1A, p. 381–390.
1983b: Reconnaissance vegetation studies on western Victoria Island, Canadian Arctic Archipelago; Geological Survey of Canada, Paper 83-1B, p. 75–81.

- Edlund, S.A.** (cont.)
 1983c: Vegetation of the Bathurst Island area, Northwest Territories; Geological Survey of Canada, Open File Map 888, scale 1:250 000.
 1983d: Vegetation of north-central Queen Elizabeth Islands, Northwest Territories; Geological Survey of Canada, Open File Map 887, scale 1:250 000.
 1986: Modern arctic vegetation distribution and its congruence with summer climate patterns; *in* Proceedings of Atmospheric Environment Service Workshop: Impact of Climate Change on the Canadian Arctic, (ed.) H.M. French; Atmospheric Environment Service, Downsview, Ontario, p. 84–99.
 1987a: Plants: living weather stations; *Geos*, v. 16, no. 2, p. 9–13.
 1987b: Vegetation of Melville Island, District of Franklin, Northwest Territories: western Melville Island; Geological Survey of Canada, Open File Map 1509, scale 1:250 000.
 1988: Effects of climate change on diversity of vegetation in arctic Canada; *in* Preparing for Climate Change; Proceedings of the First North American Conference on Preparing for Climate Change: a Co-operative Approach, October 27–29, 1987, Washington D.C., p. 186–193.
 1990: Bioclimatic zones in the Canadian Arctic Archipelago; *in* Canada's Missing Dimension. Science and History in the Canadian Arctic Islands. Volume I, (ed.) C.R. Harrington; Canadian Museum of Nature, p. 421–441.
 1994: The distribution of plant communities on Melville Islands, Arctic Canada; *in* The Geology of Melville Island, Arctic Canada, (ed.) R.L. Christie and N.J. McMillan; Geological Survey of Canada, Bulletin 450, p. 247–255.
- Edlund, S.A. and Alt, B.T.**
 1989: Regional congruence of vegetation and summer climate patterns in the Queen Elizabeth Island, Northwest Territories, Canada; *Arctic*, v. 42, p. 3–23.
- Edlund, S.A. and Garneau, M.**
 2000: Overview of vegetation zonation in the Arctic; *in* Environmental Response to Climate Change in the Canadian High Arctic, (ed.) M. Garneau and B.T. Alt; Geological Survey of Canada, Bulletin 529.
- Edlund, S.A. and Woo, M-k.**
 1992: Eolian deposition on western Fosheim Peninsula, Ellesmere Island, Northwest Territories during the winter of 1990–91; *in* Current Research, Part B; Geological Survey of Canada, Paper 92-1B, p. 91–96.
- Edlund, S.A., Alt, B.T., and Young, K.L.**
 1989: Interaction of climate, vegetation, and soil hydrology at Hot Weather Creek, Fosheim Peninsula, Ellesmere Island, Northwest Territories; *in* Current Research, Part D; Geological Survey of Canada, Paper 89-1D, p. 125–133.
- Edlund, S.A., Woo, M-k., and Young, K.L.**
 1990: Climate, hydrology and vegetation patterns, Hot Weather Creek, Ellesmere Island, Arctic Canada; *Nordic Hydrology*, v. 21, p. 273–286.
- Garneau, M.**
 1992: Analyses macrofossiles d'un dépôt de tourbe dans la région de Hot Weather Creek, péninsule de Fosheim, île d'Ellesmere, Territoires du Nord-Ouest; *Géographie physique et Quaternaire*, vol. 46, n° 3, p. 285–294.
- Garneau, M. and Alt, B.T. (ed.)**
 2000: Environmental response to climate change in the Canadian High Arctic; Geological Survey of Canada, Bulletin 529.
- Garneau, M., Alt, B.T., and Edlund, S.A.**
 2000: Introduction; *in* Environmental Response to Climate Change in the Canadian High Arctic, (ed.) M. Garneau and B.T. Alt; Geological Survey of Canada, Bulletin 529.
- Hopkins, A.D.**
 1920: The bioclimatic law; *Journal of the Washington Academy of Sciences*, v. X, p. 34–40.
- Hodgson, D.A., St-Onge, D.A., and Edlund, S.A.**
 1991: Surficial materials of Hot Weather Creek basin, Ellesmere Island, Northwest Territories; *in* Current Research, Part E; Geological Survey of Canada, Paper 91-1E, p. 157–163.
- Koerner, R.M.**
 1979: Accumulation, ablation and oxygen isotope variations on the Queen Elizabeth ice caps, Canada; *Journal of Glaciology*, v. 22, p. 25–41.
- Kudo, G.**
 1991: Effects of snow-free period on the phenology of alpine plants; *Arctic and Alpine Research*, v. 23, p. 436–443.
- Labine, C.L.**
 1994: Meteorology and climatology of the Alexandra Fiord Lowland; *in* Ecology of a Polar Oasis: Alexandra Fiord, Ellesmere Island, Canada, (ed.) J. Svoboda and B. Freedman; Captus University Publications, Toronto, Ontario, p. 23–39.
- Levesque, E. and Svoboda, J.**
 1992: Growth of Arctic Poppy in contrasting habitats of a polar oasis and a polar desert; *The Musk-Ox*, v. 39, p. 148–156.
 1995: Germinable seed bank from polar desert sands, central Ellesmere Island, Canada; *in* Global Change and Terrestrial Ecosystems, (ed.) T.V. Callaghan, U. Molau, M.J. Tyson, J.I. Holten, W.C. Oechel, T. Gilmanov, B. Maxwell, and B. Sveinbojornsson; August 21–26, Oppdal, Norway; Ecosystems Research Report 10, European Commission, p. 97–107.
- Levesque, E., Henry, G.H.R., and Svoboda, J.**
 in press: Phenological and growth responses of *Papaver radicum* along altitudinal gradients in the Canadian High Arctic; *Global Change Biology*.
- Muc, M., Freedman, B., and Svoboda, J.**
 1994: Vascular plant communities of a polar oasis at Alexandra Fiord, Ellesmere Island; *in* Ecology of a Polar Oasis: Alexandra Fiord, Ellesmere Island, Canada, (ed.) J. Svoboda and B. Freedman; Captus University Publications, Toronto, Ontario, p. 53–63.
- Nams, M.L.N. and Freedman, B.**
 1994: Ecology of heath communities dominated by *Cassiope tetragona*; *in* Ecology of a Polar Oasis: Alexandra Fiord, Ellesmere Island, Canada, (ed.) J. Svoboda and B. Freedman; Captus University Publications, Toronto, Ontario, p. 75–84.
- Pollard, W.H.**
 2000a: Distribution and characterization of ground ice on Fosheim Peninsula, Ellesmere Island, Nunavut; *in* Environmental Response to Climate Change in the Canadian High Arctic, (ed.) M. Garneau and B.T. Alt; Geological Survey of Canada, Bulletin 529.
 2000b: Ground-ice aggradation on Fosheim Peninsula, Ellesmere Island, Nunavut; *in* Environmental Response to Climate Change in the Canadian High Arctic, (ed.) M. Garneau and B.T. Alt; Geological Survey of Canada, Bulletin 529.
- Porsild, A.E. and Cody, W.J.**
 1980: Vascular Plants of Continental Northwest Territories, Canada; National Museums of Canada, Ottawa, Ontario, 667 p.
- Robinson, S.D.**
 2000: Thaw-slump-derived thermokarst near Hot Weather Creek, Ellesmere Island, Nunavut; *in* Environmental Response to Climate Change in the Canadian High Arctic, (ed.) M. Garneau and B.T. Alt; Geological Survey of Canada, Bulletin 529.
- Svoboda, J. and Freedman, B. (ed.)**
 1994: Ecology of a Polar Oasis: Alexandra Fiord, Ellesmere Island, Canada; Captus University Publications, Toronto, Ontario, 267 p.
- Thorsteinsson, R.**
 1971a: Geology, Eureka Sound North, District of Franklin; Geological Survey of Canada, Map 1302A, scale 1:250 000.
 1971b: Geology of Greely Fiord West, District of Franklin; Geological Survey of Canada, Map 1311A, scale 1:250 000.
- Wein, J.W. and Rencz, A.N.**
 1976: Plant cover and standing crop sampling procedures for the Canadian High Arctic; *Arctic and Alpine Research*, v. 8, no. 2, p. 139–150.
- Woo, M-k. and Young, K.L.**
 1997: Hydrology of a small basin with polar oasis environment, Fosheim Peninsula, Ellesmere Island, Canada; *Permafrost and Periglacial Processes*, v. 8, p. 257–277.
- Woo, M-k., Edlund, S.A., and Young, K.L.**
 1991: Occurrence of early snow-free zones on Fosheim Peninsula, Ellesmere Island, Northwest Territories; *in* Current Research, Part B; Geological Survey of Canada, Paper 91-1B, p. 9–14.

Woo, M-k., Young, K.L., and Edlund, S.A.

1990: 1989 observations of soil, vegetation and microclimate, and effects on slope hydrology, Hot Weather Creek basin, Ellesmere Island, Northwest Territories; *in* Current Research, Part D; Geological Survey of Canada, Paper 90-1D, p. 85–93.

Woo, M-k., Heron, R., Marsh, P., and Steer, P.

1983: Comparison of weather station snowfall with winter snow accumulation in High Arctic basins; *Atmosphere-Ocean*, v. 21, p. 312–325.

Young, K.L.

1995: Slope hydroclimatology and hydrologic responses to global change in a small High Arctic basin; Ph.D. thesis, McMaster University, Hamilton, Ontario, 167 p.

Young, K.L. and Woo, M-k.

2000: Hydrological environment of the Hot Weather Creek basin, Ellesmere Island, Nunavut; *in* Environmental Response to Climate Change in the Canadian High Arctic, (ed.) M. Garneau and B.T. Alt; Geological Survey of Canada, Bulletin 529.

Young, K.L., Woo, M-k., and Edlund, S.A.

1997: Influence of local topography, soil and vegetation on microclimate and hydrology at a High Arctic site; *Arctic and Alpine Research*, v. 29, no. 3, p. 270–284.

The insects, mites, and spiders of Hot Weather Creek, Ellesmere Island, Nunavut

F. Brodo¹

Brodo, F., 2000: The insects, mites, and spiders of Hot Weather Creek, Ellesmere Island, Nunavut; in Environmental Response to Climate Change in the Canadian High Arctic, (ed.) M. Garneau and B.T. Alt; Geological Survey of Canada, Bulletin 529, p. 145–173.

Abstract: The intermontane fauna at Hot Weather Creek is richer than expected at this latitude. In all, 232 taxa were recognized. The dominant order is Diptera, with Chironomidae being the most numerous family in terms of numbers of species and individuals. The faunal composition closely resembles that found at Lake Hazen to the northeast.

Preliminary analysis of faunal trophic levels indicates that the scavenger-detritus group, dominated by flies, is in the majority (86 species), followed by parasites (52 species), mainly Hymenoptera. There are 49 predators and only 34 herbivores.

The arctic willow, the arctic avens, louseworts, and various grasses are the favoured food plants. Only about 14 per cent of the 145 vascular plants showed arthropod damage.

Several conspicuous and easily distinguished species would be suitable for monitoring climate change. The aquatic larvae of the crane fly (*Tipula besselsi*) leave networks of lines in the silt of creek beds, thus advertising their presence and making this species a particularly useful indicator.

Résumé : La faune de la région intermontagneuse du ruisseau Hot Weather est plus riche que prévue sous cette latitude. On y a recensé un total de 232 taxons. L'ordre dominant est celui des diptères, et les chironomidés sont la famille la plus nombreuse tant au nombre d'espèces qu'au nombre d'individus. La composition faunique ressemble étroitement à celle du lac Hazen au nord-est.

L'analyse préliminaire des niveaux trophiques fauniques indique que le groupe des saprophages-microphages, dominé par les mouches (86 espèces), est le groupe majoritaire suivi par les parasites (52 espèces), surtout les hyménoptères. Il y a 49 prédateurs et seulement 34 herbivores.

Le saule arctique, le dryas arctique, les pédiculaires et diverses plantes herbacées sont les plantes alimentaires préférées. Seulement environ 14 p. 100 des 145 plantes vasculaires montraient des signes de dommages attribuables aux arthropodes.

Plusieurs espèces très visibles et faciles à distinguer pourraient servir d'indicateurs pour le changement climatique. Les larves aquatiques des tipules (*Tipula besselsi*) tracent des réseaux de lignes dans le silt du lit des ruisseaux, ce qui révèle leur présence et rend ces espèces particulièrement utiles comme indicateurs.

¹ Research Associate, Canadian Museum of Nature, Ottawa, Ontario

INTRODUCTION

Arthropods, especially insects, spiders, and mites, are a vitally important component of any ecosystem even though their presence may not be so evident at first glance. In the High Arctic, especially inland as at Hot Weather Creek, this arthropod component comprises a far greater species diversity than the more conspicuous mammals and birds. (Seven mammals and nineteen birds were found by Gould (1988) at Lake Hazen, Ellesmere Island; *see* Figure 1.) The arthropod diversity is close to the ground, in the vegetation, on or in the soil, or in the very shallow to deeper freshwater bodies in the region. Butterflies, moths, midges, and mosquitoes can be conspicuous on milder days, but even they tend to fly closer to the ground than their more southern relatives.

An inventory of insects and related arthropods was initiated formally in 1990 and continued in 1991. (Traps were set out and monitored by Dr. S.A. Edlund in 1988 and 1989 and the information from these is included in this report.) This inventory was to complement other studies (e.g. flora,

weather patterns, hydrology, geology) underway at Hot Weather Creek, a site selected for the study of global climate change.

This inventory sought to address the following questions. Which species occur at Hot Weather Creek? What are their geographic affinities? How does this fauna compare with that found in other High Arctic sites? Which species predominate in this ecosystem and what roles do they play? What differences were evidenced in the fauna between the two field seasons and how might these differences be related to the differing weather patterns? What physical evidence remains of insect-plant interactions that might persist in fossilized remains, and so provide clues to ecological relationships? Which species might be the best candidates for monitoring global climate change?

The underlying hypothesis of this research is that an inventory of the extant arthropod fauna is necessary baseline data for monitoring global climate change. Such an inventory must include relative population densities for each species. This information must be tempered with an understanding of

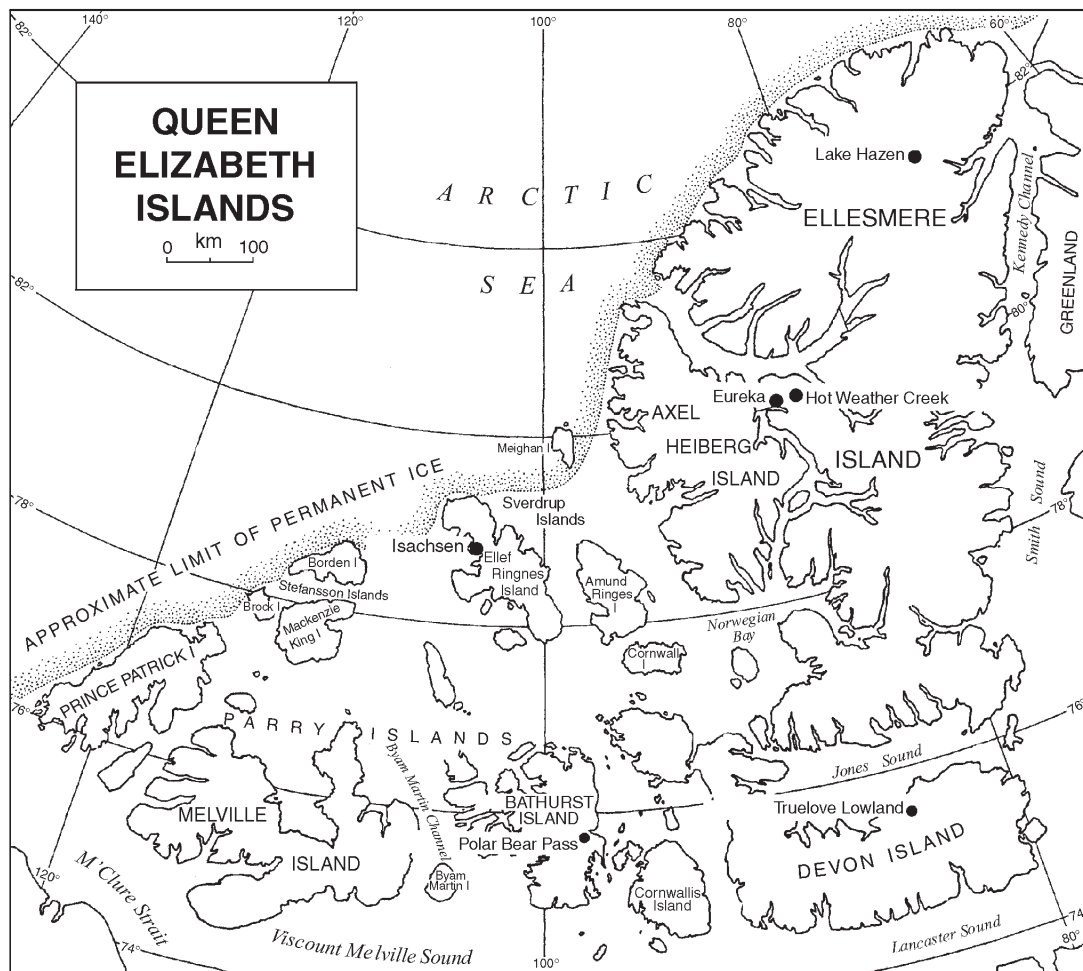


Figure 1. Queen Elizabeth Islands, Northwest Territories, showing localities where major insect collections have been made.

present annual population fluctuations in response to differing weather patterns from year to year, the so-called 'noise' in the system. It is further hypothesized that specific components of this fauna might be more sensitive to climatic changes, whether these changes are caused by stochastic weather fluctuations or whether they are anthropogenically induced. A third hypothesis is that the extant fauna provides a useful comparison with that found in fossilized or semifossilized strata to corroborate past climate fluctuations.

METHODOLOGY

A variety of traps were set up in the various habitats within easy walking distance of the camp and the contents were emptied approximately every other day. Malaise traps, flight interception traps, and yellow pitfall traps (described below) were installed in the following locations: 1) straddling a small tundra pond on the plateau west of the camp, close to the automatic weather station; 2) towards the bottom of a south-facing slope of *Cassiope tetragona* (L.)Don (arctic heather) near Picnic Lake, a small, shallow lake that freezes to the bottom during the winter (Fig. 2); 3) a fen area between Picnic Lake and Heather Creek; 4) a grassy, east-facing gully near Hot Weather Creek; 5) a temporary installation at Coal Lake, approximately a 1.5 hour walk from the base camp.

Thirty-six bright yellow plastic bowls, 27 cm in diameter and two-thirds filled with water and a few drops of detergent, were placed in a variety of habitats to trap insects alighting on the water (Fig. 3). Some bowls were dug into the ground as pitfall traps. Traps were emptied about every other day and the contents were preserved in 70 per cent ethanol and stored in plastic whorl packs or partly sorted into vials in the field. Three of these bowls were left for several weeks to simulate possible deposition of insects over the season in a shallow-water body. They produced an unusable sludge of decaying biomass.



Figure 2. Malaise trap with two yellow bowls at its base, on a heath slope near Picnic Lake, Hot Weather Creek. GSC 2000-024A

Morgan pitfall traps (Fig. 4) were placed on flatter areas bordering water bodies. These traps consisted of groupings of several 226 g (8 oz.) plastic drinking cups half-filled with water plus a drop of detergent and sunk to their rims in the terrain, separated from each other by thin, flexible, plastic strips (61 cm x 5 cm) that were half sunk into the terrain along their long axes. The long strips deflected crawling organisms towards the pitfall traps, thus sampling this fauna more effectively than isolated traps. Additional pitfall traps, without communicating plastic strips, were placed in hollows between tundra hummocks.

Aerial netting using a net modified from a design by Dr. Steve Marshall (Brodo, 1995) complemented the traps. In addition, all possible substrates, especially the vegetation, were carefully scrutinized for arthropods.

Leaf litter and topsoil samples were collected for processing through a Berlese funnel at the research station. Solar panels, which were to provide power for the 40-watt bulb, proved insufficient for the job, especially since this power



Figure 3. Yellow bowl containing butterflies (mostly *Boloria chariclea*) and other, smaller insects. GSC 2000-024B



Figure 4. Morgan traps at the muddy edge of Oxbow Lake. GSC 2000-024C

had to be shared with other projects. Additional substrate samples were collected just prior to leaving the research site, for more effective processing back in Ottawa.

Several soil quadrats, 1 m² and about 5 cm deep, were dug up and searched for invertebrates. Unlike the findings in Russia (Lantsov, 1984; Chernov, 1985), this method of sampling yielded so few specimens that it was abandoned.

RESULTS AND DISCUSSION

Several studies have documented the fact that species numbers decline with increasing latitude (Danks, 1981, 1990, 1994). The relatively small number of arthropods expected at a High Arctic research station such as Hot Weather Creek, compared with sites in boreal or temperate zones, made it feasible to attempt to inventory the entire fauna of insects and related arthropods. A list of species collected at Hot Weather Creek is provided in the appendix to this contribution.

Comparisons with other High Arctic localities

McAlpine documented a total of 55 species of spiders, mites, and insects from the northwestern Queen Elizabeth Islands (McAlpine, 1964), but only 29 from Isachsen, Ellef Ringnes Island (McAlpine, 1965a), a much harsher environment than at Hot Weather Creek. Danks (1980) found 112 species at Polar Bear Pass, on Bathurst Island, and Ryan (1977) documented 182 species of spiders, mites, and insects at Truelove Lowland, on Devon Island. Oliver (1963), collecting at Lake Hazen, Ellesmere Island, listed 239 species (plus about 25 unidentified taxa) (Fig. 1).

To date, 232 species have been recognized from the Hot Weather Creek material, including several new records for the High Arctic and one species new to science. Quite possibly other species remain to be described from this rich collection. Several important groups such as the Collembola (springtails), Chironomidae (nonbiting midges), and Braconidae (parasitic wasps) need much more work and will probably yield several dozen more species. Currently there is a lack of available taxonomic expertise in these difficult groups.

Hot Weather Creek is most similar to the Lake Hazen study site, approximately 300 km to the northwest. The Lake Hazen area was studied extensively in the 1950s and 1960s. Both are arctic oases protected from more severe weather disturbances by surrounding mountains that tend to deflect or dissipate much of the low-level cloud cover (Edlund and Alt, 1989). Lake Hazen, however, has a more varied terrain than Hot Weather Creek. Meltwater from the Mount McGill glacier provides several fast-running streams all summer (Oliver and Corbet, 1966). In contrast, the bedrock at Hot Weather Creek is composed of "poorly consolidated clastic rocks of the Eureka Sound Group which is in some places covered by younger beds of sand and silt" (Edlund et al., 1990). The region is essentially a plateau that has been undercut by the Slidre River (fed by snow and glacier melt from the Sawtooth

Range some 25 km away) and many streams fed only by snowmelt (including the creek after which the region was named). These streams are often dry by the end of July.

The greater variation in bedrock and increase in aquatic habitats might explain the somewhat richer fauna and flora at Lake Hazen. Edlund has confirmed a higher floral species diversity at Lake Hazen (S.A. Edlund, pers. comm., 1996). The birds seen at Lake Hazen (Gould, 1988) include species, such as the king eider, oldsquaw, gyrfalcon, and hoary redpoll, that are not usually seen at Hot Weather Creek. Among the insects, several recorded from the Queen Elizabeth Islands or at Lake Hazen were searched for at Hot Weather Creek, but not found, including the crane fly *Ormosia* sp., the muscid fly *Spilogona obsoleta* (Oliver, 1963; McAlpine, 1964, 1965a), the scale insect *Pulvinaria ellesmerensis* (Richards, 1964b), the aphid *Metapolophium artogenicolens* (Richards, 1964a), the geometrid moth *Psychophora sabini* Kirby, a pyralid moth *Udea torvalis* Möschl., and a pterophorid moth *Stenoptilia mengeli* Fern (Oliver, 1963; Downes, 1966). An effort was also made to collect thrips from grasses, but only a few immature individuals were found and were not identifiable to either of the two species, *Apterothrips* sp. or *Aptinothrips rufus* (Goeze), recorded from Lake Hazen (Chiasson, 1986).

Species found at Hot Weather Creek, but not at Lake Hazen, such as the two salt-tolerant flies (*see* below) may occur in habitats or niches that are rare or absent at Lake Hazen. On the other hand, some, such as the species of Sciaridae (Diptera), especially the newly described fly *Camptochaeta cladiator* Hippa & Vilkamaa and the three additional beetles, may have been included among the "at least 25 additional species of insects, not yet identified" from Lake Hazen (Oliver, 1963).

The proportional representation of different pterygote orders and of the dominant dipteran families found at several High Arctic sites are presented by Danks (1978) in two tables. Some differences between the data from Hot Weather Creek and those from Lake Hazen can be attributed to variations in collecting procedures and to differences in the ability to identify specimens. For example, Chironomidae are underrepresented in the list from Hot Weather Creek because of insufficient taxonomic analysis of the material collected, whereas the 45 mite taxa (20 per cent of the fauna) are a significant addition to this fauna, thanks to identifications by Drs. V. Behan-Pelletier, E. Lindquist, and I. Smith, Agriculture and Agri-Food Canada (1991). Only one mite was listed by Oliver (1963) and mites were omitted from the tables of Danks (1978) mentioned above.

A high proportion of Canadian High Arctic insects would be expected to show holarctic distributions (Scudder, 1979; Danks, 1981). Table 1 presents the geographic affinities of the arthropods collected at Hot Weather Creek. Of the 232 taxa listed in the appendix, 80 (35 per cent) are known to occur in the Palearctic and 29 (12 per cent) are found on Greenland, but apparently not in the Palearctic. One cannot assume that all the other taxa found at Hot Weather Creek are restricted to the Nearctic because so many of them (92, or 40 per cent) have not been determined to species and they are not

Table 1. Geographic affinities of arthropods collected at Hot Weather Creek (1989–1991).

Taxon	Nearctic distribution			Unknown	Greenland	Palearctic
	Hi	A	S			
Araneae (9) (spiders)		8	1		6	3
Acari (45) (mites)		19	5	21	9	18
Collembola (7) (springtails)		1	2	4	2	2
Anoplura (1) (sucking lice)			1			1
Homoptera (2) (plant lice and mealy bugs)	2					
Thysanoptera (1) (thrips)				1		
Coleoptera (5) (beetles)	1	3		1		2
Trichoptera (1) (caddis flies)		1			1	1
Diptera (100) (true flies)	6	56	8	30	44	39
Lepidoptera (15) (butterflies and moths)		11	4		14	12
Hymenoptera (46) (bees and wasps)		10	1	35	5	2
Total number of species	9	109	22	92	81	80

Hi = the number of species known only from the High Arctic; A = the number of species extending into the Low Arctic, north of the treeline; S = those species also found south of the treeline in the boreal region; Greenland = the number of species known from Greenland; Palearctic = the numbers of species known from the Palearctic; Unknown includes those species not completely identified and whose distribution therefore remains unknown.

completely known or catalogued. However, of the 140 species identified, 9 are only known from the High Arctic (essentially the Queen Elizabeth Islands), 109 extend into the Low Arctic, north of the treeline, and only 22 extend into the boreal region.

A high degree of endemism has been noted in the arctic fauna of the Nearctic (Scudder, 1979). As already mentioned, nine species are restricted to the High Arctic. The fossil record of the High Arctic weevil, *Isochnus arcticus*, has remained essentially unchanged throughout the Pleistocene (Anderson, 1989). At least three spiders found this far north are poor dispersers and probably survived in refugia (Leech, 1966). A refugium and possible centre of endemism has been identified and encompasses part of eastern Axel Heiberg Island and part of Ellesmere Island, including Fosheim Peninsula (Scudder, 1979), the site of Hot Weather Creek. More recent work by Bell (1996) suggests that small, ice-free islands existed in the region of Fosheim Peninsula during the last glaciation and these and other ice-free areas in the High Arctic could have served as refugia.

Habitats and feeding preferences of arthropods at Hot Weather Creek

The denser and more diverse tundra that is found in the intermontane zone of Ellesmere Island such as at Hot Weather Creek (Edlund et al., 1990) allows for a greater variety of arthropods than the more barren and exposed areas near the coast. These arthropods are generally not saltwater tolerant, but are inland forms, except for the two flies discussed below.

Most of the fauna is closely associated with water, either living in it or close by in waterlogged soils. The richest areas in terms of numbers of species as well as populations are in and around the very many shallow, standing water bodies on the plateaus (Fig. 5) and the densely vegetated fens in the lower lying areas (Fig. 6). Many aquatic species, such as some chironomid (nonbiting midge) larvae, feed on algae, desmids, diatoms, fungi, or bacteria in the water. Some, such as the dytiscid beetles (both adults and larvae) and the tanypodine larvae (also Chironomidae), are aquatic predators



Figure 5. Typical tundra pond edged with cottongrass (*Eriophorum scheutzeri*) on a plateau. GSC 2000-024D



Figure 6. Typical low-lying fen with an open pool of water in the foreground and a muskox in the background. GSC 2000-024E

of smaller animals. Other chironomids, mosquitoes, collembolans, and mites are essentially scavengers, eating decaying organic matter. Nevertheless, all these organisms depend to some degree upon the surrounding and emergent vegetation for nutrition (including eating decaying vegetation), for protection from the wind, sun, or predators, or for predators to hide from potential prey. This is probably why the most populated areas are the many shallow pools or ponds that dot the tundra, all of which have richly vegetated borders and usually some emergent plants.

Most aquatic insects, including most flies found this far north and the single species of caddisfly, have aerial adults that can be quite conspicuous because of their synchronized emergence and their mating swarms. However, aquatic beetles spend all their life stages in water, although adults may fly to neighbouring bodies of water for food or oviposition sites (Dr. A. Smetana, pers. comm., 1992).

The banks and waters of the Slidre River, which cuts a winding swath through the region before it empties into Slidre Fiord, are species poor (Fig. 7). Ice scouring in winter and fast spring flow erode the river bottom and banks, allowing almost nothing living to take hold. By mid-summer, the water level has dropped, exposing vast stretches of bare gravel. Larger streams such as Hot Weather Creek that feed into the Slidre River show a similar, but less marked, pattern. The smaller, shallower creeks in the region have siltier bottoms and stretches of richly vegetated banks that harbour a variety of arthropod life.

Other species-rich areas are the fens that develop in gullies. They are the first places to become green and they stay green longer than other habitats. Early in the season, standing water can usually be found in places. These puddles shrink, but the soil never really dries out. The fens are densely vegetated with a rich assortment of aquatic and semiaquatic plants, dominated by sedges, providing habitats for many of the same species found in the tundra ponds (e.g. dytiscid and staphylinid beetles) as well as others such as the fungal-feeding mycetophilids, which seem to be more prevalent



Figure 7. The winding Slidre River showing barren gravel banks. GSC 2000-024F

in the fens. The brightly conspicuous yellow flowers of *Ranunculus nivalis* L., *R. sulphureus* Sol., and *Saxifraga hirculis* L. var. *propinqua* (R.Br.) Simm., flowering in succession, and the two-toned, pink-flowered *Pedicularis sudetica* Willd. ssp. *albolabiata* Hultén attract the nectar seekers, especially moths and butterflies. Muskoxen were seen to feed in fens and their generous droppings probably provided nourishment for a host of mites and flies, especially the heleomyzid *Aecotheca specus*.

The hummocky tundra on the plateau and on the more gently sloping hillsides (Fig. 8) is more or less covered with arctic willow (*Salix arctica* Pall.) and arctic avens (*Dryas integrifolia* M.Vahl.), interspersed with many other flowering plants. The willow serves as the 'bread basket' of the north. Collared lemmings, the arctic weevil, and the caterpillars of most butterflies and moths eat its leaves (as well as those of the arctic avens). The willow flowers very early in the season and provides nectar and protection for several small flies, particularly the chironomid *Smittia* sp. Lemmings, the chief willow herbivores, provide food and nourishment for various insects that live in their burrows, such as winter crane flies (Trichoceridae) (McAlpine, 1965a), the bumblebee that occasionally nests in old burrows (Milliron and Oliver, 1966; Richards, 1973), and the many flies and mites that live in and around their droppings and on dead lemmings, not to mention the parasitic wasps that live on these flies. In turn, lemmings are host to at least one louse and are preyed upon by ermine; probably both are eaten by the arctic fox and arctic wolf.

The leaves and flowers of the arctic avens are also eaten by several caterpillars and the flowers are important basking places for various insects as well as necessary sources of nectar and pollen (Fig. 9). McAlpine (1965b) suggests that the absence of mosquitoes on Ellef Ringnes Island may be related to the absence of the arctic avens. The two High Arctic species of mosquitoes can facultatively mature a reduced number of eggs, without benefit of a blood meal, by getting nourishment from the nectar of *Dryas integrifolia* (Corbet, 1964). McAlpine (1965b) observed members of eight families of



Figure 8. Joyce Gould on hummocky tundra on a gently sloping hillside in late June before the emergence of leaves. GSC 2000-024G

flies imbibing nectar from seven species of plants, but primarily from *Dryas integrifolia*; in some cases, they also ate pollen. He suggests that this relationship might be of reciprocal benefit as these flies may be important pollinators this far north, even though most High Arctic plants are self-pollinators.

In several places on the plateau, encrustations of salts (Ca, Mg, NaSO₄) have leached up from the substrate, leaving barren, whitened areas on the surface where very little will grow except for scattered, salt-tolerant plants such as *Braya purpurescens* (R. Br.)Bunge, *Potentilla rubicaulis* Lehm., and the grass *Puccinellia poaceae* Th. Sor. (Fig. 10). These salt flats also harbour two very interesting species of flies that are more usually associated with coastal regions. An ephydrid fly, *Lamproscatella brunnipennis* (Malloch), was previously known from coastal Eureka; it is able to withstand osmotic pressures of salty environments. Related species are often abundant on the crystalline mud playas exposed by receding water levels in shallow, alkaline or saline lakes at more southerly sites (Mathis, 1979). The other salt-tolerant species, *Pelomyiella mallochi* (Sturtevant) in the family Tethinidae, is a new record for the High Arctic.

Nature of the fauna

In an annotated list of insects and other arthropods collected at Hot Weather Creek (see appendix), it can readily be seen that many important orders are completely missing or poorly represented. Aquatic habitats are a major component at Hot Weather Creek, yet dominant aquatic orders such as the Odonata (dragonflies and damselflies), Plecoptera (stoneflies), and Ephemeroptera (mayflies) are not found there and only one species of caddisfly (order Trichoptera) occurs this far north. The very prolific order of beetles (Coleoptera) is represented by only five species at Hot Weather Creek and it may be significant that four of these species are aquatic. Of the Hymenoptera, parasitic wasps predominate, only one species of bee was collected, and no ants occur this far north. Other important orders that are com-

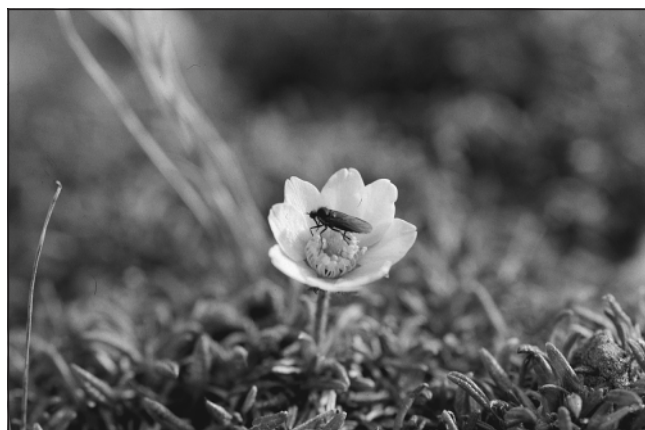


Figure 9. *Rhamphomyia filicauda* (a predaceous empidid fly) basking on, or awaiting prey on, *Dryas integrifolia* (arctic avens). GSC 2000-024H

pletely missing are the Orthoptera (grasshoppers, katydids, crickets), Hemiptera (bugs), Dictyoptera (mantids, cockroaches), and Neuroptera (fishflies, lacewings, snakeflies, antlions). In this respect, this fauna is similar to that recorded in other High Arctic regions, most notably at Lake Hazen to the north (Oliver, 1963; Danks, 1978).

Special adaptations

Most High Arctic arthropods are true arctic and tundra forms that, if they occur south of the treeline, are high-mountain extensions or relict populations (Downes, 1966). Only 22 of the species collected at Hot Weather Creek extend into the boreal zone (see Table 1). Northern insects undergo a period of diapause (suppression of development) accompanied by various physiological and behavioural mechanisms to survive the winter. These include the accumulation of cryoprotectants in the haemolymph and dehydration of cells to avoid freezing, or alternatively, to control freezing by various means (Danks, 1987, and references therein). However, Danks et al. (1994) suggest that High Arctic insects show slightly different combinations of strategies to survive in their more rigorous environment.

At lower latitudes, photoperiod is the more usual cue to trigger winter diapause. In the High Arctic, a different strategy is to use changes in temperature as a cue to enter diapause (Danks et al., 1994). At higher latitudes, continuous daylight occurs before, and extends beyond, the short growing season, making changes in photoperiod problematic as a cue for triggering winter diapause.

A related strategy is to enter diapause early to prevent development from continuing dangerously late in the summer, even when temperatures remain relatively warm. This ensures that organisms are in the appropriate state for the onset of winter. For example, only those midge larvae able to pupate early in the season without feeding will emerge in a given year. In most years, this would allow enough time for mating, egg laying, and development of winter-hardy instars before freeze-up. The large, woolly moth caterpillar



Figure 10. Surface encrustations of salts (white areas), habitat of the salt-tolerant, yellow-flowered *Potentilla rubicaulis* (in the foreground) and salt-tolerant flies. GSC 2000-024I

(*Gynaephora groenlandica*) stops feeding in mid-summer, seeks sheltered sites, and apparently goes into winter diapause (Kukal, 1990). However, caterpillars of the related *Gynaephora rossi* were found moving around again, after a hiatus of several weeks, as late as August 12, 1991 (Brodo, unpub. notes, 1991). Some had a pinkish, sticky fluid (meconium?) sticking to their hairs. (Certain insects excrete a substance called 'meconium' soon after emerging from a cocoon.) These caterpillars had apparently broken diapause, but possibly only a shorter summer diapause and not the longer winter diapause.

Another strategy is to have a lower temperature threshold for metabolism to occur. Arctic insects are generally active at much lower ambient temperatures than insects farther south. By basking in the sun, especially on the reflective white petals of the arctic avens or the yellow petals of *Arnica alpina* (Fig. 9, 11), insects have been shown to increase their body temperatures by several degrees (Danks et al., 1994). This may be offset by a diminished growth rate when body temperatures approach 30°C (Kukal et al., 1988).

Temperature variations during spring and summer, especially occasional, below-freezing temperatures, affect High Arctic organisms more significantly than the duration and degree of winter cold. Probably all life stages of High Arctic insects are freezing tolerant throughout the short growing season whereas in boreal and temperate regions, generally only one overwintering stage can withstand below-freezing temperatures. In the High Arctic, cold hardiness may be coincidental with winter diapause, but these are two independent, although related, phenomena (Danks et al., 1994). Winter mortality in the High Arctic, at least for some species, is relatively low (Kukal, 1990), apparently because the absence of solar warming for several months means that the temperature remains more stable than in the temperate zone.

Many species select relatively exposed sites for overwintering rather than the more sheltered habitats selected farther south. These sites warm up more quickly and allow for development to start earlier in the spring (Danks et al.,



Figure 11. The butterfly *Boloria chariclea* resting on *Arnica alpina*. Note the dark hairs that extend beyond the body and partly obscure the wing pattern. GSC 2000-024J

1994). Exposed sites are also the driest and resistance to desiccation is more marked among species overwintering in such sites than among those overwintering under snow cover or in other, more protected habitats.

The High Arctic growing season is short and unpredictable. Three basic strategies of development have evolved to deal with this. Some species undergo complete development rapidly within a single growing season and only one stage undergoes diapause. This strategy is used by the arctic weevil *Isochnus arcticus* and its hymenopteran parasite, *Pnigalio* sp. Female weevils lay eggs singly on newly emerged willow leaves in the spring. The larvae mine within the leaf and emerge as adult weevils, or if parasitized, an adult wasp emerges instead. Both species apparently overwinter in the leaf litter. The willow is deciduous and for insect development to be successful, it has to be completed before leaf fall.

A second strategy involves a generation time of a fixed number of years in which more than one stage undergoes diapause (or a stage is able to undergo diapause more than once before moulting). The lymantriid moth, *Gynaephora groenlandica*, overwinters in the 2nd, 3rd, 4th, 5th, and 6th larval stages and apparently takes 14 years to complete its life cycle (Kukal and Kevan, 1987). The butterfly *Boloria polaris*, which is on the wing only in odd-numbered years (Klassen et al., 1989), takes two years to develop, but its life stages are synchronized.

A third strategy, probably the more prevalent one, involves a flexible response to climate. Danks (1981, p. 281) presents various estimates of the number of years required to complete development. This strategy allows for more rapid development in favourable years and postponed development in harsher growing seasons and would prevent the elimination of a population in a particular area during a severely shortened growing season. Mosquitoes may spend one or more winters in the egg stage (Corbet, 1964). The scale insect *Pulvinaria ellesmerensis* is capable of overwintering in several nymphal stages (Richards, 1964b). *Tipula besselsi* and probably other Tipulidae may take several years to complete development, judging from the range of larval instars collected throughout the season at Hot Weather Creek. Other Tipuloidea have been recorded to take as many as five years to complete development (MacLean, 1975).

Downes (1964) noted that populations of High Arctic Lepidoptera tend to be duskier with less well developed patterns than populations to the south. This was evident in the specimens collected at Hot Weather Creek compared with specimens collected at Churchill, Manitoba, and other regions to the south. Darker insects absorb more solar heat. Downes also suggested that more energy might be expended in producing stronger patterns and that this might be a strategy to save energy. Energy may also be saved by reducing the size of the adult insect. This was documented by Hemmingsen and Jensen (1957) for the crane fly *Tipula arctica*. In size and colouring, the Hot Weather Creek flies appeared to be closer to the more southern forms on Greenland, corroborating the notion that weather patterns at Hot Weather Creek are more favourable than the latitude would indicate.

In addition to having a duller pattern than more southern populations, most butterflies, moths, and bumblebees at Hot Weather Creek are notable for their larger, heavier bodies (especially the females), thickly covered by long hairs. In the lepidopterans, hairs extend in a broad patch next to the body, along the wing bases, and on the femora and tibiae of the legs. This pattern is particularly evident in the two species of *Boloria* where dusky hairs hide the coloured wing scales (Fig. 11). The *Gynaephora* moth adults do not have hairs on their wings, but the larvae, pupae, and even the eggs are covered in long, dark hairs (Fig. 12). A female moth was observed covering eggs, as they were laid, with a coat of hairs from the tip of her own abdomen. These hairs serve to trap solar heat. For example, a 20°C increase in body temperature has been recorded on basking larvae of *Gynaephora groenlandica* (Kevan et al., 1982; Kukul et al., 1988).

Several other behavioural and physical modifications promote survival in the High Arctic. Species tend to seek habitats that absorb heat and provide shelter from winds (Danks et al., 1994). Tiny flies were seen among the woolly hairs of willow catkins and in the fuzz surrounding *Pedicularis* stems, especially on windy days (Danks, 1986; Brodo, unpub. notes, 1990). During sunny periods, flies and butterflies are often seen on various exposed substrates such as open flowers, soil, and rock surfaces, oriented to capture the sun's rays. Such basking behaviour significantly



Figure 12. Hairy pupa of *Gynaephora* sp. removed from and lying above its cocoon. GSC 2000-024K

increased body temperatures relative to ambient temperatures in High Arctic butterflies (Kevan and Shorthouse, 1970).

Trophic analysis

Information on the general food requirements for 221 of the 232 species are detailed in the appendix and summarized in Table 2. The largest trophic group, the prime recyclers in the ecosystem, feeds on algae, fungi, diatoms, detritus, or carrion. It includes 86 species, dominated by the Diptera with 54 species. However, it is far more important than these figures indicate because the most abundant species, most notably in the Culicidae and Chironomidae, belong to this group, thus producing a considerable biomass. The culicids and many chironomids form conspicuous mating swarms. The larvae and adults are a prime food source for birds and other insects and arthropods. Several birds were caught raiding the insect traps and the ruddy turnstone in particular was observed foraging for insect larvae in the shallows. The adult flies, because of their great numbers and their habit of imbibing nectar as well as basking on flowers, may be very important pollinators of many arctic plants (McAlpine, 1965b).

The parasitic insects are the next most numerous group with regard to number of species (52), but not number of individuals. This group is dominated by the Hymenoptera with 42 species (plus more to be identified from the material collected). Most wasps and the five tachinid flies are host specific and do not usually occur in large numbers. Possible exceptions are some microhymenoptera such as the weevil parasite *Pnigalio* and *Tetracyclos boreios* (Brodo, unpub. observations, 1990). The latter was reared from *Chorizococcus altoarcticus* (Richards) (as *Pseudococcus* sp., Gibson and Yoshimoto, 1981). Both hymenopteran parasites were collected in considerable numbers in the yellow bowls.

Table 2 also shows that 50 predators are known from Hot Weather Creek, 50 per cent of which are flies and 28 per cent, mites. The muscid genus *Spilogona* dominates with 13 species that apparently feed on Chironomidae (Danks, 1980). The four *Rhamphomyia* species (Empididae) were very numerous in all but the pitfall traps. Both the adults and larvae are predators of smaller flies, especially mosquitoes. Downes (1970) presented an elegant discussion of his astute observations of the feeding and mating behaviour of these flies. Predatory mites feed on smaller arthropods and arthropod eggs.

A High Arctic peculiarity documented by Danks (1986, 1990) and corroborated here is the relatively small number of herbivores. Of the 33 known herbivores, 15 are Lepidoptera, i.e. caterpillars. Probably the most numerous herbivorous species trapped was the grass leaf miner *Chromatomyia puccinelliae*, found on several species of grasses (see appendix). Even though the number of potential food plants decreases with latitude, those that are available at high latitudes seem to be underutilized (Danks, 1980, 1986; Downes, 1964). This is also the case at Hot Weather Creek.

Table 2. Trophic analysis of arthropods collected at Hot Weather Creek (1989–1991). Only larval preferences are recorded.

Taxon	Food preferences				
	Small particulates	Parasites	Predators	Herbivores	Food unknown
Araneae (9) (spiders)			(9) small flies, springtails, mites, spiders		
Acari (45) (mites)	(23) fungi, algae, mosses	(4) ectoparasites of vertebrates	(14) mites, small insects, and arthropods, including eggs	(4) <i>Lesquerella arctica</i> , <i>Salix arctica</i>	
Collembola (7) (springtails)	(6) fungi			(1) pollen	
Anoplura (1) (sucking lice)		(1) ectoparasite of lemming			
Homoptera (2) (plant lice and mealy bugs)				(2) <i>Lesquerella arctica</i> , <i>Dryas integrifolia</i>	
Thysanoptera (1) (thrips)				(1) grasses	
Coleoptera (5) (beetles)	(2) aquatic detritus		(2) aquatic organisms	(1) <i>Salix arctica</i>	
Trichoptera (1) (caddis flies)	(1) algae, detritus				
Diptera (100) (true flies)	(54) algae, fungi, detritus, carrion, dung	(5) internal parasites of Lepidoptera	(25) midges, mosquitoes, Lepidoptera	(5) grasses, <i>Erigeron</i> , <i>Melandrium</i> , <i>Papaver</i> , <i>Pedicularis</i>	11
Lepidoptera (15) (butterflies and moths)				(15) <i>Salix arctica</i> , <i>Dryas integrifolia</i> , <i>Vaccinium uliginosum</i>	
Hymenoptera (46) (bees and wasps)		(42) parasites and hyperparasites of flies, wasps and Lepidoptera		(4) <i>Salix arctica</i> , pollen, and nectar	
Total number of species	232	86	52	50	33
Numbers in parentheses indicate the total number of species within a taxon, or the number of species associated with a particular food preference. Only larval preferences are recorded.					

Dominant arthropod groups at Hot Weather Creek

Diptera (flies)

Diptera is the most abundant order of arthropods at Hot Weather Creek with 100 species (43 per cent of the total) recognized and others still to be identified. Eleven of these species are new records for the High Arctic and one, a sciarid, is new to science (Hippen and Vilkkamaa, 1994).

The family Chironomidae (nonbiting midges) is the largest in both number of species and individuals. Chironomids are ubiquitous; their larvae inhabit all water bodies and damp soils. They are mainly detritus feeders except for the Tanytopodinae, which are chiefly predators. In turn, these larvae are preyed upon by other fly larvae such as the crane fly *Tipula besselsi* (Lantsov and Chernov, 1987) and by species of the muscid genus *Spilogona* (Danks, 1980). They are also part of the food chain of the small, landlocked arctic char found in some larger ponds and of the several wading birds that breed in the area. Only part of the Hot Weather Creek

chironomid specimens have been studied and 17 species have been identified from this material. A conservative estimate suggests that 45 species probably occur there (Oliver, 1963).

Only two species of mosquitoes occur this far north, but they compensate for this lack of diversity by their abundance and their painfully irritating presence. Their natural hosts are muskoxen and birds (Corbet and Downe, 1966), the arctic wolf (Brandenburg, 1993), and probably also the other mammals found in the vicinity (collared lemming, ermine, arctic hare, arctic fox, and caribou). When vertebrate hosts are scarce, females of both species may lay a reduced number of eggs, without benefit of a prior blood meal, but nourished instead on the nectar of *Dryas integrifolia* (Corbet, 1967). These two species of mosquitoes are the only mammal-biting flies found in the area. None of the biting midges (Ceratopogonidae) at Hot Weather Creek feed on mammals.

Two blowfly species were collected, *Boreëllus atriceps* and *Protophormia terraenovae*, both carrion feeders (Fig. 13). The bird blowfly *Protocalliphora tundrae* was not

collected although it undoubtedly occurs at Hot Weather Creek. The larvae are blood-sucking parasites of the snow bunting and the savannah sparrow. The adults are difficult to catch with a net (Sabrosky et al., 1989). Snow buntings nest at Hot Weather Creek, but the nests are well camouflaged and were not found.

Five species of Tachinidae were found. *Chetogena gelida* was reared from a *Gynaephora* pupa, probably from *G. rossi* (D.M. Wood, pers. comm., 1990) (Fig. 14).

Several leaf miners (Agromyzidae) and a stem borer (Scathophagidae) were found. They are discussed in the section 'Insect damage to plants', below. Two salt-tolerant species occur in this inland community and they are discussed in an earlier section, 'Habitats at Hot Weather Creek'.



Figure 13. Adult carrion feeder fly (*Protophormia terranovae*) and several pupae from a dead fox. GSC 2000-024L



Figure 14. Pupae and two adult parasitic flies (*Chetogena gelida*, Tachinidae) from a cocoon of *Gynaephora* moth. GSC 2000-024M

Hymenoptera (bees and wasps)

Wasps are well represented by 46 species identified so far, but with two dozen or more species likely to be found among the unidentified Ichneumonidae and Braconidae. Dr. W.R.M. Mason was in the process of identifying this material and had added six new species just before his untimely death in 1991. Eight new species were added to the microhymenoptera, including four new genera, *Syrphophagus*, *Metaphycus* (Encyrtidae), *Thektogaster* (Pteromalidae), and *Entomacis* (Diapriidae). This last genus is the first record of a proctotrupid wasp in the High Arctic (L. Masner, pers. comm., 1991). Another surprise was the finding of a parasitic cynipid wasp.

Most wasps, including the microhymenoptera, are parasites or hyperparasites (parasites of parasites) of other insects and are highly species specific. Therefore, none are found in the great numbers characteristic of many of the flies. A single species of bumblebee, a pollen and nectar feeder, was collected. Several Tenthredinidae (sawflies) were found, the larvae of which are leaf rollers and gall formers in *Salix arctica*.

Acari (mites)

There is surprisingly little overlap of species lists from the various High Arctic localities (cf. Oliver, 1963; Ryan, 1977; Danks, 1980), suggesting that collecting was very patchy. Many more strategically selected soil samples would have to be collected to properly assess the richness of this fauna. Danks (1981) listed 114 species from the High Arctic. A mere 45 were recognized from the Hot Weather Creek material and yet 20 of these (44 per cent) are new records for the High Arctic.

The oribatids were the most numerous suborder both in number of species and number of specimens collected. The commonest species was *Tectocephus velatus*, followed by *Hermannia scabra* (new for the High Arctic) and *Trichoribates polaris*.

Lepidoptera (butterflies and moths)

Fifteen species were recorded from Hot Weather Creek. Eleven of these occur in both Greenland and the Palearctic. Three species (*Olethreutes mengelana*, *Gynaephora groenlandica*, and *Lasionycta leucocycla*) are found only in the Nearctic and Greenland. *Gynaephora rossi* is unique in being found in the Palearctic, but not in Greenland.

The butterfly *Boloria polaris* was collected only in 1991. It is known to have a two-year, synchronized life cycle. In northern Manitoba, it is recorded as being on the wing only in odd-numbered years (Klassen et al., 1989). In 1991, it was far less numerous than *B. chariclea* in 1991 (Brodo, unpub. data, 1991), a species with an unsynchronized, two-year life cycle that therefore is found every year. A synchronized, alternate-year life cycle is thought to be controlled by parasitism, with the parasite emerging from the larger population one

year and controlling the smaller population the following year (Wipking and Mengelkoch, 1994). Wipking and Mengelkoch (1994) state that, in the years during which both species are on the wing, the species with the synchronized, two-year life cycle should be more common. As already mentioned, this was clearly not the case at Hot Weather Creek. Regardless, it would be reasonable to assume that different parasites attack these two species. Unfortunately, no parasites emerged from the *Boloria* caterpillars that were reared.

Of the lycaenid butterflies, only one specimen of *Agriades glandon* was collected at Hot Weather Creek, whereas *Lycaena phlaeas* was common. The reverse was true at Lake Hazen: *Agriades glandon* was common and *Lycaena phlaeas* was rare (Kevan and Shorthouse, 1970).

Araneae (spiders)

Spiders apparently have a patchy distribution in the High Arctic. The most common spiders at Hot Weather Creek were *Pardosa glacialis*, *Erigone psychrophila*, and *Alopecosa exasperans*. Leech (1966), concentrating on spiders at Lake Hazen, Ellesmere Island, found *Pardosa glacialis*, *Hilaira vexatrix*, and *Erigone psychrophila*, in that order, to be the most common species. Neither Danks (1980) nor Ryan (1977) collected *Pardosa glacialis* during their High Arctic studies. Danks (1980) reported *Collinsia spetsbergensis* to be the most abundant spider at Polar Bear Pass, Bathurst Island. This species was also recorded from Devon Island (Ryan, 1977). It was rare at Lake Hazen (Leech, 1966) and not found at all at Hot Weather Creek.

Coleoptera (beetles)

This very diverse order is represented by only five species at Hot Weather Creek. The carabid *Amara alpina* Paykull, found on Devon Island (Ryan, 1977) and in semifossilized peats near Makinson Inlet, Ellesmere Island (Blake and Matthews, 1979), was not collected at Hot Weather Creek nor at Lake Hazen (Oliver, 1963), even though it was intensively sought after by Dr. Alan Morgan and the author using Morgan pitfall traps.

Two species of Dytiscidae are recorded from Hot Weather Creek, *Hydroporus polaris* Fall and *H. lapponum* Gyll. (determined by D.J. Lawson in 1996). The adults of both species were easily dislodged by stamping on the vegetation, mostly *Carex aquatilis* Wahlemb. var. *stans* (Drej.) Boott, at the edges of tundra ponds and in fens. Larvae were also collected, but not identified to species. Recently, Debruyn and Ring (1999) compared the ecology of *Hydroporus polaris* Fall and *H. morio* Aubé from Alexandra Fiord, Ellesmere Island. These were also identified by D.J. Lawson and this shows the patchiness of these beetle distributions.

Two very similar species of rove beetles were also collected in the vegetation at pond edges. They were recorded as *Atheta* sp. in Oliver (1963) and Danks (1981), but are now

included in the genus *Gnypeta*. The names by S. Ashe (A. Davies, pers. comm., 1992) remain unpublished. Larvae were collected, but not identified as to species.

A single, small, black weevil (*Isochnus arcticus*) was collected at Hot Weather Creek. See the section 'Insect damage to plants'.

Collembola (springtails)

Springtails, together with mites, are an important component of the soil fauna and were probably also insufficiently sampled at Hot Weather Creek. All the species listed were common. Fjellberg (1986) found a total of 41 species from Ellesmere Island, suggesting that many more than the seven species noted here occur at Hot Weather Creek. Identifications were based on Waltz and McCafferty (1979).

Homoptera (plant lice and mealy bugs)

Farther south, the members of this order are important pests and carriers of plant diseases. At this latitude, very few occur. Two species of aphids were collected at Lake Hazen, one on *Lesquerella arctica* (Wormskj.) S.Wats. and the other on *Salix arctica*; both were collected in significant numbers in all stages to assess their biology (Richards, 1963). Yet despite intensive efforts, none were found on a host plant at Hot Weather Creek and only a very few immature specimens were trapped. Similarly, a few male coccids were trapped, but none were found on the known food plant, *Salix arctica* (Richards, 1964b), despite much searching. Yet many specimens of *Tetracyclos boreios*, a tiny hymenopteran thought to be a parasite of scale insects (Gibson and Yoshimoto, 1981), were collected in several traps.

Trichoptera (caddisflies)

A single, circumpolar caddisfly occurs this far north, but no mayflies, stoneflies, dragonflies, or damselflies. *Apatania zonella* overwinters in unfrozen, deep pockets of water in larger ponds and lakes (Downes, 1964). Coal Lake, where this species was abundant in 1991, is known to have an unfrozen, deeper pocket (<2.5 m., P. Hamilton, pers. comm., 1991). During the growing season, the larvae apparently take advantage of the warmer, shallower water (Downes, 1964), but no sign of larvae or cases was found in the extensive shallows of Coal Lake. This primarily parthenogenetic species probably feeds on diatoms and other algae (Wiggins, 1977). It was rare in 1990.

Anoplura (sucking lice)

Collared lemmings, the host of *Hoplopleura acanthopus*, were common in 1990 as were these lice, which were removed from a trapped and dying animal. In 1991, there was practically no lemming activity at the Hot Weather Creek site.

Insect damage to plants

Insect herbivory is not as prevalent or as conspicuous in the Arctic as in the boreal or temperate zones. Insect damage is less evident (Danks, 1986; Brodo, unpub. notes, 1990). Detritivores, saprovores, parasites, and predators predominate in arctic ecosystems (Danks, 1990). There are no Orthoptera this far north and that means no grasshoppers, katydids, or crickets. There are no Hemiptera, two Homoptera, only one species of Thysanoptera (thrips), and only one herbivorous beetle. This small number of herbivorous species translates into generally healthier looking plants because fewer leaves and other vegetative parts are eaten or otherwise blemished.

Insect damage in the High Arctic is distinct enough, however, that one can reliably deduce the presence of certain herbivores by the damage left behind. These clues may be as useful for studying fossilized or semifossilized plant remains as they are for extant flora. The following damage to plants was documented at Hot Weather Creek.



Figure 15. *Salix arctica* leaves showing holes eaten out by adult weevils (*Isochnus arcticus*). Holes are approximately 1.5 mm in diameter. GSC 2000-024N

Arctic willow

The arctic willow *Salix arctica* is the dominant plant at Hot Weather Creek and probably the one that shelters and feeds the most insects.

Coleoptera

Curculionidae: The weevil *Isochnus arcticus* overwinters as an adult. In early June, or when new leaves have sprouted on the arctic willow, the adults eat out very characteristic, almost circular holes about 1.5 mm in diameter (Fig. 15). A few days later, one can find similar-sized, yellowed areas on leaves where the epidermis, top and bottom, remains intact; these indicate the presence of an egg or newly hatched larva. This larva remains within the leaf and eats the entire internal contents in its path, making an increasingly broader, discoloured patch or blotch mine, without breaking through either the upper or lower epidermis of the leaf (Fig. 16). Small, dark granules of frass are deposited within the mine as the larva feeds. Pupation occurs within the leaf and the adult beetle chews or pushes its way out and hibernates within the leaf litter. Downes (1964) discussed this beetle (as *Rhynchaenus* sp.). The subfamily was recently revised by Anderson (1989).

In 1990, weevil damage to *Salix arctica* was common and both adults and immature weevils were readily collected. About 50 per cent of these weevil larvae were found to be externally parasitized by a single, tiny wasp larva, an undescribed species of *Pnigalio* (Eulophidae) (Dr. J. Huber, pers. comm., 1990). The wasp was attached by its mouthparts to the soft-bodied beetle larva near its head end and was apparently sucking out the body contents. Both were within the blotch mine and were only visible when the mine was split open.



Figure 16. *Salix arctica* leaf with blotch mines made by larvae of the weevil *Isochnus arcticus*. Several holes made by the adult weevil are also visible. GSC 2000-024O

In 1991, weevil damage was almost nonexistent and developing larvae were very scarce. Dead adults, however, were plentiful in leaf litter from the previous year. Severe, early spring wind storms that year blew away most of the snow cover at Hot Weather Creek. It is suggested here that abrasive damage to the weevils may have been lethal. A snow cover would have kept these weevils firmly in place until spring thaw. Instead, they must have been buffeted around while in winter diapause, which might have initiated rapid ice growth through the cuticle, so killing the beetles (*see* Danks, 1994).

Hymenoptera

Tenthredinidae (sawflies): Several species of *Pontopristia* (as *Nematus* sp., Oliver, 1963) are known to attack the arctic willow. Three species of adults were collected and the smallest and most common may be a catkin eater. Two leafroller species were found, but not reared to adulthood and therefore could not be positively identified. These larvae roll up the leaf and feed from within. The larvae and pupae of one of the species remains within the leaf roll (Brodo, unpub. notes, 1991) whereas in another species, the full grown, bright green larva was found on various structures (tents, parcolls) some distance from the food plants. (Some of these larvae pupated in a vial, but did not emerge.)

Lepidoptera

Gynaephora groenlandica larvae were successfully reared on *Salix* leaves, their preferred diet (Kukal, 1990). They and the larvae of *G. rossi* tend to eat the entire leaf, starting at the edges and working their way in. Several other, unidentified, noctuid caterpillars also fed on *Salix*, but they skeletonized the leaves leaving the veins and midrib more or less intact (Fig. 17).



Figure 17. Noctuid caterpillars skeletonizing a leaf of arctic willow. Caterpillars are approximately 2.5 cm long. GSC 2000-024P

Homoptera

A species of aphid and a scale insect attach themselves to and feed on *Salix*. Small, pale, pin-point spots on the underside of *Salix* leaves indicate aphid damage. Scale insects adhere tightly to the twigs and look like tiny, brownish scabs (Richards, 1963, 1964a, b). Only a very few aphids and scales were collected in traps at Hot Weather Creek. They were not found on the host plant despite diligent searching. Presumably their populations were very low.

Diptera

Several tiny flies such as *Smittia* (Chironomidae) were found, head down close to the stem within willow catkins, sucking nectar from the nectaries. On particularly cold and windy days, these flies and others may simply be seeking shelter from the elements.

Arctic avens

The arctic avens *Dryas integrifolia* bears white flowers with yellow centres and is one of the dominant plants at Hot Weather Creek. It is particularly lush where snowbanks accumulate.

Lepidoptera

The butterfly *Boloria chariclea* (Nymphalidae) was successfully reared on *Dryas*, but seemed to prefer the petals to the leaves. Noctuid caterpillars as well as *Gynaephora groenlandica* and *G. rossi* (Lymantriidae) also ate *Dryas* petals as well as *Salix* leaves (Brodo, unpub. notes, 1990, 1991). The tortricid moth caterpillar *Olethreutes mengeliana* makes webs on *Dryas* clumps (MacKay and Downes, 1969).

Diptera

Larvae of the crane flies *Tipula arctica* and *Dactylolabis rhicnoptiloides* can be found under *Dryas* clumps; they may disturb root hairs, but seem not to inflict any visible damage.

Many other flies such as empidids, dolichopodids, and syrphids as well as butterflies and moths were seen to rest and bask on the open flowers (Fig. 9). These flowers act as parabolas, reflecting heat onto the occupant. These flies may also be taking nectar.

Pedicularis species (louseworts)

Lepidoptera

Caterpillars of the tortricid moth *Olethreutes schultzi* were found on various species of stouter stemmed *Pedicularis*, especially *P. lanata* Cham. and Schlecht., *P. arctica* R.Br., and *P. hirsuta* L. Earlier instars cloak themselves in silk-lined tunnels between the leaf bases and the stem; larger larvae make grooves and short tunnels, loosely

lined with silk, along the outside of the stem and the top of the rootstalk. These larvae were not found at Hot Weather Creek on the slender *P. capitata* Adams, although the species was found on this plant in Greenland where it does not tunnel, but lives at the bases of shoots within a loose silk covering (MacKay and Downes, 1969).

Diptera

The fly *Gonarcticus arcticus* (Scathophagidae) mines the central core of the stem in the stouter species of *Pedicularis* and pupates within the stem. Often both the moth (above) and this fly are found on the same plant, although not in contact. The fly larvae eat the pith of the stem, hollowing it out, whereas the moth eats from the outside. The presence of fly larvae or pupae is revealed in a living plant by bending the stem. If it snaps, there is a fly within; an uninhabited stem simply bends. Infested plants seem quite healthy, bearing luxuriant flowers. Perhaps seed production is affected.

Grasses

Diptera

The leaf-miner *Chromatomyza puccinellae* (Agromyzidae) was reared from several species of grasses, generally those having broader leaf blades, e.g. *Alopecurus alpinus* L., *Arctagrostis latifolia* (R.Br.) Griseb., *Dupontia fisheri* R.Br., and *Elymus alaskanus* (Schribner & Merr.) A.Love. The damage noted was a pale pocket on the leaf blade where chlorophyll was eaten away. The fly larva eats out a little enclosed pocket for itself, leaving the top and bottom epidermal surfaces of the leaf blade intact. Small black droppings (frass) within this pocket as well as the developing larva or pupa (slightly darker) may be visible.

Thysanoptera

Thripidae: Evidence of the presence of thrips was noted on several grasses although the organisms themselves were not found in situ. A few immatures were captured in traps and could not be identified to species. The damage observed was rows of minute pale spots on the leaf or grass stem, perpendicular to the stem axis — evidence of sucking by a minute insect. Two species of thrips have been collected at Lake Hazen, Ellesmere Island, *Anaphothrips* sp. and *Aptinothrips rufus* (Goeze) (Chiasson, 1986).

Nematoda

These nematodes may be mistaken for fly larvae and so are included here. Both *Arctagrostis latifolia* and the sedge *Kobresia myosuroides* (Vill.) Fiori & Paul. may have their ovaries infested with nematodes. In *Arctagrostis*, damage is seen as protruding, swollen ovaries and extended stigmas (Brodo, unpub. notes, 1991).

Arctic poppy

Diptera

A somewhat pale, blotchy mine was found on a leaf of the arctic poppy (*Papaver lapponicum* Tolm. Nordh. ssp. *occidentale* (Lundstr.) Knaben. The larva was not reared successfully, but probably was that of the agromyzid fly *Phytomyza parvicella* (Spencer, 1969). Adults of this species were collected in traps.

Fossilization of insects or of their traces

Diptera

Chironomidae (nonbiting midges)

The dominant insects of Hot Weather Creek were midges (Chironomidae), the larvae of which are aquatic or can survive in damp soils. Because of their small size and soft bodies, generally only the larval head capsules are preserved. Indeed, Garneau (1992) analyzed a peat deposit at Hot Weather Creek and found Chironomidae to be the most prevalent fossil and occurring in all strata.

Culicidae (mosquitoes)

The two species of mosquitoes breed in water, especially in the many tundra ponds and in the intervening cracks. Larval head capsules are the parts most likely to be preserved and may be part of the unidentified remains.

Tipulidae and Limoniidae (crane flies)

Larger larvae of *Tipula besselsi* (3rd and 4th instar) tunnel along just under the water in slowly moving to stagnant water bodies. They create meandering ridges along the silty substrate, but the tops of these ridges are soon eroded, leaving just grooved tracks (Fig. 18). Larvae (Fig. 19) have also been

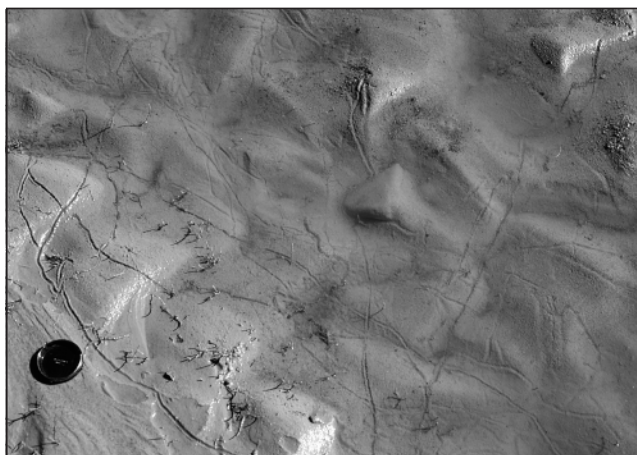


Figure 18. Eroded track of the crane fly larva *Tipula* (*Arctotipula*) *besselsi* in silt of Heather Creek. (The lens cap measures 52 mm across.) GSC 2000-024Q

observed retreating along previously formed tracks. These larval tracks are about 1 cm wide and crisscross each other; they remain in the silt and harden as the banks dry out. Bird tracks and peck marks may also be found along the larval tracks. Figure 20 shows a mating pair of a related species of adult crane flies.

The much smaller larvae of *Symplecta* (Limoniidae) (and also smaller instars of *Tipula besselsi*) make much smaller tracks, but these seem to be eroded quite easily. None of the five species of crane flies at Hot Weather Creek are found in the fens so their remains are unlikely to be found in the local peats.

Coleoptera (beetles)

Beetles are usually the best preserved insects in the fossil record. Only a few unidentified beetle remains were found in the two top strata in a peat deposit at Hot Weather Creek (Garneau, 1992).



Figure 19. *Tipula besselsi* larvae collected in net. Larvae are approximately 2.5 cm long. GSC 2000-024R

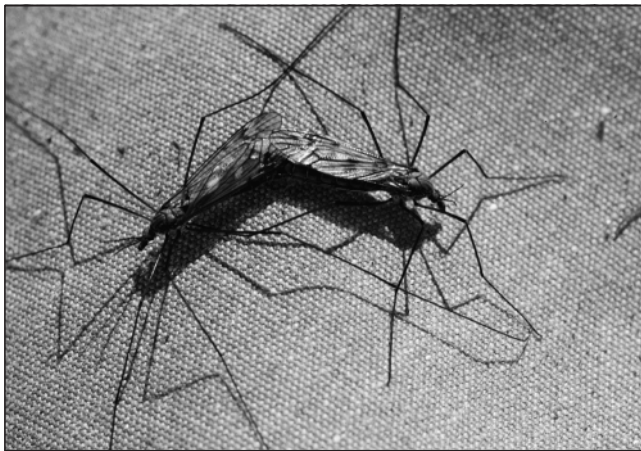


Figure 20. Mating adult crane flies (*Tipula arctica*). Wing length approximately 1.5 cm. GSC 2000-024T

Curculionidae

The weevil *Isochnus arcticus* has been found as fossils in the Northwest Territories (Anderson, 1989).

Carabidae

The ground-beetle *Amara alpina*, recognized from fossilized and semifossilized peats from the Arctic (Blake and Matthews, 1979), was not found at Hot Weather Creek or at Lake Hazen.

Dytiscidae and Staphylinidae

The two species of predaceous water beetles and two species of rove beetles were quite common at the edges of shallow ponds and in fens. Both the adults and larvae of any or all of these species might be found preserved in peats.

Influence of weather patterns on insect populations

The fact that vegetation is denser and more diverse at Hot Weather Creek than in more barren areas at this latitude (Edlund et al., 1990) and has a correspondingly richer invertebrate fauna is mainly attributable to the prevailing weather patterns on Fosheim Peninsula (Edlund et al., 1990). The ice-capped mountains to the west and east deflect or dissipate low-level clouds coming from the central Arctic Ocean and intercept some of the precipitation. They shield the interior from many cyclonic disturbances. To some extent, the ice and snow on these mountains provide an albedo affect, reflecting some heat and warming the interior.

Precipitation and temperatures measured at nearby coastal Eureka since 1947 have served to classify this region as a ‘cold desert’ (Edlund and Alt, 1989, and references therein). More recent analyses (e.g. Edlund et al., 1990) show that 30 km inland (the site of the Hot Weather Creek station), there is a significantly warmer temperature regimen, translating into a longer growing season, and that available moisture is greater than that accounted for by local precipitation.

During the warmer summers of 1988 and 1989, Edlund et al. (1990) documented increases in available moisture from melting ground ice and ice lenses in the hillsides. This melt caused quite dramatic detachments or soil slumping. Previously dried-up ponds and creeks suddenly had wet spots that developed into expanding puddles without the benefit of any precipitation. In 1990, this phenomenon was repeated, quite dramatically, as huge chunks of the bank fell with resounding crashes into Hot Weather Creek. It is postulated by Edlund et al. (1990) that it is this additional water made available in warmer years that, together with comparatively warmer temperatures and decreased wind speeds, allow this arctic oasis to flourish.

The 1991 growing season began quite differently. In early spring, wind storms had swept most of the snow from the Hot Weather Creek site. Consequently, less snowmelt was available to feed the river and streams and the water level peaked earlier (P. Wolfe, pers. comm., 1991).

The arctic weevil and signs of its presence, which had been so prevalent in 1990, were almost totally absent in 1991 as was *Phigalia*, the tiny parasitic wasp. Lack of snow cover and consequent physical damage due to ice nucleation in the overwintering adults are suggested (*see above*) as reasons for this. (Many dead adult weevils were found early in the season, negating the possibility that the parasite controlled the weevil life cycle.)

Adults of the crane flies *Tipula besselsi* and *Symplecta* sp. were scarcer in 1991 than in 1990, hampering proposed research on their life histories. These larvae live in silty substrates along the banks and shallows of streams and ponds. Those areas had dried up by mid-June in 1990, as the streams shrank and virtually disappeared. Later, puddles appeared in many places, but in the meantime, many of the larvae probably dried up or, equally likely, became more vulnerable to bird predation, especially by the ever-present ruddy turnstones.

The year 1991 was memorable also for the earlier drying up of stream beds, which inconvenienced camp personnel who had to haul water considerable distances. The weather, which had been unseasonably warm, turned colder and brought rain torrents, sleet, and some snow. Initially, rain seeped into the ground through various fissures and cracks. The ground became increasingly sodden and suddenly the streams began to flow. In fact, the waterline in the streams could be seen moving forward rapidly. The first burst of water was cloudy, indicating that organic material was being flushed out of the soil. This was soon followed by clear-running water.

This unexpected increase in water (and loss of nutrients) must have effected many organisms in the soil and water and possibly these effects would not manifest themselves until the following season. However *Gynaephora* larvae, primarily *G. rossi*, were unexpectedly found moving around on the tundra in early August. Some had their hairs matted down by a thick, pink liquid that was apparently released anally (Brodo, unpub. notes, 1991). This was rather late in the season for this species (Kukal, 1990). They may have been prematurely released from diapause by the rain.

Insects as monitors of climate change

Because of their flexible developmental rates, insects have been shown to respond rapidly to fluctuations in climate and so might serve as useful indicators of changes, for example, of global warming (Young, 1994). As it would not be reasonable to attempt to monitor this entire fauna, a few easily recognized and generally common insects might be selected.

Herbivores respond quickly to changes in the nutritional status of host plants. Such changes often result in increased fecundity (Young, 1994), which is measurable and probably more easily monitored than changes in the nutritional status of the host food plants. Herbivores that leave distinctive

marks on the vegetation could be monitored more easily in all life stages. Good choices would be the grass leaf miner fly *Chromatomya puccinelliae*, the *Pedicularis* stem-borer fly *Gonarticus arcticus*, the peripheral stem-borer moth *Olethreutes schultzi*, also on *Pedicularis*, and the arctic weevil *Isochnus arcticus*.

Interannual weather patterns have been shown to affect weevil populations dramatically from year to year (*see above*). Undoubtedly, the survival and fecundity of many other insects are equally affected. It is crucial, therefore, that a long-term monitoring program be established to separate background noise from a possible trend. As in monitoring weather patterns, the continuous monitoring of insect populations over several decades, correlated with meteorological information, will elucidate trends and tell us something of the population dynamics of these insects.

Herbivores are likely to be far more sensitive to climate changes because they are primary consumers and as such are at the bottom of the arthropod food chain. There would be a predicted lag in response by detritivores, scavengers, carrion, and microflora feeders. Microflora feeders live in water or in very moist substrates and so would be buffered somewhat by their substrates.

The three large Tipulidae would be additional good choices for monitoring global change in the High Arctic. The adults are common and collected in all kinds of traps, and all three species can be distinguished on the wing and easily netted. Of the larvae, all but the first instars are readily distinguishable and large enough to handle easily. Larvae of the aquatic species *Tipula (Arctotipula) besselsi* are the most easily collected using Morgan traps. This species has the added advantage of leaving its traces in mud, as mentioned above. Similarly, *Nephrotoma lundbecki* larvae can be trapped, but not as readily, in the soil of moist slopes, but not at the edges of ponds nor under water. The larvae of the equally abundant *Tipula arctica*, however, live in the soil of hummocky tundra and individuals are too widely dispersed in difficult terrain to make collecting feasible.

Young (1994), working with a team on Spitsbergen to develop population models for monitoring global warming, studied the most important herbivore on site, an aphid on *Dryas integrifolia*, and obtained useful results. In contrast, companion studies with Collembola were not as fruitful because these soil-inhabiting arthropods are buffered to some extent by the moist soils they inhabit. Aphids were extremely scarce at Hot Weather Creek, but apparently not at Lake Hazen. The potential array of insects at each site should be evaluated.

Chironomidae are favoured by many researchers for assessing water quality (D. Oliver, pers. comm., 1991) and could be useful for monitoring global change. However, these species are too numerous, they require special preparation before study (slides have to be made), and they are difficult to identify.

CONCLUSIONS

The vicissitudes of the weather from one year to the next are evidence of the unpredictability of the present climate. This variation and the concomitant differential effects it has on the different insect components must be taken into account when assessing possible evidence for global climate change.

Many High Arctic species require several years to complete a generation, as documented above and by Danks (1990). Usually, some individuals of each generation emerge each year except for severely intemperate years. On the other hand, species such as the butterfly *Boloria polaris* emerge only in alternate years. Perhaps other species are similarly synchronized or have an even longer development span, such as the 14 years suggested for *Gynaephora* by Kukal (1990). Most High Arctic species have flexible, extended life cycles and, in poorer seasons, few will emerge. Monitoring must, therefore, be extended over several seasons to establish patterns.

Each research site presents a slightly different facies and the terrain and its dominant inhabitants should influence species selected for environmental monitoring. For Hot Weather Creek, several common herbivores that are easy to identify could be monitored successfully as early detectors of global warming. To complement those studies, it is suggested that the three large crane fly species would be useful because of their abundance, because adults and larvae are easily recognized, and because they represent two other trophic categories. *Tipula besselsi* is a predator, principally on chironomid larvae, and the other two feed on micro-organisms or detritus. The distinctive traces left in the mud by *Tipula besselsi* add to the usefulness of this taxon as a possible indicator species.

ACKNOWLEDGMENTS

My sincere thanks to Dr. Sylvia A. Edlund who invited me to contribute to the study of Hot Weather Creek. I profited from her smoothly run research camp and I thank the many individuals who enriched my stay in this quietly beautiful place. This work was supported by two contracts from the Geological Survey of Canada and a grant from Environment Canada. As all others who have had the privilege of being under the aegis of the Polar Continental Shelf Project, I thank them for the generous logistical support that made all this possible. I also wish to acknowledge the help provided by many of my entomological colleagues who graciously identified Hot Weather Creek specimens, commented on parts of the manuscript, and taught me a lot in the process. Their names are listed elsewhere, but it must be acknowledged here that without their expertise such a study would not have been possible. For helping me sort through the thousands of specimens, I thank Rachel Paley, Elizabeth Robinson, and Andrea Svoboda. Thank you to Irwin Brodo, Hugh Danks, and John Matthews, Jr. for helpful suggestions on earlier drafts of this paper. Lastly, I wish to express my appreciation to the Cartography Section, Geological Survey of Canada, for the superb reproductions of my slides.

REFERENCES

- Anderson, R.S.**
1989: Revision of the subfamily Rhynchaeninae in North America (Coleoptera: Curculionidae); American Entomological Society Transactions, v. 115, p. 207–312.
- Arnett, R.H., Jr.**
1993: American Insects; The Sandhill Crane Press, Inc., Gainesville, Florida, 850 p.
- Bell, T.**
1996: The last glaciation and sea level history of Fosheim Peninsula, Ellesmere Island, Canadian High Arctic; Canadian Journal of Earth Sciences, v. 33, p. 1075–1086.
- Bird, C.D., Hilchie, G.J., Kondla, N.G., Pike, E.M., and Sperling, F.A.H.**
1995: Alberta Butterflies; Provincial Museum of Alberta, Edmonton, Alberta, 347 p.
- Blake, W., Jr. and Matthews, J.V., Jr.**
1979: New data on an interglacial peat deposit near Makinson Inlet, Ellesmere Island, District of Franklin; Geological Survey of Canada, Paper 79-1A, p. 157–164.
- Brandenburg, J.**
1993: To the Top of the World: Adventures with Arctic Wolves; Walker and Co., New York, 44 p.
- Brodo, F.**
1990: Crane flies (Diptera: Tipulidae) of the arctic islands; in Canada's Missing Dimension, Science and History in the Canadian Arctic Islands, Volume II, (ed.) C.R. Harington; Canadian Museum of Nature, Ottawa, Ontario, p. 471–484.
1995: Analysis and additions to the crane fly fauna of Finse, South Norway (Diptera: Tipulidae); Fauna norvegica Series B, v. 42, p. 11–20.
- Chernov, Y.I.**
1985: The Living Tundra; Cambridge University Press, Cambridge, 213 p. (Translated from Russian by D. Löve.)
- Chiasson, H.**
1986: A synopsis of the Thysanoptera (Thrips) of Canada; Lyman Entomological Museum and Research Laboratory, Memoir no. 17, 130 p.
- Corbet, P.S.**
1964: Reproduction in mosquitoes of the high arctic; Proceedings XII International Congress on Entomology, London, p. 817–818.
1967: Facultative autogeny in arctic mosquitoes; Nature, v. 215, no. 5101, p. 662–663.
- Corbet, P.S. and Downe, A.E.R.**
1966: Natural hosts of mosquitoes in northern Ellesmere Island; Arctic, v. 19, no. 2, p. 153–161.
- Cumming, J.M. and Cooper, B.E.**
1993: Techniques for obtaining adult-associated immature stages of predacious tachydromiine flies (Diptera: Empidoidea), with implications for rearing and biocontrol; Entomological News, v. 104, no. 2, p. 93–101.
- Dahl, C.**
1973: Notes on the arthropod fauna of Spitsbergen III. 14. Trichoceridae (Dipt.) of Spitsbergen; Annales Entomologici Fennici, v. 39, no. 2, p. 49–59.
- Danks, H.V.**
1978: Modes of seasonal adaptation in the insects. I. Winter survival; Canadian Entomologist, v. 110, no. 11, p. 1167–1205.
1980: Arthropods of Polar Bear Pass, Bathurst Island, Arctic Canada; Syllogeus, National Museum of Natural Sciences, no. 25, 68 p.
1981: Arctic Arthropods. A Review of Systematics and Ecology with Particular Reference to the North American Fauna; Entomological Society of Canada, Ottawa, Ontario, 608 p.
1986: Insect plant interactions in arctic regions; Revue d'entomologie du Québec, v. 31, no. 1 and 2, p. 52–75.
1987: Insect dormancy: An ecological perspective; Biological Survey of Canada (Terrestrial Arthropods), Ottawa, Ontario, 439 p.
1990: Arctic insects: instructive diversity; in Canada's Missing Dimension, Science and History in the Canadian Arctic Islands, Volume II, (ed.) C.R. Harington; Canadian Museum of Nature, Ottawa, Ontario, p. 444–470.
1994: Regional diversity of insects in North America; American Entomologist, v. 40, no. 1, p. 50–55.

- Danks, H.V., Kukal, O., and Ring, R.A.**
1994: Insect cold-hardiness: insights from the Arctic; *Arctic*, v. 47, no. 4, p. 391–404.
- Debruyn, A.M.H. and Ring, R.A.**
1999: Comparative ecology of two species of *Hydroporus* (Coleoptera: Dytiscidae) in a High Arctic oasis; *Canadian Entomologist*, v. 131, no. 3, p. 405–420.
- Downes, J.A.**
1964: Arctic insects and their environment; *Canadian Entomologist*, v. 96, no. 1/2, p. 279–307.
1966: The Lepidoptera of Greenland; some geographic considerations; *Canadian Entomologist*, v. 98, no. 11, p. 1135–1144.
1970: The feeding and mating behaviour of the specialized Empidinae (Diptera); observations on four species of *Rhamphomyia* in the high arctic and a general discussion; *Canadian Entomologist*, v. 102, no. 7, p. 769–791.
- Edlund, S.A. and Alt, B.T.**
1989: Regional congruence of vegetation and summer climate patterns in the Queen Elizabeth Islands, Northwest Territories, Canada; *Arctic*, v. 42, no. 1, p. 3–23.
- Edlund, S.A., Woo, M.-k., and Young, K.L.**
1990: Climate, hydrology and vegetation patterns: Hot Weather Creek, Ellesmere Island, Arctic Canada; *Nordic Hydrology*, v. 21, p. 273–286.
- Fjellberg, A.**
1985: Arctic Collembola I. Alaskan Collembola of the families Poduridae, Hypogastruridae, Odontellidae, Brachystomellidae and Neanuridae; *Entomologica Scandinavica Supplementum* 21, p. 1–126.
1986: Collembola of the Canadian high arctic. Review and additional records; *Canadian Journal of Zoology*, v. 64, p. 2386–2390.
- Gagné, R.J.**
1975: A revision of the nearctic species of the genus *Phronia* (Diptera: Mycetophilidae); *American Entomological Society Transactions*, v. 101, no. 2, p. 227–318.
- Garneau, M.**
1992: Analyses macrofossiles d'un dépôt de tourbe dans la région de Hot Weather Creek, péninsule Fosheim, île d'Ellesmere, Territoires du Nord-Ouest; *Géographie Physique et Quaternaire*, vol. 46, n° 3, p. 285–294.
- Gibson, G.A.P. and Yoshimoto, C.**
1981: Redescription of *Tetracyclus boreios* (Hymenoptera: Encyrtidae), with a discussion of its placement and structure; *Canadian Entomologist*, v. 113, no. 10, p. 873–881.
- Gill, G.D.**
1962: The heleomyzid flies of America north of Mexico (Diptera: Heleomyzidae); *Proceedings, United States National Museum*, v. 113, no. 3465, p. 495–603.
- Gíslason, G.M.**
1981: Predatory exclusion of *Apatania zonella* (Zett.) by *Potamophylax cingulatus* (Steph.) (Trichoptera: Limnephilidae) in Iceland; *Proceedings of the Third International Symposium on Trichoptera*, v. 20, p. 99–109.
- Gould, J.**
1988: A comparison of avian and mammalian faunas at Lake Hazen, Northwest Territories, in 1961–62 and 1981–82; *The Canadian Field-Naturalist*, v. 102, no. 4, p. 666–670.
- Griffiths, G.C.D.**
1987: Anthomyiidae, Part 2, No. 6, Cyclorrhapha II (Schizophora: Calyptratae); *Flies of the Nearctic Region*, v. 8, Schweizerbart, Stuttgart, p. 794–952.
1991: Anthomyiidae, Part 2, No. 7, Cyclorrhapha II (Schizophora: Calyptratae); *Flies of the Nearctic Region*, v. 8, Schweizerbart, Stuttgart, p. 953–1048.
- Hemmingsen, A.M. and Jensen, B.**
1957: The occurrence of *Tipula (Vestiplex) arctica* Curtis in Greenland and its decreasing body length with increasing latitude; *Meddelelser om Grønland*, v. 159, no. 1, p. 1–20.
- Hippa, H. and Vilkamaa, P.**
1994: The genus *Camptochaeta* gen. n. (Diptera, Sciaridae); *Acta Zoologica Fennica*, no. 194, 85 p.
- Hutson, A.M., Ackland, D.M., and Kidd, L.N.**
1980: Mycetophilidae (Bolitophilinae, Ditomyiinae, Diadocidiinae, Keroplatinae, Sciophilinae and Manotinae) Diptera, Nematocera; *Handbooks for the Identification of British Insects*, Royal Entomological Society of London, v. IX, no. 3, 111 p.
- Kevan, P.G. and Shorthouse, J.D.**
1970: Behavioural thermoregulation by high arctic butterflies; *Arctic*, v. 23, no. 4, p. 268–279.
- Kevan, P.G., Jensen, T.S., and Shorthouse, J.D.**
1982: Body temperatures and behavioral thermoregulation of high arctic woolly-bear caterpillars and pupae (*Gynaephora rossii*, Lymantriidae: Lepidoptera) and the importance of sunshine; *Arctic Alpine Research*, v. 14, p. 125–136.
- Klassen, P., Westwood, A.R., Preston, W.B., and McKillop, W.B.**
1989: The Butterflies of Manitoba; *Manitoba Museum of Man and Nature*, Winnipeg, Manitoba, 290 p.
- Kukal, O.**
1990: Energy budget for activity and growth of a high arctic insect, *Gynaephora groenlandica* (Wocke) (Lepidoptera: Lymantriidae); in *Canada's Missing Dimension, Science and History in the Canadian Arctic Islands Volume II*, (ed.) C.R. Harington; *Canadian Museum of Nature*, Ottawa, Ontario, p. 485–510.
- Kukal, O. and Kevan, P.G.**
1987: The influence of parasitism on the life history of a high arctic insect, *Gynaephora groenlandica* (Wöcke) (Lepidoptera: Lymantriidae); *Canadian Journal of Zoology*, v. 65, no. 1, p. 156–163.
- Kukal, O., Heinrich, B., and Duman, J.G.**
1988: Behavioral thermoregulation in the freeze-tolerant arctic caterpillar, *Gynaephora groenlandica*; *Journal of Experimental Biology*, v. 138, p. 181–193.
- Lantsov, V.I.**
1984: Ecology, morphology and taxonomy of arctic crane-flies of the genus *Prionocera* (Diptera: Tipulidae); *Zoologicheskii Zhurnal*, v. 43, no. 8, p. 1196–1204 (in Russian).
- Lantsov, V.I. and Chernov, Y.I.**
1987: Tipulid craneflies in the tundra zone; *Moscow*, 175 p. (in Russian).
- Leech, R.E.**
1966: The Spiders (Araneida) of Hazen Camp 81°49'N, 71°18'W; *Quaestiones Entomologicae*, v. 2, p. 153–212.
- MacKay, M.R. and Downes, J.A.**
1969: Arctic Olethreutinae (Lepidoptera: Tortricidae); *Canadian Entomologist*, v. 101, no. 10, p. 1048–1053.
- MacLean, S.F., Jr.**
1975: Ecology of tundra invertebrates at Prudhoe Bay, Alaska; in *Ecological Investigations of the Tundra Biome in the Prudhoe Bay Region, Alaska*, (ed.) J. Brown; *Biological papers of the University of Alaska, Special Report* 2, p. 115–123.
- Makarova O.L.**
1995: On the association of gamasid mites of the genus *Arctoseius* (Mesostigmata, Ascidae) with winter crane flies (Diptera, Trichoceridae) in the Northern Taimyr Peninsula; *Arctic Insect News*, v. 6, p. 2–4.
- Mathis, W.N.**
1979: Studies of Ephydrinae (Diptera: Ephydriidae), II: Phylogeny and Classification, and Zoogeography of Nearctic *Lamproscatella* Hendel; *Smithsonian Contributions to Zoology* no. 295, p. 1–41.
- McAlpine, J.F.**
1964: Arthropods of the bleakest barren lands: composition and distribution of the arthropod fauna of the northwestern Queen Elizabeth Islands; *Canadian Entomologist*, v. 96, no. 1/2, p. 127–129.
1965a: Insects and related terrestrial invertebrates of Ellef Ringnes Island; *Arctic*, v. 18, no. 2, p. 73–103.
1965b: Observations on anthophilous diptera at Lake Hazen, Ellesmere Island; *The Canadian Field-Naturalist*, v. 79, no. 4, p. 247–252.
1977: A revised classification of the Piophilidae, including 'Neottiophilidae' and 'Thyreophoridae' (Diptera: Schizophora); *Memoirs of the Entomological Society of Canada*, no. 103, 66 p.
- Milliron, H.E. and Oliver, D.R.**
1966: Bumblebees from northern Ellesmere Island with observations on usurpation by *Megabombus hyperboreus* (Schönh.) (Hymenoptera: Apidae); *Canadian Entomologist*, v. 98, no. 2, p. 207–213.
- Oliver, D.R.**
1963: Entomological studies in the Lake Hazen area, Ellesmere Island, including lists of species of Arachnida, Collembola, and Insecta; *Arctic*, v. 16, no. 3, p. 175–180.
- Oliver, D.R. and Corbet, P.S.**
1966: Aquatic habitats in a high arctic locality: the Hazen Camp study area, Ellesmere Island, N.W.T.; *Defence Research Board Canada, Directorate of Physical Research (Geophysics)*, Hazen 26, 115 p.

Oliver, D.R. and Roussel, M.E.

1983: The genera of larval midges of Canada (Diptera: Chironomidae). The insects and arachnids of Canada, Part 11; Agriculture Canada Publication 1746, 263 p.

Richards, K.W.

1973: Biology of *Bombus polaris* Curtis and *B. hyperboreus* Schönherr at Lake Hazen, Northwest Territories (Hymenoptera: Bombini); *Questiones Entomologicae*, v. 9, no. 2, p. 115–157.

Richards, W.R.

1963: The Aphididae of the Canadian arctic (Homoptera); *Canadian Entomologist*, v. 95, no. 5, p. 449–464.

1964a: A new arctic aphid (Homoptera: Aphididae); *Canadian Entomologist*, v. 96, no. 11, p. 1027–1029.

1964b: The scale insects of the Canadian arctic (Homoptera: Coccoidea); *Canadian Entomologist*, v. 96, no. 11, p. 1457–1462.

Ryan, J.K.

1977: Appendix 7. Invertebrates of Truelove Lowland; in *Truelove Lowland, Devon Island, Canada: A High Arctic Ecosystem*, (ed.) L.C. Bliss; University of Alberta Press, Edmonton, Alberta, p. 699–703.

Sabrosky, C.W., Bennett, G.F., and Whitworth, T.L.

1989: Bird Blow Flies (Protocalliphora) in North America; Smithsonian Institution Press, Washington, D.C., 299 p.

Savchenko, E.N., Oosterbroek, P., and Stary, J.

1992: Family Limoniidae; in *Catalogue of Palaearctic Diptera, Volume 1*, (ed.) Á. Soós, L. Papp, and P. Oosterbroek; Hungarian Natural History Museum, p. 183–369.

Schauff, M.E.

1984: The holarctic genera of Mymaridae (Hymenoptera: Chalcidoidea); *Memoirs of the Entomological Society of Washington*, no. 12, 65 p.

Scudder, G.G.E.

1979: Present patterns in the fauna and flora of Canada; in *Canada and its Insect Fauna*, (ed.) H.V. Danks; *Memoirs of the Entomological Society of Canada*, v. 108, p. 87–179.

Spencer, K.A.

1969: The Agromyzidae of Canada and Alaska; *Memoirs of the Entomological Society of Canada*, v. 64, 311 p.

Vockeroth, J.R.

1987: Scathophagidae; in *Manual of Nearctic Diptera, Volume 2*, (ed.) J.F. McAlpine; Agriculture Canada, Monograph no. 28, p. 1085–1097.

1990: Revision of the nearctic species of *Platycheirus* (Diptera, Syrphidae); *Canadian Entomologist*, v. 122, no. 7/8, p. 659–766.

Vockeroth, J.R. and Thompson, F.C.

1987: Syrphidae; in *Manual of Nearctic Diptera, Volume 2*, (ed.) J.F. McAlpine; Agriculture Canada, Monograph no. 28, p. 713–743.

Waltz, R.D. and McCafferty, W.P.

1979: Freshwater springtails (Hexapoda: Collembola) of North America; *Research Bulletin 960*, Purdue University Agricultural Experiment Station, West Lafayette, Indiana, 32 p.

Wiggins, G.B.

1977: Larvae of the North American Caddisfly Genera (Trichoptera); University of Toronto Press, 401 p.

Wipking, W. and Mengelkoch, C.

1994: Control of alternate-year flight activities in high-alpine Ringlet butterflies (*Erebia*, Satyridae) and Burnet moths (*Zygaena*, Zygaenidae) from temperate environments; in *Insect Life-Cycle Polymorphism: Theory, Evolution and Ecological Consequences for Seasonality and Diapause Control*, (ed.) H.V. Danks; Kluwer Academic Publishers, p. 313–347.

Wood, D.M., Dang, P.T., and Ellis, R.A.

1979: The mosquitoes of Canada (Diptera: Culicidae). The insects and arachnids of Canada, Part 6; Agriculture Canada Publication 1686, 390 p.

Young, S.

1994: Insects that carry a global warning; *New Scientist*, v. 142, no. 1923, p. 32–35.

APPENDIX A.

ANNOTATED LIST OF SPECIES COLLECTED AT HOT WEATHER CREEK, ELLESMERE ISLAND, NUNAVUT

F. Brodo

Species, or higher categories, designated with an asterisk (*) are new records for the High Arctic, roughly north of latitude 74°N, and are changes to the list presented in Danks (1981). The classification here is also based on that reference, with changes where noted. The full scientific name of each species is followed by its known distribution in several other important localities indicated on Figure 1. These are designated here by the following: [LH] = Lake Hazen, Ellesmere Island; [ER] = Ellef Ringnes Island; [TL] = Truelove Lowland, Devon Island; [PB] = Polar Bear Pass, Bathurst Island. In addition, North American distributions are designated by [Hi] = only known from the High Arctic, [S] = extends south of treeline, and [A] = broad arctic distribution north of treeline. [G] = occurs on Greenland and [P] = known from the Palearctic Region. This information is followed by notes on feeding behaviour or other relevant information on the species in question.

Voucher specimens will be deposited in the Canadian National Collection of Insects, Agriculture and Agri-Food Canada, unless otherwise indicated.

Order ARANEAE (spiders)¹

All spiders are predators. Leech (1966) provides information on prey.

Dictynidae

Dictyna borealis Pickard-Cambridge; [LH,TL;A;G]; feed on small flies such as Chironomidae and Ceratopogonidae.

Linyphiidae (sheet-web spiders)

Meioneta maritima (Emerton); [LH;A]; feed on Collembola, Acari.

Erigonidae

Erigone psychrophila Thorell; [LH,ER,TL,PB;A;G,P].

Hilaira vexatrix (Pickard-Cambridge); [LH,TL;A]; cannibalistic.

Minyriolus pampia Chamberlin; [LH,TL;A;G].

Savignya barbata (Koch) (= *Diplocephalus barbatus*); [LH,TL,PB;A;G,P].

Walckenaeria clavicornis (Emerton) (= *Cornicularia karpinskii* (P.-C.)); [LH;S;G,P].

Lycosidae (wolf spiders)

Alopecosa exasperans (Pickard-Cambridge) (= *Tarentula exasperans*); [LH,TL;A;G]; small flies, Collembola.

Pardosa glacialis (Thorell); [LH;A;G]; Chironomidae and other small flies, cannibalistic.

Subclass ACARI (mites)²

Trophic information supplied by Dr. V. Behan-Pelletier (Oribatei), Dr. E. Lindquist and Dr. I. Smith (Mesostigmata, Prostigmata, and Acaridiae) unless otherwise indicated; remarks concerning where or how collected are from F. Brodo (unpub. notes, 1990 and 1991).

Suborder MESOSTIGMATA

Parasitidae

Most are predators of microarthropods in soil, litter, and organic substrates; deutonymphs are phoretic on bumblebees.

**Gamasodes* near *bispinosus* (Halbert); [A;P].

**Parasitus favus* Richards; [A]; ex *Bombus polaris*.

**Parasitus perthecatus* Richards; [A]; ex *Bombus polaris*.

Ascidae

Most are predators of nematodes and vermiform microarthropods, e.g. diptera larvae. Adult ♀♀ of *Arctoseius* spp. are phoretic on adult Trichoceridae (Makarova, 1995).

Arctoseius idiodactylus Lindquist; [A;P]; ex soil.

Arctoseius weberi Evans; [PB;A;P]; ex soil.

**Arctoseius* n. sp. 1, near *weberi* Evans; [PB]; ex soil.

**Arctoseius* n. sp. 2; [PB]; ex soil on plateau.

Arctoseius sp.; ex soil.

Cheiroseius sp.; ex soil on plateau.

**Proctolaelaps parvanalis* (Thor); [A;P]; ex yellow bowl.

Phytoseiidae

Most are predators of microarthropods.

**Amblyseius* near *cree* Chant & Hansell; ex yellow bowl.

**Amblyseius* near *tibielingmiut* Chant & Hansell.

Laelapidae

**Pneumolaelaps* sp. near *fuscicolens* (Ouds.); ex *Bombus polaris*; pollen feeders, nest associates of *Bombus*.

Haemogamasidae

Haemogamasus ambulans (Thorell) (as *H. alaskensis*); [ER,TL,PB;S;P]; ex soil; facultative ectoparasite and nest associate of lemmings.

Suborder PROSTIGMATA

Alicorhagiidae

Presumed to be saprophagous (Danks, 1981).

Alicorhagia sp.; ex base of *Dryas-Salix* hummocks.

**Alicorhagidia* sp.

Nanorchestidae

Nanorchestes sp.; ex litter around *Dryas-Salix* hummocks; probably algal feeder.

Eupodidae

Mostly fungivores.

**Cocceupodes breweri* Strandtmann; [A;P]; ex leaf and soil litter.

Cocceupodes ?curviclava Thor; ex soil.

Eupodes alaskanensis Strandtman; [A]; ex soil; eats various cryptogams.

Eupodes sp.; ex yellow bowl; eats various cryptogams.

Penthaleidae

Obligate plant feeders, including algae and mosses.

Penthaleus sp. (not *P. major*); ex yellow bowl; probably feeds on algae, mosses.

Tydeidae

Tydeus sp.; [ER]; ex *Dryas-Salix* hummocks, yellow bowl; probably fungivorous.

Bdellidae

Cyta latirostris (Hermann); ex soil, yellow bowl; [S;G,P]; preys on small arthropods and arthropod eggs.

Stigmaeidae

Cheyllostigmaeus ?torulus Summers; pitfall edge of Oxbow Lake; possibly predators of microarthropods.

Tetranychidae

Obligate plant feeders.

Bryobia sp.; ex yellow bowl, *Lesquerella arctica* (Wormskj.) S. Wats., soil around *Elymus alakanus*, pitfall trap at Oxbow Lake; collected on and probably feeds on *Lesquerella arctica* (Brodo, unpub. notes, 1990).

Petrobia latens (Muller); [S;P]; ex yellow bowl, pitfall trap at Oxbow Lake; probably feeds on grasses (Danks, 1981).

Eriophyidae

**Aculops tetanothrix* (Nalepa); [A;P]; gall maker and leaf-sap feeder; collected on *Salix arctica*.

Trombidiidae

Larvae are parasitic on insects; nymphs and adults are predatory on microarthropods.

**Valgothrombium* sp.; ex pitfall at Oxbow Lake.

Sperchontidae

**Sperchon* sp.; larvae are parasites, nymphs and adults are predators of chironomid larvae.

Lebertiidae

Lebertia sp.; [LH,TL]; ex yellow bowl; larvae are parasites, nymphs and adults are predators of chironomid larvae.

Suborder ACARIDIAE**Acaridae**

Hypopodial nymph phoretic on insects; other instars feed on fungi or scavenge.

**Kuzinia* sp.; [TL]; ex *Bombus polaris* and on *Lesquerella arctica*, yellow bowl.

Suborder ORIBATEI**Hypochthoniidae**

**Hypochthonius rufulus* C.L. Koch; [A;P]; fungi and algae feeder.

Brachychthoniidae

**Liochthonius forsslundi* (Hammer); [A;P]; *Dryas-Salix* hummocks; fungivorous.

Liochthonius sellnicki (Thor) (as *L. scalaris*); [ER,TL,PB;A;G,P]; fungal feeder.

***Trhypochthoniidae**

**Trhypochthoniellus setosus canadensis* Hammer; [S;G,P]; probably fungi and algae feeder.

Hermanniidae

Hermannia reticulata Thorell; [TL;S;P]; feeder on dead plant material and fungi.

**Hermannia scabra* (L. Koch); [A;G,P]; feeder on dead plant material and fungi.

Eremaeidae

Eueremaus foveolatus (Hammer); [A]; feeder on fungi and pollen.

Tectocephidae

Tectocephus velatus (Michael); [PB;S;G,P]; fungal feeder.

Oppiidae

Oppiella clavigera (Hammer) (= *Oppia clavigera*); [A;G,P]; fungal feeder.

Oribatulidae

**Oribatula* sp.; feeder on dead plant material and fungi.

Ceratozetidae

Species listed below are feeders on algae, fungi, dead plant material, and pollen.

Diapterobates notatus Thorell?; [TL;A;G,P].

Iugoribates gracilis Sellnick; [TL,PB;A;G].

Trichoribates polaris Hammer; [TL,PB;A;G].

Order COLLEMBOLA (springtails)

Probably fungal hyphae feeders (Danks, 1980).

Onychiuridae

Onychiurus sp.

Isotomidae

Isotoma sp. 1

Isotoma sp. 2

Isotomurus palustris (Müller); [LH,TL,PB;S;G,P].

Entomobryidae

Entomobrya comparata Folsom; [TL;A]; pollen feeder (Danks, 1981).

Poduridae

Podura aquatica (L.); [LH,TL,PB;S;G,P]; characteristic species in wet habitats with some open water, Fjellberg (1985).

Sminthuridae

Sminthurides sp. (possibly *aquaticus* (Bourlet); [LH,TL].

Class INSECTA**Suborder ANOPLURA (sucking lice)****Hoplopleuridae**

Hoplopleura acanthopus (Burmeister); [ER,PB;S;P]; parasitic on collared lemming (Danks, 1980; Brodo, unpub. notes, 1990).

Order HOMOPTERA³**Aphididae** (plant lice)

?*Brevicoryne arctica* Richards; [LH;Hi]; yellow bowl; probably lives on *Lesquerella arctica* (Richards, 1963).

Pseudococcidae (mealy bugs)

Chorizococcus altoarcticus (Richards) (= *Pseudococcus altoarcticus*); [LH,TL;Hi]; yellow bowl; lives on *Dryas integrifolia* (Richards, 1964b).

Order THYSANOPTERA (thrips)**Thripidae**

Immatures only; yellow bowl; probably lives on grasses (Chiasson, 1986).

Order COLEOPTERA (beetles)**Dytiscidae** (diving water beetles)⁴

Larvae are predators on aquatic small invertebrates (Arnett, 1993).

Hydroporus lapponum (Gyllenhal); [A;P].

Hydroporus polaris Fall; [LH;A].

Staphylinidae (rove beetles)⁵

These species may be associated with decaying matter (Danks, 1981).

Gnypeta sp. 1 (as *Atheta*); [LH,TL;A]; species being monographed by Ashe.

Gnypeta sp. 2; species being monographed by Ashe.

Curculionidae (weevils)⁶

Isochnus arcticus (Korotyaev) (as *Rhynchaenus* sp.); [LH;Hi;P]; on *Salix arctica*.

Order TRICHOPTERA (caddisflies)**Limnephilidae**

Apantania zonella Zetterstedt⁷; [LH,TL;A;G,P]; diatoms (Gíslason, 1981).

Order DIPTERA (true flies)**Tipulidae** (crane flies)

Nephrotoma lundbecki (Nielsen) (= *N. arctica*); [LH,TL;A;G,P]; probably detritus (Brodo, 1990).

Tipula (Arctotipula) besselsi Osten Sacken; [A;G,P]; larvae are predators on chironomid larvae (Lantsov and Chernov, 1987).

Tipula (Vestiplex) arctica Curtis; [LH,TL;A;G,P]; probably detritus feeders (Brodo, 1990).

Limoniidae (crane flies)⁸

Dactylolabis rhinoptiloides Alexander; [LH;A]; probably detritus feeders (Brodo, 1990).

Symplecta sp. (= *Erioptera (Symplecta)* sp.); probably detritus (Brodo, 1990).

Trichoceridae (winter crane flies)

Larvae live in the microflora associated with mammals and birds (Dahl, 1973).

Trichocera borealis Lackschewitz; [LH,ER,PB;A;G,P].

Trichocera columbiana Alexander; [ER,PB;S].

Culicidae (mosquitoes)

Larvae feed on detritus, algae, other microorganisms (Wood et al., 1979).

Aedes impiger (Walker); [LH,TL;S;G,P].

Aedes nigripes (Zetterstedt); [LH,TL,PB;A;G,P].

Ceratopogonidae (biting midges)⁹

Ceratopogon sp. 1; [LH]

Ceratopogon sp. 2; [LH]

Culicoides sp.; [LH]

**Forcipomyia (Thyridomyia) monilicornis* (Coquillett); [A]; larvae probably in soil, eating mycelia (J.A. Downes, pers. comm., 1992).

Chironomidae (midges)¹⁰

Chironominae

Most larvae feed on small plants, animals and detritus (Oliver and Roussel, 1983).

**Chironomus (Chaetolabis)* n. sp.; [A].

Chironomus (Chironomus) sp.

Stictochironomus cfr. unguiculatus (Malloch)

Diamesinae

Most larvae feed on algae, primarily diatoms (Oliver and Roussel, 1983).

Diamesa geminata Kieffer; [TL;A;G,P].

Diamesa sp.

Pseudokiefferiella sp.

Orthocladiinae

Most larvae feed on micro organisms and detritus (Oliver and Roussel, 1983).

Chaetocladius sp.

Corynoneura sp.

Cricotopus sp.

Diplocladius cultriger Kieffer; [LH,ER,TL;S;P].

Limnophyes sp.

Orthocladius (Orthocladius) spp.

Orthocladius (Eudactylocladius) spp.

Smittia sp.; adults imbibe nectar from *saxifraga oppositifolia* and *salix arctica* (McAlpine, 1965b)

**Tokunagaia sp.*

Tanypodinae

Larvae are predators on other chironomid larvae (Danks, 1980).

**Arctopelopia sp.*

Procladius (Holotanypus) cfr. culiciformis (Linn.)

Mycetophilidae (fungus gnats)¹¹

Most larvae in this family are fungal feeders (J.R. Vockeroth, pers. comm., 1992).

Boletina sp.; larvae may feed on liverworts or mosses (Hutson et al., 1980).

Bolitophila sp.; [LH]; the most common fungus gnat (Brodo, unpub. notes, 1990 and 1991).

Exechia frigida (Boheman); [LH,PB;A;G,P].

Exechia sp.; [LH].

Mycomya ultima Väisänen

Phronia egregia Dziedzicki¹²; [A;P].

Phronia portschinskyi Dziedzicki; [S;P].

Phronia taczanowskyi Dziedzicki; [S;P].

Sciaridae (fungus gnats)¹³

Larvae are fungal feeders, primarily in the soil.

Bradysia sp.

**Camptochaeta cladiator* Hippa and Vilkamaa; [Hi;G,P].

**Camptochaeta consimilis* (Holmgren); [Hi;P].

**Camptochaeta delicata* (Legersdorf); [Hi;G,P].

**Camptochaeta quadriceps* Hippa and Vilkamaa; [Hi].

Corynoptera sp.

Scatopsciara sp.; [LH].

**Sciara sp.*; [LH].

**Trichosia sp.*

Cecidomyiidae (gall midges)

Micromyini: sp. 1; larvae probably feed on fungi and detritus (Arnett, 1993).

Cecidomyiidi: sp. 1; larvae probably feed on fungi and detritus (Arnett, 1993).

Empididae (empidid or dance flies)

Adults feed on smaller flies, especially chironomids and culicids (Downes, 1970); larvae feed on small arthropods, particularly fly larvae (Cumming and Cooper, 1993).

Rhamphomyia filicauda Henriksen and Lundbeck; [LH;A;G].

Rhamphomyia hoeli Frey; [LH,TL;Hi;G].

Rhamphomyia nigrita Zetterstedt; [LH,TL;A;G,P].

Rhamphomyia ursinella Melander; [LH;A].

Dolichopodidae (long-legged flies)

Both adults and larvae feed on smaller arthropods (Arnett, 1993).

Dolichopus dasyops Malloch; [LH;A].

Dolichopus humilus Van Duzee; [LH,TL;A;G].

Phoridae

Megaselia (Megaselia) sp.; [LH]; larvae are probably on carrion or fungi (Arnett, 1993).

Syrphidae (flower flies)¹¹

Adults feed on pollen and nectar of various flowers (McAlpine 1965b; Vockeroth and Thompson, 1987).
Helophilus borealis Staeger; [LH;A;G,P]; larvae in wet detritus (Vockeroth and Thompson, 1987).

Parasyrphus tarsatus (Zetterstedt) (= *Melangyna tarsata* (Zett.)); [A;P]; larvae probably predacious on soft arthropods (J.R. Vockeroth, pers. comm., 1992).

Platycheirus carinatus (Curran), new combination, Vockeroth, 1990; (= *Carposcalis carinatus*); [LH;A]; larvae probably predacious on soft arthropods (J.R. Vockeroth, pers. comm., 1992).

Piophilidae (piophilid flies)¹⁴

Larvae are scavengers on decaying proteinaceous animal and vegetable matter (McAlpine, 1977).

Arctopiophila arctica (Holmgren) (as *Allopiophila arctica*); [LH,ER,TL,PB;A;P]; adults imbibe nectar from *Dryas integrifolia* (McAlpine, 1965b).

Lasiopiophila pilosa (Staeger); [LH;A;G]; adults imbibe nectar from *Dryas integrifolia* (McAlpine, 1965b).

Parapiophila fulviceps (Holmgren); [TL;A;P].

Agromyzidae¹⁴

Chromatomyia erigerontophaga (Spencer); [A;G]; larvae form linear mines in *Erigeron* (Spencer, 1969).

Chromatomyia puccinelliae (Spencer) (= *Phytomyza puccinelliae*); [A;G]; reared from the following grasses *Elymus alakanus*, *Arctagrostis latifolia*, *Dupontia fisheri*, *Alopecurus alpinus* (Brodo, unpub. notes, 1991).

Phytomyza parvicella (Coquillett); [A;G]; leaf miner on poppy (Spencer, 1969).

Heleomyzidae

Aecothea specus (Aldrich); [TL;S]; larvae in carrion, dung (Gill, 1962).

Ephydriidae

Lamproscatella brunnipennis (Malloch); [A;G,P]; a salt-tolerant species, usually collected at coastal localities (Mathis, 1979).

***Tethinidae**¹¹

**Pelomyiella mallochi* (Sturtevant); [S;G,P].

Scathophagidae¹¹

Probably all adults in this family are predacious on other insects.

Allomyella unguiculata (Malloch); [TL;A]; larvae in wet soil, probably predacious (Vockeroth, 1987).

Gonarcticus arcticus (Becker); [LH;A;G]; larvae mine in stems of *Pedicularis* (Brodo, unpub. notes, 1990); adults probably predacious on other insects.

Scathophaga apicalis Curtis; [LH,TL;A;G,P]; larval habits unknown (J.R. Vockeroth, pers. comm., 1992).

Scathophaga multisetosa Holmgren; [LH;A;P]; larval habits unknown (J.R. Vockeroth, pers. comm., 1992).

Scathophaga nigripalpis Beck; [LH,TL;A;G]; larval habits unknown (J.R. Vockeroth, pers. comm., 1992); adults feed on pollen of *Dryas integrifolia* (McAlpine, 1965b).

Anthomyiidae¹¹

Delia polaris Griffiths (= *Delia fasciventris* (Ringdahl)); [LH,TL;A]; host plants probably *Melandrium* spp. (Griffiths, 1991).

Eutrichota tunicata (Zetterstedt) (= *Pegomya tunicata*); [LH;A;G,P]; larvae in detritus (Danks, 1980); adults are nectar feeders on *Dryas integrifolia* (McAlpine, 1965b).

Fucellia pictipennis Becker; [LH,ER,TL,PB;A;G,P]; larvae in detritus (Danks, 1980); adults are nectar feeders on *Dryas integrifolia* (McAlpine, 1965b).

Fucellia vibei Collin; [A]; larvae in detritus (Danks, 1980).

Paradelia arctica (Ringdahl) (= *Pegomya intersepta arctica* Hockett); [LH;A;G,P]; (Griffiths, 1987).

Muscidae¹⁵

Larvae in the genus *Spilogona* are predators on Chironomidae (Danks, 1980).

Drymeia groenlandica (Lundbeck) (= *Eupogonomyia groenlandica*); [LH;A;G].

Drymeia segnis (Holmgren) (= *Pogonomyoides segnis*); [LH,ER,PB;A;G,P]; pollen feeder (Danks, 1981).

Spilogona almquistii (Holmgren); [LH,TL,PB;A;G,P].

Spilogona deflorata (Holmgren); [LH,TL;A;P].

Spilogona denudata Holmgren; [LH;A;P].

Spilogona dorsata (Zetterstedt); [LH,TL,PB;A;G,P].

Spilogona extensa (Malloch); [LH,PB;A;G].

Spilogona latilamina (Collin); [LH,PB;A;G].

Spilogona melanosoma (Hockett); [TL,PB;A;G]; larvae in wet areas (McAlpine, 1965a).

“*Spilogona micans* (Ringdahl)” (not the same as *S. micans* (Ringdahl) in Europe, Danks, 1981; [PB;A].

Spilogona monocantha Collin; [LH;A;G].

Spilogona obsolata (Malloch); [LH,ER,TL,PB;A;G]; larvae in wet areas (McAlpine, 1965a).

Spilogona sanctipauli (Malloch); [LH,ER,PB;A;G,P].

Spilogona tornensis (Ringdahl); [LH;A;G,P]
Spilogona tundrae (Schnabl); [LH,TL,PB;A;G,P].

Calliphoridae (blow flies)¹⁶

Larvae in carrion and dung (Arnett, 1993).

Boreëllus atriceps (Zetterstedt); [LH,ER,TL,PB;A;G,P]; larvae in carrion, especially dead lemmings (McAlpine, 1965a; Brodo, unpub. notes, 1990); adults are nectar feeders on *Potentilla* (McAlpine 1965b).

Protophormia terraenovae (Robineau-Desvoidy); [LH,TL;S;G,P]; can cause subcutaneous myiasis in caribou but generally breed in carrion (Danks, 1981); adults may eat *Salix arctica* pollen (McAlpine 1965b).

Tachinidae¹⁷

Chetogena gelida (Coquillett); [TL;A;P]; larvae parasitic on larvae of *Gynaephora*, probably *rossii* (D.M. Wood, pers. comm., 1991); reared from *Gynaephora* sp. pupa (Brodo, unpub. notes, 1990); adults are pollen feeders (McAlpine 1965b).

Exorista n. sp.; [LH;Hi;P]; coincident with and probably parasitic on larvae of *Gynaephora groenlandica* (D.M. Wood, pers. comm., 1991).

Peleteria aenea (Staeger) (= *Peleteriopsis aenea*); [LH;A;G]; probably parasitic on noctuids (D.M. Wood, pers. comm., 1991).

Periscepsia stylata (B. & B.) (= *Petinarctia stylata* (B. & B.)); [A;G].

Trafoia arctica (Sack) (= *Tenuirostra arctica* (Sack)); [A;G,P]; probably parasitic on the geometrid *Psychophora sabini* (D.M. Wood, pers. comm., 1991).

Order LEPIDOPTERA (butterflies and moths)¹⁸

Tortricidae (tortricid moths)¹⁹

Olethreutes mengelana (Fernald); [LH,TL;A;G]; webs among leaves of *Dryas integrifolia*, MacKay and Downes, 1969).

Olethreutes schulziana (Fabricius) (= *O. inquietana* Walker, MacKay and Downes, 1969); [LH,TL;A;G,P]; a stem-borer in several species of *Pedicularis*, common at Hot Weather Creek.

Pieridae (butterflies: whites and sulphurs)

Colias hecla Lefebvre; [LH;A;G,P]; the larval plant *Astragalus* in Manitoba (Klassen et al., 1989) does not occur at Hot Weather Creek, possibly the larvae feed on *Pedicularis* species.

Lycaenidae (gossamer-winged butterflies)

Agriades glandon (de Prunner) (= *Agriades franklinii* (Curtis), *Lycaena aquilo*, *Plebeius aquilo*); [LH;S;G,P]; larvae may feed on *Saxifraga oppositifolia* (Bird et al., 1995).

Lycaena phlaeas Linnaeus (copper butterfly) (= *L. feildenii* McLach., *Rumicia phlaeas* (L.)); [LH;S;G,P]; *Oxyria digyna* is the reported food plant (Bird et al., 1995).

Nymphalidae (brush-footed butterflies)

Boloria chariclea (Schneider) (= *Clossiana chariclea*); [LH,TL;A;G,P]; on *Dryas integrifolia* and *Salix arctica* (Brodo, unpub. notes, 1990 and 1991).

Boloria polaris (Boisduval); [LH,TL;S;G,P]; larvae probably on *Dryas integrifolia* and *Salix arctica*.

Geometridae (inch worms)²⁰

Entephria polata (Duponchel) (= *Dasyuris polata*); [LH,TL;S;G,P].

[*Psychophora sabini* Kirby]; [LH,ER,TL,PB;S;G,P]; presumed to be parasitized by the fly *Trafoia arctica*, but not collected at Hot Weather Creek.

Lymantriidae

Gynaephora groenlandica (Wocke) (= *Byrdia groenlandica*); [LH,TL;A;G]; larvae on *Salix arctica* and blossoms of *Dryas integrifolia* (Kukal, 1990; Brodo, unpub. notes, 1990 and 1991).

Gynaephora rossi (Curtis); [TL;A;P]; larvae fed on *Salix arctica* and blossoms of *Dryas integrifolia* (Brodo, unpub. notes, 1991).

Noctuidae (noctuid moths)²¹

Apamea zeta (Treitske) (= *Crymodes exulis* (Duponchel)); [LH;A;G,P]; larvae on *Salix*, *Kobresia*, and grasses.

Lasionycta leucocycla (Staudinger) (= *Lasiestra leucocycla*); [LH,TL;A;G]; larvae on *Salix*, *Kobresia*, *Dryas*, and *Saxifraga*.

Polia richardsoni (Curtis) (= *Anarta richardsoni*); [LH,TL;A;G,P]; larvae on *Salix* and *Saxifraga*.

Sympistris zetterstedti (Staudinger); [LH,TL;A;G,P].

Syngrapha parilis (Hübner); [LH;A;G,P].

Order HYMENOPTERA (bees, wasps)

Tenthredinidae²²

Pontoprastia sp. 1 (= *Amauronematus amentorum* (Förster; = *Nematus* sp.); [LH;S;P].

Pontoprastia sp. 2

Pontoprastia sp. 3

Braconidae

Rogas n. sp.; [LH,TL]; reared from *Gynaephora groenlandica* (Brodo, unpub. notes, 1990).

Ichneumonidae²³

All are parasites, parasitoids or hyperparasites of other arthropods.

Atractodes spp.; [LH,TL,PB]; cyclorrhaphus dipteran cocoons.

**Bathythrix longiceps*

**Calypta arctica* Dasch

Campoletis n. spp.; [TL]; immature noctuid larvae.

Cryptus arcticus Sch.; [LH;A;G]; lepidoptera larvae.

**Dacnusa* sp.

Diplazon sp.; [LH].

Exochus pullatus Townes; [LH;A]; lepidoptera larvae.

**Glypta arctica* Dasch.

Hemitelini; spider egg sacs.

Hyposoter n. sp. near *luctus* Davis; [TL]; lepidoptera larvae.

**Ichneumon byrdiae* (Heinrich) (= *Pterocormus byrdiae*); [A].

Ichneumon lariae Curtis (= *Pterocormus lariae*); [LH,TL;A;G]; lepidoptera larvae.

Ichneumon sp.; [TL,PB].

Lissonota fuscipilis Townes; [A]; on lepidopteran larvae concealed in stems, therefore may attack the tortricid moth *Olethreutes schultzeana*, which externally mines *Pedicularis* stems.

**Lissonota trichota* Townes; [A].

**Mesochorus gelidus* Dasch; [A]; hyperparasite.

Mesoleius s.l.; [LH,TL]; sawfly larvae.

Mesoleptus sp.; [TL]; cyclorrhaphous diptera emerging from cocoons.

Microleptinae spp.

Opidus (= *Oresbius*); [LH,TL].

Orthocentrus sp.; [LH,TL]; larvae of Mycetophilidae.

Phygadeuon sp.; [LH]; pupae of cyclorrhaphus diptera.

**Pohneumon* sp.

Proclitus spp. (two species?); [LH].

Saotis n. sp.; [LH]; sawfly larvae.

Stenomacrus spp. (2 species); [LH,ER,TL,PB]; mycetophilid larvae.

**Syndipnus* n. sp.; sawfly larvae.

Tymmophorus gelidus Dasch; [A;G]; attacks adult syrphids as they emerge from pupae.

Myrmariidae²⁴

Anaphes (*Patasson*) sp.; in insect eggs (Schauff, 1984).

Eulophidae

**Pnigalio* sp. (not *kukakensis* (Ashmead); external parasite of *Isochnus arcticus* (Brodo, unpub. notes, 1990 and 1991).

**Aprostocetus* sp.

Encyrtidae

**Metaphycus* sp.

**Syrphophagus* sp.

**Tetracylos boreios* Kryger; [LH;A;G]; reared from *Chorizococcus altoarcticus* (= *Pseudococcus* sp., Gibson and Yoshimoto, 1981).

Pteromalidae

Seladerma sp.; [TL].

**Thektogaster* sp.

Cynipidae

*sp.; hyperparasite on braconid or parasite on aphid.

Diapriidae

**Entomacis* sp.; primary parasitoid of terrestrial larvae of Ceratopogonidae, possibly of *Forcipomyia* sp. (L. Masner, pers. comm., 1992).

Apidae (bees)²⁵

Bombus polaris polaris Curtis (= *Megabombus polaris*); [LH;A;G,P]; nectar and pollen from many flowers including *Arnica alpina*, *Cassiope tetragona*, *Dryas integrifolia*, *Epilobium latifolium*, *Papaver lapponicum*, *Pedicularis* spp., *Salix arctica*, *Saxifraga oppositifolia*, *Silene acaulis*, *Stellaria longipes* (Richards, 1973; Brodo, unpub. notes, 1990 and 1991).

- 1 Voucher specimens sent to and identifications by Dr. S. Koponen, Turku, Finland.
- 2 Identifications by Drs. V. Behan-Pelletier, E. Lindquist, and I. Smith, Agriculture and Agri-Food Canada
- 3 Identifications by Eric Maw. A single immature aphid, four male scales, and one immature, minute thrips slide-mounted and retained by Dr. Foottit, Agriculture and Agri-Food Canada.
- 4 Identifications by Dr. David J. Larson, Memorial University of Newfoundland.
- 5 Identification by Andrew Davies, Agriculture and Agri-Food Canada.
- 6 Identified by Dr. A. Howden, Canadian Museum of Nature. The subfamily to which this species belongs has recently been revised by Anderson (1989).
- 7 Identification confirmed by P. McCuller, Royal Ontario Museum, Toronto, Ontario.
- 8 Classification based on Savchenko et al. (1992).
- 9 Determinations by J.A. Downes, Canadian Museum of Nature, Ottawa, Ontario.
- 10 Identifications by Dr. D. Oliver and M.E. Roussel, Agriculture and Agri-Food Canada. Probably only half the species collected have been identified to date.
- 11 Identifications by Dr. R. Vockeroth, Agriculture and Agri-Food Canada.
- 12 Identifications based on Gagné (1975).
- 13 Identifications by Vilkkamaa, Helsinki, Finland. Hippa and Vilkkamaa (1994) described *quadriceps* from a single male collected at Hot Weather Creek.
- 14 Identifications by Bruce Cooper, Agriculture and Agri-Food Canada.
- 15 Manuscript keys courtesy of Dr. D.M. Wood, Agriculture and Agri-Food Canada.
- 16 Identifications by Guy Shewell, Agriculture and Agri-Food Canada.
- 17 Dr. D.M. Wood, Agriculture and Agri-Food, Canada, verified determinations and provided information on host-parasite relations.
- 18 Determinations checked by Dr. D. Lafontaine, Agriculture and Agri-Food, Canada, except where noted.
- 19 Determinations by Dr. P. Dang, Agriculture and Agri-Food Canada.
- 20 Determinations by Dr. K. Bolte, Agriculture and Agri-Food Canada.
- 21 Determinations by Dr. K. Mikkola, Helsinki, Finland and Dr. D. Lafontaine, Agriculture and Agri-Food Canada.
- 22 Identification by Dr. A. Zinoviev, St. Petersburg, Russia.
- 23 Identifications by Dr. W. Mason, retired from Agriculture Canada and deceased December 1991. Information concerning host-parasite relationships by Luc Leblanc.
- 24 Identifications of the micro-hymenopteran families by Dr. G. Gibson, Dr. J. Huber, and Dr. L. Masner, Agriculture and Agri-Food Canada.
- 25 Identifications by Louise Dumouchel, Agriculture and Agri-Food Canada.

Quaternary geology and glacial history of Fosheim Peninsula, Ellesmere Island, Nunavut

T. Bell¹ and D.A. Hodgson²

Bell, T. and Hodgson, D.A., 2000: Quaternary geology and glacial history of Fosheim Peninsula, Ellesmere Island, Nunavut; in Environmental Response to Climate Change in the Canadian High Arctic, (ed.) M. Garneau and B.T. Alt; Geological Survey of Canada, Bulletin 529, p. 175–196.

Abstract: Surficial sediments of western Fosheim Peninsula consist mainly of weathered, sedimentary bedrock (resistant to friable), Pleistocene till (stony diamicton), and Holocene raised marine and deltaic sediments (fine to coarse grained), as well as minor deposits of preglacial fluvial gravels, Quaternary glaciofluvial and fluvial material, and glacier ice.

The rolling landscape mostly postdates a long period of Late Tertiary planation. Extensive, subdued, glacial deposits record ice of both southeasterly (granitic dispersal train along Eureka Sound) and local provenance. Fossiliferous tills were generally deposited before 30 ka, but amino-acid analyses of ice-transported marine shells indicate at least two populations, the oldest of which might be early Quaternary. Local glaciation of uplands occurred during the last glacial maximum (Late Wisconsinan).

Regressive suites of locally thick, glaciomarine, marine, and deltaic sediments were deposited on an emerging land surface from the latest Pleistocene through the Holocene.

Résumé : Les sédiments de surface de l'ouest de la péninsule Fosheim se composent surtout de socle rocheux sédimentaire altéré (résistant à friable), de till pléistocène (diamicton pierreux) et de sédiments holocènes deltaïques et marins soulevés (de granulométrie fine à grossière), ainsi que de dépôts mineurs de graviers fluviaux préglaciaires, de matériaux fluviaux et fluvioglaciaires quaternaires et de glace de glacier.

Le paysage ondulé a surtout été formé suite à une longue période d'aplanissement au Tertiaire tardif. De vastes étendues planes de dépôts glaciaires témoignent de la présence de glace provenant du sud-est (traînée de dispersion granitique le long du détroit d'Eureka) et de glace locale. Les tills fossilifères ont généralement été mis en place il y a plus de 30 ka mais les analyses d'acides aminés des coquillages marins transportés par les glaces indiquent au moins deux populations, dont la plus ancienne pourrait dater du début du Quaternaire. Les hautes terres ont été englacées par endroits du dernier maximum glaciaire (Wisconsinien supérieur).

Des séries régressives de sédiments glaciomarins, marins et deltaïques, localement de forte épaisseur, ont été déposées sur des terres émergentes à partir de la toute fin du Pleistocene et pendant l'Holocène.

¹ Department of Geography, Memorial University of Newfoundland, St. John's, Newfoundland, A1B 3X9

² Geological Survey of Canada, 601 Booth Street, Ottawa, Ontario K1A 0E8

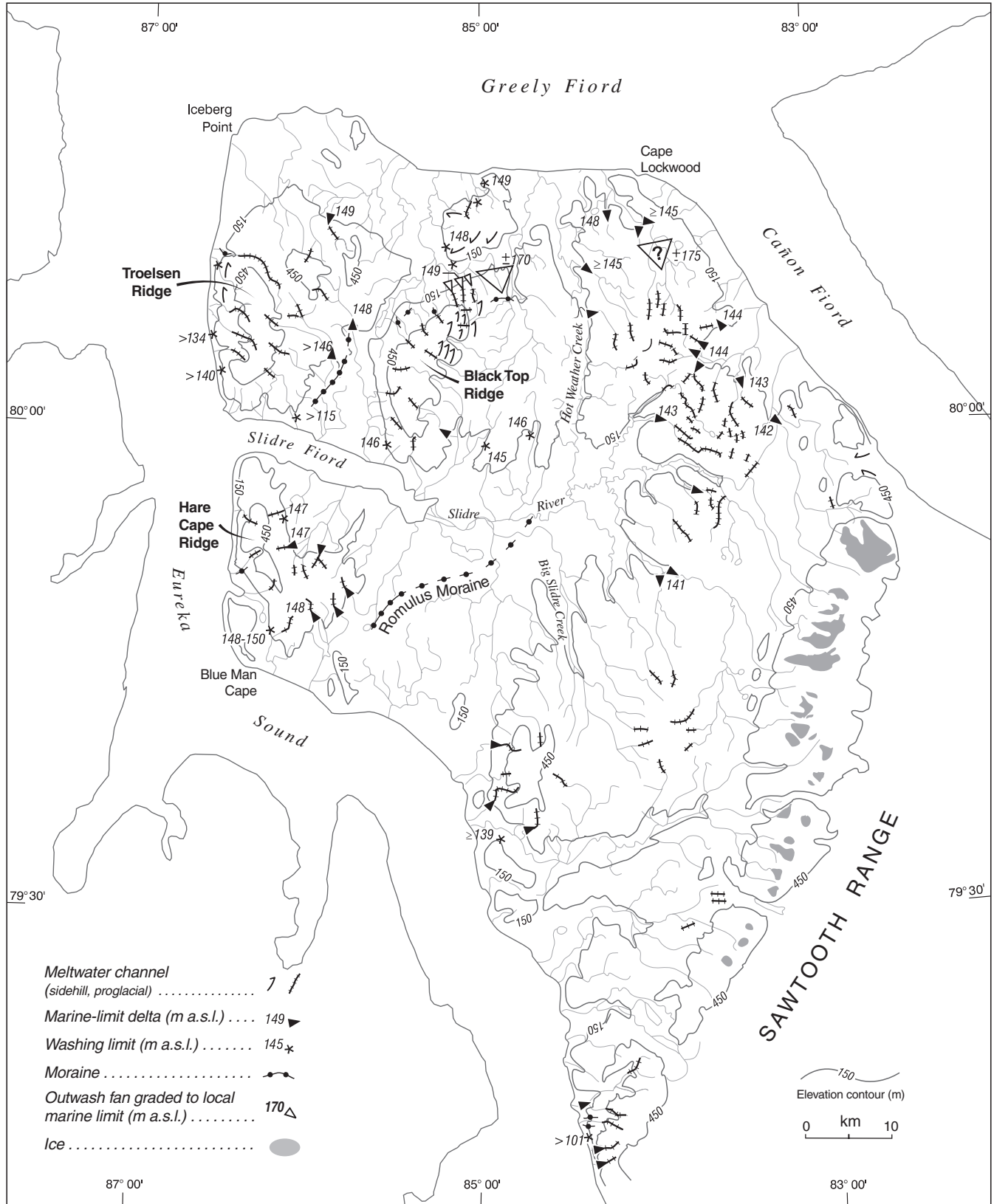


Figure 1. Northwestern Fosheim Peninsula, showing contemporary ice cover and prominent ice-marginal and marine features. Elevations were measured by altimetry; accuracy is ± 2 m.

INTRODUCTION

The surficial sediments of Fosheim Peninsula provide a record of paleoenvironmental change in an area of the Canadian High Arctic that exhibits Tertiary planation, Quaternary glaciation, marine inundation, and a variety of weathering processes. The nature and distribution of these sediments provide a geological framework for understanding current geomorphic and sedimentological activity in the region and may be used to delineate 'sensitive terrain' within the context of landscape response to future climate change.

The primary objective of this paper is to describe the surficial sediments and geomorphology related to Quaternary glaciation and sea-level change on the peninsula. The history of glacial and sea-level events is summarized from Bell (1992, 1996) and Bell and England (1993). The surficial mapping presented here was initiated in the 1970s, prompted by the discovery of oil and gas in the centre of the peninsula (Hodgson, 1974), and refined during doctoral research by the first author between 1988 and 1990 (Bell, 1992). Preliminary surficial material maps (1:125 000), together with biophysical and terrain sensitivity data, were prepared by Hodgson and Edlund (1978). Final Quaternary geology maps are in preparation.

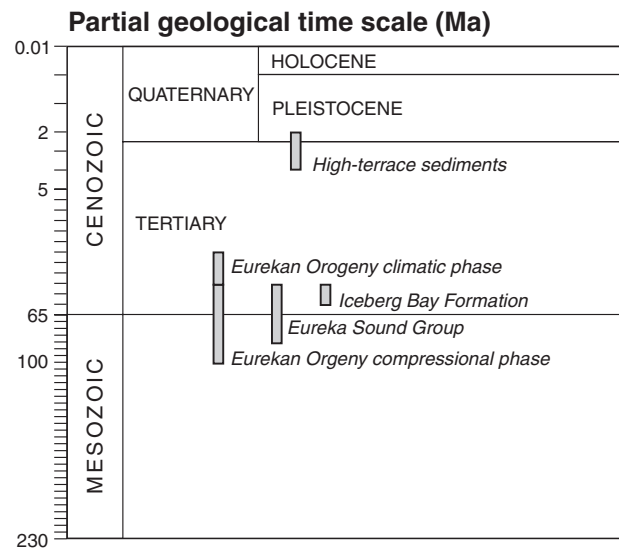
Fosheim Peninsula includes all the land west of the neck between Cañon and Bay fiords, but for the purposes of this report, the name 'Fosheim Peninsula' will be used to describe the study area, which lies northwest of the Sawtooth Range (Fig. 1).

PRE-QUATERNARY GEOLOGY

Fosheim Peninsula is underlain by folded and faulted sedimentary rocks of the Sverdrup Basin geological structure (Table 1) (Thorsteinsson and Tozer, 1970; Trettin, 1989). Mesozoic bedrock outcrops in uplands of the western peninsula including the Sawtooth Range, where it consists dominantly of fine- to medium-grained, quartzose sandstone with interbedded siltstone and shale, intruded by basic dykes and sills. The earliest phase of Eureka tectonism caused the breakup of Sverdrup Basin into a series of smaller subbasins (Table 1). One of these, the Remus Basin, occupied easternmost Axel Heiberg and west-central Ellesmere islands (Fig. 2, inset), where sandstone and shale over 3 km thick make up the Eureka Sound Group (Miall, 1986; Ricketts, 1988). The most commonly exposed geological unit on Fosheim Peninsula, the Iceberg Bay Formation (early Tertiary), consists predominantly of fine- to coarse-grained, poorly cemented, quartzose sandstone with interbeds of shale, siltstone, and coal. Coal-bearing strata may include petrified logs and stumps indicative of a broad-leaved, deciduous forest (Basinger, 1991).

Although the Iceberg Bay Formation represents the final depositional event of the Remus Basin prior to its uplift and thrusting during the Paleogene Eureka Orogeny (Table 1), the basin was partly rejuvenated during the Pliocene when

Table 1. Subdivisions of the Phanerozoic geological time scale and approximate ages of geological events described in the text.



fluvial sediments prograded across west-central Ellesmere Island and eastern Axel Heiberg Island. These sediments, originally included in the Beaufort Formation of the Arctic Coastal Plain (Tozer, 1956; Thorsteinsson and Tozer, 1970), are referred to here as 'high-terrace sediments', following Craig and Fyles (1960) and Fyles (1990).

PHYSIOGRAPHY

Roots (1963) divided the physiography of Fosheim Peninsula into two zones, the ridges and valleys of the Central Mountain Belt and the Eureka Sound Uplands. The ridge and valley zone includes the Sawtooth Range and the mountainous region farther south, where parallel to subparallel ridges are separated by linear valleys oriented northeast-southwest (local relief over 1000 m). Small ice caps and cirque glaciers are common on these ridges. Drainage systems have either parallel or trellis networks with short tributaries. River gradients are low in the main valleys, but it is apparent that significant incision has occurred because late Tertiary fluvial deposits are perched over 300 m above the valley floors.

The Eureka Sound Uplands occupies the western half of the peninsula. The name is an inappropriate description of a generally topographically subdued landscape, more than half of which is below 200 m a.s.l., with isolated ridges up to 840 m a.s.l. The region generally exhibits a dendritic drainage system. Slide River drains the largest catchment, including some glacierized basins in the Sawtooth Range (Fig. 1). Many rivers have incised meanders in their lower reaches and whereas some have reoccupied paleochannels, others have cut into bedrock during the Holocene. Gullying of poorly consolidated bedrock and raised, marine, fine-grained sediment has resulted in local badland topography.

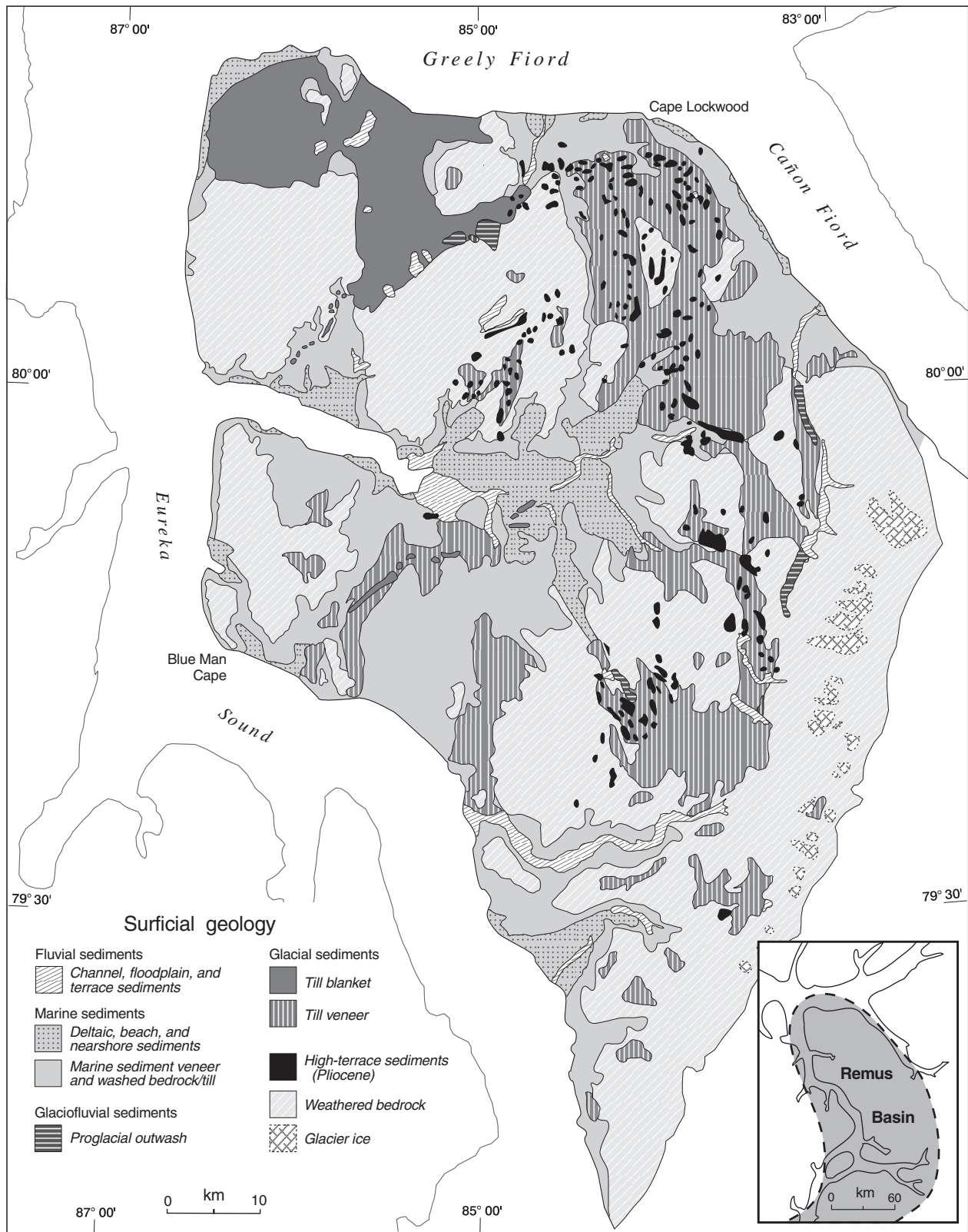


Figure 2. Summary surficial geology map of northwestern Fosheim Peninsula. For cartographic reasons, sediment units of limited areal extent have been combined or omitted (see text); more detailed maps have been published by Hodgson and Edlund (1978). Inset shows the extent of Remus Basin on eastern Axel Heiberg Island and west-central Ellesmere Island (after Miall, 1986).

SURFICIAL MATERIALS AND GEOMORPHIC FEATURES

Weathered bedrock

Weathered bedrock is the most common surficial unit on Fosheim Peninsula (Fig. 2). Advanced surface weathering, including pitting, flaking, and tafoni development, is present on many bedrock outcrops and glacial erratics. Residuum is reported to be 1 to 2 m thick in various parts of the peninsula (Hodgson et al., 1991) and although its texture reflects the lithology of the underlying rock formation, there is some surface reworking and mixing of grain sizes. Below the Holocene marine limit, bedrock surfaces have been washed and residuum reworked with littoral and nearshore sediment. Eolian activity has also modified residuum through the deflation of fine-grained sediment, as evidenced by surface lags and incipient stone pavement. Slope processes have produced sorted and nonsorted stripes in residuum and gelifluction lobes commonly incorporate residual material.

The duration of bedrock weathering on Fosheim Peninsula is difficult to assess because weathering processes in cold, arid environments are poorly understood and rates may vary through time, depending on climatic conditions. For example, the depth of weathered bedrock recorded from drill sites on the peninsula exceeds the present depth of the active layer, likely indicating that this deeper weathering formed during a warmer period when the active layer was deeper (Hodgson, 1989; Hodgson and Nixon, 1998). The occurrence of lowland tors (Fig. 3), intensely weathered bedrock, and rooted, coalified tree stumps projecting over 1 m from the ground (*see* McMillan, 1963) suggests that considerable landscape dissection and substantial subaerial weathering have occurred since the last extensive glaciation of the peninsula.



Figure 3. Sandstone tor (about 1 m high) at 183 m a.s.l. surrounded by weathered bedrock and scattered glacial erratics east of Big Slide Creek, on Fosheim Peninsula. This site lay beyond the proposed limit of local ice advance during the last glaciation. High-terrace sediments in the right background are shown in more detail in Figure 4. GSC 2000-023A

High-terrace sediments

Craig and Fyles (1960) and Fyles (1962) first reported unconsolidated deposits beneath widespread high terraces on west-central Ellesmere Island. They consist of horizontally stratified, unconsolidated sand, silty sand, and gravel lying beneath gently sloping, gravelly terraces up to 600 m a.s.l. (Fyles, 1989). The main surfaces are remnants of a fluvial plain that conformed to the present regional topographic framework (Craig and Fyles, 1960); lower, inset flights of terraces may be significantly younger (Fig. 4). High-terrace sediments contain wood, peat, mammalian bones, and other organic remains indicative of boreal forest to forest-tundra conditions (Fyles, 1989; C.R. Harington, pers. comm, 1997). Matthews and Ovenden (1990) used floral evidence to suggest an early Pliocene to early Quaternary age for these deposits.

Although exposures of terrace sediments are rare, Hodgson et al. (1991) reported the presence of a 27 m thick section in a deep gully near Hot Weather Creek. The exposure contained “generally planar-bedded, in places crossbedded, fine sand, subordinate sandy silt, granule beds, and coal fragments” overlain by a veneer of bouldery gravel. In the absence of sediment outcrops, high-terrace remnants overlain by gravelly diamicton are indistinguishable from glaciofluvial landforms composed of gravelly outwash. On northeastern Fosheim Peninsula, for example, mesas and flat-topped terraces resemble a dissected outwash plain that grades to about 175 m a.s.l. on the Cañon Fiord–Greely Fiord coastal lowlands. Wood (described as ‘driftwood’) collected from the top of one of these terraces was dated >33 000 BP (L-266C; Broecker et al., 1956). Although the surficial geology map portrays these landforms as high-terrace sediments (Fig. 2), they are likely glaciofluvial deposits reworked from high-terrace sediments. Further investigation is needed to resolve a more detailed classification.

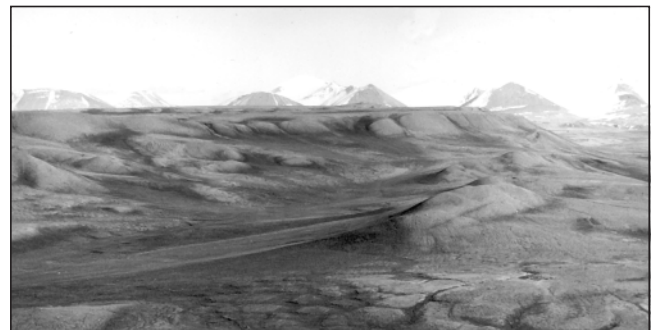


Figure 4. View of high-terrace sediments at about 330 m a.s.l. on Fosheim Peninsula. The distinct, planar surface, sloping to the north, is the remnant of a Pliocene fluvial plain (*see* Fyles, 1989). Unaltered wood samples indicative of boreal-forest to forest-tundra conditions have been recovered from these sediments. Lower, inset terraces are likely glaciofluvial in origin and may be significantly younger. Cirque glaciers in the Sawtooth Range are visible in the background. GSC 2000-023B

Till

Till on Fosheim Peninsula is divided into two mappable units, blanket and veneer (Fig. 2). Till blanket is sufficiently thick (>2 m) to completely obscure the underlying bedrock structure (Fig. 5), whereas the surface of till veneer mimics the underlying rock surface. Regionally extensive blankets and veneers of stony diamicton are rarely formed into characteristic glacial landforms, but are interpreted as till for the following reasons: the base of the diamicton, where observed, commonly forms an abrupt, planar contact with the underlying sediment and is considered to be erosional; subdiamicton sediments are penetratively deformed consistent with glacial shearing and loading; diamicton contains incorporated clasts and/or rafts of underlying sediment; and diamicton contains striated, regional erratics and, in some cases, transported marine shell fragments (some erratics are too large to be derived from fluvially transported, high-terrace deposits) (Bell, 1996).

Extensive till blankets are restricted to lowland areas where they are up to 15 m thick (e.g. Iceberg Point; Hodgson and Edlund, 1978). In section, the till is commonly matrix supported, fine grained, and compact. In places, it displays evidence of subglacial, tectonic shear, including stacking and rotation of subfill sand rafts and attenuation of sand laminae in the direction of shear (e.g. west and northwest near Hot Weather Creek). Shell fragments from subfill sand near Iceberg Point provided a radiocarbon date of $45\,850 \pm 980$ BP (TO-2228; Bell, 1992), whereas peat overlying diamicton in 'Big Slide Creek' valley was dated at $>41\,200$ BP (GSC-268; Dyck et al., 1965; Hodgson, 1985); neither of these dates is considered finite.

Till contains clasts that may have either regional or local provenance. Regional till contains foreign erratics, transported into the area, whereas local till contains only native erratics eroded from outcrops within the area. Limestone, dolomite, sandstone, diabase, and chert-pebble conglomerate may originate on the peninsula, whereas quartzite and granite erratics have their nearest source 100 km to the southeast, in



Figure 5. An example of the fine-grained till that is locally restricted to low-lying areas on Fosheim Peninsula. In contrast, upland areas are dominated by weathered bedrock with scattered glacial erratics. GSC 2000-023C

the northernmost Canadian Shield on Ellesmere Island. Quartzite erratics, which are widespread on the peninsula, are typically subrounded, displaying crescentic scars like percussion marks or chattermarks. Because glacial modification (e.g. striations, facetting) is apparently minimal, the erratics may have been glacially reworked from Pliocene fluvial sediments on the peninsula. In contrast, granite erratics are commonly angular to subangular and up to 3 m in diameter. They are distributed in a long, relatively narrow belt along the western fringe of the peninsula, roughly coincident with northern Eureka Sound. On the basis of earlier observations, the dispersal pattern can be extended southward along Eureka Sound and westward through Bay Fiord from the Canadian Shield (Prince of Wales Mountains; Fyles, 1962; Hodgson, 1985).

Discontinuous, fossiliferous till was observed along the northern and western margins of the peninsula and on eastern Axel Heiberg Island. Whole and fragmented marine shells scattered over weathered bedrock and patchy till on 'Hare Cape Ridge' (up to 627 m a.s.l.) provided a range of radiocarbon dates between $36\,300 \pm 2000$ BP (GSC-111; Dyck and Fyles, 1964) and $19\,500 \pm 1100$ BP (L-548; Sim, 1961) (see Appendix A), which prompted J.G. Fyles to conclude that the dates were minimum estimates (Fyles in Dyck and Fyles, 1964) and that the shells were probably transported by an extensive, pre-Wisconsinan glaciation (Fyles in Jenness, 1962). Surface shell samples from fossiliferous till were subjected to amino-acid analysis (Appendix B). On the basis of amino-acid ratios, specifically the ratio of alloisoleucine to isoleucine, it can be demonstrated that two shell populations, with mutually exclusive ratios, can be identified according to till location (Fig. 6, Table 2) (Bell, 1992). The highest ratios (Group I) and, consequently, the oldest shells, are associated with till on the northwestern and southwestern corners of the peninsula. Lower ratios (Group II) are confined to till on Hare Cape Ridge and the adjacent lowland and in west-central

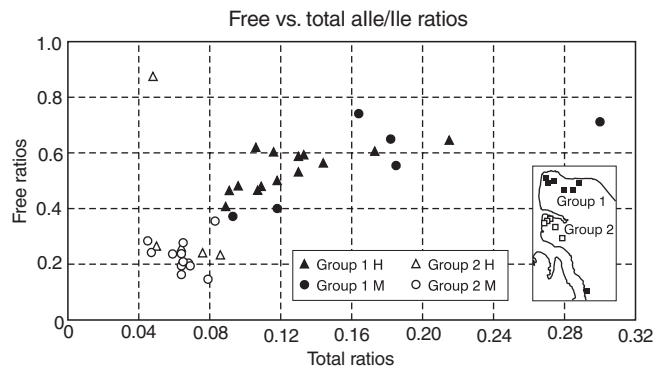


Figure 6. Plot of free versus total alle/Ile ratios for ice-transported marine shells collected from the surface of till samples in the study area. Two groups are identified according to sample location (see inset and Appendix B). For comparison, only the results from *Hiatella arctica* (H) and *Mya truncata* (M) are shown. Samples with mixed populations are not plotted (see Appendix B).

Table 2. Summary group statistics for alle/lle ratios from ice-transported shells in regional till on Fosheim Peninsula (Bell, 1992).

	GROUP I		GROUP II		GROUP III	
	Free	Total	Free	Total	Free	Total
range	0.372–0.741	0.089–0.185	0.146–0.355	0.047–0.086	0.285–0.417	0.041–0.090
x	0.37	0.127	0.232	0.065	n.a.	n.a.
S _x	0.102	0.032	0.049	0.011	n.a.	n.a.
CV	19%	25%	21%	17%	n.a.	n.a.
n	19	17	17	20	4	4

Notes: Some ratios were not used in data reduction or analysis because of taxonomic differences, anomalously high ratios from 'old' shells, or inconsistent free and total ratios suggesting analytical error. See Appendix B for complete data set.
n.a. = not applicable
CV = coefficient of variation (S_x/x)

Eureka Sound. Samples with mixed populations (Group III) are found near Cape Lockwood on the Greely Fiord coast and at the southern margin of the Sawtooth Range.

The lowland southeast of Slidre Fiord contains one of the most significant glacial landforms on the peninsula. A 25 to 30 km long, arcuate ridge between 134 and 57 m a.s.l. runs diagonally across the lowland to Slidre River (Fig. 2, 7), where it is partly buried by Holocene marine sediments. The ridge is draped with a bouldery gravel lag that in places has been reworked into well defined beach ridges. Where the lag is thin or discontinuous, a fossiliferous, fine-grained diamicton is exposed at the surface; it seems to be an extension of the till that mantles the adjacent lowland. Towards Slidre River, ridge sediments become nonfossiliferous and the proportion of carbonate clasts increases, resembling that of till from the interior of the peninsula. Pockets of Holocene marine silt drape the ridge to within 10 to 15 m of its crest (8230 ± 80 BP, GSC-4957). The ridge is interpreted to be a moraine (Romulus Moraine) deposited by north- and west-flowing ice.

Two other locally prominent moraines were mapped on the peninsula. One runs southwest to northeast across the lowland north of Slidre Fiord (Fig. 2, 8). It has an elevation between 176 m and 185 m a.s.l. although shorter segments and terraces are found at lower elevations (165–170 m a.s.l.) and show evidence of marine washing. A discontinuous, gravelly moraine ridge, mantled with large sandstone blocks, crosses the lowland northeast of Black Top Ridge (Fig. 2).

Much smaller, less continuous moraines are restricted to valleys with significant upland catchments. Subdued gravel ridges on the lowland northwest of Black Top Ridge form discontinuous moraine loops grading from 230 m to 170 m a.s.l. Till and alluvial gravel on the proximal side of the moraines are composed of native erratics, whereas the lowland distal to the moraines is mantled with fossiliferous till containing foreign erratics. Similar crosscutting relationships are recorded by moraines in valleys draining uplands along Eureka Sound. These moraines demarcate the boundary between locally derived till in valley bottoms and regional till on adjacent slopes. In general, moraines descend from a maximum elevation of 220 m to between 80 and 120 m on the coastal lowland.



Figure 7. Oblique view of part of Romulus Moraine looking southwest towards Eureka Sound. The proximal side is to the left. Beach ridges on the moraine surface indicate marine washing. Bedrock is exposed on the lowland in the left background. The moraine was deposited by north- and west-flowing ice from Eureka Sound and central Ellesmere Island, respectively. GSC 2000-023D



Figure 8. View along a prominent moraine (185 m a.s.l.) north of Slidre Fiord. The lower parts of the moraine (<170 m a.s.l.) look to be marine washed. GSC 2000-023E

Glaciofluvial sediments

Meltwater channels are the most widespread landform related to glaciation. Many channels are considered polycyclic and, in some cases, periods of activity can be distinguished on the basis of lithology and associated relative sea level. For example, ice-marginal channels up to 600 m a.s.l. on the northern end of Black Top Ridge were originally formed during the systematic retreat of a regional ice cover (Hodgson, 1985) and are related to the deposition of a moraine and related outwash complex approximately 170 m a.s.l. on the adjacent lowland (Bell, 1992). During local glaciation, some of these channels were reoccupied in a proglacial setting, draining meltwater from an upland ice cap to fans, graded to about 150 m a.s.l. Outwash from this former ice cap is characteristically darker on airphotos than that associated with the older, regional ice cover because it contains a higher proportion of local shale and diabase. Elsewhere, proglacial channels are preserved as either overfit stream valleys on upland slopes or abandoned channels on till-covered lowlands. Typically, they form a radial pattern around local uplands and grade to marine limit (Fig. 1).

Apart from extensive gravel deposits on northeastern Fosheim Peninsula, which are mapped as high-terrace sediments, but suspected to be of glaciofluvial origin (see above), the only other significant outwash deposit occurs near the head of Big Slide Creek. A narrow outwash plain composed of pebble to boulder gravel over 5 m thick, resting on bedrock, grades downvalley from 232 m to 185 m a.s.l.

Marine sediments

Coastal and interior lowlands on Fosheim Peninsula were shallow inlets and basins during periods of higher sea level and collected an extensive record of sedimentation related to local glacial and sea-level history (Fig. 2) (Bell, 1996). The most extensive marine deposits are contained in the lower Slidre River basin, which covers an area of about 250 km² and received meltwater from surrounding ice caps and more distal

cirque glaciers in the Sawtooth Range during the late Pleistocene and Holocene (Fig. 9). Basin sediments form discrete wedges in tributary valleys, reaching a maximum thickness of about 36 m in the lower Slidre River valley. The basin fill has a consistent upper limit between 125 and 130 m a.s.l. that commonly onlaps bedrock. In section, the lower contact of the fill is obscured by either colluvium or massive ground ice that formed in situ following marine regression (Pollard, 1991, 2000). The surface of the fill consists of a lightly vegetated, silty sand that, in places, is actively deflating (Fig. 9).

Structureless to laminated mud and/or interbedded mud and fine sand dominate the sedimentary sequences of the Slidre River basin, recording deposition by suspension settling and from low-density turbidity currents in a prodeltaic environment (Bell, 1996; Aitken and Bell, 1998). Sediment texture coarsens upward, reflecting increasing proximity to sediment sources as deltas prograded during Holocene marine regression. Paired and single valves of *Hiattella arctica* and *Mya truncata*, collected between 59 and 137 m a.s.l. on the fill surface, provided an age range of 8000 to 9000 years (n = 13; Bell, 1996) (see Appendix A).

Elsewhere on the peninsula, Holocene marine sediments accumulated on coastal lowlands, downvalley from marine-limit deltas (Fig. 2). In general, deposits are 5 to 10 m thick, but may reach 35 m in thickness in valleys with significant upland catchments (Fig. 10). Coastal sites more distal to meltwater outlets commonly consist of weathered bedrock or diamicton, either marine washed or draped by a thin veneer (<0.5 m thick) of marine sediment (Fig. 2).

In some places, the Holocene fill possibly buried older Quaternary deposits (see McMillan, 1963; Hodgson, 1985; Hodgson et al., 1991; Bell, 1992). For instance, a *Salix* twig dated at 44 420 ± 840 BP (TO-2242) from ripple-bedded sand underlying Holocene marine rhythmites on the Greely Fiord coast may indicate the presence of older marine sediments.



Figure 9. View looking southeast across the featureless, fine-grained surface of the sediment fill in Slidre River valley. During the Holocene high sea level, this interior lowland acted as a shallow-marine basin, collecting an extensive record of sedimentation related to local glacial and sea-level history (Bell, 1996; Aitken and Bell, 1998). The Sawtooth Range in the background is 35 km away. GSC 2000-023F

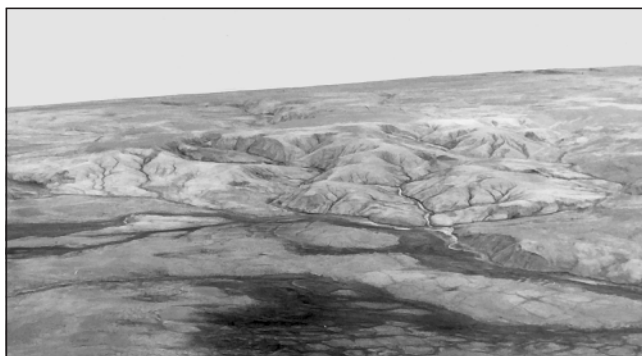


Figure 10. An example of a thick marine deposit downvalley from a glacierized catchment during the last glaciation. The deposit, located below 70 m a.s.l. on the Greely Fiord coast, consists of about 35 m of marine rhythmites dated between 9.1 and 7.9 ka, underlain by bedded sand containing terrestrial organic material dated at 44 ka (Bell, 1996). Adjacent coastal sites that did not act as meltwater outlets are typically only marine washed or draped by a thin veneer of marine sediment. GSC 2000-023G

Fluvial sediments

Fluvial gravel and sand comprise a minor surficial unit on the peninsula (Fig. 2). Two types are identified, deposits that lie within the active floodplain and deposits that are perched above it. The former are flooded periodically from single to multiple channels. Inactive alluvium is separated from the floodplain by a distinct bluff and ice-wedge polygons are common on its surface. In some valleys, the highest inactive alluvium consists of proglacial outwash. Flow regimes are generally nival, but some rivers have Sawtooth Range glaciers in their headwaters (e.g. Slidre River).

Eolian sediments

Wind-blown sand and coarse silt lie adjacent to poorly vegetated, fluvial sediments in the study area. The largest deposit is on the north side of the lower Slidre River floodplain. Eolian landforms consist mainly of ripples and low dunes. It has been demonstrated that eolian erosion and deposition are significant processes during the winter on Fosheim Peninsula (Edlund and Woo, 1992). Although snow cover protects most surfaces, redistribution of snow by wind can create bare patches that become critical sites for eolian activity. In some cases, sand and gravel (including platy clasts with long axis up to 60 mm) have been transported over 1 km during wind storms, when gusts exceeded 90 km/h (Edlund and Woo, 1992). Eolian sediments are minor surficial materials in the study area and their distribution is not shown on Figure 2.

Organic deposits

Thin, organic deposits (peat) composed of mosses and vascular plants are accumulating in abandoned stream valleys and surface depressions (Edlund et al., 1989; Garneau, 1992, 2000). Thicker deposits (0.5 m to over 5 m) exposed by

stream incision are commonly mid-Holocene (Hodgson et al., 1991). This does not, however, necessarily indicate a more favourable paleoclimate at that time; instead, it may reflect a bias in the dated samples that were readily obtained from the Slidre River valley fill (Hodgson et al., 1991). The dates, therefore, may be more representative of local emergence than of a climatic optimum. Organic deposits are minor surficial materials in the study area and their distribution is not shown on Figure 2.

Colluvium

Most unconsolidated deposits on slopes undergo a degree of mass wasting that can materially alter composition or structure. The dominant processes are solifluction and rill washing, with slope failures locally significant on fine-grained materials. Colluvium is a minor surficial material in the study area and its distribution is not shown on Figure 2.

TERTIARY LANDSCAPE HISTORY

Rivers carried sediment from all directions into the Early Tertiary Remus Basin where it was deposited as the Eureka Sound Group. When the Middle Tertiary Eureka Orogeny reached its climactic phase, rivers continued to flow to the Remus Basin as antecedent drainage through the uplifting Sawtooth Range. Remnants of these river valleys may be preserved as wind gaps in the modern Sawtooth Range and as high-terrace sediments. The later development of interisland channels and fiords, by whatever process (Bell, 1992), caused the breakup of the contiguous Remus Basin, the truncation of the antecedent drainage system, and the evolution of the present drainage pattern, which parallels the ridge-and-valley topography on southern Fosheim Peninsula. Subsequent channel incision to modern base level has isolated fluvial (high-terrace) sediments up to 300 m above present valley floors.

QUATERNARY HISTORY

Quaternary glacial and sea-level history is synthesised here from Bell (1992, 1996) and Bell and England (1993). Obviously, numerous hiatuses exist in the known geological record of Fosheim Peninsula from the Late Tertiary through much of the Quaternary. Two distinct glacial styles and at least one marine event are recognized from the geomorphology and sedimentology (Fig. 11): ice advances from regional sources that inundated the peninsula; growth of local upland ice caps and expansion of cirque glaciers in the Sawtooth Range; and sea-level transgression in the latest Pleistocene followed by regression through the Holocene.

Regional glaciation

Erratics are widely distributed on Fosheim Peninsula and although they need not represent a single glacial event, high-elevation erratics could only have been deposited by ice

that covered the entire peninsula (Fig. 11). Erratics' dispersal patterns document former ice-flow direction. Till containing granite erratics forms a long, narrow, northward dispersal train on the western fringe of the peninsula, roughly coincident with northern Eureka Sound. It represents a regional ice source, probably originating from the northernmost Canadian Shield of southeastern Ellesmere Island, that advanced across the high summits of western Fosheim Peninsula and eastern Axel Heiberg Island into Greely Fiord. The pattern resembles a Dubawnt-type dispersal train, as described by Dyke and Morris (1988). Other erratics, mainly quartzite, are widespread across the peninsula, including the highest summits, and most likely represent a westerly and northwesterly ice flow from central and south-central Ellesmere Island. Both flows were contemporaneous across the peninsula. With the exception of a few coastal sites, ice-transported marine shells are found only in till associated with the granite dispersal train.

Regional ice retreat across the peninsula is recorded by high-elevation meltwater channels (e.g. Black Top Ridge), moraines (e.g. Romulus Moraine), and outwash deposits. Together, they show the progressive southward and south-eastward retreat of ice towards central Eureka Sound and Cañon Fiord, respectively (Fig. 11). Deglacial sea levels are recorded by remnants of outwash fans graded to 170 and 175 m a.s.l. on Greely and Cañon fiord coasts, respectively, and marine-washed segments of an end moraine north of Slidre Fiord (170 m a.s.l.).

Although different glacial episodes of regional glaciation could not be recognized from field mapping, amino-acid ratios from ice-transported shells in regional till demonstrate that two shell populations, with mutually exclusive ratios, can be identified according to till location. Group I, the oldest shells, is associated with till on the northwestern and southwestern corners of the peninsula; the younger shells of Group II are confined to till on Hare Cape Ridge and adjacent lowland and west-central Eureka Sound. The occurrence of two tills with ice-transported shells of discrete, relative ages can

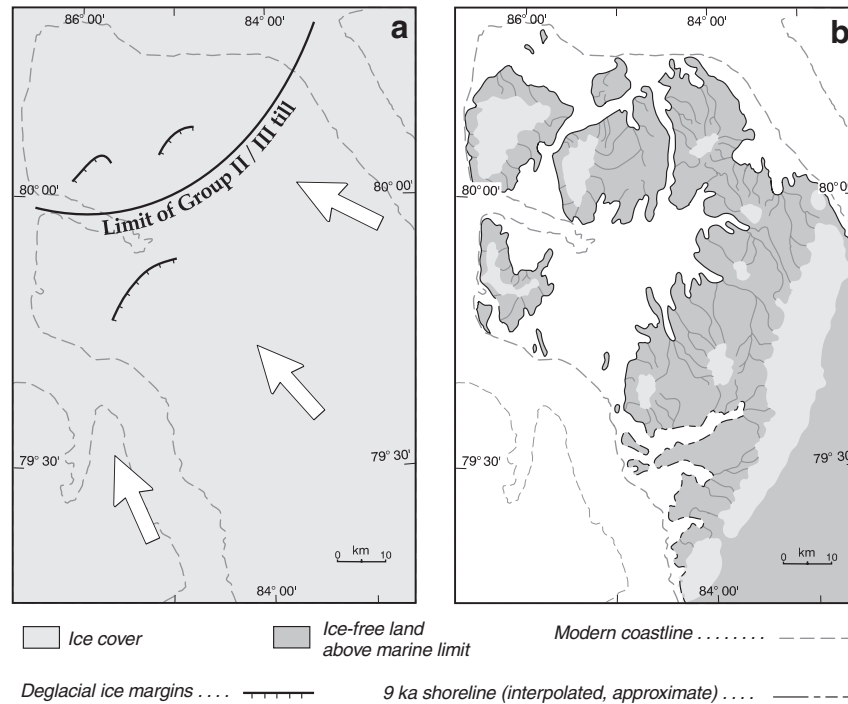


Figure 11. Paleogeography of northwestern Fosheim Peninsula during **a**) regional glaciation and **b**) local glaciation (about 9 ka). Open arrows show the direction of regional ice movement as reconstructed from the distribution of glacial erratics. The positions of deglacial ice margins are mapped from moraines and meltwater channels. The line that curves across the peninsula from Slidre Fiord to Cape Lockwood represents the northwestern limit of till containing younger (Group II) or mixed (Group III) shell populations that may represent a discretely younger glacial advance (see text for discussion). Map **b**) at about 9 ka is a schematic depiction of ice caps in areas that are now ice free and of more extensive glaciers in the Sawtooth Range. The shoreline at marine limit is interpolated between measured sites (broken line where speculative). The present shoreline is represented by a broken line.

be reasonably explained in terms of two glacial advances, one that inundated the entire peninsula and another that terminated north of Hare Cape Ridge (Fig. 11). However, no geomorphic expression of such an ice margin exists, although till provenance changes abruptly on either side of Slidre Fiord.

Local glaciation

The limit of local till, commonly marked by moraines, records the maximum position of small ice tongues draining local ice caps on the peninsula. Meltwater channels show a radial distribution around uplands, related to individual ice caps on Troelsen, Hare Cape, Black Top, and several unnamed ridges (Fig. 1, 11). Glaciers advanced onto adjacent lowlands from cirque basins in the Sawtooth Range. In most cases, ice terminated on land as indicated by the pattern of proglacial meltwater channels leading to marine-limit deltas (Fig. 1); however, outlet glaciers draining ice caps along Eureka Sound entered a higher relative sea level and calved. Marine-limit deltas associated with the local ice limit show a pattern of smoothly decreasing elevation, from 149 m in northern Eureka Sound and Greely Fiord to 139 m or more and 142 m in central Eureka Sound and Cañon Fiord, respectively (Fig. 1). A synchronous marine limit is implied where the ice limit was inland of the sea. Radiocarbon dates from either surface shells collected immediately below marine limit or in situ shells from fine-grained deposits downvalley from marine-limit deltas suggest that this marine limit was likely established by 10.6 ka, with the sea level remaining high (within 10 m of the marine limit) until 8.7 ka or later (Bell, 1996). Coastal and interior lowlands on the peninsula acted as shallow marine basins, collecting an extensive record of sedimentation related to local glacial and sea-level history.

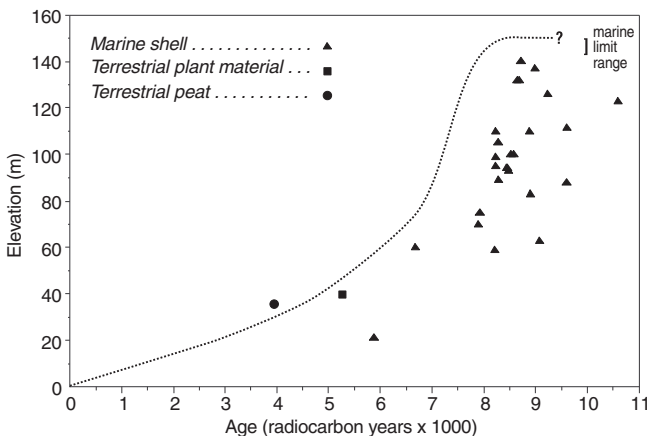


Figure 12. Provisional sea-level curve for northwestern Fosheim Peninsula. Emergence data are based on 27 radiocarbon dates on marine shell and terrestrial peat and plant material presented in Bell (1996) and Hodgson et al. (1991) (see Appendix A). Because the corresponding sea level for many dated samples is unknown, a curve consistent with the unloading history of a site beyond the last ice margin is fit to the data. See Bell (1996) for discussion.

From oldest to youngest, these sediments have been interpreted to represent the following: a deepening of the submerged basins as sea level transgressed to marine limit; marked increases in sedimentation rate in response to increased ablation on local ice caps (9.5 ka); and marine regression and shallowing of the marine basins (Bell, 1996).

Glacial chronology and correlations

The crosscutting relationship of local and regional till, the pattern of moraines and meltwater channels, and the relative sea-level history indicate that local ice advance postdated regional ice retreat. Using amino-acid analyses, ratios from the total acid hydrolysate of shells in Group I till are seen to be similar to those from the oldest marine sediments of the Kap København Formation, northern Greenland, dated 3.2 to 2.4 Ma (Funder et al., 1985). Because redeposited shells reflect the age of sediments incorporated during glacial advance, they provide only a maximum date for glaciation. Hence, 2.4 Ma is a maximum date for regional glaciation of the peninsula. If Group I and II shell populations, with their mutually exclusive amino-acid ratios, indicate two discrete regional glaciations of the peninsula, then Group II ratios can provide a minimum estimate for the age of Group I glaciation. Group II ratios are similar to those from the Robeson aminozone (mean total ratio = 0.063) on northeastern Ellesmere Island, which is thought to predate 70 ka (Retelle, 1986). Although the age of regional glaciation cannot be established precisely, it is proposed that the regional ice advance responsible for Group I till deposition predated the last glacial maximum and may be as old as 2.4 Ma. The timing of Group II till deposition cannot be determined from the available data.

The paleogeography of Fosheim Peninsula at ca. 9 ka shows the presence of local upland ice caps in areas that are now ice free, more extensive glaciers in the Sawtooth Range, and the sea occupying extensive coastal and interior lowlands (Fig. 11). Deglaciation of the peninsula was underway by 9.5 ka (Bell, 1996), which is similar to deglacial records from Bay Fiord, central Eureka Sound (Hodgson, 1985), and outer Cañon Fiord (England, 1990). Sea level was at, or close to, the marine limit (142–149 m a.s.l.) from at least 10.6 to 8.7 ka. Initial rapid emergence caused relative sea level to fall to about 80 m a.s.l. by 7 ka, but this was followed by a steadily declining rate of emergence in the middle to late Holocene (Fig. 12).

CONCLUSIONS

Surficial mapping of western Fosheim Peninsula shows the most extensive unit to be weathered bedrock derived from highly friable to moderately resistant sedimentary (very minor igneous) bedrock. Small deposits of Pliocene unconsolidated sand, silt, and gravel are remnants of a formerly extensive, Late Tertiary peneplain.

A discontinuous, stony diamicton on the peninsula indicates inundation by at least one glaciation. A regional till containing foreign erratics is present on the west side of the

peninsula, adjacent to Eureka Sound. The presence of granites in this till indicates ice dispersal from the Canadian Shield, which is at its northernmost limit in southeastern Ellesmere Island. Regional till without indicator erratics covered the central and eastern peninsula, leaving now subdued end moraines marking a southward retreat. Erratics in regional till include marine bivalves that yield probably infinite radiocarbon ages. On the basis of amino-acid ratios from shells in regional till, which indicate two discrete shell populations according to till location, regional glaciation is subdivided into two advances on the peninsula. The earliest and most extensive of these likely predated the last glaciation and may be Early Quaternary, on the basis of comparisons with amino-acid ratios from the independently dated Kap København Formation in northern Greenland.

Drainage channels and rare end moraines record local glaciation of ridges and plateaus. Outwash in places grades to the latest Pleistocene–Holocene marine limit. The marine limit, defined by strandlines and trimlines, is at a maximum of 150 m in the northwestern part of the peninsula and falls to the southeast. Thick marine and deltaic sediments record the regressing shoreline and prograding rivers in larger river basins (particularly Slidre River). Uplift has resulted in most rivers incising their channels, except where confining sediments are unconsolidated and finer grained (again, the lower Slidre River). Sandy terraces adjacent to such anastomosing channels are subject to eolian processes.

ACKNOWLEDGMENTS

We are grateful for the encouragement to work on the Fosheim Peninsula provided by John England (University of Alberta) to T. Bell in 1988 and by John Fyles (Geological Survey of Canada) to D.A. Hodgson in 1972. Fieldwork was funded by the Natural Sciences and Engineering Research Council (grant A6880 to John England), the Canadian Circumpolar Institute, University of Alberta (BAR grant), and an Energy, Mines, and Resources Research Agreement (no. 171). Logistical support was provided by the Polar Continental Shelf Project, Natural Resources Canada. Strong support in the field was provided by R.J. Richardson, Richard England, Scott Lamoureux, and Gillian Davidge. Roger McNeely (Geological Survey of Canada) provided information on radiocarbon dates from the Survey's Date Locator File. Gary McManus and Charles E. Conway (Memorial University of Newfoundland Cartographic Laboratory) prepared the figures. Drs. Alec Aitken and Michelle Garneau provided constructive comments on the manuscript.

REFERENCES

Aitken, A.E. and Bell, T.

1998: Holocene glacial marine sedimentation and macrofossil palaeoecology in the Canadian High Arctic: environmental controls; *Marine Geology*, v. 145, p. 151–171.

Basinger, J.F.

1991: The fossil forests of the Buchanan Lake Formation (Early Tertiary), Axel Heiberg Island, Canadian Arctic Archipelago: Preliminary floristics and paleoclimate; *Geological Survey of Canada, Bulletin* 403, p. 39–65.

Bell, T.

1992: Glacial and sea level history of western Fosheim Peninsula, Ellesmere Island, Arctic Canada; Ph.D. thesis, University of Alberta, Edmonton, Alberta, 172 p.

1996: The last glaciation and sea level history of Fosheim Peninsula, Ellesmere Island, Canadian High Arctic; *Canadian Journal of Earth Sciences*, v. 33, p. 1075–1086.

Bell, T. and England, J.

1993: Extensive glaciations of Ellesmere Island: tentative age estimates based on amino acid ratios and paleoenvironmental implications; *in* 23rd Arctic Workshop Program and Abstracts; Byrd Polar Research Center Miscellaneous Series Publications No. 322, Byrd Polar Research Center, The Ohio State University, Columbus, p. 90–92.

Broecker, W.S., Kulp, J.L., and Tucek, C.S.

1956: Lamont natural radiocarbon measurements III; *Science*, v. 124, p. 154–165.

Craig, B.C. and Fyles, J.G.

1960: Pleistocene geology of Arctic Canada; Geological Survey of Canada, Paper 60-10, 21 p.

Dyck, W. and Fyles, J.G.

1964: Geological Survey of Canada radiocarbon dates III; *Radiocarbon*, v. 6, p. 167–181.

Dyck, W., Fyles, J.G., and Blake, W., Jr.

1965: Geological Survey of Canada radiocarbon dates IV; *Radiocarbon*, v. 7, p. 24–46.

Dyke, A.S. and Morris, T.F.

1988: Drumlin fields, dispersal trains, and ice streams in Arctic Canada; *Canadian Geographer*, v. 32, p. 86–90.

Edlund, S.A. and Woo, M-k.

1992: Eolian deposition on western Fosheim Peninsula, Ellesmere Island, Northwest Territories during the winter of 1990–91; *in* Current Research, Part B; Geological Survey of Canada, Paper 92-1B, p. 91–96.

Edlund, S.A., Alt, B.T., and Young, K.L.

1989: Interaction of climate, vegetation, and soil hydrology at Hot Weather Creek, Fosheim Peninsula, Ellesmere Island, Northwest Territories; *in* Current Research, Part D; Geological Survey of Canada, Paper 89-1D, p. 125–133.

England, J.

1990: The late Quaternary history of Greely Fiord and its tributaries, west-central Ellesmere Island; *Canadian Journal of Earth Sciences*, v. 27, p. 255–270.

Funder, S., Abrahamsen, N., Bennike, O., and Feyling-Hanssen, R.W.

1985: Forested Arctic: evidence from North Greenland; *Geology*, v. 13, p. 542–546.

Fyles, J.G.

1962: Surficial geology, Axel Heiberg–Ellesmere Island, 1961; *in* Fieldwork 1961, (ed.) S.E. Jenness; Geological Survey of Canada, Information Circular 5, p. 4–6.

1989: High terrace sediments, probably of Neogene age, west-central Ellesmere Island, Northwest Territories; *in* Current Research, Part D; Geological Survey of Canada, Paper 89-1D, p. 101–104.

1990: Beaufort Formation (late Tertiary) as seen from Prince Patrick Island, Arctic Canada; *Arctic*, v. 43, p. 393–403.

Garneau, M.

1992: Analyses macrofossiles d'un dépôt de tourbe dans la région de Hot Weather Creek, péninsule de Fosheim, île d'Ellesmere, Territoires du Nord-Ouest; *Géographie physique et Quaternaire*, v. 46, p. 285–294.

2000: Peat accumulation and climatic change in the High Arctic; *in* Environmental Response to Climate Change in the Canadian High Arctic, (ed.) M. Garneau and B.T. Alt; Geological Survey of Canada, Bulletin 529.

Hodgson, D.A.

1974: Surficial geology, geomorphology and terrain disturbance, central Ellesmere Island, District of Franklin; *in* Report of Activities, Part A; Geological Survey of Canada, Paper 74-1A, p. 247–248.

1985: The last glaciation of west-central Ellesmere Island, Arctic Archipelago, Canada; *Canadian Journal of Earth Sciences*, v. 22, p. 347–368.

Hodgson, D.A. (cont.)

1989: Quaternary geology of the Queen Elizabeth Islands; *in* Chapter 6, Quaternary Geology of Canada and Greenland (ed.) R.J. Fulton; Geological Survey of Canada, Geology of Canada, no. 1, p. 441–459 (also Geological Society of America, The Geology of North America, v. K-1, p. 441–459).

Hodgson, D.A. and Edlund, S.A.

1978: Biophysical regions, western Fosheim Peninsula and eastern Axel Heiberg Island; Geological Survey of Canada, Open File 501.

Hodgson, D.A. and Nixon, F.M.

1998: Ground ice volumes determined from shallow cores from western Fosheim Peninsula, Ellesmere Island, Northwest Territories; Geological Survey of Canada, Bulletin 507, 178 p.

Hodgson, D.A., St-Onge, D.A., and Edlund, S.A.

1991: Surficial materials of Hot Weather Creek basin, Ellesmere Island, Northwest Territories; *in* Current Research, Part E; Geological Survey of Canada, Paper 91-1E, p. 157–163.

Jenness, S.E.

1962: Fieldwork 1961; Geological Survey of Canada, Information Circular 5.

Matthews, J.V., Jr. and Ovensen, L.E.

1990: Late Tertiary plant macrofossils from localities in northern North America (Alaska, Yukon, and Northwest Territories); *Arctic*, v. 43, p. 364–392.

McMillan, N.J.

1963: Slide River; *in* Geology of the North-Central Part of the Arctic Archipelago, Northwest Territories (Operation Franklin), (ed.) Y.O. Fortier; Geological Survey of Canada, Memoir 320, p. 400–407.

Miall, A.D.

1986: The Eureka Sound Group (Upper Cretaceous–Oligocene), Canadian Arctic Islands; *Bulletin of Canadian Petroleum Geology*, v. 34, p. 240–270.

Pollard, W.H.

1991: Observations on massive ground ice on Fosheim Peninsula, Ellesmere Island, Northwest Territories; *in* Current Research, Part E; Geological Survey of Canada, Paper 91-1E, p. 223–231.

Pollard, W.H. (cont.)

2000: Distribution and characterization of ground ice on Fosheim Peninsula, Ellesmere Island, Nunavut; *in* Environmental Response to Climate Change in the Canadian High Arctic, (ed.) M. Garneau and B.T. Alt; Geological Survey of Canada, Bulletin 529.

Retelle, M.J.

1986: Glacial geology and Quaternary marine stratigraphy of the Robeson Channel area, northeastern Ellesmere Island, NWT; *Canadian Journal of Earth Sciences*, v. 23, p. 1001–1012.

Ricketts, B.D.

1988: The Eureka Sound Group: alternative interpretations of the stratigraphy and paleogeographic evolution — Reply; *in* Current Research, Part D; Geological Survey of Canada, Paper 88-1D, p. 149–152.

Roots, E.F.

1963: Physiography; *in* Geology of the North-Central Part of the Arctic Archipelago, Northwest Territories (Operation Franklin), (ed.) Y.O. Fortier; Geological Survey of Canada, Memoir 320, p. 418–426.

Sim, V.W.

1961: A note on high-level marine shells on Fosheim Peninsula, N.W.T.; *Geographical Bulletin*, v. 16, p. 120–123.

Thorsteinsson, R. and Tozer, E.T.

1970: Geology of the Arctic Archipelago; *in* Geology and Economic Minerals of Canada, (ed.) R.J.W. Douglas; Geological Survey of Canada, Economic Geology Report No. 1, p. 547–590.

Tozer, E.T.

1956: Geological reconnaissance, Prince Patrick, Eglinton, and western Melville islands, Arctic Archipelago, Northwest Territories; Geological Survey of Canada, Paper 55-5, 32 p.

Trettin, H.P.

1989: The Arctic Islands; *in* The Geology of North America - An Overview, (ed.) A.W. Bally and A.R. Palmer; Geological Society of America, The Geology of North America, v. A; Boulder, Colorado, p. 349–370.

ADDENDUM

As noted above, most previous studies of Ellesmere and adjacent islands have supported a restricted Late Wisconsinan glaciation for the area (with the exception of Blake, 1970). However, recent studies to the northwest of Fosheim Peninsula, along the shores of Nansen Sound (Bednarski, 1998), to the east (England, 1999), to the immediate south (Ó Cofaigh et al., 2000), and farther south (Dyke, 1999), infer pervasive ice over the peninsula.

Bednarski, J.

1998: Quaternary history of Axel Heiberg Island bordering Nansen Sound, Northwest Territories, emphasising the Last Glacial Maximum; *Canadian Journal of Earth Sciences*, v. 35, p. 520–533.

Blake, W., Jr.

1970: Studies of glacial history in Arctic Canada. I. Pumice, radiocarbon dates, and differential postglacial uplift in the eastern Queen Elizabeth Islands; *Canadian Journal of Earth Sciences*, v. 7, p. 634–664.

Dyke, A.S.

1999: Last Glacial Maximum and deglaciation of Devon Island, Arctic Canada: support for an Inuitian Ice Sheet; *Quaternary Science Reviews*, v. 18, p. 393–420.

England, J.

1999: Coalescent Greenland and Inuitian ice during the Last Glacial Maximum; revising the Quaternary of the Canadian High Arctic; *Quaternary Science Reviews*, v. 18, p. 421–456.

Ó Cofaigh, C., England, J., and Zreda, M.

2000: Late Wisconsinan glaciation of southern Eureka Sound: evidence for extensive Inuitian ice in the Canadian High Arctic during the Last Glacial Maximum; *Quaternary Science Reviews*, v. 19, p. 1319–1341.

Appendix A. Radiocarbon dates from Fosheim Peninsula, T. Bell¹ and D. Hodgson².

Age (years BP) ³	$\delta^{13}\text{C}$ (‰)	Laboratory no. ⁴	Field sample no.	Material/Taxa	Sample elevation (m)	Related sea level (m)	Geological environment	Comments	Lat. N	Long. W	Collector/Year	References
45 850 ± 980	—	TO-2228	FP-02-S-9029	Shells	98	—	Deformed sand underlying glacial diamicton	Sample subjected to amino acid analysis (AGL-1862; Appendix B)	80°15'	86°19'	T. Bell, 1990	Bell (1992)
44 420 ± 840	—	TO-2242	FP-55-O-9008	<i>Salix</i> twig	34	—	Bedded sand underlying thick section of marine rhythmites; contact obscured	See also TO-2236 and TO-2243.	80°15'	84°39'	T. Bell, 1990	Bell (1992)
> 41 200*	—	GSC-2688 5L	FG-61-195d	Sedge and moss peat	259	—	Peat underlying gravel terrace	Overlying gravel may be colluvial or fluvial	79°43'	84°25'	J.G. Fyles, 1961	Blake (1974), Dyck et al. (1965)
38 100 ± 380	—	TO-1200		Shell fragments	167	≥167	Surface of clast-poor silt	Marine sediments (possibly reworked?)	79°33'	81°48'	V. Sloan, 1988	Sloan (1990)
> 37 000 > 37 000	-27.1	GSC-5067 5L GSC-5067 2L	SV-90-2	Peat	—	—	Sand	Material does not date a Holocene terrace as assumed; twigs show no evidence of transport (i.e. rounded edges)	79°59'	84°25'	D.A. St-Onge, 1990	McNeely and Jorgensen (1993)
36 300 ± 2000*	—	GSC-111 IF	FG-61-174a	<i>Hiatella arctica</i> , <i>Mya truncata</i> , and <i>Astarte</i> sp.	625	—	Summit ridge of weathered rock and erratic stones	Likely glacially transported; sample consisted of whole shell valves and fragments	79°55'	86°22'	J.G. Fyles, 1961	Dyck and Fyles (1964)
>36 000*	—	GSC-2688 BE	FG-61-195d	Sedge and moss peat	259	—	Same sample as GSC-2688 5L	Same sample as GSC-2688 5L	79°43'	84°25'	J.G. Fyles, 1961	Blake (1974), Dyck et al. (1965)
34 950 ± 340**	—	TO-1201		Shell fragments	167	≥167	Same site as TO-1200	Same site as TO-1200	79°33'	81°48'	V. Sloan, 1988	Sloan (1990)
> 33 000*	—	L-266C		Wood	—	—	On gravel ridge		—	—	P.F. Bruggeman	Broecker et al. (1956)
30 300 ± 1600*	—	GSC-111 OF	FG-61-174a	<i>Hiatella arctica</i> , <i>Mya truncata</i> , and <i>Astarte</i> sp.	625	—	Same sample as GSC-111 IF	Same sample as GSC-111 IF	79°55'	86°22'	J.G. Fyles, 1961	Dyck and Fyles (1964)
29 380 ± 230**	—	TO-1198		Shell fragments	132	≥132	Surface of diamicton	Marine sediments (possibly reworked?)	79°32'	81°40'	V. Sloan, 1988	Sloan (1990)
28 700 ± 600*	—	GSC-51	FG-61-207h	<i>Hiatella arctica</i> fragments	191	—	Hillock of weathered rock, erratic stones	Likely glacially transported; highest evidence of marine overlap around Slidre Fiord is at 160 m	79°51'	85°42'	J.G. Fyles, 1961	Dyck and Fyles (1962)
19 500 ± 1100*	—	L-548		<i>Hiatella arctica</i> <i>Mya truncata</i>	607	—	Same site as GSC-111	Same site as GSC-111	79°54'	86°20'	V.W. Sim, 1955	Andrews and Drapier (1967), Sim (1961)
12 750 ± 240	—	UL-1005		Herbaceous and twiggy organic debris	140	—	Eroded section in polygon field; 190-195 cm depth	Site 21 in Garneau, 2000	79°58'	84°28'	M. Garneau, 1992	Gajewski et al. (1995)
10 600 ± 90	+1.04	GSC-4784	EJ-88-92S	<i>Hiatella arctica</i>	122-123	>123	Silt strata with abundant shells exposed on surface by deflation	Oldest dated shell sample from marine silt on Fosheim Peninsula	80°00'	84°30'	S.A. Eklund and J.G. Fyles, 1988	Hodgson et al. (1991), McNeely and Jorgensen (1992)
9560 ± 90	—	TO-2240	FP-49-S-9006	<i>Portlandia arctica</i>	90	>88 ≤141	Marine rhythmites in 17 m thick section	Sample from same section as TO-2611 and considered more reliable	79°56'	84°17'	T. Bell, 1990	Bell (1996)
9550 ± 250*	—	L-647B		Marine pelecypods	110	>110	Surface	Note GSC-1800 is higher and younger in this area	79°58.8'	85°34.8'	F. Müller, 1959, 1960?	Müller (1963)

9280 ± 120	+2.40	GSC-1800	HCA-72-22-7-5B	<i>Mya truncata</i>	124	>125	In situ shells within interbedded sand and clayey silt, below gravel beach; shells similar those at 129 m	Highest nearby beaches at 140 m; wave-cut notch and washing limit at 160 m	79°59'	85°37'	D.A. Hodgson, 1972	Hodgson (1985)
9260 ± 130		UL-1037		Moss peat	140	>126 ≤145	Eroded section in polygon field; 180–183 cm depth	Site 21 in Garneau, 2000	79°58'	84°28'	M. Garneau, 1992	Gajewski et al. (1995)
9230 ± 100	—	TO-1963	SP-02-S-8917	<i>Poritandia arctica</i>	126		Bottomsets	Dates delta upvalley at 143 m a.s.l.	79°59'	84°05'	T. Bell, 1989	Bell (1996)
9220 ± 140		UL-1008		Moss and sedge peat	140		Eroded section in polygon field; 95–98 cm depth	Site 21 in Garneau, 2000	79°58'	84°28'	M. Garneau, 1992	Gajewski et al. (1995)
8080 ± 80	—	TO-2236	FP-22-S-9025	<i>Poritandia arctica</i>	63	>63 ≤149	Marine rhythmites; same site as TO-2242 and TO-2243	Together with TO-2243, these dates provide an average sedimentation rate of 6 mm/a between 9.1 and 7.9 ka BP at this site	80°15'	84°39'	T. Bell, 1990	Bell (1996)
8990 ± 80	—	TO-2232	FP-15-S-9017	<i>Hiatella arctica</i>	137	>137 ≤149	Surface of stony silt	Shells collected within 12 m of Holocene marine limit	80°11'	85°28'	T. Bell, 1990	Bell (1996)
8920 ± 110	-28.1	GSC-5948	ES-20-0-9422	Organic material	86	—	Discrete lenses of ice-rich, sandy clay overlain by sand and gravel forming marine terrace	Sample provides maximum date on marine limit at 95 m	79°35'	87°27.5'	A. Altken, 1994	
8900 ± 90	—	TO-2611	FP-50-B-9006	Echinoderm spicules	86.5	>83 ≤141	Near base of 17 m thick section of marine mud	Dated material considered less reliable than TO-2240, 3.5 m higher in section	79°56'	84°17'	T. Bell, 1990	Bell (1996)
8880 ± 90	—	TO-2235	FP-21-S-9025	<i>Hiatella arctica</i>	110	>110	Surface of stony silt	Minimum date on deglaciation of adjacent ridge top	80°04'	86°34'	T. Bell, 1990	Bell (1996)
8710 ± 140*	—	GSC-254	FG-61-209c	<i>Hiatella arctica</i>	140	>140	Surface of marine silt	Highest Holocene shells recorded from Queen Elizabeth Island; also see GSC-243	79°48'	86°15'	J.G. Fyles, 1961	Dyck et al. (1965), Hodgson (1985)
8680 ± 80	+1.03	GSC-5156	FP-28-S-9026	<i>Hiatella arctica</i>	132	>132 ≤150	Surface of stony silt	Considered to be same site as GSC-254	79°48'	86°18'	T. Bell, 1990	Bell (1996)
8640 ± 80	—	TO-2237	FP-28-S-9026	<i>Hiatella arctica</i>	132	>132 #150	Surface of stony silt	Considered to be same site as GSC-254	79°48'	86°18'	T. Bell, 1990	Bell (1996)
8570 ± 120	+1.10	GSC-5155	FP-26-S-8906	<i>Mya truncata</i>	100	>100 ≤145	Surface of marine silt	Minimum date on establishment of local marine limit at 145 m	79°58'	84°26'	T. Bell, 1989	Bell (1996), McNeely and Jorgensen (1993)
8570 ± 100	—	TO-4588	FP-59-S-9313	<i>Mya truncata</i>	99	>99 ≤143	From base of marine rhythmites overlying massive ground ice	Maximum date on age of ground ice (segregated) formation	79°56'	84°15'	T. Bell and W. Pollard, 1993	
8520 ± 80	+1.25	GSC-4708	LC-4-S-88	<i>Mya truncata</i>	100	>111 ≤146	Marine silt	Fossiliferous silt was likely deposited during melting of local ice cap upvalley	79°57'	85°21'	T. Bell, 1988	Bell (1996), McNeely and Jorgensen (1992)
8480 ± 80	—	TO-2241	FP-52-S-8914	<i>Mya truncata</i>	93	>93 ≤147	Marine silt	Minimum date on marine occupation of lowland south of Romulus Lake	79°50'	85°13'	T. Bell, 1989	Bell (1996)

¹ Department of Geography, Memorial University of Newfoundland, St. John's, Newfoundland A1B 3X9

² Terrain Sciences Division, Geological Survey of Canada, 601 Booth Street, Ottawa, Ontario K1A 0E8

³ The error for GSC dates represents 95% probability; for all others, it represents 68.3% probability. The $\delta^{13}\text{C}$ base for GSC dates is given where the age is corrected for isotopic fractionation. A single asterisk denotes an uncorrected GSC date. The GSC standard values for marine shells and wood are 0.0‰ and -25‰, respectively. Most IsoTrace dates have been corrected for isotopic fractionation to a base of $\delta^{13}\text{C} = -25\text{‰}$ and, in the case of marine shells, they have also been adjusted for a reservoir effect of 410 years, which is roughly equivalent to a fractionation correction to a base of $\delta^{13}\text{C} = 0.0\text{‰}$. A double asterisk denotes IsoTrace dates that have been corrected for isotopic fractionation to a base of $\delta^{13}\text{C} = 0\text{‰}$, but with no adjustment for the marine reservoir effect.

⁴ Laboratory designations: Beta, Beta Analytic Inc.; GSC, Geological Survey of Canada Radiocarbon Laboratory; L, Lamont Radiocarbon Laboratory; TO, IsoTrace Radiocarbon Laboratory; UL, Universit  Laval

Appendix A. (cont.)

Age (years BP) ³	$\delta^{13}\text{C}$ (‰)	Laboratory no. ⁴	Field sample no.	Material/Taxa	Sample elevation (m)	Related sea level (m)	Geological environment	Comments	Lat. N	Long. W	Collector/Year	References
8450 ± 140*	—	GSC-243	FG-01-209c	<i>Hiatella arctica</i>	140	>140	Surface of marine silt	Second preparation; see GSC-254	79°48'	86°15'	J.G. Fyles, 1961	Dyck et al. (1965), Hodgson (1985)
8450 ± 80	—	TO-2229	FP-06-S-8927	<i>Mya truncata</i>	94	>94 ≤149	Surface of stony silt	Minimum date on marine limit in this area	80°15'	85°02'	T. Bell, 1989	Bell (1996)
8440 ± 80	—	TO-2233	FP-19-S-9025	<i>Mya truncata</i>	94	>94	Surface of marine silt	Minimum date on retreat of outlet glacier from upland ice cap	80°11'	86°33'	T. Bell, 1990	Bell (1996)
8430 ± 70	—	TO-2245	FP-88-S-9012	<i>Hiatella arctica</i>	101	>101	Silt	Minimum date on marine overlap in area	79°14'	85°30'	T. Bell, 1990	Bell (1996)
8280 ± 80	—	TO-2238	FP-35-S-9030	<i>Mya truncata</i>	89	>89 ≤148	Deflating silt surface	Provides minimum date on establishment of marine-limit delta upvalley at 148 m a.s.l.	79°46'	85°52'	T. Bell, 1990	Bell (1996)
8270 ± 80	—	TO-2234	FP-21-S-8929	<i>Mya truncata</i>	105	>105 ≤141	Sandy silt	From surface of Holocene sediment fill in Slidre River valley	79°56'	84°12'	T. Bell, 1989	Bell (1996)
8230 ± 80	+2.11	GSC-4957	RL-14-S-8915	<i>Mya truncata</i>	110	>124	Stony marine silt	Marine silt drapes distal side of moraine considered to predate the last glaciation	79°51'	85°17'	T. Bell, 1989	Bell (1992, 1996), McNeely and Jorgensen (1993)
8230 ± 80	—	TO-1964	SR-11-S-8929	<i>Mya truncata</i>	95	>95 ≤141	Silt surface	From surface of Holocene sediment fill in Slidre River valley	79°56'	84°12'	T. Bell, 1989	Bell (1996)
8230 ± 70**	—	TO-1242	ER-05-S-88	<i>Mya truncata</i>	99	>99 ≤148	Silt	Minimum date on local marine limit	79°44'	85°47'	T. Bell, 1988	Bell (1996)
8210 ± 80	—	TO-2231	FP-08-S-9002	<i>Mya truncata</i>	59	>59	Silt	Provides date on glacier runoff from upland ice cap	80°05'	86°33'	T. Bell, 1990	Bell (1996)
8190 ± 110	+2.22	GSC-1822	HCA-72-23-7-2	<i>Mya truncata</i>	91	>91	Surface of gravel and sand beach ridges	Highest nearby beaches at 136 m	80°15.5'	84°17.5'	D.A. Hodgson, 1972	Hodgson (1985)
7970 ± 90	—	TO-1966	GF-06-T-8930	Narwhal tusk	5	>5 ≤149	Diamicton	Tusk recovered from colluvial deposits in deep gully	80°17'	84°18'	T. Bell, 1989	Bell (1996)
7930 ± 70	+1.36	GSC-4697	IB-BTP-27/0788	<i>Mya truncata</i>	90	≥120	Marine silt	Dates local marine limit marked by terrace at 120 m	79°42'	81°40'	J. England and V. Sloan, 1988	England (1992), Sloan (1990)
7920 ± 100	+0.49	GSC-5119	FP-30-S-9027	<i>Hiatella arctica</i>	75	>75	Glaciomarine mud overlain by beaches to 106 m	Minimum date on retreat of outlet glacier from local ice cap	79°51'	86°25'	T. Bell, 1990	Bell (1996), McNeely and Jorgensen (1993)
7940 ± 90	-27.3	GSC-5066 5L	SV-90-1	Basal peat	60	>80	From drained, dissected wetland in a pre-existing valley	Sample from base of same section that yielded GSC-2005. Age of sample conflicts with local emergence history; see Bell (1996). See also GSC-5066-2L	79°56'	84°32'	D.A. St-Onge, 1990	Hodgson et al. (1991)
7910 ± 120	-27.3	GSC-5066 2L	SV-90-1	Sedge peat	60	>80	Eroded section in polygon field; 285–288 cm depth	Site 5 in Garneau, 2000	79°58'	84°32'	D.A. St-Onge, 1990	Gajewski et al. (1995)
7910 ± 100	—	UL-1007	—	Moss peat	140	—	Eroded section in polygon field; 90–93 cm depth	Site 21 in Garneau, 2000	79°58'	84°28'	M. Garneau, 1992	Gajewski et al. (1995)
7900 ± 100	+1.42	GSC-4741	STV-3-5-88	<i>Mya truncata</i>	65	>64 ≤141	Marine silt	Minimum estimate on retreat of local ice in northern Sawtooth Range	79°54'	82°34'	J. England and T. Bell, 1988	England (1990)

7890 ± 80	—	TO-2243	FP-56-S-9008	<i>Mya truncata</i>	70	>70 ≤149	Surface of 36 m thick section of marine rhythmites; same site as TO-2242 and TO-2232	80°15'	84°39'	T. Bell, 1990	Aitken and Bell (1998), Bell (1996)
7680 ± 70		Beta-62286		Shells	100		Raised beach	79°58'	84°28'	M. Garneau and K. Gajewski, 1992	
7420 ± 100	+0.87	GSC-5549	92.25.7.9.2	<i>Mya truncata</i>	100		Raised beach	79°58'	84°28'	M. Garneau and K. Gajewski, 1992	
7120 ± 80	-27.0	GSC-5180	FP-23.07.90.05	Basal peat	122	—	Polygon eroded by landslide; 280–283 cm depth; peat overlying sand	79°59'	84°08'	C. B. égin and Y. Michaud, 1990	Gajewski et al. (1995), McNeely and Atkinson (1996)
7040 ± 90	—	TO-4589	FP-68-S-9317	<i>Bathycarca</i> sp.	25	—	Marine rhythmites	79°28'	84°23'	T. Bell, 1993	Aitken and Bell (1998)
6670 ± 70	—	TO-2230	FP-06-S-9001	<i>Astarte</i> sp.	60	>60 ≤149	Surface of marine silt	80°14'	85°18'	T. Bell, 1990	Aitken and Bell (1998), Bell (1996)
6540 ± 290		TO-3879		Lake sediment, gyttja	305		Solstice lake; 92–93 cm interval from 100.5 cm core	79°25'	84°07'	A. Wolfe, 1992	Wolfe (1994)
6490 ± 90	+2.15	GSC-5713	FP-03-S-9327	<i>Astarte</i> sp.	44–51	—	Deflating marine silt	79°42'	85°30'	T. Bell and W. Pollard, 1993	
6480 ± 70	—	TO-2244	FP-85-S-9012	<i>Mya truncata</i>	16	≥30	Bottomsets underlying delta foresets	79°19'	85°32'	T. Bell, 1990	Bell (1996)
6430 ± 50		Beta-77037		Moss peat	60		Eroded section in polygon field; 51–58 cm depth	79°58'	84°28'	M. Garneau, 1991	Gajewski et al. (1995), Garneau (1992)
6380 ± 70	+1.65	GSC-5959	CF-01-S-2993	<i>Mya truncata</i> <i>Hiatella arctica</i>	30	>30	Sandy mud associated with marine delta	79°39'	81°44'	A. Aitken, 1993	
6350 ± 90	+1.54	GSC-5117	FP-90-S-9012	<i>Hiatella arctica</i>	28	≥30	Gravel foresets	79°14'	85°38'	T. Bell, 1990	Bell (1996), McNeely and Jorgensen (1993)
6250 ± 70		TO-2677		<i>Cassiope</i> leaf fragments	120	—	Polygon eroded by landslide; surface sample	79°59'	84°08'	C. Bégin and Y. Michaud, 1990	Gajewski et al. (1995)
6040 ± 170*	—	GSC-5081	HCA-90-8-8-1	<i>Salix</i> sp. twigs	15	>44?	Detrital organic material in clayey silt	79°55'	84°38'	D.A. Hodgson, 1990	Hodgson et al. (1991)

1 Department of Geography, Memorial University of Newfoundland, St. John's, Newfoundland A1B 3X9

2 Terrain Sciences Division, Geological Survey of Canada, 601 Booth Street, Ottawa, Ontario K1A 0E8

3 The error for GSC dates represents 95% probability; for all others, it represents 68.3% probability. The $\delta^{13}\text{C}$ base for GSC dates is given where the age is corrected for isotopic fractionation. A single asterisk denotes an uncorrected GSC date. The GSC standard values for marine shells and wood are 0.0‰ and -25‰, respectively. Most IsoTrace dates have been corrected for isotopic fractionation to a base of $\delta^{13}\text{C} = -25\text{‰}$, and, in the case of marine shells, they have also been adjusted for a reservoir effect of 410 years, which is roughly equivalent to a fractionation correction to a base of $\delta^{13}\text{C} = 0.0\text{‰}$. A double asterisk denotes IsoTrace dates that have been corrected for isotopic fractionation to a base of $\delta^{13}\text{C} = 0\text{‰}$, but with no adjustment for the marine reservoir effect.

4 Laboratory designations: Beta, Beta Analytic Inc.; GSC, Geological Survey of Canada Radiocarbon Laboratory; L, Lamont Radiocarbon Laboratory; TO, IsoTrace Radiocarbon Laboratory; UL, Université Laval

Appendix A. (cont.)

Age (years BP) ³	$\delta^{13}\text{C}$ (‰)	Laboratory no. ⁴	Field sample no.	Material/Taxa	Sample elevation (m)	Related sea level (m)	Geological environment	Comments	Lat. N	Long. W	Collector/Year	References
6010 ± 70	+3.54	GSC-5738	FP-67-S-9317	<i>Astarte</i> sp.	33	—	Marine silt	Prodeltaic deposit along Eureka Sound	79°28'	84°24'	T. Bell, 1993	
5870 ± 80	—	TO-1965	BSC-07-S-8909	<i>Portlandia arctica</i>	21	>21	Marine rhythmites	Sample overlain by another 12 m of rhythmites, which were deposited prior to 4 ka BP. Average sedimentation rate for this period was ≥ 6.4 mm/a.	79°53'	84°37'	T. Bell, 1989	Bell (1996)
5830 ± 100		Beta-51988		Peat	120		Polygon eroded by landslide; 180–183 cm depth	Site 19 in Garneau, 2000	79°59'	84°08'	C. Bégin and Y. Michaud, 1990	Gajewski et al. (1995)
5560 ± 60		UL-1006		Moss and sedge peat	140		Eroded section in polygon field; 35–38 cm depth	Site 21 in Garneau, 2000	79°58'	84°28'	M. Garneau, 1992	Gajewski et al. (1995)
5420 ± 100		UL-1009		Herbaceous and twiggy organic debris	120		Polygon eroded by landslide; 200–203 cm depth	Site 19 in Garneau, 2000	79°59'	84°08'	M. Garneau, 1991	Gajewski et al. (1995)
5280 ± 60	-26.7	GSC-3148	HCA-78-B/7-3c (I)	Wood	40	≥ 44 ?	Delta-front deposits; sample from 26 m above base of 30 m exposure	Provides possible date for former sea level at 44 m a.s.l. (top of section)	79°54'	84°42'	D.A. Hodgson, 1978	Hodgson et al. (1991)
5200 ± 90	+1.39	GSC-5147	FP-82-S-9012	<i>Hiatella arctica</i>	14	≥ 16	Gravel foresets; upper contact truncated	Provides date on former sea level higher than 16 m above present level	79°19'	85°31'	T. Bell, 1990	McNeely and Jorgensen (1993)
5070 ± 70		TO-3039		Sedge peat	60		Eroded section in polygon field; 300 cm depth	Site 5 in Garneau, 2000	79°58'	84°28'	M. Garneau, 1991	Gajewski et al. (1995)
4990 ± 70		TO-3037		Moss peat	60		Eroded section in polygon field; surface sample	Site 5 in Garneau, 2000	79°58'	84°28'	M. Garneau, 1991	Gajewski et al. (1995)
4970 ± 60		Beta-77034		Moss peat	60		Eroded section in polygon field; 163–165 cm depth	Site 6 in Garneau, 2000	79°58'	84°28'	M. Garneau, 1991	Gajewski et al. (1995), Gajewski (1992)
4950 ± 60*	—	GSC-2005	HCA-72-117-3a	Rhizome moss peat	60	>20	Drained, dissected wetland in pre-existing valley	Sample 6 cm thick from 30 cm below top of 2.2 m peat. in same exposure as GSC-5066	79°56'	84°35'	D.A. Hodgson, 1972	Ovenden (1988)
4940 ± 80		Beta-51990		Peat	45		Eroded section in polygon field; surface sample	Site 4 in Garneau, 2000	79°58'	84°28'	C. Bégin and Y. Michaud, 1990	Gajewski et al. (1995)
4900 ± 70	-32.0	GSC-5570	91-10-B10	Mixture of moss and sedge peat	60		Eroded section in polygon field; 148–151 cm depth	Site 5 in Garneau, 2000	79°58'	84°28'	M. Garneau, 1991	Gajewski et al. (1995)
4860 ± 80		Beta-77033		Moss peat	60		Eroded section in polygon field; 75–78 cm depth	Site 6 in Garneau, 2000	79°58'	84°28'	M. Garneau, 1991	Gajewski et al. (1995), Gajewski (1992)
4850 ± 80		UL-1012		Sedge peat	60		Eroded section in polygon field; 10–12 cm depth	Site 6 in Garneau, 2000	79°58'	84°28'	M. Garneau, 1991	Gajewski et al. (1995), Gajewski (1992)
4840 ± 100		Beta-77035		Sedge peat	60		Eroded section in polygon field; 173–178 cm depth	Site 6 in Garneau, 2000	79°58'	84°28'	M. Garneau, 1991	Gajewski et al. (1995), Gajewski (1992)

4820 ± 70	-27.9	GSC-4822	EJ-88-128A	Peat	114	>20	Sample from 1.5 m depth, exposed by erosion along frost fissure	Drained wetland; see also GSC-4838	79°59'	84°29'	S.A. Edlund, 1988	Hodgson et al. (1991)
4590 ± 60		Beta-77036		Moss peat	60		Eroded section in polygon field; 35–42 cm depth	Site 6 in Garneau, 2000	79°58'	84°28'	M. Garneau, 1991	Gajewski et al. (1995), Garneau (1992)
4500 ± 70		TO-3038		Moss peat	60		Eroded section in polygon field; 20–23 cm depth	Site 5 in Garneau, 2000	79°58'	84°28'	M. Garneau, 1991	Gajewski et al. (1995)
4500 ± 90	+1.38	GSC-4755	STV-2-5-88	<i>Hiatella arctica</i> <i>Mya truncata</i>	6	—	Marine silt and clay		79°54'	82°32'	J. England and T. Bell, 1988	McNeely and Jorgensen (1992)
4310 ± 80	-29.4	GSC-5554	91.10.B7.100	Moss peat	60		Eroded section in polygon field; 100–103 cm depth	Site 5 in Garneau, 2000	79°58'	84°28'	M. Garneau, 1991	Gajewski et al. (1995)
4220 ± 130*	—	GSC-592	FG-61-210c	<i>Astarte</i> sp.	11	>11	Beach surface, gravely silt	Sample part of Slidre Fjord series; see also GSC-589 and GSC-590	79°59'	85°37'	J.G. Fyles, 1961	Hodgson (1985)
4050 ± 60	-29.5	GSC-4838	EJ-88-127C	Peat	84 ft? 26	>10	Sample near base of 2 m peat (over rock) exposed by erosion along frost fissures	Drained wetland; see also GSC-4822	79°58'	84°28'	S.A. Edlund, 1988	Hodgson et al. (1991)
3970 ± 80*	—	GSC-2039	HCA-72-3/8-2c	Rhizome-moss peat	35? 40	>10	Delta wetland over delta-front deposit over prodelatic sand and silt	This peat sample used to constrain relative sea level history; see TO-1965	79°54'	84°38'	D.A. Hodgson, 1972	Hodgson et al. (1991), Ovenden (1988)
3930 ± 80	-29.2	GSC-5547	91.10.A3.45	Moss peat	60		Eroded section in polygon field; 45–48 cm depth	Site 5 in Garneau, 2000	79°58'	84°28'	M. Garneau, 1991	Gajewski et al. (1995)
3870 ± 80		UL-1004		Moss peat — <i>Calliergon</i> sp.	45	—	Eroded section in polygon field; 50–53 cm depth	Site 4 in Garneau, 2000	79°58'	84°28'	M. Garneau, 1992	Gajewski et al. (1995)
3860 ± 80		Beta-51989		Peat	45	—	Eroded section in polygon field; 135–138 cm depth	Site 4 in Garneau, 2000	79°58'	84°28'	C. Bégin and Y. Michaud, 1990	Gajewski et al. (1995)
3850 ± 80		Beta-51994		Moss peat	60		Eroded section in polygon field; surface sample	Site 5 in Garneau, 2000	79°58'	84°28'	M. Garneau, 1991	Gajewski et al. (1995)
3620 ± 160	—	TO-3759		<i>Portlandia arctica</i>	—	—	Sample from 70 cm below Romulus Lake bottom in laminated mud	Maximum age of isolation of Romulus Lake (~8 m a.s.l.) from the sea	79°53'	85°05'	G. Davidge, 1992	Davidge (1994)
3420 ± 130*	—	GSC-589	FG-61-210b	<i>Astarte</i> sp.	3.5	>3.5	Beach surface, gravely silt	Sample part of Slidre Fjord series; see also GSC-592 and GSC-590	79°59'	85°37'	J.G. Fyles, 1961	Hodgson (1985)
3210 ± 110		UL-1036		Moss peat with herbs	45	—	Eroded section in polygon field; 85–88 cm depth	Site 4 in Garneau, 2000	79°58'	84°28'	M. Garneau, 1992	Gajewski et al. (1995)
3140 ± 110	-25.8	GSC-5586	92.14H.120	Herbaceous and twiggly organic debris	45	—	Eroded section in polygon field; 120–125 cm depth	Site 4 in Garneau, 2000	79°58'	84°28'	M. Garneau, 1992	Gajewski et al. (1995)
2930 ± 60		TO-3040		Salix fragments and <i>Carex</i> seeds	50	—	Cored section in polygon field; 150–153 cm depth	Site 13 in Garneau, 2000	79°58'	84°28'	M. Garneau, 1991	Gajewski et al. (1995)

1 Department of Geography, Memorial University of Newfoundland, St. John's, Newfoundland A1B 3X9

2 Terrain Sciences Division, Geological Survey of Canada, 601 Booth Street, Ottawa, Ontario K1A 0E8

3 The error for GSC dates represents 95% probability; for all others, it represents 68.3% probability. The $\delta^{13}\text{C}$ base for GSC dates is given where the age is corrected for isotopic fractionation. A single asterisk denotes an uncorrected GSC date. The GSC standard values for marine shells and wood are 0.0‰ and -25‰, respectively. Most IsoTrace dates have been corrected for isotopic fractionation to a base of $\delta^{13}\text{C} = -25\text{‰}$ and, in the case of marine shells, they have also been adjusted for a reservoir effect of 410 years, which is roughly equivalent to a fractionation correction to a base of $\delta^{13}\text{C} = 0.0\text{‰}$. A double asterisk denotes IsoTrace dates that have been corrected for isotopic fractionation to a base of $\delta^{13}\text{C} = 0\text{‰}$, but with no adjustment for the marine reservoir effect.

4 Laboratory designations: Beta, Beta Analytic Inc.; GSC, Geological Survey of Canada Radiocarbon Laboratory; L, Lamont Radiocarbon Laboratory; TO, IsoTrace Radiocarbon Laboratory; UL, Université Laval

Appendix A. (cont.)

Age (years BP) ³	$\delta^{13}\text{C}$ (‰)	Laboratory no. ⁴	Field sample no.	Material/Taxa	Sample elevation (m)	Related sea level (m)	Geological environment	Comments	Lat. N	Long. W	Collector/Year	References
2710 ± 130*	—	GSC-590	FG-61-210a	<i>Astarte</i> sp.	1.5	>1.5	Beach surface, gravely silt	Sample part of Sidre Fiord series; see also GSC-592 and GSC-589	79°59'	85°37'	J.G. Fyles, 1961	Hodgson (1985)
2700 ± 70	-26.2	GSC-5577	92.14F100	Sedge peat	45	—	Eroded section in polygon field; 100–103 cm depth	Site 4 in Garneau, 2000	79°58'	84°28'	M. Garneau, 1992	Gajewski et al. (1995)
2640 ± 70	-27.5	GSC-5137	FP-25.07.90-02	<i>Salix</i> fragments and <i>Carex</i> seeds	50	—	Cored section in polygon field; 110–113 cm depth	Site 13 in Garneau, 2000	79°56'	84°30'	M. Garneau, 1991	Gajewski et al. (1995), McNeely and Atkinson (1996)
2580 ± 60	-26.8	GSC-5589	92.29.7.15.3	Sedge peat	110	—	Surface of polygon eroded by landslide	Site 20 in Garneau, 2000	79°58'	84°28'	M. Garneau, 1992	Gajewski et al. (1995)
2510 ± 70	-31.1	GSC-5575	92.14B.60	Moss peat — <i>Calliergon</i> sp.	45	—	Eroded section in polygon field; 58–61 cm depth	Site 4 in Garneau, 2000	79°58'	84°28'	M. Garneau, 1992	Gajewski et al. (1995)
1910 ± 60	-27.9	GSC-5280	FP-23.07.90-01	Peat	122	—	Polygon eroded by landslide; surface sample	Site 19 in Garneau, 2000	79°59'	84°08'	C. Bégin and Y. Michaud, 1990	Gajewski et al. (1995), McNeely and Atkinson (1996)
1890 ± 80	—	Bela-51992	—	Peat	50	—	Cored section in polygon field; 50–53 cm depth	Site 13 in Garneau, 2000	79°58'	84°28'	C. Bégin and Y. Michaud, 1990	Gajewski et al. (1995)
1350 ± 50	—	TO-3878	—	Lake sediment, <i>gyttja</i>	305	—	Solstice Lake; 33–34 cm interval from 100.5 cm core	See Wolfe (2000)	79°25'	84°07'	A. Wolfe, 1992	Wolfe (1994)
930 ± 60	—	Bela-51993	—	Peat	50	—	Cored section in polygon field; 20–23 cm depth	Site 13 in Garneau, 2000	79°58'	84°28'	C. Bégin and Y. Michaud, 1990	Gajewski et al. (1995)
450 ± 60	—	TO-4587	FP-29-S-9306	<i>Colus</i> sp.	143	—	Surface sample on silty sand at marine limit	According to this date, sample was carried from lower elevation to sample site	80°04'	83°40'	T. Bell, 1993	—
330 ± 50	-27.9	GSC-4734	SAW 1	Peat	450	—	Peat overlain by till in front of glacier in Sawtooth Mountain Range	Date confirms glacier readvance during Little Ice Age	79°54'	83°14'	B.H. Luckman, 1988	McNeely and McCuaig (1991)
150 ± 50	-28.8	GSC-3200	HCA-78-247-5	Plant: <i>Dryas integrifolia</i>	-150	—	In situ (dead?) plants on bedrock 1–2 m from snout of retreating glacier	Recently deglaciated	79°04.5'	80°56'	D.A. Hodgson, 1978	Blake (1981, 1982)

¹ Department of Geography, Memorial University of Newfoundland, St. John's, Newfoundland A1B 3X9

² Terrain Sciences Division, Geological Survey of Canada, 601 Booth Street, Ottawa, Ontario K1A 0E8

³ The error for GSC dates represents 95% probability, for all others, it represents 68.3% probability. The $\delta^{13}\text{C}$ base for GSC dates is given where the age is corrected for isotopic fractionation. A single asterisk denotes an uncorrected GSC date. The GSC standard values for marine shells and wood are 0.0‰ and -25‰, respectively. Most IsoTrace dates have been corrected for isotopic fractionation to a base of $\delta^{13}\text{C} = -25\text{‰}$ and, in the case of marine shells, they have also been adjusted for a reservoir effect of 410 years, which is roughly equivalent to a fractionation correction to a base of $\delta^{13}\text{C} = 0.0\text{‰}$. A double asterisk denotes IsoTrace dates that have been corrected for isotopic fractionation to a base of $\delta^{13}\text{C} = 0\text{‰}$, but with no adjustment for the marine reservoir effect.

⁴ Laboratory designations: Beta, Beta Analytic Inc.; GSC, Geological Survey of Canada Radiocarbon Laboratory; L, Lamont Radiocarbon Laboratory; TO, IsoTrace Radiocarbon Laboratory; UL, Université Laval

Appendix B. Amino-acid ratios from ice-transported shells on Fosheim Peninsula, Ellesmere Island, Nunavut. Compiled by T. Bell

Laboratory number ^a	Genus ^b	alle/Ile ratios ^c		Enclosing material	Sample elev. (m)	Lat. N	Long. W	Comments
		Free	Total					
GROUP I^d								
AGL-1688A	<i>H.a.</i>	0.593	0.133	Till surface	198	80°13'	86°17'	Abundant granite erratics on till surface.
B	<i>H.a.</i>	0.620	0.106					
C	<i>H.a.</i>	0.466	0.107					
AGL-1704A	<i>M.t.*</i>	0.555	0.185	Till	134	80°14'	85°57'	Granite erratics present.
B	<i>M.t.*</i>	0.510	0.058					
C	<i>M.t.*</i>	0.712	0.300					
D	<i>H.a.*</i>	0.606	0.173					
AGL-1710A	<i>H.a.</i>	0.465	0.091	Till(?)	98	80°15'	86°15'	Till overlies sand (AGL-1862). Granite erratics present.
B	<i>M.t.</i>	0.372	0.093					
C	<i>Ast.*</i>	0.532	0.130					
AGL-1862A	fragments	0.599	–	Subtill sand	98	80°15'	80°19'	Shells dated 45 850 ± 980 BP (TO-2228) (Bell, 1992)
AGL-1684A	<i>H.a.</i>	0.408	0.089	Till surface	157	80°10'	85°30'	Sample included whole valves. No granite erratics observed.
B	<i>H.a.</i>	0.480	0.109					
C	<i>H.a.</i>	0.482	0.096					
AGL-1863A	<i>M.t.</i>	0.741	0.164	Till surface	165	80°11'	85°00'	Till overlain by outwash graded to 170 m a.s.l.
B	<i>M.t.</i>	0.650	0.182					
C	<i>Ast.</i>	0.646	0.215					
AGL-1700A	<i>M.t.*</i>	0.400	0.118	Beach sand and gravel	129	80°13'	84°50'	Beach material reworked from underlying till. No granite erratics observed.
AGL-1701A	<i>H.a.</i>	0.501	0.118	Till surface	225	79°19'	85°32'	No granite erratics observed.
B	<i>H.a.</i>	0.564	0.144					
C	<i>H.a.</i>	0.604	0.116					
D	<i>H.a.</i>	0.588	0.130					

¹ Department of Geography, Memorial University of Newfoundland, St. John's, Newfoundland, A1B 3X9

a Shell samples were analyzed at the Amino Acid Geochronology Laboratory, University of Massachusetts. The letters A to E refer to individual valves or fragments analyzed from each sample.

b Shells: *H.a.*, *Hiattella arctica* *Ast.*, *Astarte* sp.

M.t., *Mya truncata*

* denotes fragments that were identified by their characteristic amino acid content.

c Each ratio is a mean value for at least three individual analyses on each valve or fragment.

d Till samples were grouped by location and amino acid ratios. See Bell (1992) and text for explanation.

REFERENCES

Bell, T.

1992: Glacial and sea-level history of western Fosheim Peninsula, Ellesmere Island, Arctic Canada; Ph.D. thesis, University of Alberta, Alberta, 172 p.

Dyck, W. and Fyles, J.G.

1964: Geological Survey of Canada radiocarbon dates III; Radiocarbon, v. 6, p. 167–181.

Dyck, W., Fyles, J.G., and Blake, W., Jr.

1965: Geological Survey of Canada radiocarbon dates IV; Radiocarbon, v. 7, p. 24–46.

Sim, V.W.

1961: A note on high-level marine shells on Fosheim Peninsula, N.W.T.; Geographical Bulletin, v. 16, p. 120–123.

Appendix B. (cont.)

Laboratory number ^a	Genus ^b	alle/le ratios ^c		Enclosing material	Sample elev. (m)	Lat. N	Long. W	Comments
		Free	Total					
GROUP II								
AGL-1707A B C	<i>M.t.</i> <i>M.t.</i> <i>M.t.</i>	0.206 0.163 0.204	0.065 0.064 0.068	Till surface	612–626	79°54'	86°20'	28 700 ± 600 BP (GSC-51) (Dyck and Fyles, 1962) 30 000 ± 1600 BP (GSC-111-OF) 36 300 ± 2000 BP (GSC-111-IF) (Dyck and Fyles, 1964)
AGL-1687A B C	<i>M.t.*</i> <i>M.t.*</i> <i>M.t.*</i>	0.242 0.146 0.237	0.047 0.079 0.059	Till surface	324	79°54'	86°13'	Granite erratics observed
AGL-1685A B C	<i>M.t.</i> <i>M.t.</i> <i>M.t.</i>	0.194 0.209 0.194	0.064 0.065 0.069	Till surface	272	79°51'	86°00'	19 500 ± 1100 BP (L-548) (Sim, 1961). Granite erratics observed.
AGL-1690A B C D E	<i>H.a.</i> <i>H.a.</i> <i>H.a.</i> <i>M.t.</i> <i>M.t.</i>	0.241 0.265 0.234 0.238 0.355	0.076 0.050 0.086 0.064 0.083	Till surface	145	79°45'	85°12'	Granite erratics observed.
AGL-1686A B C D	<i>H.a.</i> <i>H.a.</i> <i>M.t.</i> <i>M.t.</i>	0.262 0.875 0.277 0.284	0.064 0.048 0.065 0.045	Till surface	469	79°11'	86°02'	Granite erratics present.
AGL-1689A B C	<i>M.t.</i> <i>M.t.</i> <i>M.t.</i>	– – –	0.059 0.067 0.052	Till surface	96–116	79°46'	85°39'	Valves more fragmented inland from Eureka Sound. Rare granites present.
GROUP III								
AGL-1706A B C	<i>H.a.</i> <i>H.a.</i> <i>H.a.</i>	0.285 0.379 0.358	0.049 0.041 0.089	Till surface	142	80°14'	84°16'	No granites observed.
AGL-1703A B C	<i>Ast.</i> <i>Ast.</i> <i>M.t./H.a.</i>	0.200 0.615 0.417	0.059 0.055 0.090	Till surface	174	79°17'	85°37'	No granites observed. Till overridden by cirque glacier during last glaciation.
INTERNATIONAL LABORATORY STANDARDS (March–June 1992)								
		Free	Total					
ILC-A Saxidomus		0.439	0.161 ± 0.0056 (n=2)					
ILC-B Mercenaria		0.940	0.500 ± 0.0300 (n=2)					
ILC-C Mercenaria		1.320	1.052 ± 0.0250 (n=2)					
AGL ANALYTICAL STANDARDS								
For the periods:								
3/24–4/16, 1992		0.097 ± 0.0020	C.V. = 2.1%					
4/23–6/6, 1992		0.234 ± 0.0045	C.V. = 1.8%					

Preliminary results on the Quaternary sedimentary environment and benthos of part of Cañon Fiord, Fosheim Peninsula, Ellesmere Island, Nunavut

R. Gilbert¹ and A.E. Aitken²

Gilbert, R. and Aitken, A.E., 2000: Preliminary results on the Quaternary sedimentary environment and benthos of part of Cañon Fiord, Fosheim Peninsula, Ellesmere Island, Nunavut; in Environmental Response to Climate Change in the Canadian High Arctic, (ed.) M. Garneau and B.T. Alt; Geological Survey of Canada, Bulletin 529, p. 197–205.

Abstract: Acoustic profiling in Cañon Fiord revealed two acoustic facies. The lower facies, mostly 10 to 30 m thick, was deposited near or beneath glaciers that formerly extended down the fiord. A central ridge of these sediments along the fiord floor may represent the late Pleistocene ice limit. Overlying, acoustically transparent to layered sediments are up to 50 m thick. These conformable glaciomarine deposits resulted from suspension settling and from gravity flows (probably turbidity currents). Accumulation rates are estimated at 1 to 2 mm/a, with the higher rates towards the fiord head.

Cluster analysis based on mollusc species from dredge samples defines three assemblages: a diverse *Astarte* assemblage in mud, sand, and gravel substrates in shallow (5–40 m) deltaic environments; a low-diversity *Portlandia arctica* assemblage in muddy substrates at 10–20 m depth; and a low-diversity *Astarte crenata* assemblage in sandy mud substrates in deep water (40–80 m). These associations broadly resemble others in similar situations throughout the Arctic Archipelago and northern Greenland.

Résumé : Des profils acoustiques effectués dans le fjord Cañon ont révélé deux faciès acoustiques. Le faciès inférieur, généralement de 10 à 30 m d'épaisseur, représente des dépôts périglaciaires ou sous-glaciaires associés aux glaciers qui s'avançaient autrefois dans le fjord. Une crête centrale sur le fond du fjord composée de ces sédiments pourrait représenter la limite des glaces du Pléistocène supérieur. Des sédiments sus-jacents acoustiquement transparents ou stratifiés ont jusqu'à 50 m d'épaisseur. Ces sédiments glaciomarins concordants proviennent du dépôt de sédiments fins en suspension et de coulées de masse (probablement des courants de turbidité). On estime que les taux d'accumulation étaient de 1 à 2 mm/a et que l'accumulation était plus forte vers l'extrémité intérieure du fjord.

Des analyses typologiques des espèces de mollusques recueillis dans les échantillons prélevés à la drague révèlent trois assemblages : un assemblage varié d'*Astarte* dans les substrats boueux, sablonneux et graveleux dans des milieux deltaïques peu profonds (de 5 à 40 m); un assemblage peu diversifié de *Portlandia arctica* dans les substrats boueux à 10 à 20 m de profondeur; et un assemblage peu diversifié d'*Astarte crenata* dans les substrats de boue sablonneuse en eau profonde (de 40 à 80 m). Ces associations ressemblent généralement à celles que l'on retrouve dans des environnements similaires partout dans l'archipel Arctique et dans le nord du Groenland.

¹ Department of Geography, Queen's University, Kingston, Ontario K7L 3N6

² Department of Geography, University of Saskatchewan, Saskatoon, Saskatchewan S7N 0W0

INTRODUCTION

Cañon Fiord borders the eastern side of Fosheim Peninsula on Ellesmere Island. The inner 40 km of the fiord between a narrows north of South Bay and a calving glacier filling the fiord head (Fig. 1) were examined in a reconnaissance survey in 1993. Our purpose was to extend understanding of High Arctic physical and biological glaciomarine environments (Lemmen, 1990; Gilbert et al., 1993; Aitken and Gilbert, 1996) and to assess interpretations of Quaternary glacial history derived from the terrestrial records in the region (England, 1992).

Of the 5012 km² drainage basin tributary to Cañon Fiord east of the 'Narrows', 46 per cent of which is glacier covered, almost one half (2323 km²; 77 per cent glacier covered) drains the southwestern portion of the Agassiz Ice Cap to the fiord head via 'Cañon Glacier'. This is the main source of water and sediment to the fiord. Other significant sources are found at South Bay (1067 km²; 6.5 per cent glacier covered) and 'East Bay' (860 km²; 24 per cent glacier covered).

The fiord is ice-covered 11 to 12 months a year. Numerous icebergs from the calving glaciers move about the fiord during open water, but they are relatively clean and are probably not significant agents of ice rafting. As well, tidal currents are weak because the mean tide (mixed, mainly diurnal) is less than 0.4 m as measured during the field study.

METHODS

Echo soundings and 85 km of subbottom acoustic survey with a Datasonics 3.5 kHz subbottom profiler were conducted from inflatable boats during a brief period in August. The benthos was sampled at 17 sites in depths of 5 to 80 m in South

Bay (Fig. 1), using a clam shell sampler and a Kolquitz dredge fitted with a 1 mm mesh. The clam shell sampler was ineffective, recovering only small quantities of sediment barren of macrofauna at sites A5, A6, and A7. Elsewhere, the Kolquitz dredge was towed across the seafloor until it could not be moved. The samples were sieved on site through a 0.5 mm screen in seawater and the material retained was preserved in buffered formalin. In the laboratory the marine invertebrates were sorted under a binocular microscope and identified to species level where possible.

The presence of molluscs in each dredge sample was recorded and entered in a data matrix. The data matrix was reduced to include only those species present at two or more stations, then evaluated by cluster analysis using SAS/STAT Version 6 clustering procedures (SAS Institute Inc., 1989). Jaccard's coefficient was used to create a similarity matrix. Clusters present within the similarity matrix were determined by Ward's method as recommended by Jones (1988).

Locations of all acoustic transects and benthic samples were read from global positioning system receivers. Stormy weather following unfavourable sea-ice conditions restricted the benthic sampling to the region of South Bay and prevented sediment coring in the fiord.

ACOUSTIC RESULTS AND GLACIOMARINE ENVIRONMENT

Cañon Fiord was previously unsurveyed except for six points sounded by the Defense Research Board expeditions between 1963 and 1969 (Canadian Hydrographic Survey, 1986). Our results show that the inner fiord is a simple trench with a maximum measured depth of 357 m in the west decreasing to 280 m 4.5 km from the glacier front (Fig. 1). Depths are

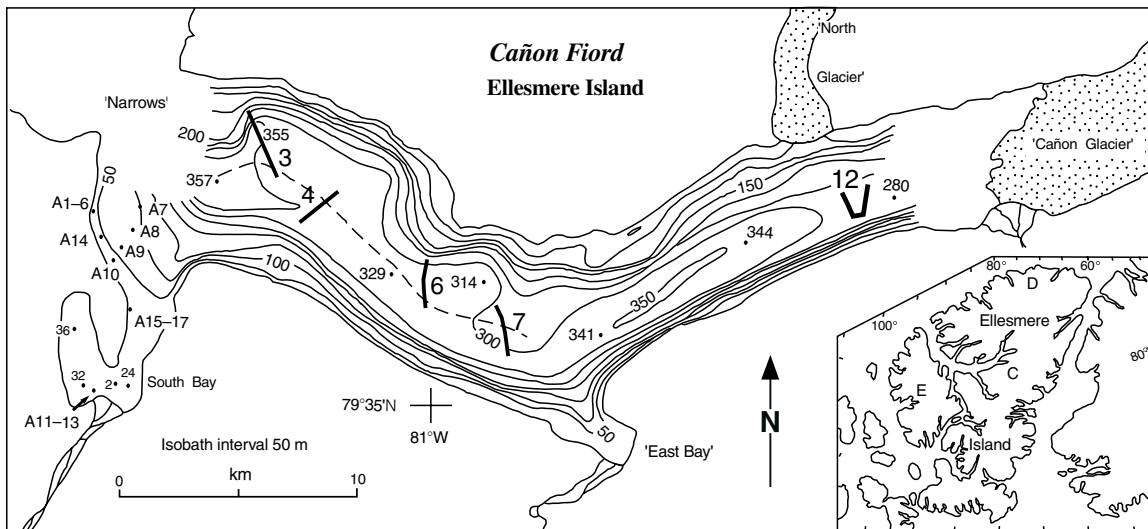


Figure 1. Bathymetry of inner Cañon Fiord determined from 13 subbottom profiles across the fiord. Spot depths are in metres. The dashed line shows the location of the mid-fiord ridge. The locations of profiles presented in Figure 2 are numbered. Benthic sampling sites are prefixed by A. Names in quotation marks are unofficial. On the inset map, C, D, and E refer respectively to Cañon, Disraeli, and Expedition fiords.

probably about 100 to 200 m at the front (104 m according to the Defense Research Board). The Defense Research Board measurement of 223 m near the Narrows indicates shallower water and possibly a sill, but this sounding does not necessarily represent sill depth; the maximum depth may be greater or the sounding may be off the sill, which may be shallower.

Two acoustic facies are seen in the subbottom records (Fig. 2): a lower, poorly resolved unit (facies 1) and an upper, thin cover of easily penetrated material (facies 2).

Facies 1 has a strongly reflecting, irregular, upper surface with local relief of about 1–5 m. Sound penetration is poor, but there are some reflectors 10–30 m (a few to 50–80 m) below this surface (e.g. Fig. 2c), suggesting that facies 1 is probably a coarse-grained material deposited directly from, or close to, a glacier. Facies 1 forms an irregular, multicrested ridge along the floor of the fiord (Fig. 1). The height of the ridge varies from over 50 m on transect 7 (Fig. 2d) to about 10 m on transect 4 (Fig. 2b). Medial ridges are uncommon in fiords or fiord lakes where cross-sections are normally U-shaped due to glacial erosion and partial filling by glaciomarine or glaciolacustrine sediment. The ridge in Cañon Fiord may represent a moraine at the grounding line or

calving line at the last glacial limit in the fiord. This limit was suggested by England (1992) to extend from the promontory north of East Bay to the north shore at the Narrows. A central ridge does not appear east of East Bay where a single ice stream, filling the valley from wall to wall, would have been fed by ice from Cañon and North glaciers. The greater height and width of the ridge on transect 7 may relate to the confluence of an expanded Cañon Glacier from the east with local glaciers from the north side of the fiord.

Facies 2 covers all of the floor and parts of the sides of the fiord. It consists of acoustically transparent and layered glaciomarine sediment up to 50 m thick (Fig. 3). Across much of the fiord, facies 2 conforms to the surface of facies 1 and contains few strong acoustic reflectors (Fig. 2a, c, d, e). These characteristics suggest that it was deposited from suspension and that slope processes (including gravity flows) have been relatively unimportant over large areas of the fiord (*see* Syvitski and Shaw, 1995). However, in the deepest mid-basin parts, deposition was greater; the fill smooths the surface below and the many nearly horizontal acoustic reflectors can be traced for hundreds of metres (Fig. 2a, b, c). This ponding of sediment suggests that gravity-flow processes, especially turbidity currents, are locally active agents of deposition

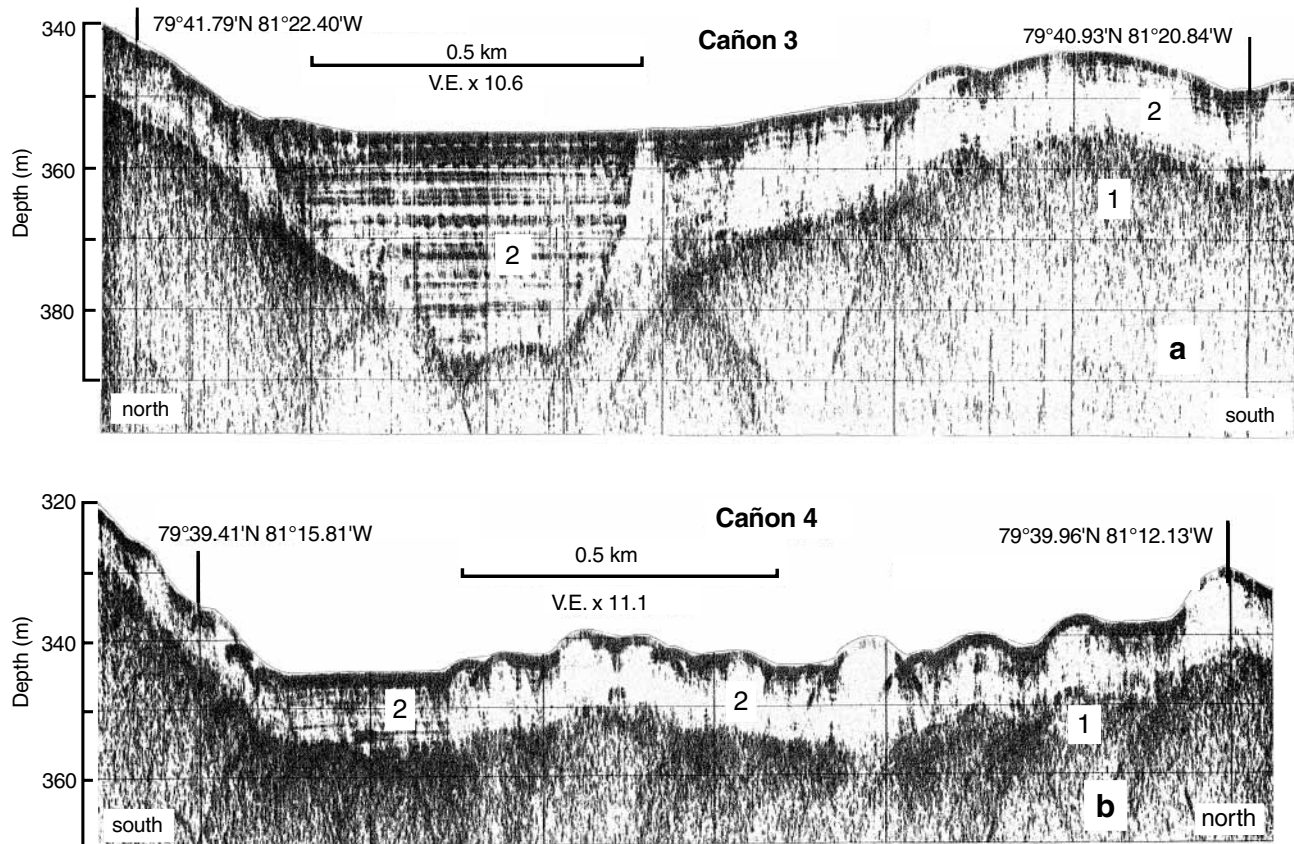


Figure 2. Segments of 3.5 kHz subbottom profiles across inner Cañon Fiord. Locations are shown in Figure 1. Depth scales assume sound velocity in water and sediment of 1460 m/s. Numbers 1 and 2 refer to acoustic facies described in the text. There are no multiples on these records, although side echos appear as parabolic images where the seafloor is irregular. Note the scale change on transect 12 (e).

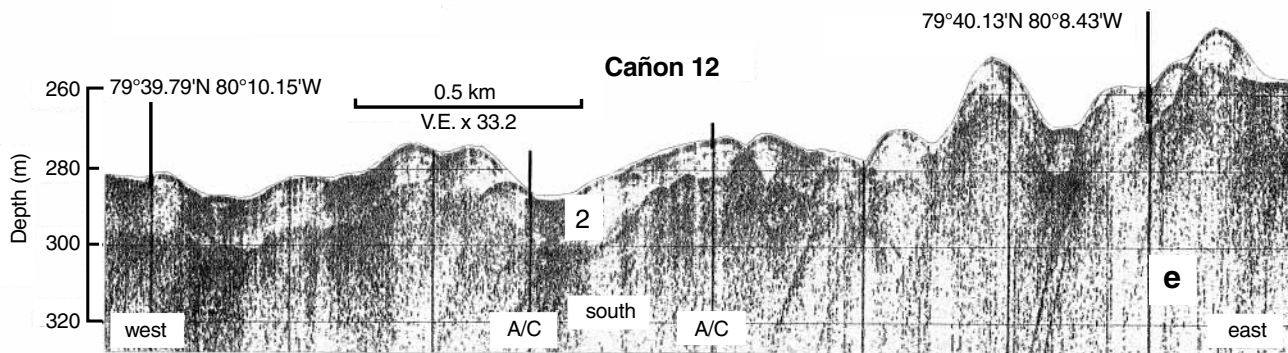
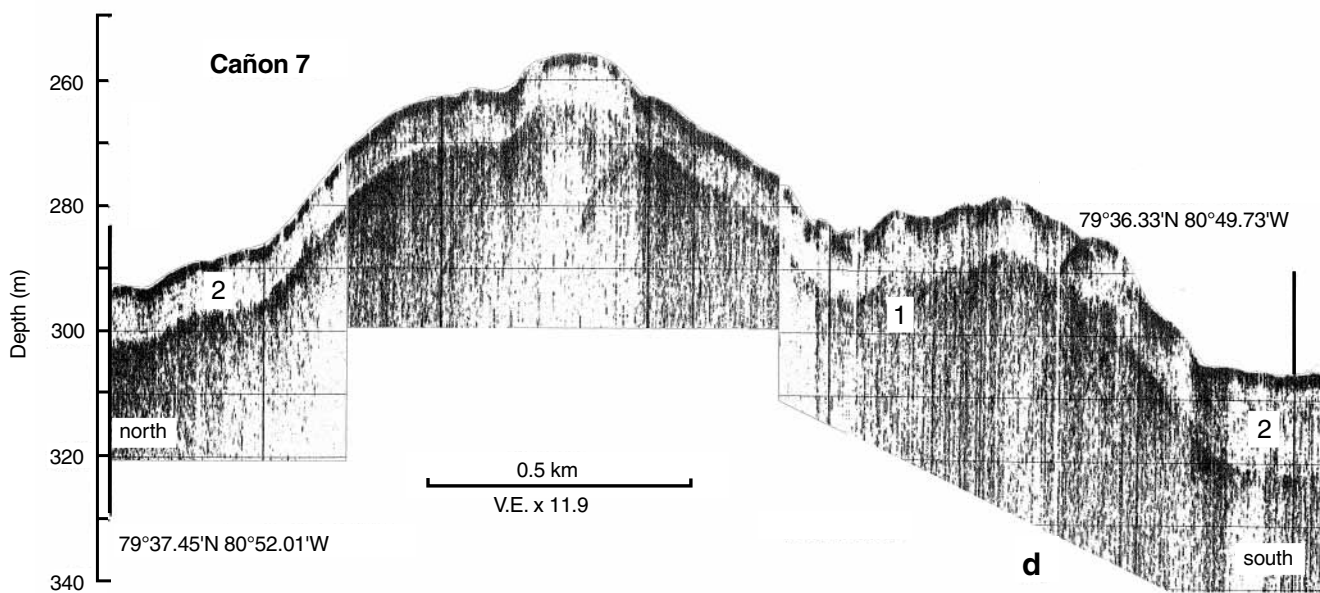
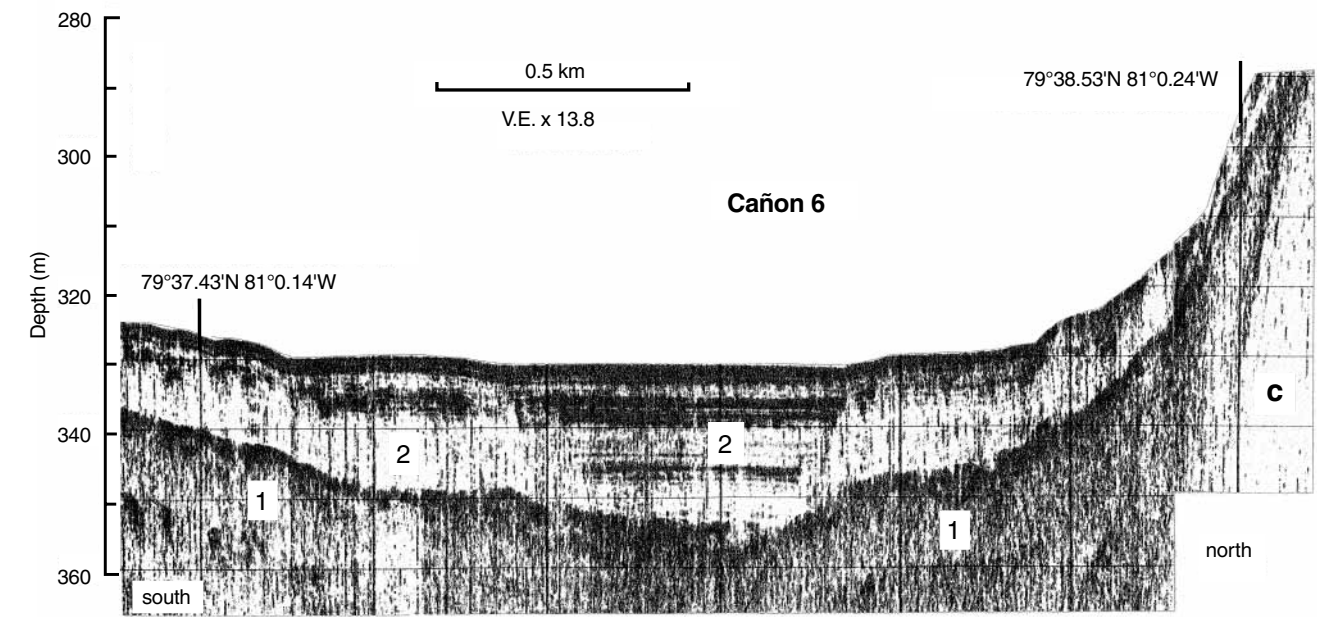


Figure 2. (cont.)

along the thalweg of the fiord. There is no evidence that these currents created trenches on the fiord floor as has been reported elsewhere (e.g. Gilbert, 1983).

The thickness of facies 2 varies significantly along the transects (Fig. 3) and so it cannot yet be mapped throughout the fiord. Sedimentation is greater on the north (right hand) side of the fiord, despite higher inputs on the south side at South and East bays. This suggests some control of sediment transport by the Coriolis effect (*see* Gilbert, 1983; Görlich, 1986). The mean thickness of facies 2 generally decreases downfiord (Fig. 4) from 14 m within 6 km of Cañon Glacier to 8.5 m in mid-basin, in response to the sediment sources in Cañon and North glaciers at the head. The uniform exponential decrease in accumulation downfiord reported elsewhere (Gilbert et al., 1993; Syvitski and Shaw, 1995) does not occur in Cañon Fiord. The greater mean thickness of sediments on

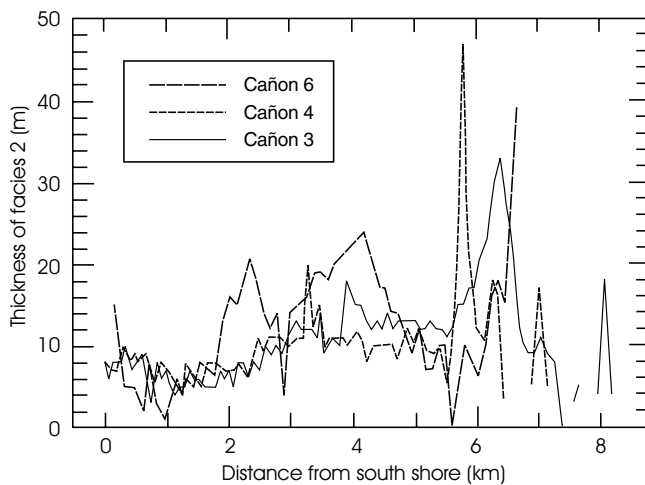


Figure 3. Thickness of facies 2 in three transects from shore to shore in Cañon Fiord. In each case the view is downfiord.

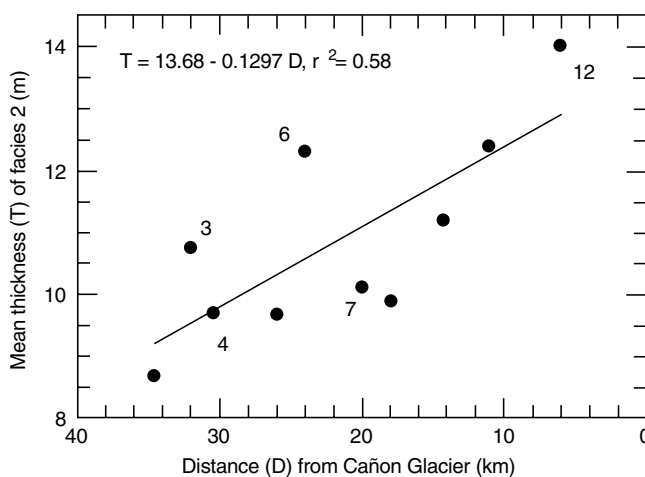


Figure 4. Mean thickness of the surficial layer of glaciomarine sediment from subbottom transects across inner Cañon Fiord. The numbers refer to transects shown in Figures 1 and 2.

transects 3 and 6 may arise from sedimentary sources at South and East bays and, to a lesser extent, from the small outlet glaciers from Agassiz Ice Cap along the north side of the fiord.

The thickness of facies 2 is nearly the same as that of the comparable glaciomarine unit in Expedition Fiord, Axel Heiberg Island (Fig. 1), where in mid-fiord the mean thickness is about 10 m, whereas close to the delta at the head the thickness is over 20 m and 50 m under the delta lip. However, the thickness is much less than in most other fiords (Syvitski and Shaw, 1995, Table 5-3). Assuming a period of at least 8000 years of marine incursion in Cañon Fiord (England, 1992), the rates of sedimentation are about 1 to 1.5 mm/a in mid-fiord and close to 2 mm/a in the inner fiord. These values are at the low end of the range of glacially fed fiords in the mid-Arctic and temperate regions (Eyles et al., 1985; Syvitski and Shaw, 1995, Table 5-4), but are an order of magnitude greater than in Disraeli Fiord on northern Ellesmere Island (Lemmen, 1990).

BENTHOS

Our knowledge of the biology of Canadian High Arctic fiords is in its infancy. Benthic sampling near Ellesmere and Axel Heiberg islands (Greig, 1909; Curtis, 1972; Hunter and Leach, 1983; Dale, 1985; Aitken and Gilbert, 1996) has contributed to our understanding of marine invertebrate ecology and zoogeography of the region, mainly that of molluscs and polychaetes. The material collected from Cañon Fiord includes a variety of marine invertebrates such as polychaetes, molluscs (gastropods and bivalves), crustaceans (amphipods and cumaceans), echinoderms (echinoids [sea urchins], holothurians [sea cucumbers], and ophiuroids [brittlestars]). In this paper we compare the distribution of molluscs in Cañon Fiord with distributions of other molluscan macrofaunas inhabiting the marine environments of the Canadian Arctic Archipelago and northern Greenland.

The molluscan macrofauna dredged from Cañon Fiord is listed in Table 1. Macpherson (1971) and Lubinsky (1980) noted the similarity in species composition of molluscan macrofaunas inhabiting high-latitude continental shelves in the northern hemisphere. Table 2 shows that the marine molluscs inhabiting Cañon Fiord are distributed widely in High Arctic estuarine and continental-shelf environments.

Several mollusc associations can be recognized on the basis of the presence or absence of species in dredge samples from Cañon Fiord. An *Astarte* association, characterized by the presence of *Astarte borealis*, *Hiatella arctica*, *Macoma loveni*, *Musculus discors*, *Mya truncata*, and *Portlandia arctica*, inhabits heterogeneous substrates of mud, sand, and gravel at depths of 5–30 m (A4, A11, A14, A15, A16, A17 in Fig. 5a). The species composition of the *Astarte* association inhabiting shallow waters in South Bay is similar to that of the *Astarte* association from Expedition Fiord on Axel Heiberg Island, described by Aitken and Gilbert (1996), and the *Astarte* association on the inner continental shelf of eastern Baffin Island, described by Thomson et al. (1986). In the last two areas, this association inhabits mixed substrates of sand and mud at depths of 5 to 50 m. The absence of the *Astarte*

Table 1. Marine molluscs recovered in dredge samples from Cañon Fiord, Ellesmere Island.

	Site													
	A1	A2	A3	A4	A8	A9	A10	A11	A12	A13	A14	A15	A16	A17
	Depth (m)													
	5	5	10	20	80	60	40	5	10	20	30	5	10	15
Bivalvia														
<i>Astarte borealis</i>				X								X	X	X
<i>Astarte crenata</i>					X	X	X							
<i>Clinocardium ciliatum</i>	X	X	X											
<i>Delectopecten greenlandicus</i>				X										
<i>Hiatella arctica</i>								X			X	X	X	
<i>Macoma loveni</i>												X	X	
<i>Musculus discors</i>												X	X	
<i>Mya truncata</i>				X				X				X	X	
<i>Nuculana pernula</i>														X
<i>Portlandia arctica</i>								X	X	X		X	X	X
<i>Thyasira gouldi</i>														X
<i>Yoldiella</i> spp.					X	X	X		X	X				
Gastropoda														
Naticidae (egg cases)	X	X	X											

Table 2. Depth distribution of molluscs recovered from High Arctic fiord and continental-shelf environments.

	Axel Heiberg Island		Ellesmere Island		Greenland		Svalbard
	A	B	C	D	E	F	G
Bivalvia							
<i>Astarte borealis</i>	3–45 m			5–20 m	12–52 m	6–16 m	15–25 m
<i>Astarte crenata</i>				40–80 m		30–190 m	
<i>Astarte warhami</i>	3–53 m					6–47 m	
<i>Clinocardium ciliatum</i>	9–20 m			5–10 m	12–52 m		15–18 m
<i>Cuspidaria arctica</i>	9–14 m					30–80 m	
<i>Delectopecten greenlandicus</i>	14–67 m	152 m, 180 m		20–30 m		10–190 m	
<i>Hiatella arctica</i>	3–40 m		Intertidal	5–30 m	8–64 m	2–45 m	1–25 m
<i>Macoma calcarea</i>	4–16 m		Intertidal		8–64 m	2–16 m	
<i>Macoma loveni</i>	3–32 m			5–10 m		6–38 m	
<i>Mya truncata</i>	3–32 m		Intertidal	5–20 m	8–64 m	2–40 m	12–15 m
<i>Portlandia arctica</i>	4–81 m			5–20 m		3–18 m	
<i>Nuculana pernula</i>	9–40 m			15 m	40–54 m	30–80 m	
<i>Thracia devexa</i>	4–16 m					16–140 m	
<i>Thyasira gouldi</i>	5–82 m			15 m		8–16 m	
<i>Thyasira dunbari</i>	8–10, 57 m					19–47 m	
<i>Yoldiella fraterna</i>	32–45 m	152 m					
<i>Yoldiella intermedia</i>	34–66 m	160 m, 425–604 m				45–190 m	
<i>Yoldiella lenticula</i>	9–82 m	180–604 m				30–50 m	
Scaphopoda							
<i>Siphonodentalium lobatum</i>	48–72 m	175 m, 487 m				50–80 m	
Gastropoda							
<i>Cylichna alba</i>	18–20 m		Intertidal			5–190 m	15–18 m
<i>Cylichna occulta</i>	4–32 m					3–80 m	15–18 m
<i>Lepeta caeca</i>	34–40 m				54 m	15–35 m	1–10 m
<i>Oenopota cinerea</i>	4–6 m						
<i>Oenopota decussata</i>	30–32 m						
<i>Oenopota novajasemliensis</i>	9–65 m					6–40 m	
<i>Oenopota reticulata</i>	8–10 m					3–50 m	
<i>Trichotropis borealis</i>	4–32 m				18–45 m	2,68,140 m	
Sources of information: A – Expedition Fiord, Aitken and Gilbert (1996); B – Axel Heiberg Island continental shelf, Wagner (1964) and unpublished data; C – Cape Herschel and Alexandra Fiord, Dale (1985); D – Cañon Fiord, present study; E – continental shelf off Thule, northwest Greenland (Vibe, 1939, 1950); F – Jørgen Brønlund Fjord, Greenland (Schjømte, 1989); G – Van Keulen Fjord, Spitsbergen, Svalbard, Rózycki (1984).							

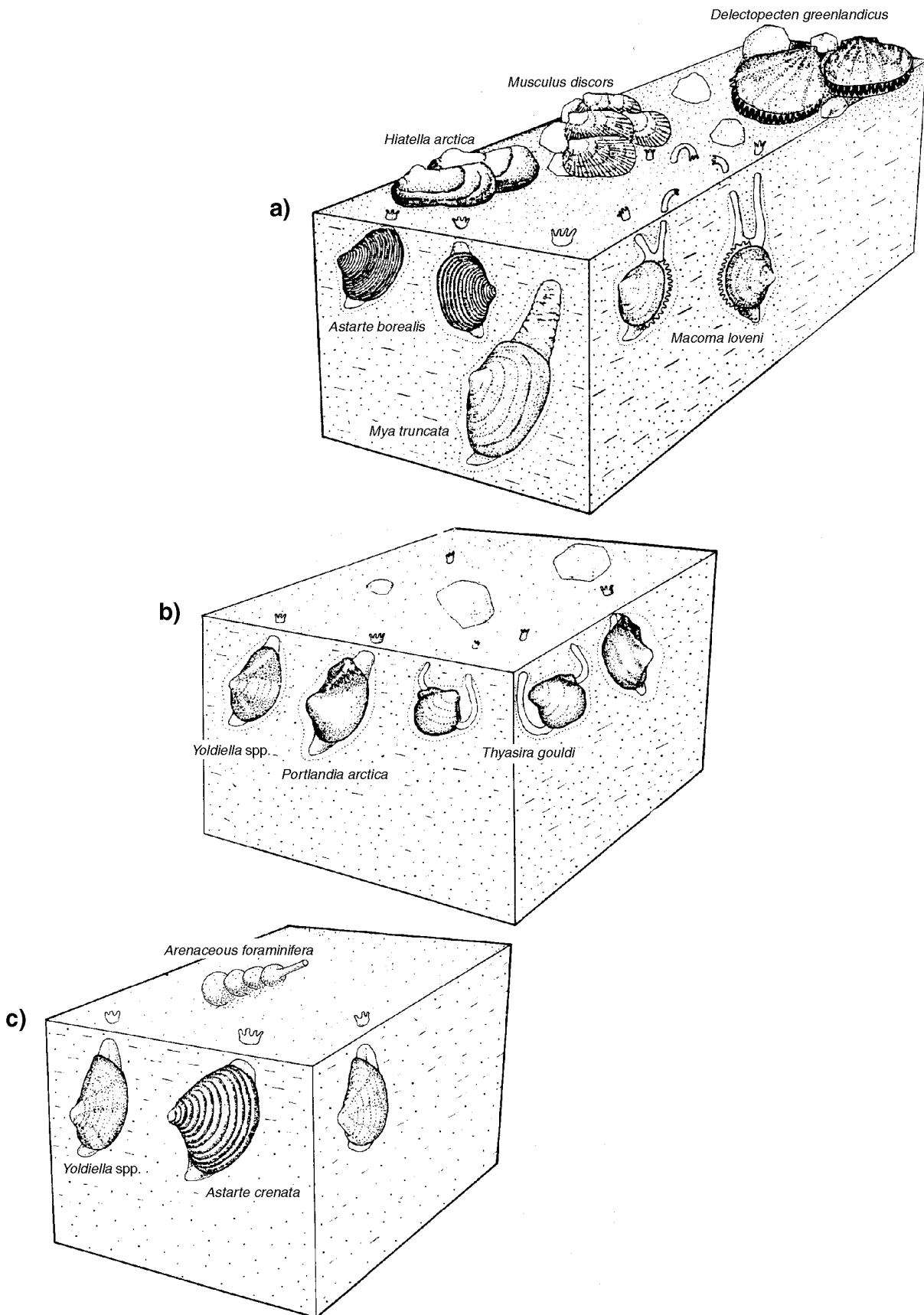


Figure 5. Benthic assemblages in Cañon Fiord. a) *Astarte* assemblage on heterogeneous mud, sand and gravel substrates from 5 to 40 m depth. b) *Portlandia arctica* assemblage on muddy sand substrates on prodeltaic slopes from 10 to 30 m depth. c) *Astarte crenata* assemblage on sandy mud in deep-water environments from 40 to 80 m depth.

association in prodeltaic environments in the study area most probably relates to the intolerance of suspension-feeding molluscs such as *Astarte*, *Hiattella*, *Musculus*, and *Mya* for the elevated suspended-sediment concentrations encountered in these environments.

An association characterized by an abundance of juvenile cockles (*Clinocardium ciliatum*) and pectens (*Delectopecten* sp.) and naticid (moon snail) egg cases occurs on muddy sand substrates at depths of 5 to 10 m on the slope of the delta at A1, A2, and A3 (Fig. 1). This area appears to serve as a nursery ground for molluscs in South Bay.

An actively prograding delta in South Bay provides a large input of fresh water and sediment to Cañon Fiord. In the prodeltaic environment, a *Portlandia arctica* association inhabits sandy mud substrates at depths of 10 to 30 m (A12, A13 in Fig. 5b). *Portlandia arctica* and *Yoldiella* spp. are common species in this association. Similar low-diversity *Portlandia* associations have been recorded from fiord-head environments characterized by high suspended-sediment concentrations, rapid sedimentation rates, cold temperatures, and variable salinities in Coronation Fiord (Syvitski et al., 1989) and Pangnirtung Fiord (Dale et al., 1989) on eastern Baffin Island and in Expedition Fiord on Axel Heiberg Island (Aitken and Gilbert, 1996). In the last two fiords, *Nucula belloti*, *Nuculana pernula*, and *Thyasira* spp. are common members of the molluscan macrofauna.

At depths greater than 40 m, an *Astarte crenata* association characterized by the presence of *Astarte crenata*, *Yoldiella* spp., and arenaceous foraminifera inhabits sandy mud substrates (A8, A9, A10 in Fig. 5c). Elsewhere, *A. crenata* and *Yoldiella* spp. occur commonly within the *Astarte crenata*–*Bathyarca glacialis* association that is found on muddy substrates at depths of 45–200 m in Greenland fiords (Spärck, 1933; Thorson, 1934) and the Onuphid and Maldanid (= *Astarte crenata*–*Bathyarca glacialis*) associations that inhabit mixed substrates of gravel, sand, and mud at depths of 125 to 750 m in Baffin Island fiords (Syvitski et al., 1989; Aitken and Fournier, 1993).

CONCLUSIONS AND FURTHER WORK

These preliminary results from Cañon Fiord, along with the studies at Expedition and Disraeli fiords (Lemmen, 1990; Gilbert et al., 1993), are the beginnings of what may be interpreted as a consistent pattern of sedimentation in Canadian High Arctic fiords as distinct from the patterns of mid-arctic fiords. Postglacial sedimentation rates are low, generally less than about 2 mm/a except near points of inflow, and the total sediment accumulation is normally less than a few tens of metres. Processes of sedimentation are dominated by settling from suspension supplemented by relatively weak gravity flows depositing sediment especially in the deepest regions of the basin. Reworking of sediments by slumping is relatively unimportant. For these reasons, it is probable that high-resolution, long-term records of the sedimentary environment could be obtained from cores recovered through the sea ice (see Gilbert et al., 1993). It is anticipated that these

would record changes in the glacial, hydrological, biological, and climatic regimes that would supplement the assessments of Quaternary environments from the terrestrial records (e.g. England, 1992). Resurvey with more powerful acoustic sources would better resolve facies 1 and associated deposits to more fully address the extent of Quaternary glaciation and the proglacial environment. As well, we suggest that extending the study to outer Cañon Fiord and to Nansen Sound and Greely Fiord is important to complete the regional picture of glaciation and marine sedimentation by linking to the studies on the polar continental shelf (van Wagoner et al., 1989; Hein et al., 1990).

The molluscs recovered from Cañon Fiord are also distributed widely within high-latitude estuaries and across the continental shelves bordering the Arctic Ocean. It is not surprising, therefore, that the species composition of the various mollusc associations present in Cañon Fiord is broadly similar to that of mollusc associations occurring over the same bathymetric range on similar substrates in estuarine and shelf environments within the Canadian Arctic Archipelago and along northern and eastern coastlines of Greenland. Water temperature, salinity, dissolved oxygen, and particulate organic carbon content amongst others, have been demonstrated to influence the distribution of benthic organisms in high-latitude estuarine and shelf environments (Dunbar, 1951; Ockelmann, 1958; Carey and Ruff, 1977; Dale et al., 1989; Syvitski et al., 1989; Carey, 1991). Their specific influences on the distribution of molluscs within Cañon Fiord remains to be investigated. Advancing our knowledge of the ecology of modern marine molluscs will facilitate the study of Quaternary environmental change in high-latitude environments. Aitken (1990) has demonstrated that marine molluscs, amongst all the marine invertebrates, have the greatest potential for preservation in Quaternary glaciomarine sediments and their usefulness in the study of paleoceanography has been demonstrated (Hillaire-Marcel, 1980; Thomsen and Vorren, 1986; Rodrigues, 1988; Lemmen et al., 1994; Dyke et al., 1996).

ACKNOWLEDGMENTS

The work was supported by research and equipment grants from the Natural Sciences and Engineering Research Council of Canada. The Polar Continental Shelf Project provided logistic support and the Northern Scientific Training Grants Program of Indian and Northern Affairs Canada assisted students M. Dance, J. Hartshorn, L. Liblik, and A.P. Wolfe, whose help in the field was invaluable. We appreciate a careful review of the paper by A.S. Dyke.

REFERENCES

- Aitken, A.E.
1990: Fossilization potential of arctic fjord and continental shelf benthic macrofaunas; in *Glaciomarine Environments: Processes and Sediments*, (ed.) J.A. Dowdeswell and J.D. Scourse; The Geological Society Special Publication No. 53, London, p. 155–176.

- Aitken, A.E. and Fournier, J.**
1993: Macrobenthos communities of Cambridge, McBeth and Iirbilung fiords, Baffin Island, Northwest Territories, Canada; *Arctic*, v. 46, p. 60–71.
- Aitken, A.E. and Gilbert, R.**
1996: Marine mollusca from Expedition Fiord, western Axel Heiberg Island, Northwest Territories, Canada; *Arctic*, v. 48, p. 29–43.
- Canadian Hydrographic Survey**
1986: Nansen Sound and Greely Fiord; Chart 7941 (scale 1:300 000).
- Carey, A.G., Jr.**
1991: Ecology of North American arctic continental shelf benthos: a review; *Continental Shelf Research*, v. 11, p. 865–883.
- Carey, A.G., Jr. and Ruff, R.E.**
1989: Ecological studies of the benthos in the western Beaufort Sea with special reference to the bivalve molluscs; *in* *Polar Oceans*, (ed.) M.J. Dunbar; Arctic Institute of North America, Washington D.C., p. 505–530.
- Curtis, M.A.**
1972: Depth distributions of benthic polychaetes in two fiords on Ellesmere Island, N.W.T.; *Journal of the Fisheries Research Board of Canada*, v. 29, p. 1319–1327.
- Dale, J.E.**
1985: Recent intertidal molluscs from the east-central coast of Ellesmere Island, Northwest Territories; *in* *Current Research, Part B*; Geological Survey of Canada, Paper 85-1B, p. 319–324.
- Dale, J.E., Aitken, A.E., Gilbert, R., and Risk, M.J.**
1989: Fauna of arctic fiords; *Marine Geology*, v. 81, p. 331–358.
- Dunbar, M.J.**
1951: Eastern arctic waters; *Bulletin of the Fisheries Research Board of Canada*, v. 88, 131 p.
- Dyke, A.S., Dale, J.E., and McNeely, R.N.**
1996: Marine molluscs as indicators of environmental change in glaciated North America and Greenland during the last 18 000 years; *Géographie physique et Quaternaire*, v. 50, p. 125–184.
- England, J.**
1992: Postglacial emergence in the Canadian High Arctic: integrating glacioisostasy, eustasy, and late deglaciation; *Canadian Journal of Earth Sciences*, v. 29, p. 984–999.
- Eyles, C.H., Eyles, N., and Miall, A.D.**
1985: Models of glaciomarine sedimentation and their applications to the interpretation of ancient glacial sequences; *Palaeogeography, Palaeoclimatology, Palaeoecology*, v. 51, p. 15–84.
- Gilbert, R.**
1983: Sedimentary processes of Canadian arctic fjords; *Sedimentary Geology*, v. 36, p. 147–175.
- Gilbert, R., Aitken, A.E., and Lemmen, D.S.**
1993: The glaciomarine sedimentary environment of Expedition Fiord, Canadian High Arctic; *Marine Geology*, v. 110, p. 257–273.
- Görllich, K.**
1986: Glaciomarine sedimentation of muds in Hornsund fjord, Spitsbergen; *Annales Societatis Geologorum poloniae*, v. 56, p. 433–477.
- Greig, J.A.**
1909: Brachiopods and molluscs with a supplement to the echinoderms; Report of the second Norwegian Arctic Expedition in the *FRAM*: 1898–1902; Videnskab-Selskabet, Kristiania, no. 20, 38 p.
- Hein, F.J., van Wagoner, N.A., and Mudie, P.J.**
1990: Sedimentary facies and processes of deposition: ice island cores, Axel Heiberg Shelf, Canadian Polar Continental Margin; *Marine Geology*, v. 93, p. 243–265.
- Hillaire-Marcel, C.**
1980: Les faunes des mers post-glaciaires du Québec : quelques considérations paléocéologiques; *Géographie physique et Quaternaire*, vol. 1, p. 3–59.
- Hunter, J.C. and Leach, S.T.**
1983: Hydrographic data collected during fisheries activities of the Arctic Biological Station, 1960 to 1979; *Canadian Data Report of Fisheries and Aquatic Sciences*, v. 414, 87 p.
- Jones, B.**
1988: Biostatistics in Paleontology; *Geoscience Canada*, v. 15, p. 3–22.
- Lemmen, D.S.**
1990: Glaciomarine sedimentation in Disraeli Fiord, high arctic Canada; *Marine Geology*, v. 94, p. 9–22.
- Lemmen, D.S., Aitken, A.E., and Gilbert, R.**
1994: Early Holocene deglaciation of Expedition and Strand fiords, Canadian High Arctic; *Canadian Journal of Earth Sciences*, v. 31, p. 943–958.
- Lubinsky, I.**
1980: Marine bivalve molluscs of the Canadian Central and Eastern Arctic: faunal composition and zoogeography; *Canadian Bulletin of Fisheries and Aquatic Sciences*, Bulletin 207, 111 p.
- Macpherson, E.**
1971: The marine molluscs of arctic Canada; *National Museums of Canada, Publications in Biological Oceanography*, 3, 149 p.
- Ockelmann, W.K.**
1958: Marine lamellibranchiata; *Meddelelser om Grønland*, v. 122(4), 248 p.
- Rodrigues, C.G.**
1988: Late Quaternary invertebrate faunal associations and chronology of the western Champlain Sea basin; *in* *The Late Quaternary Development of the Champlain Sea Basin*, (ed.) N.R. Gadd; Geological Association of Canada Special Paper 35, p. 155–176.
- Rózycki, O.**
1984: Distribution of bivalves in the Van Keulen Fjord (Spitsbergen, Bellsund); *Polskie Archiwum Hydrobiologii*, v. 31, p. 83–89.
- SAS Institute Inc.**
1989: SAS/STAT® User's Guide, Version 6, Fourth Edition, Volumes 1 and 2; Cary, North Carolina, SAS Institute Inc., 1686 p.
- Schiøtte, T.**
1989: Marine mollusca from Jørgen Brønlund Fjord, northern Greenland, including the description of *Diaphana vedelsbyae* n. sp.; *Meddelelser om Grønland, Bioscience*, v. 28, 24 p.
- Spärck, R.**
1933: Contributions to the animal ecology of the Franz Joseph Fjord and adjacent East Greenland waters; *Meddelelser om Grønland*, v. 100(1), p. 1–40.
- Syvitski, J.P.M. and Shaw, J.**
1995: Sedimentology and geomorphology of fjords; *in* *Geomorphology and Sedimentology of Estuaries*; (ed.) G.M.E. Perillo; Elsevier Science, Developments in Sedimentology 53, Amsterdam, p. 113–178.
- Syvitski, J.P.M., Farrow, G.E., Atkinson, R.J.A., Moore, P.G., and Andrews, J.T.**
1989: Baffin Island fjord macrobenthos: bottom communities and environmental significance; *Arctic*, v. 42, p. 232–247.
- Thomsen, E. and Vorren, T.O.**
1986: Macrofaunal palaeoecology and stratigraphy in Late Quaternary shelf sediments off northern Norway; *Palaeogeography, Palaeoclimatology, Palaeoecology*, v. 56, p. 103–150.
- Thomson, D.H., Martin, C.M., and Cross, W.E.**
1986: Identification and characterization of arctic nearshore benthic habitats; *Canadian Technical Report of Fisheries and Aquatic Sciences*, v. 1434, 70 p.
- Thorson, C.**
1934: Contributions to the animal ecology of Scoresby Sound Fjord complex (East Greenland); *Meddelelser om Grønland*, v. 100(3), p. 1–67.
- van Wagoner, N.A., Mudie, P.J., Cole, F.E., and Daborn, G.**
1989: Siliceous sponge communities, biological zonation, and Recent sea-level change on the arctic margin: Ice Island results; *Canadian Journal of Earth Sciences*, v. 26, p. 2341–2355.
- Vibe, C.**
1939: Preliminary investigations on shallow water animal communities in the Upernavik and Thule districts (northwest Greenland); *Meddelelser om Grønland*, v. 124(2), p. 1–42.
1950: The marine mammals and the marine fauna in the Thule district (northwest Greenland) with observations on ice conditions in 1939–1941; *Meddelelser om Grønland*, v. 150(6), p. 1–115.
- Wagner, F.J.E.**
1964: Faunal report II, Marine geology program, Polar Continental Shelf Project, Isachsen, District of Franklin; Geological Survey of Canada, Bedford Institute of Oceanography Report 64-1, 15 p.

Distribution and characterization of ground ice on Fosheim Peninsula, Ellesmere Island, Nunavut

W.H. Pollard¹

Pollard, W.H., 2000: Distribution and characterization of ground ice on Fosheim Peninsula, Ellesmere Island, Nunavut; in Environmental Response to Climate Change in the Canadian High Arctic, (ed.) M. Garneau and B.T. Alt; Geological Survey of Canada, Bulletin 529, p. 207–233.

Abstract: The widespread occurrence of ground ice in the Eureka Sound lowlands, western Fosheim Peninsula, is described. Of particular importance are the distribution and thickness of ice-rich sediments and massive ice. Outside of the Mackenzie Delta and Yukon Coastal Plain, few areas in the Canadian Arctic report such extensive massive ice.

Field investigations from 1990 to 1995 identified seven ice-rich areas in the Eureka Sound lowlands, six on Fosheim Peninsula and the seventh, on eastern Axel Heiberg Island. Bodies of massive ice occur mostly in fine-grained, marine sediments as either shallow bodies of pure ice interbedded with layers of icy sediment, or as deep, thick layers of horizontally layered, clear to white ice. Massive ice is interpreted as intrasedimental in origin and is probably the result of rapid permafrost aggradation into recently emerged marine sediments. The widespread occurrence of stabilized retrogressive thaw slumps suggests that ground ice was even more common in the past.

Résumé : L'auteur décrit la présence généralisée de glace de sol dans les basses terres du détroit d'Eureka, dans l'ouest de la péninsule Fosheim. La présence généralisée et l'épaisseur des sédiments riches en glace et de la glace massive sont des points particulièrement importants. En dehors du delta du Mackenzie et de la plaine côtière du Yukon, il y a peu d'endroits de l'Arctique canadien où l'on peut observer de telles étendues de glace massive.

Les études sur le terrain de 1990 à 1995 ont permis de reconnaître sept zones riches en glace dans les basses terres du détroit d'Eureka, six sur la péninsule Fosheim et une dans l'est de l'île Axel Heiberg. Les corps de glace massive se rencontrent surtout dans des sédiments marins à grain fin, soit à faible profondeur, sous la forme de corps de glace pure interstratifiée avec des couches de sédiments riches en glace, soit à plus grande profondeur, sous la forme d'épaisses couches horizontales de glace claire ou blanchâtre. On interprète la glace massive ayant une origine intrasédimentaire; elle est probablement le produit de l'aggradation rapide de pergélisol dans des sédiments marins récemment émergés. La présence généralisée de glissements régressifs dus au dégel, maintenant stabilisés, porte à croire que la glace de sol était encore plus abondante dans le passé.

¹ Department of Geography, Centre for Climate and Global Change Research, McGill University, 805 Sherbrooke Street West, Montréal, Québec H3A 2K6

INTRODUCTION

Ground ice is an important constituent of surficial deposits in the Fosheim Peninsula area of western Ellesmere Island. It is particularly abundant in the lowlands surrounding Eureka Sound, Slidre Fiord, and the Slidre River valley, where it commonly occurs as extensive bodies of massive, tabular ice. Ice wedges also constitute a significant part of the total volume of ground ice in the upper 5 to 10 m of permafrost, where only small amounts of buried ice exist. The formation of various types of ground ice is closely related to permafrost aggradation and seasonal temperature perturbations in the upper part of the permafrost profile. A variety of sedimentological and depositional processes might also play an active role in the formation of ground ice, particularly in the case of buried massive ice. On Fosheim Peninsula, the late Quaternary evolution of climate, glacial activity, and sea-level change combine to determine the nature and distribution of ground ice.

Ground ice remains one of the most problematic aspects of permafrost and a major obstacle to development in arctic regions. Knowledge of ground ice, particularly massive ice and ice-rich sediments, is necessary not only to understand the evolution of the Late Quaternary landscape in this region, but also to assess the potential geomorphic response of the landscape to natural and anthropogenic disturbances of permafrost regimes. Thermokarst and erosion associated with the Eureka weather station and the Panarctic Gemini E-10 well site reflect the sensitive nature of surficial sediments and icy permafrost in this part of the Arctic. Concern that global warming will not only cause a shift in the pattern of permafrost distribution, but will also induce widespread thermokarst in areas underlain by ice-rich sediments, provides additional impetus for the investigation of ground ice. Ground-ice studies may also provide useful proxy information on paleoclimates and paleogeomorphology.

Objective

The primary objective of this report is to describe ground-ice conditions in the Fosheim Peninsula area, Ellesmere Island, with particular reference to exposures of massive ice in the Eureka Sound lowlands. Specific goals include providing a comprehensive overview of ground-ice studies on Fosheim Peninsula by synthesizing published and unpublished material; documenting the nature and distribution of massive ice and ice-rich sediments; documenting the stratigraphy, structure, and chemistry of massive ice; and explaining the origin of massive ice and its significance with respect to Late Pleistocene and Holocene changes on Fosheim Peninsula.

Nature and terminology of ground ice

Many processes and landforms unique to permafrost regions are directly related to the aggradation and degradation of ground ice (Fig. 1). Ice is unique among the minerals that comprise the Earth's crust in that over its entire range of occurrence, it is close to its melting point and thus highly unstable (Fig. 1b). Ice is interesting for two other reasons,

firstly because it is the only common mineral that increases in volume when it changes from liquid to solid and secondly, because it has a density of less than 1 and is highly plastic under any degree of applied stress. It has several other physico-chemical properties that contribute to its geological significance, including the tendency to reject solutes and impurities during freezing.

The term 'ground ice' refers to "all types of ice formed in freezing and frozen ground" (Permafrost Subcommittee, 1988, p. 46). A widely used ground-ice classification developed by Mackay (1972) identifies three primary sources of water leading to ten genetically distinct types of ice, ranging from disseminated ice crystals in a soil matrix (pore ice) to thick (10–20 m), horizontally layered bodies of nearly pure ice that cover several square kilometres (Fig. 2, 3). Of the many types of ground ice that are recognized, pore ice, wedge ice, intrasedimental ice (i.e. segregated and intrusive ice), and buried ice are thought to be most significant in terms of volume and frequency of occurrence. The formation of ground ice is a complex process in which temperature, soil grain size and water content, chemistry, and transfer processes combine to determine the type and rate of ice formation. In general, ice content is highest at and immediately below the permafrost table and decreases with depth (Pollard and French, 1980). In places, ground-ice content exceeds the saturated-moisture content of the host sediments, producing a condition called

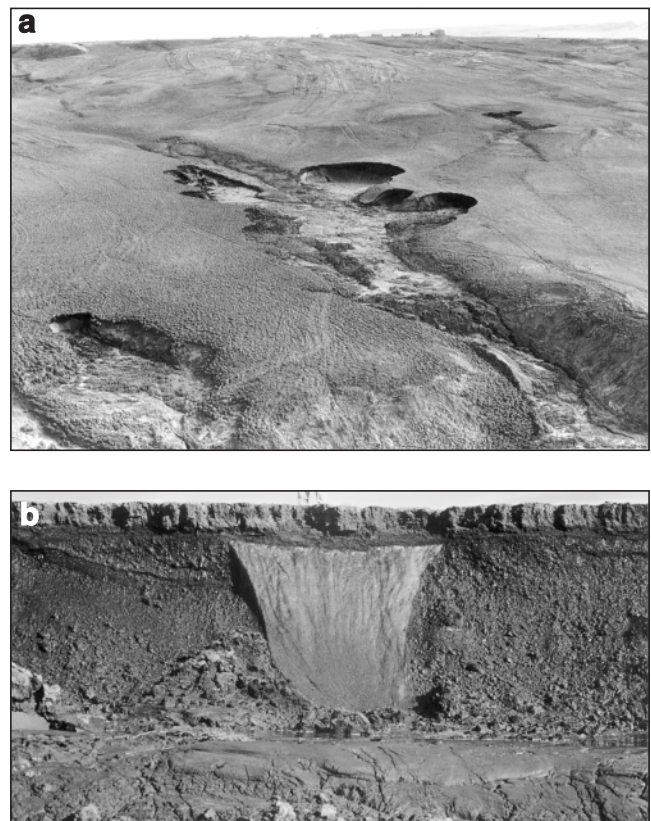


Figure 1. *a*) Thermokarst (GSC 2000-022A) and *b*) an ice wedge (GSC 2000-022B) in the Eureka area of Fosheim Peninsula.

'excess ice'. When permafrost containing excess ice thaws, the ground surface will settle in proportion to the volume of excess ice. This process and the landforms it produces are termed 'thermokarst'. Thermokarst plays an important role in the evolution of landscapes underlain by ice-rich permafrost and occurs in response to both natural and anthropogenic disturbances.

Massive ice

The highest excess ice contents and thus the greatest potential for thermokarst are associated with massive ice (Fig. 4a, b). Massive ice is "a large mass of ground ice having a gravimetric ice content >250%" (Mackay, 1989, p. 6). According to Mackay (1989), massive ice can be divided into two main types, intrasedimental ice and buried surface ice. Intrasedimental ice, or ice formed by in situ freezing of

ground water, includes segregation and intrusive ice as well as all intermediate forms. Buried surface ice forms when a mass of surface ice (e.g. river, lake, sea, snowbank, and glacier ice) is buried and preserved in permafrost. Glacier ice is a potentially significant source of buried ice and has been observed at several locations in the Canadian Arctic (Lorrain and Demeur, 1985; St-Onge and McMartin, 1995). Many modern moraine systems on Ellesmere and Axel Heiberg islands are ice cored and although the origin of this ice has not been confirmed, it is most likely buried glacier ice.

Central to the discussion of ground ice is the measurement of ice content. Ice content can be expressed either gravimetrically or volumetrically. Gravimetric ice content refers to the weight of ice in a sample as a percentage of either total sample weight or dry sample weight. Volumetric ice content refers to the volume of ice as a proportion of the volume of the total sample. Gravimetric ice contents are more

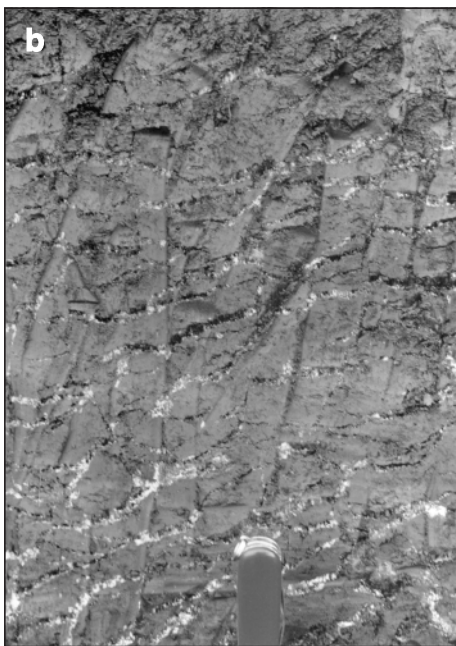
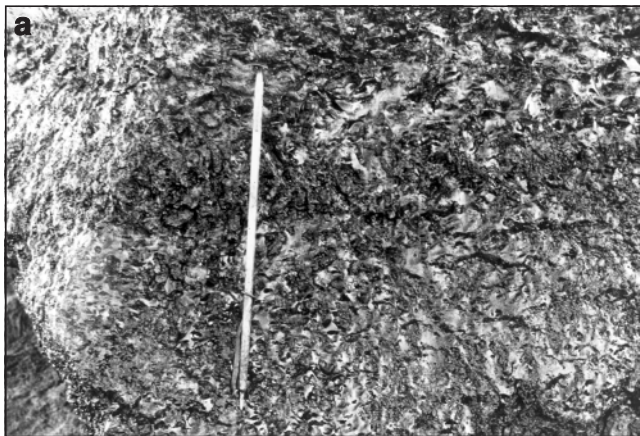


Figure 2. Cryogenic textures in *a*) massive pore ice (GSC 2000-022C) and *b*) reticulated ice (GSC 2000-022D).

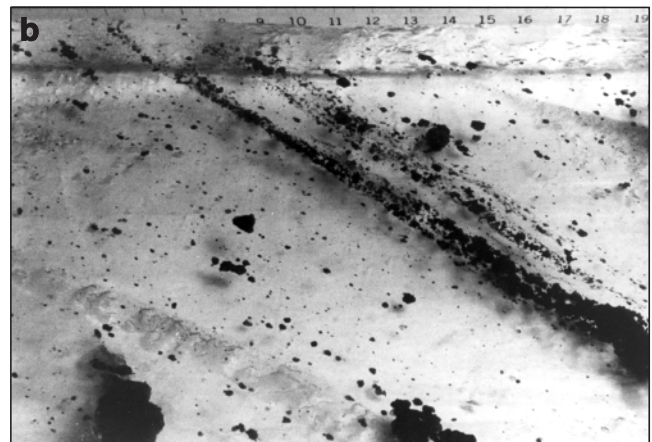
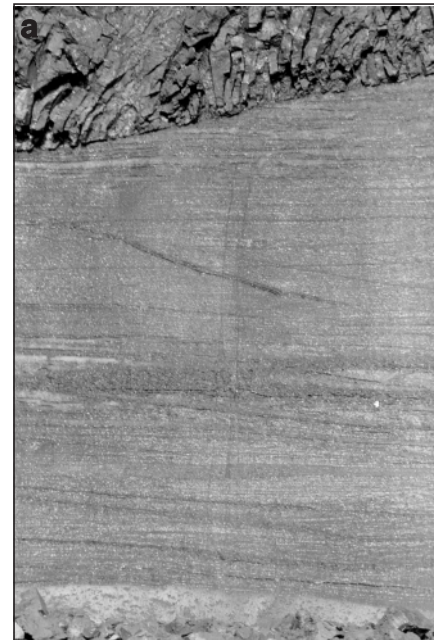


Figure 3. Massive ice in *a*) section (GSC 2000-022E) and *b*) thin section (GSC 2000-022F).

common because they are easy to compute; however, volumetric ice contents allow the calculation of excess ice and thus of potential thaw subsidence (e.g. Pollard and French, 1980). In this report, all ice content is expressed volumetrically. For example, Figures 4a and 4b show massive ice with a volumetric ice content on the order of 70 to 98 per cent.

Significance of ground ice

Ground ice is significant because of its geomorphic and geological role in the development of past and future landscapes, including various processes and landforms associated with ground-ice aggradation, such as frost heave or the formation of ice-cored landforms, and degradation, particularly thermokarst. These processes produce a variety of diagnostic stratigraphic and sedimentological structures that can be used to reconstruct the evolution of the ground-ice system. Since the presence of ground ice is most often indicative of freezing and permafrost formation, the analysis of its stratigraphic context and topographic setting provides valuable information on climate and landscape change. Therefore, ground-ice studies may also provide useful proxy information on arctic paleoclimates and paleogeomorphology and thus may play a

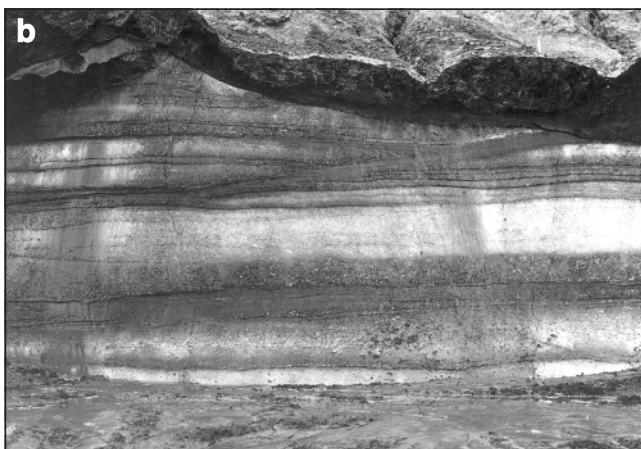
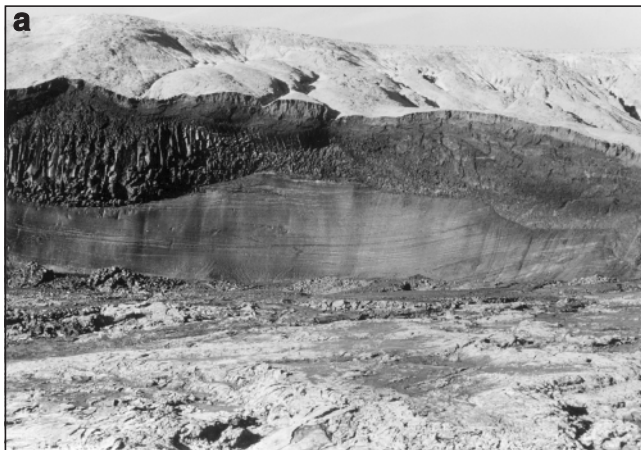


Figure 4. Exposures of massive ice exposed in **a**) the Eureka (GSC 2000-022G) and **b**) Slidre River (GSC 2000-022H) areas.

valuable role in environmental reconstruction. Information on the nature and distribution of ground ice on Fosheim Peninsula and in the High Arctic in general is important if we hope to predict terrain changes in response to recent predictions of warming and increased precipitation for arctic environments that are associated with global climate change (Schlesinger and Mitchel, 1987; Houghton et al., 1990).

Since ground ice is inherently unstable, it is also significant for geotechnical reasons. Many geotechnical issues identified in the early 1940s (Muller, 1945) are still the source of considerable concern for northern development (French, 1994). Changes to surface conditions may modify ground thermal regimes and moisture conditions sufficiently to induce highly destructive processes such as frost heave, thermokarst, and gully erosion.

BACKGROUND

General

Ground ice occurs throughout the permafrost zone of Canada and is generally present in most permafrost materials with the exception of impermeable bedrock. Massive ice has been reported in many parts of the Canadian Arctic (Lamothe and St-Onge, 1961; Mackay, 1966, 1971, 1973; French et al., 1982, 1986; Edlund et al., 1989; Egginton and Hodgson, 1990; Pollard, 1990), northern Alaska (Lawson, 1986), Russia (Solomatina, 1986), and China. The main body of detailed information on ground-ice characteristics in Canada has focused on occurrences in the Mackenzie Delta and northern Yukon Territory (Mackay, 1963, 1973; Pollard and French, 1980; Dallimore and Wolfe, 1988; Harry et al., 1988; Pollard and Dallimore, 1988; Mackay and Dallimore, 1992). Massive ice has been described on Banks Island (French et al., 1982, 1986), Victoria Island (Lorrain and Demeur, 1985), and Melville Island (Sharp, 1992). Until recently, however, very little information has been available on ice-rich permafrost and massive ice in the High Arctic. Previously, ground ice was not thought to be important under the extreme dry and cold conditions typical of High Arctic polar deserts because of the apparent lack of groundwater to feed ground-ice processes. Since ground ice is now seen to be locally significant in parts of the High Arctic, an important part of this paper is to explain water source and transfer processes.

High Arctic

Since the establishment in 1988 of the Hot Weather Creek High Arctic observatory by the Terrain Sciences Division of the Geological Survey of Canada, several researchers have reported on ground-ice conditions on Fosheim Peninsula (Edlund, 1989; Pollard, 1991; Barry and Pollard, 1992; Robinson, 1994; Hodgson and Nixon, 1998). Prior to this, however, only a few published reports described ground-ice conditions in the Canadian High Arctic. Of note, St-Onge (Lamothe and St-Onge, 1961; St-Onge, 1964) documented ground ice as part of a description of surficial materials in the Isachsen area of Ellef Ringnes Island. Similarly, Christie

(1964) described various types of ground ice in the Lake Hazen area of northern Ellesmere Island, including segregated ice in bedded silts, ice-wedge ice, and extensive buried glacier ice. Kalin (1971) documented buried glacier ice in the terminal moraine system of the White and Thompson glaciers at Expedition Fiord on west-central Axel Heiberg Island. Ground ice is mentioned in a number of geological and consultants' reports in the context of Quaternary geology or material properties (e.g. Hodgson, 1973a, b, 1974). Hodgson (1974), Hodgson and Edlund (1975), and Edlund (1989) briefly describe ground ice with respect to geomorphology, terrain disturbance, and vegetation in central Ellesmere Island.

Study area

The focus of this report is the west-central portion of Fosheim Peninsula on western Ellesmere Island and May Point on western Axel Heiberg Island (Fig. 5). This area forms a large, rolling lowland surrounded by glacierized mountains that rise to over 500 m a.s.l. The landscape is incised by numerous short river channels. Ice-wedge polygons are ubiquitous in areas of sediment cover and active-layer detachment and retrogressive thaw-slump scars are also common. The area is underlain by poorly lithified Mesozoic and Cenozoic clastic rocks of the Savik, Awingak, Deer Bay, Isachsen,

Christopher, Hassel, Kankuk, and Eureka Sound formations (oldest to youngest). Outcrops of weathered bedrock are widespread at elevations above the marine limit and resistant sandstones of the Heiberg Formation form steep ridges over 500 m a.s.l. Fosheim Peninsula lies east of and thus beyond a belt of glacial drift that marks the Late Pleistocene glacial limit (Hodgson, 1985). Approximately 30 per cent of the peninsula lies below the Holocene marine limit, which is placed at approximately 140 to 150 m a.s.l. (Hodgson, 1985; Egginton and Hodgson, 1990). Below this elevation, a blanket of fine sediment of variable thickness containing sandy silt and silty clay covers much of the surface. This sediment contains whole shells (some valves are articulated) and shell fragments and thus is interpreted initially as marine in origin. Coarse sand and gravel occur in isolated layers and in raised beach and surface lag deposits. Scattered cobbles and boulders also occur on most surfaces. A fine-grained till and diamicton overlying bedrock are described by Hodgson (1985, p. 361) in the northern part of Fosheim Peninsula. The Quaternary history and the extent of Pleistocene glaciation in this area are still poorly understood (Hodgson, 1985) and could have a strong bearing on the interpretation of the origin of ground ice, its age, and the possible preservation of buried glacier ice. Thus, a particular concern of field mapping and section descriptions is the identification of fine till or diamicton units and their association with massive ice.

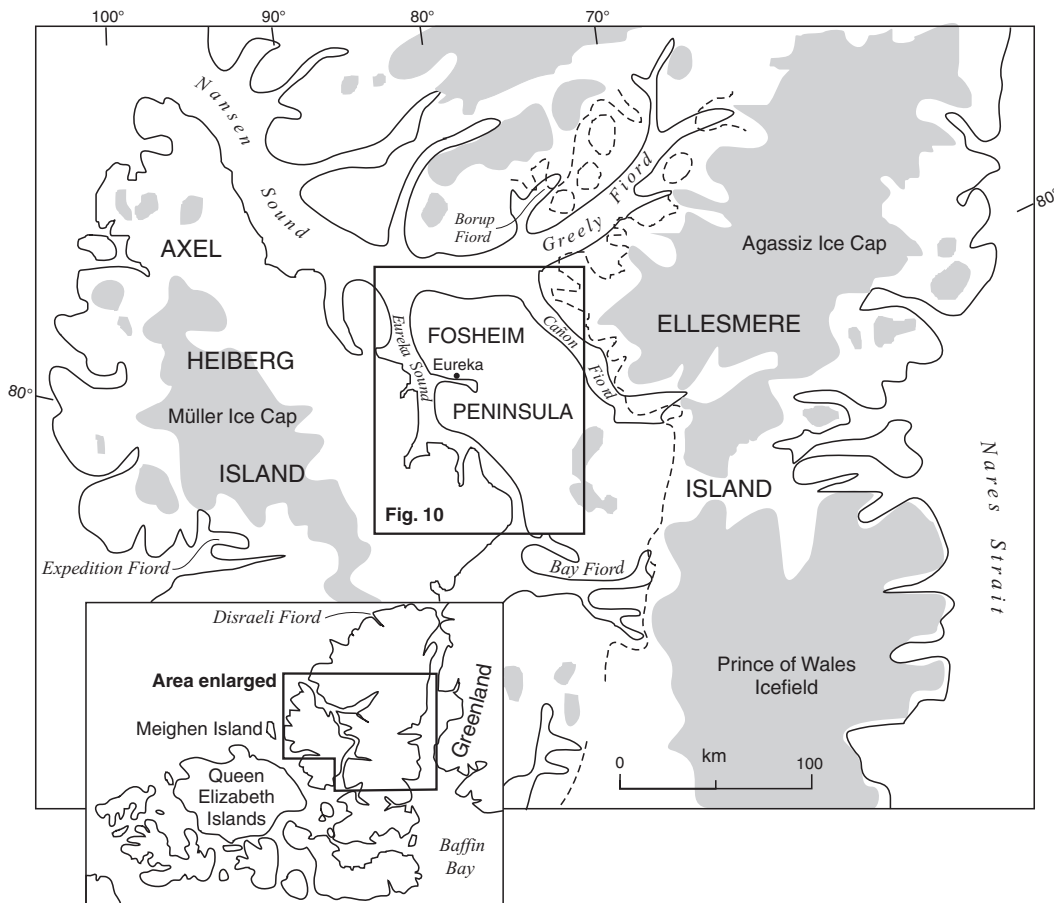


Figure 5. Map of the study area.

GROUND ICE ON FOSHEIM PENINSULA

Various forms of ground ice occur in surficial materials on Fosheim Peninsula. Pore ice is present in virtually all perennially frozen, unconsolidated sediments and in places is a source of excess ice. Similarly, ice-wedge polygons are found on most surfaces except resistant bedrock outcrops and ridges (e.g. Black Top Ridge). High-centred polygons are most common and polygon dimensions are highly varied, ranging from 7 to 20 m in diameter depending on setting and materials. In low-lying areas, ice-wedge troughs are usually well developed, but at higher elevations and in coarse-grained materials, they are poorly defined. Ice-wedge dimensions are also highly varied and depend on a combination of setting, age, and water supply. In the Eureka area, for example, ice wedges range from small fissures 10 to 30 cm wide and 100 to 200 cm deep to classic, V-shaped wedges 100 to 200 cm wide and 350 cm deep (Fig. 1b). The average width of an ice-wedge trough, based on the measurement of 350 wedges in five different areas, is 130 cm. Following the method described in Pollard and French (1980, equation 8), ice-wedge ice is estimated to make up approximately 10 to 12 per cent of the upper 5 m of permafrost; this is comparable with estimates from the Mackenzie Delta and Yukon Territory coast. Segregated ice ranges through a full spectrum of forms, from thin, discontinuous ice lenses, to fully developed, reticulate textures, to thick, tabular bodies of massive ice (Fig. 2, 3). It is particularly significant in fine-grained marine silts, silty clays, and sandy silts that were deposited during the late Quaternary and subsequently exposed to cold, subaerial permafrost conditions (Bell, 1996). Roughly 25 to 30 per cent of Fosheim Peninsula lies below the Holocene marine limit, which is approximately 150 m a.s.l. Above this elevation, weathered, coarse-grained, Tertiary deposits are widespread; however, even though they display widely spaced ice-wedge polygons, they do not seem to contain significant amounts of other forms of ground ice, particularly massive ice. Elevated, more resistant bedrock surfaces show no evidence of ground ice, although at Hot Weather Creek thick layers of pure ice were observed at depth in consolidated rock strata of the Eureka Sound Formation (*see below*). Buried ice is present in relatively small quantities as buried snowbank deposits in the stabilized headwalls of retrogressive thaw slumps. Buried glacier ice could be present in various till deposits, but to date has not been observed in this area.

A full understanding of the nature of ground ice requires an in-depth examination of its stratigraphic and physical characteristics. A general overview of ground ice can be inferred from airphotos, but detailed information on ground ice on Fosheim Peninsula comes from two other sources. The first is a regional coring program in the mid 1970s associated with mapping of surficial geology and Quaternary deposits (Hodgson et al., 1991; Hodgson and Nixon, 1998) and the second is a series of site-specific projects concerned with massive ice and thermokarst (Pollard, 1991; Barry, 1992; Robinson, 1994). Recent work by Bell (1992, 1996, Appendix B *in* Bell and Hodgson, 2000) on late Quaternary glaciation and sea-level history has also been very useful in the interpretation of ground ice.

Airphoto evidence

Fosheim Peninsula presents numerous surface features that reflect the presence and often unstable nature of ground ice. A general indication of the abundance and distribution of ground ice can be inferred from a variety of landforms and geomorphic evidence, much of which is visible on airphotos. For example, on an airphoto taken in 1959 (Fig. 6), ice-wedge polygons, thermokarst, and mass-wasting features are clearly visible at lower elevations and entirely absent from higher surfaces. Low-plateau features composed of marine sediments that host many of the thicker ground-ice bodies are also clearly visible. On a 1973 airphoto of the Panarctic Oils Gemini well site (Fig. 7), a large, retrogressive thaw slump with a 150–200 m long headwall, together with several smaller slumps, tundra ponds, ice-wedges troughs, and active-layer detachment scars dominate the landscape. Melting ground ice is visible as a dark band along retrogressive thaw-slump headwalls and runoff has created several large ponds up to 50 m wide. Similarly, 1986 airphotos of the area surrounding the Eureka weather station (Fig. 8a, b) show widespread thermokarst and erosion associated with terrain disturbance caused by construction and maintenance of the station airstrip. The numerous, large, retrogressive thaw-slump scars adjacent to Station and Airstrip creeks, however, clearly predate construction of the airstrip. Marine sediments forming relatively low, flat, undifferentiated terraces flank Station Creek. Numerous large, cusp-shaped scars and deep gully erosion reflect the unstable nature of these features. Extensive gully erosion also marks areas that were disturbed during construction of the airstrip. The present airstrip was built in 1951 after an airstrip built in 1947 was abandoned. A low-level airphoto (Fig. 9) of the abandoned airstrip shows the development of a modified vegetation cover, thaw degradation along ice-wedge troughs, and local ponding along ice-wedge polygons. Coring by Hodgson and Nixon (1998) encountered considerable ground ice in this area including ice wedges 5 m deep.

Drill/core data

In 1972, 1973, and 1974, D. Hodgson and M. Nixon drilled 152 holes to depths ranging from 1 to 8 m on central Ellesmere Island, using a variety of hand-held corers and drills. Although the purpose of the coring was to assist stratigraphic studies and mapping of Quaternary deposits on western Fosheim Peninsula, the nature and content of ground ice were of central interest. The primary aim of coring was to measure ice content in the main groups of surficial material near Eureka while focusing on materials known to contain excess ice and on disturbed areas. At the time “interest in ground ice was stimulated by terrain performance and disturbance associated with oil and gas exploration” (Hodgson and Nixon, 1998, p. 3). Such exploration was carried out on Fosheim Peninsula and eastern Axel Heiberg Island from the late 1960s to the mid 1970s. Figure 10 shows the location of drill sites mentioned in Hodgson and Nixon (1998). Hodgson and Nixon (1998) also report that visible ice was observed in shot holes during seismic reflection investigations carried out in the area by Panarctic Oils Ltd.

Approximately 61 per cent of the holes were drilled in Holocene marine sediments and marine veneer, 30 per cent in weathered bedrock, 6 per cent in till, and the remaining 5 per cent in peat and other materials. Most holes were drilled below the Holocene marine limit. Approximately 18 per cent of the holes were drilled at sites of known anthropogenic disturbance, 25 per cent in ice-wedge troughs, and 33 per cent in ice-wedge-polygon centres. Hodgson and Nixon found that for all the holes, the mean volumetric ice content was 53 per cent, i.e. ranging from 30 per cent for 10 holes drilled in

coarse rock material to 84 per cent for the 38 holes drilled in ice-wedge troughs. A mean ice content of 64 per cent was obtained for the 90 holes drilled in marine sediments. However, this value could be misleading because it includes the majority of holes drilled in ice-wedge troughs that by nature have a high probability of encountering massive ice. The average ice content for 50 holes drilled in polygon centres was 47 per cent; however ice content was under 25 per cent in 17 of the holes. Hodgson and Nixon also found gradational contacts between sediments and ice (denoted by reticulate

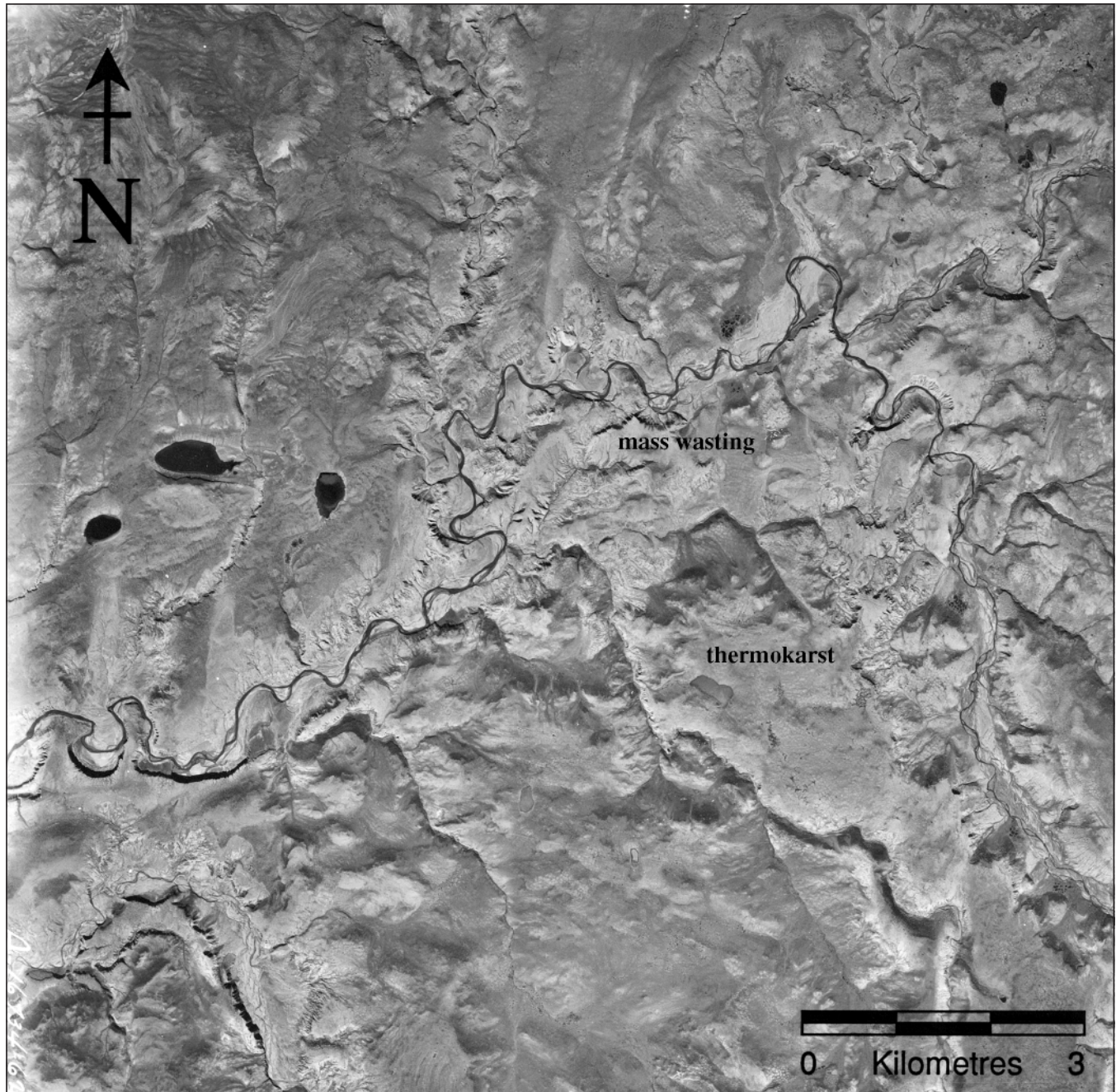


Figure 6. Airphoto of the Slidre River area showing ice-wedge polygons, thermokarst, and mass-wasting features at lower elevations (scale: 1:60 000). NAPL A16734-62

cryogenic structure) as well as horizontal stratification within the ice. They also noted vertical elongation of gas inclusions in massive ice.

Coring by Hodgson and Nixon in the immediate Eureka area encountered considerable ground ice, including 3 m of pure and silty ice 50 to 150 cm beneath the ground surface in

polygon centres and pure ice to 4.5 m beneath an ice-wedge trough at the old airstrip. At the new airstrip, massive ice was encountered beneath ice-wedge troughs, but not elsewhere. However, as will be mentioned in the discussion on ground-ice stratigraphy, massive ice is also present near the new airstrip, but is stratigraphically deep (Pollard, 1991). The thick bodies of massive ice described by Pollard (1991) hold

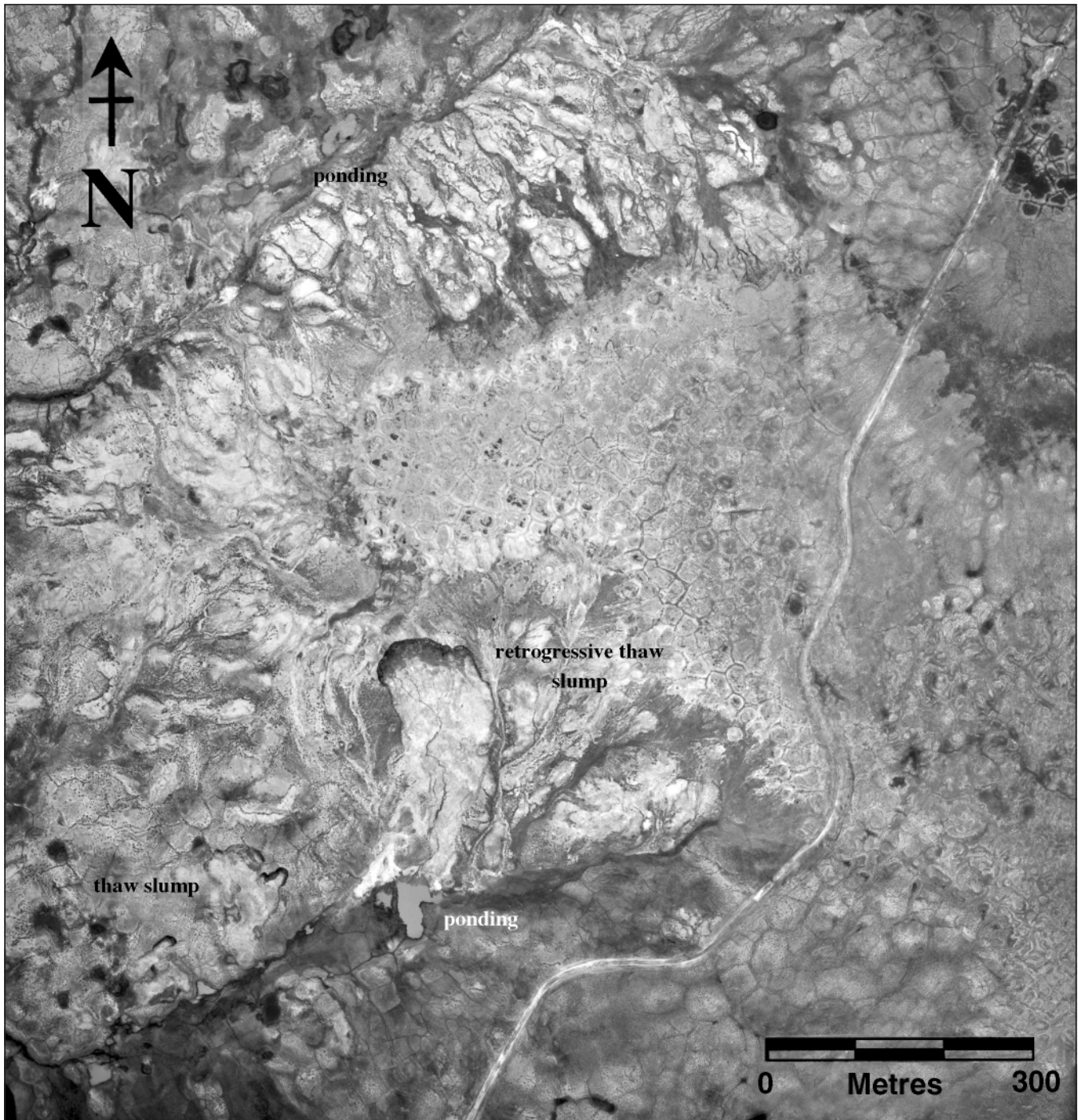


Figure 7. Airphoto of Panarctic Oils Gemini well site, showing a large retrogressive thaw slump, several smaller slumps, tundra ponds, ice-wedge troughs, and active-layer detachment scars (scale: 1:5500). NAPL A30859-47

significant potential for thermokarst; however, the bed of coarser grained material and aggregate that currently underlies the airstrip allows free drainage and provides insulation against thaw subsidence.

Barry (Barry, 1992; Barry and Pollard, 1992) drilled a series of shallow holes using a United States Army Cold Regions Research and Engineering Laboratory coring kit in

support of geophysical investigations near Hot Weather Creek and Eureka. At Hot Weather Creek, Barry encountered ice-rich strata and laminated, cryogenic structure immediately below the base of the active layer, adjacent to a retrogressive thaw slump, and along the tops and sides of ice wedges. Shallow drilling at Eureka defined ice-lens formation during active-layer freezeback and found ice-rich sediments at the base of the active layer.

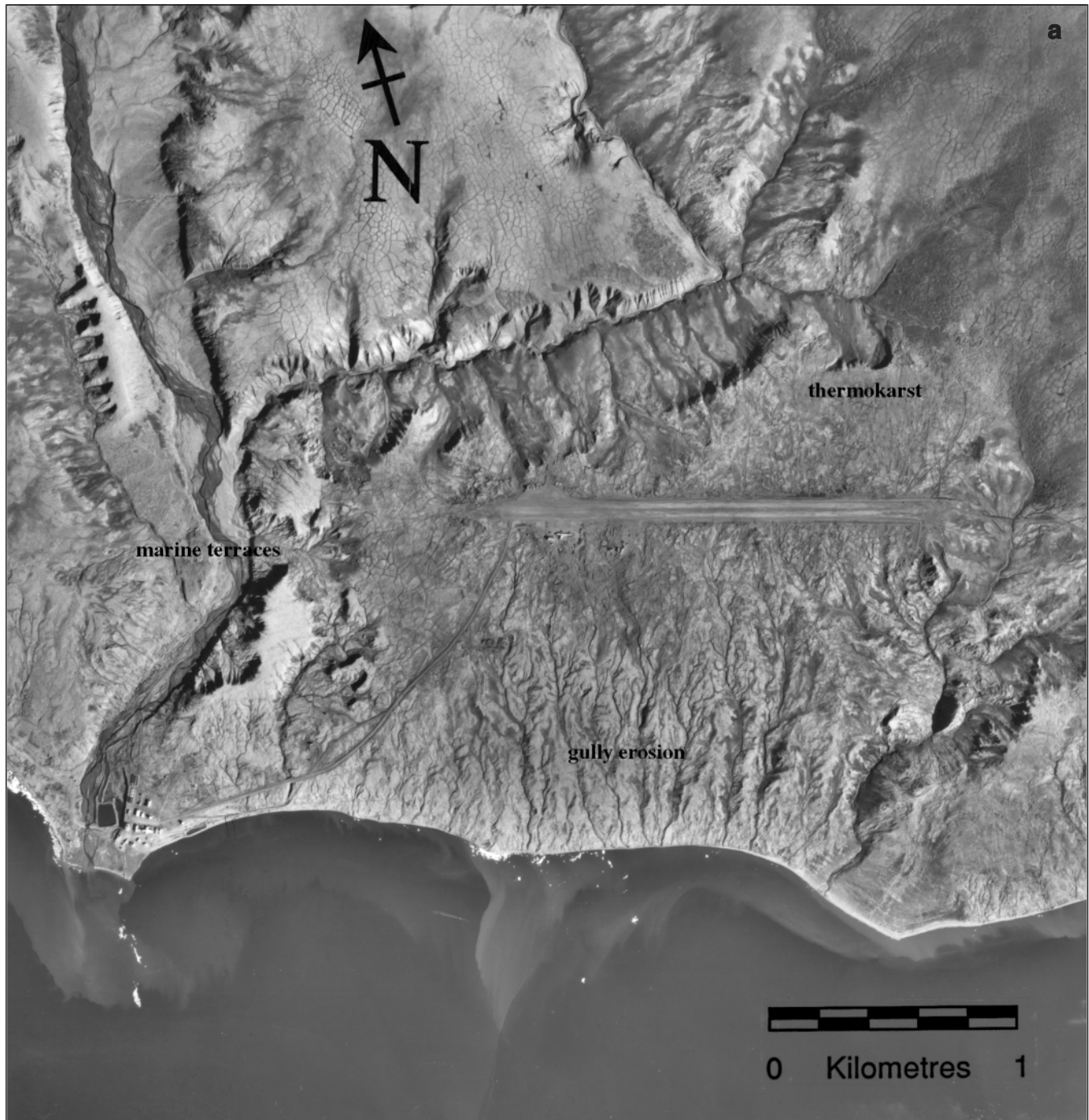


Figure 8. Area around the Eureka weather station showing marine terraces and thermokarst; **a)** scale of 1:60 000 (NAPL A27038-24); **b)** scale: 1:7000 (NAPL A27038-112).

Robinson (1993) drilled 18 shallow boreholes using a United States Army Cold Regions Research and Engineering Laboratory permafrost corer in support of geophysical investigations at 'Hacker Creek', a small, ephemeral tributary of Slidre River that drains an ice-rich plateau composed of

marine sediments. This area is approximately 4 to 5 km south-east of Hot Weather Creek and 3 km south of the Gemini well site and lies within the Slidre River valley ground-ice area. Drilling at undisturbed plateau surfaces failed to encounter massive ice before holes bottomed out at depths of 2.34 to

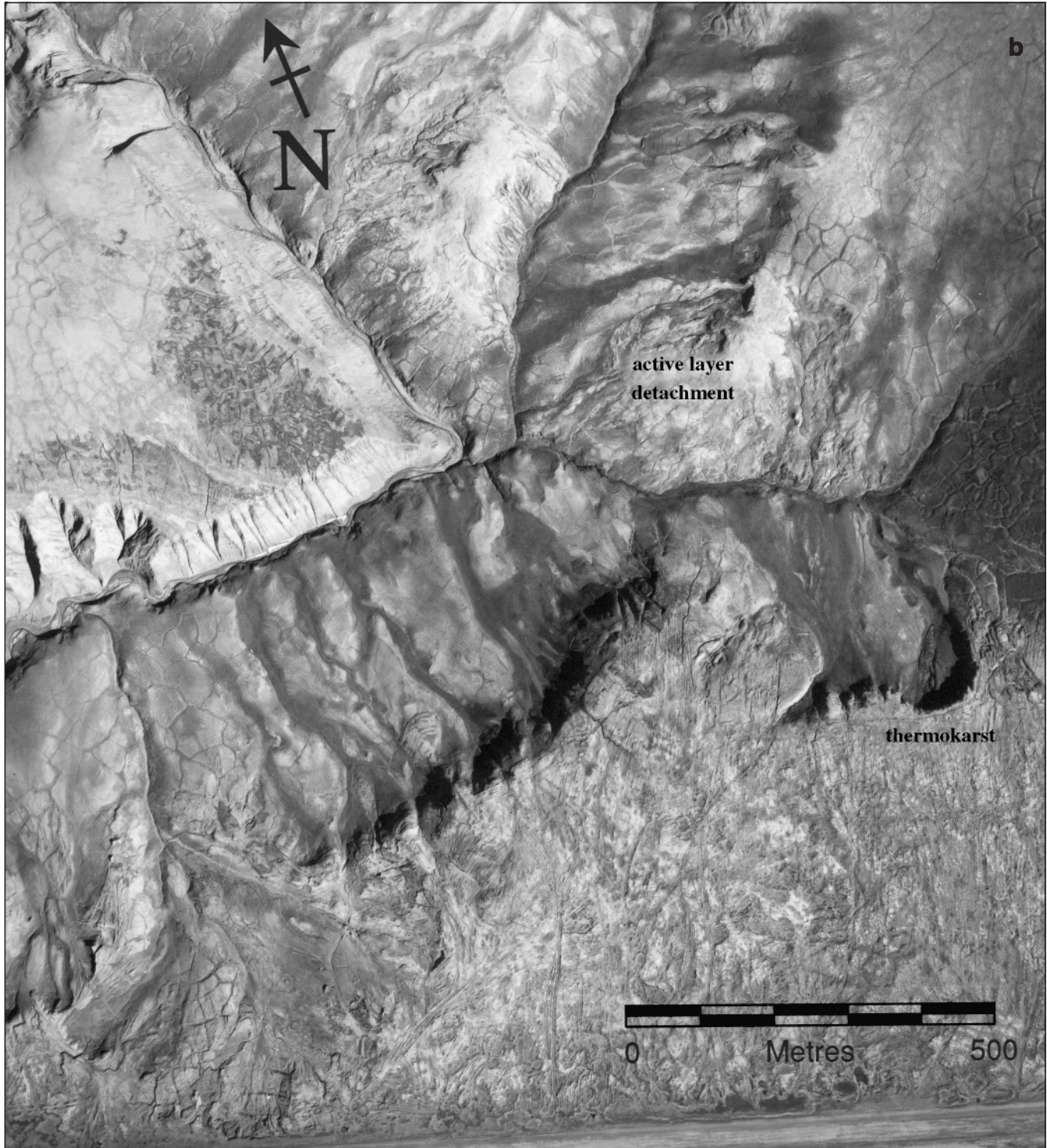


Figure 8b.

2.54 m. At lower elevations, however, Robinson encountered ice at depths between 0.85 and 2.45 m. Ice in these holes was only slightly thicker than 1 m, which is technically less than the limiting minimum thickness for massive ice (Mackay, 1989).

Geophysical investigations

Both Barry (1992) and Robinson (1993) focused on the application of geophysical techniques to delineate ground-ice conditions. Barry used ground-penetrating radar whereas Robinson used gravity and electromagnetic surveys in addition to ground-penetrating radar. The ground-penetrating-

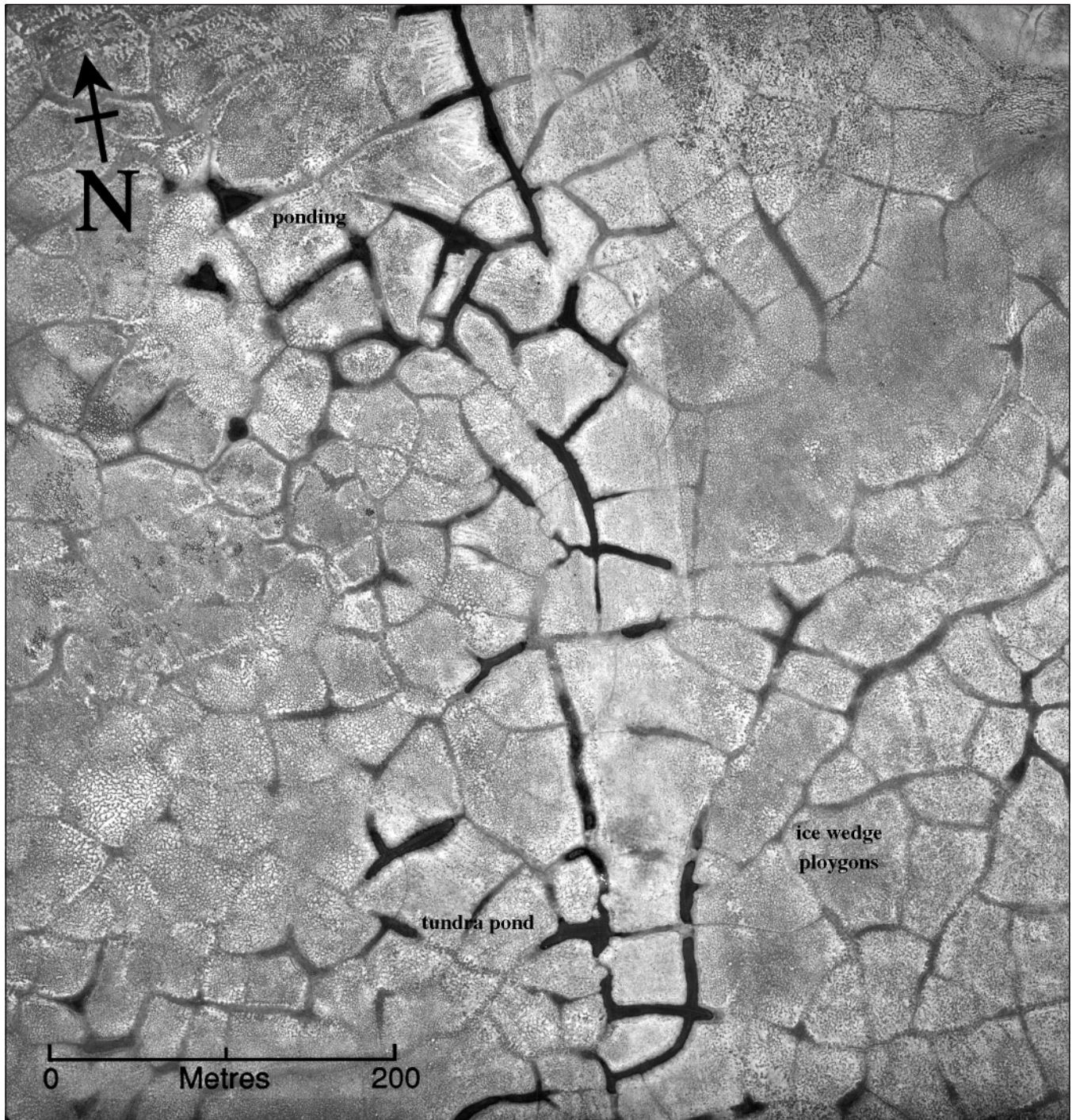


Figure 9. Low-level airphoto of the old Eureka airstrip showing the development of a modified vegetation cover, thaw degradation along ice-wedge troughs, and local ponding along ice-wedge polygons (scale: 1:2000). NAPL A30860-174

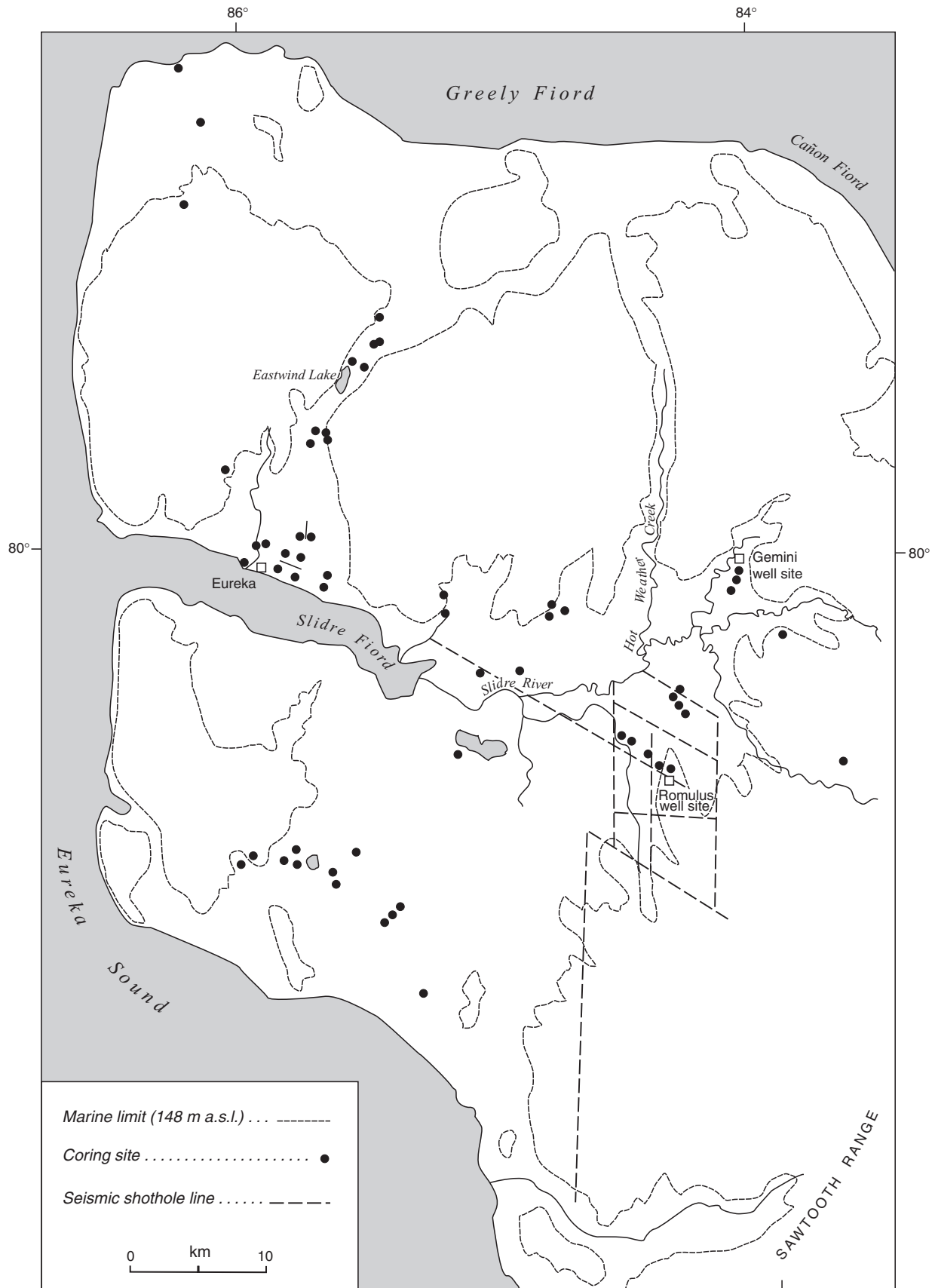


Figure 10. Map of western Fosheim Peninsula showing the distribution of ice-coring data (from Hodgson and Nixon, 1998).

radar technique involves the transmission of short pulses of high-frequency, electromagnetic energy into the ground; reflections are produced when the energy encounters interfaces with contrasting properties. Permafrost usually provides an ideal transmission medium, but in this area the conductive nature of thawed sediments in the active layer and the high salt content of the marine sediments caused signal attenuation and generally poor results. However, despite limited success, both Barry and Robinson demonstrated that many areas are underlain by extensive ground ice. In particular, Robinson used gravity profiles to show that a terrace of laminated sandy silt and silty clay was cored by massive ice up to 17 m thick. The terrace in question is within the area designated as massive-ice site 3 (Fig. 11, massive-ice site 3). In addition to gravity profiles, Robinson also provides a series of stratigraphic descriptions and detailed observations on thermokarst.

Natural sections

Spatial patterns in ground-ice content and morphology are highly varied (Pollard and French, 1980). This reflects not only the discrete nature of some ground-ice features such as ice wedges and frost mounds or buried surface ice, but also the very complex nature of processes associated with epigenetic ground-ice formation. Coring provides a point indication of ground ice and limited stratigraphic information, but rarely provides information on the lateral extent of ground ice unless a series of closely spaced cores is obtained. Geophysical surveys on the other hand provide useful spatial information, but lack detail. Both are subject to technical problems and limitations. Although considerable general information is obtained from coring and geophysical surveys, the most detailed information on ice morphology, structure, stratigraphy, and sediment character comes from the examination of natural, vertical exposures of sediment. The unstable nature of ground ice contributes to accelerated erosion and inevitably results in thaw-related disturbances where excess ice is present. As a result, most areas containing massive ice or ice-rich permafrost develop natural exposures, which in some cases are 20–30 m high. The most useful sediment exposures are found in the headwalls of active retrogressive thaw slumps, or active-layer detachments, and along river channels. Studies of ground ice on Fosheim Peninsula involved measuring several sections at each exposure of ground ice and sampling major sediment and ice units. In addition to mapping lithological and sedimentological variations and structures, contact relationships between massive ice and its enclosing sediments, sediment layers contained within ice units, and ice-inclusion (both sediment and gas) patterns were studied in detail.

MASSIVE ICE

Distribution and setting

Reconnaissance of the Fosheim Peninsula–Eureka Sound area in 1991, 1992, and 1994 identified seven separate areas, each characterized by several exposures (sites) with massive

ice (massive-ice sites), as well as both active and inactive thermokarst features and tundra ponds (Fig. 11). The seven areas are as follows: Eureka (lat. 80°00'N, long. 85°57'W); south Slidre Fiord (lat. 79°56'N, long. 86°05'W and lat. 79°54'N, long. 85°30'W); Slidre River (lat. 79°55'N, long. 84°14'W), including Hot Weather Creek (lat. 79°59'N, long. 84°28'W) and the Gemini well site (lat. 79°58'N, long. 84°10'W); Blue Man Cape (latitude 79°44'N, long. 85°57'W); Eureka Sound (lat. 79°43'N, long. 84°30'W); south Fosheim (lat. 79°28'N, long. 84°20'W); and May Point (lat. 79°25'N, long. 84°29'W). The May Point area is on eastern Axel Heiberg Island, directly across Eureka Sound from the south Fosheim site. It lies on the western edge of the intermontane basin marking the physiographic unit that characterizes Fosheim Peninsula. It has most of the same geomorphic and stratigraphic characteristics as sites on Fosheim Peninsula and is therefore relevant to this study. Two other areas, Romulus Lake (lat. 79°52'N, long. 84°55'W; RL in Fig. 11) and the Depot Point airstrip (lat. 79°22'N, long. 86°24'W and lat. 79°24'N, long. 86°00'W; DP in Fig. 11), also have widespread thermokarst, similar surficial geology, and most of the same topographic characteristics, but currently lack exposures of massive ice. A number of isolated exposures of massive ice and retrogressive thaw slumps were also mapped. Retrogressive thaw slumps, although not always containing massive ice, indicate the presence of relatively large bodies of icy permafrost and excess ice. The distribution of massive ice corresponds closely with that of fine-grained, marine sediments identified by Bell (1996). The nature of the ice is also stratigraphically controlled by these and other surficial materials. The most significant ice exposures, however, occur where thick marine deposits form flat to gently dipping plateaus. The only massive-ice location lacking this type of landform is the Blue Man Cape site.

During this study, 73 sections containing massive ice and ice-rich sediments were examined. In many places, small slumps are associated with exposures of wedge ice. Ice-wedge ice is a common constituent of surface materials, with ice wedges occurring everywhere surface deposits are thick enough to allow thermal contraction cracking; however, sites where ice wedges were the only type of ice exposed are not included. In cases where ice wedges are exposed parallel to their longitudinal axis, their horizontally layered ice is easily mistaken for segregated ice.

On the basis of aerial reconnaissance in 1994, there are an estimated 150+ stabilized retrogressive thaw slumps and sites marked by thermokarst topography. Although many of these inactive features (approximately 60 per cent) occur near active slumps and ice exposures (i.e. massive-ice sites 1–7 in Fig. 11), they also occur in numerous other locations characterized by fine-grained, marine sediments. The Romulus Lake and Depot Point airstrip sites each contain numerous, large, stabilized slump scars in laminated, marine sediments. In places, seepage from thawing ice produces localized ponding, but no ice was visible at the time.

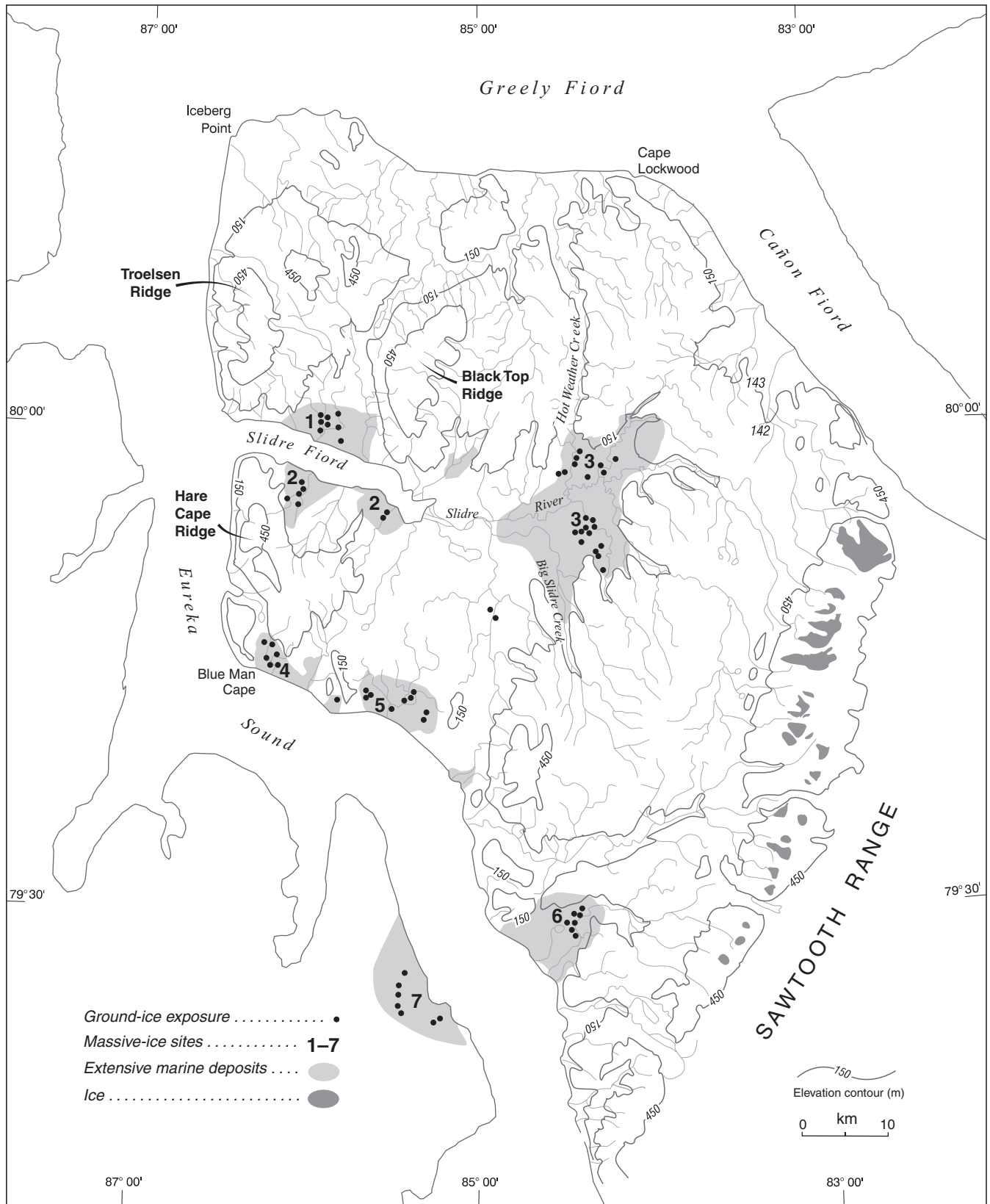


Figure 11. Map showing the distribution of areas and exposures of massive ground ice.

Ice-content profiles

The vertical distribution of ground ice, combined with the ground thermal regime (as defined by active-layer dynamics), determines the relative sensitivity of permafrost materials. Since the nature and distribution of ground ice is a function of freezing history, water supply, sediment lithology, stratigraphy, and localized processes such as thermal contraction cracking, it is not surprising that ice content varies considerably over relatively short distances. However, on Fosheim Peninsula, the pattern of ground-ice content is closely linked to the thickness of marine sediments and, although considerable variation exists both locally and regionally, the presence of terraced marine deposits proved to be an extremely good indicator of massive ice.

Several sections at each massive-ice site were analyzed for ice content. For convenience, ice content is expressed as a percentage by volume, although most measurements were done gravimetrically. Gravimetric ice content was converted to volumetric ice content following a procedure outlined in Pollard and French (1980). The base of the active layer formed the top of most measured profiles. Active-layer depths vary considerably, ranging from 60 to 70 cm for dry, south-facing surfaces to 30 to 40 cm for damp, north-facing or shaded locations. In much of Fosheim Peninsula, particularly above the marine limit where surficial materials are coarse grained, permafrost is quite dry and ice content averages 3 to

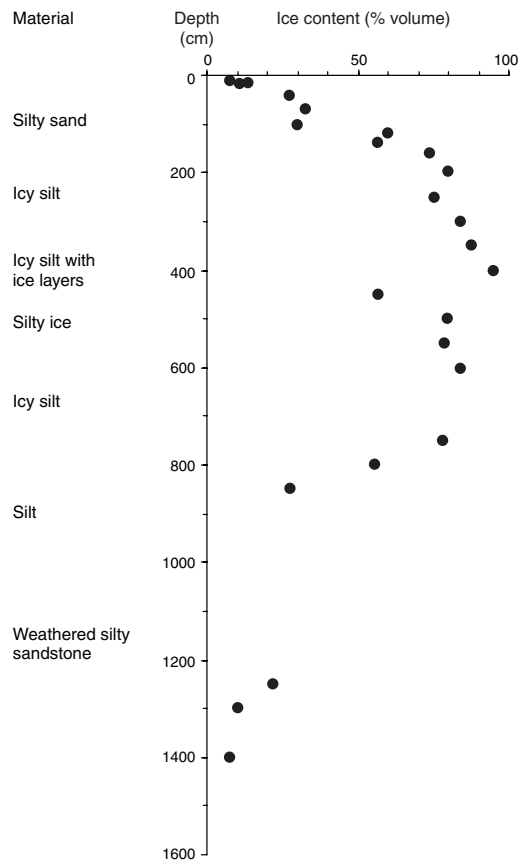


Figure 12. Ice-content profile, pattern 1, for a site in the Eureka Sound area.

10 per cent by volume. However, in the ice-rich areas below the marine limit, ice-content profiles form three patterns. The first, illustrated in Figure 12, is marked by moderately high ice content (20–30 per cent), with the ice occurring as pore ice and thin, discontinuous ice lenses and layers near the base of the active layer. Beneath the active layer, ice content increases sharply so that at depths of roughly 1.0 to 1.3 m, it reaches 60 to 99 per cent where layers of pure ice and muddy ice predominate; the sediment in the ice is mainly silt or clay sized. In this pattern, ice content is high at depths from 2 to 7 m to 8 to 9 m. In only a few instances is it possible to obtain data below the base of the massive-ice zone and, in such cases, the ice content drops dramatically (10–30 per cent). Pore ice and lens ice occur where the lithology changes to coarse, sandy material or weathered bedrock. Figure 12 shows the relationship between ice content and stratigraphy in a section at the Eureka Sound ground-ice area. Figures 13a and b show sections of massive ice from Hot Weather Creek (Slidre River ground-ice area) and Eureka, respectively.

The second pattern is marked by a layer of weakly laminated, sandy silt 5 to 7 m thick with ice content ranging from 8 to 15 per cent near the base of the active layer, to 12 to 17 per cent at depths of 2 to 3 m. Near the base of the unit, ice content increases to 30 to 40 per cent as clay and silt contents increase.

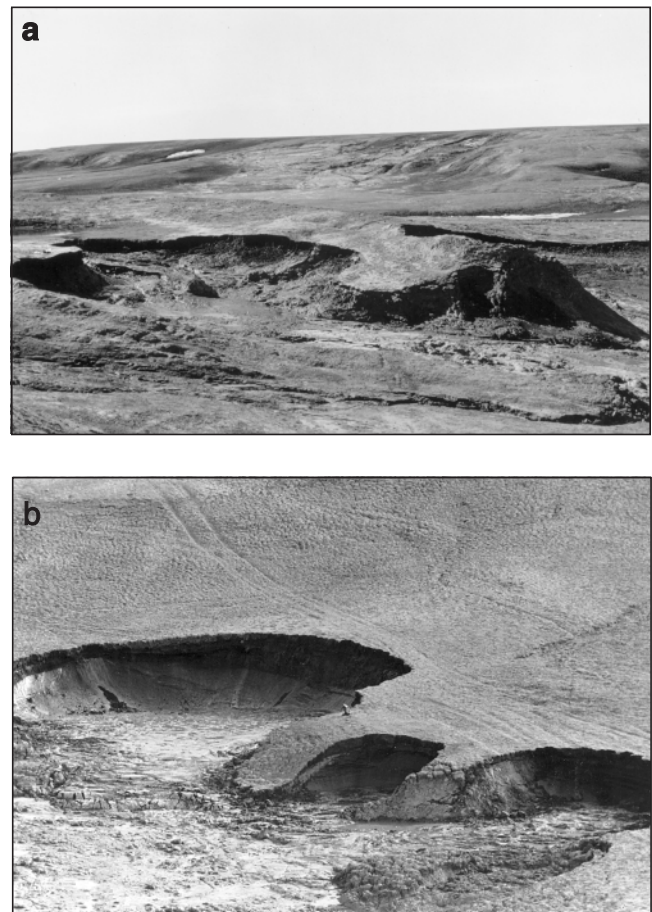


Figure 13. Exposures of massive ice at **a**) Hot Weather Creek (GSC 2000-0221) and **b**) Eureka (GSC 2000-022J).

Pore ice and lens ice grade into more regular, vertical and reticulate ice veins. At depths ranging from 7 to 10 m, faintly laminated, silty clay changes abruptly to massive ice containing fragments or layers of silty clay (60–70 per cent ice) to pure, horizontally foliated, massive ice (90–100 per cent ice). Figure 14 shows an ice-content profile and Figure 15, sections of massive ice from the Eureka area.

The third pattern is intermediate between the first and second. Ice content increases gradually (15–30 per cent) with depth and usually reflects an increase in silt content. At a depth of roughly 4 to 5 m, interbedded layers of silty ice and icy silt with ice contents of 65 to 78 per cent (locally higher) predominate for up to 5 m. At a depth of 9 to 10 m, ice content decreases to 50 to 60 per cent; below this depth, ice content drops off dramatically (5–10 per cent) as materials grade into a weathered bedrock substrate. Figure 16 shows an ice-content profile and Figure 17, an exposure of ground ice from the Blue Man Cape area.

Association with marine sediments

These three patterns reflect a combined effect of local differences in permafrost aggradation, lithology, and water supply on epigenetic ground-ice formation. For example, within areas where laminated marine deposits form flat to gently

dipping terraces and plateaus, the first pattern is most common (Fig. 18a, b, c, d). In such areas, thick massive ice with a volumetric ice content of 85 to 99 per cent occurs as uniform, tabular bodies at the unconformable contact between fine-grained marine sediments and underlying, coarse-grained, transgressive deposits and weathered bed-



Figure 15. Exposure of massive ice in the Eureka area. GSC 2000-022K

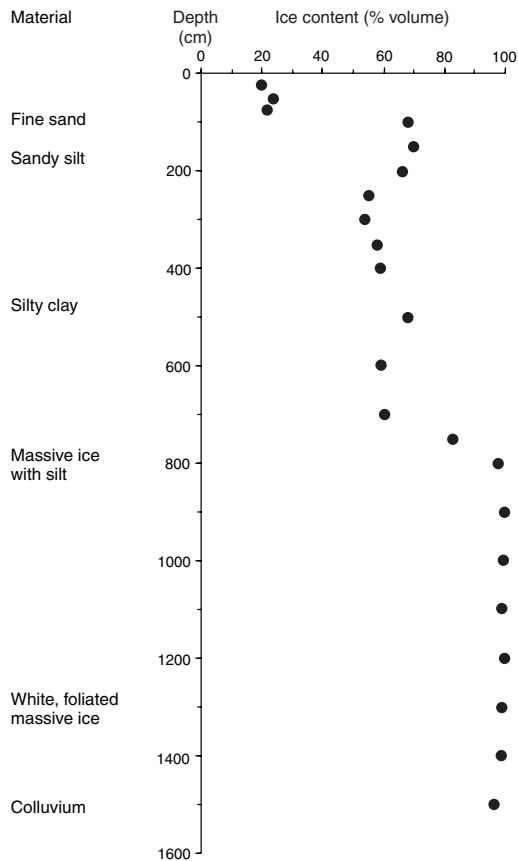


Figure 14. Ice-content profile, pattern 2, for a site in the Eureka area.

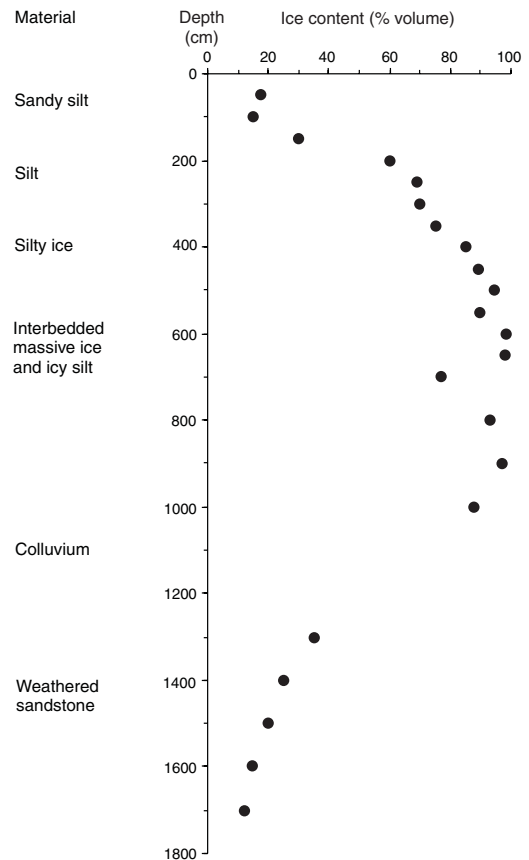


Figure 16. Ice-content profile, pattern 3, for a site near Blue Man Cape.



Figure 17. Exposure of ground ice at Blue Man Cape. GSC 2000-022L

rock. At several locations, a thin band of oxidized sand marking this unconformity can be seen at the contact between the massive ice and the overlying marine deposits. The presence of oxidized sand and thin layers of marine sediment in the upper part of the massive ice indicates that ground ice formed as the freezing front of aggrading permafrost reached this depth. The low hydraulic conductivities and impermeable nature of the fine-grained marine sediments do not permit sufficient water migration for massive ice to form within the deposit. As a result, in situ freezing produces pore ice, small ice lenses, or discontinuous ice layers. Water is readily drawn to the freezing front as the front approaches the underlying weathered bedrock and sandy material associated with marine transgression. As long as the water supply balances freezing associated with permafrost aggradation, ice will continue to form. Even though climates were extremely arid during the time of permafrost aggradation, two potential sources of water did exist. During the first half of the Holocene, both runoff from the melting of local ice caps and brackish seawater were available to recharge local



Figure 18. Massive ice exposed in marine sediments forming flat terraces at **a)** Eureka (GSC 2000-022M), **b)** and **c)** Slidre River (GSC 2000-022N, -022O), and **d)** Slidre Fiord (GSC 2000-022P).

groundwater systems of emerging landscapes. In the latter part of the Holocene, seawater remains the only significant source of water for the formation of ground ice.

Ice in bedrock

In 1992, undercutting of a meander bend by Hot Weather Creek a few hundred metres downstream from the Hot Weather Creek base camp created a particularly interesting exposure 25 to 30 m in height (Fig. 19). This section contained 1.8 m of massive ice and icy sand in bedded sands (Fig. 20) and also several ice sills 30 to 60 cm thick within intact bedrock of the Eureka Sound Group (Fig. 21a, b). The upper sand unit is horizontally bedded and locally

crossbedded and contains a series of thin, clay-silt and coal layers. Massive ice occurs with a band of silty sand and its upper and lower contacts are gradational. Deformation of the ice is apparently related to a diapiric uplift beneath a large ice wedge. Although massive ice in sand is unusual, it is the presence of ice in bedrock that is significant since it was not seen elsewhere during this study. The presence of 16 to 18 m of sand, silty sand, and ice overlying the ice-bearing bedrock is also significant. At this location, the Eureka Sound Group consists of fine- to medium-grained, white sandstone with thick bands of coal and grey, muddy sandstone. The ice occurs as a series of sills of varied thickness that extend 20 to 30 m horizontally. It is relatively clean in appearance and, in



Figure 19. Ground ice in bedrock at Hot Weather Creek. GSC 2000-0220



Figure 20. Upper part of the section in Figure 19 showing massive ice in bedded sand. GSC 2000-022P



Figure 21. Ice sills in bedrock. **a)** GSC 2000-022S, **b)** GSC 2000-022T

all cases, it forms a sharp contact with the enclosing rock. The water source for this ground ice would have been deep groundwater.

Ice in till/diamicton

According to Bell (1992, 1996), the highland ice caps of the last glaciation produced small, localized moraines and a thin till veneer. Localized glacial deposits (till and diamicton) associated with a more pervasive, pre-Wisconsinan glaciation also cover parts of Fosheim Peninsula, although mainly above the Holocene marine limit. However, the presence of localized glacial deposits — no matter how thin — introduces the potential for buried glacier ice. Of the seven massive ground-ice areas identified, none are above the marine limit where most till deposits occur and only one, the Blue Man Cape area, is below the marine limit where glacial deposits have been mapped (Bell, 1992). Ground ice at the Blue Man Cape (massive-ice site 4) is, however, quite different from ice observed in all other areas. At this location, sediment-rich massive ice is overlain unconformably by a bouldery diamicton. Horizontal to gently dipping bands of silty sand produce foliations within the ice body; large boulders and cobbles are found locally (Fig. 22). Material contained in the ice is the same as the overlying sediments. The unconformable nature of the upper contact is not unusual for such a shallow ground-ice deposit. Neither chemical nor petrographic analyses could demonstrate conclusively a glacial origin for this ice mass; rather, traces of NaCl in the ice tend to refute a glacial origin. If this were glacier ice, one would expect the internal structure to reflect an orientation other than one parallel to the ground surface; moreover, one would not expect to find such a strong similarity between enclosing and contained sediments. Therefore, it would seem that the ice shown in Figure 22 was formed in situ as permafrost aggradated into reworked glacial deposits and is thus intrasedimental in origin.



Figure 22. Massive ice in bouldery diamicton at Blue Man Cape. GSC 2000-022U

GROUND-ICE STRATIGRAPHY

Methods

Stratigraphic descriptions were derived from two or three measured sections at approximately 30 locations; in some cases, steep, unstable exposures limited access to upper parts of the section. Wherever possible, contact relationships between units, particularly between the massive ice and enclosing sediments, were documented in detail. Since most information in this study comes from natural sections, only the upper massive-ice contacts were documented at all sites. Lower contacts are rarely seen in retrogressive thaw slumps and, in this study, they were documented only where secondary erosional processes (e.g. river or coastal erosion) removed flow deposits produced by thermokarst and underlying sediments. At locations where basal contacts were not accessible, the examination of sediments contained in the ice and the analysis of nearby sections with no massive ice indicated that deep bodies form at or near the contact between marine deposits and the underlying bedrock. Stratigraphic units were defined using a combination of sedimentology and cryogenic texture (Pollard, 1991). Samples were taken from each unit for grain size, moisture content, and hydrochemical analyses. Conductivity, salinity, and pH of melted ice samples were measured on site; all other analyses were carried out at McGill University, Montréal, Quebec. Shell and organic materials were sampled for identification and dating. Large, oriented block samples of massive ice were excavated from ice faces to document gas and sediment inclusions. Exposure to direct solar radiation induces intercrystalline melting and the formation of Tyndall figures, which allow preliminary observations on crystal texture. Twenty-two oriented block samples were transported to the author's geocryology laboratory at McGill University for petrographic analyses.

Cryostratigraphy

Detailed stratigraphic analyses involving measured sections, sampling of ice and sediments, and elevation measurements show that the stratigraphic nature of ground ice is highly varied, reflecting primarily the thickness, structure, and grain-size characteristics of marine sediments. The ground ice observed occurs primarily in sandy silt and silty clay of marine origin. The elevations of the study sites range from 25 m to approximately 140 m a.s.l., and are therefore all below the Holocene marine limit. At the Eureka Sound site (massive-ice site 5) articulated shells, including *Mya truncata* and *Hiatella arctica*, occur in situ within the sediments that directly overlie the massive ice.

Bodies of massive ground ice exposed at Eureka (massive-ice site 1), Slidre Fiord (massive-ice site 2), Slidre River (massive-ice site 3), Eureka Sound (massive-ice site 5), and south Fosheim (massive-ice site 6) are similar in appearance and stratigraphic position. In each case, thick, clear to white ice bodies occur below several metres of laminated, sandy, marine silts and clays. Horizontal laminations are 1 to 2 cm thick and a reticulate cryogenic texture occurs in silty clay immediately overlying the massive ice. At undisturbed sites, the upper contacts are abrupt, but gradational.

Hydrochemical and isotopic analyses of ice from massive ice and overlying sediment indicate a common water source and sediment contained in the upper part of the ice mass is the same as the overlying material. In several instances, however, upper contacts are truncated by thaw unconformities associated with earlier thermokarst activity (Fig. 23).

A section along Station Creek at Eureka (Fig. 23) typifies the stratigraphic relationships found in many deep ice sections. A layer of fine sediment (unit A) ranging from 3 m to over 7 m in thickness overlies massive ice (unit B) containing horizontally layered, white and dark ice interbedded with laminae of icy sediment. The body of ice is exposed near the base of steep-sided stream valleys and sediment thickness is estimated from a composite of several sections. Unit A consists of dark brown, sandy silt with silty clay and clay layers grading into massive grey clay. Shells and shell fragments litter the ground and are found in the upper part of unit A. The upper 11.5 m of this unit (below a 40 cm thick active layer) has a relatively low ice content, with ice films, pore ice, and thin, discontinuous, horizontal ice lenses making up less than 15 per cent of the total volume. From roughly 1.5 to 2.0 m below the ground surface to the top of the ice unit, a distinct, reticulate texture is dominant. Variations in the size and spacing of vertical and horizontal ice veins produces two or three textural variations (cryofacies). In general, the clay-rich sediment blocks between ice veins are free of visible ice and are highly consolidated when thawed. Ice content within this part of unit A is roughly 20 to 22 per cent. The contact between units A and B is generally abrupt and, in most places, gradational, as is inferred from the inclusion of clay fragments from unit A in the upper 10 cm of the massive ice, the manner in which folia in the massive ice are more or less parallel to the upper contact, and the absence of fine particles from unit A in gas inclusions or along intercrystalline boundaries in massive ice immediately below the contact. Part of the contact that is clearly unconformable (broken line in Figure 23) is a thaw unconformity separating mudflow deposits without a reticulate texture from the underlying ice. Together with the truncation of primary structures in the

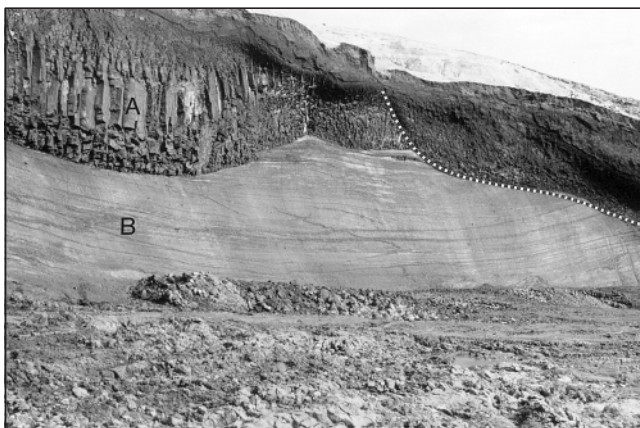


Figure 23. Massive-ice section with a thaw unconformity (dotted line) at Station Creek in the Eureka area. GSC 2000-022V

massive ice, this massive texture suggests that an earlier thermokarst event, possibly a retrogressive thaw slump or a thaw lake, caused deep thaw and produced a thaw unconformity.

A number of ice wedges in unit A are visible in a section in a nearby tributary valley. They are 0.7 to 1.5 m wide and up to 3 m deep and their tops are at a depth of 80 to 90 cm.

Unit B is composed of deformed, horizontally foliated, massive ice. The foliated appearance is produced by alternating layers of dark (clear) and white (bubble-rich) ice together with thin, discontinuous clay laminae. The volumetric ice content of unit B ranges from 98 per cent in samples from the white ice to 79 per cent in samples containing dark ice and clay laminae. In places, thicker layers of sediment and higher concentrations of suspended sediment result in a drop in ice content to 65 per cent. Figure 24 shows four exposures of massive ice in the Slidre River valley that have many of the same characteristics.

However, ice bodies at Hot Weather Creek (massive-ice site 3, Fig. 25a) and Blue Man Cape (massive-ice site 4, Fig. 25b) occur in a distinctly different stratigraphic setting. As described in the discussion on ice content, these sites have relatively shallow bodies of dirty massive ice. Overlying sediments tend to be fairly massive and ice-rich. The massive ice unit is composed of alternating layers of clean ice, dirty ice, and icy sediment. Ice-rich sediments beneath the active layer grade into the massive-ice body with no clear upper contact. At Hot Weather Creek, massive ground ice and icy sediments are exposed in the headwall of a bimodal retrogressive thaw slump, described by Edlund et al. (1989), and in a thermal erosional niche at the base of the stream bank. Both occur on the outside of a large meander loop of Hot Weather Creek that is cutting back into either a former tundra pond or a stabilized retrogressive thaw slump. In June 1990, the east bowl of the slump had a 2.8 to 3.1 m high headwall that contained 90 to 100 cm of sandy silt grading into 20 to 30 cm of grey clay overlying 1.6 to 1.9 m or more of massive ice. The silty sand unit varies from massive to finely bedded with thin clay bands. In places, the bedding is contorted and faulted. Visible pore ice and thin ice lenses occur below the base of the active layer and yield low ice contents (under 20 to 25 per cent by volume). Larger ice lenses are associated with clay bands. The grey clay unit is icy (ice content from 25 to 35 per cent) and contains pore ice, thin, discontinuous, horizontal ice layers (laminated texture), and zones of reticulate ice veins. The massive-ice unit consists of horizontal to gently dipping layers of clear ice, 15 to 30 cm thick, and thin, irregular, undulating bands of sediment. The contact between the massive ice and the overlying clay is abrupt and unconformable; it truncates ice/sediment bands and cloudy, elongated gas bubbles.

Cryogenic textures

The aggradation or inclusion of ground ice in a stratigraphic sequence results in distinct textures being superimposed on the primary sedimentary structure. The resultant textures reflect the process of permafrost aggradation and moisture redistribution associated with an advancing freezing plane, of

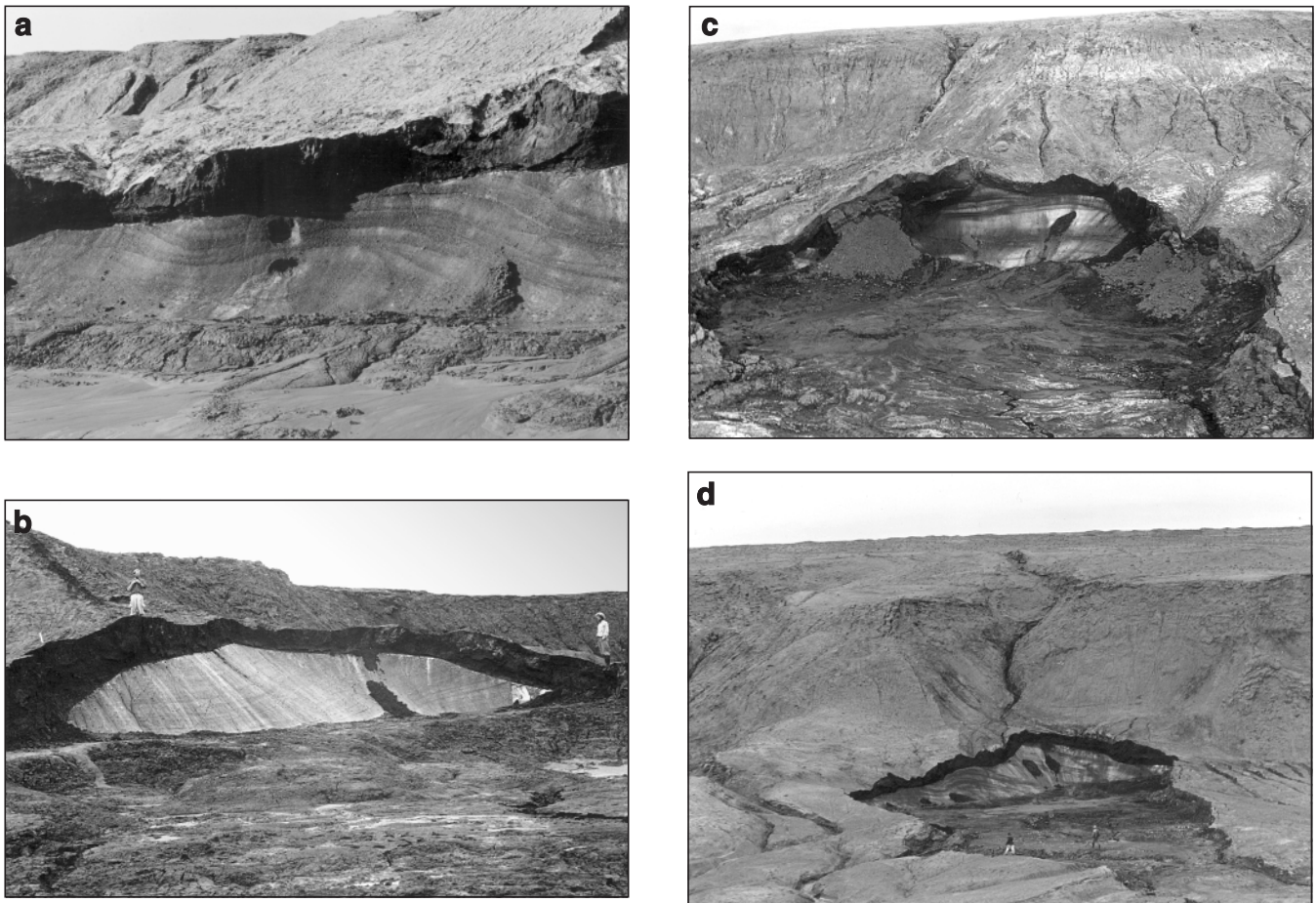


Figure 24. Ice sections showing horizontally foliated, massive white ice in the Slidre River valley. **a)** GSC 2000-022W, **b)** GSC 2000-022X, **c)** GSC 2000-022Y, **d)** GSC 2000-022Z

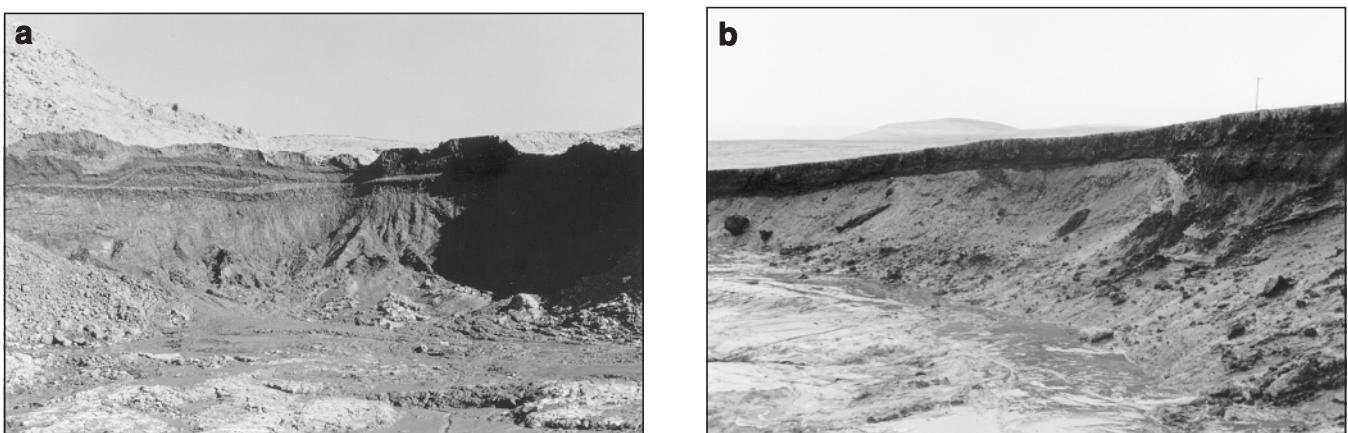


Figure 25. Dirty, massive ice at **a)** Hot Weather Creek (GSC 2000-022AA) and **b)** Blue Man Cape (GSC 2000-022BB).

freezing and thawing of ice-rich sediments. The terms 'cryotexture' or 'cryogenic texture' are used to describe these phenomena (Demek, 1978; Permafrost Subcommittee, 1988). An integrated classification of terms exists in Russian literature to describe cryogenic textures; however, in North America, the closest equivalent are field classifications developed by Pihlainen and Johnston (1963) and Murton and French (1994). The following description combines Russian cryogenic terminology (e.g. Demek, 1978, p. 145) and genetic and descriptive North American ground-ice terminology (e.g. Pihlainen and Johnston, 1963; Mackay, 1989; Pollard, 1991).

At least four distinct cryogenic textures are seen in sections on Fosheim Peninsula, including massive ice (includes foliated, segregated ice and wedge ice), reticulate ice (rectangular and irregular), laminated ice, and ice-bonded or ice-fused sediment. Massive ice is defined by the Permafrost Subcommittee (1988) as a large, usually tabular mass of ground ice with a gravimetric ice content over 250 per cent. Two types of massive ice commonly occur in permafrost, intrasedimental ice formed in situ by the freezing of groundwater and buried ice. Intrasedimental ice includes segregated ice, which can vary considerably in appearance (e.g. Mackay, 1989; Pollard, 1990). The recognition of massive ice as a cryogenic texture requires further clarification. On Fosheim Peninsula, three forms of intrasedimental ice are documented, but they are considered to be variants of the same cryotexture. They are horizontally foliated, clear to white, intrasedimental ice; dirty, massive to horizontally layered ice and icy sediment; and wedge ice. Massive ice at Eureka, Slidre River, Eureka Sound, and south Fosheim consists of extensive bodies (vertical exposures up to 7 m high and horizontally continuous for over 35 m) of horizontally foliated, segregated ice with thin bands and laminae of fine-grained sediment. Bands of white ice contained oval to vertically elongated gas inclusions up to 11 mm long. The layers of white ice vary considerably in thickness and are wavy in appearance. The dark ice contains small, randomly spaced inclusions of gas and sediment. Gas content is much lower than in the white ice and gas inclusions occur as small, circular bubbles. Thin, discontinuous sediment laminae and bands up to 25 mm thick contribute to the foliated appearance of the ice.

Ice wedges form discrete bodies of massive ice and, depending on wedge orientation and perspective, may generate different textural patterns. Large ice wedges are exposed near Eureka (massive-ice site 1), Slidre River (massive-ice site 3), and south Fosheim (massive-ice site 6). In normal section, ice wedges are vertically foliated, wedge-shaped bodies of clear (dark) and dirty ice. However, in sections parallel to the axis of the wedge, the ice appears horizontally foliated and is easily confused with intrasedimental ice.

Complex patterns of ice veins are common in fine sediments immediately overlying massive-ice bodies, particularly deep massive ice (pattern 1). These ice veins often grade from a random pattern of vertical and horizontal veins to a regular pattern of vertical and horizontal veins. Reticulate ice veins can be subdivided into a hierarchy of primary and secondary veins depending on whether they extend beyond or

terminate at points of intersection (Mackay, 1974). Two reticulate textural variations are recognized, a rectangular reticulate texture with a well developed network of straight, primary and secondary ice veins oriented respectively normal and parallel to the top of the massive ice and a network of irregular, secondary ice veins with no obvious preferred orientation. In the first case, the texture is initially poorly developed and characterized by a primary network of thin, straight, unevenly spaced, vertical ice veins and a weak secondary network of horizontal ice veins. With increasing depth, the pattern becomes rectangular with large, vertical, primary ice veins up to 3.0 cm thick spaced 14 to 16 cm apart and smaller, horizontal, secondary ice veins up to 50 cm apart. Immediately above the massive ice, the pattern of ice veins is irregular and more closely spaced; the distinction between primary and secondary ice veins is not as clear. The rectangular pattern also forms larger cells. As ice veins become progressively larger and sediment blocks occupy lower volumes, reticulate cryogenic textures give way to an ice-sediment breccia, termed a 'brecciated cryogenic texture', that is found in many of the deep massive-ice sections and was observed at all sites except near Blue Man Cape and May Point.

Laminated cryogenic textures consist of thin, discontinuous to semicontinuous, parallel, horizontal, concordant ice lenses and layers. Variation in freezing rate, material, and soil water conditions will produce several textural variations or

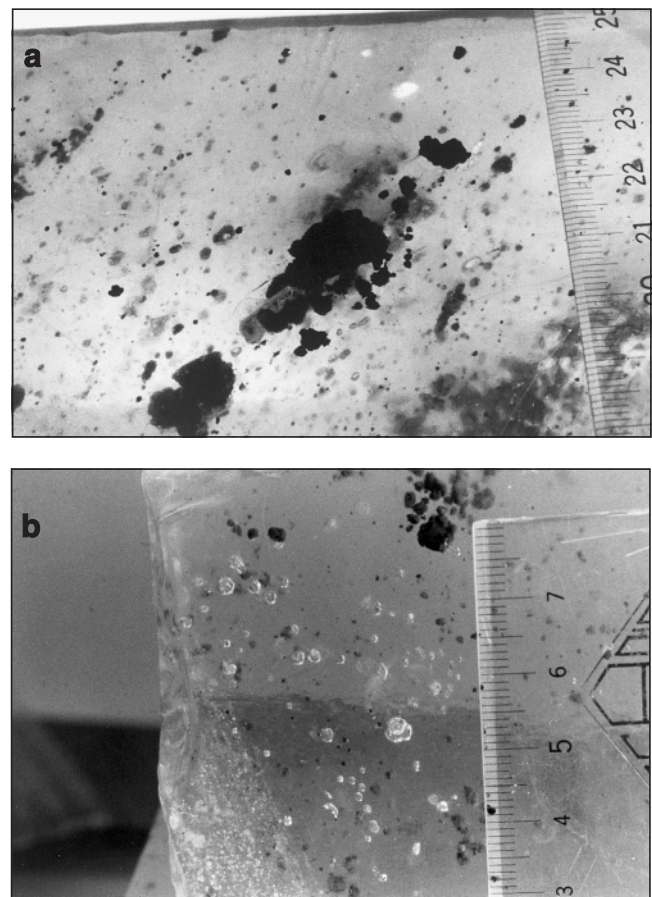


Figure 26. Inclusions of a) sediment and b) gas in ice.

cryofacies; for example, a gradation from fine ice lenses to larger, more closely spaced lenses (lenticular) to rhythmic ice banding may simply reflect subtle fluctuations in the dynamic balance of conditions. At Hot Weather Creek, a lenticular, laminated cryogenic texture containing small (1–2 mm thick and 10–12 mm long), wavy ice lenses characterizes the 30 cm grey clay layer that unconformably overlies massive ice.

Ice-bonded or fused textures include the Nb, Nbn, Nbe, Vx, and Vc ice types of Pihlainen and Johnston (1963) and consist primarily of ice coatings, pore ice, and matrix ice that is commonly so fine that it is not readily visible. As a result, ice-bonded or fused textures lack a distinct pattern and often require close examination to identify. Ice-bonded textures are found in the upper part of sections where ground ice is relatively shallow. At some sites near Eureka, Hot Weather Creek, Blue Man Cape, Eureka Sound, and May Point, massive ice-bonded cryotextures are found immediately below the active layer.

ICE CHARACTERISTICS

Appearance and petrographic characteristics of ice

The colour and appearance of massive ice reflects the nature and pattern of gas and sediment inclusions (Fig. 26a, b) in the ice. Patterns and structures of inclusions in massive ice, along

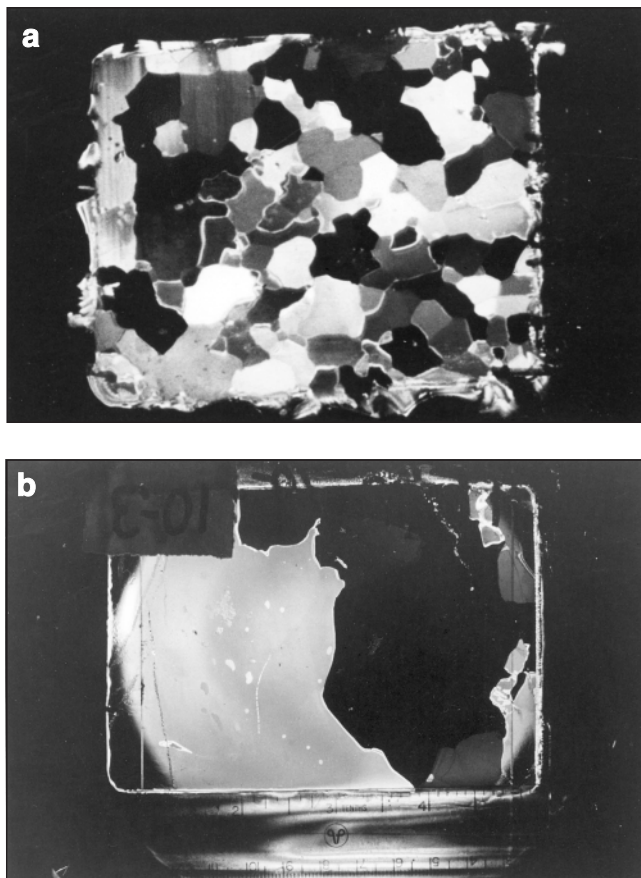


Figure 27. Thin sections of ice under crosspolarized light.

with stratigraphic relationships, provide information on the origin of the ice. This information, when combined with information on petrography and chemistry, provides a rough picture of the freezing process. For example, many deep bodies of massive ice contain numerous gas inclusions, giving the ice a very distinctive white appearance. The arrangement of inclusions into distinct planes produces foliations that parallel major internal structures and contacts. The crystal structure includes medium to large, subhedral and anhedral (Fig. 27) crystals with fabrics dominated by vertical to steeply dipping c-axes (Fig. 28).

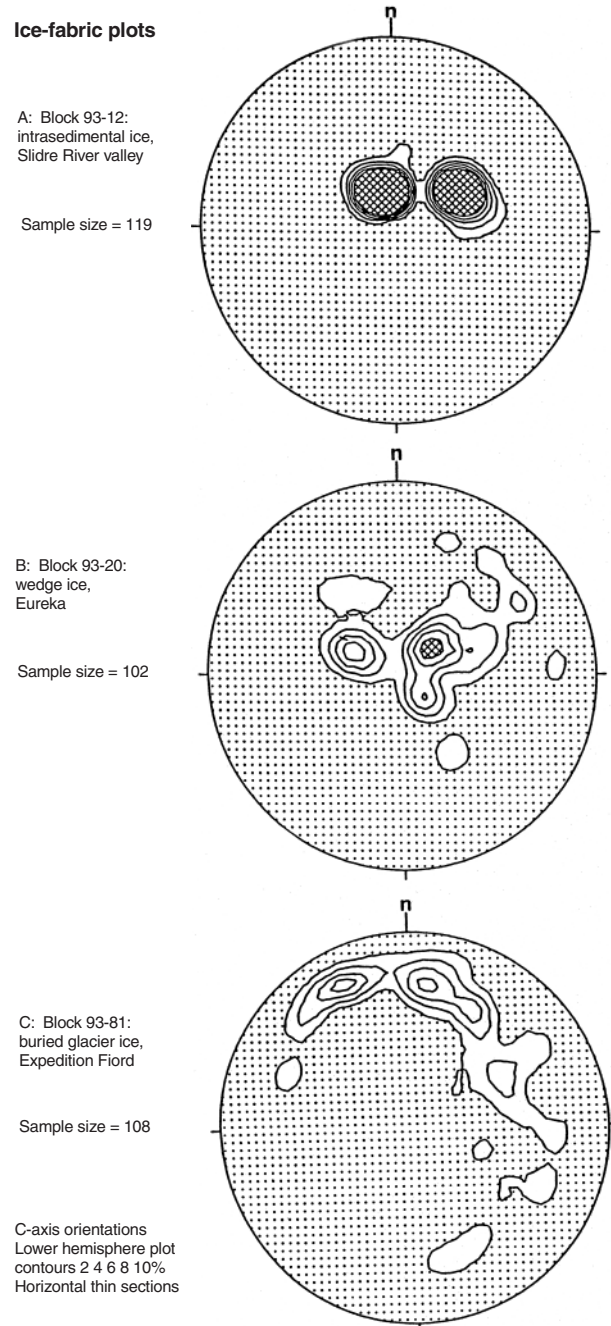


Figure 28. Fabric diagrams of c-axis orientations for a) intrasedimental, b) wedge, and c) glacier ice.

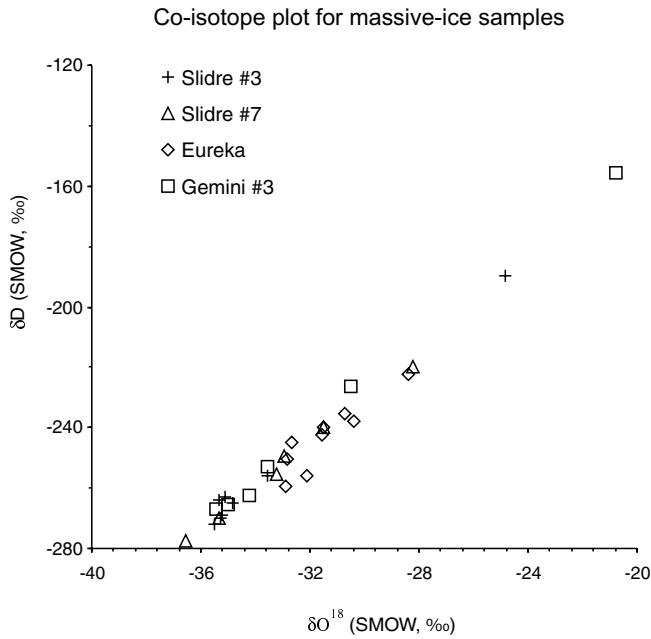


Figure 29. Co-isotope plot for massive-ice samples from the Slidre River and Eureka areas.

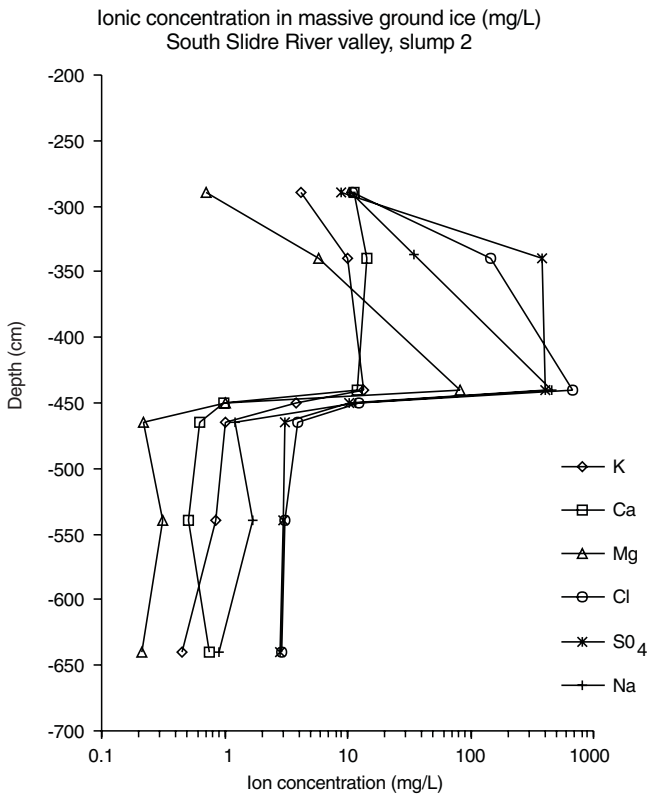


Figure 30. Plot of ionic concentrations in massive ground ice.

Chemical composition

Massive ice contains relatively high concentrations of dissolved ions and both ionic chemistry and stable isotopes are constant with depth and show little evidence of fractionation. Co-isotope plots have slopes ranging from 5 to 7.5 (Fig. 29). Data for ice samples taken from overlying sediments are similar to those from the ice unit. They indicate slow ice formation with a reasonably constant supply of subpermafrost groundwater. Higher salinity values (Fig. 30) in the overlying sediments and in ice immediately below upper contacts (sediment–ice) reflect the marine origin of the sediments and diffusion into the ice body. By comparison, data for shallow ground ice indicate rapid freezing of suprapermafrost water.

An analysis of gas chemistry has provided conflicting results. Bulk ice samples analyzed at the Gas Chemistry Laboratory of Dr. M. Whelan at the SCRIPPS Institution for Oceanography yielded high concentrations (ranging from 442 to 13 000 ppm CO₂ and 4.9 to 16.1 ppm CH₄) for both CO₂ and CH₄ in gas bubbles in the ice, well above normal atmospheric background levels. However, recent analyses conducted at McGill University suggest that concentrations of both CO₂ and CH₄ in gas bubbles within the ice are below background levels. The high values are difficult to explain, other than through sample contamination, although they may relate to the effects of regional geology on groundwater chemistry or a possible contribution from hydrocarbon deposits. If these values are accurate, then the potential contribution of greenhouse gases associated with melting permafrost may be higher than previously expected.

DISCUSSION

Ground ice is an important component of unconsolidated material below the marine limit on Fosheim Peninsula. Observations over five seasons indicate that it is much more widely distributed than what was previously documented. Cryostratigraphic analyses suggest that massive segregated ice forms large, tabular bodies beneath a thick sequence of marine sediments. The vertical pattern and distribution of cryogenic textures, together with petrographic and inclusion characteristics of ground ice, provide the basis for the following model of aggradation.

Shortly after emergence, a period of rapid permafrost aggradation froze relatively dry surficial sediments, producing a fused or ice-bonded cryogenic texture. With increasing depth, freezing continued either at a progressively slower rate or at the same rate into finer sediments with slightly higher water contents, causing the formation of shrinkage cracks and primary and secondary ice veins in a reticulate cryogenic texture. The formation of primary and secondary ice veins implies colder surface temperatures. With greater depth, the rate of advance of the freezing plane slowed, allowing moisture to be drawn towards the freezing plane at a rate that effectively created a balance between water supply and freezing; this resulted in the formation of massive segregated ice. On

the basis of data from the Mackenzie Delta–Tuktoyaktuk Peninsula area, it seems highly probable that the massive-ice bodies on Fosheim Peninsula are underlain by coarse-grained sediments with hydraulic conductivities higher than those of the fine-grained material overlying the ice. Following the formation of permafrost, local thaw events associated with retrogressive thaw slumps or the formation of tundra ponds disrupted the primary cryogenic textures and, in places, induced the reworking of material. Ice-wedge polygons are common in unconsolidated sediments. Ice wedges have also formed over primary cryogenic textures. Clearly, this model represents only a working hypothesis and more research is required to either confirm or refute it.

Ground ice was observed at only one location within the Eureka Sound Group; however, the tentative identification on airphotos of features resembling retrogressive thaw slumps in weathered bedrock suggests that it could be present in significant volumes.

Origin of massive ice

Several complementary lines of evidence lead to the conclusion that massive ice on Fosheim Peninsula is primarily intrasedimental in origin. The stratigraphy and elevation of nearly all bodies of massive ice place the ice within marine sediments deposited during the Holocene. Ground-ice chemistry suggests that massive ice formed from groundwater or seawater that contained significant amounts of dissolved minerals. Its petrography is consistent with slow epigenetic formation associated with permafrost aggradation.

Implications for climate change

From 1990 to 1995, 73 natural exposures of massive ice were documented. In some cases, layers of nearly pure ice 5 to 7 m thick underlie plateau structures covering several square kilometres. Degradation of massive ice and ice-rich permafrost produces extensive thermokarst (Robinson, 2000). The hundreds of active and inactive retrogressive thaw slumps and active-layer detachments attest to the widespread nature of ground ice and its role in the development of slopes and landscapes. However, thermokarst is a natural process in areas underlain by ice-rich permafrost. The magnitude of active thermokarst reflects a combination of summer temperature and disturbance regime. Thus, an increase in either summer temperature or disturbance regime will likely bring about an increase in the magnitude of thermokarst. Natural disturbances that may initiate thermokarst include river and gully erosion and active-layer detachments (Lewkowitz, 1992; Harris and Lewkowitz, 1993). The latter are a form of slope instability that can be related to thawing of ice-rich permafrost. Active-layer detachments may also trigger more extensive thermokarst by removing surficial sediments and bringing ice-rich permafrost into range of the new active layer.

CONCLUSIONS

Two main conclusions can be drawn from this work. Firstly, massive ice is a fairly common constituent of High Arctic permafrost where it occurs as intrasedimental massive ice in marine sediments below the Holocene marine limit. Secondly, its aggradation and degradation have played a significant role in the evolution of Holocene landscapes in this part of the High Arctic. By using the Holocene emergence history as a proxy for time, it is possible to estimate periods when ground ice formed.

ACKNOWLEDGMENTS

This work was supported by research grants from the Natural Science and Engineering Research Council of Canada, the Department of Energy, Mines, and Resources (EMR Research Agreement 227-4-91), and the Atmospheric Environment Service. The author wishes to express sincere appreciation to the Polar Continental Shelf Project (PCSP/ÉPCP 00697) for its generous field support. The author thanks Dr. Trevor Bell and Dr. Sylvia Edlund for their helpful discussions and insight. The field assistance of Craig Forcese, Peter Barry, Ray Shannon, and Nora Jackson is gratefully acknowledged. Student assistants were funded in part through the Northern Scientific Training Program (Department of Indian Affairs and Northern Development).

REFERENCES

- Barry, P.**
1992: Ground ice characteristics in permafrost on Fosheim Peninsula, Ellesmere Island, N.W.T.: a study utilizing ground probing radar and geomorphic techniques; M.Sc. thesis, McGill University, Montréal, Quebec, 120 p.
- Barry, P. and Pollard, W.H.**
1992: Ground probing radar investigation of ground ice on the Fosheim Peninsula, Ellesmere Island, N.W.T.; *The Musk-Ox*, v. 39, p. 59–67.
- Bell, T.**
1992: Glacial and sea level history of western Fosheim Peninsula, Ellesmere Island, Arctic Canada; Ph.D. thesis, University of Alberta, Edmonton, Alberta, 172 p.
1996: The last glaciation sea level history of Fosheim Peninsula, Ellesmere Island, Canadian High Arctic; *Canadian Journal of Earth Sciences*, v. 33, p. 1075–1086.
- Bell, T. and Hodgson, D.A.**
2000: Quaternary geology and glacial history of Fosheim Peninsula, Ellesmere Island, Nunavut; *in* Environmental Response to Climate Change in the Canadian High Arctic, (ed.) M. Garneau and B.T. Alt; Geological Survey of Canada, Bulletin 529.
- Christie, R.L.**
1964: Reconnaissance of the surficial geology of northeastern Ellesmere Island, Arctic Archipelago; Geological Survey of Canada, Bulletin 138, 50 p.
- Dallimore, S.A and Wolfe, S.**
1988: Massive ground ice associated with glaciofluvial sediments, Richards Island, N.W.T., Canada; *in* Permafrost, Fifth International Conference Proceedings, v. I; Tapir Publishers, Trondheim, Norway, p. 127–131.

- Demek, J.**
1978: Periglacial geomorphology: present problems and future prospects; *in* *Geomorphology*, (ed.) C. Emberton, D. Brunsden, and D. Jones; Oxford University Press, Oxford, United Kingdom, p. 139–153.
- Edlund, S.A.**
1989: Vegetation indicates potentially unstable Arctic terrain; *Geos*, v. 18, no. 3, p. 9–13.
- Edlund, S.A., Alt, B.T., and Young, K.L.**
1989: Interaction of climate, vegetation, and soil hydrology at Hot Weather Creek, Fosheim Peninsula, Ellesmere Island, Northwest Territories; *in* *Current Research, Part D*; Geological Survey of Canada, Paper 89-1D, p. 125–133.
- Egginton, P. and Hodgson, D.**
1990: Preliminary assessment of selected drainage basins in western Fosheim Peninsula, Ellesmere Island, as sites for global change studies; *in* *Current Research, Part D*; Geological Survey of Canada, Paper 90-1D, p. 71–77.
- French, H.M.**
1994: Living on ice: problems of urban development in Canada's North; *Geoscience Canada*, v. 21, no. 4, p. 163–175.
- French, H.M., Bennet, L., and Hayley, D.W.**
1986: Ground ice conditions at Rae Point and Sabine Peninsula, Eastern Melville Island; *Canadian Journal of Earth Sciences*, v. 22, p. 1389–1400.
- French, H.M., Harry, D.G., and Clark, M.J.**
1982: Ground ice stratigraphy late-Quaternary events, southwest Banks Island, Canadian Arctic; *in* *Proceedings Fourth Canadian Permafrost Conference*, Calgary, Alberta; National Research Council of Canada, Ottawa, p. 81–90.
- Harris, C.H. and Lewkowicz, A.G.**
1993: Form and internal structure of active-layer detachment slides, Fosheim Peninsula, Ellesmere Island, Northwest Territories, Canada; *Canadian Journal of Earth Sciences*, v. 30, p. 1708–1714.
- Harry, D.G., French, H.M., and Pollard, W.H.**
1988: Massive ground ice and ice-cored terrain near Sabine Point, Yukon Coastal Plain; *Canadian Journal of Earth Sciences*, v. 25, p. 1846–1856.
- Hodgson, D.A.**
1973a: Terrain performance, central Ellesmere Island, District of Franklin; *in* *Report of Activities, Part A*; Geological Survey of Canada, Paper 73-1A, p. 185.
1973b: Surficial geology and geomorphology of central Ellesmere Island; *in* *Report of Activities, Part A*; Geological Survey of Canada, Paper 73-1A, p. 203.
1974: Surficial geology, geomorphology and terrain disturbance, central Ellesmere Island; *in* *Report of Activities, Part A*; Geological Survey of Canada, Paper 74-1A, p. 247–248.
1985: The last glaciation of west-central Ellesmere Island, Arctic Archipelago, Canada; *Canadian Journal of Earth Sciences*, v. 22, p. 347–368.
- Hodgson, D.A. and Edlund, S.A.**
1975: Surficial geology, geomorphology and terrain disturbance, central Ellesmere Island; *in* *Report of Activities, Part A*; Geological Survey of Canada, Paper 75-1A, p. 4–11.
1977: Biophysical regions, western Fosheim Peninsula and Eastern Axel Heiberg Island; Geological Survey of Canada, Open File 501.
- Hodgson, D.A. and Nixon, F. M.**
1998: Ground ice volumes determined from shallow cores from western Fosheim Peninsula, Ellesmere Island, Northwest Territories; *Geological Survey of Canada, Bulletin* 507, 178 p.
- Hodgson, S.A., St-Onge, D.A., and Edlund, S.A.**
1991: Surficial materials of Hot Weather Creek basin, Ellesmere Island, Northwest Territories; *in* *Current Research, Part E*; Geological Survey of Canada, Paper 91-1E, p. 157–163.
- Houghton, J.T., Jenkins, G.J., and Ephraums, J.J.**
1990: *Climate Change: The IPCC Scientific Assessment*; published for the Intergovernmental Panel on Climate Change, Cambridge University Press, Cambridge, 364 p.
- Kalin, M.**
1971: The active push moraine of the Thompson Glacier, Axel Heiberg Island, Canadian Arctic Archipelago; McGill University, Axel Heiberg Island Research Reports, *Glaciology* no. 4, 68 p.
- Lamothe, C. and St-Onge, D.**
1961: A note on a periglacial erosional process in the Isachsen area, Northwest Territories; *Geographical Bulletin*, no. 16, p. 104–113.
- Lawson, D.**
1986: Ground ice in perennially frozen sediments, northern Alaska; *in* *Proceedings, Permafrost, Fourth International Conference*, Washington, D.C.; National Academy Press, p. 695–700.
- Lewkowicz, A.G.**
1992: Factors influencing the distribution of active layer detachment slides on Ellesmere Island, Arctic Canada; *in* *Periglacial Geomorphology*, (ed.) J.C. Dixon and A.D. Abrahams; The Binghampton Symposia in Geomorphology, International Series no. 22; John Wiley and Sons Ltd., Chichester, United Kingdom, p. 223–250.
- Lorrain, R.D. and Demeur, P.**
1985: Isotopic evidence for relic Pleistocene glacier ice on Victoria Island, Canadian Arctic Archipelago; *Arctic and Alpine Research*, v. 17, p. 89–98.
- Mackay, J.R.**
1963: The Mackenzie Delta area, N.W.T.; *Geographical Branch, Memoir* 5, 202 p.
1966: Segregated epigenetic ice and slumps in permafrost, Mackenzie Delta area, N.W.T.; *Geographical Bulletin*, v. 8, no. 1, p. 59–80.
1971: The origin of massive icy beds in permafrost, western Arctic, Canada; *Canadian Journal of Earth Sciences*, v. 8, no. 4, p. 397–422.
1972: The world of underground ice; *Annals Association American Geographers*, v. 62, no. 1, p. 1–22.
1973: Problems in the origin of massive icy beds, western Arctic coast, Canada; *in* *Proceedings Second International Conference on Permafrost*, Yakutsk, U.S.S.R.; North American Contribution, United States National Academy of Sciences, Washington, D.C., p. 223–228.
1974: Reticulate ice veins in permafrost, Northern Canada: Reply; *Canadian Geotechnical Journal*, v. 12, p. 163–165.
1989: Massive ice: some field criteria for the identification of ice types; *in* *Current Research, Part G*; Geological Survey of Canada, Paper 89-1G, p. 5–11.
- Mackay, J.R. and Dallimore, S.R.**
1992: Massive ice of the Tuktoyaktuk area, western Arctic coast, Canada; *Canadian Journal of Earth Sciences*, v. 29, p. 1235–1249.
- Muller, S.W.**
1945: Permafrost or permanently frozen ground and related engineering problems; United States Engineers Office, Strategic Engineering Study, Special Report no. 62, 136 p.
- Murton, J.B. and French, H.M.**
1994: Cryostructures in permafrost, Tuktoyaktuk coastlands, western arctic Canada; *Canadian Journal of Earth Sciences*, v. 31, p. 737–747.
- Permafrost Subcommittee**
1988: Glossary of permafrost and related ground-ice terms; Associate Committee on Geotechnical Research, National Research Council of Canada, Technical Memorandum no. 142, Ottawa, 156 p.
- Pihlainen, J.A. and Johnston, G.H.**
1963: Guide to a field description of permafrost; Associate Committee on Snow and Soil Mechanics, National Research Council of Canada, Technical Memorandum no. 79, Ottawa, 21 p.
- Pollard, W.H.**
1990: The nature and origin of ground ice in the Herschel Island area, Yukon Territory; *in* *Permafrost Canada, Proceedings of the Fifth Canadian Permafrost Conference*; Collection Nordica, Centre d'études nordiques, Université Laval, Quebec, p. 23–30.
1991: Observations on massive ground ice on Fosheim Peninsula, Ellesmere Island, Northwest Territories; *in* *Current Research, Part E*; Geological Survey of Canada, Paper 91-1E, p. 223–231.
- Pollard, W.H. and Dallimore, S.R.**
1988: Petrographic characteristics of massive ground ice, Yukon Coastal Plain, Canada; *in* *Proceedings, Permafrost, Fifth International Conference*, v. I; Tapir Publishers, Trondheim, Norway, p. 224–229.
- Pollard, W.H. and French, H.M.**
1980: A first approximation of the volume of ground ice, Richards Island, Pleistocene Mackenzie Delta, Northwest Territories, Canada; *Canadian Geotechnical Journal*, v. 17, no. 4, p. 509–516.
- Robinson, S.D.**
1993: Geophysical and geomorphological investigations of massive ground ice, Fosheim Peninsula, Ellesmere Island, Northwest Territories; M.Sc. thesis, Department of Geography, Queen's University, Kingston, Ontario, 171 p.
1994: Geophysical studies of massive ground ice, Fosheim Peninsula, Ellesmere Island, Northwest Territories; *in* *Current Research, Part B*; Geological Survey of Canada, Paper 94-1B, p. 11–18.

Robinson, S.D. (cont.)

2000: Thaw-slump-derived thermokarst near Hot Weather Creek, Ellesmere Island, Nunavut; *in* Environmental Response to Climate Change in the Canadian High Arctic, (ed.) M. Garneau and B.T. Alt; Geological Survey of Canada, Bulletin 529.

Schlesinger, M.E. and Mitchel, J.F.B.

1987: Climate model simulations of equilibrium climate response to increased carbon dioxide; *Review of Geophysics*, v. 25, p. 760–798.

Sharp, D.R.

1992: Quaternary geology of the Wollaston Peninsula, Victoria Island, Northwest Territories; Geological Survey of Canada, Memoir 434, 84 p.

Solomatin, V.I.

1986: The petrogenesis of underground ice, Novosibirsk; U.S.S.R. Academy of Sciences, 215 p.

St-Onge, D.A.

1964: La géomorphologie de l'île Ellef Ringnes, Territoires du Nord-Ouest, Canada. Étude de la géographie; ministère des Mines et Rélevés techniques, Ottawa, Ontario, 46 p.

St-Onge, D.A. and McMartin, I.

1995: Quaternary geology of the Inman River area, Northwest Territories; Geological Survey of Canada, Bulletin 446, 59 p.

Woo, M-k., Young, K.L., and Edlund, S.A.

1990: 1989 observations of soil, vegetation, and microclimate, and effects on slope hydrology, Hot Weather Creek basin, Ellesmere Island, Northwest Territories; *in* Current Research, Part D; Geological Survey of Canada, Paper 90-1D, p. 85–93.

Physical, chemical, and biological characteristics of lakes from the Slidre River basin on Fosheim Peninsula, Ellesmere Island, Nunavut

P.B. Hamilton¹, K. Gajewski², R. McNeely³, and D.R.S. Lean⁴

Hamilton, P.B., Gajewski, K., McNeely, R., and Lean, D.R.S., 2000: *Physical, chemical, and biological characteristics of lakes from the Slidre River basin on Fosheim Peninsula, Ellesmere Island, Nunavut*; in *Environmental Response to Climate Change in the Canadian High Arctic*, (ed.) M. Garneau and B.T. Alt; Geological Survey of Canada, Bulletin 529, p. 235–248.

Abstract: Significant changes in lake pH, sodium, calcium, magnesium, dissolved inorganic carbon, organic content of sediments, and benthic diatom community structure were observed along an elevational transect of lakes through the Slidre River basin. Water solutes varied from dilute calcium bicarbonate in headwater lakes to sodium chloride in lakes at the estuarine mouth. Calcium, sodium, and sulfate levels varied depending on the type of surficial materials in the basin and proved to be a useful proxy for defining marine limits in the region. A general shift from species-poor headwater lakes dominated by *Fragilaria* spp. to a more diverse flora dominated by *Cymbella-Navicula-Denticula-Epithemia* in the middle reaches was observed. Lakes closer to the estuarine mouth of the Slidre River basin contained high concentrations of solute-loving taxa (e.g. *Amphora* spp.). The saline Romulus Lake and unnamed 'lake 8' were devoid of diatoms, suggesting the possibility of dissolution in these saline waters in association with high pH. An increase in the organic matter of the sediments from coastal to upland lakes indicates larger drainage catchments with higher allochthonous and autochthonous input in the headwater lakes.

Résumé : On a observé des changements importants du pH, des concentrations de sodium et de magnésium, de la quantité de carbone inorganique dissout, du contenu organique des sédiments et de la structure de la communauté de diatomées benthiques des lacs présents le long d'un transect ascendant de lacs dans le bassin versant de la rivière Slidre. Les solutés dans l'eau varient : en amont, les eaux des lacs présentent des solutions dilués de bicarbonate de calcium et près de l'embouchure de l'estuaire, les eaux des lacs sont dominés par des solutions de chlorure de sodium. Les concentrations de calcium, de sodium et de sulfates fournissent une idée des types de matériaux de surface présents dans le bassin et constituent des indicateurs utiles pour définir les limites marines. On observe une transition générale depuis les lacs à la tête du bassin versant à population peu diversifiée, dominée par *Fragilaria* sp., vers une flore plus diversifiée dominée par les espèces *Cymbella-Navicula-Denticula-Epithemia* en altitude moyenne. Les lacs situés près de l'embouchure de l'estuaire contiennent de fortes concentrations de taxons aimant les solutions plus concentrés. Le lac Romulus et le «lac 8» ne contenaient pas de diatomées, ce qui suggère la possibilité de leur dissolution dans ces eaux salines au pH plus élevé. Une augmentation de la quantité de matière organique dans les sédiments des lacs en altitude par rapport aux lacs situés près des côtes témoigne de bassins de captage plus étendus accompagnés d'apports allochtones et autochtones plus élevés pour les lacs en amont.

¹ Research Division, Canadian Museum of Nature, P.O. Box 3443, Station D, Ottawa, Ontario K1P 6P4

² Département de géographie, Université d'Ottawa, Ottawa, Ontario K1N 6N5

³ Geological Survey of Canada, Terrain Sciences Division, 601 Booth Street, Ottawa, Ontario K1A 0E8

⁴ Department of Biology, University of Ottawa, Ottawa, Ontario K1N 6N5

INTRODUCTION

Ecosystems of the Canadian Arctic Archipelago are strongly influenced by climate and geology (Edlund and Alt, 1989; Edlund et al., 1989; Bell, 1992; Edlund, 1992; Etkin and Agnew, 1992). Across the Arctic Archipelago, summer temperature generally decreases towards the northwest. However, within the arctic islands there are deviations from this pattern. For example, the orientation of mountain ranges enclosing the interior of Ellesmere Island creates a significantly warmer microclimate (Edlund and Alt, 1989). The Fosheim Peninsula is characterized by higher temperatures and longer freshwater ice-free periods (Edlund and Alt, 1989). Increased biological activity, especially plant growth, is found around freshwater ecosystems such as lakes, ponds, and tundra wetlands where moisture is available (Edlund et al., 1989; Edlund, 1992).

High Arctic freshwater ecosystems are sensitive to small climate changes (Bradley, 1990; Douglas et al., 1994; Gajewski et al., 1997). Consequently, the knowledge of factors that influence fresh waters on Fosheim Peninsula and in other locations on Ellesmere Island will be important in assessing the impact of future climate changes on arctic environments (Douglas et al., 2000; Wolfe, 2000).

Fosheim Peninsula has 10 distinct hydrometric basins. Lakes, ponds, and wetlands are limited, with lotic systems dominating the freshwater resources (Fig. 1). Surface-water retention time for lotic systems is short with fresh waters draining quickly to the fiord, especially during snowmelt. Conversely, lake systems typically have basin entrapments with long water-retention times (Davidge, 1994).

Two geological features, the Franklinian Mobile Belt and the Sverdrup Basin, underlie Fosheim Peninsula (Thornsteinsson, 1971; Bell, 1992). Sverdrup Basin rocks and the overlying marine sediments are important factors affecting local biological diversity. The Eureka Sound Formation is a predominant component of the Sverdrup Basin and is dominated by extensive coal beds. Coal deposits introduce particulate organic carbon (POC) to the lake sediments and may cause elevated per cent organic carbon levels. Indeed, coal from the Eureka Sound Formation has introduced old pollen that affects the analysis of present-day pollen records (Garneau, 1992; Gajewski et al., 1995). In addition, marine deposits represent at least a third of Fosheim Peninsula's surface sediments and alter the ion composition of the freshwater ecosystems of western Fosheim Peninsula.

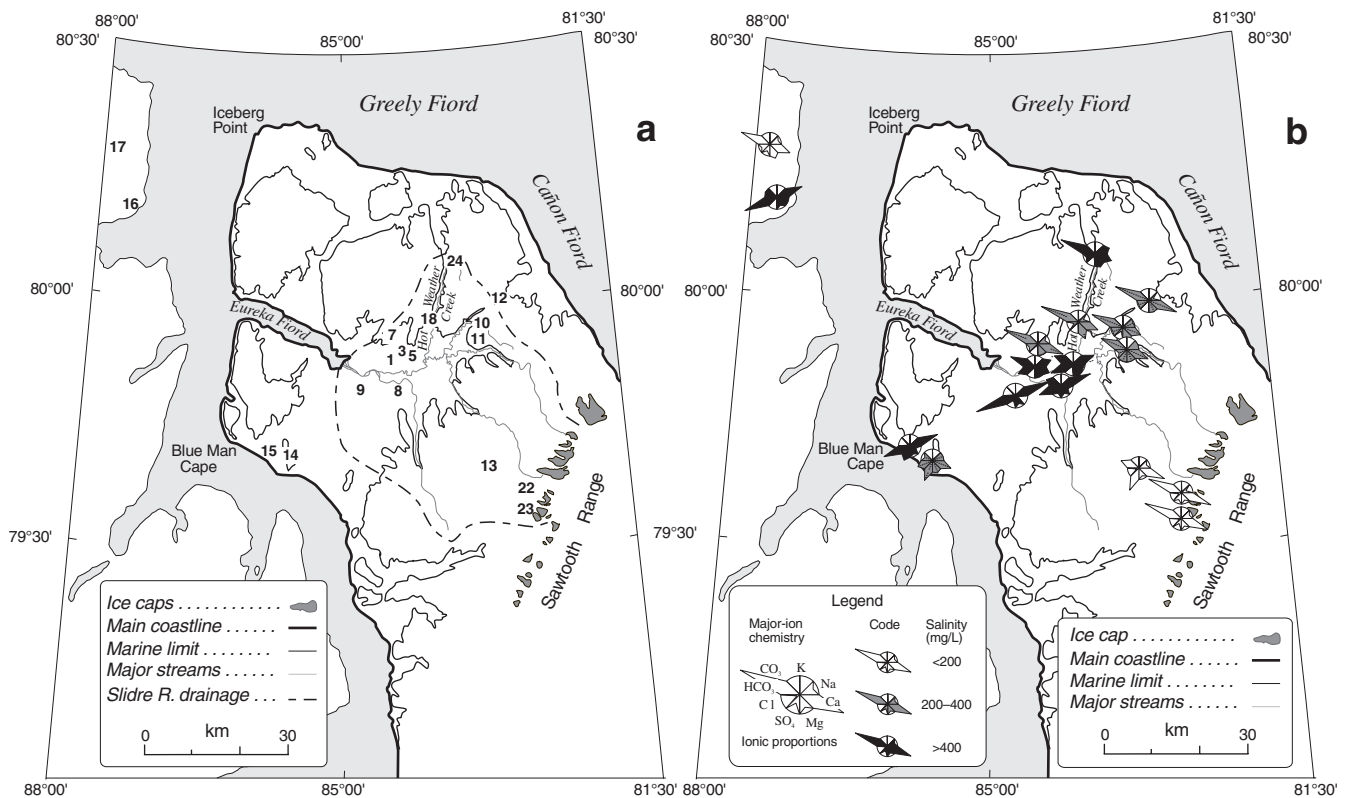


Figure 1. Map of Fosheim Peninsula (Ellesmere Island) outlining the Slidre River basin. **a)** The study lakes are numbered. Lake 17 is part of a small basin on Axel Heiberg Island. Lakes 14 and 15 are part of a small basin southeast of Blue Man Cape. Lake 12 is part of a small basin on the northeast side of the peninsula draining into Cañon Fiord. **b)** Major-ion proportional compositions for the study lakes on Fosheim Peninsula and on the west coast of Axel Heiberg Island.

The objective of this study was to examine the chemical composition, nutrients, and diatom diversity of lakes and ponds in the largest watershed, the Slidre River basin, on Fosheim Peninsula. It is proposed that i) varying chemical conditions within the basin alter biological characteristics and diversity of the system and ii) basin morphometry, water chemistry, nutrients, and finally climate control algal biodiversity in the lakes and ponds on Fosheim Peninsula.

STUDY AREA

The area is on Fosheim Peninsula along the west coast of Ellesmere Island at latitude 80° N. Eighteen lakes and large ponds from five different drainage basins were studied (Table 1). Thirteen lakes were within the Slidre River watershed and one was in a basin to the northeast draining into Cañon Fiord (lake 12, Fig. 1). Two additional lakes in a small drainage area southwest of the Slidre River (lakes 14, 15) and two lakes from different basins (lakes 16, 17) along the east coast of Axel Heiberg Island across Eureka Sound were also sampled (Fig. 1). Four lakes (7, 10, 18, 24) had water depths of less than 3.0 m and are referred to as 'ponds' because of the potential of complete freezing during winter (Hobbie, 1973).

The Slidre River basin is the largest watershed on Fosheim Peninsula and drains 3700 km². It covers 28 per cent of Fosheim Peninsula. The headwaters of the Slidre River originate at elevations over 500 m in the Sawtooth Range. There are relatively few (about 25) large (>0.05 km²) water bodies in the Slidre River basin, with some having depths of less than 1.5 m. Two of the four major rivers originate in polygon wetlands whereas the others are glacier fed.

A smaller basin just south of the Slidre River covers 91.6 km² and contains two lakes within 2.8 km of the coast (lakes 14, 15, Fig. 1). Lake 14 is slightly above the marine sediment limit, whereas lake 15 is underlain by marine sediments. To the northeast, a headwater lake 8.5 km from the coast is in a small watershed draining 28 km² into Cañon Fiord (lake 12, Fig. 1). Lake 12 is above the marine sediment limit. Two other lakes (lakes 16, 17, Fig. 1) on Axel Heiberg Island are in small basins that drain 42 km² and 32 km² of the western coastal plains, respectively. Both lakes on Axel Heiberg Island are within 4.5 km of Eureka Sound.

METHODS

Eighteen lakes and large ponds on Fosheim Peninsula and Axel Heiberg Island were examined during middle to late July 1990 and 1992. At each lake, samples were collected for water chemistry, phytoplankton, and benthic diatom analyses.

Conductance and temperatures were measured in the field using a YSI Model 33 S-C-T meter. Conductance and pH measurements were repeated at the base camp. Two-liter water samples were collected at 0.6 to 0.8 m depth for water chemistry and phytoplankton analyses. Immediately upon collection, an aliquot for phosphorus was preserved with 1% ulfuric acid. Particulate carbon and nitrogen samples were filtered at the base camp, dried (about 60°C for a minimum of two hours), and stored dry. Chlorophyll-*a* samples were collected on glass fiber filters and stored frozen in either a propane refrigerator or a 'permafrost' ice freezer. During transport (about two weeks), samples for chemical analyses

Table 1. Location and physical and chemical data for the 18 lakes sampled for this study.

Lake	Common name	Latitude (N)	Longitude (W)	Date sampled (yy/mm/dd)	Elevation (m)	Surface area (Ha)	Depth (m)	Temperature (°C)	pH	Conductance (µS/cm)	Soluble reactive phosphorus (µg/L)
1	Two Basin	79°55.5'	84°40'	92/07/23	60	14.2	9.5	3.5	8.2	566	0.7
3	Ridge	79°55.9'	84°36'	92/07/24	70	28.1	5.0	6.3	8.2	506	0.8
5	Coal	79°55.6'	84°32'	92/07/25	70	20.2	7.0	8.5	8.5	1073	0.9
7	Lake 7	79°56.0'	84°46'	92/07/26	150	0.54	2.5	10.0	8.4	288	0.6
8	Lake 8	79°53.5'	84°48'	92/07/27	30	21.9	6.5	7.5	8.6	>2000	0.8
9	Romulus	79°52.0'	85°03'	92/07/27	10	229.0	55.0	≈ 6	8.4	>2000	1.3
10	Gemini	79°59.6'	84°08'	92/07/28	100	16.8	1.0	0.9	8.2	379	1.0
11	Lake 11	79°58.4'	84°03'	92/07/28	120	≈15	3.2	2.8	8.2	416	0.5
12	Lake 12	80°01.0'	83°23.2'	92/07/30	200	8.7	3.7	0.7	8.3	366	0.7
13	Lake 13	79°43.9'	83°28.1'	92/07/30	400	9.3	4.5	4.1	7.7	126	0.4
14	Lake 14	79°44.1'	85°48.4'	92/07/30	140	8.6	1.3	1.9	7.8	524	0.5
15	Lake 15	79°44.6'	85°59.6'	92/07/30	140	3.1	3.5	1.2	8.3	>2000	1.8
16	Lake 16	80°10.9'	87°41.2'	92/07/31	90	12.2	3.7	2.5	8.0	998	0.3
17	Lake 17	80°15.6'	87°46.3'	92/07/31	140	18.7	3.5	2.5	8.0	293	0.4
18	Lake 18	80°00.0'	84°26'	92/08/02	70	0.45	0.5	0.9	8.5	405	1.2
22	Lake 22	79°43.1'	83°31'	92/08/03	365	5.0	5.5	0.9	7.4	78	0.2
23	Lake 23	79°42.9'	83°30'	92/08/03	375	7.8	9.0	3.0	7.5	98	0.3
24	Lake 24	80°08.0'	84°23'	90/07/01	150	3.9	8.5	8.0	8.2	255	5.3

were stored under cold, dark conditions. Analyses were carried out at the National Water Research Institute (Burlington, Ontario) following standard methods (Environment Canada, 1979). The nutrients analyzed include nitrite (NO₂), nitrate (NO₃), ammonium (NH₃), particulate nitrogen (PN), soluble reactive phosphorus (SRP), filtered phosphorus (FP), total particulate phosphorus (TPP), dissolved inorganic carbon (DIC), dissolved organic carbon (DOC), and particulate organic carbon (POC). Ions analyzed included calcium (Ca), magnesium (Mg), sodium (Na), potassium (K), chloride (Cl), sulfate (SO₄), and silica (SiO₂). Deep-water samples were collected from directly above the benthic sediment in three lakes (lakes 3, 5, 7, Table 1), at 9.0 m, 4.0 m, and 6.0 m respectively, using a Kemmerer sampler.

Phytoplankton samples were preserved in the field with 1% to 2% acidified Lugol's solution (Thronsen, 1978). In the laboratory, subsamples of phytoplankton were processed for diatom analysis, by reducing 60 mL samples, digesting with 40% hydrogen peroxide, washing six times, and then storing in 10 mL of distilled water. A 0.4 mL slurry was dried on a coverslip and mounted onto slides using Hyrax[®]. A Leitz Diaplan microscope equipped with brightfield, phase contrast, and differential interference contrast optics using Plan Apo (63X, 1.4) and fluotar (50X, 1.00; 100X, 1.32) objectives was used. Randomly selected transects were counted and, whenever possible, a minimum of 600 valves were counted; however, some lakes had few to no diatoms present. Taxonomic identifications followed the floras of Ehrenberg (1854), Van Heurck (1880–1885), Hustedt (1930–1966), Patrick and Reimer (1966, 1975), Foged (1981), and Krammer and Lange-Bertalot (1986, 1988, 1991a, b).

Lake surface sediments were collected using either an Ekman dredge or a modified Livingstone sampler. Freeze-dried sediment samples were used for diatom analysis; aliquots varying from 0.1 to 0.5 g dry weight were treated with 10% HCl, washed, and then digested by boiling in H₂SO₄:NH₃. The digested samples were washed at least five times and subsample slurries were dried onto coverslips and mounted as above. Representative sediment and phytoplankton samples (CANA 52330–52364) are part of the national collection at the Canadian Museum of Nature, Ottawa, Canada. The organic content of the sediment was estimated by loss-on-ignition using 1 cc (9–10 g wet) of sediment (Dean, 1974).

Total ion balances were calculated and ion-proportion diagrams were generated using the procedures of Maucha (Hutchinson, 1957). This methodology for examining ion proportions in aquatic systems was used by McNeely and Gummer (1984) to study environmental chemistry in east-central Ellesmere Island. As indicated by the bicarbonate-carbonate equilibrium in fresh waters below pH 8.4, the measurable carbonate ion level is negligible. Magnesium was not measured at three lakes. A linear regression of magnesium against conductivity using available Ellesmere Island data gave a relationship of $(\ln \text{conductance}) = 3.96 + 0.81 * (\ln$

magnesium) ($r^2 = 0.903$, Hamilton et al., 1994) and was used to calculate the missing magnesium data for these three lakes. A calculated freshwater salinity (equivalent to total dissolved solids [TDS]) was generated from the ion-balance calculations.

RESULTS

A marked change in slope occurs in the Slidre River basin at about 140 m a.s.l. (Fig. 2a). Low-elevation lakes had *Dryas-Salix* hummocky shorelines with some moss embankments and slumping, unstable slopes. In the shallow areas around the lakes, sedges and cottongrass predominate. Headwater lakes were rocky or had stable moss embankments. Purple saxifrage typically dominates the slopes surrounding these headwater lakes. No lakes at elevations from 150 to 300 m a.s.l. were available for sampling (Fig. 2b). Five of the lakes are in four other smaller watersheds (squares, Fig. 2a). Water depth (Fig. 2b) and lake surface area (Table 1) show no relationship with elevation nor with lake location within the watershed. The headwater lakes (lakes 13, 22, and 23) were approximately 50 per cent covered with a deteriorating ice sheet at the time of sampling (July 23–August 3, 1992).

Water chemistry

Lake pH increased from 7.5 to 8.5 in samples obtained from high to low elevations (Fig. 2c). This trend is also seen in the major ions, as salinity increases with decreasing elevation (Fig. 2d, Table 2). A change from a sodium-dominated to a calcium-dominated aquatic system occurs at about 140 m a.s.l., which corresponds to the change in the slope of the basin (Fig. 1b, 2d) and the Holocene marine limit. Sodium levels varied from 1.7 mg/L (lake 22) in the headwaters to 11 400 mg/L (Romulus Lake, lake 9) in the lowland (Table 2). Likewise, calcium levels varied from headwaters to lowlands and ranged from 9.9 mg/L (lake 22) to 210 mg/L (lake 15). Changes in magnesium levels were also significant and ranged from 1.5 mg/L (lake 22) to 179 mg/L (lake 15). Conductance is a good predictor of both calcium and sodium content, although the linear relationship and more diverse distribution of calcium gives a stronger correlation (Fig. 3). The headwater lakes are dominated by calcium bicarbonate with one exception (lake 13), which also has a significant amount of calcium sulfate (Fig. 1b, Table 2). Seven lakes show high conductance conditions with calculated freshwater salinities ranging from 300 to 958 mg/L (Fig. 1b, Table 2). Romulus Lake and an unnamed lake (lake 8) are moderately saline, the dominant salt being sodium chloride, with calculated total dissolved solids concentrations greater than 3000 mg/L. The headwaters of Hot Weather Creek (lake 24) are dominated by calcium-magnesium bicarbonate with minor amounts of sodium chloride. Physical factors such as surface area, depth, and temperature are not correlated with the chemical parameters of lakes in the Slidre River basin.

Lakes 14 and 15, south of the Slidre River, had calcium sulfate and sodium chloride as the dominant ions, respectively. Lake 14 is the headwater lake at or slightly above the marine limit (Fig. 1b) and is located in a fault zone with high ridges on either side (Bell, 1996). It has a raised, moss shoreline on a cobble-gravel substrate. A till deposit at the south end of the lake blocks water flow. Lake 15 had a stone-gravel shoreline with very little vegetation. The extensive littoral zone was predominantly gravel and clay. The water was cold (1.2°C), with moderately high solute levels giving a total dissolved solids salinity of 3856 mg/L.

On Axel Heiberg Island, both study lakes were cold (2.5°C), partly ice covered, and shallow (<4 m). Lake 16 had a raised, moss shoreline (embankment) with a cobble-gravel-dominated littoral benthos. The waters were

dominated by sodium chloride (Fig. 1b). Lake 17 had a rocky shoreline characterized by sparse vegetation, with a cobble-gravel-dominated littoral benthos and clay-silt at the benthic sampling station. Its waters were dominated by calcium-magnesium bicarbonate.

Nutrients

Due to the high Ca concentration, the carbon pool was dominated by dissolved organic carbon. Total carbon was greater (over 60 mg/L) at low to middle elevations in the Slidre River basin, whereas high-elevation headwater lakes had much lower levels (Fig. 4a). The buffered, alkaliphilous aquatic systems of the peninsula contain elevated amounts of dissolved organic carbon in the water column. Dissolved

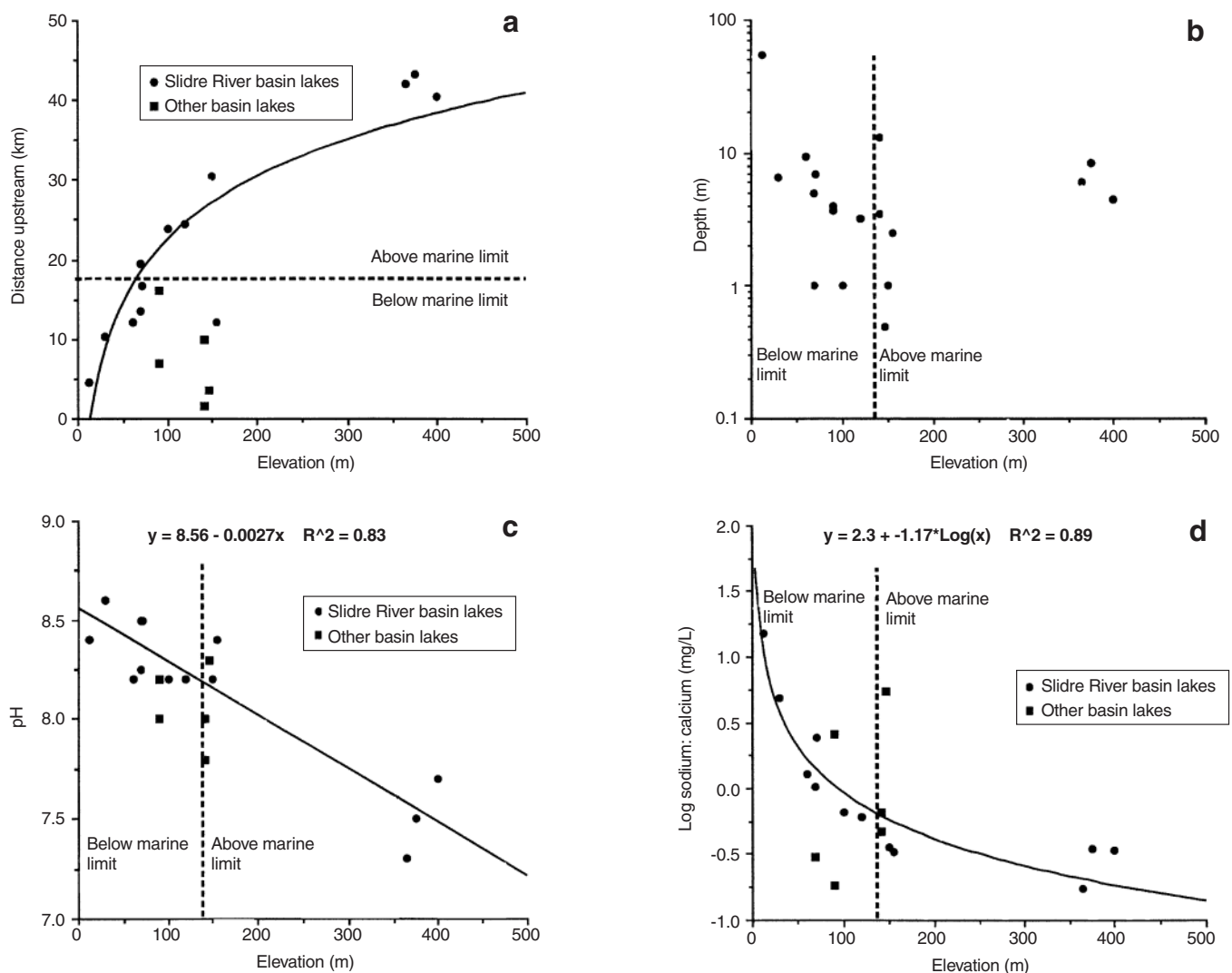


Figure 2. Relationship between physical aspects and chemical characteristics of lake waters and elevation. **a)** Relationship between lake elevation and distance upstream from the Slidre River outflow. **b)** Lake water depth plotted against elevation. **c)** Relationship between pH and elevation. **d)** The changing Na:Ca ratio in the study lake waters as a function of elevation. Values below 0 represent calcium-dominated lake solutes. Curves for Figures 2a and d are calculated using data from only the lakes of the Slidre River basin (circles).

Table 2. Water solute concentrations and ion balances calculated using the procedures of Maucha (*in* Hutchinson, 1957, p. 557). Waters with total dissolved solids (TDS) of 0 to 1000 mg/L are fresh; from 1001 to 3000 mg/L are slightly saline; and from 3001 to 10 000 mg/L are moderately saline. On the basis of total dissolved solids, all lakes except Romulus Lake and lake 15 are freshwater lakes.

Lake 1							Lake 3							
Surface			Bottom				Surface			Bottom				
Ion	Concentration mg/L	meq/L	Ion Prop. %	Concentration mg/L	meq/L	Ion Prop. %	Ion	Concentration mg/L	meq/L	Ion Prop. %	Concentration mg/L	meq/L	Ion Prop. %	
K	4.47	0.114	2.1	4.35	0.111	2.0	K	3.70	0.095	1.9	3.70	0.095	1.9	
Na	48.90	2.127	38.8	48.90	2.127	38.9	Na	38.20	1.662	32.6	38.20	1.662	32.7	
Ca	38.20	1.906	34.8	38.10	1.901	34.7	Ca	37.10	1.851	36.3	36.70	1.831	36.1	
Mg	16.20	1.332	24.3	16.20	1.332	24.3	Mg	18.10	1.488	29.2	18.10	1.488	29.3	
CO ₃	0.00	0.000	0.0	0.00	0.000	0.0	CO ₃	0.00	0.000	0.0	0.00	0.000	0.0	
HCO ₃	207.99	3.409	57.9	210.44	3.449	58.3	HCO ₃	221.10	3.623	67.0	206.90	3.391	65.3	
Cl	82.90	2.338	39.7	82.20	2.318	39.2	Cl	57.90	1.633	30.2	58.00	1.636	31.5	
SO ₄	6.90	0.144	2.4	7.00	0.146	2.5	SO ₄	7.40	0.154	2.8	7.80	0.162	3.1	
Cation sum			5.48 meq/L	Cation sum			5.47 meq/L	Cation sum			5.10 meq/L	Cation sum		5.08 meq/L
Anion sum			5.89 meq/L	Anion sum			5.91 meq/L	Anion sum			5.41 meq/L	Anion sum		5.19 meq/L
Difference			0.41 meq/L	Difference			0.44 meq/L	Difference			0.31 meq/L	Difference		0.11 meq/L
Salinity ¹			11.30 meq/L	Salinity			11.32 meq/L	Salinity			10.43 meq/L	Salinity		10.20 meq/L
			401.40 mg/L				402.98 mg/L				379.08 mg/L			365.26 mg/L
Lake 5							Lake 7			Lake 8				
Surface			Bottom				Ion	Concentration mg/L	meq/L	Ion Prop. %	Concentration mg/L	meq/L	Ion Prop. %	
K	10.00	0.256	2.5	10.20	0.261	2.5	K	1.81	0.046	1.6	13.80	0.353	1.9	
Na	110.00	4.785	46.5	111.00	4.828	46.6	Na	10.90	0.474	16.5	281.00	12.223	65.6	
Ca	45.90	2.290	22.2	46.20	2.305	22.3	Ca	33.09	1.651	57.4	57.40	2.864	15.4	
Mg	36.10	2.969	28.8	36.00	2.961	28.6	Mg	8.60	0.707	24.6	38.70	3.183	17.1	
CO ₃	0.00	0.000	0.0	0.00	0.000	0.0	CO ₃	0.00	0.000	0.0	0.00	0.000	0.0	
HCO ₃	277.50	4.548	43.0	281.60	4.615	43.1	HCO ₃	147.90	2.424	77.1	254.20	4.166	33.6	
Cl	190.00	5.358	50.7	192.50	5.429	50.7	Cl	21.70	0.612	19.5	217.00	6.120	49.4	
SO ₄	31.70	0.660	6.2	32.20	0.670	6.3	SO ₄	5.10	0.106	3.4	101.00	2.103	17.0	
Cation sum			10.30 meq/L	Cation sum			10.35 meq/L	Cation sum			2.88 meq/L	Cation sum		18.62 meq/L
Anion sum			10.57 meq/L	Anion sum			10.71 meq/L	Anion sum			3.14 meq/L	Anion sum		12.39 meq/L
Difference			0.27 meq/L	Difference			0.36 meq/L	Difference			0.26 meq/L	Difference		6.23 meq/L
Salinity			20.77 meq/L	Salinity			20.98 meq/L	Salinity			5.97 meq/L	Salinity		30.93 meq/L
			695.65 mg/L				704.07 mg/L				226.14 mg/L			958.02 mg/L
Lake 9			Lake 10				Lake 11			Lake 12				
Ion	Concentration mg/L	meq/L	Ion Prop. %	Concentration mg/L	meq/L	Ion Prop. %	Ion	Concentration mg/L	meq/L	Ion Prop. %	Concentration mg/L	meq/L	Ion Prop. %	
K	35.00	0.895	1.5	3.42	0.087	2.3	K	2.99	0.076	1.9	1.62	0.041	1.2	
Na	1020.00	44.367	75.3	20.30	0.883	22.9	Na	23.20	1.009	25.4	8.22	0.358	10.0	
Ca	67.50	3.368	5.7	30.80	1.537	39.9	Ca	38.30	1.911	48.1	45.10	2.250	62.7	
Mg	125.00	10.280	17.4	16.40	1.349	35.0	Mg	11.90	0.979	24.6	11.40	0.937	26.1	
CO ₃	0.00	0.000	0.0	0.00	0.000	0.0	CO ₃	0.00	0.000	0.0	0.00	0.000	0.0	
HCO ₃	122.50	2.008	4.0	171.80	2.815	68.7	HCO ₃	140.90	2.309	56.5	180.95	2.965	75.4	
Cl	1500.00	42.301	85.1	32.70	0.922	22.5	Cl	26.30	0.742	18.2	31.80	0.897	22.8	
SO ₄	260.00	5.413	10.9	17.30	0.360	8.8	SO ₄	49.70	1.035	25.3	3.40	0.071	1.8	
Cation sum			58.91 meq/L	Cation sum			3.86 meq/L	Cation sum			3.98 meq/L	Cation sum		3.59 meq/L
Anion sum			49.72 meq/L	Anion sum			4.10 meq/L	Anion sum			4.09 meq/L	Anion sum		3.93 meq/L
Difference			9.19 meq/L	Difference			0.24 meq/L	Difference			0.11 meq/L	Difference		0.35 meq/L
Salinity			108.59 meq/L	Salinity			7.90 meq/L	Salinity			8.01 meq/L	Salinity		7.46 meq/L
			3127.55 mg/L				289.28 mg/L				290.47 mg/L			278.87 mg/L

¹ Salinity = Sum [potassium + sodium + calcium + magnesium + carbonate + chloride + sulphate] + 0.98 [bicarbonate] (*see* Hutchinson, 1957, p. 557)

Lake 13				Lake 14			Lake 15			Lake 16				
Ion	Concentration		Ion Prop.	Concentration		Ion Prop.	Ion	Concentration		Ion Prop.	Concentration		Ion Prop.	
	mg/L	meq/L	%	mg/L	meq/L	%		mg/L	meq/L	%	mg/L	meq/L	%	
K	1.46	0.037	3.4	3.86	0.099	2.3	K	61.40	1.570	2.1	4.17	0.107	1.4	
Na	4.55	0.198	17.8	24.60	1.070	24.9	Na	1140.00	49.587	64.9	101.00	4.393	55.8	
Ca	13.50	0.674	60.5	37.70	1.881	43.7	Ca	210.00	10.479	13.7	38.90	1.941	24.6	
Mg	2.49	0.205	18.4	15.20	1.250	29.1	Mg	179.00	14.720	19.3	17.50	1.439	18.3	
CO ₃	0.00	0.000	0.0	0.00	0.000	0.0	CO ₃	0.00	0.000	0.0	0.00	0.000	0.0	
HCO ₃	24.90	0.408	42.0	43.71	0.716	18.2	HCO ₃	145.40	2.383	4.3	127.10	2.083	26.6	
Cl	1.94	0.055	5.6	48.30	1.362	34.6	Cl	1195.00	33.700	60.8	202.00	5.697	72.8	
SO ₄	24.40	0.508	52.3	89.40	1.861	47.2	SO ₄	928.00	19.321	34.9	2.10	0.044	0.6	
Cation sum			1.11 meq/L	Cation sum			4.30 meq/L	Cation sum			76.36 meq/L	Cation sum		7.88 meq/L
Anion sum			0.97 meq/L	Anion sum			3.94 meq/L	Anion sum			55.40 meq/L	Anion sum		7.82 meq/L
Difference			0.14 meq/L	Difference			0.36 meq/L	Difference			20.95 meq/L	Difference		0.06 meq/L
Salinity ¹			2.08 meq/L	Salinity			8.23 meq/L	Salinity			131.71 meq/L	Salinity		15.66 meq/L
			72.74 mg/L				261.90 mg/L				3855.89 mg/L			490.23 mg/L
Lake 17				Lake 18			Lake 22							
Ion	Concentration		Ion Prop.	Concentration		Ion Prop.	Ion	Concentration		Ion Prop.				
	mg/L	meq/L	%	mg/L	meq/L	%		mg/L	meq/L	%				
K	1.10	0.028	1.1	3.38	0.086	2.2	K	0.59	0.015	2.1				
Na	11.40	0.496	19.5	11.10	0.483	12.0	Na	1.71	0.074	10.5				
Ca	24.10	1.203	47.4	37.00	1.846	46.0	Ca	9.90	0.494	69.7				
Mg	9.86	0.811	32.0	19.40	1.595	39.8	Mg	1.52	0.125	17.6				
CO ₃	0.00	0.000	0.0	0.00	0.000	0.0	CO ₃	0.00	0.000	0.0				
HCO ₃	100.14	1.641	66.6	219.10	3.591	87.2	HCO ₃	29.48	0.483	77.3				
Cl	16.30	0.460	18.6	15.10	0.426	10.3	Cl	1.40	0.039	6.3				
SO ₄	17.50	0.364	14.8	4.90	0.102	2.5	SO ₄	4.90	0.102	16.3				
Cation sum			2.54 meq/L	Cation sum			4.01 meq/L	Cation sum			0.71 meq/L			
Anion sum			2.47 meq/L	Anion sum			4.12 meq/L	Anion sum			0.62 meq/L			
Difference			0.07 meq/L	Difference			0.11 meq/L	Difference			0.08 meq/L			
Salinity			4.97 meq/L	Salinity			8.06 meq/L	Salinity			1.32 meq/L			
			178.40 mg/L				305.60 mg/L				48.91 mg/L			
Lake 23				Lake 24										
Ion	Concentration		Ion Prop.	Concentration		Ion Prop.								
	mg/L	meq/L	%	mg/L	meq/L	%								
K	0.52	0.013	1.4	6.84	0.175	3.5								
Na	4.21	0.183	18.8	36.10	1.570	31.4								
Ca	12.10	0.604	62.1	36.00	1.796	35.9								
Mg	2.10	0.173	17.8	17.70	1.456	29.1								
CO ₃	0.00	0.000	0.0	0.00	0.000	0.0								
HCO ₃	45.20	0.741	84.1	263.30	4.315	75.6								
Cl	1.28	0.036	4.1	38.40	1.083	19.0								
SO ₄	5.00	0.104	11.8	14.90	0.310	5.4								
Cation sum			0.97 meq/L	Cation sum			5.00 meq/L							
Anion sum			0.88 meq/L	Anion sum			5.71 meq/L							
Difference			0.09 meq/L	Difference			0.71 meq/L							
Salinity			1.84 meq/L	Salinity			10.62 meq/L							
			69.51 mg/L				407.97 mg/L							

¹ Salinity = Sum [potassium + sodium + calcium + magnesium + carbonate + chloride + sulphate] + 0.98 [bicarbonate] (see Hutchinson, 1957, p. 557)

organic carbon was negatively correlated with secchi depth (Fig. 5a) whereas dissolved inorganic carbon decreased with distance upstream (Fig. 5b). Although a general increase in dissolved organic carbon was evident when plotted against particulate organic carbon, no correlation was noted. Levels of particulate organic carbon range from 300 to 950 µg/L and show a positive correlation with total phosphorus (TP, Fig. 5c). No relationship between particulate organic carbon and lake elevation was observed in the water column (Fig. 6a), although the organic content of the benthic sediments was higher in the headwater lakes (Fig. 6c).

The total nitrogen (TN) to phosphorus ratio varies from 15 to 90. Nitrate generally dominated the soluble nitrogen pool, although ammonium levels were high in lake 12 (21 µg/L, not shown). Particulate carbon levels were strongly correlated with particulate nitrogen, with a mean POC:PN ratio of 7.1 (Fig. 6b). Phosphorus levels were low (<12 µg/L) with filtered phosphorus (TFP) dominating (Fig. 4c). Exceptions were Lakes 12 and 14 where particulate phosphorus (TPP)

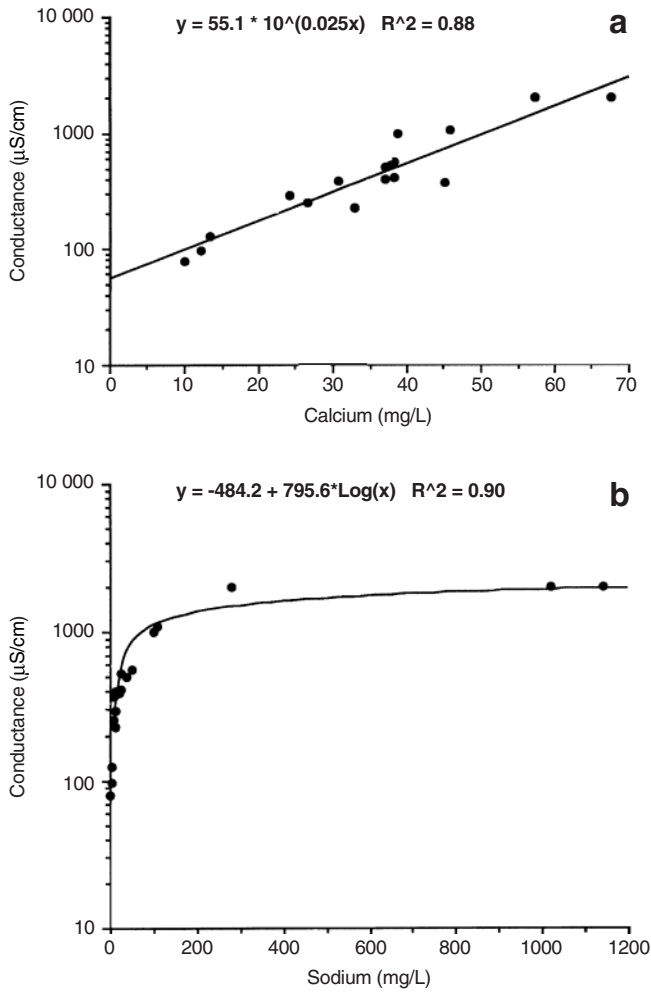


Figure 3. Comparison of calcium and sodium concentrations and conductance for all the lakes studied on Fosheim Peninsula. **a)** Log conductance plotted against calcium. **b)** Log conductance plotted against sodium.

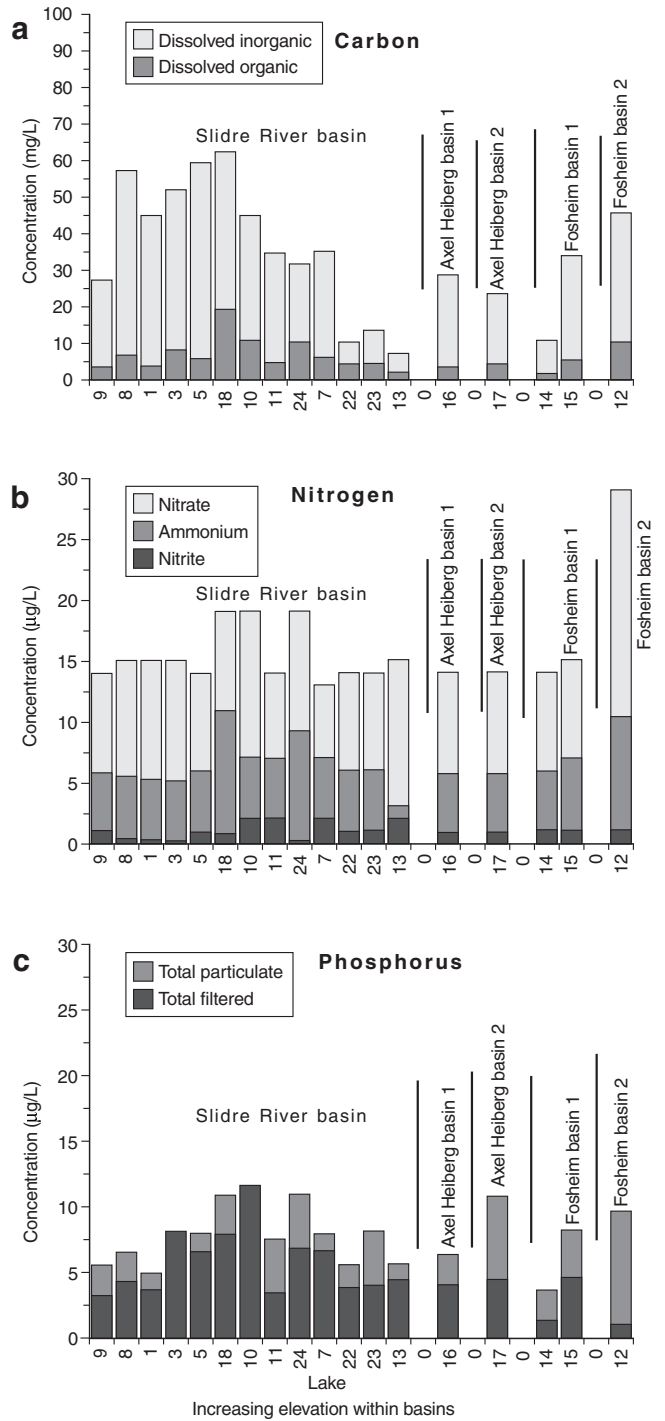


Figure 4. Lake-water nutrient pools on Fosheim Peninsula. Relationship of **a)** carbon, **b)** nitrogen, **c)** phosphorus to elevation. The lakes are sorted by drainage basin (Slidre River basin, Axel Heiberg basin 1, Axel Heiberg basin 2, Fosheim basin 1, Fosheim basin 2).

dominated. Particulate organic carbon did not correlate with particulate phosphorus, nor was there any relation between soluble reactive phosphorus (SRP) and total phosphorus. In temperate lakes, dissolved phosphorus is typically correlated with total available phosphorus (Rigler, 1956).

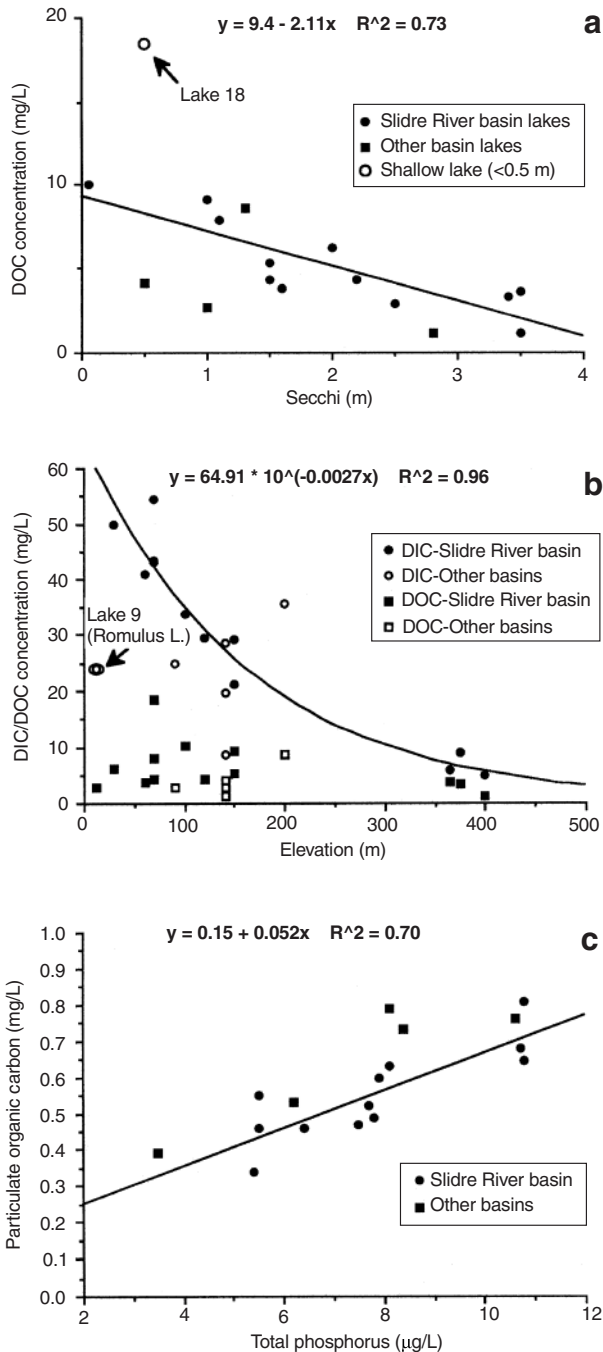


Figure 5. Carbon composition of lake waters. **a**) Dissolved organic carbon (DOC) plotted against Secchi depth. Lake 18 was excluded from the Slidre River basin regression because of lake depth. **b**) DOC/DIC (dissolved inorganic carbon) as a function of elevation. **c**) Particulate organic carbon (POC) plotted against total phosphorus (TP).

Phytoplankton

Pelagic diatom densities were low in all lakes, ranging from absent to 250 000 frustules/L. The lowland lakes (<30 m a.s.l.) had no diatoms in the phytoplankton assemblage. The lakes at 60–70 m of elevation had assemblages dominated by centric diatoms, specifically *Cyclotella bodanica* var. *lemanica* O. Müller. At higher elevations, the plankton community was dominated by araphid taxa, such as *Fragilaria*

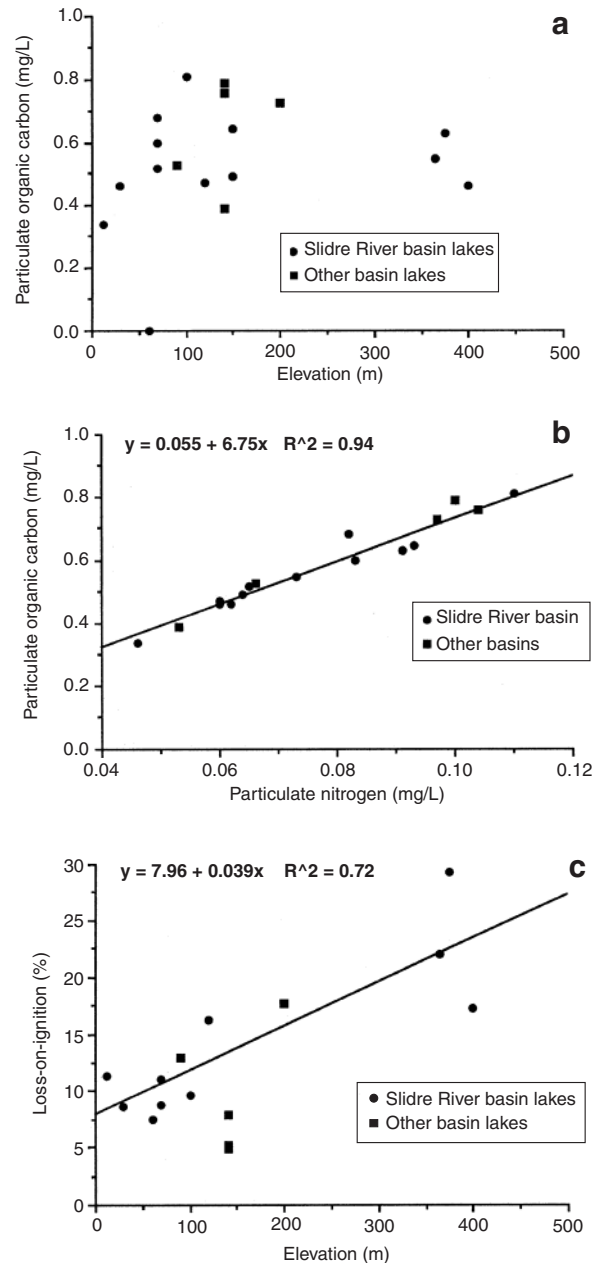


Figure 6. Carbon compositions for lake waters and benthic sediments. **a**) Lake-water particulate organic carbon plotted against elevation. **b**) Relationship between lake-water particulate organic carbon and particulate nitrogen. **c**) Relationship between sediment per cent loss-on-ignition and elevation.

pinnata Ehrenberg, with counts ranging up to 118 500/L. Other phytoplankton present include taxa from all algal divisions, but the assemblages were dominated by Chrysophyta (Hamilton, unpub. data, 1997). The naked chrysophytes were predominant whereas scaled and loricated chrysophytes were present in lower numbers.

Benthic diatoms

A clear difference in benthic diatom assemblages was observed within the Slidre River basin. At low elevations, in lakes with high pH and moderate salinity (>3000 mg/L), almost no intact diatoms were observed in the sediments (Fig. 7). At elevations between 60 and 70 m, the diatom assemblage was dominated by *Amphora pediculus* (Kützing) Grunow, *A. inariensis* Krammer, and *A. copulata* (Kützing) Schoeman & Archibald (Fig. 7). At elevations ranging from 100 to 150 m (lakes 7, 11, 24), benthic sediments had varied diatom compositions dominated by *Fragilaria* or *Amphora* taxa. An exception is Gemini Lake (Lake 10), a shallow lake about 100 m above sea level, in which there were no intact diatoms in the sediments and diatom fragments were rare. At high elevations, the benthic diatom flora was dominated by *Fragilaria* spp., specifically *Fragilaria pinnata* (Fig. 7). The small, elliptical to oval form of *F. pinnata* was dominant with *F. cf. pinnata* var. *intercedens* (Grunow) Hustedt occurring as a rarer form. *Fragilaria construens* (Ehrenberg) Grunow was also common in middle- to high-elevation lakes

(120–200 m a.s.l.), although not observed in abundance at the high elevations. A more diverse flora was evident at middle elevations and included *Amphora* and *Fragilaria* taxa as well as other distinct forms such as *Achnanthes flexella* (Kützing) Brun, *Achnanthes lanceolata* (Brébisson) Grunow, *Diploneis smithii* (Brébisson) Cleve, *Caloneis bacillum* (Grunow) Cleve, *Encyonema minutum* (Hilse) Mann, *Epithemia* cf. *turgida* (Ehrenberg) Kützing, *Denticula kuetzingii* Grunow, *Nitzschia perminuta* (Grunow) M. Peragallo, *Navicula elginensis* (Gregory) Ralfs, and *N. cf. vulpina* Kützing (Fig. 7).

Benthic diatom assemblages in lakes 12, 14, 15, and 17 varied from *Amphora* spp. to *Fragilaria pinnata* (Fig. 7). Other taxa including *Denticula kuetzingii* and *Navicula* spp were also prominent in coastal lakes below the marine limit (Fig. 7).

DISCUSSION

The topography of the Slidre River basin ranges from bed-rock in the headwater region to raised marine sediments in the lower reaches. This variation in materials affects the chemistry of the lakes, which range from dilute, calcium-bicarbonate-dominated headwater lakes to slightly or moderately saline, low-elevation lakes. Field conductance effectively summarizes these changing solute levels throughout the basin, especially the carbonate concentrations (Fig. 4a).

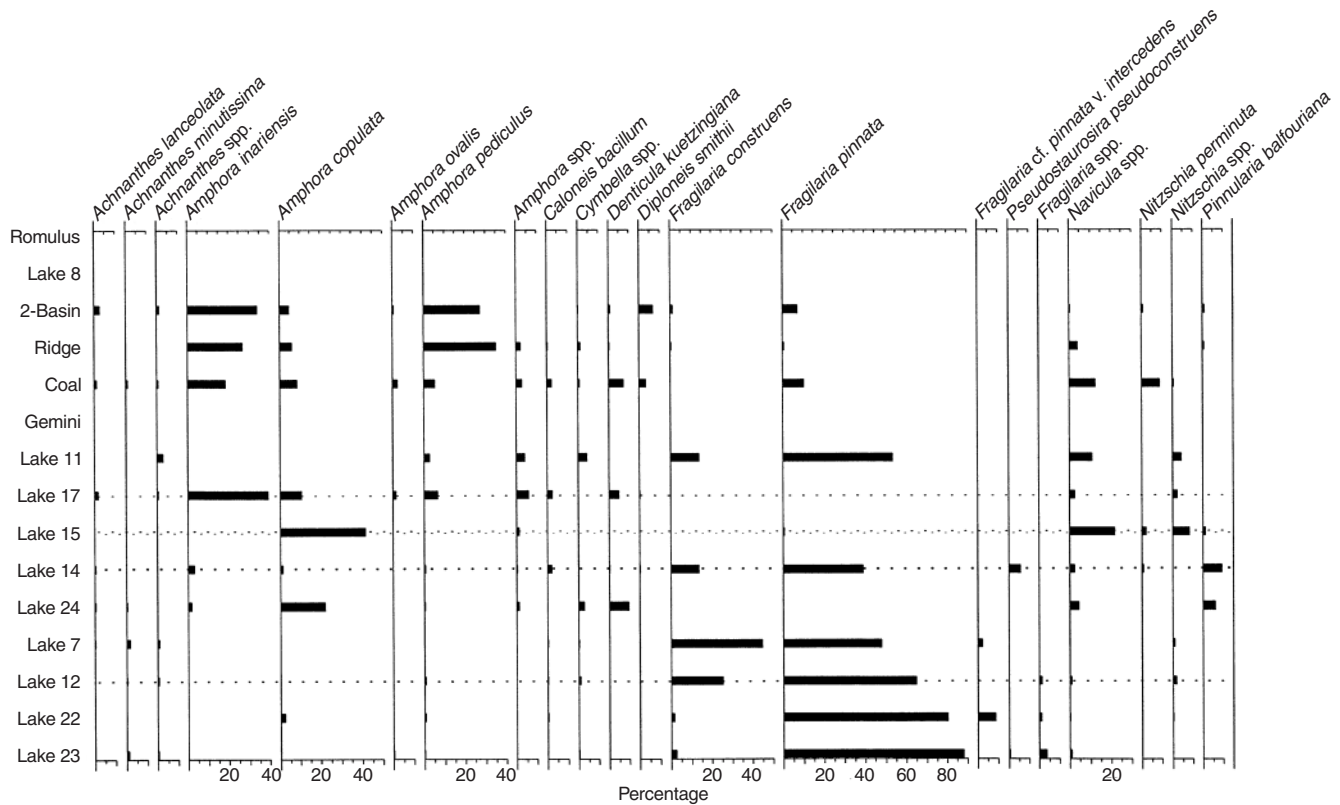


Figure 7. Per cent composition of the benthic diatom assemblages plotted against elevation. The lakes are ordered by increasing elevation with the lowest elevations at the top.

Lowland and coastal lakes can also be influenced by marine aerosols (McNeely and Gummer, 1984), whereas inland lakes are more strongly influenced by the composition of surficial sediments.

Within the Slidre River basin, the type of surficial material is reflected by the water chemistry of the lakes (Fig. 1b). The headwater lakes (sites 22 and 23) are essentially dilute calcium bicarbonate waters typical of snow and glacial meltwaters. The chemistry of lake 13, downstream from the headwater lakes, indicates low solute concentrations with calcium sulfate (gypsum) present in the lake water. Since no gypsum bedrock occurs in the immediate area nor in the Sawtooth Range, the water chemistry of this lake suggests glacial transport of sediments from local gypsum sources to the southwest (T. Bell and D.A. Hodgson, pers. comm., 1997).

In the middle basin area (Fig. 1b, lakes 10 and 11), the water chemistry is similar to that of the headwater lakes except for an increase in solutes (Table 2). Lake 10 (Gemini Lake) and lake 18 show evidence of dolomite in the surficial materials with calcium-magnesium bicarbonate being the dominant ions. Lake 24, at the headwaters of Hot Weather Creek, not only shows the influence of dolomite, but also indicates an increase in sodium and chloride, with enhanced solute levels. This would suggest that the lake is close to or slightly below the marine limit in the area.

Lakes 1 and 5 illustrate the marked influence of surface sediments on solute levels, especially where the sediments represent Holocene marine deposits and sodium chloride becomes the dominant ion pair (Fig. 1b). Lake 8 and Romulus Lake (lake 9) are moderately saline as indicated by total dissolved solids of >3000 mg/L. The elevated solute levels in these lakes and the enhanced magnesium versus calcium concentrations suggest that the lake waters are diluted trapped seawater (Davidge, 1994) rather than derived from the leaching of surficial materials (sites 1 and 5, Fig. 1b). The persistent high solute levels in these lakes attest to their low flushing rates since the time of their isolation from the sea, which is due to their physiographic setting (small headwater catchments) and an arctic climatic regime (low precipitation).

Lake 7 helps to define the extent of marine limit on the north side of the Slidre River, in that it has a low solute content and is dominated by calcium bicarbonate and not sodium chloride. This suggests that the marine limit is below 140 m along the edge of Black Top Mountain. Lake waters below the marine limit defined by Bell (1992) are dominated by sodium chloride (Fig. 2, 3). Although dust storms blow sediment throughout the basin, as evidenced by the accumulation of sediments around local hummocks (S.A. Edlund, pers. comm., 1996), no evidence was found of either marine aerosols or sediment being moved from the coastal lowlands to the headwater lakes in the Sawtooth Range.

Bedrock and surficial influences on water chemistry are further evident in the basin south of the Slidre River, in which lakes 14 and 15 both have enhanced levels of calcium sulfate (Fig. 1b, Table 2). These levels indicate that there is gypsum in the local surficial materials, suggesting the potential of glacial transport (T. Bell and D.A. Hodgson, pers. comm.,

1997). Lake 14, with only a moderate solute content, shows some evidence of sodium chloride enrichment, which may be related to marine aerosols or more likely due to the marine sediment observed around the lake. Lake 14 is judged to be above the marine limit, whereas lake 15 is downstream and below the marine limit. Lake 15 not only exhibits calcium sulfate from the surficial gypsum, but also shows high sodium chloride levels (Fig. 1b, Table 2), which may have been derived from underlying marine deposits and possibly enhanced by aerosols, as a result of the lake's proximity to the coast.

Lakes 16 and 17 are on the coastal lowlands of western Axel Heiberg Island, but as suggested by their water chemistry, lake 16 is below the marine limit and dominated by sodium chloride, whereas lake 17 is above the marine limit on surficial materials derived from dolomitic bedrock. The slightly enhanced levels of sodium chloride in lake 17 are probably indicative of dust and aerosol transport.

These lakes are oligothermic, alkaliphilous, and oligotrophic. Total nitrogen to phosphorus ratios greater than 15 indicate significant phosphorus limitation (Lean et al., 1989). A positive total phosphorus to particulate organic matter relationship is also indicative of phosphorus limitation, especially when considering that a POC:PN ratio of 7.1 shows a mid-range chemical system for healthy phytoplankton growth (Lean et al., 1989). Nitrate, nitrite, and soluble reactive phosphorus levels are commonly below their detection limit (>0.005, >0.001, and >0.002), as has been observed in other studies (Schindler et al., 1974; McNeely and Gummer, 1984).

The higher DOC:DIC ratio in upland lakes relates to a decrease in dissolved inorganic carbon rather than an increase in dissolved organic carbon. In fact, a reduction in dissolved inorganic carbon can be attributed directly to lower solute levels in the upland lakes (Fig. 1b, Table 2). This observation is further supported by the absence of any association between these two variables (Fig. 5b). Although dissolved inorganic carbon dominates, levels of dissolved organic carbon are unexpectedly high for the tundra and are comparable to those of temperate lakes (Scully and Lean, 1994). The negative relationship between Secchi disc depth and dissolved organic carbon defined here is also reported for southern Canadian lakes (E. Benzen, pers. comm., 1997). It may be that a certain amount of the visible light that is reflected back from the Secchi disc is absorbed by the dissolved organic carbon or that those factors contributing to the dissolved organic carbon correlate by chance with the attenuation of visible light. For example, drainage basin area is a good predictor of dissolved organic carbon export, but it is also a good predictor of total phosphorus export and the biomass of organisms that are responsible for the attenuation of visible light (Rasmussen et al., 1989).

Particulate organic carbon levels are similar to levels observed in Lake Ontario (Stevens and Neilson, 1987). Given the differences in drainage areas, growing seasons, and general climatic conditions, the similarities in particulate organic carbon levels are worthy of further study. The variation in

particulate organic carbon levels from lake to lake indicates a lack of association with lake elevation or lake location within the Slidre River basin.

The organic content of lake sediments increases with distance upstream (Fig. 6c). Wolfe (2000) has also noted high organic carbon levels in the sediments of Solstice Lake, a headwater lake (305 m a.s.l.). The organic carbon in the sediments of these ice-free headwater lakes is a function of both allochthonous and autochthonous input. Compared to the lowland lakes, these headwater lakes typically have large catchments, which can supply allochthonous input (both nutrients and detritus), especially from the wetlands at the base of the Sawtooth Range. Hobbie (1973) has shown that leaching of terrestrial materials may contribute significant allochthonous nutrients to lakes, although this does not appear to be occurring in the larger lakes of Fosheim Peninsula. An example from the Arctic Archipelago is a coastal lake on Devon Island with no terrestrial organic carbon input, but with enough autochthonous carbon production to assist varved benthic sedimentation (Gajewski et al., 1997). The development of benthic algal and vascular plant mats, as observed in lake 12, also indicates the importance of benthic autochthonous carbon production. Allochthonous input of organic carbon may account for higher productivity in shallow ponds associated with polygon wetlands (Hamilton, pers. obs., 1997).

In the Fosheim Peninsula region, surface waters can carry significant sediment loads, especially during freshets (Lewkowitz and Wolfe, 1994). The high relief around the headwater lakes may create runoff with sufficient velocity to move significant amounts of detrital matter into the local, open-water lakes (typically spring ice-covered moats) thus increasing the levels of organic carbon. However, large, permanently ice-covered lakes in the middle of the Sawtooth Range have sediments with low organic content and only a few diatoms (i.e. low autochthonous production, Hamilton, pers. obs., 1997). These frozen lakes are not collection basins for organic matter because sediment-laden water either deposits its load in a nearshore delta or the flow passes through the lake basin.

The catchments of the lowland lakes, which are the source areas for organic detritus, are substantially smaller than those of the upland lakes, and the amount of clastic sediment both eroding from shorelines, including slumping, and being blown in by dust storms is potentially high (Hamilton, pers. obs., 1996). This leads to a dilution of the organic matter in the sediments and, therefore, measurements of organic matter will indicate an apparent low organic content even if the flux were as high as in the upland lakes. Another possible explanation for the low organic sediment in the downstream lakes is related to the suppression of terrestrial plant growth by windblown sediments that smother the vegetation (S.A. Edlund, pers. comm., 1996), thus reducing the amount of both allochthonous nutrient and detrital organic matter contributed to these lakes.

Benthic diatoms varied from araphid taxa in the headwater lakes to larger raphid taxa in the lowland lakes (Fig. 7). The presence of large raphid diatoms in aquatic systems at

low elevations has been reported in other regions of the Arctic (Douglas and Smol, 1993; Gajewski et al., 1997). *Amphora* taxa can dominate in lakes and ponds with higher solute levels (Foged, 1953, 1955, 1981). Upland lakes on Fosheim Peninsula contain more diverse assemblages, from large raphid forms such as *Amphora*, *Navicula*, *Denticula*, and *Cymbella* under alkaline to circumneutral conditions to the smaller araphid *Fragilaria* in circumneutral to acidic conditions. The headwater lakes or higher elevation lakes are dominated by *Fragilaria pinnata* (see also Wolfe 2000). Smol (1983) suggests that *Fragilaria* taxa are more abundant in arctic lakes under cold conditions. This is supported by the dominance of *Fragilaria pinnata* in the colder headwater lakes. Changes from the araphid *Fragilaria* to raphid taxa such as *Amphora*, *Pinnularia*, *Cymbella*, and *Navicula* in recent sediment deposition (<200 years) (Douglas et al. 1994; Doubleday et al., 1995; Gajewski et al. 1997; Douglas et al., 2000; Wolfe, 2000) correlate well with increasing temperatures interpreted from ice cores from northern ice caps (sensu Gajewski et al., 1997). Floral differences related to elevation and possibly temperature have also been observed in arctic lotic systems (Hamilton and Edlund, 1994).

Differences in lake diatom assemblages within the smaller coastal basins are evident in this study (Fig. 7). These lakes, within 13 km of the coast, clearly show the importance of surficial sediments on water chemistry and biodiversity as evidenced by the changing diatom assemblages in the Slidre River basin. Lakes above the marine limit (lakes 12, 14) have araphid-dominated assemblages, whereas lakes underlain by marine sediments are dominated by *Amphora* and *Navicula* species. Lake location, lake chemistry, and climate are important variables that must be considered when reconstructing regional paleohistories. In the case of central Ellesmere Island, including the Lake Hazen region, limnological data sets must include water bodies of both high and low solute levels for an effective evaluation of diatom biodiversity.

Dissolution of diatom valves can be a significant problem in brackish lakes with elevated pH. The general problems of dissolution are reviewed by Jørgensen (1955) and Barker et al. (1994). Romulus Lake (lake 9) and lake 8 are examples of moderately saline lakes with diatom fossils missing or absent. The absence of diatom fragments further suggests dissolution as the problem. Although pH readings are only available for surface waters, the salinity and pH levels of Romulus Lake and lake 15 are indicative of conditions favourable for silica dissolution. Coastal arctic lakes with elevated pH and salinity (especially those formed by trapped seawater) may not provide microfossils suitable for environmental assessments.

We have identified some of the factors influencing the composition of diatoms on Fosheim Peninsula. The high organic carbon levels within some lake systems may reflect new production or simply the movement of existing organic material into the headwater lakes. The relative importance of these sources is not fully understood, although without this organic matter, aquatic bacterial activity would be significantly reduced. Chemical factors that influence diatom composition vary spatially as a result of differences in physiography and surficial bedrock geology. Many of these

factors vary in time because of changes in the hydrological cycle, the climate, or the vegetation and will thus influence diatom composition.

ACKNOWLEDGMENTS

The authors wish to thank Dr. S.A. Edlund for discussion and technical support, especially while staying at the Hot Weather Creek base camp on Fosheim Peninsula. The Polar Continental Shelf Project provided extensive logistical field support. Further thanks are extended to Dr. T. Bell for providing the Fosheim Peninsula base map and to D. Atkinson for making modifications to the base map. M. Rejhon developed the PASCAL program used to assess ion balances and produce the ionic proportion diagrams.

This work is supported by an Natural Sciences and Engineering Research Council of Canada (NSERC) Research Grant to K. Gajewski and is a contribution to Project 4 of the Climate System History and Dynamics Project funded by NSERC and the Atmospheric Environment Service (AES). Additional financial support was provided by the Canadian Museum of Nature.

REFERENCES

- Barker, P., Fontes, J.-C., Gasse, F., and Druart, J.-C.**
1994: Experimental dissolution of diatom silica in concentrated salt solutions and implications for paleoenvironmental reconstruction; *Limnology and Oceanography*, v. 39, p. 99–110.
- Bell, T.**
1992: Glacial and sea level history of western Fosheim Peninsula, Ellesmere Island, Arctic Canada; Ph.D. thesis, University of Alberta, Edmonton, Alberta, 163 p.
1996: The last glaciation and sea level history of Fosheim Peninsula, Ellesmere Island, Canadian High Arctic; *Canadian Journal of Earth Sciences*, v. 33, p. 1075–1086.
- Bradley, R.S.**
1990: Holocene paleoclimatology of the Queen Elizabeth Islands, Canadian High Arctic; *Quaternary Science Reviews*, v. 9, p. 365–384.
- Davidge, G.**
1994: Physical limnology and sedimentology of Romulus Lake: meromictic lake in the Canadian High Arctic; M.Sc. thesis, Queen's University, Kingston, Ontario, 114 p.
- Dean, W.E., Jr.**
1974: Determination of carbonate and organic matter in calcareous sediment and sedimentary rock by loss on ignition: comparison with other methods; *Journal of Sedimentary Petrology*, v. 44, p. 241–248.
- Doubleday, N., Douglas, M.S.V., and Smol, J.P.**
1995: Paleoenvironmental studies of black carbonaceous particles in the High Arctic: a case study from northern Ellesmere Island; *The Science of the Total Environment*, v. 160/161, p. 661–668.
- Douglas, M.S.V. and Smol, J.P.**
1993: Freshwater diatoms from high arctic ponds (Cape Herschel, Ellesmere Island, N.W.T.); *Archiv für Hydrobiologie*, v. 131, p. 401–434.
- Douglas, M.S.V., Smol, J.P., and Blake, W., Jr.**
1994: Marked post-18th century environmental change in high arctic ecosystems; *Science*, v. 266, p. 416–419.
2000: Summary of paleolimnological studies at High Arctic ponds at Cape Herschel, east-central Ellesmere Island, Nunavut; *in Environmental Response to Climate Change in the Canadian High Arctic*, (ed.) M. Garneau and B.T. Alt; Geological Survey of Canada, Bulletin 529.
- Edlund, S.A.**
1992: Climate change and its effects on Canadian arctic plant communities; *in Proceedings of a symposium held at McMaster University, Arctic Environments: Past Present and Future*, (ed.) M-k. Woo and D.J. Gregor; McMaster University, Department of Geography, Hamilton, Ontario, p. 121–137.
- Edlund, S.A. and Alt, B.T.**
1989: Regional congruence of vegetation and summer climate patterns in the Queen Elizabeth Islands, Northwest Territories, Canada; *Arctic*, v. 42, p. 3–22.
- Edlund, S.A., Alt, B.T., and Young, K.L.**
1989: Interaction of climate vegetation and soil hydrology at Hot Weather Cr., Fosheim Peninsula, Ellesmere Island, Northwest Territories; *in Current Research, Part D; Geological Survey of Canada, Paper 84-1A*, p. 279–285.
- Ehrenberg, C.G.**
1854: Zur Mikrogeologie. Das Erden und Felsen schaffende Wirken des unsichtbar klein selbständigen ebens auf der Erde; Leopold Voss, Leipzig, 374 p.
- Environment Canada**
1979: Analytical Methods Manual; Environment Canada, Ottawa, Ontario, 340 p.
- Etkin, D. and Agnew, T.**
1992: Arctic climate in the future; *in Proceedings of a symposium held at McMaster University, Arctic Environments: Past Present and Future*, (ed.) M-k. Woo and D.J. Gregor; McMaster University, Department of Geography, Hamilton, Ontario, p. 17–34.
- Foged, N.**
1953: Diatoms from West Greenland collected by Tyge W. Bocher; *Meddelelser om Grønland*, v. 147, p. 1–86.
1955: Diatoms from Peary Land, North Greenland, collected by Kjeld Holmen; *Meddelelser om Grønland*, v. 128, p. 1–90.
1981: Diatoms in Alaska; *Bibliotheca Phycologica*, v. 53, p. 1–317.
- Gajewski, K., Garneau, M., and Bourgeois, J.**
1995: Paleoenvironments of the Canadian High Arctic derived from pollen and plant macrofossils: problems and potentials; *Quaternary Science Review*, v. 14, p. 609–629.
- Gajewski, K., Hamilton, P.B., and McNeely, R.**
1997: Annually laminated sediments from an oligotrophic lake on Devon Island, Nunavut, Canada; *Journal of Paleolimnology*, v. 17, p. 215–225.
- Garneau, M.**
1992: Analyses macrofossiles d'un dépôt de tourbe dans la région de Hot Weather Creek, péninsule de Fosheim, île d'Ellesmere, Territoires du Nord-Ouest; *Géographie physique et Quaternaire*, vol. 46, p. 285–294.
- Hamilton, P.B. and Edlund, S.E.**
1994: Occurrence of *Prasiola fluviatilis* (Chlorophyta) on Ellesmere Island in the Canadian Arctic; *Journal of Phycology*, v. 30, p. 217–221.
- Hamilton, P.B., Lean, D.R.S., and Poulin, M.**
1994: The physicochemical characteristics of lakes and ponds from the northern regions of Ellesmere Island; *in Proceedings of the Fourth Arctic-Antarctic Diatom Symposium (workshop)*, (ed.) P.B. Hamilton; Canadian Museum of Nature, Ottawa, Ontario; Canadian Technical Report of Fisheries and Aquatic Sciences 1957, p. 57–63.
- Hobbie, J.E.**
1973: Arctic limnology: a review; *in Alaska Arctic Tundra*, (ed.) M.E. Britton; The Arctic Institute of North America, Technical Paper no. 25, Washington D.C., p. 127–168.
- Hustedt, F.**
1930–1966: Die Kieselalgen Deutschlands, Österreichs und der Schweiz unter Berücksichtigung der Übrigen Länder Europas sowie der angrenzenden Meeresgebiete; *in Kryptogamen-Flora von Deutschland, Österreich und der Schweiz, Band 7, Teil 2, Lief. 1*, p. 1–176, Fig. 543–682, (ed.) L. Rabenhorst; Verlagsgesellschaft m. b. h. Leipzig.
- Hutchinson, G.E.**
1957: *A Treatise on Limnology*, v. 1, Geography, Physics and Chemistry; J. Wiley and Sons, New York, 1015 p.
- Jørgensen, E.G.**
1955: Solubility of the silica in diatoms; *Physiologica Plantarum*, v. 8, p. 846–851.

Krammer, K. and Lange-Bertalot, H.

- 1986: Bacillariophyceae (Teil 1: Naviculaceae); *in* Süßwasserflora von Mitteleuropa, Band 2/1, (ed.) H. Ettl, J. Gerloff, H. Heynig, D. Mollenhauer; G. Fisher Verlag, Stuttgart, 876 p.
- 1988: Bacillariophyceae (Teil 2: Bacillariaceae, Epithemiaceae, Surirellaceae); *in* Süßwasserflora von Mitteleuropa, Band 2/2, (ed.) H. Ettl, J. Gerloff, H. Heynig, D. Mollenhauer; G. Fisher Verlag, Stuttgart, Germany, 596 p.
- 1991a: Bacillariophyceae (Teil 3: Centrales, Fragilariaceae, Eunotiaceae); *in* Süßwasserflora von Mitteleuropa, Band 2/3, (ed.) H. Ettl, J. Gerloff, H. Heynig, D. Mollenhauer; G. Fisher Verlag, Stuttgart, Germany, 576 p.
- 1991b: Bacillariophyceae (Teil 4: Achnantheaceae, Kritische Ergänzungen zu *Navicula* (Lineolatae) und *Gomphonema* Gesamtliteraturverzeichnis Teil 1–4); *in* Süßwasserflora von Mitteleuropa, Band 2/4, (ed.) H. Ettl, J. Gerloff, H. Heynig, D. Mollenhauer; G. Fisher Verlag, Stuttgart, Germany, 437 p.

Lean, D.R.S., Pick, F.R., Mitchell, S.F., Downes, M.T., Woods, P.T., and White, E.

- 1989: Plankton P and N deficiency in Lake Okaro NZ; *Archiv für Hydrobiologie beiheft Ergebnisse der Limnologie*, v. 32, p. 195–211.

Lewkowitz, A.G. and Wolfe, P.M.

- 1994: Sediment transport in Hot Weather Cr, Ellesmere Island, N.W.T., Canada 1990–1991; *Arctic and Alpine Research*, v. 26, p. 213–226.

McNeely, R. and Gummer, W.D.

- 1984: A reconnaissance survey of the environmental chemistry in east-central Ellesmere Island, N.W.T.; *Arctic*, v. 37, p. 210–223.

Patrick, R. and Reimer, C.W.

- 1966: The diatoms of the United States, exclusive of Alaska and Hawaii; *Academy of Natural Sciences of Philadelphia*, v. 1, Monograph 13, 688 p.
- 1975: The diatoms of the United States, exclusive of Alaska and Hawaii; *Academy of Natural Sciences of Philadelphia*, v. 2, pt. 1, Monograph 13, 214 p.

Rasmussen, J.B., Godbout, L., and Schallenberg, M.

- 1989: The humic content of lake water and its relationship to watershed and lake morphometry; *Limnology and Oceanography*, v. 34, p. 1336–1343.

Rigler, F.H.

- 1956: A tracer study of the phosphorus cycle in lake water; *Ecology*, v. 37, p. 550–562.

Schindler, D.W., Welch, H.E., Kalff, J., Brunskill, G.J., and Kritsch, N.

- 1974: Physical and chemical limnology of Char Lake, Cornwallis Island (75°N Lat.); *Journal of the Fisheries Research Board of Canada*, v. 31, p. 585–607.

Scully, N.M. and Lean, D.R.S.

- 1994: The attenuation of UV radiation in temperate lakes; *Archiv für Hydrobiologie beiheft Ergebnisse der Limnologie*, v. 43, p. 135–144.

Smol, J.P.

- 1983: Paleophycology of a high arctic lake near Cape Herschel, Ellesmere Island; *Canadian Journal of Botany*, v. 61, p. 2195–2204.

Stevens, R.J.J. and Neilson, M.A.

- 1987: Response of Lake Ontario to reductions in phosphorus loading, 1967–1982; *Canadian Journal of Fisheries and Aquatic Sciences*, v. 44, p. 2059–2068.

Thornsteinsson, R.

- 1971: Revised geological map, Fosheim Peninsula, District of Franklin (E.S.N. 1302A); *Geological Survey of Canada*, Ottawa, Ontario, scale: 1:125 000.

Thronsen, J.

- 1978: Preservation and storage; *in* *Phytoplankton Manual*, (ed.) A. Sournia; United Nations Educational, Scientific, and Cultural Organization; Page Brothers Ltd., Paris, p. 69–75.

Van Heurck, H.

- 1880–1885: *Synopsis des Diatomées de Belgique*; Anvers, 235 p., 135 pl.

Wolfe, A.P.

- 2000: A 6500 year diatom record from southwestern Fosheim Peninsula, Ellesmere Island, Nunavut; *in* *Environmental Response to Climate Change in the Canadian High Arctic*, (ed.) M. Garneau and B.T. Alt; *Geological Survey of Canada, Bulletin 529*.

A 6500-year diatom record from southwestern Fosheim Peninsula, Ellesmere Island, Nunavut

A.P. Wolfe¹

Wolfe, A.P., 2000: A 6500-year diatom record from southwestern Fosheim Peninsula, Ellesmere Island, Nunavut; in *Environmental Response to Climate Change in the Canadian High Arctic*, (ed.) M. Garneau and B.T. Alt; Geological Survey of Canada, Bulletin 529, p. 249–256.

Abstract: Diatom analyses were conducted on a 105.5 cm sediment core from a small upland lake on southwestern Fosheim Peninsula, Ellesmere Island. The core represents approximately 6500 years of continuous deposition. Diatom floras were consistently dominated by *Fragilaria* sp. Three diatom zones can be identified that broadly reflect regional paleoclimatic conditions inferred independently. Diatom concentrations were high in the oldest sediments and assemblages were dominated by *Fragilaria construens* var. *venter*. Subsequently, after ca. 4000 BP, diatom concentrations decreased, frequencies of the *F. pinnata* complex expanded at the expense of *F. construens* var. *venter*, and several additional benthic taxa became increasingly common. The greatest diatom changes of the entire record took place in the upper 3 cm, when diatom concentrations and diversity rose dramatically. The diatom stratigraphy indicates significant differences between the character of the two warm paleoclimatic periods encompassed by the record, the relatively wet early to middle Holocene and the arid twentieth century.

Résumé : On a fait des analyses de diatomées provenant d'une carotte de sédiments de 105,5 cm tirée d'un petit lac en élévation situé dans le sud-ouest de la péninsule Fosheim, dans l'île d'Ellesmere. La carotte représente environ 6 500 ans de sédimentation ininterrompue. De façon uniforme, les flores de diatomées étaient dominées par des espèces du genre *Fragilaria*. On peut reconnaître trois zones de diatomées qui reflètent de manière générale les conditions paléoclimatiques régionales déduites autrement. Dans les sédiments les plus anciens, les concentrations de diatomées étaient élevées et les assemblages étaient dominés par *Fragilaria construens* var. *venter*. À compter d'il y a 4000 ans, les concentrations de diatomées ont diminué et la fréquence de complexes dominés par *F. pinnata* a augmenté au dépens de *F. construens* var. *venter*, et plusieurs autres taxons benthiques sont devenus de plus en plus abondants. Les plus grands changements chez les diatomées qui ont été observés dans toute la carotte sont observés dans les 3 cm supérieurs alors que les concentrations et la diversité des diatomées ont augmenté de manière saisissante. La stratigraphie des diatomées révèle des différences importantes entre les deux périodes de réchauffement paléoclimatiques qu'elle couvre, soit la période relativement humide de l'Holocène supérieur à moyen et la période aride du vingtième siècle.

¹ Institute of Arctic and Alpine Research, Campus Box 450, University of Colorado, Boulder, Colorado, 80309-0450

INTRODUCTION

Paleolimnological studies on Ellesmere Island have been few to date, although the number of sites investigated has increased recently (Smol, 1983; Douglas et al., 1994; Doubleday et al., 1995; Smith, 1995). The ubiquity of lakes and ponds throughout most of the High Arctic implies that paleolimnology should provide the most accessible and reliable continuous records of postglacial environmental change. Other paleoecological repositories, such as peats, exist in some areas, but are generally infrequent and present records of mostly local paleoenvironmental conditions (Lafarge-England et al., 1991; Garneau, 1992). Because of extremely low pollen concentrations in sediments and the low pollen production rates of most endemic High Arctic plants, palynology can be problematic at these latitudes (Funder and Abrahamsen, 1988; Gajewski et al., 1995), although several diagrams may nonetheless be interpreted in the context of Holocene paleoclimatic conditions (Hyvärinen, 1985; Fredskild, 1995). A strong case can be made for the usefulness of diatom-based paleolimnological studies, as diatoms are generally abundant and well preserved in the sediments of High Arctic lakes, with noteworthy exceptions (e.g. Björck et al., 1994). Although the taxonomic and ecological positions of certain taxa remain enigmatic, much progress has been made in arctic freshwater-diatom ecology (Douglas and Smol, 1993, 1995). By reporting a new diatom stratigraphy from southwestern Fosheim Peninsula, this paper contributes to the growing body of paleoecological studies from Ellesmere Island. These studies are beginning to define how High Arctic ecosystems responded to Holocene climatic variability.

STUDY SITE

Solstice Lake (unofficial name) is situated at latitude $79^{\circ}25'N$, longitude $84^{\circ}07'W$ on southwestern Fosheim Peninsula, Ellesmere Island (Fig. 1). It is 305 m a.s.l. and occupies a small, bedrock-controlled, comma-shaped depression approximately 600 m long. It was visited only once, on June 21, 1992, at which time lake-water pH was 7.3 and electrical conductivity was $46 \mu S/cm$ (both measurements from a depth of 3.0 m). Ice thickness was 1.8 m. Because of nearly complete snow cover in the catchment, no observations of local vegetation or other site characteristics were possible. Adjacent uplands are windswept, nearly barren, and characterized by numerous tor-like features. Cretaceous sedimentary rocks, primarily quartzose sandstones, constitute the local rocks (Okulitch, 1991). Older, clastic, Triassic to Jurassic formations rise to over 1000 m a.s.l. in the Sawtooth Range immediately to the southeast. These mountains support the only extant glaciers on Fosheim Peninsula, the closest of which is 15 km east of the study site. Solstice Lake occupies a foothill plateau north of a large, fault-controlled valley that contains three large lakes, the largest of which is over 80 m deep. Abundant coal is present in this valley, originating from poorly consolidated sedimentary rocks within the Eureka Sound Group (Campanian to Eocene) that outcrop in Wolf Valley to the south (Miall, 1991). Although no coal was seen

in the immediate vicinity of Solstice Lake, its nearby presence implies the potential for eolian redistribution and this is of direct relevance to the reliability placed on radiocarbon dates. Owing to its intermontane position, Fosheim Peninsula has an arid, continental climate. Annual precipitation at the Eureka station, 70 km north of Solstice Lake, is a mere 64 mm, whereas the mean annual temperature range is $43^{\circ}C$. The mean summer temperature of $5.4^{\circ}C$ is anomalously high for this latitude (Atmospheric Environment Service, 1982).

MATERIALS AND METHODS

A 100.5 cm core was obtained from Solstice Lake using a modified portable percussion-coring device (Gilbert and Glew, 1985). The core was taken in 6.0 m of water, which, from adjacent depth soundings, seems to be the lake's maximum depth. The core was securely packed in the field and, once returned to the laboratory, it was split, logged, and stored at $4^{\circ}C$. Organic matter and carbonate content were estimated by loss-on-ignition (Dean, 1974). Two mixed macrofossil samples were removed from the 33 to 34 and the 92 to 93 cm intervals for AMS radiocarbon dating at the IsoTrace Laboratory, University of Toronto, Toronto, Ontario.

For diatom analyses, 27 sediment subsamples 1 cm thick and with a wet-sediment volume of $1 cm^3$ were taken from the core, generally at 5 cm intervals, but more closely spaced towards the top (every 1 cm from 0 to 5 cm) and the bottom

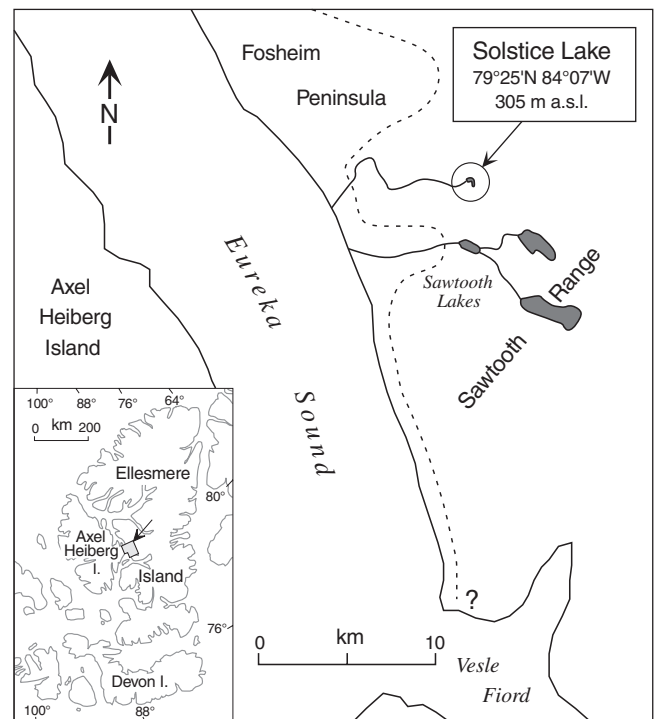


Figure 1. Location map of Solstice Lake on southwestern Fosheim Peninsula. The dashed line represents the approximate position of the postglacial marine limit (Bell, 1992).

(every 2 or 3 cm below 90 cm) of the core. For simplicity, all sample depths mentioned hereafter refer to the depth in the core at the top of the sample (e.g. sample from 3 cm is actually 3–4 cm). These samples were processed first with 30% H_2O_2 , then with a strong acid digest (H_2SO_4 and $K_2Cr_2O_7$). Washed slurries were spiked with a known quantity of exotic markers (*Eucalyptus* pollen) to enable calculations of diatom concentrations (Kaland and Stabell, 1981). Dilutions of these slurries were dried on coverslips and mounted in Naphrax. Because of generally low diatom concentrations, relatively undiluted (thick) suspensions were mounted. Diatom valves and chrysophyte cysts were counted in transects at 1000x under oil immersion. Diatoms were identified using primarily the floras of Hustedt (1959), Patrick and Reimer (1966, 1975), Foged (1981), Germain (1981), and Kramer and Lange-Bergamot (1986, 1991).

RESULTS

Sediments and chronology

The Solstice Lake core contains three lithological units (Fig. 2). The base of the core, from 93 to 100.5 cm, is an organic, brown, silty sand (Mainsail 10YR 5/4) with infrequent macrofossil. A gradual transition to highly compacted gadget is centered at 93 cm. This 'granular' gadget (10YR 4/2) extends to 57 cm and resembles the sediments illustrated by Funder and Abrahamsen (1988) from eastern North Greenland. Macrofossil are abundant throughout this

portion of the core. Between 57 cm and the core top, sediments are a uniform silt gadget (10YR 4/4). This material is structure less except for major macrofossil assemblages at 34 to 36 cm and 45 to 46 cm, which form continuous horizons across the core. Dispersed plant macrofossil also occur throughout the unit. Loss-on-ignition results illustrate the higher organic content of the lower gadget, as well as the presence of some carbonate material (2–4 per cent) throughout the sequence.

The radiocarbon dating results, reported in uncalibrated radiocarbon years before present, are 1390 ± 50 BP (TO-3878) from 33 to 34 cm and 6540 ± 290 BP (TO-3879) from 92 to 93 cm. If these ages are assumed to be correct, then, by linear interpolation, sediment accumulation rates were more than twice as high in the silt gadget above 33 cm (24.1 cm/ka) than in the more organic underlying gadget (11.5 cm/ka). However, the lower organic sediments appear strongly compacted.

Diatom record

The diatom record of the Solstice Lake core contains 43 taxa (Table 1), all of which have been documented from the Canadian Arctic Archipelago (see Hamilton et al., 1994). Not a single centric diatom was encountered. Diatom concentrations are low, even for this latitude (cf. Smol, 1983; Blake et al., 1992), so much so that routine diatom sums totaling 500 to 750 valves were not reached in some samples. In such samples, diatom sums were reduced to 300 (85 and 92 cm), 200 (3 cm),

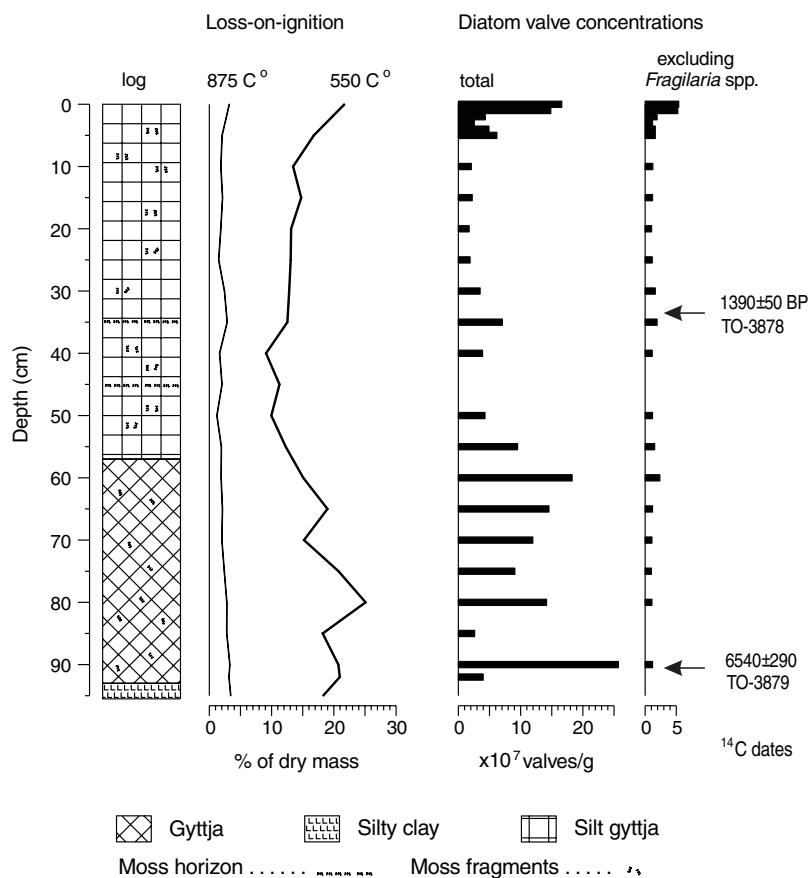


Figure 2.

Stratigraphic log, loss-on-ignition, diatom valve concentrations (expressed per gram of dry sediment), and radiocarbon dates from the Solstice Lake core.

and 100 (20 and 25 cm). Two samples were completely barren of diatoms (45 cm and 99 cm), whereas only trace numbers of valves (i.e. <10), belonging to species of *Fragilaria*, were observed at 94 and 97 cm.

The most salient feature of the Solstice Lake diatom stratigraphy (Fig. 3) is the consistent dominance of species of *Fragilaria* (*Staurosira*, *Staurosirella*, and *Pseudostaurosira*

sensu Round et al., 1990) throughout the sequence. *Fragilaria pinnata* (including varieties *pinnata* and *intercedens* and fo. *subrotunda*) and *F. construens* var. *venter* (*sensu* Blake et al., 1992) never accounted for less than 60 per cent of any sample. Nonetheless, three distinct fossil zones can be identified in the diatom stratigraphy (Fig. 3), on the basis of the characteristics described below. The boundary depth between zones 1 and 2 is inferred.

Table 1. Taxonomic list of diatoms encountered in the Solstice Lake core.

<i>Achnanthes flexella</i> (Kützing) Brun	<i>Gomphonema</i> spp.
<i>A. linearis</i> (W. Smith) Grunow	<i>Navicula capitata</i> var. <i>hungarica</i> (Grunow) Ross
<i>A. minutissima</i> Kützing	<i>N. contenta</i> Grunow
<i>A. oestrupii</i> (Cleve-Euler) Hustedt	<i>N. dicephala</i> Ehrenberg
<i>A. peragalli</i> Brun & Héribaud	<i>N. explanata</i> Hustedt
<i>Amphora libyca</i> Ehrenberg	<i>N. cf. laevisissima</i> Kützing
<i>A. perpusilla</i> Grunow	<i>N. minuscula</i> Grunow
<i>Cymbella</i> cf. <i>angustata</i> (W. Smith) Cleve	<i>N. perpusilla</i> (Kützing) Grunow
<i>C. behrei</i> Foged	<i>N. pseudoscutiformis</i> Hustedt
<i>C. cymbiformis</i> Agardh	<i>N. schmassmannii</i> Hustedt
<i>C. gaemannii</i> Meister	<i>N. vulpina</i> Kützing
<i>C. minuta</i> Hilse ex. Rabenhorst	<i>Neidium</i> spp.
<i>C. minuta</i> fo. <i>latens</i> (Krasske) Reimer	<i>Nitzschia frustulum</i> var. <i>perminuta</i> (Rabenhorst) Grunow
<i>Denticula elegans</i> Kützing	<i>Pinnularia balfouriana</i> Grunow ex. Cleve
<i>Eunotia praerupta</i> Ehrenberg	<i>P. borealis</i> Ehrenberg
<i>Fragilaria construens</i> var. <i>venter</i> (Ehrenberg) Grunow	<i>P. nodosa</i> (Ehrenberg) W. Smith
<i>F. pinnata</i> Ehrenberg	<i>Reimeria sinuata</i> (Gregory) Kociolek & Stoermer
<i>F. pinnata</i> var. <i>intercedens</i> (Grunow) Hustedt	<i>Stauroneis anceps</i> Ehrenberg
<i>F. pinnata</i> fo. <i>subrotunda</i> Mayer	<i>S. phoenicenteron</i> (Nitzsch) Ehrenberg
<i>F. pinnata</i> var. <i>ventriculosa</i> (Schumann) Mayer	<i>S. smithii</i> Grunow
<i>F. pseudoconstruens</i> Marciniak	<i>Synedra parasitica</i> (W. Smith) Grunow
<i>F. vaucheriae</i> (Kützing) Petersen	

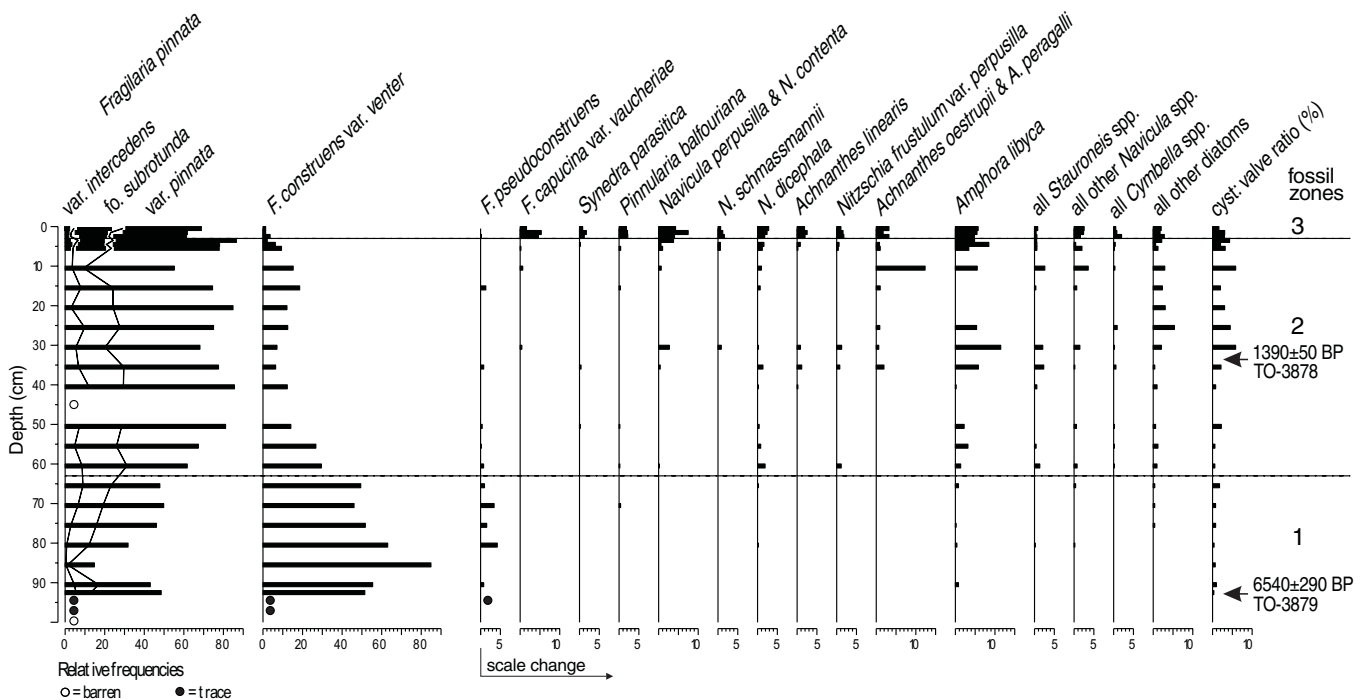


Figure 3. Relative-frequency diagram of the dominant diatoms encountered in the Solstice Lake core and zonation of fossil assemblages.

Zone 1 (93–62.5 cm)

Fragilaria construens var. *venter* is more abundant than the *F. pinnata* complex in this portion of the core. *Fragilaria pseudoconstruens* is the only other common diatom. Chrysophyte cysts are consistently represented, but infrequent. Diatoms other than the stated taxa do not exceed 2 per cent in this zone, although diatom concentrations are generally high.

Zone 2 (62.5–3 cm)

The *F. pinnata* complex expands at the expense of *F. construens* var. *venter* in this zone, and *F. pseudoconstruens* is far less common than in underlying sediments. Several additional benthic diatoms begin to appear consistently, such as *Amphora libyca* and species of *Achnanthes*, *Cymbella*, *Navicula*, *Nitzschia*, and *Stauroneis*. In most samples within this zone, these taxa collectively account for between 10 and 30 per cent of the assemblage. Chrysophyte cysts are also more frequent in this zone (1–5 per cent of the diatom sum). However, diatom concentrations are low (<10⁸ valves per gram) throughout zone 2, which includes a somewhat enigmatic barren sample at 45 cm.

Zone 3 (3–0 cm)

Within the uppermost three samples, a significant floristic shift occurred. Diatoms other than species of *Fragilaria* unprecedentedly exceed 30 per cent of the assemblage. The taxa that appeared in zone 2 remain represented in similar frequencies, but several additional taxa increase markedly in number. This group includes *Fragilaria capucina* var. *vaucheriae*, *Synedra parasitica*, *Pinnularia balfouriana*, *Navicula perpusilla* and *N. contenta* (*Diadesmis sensu* Round et al., 1990), and, to a lesser extent, *Navicula schmassmannii*, *N. dicephala*, and *Achnanthes linearis*. Diatom concentrations also rise abruptly within this zone. The peak concentrations of diatoms other than *Fragilaria* in zone 3 is over three times greater than in any of the previous assemblage (Fig. 2).

DISCUSSION

On *Fragilaria*

Floras dominated by species of *Fragilaria*, sustained over the entire postglacial or postemergent history of a given lake, are not unusual in the Canadian High Arctic and adjacent Greenland (Foged, 1972; Wolfe, 1991; Blake et al., 1992; Douglas et al., 1994). However, diatom assemblages from other sites show several marked changes throughout the Holocene (Smol, 1983), implying that the floras of some lakes are more sensitive to changing environmental conditions than others. The *Fragilaria* assemblage may be sustained in lakes that remain well buffered throughout the Holocene, for example through geological inputs from carbonate bedrock or surficial deposits. Indeed, the taxa from Solstice Lake indicate a

circumneutral to slightly alkaline environment, with no convincing indication of past changes in lake-water chemistry. On the other hand, arctic lakes within poorly buffered granitic or driftless catchments are highly sensitive to subtle variations in alkalinity production and hence their diatom histories imply past fluctuations in lake-water pH, notably a trend of gradual pH decline (Smol, 1983; Wolfe, 1994).

These general comments do not address the ecological aspects of individual *Fragilaria* taxa, which are frequently labelled collectively as benthic alkaliphilous forms. However, the successional patterns of this genus contain strong evidence that there are indeed ecological differences between congeners. This type of pattern was observed at Solstice Lake (zones 1 and 2, Fig. 3) and has been reported from other High Arctic sites (Blake et al., 1992; Douglas et al., 1994), as well as from early postglacial sediments of temperate lakes (e.g. Lortie and Richard, 1986). It may prove difficult to identify the environmental optima of individual *Fragilaria* taxa, as modern samples containing the full range of assemblage compositions manifested in fossil material may not be present (e.g. Douglas and Smol, 1993). The stratigraphic record is of little assistance because the order of successive dominance by taxa such as *F. pinnata* and *F. construens* var. *venter* often differs between published sites. Subtle competitive factors, operating at the scale of individual lakes, may be responsible for these trends.

Marked recent diatom changes

The most significant features of the diatom stratigraphy from Solstice Lake are the changes that occurred in the upper 3 cm of sediment deposition (zone 3). These changes are directly comparable to those described by Douglas et al. (1994) from Cape Herschel, 120 km to the east, thus strengthening their argument that the signal is of regional significance. It is possible that additional records from Ellesmere (Doubleday et al., 1995) and northern Baffin (Wolfe, 1991) islands may also be tracking the same environmental changes. Shifts to a more diverse and productive diatom flora imply an improved photosynthetic regime and/or a prolonged ice-free period (see Smol, 1988), whereas increases among aerophilous and moss epiphytic taxa (*Pinnularia balfouriana*, *Navicula perpusilla*, and *N. contenta*) suggest enhanced littoral and terrestrial production.

Interpolation of the available chronological data suggests that these changes occurred within the last 125 years, although this estimate remains tentative in the absence of supplemental dating control. The AMS dates from Solstice Lake are compromised since the dated macrofossil were not identified and likely combined terrestrial and aquatic materials; the latter may introduce significant, hard-water effects if old carbon is present (Snyder et al., 1994). The presence of coal in the Solstice Lake catchment is questionable (none was observed), but certainly possible. In the absence of additional chronological data, the two available dates are considered a first approximation of the Solstice Lake core chronology.

Colonization, dissolution, and barren samples

Because most Solstice Lake diatoms were present in assemblages well before any of the observed stratigraphic changes, colonization processes cannot be invoked as a possible cause of these changes, as detailed elsewhere (Smol, 1983; Douglas et al., 1994). Partial dissolution of diatom valves was observed in some of the larger taxa (*Amphora libyca*, *Neidium* spp., *Navicula dicephala*), but valves of small and delicate forms (e.g. *Achnanthes peragalli*, *Navicula perpusilla*, *Nitzschia frustulum* var. *perpusilla*) appeared unaffected, as did the valves of *Fragilaria*. It is therefore doubtful that diatom stratigraphic trends were modified by selective dissolution. Barren and diatom-poor samples at the base of the core are consistent with the unproductive or even ephemeral state of the lake during its earliest development. The barren sample at 45 cm is more difficult to interpret and may indeed represent silica dissolution. However, barren samples may also be attributable to the complete absence of diatom production (Doubleday et al., 1995).

Paleoclimatic implications

Prevalent Holocene paleoclimatic conditions over Ellesmere Island, as synthesized by Bradley (1990), include an early Holocene thermal maximum (9000–7000 BP) and conditions as warm or warmer than today between 10 000 and 4000 BP. In the early Holocene, decreased volumes of sea ice probably led to increased precipitation in areas such as Fosheim Peninsula, so that, despite nearly maximum Holocene summer temperatures, local ice caps in the Sawtooth Range were sustained until 5200 BP (Bell, 1992). The climate deteriorated significantly after 3500 BP (Bradley, 1990) and many Ellesmere Island glaciers advanced between 3000 and 1000 BP (e.g. Blake, 1981, 1989). This Neoglacial cooling culminated about 400 to 100 BP (Little Ice Age; AD 1550 to 1900), in what may have been the coldest period in the entire Holocene (Bradley, 1990). Further glacial advances occurred during this interval (Blake, 1981; Bergsma et al., 1984). Compared with the rest of the late Holocene, climate since ca. AD 1925 has been exceptionally warm, as illustrated by the summer melt record of the Agassiz Ice Cap (Koerner and Fisher, 1990).

Because these regional inferences are quite solidly supported by several independent lines of evidence (*see also* Beltrami and Taylor, 1995), it seems appropriate to evaluate the Solstice Lake diatom stratigraphy within this proposed paleoclimatic context. Solstice Lake infilled and became a permanent feature ca. 6500 BP, likely as a result of decreased aridity. Warm conditions engendered high diatom production, as inferred from valve concentrations, as well as primarily autochthonous, organic sedimentation. Species of *Fragilaria*, notably *F. construens* var. *venter*, were strongly dominant once established (i.e. above 92 cm). Other diatoms may have been outcompeted by this genus, for example with respect to nutrients such as silica.

Subsequently, diatom concentrations and sediment organic content decreased. The radiocarbon dates place this transition between 4000 and 3000 BP, so that these changes

may well correlate with Neoglacial cooling. Decreased diatom paleoproductivity is envisaged for this entire period (Fig. 2). However, the flora diversified, suggesting that the competitive advantage previously held by *Fragilaria* was less effective during Neoglacial cooling. Peak abundances of chrysophyte cysts also occurred in these sediments, perhaps reflecting the potentially advantageous nutritional strategies of chrysophyte algae (flagellar motility, heterotrophy) over diatoms in extreme environments (*see* Smol, 1983). The indication of increased sediment accumulation rates, at least in the latter part of this period, can be reconciled with more significant input of allochthonous minerals, primarily from erosion and eolian processes within an unstable catchment basin. Low diatom concentrations since ca. 1000 BP may thus be attributable in part to enhanced mineral sedimentation.

Finally, Solstice Lake apparently recorded recent climate warming through paleolimnological expressions of increased diatom production, floristic diversification, and expanded habitat availability. These changes are consistent with warming following the Little Ice Age. However, core chronology is insufficient to state whether the reorganization of diatom communities was initiated in the last 100 (Bradley, 1990) or 200+ (Douglas et al., 1994) years.

An interesting exercise is to compare the diatom assemblages associated with the two independently inferred periods of warm Holocene paleoclimate, prior to 4000 BP and in the twentieth century (cf. diatom zones 1 and 3). Whereas conditions seem to have been 'warm and wet' in the early to middle Holocene, recent conditions have likely been relatively warm and arid. This explanation reconciles, for example, the persistence of expanded glaciers in the early and middle Holocene (Bell, 1992) with the presently negative mass balances of many Ellesmere Island glaciers (e.g. Bergsma et al., 1984). In the last few decades, warm temperatures would have prolonged the diatom growing season and resulted in habitat expansion, whereas enhanced aridity would have increased the distribution of drier habitats available to aerophilous forms. This model is entirely compatible with the observations from Solstice Lake. Further research should be directed at refining core chronology and ascertaining whether paleolimnological changes are manifested in other biota, particularly local vegetation. Since the Solstice Lake core has abundant macrofossil, the opportunity exists to address both these remaining questions.

ACKNOWLEDGMENTS

This research was supported by Natural Sciences and Engineering Research Council of Canada research grants to R. Gilbert (Queen's University) and a postdoctoral fellowship to the author. Logistical support from the Polar Continental Shelf Project (Natural Resources Canada) made fieldwork possible. R. Edgecombe provided able field assistance. I especially thank S.A. Edlund and the Hot Weather Creek team of 1992 for their support, as well as J.-S. Vincent for inviting this contribution. W. Blake, Jr., and M.S.V. Douglas provided many useful comments on the manuscript.

REFERENCES

Atmospheric Environment Service

1982: Canadian climate normals 1951–1980: temperature and precipitation. The North: Yukon Territory and Northwest Territories; Environment Canada, Downsview, Ontario, 55 p.

Bell, T.

1992: Glacial and sea level history of western Fosheim Peninsula, Ellesmere Island, Arctic Canada; Ph.D. thesis, University of Alberta, Edmonton, Alberta, 172 p.

Beltrami, H. and Taylor, A.E.

1995: Records of climatic change in the Canadian Arctic: towards calibrating oxygen isotope data with geothermal data; *Global and Planetary Change*, v. 11, p. 127–138.

Bergsma, B.M., Svoboda, J., and Freedman, B.

1984: Entombed plant communities released by a retreating glacier at Alexandra Fiord; *Arctic*, v. 37, p. 49–52.

Björck, S., Bennike, O., Ingólfsson, Ó., Barnekow, L., and Penney, D.N.

1994: Lake Boksehandsen's earliest postglacial sediments and their paleoenvironmental implications, Jameson Land, east Greenland; *Boreas*, v. 23, p. 459–472.

Blake, W., Jr.

1981: Neoglacial fluctuations of glaciers, southeastern Ellesmere Island, Canadian Arctic Archipelago; *Geografiska Annaler*, v. 63A, p. 201–218.

1989: Application of ¹⁴C AMS dating to the chronology of Holocene glacier fluctuations in the High Arctic, with special reference to Leffert Glacier, Ellesmere Island, Canada; *Radiocarbon*, v. 31, p. 570–578.

Blake, W., Jr., Boucherle, M.M., Fredskild, B., Janssens, J.J., and Smol, J.P.

1992: The geomorphological setting, glacial history, and Holocene development of 'Kap Inglefield Sø', Inglefield Land, northwestern Greenland; *Meddelelser om Grønland Geoscience*, v. 127, p. 1–42.

Bradley, R.S.

1990: Holocene paleoclimatology of the Queen Elizabeth Islands, Canadian High Arctic; *Quaternary Science Reviews*, v. 9, p. 365–384.

Dean, W.E., Jr.

1974: Determination of carbonate and organic matter in calcareous sediment and sedimentary rock by loss on ignition: comparison with other methods; *Journal of Sedimentary Petrology*, v. 44, p. 241–248.

Doubleday, N.C., Douglas, M.S.V., and Smol, J.P.

1995: Paleoenvironmental studies of black carbonaceous particles in the High Arctic: a case study from northern Ellesmere Island; *The Science of the Total Environment*, v. 160/161, p. 661–668.

Douglas, M.S.V. and Smol, J.P.

1993: Freshwater diatoms from High Arctic ponds (Cape Herschel, Ellesmere Island, N.W.T.); *Nova Hedwigia*, v. 57, p. 511–552.

1995: Periphytic diatom assemblages from high arctic ponds; *Journal of Phycology*, v. 31, p. 60–69.

Douglas, M.S.V., Smol, J.P., and Blake, W., Jr.

1994: Marked post-18th century environmental change in high arctic ecosystems; *Science*, v. 266, p. 416–419.

Foged, N.

1972: The diatoms of four postglacial deposits in Greenland; *Meddelelser om Grønland Band 194*, no. 4, p. 1–66.

1981: Diatoms in Alaska; *Bibliotheca Phycologica Band 53*; J. Cramer Verlag, Vaduz, 317 p.

Fredskild, B.

1995: Palynology and sediment slumping in a high arctic Greenland lake; *Boreas*, v. 24, p. 345–354.

Funder, S. and Abrahamsen, N.

1988: Palynology in a polar desert, eastern North Greenland. *Boreas*, v. 17, p. 195–207.

Gajewski, K., Garneau, M., and Bourgeois, J.C.

1995: Paleoenvironments of the Canadian High Arctic derived from pollen and plant macrofossils: problems and potentials; *Quaternary Science Reviews*, v. 14, p. 609–629.

Garneau, M.

1992: Analyses macrofossiles d'un dépôt de tourbe dans la région de Hot Weather Creek, péninsule de Fosheim, île d'Ellesmere, Territoires du Nord-Ouest; *Géographie physique et Quaternaire*, vol. 46, p. 285–294.

Germain, H.

1981: Flore des diatomées, eaux douces et saumâtres du Massif Armoricaïn et des contrées voisines d'Europe occidentale; Société Nouvelle des Éditions Boubée, Paris, 444 p.

Gilbert, R. and Glew, J.R.

1985: A portable percussion coring device for lacustrine and marine sediments; *Journal of Sedimentary Petrology*, v. 55, p. 607–608.

Hamilton, P.B., Douglas, M.S.V., Fritz, S.C., Pienitz, R., Smol, J.P., and Wolfe, A.P.

1994: A compiled freshwater diatom taxa list for the arctic and subarctic regions of North America; *Proceedings of the fourth Arctic-Antarctic Diatom Symposium*, (ed.) P.B. Hamilton; Canadian Technical Report of Fisheries and Aquatic Sciences 1957, Ottawa, Ontario, p. 85–102.

Hustedt, F.

1959: Die Kieselalgen Deutschlands, Österreichs und der Schweiz, Teil II. Rabenhorst's Kryptogamen-Flora von Deutschland, Österreich und der Schweiz; *Academische Verlagsgesellschaft*, Leipzig, 845 p.

Hyvärinen, H.

1985: Holocene pollen stratigraphy of Baird Inlet, east-central Ellesmere Island; *Boreas*, v. 14, p. 19–32.

Kaland, P.E. and Stabell, B.

1981: Methods for absolute diatom frequency analysis and combined diatom and pollen analysis in sediments; *Nordic Journal of Botany*, v. 1, p. 697–700.

Koerner, R.M. and Fisher, D.A.

1990: A 10 000 year record of summer climate: Agassiz Ice Cap, northern Ellesmere Island, Northwest Territories, Canada; *Nature*, v. 343, p. 630–633.

Krammer, K. and Lange-Bertalot, H.

1986: Bacillariophyceae 1. Teil: Naviculaceae; Süßwasserflora von Mitteleuropa, (ed.) H. Ettl, H. Gerloff, H. Heynig, D. Mollenhauer; Gustav Fischer, Stuttgart, 876 p.

1991: Bacillariophyceae 3. Teil: Centrales, Fragilariaceae, Eunotiaceae; Süßwasserflora von Mitteleuropa, (ed.) H. Ettl, H. Gerloff, H. Heynig, D. Mollenhauer; Gustav Fischer, Stuttgart, 576 p.

Lafarge-England, C., Vitt, D.H., and England, J.

1991: Holocene soligenous fens on a high arctic fault block, northern Ellesmere Island; *Arctic and Alpine Research*, v. 23, p. 80–98.

Lortie, G. and Richard, P.J.H.

1986: Late-glacial diatom and pollen stratigraphy from Lake Boucané, southeastern Quebec, Canada; *Proceedings of the Eighth International Diatom Symposium*, (ed.) M. Ricard; Koeltz, Koenigstein, p. 687–697.

Miall, A.D.

1991: Late Cretaceous and Tertiary basin development and sedimentation, Arctic Islands; *in* Chapter 15 of *Geology of the Inuitian Orogen and Arctic Platform of Canada and Greenland*, (ed.) H.P. Trettin; Geological Survey of Canada, *Geology of Canada*, no. 3, p. 437–458 (*also* *Geological Society of America, The Geology of North America*, v. E, p. 437–458).

Okulitch, A.V. (comp.)

1991: *Geology of the Canadian Archipelago and North Greenland*; Figure 2; *in* *Geology of the Inuitian Orogen and Arctic Platform of Canada and Greenland*, (ed.) H.P. Trettin; Geological Survey of Canada, *Geology of Canada*, no. 3 (*also* *Geological Society of America, The Geology of North America*, v. E), scale 1:2 000 000.

Patrick, R. and Reimer, C.W.

1966: The diatoms of the United States exclusive of Alaska and Hawaii, volume 1; *Academy of Natural Sciences of Philadelphia Monograph* 13, 688 p.

1975: The diatoms of the United States exclusive of Alaska and Hawaii, volume 2, part 1; *Academy of Natural Sciences of Philadelphia Monograph* 13, 214 p.

Round, F.E., Crawford, R.M., and Mann, D.G.

1990: The diatoms. Biology and morphology of the genera; Cambridge University Press, Cambridge, United Kingdom, 747 p.

Smith, I.R.

1995: Late Quaternary glaciation and ice dynamics on the Hazen plateau, northern Ellesmere Island; Canadian Quaternary Association–Canadian Geomorphology Research Group joint conference abstracts, St. John's, Newfoundland, p. CA46.

Smol, J.P.

1983: Paleophycology of a high arctic lake near Cape Herschel, Ellesmere Island; Canadian Journal of Botany, v. 61, p. 2195–2204.

1988: Paleoclimate proxy data from freshwater arctic diatoms; Verhandlungen der Internationalen Vereinigung von Limnologen, v. 23, p. 837–844.

Snyder, J.A., Miller, G.H., Werner, A., Jull, A.J.T., and Stafford, T.W.

1994: AMS-radiocarbon dating of organic-poor lake sediments, an example from Linnévatnet, Spitsbergen; The Holocene, v. 4, p. 413–421.

Wolfe, A.P.

1991: Mid and late Holocene diatoms from 'Water Supply Lake', Baffin Island, N.W.T., Canada; Journal of Paleolimnology, v. 6, p. 199–204.

1994: A paleolimnological assessment of late Quaternary environmental change on southwestern Cumberland Peninsula, Baffin Island, N.W.T.; Ph.D. thesis, Queen's University, Kingston, Ontario, 161 p.

Summary of paleolimnological investigations of High Arctic ponds at Cape Herschel, east-central Ellesmere Island, Nunavut

M.S.V. Douglas¹, J.P. Smol², W. Blake, Jr.³

Douglas, M.S.V., Smol, J.P., and Blake, W., Jr., 2000: Summary of paleolimnological investigations of High Arctic ponds at Cape Herschel, east-central Ellesmere Island, Nunavut; in Environmental Response to Climate Change in the Canadian High Arctic, (ed.) M. Garneau and B.T. Alt; Geological Survey of Canada, Bulletin 529, p. 257–269.

Abstract: This overview summarizes limnological and paleolimnological studies carried out at 36 reference ponds as part of the Cape Herschel Project on Ellesmere Island. Marked relief, proximity to the sea, and drainage-basin composition cause pronounced interpond differences in microclimate, water chemistry, and vegetation. The ponds freeze completely for 9 to 10 months of the year; in summer, water temperatures fluctuate diurnally. Ponds are shallow, clear, oligotrophic, and, with one exception, alkaline. Conductivity values fluctuate seasonally. Such High Arctic ponds may be especially sensitive monitors of future environmental change.

Over 130 diatom taxa from 28 genera were identified. Benthic diatoms were abundant and exhibited varying degrees of microhabitat specificity; planktonic taxa were absent. Other biological indicators, such as chrysophytes and invertebrates, were also studied.

Paleolimnological data indicate that diatom assemblages were relatively stable over the last few millennia, then underwent unparalleled changes beginning in the nineteenth century. The environmental factors causing these changes may be related to recent climatic warming.

Résumé : Cet article résume les résultats d'études limnologiques et paléolimnologiques effectuées à 36 étangs dans le cadre du projet du cap Herschel dans l'île d'Ellesmere. Le relief accidenté, la proximité à la mer et la composition des bassins de drainage engendrent de grandes différences entre les étangs quant au microclimat, à la chimie de l'eau et à la végétation. Les étangs gèlent complètement de 9 à 10 mois par année; l'été, la température de l'eau fluctue de façon diurne. Les étangs sont peu profonds, limpides, oligotrophes et, sauf pour une exception, alcalins. Les valeurs de conductivité varient de façon saisonnière. De tels étangs situés dans l'extrême Arctique pourraient servir d'indicateurs très sensibles aux futurs changements environnementaux.

On a identifié plus de 130 taxons de diatomées de 28 genres. Les diatomées benthiques sont abondantes et présentent divers degrés de spécificité des micro-habitats. Les taxons planctoniques sont absents. On a également étudié d'autres indicateurs biologiques (chrysophytes et invertébrés).

Les données paléolimnologiques indiquent que les assemblages de diatomées ont été relativement stables lors des quelques derniers millénaires mais qu'ils ont ensuite subi de vastes transformations à partir du dix-neuvième siècle. Les facteurs environnementaux qui ont causé ces variations pourraient être reliés au réchauffement climatique récent.

¹ Department of Geology, University of Toronto, 22 Russell Street, Toronto, Ontario M5S 3B1

² Paleoeological Environmental Assessment and Research Laboratory, Department of Biology, Queen's University, Kingston, Ontario K7L 3N6

³ Geological Survey of Canada, 601 Booth Street, Ottawa, Ontario K1A 0E8

INTRODUCTION

Cape Herschel, a promontory on the east-central coast of Ellesmere Island (Fig. 1, 2, 3), is the site of a scientific field station established in 1973 as part of the North Water Project by the late professor Fritz Müller, a Swiss glaciologist who was associated with McGill University. The project's mandate was to examine the North Water polynya in Smith Sound and northernmost Baffin Bay (Fig. 2) and to determine its effects upon weather, climate, and the flora and fauna (Müller et al., 1977).

The Cape Herschel Project, directed by W. Blake, Jr., was supported by the Geological Survey of Canada and the Polar Continental Shelf Project. Following a reconnaissance aboard the C.S.S. *Hudson* in 1974, research was conducted in the region every year from 1977 through 1991. The station was re-opened by M.S.V. Douglas, J.P. Smol, and J.R. Glew in 1995 and 1998 and we plan future work on these sites. Initially, the main goals were to unravel details of the glacial history of east-central Ellesmere Island and to establish a chronology of Pleistocene and Holocene events. Coring of lacustrine sediments and investigations of the ponds and lakes themselves formed an integral part of this work.

The Cape Herschel peninsula is characterized by a large number of ponds. A considerable amount of research on the neolimnology (present-day limnology) and paleoecology of these ponds has been carried out since 1983, and results from most of this research have been published in a diverse array of biological and limnological journals. The main objective of this paper is to collate and summarize these studies.

Much of our work on Cape Herschel had a paleolimnological focus. Paleolimnology, which has seen considerable advances over the last decade, can potentially provide important paleoclimatic proxy data for arctic regions (e.g. Smol et al., 1994). The research on Cape Herschel provides an important regional comparison with similar work at Hot Weather Creek, on Fosheim Peninsula (Fig. 1), synthesized elsewhere in this bulletin.

SITE DESCRIPTION

Cape Herschel (lat. $78^{\circ}37'N$, long. $74^{\circ}42'W$), on the east-central coast of Ellesmere Island facing Smith Sound (Fig. 1), is a rugged peninsula approximately 2 km wide by 5 km long, of moderate relief, with the high point being 285 m a.s.l. The local bedrock consists principally of massive, reddish orthopyroxene granite (Frisch, 1984), overlain by patches of carbonate-rich till, chiefly derived from the Paleozoic terranes to the north and northwest (Blake, 1977).

Terrestrial vegetation on the cape is scant and consists mainly of mosses, lichens, grasses, sedges, *Salix*, and a few other flowering plants. Bridgland and Gillett (1983) considered the flora to be moderately rich and concluded that climate was the principal factor affecting diversity.

Although no glaciers are on the cape proper, evidence of the former passage of glacier ice is abundant (e.g. Blake, 1977, 1992a). Many small patches of snow persist throughout the summer and major outlet glaciers from the Prince of Wales Icefield are present immediately north and south of Cape Herschel (Fig. 2).

Cape Herschel lies close to the northern limit of the North Water polynya (Fig. 2; Dunbar, 1969; Barr, 1985), which has a moderating effect on local climate. Maximum summer air temperatures at the station are frequently between 0° and $5^{\circ}C$, but may attain $14^{\circ}C$ (Douglas and Smol, 1994). Significant interyear differences are also apparent. These annual variations are slight in absolute terms, but they have important implications when one considers the brevity (only a few weeks) of the 'summer' growing season. Even modest weather changes can profoundly influence the time the ponds will begin to thaw and when aquatic primary production will begin (Douglas and Smol, 1994).

GLACIAL HISTORY

Following a few incidental observations on glacial and postglacial features in the region (Prest, 1952; Christie, 1962), Blake (1977) described the glacial sculpture along the narrow, ice-free margin of the east-central coast of Ellesmere Island. In a subsequent series of papers, he outlined the glacial and postglacial history of the Smith Sound region, focusing on the area around Cape Herschel. Evidence is presented for an ice stream having flowed southward from Kane Basin to northernmost Baffin Bay (Blake, 1992a; Blake et al., 1992). Blake (1992b, 1993) produced an emergence curve for the Cape Herschel area based on radiocarbon dates from



Figure 1. Map of central and southern Ellesmere Island showing the location of Cape Herschel relative to Fosheim Peninsula. The arrows indicate the former direction of the Smith Sound Ice Stream in the southern part of Nares Strait.

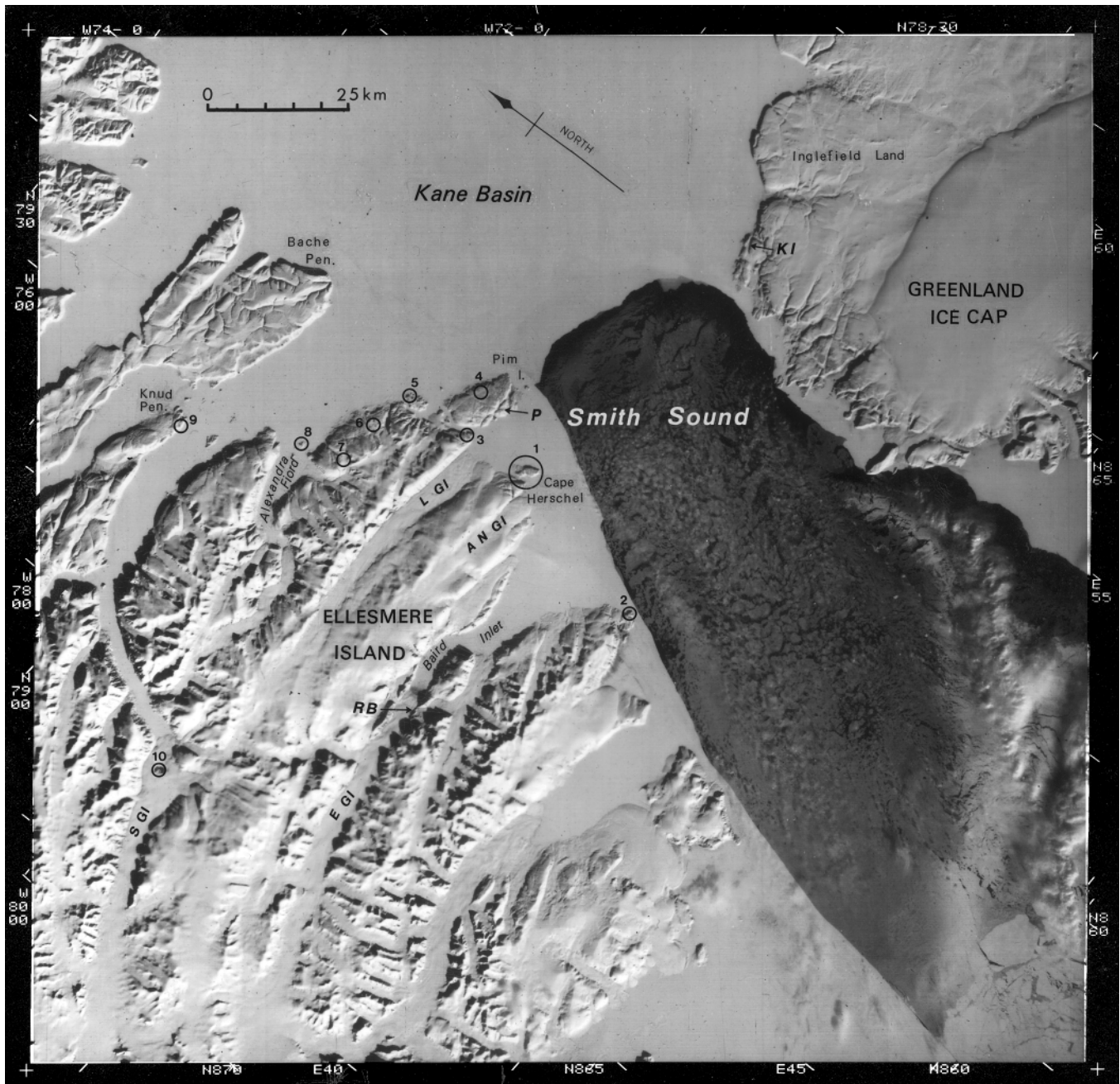


Figure 2. LANDSAT image showing the development of the North Water polynya in Smith Sound on April 4, 1973. The whole of Cape Herschel Peninsula is circled and all other sites where cores of frozen pond sediment were recovered are indicated: 2, Cape Isabella; 3, Rice Strait pond; 4, pond on the north slope of Pim Island; 5, Cape Rutherford pond; 6, Saate Glacier pond; 7, a pond on the plateau above Alexandra Fiord; 8, Skraeling Island pond; 9, Knud Peninsula delta pond; 10, Stygge Glacier nunatak pond. The initials indicate the location of lakes and glaciers mentioned in the text: RB, Rock Basin Lake at the head of Baird Inlet; P, Proteus Lake on Pim Island; KI, Kap Inglefield S, near the northwest coast of Inglefield Land; S Gl, Stygge Glacier; L Gl, Leffert Glacier; A N Gl, Alfred Newton Glacier; E Gl, Ekblaw Glacier. Landsat image E-10255-18054, spectral band 7.

Figure 3.

Oblique aerial view southeastward from Rosse Bay at Cape Herschel Peninsula and Elison Pass, with Smith Sound and Greenland beyond. Note the gentler slopes on the northwestern side of the peninsula, where many of the ponds are located. Photograph by W. Blake, Jr., July 29, 1988. GSC 1996-121B



Figure 4.

Coring of frozen sediment at Beach Ridge pond (see Fig. 6) using a motor-driven (Stihl), 30 cm long coring barrel (7.6 cm inner diameter) equipped with tungsten carbide teeth. View northeastward across Rosse Bay to Pim Island. Photograph by W. Blake, Jr., May 22, 1978. GSC-175227

Figure 5.

An example of the uppermost increment from two cores of frozen pond sediment recovered from Camp pond at Cape Herschel (see Fig. 6, 9). All cores tended to break approximately 1 cm above the ice-sediment contact, as illustrated in the lower core; in the upper core, 6 cm of ice is present (out of a total of 19 cm). In both cases the surface sediment is recovered 100 per cent intact. Photograph by W. Blake, Jr., May 27, 1979. GSC 1996-122F



molluscs, driftwood, marine mammal bone and tusk, charred material from archaeological sites, and organic sediment from ponds. Approximately 135 m of emergence have taken place over the last 8700 to 8500 radiocarbon years, with two thirds of the emergence occurring in the first 2000 years.

Numerous cores of Holocene sediments have been examined from small ponds on Cape Herschel Peninsula to obtain minimum ages for deglaciation or postglacial emergence (Blake, 1978). These cores were extracted during a series of spring expeditions (Fig. 4, 5), when the ponds were frozen to the bottom; 100 per cent recovery of the sediment was achieved using specially designed equipment (Blake, 1978, 1982). The first ponds to be cored were chosen because they were located below the limit of Holocene marine submergence and, in the absence of driftwood, provided alternative material for radiocarbon dating. Lichti-Federovich (S. Lichti-Federovich, unpub. GSC diatom rept., 1978, 1979, 1981) did not find marine littoral diatoms at any depths in these cores. Other ponds and lakes at higher elevations have since been cored. Radiocarbon dates from the basal sediments of these ponds and lakes provide minimum ages for deglaciation and for the onset of organic accumulation (Blake, 1981, 1987).

CONTAMINANTS

An assessment of snow quality and the extent of anthropogenic pollution (McNeely and Gummer, 1984) indicated that a variety of pesticide residues are dispersed globally via the atmosphere and are deposited at sites even as remote as Cape Herschel. Concentrations, however, were low. J. Blais (McGill University, unpub. data, 1993) examined ratios of the lead isotopes ^{206}Pb and ^{207}Pb in Cape Herschel pond sediments, but could not track any significant anthropogenic signal. On the basis of these limited data, the Cape Herschel region is apparently (not surprisingly) relatively pristine with respect to atmospherically deposited contaminants.

LIMNOLOGY OF THE CAPE HERSCHEL PONDS

The abundance of ponds on the Cape Herschel peninsula (Fig. 6) makes it ideal for limnological study. We selected 36 reference ponds to represent as broad an environmental spectrum as possible (Douglas, 1989; Douglas and Smol, 1994). The variable local relief and exposure results in significant interpond differences in microclimate and vegetation. For example, the sites with the highest elevations (e.g. Plateau ponds 1 and 2, Fig. 6), both over 200 m a.s.l., have shorter ice-free geological seasons. In addition, proximity to the sea and the geological variations within drainage basins (Precambrian orthopyroxene granite bedrock, with the overlying till containing Paleozoic carbonate material) affect the chemical composition of the water of each pond.

We monitored limnological changes over parts of four field seasons (1983, 1984, 1986, 1987) in the 36 study ponds (Douglas and Smol, 1994). The ponds are described in detail in Douglas (1989). Two additional field seasons have been completed (1995, 1998), but the data have not yet been fully analyzed. The main objectives of these studies were to describe and interpret seasonal changes in limnological variables and to compare these data with those from other regions. The ponds freeze completely for nine to ten months of the year; however, during the short summers, water temperatures increase substantially (to a recorded maximum of 17°C) and fluctuate diurnally, tracking ambient air temperatures.

All the ponds are shallow ($Z_{\text{max}} < 2$ m), clear, and oligotrophic. With the exception of Paradise pond (Fig. 6), with a $\text{pH} \leq 6.5$, the ponds are alkaline (pH range of 7.4 to 8.6), reflecting the presence of carbonate-rich till. Conductivity values fluctuated seasonally, but were generally between 100 and 300 μS . The only exceptions were tidally influenced, Brackish pond (Fig. 6), with conductivity up to 10 393 μS , and dilute Paradise pond (Fig. 6), with a minimum conductivity of 22 μS . Major-ion concentrations are relatively similar among the remaining sites, although environmental gradients exist (reflecting, for example, differences in local drainage basins and proximity to the sea). The major cations are Ca^{2+} and Na^{+} , whereas the major anion is Cl^{-} . Ionic concentrations change over the summer as a result of the combined effects of cryoconcentration, snowmelt dilution, evaporation, and other variables. High Arctic ponds such as these may be especially sensitive monitors of future environmental change.

PRESENT-DAY POND COMMUNITIES

Diatoms

A major objective of the Cape Herschel Project was to decipher past environmental changes from the paleolimnological record preserved in pond sediments. Because diatom frustules are the primary paleolimnological indicators used, much of our research focused on the taxonomic description and ecological characterization of modern diatom flora (Douglas, 1989; Douglas and Smol, 1993, 1995a). Diatoms are excellent paleolimnological indicators, as they are often very abundant and well preserved in sediments. In addition, they have well defined optima and tolerances to environmental variables (Smol, 1987; Smol et al., 1994).

Epiphytic, epilithic, and surface-sediment diatom assemblages were identified and enumerated for each of the Cape Herschel study ponds (Douglas and Smol, 1993, 1995a). Benthic diatoms were abundant, whereas planktonic taxa were absent. Species richness was high overall, but was generally low within each pond. Over 130 diatom taxa from 28 genera were identified in the periphyton samples, with marked differences in species composition evident among the ponds. Moreover, many of the diatoms exhibited varying degrees of microhabitat specificity (Douglas and Smol, 1995a). Variance partitioning by canonical correspondence

analysis showed that 26 per cent of the total variance exhibited by diatom species composition could be accounted for by the measured environmental variables (i.e. 10.2 per cent by habitat and 15.8 per cent by chemical composition of water). Pond water alkalinity best explained the distribution of taxa, and weighted averaging regression and calibration were used to develop a transfer function to infer pond water alkalinity from the diatom assemblages. Other important environmental variables included $[Na^+]$ for the epilithic and $[SiO_2]$ for the epiphytic assemblages.

Chrysophyte cysts

The siliceous resting stages of chrysophyte algae, known as 'cysts' or 'stomatocysts', are being used increasingly in paleolimnological studies (Duff et al., 1995). The taxonomy and ecology of High Arctic cyst floras were largely unknown, so a study parallel to the diatom study was initiated to describe the taxonomy and present-day distributions of these as yet underutilized paleoindicators.

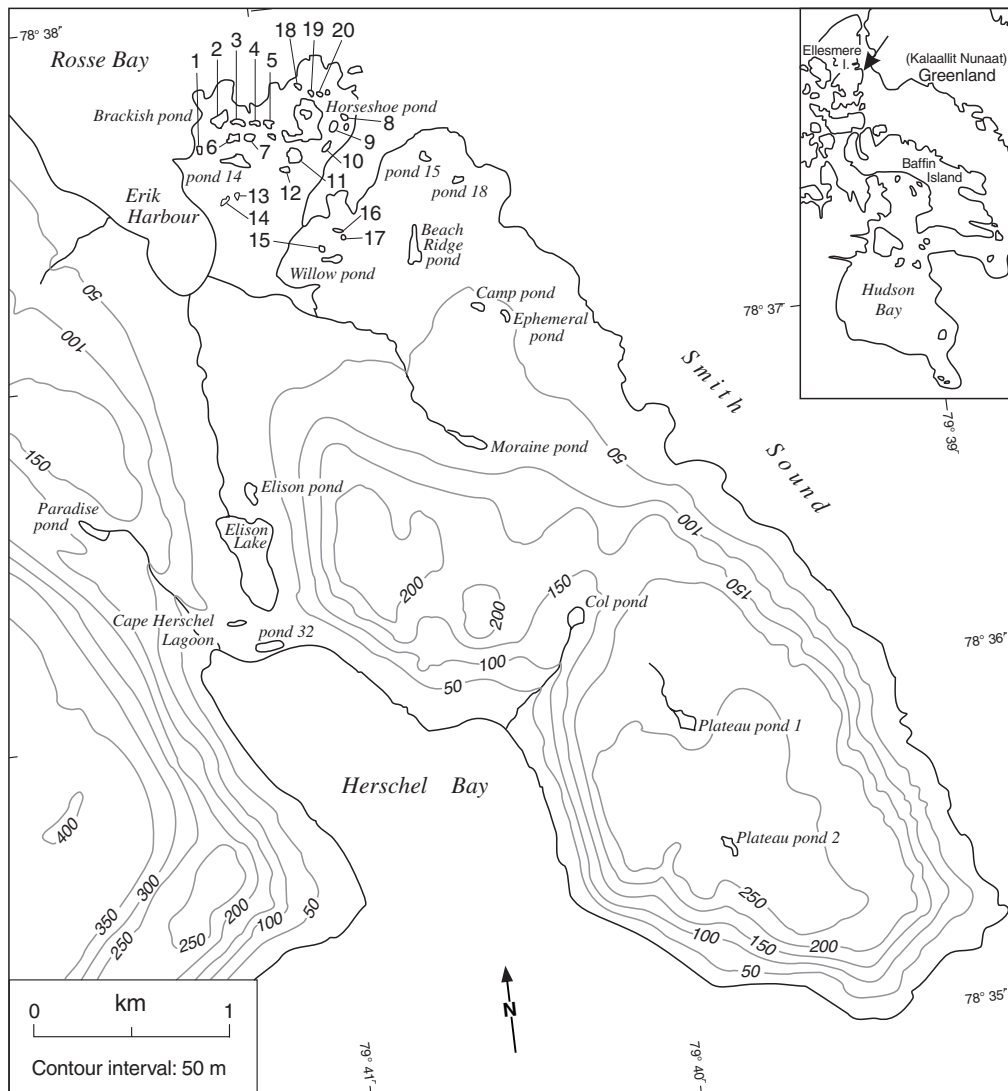


Figure 6. Map of Cape Herschel showing the major study sites (modified from Douglas and Smol, 1994). All pond names are unofficial except for *Elison Lake*. Topographic data courtesy of G. Holdsworth. Numbers on the map correspond to the following pond names: 1, Cold pond; 2, Brackish pond; 3, pond 1; 4, pond 10; 5, pond 8; 6, pond 13; 7, pond 12; 8, pond 26; 9, pond 24; 10, pond 6; 11, pond 7; 12, pond south of 7; 13, pond 27; 14, pond 28; 15, pond northwest of Willow; 16, pond 2; 17, pond 3; 18, Ephemeral pond; 19, pond northwest of Horseshoe; 20, Poppy pond.

Duff et al. (1992) identified 35 chrysophyte stomatocyst morphotypes from the ponds. Many of these cysts had not been described previously. In a subsequent analysis focusing on habitat specificity, Douglas and Smol (1995b) found that chrysophyte cysts were relatively more common in moss periphytic and epilithic habitats than in surface sediment samples, with the highest percentages of cysts relative to diatoms found in the semiaquatic mosses. This was surprising, as chrysophytes are generally considered to be planktonic, but apparently periphytic taxa may be common at high latitudes. As discussed in Douglas and Smol (1995b), the ratio of diatom frustules to chrysophyte cysts in arctic sediment cores may track different environmental variables than paleolimnologists may intuitively expect on the basis of observations from more temperate regions. Moreover, these data may be useful in interpreting chrysophyte cyst assemblages preserved in High Arctic fossil peat deposits (Brown et al., 1994). A subsequent study of these same sites (Wilkinson et al., 1997) specifically examined the cysts present in periphytic habitats and confirmed that, for example, the mosses in these High Arctic ponds support distinctive chrysophyte assemblages.

Invertebrates

A characteristic feature of the study ponds is the abundance of aquatic invertebrates (e.g. cladocerans, copepods, chironomids), possibly reflecting the absence of fish. Parsons (1985) examined zooplankton populations in three ponds, Horseshoe, Willow, and Camp. For reasons not yet apparent, great differences existed between populations in two of the ponds. The rotifer fauna from five small alkaline ponds on Cape Herschel (Beachridge, Brackish, Camp, Horseshoe, and Willow) was examined by Nogrady and Smol (1989). The relatively diverse assemblage of 33 taxa yielded one new species. Douglas and Smol (1987) used some of the pond surface sediments to complete a survey of siliceous protozoan indicators.

PALEOLIMNOLOGY OF HIGH ARCTIC PONDS

Several independent lines of evidence (Douglas, 1993; Douglas et al., 1994) indicate that the sediment profiles of the Cape Herschel ponds are not seriously disrupted by cryoturbation or other mixing processes. For example, after watching the summer thaw and subsequent freeze-up of the ponds over several field seasons, it is evident that the sediments are not disturbed by certain processes associated with mixing in some subarctic lakes (e.g. Nichols, 1967). Further physical evidence that the sediment profiles are relatively undisturbed is that the outline of holes left by coring while the ponds were completely frozen could still be seen once the ponds had thawed. Perhaps the strongest data supporting the veracity of the paleolimnological records are the changes in the diatom

profiles themselves (e.g. Douglas et al., 1994). For example, if cryoturbation were a serious problem, then it would not be possible to record the striking diatom changes, all within a few centimetres or even within a 1 cm thick section, that our studies revealed. Similarly, the ^{210}Pb profiles obtained for the cores also indicate that the pond sediments are relatively undisturbed (Douglas et al., 1994).

Paleolimnological data from the study ponds consistently show that diatom assemblages were relatively stable over the last few millennia, but then experienced unparalleled changes, likely beginning in the nineteenth century (Douglas et al., 1994). A typical example of the magnitude and abruptness of the diatom changes is shown in Figure 7, which depicts diatom profiles from Col pond, 135 to 140 m a.s.l. (Fig. 6, 8). The core may represent as much as 8000 years of deposition. Col pond's diatom flora was overwhelmingly dominated by small benthic *Fragilaria* taxa until the early nineteenth century, at which time the flora shifted abruptly to a relatively diverse assemblage of *Achnanthes*, *Caloneis*, *Cymbella*, *Navicula*, *Nitzschia*, and *Kraskella* species. Dating by ^{210}Pb indicates that the above successional changes probably began in the nineteenth century (Douglas et al., 1994).

Figure 7a is based on an analysis of sample 82-44, core 2 (155 cm), and is a simplified version of previously published examples from Douglas et al. (1994). Figure 7b, based on an analysis of sample 81-12, core 1 (233 cm), documents diatom data from selected intervals in a replicate core for Col pond. A comparison of these two profiles indicates that the changes in diatom flora through time are reproducible.

Similarly abrupt changes occurred in the other cores analyzed (Douglas, 1993; Douglas et al., 1994). For example, Camp pond, at 58.5 m a.s.l., (Fig. 6, 9) is one of the smallest and hence perhaps one of the more sensitive sites on the cape. Bulk dating of the organic fraction (sample 78-4, core 12, 104–100 cm) indicates that the core we report on here (Fig. 4) covers 4890 ± 70 ^{14}C years (GSC-2838) or 5661 to 5583 calibrated years (R.P. Beukens, pers. comm., 1991) of sediment accumulation. Its diatom history (Fig. 10) is dominated by *Denticula kuetsingii*, *Fragilaria pinnata*, *Nitzschia frustulum*, as well as other *Nitzschia* species. The recent sediments, however, record a striking shift to dominance by *Achnanthes* spp.

The sediment core (Fig. 11) from Elison Lake, 16.5 m a.s.l. (Fig. 6, 12), the largest water body on the cape, covers 3850 ± 100 ^{14}C years (GSC-3170) or 4417 to 4140 calibrated years of sediment accumulation (sample 78-27, core 1, 50–47 cm). For almost all of its history, the Elison Lake diatom flora was dominated by the pioneering *Fragilaria construens/pinnata* complex, similar to the one recorded in Col pond. However, the moss epiphyte *Pinnularia balfouriana*, which represented about 10 per cent of the assemblage throughout the core, increased dramatically in number in post-eighteenth century sediments (Fig. 11).

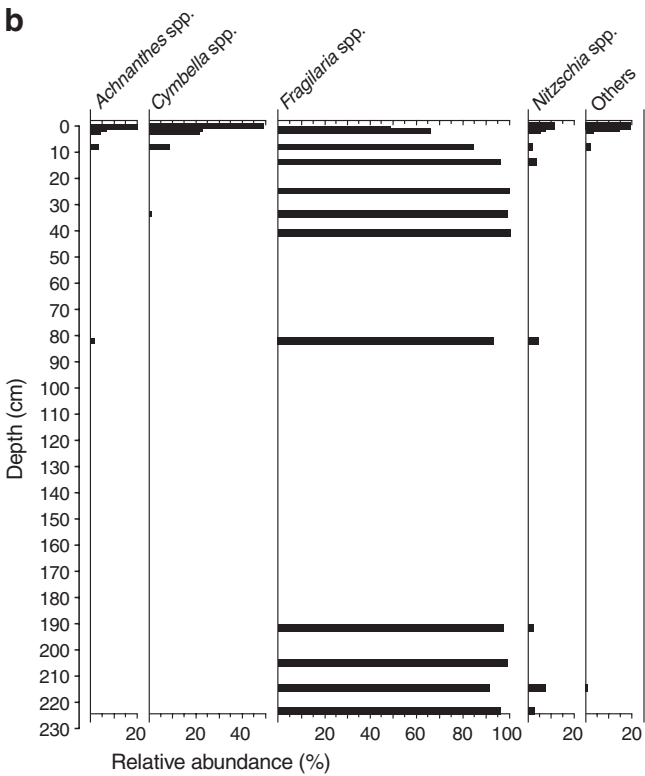
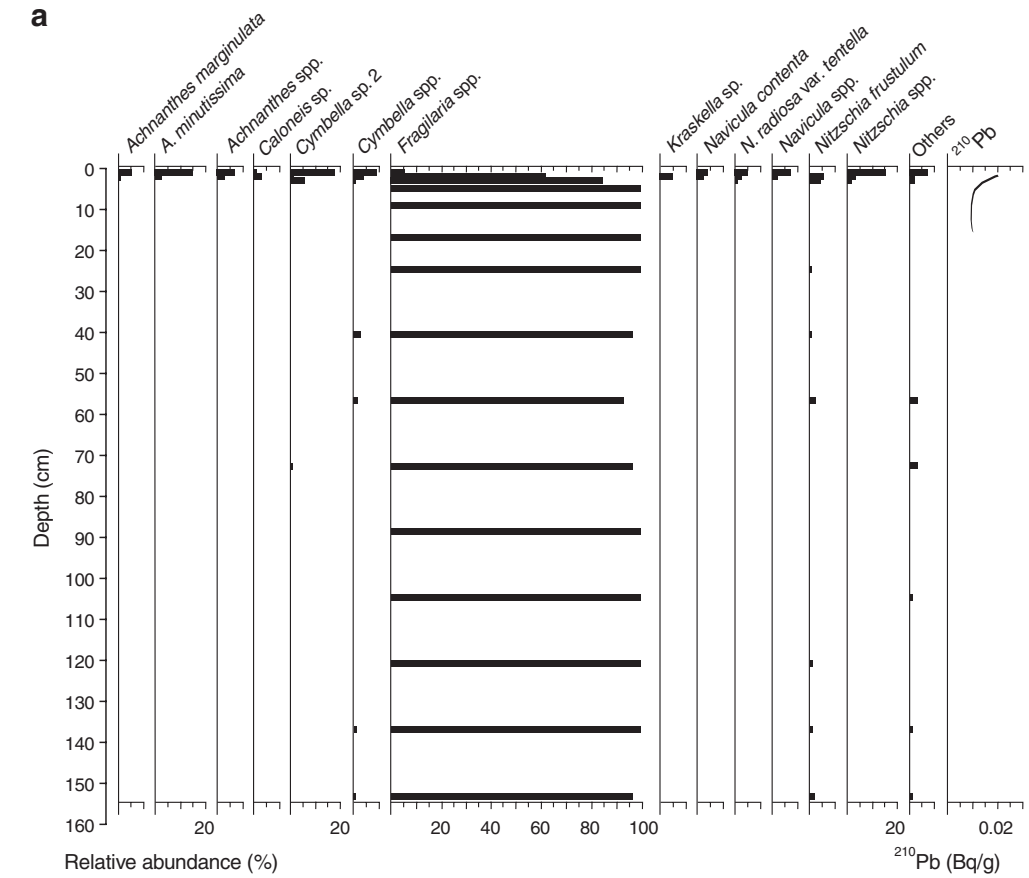


Figure 7.

Relative frequency diagram summarizing some of the dominant changes in diatom assemblages from Col pond. **a**) Modified from Douglas *et al.* (1994). **b**) Diatom changes from selected intervals of a replicate core. Note that certain species have been grouped to the generic level in some profiles (see Douglas *et al.*, 1994, and Douglas, 1993, for more detailed stratigraphies). Note how strikingly similar the diatom changes are in the two cores. On the basis of ^{210}Pb dating (Douglas *et al.*, 1994), the marked species changes occurred in the nineteenth century.

Compared to the abrupt, recent changes in diatom assemblages, species changes in the older sediments seem modest. As noted in Douglas et al. (1994), these earlier changes may also be climate related, but because of poor dating control, it is difficult to interpret them at present.

As discussed in Douglas et al. (1994), the causes of the marked diatom changes recorded over the last two centuries cannot be determined with certainty. However, preservation of artifacts, immigration of new taxa, local disturbances, and increased doses of ultraviolet radiation are not viable hypotheses to explain these changes (Douglas et al., 1994). The diatom shifts recorded (e.g. increased diversity, shifts to more complex periphytic assemblages, increases in moss epiphytes) are similar to what one would expect with climatic warming (Douglas and Smol, 1993). Regardless of the cause, these High Arctic ponds have clearly changed dramatically in the recent past.

PALEOLIMNOLOGICAL RESEARCH FROM SITES NEAR CAPE HERSCHEL

In addition to the work completed and in progress for Cape Herschel, studies have been carried out at a number of nearby sites. For example, Rock Basin Lake (site RB, Fig. 2), a small, 14.5 m deep lake 295 m a.s.l. near the head of Baird Inlet, some 50 km west-southwest of Cape Herschel, has been the subject of several paleolimnological investigations. Organic sediments yielded a maximum age of 8970 ± 160 BP (GSC-3051) (Blake 1981, 1987). Four local pollen zones were recognized by Hyvärinen (1985) when he constructed the first Holocene diagram for Ellesmere Island. The most recent zone indicated a climatic deterioration beginning 3500 to 4000 radiocarbon years ago. Analysis of the same core for diatoms (Smol, 1983) revealed that most of the 55 taxa were littoral, benthic, oligotrophic, and acidophilous species. Smol concluded that climate was an overriding factor in controlling past diatom assemblages. Climate changes were closely linked to the extent of lake ice cover and this, in turn, determined which



Figure 8.

View southwestward at Col pond from the slope leading to the high plateau on Cape Herschel Peninsula. Note the boulders in this extremely shallow (18–26 cm) pond at 135 to 140 m a.s.l. In the distance is Alfred Newton Glacier (arrow), an outlet glacier from the Prince of Wales Icefield (see Fig. 2). Photograph by W. Blake, Jr., July 20, 1988. GSC 1996-120G

Figure 9.

Oblique aerial view westward at Camp pond (black arrow) and the Cape Herschel base station (black arrow) and the Cape Herschel base station. Camp pond is at 58.5 m a.s.l. In the distance, at the northern end of Elison Pass, is Erik Harbour (open arrow), the innermost part of Rosse Bay (see Fig. 6). Photograph by W. Blake, Jr., July 28, 1988. GSC 1996-120B



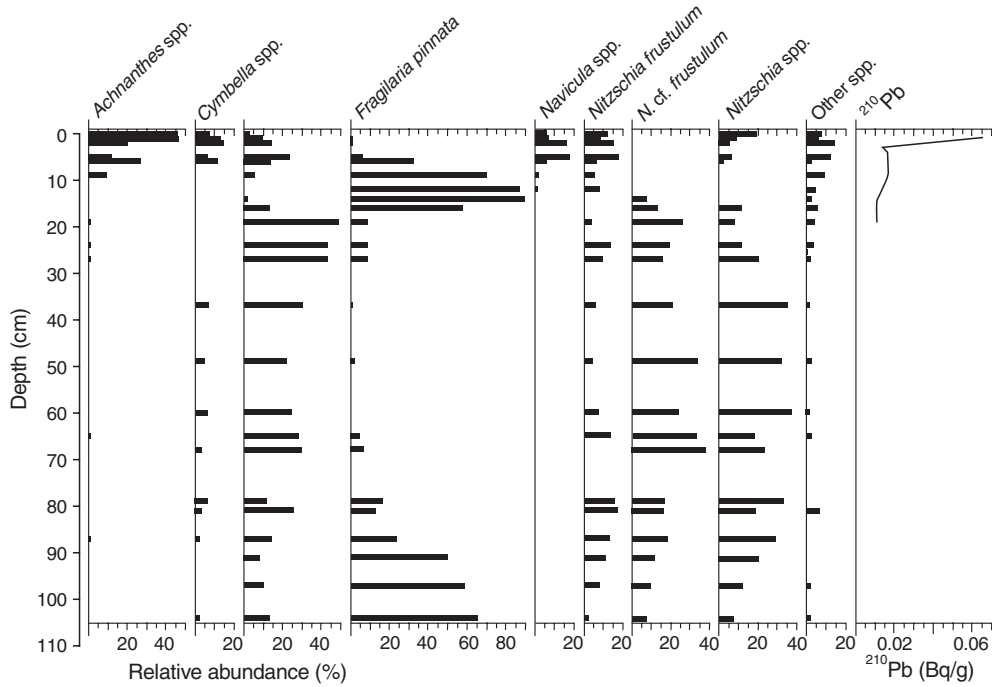


Figure 10. Relative frequency diagram summarizing some of the dominant changes in diatom assemblages from Camp pond (modified from Douglas et al., 1994). On the basis of ^{210}Pb dating, the marked species changes occurred in the nineteenth century.

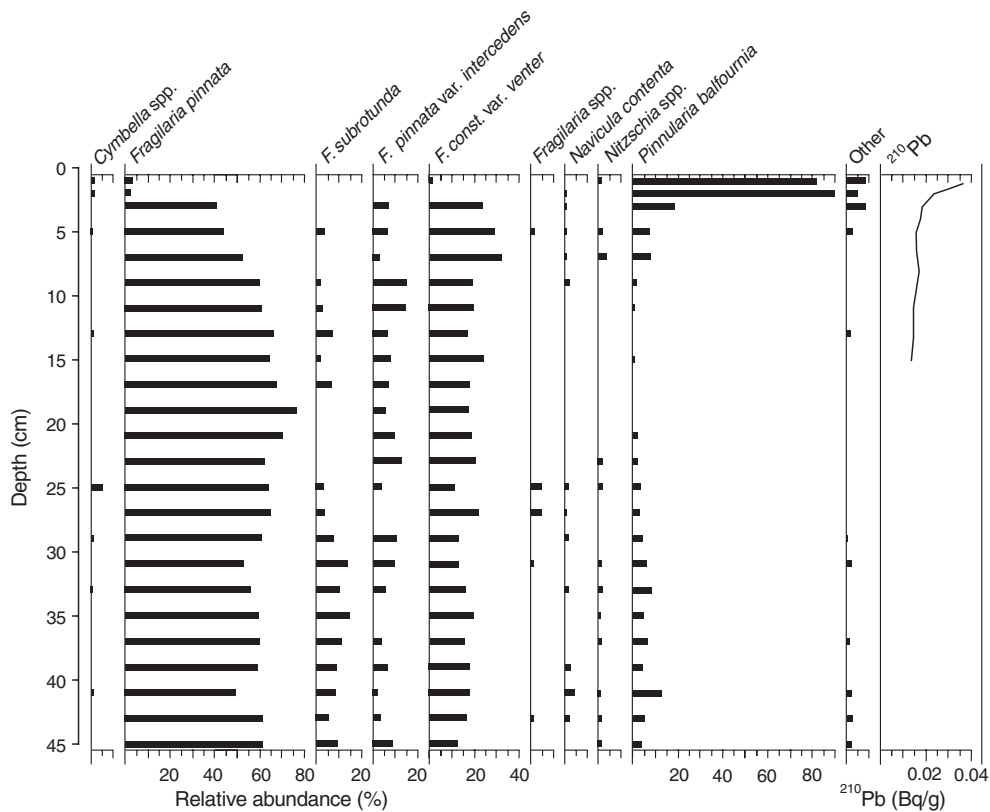


Figure 11. Relative frequency diagram summarizing some of the dominant changes in diatom assemblages from Elison Lake (modified from Douglas et al., 1994). On the basis of ^{210}Pb dating, the marked species changes occurred in the nineteenth century.



Figure 12.

View westward at the southern part of *Elison Lake* and innermost *Herschel Bay* (see Fig. 6) from the *Cape Herschel plateau*. The core of frozen sediment was extracted fairly close to the end moraine, now reworked into beaches, that dams the lake at its southern end. *Elison Lake*, at 16.5 m a.s.l., is approximately 500 m long; depth at the coring site was about 95 cm. The arrow shows *Cape Herschel lagoon* (see Fig. 6). Photograph by W. Blake, Jr., August 2, 1981. GSC 203107-D

habitats in the lake were available for algal growth. This hypothesis has since been further refined (Smol, 1988). Duff and Smol (1988) later described 26 chrysophycean stomatocyst morphotypes from the same core, demonstrating the utility of these new microfossils in paleolimnological reconstructions from High Arctic regions.

Howard (1989) studied the diatom microfossils in a core from *Proteus Lake*, an 8 m deep lake 390 m a.s.l. on *Pim Island*, 13 km east-northeast of *Cape Herschel* (site P, Fig. 2). Earlier, *Lichti-Federovich* has undertaken several preliminary studies on diatoms from cores in the area (*S. Lichti-Federovich*, unpub. GSC diatom rept., 1979) as well as on snow samples from *Ellesmere Island* and north-west *Greenland*. These investigations are summarized in *Douglas* (1989) and *Douglas and Smol* (1993). Two additional studies deal with diatom taxa found in precipitation samples at *Cape Herschel* (*Lichti-Federovich*, 1985, 1986). Other investigations from *Ellesmere Island* are summarized elsewhere in this volume (e.g. *Hamilton et al.*, 2000; *Wolfe*, 2000).

Across *Smith Sound*, *Blake et al.* (1992) completed a multidisciplinary paleolimnological investigation of the Holocene sediments from a lake on *Inglefield Land*, *Greenland*, 50 km east of *Cape Herschel* (site KI, Fig. 2). The Holocene diatom flora was dominated by small benthic *Fragilaria* taxa, similar to the pre-eighteenth century assemblages recorded in the *Cape Herschel ponds*. Past climatic changes were believed responsible for most of the changes recorded in pollen, algal, and invertebrate assemblages. For example, a striking change in green algal microfossils from *Scenedesmus* to *Pediastrum*, some 4000 radiocarbon years ago, suggested a climatic deterioration. Other paleoclimatic indicators suggest a similar cooling in other arctic regions, as summarized by *Bradley* (1990). *Brown et al.* (1994) studied siliceous microfossils preserved in a 2 m long peat core (*Brassard and Blake*, 1978) from the summit plateau of the largest of the *Carey Islands* (*Øer*), *Greenland* (Fig. 1). They found marked fluctuations in diatoms, chrysophytes, and protozoan plates,

which they speculated may have been caused by climatic changes between 6300 ± 80 BP (GSC-2368) and 4390 ± 140 BP (GSC-2415).

CONCLUSIONS AND RECOMMENDATIONS

Paleolimnological approaches, using biological indicators preserved in dated pond and lake sediments, offer exciting possibilities for reconstructing past climatic and environmental trends. Much of this work, however, is still exploratory and considerable additional research will be required to define more accurately the ecological optima and tolerances of various indicators, such as diatoms.

Paleolimnological work in High Arctic environments, however, is not without its problems. Compared with other lakes and ponds, High Arctic sites tend to have very slow sedimentation rates, thus limiting the temporal resolution that can be achieved. Suitable material for AMS ^{14}C dating has been notoriously difficult to find in some cores. Moreover, in lakes and ponds of certain morphometries, problems associated with sediment mixing due to ice push and other mixing processes may occur. Fortunately, many of these potential problems can be addressed and the extent of any problems can be assessed using independent measures. As a result, many sedimentary profiles yield valuable information on past environmental change.

Shallow arctic ponds may be especially sensitive bellwethers of environmental change. New paleolimnological studies should be initiated in other High Arctic regions to determine if the striking successional changes recorded in the post-eighteenth century sediments of the *Cape Herschel ponds* have occurred elsewhere and, if so, did these changes occur synchronously? Indeed, *Wolfe* (2000) suggests that similar environmental changes may have occurred at *Hot Weather Creek* and *Douglas* (1993, Appendix L) has recorded marked diatom shifts in the most recent sediments of *Lake Hazen*, north of the *Agassiz Ice Cap* (Fig. 1).

There are now more long-term limnological data for the Cape Herschel study ponds than for any other comparable High Arctic region. Continued monitoring of these sites will undoubtedly lead to important new insights into the causes and nature of environmental change.

ACKNOWLEDGMENTS

We gratefully acknowledge research support from the Geological Survey of Canada, the Polar Continental Shelf Project, the Northern Studies Training Grants, the Natural Sciences and Engineering Research Council of Canada, the Arctic Institute of North America, and a Jennifer Robinson Memorial Scholarship (AINA) to M.S.V. Douglas. B. Risto and R.J. Cornett performed ^{210}Pb dating at Atomic Energy Canada, Ltd. D. Lemmen provided many useful comments on the manuscript. This paper is contribution no. 61 from the Cape Herschel Project.

REFERENCES

- Barr, W.**
1985: The expeditions of the first international polar year, 1882–83; The Arctic Institute of North America, Technical Paper no. 29; University of Calgary, Calgary, Alberta, 222 p.
- Blake, W., Jr.**
1977: Glacial sculpture along the east-central coast of Ellesmere Island, Arctic Archipelago; *in* Report of Activities, Part C; Geological Survey of Canada, Paper 77-1C, p. 107–115.
1978: Coring of Holocene pond sediments at Cape Herschel, Ellesmere Island, Arctic Archipelago; *in* Current Research, Part C; Geological Survey of Canada, Paper 78-1C, p. 119–122.
1981: Lake sediment coring along Smith Sound, Ellesmere Island and Greenland; *in* Current Research, Part A; Geological Survey of Canada, Paper 81-1A, p. 191–200.
1982: Coring of frozen pond sediments, east-central Ellesmere Island: a progress report; *in* Current Research, Part C; Geological Survey of Canada, Paper 82-1C, p. 104–110.
1987: Lake sediments and glacial history in the High Arctic; evidence from east-central Ellesmere Island, Arctic Canada, and from Inglefield Land, Greenland; *Polar Research*, v. 5, p. 341–343.
1992a: Shell-bearing till along Smith Sound, Ellesmere Island–Greenland: age and significance; *in* Quaternary Stratigraphy, Glacial Morphology, and Environmental Change, (ed.) A.-M. Robertsson, B. Ringberg, U. Miller, and L. Brunnberg; Sveriges Geologiska Undersökning, Ser. Ca. 81, p. 51–58 (Festschrift for Professor Jan Lundqvist).
1992b: Holocene emergence at Cape Herschel, east-central Ellesmere Island, Arctic Canada: implications for ice sheet configuration; *Canadian Journal of Earth Sciences*, v. 29, p. 1958–1980.
1993: Holocene emergence along the Ellesmere Island coasts of northernmost Baffin Bay; *Norsk Geologisk Tidsskrift*, v. 73, p. 147–160.
- Blake, W., Jr., Boucherle, M.M., Fredskild, B., Janssens, J.A., and Smol, J.P.**
1992: The geomorphological setting, glacial history and Holocene development of ‘Kap Inglefield Sø’, Inglefield Land, North-West Greenland; *Meddelelser om Grønland, Geoscience*, Nr. 27, 42 p.
- Bradley, R.S.**
1990: Holocene paleoclimatology of the Queen Elizabeth Islands, Canadian High Arctic; *Quaternary Science Reviews*, v. 9, p. 365–384.
- Brassard, G.R. and Blake, W., Jr.**
1978: An extensive subfossil deposit of the arctic moss *Aplodon wormskioldii*; *Canadian Journal of Botany*, v. 56, p. 1852–1859.
- Bridgland, J. and Gillett, J.M.**
1983: Vascular plants of the Hayes Sound region, Ellesmere Island, Northwest Territories; *The Canadian Field-Naturalist*, v. 97, p. 279–292.
- Brown, K.M., Douglas, M.S.V., and Smol, J.P.**
1994: Siliceous microfossils in a Holocene High Arctic peat deposit (Nordvestø, Northwest Greenland); *Canadian Journal of Botany*, v. 72, p. 208–216.
- Christie, R.L.**
1962: Geology, Alexandra Fiord, Ellesmere Island, District of Franklin; Geological Survey of Canada, map 9-1962 (scale 1:253 440).
- Douglas, M.S.V.**
1989: Taxonomic and ecological characterization of freshwater diatoms from the sediments of 36 High Arctic ponds (Cape Herschel, Ellesmere Island, NWT, Canada); M.Sc. thesis, Department of Biology, Queen’s University, Kingston, Ontario, 173 p.
1993: Diatom ecology and paleolimnology of High Arctic ponds; Ph.D. dissertation, Department of Biology, Queen’s University, Kingston, Ontario, 161 p.
- Douglas, M.S.V. and Smol, J.P.**
1987: Siliceous protozoan plates in lake sediments; *Hydrobiologia*, v. 154, p. 13–23.
1993: Freshwater diatoms from high arctic ponds (Cape Herschel, Ellesmere Island, N.W.T.); *Nova Hedwigia*, v. 57, p. 511–552.
1994: Limnology of high arctic ponds (Cape Herschel, Ellesmere Island, N.W.T.); *Archiv für Hydrobiologie*, v. 131, p. 401–434.
1995a: Periphytic diatom assemblages from high arctic ponds; *Journal of Phycology*, v. 31, p. 60–69.
1995b: Paleolimnological significance of chrysophyte cysts in arctic environments; *Journal of Paleolimnology*, v. 13, p. 79–83.
- Douglas, M.S.V., Smol, J.P., and Blake, W., Jr.**
1994: Marked post-18th century environmental change in high arctic ecosystems; *Science*, v. 266, p. 416–419.
- Duff, K.E. and Smol, J.P.**
1988: Chrysophycean statospores from the postglacial sediments of a High Arctic lake; *Canadian Journal of Botany*, v. 66, p. 1117–1128.
- Duff, K.E., Douglas, M.S.V., and Smol, J.P.**
1992: Chrysophyte cysts in High Arctic ponds; *Nordic Journal of Botany*, v. 12, p. 471–499.
- Duff, K.E., Zeeb, B.A., and Smol, J.P.**
1995: *Atlas of Chrysophycean Cysts*; Kluwer Academic Publishers, Dordrecht, 189 p.
- Dunbar, M.**
1969: The geographical position of the North Water; *Arctic*, v. 22, p. 438–441.
- Frisch, T.**
1984: Geology, Prince of Wales Mountains, District of Franklin, Northwest Territories; Geological Survey of Canada, Map 1572A, scale 1:250 000.
- Hamilton, P.B., Gajewski, K., McNeely, R., and Lean, D.R.S.**
2000: Physical, chemical, and biological characteristics of lakes from the Slide Basin on Fosheim Peninsula, Ellesmere Island, Nunavut; *in* Environmental Response to Climate Change in the Canadian High Arctic, (ed.) M. Garneau and B.T. Alt; Geological Survey of Canada, Bulletin 529.
- Howard, S.M.**
1989: The postglacial history and present-day diatom assemblages of Proteus Lake, Pim Island, Canadian High Arctic; B.Sc. thesis, Department of Biology, Queen’s University, Kingston, Ontario, 42 p.
- Hyvärinen, H.**
1985: Holocene pollen stratigraphy of Baird Inlet, east-central Ellesmere Island, arctic Canada; *Boreas*, v. 14, p. 19–32.
- Lichti-Federovich, S.**
1985: Diatom dispersal phenomena: diatoms in rime frost samples from Cape Herschel, Ellesmere Island, N.W.T.; *in* Current Research, Part B; Geological Survey of Canada, Paper 85-1B, p. 391–399.
1986: Diatom dispersal phenomena: diatoms in precipitation samples from Cape Herschel, east-central Ellesmere Island, N.W.T. — a quantitative assessment; *in* Current Research, Part B; Geological Survey of Canada, Paper 86-1B, p. 263–269.
- McNeely, R. and Gummer, W.D.**
1984: A reconnaissance survey of the environmental chemistry in east-central Ellesmere Island, N.W.T.; *Arctic*, v. 37, p. 210–223.

Müller, F., Ohmura A., and Braithwaite, R.

1977: The North Water Project (Canadian High Arctic); *Polar Geography*, v. 1, p. 75–85.

Nichols, H.

1967: The distribution of arctic lake sediments by ‘bottom ice’: a hazard for palynology; *Arctic*, v. 20, p. 213–214.

Nogrady, T. and Smol, J.P.

1989: Rotifers from five High Arctic ponds (Cape Herschel, Ellesmere Island, N.W.T.); *Hydrobiologia*, v. 173, p. 231–242.

Parsons, D.

1985: Patterns of growth and relative abundance of cladocerans in two high arctic ponds; B.Sc. Honours thesis, Department of Biology, Queen’s University, Kingston, Ontario, 50 p.

Prest, V.K.

1952: Notes on the geology of parts of Ellesmere and Devon islands, Northwest Territories; Geological Survey of Canada, Paper 52-32, 15 p.

Smol, J.P.

1983: Paleophycology of a high arctic lake near Cape Herschel, Ellesmere Island; *Canadian Journal of Botany*, v. 61, p. 2195–2204.

1987: Methods in Quaternary ecology – freshwater algae; *Geoscience Canada*, v. 14, p. 208–217.

1988: Paleoclimate proxy data from freshwater Arctic diatoms; *Verhandlungen Internationale Vereinigung für Theoretische und Angewandte Limnologie*, v. 23, p. 837–844.

Smol, J.P., Cumming, B.F., Douglas, M.S.V., and Pienitz, R.

1994: Inferring past climatic changes in Canada using paleolimnological techniques; *Geoscience Canada*, v. 21, p. 113–118.

Wilkinson, A.N., Zeeb, B.A., Smol, J.P., and Douglas, M.S.V.

1997: Chrystophyte stomatocyst assemblages associated with periphytic habitats from High Arctic pond environments; *Nordic Journal of Botany*, v. 17, p. 95–112.

Wolfe, A.P.

2000: A 6500 year diatom record from southwestern Fosheim Peninsula, Ellesmere Island, Nunavut; *in* Environmental Response to Climate Change in the Canadian High Arctic, (ed.) M. Garneau and B.T. Alt; Geological Survey of Canada, Bulletin 529.

Present and past environments inferred from Agassiz Ice Cap ice-core records

J.C. Bourgeois¹, R.M. Koerner¹, B.T. Alt², and D.A. Fisher¹

Bourgeois, J.C., Koerner, R.M., Alt, B.T., and Fisher, D.A., 2000: Present and past environments inferred from Agassiz Ice Cap ice-core records; in Environmental Response to Climate Change in the Canadian High Arctic, (ed.) M. Garneau and B.T. Alt; Geological Survey of Canada, Bulletin 529, p. 271–282.

Abstract: Six surface-to-bedrock ice cores from the Agassiz Ice Cap were analyzed primarily for oxygen isotope ratios, melt-layer percentage, volcanic acidity layers, and pollen concentrations. The pre-Holocene section contains ice from both the last glacial period and the last interglaciation. Melt concentration and $\delta^{18}\text{O}$ records indicate that summer temperatures were 2 to 2.5°C warmer in the early Holocene than now. Gradual cooling has occurred in summer since approximately 8000 years ago, with a minimum about 100 to 200 years ago.

Short cores and snow-pit samples from the borehole area were used for chemical and pollen analyses. Contaminant concentration in the snow has increased since the 1950s in association with a marked increase in SO_2 emissions in Eurasia. Pollen assemblages show seasonal and annual variations and are compared with meteorological records from automatic weather stations. These meteorological records are considered essential for transfer functions for both the ice-core results and the long-term, mass-balance survey.

Résumé : Six carottes de glace allant de la surface jusqu'au substratum rocheux ont été prélevées sur la calotte glaciaire Agassiz et analysées surtout pour déterminer les rapports des isotopes d'oxygène, le pourcentage des couches de fonte, les couches d'acidité volcanique et les concentrations de pollen. La section antérieure à l'Holocène contient de la glace datant de la dernière période glaciaire et de la glace remontant à la dernière période interglaciaire. Les données sur la concentration de fonte et $\delta^{18}\text{O}$ indiquent que les températures estivales à l'Holocène inférieur étaient de 2 à 2,5 °C plus élevées que les températures contemporaines. Un refroidissement estival graduel a commencé il y a environ 8 000 ans et a atteint un minimum il y a environ 100 à 200 ans.

Des carottes courtes et des échantillons creusés dans la neige, prélevés à proximité des sondages, ont été utilisés pour des analyses polliniques et chimiques. Une augmentation de la concentration des contaminants dans la neige depuis les années 1950 est associée avec une augmentation marquée des émissions de SO_2 en Eurasie. Les assemblages de pollen montrent des variations annuelles et saisonnières que l'on compare avec les enregistrements météorologiques provenant de stations météorologiques automatisées. On considère que ces observations météorologiques sont essentielles pour l'établissement de fonctions de transfert pour les données tirées des carottes de glace et pour le bilan de masse à long terme.

¹ Terrain Sciences Division, Geological Survey of Canada, 601 Booth Street, Ottawa, Ontario K1A 0E8

² Balanced Environments Associates, 5034 Leitrim Road, Carlsbad Springs, Ontario K0A 1K0

INTRODUCTION

The northern part of the Agassiz Ice Cap (Fig. 1), on Ellesmere Island, has been the site of glaciological investigations since 1974. Six surface-to-bedrock ice cores have been drilled, providing long records of past environmental changes. The cores are referred to as A77, A79, A84, A87, A93.1, and A93.2, the number representing the year they were drilled. In addition, several shorter cores have been extracted near the deep ice core sites. The area around the borehole sites has been monitored extensively over the years and snow-pit samples have been analyzed for contaminants (both natural and anthropogenic). Mass-balance measurements, which determine the difference between the amount of accumulation (usually snow) and the amount of ablation (melting of ice and snow), have been taken every spring since 1977 near the borehole sites and on a nearby glacier.

Because of the substantial amount of information available on the Agassiz Ice Cap, the site has been used to test new instruments or methods. In 1988, an experimental automatic weather station (autostation) was installed near the A77 borehole site and two more stations have since been placed at other locations. Many problems inherent to remote arctic locations remain to be solved, but the available data are being used to relate the various parameters being studied on the ice cap to climate variables.

This paper summarizes some of the modern and paleoenvironmental records obtained thus far from the Agassiz Ice Cap ice cores and snow surveys. Some of these

records may be regarded as climate proxies whereas others reveal changes in the composition of the atmosphere over the ice cap through time. The paleoenvironmental records discussed are primarily 1) stable oxygen isotope ratios (the ratio of the concentrations of heavy and light isotopes in a sample is measured in terms of its deviation from the ratio of the standard mean ocean water (SMOW), expressed as δ and measured in parts per thousand (‰), presented as $\delta^{18}\text{O}$, in which the variations in the records are essentially interpreted as changes in temperature; 2) ice-melt stratigraphy (percentage of melt layers in core sections), which provides a record of past summer conditions at the site and through relation to mass-balance survey results over the ice cap in general; 3) the acidity record determined by solid electrical conductivity measurements, that provides seasonal acidity variations in which high-acidity peaks are associated with major volcanic eruptions; and 4) pollen spectra, composed of both regional tundra types and extraregional types (mainly tree pollen), which are used to trace the possible origin of the air masses reaching the ice cap and can provide additional climate information when combined with other core parameters.

This review of the Agassiz Ice Cap snow and ice core records is divided into three sections, the pre-Holocene, the Holocene, and the modern record. The pre-Holocene refers to the section between the late Pleistocene-Holocene transition and the bedrock. It represents less than 10 per cent of the total core length, but probably close to 90 per cent of the time period covered by the ice cores. The resolution is low in the early Holocene, but improves in younger sections. The most recent part of the Holocene (the modern record) is presented separately. With the exception of the meteorological and mass-balance records, the data were obtained primarily for monitoring levels of contaminants and the samples were recovered from snow pits and shallow cores.

BOREHOLES AND ICE CAP

The Agassiz Ice Cap, approximately 16 000 km², covers central Ellesmere Island between latitudes 79°45'N and 81°N. It is drained by glaciers that penetrate the surrounding mountains, the larger ones reaching sea level. The boreholes are in the northern part of the ice cap, at latitude 80°40'N, longitude 73°30'W. The first core (A77), drilled in 1977 to a depth of 338 m, is from about 1 km downslope from a local ice divide at an elevation of 1670 m (Fig. 2). Core A79 (139 m deep and located about 30 m higher) is 200 m down the opposite side of the ice divide; cores A84 and A87 (both 127 m deep) are 30 m apart at the top of the flow line, which is a local ice dome. In 1993, two more cores (A93.1, A93.2) were drilled, only a few metres apart, at the top of that local dome. However, with one exception (Zheng et al., 1998), the results obtained from cores A93.1 and A93.2 are unpublished and since these two cores are only tens of metres away from the A87 borehole site, they are not discussed in this paper. Information on the various core parameters is presented in Table 1.

The Agassiz Ice Cap lies in the Eastern Canadian Arctic within the Arctic mountains and fiords climate region as defined in Alt and Maxwell (2000, Fig. 5 and 7). It faces the



Figure 1. Drill sites on the Agassiz Ice Cap. HWC = Hot Weather Creek.

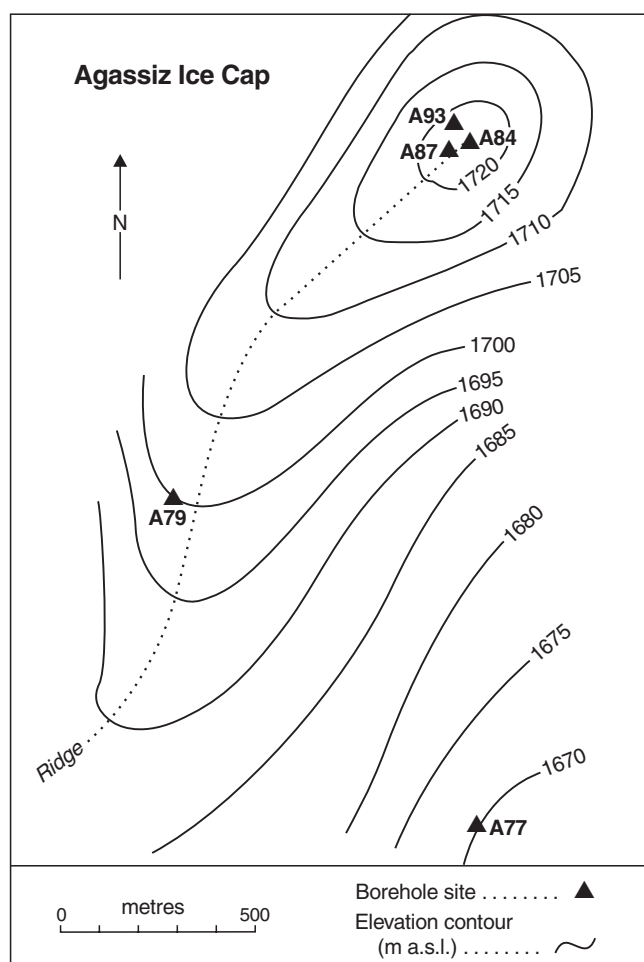


Figure 2. Borehole sites on the Agassiz Ice Cap. The site number indicates the year of drilling.

anomalously warm, dry intermontane region to the west (Alt and Maxwell, 2000, Fig. 14) and the contrastingly wet regime of northern Baffin Bay to the southeast as reflected by Koerner's regional accumulation map (Koerner, 1979) reproduced in Alt and Maxwell (2000, Fig. 19). It is somewhat protected from cold, wet Arctic Ocean air masses by the mountains of northern Ellesmere Island. The automatic weather station (autostation), installed near the site of the A77 borehole in 1988, is in the area where these three climate regions would be expected to converge. The station records temperature, changes in relative snow-surface height, wind speed and direction, relative humidity, and incoming solar radiation. Preliminary reports on the data and on instrumentation problems associated with remote Arctic locations are presented by Alt et al. (1992) and Labine et al. (1994). At the A77 site, during the six years of record (1988–1993), monthly mean screen-level temperatures for July varied from +0.5°C to -4.9°C and for January from -32.4°C to -39.3°C (Table 2). Mean annual temperatures for this period lie in the -22.5 to -21.5°C range. The highest screen-level temperature recorded was 12.7°C, but this was undoubtedly produced by overheating of the screen. The lowest recorded temperature

Table 1. Properties of Agassiz Ice Cap ice cores.

Core number	Elevation (m a.s.l.)	Core length (m)	Ice accumulation (m/a)	Melt average (%)
A77	1670	338	0.175	3.1
A79	1700	139	0.115	-
A84	1730	127	0.098	5.1
A87	1730	127	0.098	5.1
A93.1 and A93.2	1730	123	0.098	5.1

Table 2. Preliminary values of positive degree day (PDD) totals for summers in the A77 autostation record and mean monthly July and January screen-level temperatures calculated from 24 hourly values (Tm24)* and by the traditional method of maximum+minimum/2 (Tmxn).

YEAR	PDD (°C)		July mean (°C)		January mean (°C)	
	Tm24	Tmxn	Tm24	Tmxn	Tm24	Tmxn
1988	31.7	47.3	0.1	0.5	-39.3	-39.1
1989	11.0	11.5	-3.6	-3.5	-32.4	-32.3
1990	8.2	16.1	-4.0	-4.5	-38.3	-37.9
1991	4.1	3.3	-3.5	-3.8	-35.8	-35.6
1992	0.1	1.9	-4.6	-4.9	-35.7	-35.7
1993	6.3	9.1	-3.2	-3.2	-35.1	-35.0
1994						
1995						

*Differences between the Tm24 and traditional Tmxn methods of calculating daily mean temperatures are discussed in detail in Alt and Maxwell (2000). Note that for ice-cap conditions, the difference in total PDD between the two methods can be quite significant (see for instance 1990).

of -51.2°C may be a result of radiative cooling of the sensor. Above-freezing temperatures were experienced every summer in the record. The resulting positive degree-day (PDD) totals ranged from 47.3°C to 0.1°C (Table 2).

In the northern part of the ice cap, annual precipitation is about 0.175 m/a, ice equivalent (Fisher et al., 1983). Most precipitation falls as snow in early winter. However, due to the presence of a ridge in the borehole area, wind turbulence is common and causes the removal or scouring of the soft winter snow (Fisher et al., 1983; Fisher and Koerner, 1988). Borehole sites A79, A84, A87, and A93 are currently most affected by this process, but not the A77 site. As a result, accumulation at the three scoured sites is about 65 per cent of that at the A77 site. South of the A77 site, accumulation rates vary much less (Fisher et al., 1983). The removal of some winter snow also affects the $\delta^{18}\text{O}$ record since some of the cold winter peaks (most negative δ values) are truncated. The cores from the top of the ridge (A79, A84, A87, A93) give on average 2.5‰ less negative δ values than the core drilled 1 km down the ridge (A77) (Fisher et al., 1983, 1995). These differences must be considered in the interpretation of the Holocene records. At the A77 site, ice migration down the flow line presents another problem because some of the oldest ice comes from the scouring zone.

Melting is minimal at high elevations on the ice cap and when it does occur, it is recorded as ice layers in the firn. It currently represents approximately 3 per cent of the annual precipitation at the A77 site and 5 per cent at the top of the ridge. The difference is due to the thinner annual layer at the top that results from removal of some of the winter snow on the ridge. The thickness of the summer melt layers in the ice cores provides a good indicator of past summer temperatures and is used by Koerner and Fisher (1990) to produce a Holocene summer temperature record for the Agassiz Ice Cap.

TIME SCALES

Several techniques are used to establish ice-core time scales. These and related problems are documented in a series of papers edited by Oeschger and Langway (1989). Some are based on ice-flow modelling, which provides an approximate age-depth chronology, whereas others are based on annual and seasonal variations of various components found in snow and ice, the most frequently used of which are variations in isotopic composition, dust, acidity, and trace substances. However, the lower the accumulation, the more likely the annual and seasonal snow layers will be disturbed by surface winds and the more rapidly the annual layers will thin out to the point where they cannot be identified. Calibration between cores can also be made using well known volcanic events. These are detected in ice cores as layers of high acidity.

On the Agassiz Ice Cap, the precipitation rate is relatively low; nevertheless, the time scales are felt to be accurate to within 10 per cent for the past 7000 years (Fisher et al., 1983). Note that the chronology used in this paper is in calendar years and not in ^{14}C years. The initial theoretical time scales were checked by comparison with the volcanic acid layers in the cores (Fisher et al., 1983, 1995). These volcanic events are well dated in the finer resolution Greenland cores. A major shift in $\delta^{18}\text{O}$ values, which occurs at a few metres above bedrock on the Agassiz Ice Cap, is correlated with a similar shift in the Greenland cores. Assuming that the more negative the $\delta^{18}\text{O}$ values, the colder the period, then this shift marks the transition between the late Pleistocene and the Holocene. In the recently drilled ice cores from the Summit area of Greenland, this transition occurs at 1400 m above bedrock and is assigned an age of 11 550 calendar years (Johnsen et al., 1992). The Agassiz ice Cap ice cores are not dated unequivocally beyond this transition.

PRE-HOLOCENE RECORD

In all Agassiz Ice Cap ice cores, the pre-Holocene record is limited to the bottom 8 to 11 m of ice near bedrock. Studies of ice properties (Koerner et al, 1981; Fisher and Koerner, 1986; Fisher, 1987) and of the origin of the basal ice (Gemmell et al., 1986; Koerner et al., 1987, 1988; Koerner, 1989) have been conducted. The latter studies are of importance for establishing the timing of the initial growth of the present ice cap. The much compressed record does not allow for

high-resolution studies, but because of the shallow ice depth, the pre-Holocene ice is easily accessible for bulk sampling (Koerner et al., 1988, 1991).

In the pre-Holocene $\delta^{18}\text{O}$ records shown in Figure 3, a section with very negative δ values (cold climate) is found below the late Pleistocene-Holocene transition and another relatively warm section is found near bedrock. Core A79 and to a lesser extent the other cores at the top of the flow line have a layer of very 'silty' ice near the bed. Radioecho sounding (Walford and Harper, 1981) shows that this silty ice layer is characteristic of the basal ice over most of the bedrock hill underlying the ice divide and extends for over 1 km northeast from hole A79. At the A79 hole, core recovery was poor in that particular section (only about 10 per cent) and most of the ice was brought to the surface as meltwater produced by the thermal drill. The origin of this particle-rich bottom layer is problematic and two hypotheses are proposed for its formation.

Koerner et al. (1987) consider this silty ice to be of Ice Age origin. The warm δ values (normally indicative of a warm climate) are attributed to basal melting in a deep bedrock valley south of the borehole site at a time when the ice cap was much thicker than at present, such as at an early stage of the Sangamon Interglaciation. The warmer δ values could result from fractionation during refreezing as the ice flowed up the bedrock slope towards the borehole area. The ice could have incorporated the dirt at that time, as suggested by Gemmell et al. (1986).

On the basis of pollen analyses of the pre-Holocene ice (summarized in Fig. 4), Koerner et al. (1988) had to reconsider this hypothesis. They analyzed several large ice samples from early Holocene and pre-Holocene sections in core A79 to resolve the stratigraphy in the older, undated section of the

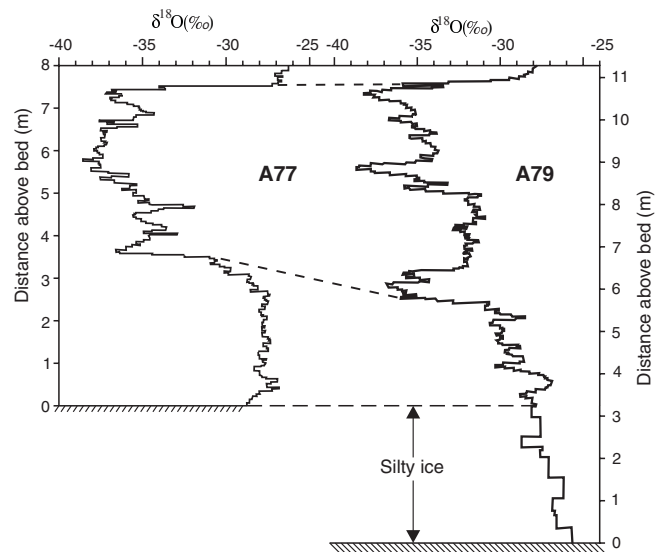


Figure 3. Oxygen isotope ratio ($\delta^{18}\text{O}$) for the lowermost section of cores A77 and A79. The late Pleistocene-Holocene transition is at 7.5 m (A77) and 10.8 m (A79) above the bed.

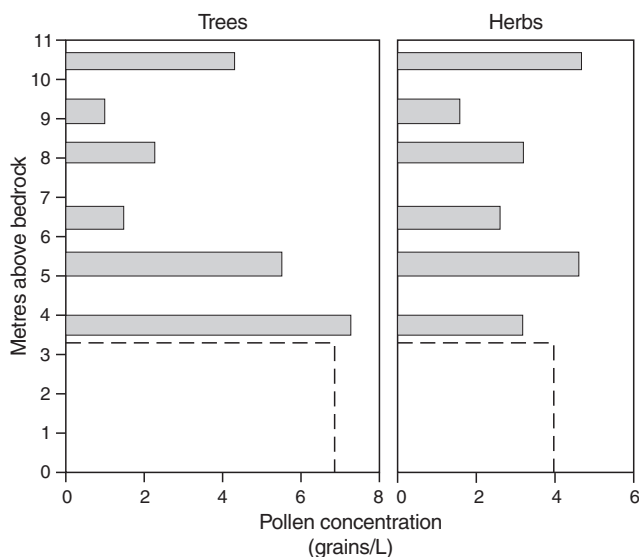


Figure 4. Summary pollen concentration diagram for the pre-Holocene section of core A79. Below the late Pleistocene-Holocene transition (top of diagram), the samples are not dated and only their approximate location above the bed is presented. The thickness of the bars indicates the thickness of the samples. The bottom sample (dotted line) is from the meltwater tank of the thermal drill and the pollen concentration is probably too low (see text).

core. To obtain an adequate pollen sum, they melted, laterally, 30 to 40 kg ice samples from the bottom of the hole and pumped the water to the surface. However, they could not obtain samples from the bottom 3 m and instead used the meltwater samples recovered with the thermal drill in 1979. It has since been established that this type of sample (from the tank of the thermal drill) produces abnormally low pollen concentrations (Koerner et al., 1988). Even so, the pollen concentration from the meltwater is as high as the modern values. A second set of pollen samples, retrieved from the A87 borehole using the first procedure (Bourgeois, unpub. data, 1991), shows higher concentrations than today in the bottom ice samples. The results obtained from pollen analyses, together with the oxygen-isotope signatures, are for Koerner et al. (1988) evidence that the ice near bedrock was formed in a relatively warm period, probably towards the end of the last interglaciation. Consequently, the ice cap must have melted completely or extensively in an earlier stage of the same interglaciation. From similar ice properties found at the bottom of Camp Century and Dye 3 ice cores in Greenland, Koerner (1989) concludes that these sites must also have been ice free during part of the last interglaciation.

Other oxygen isotope variations that occur in the pre-Holocene section of the cores have not been studied in detail, but a comparative study of $\delta^{18}\text{O}$ values for the bottom part of all Agassiz Ice cap cores is in progress. The characteristics of the pre-Holocene Agassiz Ice Cap ice have been studied from cores and from borehole measurements (Fisher and Koerner, 1986; Fisher, 1987). The studies reveal several differences between Wisconsinan and Holocene-interglacial

stage ice. Ice Age ice contains more microparticles, is much 'softer' than interglacial ice, and deforms more readily in borehole tilt and closure measurements. Furthermore, because of the alkaline nature of the Ice Age ice, the solid conductivity, which is used as an indicator of volcanic acid layers in cores, is extremely low in this type of ice, compared to Holocene ice.

Other than the relatively high pollen concentration found in the lowermost ice samples of cores A79 and A87, there are no significant pollen variations in the pre-Holocene section (Koerner et al., 1988). Furthermore, the difference between the glacial period and the Holocene (based on the results of pollen analysis) is not well defined. To what extent this lack of variations is due to a different (i.e. stronger) atmospheric circulation during the Ice Age and/or lower snow accumulation and therefore higher pollen concentration is still to be determined. Results obtained from chemical and particle analyses of Agassiz Ice Cap pre-Holocene ice should help elucidate this problem.

Holocene Record

Holocene records of oxygen isotopes, melt percentages, electrical conductivity, and pollen concentration for the Agassiz Ice Cap are reported by Fisher et al., (1983, 1995), Bourgeois (1986), Fisher and Koerner (1988), Koerner and Fisher (1990), and Zheng et al (1998). Furthermore, Fisher and Koerner (1994) present a detailed record of the last 1000 years of melt, $\delta^{18}\text{O}$ values, and electrical conductivity; Taylor (1991) compares, for the same period, $\delta^{18}\text{O}$ (temperature) profiles from the Agassiz Ice Cap ice cores with deep ground-temperature profiles from three wells southwest of the Agassiz Ice Cap borehole sites.

All Agassiz Ice Cap ice cores, including the two A93 cores, were analyzed for $\delta^{18}\text{O}$ (at the University of Copenhagen). The record, usually presented in 50-year averages, is interpreted as a proxy temperature record, where a change in the isotope ratio of 0.62‰ is equal to a 1°C temperature change (Dansgaard et al., 1971). However, in core A77, the winter snow contributing the most negative $\delta^{18}\text{O}$ values was removed by scouring until about 8000 years ago, by which time ice movement had moved the borehole site from the scouring zone into the non-scouring zone lower down. Consequently, the early Holocene part of core A77 is mainly a summer-dominated record of snow accumulation, whereas the most recent part is representative of all seasons; therefore the average δ values in the latter are 'colder'. The differences between ice cores and the distinction between the climatic signal and noise attributed, for example, to snow drifting are considered by Fisher and Koerner (1994) and Fisher et al. (1995) in the interpretation of these records.

Following the large, abrupt change in stable-isotope ratios marking the end of the last glaciation, Agassiz Ice Cap ice core $\delta^{18}\text{O}$ profiles (Fig. 5a) show a rapid warming trend that reaches a maximum between approximately 8000 and 9000 years ago. This is followed by gradual cooling that increased 1500 years ago. The coldest values of the entire Holocene

were reached approximately 100–200 years ago. This was followed by a pronounced warming into the present century. Koerner and Fisher (1990) consider that since the early Holocene, the change in $\delta^{18}\text{O}$ values corresponds to a cooling of the average temperature of approximately 2.5°C . Changes in the elevation of the ice cap are not considered in this estimate as Koerner (1979) shows that in the Canadian Arctic, $\delta^{18}\text{O}$ values are unaffected by elevation.

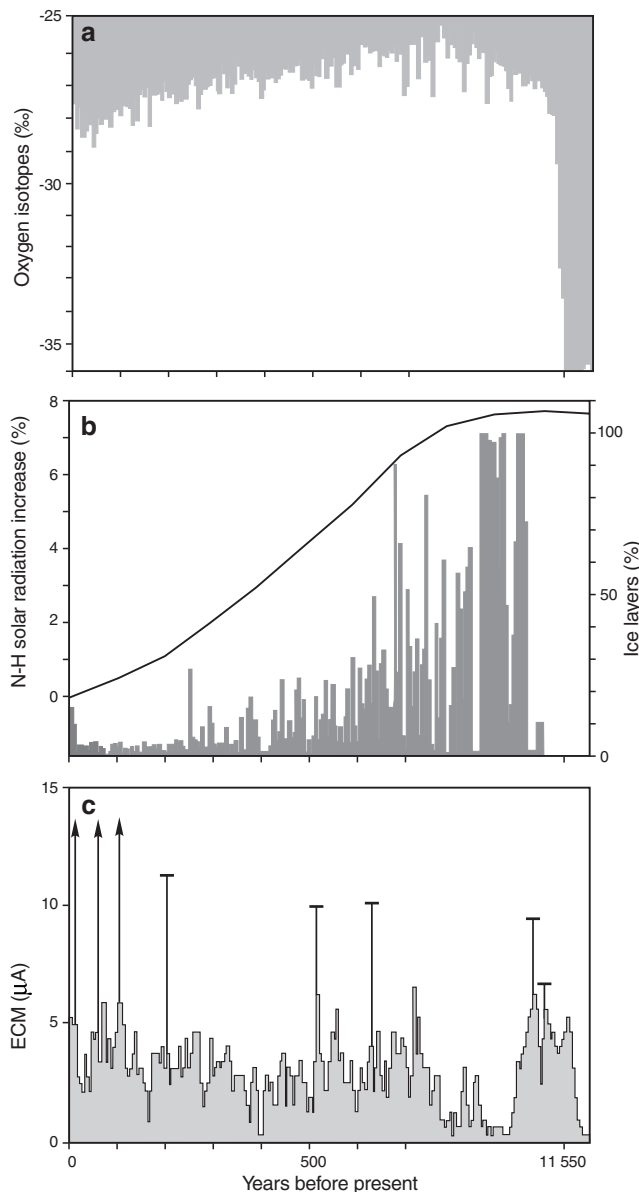


Figure 5. *a*) Oxygen isotopes ($\delta^{18}\text{O}$), *b*) melt-layer concentration, and *c*) ECM (electrical conductivity measurements) for the Holocene section of core A84. The lines in (a) correspond to the major volcanic eruptions. For a comparison of the four Agassiz Ice Cap ice core records, see Fisher and Koerner (1994) and Fisher et al. (1995).

The changing concentration of melt layers with depth is a good indicator of past summer conditions (Koerner and Fisher, 1990). Melt layers, recognized in the cores by their bubble-free texture, are formed by melting on the snow-pack surface, which produces water that percolates down and refreezes in the colder snow layers below. The warmer the summers, the greater the number of melt layers produced. The melt percentage is established by measuring the thickness of melt layers in a core and expressing it in terms of a varying percentage of the annual layer ice-equivalent thickness. Although a warmer climate would most likely lead to an increase in the amount of precipitation on the ice cap, it would probably also lead to an increase in the amount of melt.

The Holocene melt record is presented in Figure 5b. The resolution is poor in the oldest section, but nevertheless four features are significant in this record: very high melt from approximately 9500 to 8500 years ago; decreasing melt from 8500 to about 2500 years ago; very low melt from 2500 to 100 years ago; and a moderate increase in melt during the last 100 years. Presently, melting occurs almost every summer at the Agassiz Ice Cap drill sites. The meltwater percolates down into the snow, refreezes, and forms an ice layer. This represents only about 5 per cent of the annual accumulation (Koerner and Fisher, 1990). By comparison, in the early Holocene, melt layers often formed 100 per cent of the annual layer, which means that the entire annual layer melted during the summer. In the absence of runoff, this would be equivalent to the formation of a 10 cm ice layer in the snow pack each year. If runoff did occur, some years would have had a negative mass balance at the drill site. Presently in the Queen Elizabeth Islands, 10 cm melt (the equivalent of early Holocene melt at the top) occurs each year at an elevation 200 m lower than the borehole site (Koerner, 1979). This can be interpreted as a minimum summer cooling of 2°C from the early Holocene to the present (Koerner and Fisher, 1990) and is comparable to the drop of 2.5°C indicated by the oxygen-isotope record.

A comparison of Holocene $\delta^{18}\text{O}$, melt, and electrical conductivity records for four of the Agassiz Ice Cap cores (Fisher et al., 1995; Zheng et al., 1998) reveals significant differences in δ records in the early part of the Holocene. For the same period, the volcanic acid (electrical conductivity) record is noticeably flat (Fig. 5c), whereas the amount of summer melt is high. According to Fisher et al. (1995), the very high summer melt and noise in the δ values between ca. 11 550 and 8000 calendar years could indicate that at that time or possibly earlier, the site had a negative balance and, therefore, some very early Holocene ice might be missing. However, the presence in all four cores of the Younger Dryas oscillation suggests that the site was not in the ablation zone long enough for the Wisconsinan ice to be eroded. In a comparative study of circumpolar Arctic ice cap $\delta^{18}\text{O}$ and melt records, Koerner and Fisher (1995) conclude that glacier retreat was widespread in the early Holocene and some smaller ice caps (e.g. Meighen and Melville) disappeared at that time. These findings are consistent with several other proxy records from the High Arctic showing maximum warmth at the beginning of the Holocene (e.g. Bradley, 1990; Dyke et al., 1996) and with the solar radiation curve (Fig. 5b). However, they are more

difficult to reconcile with some glacial geology records from Ellesmere Island that show limited glacier retreat in the early Holocene (e.g. England, 1983, 1990, 1996). According to Koerner and Fisher (1995), the cooling that followed the second half of the Holocene promoted the expansion and regrowth of glaciers and ice caps.

Pollen analysis was carried out on the meltwater tank samples produced during drilling of core A77. For every 1.5 m increment drilled, the heating element of the thermal drill melted between 12 to 15 L of water. Field and laboratory procedures were developed to minimize the loss of pollen grains (Bourgeois, 1986). Even so, the pollen content of the melt tank samples was extremely low (usually <1 grain/L). A pollen concentration diagram was constructed for the Holocene by combining samples to produce 500 year increments. The pollen grains found in the samples were assigned to two groups on the basis of their most probable origin, regional (from the High Arctic tundra) and exotic (long distance), pollen from the latter group consisting predominantly of tree and shrub (alder, birch, pine, spruce) pollen from the boreal forest and Low Arctic tundra.

The resulting pollen concentration diagram (Bourgeois, 1986) shows that the maximum concentration of regional pollen types lags behind the temperature maximum (as recorded in the melt and $\delta^{18}\text{O}$ records) by several thousand years. A small increase occurs approximately 6000 years ago and the maximum is reached 3000 years ago. The number of tundra taxa then begins to decrease slightly. The concentration of pollen from tree taxa is also very low in the early Holocene. The concentration of alder and birch pollen starts to increase at 7500 calendar years. The two taxa reach a maximum 1500 years ago, for which there is no adequate explanation. Pine and spruce pollen, although regularly present in small amounts throughout the Holocene, does not follow the same trend as pollen from the above taxa.

The A77 pollen diagram was the first produced from ice cores on the Agassiz Ice Cap. Subsequent analyses of surface samples (Bourgeois et al., 1985; Bourgeois, 1990) and pre-Holocene bulk samples obtained by melting down the borehole and pumping the water to the surface (Koerner et al., 1988) consistently showed higher pollen concentrations than those obtained from the melt tank of the thermal drill. Pollen concentration is always extremely low on the Agassiz Ice Cap, but the difference between the melt tank and other types of samples is significant (<1 grain/L in melt-tank samples compared to average values of 2 to 20 grains/L for other types of samples). We do not know the cause for this, but the difference also applies to chemical analyses of samples obtained from melt tanks and from core segments. Because of these significant variations between the pollen content of melt-tank samples and other types of snow or ice samples from the same ice cap, it is impossible to validate the pollen record obtained from the A77 site. Furthermore, other pollen diagrams produced from analysis of the A87 ice core and selected sections of the A84 core reveal high pollen concentrations in the early Holocene, with profiles similar to $\delta^{18}\text{O}$ and melt records for the same periods (Bourgeois, unpub. data, 1996).

MODERN RECORDS

A large number of surface (and near surface) samples have been collected on the Agassiz Ice Cap to 1) monitor levels of contaminants in the snow, including seasonal and spatial variations, 2) monitor climate variability (using proxy data), and 3) provide modern values for various components being studied in the ice cores. Studies related to the chemical content of snow, based on accumulation over a few years, are provided by Duchesneau (1992), Nriagu et al. (1994), and Goto-Azuma et al. (1997). Koerner and Fisher (1982), Barrie et al. (1985), Gregor et al. (1995, 1996), Peters et al. (1995), and Koerner et al. (1999) contribute longer modern records. Peters et al. (1997) investigated the annual deposition of ^{210}Pb to the ice cap for the 1963 to 1993 period to determine the temporal trend and to test the accuracy of ^{210}Pb dating methodology. A detailed, 35-year record of radioactivity related to nuclear bomb tests has also been developed from the firm layers of the Agassiz Ice Cap (A. Kudo, unpub. data, 1996). In addition, the biological content (pollen and bacteria) of the snow is the subject of studies by Bourgeois (1990) and Handfield (1992). The data on temperature and surface elevation changes during the summer months are used by Alt and Bourgeois (1995) to determine the timing of precipitation events and pollen deposition on the ice cap. This information is also being used for similar studies on stable isotopes and snow chemistry. Some data obtained from the Agassiz Ice Cap are used in spatial studies of High Arctic glacier mass balance (Koerner and Lundgaard, 1995), pollen influx (Bourgeois et al., 1985), and contaminants (Koerner, 1994). The findings, particularly those related to ice-core studies, are reviewed below.

Chemical analyses

Koerner and Fisher (1982) were the first to notice increasing acid levels in Arctic ice cores from analyses of Agassiz Ice cap ice samples. Their measurements of pH and conductivity on core A77 and shallow cores reveal a significant increase in acidity and conductivity beginning in the early 1950s, compared with the preceding 5000 years. Barrie et al (1985) reviewed the same data, dating back to 1912, along with a 10 m core from the Mount Oxford area in northwest Ellesmere Island. They correlated the concentrations with those obtained from aerosol samples collected at Alert on the northern coast of Ellesmere Island. Results show that since 1956, there has been a 75 per cent increase in Arctic air pollution that can be associated with a marked increase in SO_2 and NO_x emissions in Europe (Fig. 6). More recently, Koerner et al. (1999) measured the influx of these two major pollutant ions in two shallow ice cores from the Agassiz Ice Cap. The cores, one from a snow-scoured zone and the other from an unscoured zone, cover close to 100 years of snow deposition. The record, which ends in 1989, shows no evidence of decreasing concentration of these aerosols (Fig. 6), despite decreasing emissions due to improved industrial fuel-emission technology in western Europe and North America in the last two decades. According to Koerner et al. (1999), this suggests that the dominant source of pollutants to northern Ellesmere Island is Russia. Indeed, a spatial study on snow chemistry

conducted in the Canadian Arctic (including the Agassiz Ice Cap), the Russian Arctic, and the Arctic Ocean effectively shows a decreasing concentration of pollutants from the Russian side to the Canadian Arctic (Koerner, 1994).

In 1993, an 8.3 m pit was excavated at a site approximately 1.7 km north of the Agassiz Ice Cap drill sites to study the depositional trends of polycyclic aromatic hydrocarbons (PAHs), elemental carbon (also called 'black carbon', 'graphitic carbon', 'charcoal', or 'soot'), and polychlorinated biphenyls (PCBs). The 30-year record shows that the flux of PAHs to the Agassiz Ice Cap has remained relatively constant for the period 1972–1973 to 1992–1993, with a mean value of $11 (\pm 6) \mu\text{g}/\text{m}^2/\text{year}$ (Gregor et al., 1995; Peters et al., 1995). A greater flux (mean value of $74 (\pm 20)$) was obtained for the period prior to 1972. This change in flux magnitude may reflect changes in the global use of fossil fuels (Peters et al., 1995). Elemental-carbon flux shows no trend during the same period and there seems to be no relationship between elemental carbon and PAH concentrations or deposition. However, as mentioned by Peters et al. (1995), problems were encountered during the analysis of elemental carbon and these results should be regarded with caution. Similarly, the flux of PCBs to the Agassiz Ice Cap shows no well defined trends and records obtained thus far disagree. In the study by Gregor et al. (1995), fluxes show large interannual variability during the 30-year period. Deposition was generally higher in the 1960s (maximum of $930 \text{ ng}/\text{m}^2/\text{year}$ in 1967–1968), decreased in

1968–1969, increased to 1979–1980, and reached a minimum in 1980–1981 ($91 \text{ ng}/\text{m}^2/\text{year}$). The flux has since increased, although interannual variations are still considerable. In 1987, a 17-year record was obtained at another Agassiz Ice Cap location. Gregor et al. (1996) conclude that at the site, PCB deposition has been decreasing since the early 1970s. These results demonstrate the need for more research on the analytical methods and postdepositional processes affecting certain types of organic contaminants in the Arctic.

In the first chemical analysis of ice samples from the Agassiz Ice Cap, Koerner and Fisher (1982) noticed a seasonal cycle in which higher acidity levels are reached in late winter–early spring. This seasonality and the spatial variations in snow chemistry (Cl^- , SO_4^{2-} , NO_3^-) on the Agassiz Ice Cap have been studied in detail by Goto-Azuma et al. (1997) and Koerner et al. (1999) from snow-scoured zones and from the unscoured zone. Seasonal ion peaks are clearly evident in both zones even though a large part of the winter snow is removed from the scoured zones. This fact suggests that on the ice cap, dry deposition of pollutants, as opposed to wet deposition (i.e. in snowfall), is the primary form of deposition in midwinter. Furthermore, the SO_4^{2-} and NO_3^- peaks in late winter–early spring are enhanced by anthropogenic inputs.

Pollen

Bourgeois (1990) studied annual and seasonal variations in pollen grains in the snow layers of the Agassiz Ice Cap to gain a better understanding of the relationship between pollen concentration in snow/ice and climate. An eight-year pollen concentration record (Fig. 7) was obtained from pits excavated near the A77 borehole site. Tree pollen shows less variation than regional pollen and exceptionally high (low) concentrations are apparently related to particular synoptic conditions at the time of flowering. For example, the high concentration of tree pollen in the 1982 and 1983 spring and summer snow layers occurred when synoptic conditions promoted a strong, direct flow of air from the south to the Arctic Islands. Conversely, a strong northwesterly flow over the islands in the spring of 1986 resulted in very low tree pollen concentrations in snow deposited at that time. Regional pollen types show larger seasonal and interannual variations. A higher concentration is normally found in a loose, granular snow layer formed on top of the summer melt layer (referred to as the 'a' layer for representing the first snow of the balance year). Bourgeois (1990) considered this layer to be formed in late summer or early autumn. However, Alt and Bourgeois (1995) studied the timing of deposition of that particular snow layer on the basis of meteorological records from the nearby autostation and found that it could be deposited as early as mid-July. At that time, melting may have ceased on top of the ice cap, but plants are still flowering on the tundra. If the first snowstorms of the season are sufficiently well developed (as in the summer of 1988 and 1991), they could potentially transport relatively large amount of tundra pollen to the ice cap as well as scavenge pollen in the atmosphere above the ice cap. According to Alt and Bourgeois (1995), extreme regional pollen concentrations reflect the conditions of the intermontane region southeast of the ice cap. However, longer records are needed to confirm this relationship.

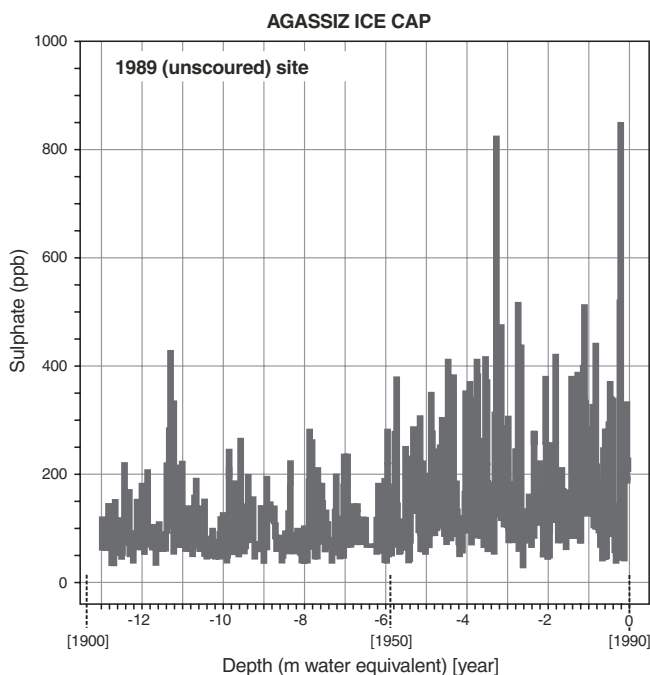


Figure 6. Sulphate concentration (ppb) in a shallow core recovered from the unscoured zone of the Agassiz Ice Cap. A high sulphate concentration at approximately 11 m depth is associated with the Katmai volcanic eruption, dated at 1912. The marked increase in concentration in the middle of the twentieth century (approximately 6 m depth) is attributed to anthropogenic pollutants.

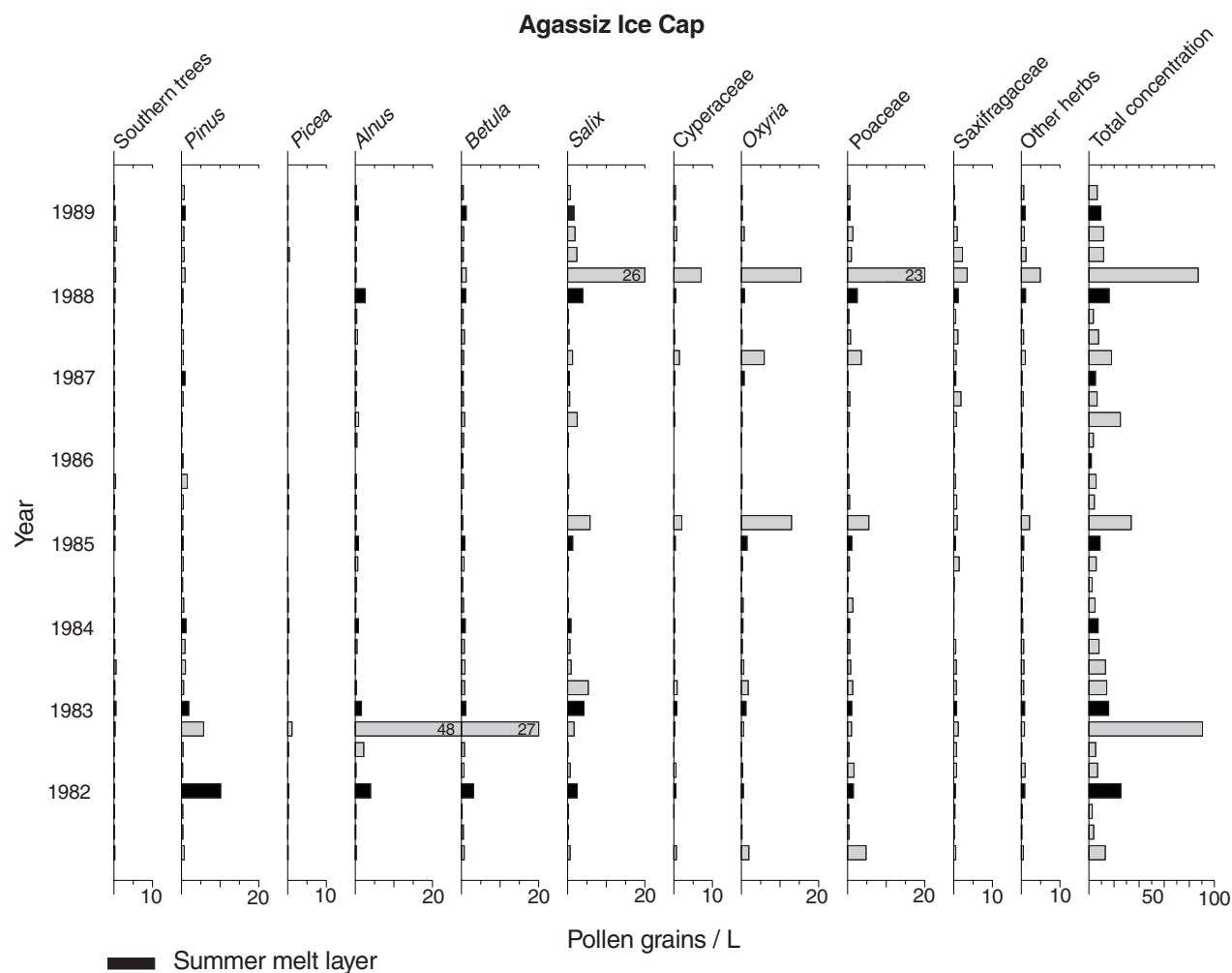


Figure 7. Seasonal pollen variations (number of grains/L) in the snow layers of the Agassiz Ice Cap during an eight-year period.

Mass balance

Since 1977, mass-balance measurements have been made each year on the northeast part of the Agassiz Ice Cap. The measurements form two data sets, but they cannot be used to compile a real mass-balance record as the area for each elevation interval remains unknown. The first data set is from a line of 18 poles set between the drill sites and a ridge that forms the eastern part of the ice cap in this general area. It represents accumulation in the uppermost regions of the ice cap, which is in the percolation zone (where summer melt refreezes within the current surface layer). Pole measurements on their own introduce errors because the snow between the surface and the bottom of the pole settles whereas the pole cannot. Therefore, in the accumulation zone, a board is placed on the surface each spring. The depth and density of the snow overlying this board is then measured the following spring. The second set begins just above the firn line, above the 'Drambuie Glacier', and runs down that glacier to the east-northeast and into the ablation zone. In the ablation and superimposed ice zones, the distance from the top of the stake to the surface of the ice is measured each spring to determine the ice gain or loss since the previous spring.

The record from the Agassiz Ice cap is only 20 years long. No trends are appearing, which is consistent with what has been found for four other ice caps in the High Arctic (Koerner and Lundgaard, 1995).

Synoptic climate

Preliminary results from the A77 site autostation show that, in summer, the ice cap is approximately 12°C cooler than the interior of the Fosheim Peninsula to the west (cf. Table 2 and Alt et al., 2000, Table 1 for Hot Weather Creek). The mean July atmospheric lapse rates between the two stations range from 0.6°C to 0.9°C/100 m, which shows the cooling effect of the ice cap relative to the 'standard atmospheric' lapse rate of 0.6°C. In winter, the lapse rate is reversed (-0.2 to -0.5°C/100 m), as would be expected from the persistence of temperature inversions in the radiosonde records for High Arctic stations during this season (Bradley et al., 1992, 1993; Alt et al., 2000). An examination of the daily temperature records for Hot Weather Creek (see Alt et al., 2000, Fig. 13) and A77 on the Agassiz Ice Cap (B.T. Alt, unpub. data, 1998) shows that the inversion breaks down during warm intrusions, which are frequent some winters and not others (see Alt

SNOW DEPTH AT END OF MONTH / SNOWFALL
AGA(A77)/HWC(AWS)/EU(AES): April 1988–March 1995

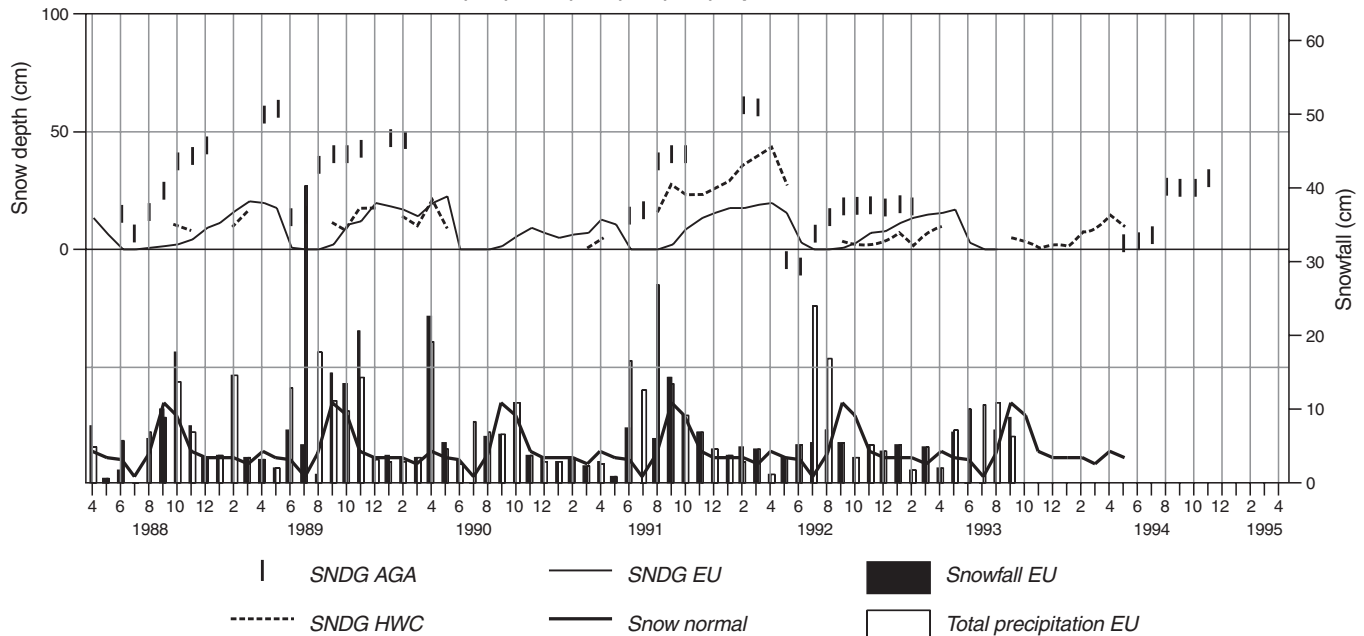


Figure 8. Top: Snow depth (in centimetres) at the end of each month measured using an autostation snow-depth sounder at site A77 on the Agassiz Ice Cap (vertical bars) and at Hot Weather Creek (dashed line) and a ruler at Eureka (solid line). Bottom: Total monthly precipitation (in millimetres; open bars), total monthly snowfall (in centimetres; solid bars), and 30-year normal monthly snowfall for Eureka for comparison. SNDG = snow on the ground; AGA = Agassiz Ice Cap; HWC = Hot Weather Creek; EU = Eureka; Snow normal = 30-year normal snowfall; HWC(AWS) = Hot Weather Creek automatic weather station; EU(AES) = Atmospheric Environment Service Eureka station

et al., 2000, for further discussion). The potential breakdown of the winter inversion conditions has obvious ramifications for the interpretation of the paleotemperature record relative to sea-level tundra locations. An absence of temperature inversions in paleorecords would suggest more direct transport of pollen and pollutants to the ice cap with the mid-latitude systems.

The ice cap snow-depth records for Agassiz Ice Cap core site A77 (Fig. 8), as well as Hot Weather Creek and Eureka on Fosheim Peninsula (Fig. 1), show considerable variation in accumulation rates and patterns from year to year. The snow-depth records, combined with the analysis of synoptic weather conditions, provide vital information regarding source, timing, and method of deposition of the various components measured in detailed snow-pit studies (Alt and Bourgeois, 1995), such as chemical composition (Goto-Azuma et al., 1997). The autostation records also provide the data necessary to calculate transfer functions for summer melt (*see* 'Mass balance' above). Comparative studies of the modern record are essential to interpret the deep ice core results.

SUMMARY

Several ice cores and sets of snow-pit samples have been collected on the Agassiz Ice Cap for environmental/climatological studies. The records obtained thus far suggest that 1) the

borehole area was free of ice for part of the last interglacial stage and the present ice cap probably started to grow towards the end of that interglacial stage; 2) Pleistocene ice is limited to a few metres near the bed, but this ice shows the major $\delta^{18}\text{O}$ steps seen in higher resolution cores; 3) the early Holocene was apparently the warmest part of the Holocene; 4) since 8000 BP, summer temperatures have cooled by 2 to 2.5°C; 5) the coldest period of the Holocene occurred approximately 100 to 200 years ago; and 6) the concentration of pollutants in snow on the Agassiz Ice Cap has been increasing since the middle of the twentieth century.

The drilling of four ice cores within a few tens of metres of one another and of two other cores approximately 1 km away has allowed us to study the effect of wind scouring and summer melt on ice-core paleoclimatic records. It has also allowed us to experiment and compare results of pollen analysis obtained from meltwater, core segments, and downhole melting devices. Spatial and temporal chemical surveys from shallow cores and snow pits have provided valuable information on the reproducibility of data and on the process of dry deposition. Automatic weather stations installed at several locations on the ice cap are providing meteorological data sets that are being used for mass-balance, snow-chemistry, pollen, and stable-isotope studies.

REFERENCES

Alt, B.T. and Bourgeois, J.C.

1995: Establishing the chronology of snow and pollen deposition events on Agassiz Ice Cap (Ellesmere Island, Northwest Territories) from autostation records; *in* Current Research 1995-B; Geological Survey of Canada, p. 71–79.

Alt, B.T. and Maxwell, B.

2000: Overview of the modern arctic climate; *in* Environmental Response to Climate Change in the Canadian High Arctic, (ed.) M. Garneau and B.T. Alt; Geological Survey of Canada, Bulletin 529.

Alt, B.T., Labine, C.L., Atkinson, D.E., Headley, A.N., and Wolfe, P.M.

2000: Automatic weather station results from Fosheim Peninsula, Ellesmere Island, Nunavut; *in* Environmental Response to Climate Change in the Canadian High Arctic, (ed.) M. Garneau and B.T. Alt; Geological Survey of Canada, Bulletin 529.

Alt, B.T., Labine, C.L., Headley, A., Koerner, R.M., and Edlund, S.A.

1992: High Arctic IRMA (Integrated Research and Monitoring Area) automatic weather station field data 1990–91, parts 1, 2, and 3; Geological Survey of Canada, Open File 2562, 274 p.

Barrie, L.A., Fisher, D., and Koerner, R.M.

1985: Twentieth century trends in Arctic air pollution revealed by conductivity and acidity observations in snow and ice in the Canadian High Arctic; *Atmospheric Environment*, v. 19, p. 2055–2063.

Bourgeois, J.C.

1986: A pollen record from the Agassiz Ice Cap, northern Ellesmere Island, Canada; *Boreas*, v. 15, p. 345–354.

1990: Seasonal and annual variation of pollen content in the snow of a Canadian High Arctic ice cap; *Boreas*, v. 19, p. 313–322.

Bourgeois, J.C., Koerner, R.M., and Alt, B.T.

1985: Airborne pollen: a unique air mass tracer, its influx to the Canadian High Arctic; *Annals of Glaciology*, v. 7, p. 109–116.

Bradley, R.S.

1990: Holocene paleoclimatology of the Queen Elizabeth Islands, Canadian High Arctic; *Quaternary Science Reviews*, v. 9, p. 365–384.

Bradley, R.S., Keimig, F.T., and Diaz, H.F.

1992: Climatology of surface-based inversions in the North American Arctic; *Journal of Geophysical Research*, v. 97(D14), p. 15699–15712.

1993: Recent changes in the North American Arctic boundary layer in winter; *Journal of Geophysical Research*, v. 98(D5), p. 8851–8858.

Dansgaard, W., Johnsen, S.J., Clausen, H.B., and Langway, C.C.

1971: Climatic record revealed by the Camp Century ice core; *in* The Late Cenozoic Glacial Ages, (ed.) K.K. Turekian; Yale University Press, p. 37–56.

Duchesneau, M.

1992: La calotte de glace Agassiz : profil physico-chimique et échanges neige-atmosphère; *The Musk-Ox*, v. 39, p. 86–92.

Dyke, A.S., Hooper, J., and Savelle, J.M.

1996: A history of sea ice in the Canadian Arctic Archipelago based on postglacial remains of the bowhead whale (*Balaena mysticetus*); *Arctic*, v. 49, p. 235–255.

England, J.

1983: Isostatic adjustments in a full glacial sea; *Canadian Journal of Earth Sciences*, v. 20, p. 895–917.

1990: The late Quaternary history of Greely Fiord and its tributaries, west-central Ellesmere Island; *Canadian Journal of Earth Sciences*, v. 27, p. 255–270.

1996: Glacier dynamics and paleoclimatic change during the last glaciation of eastern Ellesmere Island, Canada; *Canadian Journal of Earth Sciences*, v. 33, p. 779–799.

Fisher, D.A.

1987: Enhanced flow of Wisconsin ice related to solid conductivity through strain history and recrystallization; *in* The Physical Basis of Ice Sheet Modelling; Proceedings of the Vancouver Symposium, August 1987; International Association of Hydrological Sciences Publication no. 170, p. 45–51.

Fisher, D.A. and Koerner, R.M.

1986: On the special rheological properties of ancient microparticle-laden northern hemisphere ice as derived from borehole and core measurements; *Journal of Glaciology*, v. 32, p. 501–510.

1988: The effect of wind on $\delta(^{18}\text{O})$ and accumulation give an inferred record of seasonal δ amplitude from the Agassiz Ice Cap, Ellesmere Island, Canada; *Annals of Glaciology*, v. 10, p. 34–37.

1994: Signal and noise in four ice-core records from the Agassiz Ice Cap, Ellesmere Island, Canada: details of the last millennium for stable isotopes, melt, and solid conductivity; *The Holocene*, v. 4, p. 113–120.

Fisher, D.A., Koerner, R.M., Paterson, W.S.B., Dansgaard, W., Gundestrup, N., and Reeh, N.

1983: Effect of wind scouring on climatic records from ice-core oxygen-isotope profiles; *Nature*, v. 301, p. 205–209.

Fisher, D.A., Koerner, R.M., and Reeh, N.

1995: Holocene climatic records from Agassiz Ice Cap, Ellesmere Island, N.W.T., Canada; *The Holocene*, v. 5, p. 19–24.

Gemmell, A.M.D., Sharp, M.J., and Sugden, D.E.

1986: Debris from the basal ice of the Agassiz Ice Cap, Ellesmere Island, Arctic Canada; *Earth Surface Processes and Landforms*, v. 11, p. 123–130.

Goto-Azuma, K., Koerner, R.M., Nakawo, M., and Kudo, A.

1997: Snow chemistry on the Agassiz Ice Cap, Ellesmere Island, Northwest Territories, Canada; *Journal of Glaciology*, v. 43, p. 199–206.

Gregor, D.J., Dominik, J., Vernet, J.-P.

1996: Recent trends of selected chlorohydrocarbons in the Agassiz Ice Cap, Ellesmere Island, Canada; *in* Proceedings of the 8th International Conference on Global Significance of the Transport and Accumulation of Polychlorinated Hydrocarbons in the Arctic, (ed.) R.G. Shearer and A. Bartonova; Comité arctique international, Oslo, Norway.

Gregor, D.J., Peters, A.J., Teixeira, C., Jones, N., and Spencer, C.

1995: The historical residue trend of PCBs in the Agassiz Ice Cap, Ellesmere Island, Canada; *The Science of the Total Environment*, v. 160/161, p. 117–126.

Handfield, M.

1992: Seasonal fluctuation patterns of microflora on the Agassiz Ice Cap, Ellesmere Island, Canadian Arctic; *The Musk-Ox*, v. 39, p. 119–123.

Johnsen, S.J., Clausen, H.B., Dansgaard, W., Fuhrer, K.,**Gundestrup, N., Hammer, C.U., Iversen, P., Jouzel, J., Stauffer, B., and Steffensen, J.P.**

1992: Irregular glacial interstadials recorded in a new Greenland ice core; *Nature*, v. 359, p. 311–313.

Koerner, R.M.

1979: Accumulation, ablation, and oxygen isotope variations on the Queen Elizabeth Islands ice caps, Canada; *Journal of Glaciology*, v. 22, p. 25–41.

1989: Ice core evidence for extensive melting of the Greenland Ice Sheet in the last interglacial; *Science*, v. 244, p. 964–968.

1994: Past and present contaminants in the Russian and Canadian High Arctic; Synopsis of research conducted under the 1993–1994 Northern Contaminants Program, Department of Indian Affairs and Northern Development, Environmental Studies Series no. 72, p. 62–72.

Koerner, R.M. and Fisher, D.A.

1982: Acid snow in the Canadian high Arctic; *Nature*, v. 295, p. 137–140.

1990: A record of Holocene summer melt from a Canadian High-Arctic ice core; *Nature*, v. 343, no. 6259, p. 630–631.

1995: The Greenland Ice Sheet record: insensitive to Holocene climatic change?; *Proceeding of the Wadati Conference on Global Change and Polar Climate*, Japan, 1995, p. 74–78.

Koerner, R.M. and Lundgaard, L.

1995: Glaciers and global warming; *Géographie physique et Quaternaire*, v. 49, p. 429–434.

Koerner, R.M., Alt, B.T., Bourgeois, J.C., and Fisher, D.A.

1991: Canadian ice caps as sources of environmental data; *Proceedings of International Conference on the Role of the Polar Regions in Global Change*, v. II (Fairbanks, 1990), p. 576–581.

Koerner, R.M., Bourgeois, J.C., and Fisher, D.A.

1988: Pollen analysis and discussion of time-scales in Canadian ice cores; *Annals of Glaciology*, v. 10, p. 85–91.

Koerner, R.M., Fisher, D.A., and Goto-Azuma, K.

1999: A 100 year record of ion chemistry from Agassiz Ice cap, northern Ellesmere Island, N.W.T., Canada; *Atmospheric Environment*, v. 33, p. 347–357.

Koerner, R.M., Fisher, D.A., and Parnandi, M.

1981: Bore-hole video and photographic cameras; *Annals of Glaciology*, v. 2, p. 34–38.

Koerner, R.M., Fisher, D.A., and Paterson, W.S.B.

1987: Wisconsinan and pre-Wisconsinan ice thicknesses on Ellesmere Island, Canada: inferences from ice cores; *Canadian Journal of Earth Sciences*, v. 24, p. 296–301.

Labine, C.L., Alt, B.T., Atkinson, D., Headley, A., Koerner, R.M., Edlund, S.A., and Waszkiewicz, M.

1994: High Arctic IRMA automatic weather station field data 1991–92; Geological Survey of Canada, Parts 1 and 2; Open File 2898, 52 p.

Nriagu, J.O., Lawson, G.S., and Gregor, D.J.

1994: Cadmium concentrations in recent snow and firn layers in the Canadian Arctic; *Bulletin of Environmental Contamination and Toxicology*, v. 52, p. 756–759.

Oeschger, H. and Langway, C.C. (ed.)

1989: *The Environmental Record in Glaciers and Ice Sheets*; Dahlem Workshop Reports, Berlin, 1988; John Wiley & Sons, Chichester, England, 400 p.

Peters, A.J., Gregor, D.J., Teixeira, C.F., Jones, N.P., and Spencer, C.

1995: The recent depositional trend of polycyclic aromatic hydrocarbons and elemental carbon to the Agassiz Ice Cap, Ellesmere Island, Canada; *The Science of the Total Environment*, v. 160/161, p. 167–179.

Peters, A.J., Gregor, D.J., Wilkinson, P., and Spencer, C.

1997: Deposition of ^{210}Pb to the Agassiz Ice Cap, Canada; *Journal of Geophysical Research*, v. 102(D5), p. 5971–5978.

Taylor, A.E.

1991: Holocene paleoenvironmental reconstruction from deep ground temperatures: a comparison with paleoclimate derived from the $\delta^{18}\text{O}$ record in an ice core from the Agassiz Ice Cap, Canadian Arctic Archipelago; *Journal of Glaciology*, v. 37, p. 209–219.

Walford, M.E.R. and Harper, M.F.L.

1981: The detailed study of glacier beds using radio-echo techniques; *Geophysical Journal of the Royal Astronomical Society*, v. 67, p. 487–514.

Zheng, J., Kudo, A., Fisher, D.A., Blake, E.W., and Gerasimoff, M.

1998: Solid electrical conductivity (ECM) from four ice cores, Ellesmere Island, N.W.T., Canada: high-resolution signal and noise over the last millenium and low resolution over the Holocene; *The Holocene*, v. 8, p. 413–421.

Peat accumulation and climatic change in the High Arctic

M. Garneau¹

Garneau, M., 2000: Peat accumulation and climatic change in the High Arctic; in Environmental Response to Climate Change in the Canadian High Arctic, (ed.) M. Garneau and B.T. Alt; Geological Survey of Canada, Bulletin 529, p. 283–293.

Abstract: Forty-eight peat deposits from the Hot Weather Creek basin, Fosheim Peninsula, were sampled to determine if accumulation rates were higher during certain parts of the Holocene than today. Twenty-two sections ≥ 50 cm thick with stratigraphy exposed by erosion were described and sampled. Three of these showed bryophyte accumulations ≥ 200 cm thick. Thirty-seven radiocarbon dates were obtained from these deposits.

To compare modern and Holocene rates of accumulation of organic material, 24 surface sites with criteria favourable for organic accumulation were also sampled. All had bryophyte deposits less than 40 cm thick. Modern summers on Fosheim Peninsula are too arid and continental and evaporation is too strong to enhance bryophyte accumulation in soils.

Results demonstrate that although peat accumulation was greater during the middle Holocene in the Arctic, it was not exclusive to that time. Results confirm the absence of large bryophyte deposits when all factors required for such accumulations are not present.

Résumé : On a échantillonné 48 dépôts de tourbe du bassin du ruisseau Hot Weather, péninsule Fosheim, afin de déterminer si les taux passés d'accumulation de tourbe ont été plus élevés durant certaines périodes de l'Holocène que les taux contemporains. On a décrit et échantillonné 22 sections (≥ 50 cm d'épaisseur) dont la stratigraphie a été exposée par l'érosion. Trois de ces sections présentaient des dépôts de bryophytes ≥ 200 cm d'épaisseur. On a obtenu 37 datations au radiocarbone à partir de ces dépôts.

Afin de comparer les taux contemporains d'accumulation de matériel organique avec les taux holocènes, on a également échantillonné 24 sites de surface présentant des critères favorables pour l'accumulation de matériel organique. Tous présentaient des accumulations de bryophytes inférieures à 40 cm d'épaisseur. Les étés contemporains sur la péninsule Fosheim sont trop arides et continentaux et l'évaporation y est trop forte pour favoriser l'accumulation de bryophytes dans les sols.

Les résultats démontrent que malgré que l'accumulation de tourbe ait été plus grande durant l'Holocène moyen dans l'Arctique, elle n'a pas été limitée à cette période. Ils confirment l'absence d'importants dépôts de bryophytes quand tous les facteurs requis pour une telle accumulation ne sont pas réunis.

¹ INRS-Eau, 2800, rue Einstein, C.P. 7500, Sainte-Foy, Québec G1V 4C7

INTRODUCTION

Peat accumulates when environmental conditions (principally climate and drainage) are more favourable to the accumulation of organic fragments in soils than to their decomposition. In the Canadian Arctic, the supply of water influencing wetlands development originates from atmospheric precipitation, drainage basins, and permafrost melting. The physical and mineralogical composition of surficial deposits also influence peat accumulation. The texture of a soil affects its permeability and, hence, the amount of water that infiltrates through it. Dense material such as bedrock, fine-textured soils (silt and clay), or permafrost allow only a small amount of water to penetrate, with most water remaining on the surface.

Climatic conditions favourable to the formation of wetlands are characterized by cold winters, cool summers, and low mean annual precipitation (Ovenden, 1990). In the present-day Canadian High Arctic, thermal and precipitation regimes are very low, which limits the growth of vegetation affecting peat accumulation (Tarnocai and Zoltai, 1988). Peatlands are confined to basins and seepage slopes that comprise less than 5 per cent of the landscape (Zoltai and Pollett, 1974; National Wetlands Working Group, 1988; Lafarge-England et al., 1991). Topogenous fens (Gore, 1983) in basins have peat accumulations averaging less than 0.5 m. Soligenous fens (Gore, 1983) on slopes with persistent seepage from the active layer and snowmelt have peat accumulation averaging 0.2 m. Recent studies on Ellesmere Island (Lafarge-England et al., 1991; Garneau, 1992; Gajewski et al., 1995) confirm these modern accumulation rates.

In the Hot Weather Creek area on Fosheim Peninsula, 48 peat sections were analyzed and dated during the summers of 1991 and 1992. This project was part of the multidisciplinary approach used at the High Arctic observatory to detect impacts of climatic change at arctic latitudes. Paleoecological reconstructions based on the analysis of macrofossils, radiocarbon dating, and the calculation of accumulation rates in peat sections allowed the identification and dating of environmental changes that occurred during the Holocene following postglacial emersion (<7000 BP, Hodgson et al., 1991; Garneau, 1992; Bell, 1992, 1996; Gajewski et al., 1995; Bell and Hodgson, 2000).

The objective of this paper is to demonstrate that peat accumulated during the Holocene under the influence of many factors, all of which may vary with climate. Lafarge-England et al. (1991) stated that rates of net organic accumulation varied considerably in equivalent intervals within adjacent peat deposits on northern Ellesmere Island. This variation indicates that changes in local hydrology and slope processes may have predominated over changes in microclimate. Combinations of allogenic and/or autogenic factors affecting peat accumulation in the High Arctic are discussed herein.

REGIONAL SETTING

On Fosheim Peninsula, the physiographic framework that influenced the setting and accumulation of peat deposits is found in the Hot Weather Creek basin (latitude 79°58'N, longitude 84°28'W) and surrounding area (Fig. 1). This peninsula is an unusually warm, well vegetated, intermontane region with terrain and biota highly sensitive to climatic fluctuations (Edlund and Alt, 1989). Its tundra and sedge-meadow vegetation is more dense and diverse than what would be expected at a latitude of 80°N (Hopkins, 1920; Edlund et al., 2000). A total of 140 vascular plant species are found in the Hot Weather Creek basin alone (*see* Appendix A in Edlund and Garneau, 2000), which is equal to the richness of the vegetation in the southern regions of the Queen Elizabeth Islands (Edlund et al., 1990, 2000).

The Hot Weather Creek basin covers about 130 km² and is 20 to 300 m above present sea level. This lowland sector is approximately 30 km from the Eureka weather station. Anomalously high summer temperatures (mean 5.4°C; Atmospheric Environment Service, 1982; Alt et al., 2000) make the region the garden spot of the Arctic (Porsild and Cody, 1980). Others (Bliss, 1977; Henry et al., 1986; Svoboda and Freedman, 1981; Freedman et al., 1994; Young and Woo, 2000) define the region as a polar oasis, which is a small, discrete oasis of relatively high biological productivity within the typically barren polar desert climate regime (Labine, 1994). Polar oases are locally fertile areas whose existence is due to either thermal or moisture enhancement or a combination of the two (Edlund and Alt, 1989; Labine, 1994; Edlund et al., 2000). Whether the study area actually is a polar oasis or not remains controversial, but at least it is recognized as a regional enhancement of a large-scale, warmer climate regime. The thick peat deposits described by Lafarge-England et al. (1991) north of Lake Hazen (latitude 82°N) lie in a foothills region where biotic productivity is also enhanced by warmer summer temperatures and would constitute a distinct thermal oasis as well.

On Fosheim Peninsula, moderate to well drained slopes of weathered and colluviated bedrock covered by sandy and silty deposits are colonized by an average of 40 vascular plant species, mainly *Salix arctica* and *Dryas integrifolia*. Vegetation covers over 50 per cent of the slopes. Its density is linked to drainage conditions and decreases from the base to the top of the slopes. Wetlands are common around ponds and lakes and at the heads of gullies and rivers. They are characterized by approximately 50 species of vascular plants and by bryophytes represented exclusively by mosses. Vascular-plant assemblages are dominated mainly by *Carex aquatilis* var. *stans* and *Eriophorum scheuchzeri*, accompanied by various sedges, grasses, and other herbs whose biogeographic distribution do not match the rigorous climate at latitude 80°N, such as *Hierochloa pauciflora*, *Cardamine pratense*, *Saxifraga hieracifolia*, and *Epilobium arcticum* (Edlund et al., 1990, 2000). Bryophytes are also present in these assemblages. The bottoms of shallow lakes and ponds are colonized by a mixture of aquatic and/or emergent vascular plants and bryophytes.

The dominant surface material of the Hot Weather Creek basin is weathered and colluviated bedrock and silty sands and clasts derived from poorly consolidated clastic rocks of the upper Cretaceous–lower Tertiary Eureka Sound Group (Thorsteinsson, 1971). The postglacial marine limit has been recognized at 139 m above present sea level (Hodgson, 1985; Bell, 1992, 1996; Bell and Hodgson, 2000). Marine inundation left discontinuous marine and fluvial sediments that in places are 30 m thick or more and that were dissected during a subsequent fall in base level that began at approximately 7000 BP (Hodgson, 1985; Bell and Hodgson, 2000). Marine regression exposed a landscape of low hills dissected by a network of polygons averaging 30 m in diameter. Depending on their morphology, the polygons are characterized by hummocky centres 10 to 50 cm high, by wet centres, or by the presence of water ponds.

Thermokarst ponds also develop along ice wedges and create a network for spring runoff. Several tributaries of Hot Weather Creek meander through the region. In places, fluvial processes eroded thick deposits of peat that accumulated in depressions beneath the Holocene marine limit. These deposits are dominated mainly by mosses and vascular plants among which grow sparse, low shrubs. The onset of peat accumulation followed the postglacial marine emersion of the region (Hodgson et al., 1991; Bell, 1992) and is related to a major period of peat accumulation in the Arctic (Stewart and England, 1983; Ritchie, 1984, 1987; Edlund, 1986; Ovenden, 1988, 1990).

In the Canadian Arctic, Stewart and England (1983), Ovenden (1988, 1990), and Bradley (1990) were the first to interpret peat deposits within the context of their growth and accumulation. Lafarge-England et al. (1991) and Garneau (1992) carried out detailed analyses of macrofossils from peat

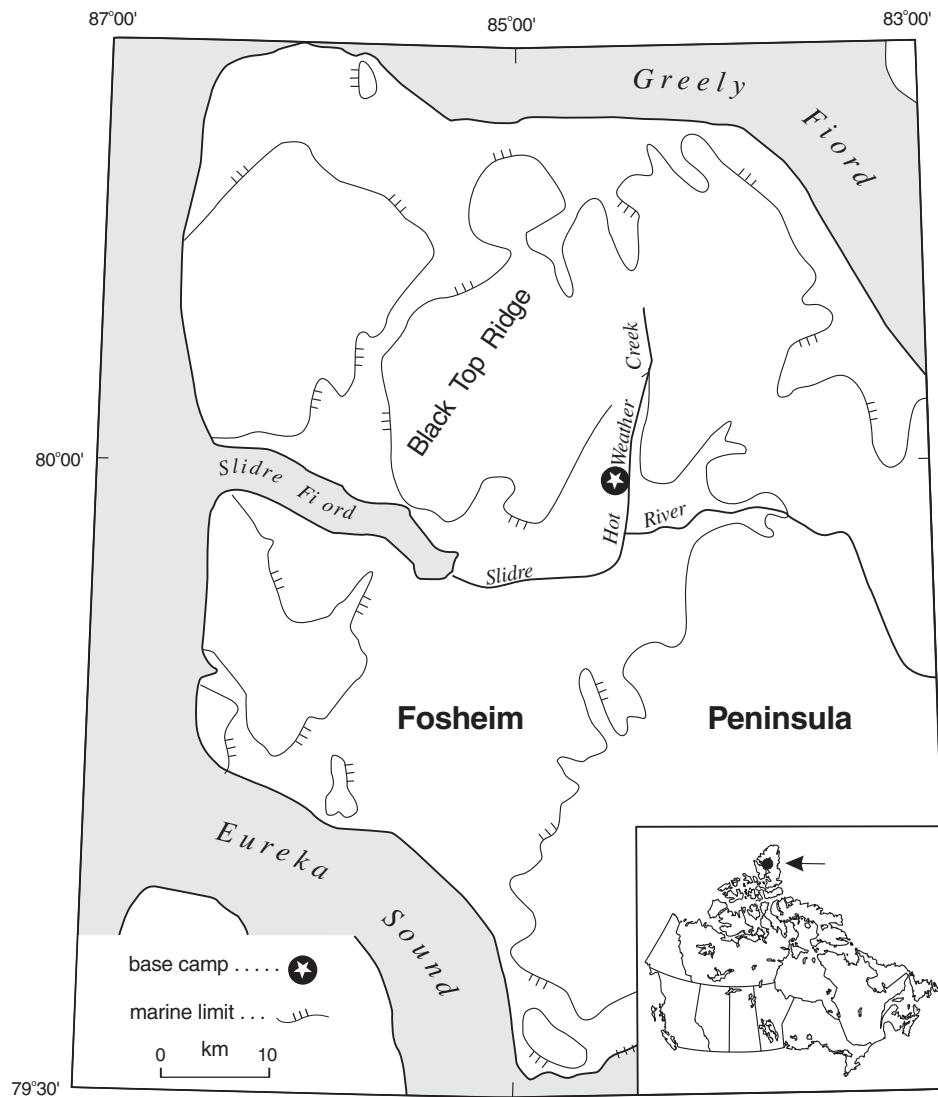


Figure 1. Hot Weather Creek basin and surrounding area.

sections 2 to 4 m thick on Ellesmere Island (between latitudes 80° and 82°N). Results from other macrofossil analyses have been published for sections at equivalent latitudes in Greenland (Fredskild, 1973, 1983, 1985; Brassard and Blake, 1978; Bennike, 1983) and Spitzbergen (Holyoak, 1984; van der Knapp, 1985, 1989; Birks, 1991). Recently, Gajewski et al. (1995) presented methodology and interpretation limits for the study of such deposits in the High Arctic.

SITE LOCATION AND DESCRIPTION OF PEAT SEQUENCES

Present-day organic accumulations are thin and locally concentrated in the Arctic Archipelago. They are restricted to saturated lowlands rich in nutrients that influence the development of fens. Concentrations of wetlands have been observed on western Banks Island, on the northeast coast of Victoria Island, on the east coast of Norwegian Bay (Graham and Cornwall islands), in the central lowlands of Bathurst Island, in lowlands in the Queen Maude Gulf, in Native Bay and on Boas Plain on Southampton Island, in the Truelove Lowlands on northern Devon Island, around Lake Hazen and on Fosheim Peninsula on Ellesmere Island, in the Murchison Lowlands on Boothia Peninsula, around Creswell Bay on Somerset Island, in some parts of Prince Charles, Spicer, Rowley, and Air Force islands, and on the Greater Plain of the Koukdjuak on southwestern Baffin Island (Tarnocai and Zoltai, 1988).

Arctic summers are currently too cold, too short, too dry, and too variable for extensive peat development (Janssens, 1990). However, thick peat deposits did accumulate through the Holocene in the Canadian Arctic. Ovenden (1988) recorded over 50 fossil deposits with thicknesses ranging from 40 to 900 cm, suggesting that past climates would have been wetter or warmer than they are now. In 17 sections in which both upper and lower peat layers have been dated, the average duration of peat growth has been estimated at 2.7 ka (Ovenden, 1988). Bradley (1990) disputed Ovenden's interpretation of climate as the cause of the onset and cessation of peat growth. He argues that a sampling bias against young peat sections makes it difficult to determine whether or not a real decline in peat accumulation occurred. He mentions that sections less than 200 cm thick and therefore younger than 2500 years (assuming from Ovenden (1988, 1990) that the mean accumulation rate was approximately 1 mm/year) have been subjectively omitted at the expense of more uncommon thick sections. Lafarge-England et al. (1991) investigated four autochthonous peat deposits on northern Ellesmere Island (latitude 82°N) with a chronology indicating a minimal age of 6410 ± 50 BP for peat accumulation and 760 ± 75 BP for the youngest section. They assumed that this variability through the Holocene indicates that changes in local hydrology and slope processes predominated over changes in microclimate.

Forty-eight peat sections (modern and fossil) were sampled on Fosheim Peninsula during the summers of 1991 and 1992 to determine whether past rates of accumulation were greater during certain periods of the Holocene than they are at

present. A total of 22 sections with thicknesses ≥ 50 cm (Fig. 2, sites 1 to 22) that have been exposed by erosion were described and sampled. Three of these (sites 5, 6, and 21) had accumulations ≥ 200 cm thick (bryophyte peat dominated by *Drepanocladus* sp., *Calliargon* sp., and *Scorpidium* sp.). Sites 5 and 6 were sampled from eroded sections in a polygon field southeast of Ridge Lake. Detailed macrofossil analyses indicated a predominance of bryophytes whose density increases then progressively decreases from the base to the top of the section. A series of mineral horizons throughout the deposit indicate recurrent eolian or alluvial activity during peat accumulation (Garneau, 1992; Gajewski et al., 1995). Different levels of these sections have been radiocarbon dated with ages ranging from approximately 7500 to 4000 BP for the 2.85 m (site 5) and 2.35 m (site 6) thick accumulations of organic material (Table 1).

Site 21 presents a 2.05 m section exposed by fluvial erosion of a polygon field. A basal age of 12 750 BP ($12\,750 \pm 240$ BP) has been obtained from sedge remnants. An environment

Table 1. Radiocarbon dates from Fosheim Peninsula. Site locations are shown in Figure 2.

Site	Depth (cm)	Age (¹⁴ C years BP)	Laboratory number
4	surface	4940 ± 80	Beta-51990
	50–30	3870 ± 80	UL-1004
	58–61	2510 ± 70	GSC-5575
	85–88	3210 ± 110	UL-1036
	100–103	2700 ± 70	GSC-5577
	120–125	3140 ± 110	GSC-5586
5	135–138	3860 ± 80	Beta-51989
	surface	3850 ± 80	Beta-51994
	surface	4990 ± 70	TO-3037
	20–23	4500 ± 70	TO-3038
	45–48	3930 ± 80	GSC-5547
	100–103	4310 ± 80	GSC-5554
	148–151	4900 ± 70	GSC-5570
	285–288	7910 ± 120	GSC-5066
	300	5070 ± 70	TO-3039
	10–12	4850 ± 80	UL-1012
6	35–42	4590 ± 60	Beta-77036
	51–58	6430 ± 50	Beta-77037
	75–78	4860 ± 80	Beta-77033
	163–165	4970 ± 60	Beta-77034
	173–178	4840 ± 100	Beta-77035
13	20–23	930 ± 60	TO-3040
	50–53	1890 ± 80	Beta-51993
	110–113	2650 ± 70	Beta-51992
	150–153	2930 ± 60	GSC-5137
19	surface	6250 ± 70	TO-2677
	surface	1910 ± 60	GSC-5280
	180–183	5830 ± 100	Beta-51988
	200–203	5420 ± 100	UL-1009
	280–283	7120 ± 80	GSC-5180
21	35–38	5560 ± 80	UL-1006
	90–93	7910 ± 100	UL-1007
	95–98	9220 ± 140	UL-1008
	180–183	9260 ± 130	UL-1037
	190–193	12 750 ± 240	UL-1005
	surface	7680 ± 70	Beta-62286
Ridge Lake (raised beach)	surface	7420 ± 100	GSC-5549

dominated by *Drepanocladus* sp. followed this herb meadow at about 10 000 BP and lasted until 7000 BP. Macrofossil analyses indicate that there was a recurrence of herb and sedge assemblages between 7000 and 6000 BP, followed by bryophyte assemblages at 6000 BP (5560 ± 80 BP); the bryophyte cover underwent fluvial erosion approximately 500 years later and peat growth stopped at the site. In the same polygon field, approximately 30 m east of site 21, site 22 presents a totally different stratigraphy over a 100 cm core. The deposit is of mostly mineral composition, with mixed herb layers 10 cm thick or less.

The other sampled sections have bryophyte accumulations under 200 cm thick (Fig. 2). Site 1 is characterized by organic sections 100 to 150 cm thick exposed by fluvial erosion of a polygon field. A radiocarbon age of 4120 ± 60 BP was obtained by Edlund (Hodgson et al., 1991) from an organic layer composed of sedge and grass fragments at a depth of approximately 200 cm. An adjacent section (site 2)

was sampled during the summer of 1991 and has an equivalent stratigraphy at a depth of 200 cm with sedge fragments at its base. At a depth of between 85 and 60 cm, herb fragments were mixed in a silty-sandy matrix. A moss-dominated horizon (mainly *Calliergon* sp. and *Drepanocladus* sp.) overlies the unit. The end of peat growth is associated with fluvial erosion of the polygon field at approximately 500 BP (radiocarbon years extrapolated).

Site 3 was also sampled by Edlund (Hodgson et al., 1991); sedge fragments from a depth of 110 cm provide an age of 4870 ± 70 BP. From bottom to top, the section is characterized by 60 cm of sedge debris overlain by 30 cm of bryophytes (mainly *Drepanocladus* sp.). An age of 500 BP has been extrapolated and marks the end of peat growth, probably as a result of fluvial erosion into the polygon field. At site 4, 2.5 km from the base camp, a fluvial valley eroded another polygon field and exposed organic sections up to 135 cm thick. A sampled sequence studied in 1992 indicates a basal

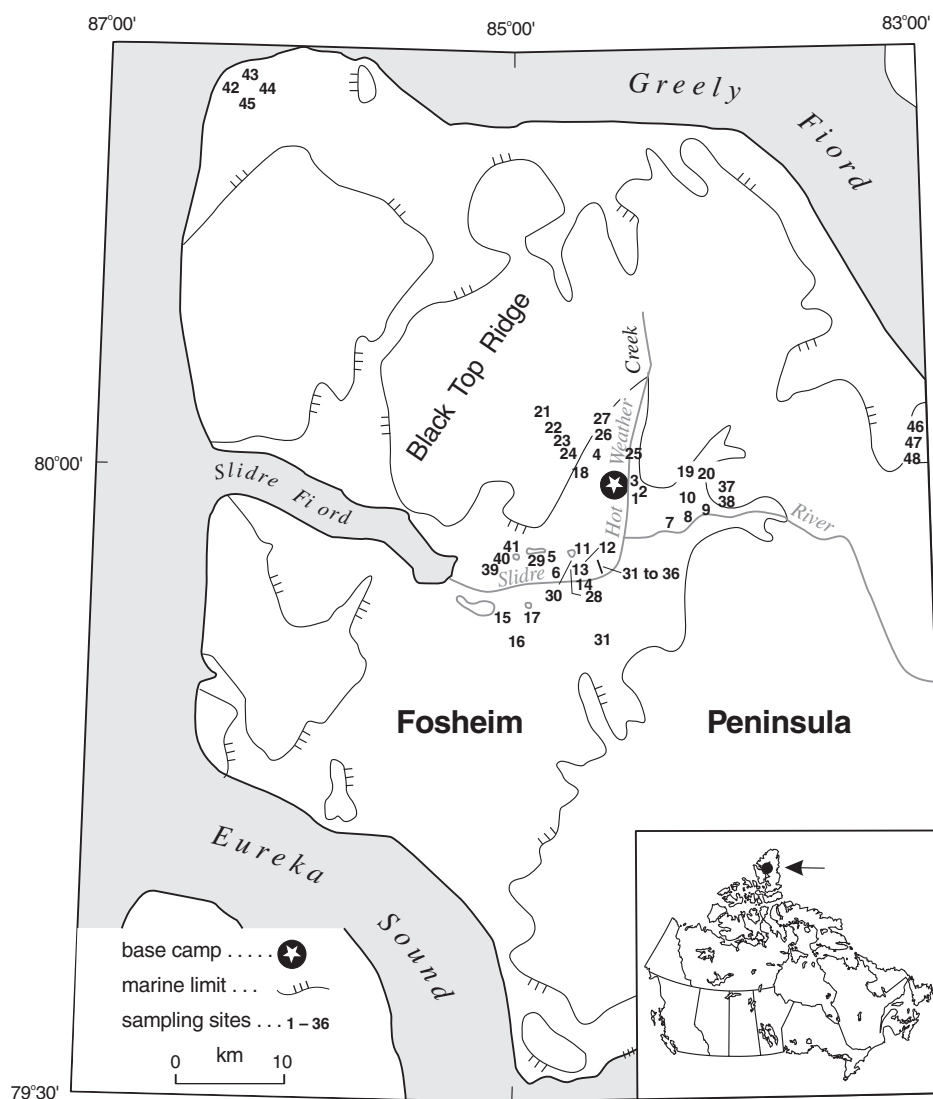


Figure 2. Location of the sampled peat deposits.

horizon dominated by herb fragments mixed in a silty matrix and dated at 3860 ± 80 BP. This horizon is covered by a moss horizon (mainly *Drepanocladus* sp.) 55 cm thick. Three other layers give radiocarbon ages of 3140 ± 70 BP at 125 to 120 cm, 2700 ± 70 BP at 103 to 100 cm, and 2510 ± 70 BP at 61 to 58 cm; peat growth is estimated to have stopped at 1500 BP due to fluvial erosion in or through the polygon field.

Four other sites (sites 7, 8, 9, and 10) were sampled from natural sections along the Slidre River. Steep slopes expose stratigraphy showing fossil polygon networks with organic accumulations between 75 and 55 cm thick. These organic horizons are composed mainly of herbs with sparse bryophytes or *Salix* fragments. Fortier et al. (1963) described equivalent sites and linked them to pre-Holocene dynamics. Two of these four sites showed marks of earlier sampling, although nothing confirmed that they were the sites mentioned by Fortier et al. (1963). Should they be the sites, then these authors' interpretation of pre-Holocene sites is erroneous, since buried organic layers are produced by surface subsidence following headwall retreat due to melting of polygon ice wedges. Pollen analyses by Terasmae (*in* Fortier et al., 1963) provide results equivalent to our previous studies (Garneau, 1992; Gajewski et al., 1995) with abundant Quaternary and Tertiary tree pollen and spores eroded from regional geological formations. Contamination due to weathering or erosion was mentioned to explain the presence of such pollen and spores in Holocene peat sections, as is observed elsewhere in the Arctic (Boulton et al., 1976; Pissart et al., 1977; Andrews et al., 1979). The species identified are *Picea*, *Pinus*, *Betula*, *Quercus*, *Ulmus*, *Fraxinus*, *Alnus*, *Myrica*, and some ericaceous taxa.

Less than 1 km south-southwest of Coal Lake and Ridge Lake, a valley created by a former Ridge Lake spillway (Garneau, 1992) is now covered by a polygon field. The surface vegetation is dominated by grasses and sedges with *Eriophorum* sp., Scrophulariaceae, *Dryas integrifolia*, *Luzula* sp., and *Pedicularis* sp. Four sampled sections (sites 11, 12, 13, and 14) showed organic accumulations 150 to 500 cm thick. Two of these sections (sites 11 and 12) were sampled using a SIPRE corer and a third (site 13), with a chainsaw. Sampling of the 500 cm section (site 14) exposed downvalley at the confluence of Hot Weather Creek was facilitated by the fact that the entire section is exposed on one slope. The botanical composition of these four sections is characterized by the predominance of herb fragments and the absence of bryophytes as observed on the present-day surface. The sequence chronology of site 13 has been described by Garneau (1992) and an age of 2930 ± 60 BP was obtained at its base.

Three other sampled sites (sites 15, 16, and 17) around Romulus Lake had no thick organic deposits. Along a 10 km northeast-southwest transect from Romulus Lake to Lake 1 (Hamilton et al., 2000), many sections exposed by fluvial erosion were investigated, but no thick deposits were observed.

Two landslide scars were also sampled (sites 18 and 19). At site 18, the landslide created a 1 km scar in a polygon field where many organic horizons up to 35–40 cm thick were exposed. Five of these sections were sampled, but none were

radiocarbon dated. A mineral horizon approximately 20 cm thick overlies the organic sequences. The organic horizons are composed of a mixture of herbs and bryophytes, with herbs dominating. Peat growth likely stopped when the landslide occurred. Site 19 is characterized by a large, 8 km scar from an old landslide. A residual polygon section from around the scar was sampled and dated. Wall subsidence disrupted stratigraphy as shown by alternating mineral and organic horizons over 300 cm thick. A basal age of 712 ± 80 BP was obtained from sedge fragments (Y. Michaud, C. Bégin, and M. Garneau, unpub. rept., 1992) and a radiocarbon age of 5420 ± 100 BP, from herb fragments from a depth of 200 cm. Radiocarbon age inversions are explained in part by the disturbance of horizons in this section (Gajewski et al., 1995). An age of 2580 ± 60 was obtained from a polygon surface (site 20) near this residual core and probably marks the end of peat accumulation (which reached a thickness of over 50 cm) following the landslide.

To compare modern and Holocene rates of organic accumulation, 24 surface sites (sites 23 to 47) that showed favourable criteria for organic accumulation were sampled from near Hot Weather Creek to the Sawtooth Range. Site 23 is a depression created by the melting of an ice wedge between two polygons. The vegetation is characterized by *Carex* sp., *Eriophorum triste*, and *Pleuropogon sabinei*. The accumulation of organic matter in the profile does not exceed 10 cm at this site. A saturated polygon network at site 24 reveals organic accumulations on the mineral surface that do not exceed 20 cm. Surface vegetation comprises *Equisetum* sp., *Dupontia fisheri*, *Alopercurus alpinus*, *Carex aquatilis* var. *stans*, *Eriophorum triste*, and *E. scheuzeri*. Sites 25 and 26 are valley bottoms produced by the erosion of polygon fields. At site 25, seepage water carrying nutrients favoured the development of a fen in which 30 to 40 cm of organic material accumulated on the mineral surface. Vegetation in ponds (site 27) created by the melting of ice wedges is dominated by *Hygrohypnum* mosses rooted through a 5 cm thick organic horizon.

The polygon field at the modern Ridge Lake level (site 28) is characterized by saturated drainage conditions. Surface vegetation is dominated by *Deschampsia ceaspitosa* sp. *braevifolia*, *Alopercurus alpinus*, *Arctagrostis latifolia*, *Carex aquatilis*, *C. maritima*, *Eriophorum scheuzeri*, *E. triste*, *Kobresia myosuroides*, *Juncus biglumis*, *Saxifraga hirculis*, and *Equisetum variegatum*, as well as by *Salix arctica* and *Dryas integrifolia* in well drained areas. The first terrace level surrounding the lake (site 29) is also covered by polygons where sedges and grasses grow over an organic horizon under 30 cm thick. The topography along the south shore of the lake is similar to that of organic lawns, but with less than 30 cm of organic material over the mineral substrate. Around Coal Lake (site 30), saturated, low-centred, ice-wedge polygons seem to be the modern analogs of the polygons that were downcut by the early Ridge Lake spillway and in which over 2 m of peat accumulated approximately 6000 years ago (sites 5 and 6). Most low-centered polygons developed into ponds colonized by *Hippuris vulgaris* and *Ranunculus aquatilis* var. *eradicatus*. A survey of surface vegetation was carried out along a 250 m transect and five

sites (sites 31 to 35) with different drainage conditions (from saturated to well drained) were cored. None of the five cores showed organic deposits over 30 cm thick. Two of the five were taken to a depth of over 1 m (sites 33 and 34) in an unsuccessful attempt to detect the recurrence of organic horizons. The banks of Coal Lake, like those of Ridge Lake, are surrounded by organic lawns (site 36) that were also sampled. Results show organic horizons 20 to 30 cm thick over the mineral surface.

Drowned polygons around Gemini Lake (site 37) and lake 11 (site 38) (Hamilton et al., 2000) were also sampled, but none had organic deposits over 25 cm thick. These horizons are characterized from base to top by a 5 cm layer composed of herb debris and woody fragments of *Salix* sp., overlain by a 20 cm thick bryophyte mat (mainly *Drepanocladus* sp.). Lakes 13 (site 39), 22 (site 40), and 23 (site 41) (Hamilton et al., 2000) were also sampled in areas with characteristics favourable for peat accumulation. Each of these three sites had organic deposits over 30 cm thick. These same conditions are found at sites 42 to 45 (Iceberg Point), where recent polygons had accumulations of organic material (mainly herbs) 15 to 25 cm thick. In the foothills of the Sawtooth Range (sites 46, 47, and 48), organic material (mainly mosses) accumulated at a line of lakes under saturated drainage conditions favourable to fen development and the accumulation of large quantities of organic material. Coring through these profiles revealed accumulations less than 30 cm thick.

DISCUSSION

Results from the sampling of 48 peat deposits on Fosheim Peninsula show the wide variations in rates of peat accumulation during the Holocene and, hence, the necessity of considering a combination of autogenic and allogenic factors to explain the presence and persistence of these deposits. Earlier studies in the Arctic (Tarnocai, 1978; Stewart and England, 1983; Ritchie, 1984, 1987; Edlund, 1986; Ovenden, 1988; Tarnocai and Zoltai, 1988) suggested that high rates of peat accumulation during the early to middle Holocene were associated with warmer and wetter climate conditions, which agrees with the interpretation of the results of various proxy data (Blake, 1972, 1989; Harington, 1975; Stewart and England, 1983; Hyvarinen, 1985; Bednarski, 1990; Bradley, 1990). Seppälä et al. (1991) and Bradley (1990) associated the accumulation of peat with the duration of a complete tundra polygon cycle during which peat accumulates in a waterlogged environment, then is lifted and exposed, resulting in the cessation of peat formation. Bradley agreed with these assumptions without considering the range of thicknesses of past peat accumulations compared with present-day values. Ovenden (1990) assessed the effect of climate on peat accumulation in Canada, but concentrated more on boreal and subarctic than on arctic peatlands. She presents mean accumulation rates of between 0.23 and 0.7 mm/year, except for the Arctic Archipelago, where rates were estimated at over 1 mm/year. She associates these high rates with high ice or mineral sediment contents in the dated organic deposits. Calculations of net

organic accumulation (NOA) as done by Lafarge-England et al. (1991) will be essential in future studies to determine real rates of accumulation at these latitudes.

As observed through our results, many stratigraphic changes in peat deposits are probably due to site-specific development (buildup of polygons), whereas those that occurred simultaneously in many basins in a region (e.g. rise in eolian activity) probably reflect climatic change. The vegetation succession identified in the sections shows alternating layers dominated by herbs or mosses, which can be associated with the colonization of ponds or polygons (bottoms or edges). Even though gross organic accumulation (GOA) and bulk density were not calculated and no sand and ice layers were observed in the horizons, we can confirm that the large thickness of peat has no modern analog. The hypothesis of tundra polygon cycles is to be considered, except that allogenic factors such as moisture regime (runoff, atmospheric precipitation, and ground-ice melting) probably influenced the rate of accumulation in the past.

All sites sampled on Fosheim Peninsula with bryophyte accumulations over 50 cm thick gave radiocarbon ages between 7500 and 2500 BP (Table 1). In general, the duration of accumulation calculated from two or more radiocarbon ages is between 1500 and 3000 years. Rates of accumulation for several peat deposits sampled on Fosheim Peninsula exceed 1 mm/a during the middle Holocene (sites 5 and 6). For the Grant Land Mountain area (latitude 82°N), Lafarge-England et al. (1991) calculated a net organic accumulation of peat of between 0.4 and 2.6 mm/year and a gross organic accumulation of peat of between 0.5 and 3.8 mm/year for four deposits composed mainly of bryophytes and with radiocarbon ages between 6410 ± 50 BP and 760 ± 75 BP. This sector was first studied by Lafarge-England (1989) and then by Lafarge-England et al. (1991) and has particular physiographic characteristics. It is subject to orographic precipitation that moderates the surrounding polar desert. It is located in a valley between the Hazen Plateau to the south and the glaciated Grant Land Mountains to the north and east. Glacier runoff is a source of moisture, which explains the presence of large, surficial bryophyte assemblages. Lafarge-England (1989) stated that slope gradient and soil moisture were the most important factors influencing the distribution of moss assemblages. Contrary to what was observed on Fosheim Peninsula, the four deposits studied by Lafarge-England et al. (1991) are also associated with seepage slopes that were sufficient steep to allow saturated conditions in specific areas where large bryophyte deposits accumulated. Even if climate were not the key element that influenced peat accumulation, moisture sources are directly related to climate through melting of permafrost, runoff, and atmospheric precipitation.

Our studies show that peat accumulation is associated with particular climatic conditions (Edlund and Alt, 1989; Alt and Maxwell, 1990, 2000). Fosheim Peninsula's favourable present-day summer climate is a direct result of its topographic setting in which surrounding highlands prevent the incursion of cold Arctic Ocean air masses and cyclonic activity from Baffin Bay (Edlund and Alt, 1989; Alt and Maxwell, 1990). Soil moisture traditionally associated with

atmospheric precipitation and spring runoff is due mainly to melting ground ice, which influences the present-day vegetation dynamics (growth and distribution); this influence was probably stronger when temperatures were warmer (up to 2.5° C; Koerner and Fisher, 1990).

During the last glaciation, the Eureka Sound intermontane region on Fosheim Peninsula remained ice-free because climatic hyperaridity (Edlund and Alt, 1989) prevented extensive ice buildup (England, 1987; Lemmen, 1989). However, ice caps grew at lower elevations, reflecting specific meteorological conditions in the region (Bell, 1996). The retreat of local ice caps was delayed, even through the warmest period of the Holocene (between 11 000 and 8000 BP), and led to positive or at most slightly negative glacier mass balance. High summer temperatures reduced the sea-ice cover on marine channels, thereby increasing moisture available for summer fog and early winter snowfall (Koerner, 1977). Sea level remained high until 8700 BP or later. Marine inundation produced a large, shallow bay in the heart of the peninsula that, sea-ice conditions permitting, likely imparted a strong maritime influence on local climate, with increased precipitation and summer fog. A combination of these climatic parameters probably influenced the growth of bryophytes at specific sites that were topographically suitable for the accumulation of mosses and that lack modern analogs, for example a depression south of the early Ridge Lake (sites 5 and 6: 2.85 m and 2.35 m thick) where peat accumulation began following postglacial marine emergence (approximately 7000 BP; Hodgson, 1985). The physiographic context suggests that peat accumulated initially in an open meadow dominated by sedges and grasses that record a pioneer stage following emersion. This meadow was modified subsequently by the formation of a low-centred polygon. Bryophytes colonized the wet depression and a peat deposit over 2.5 m thick developed between 7000 and 4000 BP (Garneau, 1992). On Norvesto Island, one of the Carey Islands of northwestern Greenland, Brassard and Blake (1978) found a 2.6 m thick peat deposit composed mainly of a single moss species, *Aplodon wormskioldii*. Radiocarbon ages from the base (6300 ± 80 BP) and the top (4390 ± 180 BP; 15–18 cm deep) of this deposit indicate a mean accumulation rate of 1.3 mm/year in less than 2000 years during this warmer and probably wetter period. The analysis of microfossils (diatoms and cysts of Chrysophyceae) from this section (Brown et al., 1993) shows interesting trends in the peat stratigraphy that indicate that paleoecological conditions were not uniform during the 2000 years of accumulation. At 5000 BP, the peat was wetter because of increased snow accumulation or wetter summers (Brown et al., 1993), or possibly because of local polygon transformation with ice-wedge growth, since the section was cored from a polygon field. Hattersley-Smith and Long (1967) also found a 2 m thick organic deposit on Tanquary Fiord (northern Ellesmere Island) that gave a basal age of 6480 ± 200 BP (SI-468).

Other proxy data summarized by Bradley (1990) confirm these high summer temperatures in the early to middle Holocene. Stewart and England (1983) mentioned an increase in plant productivity between 6000 and 4200 BP. Björck and Persson (1981) reported a similar increase in

vegetation productivity in Greenland between 6000 and 5000 BP followed by a decrease in productivity. Increased plant productivity has also been noted from the analysis of lake cores (Wolfe, 2000; Douglas et al., 2000) in which diatom concentrations were higher at 6000 BP and fell progressively until the nineteenth century. Blake (1989) mentioned the presence of the green algae *Mougeotia* sp. at 5730 ± 70 BP (TO-530) at Rundfjeld Mountain, Ellesmere Island, which indicates that the lake was probably completely open for an unspecified period of time during the warmest part of the middle Holocene, which also corresponds to the period of maximum reduced sea ice where a greater expanse of open water due to summer warmth has influenced moisture and atmospheric precipitation. This increased humidity might also explain the existing lag between maximum pollen concentration in ice cores and peak plant productivity, since precipitation inhibits the transportation of pollen in the atmosphere (Bourgeois et al., 2000). This increased moisture balance has also been interpreted by Bell (1996) from high marine sedimentation rates between 5900 and 4000 BP that were associated with increased runoff from snowmelt that eroded emerging marine sediments. Evidence for warmer conditions in the early to middle Holocene is also recorded in $\delta^{18}\text{O}$ values from ice cores from the Agassiz and Devon ice caps. Summer climate has deteriorated over the last 3.5 ka (Bradley, 1990). There has been a pronounced 1.5 to 2 per cent decrease in $\delta^{18}\text{O}$ values in all ice cores from the Agassiz and Devon ice caps. The melt record from the Agassiz ice core indicates a decrease in summer temperatures since 5000 BP and especially after 2000 BP. Ice cores reveal a cooling trend with warmer intervals over the past 4500 years, with a negative mass balance between approximately 2500 BP and 660 BP. Despite this late Holocene cooling trend these climate variations in specific areas could explain the persistence of bryophyte accumulations recognized by Lafarge-England et al. (1991) on northern Ellesmere Island (latitude 82°N) where they calculated accumulation rates from 0.4 to 2 mm/year between 5000 and 700 BP.

Unlike the results of Lafarge-England et al. (1991), results from Fosheim Peninsula do not indicate that a major phase of peat accumulation occurred as climate deteriorated. The maximum thickness of organic deposits from 5000 to 2000 BP does not exceed 55 to 65 cm and accumulation rates average 0.15 to 0.55 mm/year. At site 13, peat accumulation began at 2930 ± 60 BP and the deposit is composed mostly of sedge peat. Three other sections (sites 11, 12, and 14) were cored near site 13 in areas where surface conditions seemed favourable to peat accumulation, but no organic deposit over 30 cm thick was found. This decrease in accumulation rates of organic material matches the cooling and drying trends now observed in the region (Alt and Maxwell, 1990, 2000). Cooling culminated with the Little Ice Age at approximately 400 BP, as recorded in the ice cores (ca. 400–100 BP), and was followed by marked warming during the first half of the twentieth century. Peat accumulation stopped under the influence of increased fluvial erosion of polygon fields during the late Holocene. Contacts between organic horizons and overlying mineral sequences can be seen clearly. These mineral horizons represent increased eolian processes associated with increased aridity in the region (Lewkovicz, 1991).

None of the 19 recent peat deposits surveyed on Fosheim Peninsula had bryophyte accumulations over 40 cm thick. The growth of bryophytes at the present-day surface has probably been influenced by the warming trend of the first half of the twentieth century as the moisture required likely originates from the summer melting of massive ground ice. Otherwise conditions on Fosheim Peninsula are too arid and continental and summer evaporation is too strong (Alt and Maxwell, 1990) to permit thick accumulations of bryophytes in soils. On north-central Ellesmere Island (Lake Hazen, Tanquary Fiord, and southern Piper Pass), 114 to 125 different species of surface mosses have been identified (Brassard, 1971, 1976; Lafarge-England, 1989) in sectors where moisture sources (atmospheric and soil moisture) are enhanced particularly by the presence of glaciers. Physiographic and climatic conditions in these sectors are more favourable even today to the accumulation of bryophytes and probably explain the production of such accumulations even during the cooling period following the middle Holocene.

CONCLUSIONS

Results from this study demonstrate that even though peat accumulation in the Arctic was greater during the middle Holocene, it did not occur exclusively during that time. Hence, results described by Tarnocai (1978), Stewart and England (1983), Ovenden (1988), and even Bradley (1990) need to be qualified. Ovenden (1990) and Lafarge-England et al. (1991) integrated net organic accumulation calculations in order to discuss peat accumulation rates in the Arctic. By integrating different environmental processes, we can understand the global dynamics that influenced this accumulation of organics during certain parts of the Holocene in the High Arctic. First, as mentioned by Bradley (1990), bryophyte accumulation likely depends on the internal dynamics of polygons and is then associated with a combination of cold-region geomorphic processes. Indeed, at almost every site for which radiocarbon dates were obtained from the top and the base of a deposit, the duration of peat accumulation was estimated at between 1000 and 3000 years, which corresponds to values presented by Seppälä et al. (1991). More detailed stratigraphic analyses of deposits indicate the successive development of ponds and high banks (Garneau, 1992). However, conditions for the accumulation of over 2 m of peat require a combination of several favourable environmental factors such as a rise in summer temperatures and a source of moisture (atmosphere, runoff, and ground-ice melt). Contrary to what Bradley (1990) thought, a global reduction in peat growth did indeed occur with late Holocene cooling and there was no sampling bias against young peat sections. Spectacular sections 200 to 900 cm thick were exposed by fluvial erosion of polygon ice wedges in the Arctic Archipelago. Our coring results confirm the absence of large bryophyte deposits in areas where all the elements required for such an accumulation are absent. The Little Ice Age cooling seems to have been a determining factor for peat accumulation in the Arctic, as climate conditions since have been too cold, too dry, and too varied to allow for extensive peat development (Janssens, 1990) and accumulation.

Because of the absence of peat accumulation in the present-day Arctic, there is a need for the development of transfer functions using surface bryophyte calibration sets. A potential advantage of using peat profiles as paleoecological archives is that even at these latitudes, peat accumulated much faster than lake sediments. Peat profiles can therefore provide stratigraphic information at a much finer temporal resolution than paleolimnological studies once the different limits of interpretation have been recognized (Gajewski et al., 1995).

REFERENCES

- Alt, B.T. and Maxwell, B.**
1990: The Queen Elizabeth Islands: a case study for arctic climate data availability and regional climate analysis; *in* Symposium on the Canadian Arctic Islands, Canada's Missing Dimension, (ed.) C.R. Harington; National Museum of Natural Science, Special Publication, p. 294–326.
- 2000: Overview of the modern arctic climate; *in* Environmental Response to Climate Change in the Canadian High Arctic, (ed.) M. Garneau and B.T. Alt; Geological Survey of Canada, Bulletin 529.
- Alt, B.T., Labine, C.L., Atkinson, D.E., Headley, A.N., and Wolfe, P.M.**
2000: Automatic weather station results from Fosheim Peninsula, Ellesmere Island, Nunavut; *in* Environmental Response to Climate Change in the Canadian High Arctic, (ed.) M. Garneau and B.T. Alt; Geological Survey of Canada, Bulletin 529.
- Andrews, J.T., Webber, P.J., and Nichols, H.**
1979: A late Holocene pollen diagram from Pangnirtung Pass, Baffin Island, N.W.T., Canada; *Review of Palaeobotany and Palynology*, v. 27, p. 1–28.
- Atmospheric Environment Service**
1982: Canadian Climate Normals 1951–1980: Temperature and Precipitation. The North: Yukon Territory—Northwest Territories; Environment Canada, Downsview, Ontario, 55 p.
- Bednarski, J.**
1990: An early Holocene Bowhead whale in Nansen Sound, Canadian Arctic Archipelago; *Arctic*, v. 43, p. 50–54.
- Bell, T.**
1992: Glacial and sea level history, western Fosheim Peninsula, Ellesmere Island, Arctic Canada; Ph.D. thesis, University of Alberta, Edmonton, Alberta, 172 p.
- 1996: The last glaciation and sea level history of Fosheim Peninsula, Ellesmere Island, Canadian High Arctic; *Canadian Journal of Earth Sciences*, v. 33, p. 1075–1086.
- Bell, T. and Hodgson, D.A.**
2000: Quaternary geology and glacial history of Fosheim Peninsula, Ellesmere Island, Nunavut; *in* Environmental Response to Climate Change in the Canadian High Arctic, (ed.) M. Garneau and B.T. Alt; Geological Survey of Canada, Bulletin 529.
- Bennike, O.**
1983: Palaeoecological investigations of a Holocene peat deposit from Vlvedal, Peary Land, North Greenland; *Rapport Grønlands Geologiske Undersøgelse*, v. 115, p. 15–20.
- Birks, H.H.**
1991: Holocene vegetational history and climatic change in west Spitsbergen — plant macrofossils from Skardtjarna, an Arctic lake; *The Holocene*, v. 1, p. 209–218.
- Björk, S. and Persson, T.**
1981: Late Weichselian and Flandrian biostratigraphy and chronology from Hochstetter Forland, northeast Greenland; *Meddelelser om Grønland, Geoscience*, v. 5, p. 19.
- Blake, W., Jr.**
1972: Climatic implications of radiocarbon-dated driftwood in the Queen Elizabeth Islands, Arctic Canada; *in* Climatic Changes in Arctic Areas During the Last Ten Thousand Years, (ed.) Y. Vasari, H. Hyvarinen, and S. Hicks; Proceedings of a symposium held at Oulanka and Kevo, Finland, October 1971; *Acta Universitatis Ouluensis*, ser. A, *Scientiae Rerum Naturalium*, No. 3, *Geologia* No. 1, p. 1025–1042.

Blake, W., Jr. (cont.)

1989: Inferences concerning climatic change from a deeply frozen lake on Rundfjeld, Ellesmere Island, Arctic Canada; *Journal of Paleolimnology*, v. 2, p. 41–54.

Bliss, L.C. (ed.)

1977: Truelove Lowland, Devon Island, Canada: a high Arctic ecosystem; University of Alberta Press, Edmonton, Alberta, 714 p.

Boulton, G.S., Dickson, J.H., Nichols, H., Nichols, M., and Short, S.

1976: Late Holocene glacier fluctuations and vegetation changes at Maktak Fjord, Baffin Island, N.W.T., Canada; *Arctic and Alpine Research*, v. 8, p. 343–356.

Bourgeois, J.C., Koerner, R.M., Fisher, D.A., and Alt, B.T.

2000: Present and past environments inferred from Agassiz Ice Cap ice-core records; in *Environmental Response to Climate Change in the Canadian High Arctic*, (ed.) M. Garneau and B.T. Alt; Geological Survey of Canada, Bulletin 529.

Bradley, R.S.

1990: Holocene paleoclimatology of the Queen Elizabeth Islands, Canadian High Arctic; *Quaternary Sciences Review*, v. 9, p. 365–384.

Brassard, G.R.

1971: The mosses of northern Ellesmere Island, Arctic Canada, with an analysis for the Queen Elizabeth Islands; *The Bryologist*, v. 74, p. 234–281.

1976: The mosses of northern Ellesmere Island, Arctic Canada. III. New or additional records; *The Bryologist*, v. 79, p. 480–487.

Brassard, G.R. and Blake, W., Jr.

1978: An extensive subfossil deposit of the arctic moss *Aplodon wormskioldii*; *Canadian Journal of Botany*, v. 56, p. 1852–1859.

Brown, K.M., Douglas, M.S.V., and Smol, J.P.

1993: Siliceous microfossils in a Holocene, High Arctic peat deposit (Nordvestø, northwest Greenland); *Canadian Journal of Botany*, v. 72, p. 208–216.

Douglas, M.S., Smol, J.P., and Blake, W., Jr.

2000: Summary of paleolimnological investigations of High Arctic ponds at Cape Herschel, east-central Ellesmere Island, Nunavut; in *Environmental Response to Climate Change in the Canadian High Arctic*, (ed.) M. Garneau and B.T. Alt; Geological Survey of Canada, Bulletin 529.

Edlund, S.A.

1986: Modern Arctic vegetation distribution and its consequence with summer climate patterns; *Proceedings of a Canadian Climate Program Workshop*, March 3–5, Ontario, p. 84–99.

Edlund, S.A. and Alt, B.T.

1989: Regional congruence of vegetation and summer climate patterns in the Queen Elizabeth Islands, Northwest Territories, Canada; *Arctic*, v. 42, no. 1, p. 3–23.

Edlund, S.A. and Garneau, M.

2000: Overview of vegetation zonation in the Arctic; in *Environmental Response to Climate Change in the Canadian High Arctic*, (ed.) M. Garneau and B.T. Alt; Geological Survey of Canada, Bulletin 529.

Edlund, S.A., Alt, B.T., and Garneau, M.

2000: Vegetation patterns on Fosheim Peninsula, Ellesmere Island, Nunavut; in *Environmental Response to Climate Change in the Canadian High Arctic*, (ed.) M. Garneau and B.T. Alt; Geological Survey of Canada, Bulletin 529.

Edlund, S.A., Woo, M.-k., and Young, K.L.

1990: Climate, hydrology and vegetation patterns, Hot Weather Creek, Ellesmere Island, Arctic Canada; *Eighth International Northern Research Basins, Symposium and Workshop*, v. 1, Abisko, Sweden, 14 p.

England, J.

1987: Glaciation and the evolution of the Canadian High Arctic landscape; *Geology*, v. 15, p. 419–424.

Fortier, Y.O., Blackadar, R.G., Glenister, B.F., Grenier, H.R., McLaren, D.J., McMillan, N.J., Norris, A.W., Roots, E.F., Souther, J.G., Thorsteinsson, R., and Tozer, E.T.

1963: Geology of the north-central part of the Arctic Archipelago, Northwest Territories (Operation Franklin); Geological Survey of Canada, Memoir 320, 671 p.

Fredskild, B.

1973: Studies in the vegetational history of Greenland; *Meddelelser om Grnland*, v. 198, no. 4, 245 p.

1983: The Holocene vegetational development of the Godthåbsfjord area, west Greenland; *Meddelelser om Grnland, Geoscience*, v. 10, p. 1–28.

1985: The Holocene vegetational development of Tugtulligssuaq and Qeqertat, northwest Greenland; *Meddelelser om Grnland, Geoscience*, v. 14, p. 1–20.

Freedman, B., Svoboda, J., and Henry, G.H.R.

1994: Alexandra Fiord—An ecological oasis in the Polar Desert; in *Ecology of a Polar Oasis: Alexandra Fiord, Ellesmere Island, Canada*, (ed.) J. Svoboda and B. Freedman; Captus University Publications, Toronto, Ontario, p. 1–9.

Garneau, M.

1992: Analyses macrofossiles d'un dépôt de tourbe dans la région de Hot Weather Creek, péninsule de Fosheim, île d'Ellesmere, Territoires du Nord-Ouest; *Géographie physique et Quaternaire*, vol. 46, p. 285–294.

Gajewski, K., Garneau, M., and Bourgeois, J.C.

1995: Paleoenvironments of the Canadian High Arctic derived from pollen and plant microfossils: problems and potentials; *Quaternary Science Review*, v. 14, p. 609–629.

Gore, A.J.P.

1983: Introduction; in *Ecosystems of the World*. 4A. Mires: Swamp, Bog, Fen, and Moor, (ed.) A.J.P. Gore; Elsevier, Amsterdam, p. 1–34.

Hamilton, M.S., Gajewski, K., McNeely, R.N., and Lean, D.R.S.

2000: Physical, chemical, and biological characteristics of lakes from the Slide River basin on Fosheim Peninsula, Ellesmere Island, Nunavut; in *Environmental Response to Climate Change in the Canadian High Arctic*, (ed.) M. Garneau and B.T. Alt; Geological Survey of Canada, Bulletin 529.

Harrington, C.R.

1975: A postglacial walrus (*Odobenus rosmarus*) from Bathurst Island, N.W.T.; *The Canadian Field Naturalist*, v. 89, p. 249–261.

Hatterley-Smith, G. and Long, A.

1967: Postglacial uplift at Tanquary Fiord, northern Ellesmere Island, N.W.T.; *Arctic*, v. 19, p. 255–260.

Henry, G., Freedman, B. and Svoboda, J.

1986: Survey of vegetated areas and muskox populations in east-central Ellesmere Island; *Arctic*, v. 39, p. 78–81.

Hodgson, D.A.

1985: The last glaciation of west-central Ellesmere Island, Arctic Archipelago; *Canadian Journal of Earth Sciences*, v. 22, p. 347–368.

Hodgson, D.A., St-Onge, D., and Edlund, S.A.

1991: Surficial materials of Hot Weather Creek Basin, Ellesmere Island, N.W.T.; in *Current Research, Part E; Geological Survey of Canada, Paper 91-1E*, p. 157–163.

Holyoak, D.T.

1984: Taphonomy of prospective plant macrofossils in a river catchment on Spitsbergen; *New Phytologist*, v. 98, p. 405–423.

Hopkins, A.D.

1920: The bioclimatic law; *Journal of the Washington Academy of Sciences*, v. X, p. 34–40.

Hyvarinen, H.

1985: Holocene pollen stratigraphy of Baird Inlet, east-central Ellesmere Island, Arctic Canada; *Boreas*, v. 14, p. 19–32.

Janssens, J.A.

1990: Methods in Quaternary ecology. No 11. Bryophytes; *Geoscience Canada*, v. 17, p. 13–24.

Koerner, R.M.

1977: Ice thickness measurements and their implication with respect to past and present ice volumes in the Canadian High Arctic ice caps; *Canadian Journal of Earth Sciences*, v. 14, p. 2697–2705.

Koerner, R.M. and Fisher, D.A.

1990: A record of Holocene summer climate from a Canadian high-arctic ice core; *Nature*, v. 343, p. 630–631.

Labine, C.L.

1994: Meteorology and climatology of the Alexandra Fjord Lowland; in *Ecology of a Polar Oasis*, (ed.) J. Svoboda and B. Freedman; Captus University Publications, Toronto, Ontario, p. 23–29.

Lafarge-England, C.

1989: The contemporary moss assemblages of a high arctic upland, northern Ellesmere Island, N.W.T., Canada; *Canadian Journal of Botany*, v. 67, p. 491–504.

Lafarge-England, C., Vitt, D.H., and England, J.

1991: Holocene soligenous fens on a High Arctic fault block, northern Ellesmere Island (82°N), N.W.T., Canada; *Arctic and Alpine Research*, v. 23, no. 1, p. 80–98.

Lemmen, D.S.

1989: The last glaciation of Marvin Peninsula, northern Ellesmere Island, High Arctic Canada; *Canadian Journal of Earth Sciences*, v. 26, p. 2578–2590.

Lewkowicz, A.G.

1991: Observations of aeolian transport and niveo-aeolian deposition at three lowland sites, Canadian Arctic Archipelago; *Permafrost and Periglacial processes*, v. 2, p. 197–210.

National Wetlands Working Group

1988: Wetlands of Canada; Ecological Land Classification Series, No 24; Sustainable Development Branch, Environment Canada, Ottawa, Ontario, and Polyscience Publications Inc., Montréal, Quebec, 452 p.

Ovenden, L.

1988: Holocene proxy-climate data from the Canadian Arctic; Geological Survey of Canada, Paper 88-22, 11 p.

1990: Peat accumulation in northern wetlands; *Quaternary Research*, v. 33, p. 377–386.

Pissart, A., Vincent, J.-S. et Edlund, S.A.

1977: Dépôts et phénomènes éoliens sur l'île de Banks, Territoires du Nord-Ouest, Canada; *Journal canadien des sciences de la Terre*, vol. 14, p. 2462–2480

Porsild, A.E. and Cody, W.J.

1980: Vascular plants of continental Northwest Territories; National Museum of Natural Sciences, Ottawa, Ontario, 667 p.

Ritchie, J.C.

1984: Past and Present Vegetation of the Far Northwest of Canada; University of Toronto Press, Toronto, Ontario, 251 p.

1987: Postglacial Vegetation of Canada; Cambridge University Press, New York, 178 p.

Seppälä, M., Gray, G., and Ricard, J.

1991: Development of a low-centred ice wedge polygon in the northernmost Ungava Peninsula, Quebec, Canada; *Boreas*, v. 20, p. 259–282.

Stewart, T.G. and England, J.

1983: Holocene sea-ice variations and paleoenvironmental change, northernmost Ellesmere Island, N.W.T., Canada; *Arctic and Alpine Research*, v. 15, p. 1–17.

Svoboda, J. and Freedman, B. (ed.)

1981: Ecology of a high Arctic Lowland oasis, Alexandra Fiord (78°53'N; 75°55'W), Ellesmere Island, N.W.T., Canada; Progress Report of Alexandra Fiord Lowland Ecosystem Study; University of Toronto, Toronto, Ontario, and Dalhousie University, Halifax, Nova Scotia, 245 p.

Tarnocai, C.

1978: Genesis of organic soils in Manitoba and the Northwest Territories; *in* Third York University Symposium on Quaternary Research, Geographical Abstracts, Norwich, United Kingdom, p. 453–470.

Tarnocai, C. and Zoltai, S.C.

1988: Wetlands of Arctic Canada; *in* Wetlands of Canada; National Wetlands Working Group, Environment Canada, Ottawa, Ontario, p. 29–53.

Thorsteinsson, R.

1971: Geology, Eureka Sound north, District of Franklin; Geological Survey of Canada, Map 1302A, scale 1:250 000.

van der Knaap, W.O.

1985: Human influence on natural arctic vegetation in the seventeenth century and climatic change since AD 1600 in northwest Spitsbergen: a paleobotanical study; *Arctic and Alpine Research*, v. 17, p. 371–387.

1989: Past vegetation and reindeer on Edgeya (Spitsbergen) between c. 7900 and c. 3800 BP, studied by means of peat layers and reindeer faecal pellets; *Journal of Biogeography*, v. 16, p. 379–394.

Wolfe, A.P.

2000: A 6500 year old diatom record from southwestern Fosheim Peninsula, Ellesmere Island, Nunavut; *in* Environmental Response to Climate Change in the Canadian High Arctic, (ed.) M. Garneau and B.T. Alt; Geological Survey of Canada, Bulletin 529.

Young, K.L. and Woo, M.-k.

2000: Hydrological environment of the Hot Weather Creek basin, Ellesmere Island, Nunavut; *in* Environmental Response to Climate Change in the Canadian High Arctic, (ed.) M. Garneau and B.T. Alt; Geological Survey of Canada, Bulletin 529.

Zoltai, S.C. and Pollett, F.C.

1974: Wetlands in Canada: their classification, distribution, and use; *in* Mires: Swam, Bog, Fen, and Moor, B. Regional Studies, (ed.) A.J.P. Gore; Elsevier, Amsterdam, p. 245–268.

Late Tertiary plant and arthropod fossils from the high-terrace sediments on Fosheim Peninsula, Ellesmere Island, Nunavut

J.V. Matthews, Jr.¹ and J.G. Fyles²

Matthews, J.V. and Fyles, J.G., 2000: Late Tertiary plant and arthropod fossils from the high-terrace sediments of Fosheim Peninsula, Ellesmere Island, Nunavut; in Environmental Response to Climate Change in the Canadian High Arctic, (ed.) M. Garneau and B.T. Alt; Geological Survey of Canada, Bulletin 529, p. 295–317.

Abstract: Macroremains of bryophytes, vascular plants, and arthropods have been found in the 'high-terrace sediments' on Fosheim Peninsula. They show that no site predates the early Pliocene and that some may date from one of the Pleistocene interglacial stages. They help bracket the age of high-terrace sediments on Fosheim Peninsula and provide information on late Tertiary environments of the region. Climate here was significantly warmer during deposition than at present, and at times the region was occupied by open forests. These open forests, even those forming the treeline, were more diverse than modern taiga, whose northern limit is now 1000 km or more to the south.

The late Tertiary fossils discussed here are important for studying Quaternary sites in the region because knowing the taxonomic content of late Tertiary fossil assemblages is essential to recognizing Quaternary assemblages. Although some samples described herein seem to come from typical high-terrace deposits, they are apparently Quaternary rather than Tertiary.

Résumé : On a trouvé des macrorestes de bryophytes, de plantes vasculaires et d'arthropodes dans les sédiments de hautes terrasses dans la péninsule Fosheim. Ces fossiles indiquent qu'aucun des sites est antérieur au Pliocène précoce et que certains remontent probablement à un des stades interglaciaires du Pléistocène. Ils facilitent la datation plus précise des sédiments et fournissent de l'information sur les environnements du Tertiaire tardif dans la région. À l'époque du dépôt des sédiments, le climat était beaucoup plus chaud qu'aujourd'hui et pendant certaines époques, la région était recouverte de forêts clairsemées. Ces forêts clairsemées, même celles qui formaient la limite de croissance des arbres, étaient plus diversifiées que la taïga moderne, dont la limite actuelle se situe à 1000 km ou plus vers le sud.

Les fossiles du Tertiaire tardif dont nous discutons ici sont importants pour l'étude des sites quaternaires de la région, car ce n'est qu'en connaissant le contenu taxonomique des assemblages de fossiles du Tertiaire tardif que nous pouvons reconnaître les assemblages du Quaternaire. Bien que certains des échantillons décrits ici semblent provenir de dépôts typiques de hautes terrasses, ils remonteraient au Quaternaire plutôt qu'au Tertiaire.

¹ Ohana Productions, 23 Sherry Lane, Nepean, Ontario K2G 3L4

² Geological Survey of Canada, 601 Booth Street, Ottawa, Ontario K1A 0E8

INTRODUCTION

For several years, the Geological Survey of Canada maintained an environmental monitoring site on the Fosheim Peninsula at Hot Weather Creek, near the Eureka weather station (Garneau et al., 2000) (Fig. 1). Numerous studies have been carried out at this site, including several that deal with Holocene paleontology and environments. Reconstructing Holocene environments using fossils is highly dependent on identifying fossils that have been transported from other (older?) deposits. In the Canadian High Arctic, the problem of reworked fossils is much more serious than farther south, for two reasons, 1) the production of contemporary and Holocene organic remains is much lower than at sites farther south and 2) many High Arctic areas are underlain by late Tertiary

deposits containing abundant fossils of plants and animals almost as well preserved as their Quaternary counterparts. Whereas some of these fossils, such as conifer needles, are clearly not of Holocene origin, for others, such a distinction is much harder to make.

This paper describes the existence of a number of late Tertiary fossiliferous sites on the Fosheim Peninsula (Fig. 1) and provides lists of fossils isolated and identified from these deposits. Almost all the deposits are or seem to be part of the distinctive suite of sediments informally known as the 'high-terrace sequence'. Fossils from the high-terrace sites aid in recognizing Quaternary fossil assemblages. They also reveal details about high-latitude environments just before the advent of the arctic climate that typifies the region today.

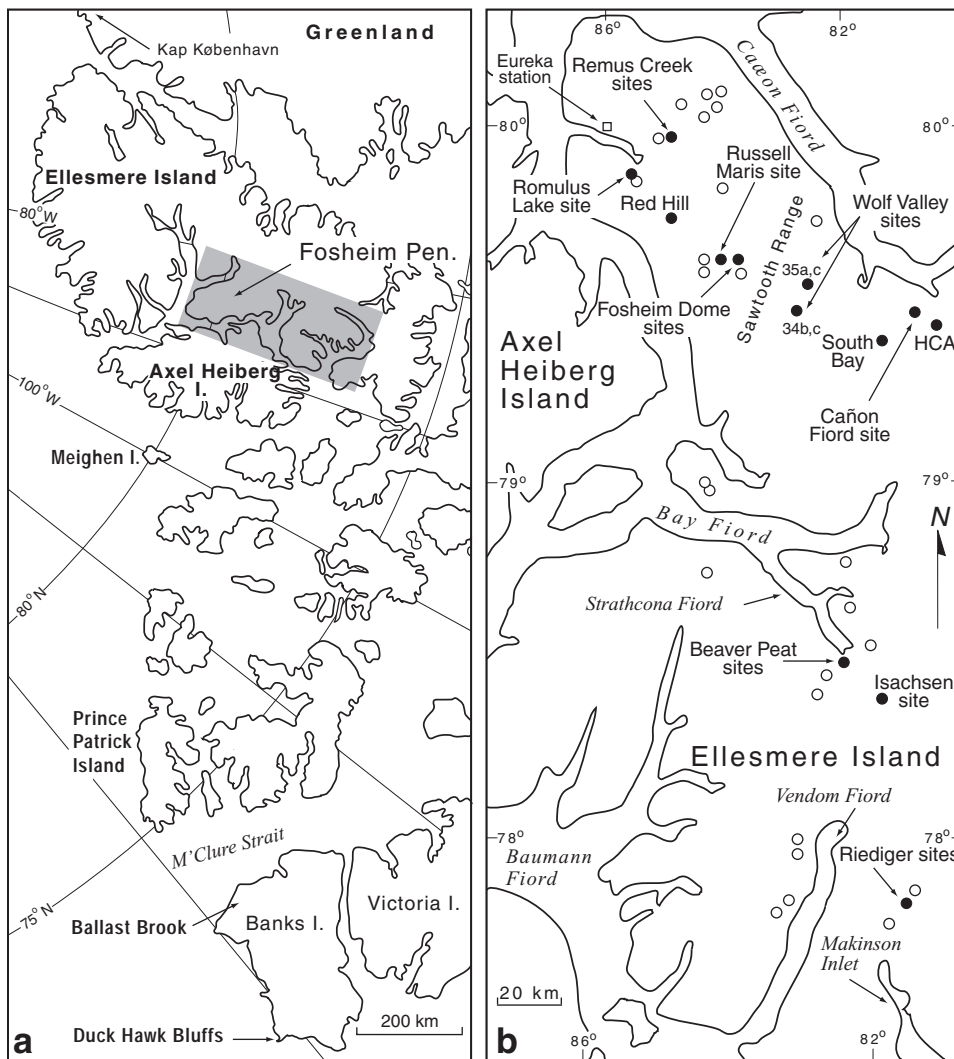


Figure 1. a) Map showing many of the sites in the Canadian Arctic Archipelago and adjacent areas that are mentioned in the text. The shaded box indicates the area shown in Figure 1b. The Kap København site in northern Greenland is actually just beyond the margin of the map. b) High-terrace sites discussed in the text (black circles) plus some others discovered by JGF. For information on the exact location of each of the studied sites, see text and appendices A and B.

METHODS AND TERMINOLOGY

Collated and updated versions of previously published lists of plant macrofossils and arthropod fossils from sites on Fosheim Peninsula and two nearby sites are provided in appendices A and B. All sampling localities discussed in this paper are shown in Figure 1. Those with an asterisk represent collections of fossil-bearing samples from the same exposure or samples of presumed equivalent age from closely spaced exposures.

Unless otherwise indicated, vascular plant taxa were identified by JVM. Bryophytes were identified by L.E. Ovenden (Pest Management Regulatory Agency, Health Canada, Ottawa, Ontario). Vascular plant fossils, consisting mostly of seeds and fruits, were identified by comparison with modern reference material in the Geological Survey of Canada seed and fruit reference collection and with illustrations in various publications (particularly Russian ones), and with the help and advice of various specialists on late Tertiary macrofloras from North America and northern Europe. A valuable aid in identifying some plant macrofossils has been the study of degraded and transported seeds and fruits from modern alluvium, lacustrine deposits, and various types of mires and swamps.

The term 'florule' is used here informally to denote macrofloral remains from a specific level or horizon at a single locality. The term 'flora' generally refers to a collection of florules, commonly from different sites in the same region. The terms 'faunule' and 'fauna' are applied in the same sense for insect and other arthropod fossils.

Most fossils of insects and other arthropods are unaltered fragments of beetles (Coleoptera), which were identified using the synoptic reference collection at the Geological Survey of Canada, by comparison with the extensive collections in Agriculture Canada's Canadian National Collection of Insects, and by consultation with various specialists. In addition to insects, several other arthropod groups are represented, the most common of which are oribatid mites.

Many vascular plant and insect fossils are identified only to the generic level or tentatively ('cf.') to the species level. In view of the existence of the Bering Land Bridge during the Tertiary and the occurrence of obvious Asian taxa in these North American assemblages, it is highly probable that many plant fossils listed herein have already been found in some of the rich fossil floras from Russia. Many new species have been described from collections at Russian sites. This means that the definitive identification of fossils from the Canadian Arctic must await comparison with Russian type specimens. Until such time as that is done, we refrain from describing new taxa and further complicating an already overburdened nomenclature (Tiffney, 1989). There are, however, a few fossils for which the specific identity is obvious. This is true for many bryophyte fossils, the majority of which cannot be distinguished from extant species (Matthews and Ovenden, 1990).

Most arthropod fossils in late Tertiary sites from Fosheim Peninsula can be readily assigned to extant genera and many appear closely related to extant species. A few specimens apparently represent extinct species; however, caution is required in drawing such a conclusion if the modern fauna is poorly documented. Species thought to be extinct have subsequently been found living in poorly collected regions.

It is only possible to assess the climatic implications of fossils listed here if their modern distribution is known. In the High Arctic where the climatic regime restricts the distribution of whole plant groups more than elsewhere, the occurrence of even a single fragment of wood can have paleoclimatic implications, because some areas of the region are currently beyond the limit of all woody plants, even prostrate shrubs (Edlund and Alt, 1989). The Fosheim Peninsula is within the limit of woody plants today, but, like the rest of Ellesmere Island, it has probably been beyond the limit of trees, particularly conifers, since the late Pliocene (Matthews, unpub. data). Therefore, the occurrence of any conifer wood or other conifer fossils has immediate climatic implications regardless of the exact identity of the fossil. However, one must always be cautious in drawing paleoenvironmental conclusions on the basis of wood remains alone because wood readily survives recycling from older sediments. The same is not as true of other, more delicate fossils such as leaves and needles, especially charred needles, which are extremely fragile.

Knowledge of the distribution of modern insects is just as important as data on plant distribution for reconstructing climate using fossil evidence. Unfortunately, data on the distribution of arctic insects are less well known than those for plants. Nevertheless, as with plants, whole insect groups are missing from large areas of the Arctic, making even nondescript fossils potentially significant. For example, ground-beetles (Carabidae) are one of the most common beetle groups world wide, but are not found anywhere on Ellesmere Island today. This makes any carabid fossil from Fosheim Peninsula a significant climatic indicator.

The best available information on the arctic distribution of many of the insects listed here is Danks' (1981) comprehensive review of arctic insects. The study of the Fosheim Peninsula site is further aided by the fact that the present insect fauna at Hot Weather Creek — the warmest area of the entire peninsula and perhaps of all of Ellesmere Island (Edlund, 1992) — has been inventoried in detail (Brodo, 2000).

ELLESMERE ISLAND HIGH-TERRACE SEDIMENTS

The Beaufort Formation in the western arctic islands has traditionally been recognized as the prime source of late Tertiary plant and arthropod fossils in the Canadian Arctic. Ongoing studies of the high-terrace sediments on Ellesmere Island show that they are equally rich sources of well preserved plant and insect fossils. The high-terrace sands, gravels, and peat generally underlie glacial deposits and cap the sediments of the Cretaceous–early Tertiary Eureka Sound Group. As their

name implies, typical high-terrace sediments occur high up on valley sides. They were obviously deposited prior to significant uplift and fiord formation. Moreover, they may have been deposited at a time when many of the channels now separating the islands of the archipelago did not exist, making them the thin edge of the thick wedge of Tertiary sediments that in part constitutes the Beaufort Formation on the western islands. In fact, in some previous publications, the high-terrace sediments are referred to the Beaufort Formation. Fyles (1990) suggests it is more appropriate to recognize the high-terrace sediments as a separate formation and only then make judgments regarding its correlatives.

FOSSIL ASSEMBLAGES

This paper concerns nine sites or closely spaced groups of sites among the more than 21 localities studied by JGF on Fosheim Peninsula (Fig. 1b). Some sites are poorly understood in terms of stratigraphy and require additional study. In a few cases, the samples studied were so small as to permit only a preliminary estimate of their actual fossil content. Despite these deficiencies, the various assemblages discussed here can be divided into two groups, those of probable late Tertiary age and those possibly as young as the Quaternary.

The late Tertiary assemblages are easily recognized since they consistently contain one or more of several plant and insect 'index' fossils (Plate 1). These same index fossils occur at other dated, late Tertiary sites in the Canadian High Arctic (Matthews, unpub. data; Fyles et al., 1991). It is much more difficult to assign a Quaternary age to a site, because such a conclusion is based largely on negative evidence.

LATE TERTIARY FLORAS AND FAUNAS

Remus Creek sites

The Remus Creek sites are located along approximately 100 m of a gently sloping outcrop slightly east of Remus Creek (lat. 79°59'N, long. 84°51'W). The elevation of the three samples discussed here ranges from 235 to 255 m a.s.l. Plant and arthropod fossils from individual levels are listed in Table 1.

Sample 31c comes from a 5 cm thick zone of plant detritus and wood within a 50 cm thick unit of sand and contains a number of important plant and insect fossils. *Decodon* (Matthews and Ovenden, 1990, Fig. 4-8) is present among the plants, which alone suggests that the unit is no younger than late Pliocene (Fyles et al., 1994; Matthews, unpub. data), and this is confirmed as well by the presence of leaves of cedar (*Thuja*) and a species of five-needle pine in addition to larch (*Larix*) and spruce (*Picea*). The presence of these tree fossils plus the fact that all of the birch samaras resemble those from tree birches suggests that the site was completely forested at the time of deposition.

Table 1. Fossils of plants and animals (arthropods and other invertebrates) from the Remus Creek site.

FOSSILS	SAMPLE NUMBER		
	14b	33a	31c
PLANTS AND RELATED REMAINS			
Coal and/or amber	+		+
Bryophytes	++		
Bryales			
<i>Meesia triquetra</i> (Richt.) Aongstr.		+	
Hypnobryales			
<i>Calliergon giganteum</i> (Schimp.) Kindb.		+	
<i>Drepanocladus</i> spp.		+	
<i>Scorpidium scorpioides</i> (Hedw.) Limpr.		++	
Vascular plants			
Equisetaceae			
<i>Equisetum</i> sp.			+
Pinaceae			
<i>Larix</i> sp.	+	+	+
<i>Picea</i> sp.	+	+	+
<i>Pinus</i> five-needle type	+		+
Cupressaceae			
<i>Thuja</i> sp.	++		+
Arctopterygaceae			
<i>Arctopteryx</i> sp.			+
Potamogetonaceae			
<i>Potamogeton</i> spp.		+	+
<i>P. diversifolius/spirillus</i> type		+	
Cyperaceae			
<i>Carex</i> spp.	+	+	+
<i>Carex</i> sect. <i>Paludosae</i>		+	
<i>Rhynchospora</i> sp.		cf.	
Myricaceae			
<i>Comptonia</i> sp.			+
<i>Comptonia peregrina</i> B.B., Small, Rydb.			+
Betulaceae			
<i>Alnus</i> sp.	+		
<i>Alnus incanac</i> type			
<i>Betula</i> sp. arboreal type	+		+
Nymphaeaceae			
<i>Nymphaea</i> sp.		++	
Ranunculaceae			
<i>Ranunculus hyperboreus</i> type		+	
Lythraceae			
<i>Decodon globosus</i> type			+
Haloragaceae			
<i>Hippuris</i> sp.		+	+
Ericaceae			
<i>Andromeda polifolia</i> L.		+	+
Cornaceae			
<i>Cornus stolonifera</i> Michx.			+
Gentianaceae			
<i>Menyanthes trifoliata</i> L.	+	+	
ARTHROPODS AND OTHER ANIMALS			
BRYOZOA			
<i>Cristatella mucedo</i> L.		+	
ARTHROPODA			
INSECTA			
HEMIPTERA			
Pentatomidae			
Genus?		+	
NEUROPTERA			
<i>Sialis</i> sp.			+
COLEOPTERA			
Carabidae			
<i>Blethisa</i> sp.	+		
<i>Dyschirius tridentatus</i> group	+		
<i>Notiophilus</i> sp.	+		
<i>Tachys</i> sp.			+
Micropeplidae			
<i>Micropeplus tesseraula</i> Curtis			+
Gyrinidae			
<i>Gyrinus</i> sp.		+	
Lathridiidae			
Genus?		+	
Chrysomelidae 'leaf beetles'			
Donacinae		+	
Curculionidae			
<i>Grypius</i> sp.	+		
Remus Creek site: east of Remus Creek (lat. 79°59'N, long. 84°51'W), Fosheim Peninsula, east of Slidre Fiord. 14b = Sample FG 88-14b, collected by J.G. Fyles, July 14, 1988 (fieldbook 1-14), "from peat mat (containing modern rootlets) immediately above shale of the Eureka Sound Formation (exposure slumped)". 33a = Sample FG 88-33a, collected by J.G. Fyles, July 19, 1988 (fieldbook 1-33), "peat bed up to 40 cm thick. Sample combines upper mossy part and lower earthy with wood". 31c = Sample FG 88-31c, collected by J.G. Fyles, July 19, 1988 (fieldbook 1-31), "close to level of 31a from N section, 20 cm below 31d. Contains pelecypod shells."			

One of the sample 31c plant fossils is *Comptonia* (Plate 1c), included in the genus *Myrica* by some taxonomists. *Comptonia* seeds or endocarps occur in some other Fosheim Peninsula samples and are found in most late Pliocene samples from the Canadian Arctic. A few *Comptonia* seeds from sample 31c are so well preserved that they still possess the enclosing bracts. This suggests that *Comptonia* was growing at or very near the site. The fossils resemble fruits from the extant species *C. asplenifolia*. A similar form is also found in one of the Ballast Brook Beaufort samples from northern Banks Island (Fig. 1a) (Fyles et al., 1994). Together, they show that the modern form may have a long lineage and that it is not derived from any of the late Tertiary fossil species. The appearance of this apparently modern form of *Comptonia* at the Remus Creek site may also mean that the site is slightly younger than the other Pliocene sites discussed in this report or in Matthews and Ovenden (1990).

A peculiar plant fossil in sample 31c is similar to fossils found rarely at some of the Beaufort Formation localities (Plate 1a) and once thought by JVM to represent leaves of the Japanese umbrella pine, *Sciadopitys* (Matthews et al., 1990). *Sciadopitys* survived in Europe until quite late in the Pliocene (van der Hammen et al., 1971) and therefore its presence in the Tertiary of the Canadian High Arctic was not a great surprise, especially since the plant assemblages from that region contain some of the same taxa found in the late Tertiary of northern Europe (Matthews, unpub. data). However, it is now known that the presumed *Sciadopitys*-type leaves seen at Remus Creek and other sites are probably reworked from lower Cretaceous deposits such as those occurring on Baffin Island, Greenland, and Spitsbergen (Bose and Manum, 1990). Rather than being a plant related to *Sciadopitys* or any other member of the family Taxodiaceae, they are referred by Bose and Manum (1990) to an extinct conifer within the extinct family Arctopityaceae. While Quaternary sites in the Canadian Arctic can be contaminated by late Tertiary fossils that are difficult to distinguish from their younger counterparts, the *Sciadopitys*-like needles are an example of Mesozoic or early Tertiary fossils playing the same role in late Tertiary fossil assemblages.

Arthropod fossils are not abundant in sample 31c. Nevertheless, most of them represent groups that do not occur on Ellesmere Island today, signifying a much warmer climate at the time of deposition. Most of the taxa listed in Table 1 have been found at other Pliocene sites in the Canadian Arctic, the one exception being the tiny beetle, *Micropeplus tesserula*. The presence of its fossils is not surprising because it lives in the modern boreal forest at sites very much like the peaty ponds that must have existed at Remus Creek (Campbell, 1968). A few fossils of gastropods occur in this sample — a subject for future study.

Sample 33a comes from a mossy peat at a section slightly south of the site of sample 31c and at the same elevation. It consists of peat in gravel only about 2 m above the top of the Late Cretaceous–early Tertiary Eureka Sound Group. L.E. Ovenden (unpub. rept., 1991) examined moss fossils from this sample and found an abundance of *Scorpidium scorpioides* as well as a few fragments of *Meesia triquetra* and *Calliergon giganteum*. All three grow widely in boreal

and arctic regions and so say little about details of past climate. *Scorpidium* occurs in minerotrophic peaty pools or shallow ponds.

The vascular plant macrofossils from sample 33a, though not abundant, attest to a local origin for the *Scorpidium* fossils and the autochthonous nature of the peat since they include numerous remains of aquatic and emergent aquatic plants, such as fruits of *Nymphaea*, achenes of a species of *Carex* similar to *C. rhynchophysa*, and fruits of several types of *Potamogeton*. One type of *Potamogeton* is very small and probably represents the species *P. diversifolius* or *P. spirillus*. Further testimony to the local origin of these aquatic plant fossils is that many of the *Potamogeton* fruits are exceptionally well preserved. The peat evidently represents the margin of a small pond.

The few arthropod fossils in the assemblage also suggest the presence of a small pond. Among them are fragments of a whirligig beetle (*Gyrinus*) and the leaf-beetle *Donacia* the larvae and adults of which are associated with aquatic species of *Carex*.

An unusual feature of this sample 33a is the abundance of larch (*Larix*) seeds. Normally, larch needles dominate and seeds are rare. The number of seeds probably means that larch was growing near the pond site, but spruce (*Picea*) must also have occurred in the region, because the sample yielded a few charred needles. These needles lack resin canals, ruling out red or black spruce. They probably represent white spruce (*Picea glauca*) or *P. banksi*, a closely related, extinct species (Hills and Gilvie, 1970).

The absence of pine needles and other late Tertiary fossils, such as *Decodon*, which occur in other Remus Creek samples, is almost certainly due to the autochthonous character of the peat. Sample 31c from essentially the same level at an adjacent part of the exposure contains macrofossils of pine and eastern cedar (*Thuja*).

Many of the fossils from sample 33a represent plants and insects that are not found today on any of the islands of the Arctic Archipelago. For example, *Nymphaea* barely reaches the present-day treeline (Porsild and Cody, 1980) and beetles of the genus *Gyrinus* barely occur beyond the regional treeline. Evidently, climate at the time of deposition of the sample 33a peat was much warmer than at present.

Sample 14b comes from a peat mat resting on the shale of the Eureka Sound Group, placing it 2–5 m below the other two samples. Leaf fragments of *Thuja* are abundant as are leaf fragments of five-needle pine, larch, and spruce. The other plant fossils add little to the information provided by the other two samples and give no reason to suspect that sample 14b is significantly older than the other two.

Fossil insects from sample 14b are more diverse than in the other two samples. Unlike those of sample 33a, they include taxa (the carabid beetles *Notiophilous* and *Blethisa*) that ordinarily would not be found in the same biotope, so the peat must be somewhat detrital. Another ground-beetle, *Dyschirius* is from the *tridentatus* group that, with one exception, is found today only west of the Rocky Mountains and not in the subarctic region (Bousquet, 1988). However, fossils

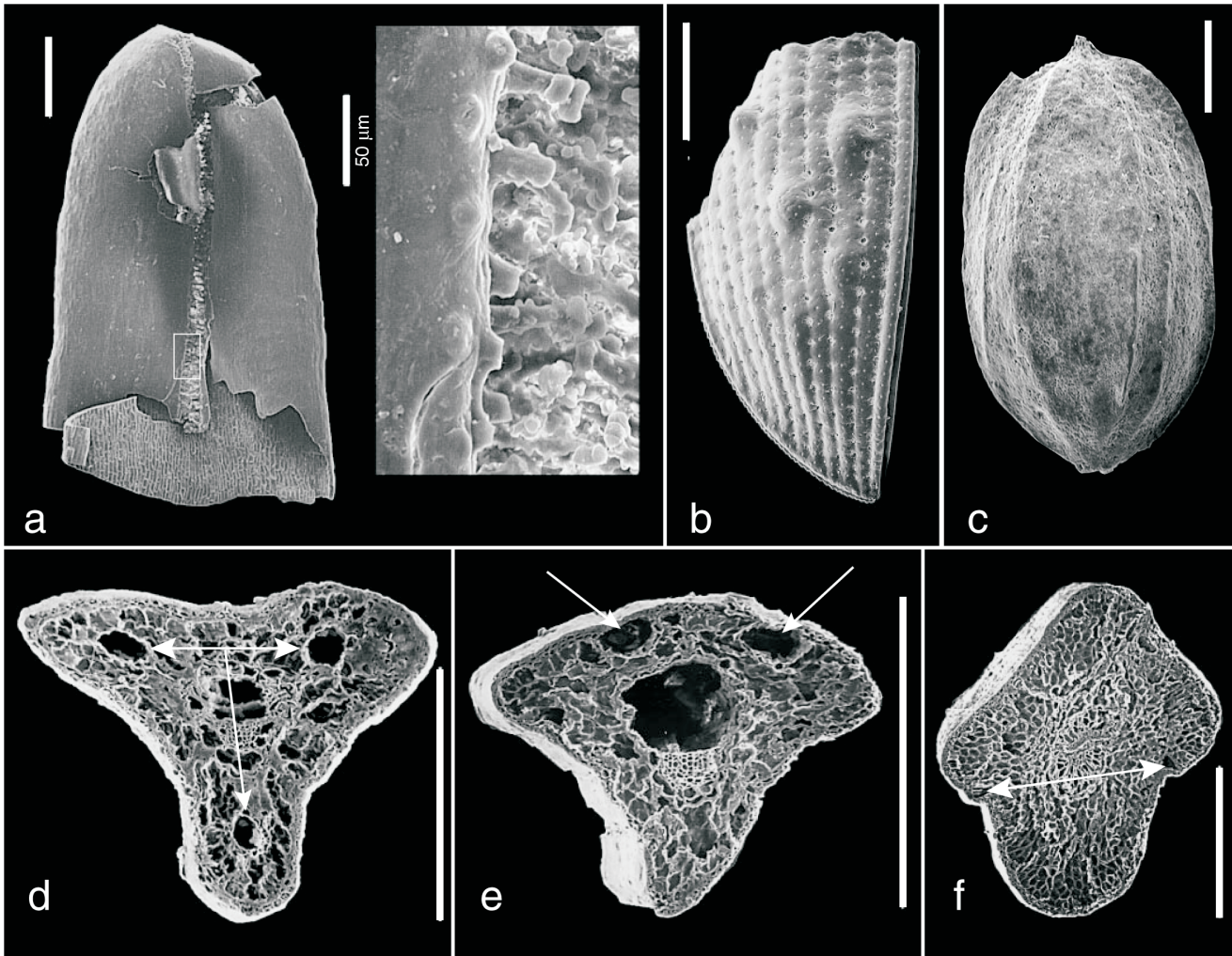


Plate 1. Scanning electron micrographs of plant and insect macrofossils from the high-terrace sediments on Fosheim Peninsula and similar fossils from other sites in the Canadian High Arctic. All scale bars are 0.5 mm unless otherwise indicated. **a**) *Arctopitys* type 'needle' similar to the type seen at the Remus Creek site. The fossil comes from the Pasley River site on Boothia Peninsula (Dyke and Matthews, 1987). The image on the left shows the apical part of the needle, the medial groove on the lower surface, and the inner surface of the cuticle on the upper surface. The image on the right is a magnified view of the area shown in the white box and shows the characteristics of the papillae along the left margin of the median groove. See Bose and Manum (1990) for a detailed study of *Arctopitys* and *Sciadopitys*. In addition to Remus Creek, fossils such as the one shown are found at several Beaufort Formation sites in the Canadian Arctic. **b**) *Helophorus meighensis* Matth. from the South Bay site. The fossil is the apical third of the left elytron and shows the development of elytral tubercules typical of this extinct species. The same species is found at the Beaver Peat site on Strathcona Fiord, at the Riediger Site (see text), and in the Beaufort Formation on Meighen Island (Matthews, 1976); it is one of the 'index fossils' that show that some Fosheim Peninsula high-terrace sites are early Late Pliocene. **c**) *Comptonia endocarp* similar to those seen at several Fosheim Peninsula high-terrace sites. The type shown differs from the endocarp of the only extant species, *C. asplenifolia*, a fossil of which occurs at the Remus Creek site. The fossil shown is from sample FG88-53b at the Beaver Peat site on Strathcona Fiord (Fig. 1 and text). **d**) Cross-section of a needle (abaxial surface at top) of the *Pinus (Strobus) subsect. Cembrae* type. Note the three resin canals located in a medial position (Critchfield, 1986). Pines with this type of leaf anatomy do not now grow in North America, but did grow in the Canadian High Arctic (including Fosheim Peninsula) during the later Tertiary. This needle type is one of the index fossils for the later Tertiary in Arctic Canada. The fossil shown (GSC-99132) comes from sample FG88-10c from the Isachsen site, approximately 20 km southeast of the Beaver Peat site (Fig. 1b) (Matthews, unpub. data). **e**) Cross-section of a needle (abaxial surface at top) of the *Pinus (Strobus) subsect. Eustrobi* type. Note the two resin canals (arrows) in 'external' position (Critchfield, 1986). This type of needle is found at a number of high-terrace sites as well as at the Beaufort Formation and other late Tertiary sites in northern North America (Matthews, unpub. data). Modern white pines in North America have needles with similar anatomy in cross-section (Critchfield, 1986). The fossil in the micrograph (GSC-99131) comes from sample FG88-51b from the Beaver Peat site on Strathcona Fiord (see text and Fig. 1b). **f**) Laterally compressed cross-section of a needle (abaxial surface at top) of the *Picea mariana/rubra* type. Note the two small resin canals (arrows). Similar spruce needles are found at a number of high-terrace and Beaufort Formation sites and are particularly abundant at the Russell Maris site on Fosheim Peninsula (see text and Fig. 1b). The fossil shown comes from sample FG88-51b from the Beaver Peat site on Strathcona Fiord (see text and Fig. 1b).

representing at least two species in this group occur in the Beaufort Formation on Meighen Island (Fig. 1a) (Matthews, 1979, unpub. data). Like many of the other insect fossils from Remus Creek, *Dyschirius* is a genus whose present northern limit is south of the regional treeline, hence nearly 1000 km south of Fosheim Peninsula.

Fossils of the weevil *Grypius*, which occurs in sample 14b, are also abundant in Meighen Island assemblages (Matthews, 1977, unpub. data). Today they occur along sandy shorelines of rivers in the northern boreal forest. They also show that sample 14b peat is detrital, because such fossils would not occur in an autochthonous peat.

Remus Creek is one of the few sites reported here for which pollen data exist. A study of a sample from FG 88-31c (M. Frappier, unpub. rept., 1995) shows a dominance of spruce pollen (32 per cent), then pine (21 per cent), birch (23 per cent), alder (9 per cent), and *Salix* (5 per cent). Traces of *Typha* and *Nuphar* pollen are also recorded.

Remus Creek sediments apparently do represent an open, tundra-like environment such as is implied by the Beaver Peat sediments from Strathcona Fiord (see below). On this basis, we argue that the Remus Creek site may be either older or younger than the Beaver Peat and associated deposits. Some of the plant fossils suggest that the Remus Creek sediments may be slightly younger than those of the Beaufort Formation near Bjaere Bay on Meighen Island (Fig. 1a) (Matthews, unpub. data; Fyles et al., 1991) and, if true, then the Remus Creek site could be between 3.1 and 2.5 Ma.

While the Remus Creek sites obviously represent a time when the climate of Ellesmere Island, and Fosheim Peninsula in particular, was markedly warmer than at present, it is difficult to estimate the particulars of that climatic regime because oceanic conditions were different (e.g. probably no perennial ice in the Arctic Ocean (Repenning and Brouwers, 1992); some major vegetation types of the time lack a modern analogue (Matthews, unpub. data); and regional geography was different (Fyles, 1990, and pers. comm., 1997)). All that can be said with some certainty is that diverse coniferous forests evidently existed on Fosheim Peninsula and this means that the mean July temperature was likely over 5°C warmer than at present.

The Remus Creek site deserves to be a prime target for future research. Not only does it contain both autochthonous and allochthonous deposits, enhancing the probability of learning important details about both local and regional biota, but it is located only a short distance from the Eureka base and weather station, simplifying logistical problems.

Wolf Valley sites

Plant fossils including tree species similar to those described above from Fosheim Peninsula also occur in high-terrace sediments in Wolf Valley (Fig. 1). Wolf Valley drains northward into Cañon Fiord along the east side of the north-trending Sawtooth Range, which borders the high eastern margin of Fosheim Peninsula. The five Wolf Valley samples reported here (Table 2) are from two localities south of Cañon Fiord,

separated by about 8 km, on the east wall of the Wolf River valley (lat. 79°31'N, long. 83°00'W). Four of the samples come from detrital organic zones or peats in a 30 m thick sequence of sand and silt beneath 15 m of gravel with wood. Sample 38c is a collection of sticks found in the creek bed and thus may come from any level of the exposure.

Samples 35c and 35a are correlative, both coming from different locations along a 3 m thick unit of compressed organic material at the base of the high-terrace gravel and sand. Thus, they are probably of about the same age. Samples 34b and 34c come from fine plant detritus approximately 20 m lower than samples 35a and 35c.

Plant remains are relatively abundant in samples 35c and 35a and since both come from the same horizon, they could be pooled to form an even larger and more informative assemblage. The fossils referred to the *Betula glandulosa* type are samaras with very small wings. No birch grows in the region today, so these fossils suggest a slightly warmer climate. Even warmer conditions are suggested by remains of *Alnus*, *Glyceria*, *Sparganium hyperboreum*, and *Menyanthes*. *Menyanthes* (buckbean) seeds are relatively abundant. They float well, are readily transported by streams and rivers, and consequently are common fossils in alluvium, but only in sediments that were deposited in subarctic and Low Arctic tundra regions. Most *Menyanthes* seeds are larger than 2 mm, like the modern *M. trifoliata*, but, as noted in Table 2, a few are smaller. Some European workers have described such forms as a separate, extinct species (Jentys-Szaferowa and Truchanowiczowna, 1953). However, it seems more likely that they represent an ecotype or at most a subspecies. The youngest deposits in which JVM has seen *Menyanthes* seeds as small are the last interglacial beds at Chi'jee's Bluff in the northern Yukon Territory (Matthews et al., 1990b). Thus, although the 'small type' *Menyanthes* may not be from an extinct species, they may in fact represent an ecotype that is not currently found in northern regions.

Like many of the *Carex* fossils, bur-reed (*Sparganium*) fossils are so well preserved that they must have grown locally. Currently, *Sparganium* is absent from even the most southern islands of the Arctic Archipelago (Porsild and Cody, 1980).

Sample 34b contains a single endocarp of *Comptonia*. *Comptonia* endocarps are very rugged and likely to survive reworking from older units. That this may be the origin of the fossil in sample 34b is indicated by its poor state of preservation compared to fossils from other Fosheim Peninsula sites. However, this is probably not the explanation for the presence of seeds of *Nuphar* (pond lily). Currently, pond lily does not grow much beyond the treeline (Porsild and Cody, 1980); consequently, when the sediments of sample 34b were deposited, the Fosheim Peninsula climate must have been as warm as at the southern fringe of the hypoarctic tundra zone. This may explain the presence of a few needles of larch and spruce in sample 34b as well as that of several types of conifer wood among the fragments found in the creek valley below the exposure (sample 38c).

Arthropod and related fossils are rare in all Wolf Valley samples, but those present have clear environmental implications. Most of the taxa in Table 2 do not occur on Ellesmere Island today. In some cases, the fossils represent whole groups of insects (e.g. Odonata in sample 35c) that do not occur anywhere on Ellesmere Island, much less on Fosheim Peninsula.

Taken together, the arthropod and plant fossils from Wolf Valley show clearly that climate was significantly warmer than at present, i.e. that it was more like that of the southern part of the hypoarctic tundra zone. The treeline may have crossed Fosheim Peninsula at the time of deposition and, if so, mean July temperatures were 3 to 5°C warmer than at present (Etkin and Agnew, 1992; Edlund, 1992. However, the plant

and insect fossils apparently do not represent a climate as warm as the one that characterized the region 3 Ma or so ago when a diversity of conifers grew in the High Arctic.

The Wolf Valley fauna and flora appears to be impoverished compared to other undoubtedly late Tertiary high-terrace assemblages from the region and elsewhere on Ellesmere Island. In particular, note the absence of fossils of the plants *Decodon*, *Physocarpus*, *Cornus stolinifera*, and *Aracites*. All occur at many other Pliocene sites (Fyles et al., 1994). Conifer fossils are also rare and are restricted to a few spruce and larch needles in only one sample and a few fragments of conifer wood from an unknown part of the section. Of particular note is the complete absence of needles of pine, the most common conifer fossil after *Larix*, at many other high-terrace sites. These omissions may be a sign that the

Table 2. Fossils of plants and animals (arthropods and other invertebrates) from the Wolf Valley site.

FOSSILS	SAMPLE NUMBER					FOSSILS	SAMPLE NUMBER				
	35c	35a	34b	34c	38c		35c	35a	34b	34c	38c
PLANTS AND RELATED REMAINS						ARTHROPODS AND OTHER ANIMALS					
Coal and/or amber			+			Gentianaceae					
Actinorhizal nodules			+			<i>Menyanthes trifoliata</i> L.	+		+		
Fungal sclerotia	+	+		+		<i>Menyanthes</i> 'small type'	+				
Bryophytes		+				ARTHROPODS AND OTHER ANIMALS					
Equisetaceae						BRYOZOA					
<i>Equisetum</i> sp.	+	?				<i>Cristatella mucedo</i> L.		+	+		
Pinaceae						ARTHROPODA					
<i>Larix</i> sp.			+			INSECTA					
<i>Picea</i> sp.			+		+	ODONATA					
<i>Pinus (Strobus) monticola</i> type (wood)*			+		+	Genus?	+				
Sparganiaceae						COLEOPTERA					
<i>Sparganium hyperboreum</i> type	+					Carabidae					
Potamogetonaceae						<i>Carabus</i> sp.	+				
<i>Potamogeton</i> spp.		+	+			<i>Bembidion umiatense</i> Lth.		cf.			
Gramineae						<i>Bembidion</i> sp.	+	+			
<i>Glyceria</i> sp.	+					<i>Bembidion sordidum</i> Kby.		cf.			
Cyperaceae						<i>Pterostichus (Cryobius)</i> spp.		+	+		
<i>Carex</i> spp.	+	+		+		<i>Pterostichus haematopus</i> Dej.		cf.			
<i>Eriophorum</i>	?					<i>Amara alpina</i> Payk.		cf.			
Salicaceae						Dytiscidae					
<i>Salix</i> sp. (wood)					+	Genus?	+	+			
Myricaceae						<i>Colymbetes</i> sp.	+				
<i>Comptonia</i> sp.			+			Staphylinidae					
Betulaceae						<i>Micropeplus sculptus</i> LeC.	+				
<i>Alnus</i> sp.		+	+			<i>Stenus</i> sp.		+			
<i>Betula glandulosa</i> type	+	+				<i>Tachinus</i> sp.		+			
<i>Betula</i> sp.	+		+			Byrrhidae					
<i>Betula</i> sp. (wood)					+	<i>Simplocaria</i> sp.	+				
Chenopodiaceae						Lathridiidae					
<i>Chenopodium</i> sp.		+				Genus?		+			
Nymphaeaceae						Chrysomelidae					
<i>Nuphar</i> sp.			+			Galerucinae		+			
Ranunculaceae						Curculionidae					
<i>Caltha</i> sp.	?					<i>Apion</i> sp.		+			
<i>Ranunculus</i> sp.		+				<i>Phyllobius</i> sp.	?	+			
Rosaceae						<i>Hypera</i> sp.		?			
<i>Dryas</i> sp.		+	+			<i>Rhynchaenus</i> sp.		?			
<i>Potentilla palustris</i> (L.) Scop.	+	+				Genus?			+		
<i>Potentilla</i> sp.		+	+			HYMENOPTERA					
Haloragaceae						Family?		+			
<i>Hippuris</i> sp.	+					ARACHNIDA					
Ericaceae						Araneae					
<i>Andromeda polifolia</i> L.	+					Family?		+			

Wolf Valley site: Wolf Valley (lat. 79°36'N, long. 82°31' W), Fosheim Peninsula, 25 km from Cañon Fiord, approximately 380 m a.s.l. "same site as 1961 station 3-29-6".
 35c = Sample FG 88-35c/2 collected by J.G. Fyles, July 20, 1988 (fieldbook 1-35), "Sample from west 1/2 m of 3 m organic unit".
 35a = Sample FG 88-35a collected by J.G. Fyles, July 20, 1988. (fieldbook 1-35), "west exposure, 0.5 to 1 m above base of 3 m organic unit".
 34b = Sample FG 88-34b collected by J.G. Fyles, July 20, 1988. (fieldbook 1-34).
 34c = Sample FG 88-34c collected by J.G. Fyles, July 20, 1988. (fieldbook 1-34), "sample a, b, and c from 30+ m sequence of sand and silty sand beneath 15 m gravel with wood".
 38c = Wood samples from various localities in the valley bottom. Not in situ. Samples identified as 'wood' come from FG 89-38c and were identified by H. Jetté (unpub. rept., 1994)

Wolf Valley site is younger than the typical high-terrace deposits. For example, it may be correlative with the late Pliocene Kap København Formation on northern Greenland (Fig. 1a) (Bennike, 1990), which also represents a time when trees existed in the High Arctic but apparently postdates the extinction of five-needle pine from that region. On the other hand, Wolf Valley sites might correspond to the early Quaternary Fishcreekian Transgression of the northern Alaskan coast (McDougall, 1995), which occurred between 1.7 and 1.2 Ma.

Russell Maris site

The Russell Maris site is located between Fosheim Dome and the Sawtooth Range (lat. 79°39'N, long. 83°52'W). Unlike most of the deposits discussed herein, it is an autochthonous forest bed with trees in growth position. Like most autochthonous deposits, the peat contains a low diversity of fossils and is dominated by several types. In this case, the most abundant vascular plant fossils are needles of spruce (*Picea*) and seeds of larch (*Larix*). In cross-section, some spruce needles show the type of resin canals typical of black spruce (*Picea mariana*) or red spruce (*Picea rubra*) (Plate 1f). We suspect that most of the needles represent black spruce, although this remains to be confirmed by more detailed anatomical study.

Several needles of a five-needle pine also occur in the assemblage. Their cross-sections reveal the externally positioned resin canals (Plate 1e) that are typical of the subsection *Eustrobi*, which includes the western white pine, *P. monticola* (Critchfield, 1986).

The presence of a few leaves of bog cranberry (*Oxycoccus*) and *Ledum* agrees with the evidence from fossil mosses (see below), suggesting the forest developed under damp, boggy conditions. *Shepherdia* is not normally found in such environments, yet its distinctive seeds also occur in the assemblage, the first of their type to be found at any High Arctic site. The *Shepherdia* species growing today in northern forests (*S. canadensis*, soapberry) is a shrub of dry, open sites within conifer forests. The fossil seeds in this sample differ from those of *S. canadensis* and therefore may represent another species, possibly an extinct one with site requirements quite different from *S. canadensis*.

Endocarps of *Myrica* also occur in the Russell Maris sample. They lack the distinctive lateral lobes, but obviously represent a species in the *Gale* group. Fossils of this type are common in late Tertiary deposits from Arctic Canada (Matthews and Ovenden, 1990; Matthews, unpub. data). They probably refer to the extinct species *Myrica arctogale* described from the Kap København site in northern Greenland (Fig. 1b) (Bennike, 1990).

Actinorhizal nodules are also present (Burgess and Peterson, 1987). These delicate structures form on the roots of alders and myricaceous plants and are another indication that Russell Maris peat is autochthonous.

Fossil mosses have low diversity and represent an in situ woodland floor (L.E. Ovenden, unpub. rept., 1990). *Tomenthypnum nitens*, the dominant form, and *Dicranum leioneuron* typically grow in fens and bogs whereas *Hylocomium* and *Rhytidiadelphus* grow on old logs within conifer forests and less frequently in peat lands. These last two are members of the group of feather mosses that are common in conifer forests (L.E. Ovenden, unpub. rept., 1990). Neither *R. triquetrus* nor *Dicranum leioneuron* occur today in the arctic islands; therefore, like the vascular plants, they indicate a warmer climate than at present.

Very few insects are found in this sample, as is typical of autochthonous deposits. At least one of them, probably from the Coleoptera family Anobiidae, is a type not recorded in any other arctic or subarctic deposit, whether Quaternary or Late Tertiary.

Romulus Lake site

The Romulus Lake site is 3 km south of the southwestern end of Romulus Lake at the head of Slidre Fiord (lat. 79°52'N, long. 85°15'W; elevation: 79 m) (Fig. 1b). The sample (FG-88-44b) discussed here consists of plant detritus and wood from a 20 cm zone within sands 4 m below the surface. The site differs from the others discussed here in that it is much lower than typical high-terrace deposits, yet the fossil content is very similar to assemblages from typical high-terrace sites.

Plant macrofossils clearly suggest that the sediments and plant fossils are late Tertiary. Among them are abundant seeds and needles of spruce, a few needles of a white pine, well preserved endocarps of *Comptonia*, *Decodon*, and *Aracites*, and possibly even a few seeds of *Physocarpus*. As with many Quaternary samples, *Dryas* leaves are abundant, but the difference in this case is that not all of them appear to be of the *D. integrifolia* type as is always the case for virtually all Quaternary samples from the High Arctic. Some *Dryas* leaves resemble those of the *D. octopetula* type seen in the late Pliocene deposits at Kap København in northern Greenland (Fig. 1b) (Bennike, 1990).

A nearby site (lat. 79°51.5'N, long. 85°17'W; sample HCA-72 5/8-1) reveals horizontally stratified sand with beds of woody debris in contact with tilted fine white sand resting on black shale. The pollen from the horizontally bedded sand includes many Tertiary types (R.J. Mott, unpub. rept., 1973). Wood from the site has been identified as *Picea* and *Larix*, one of the *Larix* pieces being a log 2 m long with a diameter of 40 cm (R.J. Mott, unpub. rept., 1973). The beds at this site may be equivalent to the ones seen at the Romulus Lake site, but no macrofossil samples have been examined to test this conclusion.

South Bay site

The South Bay site is 16 km south of South Bay on Cañon Fiord (lat. 79°26'N, long. 81°42'W) at an elevation of 500 m. The sample discussed here comes from a 50+ cm zone of silty, woody peat.

Plant macrofossils from this site are well preserved. Needles of a five-needle pine of the *Cembrae* type (two resin canals located in a medial position, Plate 1d) (Critchfield, 1986) are abundant, as are pine seeds. Many spruce needles are also present. Some of them were examined in cross-section and lack resin canals, which means that they are probably white spruce (*Picea glauca*) or a related extinct species, such as *P. banksi* (Hills and Ogilvie, 1970). *Larix* needles are also present, but are rarer than either spruce or pine. Some conifer needles are charred, which means that they are unlikely to have survived reworking. This and the excellent state of preservation of the other fossils shows that the fossils were deposited in place or, if reworked, are not from significantly older deposits.

A striking characteristic of the macroflora from South Bay is the abundance of endocarps of *Comptonia*. This plant is practically an indicator of late Tertiary age for samples from the Canadian Arctic. At South Bay, the endocarps display a striking range of sizes and forms, possibly signifying that several different species are represented.

Another plant that seems to be typical of late Tertiary deposits in the Arctic is *Physocarpus* or nine bark (Fyles et al., 1994, Table 5). *Physocarpus* is not abundant in the South Bay assemblage, but it is definitely present and just as well preserved as the other fossils. Even though the South Bay site contains plants found in virtually all other late Tertiary assemblages, there are some puzzling omissions, e.g. *Myrica arctogale* and *Aracites globosa*.

Insect fossils are not abundant in the South Bay sample, but they do contain a very significant fragment, the apical third of the elytron of the water scavenger beetle *Helophorus* (Plate 1b). It exhibits characteristics seen in the extinct *H. meighensis* (Matthews, 1976), previously described from the Beaufort Formation on Meighen Island. This fossil, like some of the plants, shows that the South Bay site is late Tertiary ((?)Pliocene).

A single pollen sample was studied from the South Bay site. It is dominated by *Betula* (47 per cent), alder (14 per cent), spruce (17 per cent), and pine (12 per cent). Since pine macrofossils show that five-needle pines grew in the region, the low percentage of pine pollen is puzzling, although it is a characteristic of other Ellesmere Island samples containing pine macrofossils and may mean that the reproductive physiology of pines in the late Tertiary Arctic differed from that of modern pines. However, it should be noted that even some modern surface samples from sites adjacent to stands (Hughes et al., 1981) as well as late Quaternary fossil samples containing needles of white pine (Mayle and Cwynar, 1995) also show unexpectedly low percentages of pine pollen.

QUATERNARY FLORAS AND FAUNAS

All the sites mentioned above contain fossils of plants or insects that have been found in the Pliocene Beaufort Formation and at other Ellesmere Island high-terrace sites known to be older than Quaternary (*see below*). Only the Wolf Valley site stands apart from the others, but it too seems to be no

younger than latest Tertiary or possibly earliest Quaternary. The sites discussed below all share characteristics that suggest they are much younger — either Holocene or one of the other Quaternary interglacial stages.

Fosheim Dome site

The Fosheim Dome site (Fig. 1b) is in a small, unnamed valley (lat. 79°37'N, long. 83°47'W) between Fosheim Dome and the Sawtooth Range. The five samples discussed here come from a 17 m unit of fine- to medium-grained, cross-stratified sand overlying the typical sand and gravel of the high-terrace sediments on the north wall of the valley. Are these sands simply a rarely seen facies of the high-terrace sediments or are they a distinctly younger unit? Although the sands contain very little organic material, the fossils listed in Table 3 help to answer this question.

One of the Fosheim Dome samples contains five-needle pine, an index fossil for late Tertiary samples in the Arctic. In this case, the fossil is a single, poorly preserved needle fragment and is not accompanied by any of the other typical late Tertiary fossils, e.g. *Comptonia*, *Myrica*, *Aracites*, or *Physocarpus* (Fyles et al., 1994, Table 5). This means that the pine-needle fragment is probably reworked from older deposits.

Leaves of mountain aven, *Dryas integrifolia*, a plant now abundant on Fosheim Peninsula, are abundant in some samples. The assemblage also includes a few plants not currently found on Fosheim Peninsula. For example, sample 38e, one of the most diverse of the group, contains both *Menyanthes trifoliata* and *Nuphar*, neither of which grows on Ellesmere Island today (Porsild and Cody, 1980). While the possibility that these fossils are reworked from older deposits cannot be completely discounted, their presence at least suggests that climate at the time of deposition was warmer than at present.

The arthropod fossils from sample 38e and particularly sample 5a also indicate a warmer climate. Among them are a number of ground-beetles (Carabidae), a family that is not found on Ellesmere Island today (Danks, 1981; Brodo, 2000). None of the taxa are restricted to forested areas, but species such as *P. (Cryobius) brevicornis* currently do not live much beyond the treeline (Lindroth, 1966). The same is true of all species of the genus *Notiophilous* and the species in the *Bembidion sordidum* group (Lindroth, 1961, 1963). Although insect fossils are rarer in samples 5d and 5b, these samples also contain taxa that are not found on Ellesmere Island today.

Sample 5a is the only one in which bryophyte fossils have been studied in detail. The 5a assemblage is unusually rich in species from damp (not wet) tundra, with minor amounts of species more likely to occur along streams or on fresh alluvium (L.E. Oviden, unpub. rept., 1989), probably a reflection on the origin of the sands from which the samples come (several of the insects, e.g. *Bembidion sordidum* group, also suggest an alluvial site). *Pleurozium schreberi* in sample 5a is not in accord with the other fossils since it usually is found within forested areas, but we believe that this indicates only that the regional environment at the time of deposition was similar to the present-day Low Arctic tundra. If this is the

Table 3. Fossils of plants and animals (arthropods and other invertebrates) from the Fosheim Dome locality.

FOSSILS	SAMPLE NUMBER					FOSSILS	SAMPLE NUMBER				
	5a	5d	5c	38e	5b		5a	5d	5c	38e	5b
PLANTS AND RELATED REMAINS						Hippuridaceae					
Amber	+					<i>Hippuris</i> sp.			+	+	+
Fungal sclerotia	+	+	+	+		Empetraceae					
BRYOPHYTA						<i>Empetrum nigrum</i>				+	
Dicranales						Ericaceae					
<i>Ceratodon purpureus</i> (Hedw.) Brid.	+					Genus?	+				
<i>Distichium inclinatum</i> (Hedw.) BSG	+					<i>Vaccinium</i> sp.	+				
<i>Ditrichum flexicaule</i> (Schwaegr.) Hampe	+					Gentianaceae					
Pottiales						<i>Menyanthes trifoliata</i> L.	+				
<i>Tortula ruralis</i> (Hedw.) Gaertn.	+					ARTHROPODS AND OTHER ANIMALS					
Bryales						TUBELLARIA					
<i>Bryum</i> spp.	+					BRYOZOA					
Hypnobryales						<i>Cristatella mucedo</i> L.	+		+	+	
<i>Calliergon giganteum</i> (Schimp.) Kindb.	+					ARTHROPODA					
<i>C. richardsonii</i> (Mott.) Kindb. ex Warnst.	+					INSECTA					
<i>Campylium</i> sp.	+					PLECOPTERA					
<i>Drepanocladus aduncus</i> (Hedw.) Warnst.	+					Family?				+	
<i>D. fluitans</i> (Hedw.) Warnst.	+					HEMIPTERA					
<i>D. revolvens</i> (Sw.) Warnst.	+					Saldidae					
<i>Hygrohypnum bambergi</i> Schimp.	+					<i>Salda</i> ?					
<i>Hypnum</i> sp.	+					Genus					+
<i>Myurella tenerrima</i> (Brid.) Lindb.	+					HOMOPTERA					
<i>Thuidium abietinum</i> (Hedw.) B.S.G.	+					Cicadellidae					
<i>Tomenthypnum nitens</i> (Hedw.) Loeske	+					Genus?	+				
<i>Pleurozium schreberi</i> (Brid.) Mitt.	+					COLEOPTERA					
Polytrichales						Carabidae					
<i>Polytrichum</i> sp.	+					<i>Notiophilus</i> sp.	+				
VASCULAR PLANTS						<i>Bembidion</i> sp.	+	+			
Equisetaceae						<i>Bembidion sordidum</i> grp.	+		+		
<i>Equisetum</i> sp.						<i>Bembidion umiatense</i> type				+	
Pinaceae						<i>Pterostichus (Cryobius) ventricosus</i> grp.	+				
<i>Pinus (Strobus)</i> subsect. <i>Eustrobi</i>					+	<i>Pterostichus (Cryobius) brevicornis</i> Kirby		+	+		+
Potamogetonaceae						<i>Pterostichus (Cryobius)</i> sp.				+	
<i>Potamogeton</i> sp.						<i>Pterostichus vermiculosus</i> Men.	+				
<i>Potamogeton filiformis</i>	+				+	<i>Pterostichus</i> sp.		+			
Gramineae						<i>Amara</i> sp.	+				
Genus?	+					<i>Amara glacialis</i> Mann.	+				
Cyperaceae						Dytiscidae					
<i>Carex aquatilis</i> Wahlenb.	+				+	<i>Hydroporus</i> sp.	+	+			+
<i>Carex</i> spp.	+	+	+		+	<i>Agabus</i> sp.					?
<i>Eriophorum</i> sp.	+		?			<i>Colymbetes</i> sp.		+			
<i>Kobresia</i> sp.	?				+	Staphylinidae					
Betulaceae						<i>Stenus</i> sp.	+	+			
<i>Betula</i> dwarf shrub type					+	Aleocharinae					
Salicaceae						Curculionidae					
<i>Salix</i> sp.	+				+	Genus?	+				
Betulaceae						DIPTERA					
<i>Betula</i> sp.	+					Tipulidae					
Polygonaceae						Genus?	+				
<i>Oxria digyna</i> (L.) Hill	++				+	Culicidae					
<i>Polygonum</i> sp.					+	Genus	+				
<i>Rumex</i> sp.	?					Chironomidae					
Nymphaeaceae						<i>Chironomus</i> sp.		+			
<i>Nuphar</i> sp.					+	Family?			+		+
Ranunculaceae						HYMENOPTERA					
<i>Ranunculus</i> sp.	+					Ichneumonidae					
<i>Ranunculus hyperboreus</i> type					+	Genus?	+				
Cruciferae						CRUSTACEA					
Genus?						Notostraca					
Saxifragaceae						<i>Lepidurus</i> sp.	+				
<i>Saxifraga oppositifolia</i> L.	+					ARACHNIDA					
<i>Saxifraga</i> sp.					+	Acari					
Rosaceae						Oribatei	+	+			+
<i>Dryas</i> sp.	++				+	Araneae					
<i>Dryas integrifolia</i>						Lycosidae	+				
<i>Potentilla</i> sp.					+						
<i>Potentilla palustris</i> (L.) Scop.	cf.				+						

Fosheim Dome site: north wall of a small valley between the Fosheim Dome and the Sawtooth Range (lat. 79°37'N, long. 83°47'W); elevation approximately 320–334 m a.s.l. Samples are listed from approximately lowest (5a) to highest (5b).
 5a = Sample FG 88-5a, collected by J.G. Fyles, July 10, 1988 (fieldbook 1-5). "Plant detritus (and detrital coal) in organic lens in medium sand capping gravel and sand...7 m below top of 17 m of sand".
 5d = Sample FG 88-5d, collected by J.G. Fyles, July 10, 1988 (fieldbook 1-5). "Blocks of peat (not in place but certainly from the exposure) from a 17 m unit of fine to medium sand capping gravel and sand. The peat blocks have rolled down slope but source bed not seen".
 5c = Sample FG 88-5c, collected by J.G. Fyles, July 10, 1988 (fieldbook 1-5). Detrital plant material "4 m below top of a 17 m sand in horizon. bed of medium sand."
 38e = Sample FG 89-38e, collected by J.G. Fyles, July 24, 1989 (fieldbook 89-1(39)). Silty layers in sand with lenses of peat and lenses of plant detritus; "high terrace site but cannot prove whether the exposed sands are reworked and contain younger organics."
 5b = Sample FG 88-5b, collected by J.G. Fyles, July 10, 1988 (fieldbook 1-5). Sparse detrital plant material 2 m below top of 17 m unit of fine to medium sand capping sand and gravel.

case, then it implies climate warming of more than 3°C (mean July temperature), which is probably more than occurred during the Holocene. Thus, the sands of the Fosheim Dome probably represent one of the Pleistocene interglacial stages.

Sample HCA 78-13/7-5 from near Cañon Fiord

This sample was taken 5 m from the top of a 20 m unit of deltaic/lacustrine gravel, sand, silt, and clay at a site 20 km south of the southernmost bay on Cañon Fiord (lat. 79°24'N, long. 80°51'W) at 200 m a.s.l. (Hodgson, 1985).

With the exception of *Potamogeton* and *Betula*, all of the taxa found in the deposit (Appendix A) are likely to occur on northern Ellesmere Island today. *Potamogeton* is not a High Arctic plant. *Potamogeton filiformis* is the most northern species in the genus, yet it has not been reported on Ellesmere Island, or for that matter on any other island of the Arctic Archipelago except at Iqaluit (Porsild and Cody, 1980). This suggests a warmer climate. A single, poorly preserved betulaceous samara (probably *Betula*) is also evidence of a warmer climate, especially if it represents *Alnus* rather than *Betula*.

The plant fossil assemblage lacks conifer needles, cone-scale fragments, *Myrica*, and other fossils typical of the Beaufort Formation on Meighen Island (Fig. 1a) or other high-terrace sites. Thus it is unlikely that the *Potamogeton* and (?)*Betula* fossils are reworked.

The conclusion that climate was warmer during deposition is also supported by some insect fossils (Appendix B). *Amara alpina*, a ground-beetle (Carabidae), is the northernmost representative of the group; its present northern limit is Devon Island (Lindroth, 1968; Danks, 1981). Not only does the ground-beetle *Elaphrus tuberculatus* (identified by H. Goulet, Eastern Cereal and Oilseed Research Centre, Agriculture Canada) not occur as far north as Ellesmere Island, but it is now found only west of Inuvik and the Mackenzie River. Furthermore, although it has been recorded from tundra in the Old World, it is seldom found far beyond the limit of trees in North America (Goulet, 1983).

Two other insect fossils represent ladybird beetles (family Coccinellidae). Of the two, the genus *Nephus* has the most northerly distribution, yet current records show that its distribution barely extends beyond the northern treeline (Gordon, 1985). *Nephus* is found at a pre-Holocene Quaternary site on Ellesmere Island south of Fosheim Peninsula (Blake and Matthews, 1979). The other coccinellid, *Ceratomegilla ulkei*, also is not found far beyond the present treeline (Gordon, 1985). Weevils of the genus *Lepyryus* feed on willows and poplars. Several of the species occur on tundra, but as yet none have been reported from the Arctic Archipelago (Danks, 1981).

The fossils from the HCA sample show that climate at the time of deposition was probably warm enough to allow trees to grow somewhere on Ellesmere Island, if not on Fosheim Peninsula itself. This means that the sample represents a Quaternary interglacial stage, and not the Holocene, because

wood from the site has been dated at >38 000 B.P. (Hodgson, 1985). The delta containing the fossils was built into a glacier-dammed lake (Hodgson, 1985), so the deposit is unlikely to be older than the Quaternary. However, according to the fossil evidence, the glacier responsible for the lake and the delta must have formed at a time when the climate was much warmer than at present. Its development may have been fostered by more open water conditions at the time.

Cañon Fiord site

The Cañon Fiord site is located 7 km south of Cañon Fiord and 14 km east of South Bay (lat. 79°31'N, long. 81°03'W). The sample (FG-88-39b) was taken at 578 m a.s.l. from 20 cm of mossy peat 30 cm below the top of gravel within a capping unit of gravel and sand.

Plant macrofossils are abundant and relatively well preserved (Appendix A). The two most common types are *Salix* capsules and *Ranunculus* achenes. Also present are leaf fragments and hypanthia of *Dryas integrifolia*. All the plants listed in Appendix A are found or can be expected to be found on Fosheim Peninsula today. Moreover, the assemblage lacks all fossils of trees, especially larch, spruce, or pine needles that characterize some of the other assemblages from typical high-terrace sediments. Thus, on the basis of plant fossils alone, this sample is judged to be Quaternary, possibly even as young as Holocene.

Although less abundant than plants, insect fossils (Appendix B) provide some qualifications to the above conclusion. They include one elytral fragment of the ground-beetle subgenus *Amara* (*Curtinotus*) (most likely representing the species *Amara alpina*). No species of *Amara* has been collected on Ellesmere Island or on Fosheim Peninsula (Danks, 1981; Brodo, 2000) and although the presence of this single fossil does not rule out a Holocene age, it does suggest that the Cañon Fiord peat formed during the warmest part of the Holocene.

Red Hill site

The Red Hill site is located at latitude 79°45'N, longitude 84°44'W, between the Russell Maris site and the Romulus Lake site. The sample (283 m a.s.l.) comes from a 1 to 2 cm layer of detrital plant material and wood in a 3 m exposure of fine sand, silty sand, and silt within the capping gravel and sand of the high-terrace sequence.

The sieved residue lacks fossils of conifers. However, the presence of well preserved fragments of alder, samaras of birch that approach the tree birch type, and *Chenopodium* all point to a climate that was significantly warmer than at present and warmer than expected for the middle Holocene.

Insect fossils also indicate warmer climate. Among them are elytral and pronotal fragments of carabids (ground-beetles) — *Pterostichus* (?)*ventricosus* and *P. haematopus*, both of which have their northern distribution limit in the Low Arctic tundra zone (Lindroth, 1966; Danks, 1981).

RELATED LATE TERTIARY SITES NEAR THE FOSHEIM PENINSULA

The sites discussed here represent only a few of the high-terrace macrofossil localities on Ellesmere Island. Others are mentioned in Matthews and Oviden (1990). Two of them are of special importance to this discussion.

Beaver Peat site

The Beaver Peat site is on Strathcona Fiord, a branch of Bay Fiord that forms the southern boundary of Fosheim Peninsula (Fig. 1b). The site is actually a collection of sites within 1 km of each other. The main deposit is an accumulation several metres thick of mossy peat containing beaver-chewed wood, seeds, insects, and the only Pliocene vertebrate fossils known from the Canadian Arctic (Harington, 1996). The other sites represent several different biotopes, including small ponds and bogs or fens.

Taken together, the various sample faunules provide a very complete picture of the fauna and flora of the region at the time of deposition. Note the large number of taxa listed in appendices A and B. Mammal fossils alone suggest an early Pliocene age (Harington, 1996; Hulbert and Harington, 1996). The content of plant fossils is also typical of Pliocene deposits. Significantly, one of the florules includes the small, but very distinctive, seeds referred to as the '*Paliurus* type' (Matthews and Oviden, 1990, Fig. 4-1 and 4-2; Matthews, unpub. data). This type is conspicuously absent from the Fosheim Peninsula sites or from the early Late Pliocene Beaufort Formation on Meighen Island (Fig. 1a) (Matthews, unpub. data). This shows that the Beaver Peat is probably older than the Meighen Island deposits, a conclusion also supported by the mammal fossils (Hulbert and Harington, 1996).

The Beaver Peat likely also predates all Fosheim Peninsula sites discussed herein since none of them contain *Paliurus*-type seeds. However, many of the other fossils from the Beaver Peat do occur in one or more of the Fosheim samples and it is this fact as well as the similarity of the Fosheim floras and faunas to those from the Beaufort Formation on Meighen Island that firmly date some of the Fosheim Peninsula sites as Late Pliocene.

Although the macrofossil and arthropod assemblages from the several sites grouped as the Beaver Peat include a few species that are now found far to the south, even south of the taiga zone, the overall composition of the flora and fauna suggests a forest-tundra site. For example, several beetle fossils are from species common today in tundra regions. The climate was undoubtedly much warmer than at the site today, but perhaps not much warmer than at the present treeline. The Beaver Peat, though possibly somewhat older than the Fosheim Peninsula sites, may represent a slightly colder climate. This is to be expected since the Pliocene was characterized by several major climatic fluctuations (Dowsett and Poore, 1991).

Riediger site

Another important group of sites in the high-terrace sequence is known informally as the 'Riediger site' (Fig. 1b). Although it is much farther from Fosheim Peninsula than the Beaver Peat site (see Fig. 1b), we mention it here because it contains key taxa not found so far on Fosheim Peninsula. At the Riediger site, wood- and peat-bearing sand and silty sand interbedded with cobble to boulder gravel some 20 m thick occur beneath the boulder-strewn upland surface (approx. 500 m a.s.l.) at the western margin of the Prince of Wales Ice Sheet (J.G. Fyles, pers. comm., 1996). These horizontal, undeformed, organic strata overlie an inclined and faulted succession of dark shale and somewhat indurated sandstone and conglomerate. Riediger et al. (1984) applied the name 'Beaufort Formation' to this conglomeratic sequence. In a subsequent study, Thorsteinsson et al. (1994) assign it to an upper unit of the Paleogene Eureka Sound Group.

Plant macrofossils listed in Appendix A (sample R) come from two sample localities approximately 1 km apart. Both expose woody organic sediments overlying the deformed Paleogene unit and may be of equivalent age. What is important to note here is the presence of several fossils (e.g. *Tubela*, *Aronia*, *Nymphoides*, *Epipremnum crassum*, and Cyperaceae type A) that do not occur at any of the Fosheim Peninsula sites.

Aronia (chokecherry) has only been found at this one site in the Arctic, hence its absence from the Fosheim Peninsula is not of any significance. The type referred to as 'Cyperaceae A' is found (so far) at one other place in North America — the late Miocene Canyon Village site in eastern Alaska (Matthews, unpub. data). In Europe, it occurs at a middle Miocene site in Denmark (Friis, 1985). Its presence at the Riediger site may mean that it too is Miocene. An even better indication of this is the abundance of fossils of *Epipremnum crassum* in one of the Riediger florules. The only other arctic site with a similar abundance of well preserved *Epipremnum* is the middle Miocene Ballast Brook Formation (Fyles et al., 1994) at Ballast Brook, on northern Banks Island (Fig. 1b). A few *Epipremnum* fruits are found at arctic Pliocene localities (Fyles et al., 1994; Matthews, unpub. data), but they may be reworked from older units. Farther south in Alaska and the northern Yukon Territory, abundant *E. crassum* occurs in deposits that are no older than early late Pliocene (Matthews and Oviden, 1990; Matthews, unpub. data). The absence of *E. crassum* fossils from most high-terrace sites, including all on Fosheim Peninsula, probably means that all these sites are no older than the Pliocene. *Nymphoides* is another plant that may indicate that the Riediger site is older than the Fosheim Peninsula high-terrace sites, since the only other significant occurrence of seeds of this semi-aquatic plant is also in the Ballast Brook Formation (Fyles et al., 1994).

In spite of the presence of macrofossils of five-needle pine in the Riediger samples, several pollen samples show little (less than 4 per cent) or no pine pollen, a situation also seen at several of the Fosheim Peninsula sites that yield pine macrofossils. The 'rule of thumb' that pine pollen swamps the

regional pollen rain even when pines are rare to absent apparently does not apply to some Tertiary deposits. However, we note that a few Quaternary and modern surface samples also fail to follow the 'rule' (e.g. Hughes et al., 1981; Mayle and Cwynar, 1995).

DISCUSSION

One of the objectives of this report is to put on record the many late Tertiary and probable pre-Holocene Quaternary fossil sites that exist in the high-terrace sediments found in many areas of Ellesmere Island, including Fosheim Peninsula. The fossils, when compared with dated deposits from the Beaufort Formation on the western margin of the Queen Elizabeth Islands and other high-terrace floras and faunas on Ellesmere Island, suggest that none of the Fosheim Peninsula sites discussed here are older than the Pliocene. Some are considerably younger, representing one or more Pleistocene interglacial stages or even the Holocene.

The High Arctic climate during the Pliocene was similar to that expected to occur under the $2\times\text{CO}_2$ greenhouse-gas concentration scenario (Etkin and Agnew, 1992). Therefore, a knowledge of the vegetation of the Arctic during the Pliocene provides some hints as to possible vegetation changes in the future. On the other hand, it would be wrong to draw too close a comparison since the rich coniferous forests of the Pliocene formed as a result of slow climatic deterioration throughout the Tertiary, whereas the vegetation changes of the future will be the result of nearly instantaneous climatic warming.

A second objective of the study of sites such as those discussed above is to characterize the later Tertiary floras so that they may be distinguished from those of the Quaternary (Gajewski et al., 1995). Because the late Tertiary fossils are so well preserved — in many cases as well preserved as Holocene fossils — they cannot be easily distinguished on the basis of preservation alone from their younger counterparts. There are obvious exceptions. Pine-needle fragments or even spruce-needle fragments, regardless of their preservation at Fosheim Peninsula sites, are unlikely to be Quaternary. Similarly, one can be certain that an autochthonous forest bed on Ellesmere Island (such as the Russell Maris site) must be older than Quaternary. The Kap København site in northern Greenland (Fig. 1b) (Bennike, 1990) shows that the last time such forests existed as far north was 2.5–2 Ma. Trees have almost certainly been absent from Ellesmere Island since that time. But what of other fossils, such as various species of sedge, *Dryas*, *Oxyria*, or even *Nuphar* and other aquatic plants? They can be expected in both late Tertiary and Quaternary deposits. How can such fossils be evaluated as to their paleoenvironmental significance?

In many ways, the Fosheim Peninsula samples discussed herein are a test case for resolving such a dilemma. At the outset, most seem to come from typical, high-terrace sediments (the single anomaly — Romulus Lake — remains unexplained) yet when the individual assemblages are examined, their fossils suggest that some of the samples are Quaternary.

They lack the typical fossils found in the late Tertiary samples. Even so, most of these putative Quaternary assemblages contain fossils (particularly insect fossils) indicating a level of warmth that is greater than what one might expect for the Holocene. They probably represent one or more Pleistocene interglacial stages. In other words, the study of fossils from the high-terrace sediments shows that the unit is more complex than was first thought. It contains more than late Tertiary sediments and, in some cases, it is difficult to differentiate between Tertiary and Quaternary sediments without studying the fossils.

This fact alone is reason for continuing the study of fossils from the high-terrace sediments, both on Fosheim Peninsula and elsewhere on Ellesmere Island. Not only will such investigations tell us more about the arctic realm just prior to the onset of northern hemisphere glaciation, but the study of such sites will ultimately help us better understand the course of High Arctic climate change during the Pleistocene and Holocene and perhaps even in the future.

REFERENCES

- Bennike, O.**
1990: The Kap København Formation: stratigraphy and palaeobotany of a Plio-Pleistocene sequence in Peary Land, North Greenland; *Meddelelser om Grønland*, v. 23, p. 1–85.
- Blake, W., Jr. and Matthews, J.V., Jr.**
1979: New data on an interglacial peat deposit near Makinson Inlet, Ellesmere Island, District of Franklin; *in* Report of Activities, Part B; Geological Survey of Canada, Paper 79-1B, p. 157–164.
- Bose, M.N. and Manum, S.B.**
1990: Mesozoic conifer leaves with '*Sciadopitys*-like' stomatal distribution. A re-evaluation based on fossils from Spitsbergen, Greenland and Baffin Island; *Norsk Polarinstitut, Skrifter Nr.*, v. 192, 81 p.
- Bousquet, Y.**
1988: *Dyschirius* of America north of Mexico: descriptions of new species with keys to species groups and species (Coleoptera: Carabidae); *The Canadian Entomologist*, v. 120, p. 361–387.
- Brodo, F.**
2000: The insects, mites, and spiders of Hot Weather Creek, Ellesmere Island, Nunavut; *in* Environmental Response to Climate Change in the Canadian High Arctic, (ed.) M. Garneau and B.T. Alt; Geological Survey of Canada, Bulletin 529.
- Burgess, D. and Peterson, R.L.**
1987: Development of *Alnus japonica* root nodules after inoculation with *Frankia* strain HFPAr13; *Canadian Journal of Botany*, v. 65, no. 8, p. 1647–1657.
- Campbell, M.J.**
1968: A revision of the New World Micropeplinae (Coleoptera: Staphylinidae) with a rearrangement of the world species; *The Canadian Entomologist*, v. 100, p. 225–267.
- Critchfield, W.B.**
1986: Hybridization and classification of the white pines (*Pinus* section *Strobus*); *Taxon*, v. 35, no. 4, p. 647–656.
- Danks, H. V.**
1981: Arctic Arthropods: A Review of Systematics and Ecology with Particular Reference to the North American Fauna; Entomological Society of Canada, Ottawa, 608 p.
- Dowsett, H.J. and Poore, R.Z.**
1991: Pliocene sea surface temperatures of the North Atlantic Ocean at 3.0 Ma; *Quaternary Science Reviews*, v. 10, p. 189–204.
- Dyke, A.S. and Matthews, J.V., Jr.**
1987: Stratigraphy and paleoecology of Quaternary sediments along Pasley River, Boothia Peninsula, central Canadian Arctic; *Géographie physique et Quaternaire*, v. 41, no. 3, p. 323–344.

- Edlund, S.A.**
1992: Climate change and its effect on Canadian Arctic plant communities; *in* Arctic Environment: Past, Present, and Future, (ed.) M-k. Woo and D.J. Gregor; Proceedings of a symposium held at McMaster University, November 14–15, 1991, p. 121–138.
- Edlund, S.A., Alt, B.T., and Garneau, M.**
1989: Regional congruence of vegetation and summer climate patterns in the Queen Elizabeth Islands, Northwest Territories, Canada; *Arctic*, v. 42, p. 3–23.
2000: Vegetation patterns on Fosheim Peninsula, Ellesmere Island, Nunavut; *in* Environmental Response to Climate Change in the Canadian High Arctic, (ed.) M. Garneau and B.T. Alt; Geological Survey of Canada, Bulletin 529.
- Etkin, D. and Agnew, T.**
1992: Arctic climate and the future; *in* Arctic Environment: Past, Present, and Future, (ed.) M-k. Woo and D.J. Gregor; Proceedings of a symposium held at McMaster University, November 14–15, 1991, p. 17–34.
- Friis, E.M.**
1985: Angiosperm fruits and seeds from the Middle Miocene of Jutland (Denmark); *Det Kongelige Danske Videnskaberne Selskab Biologiske Skrifter*, v. 24, no. 3, 165 p.
- Fyles, J.G.**
1990: Beaufort Formation (Late Tertiary) as seen from Prince Patrick Island, Arctic Canada; *Arctic*, v. 43, no. 4, p. 393–403.
- Fyles, J.G., Hills, L.V., Matthews, J.V., Jr., Barendregt, R., Baker, J., Irving, E., and Jetté, H.**
1994: Ballast Brook and Beaufort formations (Late Tertiary) on northern Banks Island, Arctic Canada; *in* Tertiary and Quaternary Boundaries, (ed.) T.A. Ager, J.M. White, and J.V. Matthews, Jr.; *Quaternary International*, v. 22/23, p. 141–171.
- Fyles, J.G., Marincovich, L., Jr., Matthews, J.V., Jr., and Barendregt, R.**
1991: Unique mollusc find in the Beaufort Formation (Pliocene) Meighen Island, Arctic Canada; *in* Current Research, Part B; Geological Survey of Canada, Paper 91-1B, p. 105–111.
- Gajewski, K., Garneau, M., and Bourgeois, J.C.**
1995: Paleoenvironments of the Canadian High Arctic derived from pollen and plant macrofossils: problems and potentials; *Quaternary Science Reviews*, v. 14, p. 609–629.
- Garneau, M., Alt, B.T., and Edlund, S.A.**
2000: Introduction; *in* Environmental Response to Climate Change in the Canadian High Arctic, (ed.) M. Garneau and B.T. Alt; Geological Survey of Canada, Bulletin 529.
- Gordon, R.D.**
1985: The Coccinellidae (Coleoptera) of America north of Mexico; *Journal of the New York Entomological Society*, v. 93, 912 p.
- Goulet, H.**
1983: The genera of Holarctic Elaphrini and species of *Elaphrus* Fabricius (Coleoptera: Carabidae): classification, phylogeny and zoogeography; *Quaestiones Entomologicae*, v. 19, p. 219–482.
- Harington, C.R.**
1996: Paleoecology of a Pliocene beaver pond site in the Canadian Arctic Islands; 30th International Geological Congress, Beijing, China August 4–14, 1996; Abstracts II, p. 114.
- Hills, L.V. and Ogilvie, R.T.**
1970: *Picea banksi* n.sp. Beaufort Formation (Tertiary), northwestern Banks Island, Arctic Canada; *Canadian Journal of Botany*, v. 48, p. 457–464.
- Hodgson, D.A.**
1985: The last glaciation of west-central Ellesmere Island, Arctic Archipelago, Canada; *Canadian Journal of Earth Sciences*, v. 22, p. 347–368.
- Hughes, O.L., Harington, C.R., Janssens, J.A., Matthews, J.V., Jr., Morlan, R.E., Rutter, N.W., and Schweger, C.E.**
1981: Upper Pleistocene stratigraphy, paleoecology, and archaeology of the northern Yukon interior, eastern Beringia, 1. Bonnet Plume Basin; *Arctic*, v. 34, p. 329–365.
- Hulbert, R.C. and Harington, C.R.**
1996: An early Pliocene hipparionine horse from the Canadian Arctic: biogeographic and paleoecologic implications; 56th Annual Meeting, Society of Vertebrate Paleontology, Suppl. 2, No. 3, p. 42A (abstract).
- Jentys-Szaferowa, J. and Truchanowiczowna, J.**
1953: Seeds of *Menyanthes* L. in Poland from the Pliocene to the present time. Research on the Tertiary Flores, Instytut Geologiczny, Prace 10, p. 36–59.
- Lindroth, C.H.**
1961: The ground-beetles of Canada and Alaska, 6 pts.: *Opuscula Entomologica*, Suppl. XX, p. 1–200.
1963: The ground-beetles of Canada and Alaska, 6 pts.: *Opuscula Entomologica*, Suppl. XXIV, p. 200–408.
1966: The ground-beetles of Canada and Alaska, 6 pts.: *Opuscula Entomologica*, Suppl. XXXIX, p. 409–648.
1968: The ground-beetles of Canada and Alaska, 6 pts.: *Opuscula Entomologica*, Suppl. XXXIII, p. 649–944.
- Matthews, J.V., Jr.**
1976: Evolution of the subgenus *Cyphelophorus* (Genus *Helophorus*: Hydrophilidae, Coleoptera): description of two new fossil species and discussion of *Helophorus tuberculatus* Gyll.; *Canadian Journal of Zoology*, v. 54, p. 652–673.
1977: Tertiary Coleoptera fossils from the North American Arctic; *The Coleopterists Bulletin* v. 31, p. 297–308.
1979: Late Tertiary Carabid fossils from Alaska and the Canadian Arctic Archipelago; *in* Carabid Beetles: Their Evolution, Natural History, and Classification, (ed.) C.E. Ball, T.E. Irwin, and D.R. Whitehead; W. Junk bv., The Hague, Netherlands, p. 425–445.
- Matthews, J.V., Jr. and Oviden, L.E.**
1990: Late Tertiary plant macrofossils from localities in arctic/subarctic North America: a review of the data; *Arctic*, v. 43, no. 4, p. 364–392.
- Matthews, J.V., Jr., Oviden, L.E., and Fyles, J.G.**
1990a: Plant and insect fossils from the late Tertiary Beaufort Formation on Prince Patrick Island, N.W.T.; *in* Canada's Missing Dimension: Science and History in the Canadian Arctic Islands. Vol. 1, (ed.) C.R. Harington; Canadian Museum of Nature, Ottawa, Ontario, p. 105–139.
- Matthews Jr., J.V., Schweger, C.E. and Janssens, J.J.**
1990b: The last (Koy-Yukon) interglaciation in the northern Yukon Territory: evidence from Unit 4 at Ch'ijee's Bluff exposure, Bluefish Basin; *Géographie physique et Quaternaire*, v. 44, no. 3, p. 341–362.
- Mayle, F. and Cwynar, L.C.**
1995: Impact of the Younger Dryas cooling event upon lowland vegetation of Maritime Canada; *Ecological Monographs*, v. 65, no. 2, p. 129–154.
- McDougall, K.**
1995: Age of the Fishcreekian Transgression; *Palaios*, v. 10, p. 199–220.
- Porsild, A.E. and Cody, W.J.**
1980: Vascular plants of continental Northwest Territories, Canada; Ottawa. Ottawa: National Museums of Canada, Ottawa, Ontario, 667 p.
- Repenning, C.A. and Brouwers, E.M.**
1992: Late Pliocene–Early Pleistocene ecologic changes in the Arctic Ocean borderland; United States Geological Survey, Bulletin 2036, p. 1–37.
- Riediger, C.L., Bustin, R.M., and Rouse, G.E.**
1984: New evidence for a chronology of the Eurekan Orogeny from south-central Ellesmere Island; *Canadian Journal of Earth Sciences*, v. 21, p. 1286–1295.
- Thorsteinsson, R., Harrison, J.C., and deFreitas, T.**
1994: Phanerozoic geology of the Vendom Fiord map area (NTS 48D), District of Franklin, Northwest Territories; Geological Survey of Canada Open File 2880.
- Tiffney, B.H.**
1989: The collection and study of dispersed angiosperm fruits and seeds; Phytodebris; Meeting of the paleobotanical section of the botanical Society of America, p. 97–124.
- Van der Hammen, T., Wilmstra, T.A., and Zagwijn, W.H.**
1971: The floral record of the late Cenozoic of Europe; *in* Late Cenozoic Glacial Ages, (ed.) K.K. Turekian; Yale University Press, New Haven, Connecticut, p. 391–424.

APPENDIX A

Plant macrofossils from various Fosheim Peninsula and related high-terrace site

	Sites ¹										
	RC	RM	RL	SB	BP	FD	WV	RH	CF	HCA	R
Actinorhizal nodules		+			+		+	+			+
Fungal sclerotia	+	+	+	+	+	+	+	+	+		+
Algae											
Characeae											
<i>Chara/Nitella</i> type					+						
Bryophyta ²			+		+		+		+	+	
Sphagnales											
<i>Sphagnum</i> sp.					+						
<i>S. compactum</i> DC.					+						
<i>S. imbricatum</i> Hornsch ex. Russ.											+
<i>S. lenense</i> Lindb. f. ex. Pohle											+
<i>S. magellanicum</i> Brid.					+						
<i>S. papillosum</i> Lindb.					+						
Dicranales											
<i>Ceratodon purpureus</i> (Hedw.) Brid.						+					
<i>Dicranella</i> sp.					+						
<i>Diacranum leioneuron</i> Kindb.		+									
<i>Distichium capillaceum</i> (Hedw.) B.S.G.					+						
<i>D. inclinatum</i> (Hedw.) B.S.G.						+					
<i>Ditrichum flexicaule</i> (Schwaegr.) Hampe					+	+					
Pottiales											
<i>Encalypta alpina</i> Sm.					+						
<i>Tortula ruralis</i> (Hedw.) Gaertn.						+					
<i>Tortula</i> sp.				+	+						
Bryales											
<i>Bryum</i> spp.				+	+	+					
<i>Cinclidium arcticum</i> (B.S.G.) Schimp.					+						
<i>C. latifolium</i> Lindb.				+	+						
<i>Meesia triquetra</i> (Richt.) Aongstr.	+				+						
Mniaceae											
<i>Mnium thomsonii</i> Schimp.					+						
<i>Paludella squarrosa</i> (Hedw.) Brid.					+						
<i>Pohlia</i> sp.					+						
<i>Timmia austriaca</i> Hedw.					+						
<i>T. megapolitana</i> ssp. <i>bavarica</i> (Hessl.) Brass.					+						
Hypnobryales											
<i>Amblystegium riparium</i> (Hedw.) B.S.G.					+						
<i>Calliergon giganteum</i> (Schimp.) Kindb.	+		+	+							
<i>C. richardsonii</i> (Mott.) Kindb. ex Warnst.						+					
<i>C. richardsonii</i> var. <i>robustum</i> (Lindb.&H.Arnell) Broth.					+						
<i>C. trifarium</i> (Web.&Mohr) Kindb.					+						

Note: Appearance of a taxon name in the list does not necessarily mean that the taxon was found in a particular sample. Some taxa (shown in bold face) are identified as only 'near to' (cf.) named taxon; where fossils were adequate for only a tentative identification, a '?' is used (underlined records). Consult the numerical designation for each sample.

¹ Site abbreviations: Fosheim Peninsula sites are in bold face.
BP = Beaver peat and associated deposits, Strathcona Fiord, Ellesmere Island (combination of fossils from several sites)
RM = **Remus Creek site, Fosheim Peninsula, Ellesmere Island, Nunavut**
SB = **South Bay site, Fosheim Peninsula, Ellesmere Island, Nunavut**
FD = **Fosheim Dome sites, Fosheim Peninsula, Ellesmere Island, Nunavut**
WV = **Several sites from a creek in Wolf Valley**
RL = **Romulus Lake site**
RM = **Russel Maris site**
RH = **Red Hill site**
CF = **Cañon Fiord site**
HCA = **Sample HCA 78-13/7-5 near Cañon Fiord**
R = Reidiger sites (samples FG 89-27e, FG 89-28a, and FG 89-31c are from another site 1 km away)

² Identified by L.E. Ovenden, Pest Management Regulatory Agency, Health Canada, Ottawa, Ontario

³ Identified by J.V. Matthews except for wood samples (marked by an *), which were identified by H. Jetté, Geological Survey of Canada, Ottawa, Ontario

	Sites ¹										
	RC	RM	RL	SB	BP	FD	WV	RH	CF	HCA	R
<i>Campylium arcticum</i> (Williams) Broth.				+							
<i>Campylium</i> sp.						+					
<i>C. stellatum/arcticum</i> type					+						
<i>Drepanocladus</i> spp.	+										
<i>D. aduncus</i> (Hedw.) Warnst.				+	+	+					
<i>D. crassicosatus</i> Janssens					+						
<i>D. fluitans</i> (Hedw.) Warnst.						+					
<i>D. lycopodioides</i> var. <i>brevifolius</i> (Lindb.) Mönk.						+					
<i>D. revolvens</i> (Sw.) Warnst.						+	+				
<i>Hygrohypnum bambergeri</i> Schimp.						+	+				
<i>Hypnum</i> sp.							+				
<i>Myurella tenerrima</i> (Brid.) Lindb.							+				
<i>Orthothecium chryseum</i> (Schwaegr.ex Schultes) B.S.G.						+					
<i>Scorpidium scorpioides</i> (Hedw.) Limpr.	+			+							
<i>S. turgescens</i> Auth				+							
<i>Thuidium abietinum</i> (Hedw.) B.S.G.							+				
<i>Tomenthypnum nitens</i> (Hedw.) Loeske						+	+				
<i>Pleurozium schreberi</i> (Brid.) Mitt.							+				
<i>Rhytidiadelphus triquetrus</i>		+									
Polytrichales											
<i>Pogonatum dentatum</i> (Brid.) Brid.						+					
<i>Polytrichum</i> sp.							+				
Vascular plants ³											
Equisetaceae											
<i>Equisetum</i> sp.	+					+	+				
Sellaginellaceae											
<i>Selaginella selaginoides</i> (L.) Link						+					
Pinaceae											
<i>Larix</i> sp. (needles only)	+	+	+	+	+						+
<i>L. laricina</i> type		+									
<i>L. groenlandi</i> Benn.					+						
<i>Pinus</i> five-needle undifferentiated	+		+								
<i>P. (Strobilus)</i> subsect. <i>Cembrae</i>				+	+						
<i>P. (Strobilus)</i> subsect. <i>Eustrobi</i>		+			+	+					+
<i>P. (Strobilus)</i> <i>monticola</i> type*							+				
<i>P. pumila</i> Auth?					+						
<i>Picea</i> sp.	+		+	+	+		+				+
<i>Picea</i> sp*							+				
<i>P. mariana/rubra</i> type.		+			+						
Cupressaceae											
<i>Thuja occidentalis</i> L.	+				+						+
Arctopityaceae											
<i>Arctopitys</i> sp.	+										
Sparganiaceae											
<i>Sparganium</i> sp.											+
<i>Sparganium hyperboreum</i> typ.							+				
Potamogetonaceae											
<i>Potamogeton</i> sp.			+		+	+	+				+
<i>P. filiformis</i> Pers.					+	+				+	
<i>P. diversifolius/spirillus</i> type	+										
<i>Zanichellia</i> sp.			+								
Scheuchzeriaceae											
<i>Scheuchzeria</i> sp.					+						
Gramineae											
<i>Glyceria</i> sp.					+		+				
genus?						+				+	
Cyperaceae											
<i>Cyperaceae</i> type A											+
<i>Carex</i> spp.	+		+	+	+	+	+		+	+	
<i>C. aquatilis</i> Wahlenb.					+	+				+	+

Appendix A (cont.)

	Sites ¹										
	RC	RM	RL	SB	BP	FD	WV	RH	CF	HCA	R
<i>C. sect. chordorrhizae</i>					+						+
<i>C. diandra</i> Schrank					+						
<i>C. sect. Paludosae</i> cf. <i>r hynchophysa</i>	+										
<i>Carex maritima</i> Wahlenb.										+	
<i>Eriophorum</i> sp.				+		+	+				+
<i>Rhynchospora</i> sp.	+										
<i>Kobresia</i>						+			+	+	
<i>Scirpus</i> sp.					+						
<i>S. microcarpus</i> Presl.					+						+
Araceae											
<i>Aracites globosa</i> (C.&E.Reid) Benn.	+		+		+						+
<i>Epipremnum crassum</i> C.&E. Reid											+
<i>Calla palustris</i>	+				+						
Juncaceae											
<i>Luzula/Juncus</i> type	+										
Salicaceae											
<i>Salix</i> sp.					+	+			+	+	
<i>Salix</i> sp.*							+				
<i>Populus</i> sp.											+
Myricaceae											
<i>Comptonia</i> sp.	+		+	+	+		+				
<i>C. asplenifolia</i> B.B. Small, Rydb.	+										
<i>Myrica (Gale) arctogale</i> Benn.	+	+			+						?
Betulaceae											
<i>Alnus</i> sp.	+	+		+				+			
<i>Alnus (Alnobetula)</i> sp.					+			+			
<i>Alnus incana</i> (L.) Moench	+		+								
<i>Betula</i> sp.		+		+		+					
<i>Betula</i> sp.*							+				
<i>Betula</i> dwarf shrub type				+	+	+	+			+	
<i>Betula</i> arboreal type	+				+			+			+
<i>Corylus</i> sp.				+							
<i>Tubela</i> sp.					+						+
Polygonaceae											
<i>Oxyria digyna</i> (L.) Hill	+				+	+				+	
<i>Polygonum</i> sp.					+	+					
<i>Polygonum viviparum</i> L.									+		
<i>Rumex</i> sp.						+					
Chenopodiaceae											
<i>Chenopodium</i> sp.							+	+			
Caryophyllaceae											
<i>Cerastium Beeringianum</i> Cham.&Schlect.										+	
<i>Melandrium</i> sp.									+	+	
Genus?					+						
Nymphaeaceae											
<i>Nuphar</i> sp.	+					+	+				+
<i>Nuphar (Nuparella)</i> type					+						
<i>Nymphaea</i> sp.	+										
Ranunculaceae											
<i>Caltha</i> sp.							+				
<i>Ranunculus</i> spp.					+	+	+				
<i>R. hyperboreus</i> Rottb.					+	+			+	+	
<i>R. lapponicus</i> L.			+		+						+
<i>R. trichophyllus</i> type									+		
Papaveraceae											
<i>Papaver</i> sp.											+
Cruciferae											
Cruciferae undet.						+				+	
<i>Draba</i> sp.									+		
Saxifragaceae											
<i>Saxifraga oppositifolia</i> L.					+	+					
<i>Saxifraga</i> sp.						+					

	Sites ¹										
	RC	RM	RL	SB	BP	FD	WV	RH	CF	HCA	R
Rosaceae											
<i>Aronia</i> sp.											+
<i>Dryas</i> sp.					+	+					
<i>D. octopetula</i> type			+								
<i>D. integrifolia</i>						+			+	+	
<i>Physocarpus</i> sp.			+	+	+						
<i>Potentilla</i> sp.	+					+	+	+	+	+	+
<i>P. norvegica</i> type					+						
<i>P. palustris</i> (L.) Scop.			+		+	+	+				+
<i>Rubus idaeus</i> type				+	+						+
<i>Spirea</i> sp.											+
Empetraceae											
<i>Empetrum nigrum</i> L.					+	+					
Elaeagnaceae											
<i>Shepherdia</i> sp.		+									
Rhamnaceae											
<i>Paliurus</i>					+						
Hypericaceae											
<i>Hypericum</i> sp.					+						
Lythraceae											
<i>Decodon globosus</i> type.	+		+		+						+
Haloragaceae											
<i>Myriophyllum</i> sp.											+
Hippuridaceae											
<i>Hippuris</i> sp.	+		+		+	+	+			+	+
Cornaceae											
<i>Cornus stolonifera</i> Michx.	+				+						
<i>Cornus</i> sp.		+									+
Ericaceae											
<i>Andromeda polifolia</i> L.	+		+	+	+	+	+				+
<i>Chamaedaphne</i> sp.					+						+
<i>Ledum</i> sp.		+			+						+
<i>Oxycoccus</i> sp.		+									+
<i>Vaccinium</i> sp.			+		+	+					+
<i>V. Vitis-idaea</i> L.					+						
Undet. genus?					+						
Primulaceae											
Genus?											+
Gentianaceae											
<i>Menyanthes trifoliata</i> L.	+		+		+	+	+				
<i>Menyanthes</i> (<2 mm)					+		+				
<i>Nymphoides</i> sp.											+

Note: Appearance of a taxon name in the list does not necessarily mean that the taxon was found in a particular sample. Some taxa (shown in bold face) are identified as only 'near to' (cf.) named taxon; where fossils were adequate for only a tentative identification, a '?' is used (underlined records). Consult the numerical designation for each sample.

¹ Site abbreviations: Fosheim Peninsula sites are in bold face.

BP = Beaver peat and associated deposits, Strathcona Fiord, Ellesmere Island (combination of fossils from several sites)

RM = **Remus Creek site, Fosheim Peninsula, Ellesmere Island, Nunavut**

SB = **South Bay site, Fosheim Peninsula, Ellesmere Island, Nunavut**

FD = **Fosheim Dome sites, Fosheim Peninsula, Ellesmere Island, Nunavut**

WV = **Several sites from a creek in Wolf Valley**

RL = **Romulus Lake site**

RM = **Russel Maris site**

RH = **Red Hill site**

CF = **Cañon Fiord site**

HCA = **Sample HCA 78-13/7-5 near Cañon Fiord**

R = Reidiger sites (samples FG 89-27e, FG 89-28a, and FG 89-31c are from another site 1 km away)

² Identified by L.E. Oviden, Pest Management Regulatory Agency, Health Canada, Ottawa, Ontario

³ Identified by J.V. Matthews except for wood samples (marked by an *), which were identified by H. Jetté, Geological Survey of Canada, Ottawa, Ontario

APPENDIX B

Arthropod fossils from various Fosheim Peninsula and related high-terrace site

	Sites ¹									
	RC	RM	RL	SB	BP	FD	WV	RH	CF	HCA
TUBELLARIA						+				
PORIFERA										
HAPLOSCLERINA										
Spongillidae					+					
BRYOZOA										
<i>Cristatella mucedo</i> L.	+				+	+	+			
ARTHROPODA										
INSECTA										
ODONATA										
Family?					+		+			
PLECOPTERA						+				
HEMIPTERA										
Saldidae										
<i>Salda</i> sp.						+				
HOMOPTERA										
Cicadellidae										
Genus?					+	+				
Aleyrodidae										
Genus?					+					
NEUROPTERA										
Sialidae										
<i>Sialis</i> sp.					+					
COLEOPTERA										
Trachpachidae										
<i>Trachpachus</i> sp.					+					
Carabidae										
<i>Agonum</i> sp.	+				+					
<i>Amara alpina</i> Payk.							+		+	+
<i>Amara bokeri</i> Csiki										+
<i>Amara glacialis</i> Mann.							+			
<i>Amara</i> sp.							+			
<i>Bembidion (Trepanedoris)</i> sp.						+				
<i>B. dyschirinum</i> LeC.						+				
<i>B. grapei</i> grp.						+				
<i>B. grapei</i> Gyll.						+				
<i>B. sordidum</i> grp.							+	+		
<i>B. umiatense</i> Lth.							+	+		
<i>Bembidion</i> spp.	+				+	+	+			
<i>Blethisa catenaria</i> Brown						+				
<i>Blethisa</i> sp.						+				
<i>Carabus</i> sp.								+		
<i>Carabus truncaticollis</i> Eschz.						+				
<i>Diacheila matthewsi</i> Böcher						+				

Note: Appearance of a taxon name in the list does not necessarily mean that the taxon was found in a particular sample. Some taxa are identified as only 'near to' named taxon; where fossils were adequate for only a tentative identification, a '?' is used.

¹Site Abbreviations: Fosheim Peninsula sites are in bold face

BP = Beaver peat and associated deposits, Strathcona Fiord, Ellesmere Island (combination of fossils from several sites)

RC = Remus Creek site, Fosheim Peninsula, Ellesmere Island, Nunavut

SB = South Bay site, Fosheim Peninsula, Ellesmere Island, Nunavut

FD = Fosheim Dome sites, Fosheim Peninsula, Ellesmere Island, Nunavut

WV = Several sites from a creek in Wolf Valley

RL = Romulus Lake site

RM = Russel Maris site

RH = Red Hill site

CF = Cañon Fiord

HCA = Sample HCA 78-13/7-5 near Cañon Fiord

²Identified by Nancy Williams, Scarborough College, Scarborough, Ontario

³Identified by various specialists in the Hymenoptera group, Eastern Cereal and Oilseed Research Centre, Agriculture Canada, Ottawa, Ontario

⁴Identified by E. Lundquist, Eastern Cereal and Oilseed Research Centre, Agriculture Canada, Ottawa, Ontario

⁵Identified by V. Behan-Pelletier, Eastern Cereal and Oilseed Research Centre, Agriculture Canada, Ottawa, Ontario

	Sites ¹									
	RC	RM	RL	SB	BP	FD	WV	RH	CF	HCA
<i>Dyschirius</i> sp.					+					
<i>Elaphrus tuberculatus</i> Makl.										+
<i>Notiophilus</i> sp.	+					+				
<i>Pterostichus</i> (<i>Lyperoherus</i>) sp.					+					
<i>P. haematopus</i> Dej.					+		+	+		+
<i>P. vermiculosus</i> Men.					+	+				
<i>Pterostichus</i> (<i>Cryobius</i>) spp.	+				+	+			+	
<i>P. (Cryobius) brevicornis</i> Kby.						+		+		
<i>P. (Cryobius) ventricosus</i> grp.							+			
<i>Pterostichus</i> sp.		+			+					
<i>Tachys</i> sp.	+									
Dytiscidae										
<i>Agabus bifarius</i> (Kby.)					+					
<i>Agabus</i> sp.					+	+				+
<i>Colymbetes</i> sp.					+	+				+
<i>Hydroporus</i> sp.					+	+				
Genus?	+				+					
Gyrinidae										
<i>Gyrinus</i> sp.	+				+					
Hydrophilidae										
<i>Cercyon herceus</i> Smet.					+					
<i>Cercyon</i> sp.					+					
<i>Helophorus meighensis</i> Matth.				+	+					
<i>Helophorus</i> spp.					+					
Genus?					+					
Hydraenidae										
<i>Ochthebius</i> sp.	+				+					
Staphylinidae										
<i>Acidota</i> sp.					+					
Aleocharinae	+				+		+	+	+	+
<i>Arpedium</i> sp.					+					
<i>Bledius</i> sp.	+									
<i>Gymnusa</i> sp.					+					
<i>Lathrobium</i> sp.					+					
<i>Micralymma</i> type					+					
<i>Olophrum boreale</i> (Payk).					+					
<i>O. consimile</i> Gyll.					+					
Omalinae, Coryphiini?					+					
Omalinae, genus?					+					
<i>Pycnoglypta</i> sp.					+					
<i>Stenus</i> sp.	+				+	+	+			
<i>Tachinus</i> sp.					+		+			
<i>Tachyporus</i> sp.					+					
Micropeplidae										
<i>Micropeplus nelsoni</i> Camp.					+					
<i>Micropeplus sculptus</i> LeC							+			
<i>Micropeplus tesserula</i> Curtis	+				+					
Silphidae										
<i>Silpha</i> sp.					+					
Leiodiidae										
<i>Agathidium</i> sp.					+					
<i>Colon</i> sp.										+
Genus?					+					
Ptiliidae										
<i>Acrotrichus</i> sp.					+					
Scydmaenidae										
Genus?					+					
Scarabaeidae										
<i>Aegialia</i> sp.					+					
Helodidae										
<i>Cyphon</i> sp.					+					
Byrrhidae										
<i>Byrrhus</i> sp.	+									
<i>Simplocaria</i> sp.					+	+	+			

Appendix B (cont.)

	Sites ¹									
	RC	RM	RL	SB	BP	FD	WV	RH	CF	HCA
Elateridae										
Genus?								+		
Cantharidae										
<i>Podabrus</i> sp.					+					
Anobiidae										
Genus?		+								
Anthicidae										
Genus?					+					
Coccinellidae										
<i>Nephus</i> sp.										+
<i>Ceratomegilla ulkei</i> Crotch										+
Genus?					+					
Lathridiidae										
Genus?	+				+		+			
Chrysomelidae										
<i>Donacia</i> sp.					+					
Donaciinae	+									
Galerucinae							+			
Curculionidae										
<i>Apion</i> sp.							+			
<i>Ceutorhynchus</i> sp.					+					
<i>Cylindrocopturus</i> sp.					+					
<i>Grypus equiseti</i> (Fab.)	+									
<i>Homorosoma</i> sp.					+					
<i>Hylobius</i> sp.	+									
<i>Hypera</i> sp.							+			
<i>Lepyryus</i> sp.										+
<i>Notaris</i> sp.				+	+					
<i>Phyllobius</i> sp.							+			
<i>Pissodes</i> sp.	+									
<i>Rhynchaenus</i> sp.							+			
Genus?						+				
TRICHOPTERA ²										
Limnephilidae										
<i>Limnephilus subcentralis</i> grp					+					
Calamoceratidae										
Molannidae										
<i>Molanna uniophila</i> Vorhies					+					
DIPTERA										
Tipulidae										
Genus?						+			+	
Chironomidae										
<i>Chironomus</i> type					+	+			+	
Genus?					+	+				
Xylophagidae										
<i>Xylophagus</i> sp.	+				+					
Diptera, Family?					+					
HYMENOPTERA ³										
Symphyta										
Tenthredinidae										
<i>Dolerus</i> sp.					+					
Genus?					+					
Family?					+		+			
Apocrita										
Ichneumonoidae undet.		+			+	+				
Braconidae										
Subfamily?					+					
Orthocentrinae					+					
Megaspilidae										
<i>Conostigmus</i> sp.					+					
Diapriidae										
Belytinae, genus?					+					
Formicidae										

	Sites ¹										
	RC	RM	RL	SB	BP	FD	WV	RH	CF	HCA	
<i>Formica</i> typ.		+			+						
<i>Myrmica</i> sp.					+						
Genus?	+	+			+						
Appoidea											
Genus?					+						
CRUSTACEA											
Cladocera											
<i>Daphnia</i> sp.	+				+				+		
Notostraca											
<i>Lepiduris</i> sp.						+			+		
ARACHNIDA											
Acari											
Mesostigmata											
Gamasida (Hypoaspidae)											
<i>Hypoaspis</i> sp. ⁴					+						
Prostigmata Oribatida ⁵											
Family?	+					+		+			
Eremaeidae											
<i>Eremaeus</i> sp.					+						
<i>Proteremaus macleani</i> Behan-Pelletier					+						
Astegistidae											
<i>Astegistes</i> sp.					+						
Metrioppiidae											
<i>Ceratoppia quadridentata</i> (Haller)					+						
Hydrozetidae											
<i>Hydrozetes</i> spp.					+						
Limnozeteidae											
<i>Limnozetes</i> spp.					+						
Ceratozetidae											
<i>Melanozetes meridianus</i> Sellnick					+						
<i>Neogymnobates</i> sp.					+						
<i>Trichoribates polaris</i> Hammer					+						
Mycobatidae											
<i>Mycobates conitus</i> Hammer					+						
<i>Punctoribates hexagonus</i> Berlese					+						
<i>P. quadrivertex</i> Herbert					+						
Achipteriidae											
<i>Parachiptera nivalis</i> Hammer					+						
Araneae											
Lycosidae											
Genus?					+	+					
Family?							+				

Note: Appearance of a taxon name in the list does not necessarily mean that the taxon was found in a particular sample. Some taxa are identified as only 'near to' named taxon; where fossils were adequate for only a tentative identification, a '?' is used.

¹ Site Abbreviations: Fosheim Peninsula sites are in bold face

BP = Beaver peat and associated deposits, Strathcona Fiord, Ellesmere Island (combination of fossils from several sites)

RC = Remus Creek site, Fosheim Peninsula, Ellesmere Island, Nunavut

SB = South Bay site, Fosheim Peninsula, Ellesmere Island, Nunavut

FD = Fosheim Dome sites, Fosheim Peninsula, Ellesmere Island, Nunavut

WV = Several sites from a creek in Wolf Valley

RL = Romulus Lake site

RM = Russel Maris site

RH = Red Hill site

CF = Cañon Fiord

HCA = Sample HCA 78-13/7-5 near Cañon Fiord

² Identified by Nancy Williams, Scarborough College, Scarborough, Ontario

³ Identified by various specialists in the Hymenoptera group, Eastern Cereal and Oilseed Research Centre, Agriculture Canada, Ottawa, Ontario

⁴ Identified by E. Lundquist, Eastern Cereal and Oilseed Research Centre, Agriculture Canada, Ottawa, Ontario

⁵ Identified by V. Behan-Pelletier, Eastern Cereal and Oilseed Research Centre, Agriculture Canada, Ottawa, Ontario

Preliminary results of archeological research on Fosheim Peninsula and in adjacent areas of western Ellesmere and eastern Axel Heiberg islands, Nunavut

P.D. Sutherland¹

Sutherland, P.D., 2000: Preliminary results of archeological research on Fosheim Peninsula and in adjacent areas of western Ellesmere and eastern Axel Heiberg islands, Nunavut; in Environmental Response to Climate Change in the Canadian High Arctic, (ed.) M. Garneau and B.T. Alt; Geological Survey of Canada, Bulletin 529, p. 319–324.

Abstract: An archeological survey carried out on Fosheim Peninsula and in surrounding areas during the summer of 1992 located 237 archeological sites; test excavations were carried out at six sites. Prehistoric occupation of the region apparently occurred primarily during two periods, approximately 2500 to 1000 BC and approximately AD 700 to 1700. During both periods, cultural adaptations seem to have been based largely on the hunting of land mammals, but evidence exists of increased sea-mammal hunting during the latter period. The recovery of paleobiological materials from archeological sites in the region indicates the presence in the area of species currently limited to more southern ranges.

Résumé : Un relevé archéologique effectué sur la péninsule Fosheim et dans les environs lors de l'été 1992 a permis de localiser 237 sites archéologiques. On a effectué des excavations d'essai en six emplacements. Pendant la préhistoire, la région aurait été habitée surtout pendant deux périodes, soit de 2 500 à 1 000 ans av. J.-C. et de 700 à 1 700 ans apr. J.-C. Durant ces deux périodes, les adaptations culturelles semblent avoir été en grande partie basées sur la chasse aux mammifères terrestres, mais il y a des signes que la chasse aux mammifères marins a augmenté pendant la période plus récente. Les matériaux paléobotaniques récupérés aux sites archéologiques de la région indiquent la présence d'espèces qui sont actuellement limitées à des répartitions plus méridionales.

¹ Curator, Canadian Museum of Civilization, 100 Laurier Street, Hull, Quebec, J8X 4H2

INTRODUCTION

Archeologists have traditionally linked widespread changes in prehistoric cultural patterns in Arctic Canada to environmental changes and ultimately to climatic change (McGhee, 1970; Dekin, 1972; Fitzhugh, 1972; McCartney, 1977). During the past decade, such arguments have fallen out of favour as archeologists realized that changes in climatic variables have been more complex than had been thought previously and that the dating of both climatic changes and changes in cultural patterns has generally lacked the precision necessary to argue contemporaneity between natural and cultural events (McGhee, 1981).

Despite these problems in interpretation, few archeologists would argue that climatically induced environmental change has not been an important cause of changes throughout the prehistoric record of Arctic Canada. Rather than attempting to link major and widespread changes in prehistoric cultural patterns with broad episodes of climatic change, however, it may be more feasible to undertake studies of local human adaptations to changes in local environments. Studies that concentrate on the definition and precise dating of changes in a small, local area may be expected to hold potential for understanding how prehistoric arctic hunters reacted to changes in their environment (Sutherland, 1992). The Geological Survey of Canada's Global Change Program on Fosheim Peninsula, Ellesmere Island, has provided the opportunity for initiating one such local study.

THE 1992 FIELD PROJECT

Western Ellesmere Island and eastern Axel Heiberg Island have seen relatively little archeological investigation. Archeological research carried out on Fosheim Peninsula prior to 1992 included brief helicopter and foot surveys in 1977, 1980, and 1983, as well as test excavations at a Thule Inuit site, Remus Creek (SIHq-3), in 1980 (Sutherland, unpub. rept., 1977, 1980, 1983). Work in adjacent areas was limited to preliminary foot and aerial surveys along the coasts of Borup Fiord (R. Smith, unpub. rept., 1989, 1990), an aerial survey from Whitsunday Bay on Stolz Peninsula to Schei Peninsula on eastern Axel Heiberg Island, and full-scale excavations at a Late Dorset-Thule Inuit site on Buchanan Lake in Mokka Fiord, as part of the Eureka Upland Archeological Project (Sutherland, unpub. rept., 1980, 1981, 1983).

A project of archeological survey and excavation was carried out on Fosheim Peninsula and in adjacent regions during the summer of 1992. This work constituted the archeological component of the multidisciplinary effort studying the history of environmental change in the area and was designed to document the history of occupation and adaptation to the intermontane environments of western Ellesmere Island and eastern Axel Heiberg Island.

A helicopter survey was carried out over a period of four weeks along the coasts of Eureka Sound and adjacent fiords and in selected interior regions (Fig. 1). Two hundred and thirty-seven site localities, representing all three major prehistoric occupations of the region, were inventoried during

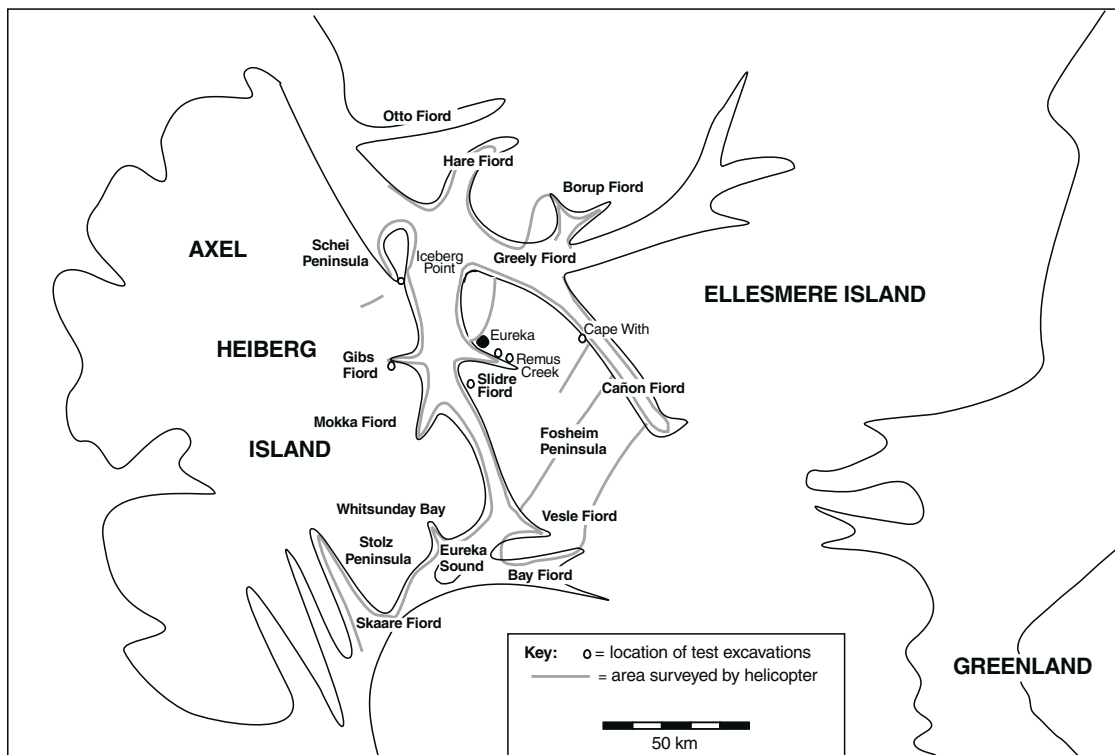


Figure 1. Map showing the routes of the 1992 helicopter survey.

the survey. Limited test excavations were carried out at six sites and more extensive excavations were conducted at Remus Creek (SIHq-3), a Thule Inuit site on Slidre Fiord. Efforts were directed particularly at the recovery of archaeological and paleobiological materials that would assist in the reconstruction of local environmental conditions over the past 4500 years.

HISTORY OF HUMAN OCCUPATION

The history of Arctic Canada is understood in terms of two sequential developments, each originating in the movements of populations with distinct cultural traditions from the western Arctic. The earlier tradition is termed 'Paleo-Eskimo' and derives from a Siberian Neolithic population that expanded across arctic North America at some time between 5000 and 4000 years ago. In the High Arctic regions of Canada and Greenland, these people developed a long-lasting way of life known as the Independence culture, which persisted until about 2000 years ago. In more southerly Arctic regions, the Paleo-Eskimos developed the Dorset culture, which continued until displaced by ancestral Inuit during the past millennium. The second eastward movement is termed 'Neo-Eskimo' and brought the direct ancestors of the Inuit to Arctic Canada about 1000 years ago. The Inuit who accomplished this movement are assigned to the Thule culture, marked by an adaptation based on the maritime hunting traditions of northern Alaska.

The 255 components now recorded from the area represent occupations related to the Independence I, Late Dorset, and Thule cultures. These occupations occurred between approximately 2500 and 1000 BC and between approximately AD 700 and 1700. No definite evidence of occupation has been found in the study area for the period between 1000 BC and AD 700, nor for the period between AD 1700 and the historic exploration period. The area may have been abandoned for at least a portion of the earlier period, as well as during the later period.

The distribution of components relating to each of the three major occupations is generally similar. All three groups apparently preferred coastal locations for the majority of their activities. Although approximately 20 per cent of the 1992 helicopter survey covered interior regions, it produced little evidence of interior settlement or hunting activities. The surveys of the interior concentrated on river valleys that would have served as transportation corridors, but where site preservation and visibility were constrained by the effects of erosion and by vegetation cover. Given the present distribution of terrestrial resources, one would expect to find indications that interior regions had been used for hunting land mammals. Nevertheless, present evidence suggests that for all three prehistoric occupations, activities and more permanent settlements were concentrated in coastal locations.

In all three periods, the coasts of Eureka Sound seem to have attracted more occupation and use than did the other coastal regions surveyed. For example, only 14 site locations were found on the coasts of Hare and Borup fiords; Cañon Fiord produced evidence of only 27 site locations; however,

over 130 sites were located along a roughly equivalent length of coastline on Eureka Sound. These differences in the density of coastal occupation may relate to differences in the seasonal distribution of sea ice, open water conditions, and the presence of sea mammals.

Despite the coastal location of most sites, the artifacts and faunal remains recovered in test excavations indicate that all three peoples concentrated their subsistence activities largely on the hunting of land mammals. The essential similarity in animal utilization is illustrated in Figure 2, which compares all faunal samples related to each major occupation of the region. It is important to note that caribou, musk-ox, and hare, which account for at least 70 per cent of the bones recovered from all three occupations, are available to hunters throughout the year in this region. Seasonally available resources such as sea mammals, birds, and fish may have been used by all three groups, but it seems apparent that the constant availability of land mammals was the most important feature of local adaptations.

Within this generally similar pattern of resource use, certain interpretations may be suggested regarding differences in the adaptations followed by each of the three major groups that occupied the area at different periods.

Independence I

A relatively wide range of styles in the artifacts recovered from sites in the Eureka Upland during past field seasons suggests lengthy occupation of the region. The components assigned in 1992 to Independence I probably relate to a period of a millennium or more of occupation. Interpretation of the functions of these artifact assemblages is limited by the poor preservation of organic artifacts from this early period. Almost all of chipped-stone artifacts seem to have functioned in general maintenance and manufacturing activities and are of types represented in most Paleo-Eskimo collections. Weapons are represented by a single point, which was probably used with a lance, and a sideblade, which may have been set into the edge of either a lance or a harpoon head; both are from SIHw-2, a settlement site in Gibs Fiord.

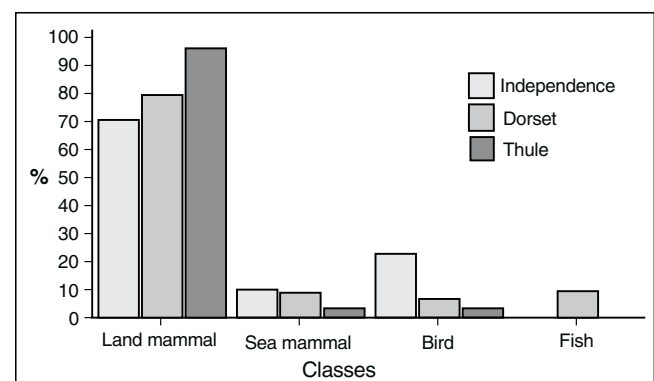


Figure 2. Classified faunal remains for sites, compared by cultural affiliation.

Faunal remains recovered from Independence I sites suggest that land mammals were the staple of the local people. None of the sites located seem to have been occupied for long periods of time. The Independence adaptation was probably based on year-round hunting of land mammals from small, temporary sites located throughout the region, supplemented seasonally by other food resources when they were available.

Late Dorset

The Late Dorset occupation of the area probably occurred over a period of a few centuries, from approximately AD 700 to perhaps as late as AD 1300 or 1400. The fact that more components can be assigned to the Dorset occupation than to the Independence occupation, which occurred over a much longer period of time, suggests that local Dorset populations were larger and their use of the area was more intense than was the case during the early Paleo-Eskimo period.

The faunal remains recovered from Dorset components show roughly the same range of animal use as that evidenced for the Independence occupation. The most interesting difference is the presence of whale bones in several Dorset components; although the Dorset people may not have hunted whales, they may have had access to the meat and bones of whales that died in the area after being trapped by ice or through other causes.

The small size of the assemblages recovered from Dorset components in 1992 precludes much interpretation of assemblage function. Three harpoon heads and one foreshaft indicate that subsistence activities included the hunting of seals. The fact that these weapons were found at three different sites suggests that sealing was a relatively important economic activity among local Dorset groups. Fishing is indicated by one small barbed spear, but as in other Dorset assemblages, we cannot identify weapons used for hunting land mammals. Other artifacts are typical of Late Dorset assemblages, including a small number of carvings and other objects that may

have been used in magical activities. Two artifacts from SIHQ-1, one with a drilled hole (which is uncharacteristic of Dorset technology) and the other resembling a Thule culture snow beater, may indicate contact with Thule Inuit immigrants to the area.

Despite the evidence suggesting that local Dorset populations were larger than those of the Independence I occupation and that the Dorset people may have had greater access to marine mammals than did their predecessors, the general pattern of adaptation seems to have been similar. A few of the Dorset settlement sites seem to have been occupied for a longer period than were any of the Independence sites identified, but no evidence has been found of permanent occupation of specific sites, nor of the storage of significant amounts of food from one season to another.

Thule Inuit

The Thule occupation of the area seems to have occurred over several centuries after about AD 1100, a span of time roughly equivalent to that of the prior Dorset occupation. The fact that over three times as many Thule as Dorset components have been identified is an indication of much more intensive use of the area by the Thule Inuit. The impression of more intensive occupation is strengthened by indications that several Thule sites are larger and were apparently occupied for significantly longer periods than were any Paleo-Eskimo sites located.

The artifacts collected from Thule components represent a wide spectrum of activities undertaken in both summer and winter. The hunting of land mammals is evidenced primarily by arrowheads and the importance of this activity is emphasized by the number of musk-ox and caribou bones found at the sites. Earlier collections from some of these sites include harpoon heads and other artifacts associated with the hunting of sea mammals, an activity that is also indicated by the presence of marine mammal bones. Winter activities are represented by a sledshoe, a portion of what is probably a snow



Figure 3.

Test excavations at the Two House site (TbHt-6). Photograph by P.D. Sutherland GSC2000-021

shovel, and mattocks used in the construction and maintenance of turf houses. In general, the assemblages are typical of those expected from Thule sites in more southerly regions of the Arctic.

Faunal remains recovered from excavated Thule sites show roughly the same range and proportion of animals as those recovered from Paleo-Eskimo sites. The presence of whale bones in local Thule sites, combined with the known ability of Thule hunters to capture bowhead whales, suggests that a significant difference in adaptation to the region, compared to that of the earlier occupants, may have been based on the utilization of this major resource.

EVIDENCE FOR PALEOBIOLOGICAL CHANGES

An analysis of animal bones recovered during previous archeological work in the area (Sutherland, unpub. rept., 1991) has produced evidence for past occupation of the area by three species that today occur only in more southerly regions: harp seal (*Phoca groenlandica*), Ross's goose (*Chen rossii*), and brown lemming (*Lemmus sibiricus*) (D. Balkwill, unpub. rept., 1982). The biological collections made in 1992 have been identified only to class level and at this stage of analysis, no species have been found that do not occur in the area under current environmental conditions, with the exception of the *cetacea* remains.

The unexpected amounts of whale bone present in local archeological sites was one of the most interesting findings of the 1992 work. These bones were found in both Late Dorset and Thule culture occupation sites at several localities. They were used as structural elements in winter houses at at least one Thule settlement site (TbHt-6). Test excavations at this site also indicated the presence of a whale vertebra; this bone element would not be expected if the whale bones had been brought to the region from elsewhere as construction material and suggests that the bones had been obtained locally (Fig. 3). The widespread occurrence of whale bones at several Late Dorset and Thule sites along the coasts of Eureka Sound suggests that bowhead whales may have appeared at least occasionally in these waters between approximately AD 700 and 1500 (see Dyke et al., 1996). The range of these large whales is currently restricted to northern Baffin Bay and eastern Jones Sound, several hundred kilometres southeast of the study area.

CONCLUSIONS

The temporal distribution of archeological sites now known from Fosheim Peninsula and surrounding areas suggests that the area was particularly attractive to human occupation during two periods, between approximately 2500 and 1000 BC and again between approximately AD 700 and 1700. Land mammals may have been relatively abundant during these periods, as they seem to have provided the basic resource for human subsistence during both periods of occupation. Evidence for maritime hunting increased during the more recent

period of occupation, perhaps because of increased maritime hunting capabilities. However, this evidence may also suggest increased populations of sea mammals and probably a decrease in the extent and seasonal duration of sea-ice cover at this time. This interpretation is supported by the amount of whale bone found at archeological sites of the period, as well as by the identification of the bones of harp seal, an animal associated with open water, from one site of this period. The recovery of remains of two other species currently associated with more southern ranges (Ross's goose and brown lemming) from the same site provides further indications of warmer local conditions about 1000 years ago.

The work undertaken to date is of a preliminary nature. Further research can be expected to provide more precise definition and dating of adaptational and paleobiological changes on Fosheim Peninsula and in adjacent areas of western Ellesmere Island and eastern Axel Heiberg Island. In turn, the understanding of prehistoric adaptations to this local region may contribute useful knowledge to our exploration of the links between environmental change and human cultural change in arctic North America.

ACKNOWLEDGMENTS

Field work in 1992 on western Ellesmere Island and eastern Axel Heiberg Island was supported by the Geological Survey of Canada's Global Change Program, the Polar Continental Shelf Project, the Prince of Wales Northern Heritage Centre, and the Royal Canadian Geographical Society. I am grateful to these agencies for their assistance. I also wish to thank Laisa Audlaluk, Margaret Bertulli, and Carol Nasmith Ramsden who so ably assisted me in the field work. The analysis of faunal remains from six archaeological sites tested during the 1992 field season and AMS dating of three of these sites were carried out with funding from the Geological Survey of Canada. I wish to thank Sylvia Edlund, co-ordinator of the Global Change Program at Hot Weather Creek, for her enthusiasm and support. I am grateful to Richard Morlan from the Archaeological Survey of Canada for reading and commenting on this paper.

REFERENCES

- Dekin, A.A.**
1972: Climatic change and cultural change: a correlative study from eastern Arctic prehistory; *Polar Notes*, v. 12, p. 11–31.
- Dyke, A.S, Hooper, J., and Savelle, J.M.**
1996: A history of sea ice in the Canadian Arctic Archipelago based on postglacial remains of the bowhead whale (*Balaena mysticetus*); *Arctic*, v. 49, no. 2, p. 235–255.
- Fitzhugh, W.W.**
1972: Environmental archaeology and cultural systems in Hamilton Inlet, Labrador; *Smithsonian Contributions to Anthropology*, v. 16, Washington, D.C., 299 p.
- McCartney, A.P.**
1977: Thule Eskimo prehistory along northwestern Hudson Bay; *Archaeological Survey of Canada, Mercury Paper 70*, Ottawa, Ontario, 485 p.
- McGhee, R.**
1970: Speculations on climatic change and Thule culture development; *Folk*, v. 11/12, p.173–184.

McGhee, R. (cont.)

1981: Archaeological evidence for climatic change over the past 5000 years; *in* *Climate and History*, (ed.) T.M.L. Wigley, M.J. Ingram, and G. Farmer; Cambridge University Press, Cambridge, United Kingdom, p. 162–179.

Sutherland, P.D.

1992: Environmental change and prehistory in Arctic Canada; *in* *Arctic Environment: Past, Present, and Future*, (ed.) M-k. Woo and D.J. Gregor; McMaster University, Department of Geography, Hamilton, Ontario, p. 139–154.

Ground-ice aggradation on Fosheim Peninsula, Ellesmere Island, Nunavut

W.H. Pollard¹

Pollard, W.H., 2000: Ground-ice aggradation on Fosheim Peninsula, Ellesmere Island, Nunavut; in Environmental Response to Climate Change in the Canadian High Arctic, (ed.) M. Garneau and B.T. Alt; Geological Survey of Canada, Bulletin 529, p. 325–333.

Abstract: Massive ground ice is common in fine-grained sediments below the Holocene marine limit in the Eureka Sound lowlands of Fosheim Peninsula. Ground-ice aggradation and degradation are closely associated with permafrost dynamics and thus contribute to the unique geomorphic nature and evolution of periglacial ecosystems on Fosheim Peninsula. Massive ice is particularly important for geomorphic, geotechnical, and paleoenvironmental reasons. During the Quaternary, extensive and localized glacial activity occurred on Fosheim Peninsula, and thus the potential for buried glacier ice exists. However, to date buried glacier ice has not been identified. A three-phase model based on the dominant landscape conditions is proposed to explain the nature of ground-ice distribution. In this model, permafrost conditions of three geomorphic environments (paraglacial, glaciated, and emergent) are considered during the last glaciation, deglaciation, and emergence. However, the emergent system is the only one containing extensive ground ice and is therefore discussed in detail.

Résumé : La glace de sol massive est une composante fréquente des sédiments marins à grain fin situés sous la limite marine de l'Holocène dans les basses terres du détroit d'Eureka de la péninsule Fosheim. L'accumulation et la dégradation de la glace de sol sont intimement associées à la dynamique du pergélisol et contribuent ainsi au caractère et à l'évolution géomorphologiques uniques des écosystèmes périglaciaires de la péninsule Fosheim. La glace massive est particulièrement importante pour des raisons géomorphologiques, géotechniques et paléoenvironnementales. Pendant le Quaternaire, la péninsule Fosheim a subi une activité glaciaire de grande envergure ainsi que locale; il est donc possible qu'il y persiste de la glace glaciaire enfouie. Toutefois, jusqu'à maintenant, on n'a pas reconnu de glace glaciaire. On propose un modèle à trois stades basé sur les conditions dominantes du paysage pour expliquer la nature de la répartition de la glace de sol. Dans ce modèle, les conditions de pergélisol dans trois environnements géomorphologiques (périglaciaire, glaciaire et émergent) sont examinées pour la dernière glaciation, pour la déglaciation et pour l'émergence. Cependant, le système émergent est le seul dans lequel il y a abondance de glace de sol et il est donc discuté de manière approfondie.

¹ Department of Geography and Centre for Climate and Global Change Research, McGill University, 805 Sherbrooke Street West, Montréal, Quebec H3A 2K6

INTRODUCTION

Ground ice forms an important component of surficial deposits in the Fosheim Peninsula area of western Ellesmere Island. It is abundant in the lowlands surrounding Eureka Sound and Slidre Fiord and in the Slidre River valley, where it commonly occurs as extensive bodies of massive ice. Ground ice is also observed locally as ice sills and dykes within intact bedrock. The formation of ground ice is related mainly to permafrost aggradation and, to a lesser degree, to the seasonal pattern in ground temperature in the upper part of the permafrost profile. Depositional processes may also play an active role in ground-ice formation, particularly in the case of buried ice. On Fosheim Peninsula, the late Quaternary evolution of climate, glacial activity, and sea-level change combine to determine the nature and distribution of ground ice.

Ground ice remains one of the most problematic aspects of permafrost and a major obstacle to development in arctic regions. Thermokarst and erosion around the Atmospheric Environment Service's Eureka weather station and sites disrupted by 1970s oil and gas exploration (e.g. the Gemini E-10 well site) reflect the sensitive nature of icy permafrost in this part of the Arctic. Knowledge about ground ice, particularly massive ice and ice-rich sediments, is necessary not only to understand landscape evolution, but also to assess the potential geomorphic response to natural and anthropogenic disturbance of permafrost. Concern that global warming will not only cause a shift in permafrost temperature and distribution, but will also induce widespread thermokarst in areas underlain by ice-rich sediments provides additional impetus for ground-ice investigation.

OBJECTIVE

The main objective of this paper is to relate ground-ice conditions on Fosheim Peninsula and information about late Quaternary environments and glacial activity to landscape development. Specific aims include 1) providing an explanation of ground-ice origin and its significance in terms of late Pleistocene and Holocene landscape change on Fosheim Peninsula and 2) in the process, introducing a simple landscape model that combines information on ground ice with glacial and sea-level histories to explain the nature of ground-ice distribution and ground-ice-related processes. Discussions about landscape evolution are meant to complement findings of process studies on thermokarst and active-layer detachments.

BACKGROUND

In general, ground-ice distribution can be viewed as the product of three environmental variables, i.e. ground temperature (which reflects the thermal balance between ground surface temperature and geothermal gradient), groundwater supply, and surficial geology. The duration and extent of ice-free conditions have significant implications for the age and extent of early permafrost conditions. It follows, therefore, that Late

Quaternary climate together with glacial and sea-level histories of Fosheim Peninsula are important factors contributing to the current patterns of permafrost and ground ice.

Eureka presently has a mean annual air temperature of -19.7°C and a mean annual temperature range of 43°C . These temperature conditions support 500+ m of permafrost. A geothermal gradient of roughly $0.038^{\circ}\text{C}/\text{m}$ exists at the Panarctic Oil Gemini E-10 well site (Taylor, 1991) located in the middle of Fosheim Peninsula approximately 40 km east of Eureka. This area is a true polar desert, receiving an average of only 64 mm of precipitation (60 per cent as snow) a year, which is the lowest recorded average in Canada. Despite the severe aridity, the Eureka Sound intermontane basin has a density and diversity of vegetation that is one of the highest in the Queen Elizabeth Islands. Paleoclimates for the Canadian High Arctic are reviewed by Bradley (1990); additional details can be obtained for central and northern Ellesmere Island from analyses of ice cores from the Agassiz Ice Cap (Fisher et al., 1983; Koerner and Fisher, 1990) and from a number of geological studies that interpret climate from various proxy indicators. In summary, these studies suggest the following three basic trends: first, a continuously warm period (with temperatures similar to current ones) prevailed in the early Holocene (10 000 to roughly 5000 BP); this was followed by a cooling trend over the last 4000 to 5000 years; finally, a marked warming since the early 1900s has seen temperatures rise by 3 to 4°C (Taylor, 1991).

Most studies of the glacial history of this part of Ellesmere Island agree that the entire region has been covered by a regional ice sheet at least once and quite possibly twice (Bell, 1996), although the timing of this glaciation remains a point of contention. England (1987) proposed that a more extensive glaciation predates the last glacial period and may have been late Tertiary, whereas others have suggested a more recent, but pre-Wisconsinan age (Fyles, 1962). There is, however, considerable debate over the extent of Late Pleistocene (Wisconsinan) ice coverage in the recent glacial geology literature for the Arctic Archipelago. This debate focuses on the strong field evidence supporting the occurrence of a series of localized ice sheets known as the Franklin Ice Complex (England, 1976, 1978, 1992; England et al., 1990) versus the evidence for a pervasive Innuitian Ice Sheet (Blake, 1970). The glacial history of Fosheim Peninsula developed by Bell (1992, 1996) and Hodgson (1985, 1989) provides strong support for the limited glaciation, 'Little Ice' model.

During the last glaciation (>9000 BP), glaciation levels were 200 to 300 m a.s.l. (Lemmen, 1989; Sloan, 1990) and the climate was colder and drier (England, 1987, 1990) than at present. These conditions gave rise to local upland ice caps that form the basis for the limited glaciation 'Little Ice' model. According to Bell (1996), the lower glacial levels during the last glacial maximum resulted in a series of small, cold-based ice caps centred upon Blacktop, Troelsen, Cape Hare and various unnamed ridges. Bell suggests that early Holocene (10 600–8700 BP) sea levels were maintained at or close to the marine limit, which is estimated at 145 to 150 m a.s.l. for central Fosheim Peninsula. Thus, the regional picture that persisted until 8700 BP or later includes a series of upland ice caps with small outlet glaciers, extensive ice-free

upland surfaces dominated by cold, dry, periglacial conditions, and an elevated sea level that inundated the central lowlands and river valleys. According to this model, much of the peninsula west of the Sawtooth Range (roughly 30–40 per cent) was inundated by a late Pleistocene–early Holocene sea that reached its maximum extent at approximately 10 600–9200 BP (Hodgson, 1985; Egginton and Hodgson, 1990; Bell, 1992, 1996). According to Bell (1992), the Holocene marine limit rises from >101 m a.s.l. in southern Fosheim Peninsula to 150 m a.s.l. near Blue Man Cape in the north-western part of the peninsula. The present study uses the 145 to 150 m contour as an approximation of marine limit and assumes that the emergence curve presented by Bell (1996) provides a time frame for permafrost formation at lower elevations. Of particular importance is the local glaciomarine deposition of fine-grained sediments transported by meltwater. A thin drape of marine sediment covers most surfaces below 150 m a.s.l.; however, extensive deposits also occur in the Slidre River valley, in an unnamed valley on southern Fosheim Peninsula, and along Slidre Fiord. In places, these marine deposits form thick, laminated terraces. Figure 1, taken from Bell (1996), shows the present distribution of marine sediments together with the location of upland glaciers, ice-free areas, and shorelines at approximately 9000 BP.

ORIGIN OF MASSIVE ICE

Between 1990 and 1994, 73 natural exposures (mostly retrogressive thaw-slump headwalls and river banks) exhibiting massive ice and ice-rich permafrost were examined in the Eureka Sound lowlands of Fosheim Peninsula and on eastern Axel Heiberg Island (Fig. 2). An examination of topographic position, stratigraphy, structure, and chemical characteristics provides strong support for an intrasedimental origin for this ice.

All the exposures are located below the Holocene marine limit and 94 per cent of them display upper contacts with fine-grained, marine sediments. In cases where the stratigraphy indicates previous thaw-slump activity, these upper contacts are abrupt and unconformable; however most contacts display a structural gradation from marine sediments to pure ice consistent with ice segregation. Lower contacts are rarely visible in this type of natural exposure. However, several sections contain an oxidized sand layer within the ice unit. In sections lacking massive ice, a similar oxidized sand occurs at the base of the lowermost marine unit at the contact with underlying weathered Tertiary bedrock. The presence of oxidized sand in the massive ice unit suggests that ice aggradation preferentially occurs at the contact between marine deposits and the underlying coarse-grained Tertiary deposits. This stratigraphic setting is similar to that of massive ice documented in the Tuktoyaktuk Peninsula area where till overlies the ice 71 per cent of the time and sand and gravel are interlayered within it 94 per cent of the time (Mackay and Dallimore, 1992).

Sediment structures within the ice display grain-size and mineralogical characteristics similar to those of the overlying sediments. Sediment and gas-inclusion layers in the ice consistently parallel the structure of the overlying deposits. Ice chemistry from reticulate ice veins and lenses immediately above the upper contacts is usually comparable with the chemical signature of the underlying body of massive ice. Petrographic data display a preferred vertical c-axis orientation for large crystals located within the ice mass, whereas smaller crystals near the upper contact and in sediment-rich layers tend to display more random fabrics. The combination of these characteristics is not only evidence of an intrasedimental origin, but effectively precludes the possibility of the ice exposures being buried glacier ice or of having formed prior to marine transgression.

LANDSCAPE MODEL

In general, two types of massive ground ice are recognized, including intrasedimental ice formed by the combined processes of ice segregation and groundwater intrusion and buried ice formed by the burial and preservation of a surface ice body (e.g. glacier ice). In the former, massive-ice formation is epigenetic and closely linked to permafrost aggradation and can thus be viewed as the product of freezing conditions at the base of permafrost. In the latter, the nature and extent of massive ice is a function of surface-ice formation and burial processes.

As previously mentioned, massive ice on Fosheim Peninsula is characteristic of intrasedimental formation as permafrost aggraded into emerging marine sediments during the Holocene. An intrasedimental origin is consistent with the conditions described by the limited-glaciation model developed by England (England et al., 1991; England, 1992), Hodgson (1974, 1985, 1989), and Bell (1992, 1996). Conditions suitable for the burial and preservation of glacier ice may have existed locally, although buried glacier ice has yet to be observed.

Observations from three oil and gas exploration wells in the Fosheim Peninsula area suggest that equilibrium permafrost depths are 500+ m for Fosheim Peninsula (Taylor et al., 1982). The age of permafrost, however, will vary depending on the Late Pleistocene and Holocene evolution of glaciers and sea levels. Since intrasedimental ice is primarily a function of permafrost aggradation (rather than being superimposed on existing permafrost), temperature and groundwater conditions at the time of permafrost formation will dictate ground-ice characteristics. Accordingly, three distinct phases of permafrost formation are suggested and correspond to 1) fully developed upland ice-cap and glacial-sea conditions, 2) ice-cap decay, and 3) emergence. The following discussion reviews permafrost and potential ground-ice conditions associated with the dominant Fosheim Peninsula permafrost/landscape systems active during each phase. This model provides environmental conditions (e.g. temperature and water supply) that explain the observed distribution of ground ice.

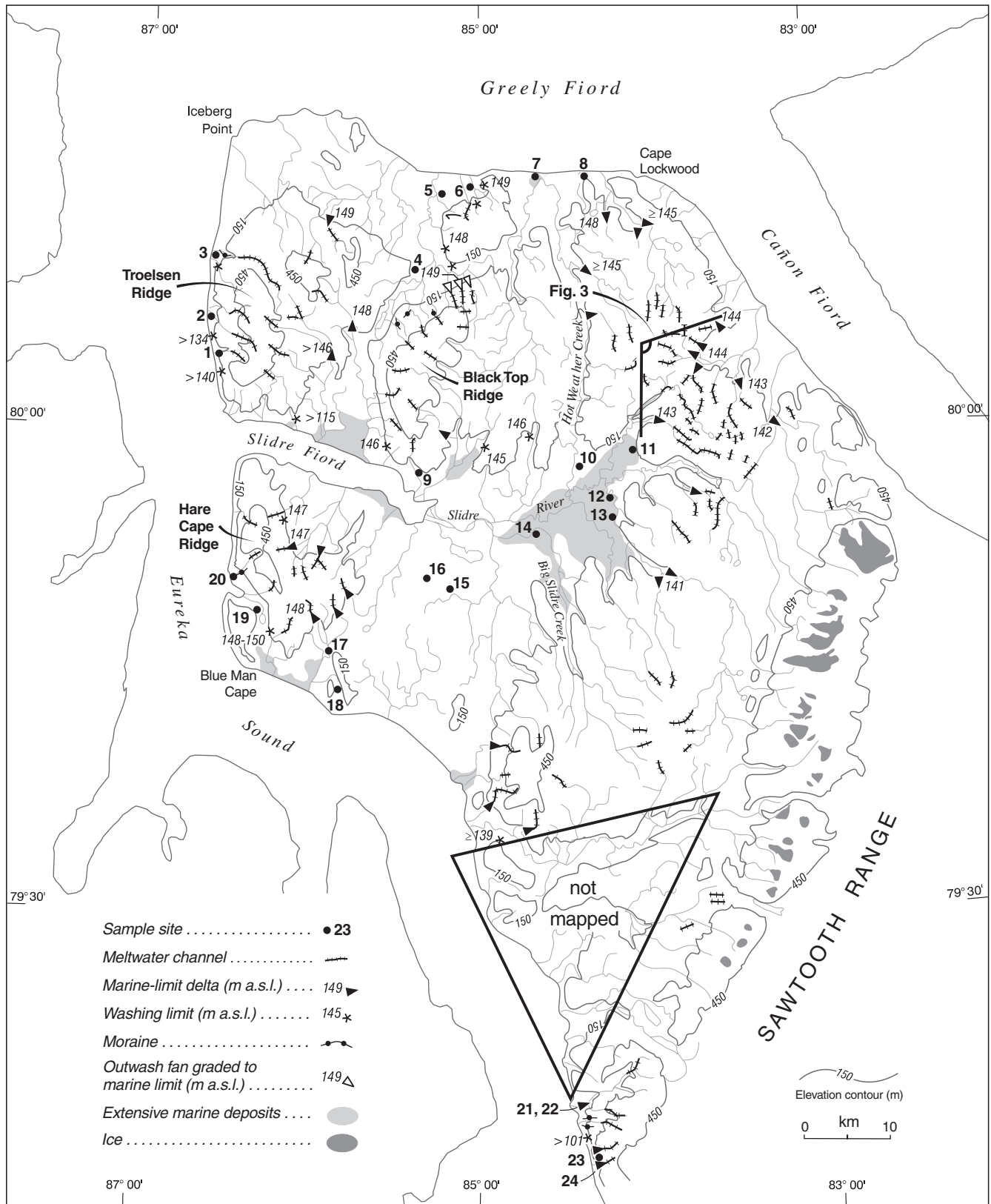


Figure 1. Map (from Bell, 1996) showing the present ice cover and prominent ice-marginal features related to the last glaciation on western Fosheim Peninsula. Site numbers and names are keyed to the original publication.

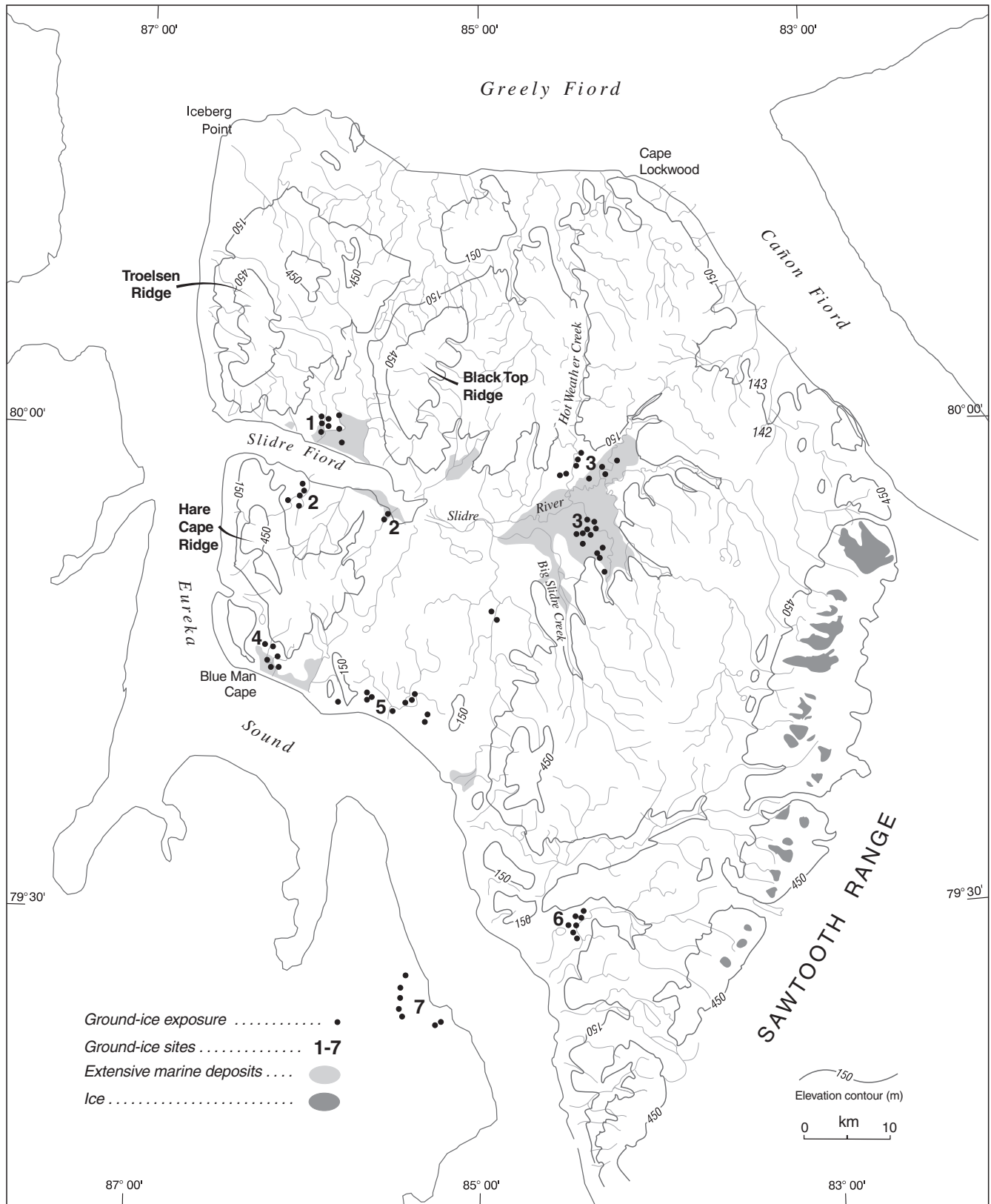


Figure 2. Map showing the distribution of exposures of massive ice in relation to deposits of marine sediments and the 150 m contour that approximates the Holocene marine limit.

During full ice-cap and glacial-sea conditions (14 000–9500 BP), the following three basic systems are involved: the area covered by upland icecaps, the cold ‘paraglacial’ upland surfaces surrounding these ice caps, and the submerged lowlands. If we disregard local variation in heat flow and geology, the deepest and oldest permafrost will exist beneath upland surfaces that remained ice free during the last glaciation. Assuming a geothermal gradient of $0.038^{\circ}\text{C}/\text{m}$, which corresponds with the Gemini well site (Taylor, 1991), and dry ‘paraglacial’ conditions 3 to 5°C colder than present, then equilibrium permafrost depths for these areas were probably 80 to 130 m deeper than present. According to Bell (1996), the upland ice caps that existed in the early Holocene were relatively thin and cold based. It follows, therefore, that permafrost underlying these ‘glaciated’ sites would initially have been the product of basal glacier temperatures. In the absence of this information, it is probably safe to assume that sub-ice-cap permafrost was much thinner than in adjacent paraglacial areas. During this phase, the permafrost that probably existed in lowland areas prior to marine transgression would slowly degrade from both the top and bottom. Taylor (1991) points out that it could take several thousand years to disappear completely. Late Pleistocene marine transgression was thought to be rapid, and the submergence duration (4000–7000 years) was probably sufficient, even near marine limit, to degrade the upper part of permafrost (depending on seabottom and permafrost temperature). Whether the period of marine transgression was long enough to completely degrade permafrost is not important in the analysis of this ground ice. The prevalence of ground ice in the upper 20 to 30 m of ground would put it within the first materials to thaw following marine transgression and the first to freeze following emergence.

The next phase corresponds to the period during which upland ice caps degraded and sea levels remained at or near the Holocene marine limit (9500–7900 BP). However, on the basis of high sedimentation rates in the submerged Big Slide Creek, Bell (1996) believes that the deglaciation phase may have lasted until 5900–4000 BP. During this time, air temperatures were warmer, causing permafrost to warm and possibly decrease in thickness. Even though permafrost was well developed (estimated 500–600 m deep) in ice-free areas, the extreme aridity would have limited potential ground-ice formation. The coarse nature of weathered Tertiary bedrock that characterizes the surficial geology of these surfaces further limits the potential for massive ground ice. There is no evidence to suggest that ground ice was ever an important component of this landscape. As deglaciation proceeded, permafrost conditions in the formerly glaciated areas would have gradually changed to correspond to conditions in paraglacial areas. Ground ice may have been preserved beneath these ice caps if it had existed prior to glaciation. However, the upland surfaces that supported ice caps during the last glaciation are dominated by bedrock and minor till deposits and are unlikely to have contained old ground ice. Local reworking of older till deposits by upland glaciers would have created conditions suitable for the burial and preservation of glacier ice — particularly in the northern part of Fosheim Peninsula where till deposits are most extensive — although buried glacier ice has not been observed. During

this time, sedimentation rates would have been high in the shallow marine basins. Bell (1996) describes the formation of four sedimentary units reflecting changes in sediment supply associated with ice-cap retreat. The rapid emergence that began at 7500 to 6500 BP would have exposed upper-level marine deposits and marked the beginning of ground-ice formation.

The third phase extends from the middle Holocene to the present and corresponds to the emergence of submerged lowland basins and the aggradation of permafrost into raised marine deposits. With middle to late Holocene temperatures as cold or colder than present, permafrost would aggrade rapidly into these deposits. During this ‘emergent’ phase, permafrost and intrasedimental ground ice form more or less simultaneously with shoreline regression. It follows, therefore, that ground ice occurring beneath and within raised marine deposits reflects the time-transgressive development of Holocene permafrost. In areas of irregular topography and varied thicknesses of marine sediments, the resulting ground-ice bodies are irregularly shaped and uneven in thickness. This type of massive ice is seen in the Eureka, south Slidre Fiord, Hot Weather Creek, Blue Man Cape, and May Point areas. Shallow ground ice like this plays an important role in thermokarst and active-layer detachment activity. However, in areas where glaciomarine deposition produced thick, flat, gently sloping, terrace-like bodies of massive to laminated sandy silt and silty clay, permafrost would have aggraded uniformly over the terrace surface. This type of deep ground ice is seen at Eureka, in the Slidre River valley, and at the Eureka Sound and south Fosheim Peninsula sites. Extensive thermokarst occurs in other locations displaying similar deposits. In both cases, as permafrost reached the base of the marine unit, a thick, uniform layer of ground ice formed from the groundwater contained in the underlying weathered bedrock. There are two possible sources of water, meltwater from glaciers and snow, or sea water. Given that areas immediately upslope would have already developed permafrost, it

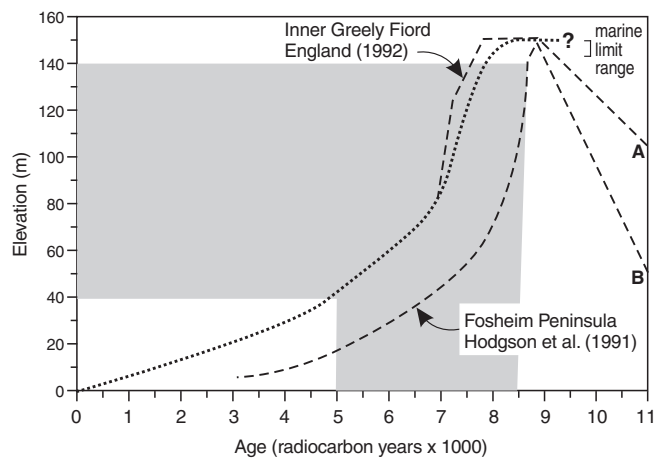


Figure 3. Provisional sea-level curve for northern Fosheim Peninsula from Bell (1996). Lines A and B refer to hypothetical transgressions to marine limit. The shaded area marks the range in elevation and corresponding age of massive-ice deposits.

seems unlikely that meltwater could sustain a sufficient groundwater system to produce the volumes of intra-sedimental ice observed. A groundwater system supported by seawater intrusion would be possible, however. The small amounts of salt that are found in ground ice in this setting support this hypothesis, although the salt could also come from the overlying marine sediments.

Of the three basic environments, i.e. glaciated, paraglacial, and emergent, the third is the most likely to contain significant ground ice because abundance of groundwater and the frost-susceptible nature of the fine-grained marine sediments. The local till deposits could contain buried glacier ice depending on their thickness, but Bell (1992) suggests that the paucity of lateral meltwater channels that would normally be associated with the upland ice caps is indicative of either in

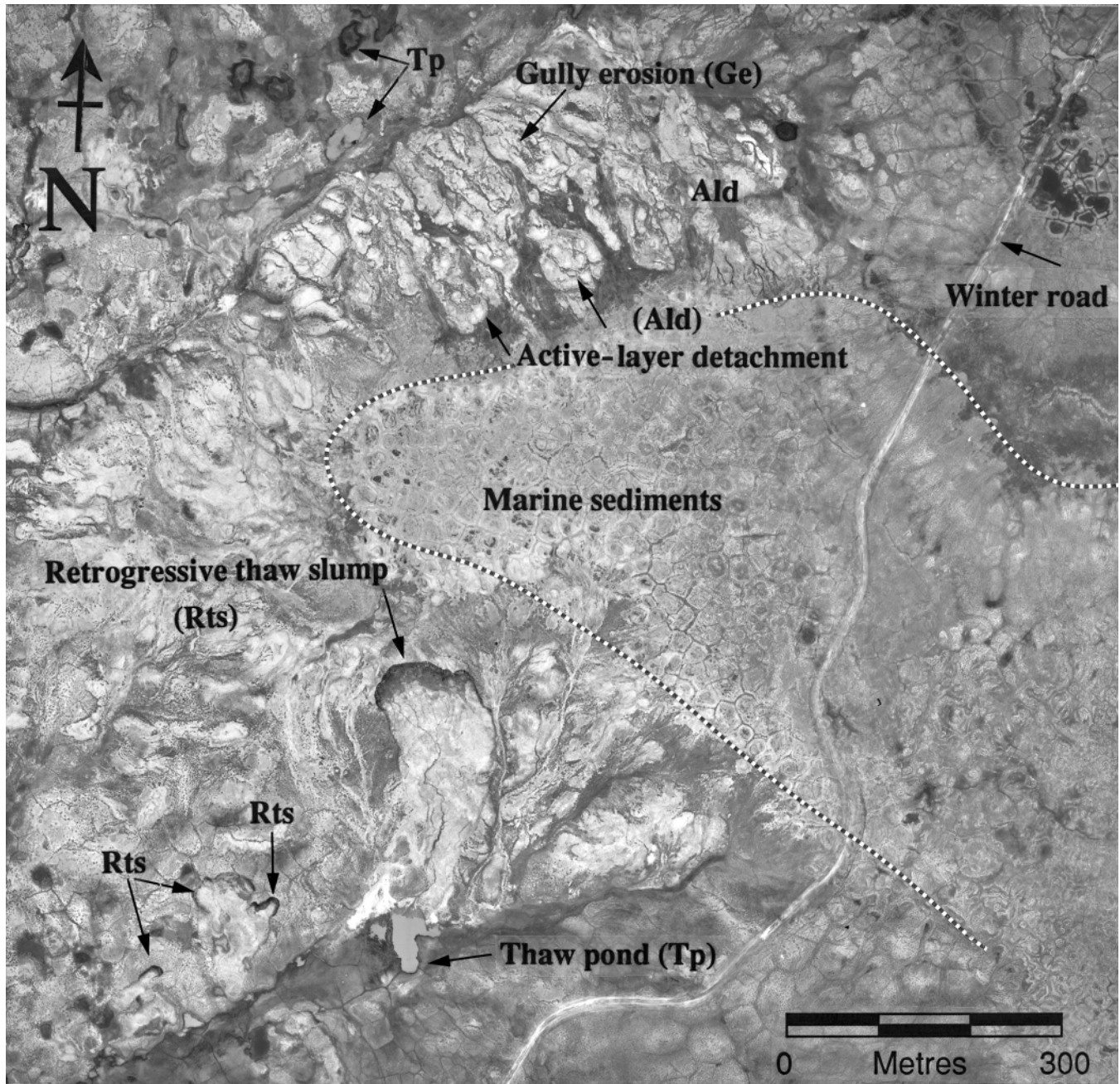


Figure 4. Airphoto of the Gemini well site in the Slidre River valley–Hot Weather Creek area showing marine sediments, retrogressive thaw slumps (Hodgson et al., 1991), and other thermokarst (both natural and anthropogenic). NAPL A308859-47

situ melting or rapid retreat, neither of which is conducive to the burial and preservation of glacier ice. For the most part, upland surfaces are composed of either bedrock or coarse-grained Tertiary deposits that are unsuitable for the formation of massive ground ice.

Elevation, age, and sea-level change

Since ground-ice formation is synchronous with emergence, then emergence history together with elevation records of ground-ice exposures provide a crude proxy record of the age of ground ice. Bell's (1996) provisional sea-level curve for Fosheim Peninsula (Fig. 3) is used here as a time frame for ground-ice history. Ground-ice exposures range in elevation from 120 m a.s.l. near the Gemini well site to 40 m a.s.l. at sites near Slidre Fiord. The elevations of ice bodies tend to cluster in the 40 to 55 m a.s.l., the 70 to 90 m a.s.l., and the 105 to 120 m a.s.l. ranges. Using Bell's sea-level curve, these ice bodies would be between 5000 and 7500 years old.

Ice degradation and thermokarst

The degradation of ground ice is another aspect of the evolution of the Fosheim Peninsula landscape. Thaw degradation, or thermokarst, is a natural part of landscape development in areas underlain by ice-rich permafrost. Despite the cold, dry nature of the climate and the deep, continuous nature of permafrost on Fosheim Peninsula, thermokarst is widespread. In many places, thermokarst is due to melt out of ice wedges, but it also occurs as retrogressive thaw slumps (73 active and 150 stabilized slumps were mapped in four years of field work), active-layer detachments, and degraded surfaces. Degraded surfaces frequently develop a 'badlands' or gullied topography. As retrogressive thaw slumps backwaste into the terraced marine deposits, extensive thermokarst topography is produced (Fig. 4). In areas where human activity has occurred, thermokarst has been accelerated; for example, the area surrounding the Eureka weather station displays several generations of anthropogenic thermokarst dating back to the late 1940s (Fig. 4). Thermokarst processes are discussed in more detail in Robinson (2000).

CONCLUSIONS

This study offers the following five basic conclusions about the origin of ground ice and landscape evolution.

Permafrost conditions are closely related to recent glacial and sea-level histories and can be divided into three phases; the first phase occurred while ice caps were fully developed, the second, during ice-cap decay, and the third, during emergence. Only the last phase is associated with the occurrence of massive ground ice.

Massive ice occurs widely below the Holocene marine limit and has an intrasedimental origin.

Massive-ice deposits are time transgressive and formed as permafrost aggraded into emerging marine sediments during the Holocene.

The intrasedimental origin is consistent with the conditions described by the limited-glaciation model proposed by England (1987) and further developed for Fosheim Peninsula by Bell (1996).

Thermokarst is an important component of the emergence phase of landscape development. Gully erosion and thaw degradation of marine-terrace deposits have produced a heavily dissected 'badlands' topography.

ACKNOWLEDGMENTS

This work was supported by research grants from the Natural Science and Engineering Research Council of Canada, the Department of Energy, Mines, and Resources (EMR Research Agreement Program), and the Atmospheric Environment Service. The author wishes to express sincere appreciation to the Polar Continental Shelf Project (PCSP/EPCP 00797) for its generous field support. The author wishes to thank Dr. Trevor Bell and Dr. Sylvia Edlund for their helpful discussions and insight. The field assistance of Craig Forcece, Peter Barry, Ray Shannon, and Nora Jackson is gratefully acknowledged. The Northern Scientific Training Program (Department of Indian Affairs and Northern Development) is acknowledged for its support of student assistants. Aerial photographs are published with the permission of the National Air Photo Library, Natural Resources Canada.

REFERENCES

- Bell, T.**
1992: Glacial and sea level history of western Fosheim Peninsula, Ellesmere Island, Arctic Canada; Ph.D. thesis, University of Alberta, Edmonton, Alberta, 172 p.
1996: The last glaciation and sea level history of Fosheim Peninsula, Ellesmere Island, Canadian High Arctic; *Canadian Journal of Earth Sciences*, v. 33, p. 1075–1086.
- Blake, W.**
1970: Studies of glacial history in Arctic Canada. I. Pumice, radiocarbon dates and differential uplift in the eastern Queen Elizabeth Islands; *Canadian Journal of Earth Sciences*, v. 7, p. 634–664.
- Bradley, R.S.**
1990: Holocene paleoclimatology of the Queen Elizabeth Islands, Canadian High Arctic; *Quaternary Science Reviews*, v. 9, p. 365–384.
- Egginton, P. and Hodgson, D.**
1990: Preliminary assessment of selected drainage basins in western Fosheim Peninsula, Ellesmere Island, as sites for global change studies; *in* Current Research, Part D; Geological Survey of Canada, Paper 90-1D, p. 71–77.
- England, J.**
1976: The late Quaternary glaciation of the eastern Queen Elizabeth Islands, N.W.T., Canada: alternative models; *Quaternary Research*, v. 6, p. 185–202.
1978: Glacial geology of northeastern Ellesmere Island, N.W.T., Canada; *Canadian Journal of Earth Sciences*, v. 15, p. 603–617.
1987: Glaciation and evolution of the Canadian high arctic landscape; *Geology*, v. 15, no. 9, p. 419–424.
1990: The late Quaternary history of Greeley Fiord and its tributaries, west-central Ellesmere Island; *Canadian Journal of Earth Sciences*, v. 27, p. 255–270.
1992: Postglacial emergence in the Canadian High Arctic: integrating glacial isostasy, eustasy, and late deglaciation; *Canadian Journal of Earth Sciences*, v. 29, p. 984–999.

England, J., Sharp, M., Lemmen, D.S., and Bednarski, J.

1991: On the extent and thickness of the Innuitian Ice Sheet: a post glacial adjustment approach: Discussion; *Canadian Journal of Earth Sciences*, v. 28, p. 1689–1695.

Fisher, D.A., Koerner, R.M., Paterson, W.S.B., Dansgaard, W., Grudenstrup, N., and Reeh, N.

1983: Effects of wind scouring on climatic records from ice-core oxygen-isotope profiles; *Nature*, v. 301, p. 205–209.

Fyles, J.

1962: Surficial geology, Axel Heiberg–Ellesmere Island, 1961; *in* Field Work, 1961, (ed.) S.E. Jenness; Geological Survey of Canada, Information Circular no. 5, p. 4–6.

Hodgson, D.A.

1974: Surficial geology, geomorphology, and terrain disturbance, central Ellesmere Island; *in* Report of Activities, Part A; Geological Survey of Canada, Paper 74-1A, p. 247–248.

1985: The last glaciation of west-central Ellesmere Island, Arctic Archipelago, Canada; *Canadian Journal of Earth Sciences*, v. 22, p. 347–368.

1989: Quaternary geology of the Queen Elizabeth Islands; *in* Chapter 6 of Quaternary Geology of Canada and Greenland, (ed.) R.J. Fulton; Geological Survey of Canada, Geology of Canada, no. 1, p. 441–459 (*also* Geological Society of America, *The Geology of North America*, v. K-1, p. 441–459).

Hodgson, D.A., St-Onge, D.A., and Edlund, S.A.

1991: Surficial materials of Hot Weather Creek basin, Ellesmere Island, Northwest Territories; *in* Current Research, Part E; Geological Survey of Canada, Paper 91-E, p. 157–163.

Koerner R.M. and Fisher, D.A.

1990: A record of Holocene summer climate from a Canadian high arctic ice core; *Nature*, v. 343, p. 630–631.

Lemmen, D.

1989: The last glaciation of Marvin Peninsula, northern Ellesmere Island, Canada; *Canadian Journal of Earth Sciences*, v. 26, p. 2578–2590.

Mackay, J.R. and Dallimore, S.R.

1992: Massive ice of the Tuktoyaktuk area, western Arctic coast Canada; *Canadian Journal of Earth Sciences*, v. 29, p. 1235–1249.

Robinson, S.D.

2000: Thaw-slump-derived thermokarst near Hot Weather Creek, Ellesmere Island, Nunavut; *in* Environmental Response to Climate Change in the Canadian High Arctic, (ed.) M. Garneau and B.T. Alt; Geological Survey of Canada, Bulletin 529.

Sloan, V.

1990: The glacial history of central Canon Fiord, west-central Ellesmere Island, Arctic Canada; M.Sc. thesis, University of Alberta, Edmonton, Alberta, 107 p.

Taylor, A.E.

1991: Holocene paleoenvironmental reconstruction from deep ground temperatures: a comparison with paleoclimate derived from the $\delta^{18}\text{O}$ record in an ice core from the Agassiz Ice Cap, Canadian Arctic Archipelago; *Journal of Glaciology*, v. 37, p. 209–219.

Taylor, A.E., Burgess, M., Judge A.S., and Allen, V.S.

1982: Canadian geothermal data collection northern wells 1981; Energy, Mines, and Resources Canada, Earth Physics Branch, Geothermal Series 13, Ottawa, Ontario, 190 p.

Thaw-slump-derived thermokarst near Hot Weather Creek, Ellesmere Island, Nunavut

S.D. Robinson¹

Robinson, S.D., 2000: Thaw-slump-derived thermokarst near Hot Weather Creek, Ellesmere Island, Nunavut; in Environmental Response to Climate Change in the Canadian High Arctic, (ed.) M. Garneau and B.T. Alt; Geological Survey of Canada, Bulletin 529, p. 335–345.

Abstract: Early Holocene marine sediments near Hot Weather Creek contain laterally extensive massive ice. Thermokarst degradation, mainly as polycyclic retrogressive thaw slumps, has already affected 12 per cent of the study area. No mechanism currently exists to expose ice in undisturbed marine sediment. With climate warming, increased snowmelt runoff leading to gullying and exposure of ice may provide the required mechanisms for future thermokarst degradation.

A strong correlation between headwall retreat and thawing degree days exists at slumps in terrain sloping at $>10^\circ$. Correlations were weaker at slumps in flatter terrain ($<5^\circ$) and poor at thaw slumps with major headwall morphology changes during the thaw season. Headwall retreat is currently 8 to 14 m/a at high-angle slumps and 5 to 9 m/a at low-angle slumps. Maximum retreat at high- and low-angle slumps is predicted to increase to about 18 and 12 m/a respectively under a 4°C summer-warming scenario.

Résumé : Les sédiments marins de l'Holocène supérieur près du ruisseau Hot Weather renferment de la glace massive de grande étendue horizontale. La dégradation thermokarstique, surtout sous la forme de glissements régressifs polycycliques dus au dégel, a déjà touché 12 p. 100 de la région à l'étude. Actuellement, il n'existe pas de mécanisme qui expose la glace dans les sédiments marins intacts. Avec le réchauffement climatique, une augmentation du ruissellement dû à la fonte de la neige pourrait entraîner le ravinement, exposant ainsi la glace, et pourrait fournir le mécanisme nécessaire pour la dégradation thermokarstique future.

On a trouvé une forte corrélation entre la retraite du front d'affaissement et le nombre de degrés jours sans gel aux glissements situés dans les terrains dont la pente est supérieure à 10° . La corrélation était plus faible dans les terrains à pente plus faible ($<5^\circ$) et elle était très faible pour les glissements dus au dégel qui présentaient de grands changements morphologiques au front d'affaissement durant la saison de dégel. Les glissements en terrain à forte pente présentent actuellement une vitesse de retraite du front d'affaissement de 8 à 14 m/a. La vitesse de retraite en terrain à pente faible est de 5 à 9 m/a. Dans un scénario avec un réchauffement estival de 4°C , on prévoit que la vitesse de retraite maximale du front d'affaissement augmentera jusqu'à environ 18 m/a pour les glissements en terrain à pente forte et jusqu'à 12 m/a pour les glissements en terrain à pente faible.

¹ Terrain Sciences Division, Geological Survey of Canada, 601 Booth Street, Ottawa, Ontario K1A 0E8

INTRODUCTION

Periglacial processes play a key role in landscape development on Fosheim Peninsula, Ellesmere Island. Large volumes of massive ground ice found in some raised marine sediments contribute to retrogressive thaw slumping and intensive slope gulying (Hodgson et al., 1991; Pollard, 1991; Barry, 1992; Robinson, 1993). In some locations, excess ice is thought to be responsible for positive topography (Robinson, 1994). Ground ice with a thin sediment overburden is prone to thermokarst development following natural or anthropogenic disturbance. Initially, interest in local ground ice was prompted by oil and gas exploration on western Fosheim Peninsula in the late 1960s to mid-1970s (Hodgson, 1974). Land use during this time was the most intensive ever experienced in the Queen Elizabeth Islands. More recently, research interest has been stimulated by predictions of 'greenhouse effect' summer warming of 4 to 6°C for this part of the Canadian Arctic (Canadian Climate Program Board, 1991). Thus, there is a need for studies examining the distribution of ground ice and thermokarst processes.

During the summers of 1991 and 1992, a joint geophysical and geomorphological study of massive ground ice was conducted. This study was undertaken as part of the Geological Survey of Canada's global-change monitoring program in the High Arctic, based at Hot Weather Creek (lat. 79°58'N, long. 84°28'W), about 25 km east of Eureka. The aim of this paper is to examine ground-ice distribution, determine current thaw rates and mechanisms, and suggest local terrain responses to potential warming. Emphasis is placed on shallow drilling, geophysical surveys, observations of ice in exposure, and the regular monitoring of retrogressive thaw-slumping rates.

REGIONAL BACKGROUND AND STUDY SITE

The west-central Fosheim Peninsula is a broad, rolling, intermontane lowland. Removed from the influence of any large water bodies and protected from the incursion of cold air masses by the surrounding mountain ranges, the Hot Weather

Creek region experiences summer temperatures that are anomalously warm for this latitude (Edlund and Alt, 1989). During the early Holocene marine inundation to approximately 148 m above present sea level, silty clay to fine sand was deposited over older Quaternary deposits or poorly consolidated clastic bedrock (Bell, 1992). In places, these marine and fluvial sediments are 30 m or more thick (Hodgson et al., 1991), with ice exposures up to 8 m thick (Fig. 1). The ground ice enclosed by the sediments is thought to be of segregated origin (Pollard, 1991; Robinson, 1993) formed following marine regression. Massive ground-ice sills have also been found in Tertiary bedrock, but are not thought to be extensive (Robinson and Pollard, 1998). Taylor et al. (1982) calculate a permafrost thickness of 502 m from thermal measurements in Gemini well, located in the extreme northeastern corner of the study area near the marine limit. The extrapolated, mean ground-surface temperature at this site is -20.8°C (Taylor, 1991). Active-layer thickness in the area generally ranges from 0.15 to 0.90 m depending upon material, moisture content, and vegetation cover.

An 80 km² area near the confluence of Hot Weather Creek and the Slidre River was selected for detailed study; only a small section of this area is above the early Holocene marine limit (Fig. 2). Marine sediments cover 58 per cent (46.2 km²) of the terrain with numerous river channels incised into the underlying bedrock. The remaining area below the marine limit consists primarily of colluvial silt and fine sand derived from weathered bedrock, marine-washed bedrock, and fluvial sediments. Detailed field studies were conducted mainly near Hacker Creek (unofficial name) (lat. 79°55.5'N, long. 84°18'W), about 6 km southeast of Hot Weather Creek. This area contains numerous ground-ice exposures and thermokarst features mainly on slopes where gulying and prior thermokarst events have removed the protective marine sediment cover. Plateau and interfluvial areas within the study region remain unaffected by thermokarst, even where ground ice is present. In a similar study, Barry (1992) mapped numerous ground-ice slumps south of Slidre Fiord. These slumps were also on valley sides; extensive lowlands and interfluvial areas did not show signs of thermokarst, even though ground ice was thought to be present.

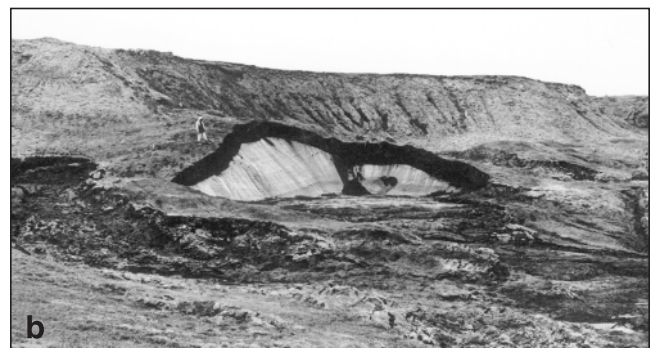


Figure 1. Photographs of **a)** Hacker West, a typical low-angle slump (GSC 2000-019), and **b)** Horkin', a high-angle slump (GSC 2000-020) (unofficial names). Note the presence of a stabilized thermokarst event in **b)** and the gradual insulation of the ice by mudflows at the sides of the slump. Photographs by S.D. Robinson

DISTRIBUTION OF MASSIVE GROUND ICE

The distribution of ground ice was investigated by visual mapping of active thaw slumps, drilling and geophysical surveys for the presence of remnant ice in thermokarst areas, and drilling and geophysical surveys for the presence of ice within undisturbed sediments.

Ground ice was found in all three investigated environments.

Active retrogressive thaw slumps

At least 20 active thaw slumps with ice exposures are found within the study region (crescent symbols in Fig. 2). Individual active slumps have affected up to 5764 m² in planimetric area, with some slump faces exposing up to 200 m² of ice

(Table 1). Sediment at the top of the ice face commonly ranges from 0.6 to 2 m thick. These ice faces are the most obvious indication of massive ice. Thaw-slump initiation may be attributed to undercutting along stream banks, local slope instability, or snowmelt gullying.

Remnant ice in thermokarst terrain

Thermokarst degradation, most notably in the form of active and stabilized retrogressive thaw slumps and some ice-wedge degradation, has affected approximately 12 per cent (5.45 km²) of the marine sediments within the study area, often resulting in the formation of badlands-type terrain (dotted regions in Fig. 2). Large volumes of ground ice may remain after slump stabilization both underneath slump mudflows and in the surrounding, undisturbed terrain.

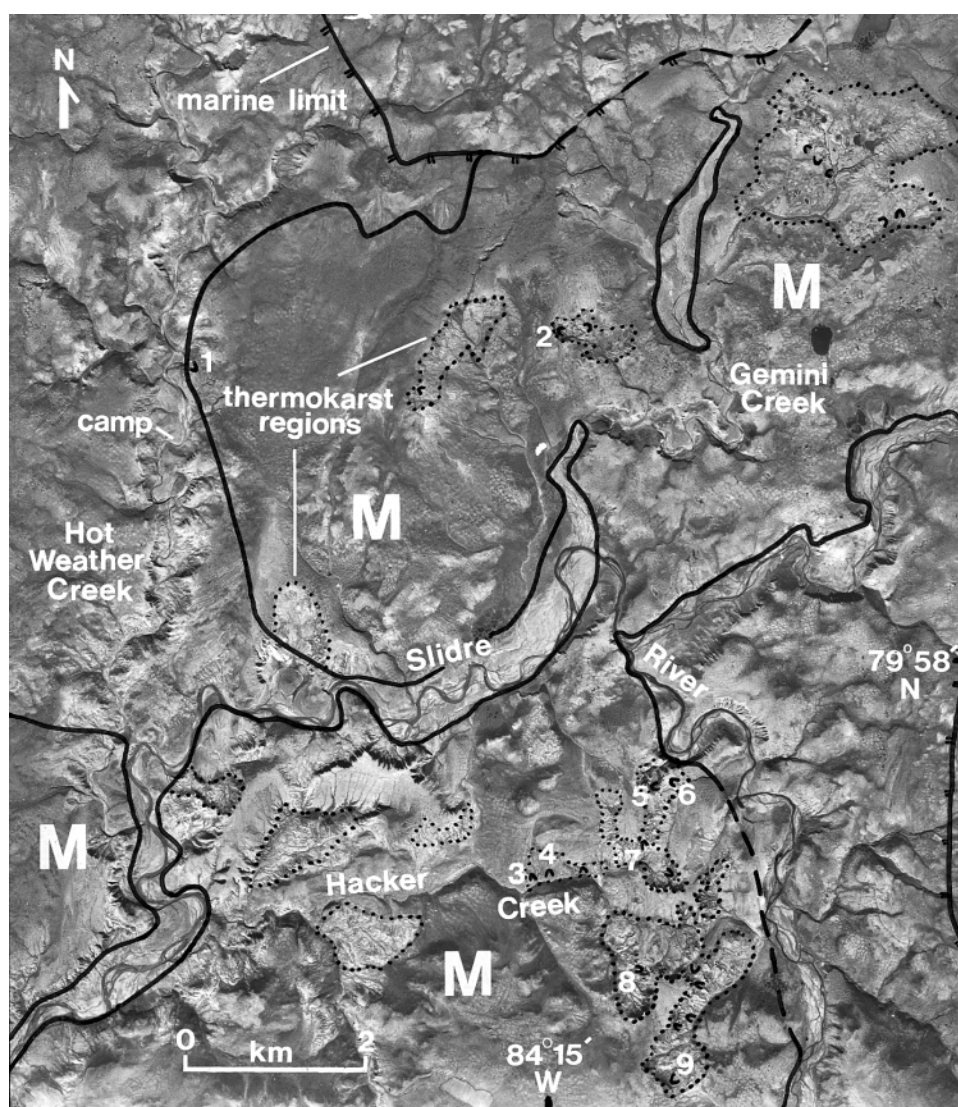


Figure 2. Airphoto of the study area, with marine sediments (M), thermokarst regions (dotted), marine limit, and active slumps with crescent-shaped outlines. Slumps selected for study are numbered. Surficial geology modified from Hodgson et al. (1991). NAPL A16734-61

Table 1. Thaw-slump morphology and measured rates of retreat.

Slump name (number refers to Figure 2 and notes below)	Type	Slump area (m ²), (maximum width, length) (m)	Ice-face azimuth (°)	Maximum ice face dimensions, (m) (width, height)	Slope mudflow, ice face, terrain (°)	1991 retreat ^a Total retreat (cm), (retreat per thawing degree day) July–August	1992 retreat ^a Total retreat (cm), (retreat per thawing degree day) full season	Midseason thaw equation	r ²
1. Base camp	Mid	4732 (74, 78)	313	52, 2.3	5, 52, 7	637 (1.58)	326 (0.76)	y=1.08x+32.6 (91) y=0.91x (92)	0.68 0.97
2. Horkin'	High	743 (23, 44)	095	47, 8.0	6, 64, 22	618 (1.75)	612 (1.45)	y=1.62x	0.85
3. Hacker West	Low	4887 (36, 150)	148	42, 1.2	2, 45, 2.5	-	608 (1.47)	y=1.53x5	0.74
4. Hacker East	Low	1193 (30,42)	187	-	2,-, 3	-	251 (0.61)	y=0.66x	0.76
5. Slide Upper	Mid	5623 (46, 210)	078	28, 3.9	6, 58 ,8	399 (1.64)	530 (1.35)	y=0.67x+51.8	0.25
6. Slide Lower	Mid	2661 (34, 130)	128	19, 3.6	8, 56, 7	500 (2.05)	543 (1.39)	y=0.83x+55.7	0.25
7. Slide South	High	1026 (30, 44)	118	28, 6.8	10, 72, 25	511 (2.42)	772 (1.87)	y=2.50x	0.85
8. West Peninsula	Low	3437 (47, 91)	298	53, 0.8	1.8, 44, 4.5	-	486 (1.19)	y=1.44x	0.74
9. East Peninsula	Low	5764 (60, 160)	064 (008)	95, 1.8	3, 23(36), 2	-	663 (1.66)	y=1.16x+33.6	0.17

^a Mean of five points of maximum retreat over the period of measurement (1991 — July and August only, 1992 — full thaw season). The figures in brackets represent headwall retreat per thawing degree day (cm/°C). Values for 1992 are averaged over the entire thaw season and include early season thaw retardation.

SLUMP NOTES

1. Located in the bowl of an old slump (stable pre-1950) on the outside of a creek meander; recent activity post-1959; rapid retreat noted in 1988–1990, much slower in 1991–1992 as the oldest headwall is approached and overburden thickens, no ice exposed in July 1993.
2. Extensive gullying throughout the old amphitheatre exposing ice at various elevations (range 12 m); present slumping initiated post-1959, slump approaching steep slope and primary sediment; upper ice very clean, some silt in lower sections, large (125 x 75 cm) gravel lens with clay matrix noted in ice in 1991.
3. The only nonpolycyclic slump, likely initiated about 1960, terrain and foot of mudflow well vegetated, no visible limits to future growth.
4. Ice covered by 20 cm of blocky silt, not exposed during the season; retreat due to ice melt beneath sediment cover and blockfall.
5. Slump about 100 m long in 1959; exposure and activity much greater in 1991 than in 1992; no ice exposed in 1993 — retreat inconsistent due to headwall changes.
6. Polycyclic slump initiated post-1959; ice-face exposure, headwall morphology, and retreat very inconsistent.
7. Initiated post-1959; slump on steep slope up to flat-topped hill; local ice up to 17 m thick (Robinson, 1994); many local, abandoned slumps at various elevations (range 16 m); ice exposed in a gully 14 m below the top of the ice body — in later season, wet sections 5 m below hilltop, especially in abandoned slumps.
8. Local slumping common on 1959 airphotos, but this slump was initiated post-1959.
9. Initiated pre-1959, complex retreat of two main headwalls; the north headwall has only a 55 cm overburden and a low ice angle; the south headwall is slightly steeper with thicker overburden; retreat is highest on the south headwall until the active layer reaches the top of the ice at the north headwall, which then promotes rapid thaw from the top of the ice as well as along the ice face.

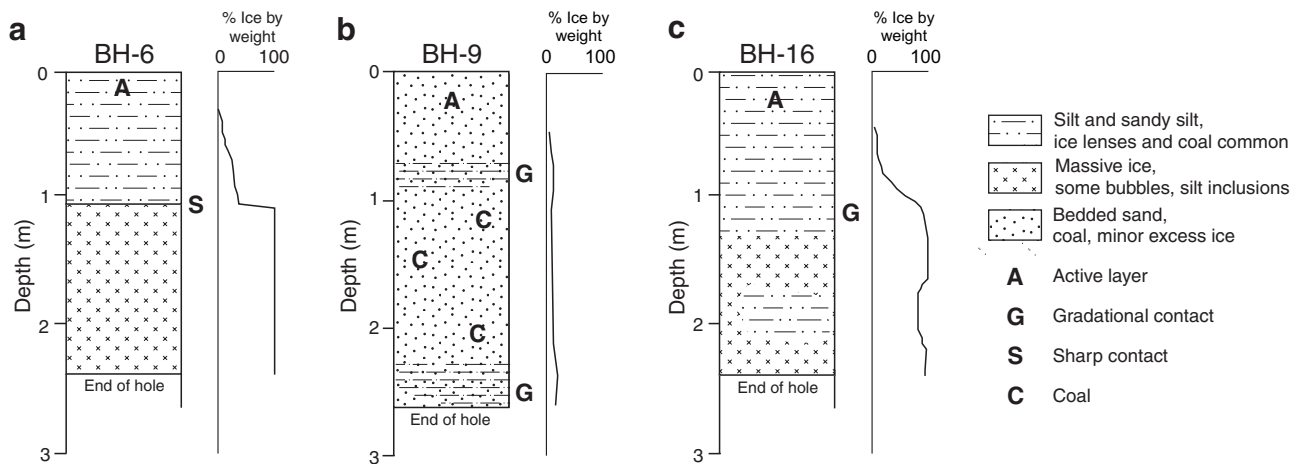


Figure 3. Borehole logs for three typical boreholes drilled in the eastern Hacker Creek region. In **a**) the sharp, thermo-erosional, sediment–ice contact typical of sediments previously affected by thermokarst is shown. **b**) Atop interfluvial areas and uplands, ice content is low and massive ice is absent in the borehole. However, gravity surveys at several of these sites have indicated the presence of ice at greater depths. **c**) Borehole log from a lowland area unaffected by thermokarst. Some massive ice occurs near the surface, with a gradational contact with the overlying sediment.

Polycyclic slumping, the development of a fresh thaw slump wholly or partly within the confines of an old slump, is very common within the area. Eight of the nine thaw slumps examined in detail have redeveloped in the mudflows of thermokarst terrain. Some locations show at least three stages of activity. This indicates a total ice thickness much greater than that exposed in any one slumping episode.

Nine shallow boreholes (maximum depth 2.87 m) were drilled in the Hacker Creek region for examination of remnant ground ice in thermokarst terrain. All boreholes penetrated 0.55 to 1.50 m thick mudflows overlying pure, massive ice (less than 5 per cent sediment by weight) extending below the borehole bottoms. The sediment-ice contact was a sharp, thermo-erosional interface in all cases (Fig. 3a). Attempts were made to map ice distribution and thickness in thermokarst areas using terrain conductivity and ground-penetrating radar. Unfortunately, the high salt content of the disturbed marine sediments overwhelmed the responses from electrical geophysical instruments (Robinson, 1994).

Intensive snowmelt gullying in 1992 revealed massive ground ice in numerous locations away from slumps. Most often occurring in the thermokarst badlands regions prone to snowdrifting, these gullies indicate that thick remnant ice is still present through much of the thermokarst-affected topography. At the Slidre South site (7 in Fig. 2), the gully exposure was in the mudflow of an active slump, 14 m lower than the top of the slump ice face. Assuming the two exposures are of the same buried ice body, 14 m may represent a minimum ice thickness. Ice exposed in the Horkin' Slump area (2 in Fig. 2) had an elevation range of 12 m.

Undisturbed ice-cored terrain

Drilling on flat-topped interfluvial hills failed to reveal ice before borehole completion at between 2.34 and 2.54 m (Fig. 3b). However, a gravity survey of one hill showed it to be cored at greater depths with up to 17 m of ice (Fig. 4; Robinson, 1994). This particular hill is surrounded on all sides by thaw slumps (including the Slidre South slump mentioned above) and badlands thermokarst terrain. Other interfluvial hills in the area are also surrounded by outcrops of ice and similar terrain, indicating that they may also be ice cored.

Boreholes drilled in lower elevation, undisturbed, and generally flatter terrain often penetrated massive ice, but with a thicker overburden than noted in thermokarst terrain. Sediment-ice contacts in undisturbed terrain were always gradational (Fig. 3c), often with reticulate ice in sediment just above the contact. This gradational contact indicates that the ice has likely not undergone any thaw. However, it is unknown whether these sediments represent little-eroded, in situ, marine deposits possibly with large ground-ice volumes at greater depths or an environment with generally lesser ground-ice volumes.

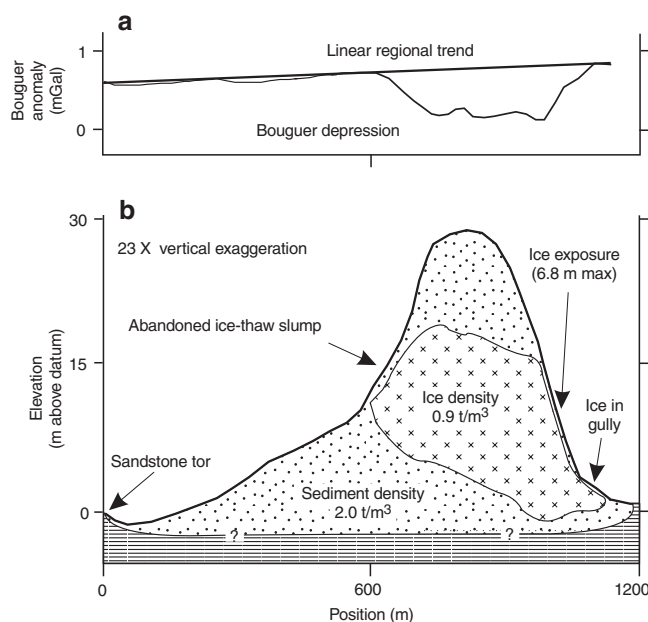


Figure 4. Calculated Bouguer anomaly (top) and topography and interpreted model of ice distribution (bottom) for a gravity survey across a plateau near Hacker Creek. The occurrence of ice in exposures on the hill flanks aided the interpretation (from Robinson, 1993).

THAW-SLUMP MORPHOLOGY

Thaw slumps are initiated following a natural or anthropogenic disturbance that exposes ice-rich permafrost. The headwall region of an active retrogressive thaw slump consists of undisturbed terrain into which the headwall is retreating, a vertical or nearly vertical headwall usually consisting of ice-poor sediment, an ablating, ice-rich face, and a mudflow of saturated material, which buries the lower portion of the ice-rich layer (Fig. 5). As the ice face ablates, sediment tumbles down the ice face and mixes with the meltwater, forming a mudflow that covers basal portions of the ice. Retrogressive thawing may be arrested if the ice face is insulated by fallen debris (Burn and Lewkowicz, 1990), due to an increase in overburden thickness or a decrease in slope. Additionally, the ice may be depleted in lateral extent. As the headwall retreats upslope, ice exposed at the sides of the slump often becomes insulated by mudflows from a slightly higher elevation (see Fig. 1). Where ice remains beneath the mudflows, subsequent disturbance may result in polycyclic slumping, which causes further depletion of the thickness of the ice body (Robinson, 1993). Ground-ice slumps within the study area have been divided into three morphological types on the basis of terrain slopes. Low-, medium-, and high-angle slumps are set in areas with terrain slopes of $<5^\circ$, 5 to 10° , and $>10^\circ$, respectively (Fig. 5). Ice-face angles in low- and high-angle slumps ranged from 23° to 45° and from 64° to 72° respectively in the study region (Table 1).

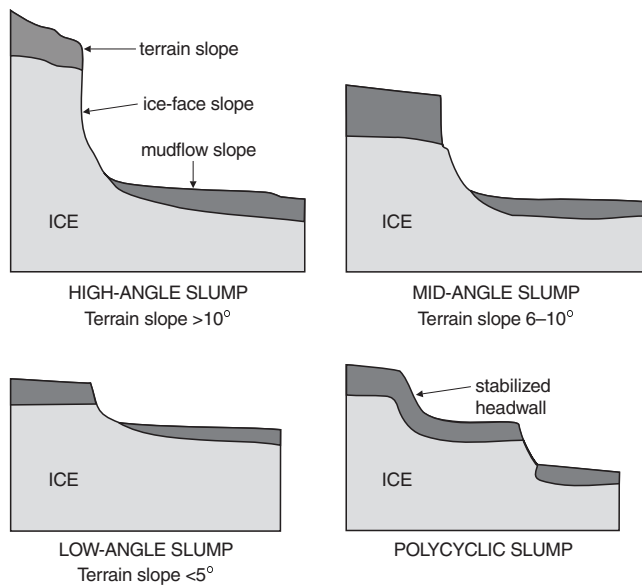


Figure 5. Retrogressive thaw-slump morphology for high-, medium-, and low-angle and polycyclic slumps.

The high-angle and some of the medium-angle slumps noted in this study are eroding into high bluffs leading to an upland interfluvial plain (Fig. 1b). The early stages of each slump exploit the thinner overburden cover of older mudflows. However, as the main bluff is approached and the headwall enters undisturbed primary sediment, the overburden thickness increases and the slump will often become stabilized. This occurred in 1993 at the Slidre Upper site (H. Taylor, pers. comm., 1993). Although the ice body extends under the plain, the greater thickness of sediment covering the ice on the hilltops and plateaus adds a degree of temporary stability to the ice body. Future degradation of the ice body may be brought about by further gully cutting, stream undercutting, or slope instability. Thus, as each individual stage of thaw is generally a backwearing process, successive stages of polycyclic slumping result in the overall decrease of ice thickness (Fig. 5). The low-angle and some medium-angle slumps are commonly found as polycyclic forms in the intensively gullied thermokarst badlands surrounding the plateaus (i.e. West Peninsula), but away from the main bluff. Others (i.e. Hacker West; Fig. 1a) are at lower elevations away from the large, ice-cored plateaus.

THAW-SLUMP HEADWALL RETREAT: RATES AND DISCUSSION

Five active retrogressive thaw slumps were monitored for headwall retreat in 1991. This was increased to nine slumps in 1992, all within 10 km of the Hot Weather Creek base camp (Fig. 2). Headwall retreat was measured using a series of wooden stakes placed 2 to 3 m apart above the headwall of each slump. Measurements were taken approximately every 7 to 10 days during the thaw season and compared to thawing-degree-day (TDD) data from the Hot Weather Creek base camp. Notes concerning any factors that may affect

slump activity (i.e. debris cover, ice-face angle, sediment thickness) were also taken during each survey. Table 1 summarizes various morphological attributes for each slump including area of thermokarst disturbance, ice-face dimensions, ice-face azimuth, slopes, and headwall retreat rates. Complete survey descriptions are available in Robinson (1993).

Rates of thaw-slump headwall retreat presented in this study are the average of the five maximum values of retreat for each survey period. This method helps eliminate the influence of point-specific events such as blockfall. Retreat in 1991 was measured only for the second half of the thaw season, whereas 1992 data include the full thaw season until August 21. For this reason, retreat results for each year presented in Table 1 are not for direct comparison. Calculated values of average headwall retreat per thawing degree day in 1991 are much higher than the 1992 values because early season thaw retardation from snowbanks remaining in the thaw bowl was not measured. Thawing degree days in 1991 and 1992 totaled 630°C and 423°C respectively. Figure 6 presents mid-season slump-retreat data from two high-angle slumps (a), two low-angle slumps (b, c), and a slump (d) in the stages of stabilization. Individual data points represent headwall retreat over a period for which thawing degree days have also been measured.

The high-angle slumps, Horkin' and South Slidre (Table 1), both show excellent midsummer correlations between average headwall retreat and thawing degree days (Fig. 6a). Early season measurements consistently fall below the regression line, showing thaw retardation due to a cover of snow and debris on the ice face. This effect is seen at all slumps, but is most pronounced in 1992 at the high-angle slumps because of thick snowdrifts in the thaw bowl. Thaw rates over the full thaw season (1992) at the Slidre South and Horkin' slumps averaged 1.87 and 1.45 cm/TDD respectively (Table 1), whereas midsummer rates were up to 2.5 cm/TDD at Slidre South. Headwall retreat in the centre of the Slidre South thaw bowl averaged 7.72 m over the 1992 thaw season (maximum retreat 8.42 m), the greatest retreat of any slump in the study (Table 1). Using the geometric relationships provided by Lewkowicz (1987), this corresponds to an average ice-face ablation of 5.65 m.

Regression lines from low-angle slumps (Fig. 6b, c) generally show a slightly lower slope than the high-angle slumps and the correlation is not as strong. Low-angle slumps are influenced to a greater degree by debris cover and blockfall. The lower ice-face and mudflow slopes retard the removal of debris from the ice face, allowing some degree of insulation. In 1992, average full-season thaw rates at low-angle slumps ranged from 1.19 to 1.47 cm/TDD. Values of headwall retreat (full-season maximum retreat of 6.08 m for Hacker West and 4.86 m for West Peninsula) and ice-face ablation (4.11 m and 3.09 m, respectively) are lower than at high-angle slumps and the actual amount of ice melt is much lower due to differences in ice-face dimensions. For each metre of headwall retreat, approximately 10 times more ice melts at Horkin' slump than at Hacker West. The ice-face orientations of Hacker West (southeast-facing) and West Peninsula (west-facing) may explain differences in their retreat rates.

Basecamp slump is a good example of a slump in the stages of stabilization. The present ice face is located in the bowl of an abandoned slump above a meander of Hot Weather Creek. The current slumping event was initiated after 1959 aerial photography and was retreating up to 1 m per week when observed from 1988 to 1990 (S.A. Edlund, pers.

comm., 1992). Measurements in 1991 and 1992 showed that slump retreat was slowing. Mudflows backed up and the debris cover became more extensive, resulting in ice exposure and retreat limited to fewer sections along the headwall. The progressive stabilization of the headwall from 1991 to

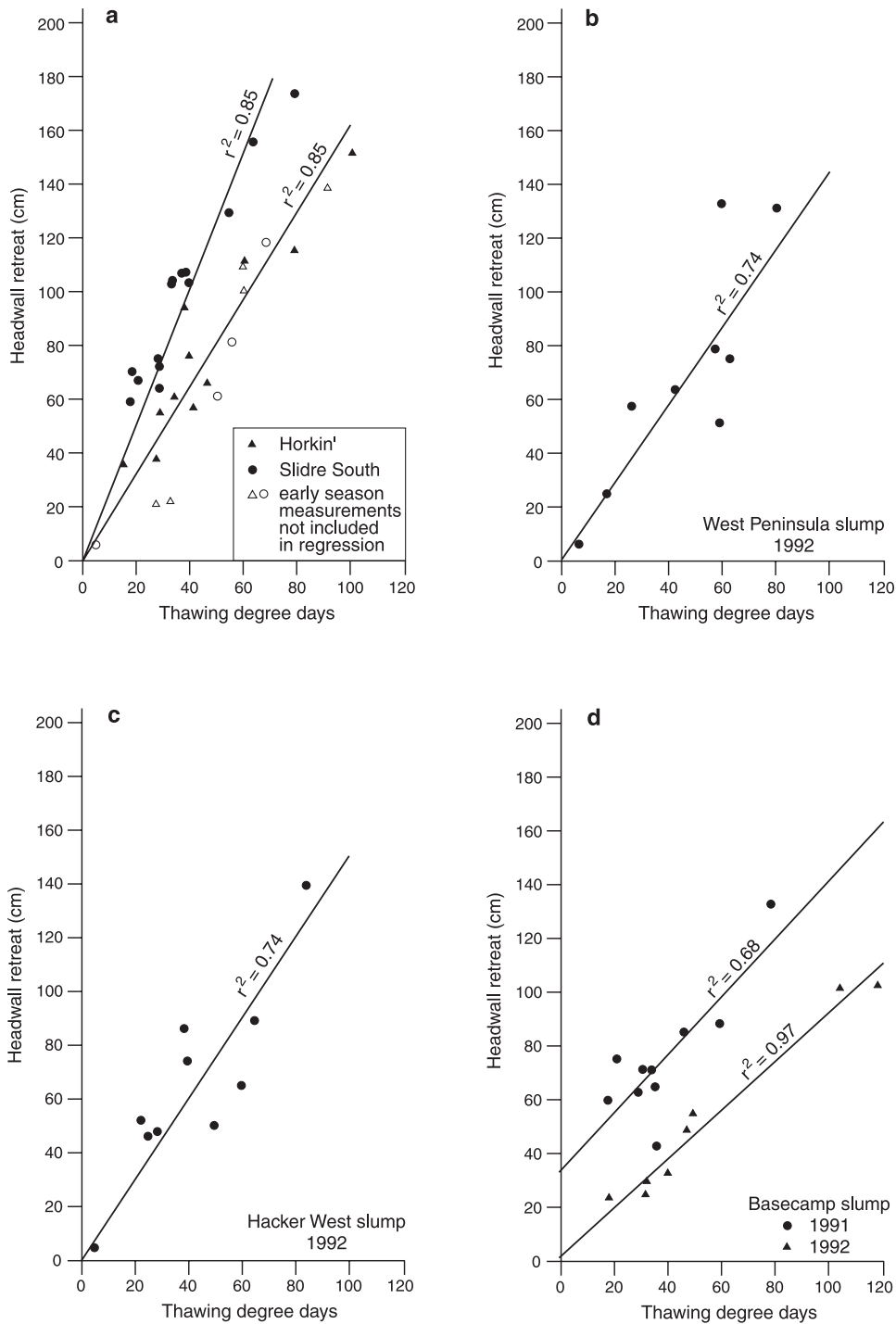


Figure 6. Midseason headwall retreat at a) Horkin' and Slidre South high-angle slumps, b) West Peninsula low-angle slump, c) Hacker West low-angle slump, and d) Basecamp slump in the stages of stabilization.

1992 is shown well in Figure 6d. No ice was visible and headwall retreat was minimal when observed in July 1993 (H. Taylor, pers. comm., 1993).

Three other slumps that were monitored within the region showed very poor correlations between headwall retreat and thawing degree days. Each of these sites (Slidre Upper (no. 5 in Table 1), Slidre Lower, (no. 6 in Table 1), and East Peninsula (no. 9 in Table 1)) underwent major changes in headwall morphology throughout the thaw season (*see* Table 1 notes). For example, at the East Peninsula site, ice was exposed early in the season only along the southeastern 25 m of the headwall. The northeastern 35 m of the headwall consisted of a low-angle (23°) ice face exposed in late season, with only 55 to 70 cm of sediment overburden. As soon as the active layer reached the top of the ice in the northeastern section, retreat became extremely rapid. Melting occurred along the sediment–ice interface as well as the exposed ice face and blocks of sediment slid off the ice face, further decreasing the exposed ice-face angle and increasing measured headwall retreat. Retreat along this section was twice that along the more stable section (thicker overburden) during late summer 1992. At the Slidre Upper and Slidre Lower sites, overburden thickness was uneven above the exposed ice face during 1992, causing differential retreat and stabilization of sections of the headwall.

Numerous researchers have examined the link between climate and thermokarst processes. Lewkowicz (1986) used a multiple regression equation to link short-term (half-hourly measurements) ice-face ablation with incoming radiation (global and diffuse), air temperature, vapour pressure, and wind speed. In turn, ablation rates were used to model headwall retreat using slump geometry (Lewkowicz, 1987), with favourable results. Although the parameters used by Lewkowicz influence short-term ice ablation, the results of this and other studies (i.e. Kerfoot, 1969; Heginbottom, 1984) suggest that a simpler thawing-degree-day model may be applicable for longer term (several days or weeks) studies. However, the dynamic nature of the headwall presents a problem for the accurate prediction of long-term retreat. Only headwall retreat at thaw slumps with relatively consistent morphologies was successfully explained using thawing degree days. Differential retreat rates, which lead to poor model results, may be a function of variations in overburden thickness, sediment content of the ice face (i.e. de Krom and Pollard, 1989), size of ice-face exposures, and periodic debris cover. As it is unlikely that a thaw slump would undergo consistent retreat throughout its existence, any modelling will become inaccurate over the long term.

Retreat measurements taken in 1991 and 1992 incorporated about 60 and 90 per cent of the total thawing degree days for the entire respective thaw seasons. Retreat data for 1991–1992 are extrapolated to the range of cumulative thawing degree days measured from 1988 to 1992 at Hot Weather Creek. This shows that high-angle slumps experience headwall retreat of between 8 and 14 m/a and low-angle slumps, of between 5 and 9 m/a. These rates are similar to those measured by Lewkowicz (9–14 m/a) (*in* Burn and Lewkowicz, 1990) elsewhere on Fosheim Peninsula. Retreat of 2.5 m in 1992 at the Hacker East site, in which the ice face

was always covered by 20 to 30 cm of debris, shows that ice only needs to be close to the surface (i.e. within the active layer) and not actually exposed for significant retreat to occur. Ice-face orientation is considered important for headwall retreat, with southerly facing slumps experiencing the greatest retreat (Lewkowicz, 1987). Although slumps of different orientations were selected for this study, too many other factors (i.e. slump geometry, overburden thickness) contribute to headwall retreat to allow for comparisons on the basis of orientation. Microscale measurements of ice-face ablation and solar radiation would facilitate these comparisons.

The thermokarst areas seem to go through cycles of activity. Only two slumps active in 1991–1992 are visibly active on 1950 and 1959 airphotos. The headwall at the Slidre Upper site has retreated approximately 120 m since 1959, a rate of 3.6 m/a. At the East Peninsula site, retreat since 1950 has been approximately 125 m, a rate of 3.0 m/a. Both of these sites are in the eastern Hacker Creek region. These rates are slower than those noted in the short time span field surveys, suggesting that cyclical retreat and periodic stabilization of slumps may be common. The western Hacker Creek area contains numerous inactive slump scars with only two areas of exposed ice. With the exception of the very active Horkin' slump, thermokarst regions in the north of the study area show signs of extensive recent thaw, but are presently less active. All other active slumps noted in the 1950 and 1959 photographs have since stabilized. Although more slumps may have been triggered in the vicinity, a relatively short life span for individual slumps is suggested. Large volumes of ground ice often remain after thermokarst stabilization, both underneath slump mudflows and in the surrounding undisturbed terrain. This maintains the potential for further degradation should the remaining ice become exposed again in the future. It should be noted that the 1950 low-level photographs (scale 1:18 000) have incomplete local coverage and 1959 photographs are at a scale of 1:60 000, thus making slump identification difficult, even on enlargements.

POTENTIAL IMPACTS OF CLIMATE CHANGE

Although the overall distribution of thick ground-ice bodies in the study areas was not determined, the distribution of ice in exposure, the presence of shallow ice in numerous boreholes, and the results of geophysical studies (Robinson, 1994) show that massive ice is a major component of surficial sediments. In addition to disturbed areas shown to have a high ground-ice content, buried ice is likely extensive under much of the undisturbed marine sediment. The few deep boreholes that have been drilled (Hodgson and Nixon, 1998), geophysical surveys (Barry, 1992; Robinson, 1994), and field observations (Pollard, 1991; Barry, 1992; Robinson, 1993) all indicate high ground-ice contents for much of the marine sediment. All this sediment, given a triggering process to expose the ice, is susceptible to thermokarst degradation. Increased snowmelt runoff leading to gullying and thickening of the active layer under climate change (Canadian Climate

Program Board, 1991) would greatly expand the triggering processes. The extremely warm summer of 1988 may provide some clues as to response to a warmer summer climate. During that summer, thicker than normal active layers resulted in the thaw of shallow ground ice and the recharge of Hot Weather Creek, water ejection features, and the triggering of numerous active-layer detachment slides (Edlund et al., 1989). Measurements at Basecamp slump indicate progressive headwall retreat of up to 1 m a week through late July. By early August, noticeable subsurface water was seeping along the base of the active layer. At one section of the headwall, channeled subsurface flow caused accelerated headwall retreat of 25 m in 38 days (Edlund et al., 1989).

Using a conservative projection of a 4°C summer warming due to climate change (Canadian Climate Program Board, 1991), annual thawing degree days will increase to approximately 750 to 1150°C from the 1988–1992 range of 422 to 740°C. This would indicate an increase in thaw-slumping rates to over 20 m/a at the South Slidre site. However, as solar radiation contributes a large proportion of the energy for ice ablation (Lewkowicz, 1987) and radiation budgets under climate change are likely to remain similar to present fluxes, utilizing thawing degree days as the sole parameter overestimates future retreat. Woo et al. (1992) suggest that higher temperatures and a longer thaw season will increase thaw-slump retreat rates by no more than 25 per cent. Using this as a guide, under a summer warming scenario, retreat rates up to about 18 m/a may be expected at slumps with a morphology similar to that presently found at the Slidre South site. Slightly lower retreat rates (up to about 12–13 m/a) may be expected at low-angle slumps. Retreat rates under the warming scenario are similar to those presently experienced at Mayo, Yukon Territory (Burn and Friele, 1989).

The triggering and propagation of thaw slumps in areas already affected by thermokarst is also likely to increase with a warmer climate. Drilling results show that sediment covering the ice in the slump mudflows is often slightly thinner than that found in undisturbed areas and is often unvegetated (Robinson, 1994). This suggests that previously disturbed terrain is susceptible to subsequent disturbance and may explain the prevalence of polycyclic slumping in the area (eight of nine slumps studied are polycyclic). Nivation and deflation may also contribute to the progressive denudation of the nonvegetated, disturbed terrain. Accelerated thermokarst has already been noted at sites where the active layer enters the top of the ice body.

A SIMPLIFIED MODEL OF ICE FORMATION AND DEGRADATION

A simplified model of ground-ice exposures in the area may be presented, based on an ice-genesis model suggested by Pollard (1991) and field observations by the author (Robinson, 1993). Following marine regression ca. 9000 BP (Hodgson et al., 1991; Bell, 1992), rapid permafrost aggradation froze the dry surficial marine sediments, creating the relatively ice-poor surface cap. With increasing depth, the drawing of water to the freezing plane from below would have been balanced by freezing rates, resulting a slower penetration of permafrost and the emplacement of thick segregated ice overlain by several metres of sediment (Mackay, 1971) (Fig. 7a). All field observations by the author in this study area support a segregational ice origin (Robinson, 1993), including the gradational upper contact between ice and sediment in undisturbed terrain and the possible presence

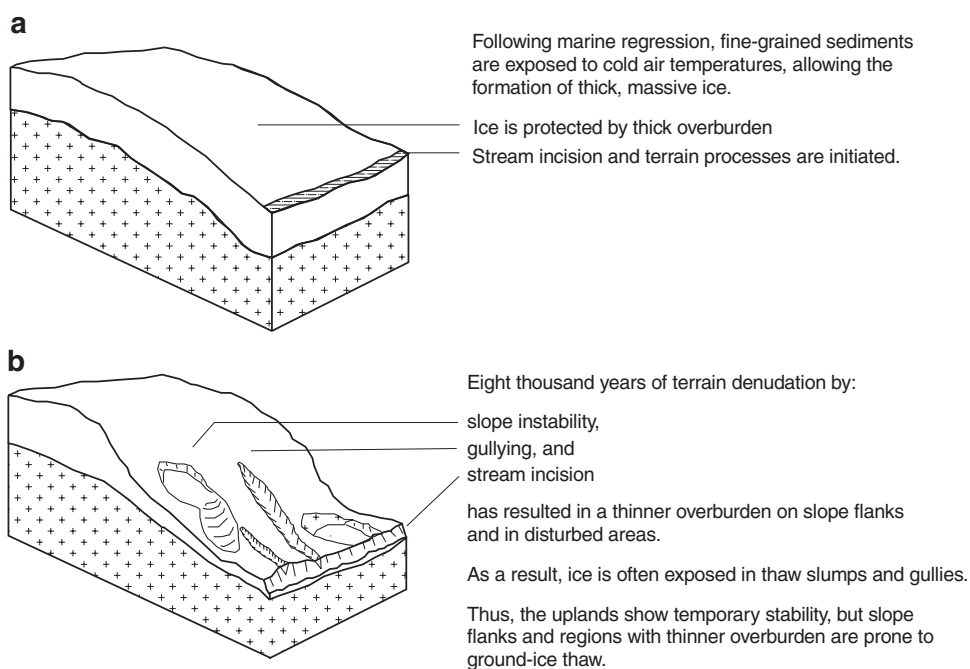


Figure 7. Simplified model for distribution and exposure of ground ice in the Hacker Creek area.

of a gravel layer below the ice to allow a constant supply of water to the freezing front. The thickness of massive ice and the elevation at which the ice formed would be dependent upon topography immediately following emergence, as well as upon freezing rates and water supply.

Altered by progressive denudation from stream incision, meltwater gulying, slope failure, and thermokarst, little of the original topography will be preserved in many areas, except for scattered ice-cored interfluvial upland areas (Fig. 7b). Diapiric uplift and contortion of the exposed ice is noted in several exposures and likely indicates local overburden unloading. Snowmelt gulying and undercutting by streams seem to be the dominant triggering mechanism of thaw slumps. Even the steep-sided, flat-topped uplands have been locally denuded by deflation. The thickness of the overburden covering the ice-cored interfluvial areas is greater than that of the disturbed terrain on the flanks. This adds temporary stability to ice under the uplands, but the ice is still subject to degradation at its sides.

CONCLUSIONS

Thick, massive ground ice is extensive throughout much of the study area in the early Holocene marine sediments, as shown by shallow drilling, geophysical studies, and the observation of ice in exposure. Thermokarst degradation, often in the form of active and stabilized retrogressive thaw slumps, has resulted in ice melt-out and scarring of approximately 12 per cent of the 80 km² study area. Large volumes of ground ice often remain after thaw-slump stabilization, both underneath slump mudflows and in the surrounding undisturbed terrain.

Ground-ice slumps within the study area are often polycyclic and can be divided into low-, medium-, and high-angle slumps set in terrain sloping at <5°, 5 to 10°, and >10° respectively. High-angle slumps, with ice-face exposures up to 8 m high, show excellent correlation between headwall retreat and thawing degree days. Low-angle slumps show lesser correlations, possibly due to the greater influence of blockfall and debris cover. High- and low-angle slump headwalls thaw at rates up to 1.87 and 1.47 cm/TDD respectively over the thaw season. Slumps with major headwall morphology changes through the thaw season show poor correlations between headwall retreat and thawing degree days. A simple thawing-degree-day model may be applicable for long-term retreat predictions, although other researchers have shown a link between short-term ice-face ablation and incoming radiation, air temperature, vapour pressure, and wind speed.

When data are extrapolated to include the full thaw season, high-angle slumps currently experience headwall retreat of 8 to 14 m/a, whereas retreat at low-angle slumps is 5 to 9 m/a. Under a summer-warming scenario, predictions based solely on increased thawing degree days will overestimate headwall retreat. More realistically, climate change is likely to increase headwall retreat to a maximum of about 18 m/a and 12 m/a for high- and low-angle slumps respectively. The frequency of slump initiation, through exposure of ice in

meltwater gullies, undercutting along stream banks, and local slope instability, is also likely to increase under climate change.

The original topography has been subjected to progressive denudation and is poorly preserved in the study area, with the exception of scattered, flat-topped hills. These ice-cored hills remain protected from thermokarst due to a thick overburden. Slope failure and gulying in the area surrounding these hills has exposed ice to thermal degradation and has resulted in a thinner overburden that provides less protection to the already disturbed ice bodies.

ACKNOWLEDGMENTS

Dr. Sylvia Edlund provided employment, friendship, and encouragement during my stays at Hot Weather Creek. Dr. Robert Gilbert capably supervised this work as part of an M.Sc. thesis at Queen's University, Kingston, Ontario. Excellent field assistance was provided by the late Paul Wolfe, Roger Edgecombe, and Chris North. The Polar Continental Shelf Project, the Science Institute of the Northwest Territories, and the Northern Science Training Program assisted both financially and logistically. Dr. Wayne Pollard and Helen Taylor provided helpful discussions and checked the field sites in 1993. Thanks are also extended to all researchers at Hot Weather Creek, Queen's University, and the Geological Survey of Canada who have helped greatly in one way or another. Reviews by Doug Hodgson and Wayne Pollard significantly improved the manuscript.

REFERENCES

- Barry, P.**
1992: Ground ice characteristics in permafrost on the Fosheim Peninsula, Ellesmere Island, N.W.T.: a study utilizing ground-probing radar and geomorphological techniques; M.Sc. thesis, McGill University, Montréal, Quebec, 135 p.
- Bell, T.**
1992: Glacial and sea level history of western Fosheim Peninsula, Ellesmere Island, Arctic Canada; Ph.D. thesis, University of Alberta, Edmonton, Alberta, 172 p.
- Burn, C.R. and Friele, P.A.**
1989: Geomorphology, vegetation succession, soil characteristics and permafrost in retrogressive thaw slumps near Mayo, Yukon Territory; *Arctic*, v. 42, no. 1, p. 31–40.
- Burn, C.R. and Lewkowicz, A.G.**
1990: Retrogressive thaw slumps; *Canadian Geographer*, v. 34, no. 3, p. 273–276.
- Canadian Climate Program Board**
1991: Climate change and Canadian impacts: the scientific perspective; *Climate Change Digest*, CCD 91-01; Canada Climate Centre, Environment Canada, 30 p.
- de Krom, V.D. and Pollard, W.H.**
1989: The occurrence of retrogressive thaw slumps on Herschel Island, Yukon Territory; *The Musk-Ox*, v. 37, p. 1–7.
- Edlund, S.A. and Alt, B.T.**
1989: Regional congruence of vegetation and summer climate patterns in the Queen Elizabeth Islands, Northwest Territories, Canada; *Arctic*, v. 42, no. 1, p. 3–23.
- Edlund, S.A., Alt, B.T., and Young, K.L.**
1989: Interaction of climate, vegetation, and soil hydrology at Hot Weather Creek, Fosheim Peninsula, Ellesmere Island, Northwest Territories; *in* Current Research, Part D; Geological Survey of Canada, Paper 89-1D, p. 125–133.

Heginbottom, J.A.

1984: Continued headwall retreat of a retrogressive thaw flow slide, eastern Melville Island, Northwest Territories; *in* Current Research, Part B; Geological Survey of Canada, Paper 84-1B, p. 363–365.

Hodgson, D.A.

1974: Surficial geology, geomorphology, and terrain disturbance, central Ellesmere Island, District of Franklin; *in* Current Research, Geological Survey of Canada, Paper 74-1A, p. 247–248.

Hodgson, D.A. and Nixon, F.M.

1998: Ground ice volumes determined from shallow cores from western Fosheim Peninsula, Ellesmere Island, Northwest Territories; Geological Survey of Canada, Bulletin 597, 180 p.

Hodgson, D.A., St-Onge, D.A., and Edlund, S.A.

1991: Surficial materials of Hot Weather Creek basin, Ellesmere Island, Northwest Territories; *in* Current Research, Part E; Geological Survey of Canada, Paper 91-1E, p. 157–163.

Kerfoot, D.E.

1969: The geomorphology and permafrost conditions of Garry Island, N.W.T.; Ph.D. thesis, University of British Columbia, Vancouver, British Columbia, 308 p.

Lewkowicz, A.G.

1986: Rate of short-term ablation of exposed ground ice, Banks Island, Northwest Territories, Canada; *Journal of Glaciology*, v. 32, no. 112, p. 511–519.

1987: Headwall retreat of ground-ice slumps, Banks Island, Northwest Territories; *Canadian Journal of Earth Sciences*, v. 24, no. 6, p. 1077–1085.

Mackay, J.R.

1971: The origin of massive icy beds in permafrost, western arctic coast, Canada; *Canadian Journal of Earth Sciences*, v. 8, no. 4, p. 397–422.

Pollard, W.H.

1991: Observations on massive ground ice on Fosheim Peninsula, Ellesmere Island, Northwest Territories; *in* Current Research, Part E; Geological Survey of Canada, Paper 91-1E, p. 223–231.

Robinson, S.D.

1993: Geophysical and geomorphological investigations of massive ground ice, Fosheim Peninsula, Ellesmere Island, Northwest Territories; M.Sc. thesis, Queen's University, Kingston, Ontario, 171 p.

1994: Geophysical studies of massive ground ice, Fosheim Peninsula, Ellesmere Island, Northwest Territories; *in* Current Research, Part B; Geological Survey of Canada, Paper 94-1B, p. 11–18.

Robinson, S.D. and Pollard, W.H.

1998: Massive ground ice within Eureka Sound bedrock, Ellesmere Island, Canada; *in* Proceedings of the Seventh International Conference on Permafrost, (ed.) A.G. Lewkowicz and M. Allard; Yellowknife, Northwest Territories, p. 949–954.

Taylor, A.E.

1991: Holocene paleoenvironmental reconstruction from deep ground temperatures: a comparison with paleoclimate derived from the $\delta^{18}\text{O}$ record in an ice core from the Agassiz Ice Cap, Canadian Arctic Archipelago; *Journal of Glaciology*, v. 37, no. 126, p. 209–219.

Taylor, A.E., Burgess, M.M., Judge, A.S., and Allen, V.S.

1982: Canadian geothermal data collection — northern wells 1981; Geothermal Series No. 13, Earth Physics Branch, Geothermal Service of Canada, 153 p.

Woo, M.-k., Lewkowicz, A.G., and Rouse, W.R.

1992: Response of the Canadian permafrost environment to climatic change; *Physical Geography*, v. 13, no. 4, p. 287–317.

Hydrological environment of the Hot Weather Creek basin, Ellesmere Island, Nunavut

K.L. Young¹ and M-k. Woo²

Young, K.L. and Woo, M-k., 2000: Hydrological environment of the Hot Weather Creek basin, Ellesmere Island, Nunavut; in Environmental Response to Climate Change in the Canadian High Arctic, (ed.) M. Garneau and B.T. Alt; Geological Survey of Canada, Bulletin 529, p. 347–374.

Abstract: Intensive hydrological studies in the Hot Weather Creek basin (1989–1991) allowed understanding of the hydrological processes in the ‘polar desert oasis’ environment, appreciation of the spatial and temporal variability of the microclimate and hydrology, and deduction of hydrological impacts due to global change.

Site values were aggregated to a basin scale. A small subbasin (Heather Creek) was divided into terrain units and hydrological quantities were aerially weighted. Integrated values of rainfall, snowmelt, sublimation, and evaporation were used, together with streamflow, to compute the basin water balance. Results suggest that this basin has hydrological attributes different from most High Arctic basins. On the basis of field and modelling information, it is surmised that a reduction in snowfall will not satisfy the basin storage capacity so that even increased rainfall will be unable to raise the streamflow. Climatic warming will increase evaporation, leading to more frequent occurrence of very low summer flows.

Résumé : Des études hydrologiques poussées du bassin du ruisseau Hot Weather (de 1989 à 1991) ont permis de mieux comprendre les processus hydrologiques de l’environnement d’un «oasis du désert polaire» et la variabilité spatiale et temporelle du microclimat et de l’hydrologie, et de déduire les effets hydrologiques dûs au changement climatique.

On a combiné les valeurs observées aux sites à l’échelle du bassin. Un petit sous-bassin (ruisseau Heather) a été divisé en unités de terrain et on a pondéré spatialement les quantités hydrologiques. On a utilisé les valeurs intégrées pour les précipitations, l’eau de fonte, la sublimation et l’évaporation ainsi que les valeurs du débit des cours d’eau pour calculer le bilan hydrologique du bassin. Les résultats démontrent que ce bassin présente des paramètres hydrologiques différents de ceux de la plupart des bassins de l’extrême Arctique. En se basant sur les résultats recueillis sur le terrain et de la modélisation, on conclut qu’une réduction des précipitations sous forme de neige ne permettrait pas de satisfaire la capacité d’emménagement du bassin et que même une augmentation des précipitations sous forme de pluie ne pourra augmenter le débit des cours d’eau. Le réchauffement climatique accroîtra l’évaporation ce qui engendrera une augmentation de la fréquence des très faibles écoulements estivaux.

¹ Department of Geography, York University, 4700 Keele Street, North York, Ontario M3J 1P3

² Department of Geography, McMaster University, Hamilton, Ontario L8S 4K1

INTRODUCTION

Northern scientists have expressed a need to better understand the linkages between atmospheric-terrestrial and hydrological processes so that future global changes to the arctic environment can be anticipated. For hydrologists, changes in energy, which is the driving force behind ground thaw, snow and ice melt, and evaporation, could ultimately influence the water storage and runoff regimes (Kane et al., 1992). To ecologists, hydrological changes in soil moisture, modifications of the soil, and nutrient dynamics can alter the present vegetation pattern, causing some plant communities to be eliminated or replaced by more resilient species (Edlund, 1992), leading to eventual changes in the grazing patterns of northern fauna. Permafrost geomorphologists are interested in knowing how climatic variability and change may induce ground thaw and trigger slope instabilities (Lewkowicz, 1992) and alter sediment loading in northern streams (Lewkowicz and Wolfe, 1994; Woo and McCann, 1994). However, progress in these directions will be hampered until the complex present-day linkages among northern terrain, geology, vegetation, water, and energy are better understood.

To date, much emphasis has been placed on how the arctic environment will change under future temperature and precipitation levels, since these are the two outputs from the global climate models that have some degree of certainty. Global climate models suggest that the Canadian arctic islands may experience summer warming of about 4°C and higher precipitation should the atmospheric concentration of carbon dioxide and other greenhouse gases be doubled. These scenarios apply to large areas since the global climate models have very low spatial resolution, often at scales far coarser than the size of most drainage basins in the arctic islands.

Compared with the lower latitudes, hydrological research in the Arctic is quite limited. Field investigations are often carried out at single points, along transects, or in small drainage basins. To provide information useful for global change studies, there exists a need to understand how the hydrological system responds to climatic forcing, permafrost, and vegetation, to depict the spatial variations of the hydrological environment at a local level, and to integrate site information for drainage-basin investigations, as part of an upscaling procedure. This study uses the Hot Weather Creek basin as an example to seek further understanding of the arctic hydrological processes that operate at several spatial scales and to explore the implications of climatic change on the arctic hydrological environment.

STUDY AREA

Hot Weather Creek, a tributary of the Slidre River, is on Fosheim Peninsula, Ellesmere Island. The basin has a drainage area of 127 km² at the stream gauging station (lat. 79°58'N, long. 84°28'W) (Fig. 1). It is underlain mostly by poorly consolidated sandstone, with lesser amounts of siltstone, conglomerate, shale, and coal of the Upper Cretaceous to Lower Tertiary Eureka Sound Formation

(Thorsteinsson, 1969). The basin likely has not been glaciated since the late Wisconsinan (Lewkowicz and Wolfe, 1994). The catchment lies within the early Holocene marine limit so that areas below 140 to 145 m have a discontinuous cover of weathered marine, estuarine, and deltaic deposits composed of medium- to fine-grained sand, silt and minor clayey silt, sandstone granules, coal fragments, detrital plant material, and molluscs (Hodgson et al., 1991). Permafrost is continuous, with active-layer depths ranging from 0.4 to 1.0 m, depending on the surface material (Young et al., 1997).

The basin is in a region that is generally warmer in the summer than other locations in the Queen Elizabeth Islands due to the surrounding mountains of Ellesmere and Axel Heiberg islands, which tend to dispel slowly moving cyclones from the Arctic Ocean and from Baffin Bay (Edlund and Alt, 1989). The lowlands of Fosheim Peninsula are part of a polar oasis favourable to the growth of tundra vegetation (Svoboda and Freedman, 1994). The inland location of Hot Weather Creek probably causes it to be even warmer than the coastal station at Eureka, only 25 km to the west.

Heather Creek (unofficial name) and a small area near the Geological Survey of Canada base camp were the principal study sites. Heather Creek is a tributary of Hot Weather Creek and has a basin area of 6.1 km², most of which is rolling topography. The creek has a beaded morphology (where narrow reaches link small pools), but generally occupies a single channel 1 to 2 m wide cut into a vegetated valley bottom. The base camp (elevation about 84 m a.s.l.) is about 0.5 km south of the mouth of Heather Creek and within about 1 km² of the intensively studied experimental sites that included a plateau location and four slopes of different aspects (east, southeast, west, and northwest). Vegetation in the study area has been described by Edlund et al. (1990). Complete cover usually occurs around thaw ponds, in fens, and in many valley bottoms and consists of grasses, sedges, cottongrass, and mosses. Plateaus tend to have higher vegetative covers (31–50 per cent) dominated by *Salix arctica* and *Dryas integrifolia* communities. Plant cover is variable on slopes, ranging from bare or under 10 per cent on sandy slopes to higher coverage below late-lying snowbeds, in soil cracks and depressions where water collects, and on the lower slopes where moisture levels tend to be high. The dominant plant cover is a *Salix arctica*–*Dryas integrifolia* complex (Woo et al., 1990).

METHODS

At the base camp, twice-daily observations of air temperature, wind speed and direction, cloud type and amount, and precipitation were reported according to the format specified by the Polar Continental Shelf Project for summer field camps (Edlund and Alt, 1989). At the experimental sites, climatological (net radiation, air and ground temperatures, wind speed, and rainfall), hydrological (soil moisture, groundwater, and slope runoff), and ground-frost data were obtained. A detailed description of the instrumentation is given in Young et al. (1997). Snow surveys were carried out at the end of winter at all the sites following the method described by Woo

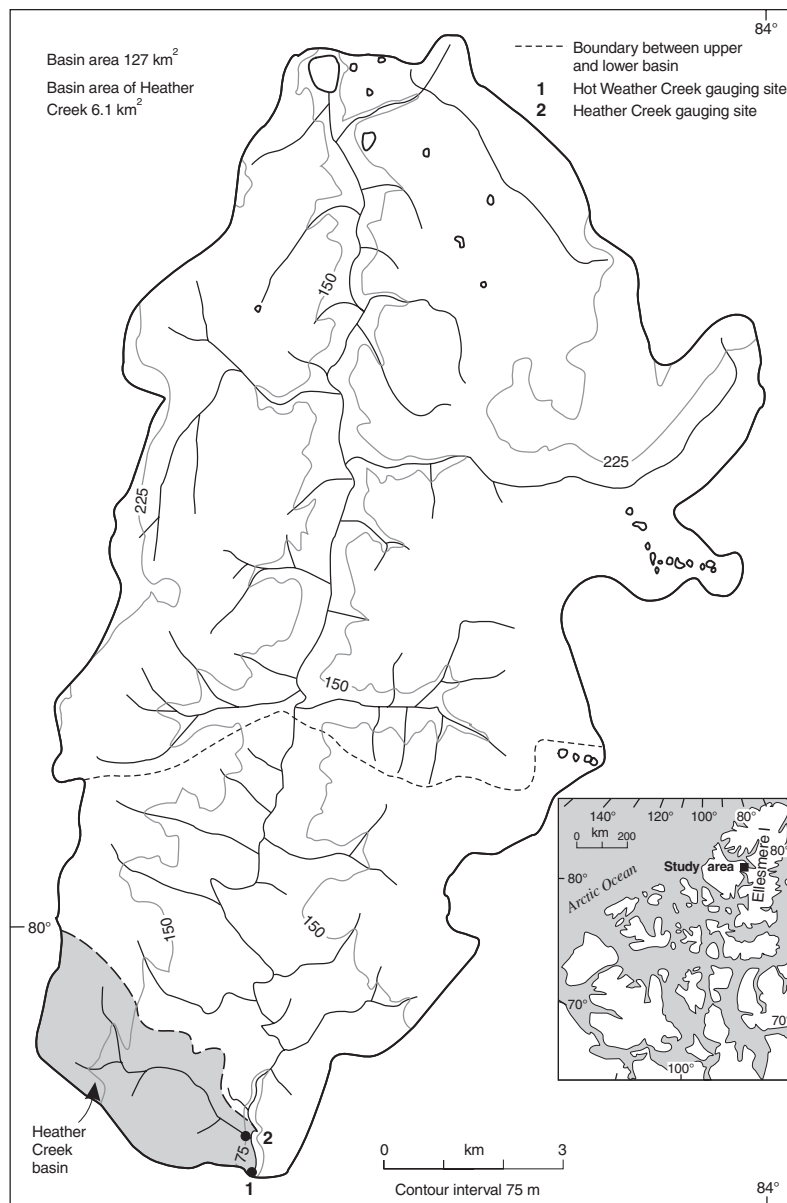


Figure 1. Hot Weather Creek and Heather Creek basins, Ellesmere Island, Nunavut.

and Marsh (1978). Daily snow ablation was determined by measuring the rate of snow-surface lowering at each experimental site. The rates of lowering were converted into water equivalent unit using measured snow-surface densities.

The stages of Hot Weather Creek and Heather Creek were recorded using Leupold-Stevens Type F water-level recorders mounted on stilling wells. The stage records were converted to discharge using rating curves empirically derived from discharge measurements (Lewkowicz and Wolfe, 1994). The levels of a small lake, several tundra ponds, and some pools in the stream channels were measured at irregular intervals in 1991.

HYDROLOGICAL PROCESSES

Snow accumulation and melt

Situated in the polar desert environment, the study area has low annual precipitation, mostly as snowfall. The long-term snowfall record at the Eureka weather station shows that the annual snowfall averages 41 mm; however, arctic snowfall is often underestimated by precipitation gauges (Goodison, 1978), particularly under conditions of blowing snow. An extensive survey of snow on the ground at the end of the winter may provide a more representative value of the total winter snowfall averaged over an area. For the winters of 1980–1981 and 1981–1982, Woo et al. (1980) found that the snow

accumulation around Eureka was two to three times greater than the snowfall at the station. Even so, the amount was lower than elsewhere in the Arctic Archipelago (Maxwell, 1980).

Snow is subject to redistribution during the long polar winter. The distribution of snow on the ground is controlled by an interaction of wind direction and topography. Thus, the snow-cover pattern varies according to the type of terrain. For Fosheim Peninsula, Woo et al. (1995) reported that the largest amount of snow accumulates in gullies, then in narrow valleys. Exposed areas such as plateaus, rolling uplands, bottomlands, lakes, and extensive valley flats have less snow. Snow on slopes is highly variable, depending on the slope aspect, steepness, and amount of concavities. At the Hot Weather Creek study sites, snow surveys carried out between 1989 and 1991 showed that the northwest-facing slope always had the greatest amount of snow because of drifting and that the west-facing slope had the least snow partly because of loss by sublimation prior to the survey (Table 1). The amount of snow received differed from winter to winter, with 1989–1990 having about three times more snow than 1990–1991.

The pattern of snow on the ground immediately prior to melting is of notable hydrological significance because it determines how much and where meltwater is available.

Snowmelt

The snowmelt season arrives late in the Arctic, about mid-May in the Fosheim Peninsula area. Table 1 lists the dates when melt began at the Hot Weather Creek base camp and the dates by which over 90 per cent of the snow has disappeared. Most years, the melt season lasts no more than three weeks.

At the beginning of the melt season, melt rates tend to be low. Later, daily snowmelt rates of 5 to 20 mm are typical. Towards the end of the melt season, melting can proceed at a

rate exceeding 50 mm/d. The energy available for snowmelt (Q_m) is contributed by net radiation (Q^*), sensible heat (Q_h) and latent heat (Q_e) fluxes, and rain-on-snow energy (Q_r).

$$Q_m = Q^* + Q_h + Q_e + Q_r \quad (1)$$

The absence of large rainfall events during the melt period renders the last term insignificant. For the melt seasons of 1989–1991, net radiation was an important source of energy for snowmelt, partly because of the large number of sunny days during the melt period. Latent heat flux, responsible for snow sublimation, was notable in the Hot Weather Creek area. Converted into water equivalent unit, sublimation loss during the melt season was 11 mm in 1989, 10 mm in 1990, and 5 mm in 1991. Sensible heat flux became more important towards the end of the melt season when some bare ground was exposed, causing sensible heat to be advected from the warmer bare soil to the snow patches.

There are areas in the Hot Weather Creek basin where the snow is covered by dust. The presence of dust greatly reduces the snow albedo and increases net radiation melt. While the snow temperature cannot rise above 0°C, the dust temperature can be much higher and this can be an additional source of heat for snowmelt and sublimation. An experiment was carried out in 1991 by adding a thin layer of dust to the snow, at a time when the air temperature was below 0°C. Snow ablation began a few hours after dusting on May 13 and the temperature at the base of the snow rose by 6°C three days after dusting, suggesting the percolation of meltwater to reach the snow–ground interface (Woo et al., 1992). By May 17, ablation at the dusted plot was 10 mm/d, whereas melting had not yet begun at the clean snow sites. The treated plot became snow-free five days earlier than the untreated plots with a similar amount of snow. This experimental result explains the occurrence of early melt zones on Fosheim Peninsula and in its vicinity, at a scale that makes it visible from satellites (Woo et al., 1991). These were areas where the snow was covered by eolian dust, which advanced the melt season and accelerated the melt rate at a regional scale.

Table 1. Precipitation characteristics at the Hot Weather Creek base camp and experimental sites.

	Experimental sites					Base camp	
	Plateau	NW	E	SE	W		
Snow water equivalent (mm)						First day ¹ of melt	Last day of melt
1989	89	181	112	51	23	147	158
1990	118	249	72	63	62	135 ²	160
1991	43	5	63	36	30	145	157
Rainfall (mm)						Number of rain days	Total rain (mm)
1989 ³	91	168	94	130	66	47	86
1990 ⁴	11	14	11	12	10	21	9
1991						46	71

¹ Dates of melt are given in Julian days
² Continuous basin-wide melt did not occur until May 29, 1989.
³ Rainfall values for experimental sites are for the period July 1 to August 22, 1989; those for the base camp are total of the entire field season.
⁴ Rainfall for experimental sites are for May 19 to August 12, 1989.

Rainfall

The amount of summer rainfall can vary greatly from year to year. For example, there were 47 rain days in 1989, 21 in 1990, and 46 in 1991. The total rainfall recorded at the base camp was 86 mm in 1989 and only 9 mm in 1990, but reached 71 mm in 1991 (Table 1).

As suggested by the 1989–1991 base-camp data, 40 per cent of the rainfall was trace events (<0.03 mm) and the median was 0.3 mm/d (Fig. 2). Rainfall of over 4.5 mm/d had an exceedance probability of 0.1, whereas rainfall greater than 10 mm/d was uncommon (exceedance probability = 0.02). Rainfall can vary noticeably within a small area, as illustrated by the data collected at the experimental sites near the base camp for the period July 1 to August 22, 1989 (Table 1). Spatial variability was less for the drier summer of 1990 when only 9 mm (cf. 95 mm in 1989) of total rainfall was recorded at the base camp. Spatial variations in rainfall are attributed to elevation and aspect of the land in relation to exposure to the rain-bearing wind (Woo et al., 1990).

Evaporation

The Penman-Monteith combination model is appropriate for calculating evaporation at the study site:

$$Q_e = [S(Q^* - Q_g) + \rho_a C_p (e_z - e_d) / r_a] / [S + \gamma(1 + r_s / r_a)] \quad (2)$$

Here, S is the slope of the saturation vapour pressure versus temperature curve at temperature T (Dilley, 1968), Q_g is the ground heat flux, ρ_a is the air density, C_p is the specific heat of air, e_z is the saturation vapour pressure at T , e_d is the saturation vapour pressure at the dew point temperature, here assumed to be the minimum of the twice-daily minimum temperature readings taken at the base camp (Jury and Tanner, 1975), γ is the psychrometric constant, and r_a and r_s are the aerodynamic and surface resistances. The ground heat flux Q_g is determined as the residual in the surface energy balance during the post-snowmelt period and is used in the force-restore scheme (Deardorff, 1978) to derive the surface temperature T_s for the snow-free season.

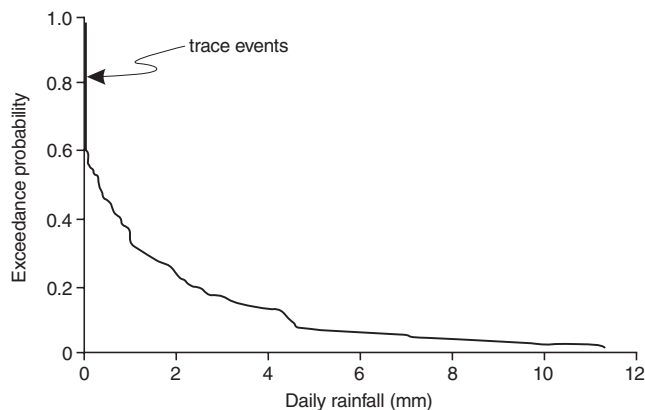


Figure 2. Exceedance probability distribution of rainfall at base camp, based on data from 1989–1991.

Figure 3a shows the seasonal daily evaporation rates for the plateau site, which is covered by tundra vegetation. High evaporation rates in May are due to sublimation losses and some condensation occurs towards the end of the melt season. The post-snowmelt rates fluctuated between zero (some days had condensation instead of evaporation) and 5 mm/d, with a general decrease after July. The very high evaporation rates were exceptional and had a low probability of occurrence. Figure 3b presents the probability distributions of daily post-snowmelt evaporation for the summers of 1989–1991. The warmer and drier summer of 1990 contributed few evaporation events of large magnitude, but the probability of occurrence of moderate evaporation rates (0.5 to 2 mm/d) was higher in the wetter summers of 1989 and 1991. The mean evaporation rates were 1.14, 0.49, and 1.23 mm/d in 1989, 1990, and 1991 respectively.

Storage change

In the course of a year, changes occur both in the amount and form of water that is being stored. Except under deep lakes, water is stored in winter as snow and ice (both ground ice and ice in ponds or on lakes). During cold summers, some residual snow may remain in shaded areas whereas in exceptionally warm summers, ground thaw may deepen the active layer to release some ground ice that is held in long-term storage (e.g. in 1988, deepening of the active layer, accompanied by melting of ground ice in permafrost, led to many slope failures, as reported by Lewkowicz, 1990).

In most years, snow accumulation constitutes the major increase in storage. This storage is released rapidly during the melt period. During this time, most of the ground remains frozen with little capacity to retain meltwater, most of which runs off. For example, in 1989, surface flow produced by snowmelt occurred between May 31 and June 7 on the north-western slope and between June 4 and 14 on the eastern slope, where snowmelt was delayed. In 1990, surface runoff was observed between May 16 and June 9 on the northwestern slope and from May 30 to June 14 on the eastern slope. As ground thaw continues, the capacity of the active layer to hold moisture increases. This storage capacity is highly variable spatially as the thaw is strongly influenced by vegetation, soil, and local heat input (Young et al., 1997). Within the thawed zone, water is retained as superpermafrost groundwater or as soil moisture in the unsaturated layer. Storage increases during rain events and decreases as water is lost to evaporation and lateral flow. Storage fluctuations are indicated by the position of the water table and by the changing soil-moisture status. Seasonal fluctuations and spatial variations at the experimental sites are reported by Young et al. (1997).

Storage fluctuations are also indicated by lake and pond levels. During the snow-free season of 1991, the levels of Picnic Lake (unofficial name), two pools along Hot Weather Creek near the base camp, a pool on Heather Creek, and two tundra ponds on the plateau were monitored (Fig. 4). All water levels showed a gradual decline as storage was depleted after snowmelt. Rainfall events in early August helped to replenish the storage, causing the water levels to rise. The

lake, with a larger storage capacity, was able to dampen its water-level fluctuations more than the pools and ponds. At the other extreme, the small ponds on the plateau have little lateral inflow to support their losses to evaporation and they dried out in midsummer until rainfall recharged their storage.

Channel storage can be significant. After a long period of drought during which flow ceases, the channels have to be filled to a certain level before flow recurs. Lewkowitz and Wolfe (1994) noted that the runoff response to an August 1991 rain event occurred 20 hours earlier at the smaller

Heather Creek than at Hot Weather Creek. They suggested that such a difference in timing was due to the larger channel storage capacity of Hot Weather Creek, which had to be replenished before flow could begin.

Basin storage buffers water input against immediate losses. The larger the storage capacity and the lower the antecedent storage level prior to recharge, the more water input can be absorbed before water is released. This increases the lag time between basin input and output.

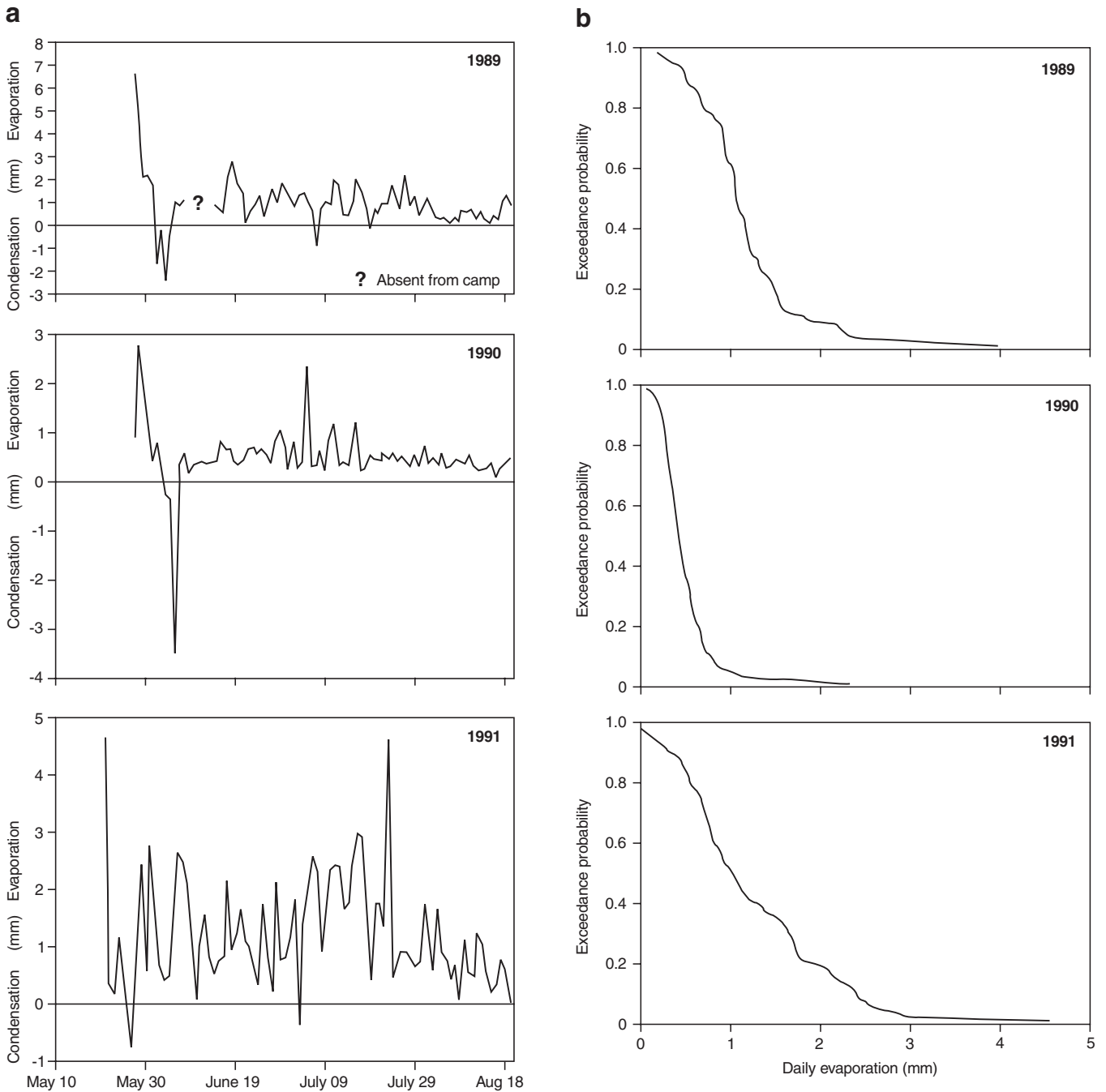


Figure 3. a) Daily evaporation and **b)** exceedance probability of daily evaporation at the plateau site, 1989, 1990, and 1991.

Streamflow

Like all rivers on Fosheim Peninsula, Hot Weather Creek and Heather Creek do not have winter flow. Their flow season lasts about three months. The initiation of flow lags behind snowmelt by several days, requiring time for the channel snowpack to saturate and for slope runoff to collect in the channels. Flow begins slowly as much meltwater is withheld within the snow or is impounded behind snowdrifts. Discharge increases as an integrated drainage network is established along the snow-filled channels. Diurnal cycles are prominent in the hydrographs, as is evident in the 1990 records from Hot Weather Creek and Heather Creek (Fig. 5a). Daily peak flows lagged behind the time of maximum daily snowmelt and the larger Hot Weather Creek showed a longer delay than the smaller Heather Creek. Daily peaks increased during a spell of substantial melt, but decreased when the melt rate dropped or when the basin snow cover was depleted towards the end of the melt season.

Streamflow did not respond readily to low rainfall events, particularly after a prolonged period of dryness when basin storage had to be replenished before flow could increase. For those rain events that could raise the streamflow, however, the hydrograph rose sharply, as is exemplified by the events of mid-August 1989 (Fig. 5b). The recession to low flow was also rapid.

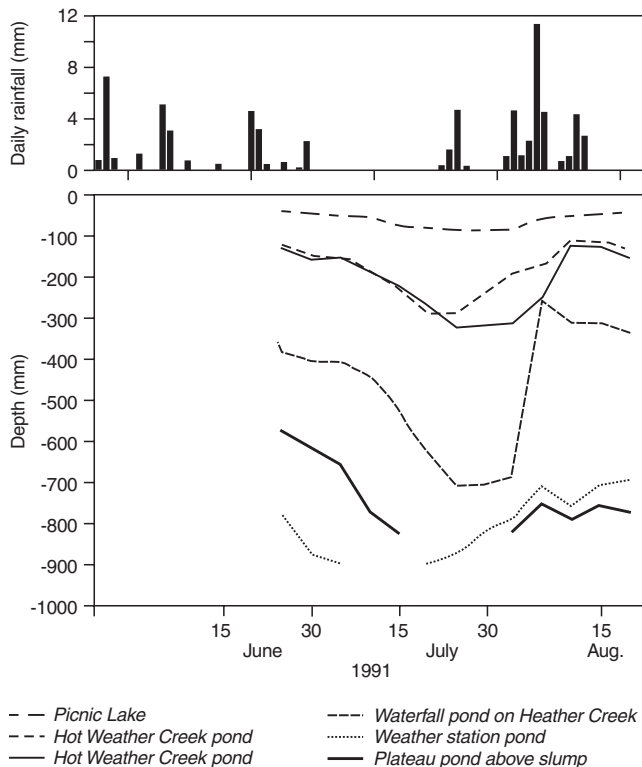


Figure 4. Daily rainfall and fluctuation of water levels in a lake, in pools along stream beds, and in tundra ponds, summer of 1991.

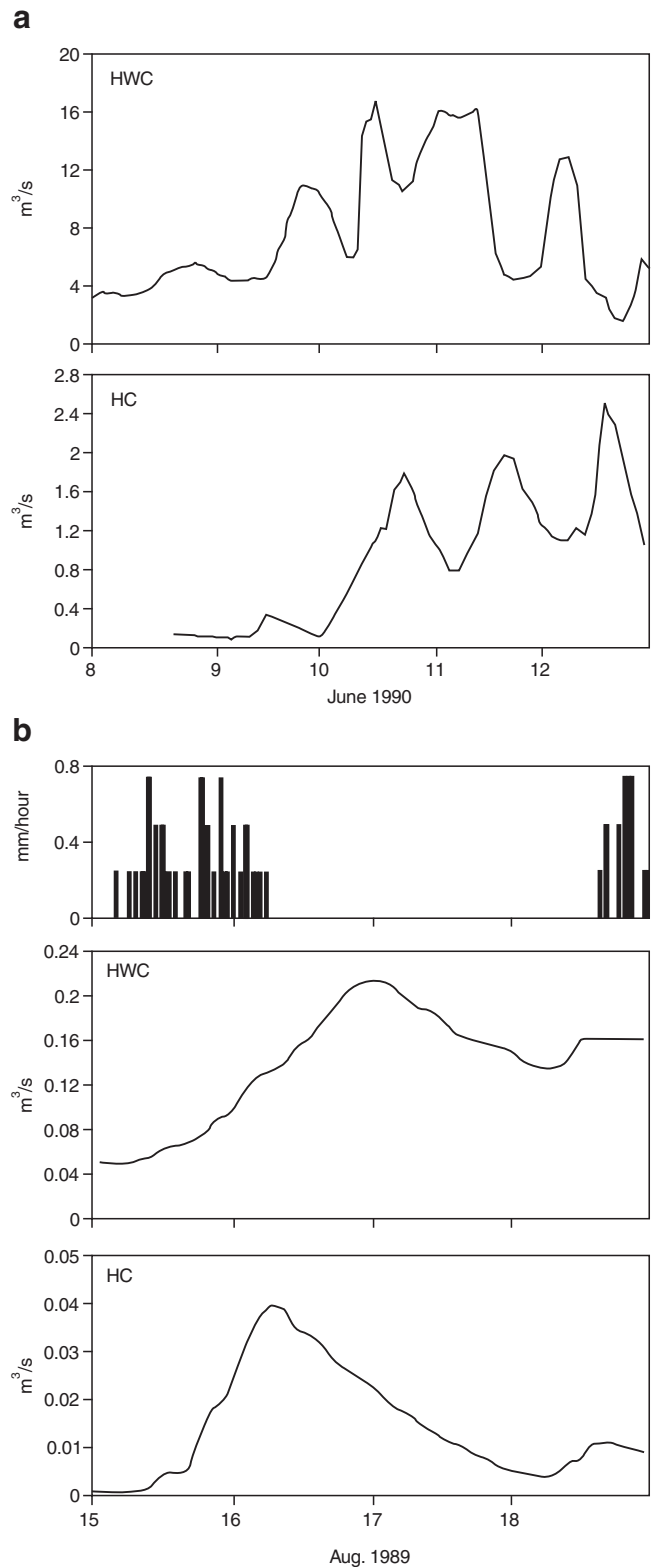


Figure 5. Response of Hot Weather Creek (HWC) and Heather Creek (HC) streamflow to a) snowmelt in 1990 and b) rainfall in 1989.

Summer has many periods of low flow. In 1990, Heather Creek did not have streamflow after the melt period whereas Hot Weather Creek had some low-flow mixed with zero-flow days. The abundance of zero flows and the prevalence of low flows in all years indicate the low level of water storage in the basins during nonrainy periods.

BASIN WATER BALANCE

Water balance components

The water budget of a basin is

$$M + R - E - Q = \Delta s \quad (3)$$

where M is snow and ice melt, R is rainfall, E is evaporation loss, Q is basin outflow, and Δs is storage change in the basin. Values of M, R, and E are obtained at specific sites. Upscaling of site information is needed to obtain aggregated values at the basin level.

The Heather Creek water balance was performed daily for 1989–1991. The basin was divided according to terrain types (Fig. 6) and the area occupied by each terrain unit was measured on a topographic map. Several attributes, including elevation, slope angle and direction, snow albedo, and ground-surface albedo for each terrain unit are given in Table 2.

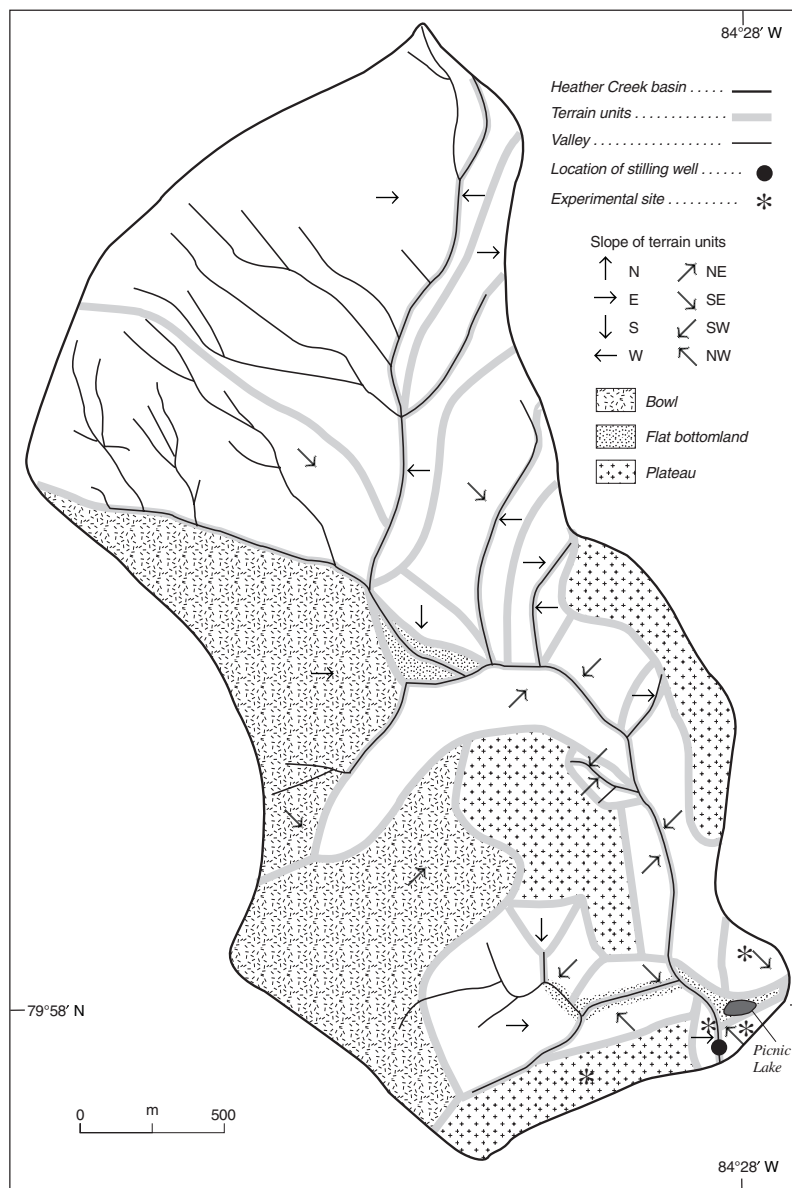


Figure 6. Terrain units in Heather Creek basin.

The computation of basin snowmelt follows the method described by Woo et al. (1983), which determines mean basin snowmelt, $M(t)$, on day t using the aerially weighted melt rate, $m_i(t)$, for various terrain units i in the catchment, as follows:

$$M(t) = \sum_{i=1}^k m_i(t) a_i / \sum_{j=1}^n a_j, k \leq n \quad (4)$$

where a_i is the area of terrain unit i , n is the total number of terrain units in the basin, with k units remaining snow covered on day t . The snow remaining in a terrain unit is updated daily by subtracting daily melt from the residual snow storage. The values of m , expressed in water equivalent unit, can be obtained from equation 1 by the following

$$m = Q_m / (\rho_w \lambda) \quad (5)$$

where ρ_w is the density of water and λ is the latent heat of fusion.

Table 2. Terrain and surface parameters used to calculate snowmelt and evaporation at Heather Creek (lat. 79°58'N, long. 84°28'W).

Unit	Slope angle (°)	Slope aspect (°)	Elevation (m a.s.l.)	Snow albedo	Ground-surface albedo 1989–1990	Area (m ²)
NE	1.1	45	130	0.8	0.10/0.15	229 203
NE	11.3	"	105	"	"	10 418
NE	"	"	100	"	"	38 201
NE*	1.0	"	115	"	"	916 814
E	3.4	90	180	"	"	1 023 497
E	2.3	"	155	"	"	76 401
E*	1.6	"	165	"	"	652 883
E	1.9	"	125	"	"	69 456
E	7.6	"	110	"	"	13 891
E	4.2/11.3 ¹	"	99	"	"	20 837
E	2.3	"	110	"	"	17 416
SE	2.3	135	170	0.8	0.13/0.16	551 477
SE	1.1	"	135	"	"	159 748
SE	11.3	"	95	"	"	31 255
SE	6.8	"	96	"	"	39 937
SE*	2.9	"	140	"	"	48 619
S	3.8	180	140	"	"	55 564
S	3.8	"	105	"	"	27 782
SW	5.7	225	110	0.8	0.10/0.16	69 456
SW	9.9	"	110	"	"	138 911
SW	11.3	"	105	"	"	6946
SW	5.7	"	108	"	"	34 728
W	2.3	270	175	"	"	69 456
W	11.3	"	145	"	"	83 347
W	1.9	"	125	"	"	83 347
W	5.7	"	130	"	"	20 837
NW	11.5	315	95	0.7	0.11/0.18	20 837
NW	11.5	"	"	"	"	48 619
P	0	0	100	0.8	0.13/0.16	213 550
P	"	"	115	"	"	368 115
P	"	"	118	"	"	236 149
BL	1.3/7	135	125	0.8	0.12 ²	34 728
BL	1.4/7	45	85	"	"	20 837
BL	1.3/7	90	85	"	"	20 837
V	1.8/4	315	180	0.7	0.15	58 667
V	1.8/7	135	180	0.8	"	"
V	"	90	110	"	"	"
V	1.8/4	270	110	"	"	"
V	"	315	95	0.7	"	"
V	1.8/7	135	95	0.8	"	"

¹ Shading occurs when sun elevation falls below a larger slope angle

² Value from Petzold and Rencz (1975)

* Within a bowl-shaped terrain

" Indicates same value as above

P = plateau; BL = bottomland; V = valley;

Various slopes identified by their cardinal directions (NE, E, SE, S, SW, W, NW)

Rainfall was measured twice daily at the base camp and daily at the experimental sites, which were clustered close to the southern boundary of the Heather Creek basin. The sites encompassed different terrain types and the rainfall measured at the base camp could be adjusted to other terrain units using ratios. Ratios were obtained between the base camp and the experimental sites (four slopes, plateau, and bottomland) using the July precipitation totals for 1989 and 1990 (Table 3). These ratios enabled an extension of daily rainfall measured at the base camp to various terrain segments in the basin. Although deviations from these ratios are expected for individual storms, the method still allows an adjustment for the spatial variations of rainfall due to topographic influences. The 'corrected' daily rainfall at various terrain units was weighted aerially to obtain the basin average.

Evaporation from different terrain units was calculated using the surface albedo and topographic parameters listed in Table 2. During the snowmelt period, only snow-free units contributed to evaporation whereas snowmelt continued at the snow-covered units. Daily evaporation computed for each unit was aerially weighted to determine the basin average.

Water balance of the Heather Creek basin

Water balance was performed for a wet summer (1989), a dry summer (1990), and a low-snow year (1991). The 1989 snowmelt period was missing because the stream gauge was not installed until the snow had melted. Otherwise, daily values of M, R, E, and Q were determined for the basin, with Δs obtained as the residual of equation 3. Figure 7 is a cumulative plot of these water-balance components.

For the years with large snow accumulation (1989 and 1990), snowmelt represented a rapid increase in liquid water storage, first within the snowpack and then in depression and detention storages as well as in the soil. In 1991, snowmelt did not significantly recharge the basin liquid water storage because of the small amount of snow available for melt (of the 50 mm of snow accumulated in the winter, 5 mm were lost to sublimation). Snowmelt runoff thus generated was small (8 mm) compared with 1990, which had 79 mm of snowmelt runoff. Although streamflow was not measured during the 1989 melt period, the flow was of a magnitude comparable to that of 1990 because both winters had much snow.

Table 3. Snow water equivalent (1990) and rainfall ratio for experimental sites, Heather Creek basin.

Terrain type	Total area (m ²)	% of basin area	Aerially weighted snow water equivalent 1990 (mm)	Rainfall ratio ¹	
				1989	1990
NE	1 194 636	19.6	22	1.3	1.7
E	2 028 381	36.5	38	1.3	1.7
SE	831 036	10.9	12	1.5	2.3
S	83 347	1.1	1	1.5	2.3
SW	250 040	3.5	4	0.8	2.4
W	298 659	4.1	5	0.8	2.4
NW	69 456	2.1	2	2.4	2.6
P	916 814	14.1	16	1.1	1.4
BL	76 401	0.9	1	1.1	1.1
V	352 001	7.2	8	1.1	1.1
Basin	6 100 771	100.0	108		

¹ Ratios are based on July rainfall at experimental sites divided by July rainfall at base camp.

Summer runoff was negligible in 1990 because of the season's very low (12 mm) rainfall. In contrast, rainfall-generated runoff was notable in the wetter summer of 1989 (103 mm of rain). Rainfall in 1991 (89 mm) was similar to that in 1989, but runoff was disproportionately low. Low runoff may be attributed to the depressed storage status of the basin.

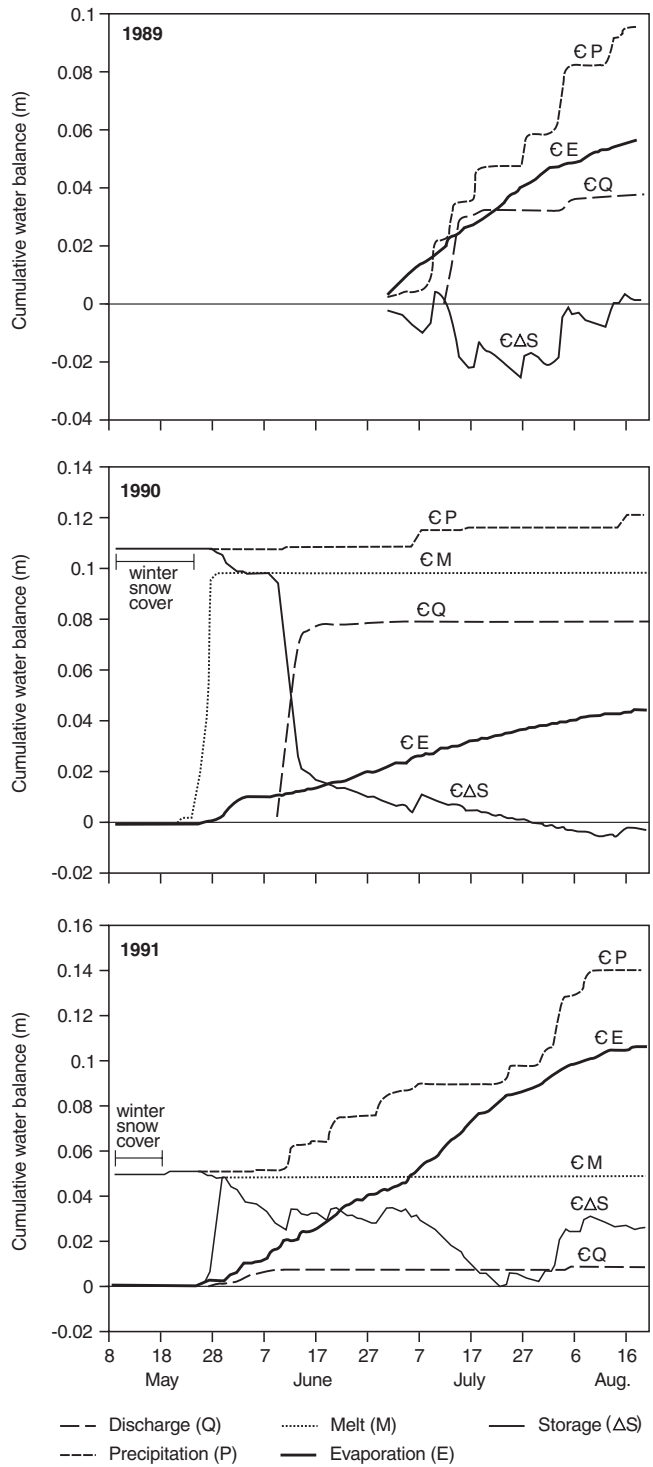


Figure 7. Cumulative plot of water-balance components for Heather Creek, 1989, 1990, and 1991.

Table 4. Water balance for Heather Creek (mm).

Year	Snow accumulation	Rainfall	Snowmelt	Sublimation	Evaporation	Streamflow
1989 (May 18– August 20)	88	103	77	11	87	38 ¹
1990 (May 21– August 20)	108	12	98	10	34	79
1991 (May 19– August 22)	50	89	45	5	101	8
¹ Calculated for the post-melt period of June 28–August 20 only.						

Since most of the meagre snowmelt was removed as streamflow, not much water was available in the spring to recharge the basin storage. Continuous depletion by evaporation gave rise to an increasingly unsatisfied storage capacity created by a thickening thawed zone. Many of the rain events failed to raise streamflow and those that did produce runoff yielded peak flows of under 0.03 m³/s.

Table 4 summarizes the various water-balance components for the Heather Creek basin. These values may be compared with other water-balance results from the Arctic Archipelago. Large year-to-year differences in snow accumulation and rainfall amounts reflect the highly variable polar desert climate. Sublimation was more important than at locations such as McMaster basin on Cornwallis Island (Woo et al., 1983), but was similar to the magnitude reported for the wetlands of Truelove Lowland on Devon Island (c, 1977). Summer evaporation was not as large as in the wetland environment of Truelove Lowland, but in 1991, it was double the average evaporation of McMaster basin. The runoff ratio (streamflow divided by precipitation) was 0.6 in 1990 and under 0.1 in 1991. These ratios were much lower than for the F2-watershed (0.7) on Baffin Island (Church, 1974) and for McMaster basin (0.8). However, they were closer to those of the Innvait basin (average 0.45) in the Alaskan Low Arctic (Kane et al., 1992). Indeed, the high percentage of vegetation cover at Heather Creek is quite distinct from the barren surfaces more frequently encountered in the High Arctic. The presence of much vegetation may have enhanced evapotranspiration and retarded runoff.

IMPLICATIONS OF GLOBAL CHANGE

Three years of intensive study provided the information and understanding that allow the hydrological implications of global change to be deduced. One approach is to use temporal variability as an analogue to furnish scenarios of hydrological responses to possible climatic changes. Caution must be exercised in this approach because it assumes 1) that no new climatic and hydrological processes, such as thunderstorms or the proliferation of pipeflows, are likely to occur, 2) that overall environmental conditions do not change drastically in the

future, for example, the loss of permafrost or the growth of trees, and 3) that the present-day variations in hydrological conditions are not sustained over long periods, although a change in climate will necessarily imply that the new conditions are long-lasting. Nevertheless, the variability witnessed in the 1989–1991 seasons covered a broad range of hydrological and climatic conditions that offer insight into the possible responses to climatic change.

Changes in the amount of snowfall will significantly affect the spring runoff and the summer water storage status of the drainage basins. For nival-regime rivers (Church, 1974) such as Hot Weather Creek and Heather Creek, the spring freshet produces the major flow events of the year. These floods will diminish if the yield from snowmelt decreases. If the snow becomes dusty, sublimation will increase and melt will begin earlier. The magnitude and timing of snowmelt runoff will be affected accordingly.

High pressure often prevails during the snowmelt period, but this may change. Should there be more rainfall events during melt, more water will become available for runoff to reinforce the freshet. An increase in summer rainfall may augment streamflow, but this depends on the storage status of the basin. When basin storage has been enriched by snowmelt, summer rain is effective in generating high runoff. Otherwise, as is illustrated by the conditions of 1991, so much of the rainfall is spent satisfying the storage capacity that little goes to streamflow. Climatic warming will likely lead to thickening of the active layer (Kane et al., 1991), increasing the liquid water storage capacity of the soil. The basin will be able to retain more rainfall input before it yields water to runoff, thereby reducing the summer streamflow.

Climatic warming may increase evaporation. A modeling approach was used to examine the sensitivity of evaporation and snowmelt to changing atmospheric and terrestrial conditions. In utilizing the sensitivity analysis, it is important to note that 1) rarely do closely related variables such as temperature, albedo, etc. change independently and 2) reasonable levels of change are needed to reflect the possible range of environmental change. The atmospheric and terrestrial conditions for 1990 were used as an example for our simulation and an arbitrarily selected 10 per cent change was applied to atmospheric aerosol content, cloud amount, temperature,

Table 5. Sensitivity of Heather Creek basin evaporation (mm) to 10 per cent changes in atmospheric and terrestrial conditions. Comparisons are made against the 1990 seasonal total (represented by values in the zero change column).

	Evaporation resulting from the following percentage changes of various factors		
	+10%	0	-10%
ATMOSPHERIC			
aerosol factor	38	34	26
temperature	37	34	31
low cloud amount	51	34	35
TERRESTRIAL			
slope albedo	33	34	34
surface resistance	32	34	37

albedo, and surface resistance to compute the possible effects on evaporation in the Heather Creek basin (Table 5). The simulation model used is presented in Young and Woo (1997).

Evaporation increases slightly when the aerosol factor is raised by 10 per cent to a maximum value of 1.0, which represents clear conditions. Higher incoming solar radiation allows more water to be evaporated. Reducing the aerosol factor by 10 per cent (reaching a level comparable to that of a large city such as Toronto, e.g. Davies et al., 1975) dampens evaporation as incoming solar radiation to the basin is impeded. A one-tenth increase in low cloud amounts over the 1990 levels increases evaporation rates higher than those produced by higher temperatures. This occurs because of the model logic, which allows the dry surface resistance (650 s/m) (*see* equation 2) to fall to 0 s/m (Young and Woo, 1997). In contrast, a one-tenth decrease in cloud amounts does not alter the rate of evaporation for the 1990 data. This suggests that a small decrease in low clouds does not modify the surface resistance, thus nullifying the effect of slight increases in solar radiation. Raising and lowering the air temperatures by 10 per cent increases and decreases evaporation by only 3 mm over 1990 conditions. In 1989 (wet summer and $r_s = 100$ s/m), similar increases and decreases in temperature altered evaporation amounts by 7 mm. This serves to indicate that perhaps large-surface resistance characteristics or fluctuations can serve to augment or nullify temperature changes. Changing surface albedo by 10 per cent does not significantly change evaporation and small changes in surface resistance do not significantly affect the evaporation rate. This limited sensitivity study reveals that the atmospheric constituents (e.g. aerosol factor, clouds) deserve much attention regarding their present and future influence on the northern hydrological environment.

DISCUSSION AND CONCLUSIONS

Results from three years of intensive field study in the Hot Weather Creek basin demonstrated the large spatial and temporal variability of the basin's hydrological variables. The two primary sources of water, snow accumulation and rainfall, vary according to the terrain. Snowmelt rate is also influenced by topography, which affects the energy available for melt. Similarly, evaporative energy varies with the terrain and also with the vegetation cover. This study shows the feasibility of upscaling point values to the drainage-basin level by aerially weighting the hydrological quantities for various facets of the terrain. The aggregation of values from point to slope and to small basins adheres to the recommendations of Church and Woo (1990) and Running et al. (1987) that to provide reliable scenarios of global change impacts, the spatial variability on a local scale should be considered.

Although the hydrological processes operating in the Hot Weather Creek basin are common to other areas of continuous permafrost (Woo, 1986), the magnitude and timing of hydrological events are much influenced by the 'polar oasis environment' of Fosheim Peninsula (Woo and Young, 1997). Sheltered by mountains from many storms, this region has lower snowfall and rainfall, large solar radiation input, and warmer summers than most other locations in the Arctic Archipelago. Compared with other High Arctic areas, the area's hydrological consequences include a reduction in water input, earlier snowmelt, higher evaporation, and lower streamflow. The milder climate relative to other polar desert areas favours the growth of vegetation, which enhances losses by evapotranspiration.

Three field seasons with different hydrological characteristics provide temporal analogues to create scenarios of hydrological responses to climatic change. In a low-precipitation area such as the Fosheim Peninsula, a decrease in snowfall will seriously reduce spring runoff. Little water will be available to add to the basin storage. Rainfall-generated runoff depends strongly on the amount of rain and the antecedent water storage in the basin. Under climatic warming, the storage capacity will increase because of the deeper and faster thawing active layer. More water is needed to satisfy the storage capacity before runoff begins. At present, streams may cease to flow during drier summers. Summer flow is apt to be much curtailed under a warmer climate as higher evaporation rates further decrease the amount of water available for streamflow. A sensitivity analysis of evaporation responses to selected atmospheric and terrestrial impacts indicates that small changes in atmospheric constituents may have a greater effect than slight modifications of the terrestrial environment.

ACKNOWLEDGMENTS

This work was funded by a research agreement with Natural Resources Canada, a grant from the Natural Sciences and Engineering Research Council, and a northern training grant from the Department of Indian Affairs and Northern Development. The logistical support of the Polar Continental Shelf Project and Dr. Sylvia Edlund is gratefully acknowledged. We thank Dr. Antoni Lewkowicz for providing some streamflow data and Mr. Angus Headley for the loan of meteorological instruments. We also thank Dr. Bea Alt, Sharon Reedyk, Tim Siferd, Kelly Thompson, and the late Paul Wolfe for their assistance in the field.

REFERENCES

- Church, M.**
1974: Hydrology and permafrost with reference to northern North America; Proceedings, Workshop Seminar on Permafrost Hydrology; Centre for National Communication, International Hydrological Decade, Environment Canada, Ottawa, Ontario, p. 7–20.
- Church, M. and Woo, M-k.**
1990: Geography of surface runoff: some lessons in research; *in* Process Studies in Hillslope Hydrology, (ed.) M.G. Anderson and T.p. Burt; Wiley, New York, p. 299–325.
- Davies, J.A., Schertzer, W., and Nunez, M.**
1975: Estimating global solar radiation; *Boundary-Layer Meteorology*, v. 9, p. 33–52.
- Deardoff, J.W.**
1978: Efficient prediction of ground surface temperature and moisture, with inclusion of a layer of vegetation; *Journal of Geophysics Research*, v. 84, p. 1889–1903.
- Dilley, A.C.**
1968: On the computer calculation of vapour pressure and specific humidity gradients; *Journal of Applied Meteorology*, v. 7, p. 717–719.
- Edlund, S.A.**
1992: Climate change and its effects on Canadian Arctic plant communities; *in* Arctic Environment: Past, Present, and Future, (ed.) M-k. Woo and D.J. Gregor; Proceedings of a symposium held at McMaster University, November 14–15, 1991, p. 121–138.
- Edlund, S.A. and Alt, B.T.**
1989: Regional congruence of vegetation and summer climate patterns in the Queen Elizabeth Islands, Northwest Territories, Canada; *Arctic*, v. 42, no. 1, p. 3–23.
- Edlund, S.A., Woo, M-k., and Young, K.L.**
1990: Climate, hydrology, and vegetation patterns, Hot Weather Creek, Ellesmere Island, Arctic Canada; *Nordic Hydrology*, v. 21, p. 273–286.
- Goodison, B.E.**
1978: Accuracy of Canadian snow gauge measurements; *Journal of Applied Meteorology*, v. 17, p. 1542–1548.
- Hodgson, D.A., St-Onge, D.A., and Edlund, S.A.**
1991: Surficial materials of Hot Weather Creek basin, Ellesmere Island, Northwest Territories; *in* Current Research, Part E; Geological Survey of Canada, Paper 91-1E, p. 157–163.
- Jury, W. A. and Tanner, C.B.**
1975: Advection modification of the Priestley and Taylor evapotranspiration formula; *Agronomy Journal*, v. 67, p. 809–812.
- Kane, D.L., Hinzman, L.D., Woo, M-k., and Everett, K.R.**
1992: Arctic hydrology and climate change; *in* Arctic Ecosystems in a Changing Climate — an Ecophysiological Perspective, (ed.) F.S. Chapin III, R.L. Jefferies, J.F. Reynolds, G.R. Shaver, J. Svoboda, and E. Chu; Academic Press, Toronto, Ontario, p. 35–57.
- Kane, D.L., Hinzman, L.D., and Zurling, P.**
1991: Thermal response of the active layer in a permafrost environment to climate warming; *Cold Regions Science and Technology*, v. 19, p. 111–122.
- Lewkowicz, A.G.**
1990: Morphology, frequency and magnitude of active layer detachment slides, Fosheim Peninsula, Ellesmere Island, N.W.T.; Proceedings of the Fifth Canadian Permafrost Conference, Québec City, Québec, p. 111–118.
1992: Climate change and permafrost landscape; *in* Arctic Environment: Past, Present, and Future, (ed.) M-k. Woo and D.J. Gregor; Proceedings of a symposium held at McMaster University, November 14–15, 1991, p. 91–104.
- Lewkowicz, A.G. and Wolfe, P.**
1994: Sediment transport in Hot Weather Creek, Ellesmere Island, N.W.T., Canada, 1990-91; *Arctic and Alpine Research*, v. 26, no. 3, p. 213–226.
- Maxwell, J.B.**
1980: The Climate of the Canadian High Arctic Islands and Adjacent Waters, v. 1; Ministry of Supply and Services, Ottawa, Ontario, 531 p.
- Petzold, D.E. and Rencz, A.N.**
1975: The albedo of selected subarctic surfaces; *Arctic and Alpine Research*, v. 7, no. 4, p. 393–398.
- Running, S.W., Nemani, R.R., and Hungerford, R.G.**
1987: Extrapolation of synoptic meteorological data in mountainous terrain and its use for simulating forest evapotranspiration and photosynthesis; *Canadian Journal of Forest Research*, v. 17, p. 472–483.
- Ryden, B.E.**
1977: Hydrology of Treelove Lowland; *in* Treelove Lowland, Devon Island, Canada: A High Arctic Ecosystem, (ed.) L.C. Bliss; University of Alberta Press, Edmonton, Alberta, p. 107–136.
- Svoboda, J. and Freedman, B.**
1994: Ecology of a Polar Oasis, Alexander Fiord, Ellesmere Island, Canada; Captus University Publications, Toronto, Ontario, 268 p.
- Thorsteinsson, R.**
1969: Geology, Greely Fiord West, District of Franklin; Geological Survey of Canada, Map 1311A, scale 1:250 000.
- Woo, M-k.**
1986: Permafrost hydrology in North America; *Atmosphere-Ocean*, v. 24, p. 201–234.
- Woo, M-k. and Marsh, P.**
1978: Analysis of error in the determination of snow storage for small High Arctic basins; *Journal of Applied Meteorology*, v. 17, p. 1537–1541.
- Woo, M-k. and McCann, S.B.**
1994: Climatic variability, climate change, runoff, and suspended sediment regimes in Northern Canada; *Physical Geography*, v. 15, p. 201–226.
- Woo, M-k. and Young, K.L.**
1997: Hydrology of a small drainage basin with polar oasis environment, Fosheim Peninsula, Ellesmere Island, Canada; *Permafrost and Periglacial Processes*, v. 8, p. 257–277.
- Woo, M-k., Edlund, S.A., and Young, K.L.**
1991: Occurrence of early snow-free zones on Fosheim Peninsula, Ellesmere Island, Northwest Territories; *in* Current Research, Part B; Geological Survey of Canada, Paper 91-1B, p. 9–14.
- Woo, M-k., Heron, R., Marsh, P., and Steer, P.**
1980: Comparison of weather station snowfall with winter snow accumulation in High Arctic basins; *Atmosphere-Ocean*, v. 21, p. 312–325.
- Woo, M-k., Marsh, P., and Steer, P.**
1983: Basin water balance in a continuous permafrost environment; Proceedings, Fourth International Conference on Permafrost, National Academy Press, Washington, D.C., p. 1407–1411.
- Woo, M-k., Rowsell, R.D., and Edlund, S.A.**
1992: Effects of manipulation of climate factors on arctic snowmelt; Ninth International Northern Research Basins Symposium/Workshop, Canada, National Hydrology Research Institute Symposium no. 10, p. 627–641.

Woo, M-k., Walker, A., Yang, D.Q., and Goodison, B.

1995: Pixel-scale ground snow survey for passive microwave study of the Arctic snow cover; Proceedings 52nd Eastern Snow Conference, Toronto, Ontario, p. 51–57.

Woo, M-k., Young, K.L., and Edlund, S.A.

1990: 1989 observations of soil, vegetation, and microclimate, and effects on slope hydrology. Hot Weather Creek basin, Ellesmere Island, N.W.T.; *in* Current Research, Part D; Geological Survey of Canada, Paper, 90-1D, p. 85–93.

Young, K.L. and Woo, M-k.

1997: Modelling net radiation in an arctic environment using summer field camp data; International Journal of Climatology, v. 17, p. 1211–1229.

Young, K.L., Woo, M-k., and Edlund, S.A.

1997: Influence of local topography, soil and vegetation on microclimate and hydrology at a High Arctic site; Arctic and Alpine Research, v. 29, no. 3, p. 270–284.

APPENDIX A

Thermal data collection available for thaw depth determinations for the Fosheim Peninsula, Ellesmere Island, Nunavut

D.T. Desrochers¹

INTRODUCTION

A great amount of thermal data has been collected on Fosheim Peninsula for the Terrestrial Program of the High Arctic Integrated Research and Monitoring Area (IRMA). These data were collected for Dr. S.A. Edlund and Dr. B.T. Alt (at the time, both with the Geological Survey of Canada) by many individuals for various purposes and at different times over the lifetime of the program.

This appendix consists of a compilation of thermal data that can lead to the determination of thaw depth for the Fosheim Peninsula and geothermal simulations for determining the potential impact of global warming on Fosheim Peninsula and the eventual implication on thaw settlement under various global warming scenarios. A site location is proposed, a brief description of available data sets is presented, and recommendations for future work are highlighted.

SITE LOCATION

The selection of a site for determining thaw depth and providing geothermal simulations used in determining the potential impact of global warming was based on an evaluation of the sensitivity of a geotechnical database for Fosheim Peninsula. Over 152 boreholes containing information on location, soils, borehole logs, and specific geotechnical descriptions were

evaluated on the basis of availability of information related to specific thaw-settlement parameters, namely amount, extent, and type of ice present in the ground.

Information on ground ice in the Fosheim Geotechnical Database was examined through a series of parameter searches within ESELog/ESEBase[®]. These searches provided a complete listing of all available information for the 152 boreholes. For thaw settlement, the only practical information obtained from the database was the following: 1) type of ground material and depth; 2) moisture content; 3) visual estimates of ice (%ICE) and excess ice; 4) active layer and frozen seasonal thaw depths; and 5) National Research Council of Canada (NRC) ice codes and comments on visible ice.

An evaluation of the database has led to five possible sites where the determination of thaw depth and geothermal simulations used in determining the potential impact of global warming can be attempted. Geotechnical, geological, microclimatic, and climatic data were compiled for each of the five sites, which were then narrowed down to one representative site for the area. Table A-1 briefly describes the location and setting of the five sites.

The study location is in the Hot Weather Creek area, west central Fosheim Peninsula, Ellesmere Island, Nunavut (Fig. A-1, A-2). Its rolling topography consists of ice-rich marine and fluvial sediments over poorly consolidated clastic bedrock (Hodgson et al., 1991). Massive ice bodies up to 10 m across have been reported in exposures (W. Pollard,

Table A-1. Site characteristics for the five sites selected from the Fosheim Geotechnical Database.

Borehole	Northing	Easting	Elevation (m a.s.l.)	Depth of borehole (m)	Active layer (m)	Setting
7303701	8880900	523250	80	4.5	0.4	150 m south of centre of Eureka airstrip
74157E1	8880900	524420	80	5.15	0.59	on 30 m polygon 10 m away from ice wedge trough near east end of Eureka airstrip
7416701E2	8883450	524490	114	6.9	0.5	polygonal patterned ground on abandoned Eureka airstrip
74217101E8	8871350	534300	5	5.25	0.55	south side of Slide River floodplain
74227102E11	8877980	542900	128	5.4	0.62	polygonal patterned ground near Hot Weather Creek

Note: northing and easting under TM Zone 16

¹ Environmental Analyses Services, 43 du Sommet, Gatineau, Quebec J8P 7W9

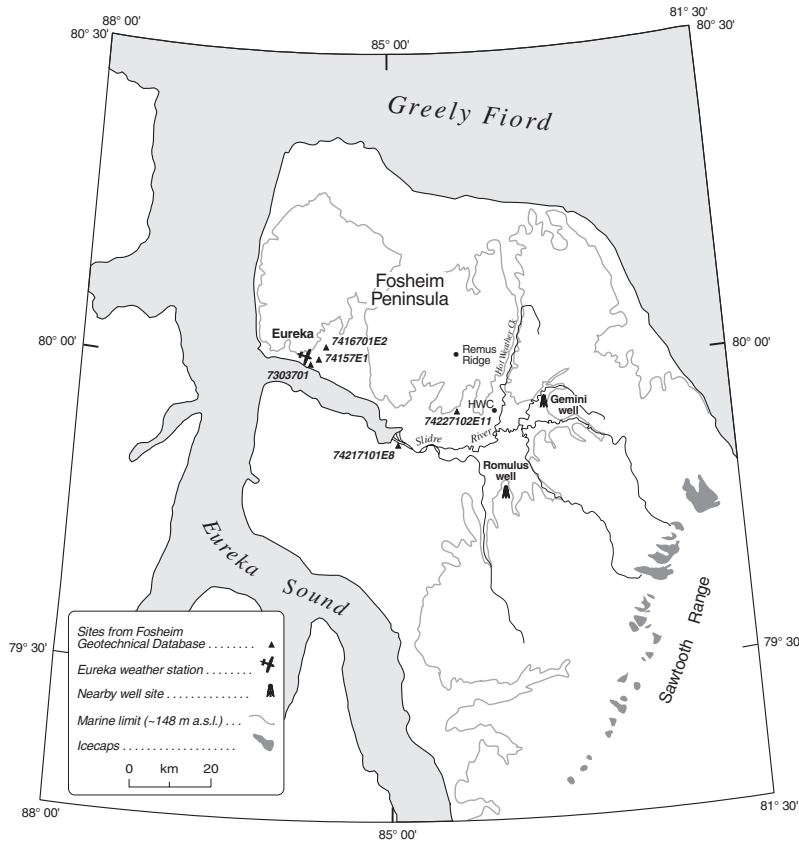


Figure A-1.

Site locations on Fosheim Peninsula, Ellesmere Island, Nunavut, from the Fosheim Geotechnical Database.

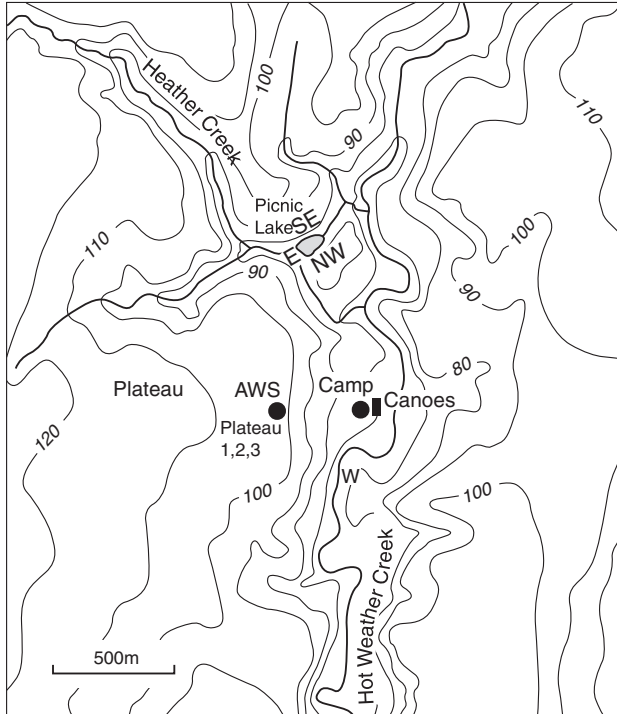


Figure A-2. Location of frost table and active layer sites near the Hot Weather Creek area (elevations in m a.s.l.).

pers. comm., 1993; Robinson, 1993). A mean ground surface temperature of -20.8°C , a mean annual temperature of -19.9°C (Eureka weather station, Atmospheric Environment Service), and a permafrost thickness of 502 m from a nearby oil well (Gemini well site, Taylor et al., 1982) are reported for Fosheim Peninsula.

The soil profile characteristics for the representative site and selected geotechnical and geothermal properties are highlighted in Table A-2. Some properties within the profile were selected from the five sites searched within the Fosheim Geotechnical Database (Hodgson and Nixon, 1998). The soil conditions consist of a fluvial layer of massive, sandy silts to a depth of 5 m. Faintly bedded silts and silty clays extend to a depth of 10 m followed by a massive-ice unit to a depth of 20 m. Since shale and sandstone are encountered in the area, they were included to a depth of 110 m.

AVAILABILITY OF DATA SETS

Various data sets with possible implications for the investigation of thaw depth exist for the Fosheim Peninsula. They include geotechnical/geological to climatic and temperature/depth information from both unpublished and published sources. A brief description of some of these data sets and their relevance to the investigation of thaw depth are provided in the following sections.

Table A-2. Soil profile characteristics and geotechnical information for a representative site selected from the Fosheim Geotechnical Database.

Soil material	Depth (m)	Thermal Conductivity (W/m)		Moisture content (%)	Unit of weight (mg/m ²)
		Unfrozen	Frozen		
Sand/silt	0–5	1.7	3.3	25	1.6
Silt	5–7.5	1.2	2.1	35	1.38
Silt/clay	7.5–10	1.548	1.935	25	1.6
Massive ice	10–20	0.59	2.09	100	0.73
Shale	20–70	0.6	0.6	20	1.74
Shale/sandstone	70–110	0.6	0.6	20	1.74

Geotechnical and geological data

Data compilation from the Fosheim Geotechnical Database

An evaluation of sensitivity and distribution of information in the Fosheim Geotechnical Database was undertaken using ESELog/ESEBase©. An assessment of the type and amount of data available in the Fosheim Geotechnical Database revealed the following:

- 14 per cent of the boreholes had excess ice;
- 16 per cent of the boreholes had moisture contents;
- 26 per cent of the boreholes had visual estimates of ice (%ICE); and

- 97 per cent of the boreholes had active layer and/or frozen seasonal thaw depths.

The database could not provide any information on such key parameters as bulk density, specific gravity, and saturation. The physical properties of soil material for the representative site were estimated in part from other strata by making comparisons with tested samples of similar soil units.

Ground-ice data

Bodies of massive ice up to 10 m across have been reported in exposures (W. Pollard, pers. comm., 1993; Robinson, 1993). According to W. Pollard (pers. comm., 1993), the ground-ice data shown in Table A-2 and used in the geothermal simulations in the section 'Ground-temperature profiles' are typical of the Fosheim Peninsula.

Climatic data

Meteorological data and information from general circulation models (GCM) as provided by the Atmospheric Environment Service's Canadian Climate Centre for this part of the High Arctic were used in this study. The Atmospheric Environment Service's 30-year normals for the Eureka weather station for the period 1961 to 1990 were used as meteorological data (Atmospheric Environment Service, 1993). Mean monthly air temperatures, total precipitation, snowfall, snow depth, rainfall, and snow density are presented in Table A-3.

Table A-3. Climate data, snow property data, and general circulation model scenarios for Fosheim Peninsula, Nunavut.

	Jan	Feb	Mar	Apr	May	Jun	Jul	Aug	Sep	Oct	Nov	Dec	Annual
30-year normals 1961-1990 Temperature (°C) Eureka	-36.6	-38.4	-37.4	-28.0	-10.9	1.9	5.4	3.0	-8.4	-22.3	-32.0	-34.5	-19.9
30-year normals 1961-1990 Total precipitation (mm)	3.0	3.0	2.4	3.5	2.9	6.6	11.0	11.6	10.2	7.7	3.3	2.9	68.1
30-year normals 1961-1990 Snowfall (cm)	3.5	3.4	2.7	4.1	3.4	3.1	1.0	4.0	10.9	9.3	4.2	3.6	53.2
½ Snowfall (cm)	1.75	1.70	1.35	2.05	1.70	1.55	0.50	2.00	5.45	4.65	2.10	1.80	26.60
Double snowfall (cm)	7.0	6.8	5.4	8.2	6.8	6.2	2.0	8.0	21.8	18.6	8.4	7.2	106.4
30-year normals 1961-1990 Snow depth (cm)	17.0	19.0	20.0	20.0	14.0	0.0	0.0	0.0	6.0	11.0	13.0	14.0	11.2
½ Snow depth (cm)	8.5	9.5	10.0	10.0	7.0	0.0	0.0	0.0	3.0	5.5	6.5	7.0	5.6
Double snow depth (cm)	34.0	38.0	40.0	40.0	28.0	0.0	0.0	0.0	12.0	22.0	26.0	28.0	22.3
30-year normals 1961-1990 Rainfall (mm)	0.0	0.0	0.0	0.0	0.0	3.7	10.0	7.9	0.9	0.0	0.0	0.0	22.5
Estimated Snow density (gm/cm ³)	0.36	0.38	0.36	-	-	-	-	-	-	-	0.33	0.34	0.35
CCC-GCM year 2050 [change from 1xCO ₂ to 2xCO ₂] Difference in temperature (°C)	7.8	7.5	6.2	4.7	3.6	2.9	8.4	5.1	2.9	12.2	5.5	7.6	6.2
[Ratio] Precipitation (%)	0.7	0.9	1.0	0.8	1.1	1.3	0.5	0.9	0.7	0.8	0.9	0.9	0.9
CCC-GCM year 2050 [Resulting scenario] Temperature (°C)	-35.7	-35.6	-31.6	-21.4	-6.4	1.1	15.6	15.0	4.2	-7.6	-26.2	-32.5	-13.4

CCC-GCM = Canadian Climate Centre's general circulation model.

Table A-4. Monthly soil temperature at the Hot Weather Creek automatic weather station between 1988 and 1993.

YEAR	MONTH	AIR TEMP	AIR R.H.	Ground temperatures (°C)					Monthly thaw depth (cm)	Mean annual thaw depth (cm)
				VEG/SURFACE	10 cm	20 cm	50 cm	100 cm		
1988	7	12.2	55.5	15.4	11.5	7.5	-0.3	-3.7	48.7	61.0
1988	8	10.1	57.1	12.1	8.2	6.0	1.7	-2.1	73.2	
1988	9	-7.2	85.5	-8.4	-6.8	-6.0	-4.4	-4.3		
1988	10	-15.7	82.5	-15.6	-13.0	-12.3	-10.7	-9.7		
1988	11	-33.5	71.2	-25.1	-20.2	-19.3	-17.2	-15.6		
1988	12	-37.1	68.0	-30.9	-24.7	-24.0	-22.0	-20.4		
1989	1	-45.1	61.0	-38.1	-31.1	-30.0	-27.2	-24.9		
1989	2	-38.5	66.5	-35.9	-32.6	-32.1	-30.6	-29.0		
1989	3	-39.4	65.4	-35.6	-31.4	-30.9	-29.7	-28.5		
1989	4	-24.1	73.8	-27.2	-27.8	-27.9	-27.9	-27.6		
1989	5	-11.7	73.9	-13.7	-18.1	-18.9	-20.4	-21.6		
1989	6	3.7	80.0	5.3	1.5	-1.2	-5.7	-9.9	16.1	
1989	7	6.6	81.3	8.0	5.9	3.4	-0.7	-4.4	46.8	
1989	8	5.0	87.4	5.8	4.5	3.2	1.1	-2.4	65.8	
1989	9	-7.4	89.2	-6.1	-3.1	-2.4	-0.7	-3.0		
1989	10	-24.7	80.5	-16.5	-11.8	-11.1	-9.1	-9.2		
1989	11	-33.9	72.2	-27.6	-20.6	-19.7	-17.6	-16.4		
1989	12	-38.1	68.4	-25.6	-22.4	-21.8	-20.4	-19.4		
1990	1	-40.9	66.3	-28.1	-24.2	-23.7	-22.4	-21.3		
1990	2	-42.4	64.8	-32.1	-27.4	-26.8	-25.2	-23.9		
1990	3	-36.4	69.3	-33.5	-29.3	-28.7	-27.3	-26.1		
1990	4	-23.0	76.0	-25.3	-25.3	-25.4	-25.3	-25.1		
1990	5	-5.4	82.2	-9.0	-14.7	-15.8	-17.8	-19.4		
1990	6	6.9	67.2	9.8	4.5	1.0	-4.5	-8.9	25.5	
1990	7	8.3	64.9	10.4	8.2	5.8	1.4	-2.9	65.9	
1990	8	6.2	72.9	7.7	5.3	3.8	1.8	-1.8	75	
1990	9	-5.6	88.0	-6.2	-3.2	-2.6	-0.6	-2.6		
1990	10	-25.6	79.7	-21.0	-15.4	-14.2	-10.9	-10.2		
1990	11	-36.8	70.1	-31.2	-25.3	-23.8	-20.5	-18.6		
1990	12	-37.9	66.8	-37.0	-32.4	-30.9	-27.7	-25.2		
1991	1	-42.5	64.3	-40.4	-36.7	-35.4	-32.5	-30.2		
1991	2	-40.5	65.3	-40.0	-37.4	-36.4	-34.3	-32.5		
1991	3	-34.6	69.7	-36.2	-35.3	-34.9	-33.8	-32.6		
1991	4	-26.1	72.1	-28.8	-30.2	-30.5	-30.4	-30.2		
1991	5	-6.5	79.0	-6.9	-12.5	-14.8	-18.2	-20.8		
1991	6	5.7	76.7	7.5	5.2	1.3	-3.4	-8.1	28.9	
1991	7	10.0	65.3	12.4	10.1	6.3	1.7	-3.7	65.7	
1991	8	4.4	84.5	4.7	4.5	3.2	5.7	-1.9	87.5	
1991	9	-6.5	94.9	-3.8	-1.1	-1.2	3.8	-2.5	80	
1991	10	-21.1	84.7	-16.0	-11.4	-11.1	-8.7	-8.4		
1991	11	-29.2	75.2	-25.7	-20.8	-19.7	-17.1	-15.6		
1991	12	-38.5	68.6	-30.5	-25.8	-24.8	-22.5	-20.9		
1992	1	-42.9	65.2	-32.1	-27.9	-27.1	-25.1	-23.8		
1992	2	-41.0	66.4	-33.9	-29.4	-28.7	-26.9	-25.7		
1992	3	-37.7	68.7	-33.3	-29.8	-29.3	-27.9	-26.9		
1992	4	-26.7	75.2	-29.0	-27.5	-27.4	-26.7	-26.3		
1992	5	-12.9	79.8	-17.2	-20.4	-21.2	-22.1	-22.9		
1992	6	2.7	76.6	4.0	0.5	-3.1	-7.8	-11.9	11.3	
1992	7	7.8	72.6	9.0	8.3	4.9	-0.3	-4.2	48.9	
1992	8	2.9	86.5	3.3	3.7	2.0	0.5	-2.6	54	
1992	9	-6.8	91.0	-7.5	-5.1	-5.2	-3.9	-4.8		
1992	10	-20.4	82.7	-16.7	-13.1	-12.8	-10.8	-10.6		
1992	11	-34.1	71.4	-30.6	-23.6	-21.9	-18.5	-17.0		
1992	12	-34.3	70.8	-32.5	-28.2	-27.0	-24.6	-23.0		
1993	1	-38.4	67.0	-36.1	-31.5	-30.2	-27.8	-26.1		
1993	2	-37.0	66.2	-36.4	-33.0	-31.9	-29.7	-28.2		
1993	3	-38.3	65.7	-37.7	-35.5	-34.6	-32.7	-31.1		
1993	4	-25.0	71.9	-27.6	-28.9	-29.0	-28.9	-28.7		
1993	5	-8.5	79.5	-10.3	-16.2	-18.0	-20.5	-22.2		
1993	6	6.7	62.7	9.7	7.1	2.1	-3.8	-8.8	30.5	
1993	7	11.7	64.6	14.3	12.2	7.7	3.6	-3.3	76.1	
1993	8	3.9	78.6	4.3	4.5	2.5	5.2	-2.0	86.2	
1993	9	-8.1	89.7	-6.7	-2.7	-3.2	0.3	-3.3	54.5	
1993	10	-18.8	84.2	-18.3	-13.8	-13.5	-10.7	-10.2		
1993	11	-35.9	69.2	-32.1	-27.3	-25.1	-20.6	-18.5		
1993	12	-37.2	68.0	-37.2	-33.8	-31.9	-28.0	-25.5		
1994	1	-34.1	65.1	-35.3	-33.9	-32.7	-30.1	-28.3		
1994	2	-38.9	64.3	-38.8	-36.9	-35.6	-32.9	-30.9		
1994	3	-39.0	63.8	-38.9	-36.2	-35.5	-33.8	-32.5		
1994	4	-26.7	70.5	-30.5	-31.3	-31.4	-31.1	-30.7		
1994	5	-6.5	79.1	-11.0	-17.2	-18.9	-21.5	-23.3		
1994	6	3.1	80.7	3.6	-3.2	-6.6	-11.0	-14.5		

Predicted endpoint data for the year 2050 from the Canadian Climate Centre's general circulation model scenario of doubled CO₂ predictions are also included in Table A-3. The doubled CO₂ scenario predictions applied in this study consisted of mean monthly air temperature and monthly total precipitation estimates for a doubling of CO₂ in the atmosphere for the Eureka weather station. A doubling of CO₂ is assumed to take place over a 50-year period. The appropriate data for the Fosheim Peninsula were obtained from gridpoint 499 of the North American window of the general circulation model (Atmospheric Environment Service, 1990). This version of the general circulation model was first generated in 1989. Upgrades of the Atmospheric Environment Service's model predictions have since been produced, but were unavailable for this report. General circulation model predictions imply an increase of 6.5°C in mean annual air temperature (Table A-3).

Thermal characteristics

Ground-temperature measurements

Ground-temperature measurements were obtained for the period 1988 to 1993 at a number of sites in the Hot Weather Creek area. Of particular interest to this study, the ground-temperature data collected at the Gemini well site stand out as the only known continuous record of its kind for the area. Figure A-3 and Table A-4 reveal monthly soil temperatures at a depth of 10, 20, 50, and 100 cm as recorded by an eight-channel Brancker datalogging system (XL-800). A detailed portion of this data set (i.e. mean daily soil temperatures between 22 June and 23 August 1992) is presented in Figure A-4. Other soil-temperature measurements at a nearby site indicate a 0.5°C to 11.0°C change in temperature between 1 January and 26 March 1991 and the same period in 1992 (Fig. A-5, A-6). The deep temperatures monitored by Taylor et al. (1982) at the Gemini well site were used as base

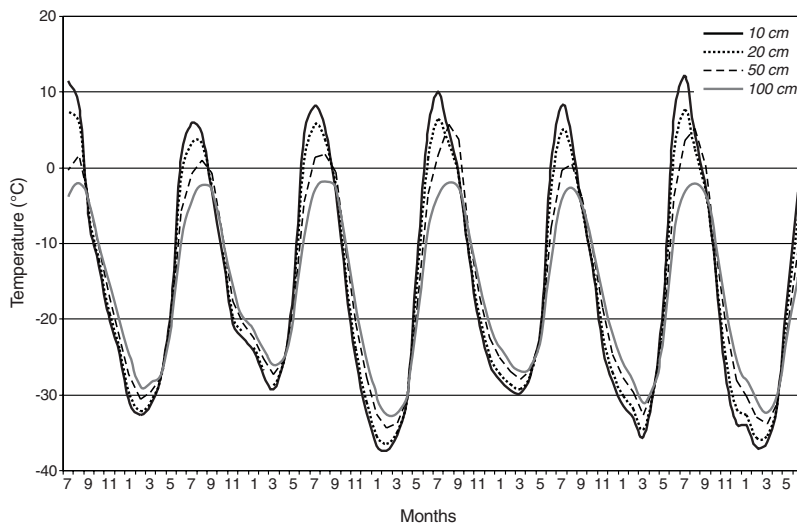


Figure A-3.

Monthly soil temperatures at the Hot Weather Creek autostation between 1988 and 1993.

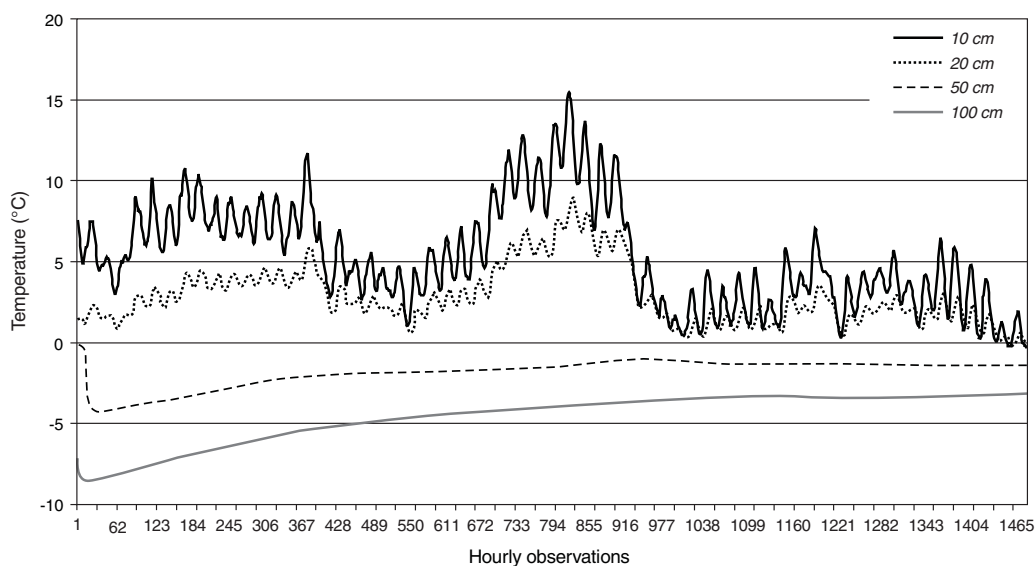


Figure A-4. Ground-temperature measurements at the Gemini well site between June 22 and August 23, 1992.

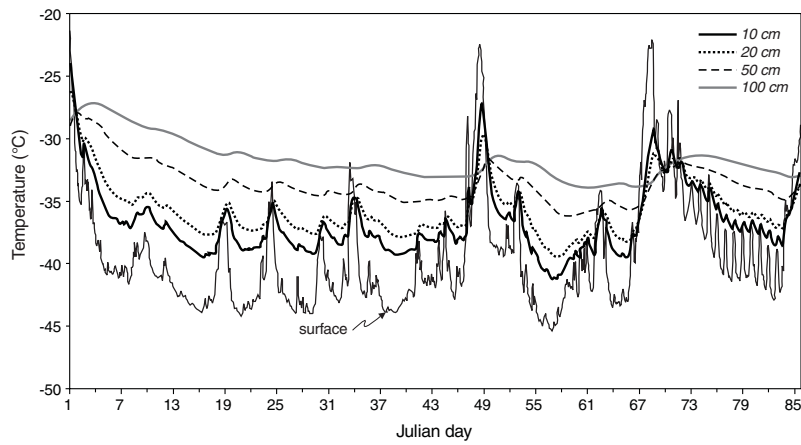


Figure A-5.
Hot Weather Creek autostation mean soil temperatures, January 1 to March 26, 1991.

Figure A-6.
Hot Weather Creek mean soil temperatures, January 1 to March 26, 1992.

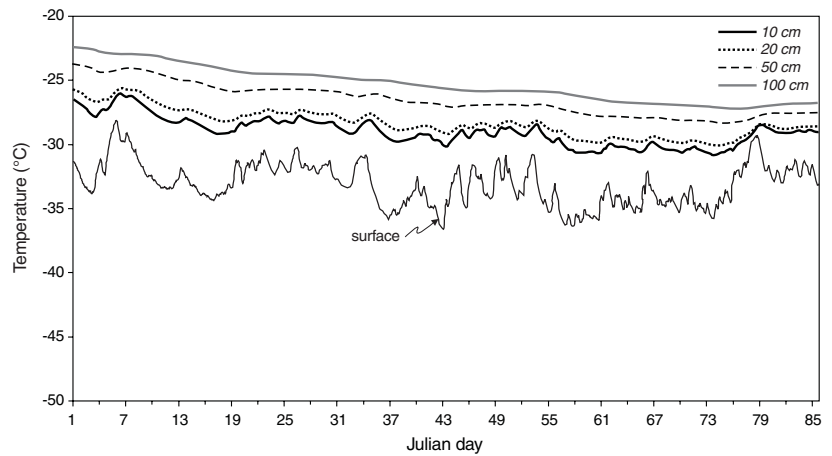


Table A-5. Summary of maximum frost table and active layer measurements in the Hot Weather Creek area (1991 and 1992).

Maximum frost table (mm) in the Hot Weather Creek area – 1991*																
Base Camp area					Plateau			Canoes							Picnic Lake	
West	East	North	South	Camp	#1	#2	#3	#1	#2	#3	#4	#5	#6	#7	East	West
890	710	920	730	655	570	565	560	730	675	680	755	755	755	785	530	390

Gemini well site – 1991															
N1	N2	N3	N4	S1	S2	S3	S4	E1	E2	E3	E4	W1	W2	W3	W4
535	580	520	530	560	520	590	630	480	505	515	600	550	630	580	570

Remus Ridge – 1991															
N1	N2	N3	N4	S1	S2	S3	S4	E1	E2	E3	E4	W1	W2	W3	W4
640	625	645	580	620	670	680	665	650	670	650	635	620	640	545	640

pond levels – 1992* (Young et al., 1997, Fig. 1)									
1	2	3	4	5	6	7	8	9	10
524	1295	465	1049	712	893	821	739	747	732

Water wells – 1992* (Young et al., 1997, Fig. 1)																								
East								West		North								South						
1-1	1	2	4-1	7-1	7	8	9	4	7-1	1-1	1	2	3	4-1	4	5	6	7-1	7	8	1-1	2	4-1	7-1
1233	756	437	675	1185	791	507	853	939	827	700	932	1180	1013	372	892	1004	927	647	1066	846	716	706	563	585

Active-layer thickness (mm) in the Hot Weather area – 1992*								
STEVENS SCREEN	AWS PLATEAU	EAST FACING	NORTH FACING	SOUTH FACING	WEST FACING	OLD WEST FACING	PICNIC LAKE BERM	MUSKOX FEN
566	572	754	754	656	686	686	382	368

*See Woo et al. (1989), Woo et al. (1992), Young (1995), Young et al. (1997), Young (1995) for site details.

condition for the preliminary geothermal simulations reported in the sections ‘Ground-temperature profiles’ and ‘Thaw depths’.

Active-layer measurements

Many sites were selected for measuring the active layer. Data sets indicate that both frost-table and active-layer measurements were taken in and around the Hot Weather Creek area (see Fig. A-2 for site locations). According to Brown and Kupsch (1974), the active layer is defined as “the top layer of ground above the permafrost table that thaws each summer and refreezes each fall” whereas the frost table is defined as “any frozen surface in the active layer that is moving down-

ward towards the permafrost table due to thawing”. The data presented in this section retain the terminology used in each data set.

The depth of the frost table was monitored in 1991 and 1992 at the Hot Weather Creek area, Gemini well site, Remus Ridge, and at many ‘pond level’ and ‘water well’ sites (see Woo et al., 1989, Fig. 1 and 2, for general view and setup of study area). Active-layer measurements were only reported for the Hot Weather Creek area in 1992. A summary of maximum frost-table and active-layer thicknesses is provided in Table A-5. The deepest maximum frost table was observed at ‘pond level’ site 2 (1295 mm) and the shallowest maximum active-layer thickness was reported at the ‘muskox fen’ site (368 mm), both in 1992.

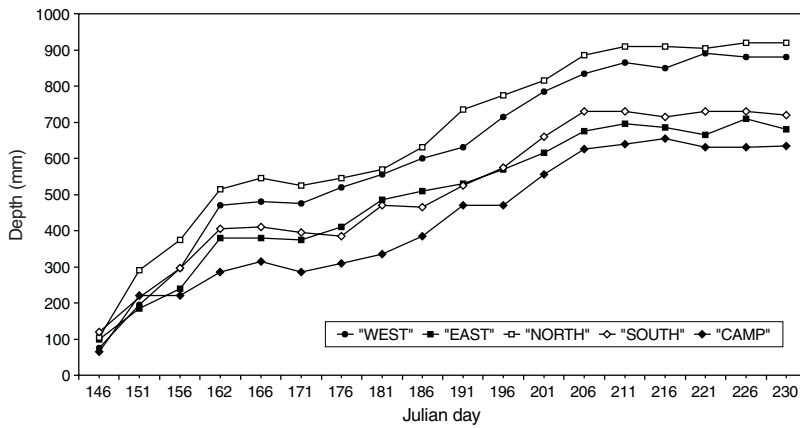


Figure A-7.
Frost tables for the Hot Weather Creek area, 1991.

Figure A-8.
Frost tables at Plateau, Hot Weather Creek area, 1991.

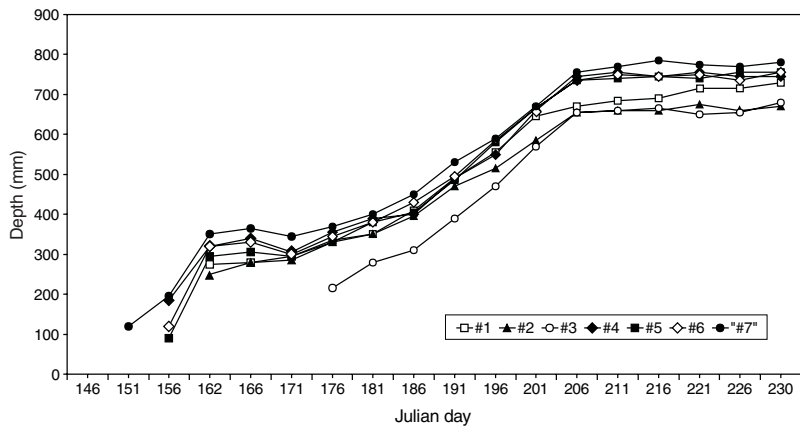
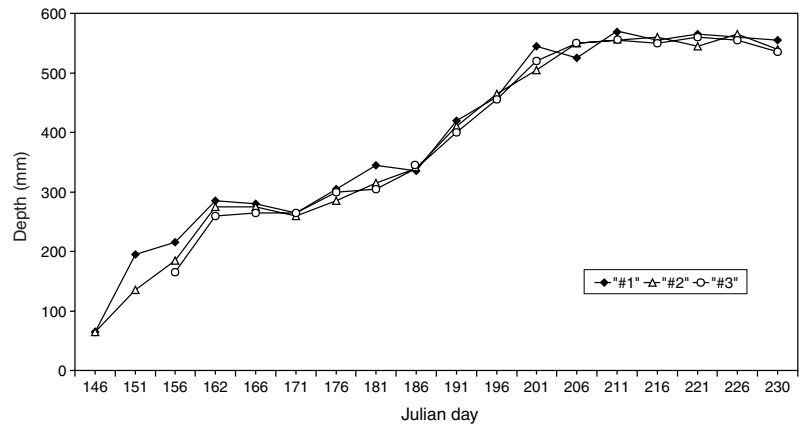


Figure A-9.
Frost tables at Canoes, Hot Weather Creek area, 1991.

The depths of the frost table for the base camp, Plateau, Canoes, Picnic Lake, Gemini, and Remus Ridge sites are plotted in Figures A-7 to A-18 and those for the 'pond level' and 'water level' sites, in Figures A-19 and A-20 respectively. Active layers for many other sites in the area are also in Figure A-21.

Ground-temperature profiles

Ground-temperature profiles as derived from geothermal simulations and under varying snow conditions were produced from base temperatures recorded at the Gemini well site. Temperature profiles for years 0 (base), 10, and 50 under

normal snow conditions, with half the normal snow, and with double the normal snow are shown in Figures A-22 to A-24 respectively.

The approach used to model the potential impact of global warming at sites with varying surficial materials in the Hot Weather Creek area consisted of running a number of one-dimensional, geothermal simulations that consider currently known thermal conditions as base condition (i.e. year 0) and then modifying surface conditions (i.e. ground surface temperatures, thermal and physical properties of ground and snow, snow depth) with time. The 30-year normals reported in Table A-3 were used in the simulations.

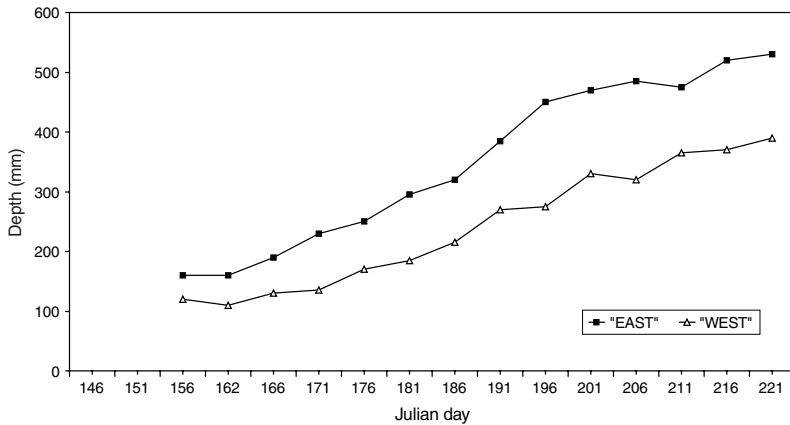


Figure A-10.
Frost tables at Picnic Lake, Hot Weather Creek area, 1991.

Figure A-11.
Frost tables at Gemini well site (north), Hot Weather Creek area, 1991.

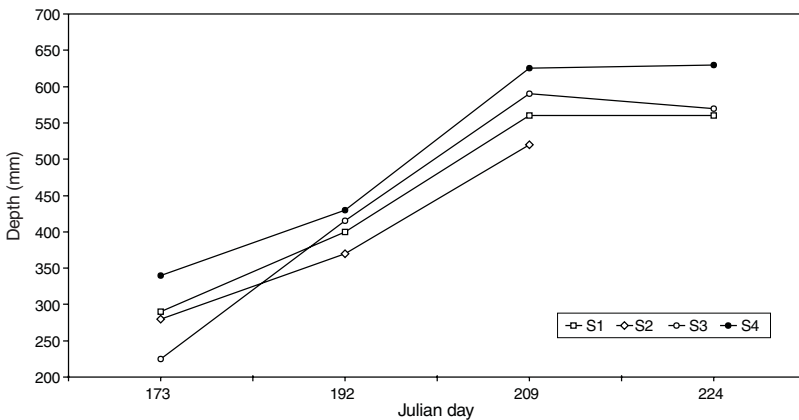
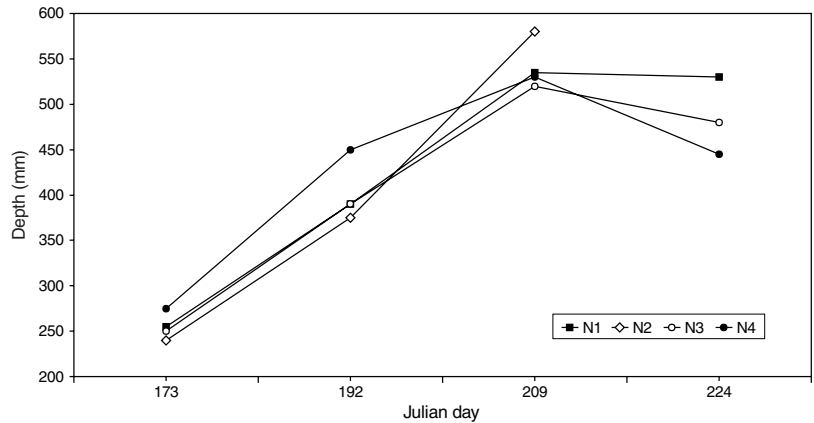


Figure A-12.
Frost tables at Gemini well site (south), Hot Weather Creek area, 1991.

Figure A-13.

Frost tables at Gemini well site (east), Hot Weather Creek area, 1991.

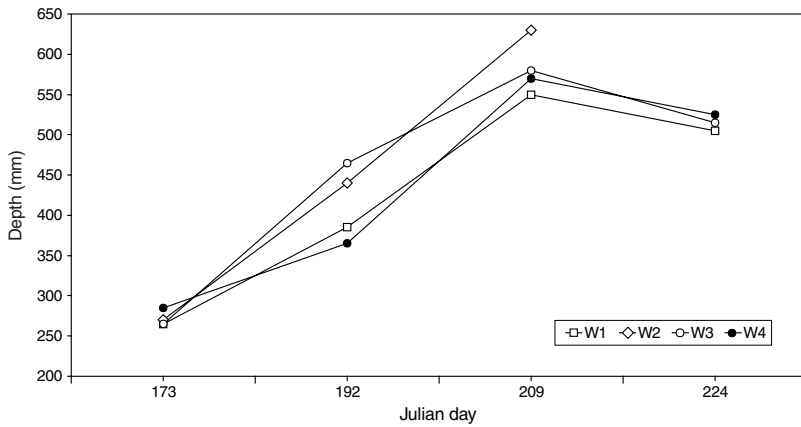
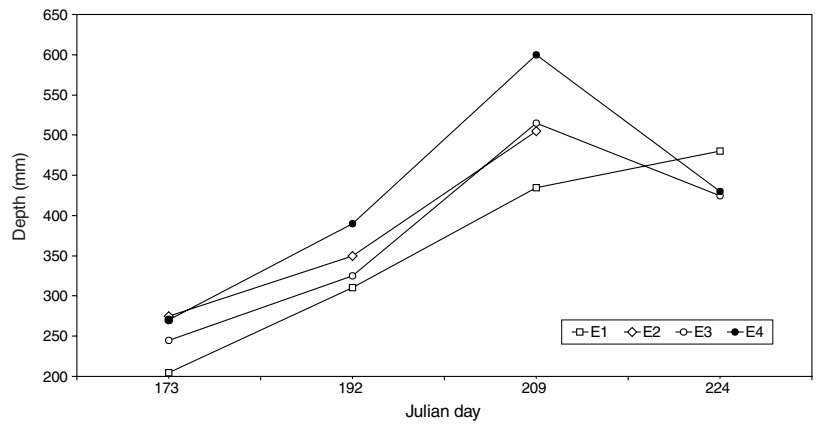


Figure A-14.

Frost tables at Gemini well site (west), Hot Weather Creek area, 1991.

Figure A-15.

Frost tables at Remus Ridge (north), Hot Weather Creek area, 1991.

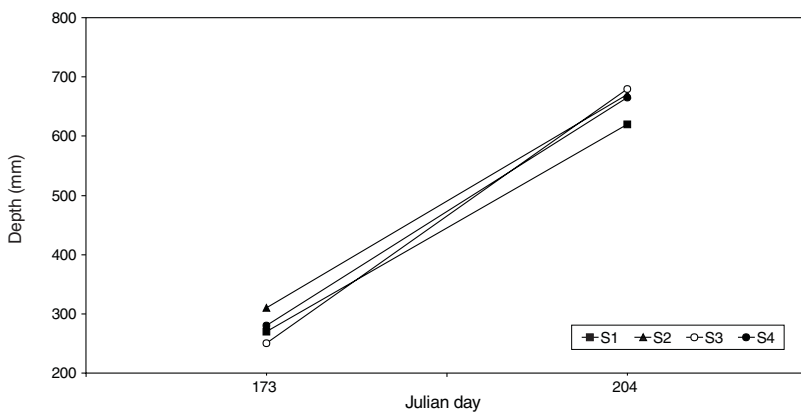
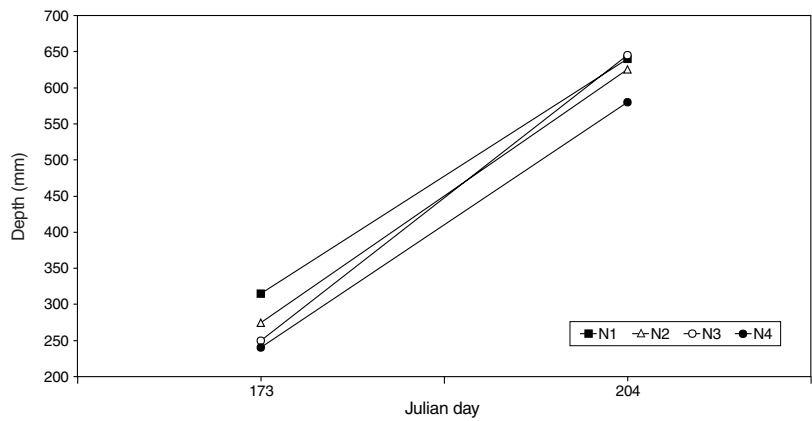


Figure A-16.

Frost tables at Remus Ridge (south), Hot Weather Creek area, 1991.

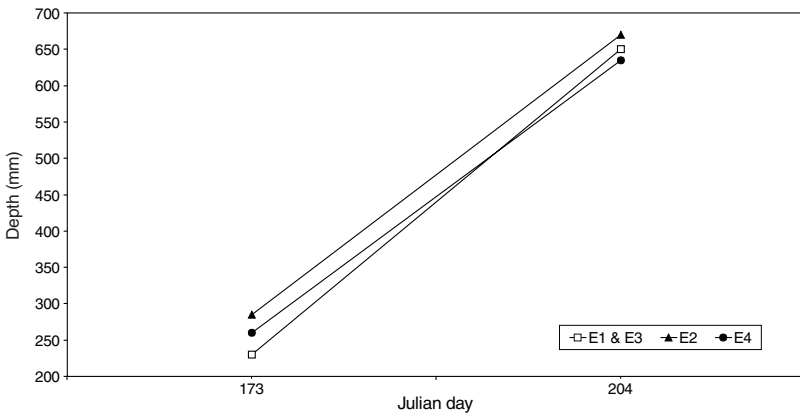


Figure A-17.

Frost tables at Remus Ridge (east), Hot Weather Creek area, 1991.

Figure A-18.

Frost tables at Remus Ridge (west), Hot Weather Creek area, 1991.

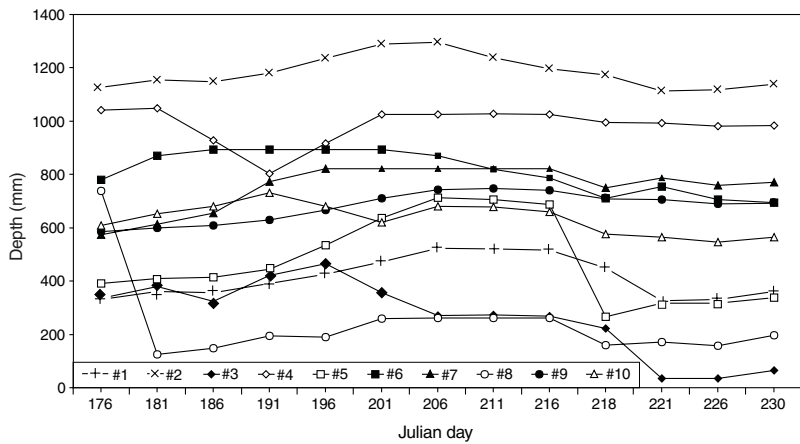
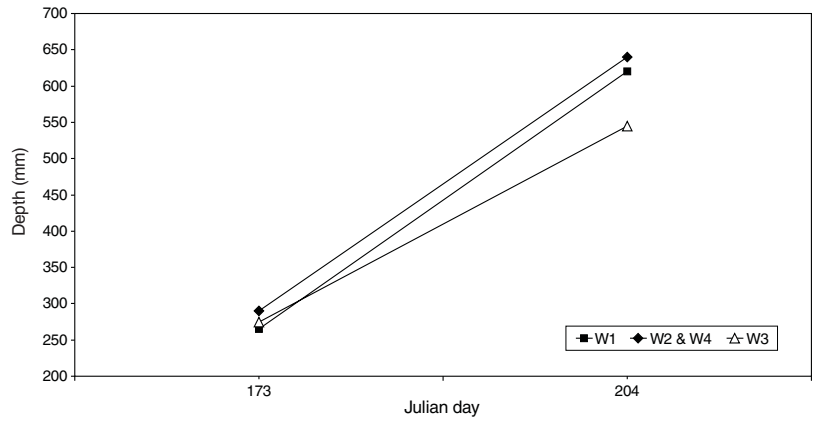
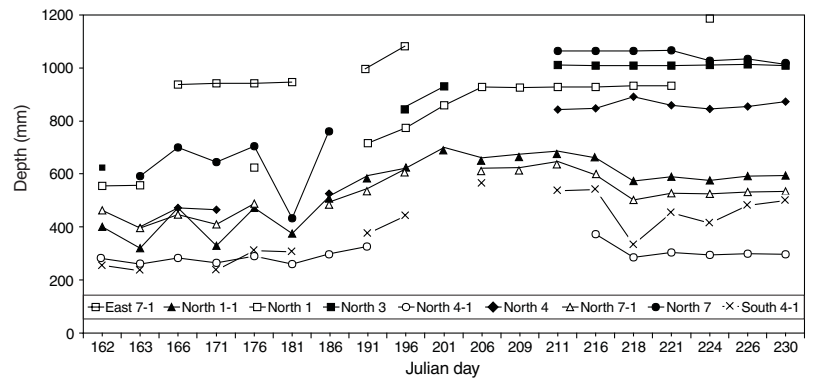


Figure A-19.

Frost tables at pond level sites, Hot Weather Creek area, between Julian days 176 and 230, 1992.

Figure A-20.

Frost tables at water level sites, Hot Weather Creek area, between Julian days 162 and 230, 1992.



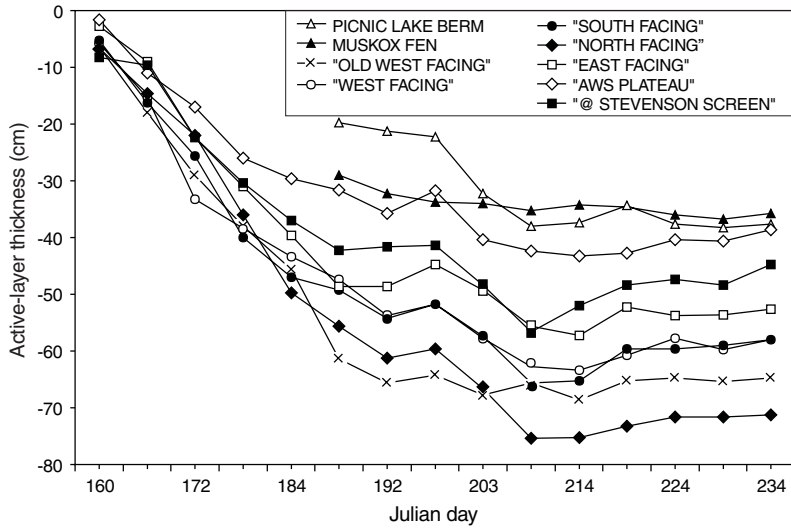


Figure A-21.
Active-layer thicknesses, Hot Weather Creek area, 1992.

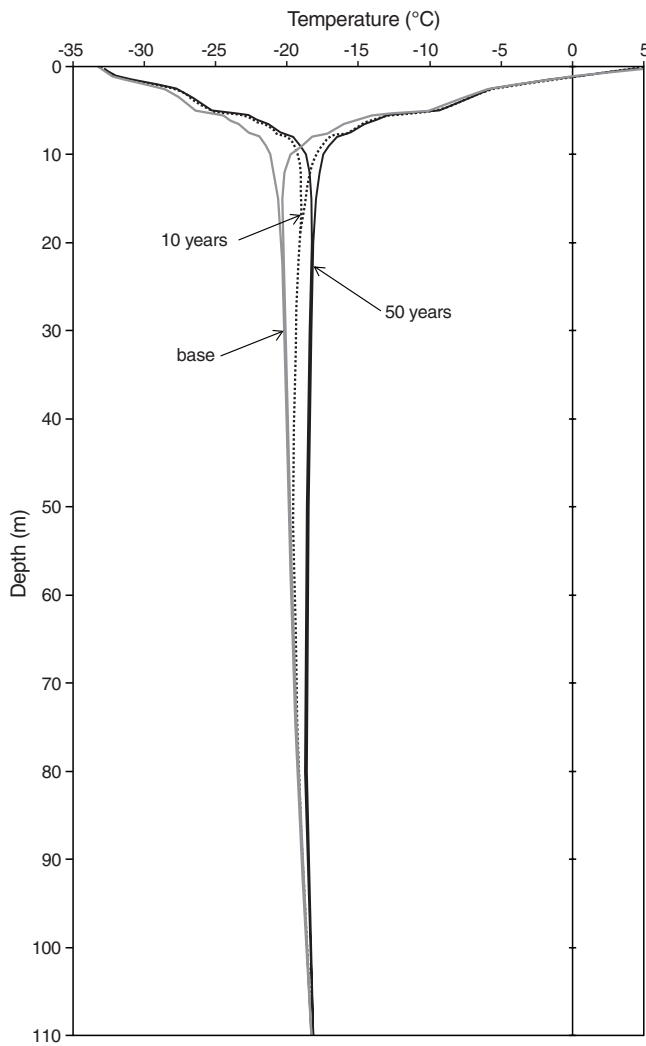


Figure A-22. Base (0), 10-, and 50-year temperature profiles under normal snow conditions for the Hot Weather Creek area.

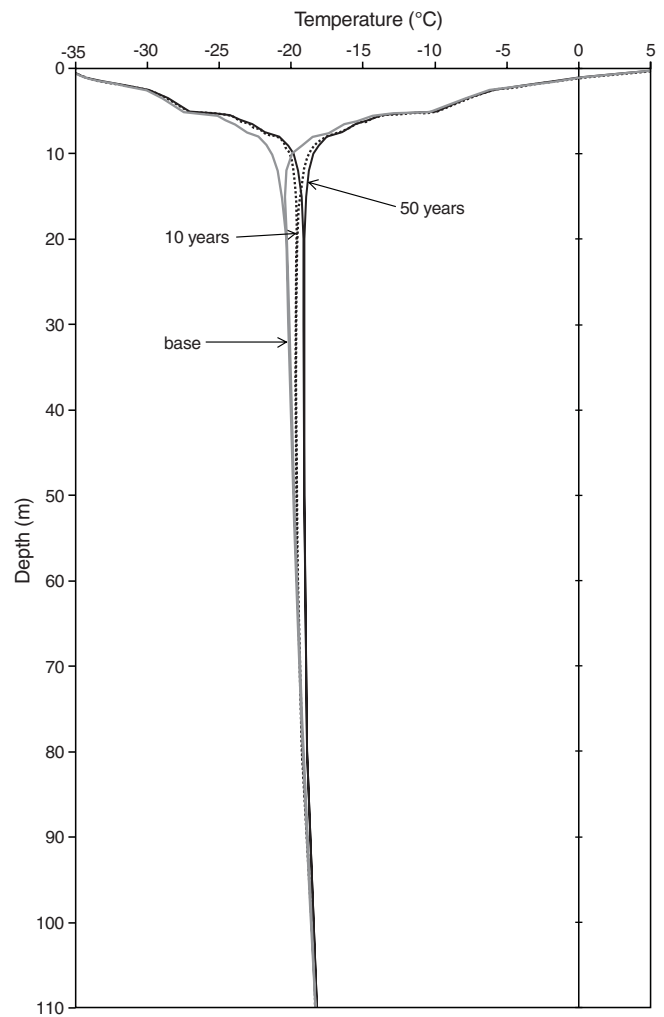


Figure A-23. Base (0), 10-, and 50-year temperature profiles with half the normal snow conditions for the Hot Weather Creek area.

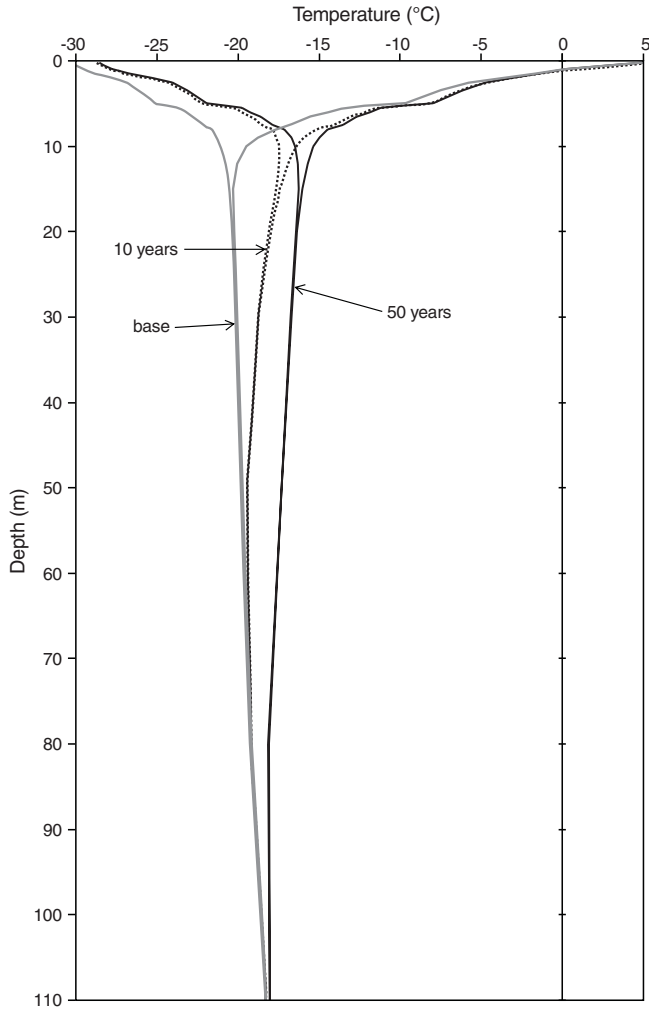


Figure A-24. Base (0), 10-, and 50-year temperature profiles with double the normal snow conditions for the Hot Weather Creek area.

Preliminary geothermal analyses were accomplished using a one-dimensional finite difference routine within GATHERM2 (Nixon Geotech Ltd.). The geotechnical and geothermal properties of a 110 m deep soil profile (as in Table A-2) were used in the model.

It should be emphasized that the general warming trend identified in Figures A-22 to A-24 is the result of changes to surface-boundary conditions. It is difficult to speculate whether such a trend suggests permafrost degradation, a return to equilibrium conditions, or both. Further simulation runs (i.e. linear conditions) may provide results that could lead to a clearer understanding of thaw depth with time.

Thaw depths

Thaw depths were calculated from the monthly soil temperatures reported in the section ‘Ground-temperature measurements’. Figure A-25 illustrates monthly and mean annual thaw depths for the Hot Weather Creek area between 1988 and 1993. Mean annual thaw depths varied from 38.1 cm to 65.5 cm for the period of observation.

Predicted thaw depths as derived from the geothermal analyses reported in the section ‘Ground-temperature profiles’ are plotted in Figure A-26. These predictions represent mean annual thaw depths from year 0 (base condition) to year 50 under varying general circulation model scenarios of snow conditions. Under the three scenarios presented, namely normal snow conditions, with half the normal snow, and with double the normal snow, mean annual thaw depths range from 31 to 40 cm within the 50-year period. Annual thaw depths also varied from 13 to 52 cm for the same period.

RECOMMENDATIONS FOR FUTURE WORK

Limitations of and recommendations on currently available geotechnical, ground-temperature, and active-layer data sets for the Hot Weather Creek area are discussed in the following sections.

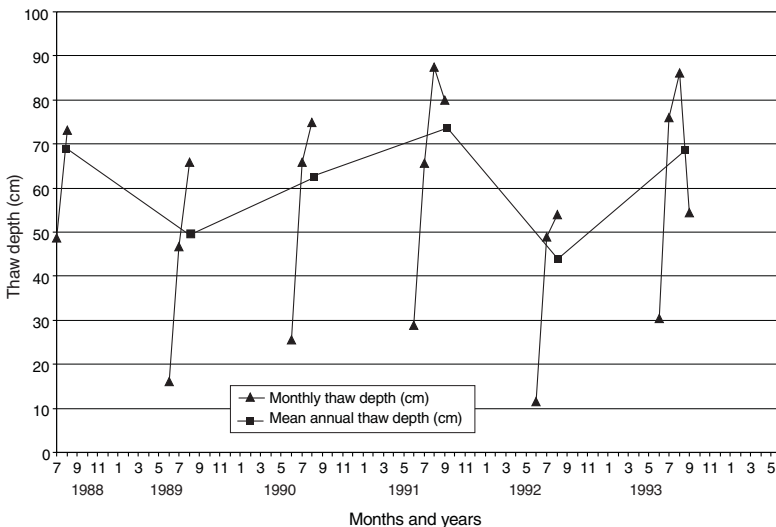


Figure A-25. Monthly and mean annual thaw depths between 1988 and 1993, Hot Weather Creek area.

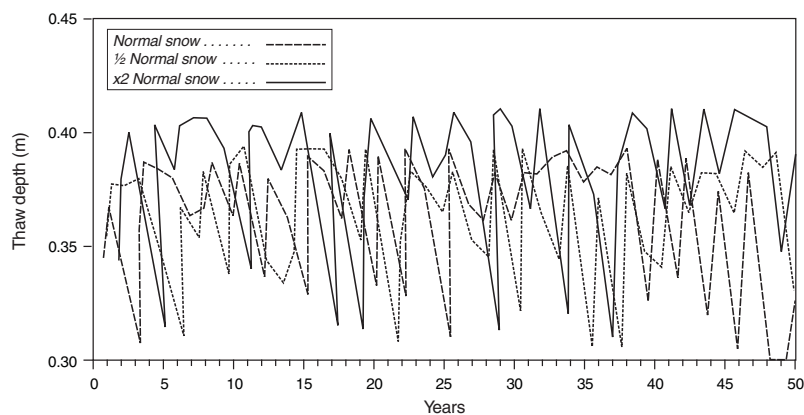


Figure A-26.

Predicted mean annual thaw depths under the Canadian Climate Centre's general circulation model scenarios for the Hot Weather Creek area.

Limitations of data sets

The greatest limitation in determining thaw settlement from the Fosheim Geotechnical Database lies on the lack of availability of certain parameters. These parameters, namely bulk density, specific gravity, moisture content, and saturation, are for the most part scarce and/or unavailable for many borehole logs in the database. As a result, physical properties of soil material have to be estimated from certain strata by making comparisons with tested samples of similar soil units.

Limitations of the ground-temperature data set have to do with continuity and data quality. Continuity has been difficult to achieve mainly because of harsh climate conditions and the resultant failure of datalogging systems. Consequently, gaps within the data set have led to poor coverage of ground-temperature conditions between late fall and early spring. The quality of available data is highly dependent on the availability of calibration files. Calibration data files do not always coincide with datalogger files. An effort should be made to correct this problem. Lastly, extrapolation of ground temperatures could resolve some continuity problems associated with the data set whereas a sensitivity analysis of all available ground-temperature data could greatly improve the quality of the data set as a whole.

Geothermal models and global warming scenarios

The Geological Survey of Canada has recently expressed the need to acquire geothermal simulations for determining the potential impact of global warming at sites with various surficial materials and the eventual implication on thaw settlement under various global-warming scenarios. Future work could emphasize an in-depth determination of thaw depth and thaw settlement on Fosheim Peninsula from geothermal analyses for varying global circulation model scenarios. With a proper geothermal model in hand, they could be generated under current conditions and moving linearly with the following conditions:

- snow depth held constant;
- snow depth at half that of current conditions;
- snow depth at twice that of current conditions.

The use of geothermal models to simulate thaw depth over a 50-year period under doubled CO₂ global warming scenarios is essential for the High Arctic Research and Monitoring Area. Since state-of-the-art one- and two-dimensional geothermal models are now available, they could be used to obtain simulated thaw depths needed to calculate thaw settlement for this area.

All future simulations should be generated from the recent version of the Canadian Climate Centre's general circulation model. Although the 1989 and current versions imply an increase of 6.5°C in mean annual air temperature, the fine-tuning of model runs has now led to differing endpoint values.

REFERENCES

Atmospheric Environment Service

- 1990: Canadian Climate Centre — General Circulation Model Monthly 1 and 2 x CO₂ Data; Canadian Climate Program, Environment Canada, Downsview, Ontario, PC version.
- 1993: Digital Canadian 1961–90 Climate Normals Atlas; Canadian Climate Program, Environment Canada, Ottawa, Ontario, CD-ROM version.
- Brown, R.J.E. and Kupsch, W.O.**
1974: Permafrost terminology; Associate Committee on Geotechnical Research, National Research Council of Canada, Technical Memorandum No. 111, NRCC 14274, 62 p.
- Hodgson, D.A. and Nixon, F.M.**
1998: Ground ice volumes determined from shallow cores from western Fosheim Peninsula, Ellesmere Island, Northwest Territories; Geological Survey of Canada, Bulletin 507, p. 178 p.
- Hodgson, D.A., St-Onge, D.A., and Edlund, S.A.**
1991: Surficial materials of Hot Weather Creek basin, Ellesmere Island, Northwest Territories; in Current Research, Part E; Geological Survey of Canada, Paper 91-1E, p. 157–163.
- Robinson, S.D.**
1993: Geophysical and geomorphological investigations of massive ground ice, Fosheim Peninsula, Ellesmere Island, Northwest Territories; M.Sc. thesis, Queen's University, Kingston, Ontario, 171 p.
- Taylor, A.E., Burgess, M.M., Judge, A.S., and Allen, V.S.**
1982: Canadian geothermal data collection — northern wells 1981; Geothermal Series No. 13, Earth Physics Branch, Geothermal Service of Canada, 153 p.
- Woo, M., Rowsell, R.D., and Edlund, S.A.**
1992: Effects of manipulation of climate factors on arctic snowmelt; in Ninth International Northern Research Basins Symposium/Workshop, Canada, National Hydrology Research Institute Symposium No. 10; p. 627–641.

Woo, M.K., Young, K.L., and Edlund, S.A.

1989: 1989 observations of soil, vegetation, and microclimate, and effects on slope hydrology. Hot Weather Creek basin, Ellesmere Island, Northwest Territories; *in* Current Research, Part D; Geological Survey of Canada, Paper 90-1D, p. 85–93.

Young, K.L.

1995: Slope hydroclimatology and hydrologic responses to global change in a small High Arctic basin; Ph.D. thesis, McMaster University, Hamilton, Ontario, 167 p.

Young, K.L., Woo, M., and Edlund, S.A.

1997: Influence of local topography, soils, and vegetation on microclimate and hydrology at a High Arctic site, Ellesmere Island, Canada; *Arctic and Alpine Research*, v. 29, no. 3, p. 270–284.

Glacier hydrology in the Sawtooth Range, Fosheim Peninsula, Ellesmere Island, Nunavut

P.M. Wolfe¹

Wolfe, P.M., 2000: Glacier hydrology in the Sawtooth Range, Fosheim Peninsula, Ellesmere Island, Nunavut; in Environmental Response to Climate Change in the Canadian High Arctic, (ed.) M. Garneau and B.T. Alt; Geological Survey of Canada, Bulletin 529, p. 375–390.

Abstract: An investigation of mass-balance conditions, superimposed-ice formation, and runoff–climate relationships was undertaken at Quviagivaa and Nirukittuq glaciers, Sawtooth Range, Fosheim Peninsula, in the summer of 1993.

Accumulation, primarily as wind-blown snow, is largely influenced by topography. Ablation, primarily as melt followed by runoff, decreases with increasing altitude, but varies greatly because of differences in surface albedo.

Superimposed ice is a major component of mass balance. Its formation showed a strong, positive relationship with initial snow water equivalent.

Runoff from the glacierized catchment was recorded for the entire season. For the main melt period, change in daily average discharge regressed against change in daily average air temperature at the glacier meteorological station (change from the average values of the previous day) produced a strong relationship.

Measurements in the Quviagivaa Creek basin suggest that the official Eureka weather station rain data cannot be applied to nearby mountainous regions, as there is the risk of greatly underestimating actual rainfall.

Résumé : Pendant l'été de 1993, on a étudié les bilans massiques, la formation de glace surimposée et la relation entre le climat et le ruissellement aux glaciers Quviagivaa et Nirukittuq chaîne Sawtooth, péninsule Fosheim.

L'accumulation de neige, surtout sous forme de neige apportée par le vent, est très influencée par la topographie. L'ablation, surtout causée par la fonte et le ruissellement, diminue si l'altitude augmente mais varie beaucoup en raison des différences d'albédo de la surface.

La glace surimposée est une composante importante du bilan de masse. Une relation très étroite existe entre sa formation et l'équivalent initial en eau de la neige.

On a enregistré le ruissellement du bassin versant du glacier pendant une saison complète. Pour la période principale de fonte, il existe une forte corrélation entre les changements du débit quotidien moyen et la variation de la température quotidienne moyenne à la station météorologique du glacier.

Les mesures effectuées dans le bassin du ruisseau Quviagivaa suggèrent qu'on ne peut pas utiliser les données officielles de la station météorologique d'Eureka pour les régions montagneuses puisqu'il y a un risque de sous-estimer grandement les précipitations réelles.

¹ Deceased

INTRODUCTION

Glacier hydrology involves the study of the accumulation, ablation, and movement of water, in both liquid and solid forms, on, under, and within glaciers. Arctic glaciers exist in a permafrost environment and most small glaciers are frozen to the bed, moving only through internal deformation, although larger glaciers (e.g. White Glacier, Axel Heiberg Island, and Laika Glacier, Coburg Island) have been shown to have a polythermal regime, whereby a temperate basal layer of ice exists in an otherwise cold glacier, allowing sliding over the bed (Blatter and Hutter, 1991). Although larger glaciers have internal drainage, as evidenced by the presence of moulins and artesian features, suggesting that water is reaching the glacier bed (e.g. John Evans and Gilman glaciers on Ellesmere Island), the hydrology of most small glaciers is simplified by the apparent lack of internal water movement. On the smallest glaciers, such as those studied in the Sawtooth Range, crevasses do not normally drain to the bed, moulins are uncommon, and runoff is concentrated in supraglacial and ice-marginal channels.

The brief summer season (June to August) is the period of greatest hydrological activity for arctic glaciers and understandably is the time frame of almost all hydrological research projects in the Arctic. Even in summer, cold temperatures result in processes that are distinct from those occurring on temperate ice masses. One of the most important features of High Arctic glaciers, which has a bearing on mass and energy balances and on runoff from the glacier, is the refreezing of meltwater on the glacier surface as 'superimposed ice' (Koerner, 1970a; Woodward, 1995). The purpose of a 1993 field expedition was to carry out measurements in one glacierized catchment in order to better understand the current regime and hydrological processes on the glaciers of the Sawtooth Range, Fosheim Peninsula. The primary objectives of the research project were as follows: to record in detail the hydrological cycle of a small High Arctic glacier in the Sawtooth Range using winter accumulation and summer ablation measurements on the glacier, meteorological data from stations on the glacier and on ice-free land 7 km west-northwest of the glacier, and a continuous discharge record from the creek draining the glacier; to examine hydrological processes occurring on the glacier, especially the extent, physical requirements for formation, and role of superimposed ice in the glacier mass balance; and to relate runoff from the glacierized basin to ablation and various hydrometeorological parameters, such as air temperature, precipitation, solar radiation, albedo, and wind speed, in order to determine the relative importance of these factors in producing glacier runoff.

This paper will discuss the main findings of the study in relation to the mass balance of the study glacier, with special reference to the formation of superimposed ice on the glacier and runoff from the study catchment.

REGIONAL SETTING AND FIELDWORK

Ellesmere Island contains approximately 80 000 km² of glacierized terrain, 53 per cent of the total glacier ice cover in Canada (Haeberli et al., 1989). Unlike most of the island, Fosheim Peninsula is largely ice-free, with the exception of the Sawtooth Range and several ice caps and glaciers on the higher land in the east. The Sawtooth Range, a 5 to 10 km wide, 85 km long mountain chain of folded and faulted, Tertiary, sedimentary rocks, trends north-northeast from the mouth of Vesle Fiord in the south to Cape With on Cañon Fiord in the north. The Sawtooth Range is home to more than 35 separate ice fields, valley glaciers, and cirque glaciers, which range in size from under 0.5 km² to 20 km² and cover approximately 75 km². Most glaciers are on the western side of the mountain range, although some that 'saddle' the divide also flow down the eastern slope. Most of the ice cover is found in the northern part of the range, where small ice caps support valley glaciers up to 5 km long. In the southern Sawtooth Range, most ice masses are small niche glaciers with limited valley extension. None of the glaciers reach much above 1300 m a.s.l. and it is likely that in warm summers, most of the ice in the range is below the average equilibrium-line altitude. Many deeply incised creeks and rivers are fed throughout the summer by melting snow and ice in the Sawtooth Range, including the headwaters of the Slide River, which drains most of western Fosheim Peninsula. Despite their close proximity to Eureka and the plenitude of research activity in the area, until 1993 no field studies had been carried out on the glaciers of Fosheim Peninsula.

An 8.7 km² glacierized catchment in the central Sawtooth Range (lat. 79°33.98'N, long. 83°20.48'W) (Fig. 1 and 2) was selected for study. The basin contains two small glaciers, Quviagivaa and Nirukittuq (unofficial names) (Fig. 3 and 4). The specifications of the catchment and the glaciers are summarized in Table 1. Quviagivaa Glacier was selected from over 35 glaciers in the Sawtooth Range for mass balance and related studies because it met the conditions of Østrem and Brugman (1991), namely that the study glacier has a well defined, highly glacierized catchment; a size comparable to adjacent glaciers, but small enough to be studied by two or three people; an elevational range from glacier terminus to upper limit as large as possible; one meltwater stream draining it; relatively easy access; few crevasses; and good maps, airphotos, and remote-sensing imagery. Quviagivaa Glacier met all considerations except the last and this was rectified in part after the 1993 field season by the creation of a topographic map of the basin from 1959 airphotos using photogrammetric methods.

Field work was undertaken between May 25 and August 11, 1993, from a camp 900 m west of the terminus of Quviagivaa Glacier. Most field work was concentrated on Quviagivaa Glacier and, to a much lesser extent, Nirukittuq Glacier. A brief visit was made to Quviagivaa Glacier on June 30, 1994, and several measurements were carried out.

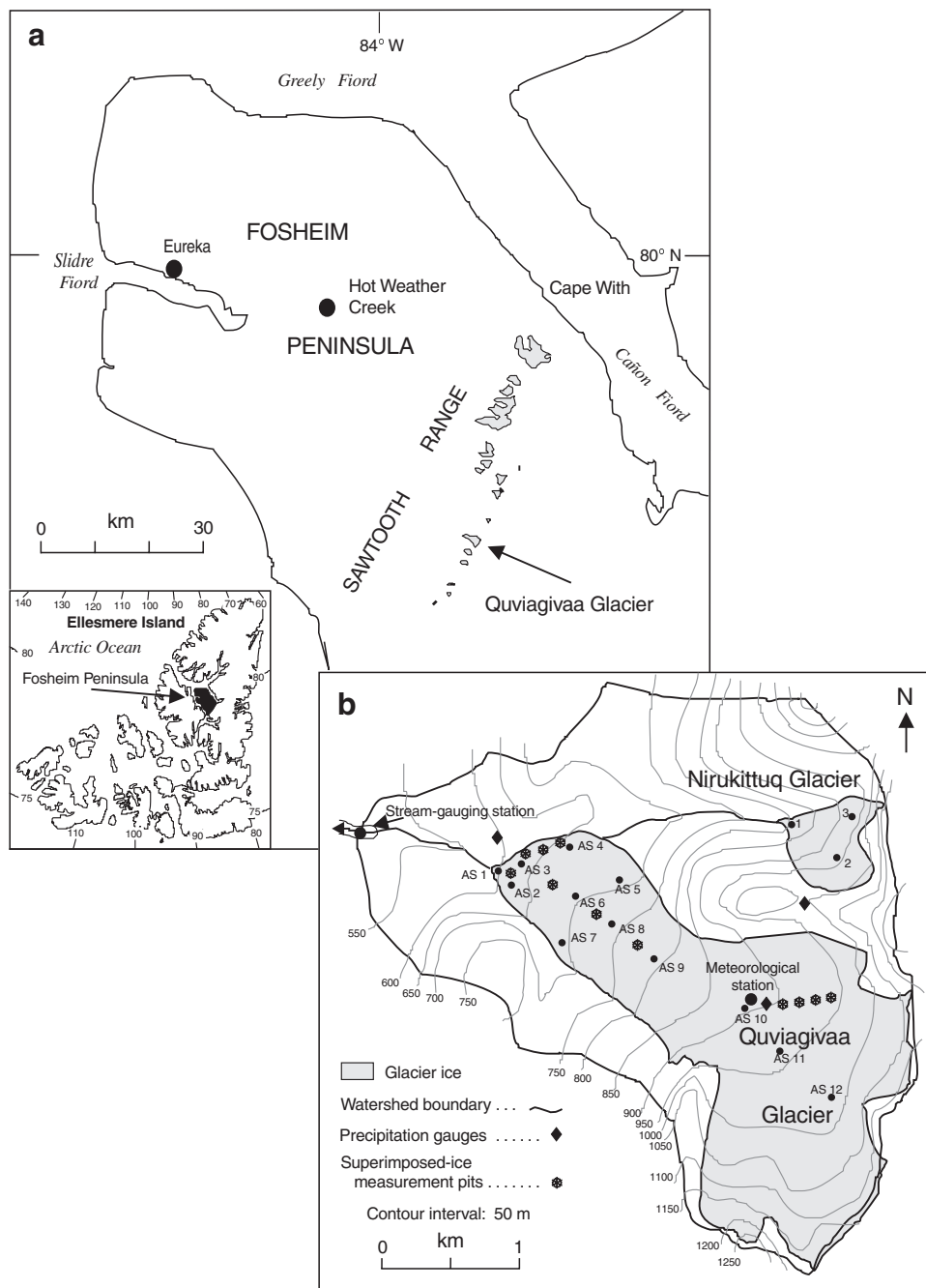


Figure 1. a) Location map of Quviagivaa Glacier on Fosheim Peninsula, Ellesmere Island. b) Topographic map of the Quviagivaa Creek basin, showing Nirukittuq and Quviagivaa glaciers and locations of measurement sites.



Figure 2. Oblique airphoto showing the central Sawtooth Range, including the Quviagivaa Creek basin. NAPL T453R-188



Figure 4. Nirukittuq Glacier, July 17, 1993. Photograph by P.M. Wolfe, GSC 2000-018B



Figure 3. Quviagivaa Glacier, July 22, 1993. Photograph by P.M. Wolfe, **a)** GSC 2000-018A1/2, **b)** GSC 2000-018A

METHODS

Accumulation and ablation

The 1992–1993 winter snow cover on Quviagivaa Glacier was measured on June 9 and 11, 1993. A total of 635 snow-depth measurements and 66 snow-pit-derived density measurements were used to draw a snow water-equivalent isomap.

Surface lowering on the glacier was measured at 12 ‘ablation stations’ throughout the summer, on alternate days at AS1 to AS10, and approximately once a week at AS11 and AS12 (see Fig. 1 for locations of AS1 to AS12). Each ablation station consisted of plastic wire strung between three, 1.8 m long aluminum stakes on each side of a 4 m triangle. The wire was marked off at 40 cm intervals, 1 m in from each stake, so as to avoid the disturbed snow and ice around the stake. Fifteen measurements were averaged to give a single value for each site.

On Nirukittuq Glacier, three, 1.8 m long, 19 mm diameter aluminum ablation stakes were installed, giving a stake density of 7.5 stakes/km². Stake measurements began prior to snowmelt and continued once a week until the end of the melt season.

A significant shortcoming of the stake network on Quviagivaa Glacier is that the elevations above 1000 m are unrepresented (although a single stake was installed at 1100 m in early August 1993), leaving 27 per cent of the glacier unmeasured. As an attempt to remedy this, the upper portion of the glacier was visited in late July and depths of firn were measured and the areal extent of superimposed ice was recorded. Although very good estimates of net ablation were made using a positive-degree-hours ablation model ($r^2 = 0.93$; $n = 16$), the mass-balance isolines for the upper portions of the glacier are less certain than those for the snout region.

Table 1. Specifications of the Quviagivaa Creek catchment and Quviagivaa and Nirukittuq glaciers.

	Quviagivaa Creek catchment	Quviagivaa Glacier	Nirukittuq Glacier
Type	proglacial	mountain valley glacier	niche glacier
Area	8.7 km ²	4.7 km ²	0.4 km ²
Elevation	491–1271 m a.s.l.	560–1250 m a.s.l.	800–1110 m a.s.l.
Latitude	79°34'N	79°34'N	79°34'N
Longitude	83°15'W	83°15'W	83°15'W
Orientation	west-northwest	west-northwest	northwest
Glacier number*		46424 C7	46424 C6
*Inland Waters Branch (1969–1972)			

During snow ablation, snow-density measurements were made to determine the water equivalent of melt by weighing a measured volume of snow from the melting portion of the snowpack. Ice-density measurements were not made and a density of 0.88 g/cm³ was applied to superimposed ice and 0.9 g/cm³, to glacier ice. The depth of the weathering rind (a surficial ice layer of lower density produced on days with high incoming solar radiation) was observed to be similar at most ablation stations at the beginning and end of the season, so a density of 0.9 g/cm³ is likely appropriate.

The standard error for each ablation station and the net mass balance is considered to be the sum of the observer and snow-density errors that gives a value of about 70 mm. This is an order of magnitude lower than the standard error of 200 to 250 mm given for the White Glacier (Cogley et al., 1995) and was attained because of the higher stake density, the glacier-wide snow survey, and the lack of inaccessible regions on Quviagivaa Glacier.

The formation of superimposed ice was monitored at all 12 ablation stations. Snow pits were dug at 10 locations prior to melt and the bottom of each pit was marked with red or blue chalk before being refilled with snow. Just prior to the total ablation of the snowpack, the snow-pit locations were excavated to the depth of the chalk layer, thereby allowing the measurement of superimposed-ice thickness. This method was not used in areas with a shallow snowpack, because of the potential for the chalk layer to absorb solar radiation and to melt the surrounding snow and ice. In firn zones, the measurement of superimposed-ice thicknesses using the two described methods can create error given the percolation of meltwater into the firn layers of previous summers. The error caused by internal accumulation is minimized on Quviagivaa Glacier because of the high regional elevation of the equilibrium line (1000–1200 m a.s.l. in the Sawtooth Range), which results in thin, high-density, icy firn on glacier surfaces not extending above this elevational range (Miller et al., 1975). Because of the low porosity of the icy firn from the summer of 1992 on Quviagivaa Glacier, it is assumed that in 1993 the superimposed ice formed preferentially on top of the firn. This assumption may not hold true for firn at the highest elevations of the glacier where measurements were not made.

Meteorology

Meteorological data were collected at the 'glacier' meteorological station at 875 m a.s.l. (Fig. 5, Table 2). Instruments were connected to a Campbell Scientific CR21X datalogger and hourly values of air temperature, wind speed and direction, incoming shortwave radiation (0.4–1.1 μm), and net radiation (0.25–60 μm) were recorded. Albedo measurements were made at each of 12 ablation stations every other day using a portable solarimeter mounted on a 75 cm long wooden rod, from which voltage was read using a multimeter. Precipitation was measured with Atmospheric Environment Service standard rain gauges at four sites within the basin: the camp meteorological station (550 m), the glacier terminus (590 m), the glacier meteorological station (875 m), and a ridge top between the two glaciers (1000 m). A second meteorological station, the 'Valley' site, was erected approximately 7 km west-northwest of the glacier site at an elevation of 230 m a.s.l. At this station, air temperature, wind speed and direction, incoming solar radiation, and soil temperature were recorded (*see* Alt et al., 2000).



Figure 5. Glacier meteorological station, July 10, 1993. Photograph by P.M. Wolfe, GSC 2000-018C

Table 2. Instrumentation of the glacier meteorological station.

Measurement	Instrument and model	Instrument height
Air temperature	Campbell Scientific Inc. 270F temperature/relative humidity	0.5 m
Wind speed and direction	R.H. Young wind monitor	0.5 m
Incoming shortwave radiation	Li-Cor LI 200SZ pyranometer	1.8 m
Net radiation	REBS Q*6 net radiometer	1.3 m
Snow-ice interface temperature	Campbell Scientific Inc. 107 temperature probe	snow-ice interface at four sites

Streamflow

A gauging station was set up in Quviagivaa Creek (the only outlet from the basin), approximately 900 m downstream from the glacier portal (Fig. 6). In a stilling well, stage was recorded using a potentiometer connected to a float and a counterweight. From June 17 to July 21, a Campbell Scientific CR21 datalogger recorded the stage every 30 minutes. Because the datalogger malfunctioned on July 21, a battery-operated Stevens Type F water-level recorder was used until the flow became too low to measure on August 8. Standard stream-gauging techniques were used to measure stream discharge. High flows on July 21 resulted in the aggradation of the streambed, necessitating two separate stage-discharge curves, one for the period of June 14 to July 21 ($r^2=0.98$, $n=15$), and one for the period of July 22 to August 10 ($r^2=0.99$, $n=13$). The main melt period was determined from the hydrograph as the period in which strong diurnal variations in stream discharge were evident. Daily discharge values were taken as the sum of hourly values from trough to trough on the hydrograph. This method accounts for the lag (<1 day) for most melt in the catchment to reach the gauging station.



Figure 6. Quviagivaa Creek stream-gauging station. The upper reaches of Nirukittuq Glacier are just visible in the upper left corner of the photograph. Photograph by P.M. Wolfe, GSC 2000-018D

SUMMARY OF RESULTS

Winter mass balance

The 1992–1993 winter accumulation of was very close to its maximum on June 9 and 11, when snow surveys were conducted on the glacier. To calculate the 1992–1993 winter mass balance, an isomap of accumulation was produced (Fig. 7), which gave an average value of 303 mm water equivalent.

The accumulation pattern is strongly influenced by the topography of the glacier. Accumulation is not highly dependent on altitude, but is most affected by the topographically influenced deposition of wind-transported snow, both during and after snowfall events. The greatest snow depths were recorded at the terminus of the glacier, which is sheltered from all winds excepting those blowing down-glacier, whereas the snowpack is significantly reduced on the central

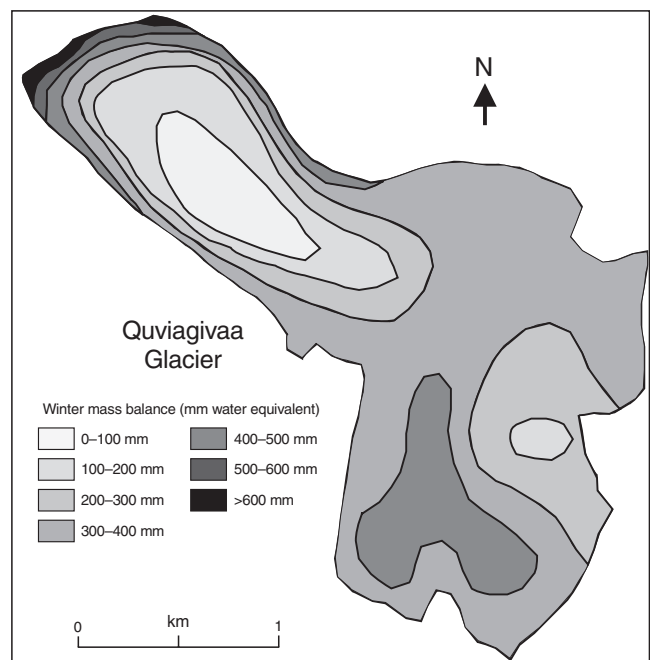


Figure 7. Map of winter mass balance, 1992–1993, for Quviagivaa Glacier.

snout of the glacier, which is convex and exposed to winds from all directions. The 1993 melt season ended on August 3 and the 1993–1994 accumulation season began abruptly on August 3 with a snowfall event followed by a week of high winds, subzero temperatures, and additional snowfall. A snow-depth survey carried out on the lower half of the glacier on August 10 determined that the pattern of accumulation after strong winds from the southeast and east on August 8 and 9 respectively closely resembles the pattern of the previous spring, with the highest accumulation at the terminus and the lowest accumulation on the central snout. This further suggests the important control exerted by glacier geometry on accumulation patterns.

Summer mass balance

Melt was first measured on June 7 at AS1 and continued almost uninterrupted from June 29 to August 3 due to consistently above-zero temperatures (except for July 2). Figure 8 shows the isomap of summer melt drawn using the 12 ablation-station data points. A regression of stake elevation and total summer ablation at ablation stations 1 to 12 shows decreasing melt with increasing altitude ($r^2 = 0.804$; $n = 12$), although total melt is not dependent on altitude alone. Ablation stations 5 to 7 are located within 5 m of elevation of each other, yet cumulative melt differs by 177 mm at AS6 and AS7. In fact, cumulative ablation varies by a similar amount across the glacier snout at an altitudinal range of 684 to 688 m a.s.l. as it does up the glacier snout from AS6 to AS9, where the altitudinal range is nearly 100 m. Much of the spatial difference in melt rate can be explained by the albedo measured at the sites. Sites at which darker glacier ice was exposed earlier (AS6 and AS9) had higher total melt values. Slush flows

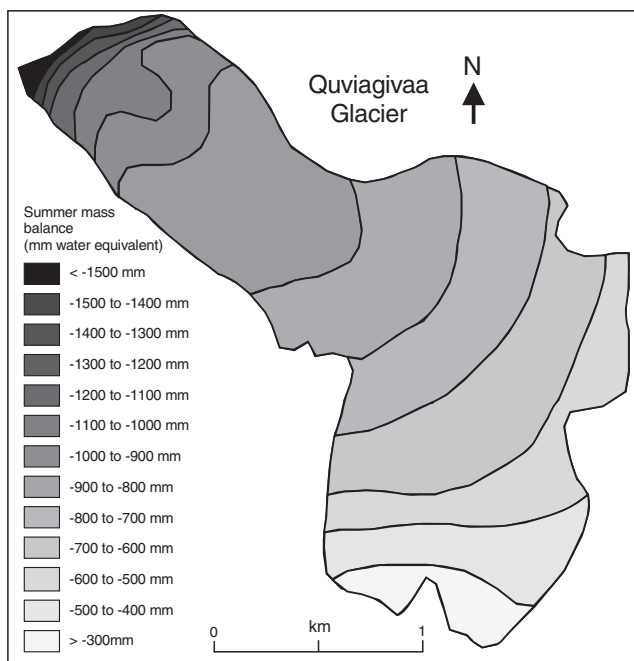


Figure 8. Map of summer mass balance, 1993, for Quviagivaa Glacier.

into the AS7 area and the north-northwest aspect of AS5 likely also contributed to the lower ablation amounts at those stations.

Net mass balance

Because of the small size of Quviagivaa Glacier, the availability of an equi-accumulation map for the winter mass balance, and the familiarity of the author with patterns of melt on the glacier through the summer, an equi-ablation map was drawn as the potentially most accurate means of calculating the net mass balance (Fig. 9). One measurement of firn accumulation at 1100 m at the end of the season gave a maximum value of accumulation on the glacier, but the graphical interpolations from 1000 to 1250 m are still problematic. To justify the placing of the equi-ablation lines in the upper portions of the glacier, a simple model was developed to estimate melt at the unmeasured elevations. Positive degree hours (PDH) were calculated as the sum of all hourly temperature values greater than 0°C during periods of measured melt at the glacier meteorological station. Although a crude method, an r^2 value of 0.93 gave very good confidence in the relationship between cumulative screen air temperature at 50 cm and melt.

Positive degree days and estimated melt were calculated at 50 m intervals to the top of the glacier using temperature lapse rates, which were taken from the difference in screen temperature between the glacier meteorological station (875 m) and the valley meteorological station (230 m). Estimated and measured melt at AS10 to AS12 agree within 2 per cent and estimated melt is likely to be within 5 per cent of actual melt at higher elevations. Using the temperature–melt relationship to calculate total summer ablation at 1100 m a.s.l.

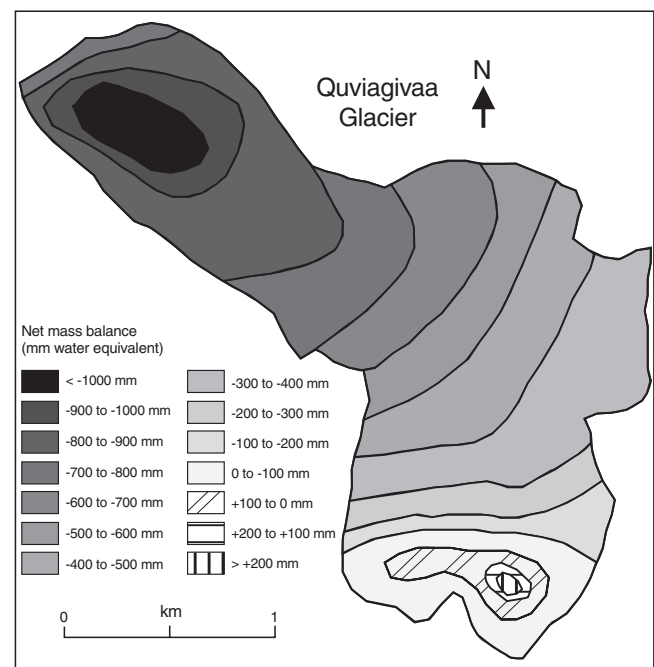


Figure 9. Map of net mass balance, 1992–1993, for Quviagivaa Glacier.

and taking into account the formation of superimposed ice gives a maximum estimated accumulation of 219 mm. This estimate is within 10 per cent of a spot measurement taken at 1100 m at the end of the field season and justifies the placement of the +200 mm isoline on the net mass-balance map. A band of net ablation was observed at the top of the glacier despite the fact that estimated positive-degree-day totals for elevations at the top of the glacier are only 30 per cent of those at the meteorological station. More heat is likely available here for melting because of heat advection from the surrounding slopes, which become snow-free in mid-July, and because of a reduction in albedo caused by rock falls, sediment carried by runoff, and eolian deposits from the adjacent rock slopes.

Climate records from Eureka (70 km west-northwest of the study site) show that the summer of 1993 had the fourth warmest July in the 46-year record. The summer of 1993 was an above-average melt year, despite the early end to melt in the first week of August as a result of a prolonged snowstorm. A dirty, net ablation surface stretched to the top of the glacier on the north side (>1100 m a.s.l.) (Fig. 10). Several small glaciers adjacent to the study catchment were visited at the end of the ablation season. All were devoid of snow and several had dirt-laden ablation surfaces extending to their upper reaches. Strongly negative mass balances were recorded on the White and Baby glaciers on Axel Heiberg Island, and on Melville and Meighen island ice caps in 1993. High melt was also recorded on the Agassiz Ice Cap in northern Ellesmere Island (R.M. Koerner, pers. comm., 1994), suggesting that the negative mass balance of the Sawtooth glaciers reflected the regional situation. Assuming that retreat at the low-angle terminus of Quviagivaa Glacier is proportional to warming, the recession (reaching a maximum of 4.3 m/a at the point of greatest retreat), as seen from 1959 and 1994 airphotos, suggests that the normal mass balance for the Sawtooth glaciers is only slightly negative (Fig. 11). The trimlines (about 40 m above the glacier surface at 850 m a.s.l.) (see Fig. 3), are assumed to represent the most recent period of maximum ice extent, most likely reached during the so-called 'Little Ice Age' (the trimline marks the border between rocks colonized by lichens and those not colonized). At that specific location,



Figure 10. Photograph of the northeast corner of Quviagivaa Glacier showing the dirty, net ablation ice surface. Note the trimline that extends to the very top of this corner of the glacier. Photograph by P.M. Wolfe, GSC 2000-018E

the height of the trimline suggests that average summer melt since the Little Ice Age has been less than half the net mass balance of -532 mm measured in 1993.

Superimposed ice

The measurement of superimposed ice on Quviagivaa Glacier showed that a positive relationship exists between initial snow water equivalent and maximum superimposed-ice formation (Fig. 12). Other factors that enhanced the

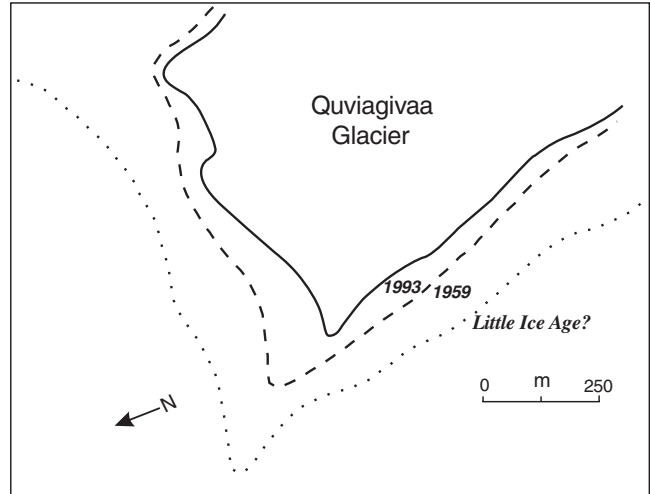


Figure 11. Terminus locations of Quviagivaa Glacier for 1993, 1959, and the estimated ice margin during the Little Ice Age.

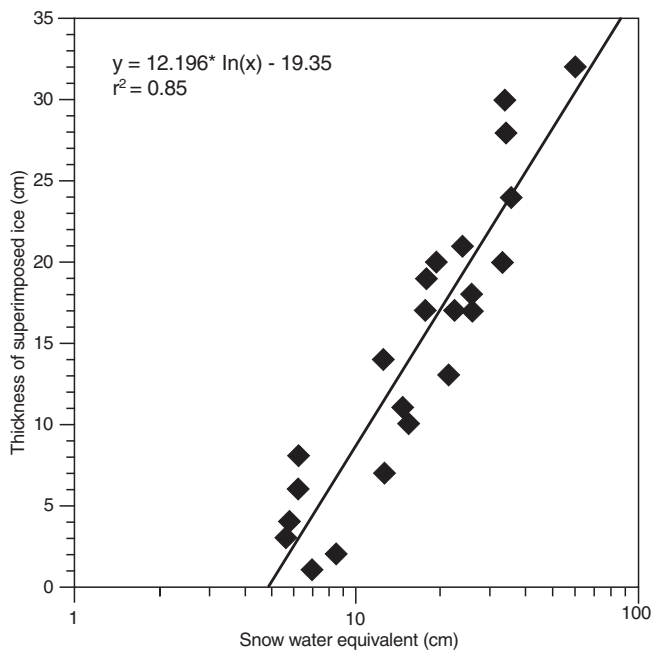


Figure 12. Maximum thickness of superimposed ice as a function of snow water equivalent at 23 sites on Quviagivaa Glacier.

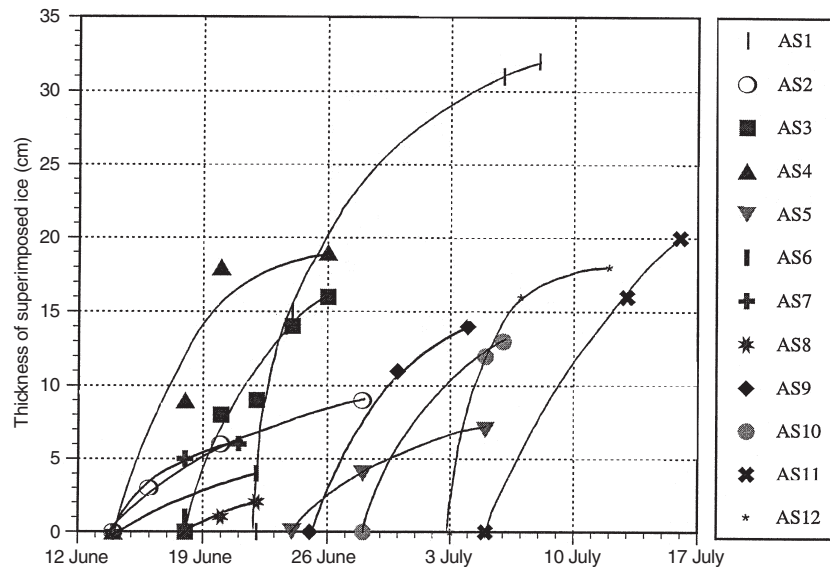


Figure 13. Superimposed-ice growth curves at ablation stations (AS) 1 to 12.

growth of superimposed ice were a cold snow–ice interface (insulated by a deep snowpack), a continuous supply of meltwater, a gentle slope, and a rough glacier surface. The growth of superimposed ice was found to follow a curve in which the most rapid accretion occurred in the first few days of formation. This rapid growth occurs when the snow–ice interface is still well below freezing and the growth curve flattens out as the snow–ice interface is warmed by the release of the latent heat of freezing, despite the greater supply of meltwater (Fig. 13). Figure 13 shows that superimposed ice did not form first at the lowest elevations, but rather at the locations with the shallowest snowpacks, likely because of the quicker arrival of meltwater at the ice surface. The maximum thickness of superimposed ice was measured near the terminus of Quviagivaa (32 cm), where initial snow depths were over 1.5 m. Areas of low superimposed-ice formation (<1 cm) were located on the central snout of the glacier, where initial snow depths were less than 15 cm. Deep snow and the accumulation of slush-flow deposits along the lower margins of both glaciers produced the thickest superimposed ice measured, some of which survived into the last half of July. At 23 sites on Quviagivaa Glacier, an average of 67 per cent of the snowpack water equivalent formed superimposed ice. The average percentage of snow water-equivalent forming superimposed ice was the same for the upper and lower portions of the glacier, although measured variability was greater on the snout of the glacier because of the greater redistribution of mass through slush flows and the larger variation in snow depth.

Figure 14 shows that at the end of the melt season, only a small patch of superimposed ice, representing less than 5 per cent of the glacier area, remained at the top of Quviagivaa Glacier. All of the superimposed ice formed in 1993 on Nirukittuq Glacier and on many of the small, neighbouring glaciers ablated by the end of the melt season. Some superimposed ice formed on approximately 95 per cent of Quviagivaa

Glacier and the areal mean maximum thickness of superimposed ice was 17.2 cm. This value suggests that if no superimposed ice formed on the glacier, the net mass balance would be 28 per cent more negative. The presence of extensive areas of superimposed ice in the upper regions of the glacier, which were exposed at the end of the melt season (likely formed in 1992 and/or in previous summers), and of patches of superimposed ice at the terminus of both study glaciers, which per-

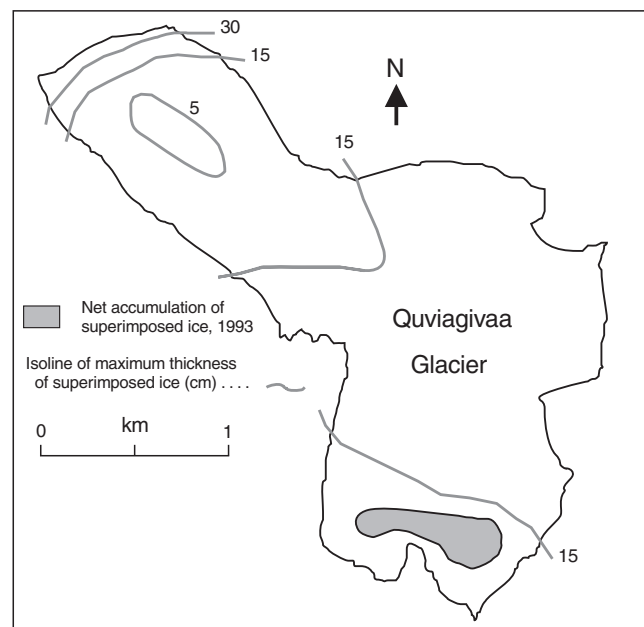


Figure 14. Map of maximum formation of superimposed ice during the melt season and coverage at the termination of the 1993 melt season.

sisted into the last week of the melt season, indicates the possibility for net accumulation of superimposed ice on up to 65 per cent of the glacier surface. The apparent location of zones of superimposed ice at the terminus of both glaciers also makes it difficult to describe a single equilibrium-line elevation.

General observations of discharge

Figure 15 shows the complete annual record of runoff for the 8.7 km² Quviagivaa Creek drainage basin and average daily meteorological elements from the glacier meteorological station for the same time period. Using the characteristics of the hydrograph and taking into account the progression of melt in

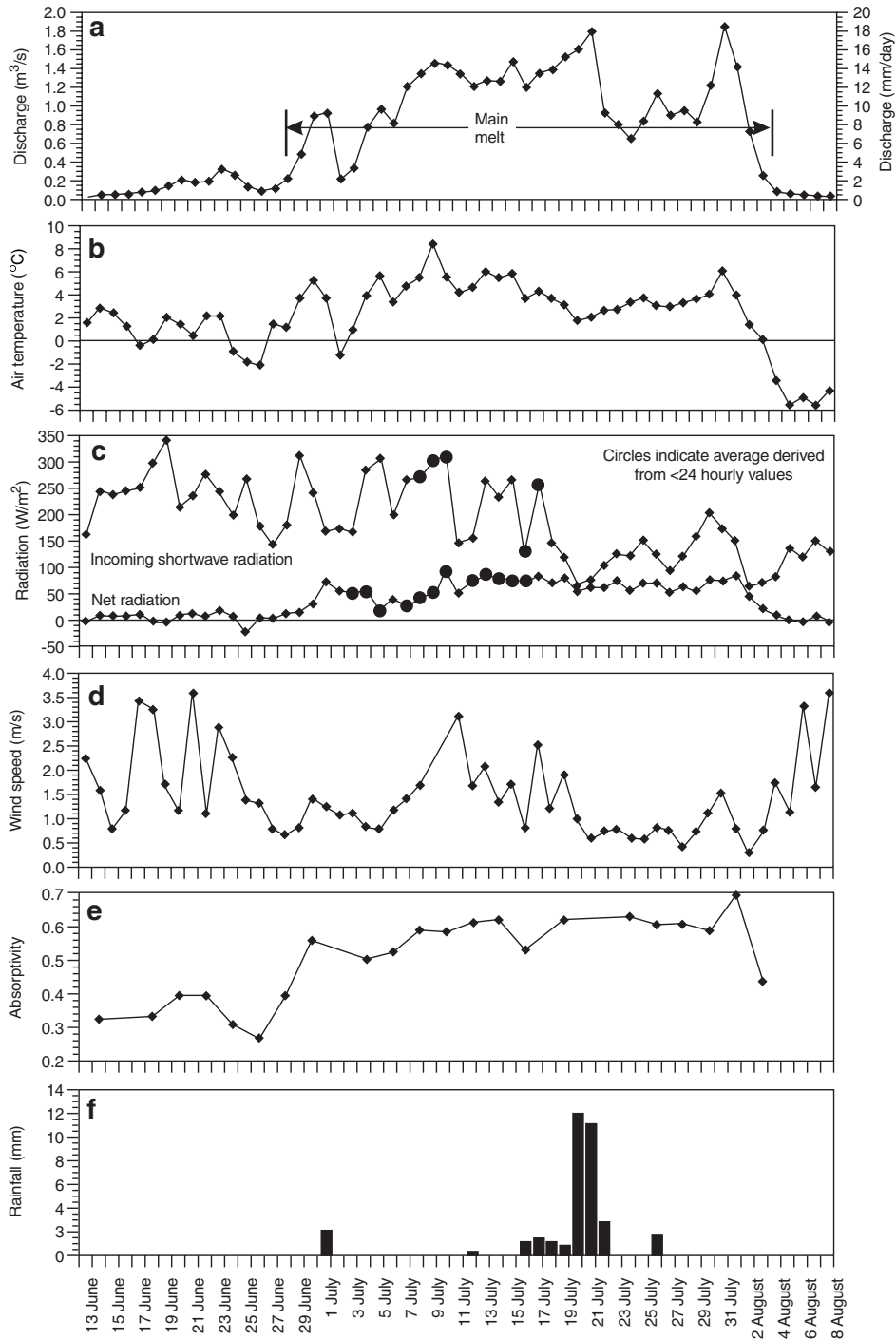


Figure 15. Plots of discharge and meteorological elements for the period of streamflow, 1993. **a)** Average daily stream discharge; **b)** average daily air temperature; **c)** average daily incoming shortwave radiation and net radiation; **d)** average daily wind speed; **e)** average daily surface absorptivity; **f)** daily precipitation.

the glacier catchment, the discharge record can be divided into three periods, early melt, main melt, and recession (Jensen and Lang, 1972). This section will deal only with the main melt period, which is the only period in which the bulk of runoff was glacier derived.

The main melt period was characterized by strong diurnal fluctuations in discharge, with daily peaks ranging from 0.5 to 3.0 m³/s. This period, lasting from June 29 to August 3, included 94 per cent of all flow measured in 1993. Synchronous discharge measurements at the glacier terminus and at the gauging station at the beginning of the main melt period (June 29) revealed that approximately 50 per cent of flow was derived from snowmelt on the nonglacierized slopes downslope from the glacier. Late on 29 June, a large slush flow (Fig. 16) occurred on the lower snout of the glacier; it fully established a pathway for flow from the northern glacier ice margin to Quviagivaa Creek and moved a large mass of saturated snow off the glacier. Because of above-freezing temperatures and high radiation values, melt proceeded rapidly from June 29 onwards and on July 5, a large slush pool that had been forming near the glacier meteorological station burst, creating numerous slush flows (Fig. 17) and opening flow pathways from the upper portions of the glacier. Comparisons of discharge measurements made at the glacier terminus and gauging station on July 9 showed that the percentage of total flow derived from snowmelt on the nonglacierized slopes downslope from the glacier had been reduced to 10 per cent.

Consistently warm temperatures in early July meant that by the middle of the month non-ice surfaces in the basin were predominantly free of snow. The seasonal peak discharge of 3.0 m³/s occurred on July 21 during a prolonged rainy period in which up to 40 mm of rain fell on the largely snow-free glacier. Reduced discharge due to low air temperature, radiation, and wind speed persisted for a week after July 21, but was followed by high melt rates and discharge values from July 30 to August 1 (*see* Fig. 15).



Figure 16. A large slush flow at the terminus of Quviagivaa Glacier, June 29, 1993. Photograph by P.M. Wolfe, GSC 2000-018F

By the beginning of August, the drainage network had extended over virtually the entire glacier, some supraglacial channels having been incised to depths of 2 m. Temperatures dropped below 0°C on August 3, ending melting in the catchment.

Hydrometeorological conditions and runoff — air temperature

The period of main melt (June 29–August 3) was used to study the relationships between runoff and individual meteorological parameters. Because of the overwhelming signal that the large precipitation event on July 20–21 had on flow, data from those dates were not used in the statistical analyses.

A scattergraph of the change in average daily air temperature versus the change in average daily discharge (from the values of the previous day) was produced for the main melt period (Fig. 18). In Figure 15, the temporal changes in the temperature-discharge relationship, which reduce the r^2 value in Figure 18, are easier to see. Although melt occurred throughout the basin from June 12 onwards, a significant lag effect was produced primarily because of snow dams in the stream bed, retention of meltwater within the snowpack and crevasses, and the formation of superimposed ice on the glacier. Primarily because of snow dams in the creek bed and a thick snowpack at the terminus of the glacier, flow during the first week of measurement (*see* Fig. 15) was confined to the nonglacierized slopes below the glacier, thereby restricting the area of contribution of flow to under 10 per cent of the drainage basin. Runoff generated from melt in the upper sections of the glacier was initially impeded (early July) by numerous transverse crevasses until they filled with water. Storage of runoff as superimposed ice was likely a major cause of low discharge values on days such as June 30 and July 5, when high temperatures did not result in peak discharges as high as for days with similar temperatures in late July. The formation of superimposed ice is widespread early in the melt season, when meltwater percolating through the winter snowpack refreezes immediately as it reaches the still



Figure 17. Advancing slush flow on the central snout of Quviagivaa Glacier, July 5, 1993. Photograph by P.M. Wolfe, GSC 2000-018G

cold (-5 to -10°C) glacier surface, and is less common when the snow has disappeared and the glacier surface has warmed to 0°C (see Fig. 13). The formation of superimposed ice varies in time and space on the glacier surface, occurring progressively later at higher elevations and in areas with deeper snowpacks (>1 m). In the ablation zone, this ice melted and contributed to runoff some two to four weeks after it was formed. In regions of net accumulation, superimposed ice will remain until the next melt season or longer.

Predicting runoff using multiple variables

The best prediction of average daily discharge during the main melt period was achieved using a multiple regression of discharge with average daily air temperature, incoming shortwave radiation, net radiation hours, and wind speed (variables are listed in order of decreasing importance to the multiple regression). The resulting equation, significant at the 99 per cent confidence interval ($r^2=0.84$), is as follows:

$$y = 0.315(T) - 0.00248(K) + 0.000217(NRH) + 0.11767(W)$$

where T = average daily air temperature (°C), K = average daily incoming shortwave radiation (W/m^2), NRH = daily net radiation hours (W/m^2), and W = average daily wind speed (m/s). Using the four variables, the resulting standard error is $\pm 0.165 m^3/s$.

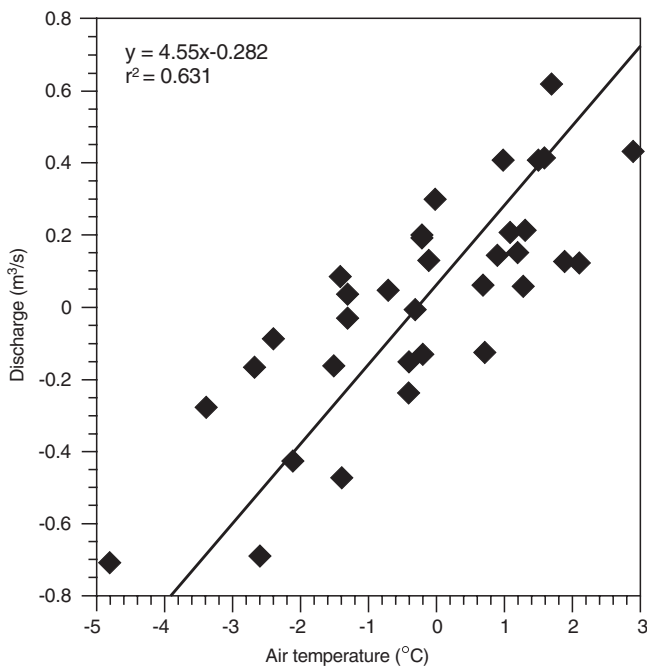


Figure 18. Scattergraph of the change in average daily air temperature and the change in average daily discharge compared to the values of the previous day.

DISCUSSION

During the last decade, no new glacier mass-balance studies have been initiated in the Canadian High Arctic and currently no other small valley glaciers are being investigated there. The closest comparable glaciers studied in the Canadian High Arctic are White and Baby glaciers on Axel Heiberg Island.

One of the most significant factors influencing the distribution of mass balance on Quviagivaa Glacier is high snow accumulation at the glacier terminus and low snow accumulation in the central portions of the snout. This pattern reduces net ablation at the terminus, thereby helping to maintain the areal extent of the glaciers, and results in a poor relationship between accumulation and altitude. This pattern has also been observed on the terminus of Icewall Glacier, an outlet of the Laika Ice Cap on Coburg Island, which, because of its lee slope and concave topography, accumulates the largest amount of firn on the entire ice cap (Blatter and Kappenberger, 1988). The high snow accumulations at the glacier terminus stop slush flows at the snout. This was especially evident on Nirukittuq Glacier, where slush mounds at the terminus measured over 80 cm deep. Baby Glacier, similar in shape to Nirukittuq, also has large snow and slush-flow deposits at its snout and this produced near-equilibrium conditions at the snout in 1991 (Dicks et al., 1992).

In 1993, the equilibrium line (ignoring the accumulation outlier) was located above the upper elevations of Quviagivaa Glacier. This situation has also occurred at other glaciers that do not reach above about 1200 m a.s.l. and for which ablation and accumulation (largely influenced by glacier geometry) are more important than elevation to the net mass balance (Blatter and Kappenberger, 1988). However, it must be noted that accumulation and especially ablation are controlled to a degree by the decrease in air temperature with elevation. During a cool summer with a positive net balance, Quviagivaa Glacier would probably have net accumulation zones at both the top and bottom of the glacier and net ablation in the exposed central snout region. This was likely the case in 1992, a cooler than average summer, as large areas of the ablation zone had net accumulations of superimposed ice. This pattern has also been found on Baby Glacier in cool years (Cogley et al., 1995). Larger glaciers such as White and Gilman, which extend several hundred metres above the highest measured equilibrium line (1444 m and 1240 m a.s.l. respectively) and have exposed terminus locations at elevations (<350 m), will not develop this mass-balance pattern (Hattersley-Smith et al., 1961; Cogley et al., 1995).

The record of superimposed-ice formation is significant in relation to the emphasis on the parametrization of mass-balance processes in ice-sheet modelling (Reeh, 1991). A value of 67 per cent of snowpack water equivalent forming superimposed ice is slightly higher than the estimate of Reeh (1991). The strong, positive relationship between initial snow water equivalent and superimposed-ice thickness, with no formation of superimposed ice for snow depths under 15 cm, is significant, but is likely only valid for areas below the

equilibrium line. It was calculated that without the formation of superimposed ice, the net mass balance of Quviagivaa Glacier would have been 28 per cent more negative in 1993. Put another way, in the absence of any formation of superimposed ice, the 1993 summer melt would have to have been reduced by 60 per cent for the glacier to be in a balanced state. This highlights the importance of superimposed ice to the mass balance in a region where snow accumulation is relatively low.

The record of discharge in this paper is significant simply because of the paucity of glacier runoff data from the Canadian arctic islands. Reasons for the small number of studies include the logistical constraints and high costs of reaching the study sites and the many difficulties involved in the collection of hydrological data in the High Arctic, such as snow-filled streams and aufeis deposits and extreme summer flows caused by rain events and high-melt periods that tend to rearrange channel geometry and wash away weirs, stilling wells, and recording devices. The only complete-season glacier discharge records from the arctic islands are from two Baffin Island glaciers, the Lewis Glacier in 1963 and the Decade Glacier in 1965 (Anonymous, 1967; Østrem et al., 1967).

Over the entire melt season, runoff from glacier basins does not correlate well with meteorological data. The complex relationship is due to the fact that only parts of the basin contribute to flow at the onset of melt and to a melt-runoff lag that varies spatially and temporally. Working in a glacierized basin in the Swiss Alps, Jensen and Lang (1972) successfully used separate regression equations to forecast discharge by subdividing the melt season into three intervals (main snowmelt, main ablation season, and reduced ablation). For this study, the relationships between discharge and meteorological elements were analyzed for the period of main melt, in which almost the entire basin contributed to runoff. In a study on Mikkaglaciaren in Arctic Sweden, Stenborg (1970) estimated that 25 per cent of the total summer discharge was delayed from the early to the middle part of the summer. The factors that give rise to this lag (Stenborg, 1970) are listed here in their approximate order of quantitative importance for Quviagivaa Glacier for the summer of 1993: 1) the formation of superimposed ice in June and early July; 2) slush pools above 875 m a.s.l. formed by rapid melting of the snowpack in early July; 3) snow dams in the glacier marginal streams and in the streambed below the glacier, which caused partial to total restriction of flow in June; 4) storage of meltwater in crevasses that do not drain to the bed; 5) the limited development of supraglacial channels at the beginning of the melt season, forcing the meltwater to move across the rough glacier surface; and 6) capillary storage of meltwater in the spring snowpack and firn.

When ablation of the snowpack is nearly complete, the capillary storage of meltwater is small and after crevasses fill up with water they no longer create a significant lag in discharge. The formation of superimposed ice is no longer widespread and flow pathways in the basin are established. The prediction of runoff from meteorological elements in this 'main melt' or 'limited lag' period then becomes more straightforward (Colbeck, 1977).

Although climate and runoff relationships are described in several arctic glacier studies (Keeler, 1964; Adams, 1966), no studies correlate unit values of stream discharge with meteorological elements in a glacierized basin. One of the most significant findings of the present study is that during the main period of melt, average discharge shows a strong, linear relationship with average air temperature on the glacier. Several studies have shown a positive relationship between temperature and runoff in alpine basins (Jensen and Lang, 1972; Østrem, 1972); however, the runoff-temperature relationship is not simple and many other factors such as albedo, radiation, wind speed, and precipitation play an important role in the production of runoff (Collins, 1984).

Net radiation is in most cases the largest source of energy for ablation on arctic glaciers (Braithwaite, 1981). However, as has been found on glaciers in the Arctic and in the Alps (Jensen and Lang, 1972), net radiation at Quviagivaa Glacier does not correlate as well with ablation or discharge as with air temperature. Konzelmann and Braithwaite (1995), while stating that net radiation is the major source of ablation energy, suggest that due to the high variability of surface albedo, spot measurements of net radiation will not give an accurate picture of the larger scale energy balance.

The importance of surface albedo to ablation is well known and van de Wal et al. (1992) have shown that variations in albedo across the snout of Hintereisferner explain most of the difference in ablation during the melt season. Since variations in surface absorptivity correlate strongly with ablation, surface absorptivity should also be the principal element determining differences in runoff.

Although in this study, wind does not show the highest correlation with discharge, it is known to cause an increase in the vertical temperature gradient and in sensible heat transfer to the glacier surface (Ohata, 1989). Working on the margin of the Greenland ice sheet, Dyonkerke and van den Broeke (1994) found that the combined katabatic (down-glacier wind) and thermal-wind (induced by the adjacent warm tundra surface) effect was to enhance the transport of sensible heat to the ice surface. Keeler (1964), working on the Sverdrup Glacier, Devon Island, found that the highest ablation rates were due to the turbulent transfer of heat during periods of high winds, high temperatures, and high humidity.

In numerous proglacial basins, rain events are related to peak annual discharges. In the White Glacier catchment in 1961, rain-induced peak flows washed out the weir, terminating stream-discharge measurements for the season (Adams, 1966). Similar peak flows also occurred in the Lewis and Decade glacier basins in 1965 and in the McCall Glacier basin in 1969 and 1970 (Anonymous, 1967; Østrem et al., 1967; Wendler et al., 1972). Cogley and McCann (1976) describe an exceptional storm that produced peak flows in the proglacial 'Sverdrup' and 'Schei' rivers at Vendom Fiord, Ellesmere Island, when 54.6 mm of rain fell July 21–23, 1973. They note that the storm would have gone unnoticed without measurements taken at research stations located away from the official High Arctic weather stations. A similar situation occurred on July 19–22, 1993, when 9.2 mm of rain were recorded at Eureka and 34.1 mm were measured at the

terminus of Quviagivaa Glacier. This suggests that brief, but significant, summer precipitation events play a much greater role in runoff in glacierized catchments than would be expected from the precipitation records from official weather stations nearly at sea level.

CONCLUSIONS

The hydrological cycles of two High Arctic glaciers were studied for the duration of the melt season in a small catchment (8.7 km²) in the Sawtooth Range. The following conclusions can be reached.

Accumulation on Quviagivaa (4.7 km²) and Nirukittuq (0.4 km²) glaciers is predominantly in the form of wind-blown snow and is controlled primarily by topography. The highest snow accumulations are at the sheltered terminus areas of each glacier. Melt is sensitive to altitude, although variations in albedo across the glacier surface strongly influence ice ablation and degrade the general relationship of decreasing ablation with increasing altitude. The net mass balance of Quviagivaa Glacier in 1992–1993 was -532 mm. Meteorological records from Eureka, a weather station 70 km west-northwest of the glacier site, show that 1993 had the fourth warmest July in the 46 years of record, thereby suggesting that the normal mass balance for the Sawtooth glaciers is less negative. A photographic comparison of the snout of Quviagivaa Glacier between 1959 and 1994 revealed a maximum retreat of 150 m at the terminus, perhaps indicating that small, negative balances were normal for the period.

The formation of superimposed ice was found to be a vital factor in the survival of Quviagivaa Glacier, as, on average, 67 per cent of the snowpack water equivalent formed superimposed ice. Maximum thicknesses of superimposed ice averaged 17 cm and ranged from 0 to 32 cm, showing a strong, positive relationship with initial snow water equivalent. A small patch of superimposed ice remaining on Quviagivaa Glacier at the end of the season represented under 5 per cent of the total glacier area, whereas all superimposed ice formed on Nirukittuq Glacier during the 1993 melt season ablated.

Runoff from the glacierized catchment was recorded from June 14 to August 9, 1993, and totaled 3 522 900 m³. The daily ablation was found to be a good predictor of daily runoff at AS2–AS11. Daily average air temperature from the glacier meteorological station was found to be the best meteorological indicator of daily runoff ($r^2 = 0.58$), although a better relationship was produced ($r^2 = 0.84$) using a multiple regression of discharge with air temperature, wind speed, incoming shortwave radiation, and net radiation hours. Precipitation was found to have the most dramatic effect on runoff, producing the highest discharge of the season on July 21. Measurements at Quviagivaa suggest that the official Atmospheric Environment Service Eureka weather station rain data cannot be applied to nearby mountainous regions, as there is the risk of greatly underestimating actual rainfall.

FUTURE WORK AND RECOMMENDATIONS

The field study at Quviagivaa Glacier lasted only one summer. However, several mass-balance stakes were installed at the end of the 1993 season and it is hoped that the stakes near the equilibrium line will be locatable when the site is next visited.

One of the main methods of reconstructing net mass balance for specific glaciers will be the analysis of ice cores from the zone of superimposed ice. A reconstruction of net mass balance from a core of superimposed ice has been achieved by one group of researchers working in Svalbard who used conductivity, microparticle concentration, and stratigraphic analysis to obtain annual resolution (Jonsson and Hansson, 1990). From the work done at the Quviagivaa Glacier, the White Glacier, and on the Devon Ice Cap, we know that the zone of superimposed ice on glaciers in the Canadian High Arctic can vary considerable in size and altitudinal extent from year to year (Koerner, 1970b; Cogley et al., 1995). As described in this paper, the net accumulation of superimposed ice on Quviagivaa Glacier in 1993 consisted of a small patch near the top of the glacier. Since some net accumulation of superimposed ice did occur even in the above-average warmth of the summer of 1993, it could be suggested that in such locations, a distinct layer of superimposed ice is formed each summer that can be counted using some of the methods used by Jonsson and Hansson (1990). Potentially, accurate dating using ¹³⁷Cs could be achieved by the identification of radioactive peaks. Radioactive peaks in polar firn and ice occur in layers laid down in 1963 as a result of atmospheric nuclear-bomb testing in the Russian Arctic and in 1986 as a result of the Chernobyl accident. The identification of these horizons would allow the calculation of 1963–present and 1986–present net mass-balance records. This method has proved successful in cores of superimposed ice using the 1963 radioactive peak (Koerner and Taniguchi, 1976; Dowdeswell and Drewry, 1989; Pinglot et al., 1996) and cores of firn/superimposed ice using the Chernobyl radioactive peak (Lefauconnier et al., 1994). Since both 1963 and 1986 were cool summers in the Canadian High Arctic, it is reasonable to assume that the radioactive peaks from those years were well preserved over a wide region in zones of superimposed ice.

A method that would speed the process of mass-balance reconstruction over a larger area involves the identification of radioactive layers in boreholes using a gamma-ray detector (Pinglot and Pourchet, 1981, 1989; Dunphy and Dibb, 1994). This time-saving method would allow relatively quick sampling on numerous glaciers. In addition, if two or more boreholes were sampled at different elevations in the zone of long-term, superimposed ice, a mass-balance gradient could be constructed from which the long-term equilibrium-line altitude could be estimated. In addition, the ablation zone can be easily identified by the concentration of radioactivity at the glacier surface (Pinglot et al., 1996). This method is especially attractive for glaciers such as those in the Sawtooth Range, many of which can become entirely net ablation surfaces in very warm summers, thereby limiting the possibility of reconstructing an annual net accumulation record.

REFERENCES

- Adams, W.P.**
1966: Ablation and run-off on the White Glacier, Axel Heiberg Island, Canadian Arctic Archipelago; *Glaciology*, No. 1, Axel Heiberg Research Reports, Jacobsen-McGill Arctic Research Expedition 1959-1962, McGill University, Montreal, 77 p.
- Alt, B.T., Labine, C.L., Atkinson, D.E., Headley, A.N., and Wolfe, P.M.**
2000: Automatic weather station results from Fosheim Peninsula, Ellesmere Island, Nunavut; *in* Environmental Response to Climate Change in the Canadian High Arctic, (ed.) M. Garneau and B.T. Alt; Geological Survey of Canada, Bulletin 529.
- Anonymous**
1967: Hydrology of the Lewis Glacier, north-central Baffin Island, N.W.T., and discussion of reliability of the measurements; *Geographical Bulletin*, v. 9, no. 3, p. 232-261.
- Blatter, H. and Hutter, K.**
1991: Polythermal conditions in Arctic glaciers; *Journal of Glaciology*, v. 37, no. 126, p. 261-269.
- Blatter, H. and Kappenberger, G.**
1988: Mass balance and thermal regime of Laika Ice Cap, Coburg Island, N.W.T., Canada; *Journal of Glaciology*, v. 34, no. 116, p. 102-110.
- Braithwaite, R.J.**
1981: On glacier energy balance, ablation, and air temperature; *Journal of Glaciology*, v. 27, no. 97, p. 381-391.
- Cogley, J.G. and McCann, S.B.**
1976: An exceptional storm and its effects in the Canadian high Arctic; *Arctic and Alpine Research*, v. 8, no. 1, p. 105-110.
- Cogley, J.G., Adams, W.P., Ecclestone, M.A., Jung-Rothenhäusler, F., and Ommann, C.S.L.**
1995: Mass balance of Axel Heiberg glaciers, 1960-1991: a reassessment and discussion; National Hydrology Research Institute Science Report No. 6, Environment Canada, Saskatoon, Saskatchewan, 168 p.
- Colbeck, S.C.**
1977: Short-term forecasting of water runoff from snow and ice; *Journal of Glaciology*, v. 19, no. 81, p. 571-587.
- Collins, D.N.**
1984: Climatic variation and runoff from alpine glaciers; *Zeitschrift für Gletscherkunde und Glazialgeologie*, Band 20, S. 127-145.
- Dicks, W., Adams, W.P., and Ecclestone, M.A.**
1992: Mass balance and ablation season processes, Baby Glacier, Axel Heiberg Island, N.W.T.; *The Musk-Ox*, v. 39, p. 15-23.
- Dowdeswell, J.A. and Drewry, D.J.**
1989: The dynamics of Austfonna, Nordaustlandet, Svalbard: surface velocities, mass balance, and subglacial melt water; *Annals of Glaciology*, v. 12, p. 37-45.
- Dunphy, P.P. and Dibb, J.E.**
1994: ¹³⁷Cs gamma-ray detection at Summit, Greenland; *Journal of Glaciology*, v. 40, no. 134, p. 87-92.
- Duynkerke, P.G. and van den Broeke, M.R.**
1994: Surface energy balance and katabatic flow over glacier and tundra during GIMEX-91; *Global and Planetary Change*, v. 9, no. 1-2, p. 17-28.
- Haerberli, W., Bosch, H., Scherler, K., Østrem, G., and Wallen, C.C.**
1989: World Glacier Inventory. Status 1988; International Association of Hydrological Sciences (International Commission on Snow and Ice) - United Nations Environment Program - United Nations Educational, Scientific, and Cultural Organization.
- Hattersley-Smith, G., Lotz, J.R., and Sagar, R.B.**
1961: The ablation season on Gilman Glacier, northern Ellesmere Island; Union Géodésique et Géophysique Internationale, Association Internationale d'Hydrologie Scientifique, Assemblée générale de Helsinki, 1960; *Commission des Neiges et Glaces*, p. 152-168.
- Inland Waters Branch**
1969-1972: *Glacier Atlas of Canada*; Department of Environment, Inland Water Directorate, Plate 7.0 (scale 1:2 000 000).
- Jensen, H. and Lang, H.**
1972: Forecasting discharge from a glaciated basin in the Swiss Alps; *The Role of Snow and Ice in Hydrology*, September, Banff, Alberta, v. 2, p. 1047-1054.
- Jonsson, S. and Hansson, M.**
1990: Identification of annual layers in superimposed ice from Storoyjokulen in northeastern Svalbard; *Geografiska Annaler*, v. 72A, no. 1, p. 41-54.
- Keeler, C.M.**
1964: Relationship between climate, ablation and runoff on the Sverdrup Glacier, 1963, Devon Island, N.W.T.; Arctic Institute of North America, Research Paper No. 27, 80 p.
- Koerner, R.M.**
1970a: Some observations on superimposition of ice on the Devon Island Ice Cap, N.W.T., Canada; *Geografiska Annaler*, v. 52A, no. 1, p. 57-67.
1970b: The mass balance of the Devon Island ice cap, Northwest Territories, Canada, 1961-66; *Journal of Glaciology*, v. 9, no. 57, p. 325-336.
- Koerner, R.M. and Taniguchi, H.**
1976: Artificial radioactivity layers in the Devon Island ice cap, Northwest Territories; *Canadian Journal of Earth Science*, v. 13, p. 1251-1255.
- Konzelmann, T. and Braithwaite, R.J.**
1995: Variations of ablation, albedo and energy balance at the margin of the Greenland ice sheet, Kronprins Christian Land, eastern North Greenland; *Journal of Glaciology*, v. 41, p. 174-182.
- Lefauconnier, B., Hagen, J.O., Pinglot, J.F., and Pourchet, M.**
1994: Mass-balance estimates on the glacier complex Kongsvegen and Sveabreen, Spitsbergen, Svalbard, using radioactive layers; *Journal of Glaciology*, v. 40, no. 135, p. 368-376.
- Miller, G.H., Bradley, R.S., and Andrews, J.T.**
1975: The glaciation level and lowest equilibrium line altitude in the high Canadian Arctic: maps and climatic interpretation; *Arctic and Alpine Research*, v. 7, no. 2, p. 155-168.
- Ohata, T.**
1989: The effect of glacier wind on local climate, turbulent heat fluxes, and ablation; *Zeitschrift für Gletscherkunde und Glazialgeologie*, Band 25, Heft 1, S. 49-68.
- Østrem, G.**
1972: Runoff forecasts for highly glacierized basins; *The Role of Snow and Ice in Hydrology*. September, Banff, Alberta, v. 2, p. 1111-1132.
- Østrem, G. and Brugman, M.**
1991: Glacier mass-balance measurements; National Hydrology Research Institute, Science Report No. 4, 224 p.
- Østrem, G., Bridge, C.W., and Rannie, W.F.**
1967: Glacio-hydrology, discharge and sediment transport in the Decade Glacier area, Baffin Island, N.W.T.; *Geografiska Annaler*, v. 49A, no. 3, p. 268-282.
- Pinglot, J.F. and Pourchet, M.**
1981: Gamma-ray bore-hole logging for determining radioactive fallout layers in snow; *in* Low-Level Counting and Spectrometry; Proceedings of an International Symposium, Berlin, 6-10 April, 1981; International Atomic Energy Agency (Proceedings Series), Vienna, p. 161-172.
1989: Détermination du bilan glaciaire en zone d'accumulation par mesures in situ de la radioactivité due à Tchernobyl; *C.R. Académie des Sciences, Paris*, vol. 309, n° 2, p. 365-370.
- Pinglot, J.F., Pourchet, M., and Lefauconnier, B.**
1997: Equilibrium line and mean annual mass balance determinations of Finsterwalderbreen by in situ and laboratory gamma ray measurements of nuclear test deposits; *in* Papers from the International Symposium of Glaciers, (ed.) I.M. Whillans, A. Fountain, J. Glen, P. Jansson, J. Kohler, M. Kuhn, and J. Moore; *Annals of Glaciology*, v. 24, p. 54-59.
- Reeh, N.**
1991: Parameterization of melt rate and surface temperature on the Greenland ice sheet; *Polarforschung*, v. 59, no. 3, p. 113-128.
- Stenborg, T.**
1970: Delay of runoff from a glacier basin; *Geografiska Annaler*, v. 52A, no. 1, p. 1-30.
- Trabant, D.C. and Mayo, L.R.**
1985: Estimation and effects of internal accumulation on five glaciers in Alaska; *Annals of Glaciology*, v. 6, p. 112-117.
- van de Wal, R.S.W., Oerlemans, J., and van der Hage, J.C.**
1992: A study of ablation variations on the tongue of Hintereisferner, Austrian Alps; *Journal of Glaciology*, v. 38, no. 130, p. 319-323.

Wendler, G., Fahl, C., and Corbin, S.

1972: Mass balance studies on McCall Glacier, Brooks Range, Alaska; Arctic and Alpine Research, v. 4, no. 3, p. 211–222.

Woodward, J.

1995: The influence of superimposed ice formation on the sensitivity of glacier mass balance to climate change; M.Sc. thesis, University of Alberta, Edmonton, Alberta, 98 p.

Summary of results and recommendations

B.T. Alt¹ and M. Garneau²

Alt, B.T. and Garneau, M., 2000: Summary of results and recommendations; in Environmental Response to Climate Change in the Canadian High Arctic, (ed.) M. Garneau and B.T. Alt; Geological Survey of Canada, Bulletin 529, p. 391–400.

Abstract: The results presented in this bulletin show the great strength of interdisciplinary studies such as those undertaken at the Geological Survey of Canada High Arctic Global Change Observatory. Such work allowed the sharing of logistics costs and field expertise and the exchange of scientific data and ideas. Many individuals and agencies participated in the field work. Some results are preliminary and others represent the culmination of decades of work in the area. An important goal of this synthesis is to provide a basis of documentation for further efforts in the area.

Most of the terrestrial component of the observatory work focused on Fosheim Peninsula, although it was also supported by results from other areas of northern Ellesmere and Axel Heiberg islands. The cryospheric component, from Agassiz Ice Cap northeast of Fosheim Peninsula, provides a temporal reference for paleoenvironmental studies and a link to changes in atmospheric constituents and climate.

Résumé : Les résultats présentés dans ce bulletin démontrent la grande efficacité d'études interdisciplinaires comme celles qui ont été effectuées à l'observatoire du changement climatique du Haut Arctique de la Commission géologique du Canada. Grâce à ces travaux, on a pu partager l'expertise et les coûts de logistique et échanger des idées et des données scientifiques. Plusieurs personnes et organismes ont participé aux travaux de terrain. Certains résultats sont préliminaires alors que d'autres représentent la culmination de plusieurs dizaines d'années de travaux dans la région. Un des objectifs principaux de cette synthèse est de fournir une base documentaire pour les futurs efforts de recherche dans la région.

La plus grande partie des travaux terrestres à l'observatoire portaient sur la péninsule Fosheim, mais ils étaient également appuyés par des résultats provenant d'autres régions du nord de l'île d'Ellesmere et de l'île Axel Heiberg. La composante cryosphérique de la calotte glaciaire Agassiz au nord-est de la péninsule Fosheim nous donne une référence temporelle pour les études paléoenvironnementales et un lien vers les changements dans les composantes atmosphériques et le climat.

¹ Balanced Environments Associates, 5034 Leirtrim Road, Carlsbad Springs, Ontario K0A 1K0

² INRS-Eau, 2800, rue Einstein, C.P. 7500, Sainte-Foy, Québec G1V 4C7

CLIMATE AND SPATIAL RELATIONSHIPS

Fosheim Peninsula has the largest interior lowland of the protected, thermally enhanced, dry, Eureka Sound intermontane area. This intermontane area, in turn, lies in the unique, circumpolar-vortex-dominated Eastern Canadian High Arctic, the climate of which is characterized by large, longitudinal temperature variations, strong and persistent temperature inversions, and widely differing precipitation totals (partly attributable to measurement error). The Eureka intermontane area is sheltered from the surface effects of the cold, moist air from the central Arctic Ocean that invades the low-lying islands of the western High Arctic. July mean temperatures at coastal stations in the area are as much as 4°C warmer than at Arctic Ocean coastal stations at the same latitude.

The climate of the Fosheim Peninsula interior lowland differs significantly from that along the ice-choked fiords. Preliminary results show that the mean monthly temperatures inland are 1.5 to 3.8°C colder in winter and 2 to 4.5°C warmer in July than at the coast. On a daily basis, the summer temperature difference between the coast and the interior can vary from 1°C to 7°C depending on synoptic weather conditions. During cold, wet spells in the summer, coastal temperatures can be the same as those inland; during warm, dry spells, hourly sampled temperatures are up to 15°C higher inland than at the coast.

The most striking feature of the winter record is the occurrence of sharp temperature peaks accompanied by strong winds and changes in snow depth. The six-year period covered by the Hot Weather Creek automatic weather station (autostation) records includes two summers of extreme warmth, two summers with temperatures well below normal (one of which was very wet), and two strongly contrasting winters. These records afford the opportunity for promising studies of future environmental change based on the integration of results from synoptic climate analyses and environmental processes.

Vegetation in the Arctic is far from homogeneous. Plant diversity and community composition vary depending on summer warmth, type of soil, and availability of moisture. In the Canadian Arctic, vascular-plant species are most diverse in the warmest regions close to the treeline and least diverse in the coldest regions. Summer warmth has the greatest influence on vegetation diversity. This control is best expressed as summations of total warmth such as positive degree days or growing degree days. Such data, however, are generally available only for the sparse network of northern weather stations. The most readily available and widespread measure of summer warmth is the mean temperature for July, the warmest month.

In the Canadian Arctic, mean July isotherms grade northward from roughly 10°C near the treeline to 1°C along the northwestern rim of the Queen Elizabeth Islands. This decline is not a simple, linear, latitudinal progression, but rather a complex pattern reflecting the interaction between solar radiation received, characteristics of the dominant air mass, topography, and the amount of open water surrounding the islands during the summer. Climate affects the diversity,

density, productivity, and growth forms of vascular plants on any given type of substrate by controlling the temperature, the length of the thaw season, the intensity and amount of precipitation, and the intensity and duration of cloud cover. Woody plants can be used as bioclimatic indicators in the Arctic the same way as trees are used in the boreal forest, and their limits coincide remarkably well with mean July isotherms drawn through sea-level coastal stations.

One issue raised by the results of the individual contributions is to determine how the conditions on the Fosheim Peninsula lowland compare with those of the intensively studied 'polar oasis' (Bliss, 1977; Henery et al., 1986; Levesque and Svoboda, 1992; Labine, 1994; Muc et al., 1994; Svoboda and Freedman, 1994) and indeed whether the study area fits the definition of an oasis, as has been suggested by a number of authors and reviewers in this volume. Polar oases have been defined as discrete lowlands bounded on all sides by polar desert and Freedman et al. (1994, p. 2) have suggested that:

Thus the Alexandra lowland is quite discrete, bounded on all sides by inhospitable terrain ranging in character from glacial ice, to upland polar desert, to frigid saltwater. This geographical aspect reinforces the impression of the lowland as a true oasis i.e. an ecological island embedded in a matrix of barren and unproductive ice, and polar desert, and semi-desert.

Freedman et al. (1994, p. 3) suggest that adiabatic warming, heating from the bare cliffs, and the regional climate are responsible for the observed mesoclimate conditions and finally conclude that:

These and other climatic indicators reinforce the conviction that the Alexandra Fiord lowland is a thermal oasis, with an ameliorated climate, in contrast to the prevailing polar desert.

The Fosheim Peninsula interior as represented by the Hot Weather Creek autostation has been shown to have higher July temperatures and produce more thawing (positive) degree days than any of the hitherto-studied polar oases (Alt et al., 2000a; Edlund et al., 2000). Summer temperatures on the rolling uplands are equivalent to those at Low Arctic sites. The area of enriched vegetation resulting from this thermal enhancement covers some 3000 km². Further enrichment in sheltered areas and wetlands is a result of local conditions. This relatively uniform, rolling, inland area is illustrated in the trimetragon photograph shown in the frontispiece. It exhibits a typical continental climate: dry, clear, and warm in the summer relative to the coast and cold in the winter. It does not rely on cliffs for additional radiation input nor is it a distinct area surrounded by inhospitable polar desert. Rather, it is the manifestation of the full potential of the relatively cloudless interior of a sheltered, regional-scale, intermontane area. Eureka's climate is modified by the ice-choked fiord, which produces cold air that is advected over the coast and low cloud and fog that reduce incoming solar radiation. In favourable synoptic years, the broad expanse of the interior is able to take full advantage of the high amounts of solar radiation available at these high latitudes.

The Fosheim Peninsula interior, as represented by the Hot Weather Creek autostation, is thus not an oasis, but rather a regional-scale enhancement of the large-scale climate. However, it is also true that, within this thermally enhanced area, local areas of available moisture, such as melting massive

ground ice, thermokarst hollows, or late snowbanks, and further thermal amelioration, such as that experienced by south-facing slopes, valley bottoms, dark materials, etc., do occur. That these are very important features of the environment cannot be denied, but on Fosheim Peninsula, they exist within an already ameliorated thermal regime. It is this regional-scale, interior, warm, summer anomaly that makes it possible for the enriched flora and fauna to survive in present conditions. It has also provided a refugium during glacial periods and, during the warmer part of the Holocene, it influenced the enhancement of different ecogeomorphological processes such as a rise in fluvial processes, less sea-ice cover, high bryophyte rate of accumulation, and high pollen and diatom concentration in sediments.

TEMPORAL RELATIONSHIPS

Dramatic evidence of past climate on Fosheim Peninsula was provided by N.J. McMillan's 1955 discovery of 'fossil forests', with stumps preserved in growth position at Hot Weather Creek (Christie and McMillan, 1991).

Evidence of climate and environmental change from the studies presented in this bulletin, including the discussion of individual extreme years during the field period, provides insight into the nature of natural and anthropogenic environmental change on Fosheim Peninsula. Holocene paleoenvironmental information is summarized in Figure 1,

starting with the ice-core results, which provide a continuous record of regional climate. Extensive reviews of the evidence from elsewhere in the Queen Elizabeth Islands are available in Bradley (1990) and Dyke et al. (1996a, b, 1997). The following discussion is limited to information from this bulletin.

Late Tertiary

Macroremains of bryophytes, vascular plants, and arthropods show that the Late Tertiary climate was significantly warmer than present-day conditions (Matthews and Fyles, 2000). At times, the region was occupied by open forests. Unlike modern taiga, which now has its northern limit thousands of kilometres farther south, the open forests of the Fosheim Peninsula, even those forming the treeline, were diverse.

The longest continuous paleoclimatic record available for the area is from the Agassiz Ice Cap to the northeast (Bourgeois et al., 2000). For an unknown period during the last interglacial stage, the climate on Agassiz Ice Cap was warmer than at any time during the present interglacial stage. Koerner and Bourgeois (1988) conclude that ice near the bedrock was formed during a relatively warm period, probably towards the end of the last interglacial stage, as the ice cap must have melted completely or extensively in an earlier stage when the landscape was still characterized by an open forest-taiga cover (Matthews and Fyles, 2000). The modern analogue of these open taiga conditions lies 1000 km south and corresponds to a mean July temperature of 10°C to 13°C.

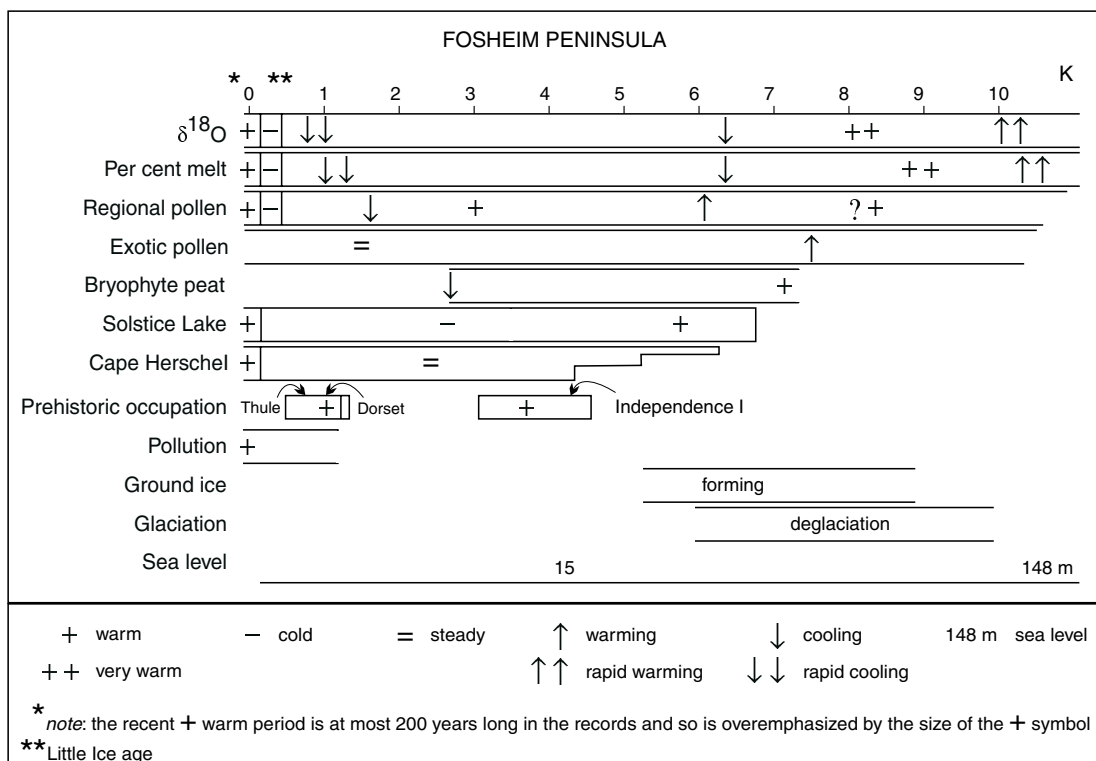


Figure 1. Summary of paleoenvironmental results from this report for Fosheim Peninsula from 10 000 BP to present.

Quaternary

Quaternary glacial history and the extent of the last glaciation in the Canadian High Arctic islands are still not fully understood (Hodgson, 1989; Bradley, 1990; Bell and Hodgson, 2000). Conditions on Fosheim Peninsula are particularly enigmatic. Bell and Hodgson (2000) provide a reconstruction of the last glaciation on Fosheim Peninsula. They suggest that despite the lowering of the paleoglaciation level by 700–800 m, ice growth was limited to the expansion of cirque glaciers and to accumulation on upland surfaces that are now free of ice (such as Black Top Ridge). Hyperaridity is suggested as the reason for limited ice growth on Fosheim Peninsula during the most recent Wisconsinan Glaciation. However, some recent studies infer a complete ice cover of the peninsula during the last glaciation (addendum to Bell and Hodgson, 2000). Marine transgression by 10 600 BP produced a marine limit that reached a maximum elevation of 148 m a.s.l. along Eureka Sound and Greely Fiord and descended southeastward to 139 to 142 m a.s.l. near the Sawtooth Range. Wisconsinan ice on Agassiz Ice Cap (Bourgeois et al., 2000) contains more microparticles, deforms more readily, and is more alkaline than Holocene ice-age ice. Pleistocene ice-age ice is limited to a few metres near the bed, but it shows the major $\delta^{18}\text{O}$ steps seen in higher resolution cores. The pollen record also indicates fluctuations in concentration and composition that could be linked to the relatively warm episodes in the $\delta^{18}\text{O}$ ice-age ice.

Holocene

Deglaciation of Fosheim Peninsula was underway by 9500 BP (Bell and Hodgson, 2000). As a result of marine transgression, much of what is now the Fosheim Peninsula interior lowland was submerged and islands of the remaining land areas were created in what is now the Fosheim interior. It is hypothesized that sea ice was reduced during this period, resulting in increased moisture availability (*see also* Bradley, 1990), which influenced for example significant accumulations of bryophytes (≥ 200 cm) whose thickness has no modern analogue (Garneau, 2000). Thus, the persistence of local ice caps through the warmest period of the Holocene to 6000–5000 BP is attributed by Bell (1996) to the fact that low-lying coastal icefields benefited from this increased moisture whereas interior highland ice caps did not.

Following a significant, abrupt change in stable-isotope ratios marking the end of the last glaciation, Agassiz ice-core $\delta^{18}\text{O}$ profiles (Bourgeois et al., 2000) show a rapid warming trend that reaches a maximum about 8000 BP. Average temperatures at this time are estimated to have been 2.5°C warmer than at present. After 8000 BP, a gradual cooling occurred that steepened at 1500 BP, reaching a minimum between 200 and 100 BP. Melt layers show maximum summer warmth, at least 2°C warmer than at present, occurring between 9500 and 8500 BP. Melt decreased until about 2500 BP, after which there was very low melt until 100 BP. Thus, both melt and $\delta^{18}\text{O}$ show maximum warmth occurring in the early Holocene (before 8000 BP) and decreasing until about 200 BP. The close correspondence between the Agassiz Ice Cap melt values and the curve of increased solar

radiation receipts from changes in orbital configuration (expressed as a per cent increase over modern values) is particularly significant (Bourgeois et al., 2000).

The initial regional pollen record, obtained from the melt tank of the thermal drill on Agassiz Ice Cap, does not begin to increase until 6000 BP and the maximum concentration is attained only at 3000 BP. This can be explained by the high atmospheric humidity (e.g. fog and precipitation) during the early and middle Holocene that inhibited pollen transportation. Alder and birch (exotic pollen) concentrations began to increase about 7500 BP and reached their maximum about 1500 BP. More recent results from downhole melting reveal high pollen concentrations in the early Holocene (Bourgeois et al., 2000) when the climate was warmer and more arid. The seasonal pollen studies on Agassiz Ice Cap show that regional pollen influx rates relate better to mean July temperature on Fosheim Peninsula than to summer temperatures (June–August) or temperatures from Alert to the north of the ice cap. Analyses of the storms responsible for the deposition of the seasonal layer also indicate that Fosheim Peninsula is the most likely source of the local pollen that reached the ice cap.

Present-day accumulations of organic matter are thin and locally concentrated in the High Arctic because, on Fosheim Peninsula, climatic conditions are too arid and continental and summer evaporation is too strong to enhance bryophyte accumulation in soils. However, thick peat deposits did accumulate in the past (between 7.5 ka and 2.5 ka) and are associated with warmer and moister climate conditions, which also agrees with the interpretation of other proxy data results.

The results of a diatom analysis of a sediment core from Solstice Lake on southwestern Fosheim Peninsula are interpreted to indicate that the lake infilled and became a permanent fixture ca. 6500 BP (Wolfe, 2000). Warm conditions engendered high diatom paleoproductivity, as inferred from valve concentrations, and increased the sedimentation of autochthonous organic material. Diversity was low, however. Wolfe (2000) suggests that the period was characterized by a warm, wet climate, as indicated by other proxy data analyses mentioned in this bulletin. Between 4000 and 3000 BP, diatom concentrations and sediment organic content decreased although species diversity increased. Decreased diatom paleoproductivity reflects cooler temperatures associated with the Neoglacial cooling starting at approximately 3500 BP (Wolfe, 2000). Low diatom concentrations since ca. 1000 BP may be attributable in part to enhanced mineral sedimentation associated with more significant allochthonous inputs from catchment erosion as many Ellesmere glaciers advanced between 3000 and 1000 BP (Blake, 1981, 1989) and also from eolian processes within the unstable basin.

By 4000 BP, emergence had slowed and Fosheim was again a peninsula.

Sutherland (2000) places the earliest evidence of prehistoric occupation of Fosheim Peninsula between 2500 and 1000 BC (Independence I period, ca. 4500–3000 BP). No definite evidence of occupation was found for the period between about 1000 BC and AD 700 (ca. 3000–1300 BP), probably because of the Neoglacial cooling that started ca.

3000 BP, as interpreted from the other proxy data. The Late Dorset occupation of the area probably occurred over a period of a few centuries, from approximately AD 700 (ca. 1300 BP) to as late as AD 1300 to 1400 (ca. 700–600 BP), which corresponds climatically to the Medieval Warm Period when the sea-ice cover was probably more open during many months of the year. The Thule (ancestors of Inuit) occupation of the area seems to have occurred over several centuries, after about AD 1100 (ca. 900 BP).

Sutherland (2000) mentions that during these periods of occupation, land animals may have been relatively abundant in the High Arctic. Evidence of increased hunting of marine animals may relate to maritime hunting capabilities or may indicate increased populations of sea mammals probably linked to a decrease in the extent of seasonal sea-ice cover. The amount of whale bones and the presence of harp seals are associated with increased open water in sea-ice areas. Remains of Ross geese and brown lemmings, which currently have more southerly ranges, provide a further indication of warmer local conditions about 1000 BP. The area may have been abandoned after AD 1700 (ca. 300 BP) following the cooling of the Little Ice Age about 100 to 200 years ago that was characterized by the lowest summers temperatures of the Holocene.

Last 100 years

Since 100 BP, $\delta^{18}\text{O}$ and melt-layer conditions in the Agassiz Ice Cap show that temperatures have increased, but are not nearly as warm as in the early Holocene.

At Solstice Creek, Wolfe (2000) found the greatest diatom changes of the entire record in the upper 3 cm of sediment, which he estimates to represent the last 125 years. Diatom concentrations and diversity rose dramatically. The diatom assemblages suggest that the warm period of the present century is more arid than that of the middle Holocene.

Paleolimnological data from Cape Herschel (Douglas et al., 2000) show unparalleled changes, likely beginning in the nineteenth century (ca. 200 BP). The recorded diatom shifts, which include increased diversity, more complex periphytic assemblages, and increases in moss epiphytes, are similar to what one would expect with climatic warming.

Last 50 years

The recent snow-pit and ice-core records indicate that pollution levels have increased on Agassiz Ice Cap and at other High Arctic sites since the 1950s. No discernable trend is apparent in either the snow and ice proxy-data parameters (such as $\delta^{18}\text{O}$ and melt layering) or the glacier mass-balance measurements for the past 30 years.

Although large areas of the Arctic do seem to be showing a warming trend, the Eastern Canadian Arctic is not (Alt and Maxwell, 2000). This is true of the summer temperatures from Eureka as well. The reason for this lack of trend is the very warm period in late 1950s and early 1960s that along with the early twentieth century warm period, overshadows the recent warm years (Alt et al., 2000a).

Period of record

As noted above, the study seasons included both wet and dry summers and periods when temperatures were well above and well below normal. The mean July temperature (9.3°C) for the six years of record was 1°C warmer than the estimated equivalent 30-year mean at the Hot Weather Creek autostation.

The summer of 1988 had the second warmest July in the 45-year record from Eureka and negligible precipitation at the Hot Weather Creek site in the interior. Environmental responses to these extreme conditions included the recharge of creeks and thaw ponds, surface seepage in the form of artesian-like features and damp spots, accelerated recession of ground-ice slumps, and the initiation of numerous active-layer detachment slides. Several species of vascular plants had second and third waves of flowering. On the basis of results from the warm summer of 1993, glaciers in the Sawtooth Range had a negative mass balance twice as high as the mean for the past 100 years. The long-term effects of prolonged periods of summer warmth of the magnitude experienced in July and August 1988 need further investigation, but some assumptions can be made. Slope instability would continue until a new equilibrium is reached. This could radically change the appearance of the landscape, both from a geomorphological and a biological view, and would provide abundant fresh habitats for colonizing plant species.

In 1989, on the other hand, a more conventional nival regime was in operation, runoff peaked in the spring, fed by adequate winter snow, and creeks were recharged from time to time by significant summer precipitation. Precipitation was well above normal. July temperatures were below normal at Eureka and the temperature difference between the coast and the interior was not as extreme as in the warm season of 1988. Some vegetation species did not produce seeds.

Although most of the paleoenvironmental indicators are measures of summer conditions (usually temperature and in some cases humidity), ice-core isotope values give annual information that can be compared with winter records. The winter of 1990–1991 was very dry, cold, and windy whereas that of 1991–1992 had good snow cover and marked warm spells. The isotope signals from these two types of winter should be identified since they would be useful in evaluating Holocene conditions.

DISCUSSION OF TEMPORAL RELATIONSHIPS

The ‘Little Ice’ model for the last glaciation on Fosheim Peninsula suggests hyperaridity to explain the lack of large ice sheets in the area. The following observations are based on the knowledge of modern synoptic conditions in the area (Alt, 1983; Alt and Maxwell, 2000; Alt et al., 2000a). The Eureka intermontane area, positioned north of the main ice sheet, was cut off from southern sources of atmospheric moisture and subject to advection of cold, dry air, not only off the ice sheet to south, but also from the frozen Arctic Ocean. Moisture from distant sources had to cross the ice sheet or the

Arctic Ocean and then penetrate the intermontane area. The most likely source of moisture, even in the case of a split jet stream, was the Beaufort Sea area, but, as is the case today, the intermontane area was protected from this westerly flow by the surrounding mountains (in contrast to northern Ellesmere and western Axel Heiberg islands). In addition, cold summer temperatures resulted in a shallow active layer, which precluded groundwater as a source of moisture even if massive ice did exist.

The reconciliation of the wide range of dates, from 9500 BP to as late as 5000 BP, for maximum melt (temperature, glacier retreat) in the Holocene requires a careful examination of the type of environmental indicator being used and the local conditions to which it corresponds. As Bradley (1990) points out, the effect of the orbital solar radiation maximum in the early Holocene is maximized by the long daylight hours of the High Arctic. The resulting melt seasons were long and intense. At sea level in the Fosheim Peninsula area, depicted at 9000 BP as isolated, ice-capped islands submerged by the sea (Bell and Hodgson, 2000), the long, intense summers resulted in a constant supply of moisture, initially from melting snow, then melting sea ice, and finally open water. Low clouds were pervasive. On windward slopes such as the south coast of Greely Fiord (given atmospheric conditions such as those suggested by Lamb (1977) and Alt (1983)), orographic precipitation nourished the glaciers. At higher elevations on extensive ice caps farther removed from the sea, melt was intense and the melt season began much earlier than at present. It should be noted that the ice-cap melt-layer values indicate only that high melt occurred in the summer. They do not necessarily represent the mass-balance conditions of the ice cap (which may very well have been less negative than melt values suggest due to enhanced accumulation at lower altitudes). On the other hand, the Fosheim ice bodies, surrounded by sea, remained near freezing because of the melting snow and sea ice (and even the open water) for most of the summer and were covered in low cloud and fog most of the time, much as is the case today for the Meighen Ice Cap. The area available to vegetation on Fosheim Peninsula was limited although existing species flourished. It seems likely that, although pollen was produced, it was rained out very close to its source by frequent, local precipitation. This pollen remained stuck to the wet ground surface, which prevented it from reaching the Agassiz Ice Cap. On the other hand, exotic pollen, which is transported at upper levels in the atmosphere, began to reach the ice cap as forests expanded in the south. It was transported into the area as a result of the more frequent southerly circulation conditions.

As the land emerged and ground ice formed each winter in the marine sediments, summers remained warm and wet. Even though solar radiation was decreasing, it was still well above modern values. By 6000 BP, the peninsula had emerged and the interior regions slowly began to dry out. Lakes infilled and sedimentation began. Diatom concentrations reached their highest values. Thermokarst was active as a result of warm summers and cold winters. Conditions for bryophyte peat accumulation were optimized by the warm, wet surface conditions and the deep active layer. Vegetation colonized newly emerged land. Existing islands of vegetation

and their resident insect population began to flourish. On the top of Agassiz Ice Cap, summer melt (and temperatures) decreased in response to decreased solar radiation and annual temperatures were lower, as reflected by $\delta^{18}\text{O}$ values. Regional pollen began to reach the ice cap, probably in isolated synoptic systems.

By 4500 BP, when the Independence I culture reached Fosheim Peninsula, the coastline was similar to today's. Summers and probably winters were still warmer than today and sea-ice conditions were favourable (open water for several months each year). Summers were warmer in the interior than on the coast. This continentality of the interior was enhanced by a decrease in the frequency of southerly atmospheric flow. The Eureka intermontane region became sheltered once again and began to dry out. Regional pollen production was greater than today and drier conditions allowed the buildup of pollen in the atmosphere and its transportation to the ice cap in a manner similar to that which occurs in favourable seasons today.

As the cold polar vortex shifted to the North American side of the Arctic Ocean, the North American trough regained dominance in the eastern Canadian Arctic. Radiation continued to decrease and summers became cooler and drier. By 2500 BP, summer conditions became more severe than those experienced today. Fosheim Peninsula was cool, dry, and unoccupied. Bryophyte accumulation slowed considerably. Diatom assemblage concentrations decreased although diversity increased.

The Late Dorset and Thule occupations occurred during the global period of climatic decline (with intervals of milder conditions, e.g. the Medieval Warm Period approximately 1000 BP) that culminated in the 'Little Ice Age' (ca. 300–150 BP). The end of the occupation corresponds to the beginning of the most severe climate. Whale and other animal remains associated with these occupations suggest that sea-ice conditions were more favourable than today. This is not reflected in the Agassiz Ice Cap ice-core summer-melt record and thus may be of a more local nature. A careful study of evidence from this period on Fosheim Peninsula and in other areas of the Arctic is needed.

The lack of occupation from AD 1700 to the present coincides with the coldest period of the Holocene, i.e. the 'Little Ice Age' discussed extensively in the literature. Results from Fosheim Peninsula are not yet sufficiently resolved to provide additional information. Presumably, the intermontane area remained sheltered and made the best possible use of the available solar radiation. Therefore, it may have been proportionally warmer than other areas of the Queen Elizabeth Islands, although this assumption requires more research.

The end of the 'Little Ice Age' was marked by the return to more favourable conditions as can be seen in all environmental indicators examined in this bulletin. The degree to which this improved climate is a reflection of industrialization is beyond the scope of this study. The importance of natural climatic change in the extremely complex reaction of climate to anthropogenic change is illustrated by the cold conditions of the 1970s in the eastern High Arctic. This, coupled with the warm 1950s and 1960s, made the period of instrumental and

field observations on Fosheim Peninsula a trendless one. The diatom records from High Arctic ponds no doubt reflect the extremely warm conditions of the 1920s and 1950s.

POSSIBLE IMPACTS OF CLIMATE WARMING

It must be stressed that climate change and climate warming are not synonymous. Climate change occurs in both directions, as witnessed by evidence of the past climate on Fosheim Peninsula. It includes warm and cold; wet and dry; clear and cloudy; calm and stormy. It is fundamental to the operation of the atmosphere-geosphere-biosphere system and not just something that man in his headlong rush for progress has recently wrought on the Earth. Pollution levels measured on the pristine arctic ice caps attest to the pervasiveness of man's indiscriminate interference with natural environmental change, but they do not rule out Nature's role in the complex interaction between environmental parameters and anthropogenic change.

Three field seasons with different hydrological characteristics provide temporal analogues to create scenarios of hydrological responses to climate change (Young and Woo, 2000). In an area of low precipitation such as Fosheim Peninsula, a decrease in snowfall will seriously reduce spring runoff. Little water will be available to add to the basin storage. Rainfall-generated runoff depends strongly on the amount of rain and the antecedent water storage in the basin. With climatic warming, the storage capacity will increase because of deeper and faster thawing of the active layer. More water will be needed to satisfy the storage capacity before runoff begins. At present, streams may cease to flow during drier summers. Summer flow is prone to be much curtailed under a warmer climate as the elevated evaporation rates further reduce the amount of water available to streamflow. A sensitivity analysis of evaporation responses to selected atmospheric and terrestrial impacts indicates that small changes in atmospheric constituents may have a greater effect than slight modifications of the terrestrial environment.

Robinson (2000) concludes that under a summer warming scenario, predictions based directly on increased thawing degrees days will overestimate headwall retreat. He also points out that, although no mechanism currently exists to expose ice in undisturbed marine sediment, with climate warming, increased snowmelt runoff leading to gullying and exposure of ice may provide the mechanisms required for future thermokarst degradation.

The impact of climate warming on the vegetation and landscape of Fosheim Peninsula are illustrated by the extreme warm summer of 1988, which witnessed extensive changes to the landscape, flourishing vegetation, high regional pollen in the Agassiz Ice Cap ice cores, and highly negative mass-balance conditions on Queen Elizabeth Islands ice caps. Other effects of warming observed from the warm summers of 1991 and 1993 include increased insect fauna, highly negative mass balance on glaciers in the Sawtooth Range, and the hydrological regime discussed above.

RECOMMENDATIONS

The breadth and diversity of the contributions in this bulletin show the potential of integrated, interdisciplinary, inter-agency studies and also point the way to future efforts in the area. In many cases, the proposals outlined below involve further analysis of existing data, which should be encouraged as a cost-effective method of advancing understanding of arctic environmental changes and their interaction processes.

Woo and Young (1997) caution that spatial and temporal variations in local environments must be considered before point measurements of frost depth, snow amount, vegetation cover, and soil moisture are upscaled for use in detecting climate change.

The preliminary results from the Hot Weather Creek autostation emphasize the need for further analysis of the autostation data, which should include a study of the thermal, wind, and precipitation regimes for the summers of 1988 to 1993 and preliminary synoptic climate studies of selected periods in the 1988–1993 record. In addition, data from the Hot Weather Creek camp and the auxiliary stations need to be incorporated into the study and all of these data compared with data from other study areas in the region.

The preliminary climate studies have also suggested a number of additional topics for further research. A detailed study of the warm intrusions and generally snow-free conditions of the winter of 1990–1991 should be compared with a similar study of the windy, cold, heavy-snow winter of 1991–1992. The extreme storm event of May 1992 offers the opportunity to study the effect of isolated storm events on the transport of pollen and contaminants to the ice cap. An areal study of surface albedo and its variation with time of year and synoptic conditions is needed not only to provide input into the ground-surface component of general circulation models, but also as ground truth for proposed remote-sensing studies. The results of the spatial temperature and albedo studies would be the first step in creating realistic areal evaluations of general circulation model grid squares.

A mesoscale spatial representation of July mean temperature variations on Fosheim Peninsula, based on geographic information system techniques, has been suggested. The study area offers the challenge of combining the records of the typical, coastal, long-term, standard weather station at Eureka with those of a wide range of nonstandard weather observations.

Standardized data-processing and documentation procedures are important for future field autostations. These should meet the criteria being developed at a national level in response to international programs such as the Global Climate Observing System.

The discussion of spatial relationships shows that a consensus is needed on the definition of 'polar oasis' and its relationship to regional climate phenomena.

Several easily identifiable common insect herbivores are suggested as early detectors of climate warming. Three large crane-fly species would be a useful complement to these.

Most High Arctic species have flexible, extended life cycles and, in poorer seasons, few will emerge. Monitoring must, therefore, be extended over several seasons in order to establish patterns.

Matthews and Fyles (2000) stress that information on Tertiary fossils from Fosheim Peninsula is also important for studying Quaternary sites in the region because fossil assemblages from such sites provide paleoecological data on climate conditions that led to the development of taiga forest cover at High Arctic latitudes. These data as well as other proxy data from the area do not preclude the need to develop transfer functions to determine the impact of global warming on High Arctic environments. In order to exclude the ice or mineral sediment content in organic accumulations, net organic accumulations and gross organic accumulations (Lafarge-England et al., 1991) need to be calculated in future studies to determine real rates of peat accumulation. Although the limits to the interpretation of past environments in the High Arctic raise some problems, Gajewski et al. (1995) have demonstrated the considerable potential for late Quaternary studies integrating different proxy data to identify the impacts of climate on arctic environments.

Additional archeological work would provide a more precise definition and dating of adaptational and paleobiological changes on Fosheim Peninsula and in adjacent areas. The results of prehistoric adaptations within this local region should be compared with those from other areas of arctic North America. Use should be made of the fact that paleoenvironmental data from the period of occupation are concentrated in the middens of early people.

The Quviagivaa Glacier should be visited as soon as possible to try to locate and measure the mass-balance stakes installed near the equilibrium line. One of the main methods proposed to reconstruct net mass balance for specific glaciers is the analysis of ice cores from the zone of superimposed ice, which vary considerably in size and altitudinal extent from year to year (Koerner, 1970; Cogley et al., 1995). Since some net accumulation of superimposed ice did occur even in the above-average warmth of the summer of 1993, it could be suggested that in such locations, a distinct layer of superimposed ice is formed each summer that can be counted using some of the methods used by Jonsson and Hansson (1990). Potentially, accurate dating could be achieved by identifying radioactive layers deposited in 1963 as a result of atmospheric nuclear-bomb testing in the Russian Arctic and in 1986 as a result of the Chernobyl accident. Since both 1963 and 1986 were cool summers in the Canadian High Arctic, it is reasonable to assume that the radioactive peaks from these years are well preserved in superimposed ice over a wide region. This would allow spatial evaluations of the 1963–present and 1986–present net mass-balance records. The identification of radioactive layers in boreholes using a gamma-ray detector would allow quick sampling on numerous glaciers. In addition, if two or more boreholes were sampled at different elevations in the zone of long-term superimposed ice, a mass-balance gradient could be constructed from which the long-term equilibrium-line altitude could be estimated.

SUMMARY OF CONCLUSIONS

Summer thermal enhancement of the Eureka intermontane area reaches its full potential in the broad expanse of the Fosheim Peninsula interior lowland, represented in the Hot Weather Creek automatic weather station records. In July, enhancement within the intermontane area averages 3°C (as high as 15°C at noon during prolonged clear periods) relative to coastal areas and over 5°C relative to similar latitudes in the western Queen Elizabeth Islands. The manifestation of this is a regional-sized area of shrub tundra within which sedge meadows are found where increased moisture is available. Regional sources of moisture include winter snow, ground ice, and, in some years, summer precipitation. Together they support the observed vegetation (which in turn supports a diverse insect fauna). They are all subject to environmental change. The impact of regional thermal enhancement is also seen in the high occurrence of thermokarst.

Within this regional-scale feature are a myriad of mesoscale, microscale, and site-specific environmental conditions and interactions. Local moisture from melting massive ground ice or late-lying snowbanks produces wetlands. Slope aspect influences local snow depth, radiative balance, and active-layer depth. Local hydrological, vegetation, and soil conditions combined with regional-scale climate influence the enhancement of primary productivity and its impact on the vegetation cover, including the development of wetlands that may influence peat accumulation in soils as well as the production of pollen, diatoms, and other micro-organisms.

The distribution of marine sediments, another important regional parameter, affects lake chemistry and ground-ice distribution. Thermokarst is largely responsible for the existing landscape in these areas. This emphasizes the importance of glacial history on present environmental conditions, on the interpretation of paleoenvironmental records and on the impact of future climate change.

The Fosheim Peninsula raises particularly interesting paleoenvironmental questions. An integration of the studies presented in this bulletin suggests some possible answers and directions for future investigations. The results include an examination of the taiga climate of the Late Tertiary and the use of transfer functions. As climate change manifests itself in the form of a change in the prevailing synoptic regime, the differences between the coast and the interior must also have changed over time. This has important ramifications for paleoenvironmental studies and for studies of future climate change. The use of transfer functions derived for paleosites in the interior using records from coastal stations must be done with care until a model is developed to produce virtual records for the interior from long-term coastal records. The modern climate of the area provides the basis for a scenario of regional hyperaridity. This in turn is used to account for limited ice cover during the last glaciation. A possible reconciliation is presented of the wide variation in timing for the Holocene maximum indicated by the various types of paleoenvironmental indicators in and around Fosheim Peninsula. The periods of prehistoric occupation of the

peninsula and the universally unfavourable conditions of the 'Little Ice Age' need further study, as does the cause of the warming that ended this period. No trend is seen in the period of instrumental records (last 50 years) because of the very warm period in the 1950s. The extreme warmth of 1988 (the first year of record from Hot Weather Creek) provides a glimpse of the possible effects of climate warming on the environment of this unique High Arctic region.

The research presented in this bulletin suggests exciting opportunities for future efforts including environmental monitoring, further analysis of existing data (much of which is provided in the appendices; *see also* Alt et al., 2000b), and continued integrated research efforts. It shows the feasibility of aggregating point data to spatial averages, of combining distributions of vegetation, landscape, and climate to produce a regional picture, and of combining diverse proxy records to reconstruct past environmental interactions and change.

REFERENCES

- Alt, B.T.**
1983: Synoptic analogs: a technique for studying climate change in the Canadian High Arctic; *in* Climate Change in Canada 3, (ed.) C.R. Harington; National Museum of Natural Sciences, Syllogeus No. 49, Ottawa, Ontario, p. 70–107.
- Alt, B.T. and Maxwell, B.**
2000: Overview of the modern arctic climate; *in* Environmental Response to Climate Change in the Canadian High Arctic, (ed.) M. Garneau and B.T. Alt; Geological Survey of Canada, Bulletin 529.
- Alt, B.T., Labine, C.L., Atkinson, D.E., Headley, A.N., and Wolfe, P.M.**
2000a: Automatic weather station results from Fosheim Peninsula, Ellesmere Island, Nunavut; *in* Environmental Response to Climate Change in the Canadian High Arctic, (ed.) M. Garneau and B.T. Alt; Geological Survey of Canada, Bulletin 529.
- Alt, B.T., Labine, C.L., Desrochers, D.T., Young, K.L., and Garneau, M.**
2000b: Climate and ground thermal data, 1988–1994: Hot Weather Creek area, Fosheim Peninsula, Nunavut; Geological Survey of Canada, Open File D3783.
- Bell, T.**
1996: Later Quaternary glacial and sea level history of Fosheim Peninsula, Ellesmere Island, Canadian High Arctic; Canadian Journal of Earth Sciences, v. 33, p. 1075–1086.
- Bell, T. and Hodgson, D.A.**
2000: Quaternary geology and glacial history of Fosheim Peninsula, Ellesmere Island, Nunavut; *in* Environmental Response to Climate Change in the Canadian High Arctic, (ed.) M. Garneau and B.T. Alt; Geological Survey of Canada, Bulletin 529.
- Blake, W., Jr.**
1981: Lake sediment coring along Smith Sound, Ellesmere Island and Greenland; *in* Current Research, Part A; Geological Survey of Canada, Paper 82-1C, p. 104–110.
1989: Inferences concerning climatic change from a deeply frozen lake on Rundfjeld, Ellesmere Island, Arctic Canada; Journal of Paleolimnology, v. 2, p. 41–54.
- Bliss, L.C.**
1977: Truelove Lowland, Devon Island, Canada: A High Arctic Ecosystem; University of Alberta Press, Edmonton, Alberta, 714 p.
- Bourgeois, J.C., Koerner, R.M., Fisher, D.A., and Alt, B.T.**
2000: Present and past environments inferred from Agassiz Ice Cap ice-core records; *in* Environmental Response to Climate Change in the Canadian High Arctic, (ed.) M. Garneau and B.T. Alt; Geological Survey of Canada, Bulletin 529.
- Bradley, R.S.**
1990: Holocene paleoclimatology of the Queen Elizabeth Islands; Canadian High Arctic; Quaternary Science Reviews, v. 9, p. 365–384.
- Christie, R.L. and McMillan, N.J.**
1991: Introduction; *in* Tertiary Fossil Forests of the Geodetic Hills, Axel Heiberg Island, Arctic Archipelago, (ed.) R.L. Christie and N.J. McMillan; Geological Survey of Canada, Bulletin 403, p. xiii–xvi.
- Cogley, J.G., Adams, W.P., Ecclestone, M.A., Jung-Rothenhauser, F., and Ommanney, C.S.L.**
1995: Mass Balance of Axel Heiberg glaciers, 1960–1991: a reassessment and discussion; Environment Canada, National Hydrology Research Institute Science Report no. 6, Saskatoon, Saskatchewan, 168 p.
- Douglas, M.S.V., Smol, J.P., and Blake, W., Jr.**
2000: Summary of paleolimnological investigations of High Arctic ponds at Cape Herschel, east-central Ellesmere Island, Nunavut; *in* Environmental Response to Climate Change in the Canadian High Arctic, (ed.) M. Garneau and B.T. Alt; Geological Survey of Canada, Bulletin 529.
- Dyke, A.S., Dale, J.E., and McNeely, R.N.**
1996a: Marine molluscs as indicators of environmental change in glaciated North America and Greenland during the last 18 000 years; Géographie physique et Quaternaire, v. 50, no. 2, p. 125–184.
- Dyke, A.S., England, J., Reimnitz, E., and Jetté, H.**
1997: Changes in driftwood delivery to the Canadian Arctic Islands: a hypothesis of postglacial oscillations of the Transpolar Drift; Arctic, v. 50, p. 1–16.
- Dyke, A.S., Hooper, J., and Savelle, J.M.**
1996b: A history of sea ice in the Canadian Arctic Archipelago based on postglacial remains of the bowhead whale (*Balaena mysticetus*); Arctic, v. 49, p. 235–255.
- Edlund, S.A., Alt, B.T., and Garneau, M.**
2000: Vegetation patterns on Fosheim Peninsula, Ellesmere Island, Nunavut; *in* Environmental Response to Climate Change in the Canadian High Arctic, (ed.) M. Garneau and B.T. Alt; Geological Survey of Canada, Bulletin 529.
- Freedman, B., Svoboda, J., and Henery, G.H.R.**
1994: Alexandra Fiord — an ecological oasis in the polar desert; *in* Ecology of a Polar Oasis: Alexandra Fiord, Ellesmere Island, Canada; (ed.) O.J. Svoboda and B. Freedman; Captus University Publications, Toronto, Ontario, p. 1–9.
- Gajewski, K., Garneau, M., and Bourgeois, J.C.**
1995: Paleoenvironments of the Canadian high Arctic derived from pollen and plant macrofossils: problems and potentials; Quaternary Science Reviews, v. 14, p. 609–629.
- Garneau, M.**
2000: Peat accumulation and climatic change in the High Arctic; *in* Environmental Response to Climate Change in the Canadian High Arctic, (ed.) M. Garneau and B.T. Alt; Geological Survey of Canada, Bulletin 529.
- Henery, G., Freedman, B., and Svoboda, J.**
1986: Survey of vegetated areas and muskox populations in east-central Ellesmere Island; Arctic, v. 39, no. 1, p. 78–81.
- Hodgson, D.A.**
1989: Quaternary geology of the Queen Elizabeth Islands; *in* Chapter 6 of Quaternary Geology of Canada and Greenland, (ed.) R.J. Fulton; Geological Survey of Canada, Geology of Canada, no. 1, p. 443–448 (*also* Geological Society of America, The Geology of North America, v. K-1, p. 443–448).
- Jonsson, S. and Hansson, M.**
1990: Identification of annual layers in superimposed ice from Storoyjokulen in northeastern Svalbard; Geografiska Annaler, v. 72A, no. 1, p. 41–54.
- Koerner, R.M.**
1970: The mass balance of the Devon Island Ice Cap, Northwest Territories, Canada, 1961–66; Journal of Glaciology, v. 9, no. 57, p. 325–336.
- Koerner, R.M. and Bourgeois, J.C.**
1988: Pollen analysis and discussion of time-scales in Canadian ice cores; Annals of Glaciology, v. 10, p. 85–91.
- Labine, C.L.**
1994: Meteorology and climatology of the Alexandra Fiord Lowland; *in* Ecology of a Polar Oasis: Alexandra Fiord, Ellesmere Island, Canada, (ed.) J. Svoboda and B. Freedman; Captus University Publications, Toronto, Ontario, p. 23–39.

LaFarge-England, C, Vitt, D.H., and England, J.

1991: Holocene soligenous fens on a high arctic fault block, northern Ellesmere Island (82°), N.W.T., Canada; *Arctic and Alpine Research*, v. 23, p. 80–98.

Lamb, H.H.

1977: *Climate: Present, Past, and Future, Volume 2, Climatic History and the Future*; London, Methuen, 835 p.

Levesque, E. and Svoboda, J.

1992: Growth of Arctic Poppy in contrasting habitats of a polar oasis and a polar desert; *The Musk-Ox*, v. 39, p. 148–156.

1995: Germinable seed bank from polar desert sands, Central Ellesmere Island, Canada; *in* *Global Change and Terrestrial Ecosystems*, (ed.) T.V. Callaghan, U. Molau, M.J. Tyson, J.I. Holten, W.C. Oechel, T. Gilmanov, B. Maxwell, and B. Sveinbojornsson; *Oppdal, Norway*, August 21–26, 1993, p. 97–107.

Matthews, J.V., Jr. and Fyles, J.G.

2000: Late Tertiary plant and arthropod fossils from the high-terrace sediments on Fosheim Peninsula, Ellesmere Island, Nunavut; *in* *Environmental Response to Climate Change in the Canadian High Arctic*, (ed.) M. Garneau and B.T. Alt; Geological Survey of Canada, Bulletin 529.

Muc M., Freedman, B., and Svoboda, J.

1994: Vascular plant communities of a polar oasis at Alexandra Fiord, Ellesmere Island; *in* *Ecology of a Polar Oasis: Alexandra Fiord, Ellesmere Island, Canada*, (ed.) J. Svoboda and B. Freedman; Captus University Publications, Toronto, Ontario, p. 53–63.

Robinson, S.D.

2000: Thaw-slump-derived thermokarst near Hot Weather Creek, Ellesmere Island, Nunavut; *in* *Environmental Response to Climate Change in the Canadian High Arctic*, (ed.) M. Garneau and B.T. Alt; Geological Survey of Canada, Bulletin 529.

Sutherland, P.D.

2000: Preliminary results of archeological research on Fosheim Peninsula and in adjacent areas of western Ellesmere and eastern Axel Heiberg islands, Nunavut; *in* *Environmental Response to Climate Change in the Canadian High Arctic*, (ed.) M. Garneau and B.T. Alt; Geological Survey of Canada, Bulletin 529.

Svoboda, J. and Freedman, B.

1994: *Ecology of a Polar Oasis: Alexandra Fiord, Ellesmere Island, Canada*; Captus University Publications, Toronto, Ontario, 267 p.

Wolfe, A.P.

2000: A 6500 year diatom record from southwestern Fosheim Peninsula, Ellesmere Island, Nunavut; *in* *Environmental Response to Climate Change in the Canadian High Arctic*, (ed.) M. Garneau and B.T. Alt; Geological Survey of Canada, Bulletin 529.

Woo, M-k. and Young, K.L.

1997: Hydrology of a small basin with polar oasis environment, Fosheim Peninsula, Ellesmere Island, Canada; *Permafrost and Periglacial Processes*, v. 8, p. 257–277.

Young, K.L. and Woo, M-k.

2000: Hydrological environment of the Hot Weather Creek basin, Ellesmere Island, Nunavut; *in* *Environmental Response to Climate Change in the Canadian High Arctic*, (ed.) M. Garneau and B.T. Alt; Geological Survey of Canada, Bulletin 529.

Young, K.L., Woo, M-k., and Edlund, S.A.

1997: Influence of local topography, soils, and vegetation on microclimate and hydrology at a High Arctic site; *Arctic and Alpine Research*, v. 29, no. 3, p. 270–284.

AUTHOR INDEX

- Aitken, A.E. 197
(e-mail: Aaitken@arts.usask.ca)
- Alt, B.T. 1, 17, 37, 129, 271, 391
(e-mail: bea.alt@sympatico.ca)
- Atkinson, D.E.. 37, 99
(e-mail: atkinson@climate.geog.uottawa.ca)
- Bell, T. 175
(e-mail: tbell@morgan.ucs.mun.ca)
- Blake, W., Jr.. 257
(e-mail: weblake@NRCan.gc.ca)
- Bourgeois, J.C.. 271
(e-mail: jcbourge@NRCan.gc.ca)
- Brodo, F. 145
(e-mail: fbrod@cyberus.ca)
- Desrochers, D.T. 361
(e-mail: eas.sae@sympatico.ca)
- Douglas, M.S.V. 257
(e-mail: msvd@opal.geology.utoronto.ca)
- Edlund, S.A. 1, 113, 129
(e-mail: sedlund@cyberus.ca)
- Fisher, D.A. 271
(e-mail: fisher@NRCan.gc.ca)
- Fyles, J.G. 295
(e-mail: jfyles@NRCan.gc.ca)
- Gajewski, K. 235
(e-mail: gajewski@aix1.uottawa.ca)
- Garneau, M. 1, 113, 129, 283, 391
(e-mail: Michelle_Garneau@INRS-Eau.quebec.ca)
- Gilbert, R. 197
(e-mail: gilbertr@qsilver.QueensU.CA)
- Hamilton, P.B. 235
(e-mail: PHAMILTON@mus-nature.ca)
- Headley, A.N. 37
- Hodgson, D.A. 175
(e-mail: dhodgson@NRCan.gc.ca)
- Koerner, R.M. 271
(e-mail: rkoerner@NRCan.gc.ca)
- Labine, C.L. 37
(e-mail: clabine@attglobal.net)
- Lean, D.S.R. 235
(e-mail: dlean@science.uottawa.ca)
- Matthews, J.V., Jr. 295
(e-mail: ohana@sympatico.ca)
- Maxwell, B. 17
(e-mail: bst.maxwell@sympatico.ca)
- McNeely, R. 235
(e-mail: mcneely@NRCan.gc.ca)
- Pollard, W.H. 207, 325
(e-mail: pollard@hawk.igs.net)
- Robinson, S.D. 335
(e-mail: srobinso@NRCan.gc.ca)
- Smol, J.P. 257
(e-mail: smolj@biology.queensu.ca)
- Sutherland, P.D. 319
(e-mail: psutherl@istar.ca)
- Wolfe, A.P. 249
(e-mail: Alexander.Wolfe@Colorado.EDU)
- Wolfe, P.M. 37, 375
(deceased)
- Woo, M-k. 347
(e-mail: woo@mcmail.cis.mcmaster.ca)
- Young, K.L. 347
(e-mail: klyoung@yorku.ca)



This volume is dedicated to the memory of our friend and colleague, Paul M. Wolfe, who worked in the Arctic with a passion we will always share.